Protein

COVID-19 is an emerging, rapidly evolving situation.
Get the latest public health information from CDC: https://www.coronavirus.gov .
Get the latest research from NIH: https://www.nih.gov/coronavirus.
Find NCBI SARS-CoV-2 literature, sequence, and clinical content: https://www.ncbi.nlm.nih.gov/sars-cov-2/.

GenPept

This record is a non-redundant protein sequence. Please read more here.

TauD/TfdA family dioxygenase [Bradyrhizobium diazoefficiens]

NCBI Reference Sequence: WP_011084309.1

Identical Proteins FASTA Graphics

Go to:

```
LOCUS       WP_011084309             295 aa            linear   BCT 27-JUL-2019
DEFINITION  TauD/TfdA family dioxygenase [Bradyrhizobium diazoefficiens].
ACCESSION   WP_011084309
VERSION     WP_011084309.1
KEYWORDS    RefSeq.
SOURCE      Bradyrhizobium diazoefficiens
  ORGANISM  Bradyrhizobium diazoefficiens
            Bacteria; Proteobacteria; Alphaproteobacteria; Rhizobiales;
            Bradyrhizobiaceae; Bradyrhizobium.
COMMENT     REFSEQ: This record represents a single, non-redundant, protein
            sequence which may be annotated on many different RefSeq genomes
            from the same, or different, species.

            ##Evidence-For-Name-Assignment-START##
            Evidence Category  :: Conserved Domain (CDD)
            Evidence Accession :: Domain architecture ID 10496218
            Evidence Source    :: NCBI SPARCLE
            ##Evidence-For-Name-Assignment-END##
            COMPLETENESS: full length.
FEATURES             Location/Qualifiers
     source          1..295
                     /organism="Bradyrhizobium diazoefficiens"
                     /db_xref="taxon:1355477"
     Protein         1..295
                     /product="TauD/TfdA family dioxygenase"
                     /calculated_mol_wt=33512
     Region          5..281
                     /region_name="TauD"
                     /note="Taurine catabolism dioxygenase TauD, TfdA family;
                     pfam02668"
                     /db_xref="CDD:335034"
ORIGIN
        1 mtiairqlqt hfvgqvsgld lrkpltpgea revesamdky avlvfhdqdi tdeqqmafal
       61 nfgqredarg gtvtkekdyr lqsglndvsn lgkdgkplak dsrthlfnlg nclwhsdssf
      121 rpipakfsll sarvvnptgg ntefadmraa ydalddetka eiedlvcehs lmysrgslgf
      181 teytdeekqm fkpvlqrlvr thpvhrrksl ylsshagkia smsvpegrll lrdlnehatq
      241 pefvyvhkwk lhdlvmwdnr qtmhrvrryd qsqprdmrra tvagteptvq qqaae
//
```


COR-AAD1-00003381
Bayer EX1008 (Part 7 of 9)

Protein

COVID-19 is an emerging, rapidly evolving situation.
Get the latest public health information from CDC: https://www.coronavirus.gov .
Get the latest research from NIH: https://www.nih.gov/coronavirus.
Find NCBI SARS-CoV-2 literature, sequence, and clinical content: https://www.ncbi.nlm.nih.gov/sars-cov-2/.

GenPept

RecName: Full=(S)-phenoxypropionate/alpha-ketoglutarate-dioxygenase; Short=SdpA; AltName: Full=(S)-dichlorprop/(S)-mecoprop dioxygenase; AltName: Full=Alpha-ketoglutarate-dependent dioxygenase; AltName: Full=Dichlorprop/alpha-ketoglutarate-dioxygenase; AltName...

UniProtKB/Swiss-Prot: P83309.2

Identical Proteins FASTA Graphics

Go to:

```
LOCUS       SDPA_DELAC               292 aa            linear   BCT 18-SEP-2019
DEFINITION  RecName:
            Full=(S)-phenoxypropionate/alpha-ketoglutarate-dioxygenase;
            Short=SdpA; AltName: Full=(S)-dichlorprop/(S)-mecoprop dioxygenase;
            AltName: Full=Alpha-ketoglutarate-dependent dioxygenase; AltName:
            Full=Dichlorprop/alpha-ketoglutarate-dioxygenase; AltName:
            Full=Mecoprop/alpha-ketoglutarate-dioxygenase.
ACCESSION   P83309
VERSION     P83309.2
DBSOURCE    UniProtKB: locus SDPA_DELAC, accession P83309;
            class: standard.
            extra accessions:Q67FS3
            plasmid:pMC1
            created: May 10, 2004.
            sequence updated: Oct 29, 2014.
            annotation updated: Sep 18, 2019.
            xrefs: AY327575.2, AAP88277.1
            xrefs (non-sequence databases): SMR:P83309, KEGG:ag:AAP88277,
            KO:K21728, BRENDA:1.14.11.43, UniPathway:UPA00348, GO:0051213,
            GO:0031418, GO:0046872, Gene3D:3.60.130.10, InterPro:IPR042098,
            InterPro:IPR003819, Pfam:PF02668
KEYWORDS    Dioxygenase; Direct protein sequencing; Iron; Metal-binding;
            Oxidoreductase; Plasmid; Vitamin C.
SOURCE      Delftia acidovorans
  ORGANISM  Delftia acidovorans
            Bacteria; Proteobacteria; Betaproteobacteria; Burkholderiales;
            Comamonadaceae; Delftia.
REFERENCE   1  (residues 1 to 292)
  AUTHORS   Schleinitz,K.M., Kleinsteuber,S., Vallaeys,T. and Babel,W.
  TITLE     Localization and characterization of two novel genes encoding
            stereospecific dioxygenases catalyzing
            2(2,4-dichlorophenoxy)propionate cleavage in Delftia acidovorans
            MC1
  JOURNAL   Appl. Environ. Microbiol. 70 (9), 5357-5365 (2004)
   PUBMED   15345421
  REMARK    NUCLEOTIDE SEQUENCE [GENOMIC DNA].;
            STRAIN=MC1; PLASMID=pMC1
            Erratum:[Appl Environ Microbiol. 2004 Nov;70(11):6948]
REFERENCE   2  (residues 1 to 292)
  AUTHORS   Schleinitz,K.M., Kleinsteuber,S., Vallaeys,T. and Babel,W.
  TITLE     Direct Submission
  JOURNAL   Submitted (??-SEP-2009) to the EMBL/GenBank/DDBJ databases
  REMARK    NUCLEOTIDE SEQUENCE [GENOMIC DNA].;
            STRAIN=MC1; PLASMID=pMC1
REFERENCE   3  (residues 1 to 292)
  AUTHORS   Schleinitz,K.M., Vallaeys,T. and Kleinsteuber,S.
  TITLE     Direct Submission
  JOURNAL   Submitted (??-SEP-2009) to the EMBL/GenBank/DDBJ databases
  REMARK    NUCLEOTIDE SEQUENCE [GENOMIC DNA].;
            STRAIN=MC1; PLASMID=pMC1
REFERENCE   4  (residues 1 to 292)
  AUTHORS   Westendorf,A., Benndorf,D., Muller,R.H. and Babel,W.
  TITLE     The two enantiospecific
            dichlorprop/alpha-ketoglutarate-dioxygenases from Delftia
            acidovorans MC1--protein and sequence data of RdpA and SdpA
```


COR-AAD1-00003382
Bayer EX1008 (Part 7 of 9)

```
  JOURNAL   Microbiol. Res. 157 (4), 317-322 (2002)
   PUBMED   12581996
  REMARK    PROTEIN SEQUENCE OF 1-25; 100-106 AND 170-182, FUNCTION, AND
            SUBUNIT.;
            STRAIN=MC1
REFERENCE   5  (residues 1 to 292)
  AUTHORS   Westendorf,A., Mueller,R.H. and Babel,W.
  TITLE     Purification and characterisation of the enantiospecific
            dioxygenases from Delftia acidovorans MC1 initiating the
            degradation of phenoxypropionate and phenoxyacetate herbicides
  JOURNAL   Acta Biotechnol. 23, 3-17 (2003)
  REMARK    FUNCTION, CATALYTIC ACTIVITY, BIOPHYSICOCHEMICAL PROPERTIES,
            COFACTOR, ACTIVITY REGULATION, PATHWAY, AND SUBSTRATE SPECIFICITY.;
            STRAIN=MC1
REFERENCE   6  (residues 1 to 292)
  AUTHORS   Benndorf,D., Davidson,I. and Babel,W.
  TITLE     Regulation of catabolic enzymes during long-term exposure of
            Delftia acidovorans MC1 to chlorophenoxy herbicides
  JOURNAL   Microbiology (Reading, Engl.) 150 (Pt 4), 1005-1014 (2004)
   PUBMED   15073309
  REMARK    INDUCTION.;
            STRAIN=MC1
COMMENT     On or before Nov 5, 2014 this sequence version replaced
            gi:75364264, P83309.1.
            [FUNCTION] Involved in the degradation of the phenoxypropionate
            herbicides. Catalyzes the enantiospecific cleavage of the ether
            bond in the herbicid S-dichlorprop
            ((S)-2-(2,4-dichlorophenoxy)propionate)(S-2,4-DP) and S-mecoprop
            ((S)-2-(4-chloro-2-methylphenoxy)propionate)(S-2,4-MCPP). It can
            also accept (RS)-2-(4-chlorophenoxy)propionate,
            (RS)-2-(m-chlorophenoxy)propionate and phenoxyacetate derivatives
            such as 2,4-dichlorophenoxyacetate (2,4-D), however it can only
            accept 2-oxoglutarate as oxygen acceptor. {ECO:0000269|Ref.5,
            ECO:0000303|PubMed:12501996}.
            [CATALYTIC ACTIVITY]
            Reaction=(S)-2-(4-chloro-2-methylphenoxy)propanoate +
            2-oxoglutarate + O2 = 2-methyl-4-chlorophenol + CO2 + pyruvate +
            succinate; Xref=Rhea:RHEA:37831, ChEBI:CHEBI:1800,
            ChEBI:CHEBI:15361, ChEBI:CHEBI:15379, ChEBI:CHEBI:16526,
            ChEBI:CHEBI:16810, ChEBI:CHEBI:30031, ChEBI:CHEBI:75285;
            EC=1.14.11.43; Evidence={ECO:0000269|Ref.5}.
            [CATALYTIC ACTIVITY] Reaction=(S)-(2,4-dichlorophenoxy)propanoate +
            2-oxoglutarate + O2 = 2,4-dichlorophenol + CO2 + pyruvate +
            succinate; Xref=Rhea:RHEA:37827, ChEBI:CHEBI:15361,
            ChEBI:CHEBI:15379, ChEBI:CHEBI:16526, ChEBI:CHEBI:16738,
            ChEBI:CHEBI:16810, ChEBI:CHEBI:30031, ChEBI:CHEBI:75287;
            EC=1.14.11.43; Evidence={ECO:0000269|Ref.5}.
            [COFACTOR] Name=Fe cation; Xref=ChEBI:CHEBI:24875;
            Evidence={ECO:0000269|Ref.5}.
            [COFACTOR] Name=L-ascorbate; Xref=ChEBI:CHEBI:38290;
            Evidence={ECO:0000269|Ref.5}.
            ACTIVITY REGULATION: Inhibited by divalent cations, most
            significantly by copper and nickel, and by diethylpyrocarbonate
            (DEPC). {ECO:0000269|Ref.5}.
            [BIOPHYSICOCHEMICAL PROPERTIES] Kinetic parameters: KM=11.5 uM for
            (RS)-2-(m-chlorophenoxy)propionate (at pH 6 and 25 degrees Celsius)
            {ECO:0000269|Ref.5}; KM=21.8 uM for S-2,4-MCPP (at pH 6 and 25
            degrees Celsius) {ECO:0000269|Ref.5}; KM=24.1 uM for
            alpha-ketoglutarate (at pH 6 and 25 degrees Celsius)
            {ECO:0000269|Ref.5}; KM=49 uM for S-2,4-DP (at pH 6 and 25 degrees
            Celsius) {ECO:0000269|Ref.5}; KM=68.3 uM for
            (RS)-2-(4-chlorophenoxy)propionate (at pH 6 and 25 degrees Celsius)
            {ECO:0000269|Ref.5}; KM=122.8 uM for 2,4-D (at pH 6 and 25 degrees
            Celsius) {ECO:0000269|Ref.5}; Note=Kcat is 50 min(-1) for
            dioxygenase activity with S-2,4-DP (at pH 6 and 25 degrees
            Celsius). Kcat is 46 min(-1) for dioxygenase activity with
            S-2,4-MCPP (at pH 6 and 25 degrees Celsius). Kcat is 36 min(-1) for
            dioxygenase activity with 2,4-D (at pH 6 and 25 degrees Celsius).
            Kcat is 17 min(-1) for dioxygenase activity with
            (RS)-2-(4-chlorophenoxy)propionate (at pH 6 and 25 degrees
            Celsius). Kcat is 15 min(-1) for dioxygenase activity with
            (RS)-2-(m-chlorophenoxy)propionate (at pH 6 and 25 degrees
            Celsius). Kcat is 1.7 min(-1) for dioxygenase activity with
            alpha-ketoglutarate (at pH 6 and 25 degrees Celsius).
            {ECO:0000269|Ref.5}; pH dependence: Optimum pH is about 6.
            {ECO:0000269|Ref.5}; Temperature dependence: Optimum temperature is
            25 degrees Celsius. {ECO:0000269|Ref.5}.
            [PATHWAY] Xenobiotic degradation; 2-(2,4-dichlorophenoxy)propanoate
            degradation. {ECO:0000305|Ref.5}.
            [SUBUNIT] Monomer. {ECO:0000269|PubMed:12501996}.
            [INDUCTION] Repressed during growth on high concentrations of
```


COR-AAD1-00003383
Bayer EX1008 (Part 7 of 9)

```
            2,4-dichlorophenoxypropionic acid (2,4-DCPP).
            {ECO:0000269|PubMed:15073309}.
            [SIMILARITY] Belongs to the TfdA dioxygenase family. {ECO:0000305}.
FEATURES             Location/Qualifiers
     source          1..292
                     /organism="Delftia acidovorans"
                     /plasmid=""
                     /db_xref="taxon:80866"
     gene            1..292
                     /gene="sdpA"
     Protein         1..292
                     /product="(S)-phenoxypropionate/alpha-ketoglutarate-
                     dioxygenase"
                     /EC_number="1.14.11.48"
                     /note="SdpA; (S)-dichlorprop/(S)-mecoprop dioxygenase;
                     Alpha-ketoglutarate-dependent dioxygenase;
                     Dichlorprop/alpha-ketoglutarate-dioxygenase;
                     Mecoprop/alpha-ketoglutarate-dioxygenase"
                     /UniProtKB_evidence="Evidence at protein level"
     Region          1..292
                     /region_name="Mature chain"
                     /note="(S)-phenoxypropionate/alpha-ketoglutarate-
                     dioxygenase. /FTId=PRO_0000097650."
     Region          5..265
                     /region_name="TauD"
                     /note="Taurine dioxygenase, alpha-ketoglutarate-dependent
                     [Secondary metabolites biosynthesis, transport and
                     catabolism]; COG2175"
                     /db_xref="CDD:225086"
     Region          6..276
                     /region_name="TauD"
                     /note="Taurine catabolism dioxygenase TauD, TfdA family;
                     pfam02668"
                     /db_xref="CDD:280777"
     Region          105
                     /region_name="Conflict"
                     /note="M -> T (in Ref. 4; AA sequence). {ECO:0000305}."
     Site            108
                     /site_type="metal-binding"
                     /note="Iron; catalytic. {ECO:0000250|UniProtKB:P37610}."
     Site            110
                     /site_type="metal-binding"
                     /note="Iron; catalytic. {ECO:0000250|UniProtKB:P37610}."
     Site            135
                     /site_type="binding"
                     /note="2-oxoglutarate. {ECO:0000250|UniProtKB:P37610}."
     Region          170
                     /region_name="Conflict"
                     /note="K -> G (in Ref. 4; AA sequence). {ECO:0000305}."
     Site            247
                     /site_type="binding"
                     /note="2-oxoglutarate. {ECO:0000250|UniProtKB:P37610}."
     Site            262
                     /site_type="metal-binding"
                     /note="Iron; catalytic. {ECO:0000250|UniProtKB:P37610}."
     Site            273
                     /site_type="binding"
                     /note="2-oxoglutarate. {ECO:0000250|UniProtKB:P37610}."
ORIGIN
        1 mqttlqitpt gatlgatvtg vhlatlddag faalhaawlq hallifpgqh lsndqqitfa
       61 krfgaierig ggdivaisnv kadgtvrqhs paewddmmkv ivgnmawhad stympvmaqg
      121 avfsaevvpa vggrtcfadm raaydaldea tralvhqrsa rhslvysqsk lghvqqagsa
      181 yigygmdtta tplrplvkvh petgrpslli grhahaipgm daaeserfle glvdwacqap
      241 rvhahqwaag dvvvwdnrcl lhraepwdfk lprvmwhsrl agrpetegaa lv
//
```


COR-AAD1-00003384
Bayer EX1008 (Part 7 of 9)

Protein

COVID-19 is an emerging, rapidly evolving situation.
Get the latest public health information from CDC: https://www.coronavirus.gov .
Get the latest research from NIH: https://www.nih.gov/coronavirus.
Find NCBI SARS-CoV-2 literature, sequence, and clinical content: https://www.ncbi.nlm.nih.gov/sars-cov-2/.

GenPept

RecName: Full=(S)-phenoxypropionate/alpha-ketoglutarate-dioxygenase; Short=SdpA; AltName: Full=(S)-dichlorprop/(S)-mecoprop dioxygenase; AltName: Full=Alpha-ketoglutarate-dependent dioxygenase; AltName: Full=Dichlorprop/alpha-ketoglutarate-dioxygenase; AltName...

UniProtKB/Swiss-Prot: Q700X4.1

Identical Proteins FASTA Graphics

Go to:

```
LOCUS       SDPA_SPHHM               287 aa            linear   BCT 12-AUG-2020
DEFINITION  RecName:
            Full=(S)-phenoxypropionate/alpha-ketoglutarate-dioxygenase;
            Short=SdpA; AltName: Full=(S)-dichlorprop/(S)-mecoprop dioxygenase;
            AltName: Full=Alpha-ketoglutarate-dependent dioxygenase; AltName:
            Full=Dichlorprop/alpha-ketoglutarate-dioxygenase; AltName:
            Full=Mecoprop/alpha-ketoglutarate-dioxygenase.
ACCESSION   Q700X4
VERSION     Q700X4.1
DBSOURCE    UniProtKB: locus SDPA_SPHHM, accession Q700X4;
            class: standard.
            created: Oct 29, 2014.
            sequence updated: Jul 5, 2004.
            annotation updated: Aug 12, 2020.
            xrefs: AJ628860.1, CAF32813.1, WP_037468461.1
            xrefs (non-sequence databases): SMR:Q700X4,
            STRING:1219045.BV98_003436, eggNOG:COG2175, OrthoDB:1742732at2,
            BRENDA:1.14.11.43, UniPathway:UPA00348, GO:0051213, GO:0046872,
            GO:0019439, Gene3D:3.60.130.10, InterPro:IPR042098,
            InterPro:IPR003819, Pfam:PF02668
KEYWORDS    Aromatic hydrocarbons catabolism; Dioxygenase; Iron; Metal-binding;
            Oxidoreductase.
SOURCE      Sphingobium herbicidovorans NBRC 16415
  ORGANISM  Sphingobium herbicidovorans NBRC 16415
            Bacteria; Proteobacteria; Alphaproteobacteria; Sphingomonadales;
            Sphingomonadaceae; Sphingobium.
REFERENCE   1  (residues 1 to 287)
  AUTHORS   Kohler,H.P.
  TITLE     Sphingomonas herbicidovorans MH: a versatile phenoxyalkanoic acid
            herbicide degrader
  JOURNAL   J. Ind. Microbiol. Biotechnol. 23 (4-5), 336-340 (1999)
   PUBMED   11423952
  REMARK    NUCLEOTIDE SEQUENCE [GENOMIC DNA], AND FUNCTION.;
            STRAIN=ATCC 700291 / DSM 11019 / NBRC 16415 / MH
REFERENCE   2  (residues 1 to 287)
  AUTHORS   Muller,T.A., Byrde,S.M., Werlen,C., van der Meer,J.R. and
            Kohler,H.P.
  TITLE     Genetic analysis of phenoxyalkanoic acid degradation in
            Sphingomonas herbicidovorans MH
  JOURNAL   Appl. Environ. Microbiol. 70 (10), 6066-6075 (2004)
   PUBMED   15466552
  REMARK    NUCLEOTIDE SEQUENCE [GENOMIC DNA].;
            STRAIN=ATCC 700291 / DSM 11019 / NBRC 16415 / MH
REFERENCE   3  (residues 1 to 287)
  AUTHORS   Muller,T.A., Fleischmann,T., van der Meer,J.R. and Kohler,H.P.
  TITLE     Purification and characterization of two enantioselective
            alpha-ketoglutarate-dependent dioxygenases, RdpA and SdpA, from
            Sphingomonas herbicidovorans MH
  JOURNAL   Appl. Environ. Microbiol. 72 (7), 4853-4861 (2006)
   PUBMED   16820486
  REMARK    FUNCTION, CATALYTIC ACTIVITY, BIOPHYSICOCHEMICAL PROPERTIES,
            SUBUNIT, COFACTOR, SUBSTRATE SPECIFICITY, AND PATHWAY.;
            STRAIN=ATCC 700291 / DSM 11019 / NBRC 16415 / MH
REFERENCE   4  (residues 1 to 287)
  AUTHORS   Muller,T.A., Zavodszky,M.I., Feig,M., Kuhn,L.A. and Hausinger,R.P.
```


COR-AAD1-00003385
Bayer EX1008 (Part 7 of 9)

```
  TITLE     Structural basis for the enantiospecificities of R- and S-specific
            phenoxypropionate/alpha-ketoglutarate dioxygenases
  JOURNAL   Protein Sci. 15 (6), 1356-1368 (2006)
   PUBMED   16731970
  REMARK    FUNCTION, CATALYTIC ACTIVITY, BIOPHYSICOCHEMICAL PROPERTIES, AND
            MUTAGENESIS OF GLU-69; GLY-97; ASN-98; GLN-162; ARG-207; HIS-208
            AND HIS-272.;
            STRAIN=Strain MH
COMMENT     [FUNCTION] Involved in the degradation of the phenoxypropionate
            herbicides. Catalyzes the enantiospecific cleavage of the ether
            bond in the herbicid S-dichlorprop
            ((S)-2-(2,4-dichlorophenoxy)propionate)(S-2,4-DP) and S-mecoprop
            ((S)-2-(4-chloro-2-methylphenoxy)propionate)(S-2,4-MCPP). It can
            also accept (RS)-2-(4-chloro-2-methylphenoxy)propionate
            ((RS)-2,4-MCPP) and phenoxyacetate derivatives such as
            2,4-dichlorophenoxyacetate (2,4-D), however it can only accept
            2-oxoglutarate as oxygen acceptor. {ECO:0000269|PubMed:16731970,
            ECO:0000269|PubMed:16820480, ECO:0000303|PubMed:11423952}.
            [CATALYTIC ACTIVITY]
            Reaction=(S)-2-(4-chloro-2-methylphenoxy)propanoate +
            2-oxoglutarate + O2 = 2-methyl-4-chlorophenol + CO2 + pyruvate +
            succinate; Xref=Rhea:RHEA:37831, ChEBI:CHEBI:1800,
            ChEBI:CHEBI:15361, ChEBI:CHEBI:15379, ChEBI:CHEBI:16526,
            ChEBI:CHEBI:16810, ChEBI:CHEBI:30031, ChEBI:CHEBI:75285;
            EC=1.14.11.43; Evidence={ECO:0000269|PubMed:16731970,
            ECO:0000269|PubMed:16820480}.
            [CATALYTIC ACTIVITY] Reaction=(S)-(2,4-dichlorophenoxy)propanoate +
            2-oxoglutarate + O2 = 2,4-dichlorophenol + CO2 + pyruvate +
            succinate; Xref=Rhea:RHEA:37827, ChEBI:CHEBI:15361,
            ChEBI:CHEBI:15379, ChEBI:CHEBI:16526, ChEBI:CHEBI:16738,
            ChEBI:CHEBI:16810, ChEBI:CHEBI:30031, ChEBI:CHEBI:75287;
            EC=1.14.11.43; Evidence={ECO:0000269|PubMed:16731970,
            ECO:0000269|PubMed:16820480}.
            [COFACTOR] Name=Fe cation; Xref=ChEBI:CHEBI:24875;
            Evidence={ECO:0000269|PubMed:16820480}.
            [COFACTOR] Name=L-ascorbate; Xref=ChEBI:CHEBI:38290;
            Evidence={ECO:0000269|PubMed:16820480}.
            [BIOPHYSICOCHEMICAL PROPERTIES] Kinetic parameters: KM=19.6 uM for
            alpha-ketoglutarate (at pH 6.75 and 30 degrees Celsius))
            {ECO:0000269|PubMed:16820480}; KM=132 uM for S-2,4-MCPP (at pH 6.75
            and 30 degrees Celsius) {ECO:0000269|PubMed:16820480}; KM=161 uM
            for S-2,4-MCPP (at pH 6.75 and 30 degrees Celsius)
            {ECO:0000269|PubMed:16731970}; KM=234 uM for (RS)-2,4-MCPP (at pH
            6.75 and 30 degrees Celsius) {ECO:0000269|PubMed:16731970};
            KM=494.8 uM for S-2,4-DP (at pH 6.75 and 30 degrees Celsius)
            {ECO:0000269|PubMed:16820480}; Note=Kcat is 229.7 min(-1) for
            dioxygenase activity with alpha-ketoglutarate (at pH 6.75 and 30
            degrees Celsius). Kcat is 284.6 min(-1) for dioxygenase activity
            with S-2,4-DP (at pH 6.75 and 30 degrees Celsius). Kcat is 303
            min(-1) for dioxygenase activity with S-2,4-MCPP (at pH 6.75 and 30
            degrees Celsius). Kcat is 899 min(-1) for dioxygenase activity with
            (RS)-2,4-MCPP (at pH 6.75 and 30 degrees Celsius). Kcat is 1010
            min(-1) for dioxygenase activity with S-2,4-MCPP (at pH 6.75 and 30
            degrees Celsius). {ECO:0000269|PubMed:16731970,
            ECO:0000269|PubMed:16820480}; pH dependence: Optimum pH is about
            6.5. {ECO:0000269|PubMed:16820480}; Temperature dependence: Optimum
            temperature is between 35 and 40 degrees Celsius.
            {ECO:0000269|PubMed:16820480}.
            [PATHWAY] Xenobiotic degradation; 2-(2,4-dichlorophenoxy)propanoate
            degradation. {ECO:0000305|PubMed:16820480}.
            [SUBUNIT] Monomer. {ECO:0000269|PubMed:16820480}.
            [SIMILARITY] Belongs to the TfdA dioxygenase family. {ECO:0000305}.
FEATURES             Location/Qualifiers
     source          1..287
                     /organism="Sphingobium herbicidovorans NBRC 16415"
                     /db_xref="taxon:1219045"
     gene            1..287
                     /gene="sdpA"
     Protein         1..287
                     /product="(S)-phenoxypropionate/alpha-ketoglutarate-
                     dioxygenase"
                     /EC_number="1.14.11.43"
                     /note="SdpA; (S)-dichlorprop/(S)-mecoprop dioxygenase;
                     Alpha-ketoglutarate-dependent dioxygenase;
                     Dichlorprop/alpha-ketoglutarate-dioxygenase;
                     Mecoprop/alpha-ketoglutarate-dioxygenase"
                     /UniProtKB_evidence="Evidence at protein level"
     Region          1..287
                     /region_name="Mature chain"
                     /note="(S)-phenoxypropionate/alpha-ketoglutarate-
                     dioxygenase. /id=PRO_0000430762."
```


COR-AAD1-00003386
Bayer EX1008 (Part 7 of 9)

```
Region          1..279
                /region_name="TauD"
                /note="Taurine dioxygenase, alpha-ketoglutarate-dependent
                [Secondary metabolites biosynthesis, transport and
                catabolism]; COG2175"
                /db_xref="CDD:225086"
Region          6..271
                /region_name="TauD"
                /note="Taurine catabolism dioxygenase TauD, TfdA family;
                pfam02668"
                /db_xref="CDD:280777"
Site            69
                /site_type="other"
                /note="Contributes to enantiospecificity.
                /evidence=ECO:0000303|PubMed:16731970."
Site            69
                /site_type="mutagenized"
                /note="E->A: The dioxygenase activity with S-2,4-MCPP and
                (RS)-2,4-MCPP is 30% and 20% of the wild-type,
                respectively. Slight increase of the affinity binding for
                S-2,4-MCPP and (RS)-2,4-MCPP.
                /evidence=ECO:0000269|PubMed:16731970."
Site            97
                /site_type="mutagenized"
                /note="G->I: The dioxygenase activity with S-2,4-MCPP and
                (RS)-2,4-MCPP is strongly reduced and there is a 18-fold
                decrease of the affinity binding for S-2,4-MCPP; when
                associated with G-98.
                /evidence=ECO:0000269|PubMed:16731970."
Site            97
                /site_type="mutagenized"
                /note="G->N: Loss of the dioxygenase activity; when
                associated with G-98.
                /evidence=ECO:0000269|PubMed:16731970."
Site            98
                /site_type="mutagenized"
                /note="N->G: The dioxygenase activity with S-2,4-MCPP and
                (RS)-2,4-MCPP is strongly reduced; when associated with
                I-97. Loss of the dioxygenase activity; when associated
                with N-97. /evidence=ECO:0000269|PubMed:16731970."
Site            order(102,104,129,257)
                /site_type="active"
                /db_xref="CDD:238154"
Site            order(102,104,257)
                /site_type="other"
                /note="iron coordination sites [ion binding]"
                /db_xref="CDD:238154"
Site            102
                /site_type="metal-binding"
                /note="Iron; catalytic.
                /evidence=ECO:0000250|UniProtKB:P37610."
Site            104
                /site_type="metal-binding"
                /note="Iron; catalytic.
                /evidence=ECO:0000250|UniProtKB:P37610."
Site            129
                /site_type="binding"
                /note="2-oxoglutarate.
                /evidence=ECO:0000250|UniProtKB:P37610."
Site            162
                /site_type="mutagenized"
                /note="Q->F: The dioxygenase activity with S-2,4-MCPP and
                (RS)-2,4-MCPP is strongly reduced.
                /evidence=ECO:0000269|PubMed:16731970."
Site            207
                /site_type="other"
                /note="Contributes to enantiospecificity.
                /evidence=ECO:0000303|PubMed:16731970."
Site            207
                /site_type="mutagenized"
                /note="R->A: The dioxygenase activity with S-2,4-MCPP and
                (RS)-2,4-MCPP is 17 and 8% of the wild-type, respectively.
                15 and 10-fold decrease of the affinity binding for
                S-2,4-MCPP and (RS)-2,4-MCPP, respectively.
                /evidence=ECO:0000269|PubMed:16731970."
Site            207
                /site_type="mutagenized"
                /note="R->V: The dioxygenase activity with S-2,4-MCPP and
                (RS)-2,4-MCPP is strongly reduced.
                /evidence=ECO:0000269|PubMed:16731970."
Site            208
```


COR-AAD1-00003387
Bayer EX1008 (Part 7 of 9)

```
                     /site_type="mutagenized"
                     /note="H->A: The dioxygenase activity with S-2,4-MCPP and
                     (RS)-2,4-MCPP is strongly reduced. 18-fold decrease of the
                     affinity binding for R-2,4-MCPP.
                     /evidence=ECO:0000269|PubMed:16731970."
     Site            242
                     /site_type="binding"
                     /note="2-oxoglutarate.
                     /evidence=ECO:0000250|UniProtKB:P37610."
     Site            257
                     /site_type="metal-binding"
                     /note="Iron; catalytic.
                     /evidence=ECO:0000250|UniProtKB:P37610."
     Site            268
                     /site_type="binding"
                     /note="2-oxoglutarate.
                     /evidence=ECO:0000250|UniProtKB:P37610."
     Site            272
                     /site_type="mutagenized"
                     /note="H->A: The dioxygenase activity with S-2,4-MCPP and
                     (RS)-2,4-MCPP is strongly reduced.
                     /evidence=ECO:0000269|PubMed:16731970."
     Site            274
                     /site_type="mutagenized"
                     /note="R->A: Loss of the dioxygenase activity.
                     /evidence=ECO:0000269|PubMed:16731970."
ORIGIN
        1 mspafdiapl datfgavvtg vkladlddag wldlqaawle yallvfpdqh ltreqqiafa
       61 rrfgplefem aaisnvrpdg slrvesdndd mmkilkgnmg whadstympv qakgavfsae
      121 vvpsvggqtg fadmraayda ldedlkarve tlqarhslhy sqsklghqtk aadgeysgyg
      181 lhdgpvplrp lvkihpetgr kslligrhah aipglepaes erllqqlidf acqppriyhh
      241 dwapgdavlw dnrcllhqat pwdmtqkrim whsriagdpa setalah
//
```


COR-AAD1-00003388
Bayer EX1008 (Part 7 of 9)

Protein

COVID-19 is an emerging, rapidly evolving situation.
Get the latest public health information from CDC: https://www.coronavirus.gov .
Get the latest research from NIH: https://www.nih.gov/coronavirus.
Find NCBI SARS-CoV-2 literature, sequence, and clinical content: https://www.ncbi.nlm.nih.gov/sars-cov-2/.

GenPept

(S)-2-(2,4-dichlorophenoxy)propionate/alpha-ketoglutarate dioxygenase [Rhodoferax sp. P230]

GenBank: ABD67501.1

Identical Proteins FASTA Graphics

Go to:

```
LOCUS       ABD67501                287 aa            linear   BCT 14-MAR-2006
DEFINITION  (S)-2-(2,4-dichlorophenoxy)propionate/alpha-ketoglutarate
            dioxygenase [Rhodoferax sp. P230].
ACCESSION   ABD67501
VERSION     ABD67501.1
DBSOURCE    accession DQ406818.1
KEYWORDS    .
SOURCE      Rhodoferax sp. P230
  ORGANISM  Rhodoferax sp. P230
            Bacteria; Proteobacteria; Betaproteobacteria; Burkholderiales;
            Comamonadaceae; Rhodoferax.
REFERENCE   1  (residues 1 to 287)
  AUTHORS   Westendorf,A., Benndorf,D., Kleinsteuber,S., Mueller,R.H. and
            Harms,H.
  TITLE     The S-enantiomer specific enzymes from Rhodoferax sp. P230 and
            Sphingobium herbicidovorans MH involved in the cleavage of
            2-phenoxypropionate (dichlorprop and mecoprop) and phenoxyacetate
            herbicides (2,4-D and MCPA), kinetic characteristics and protein
            data
  JOURNAL   Unpublished
REFERENCE   2  (residues 1 to 287)
  AUTHORS   Kleinsteuber,S.
  TITLE     Direct Submission
  JOURNAL   Submitted (17-FEB-2006) Environmental Microbiology, UFZ Centre for
            Environmental Research, Permoserstrasse 15, Leipzig 04318, Germany
FEATURES             Location/Qualifiers
     source          1..287
                     /organism="Rhodoferax sp. P230"
                     /strain="P230"
                     /db_xref="taxon:103036"
     Protein         1..287
                     /product="(S)-2-(2,
                     4-dichlorophenoxy)propionate/alpha-ketoglutarate
                     dioxygenase"
     Region          1..279
                     /region_name="TauD"
                     /note="Taurine dioxygenase, alpha-ketoglutarate-dependent
                     [Secondary metabolites biosynthesis, transport and
                     catabolism]; COG2175"
                     /db_xref="CDD:225086"
     Region          6..271
                     /region_name="TauD"
                     /note="Taurine catabolism dioxygenase TauD, TfdA family;
                     pfam02668"
                     /db_xref="CDD:280777"
     Site            order(102,104,129,257)
                     /site_type="active"
                     /db_xref="CDD:238154"
     Site            order(102,104,257)
                     /site_type="other"
                     /note="iron coordination sites [ion binding]"
                     /db_xref="CDD:238154"
     CDS             1..287
                     /gene="sdpA"
                     /coded_by="DQ406818.1:119..982"
                     /transl_table=11
ORIGIN
        1 mspafdiapl datfgavvtg vkladlddag wldlqaawle yallvfpdqh ltreqqiafa
```


COR-AAD1-00003389
Bayer EX1008 (Part 7 of 9)

```
       61 rrfgplefem aaisnvrpdg slrvesdndd mmkilkgnmg whadstympv qakgavfsae
      121 vvpsvggqtg fadmraayda ldedlkarve tlqarhslhy sqsklghqtk aadgeysgyg
      181 lhdgpvplrp lvkihpetgr kslligrhah aipglepaes erllqqlidf acqppriyhh
      241 dwapgdavlw dnrcllhqat pwdmtqkrim whsriagdpa setalah
//
```


COR-AAD1-00003390
Bayer EX1008 (Part 7 of 9)

Protein

COVID-19 is an emerging, rapidly evolving situation.
Get the latest public health information from CDC: https://www.coronavirus.gov .
Get the latest research from NIH: https://www.nih.gov/coronavirus.
Find NCBI SARS-CoV-2 literature, sequence, and clinical content: https://www.ncbi.nlm.nih.gov/sars-cov-2/.

GenPept

RecName: Full=(R)-phenoxypropionate/alpha-ketoglutarate-dioxygenase; Short=RdpA; AltName: Full=(R)-dichlorprop/(R)-mecoprop dioxygenase; AltName: Full=Alpha-ketoglutarate-dependent dioxygenase; AltName: Full=Dichlorprop/alpha-ketoglutarate-dioxygenase; AltName...

UniProtKB/Swiss-Prot: Q8KSC8.2

Identical Proteins FASTA Graphics

Go to:

```
LOCUS       RDPA_SPHHM               295 aa            linear   BCT 11-DEC-2019
DEFINITION  RecName:
            Full=(R)-phenoxypropionate/alpha-ketoglutarate-dioxygenase;
            Short=RdpA; AltName: Full=(R)-dichlorprop/(R)-mecoprop dioxygenase;
            AltName: Full=Alpha-ketoglutarate-dependent dioxygenase; AltName:
            Full=Dichlorprop/alpha-ketoglutarate-dioxygenase; AltName:
            Full=Mecoprop/alpha-ketoglutarate-dioxygenase.
ACCESSION   Q8KSC8
VERSION     Q8KSC8.2
DBSOURCE    UniProtKB: locus RDPA_SPHHM, accession Q8KSC8;
            class: standard.
            created: Oct 29, 2014.
            sequence updated: Mar 1, 2004.
            annotation updated: Dec 11, 2019.
            xrefs: AF516752.2, AAM90965.2, AJ628859.1, CAF32811.1,
            WP_031942865.1, 6D0O_A, 6D0O_B, 6D0O_C, 6D0O_D, 6D1O_A, 6D1O_B,
            6D1O_C, 6D1O_D, 6D1O_E, 6D1O_F, 6D1O_G, 6D1O_H, 6D3H_A, 6D3H_B,
            6D3H_I, 6D3H_M, 6D3I_A, 6D3I_D, 6D3I_G, 6D3I_J, 6D3J_A, 6D3M_A,
            6D3M_B, 6D3M_F, 6D3M_J
            xrefs (non-sequence databases): PDBsum:6D0O, PDBsum:6D1O,
            PDBsum:6D3H, PDBsum:6D3I, PDBsum:6D3J, PDBsum:6D3M, SMR:Q8KSC8,
            BioCyc:GCF_001598535:G1ES4-4015-MONOMER, BRENDA:1.14.11.44,
            UniPathway:UPA00348, GO:0051213, GO:0046872, GO:0019439,
            Gene3D:3.60.130.10, InterPro:IPR042098, InterPro:IPR003819,
            Pfam:PF02668
KEYWORDS    3D-structure; Aromatic hydrocarbons catabolism; Dioxygenase; Iron;
            Metal-binding; Oxidoreductase.
SOURCE      Sphingobium herbicidovorans NBRC 16415
  ORGANISM  Sphingobium herbicidovorans NBRC 16415
            Bacteria; Proteobacteria; Alphaproteobacteria; Sphingomonadales;
            Sphingomonadaceae; Sphingobium.
REFERENCE   1  (residues 1 to 295)
  AUTHORS   Kohler,H.P.
  TITLE     Sphingomonas herbicidovorans MH: a versatile phenoxyalkanoic acid
            herbicide degrader
  JOURNAL   J. Ind. Microbiol. Biotechnol. 23 (4-5), 336-340 (1999)
   PUBMED   11423952
  REMARK    NUCLEOTIDE SEQUENCE [GENOMIC DNA], AND FUNCTION.;
            STRAIN=ATCC 700291 / DSM 11019 / NBRC 16415 / MH
REFERENCE   2  (residues 1 to 295)
  AUTHORS   Schleinitz,K.M., Kleinsteuber,S., Vallaeys,T. and Babel,W.
  TITLE     Localization and characterization of two novel genes encoding
            stereospecific dioxygenases catalyzing
            2(2,4-dichlorophenoxy)propionate cleavage in Delftia acidovorans
            MC1
  JOURNAL   Appl. Environ. Microbiol. 70 (9), 5357-5365 (2004)
   PUBMED   15345423
  REMARK    NUCLEOTIDE SEQUENCE [GENOMIC DNA].;
            STRAIN=ATCC 700291 / DSM 11019 / NBRC 16415 / MH
            Erratum:[Appl Environ Microbiol. 2004 Nov;70(11):6948]
REFERENCE   3  (residues 1 to 295)
  AUTHORS   Muller,T.A., Byrde,S.M., Werlen,C., van der Meer,J.R. and
            Kohler,H.P.
  TITLE     Genetic analysis of phenoxyalkanoic acid degradation in
            Sphingomonas herbicidovorans MH
```


COR-AAD1-00003391
Bayer EX1008 (Part 7 of 9)

```
  JOURNAL   Appl. Environ. Microbiol. 70 (10), 6066-6075 (2004)
   PUBMED   15466552
  REMARK    NUCLEOTIDE SEQUENCE [GENOMIC DNA].;
            STRAIN=ATCC 700291 / DSM 11019 / NBRC 16415 / MH
REFERENCE   4  (residues 1 to 295)
  AUTHORS   Muller,T.A., Fleischmann,T., van der Meer,J.R. and Kohler,H.P.
  TITLE     Purification and characterization of two enantioselective
            alpha-ketoglutarate-dependent dioxygenases, RdpA and SdpA, from
            Sphingomonas herbicidovorans MH
  JOURNAL   Appl. Environ. Microbiol. 72 (7), 4853-4861 (2006)
   PUBMED   16820480
  REMARK    FUNCTION, CATALYTIC ACTIVITY, BIOPHYSICOCHEMICAL PROPERTIES,
            SUBUNIT, COFACTOR, SUBSTRATE SPECIFICITY, AND PATHWAY.
REFERENCE   5  (residues 1 to 295)
  AUTHORS   Muller,T.A., Zavodszky,M.I., Feig,M., Kuhn,L.A. and Hausinger,R.P.
  TITLE     Structural basis for the enantiospecificities of R- and S-specific
            phenoxypropionate/alpha-ketoglutarate dioxygenases
  JOURNAL   Protein Sci. 15 (6), 1356-1368 (2006)
   PUBMED   16731970
  REMARK    FUNCTION, CATALYTIC ACTIVITY, BIOPHYSICOCHEMICAL PROPERTIES, AND
            MUTAGENESIS OF VAL-80; LEU-83; GLN-93; ILE-106; GLY-107; PHE-171;
            TYR-221 AND ARG-285.
COMMENT     [FUNCTION] Involved in the degradation of the phenoxypropionate
            herbicides. Catalyzes the enantiospecific cleavage of the ether
            bond in the herbicid R-dichlorprop
            ((R)-2-(2,4-dichlorophenoxy)propionate)(R-2,4-DP) and R-mecoprop
            ((R)-2-(4-chloro-2-methylphenoxy)propionate)(R-2,4-MCPP). It can
            also accept (RS)-4-chlorophenoxypropanoate, however it can only
            accept 2-oxoglutarate as oxygen acceptor.
            {ECO:0000269|PubMed:16731970, ECO:0000269|PubMed:16820480,
            ECO:0000303|PubMed:11423952}.
            [CATALYTIC ACTIVITY]
            Reaction=(R)-2-(4-chloro-2-methylphenoxy)propanoate +
            2-oxoglutarate + O2 = 2-methyl-4-chlorophenol + CO2 + pyruvate +
            succinate; Xref=Rhea:RHEA:37815, ChEBI:CHEBI:1800,
            ChEBI:CHEBI:15361, ChEBI:CHEBI:15379, ChEBI:CHEBI:16526,
            ChEBI:CHEBI:16810, ChEBI:CHEBI:30031, ChEBI:CHEBI:75284;
            EC=1.14.11.44; Evidence={ECO:0000269|PubMed:16731970,
            ECO:0000269|PubMed:16820480, ECO:0000303|PubMed:11423952}.
            [CATALYTIC ACTIVITY] Reaction=(R)-(2,4-dichlorophenoxy)propanoate +
            2-oxoglutarate + O2 = 2,4-dichlorophenol + CO2 + pyruvate +
            succinate; Xref=Rhea:RHEA:37823, ChEBI:CHEBI:15361,
            ChEBI:CHEBI:15379, ChEBI:CHEBI:16526, ChEBI:CHEBI:16738,
            ChEBI:CHEBI:16810, ChEBI:CHEBI:30031, ChEBI:CHEBI:75288;
            EC=1.14.11.44; Evidence={ECO:0000269|PubMed:16731970,
            ECO:0000269|PubMed:16820480}.
            [COFACTOR] Name=Fe cation; Xref=ChEBI:CHEBI:24875;
            Evidence={ECO:0000269|PubMed:16820480}.
            [COFACTOR] Name=L-ascorbate; Xref=ChEBI:CHEBI:38290;
            Evidence={ECO:0000250|UniProtKB:Q67FR0}.
            [BIOPHYSICOCHEMICAL PROPERTIES] Kinetic parameters: KM=2.8 uM for
            alpha-ketoglutarate (at pH 6.75 and 30 degrees Celsius)
            {ECO:0000269|PubMed:16820480}; KM=98.8 uM for R-2,4-MCPP (at pH
            6.75 and 30 degrees Celsius) {ECO:0000269|PubMed:16820480};
            KM=163.7 uM for R-2,4-DP (at pH 6.75 and 30 degrees Celsius)
            {ECO:0000269|PubMed:16820480}; KM=262.4 uM for
            (RS)-4-chlorophenoxypropanoate (at pH 6.75 and 30 degrees Celsius)
            {ECO:0000269|PubMed:16820480}; KM=380 uM for R-2,4-MCPP (at pH 6.75
            and 30 degrees Celsius) {ECO:0000269|PubMed:16731970}; Note=Kcat is
            114.2 min(-1) for dioxygenase activity with R-2,4-MCPP (at pH 6.75
            and 30 degrees Celsius). Kcat is 135.6 min(-1) for dioxygenase
            activity with alpha-ketoglutarate (at pH 6.75 and 30 degrees
            Celsius). Kcat is 170.1 min(-1) for dioxygenase activity with
            R-2,4-DP (at pH 6.75 and 30 degrees Celsius). Kcat is 241.9 min(-1)
            for dioxygenase activity with (RS)-4-chlorophenoxypropanoate (at pH
            6.75 and 30 degrees Celsius). Kcat is 252 min(-1) for dioxygenase
            activity with R-2,4-MCPP (at pH 6.75 and 30 degrees Celsius).
            {ECO:0000269|PubMed:16731970, ECO:0000269|PubMed:16820480}; pH
            dependence: Optimum pH is about 6.5. {ECO:0000269|PubMed:16820480};
            Temperature dependence: Optimum temperature is between 35 and 40
            degrees Celsius. {ECO:0000269|PubMed:16820480}.
            [PATHWAY] Xenobiotic degradation; 2-(2,4-dichlorophenoxy)propanoate
            degradation. {ECO:0000305|PubMed:16820480}.
            [SUBUNIT] Homotrimer. {ECO:0000269|PubMed:16820480}.
            [SIMILARITY] Belongs to the TfdA dioxygenase family. {ECO:0000305}.
FEATURES             Location/Qualifiers
     source          1..295
                     /organism="Sphingobium herbicidovorans NBRC 16415"
                     /db_xref="taxon:1219043"
     gene            1..295
                     /gene="rdpA"
```


COR-AAD1-00003392
Bayer EX1008 (Part 7 of 9)

```
Protein         1..295
                /product="(R)-phenoxypropionate/alpha-ketoglutarate-
                dioxygenase"
                /EC_number="1.14.11.44"
                /note="RdpA; (R)-dichlorprop/(R)-mecoprop dioxygenase;
                Alpha-ketoglutarate-dependent dioxygenase;
                Dichlorprop/alpha-ketoglutarate-dioxygenase;
                Mecoprop/alpha-ketoglutarate-dioxygenase"
                /UniProtKB_evidence="Evidence at protein level"
Region          1..295
                /region_name="Mature chain"
                /note="(R)-phenoxypropionate/alpha-ketoglutarate-
                dioxygenase. /id=PRO_0000430761."
Region          13..293
                /region_name="TauD"
                /note="Taurine dioxygenase, alpha-ketoglutarate-dependent
                [Secondary metabolites biosynthesis, transport and
                catabolism]; COG2175"
                /db_xref="CDD:225086"
Region          13..24
                /region_name="Beta-strand region"
                /note="/evidence=ECO:0000244|PDB:6D3H."
Region          17..287
                /region_name="TauD"
                /note="Taurine catabolism dioxygenase TauD, TfdA family;
                pfam02668"
                /db_xref="CDD:280777"
Region          26..30
                /region_name="Beta-strand region"
                /note="/evidence=ECO:0000244|PDB:6D3H."
Region          39..52
                /region_name="Helical region"
                /note="/evidence=ECO:0000244|PDB:6D3H."
Region          53..59
                /region_name="Beta-strand region"
                /note="/evidence=ECO:0000244|PDB:6D3H."
Region          64..72
                /region_name="Helical region"
                /note="/evidence=ECO:0000244|PDB:6D3H."
Site            80
                /site_type="mutagenized"
                /note="V->A: The dioxygenase activity with R-2,4-MCPP is
                60% of the wild-type. 6-fold decrease of the affinity
                binding for R-2,4-MCPP.
                /evidence=ECO:0000269|PubMed:16731970."
Region          81..83
                /region_name="Beta-strand region"
                /note="/evidence=ECO:0000244|PDB:6D3H."
Site            83
                /site_type="mutagenized"
                /note="L->A: The dioxygenase activity with R-2,4-MCPP is
                5% of the wild-type.
                /evidence=ECO:0000269|PubMed:16731970."
Region          89..97
                /region_name="Beta-strand region"
                /note="/evidence=ECO:0000244|PDB:6D3H."
Site            93
                /site_type="mutagenized"
                /note="Q->A: The dioxygenase activity with R-2,4-MCPP is
                10% of the wild-type. 7-fold decrease of the affinity
                binding for R-2,4-MCPP.
                /evidence=ECO:0000269|PubMed:16731970."
Region          101..103
                /region_name="Beta-strand region"
                /note="/evidence=ECO:0000244|PDB:6D1O."
Site            106
                /site_type="mutagenized"
                /note="I->A: The dioxygenase activity with R-2,4-MCPP is
                30% of the wild-type. 20-fold decrease of the affinity
                binding for R-2,4-MCPP. Loss of the dioxygenase activity;
                when associated with I-107. The dioxygenase activity with
                R-2,4-MCPP is 10% of the wild-type; when associated with
                N-107. /evidence=ECO:0000269|PubMed:16731970."
Site            107
                /site_type="mutagenized"
                /note="G->I: Loss of the dioxygenase activity; when
                associated with A-106.
                /evidence=ECO:0000269|PubMed:16731970."
Site            107
                /site_type="mutagenized"
                /note="G->N: The dioxygenase activity with R-2,4-MCPP is
```


COR-AAD1-00003393
Bayer EX1008 (Part 7 of 9)

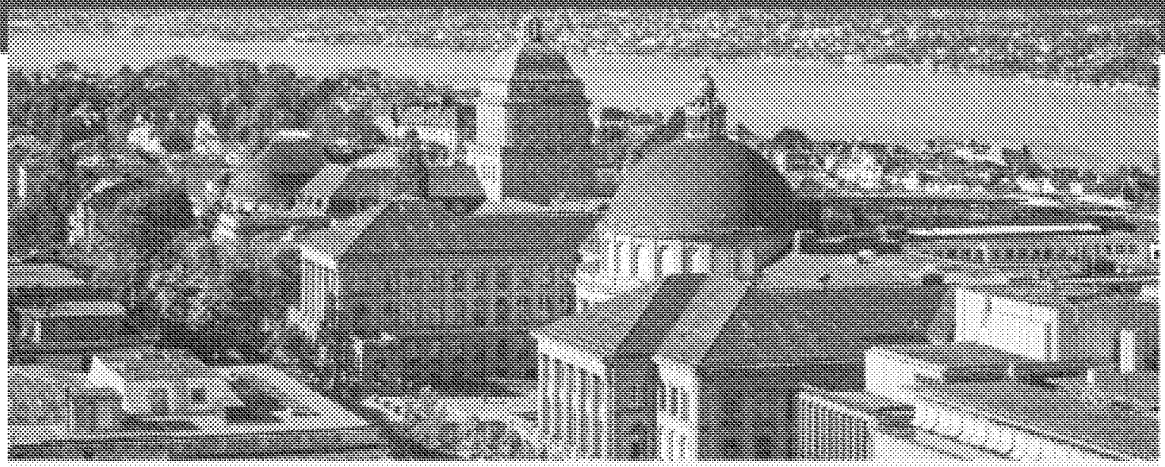
```
                10% of the wild-type; when associated with A-106.
                /evidence=ECO:0000269|PubMed:16731970."
     Region     109..111
                /region_name="Beta-strand region"
                /note="/evidence=ECO:0000244|PDB:6D3H."
     Site       111
                /site_type="metal-binding"
                /note="Iron; catalytic.
                /evidence=ECO:0000250|UniProtKB:P37610."
     Region     113..116
                /region_name="Hydrogen bonded turn"
                /note="/evidence=ECO:0000244|PDB:6D3H."
     Site       113
                /site_type="metal-binding"
                /note="Iron; catalytic.
                /evidence=ECO:0000250|UniProtKB:P37610."
     Region     117..119
                /region_name="Beta-strand region"
                /note="/evidence=ECO:0000244|PDB:6D3H."
     Region     122..130
                /region_name="Beta-strand region"
                /note="/evidence=ECO:0000244|PDB:6D3H."
     Region     133..135
                /region_name="Beta-strand region"
                /note="/evidence=ECO:0000244|PDB:6D3I."
     Region     138..142
                /region_name="Beta-strand region"
                /note="/evidence=ECO:0000244|PDB:6D3H."
     Site       138
                /site_type="binding"
                /note="2-oxoglutarate.
                /evidence=ECO:0000250|UniProtKB:P37610."
     Region     143..148
                /region_name="Helical region"
                /note="/evidence=ECO:0000244|PDB:6D3H."
     Region     152..158
                /region_name="Helical region"
                /note="/evidence=ECO:0000244|PDB:6D3H."
     Region     162..165
                /region_name="Beta-strand region"
                /note="/evidence=ECO:0000244|PDB:6D3H."
     Region     168..171
                /region_name="Helical region"
                /note="/evidence=ECO:0000244|PDB:6D3H."
     Site       171
                /site_type="mutagenized"
                /note="F->A: The dioxygenase activity with R-2,4-MCPP is
                60% of the wild-type. 4-fold increase of the affinity
                binding for R-2,4-MCPP.
                /evidence=ECO:0000269|PubMed:16731970."
     Site       171
                /site_type="mutagenized"
                /note="F->Q: The dioxygenase activity with R-2,4-MCPP is
                60% of the wild-type and the affinity binding R-2,4-MCPP
                is similar to the wild-type.
                /evidence=ECO:0000269|PubMed:16731970."
     Region     173..177
                /region_name="Helical region"
                /note="/evidence=ECO:0000244|PDB:6D3H."
     Region     178..180
                /region_name="Beta-strand region"
                /note="/evidence=ECO:0000244|PDB:6D3I."
     Region     184..186
                /region_name="Hydrogen bonded turn"
                /note="/evidence=ECO:0000244|PDB:6D3H."
     Region     192..196
                /region_name="Helical region"
                /note="/evidence=ECO:0000244|PDB:6D3H."
     Region     199..206
                /region_name="Beta-strand region"
                /note="/evidence=ECO:0000244|PDB:6D3H."
     Region     208..210
                /region_name="Hydrogen bonded turn"
                /note="/evidence=ECO:0000244|PDB:6D3H."
     Region     213..215
                /region_name="Beta-strand region"
                /note="/evidence=ECO:0000244|PDB:6D3H."
     Region     219..221
                /region_name="Hydrogen bonded turn"
                /note="/evidence=ECO:0000244|PDB:6D3H."
     Site       221
```


COR-AAD1-00003394
Bayer EX1008 (Part 7 of 9)

```
                     /site_type="other"
                     /note="Contributes to enantiospecificity.
                     /evidence=ECO:0000303|PubMed:16731970."
     Site            221
                     /site_type="mutagenized"
                     /note="Y->A: The dioxygenase activity with R-2,4-MCPP is
                     5% of the wild-type.
                     /evidence=ECO:0000269|PubMed:16731970."
     Region          222..225
                     /region_name="Beta-strand region"
                     /note="/evidence=ECO:0000244|PDB:6D3H."
     Region          230..244
                     /region_name="Helical region"
                     /note="/evidence=ECO:0000244|PDB:6D3H."
     Region          247..249
                     /region_name="Helical region"
                     /note="/evidence=ECO:0000244|PDB:6D3H."
     Region          250..253
                     /region_name="Beta-strand region"
                     /note="/evidence=ECO:0000244|PDB:6D3H."
     Site            255
                     /site_type="binding"
                     /note="2-oxoglutarate.
                     /evidence=ECO:0000250|UniProtKB:P37610."
     Region          260..264
                     /region_name="Beta-strand region"
                     /note="/evidence=ECO:0000244|PDB:6D3H."
     Region          265..267
                     /region_name="Hydrogen bonded turn"
                     /note="/evidence=ECO:0000244|PDB:6D3H."
     Region          268..272
                     /region_name="Beta-strand region"
                     /note="/evidence=ECO:0000244|PDB:6D3H."
     Site            270
                     /site_type="metal-binding"
                     /note="Iron; catalytic.
                     /evidence=ECO:0000250|UniProtKB:P37610."
     Region          275..278
                     /region_name="Hydrogen bonded turn"
                     /note="/evidence=ECO:0000244|PDB:6D3I."
     Region          281..288
                     /region_name="Beta-strand region"
                     /note="/evidence=ECO:0000244|PDB:6D3H."
     Site            281
                     /site_type="binding"
                     /note="2-oxoglutarate.
                     /evidence=ECO:0000250|UniProtKB:P37610."
     Site            285
                     /site_type="other"
                     /note="Contributes to enantiospecificity.
                     /evidence=ECO:0000303|PubMed:16731970."
     Site            285
                     /site_type="mutagenized"
                     /note="R->A: The dioxygenase activity with R-2,4-MCPP is
                     10% of the wild-type. 4-fold decrease of the affinity
                     binding for R-2,4-MCPP.
                     /evidence=ECO:0000269|PubMed:16731970."
ORIGIN
        1 mhaalsplsq rferiavqpl tgvlgaeitg vdlrepldds twneildafh tyqviyfpgq
       61 aitneqhiaf srrfgpvdpv pllksiegyp evqmirrean esgrvigddw htdstfldap
      121 paavvmraid vpehggdtgf lsmytawetl sptmqatieg lnvvhsatrv fgslyqaqnr
      181 rfsntsvkvm dvdagdretv hplvvthpgs grkglyvnqv ycqriegmtd aeskpllqfl
      241 yehatrfdft crvrwkkdqv lvwdnlctmh ravpdyagkf ryltrttvgg vrpar
//
```


COR-AAD1-00003395
Bayer EX1008 (Part 7 of 9)

ETH zürich Research Collection



Doctoral Thesis

Metabolism of phenoxyalkanoic acid herbicides in Sphingomonas herbicidovorans MH
cloning and characterization of two enantiospecific α-ketoglutarate-dependent dioxygenases and degradation pathway analysis

Author(s):
Müller, Tina Andrea

Publication Date:
2004

Permanent Link:
https://doi.org/10.3929/ethz-a-004885312

Rights / License:
In Copyright - Non-Commercial Use Permitted

This page was generated automatically upon download from the ETH Zurich Research Collection. For more information please consult the Terms of use.

ETH Library

Diss. ETH No. 15588

Metabolism of Phenoxyalkanoic Acid Herbicides in *Sphingomonas herbicidovorans* MH: Cloning and Characterization of Two Enantiospecific α-Ketoglutarate-Dependent Dioxygenases and Degradation Pathway Analysis

A dissertation submitted to the
SWISS FEDERAL INSTITUTE OF TECHNOLOGY ZURICH

for the degree of
DOCTOR OF NATURAL SCIENCES

presented by

TINA ANDREA MÜLLER
dipl. Umwelt-Natw. ETH Zurich
born March 8, 1973
citizen of Turbenthal ZH

accepted on the recommendation of
Prof. Dr. Alexander J. B. Zehnder, examiner
Prof. Dr. Hilary M. Lappin-Scott, co-examiner
Dr. Hans-Peter E. Kohler, co-examiner
Prof. Dr. Jan Roelof van der Meer, co-examiner

Zurich, 2004

COR-AAD1-00003397
Bayer EX1008 (Part 7 of 9)

Danke

Ich möchte mich ganz herzlich bei allen Leuten bedanken, die mich während diesen Jahren hier an der EAWAG auf die eine und andere Art unterstützt haben! Ich habe hier eine schöne Zeit verbracht und ich habe die angenehme Atmosphäre sehr geschätzt.

Als erstes möchte ich natürlich meinen beiden Betreuern, Hanspi und Jan Roelof, danken. Ihr habt mich immer wieder motiviert und auch während den nicht so erfolgreichen Zeiten unterstützt. Hanspi, du hast mir die Biochemie und die Welt der Enzyme nähergebracht und auch die anderen Diskussionen über Gott und die Welt haben mir Spass gemacht. Jan Roelof, vielen Dank für die Ratschläge und Tipps zur Genetik, aber auch für deinen Enthusiasmus, der mich immer wieder motiviert hat. Herzlichen Dank an euch! Thanks goes also to Hilary Lappin-Scott for being my coreferee. It was nice to talk to you and to discuss my thesis with you. Mein Dank gebührt natürlich auch Sascha Zehnder. Du hast mich immer unterstützt – auch wenn die ersten Jahre alles andere als viel versprechend waren und die 'Beaujolais nouveau'-Parties werden mir immer in Erinnerung bleiben!

Dann möchte ich mich herzlich bei Steven bedanken. Du hast dich während deiner Diplomarbeit sehr eingesetzt und es hat sich gelohnt! Thomi und Christoph; vielen Dank an euch. Ihr wart die guten Geister im Hintergrund und hattet immer ein offenes Ohr für meine kleinen und grossen Anliegen – auch wenn es ab und zu hektisch zu und her ging.

Vielen Dank an die 'Frauenclique' Caroline, Judith, Alex, Eva, Marie-Hélène und Kirsten. Caroline, merci beaucoup für deine Freundschaft, die vielen Diskussionen und lustigen Momente im und ausserhalb des Labors. Judith, auch dir herzlichen Dank für die vielen schönen und relaxenden Momente und

COR-AAD1-00003399
Bayer EX1008 (Part 7 of 9)

dir Alex für die gute Laune und das 'Tiiinscheee'. Merci Eva für die Unterstützung und es hat mich immer gefreut, mit dir (Beach)Volley zu spielen. Christoph – es war super, mit dir das Labor und Büro zu teilen und zu wissen, dass noch jemand ab und zu etwas grumlig ist… Merci auch dir Birgit für das letzte dreiviertel Jahr – es hat mich gefreut, mit dir fachzusimpeln und das Büro zu teilen. Marco, vielen Dank für die vielen aufmunternden Worten während den ersten Jahren meiner Diss und es ist kaum zu glauben aber wahr; ich habe es doch noch geschafft. Andy, vielen Dank für die lustigen Stunden in und ausserhalb der EAWAG. Nicht zu vergessen sind auch Raoul und Philippe, die mir bei meinen unzähligen Computerproblemen immer wieder geholfen haben und ohne die ich einige Male verzweifelt wäre.

Schliesslich möchte ich mich auch noch bei allen meinen Freunden ausserhalb der EAWAG und bei meiner Familie bedanken. Es war nicht immer einfach mit mir während diesen Jahren, aber ihr habt mich trotzdem immer unterstützt – obwohl euch meine Probleme wahrscheinlich ab und zu etwas unverständlich erschienen sind. Merci villmol!

TABLE OF CONTENTS

SUMMARY	**i**
ZUSAMMENFASSUNG	**v**
CHAPTER 1 GENERAL INTRODUCTION	**1**
Outline of the Thesis	2
Chirality of Pollutants – Effects on Metabolism and Fate	5
α-Ketoglutarate-Dependent Dioxygenases	47
CHAPTER 2	**69**
Genetic Analysis of Phenoxyalkanoic Acid Degradation in *Sphingomonas herbicidovorans* MH	
CHAPTER 3	**99**
Purification and Characterization of α-Ketoglutarate-Dependent *(R)*-Dichlorprop Dioxygenase RdpA from *Sphingomonas herbicidovorans* MH	
CHAPTER 4	**123**
The α-Ketoglutarate-Dependent *(S)*-Dichlorprop Dioxygenase from *Sphingomonas herbicidovorans* MH: Purification and Characterization of an Enantiospecific Enzyme	
CHAPTER 5	**145**
General Discussion and Outlook	
CHAPTER 6	**157**
Appendix	
CURRICULUM VITAE	**167**

COR-AAD1-00003401

Bayer EX1008 (Part 7 of 9)

SUMMARY

The bacterium *Sphingomonas herbicidovorans* MH is able to degrade phenoxyalkanoic acid herbicides, such as the chiral mecoprop (2-(*R,S*)-2-methyl-4-chlorophenoxypropanoic acid) and dichlorprop (2-(*R,S*)-2,4-dichlorophenoxy-propanoic acid). Strain MH degrades mecoprop and dichlorprop enantiospecific, whereby the (*S*) enantiomer is preferentially converted. This thesis work was carried out to (i) elucidate the genetic background of the mecoprop and dichlorprop degradation pathway and to (ii) characterize the two α-ketoglutarate-dependent dioxygenases that catalyze the initial degradation step and to study the features of enantioselective enzyme reactions.

To elucidate the genetic background of the phenoxyalkanoic acid degradation pathway in *S. herbicidovorans* MH, PCR- and hybridization experiments were carried out with primers and probes derived from related genes. Strain MH expressed two distinct α-ketoglutarate dependent dioxygenases, designated *(R)*- and *(S)*-dichlorprop dioxygenases (RdpA and SdpA, respectively) that converted phenoxypropanoic acid herbicides to the corresponding achiral phenols. Further breakdown of the phenol was proposed to proceed analogously to the well-studied pathway of 2,4-D (2,4-dichlorophenoxyacetic acid) in *Ralstonia eutropha* JMP134(pJP4) through a phenol hydroxylase forming a substituted catechol and further through a modified *ortho*-cleavage pathway. Several genes of this pathway were isolated: a putative phenol hydroxylase gene (*tfdB*), a putative regulatory gene (*cadR*), two genes for dichlorocatechol 1,2-dioxygenases ($dccA_{I/II}$), a complete and an incomplete gene copy for a dienelactone hydrolase ($dccD_{I/II}$), a gene for a part of a maleylacetate reductase (*dccE*) and a gene for a potential phenoxyalkanoic acid permease (*tfdK*). No gene for a chloromuconate cycloisomerase was found. In contrast to the 2,4-D pathways in other microorganisms, the *sdp*, *rdp*, and *dcc* genes of *S. herbicidovorans* MH were not located in one regulon and their expression was not tightly regulated. No coherent pattern was derived on the possible origin of the *sdp*, *rdp*, and *dcc* genes. *rdpA* from the *Alphaproteobacterium S. herbicidovorans* MH was 99% identical to *rdpA*

COR-AAD1-00003403
Bayer EX1008 (Part 7 of 9)

from the *Betaproteobacterium Delftia acidovorans* MC1. Such close resemblance is evidence for a recent gene exchange between *Alpha-* and *Betaproteobacteria.* On the contrary, $DccA_I$ and $DccA_{II}$ did not group within the known chlorocatechol 1,2-dioxygenases from *Beta-* and *Gammaproteobacteria*, but formed a separate branch in clustering analysis. This suggests a different reservoir of the genes of the modified *ortho*-cleavage pathway in *Alphaproteobacteria* from the ones in *Beta-* and *Gammaproteobacteria* and a reduced gene transfer between these bacterial groups.

We intensively investigated the two α-ketoglutarate-dependent dichlorprop-dioxygenases RdpA and SdpA, which were 30% identical to each other. The amino acid sequence of RdpA was 100% identical to the one of RdpA from the dichlorprop degrader *D. acidovorans* MC1, whereas the amino acid sequence of SdpA was only 63% identical to the one of SdpA from D. acidovorans MC1. With TfdA and TauD, the identities lay in the range of 30–37%. A conserved motif of α-ketoglutarate-dependent dioxygenases, $HXDX_{24}TX_{131}HX_{10}R$ for RdpA and $HXDX_{24}TX_{127}HX_{10}R$ for SdpA, was recognized in both proteins. In RdpA, His-111, Asp-113 and His-270 are predicted to form the 2-His-1-carboxylate facial triad involved in iron(II) binding and the residues Thr-138 and Arg-281 were putative α-ketoglutarate binding sites. The predicted iron-binding residues in SdpA were His-102, Asp-104 and His-257; and the predicted α-ketoglutarate binding residues were Thr-129 and Arg-268.

We expressed and purified both enzymes as 6xHis-tagged proteins and characterized them with respect to their physicochemical properties, their substrate, cosubstrate and cofactor specificities and enzyme kinetics. RdpA turned out to be a trimer with a subunit size of 36 kDa whereas SdpA was a monomer with a size of 32 kDa. RdpA exclusively converted the *(R)* enantiomers of dichlorprop and mecoprop whereas SdpA was specific for the *(S)* enantiomers. Both dioxygenases preferred substituted phenoxypropanoic acids to unsubstituted ones. Furthermore, RdpA and SdpA were only slightly or not active at all with phenoxyacetic and phenoxybutyric acids as substrates. RdpA activity was linearly dependent on oxygen concentration whereas SdpA showed Michalis-Menten behavior with O_2 as

COR-AAD1-00003404
Bayer EX1008 (Part 7 of 9)

the substrate with an apparent K_m-value of 159 μM. Both dioxygenases were quite specific for their cosubstrate α-ketoglutarate. The only other cosubstrate that supported activity was 2-oxoadipate. High specificity was also observed for Fe(II) which could not be replaced by any of the tested divalent cations. In the absence of ascorbate, RdpA and SdpA exhibited lower activity suggesting uncoupled decarboxylation of α-ketoglutarate.

S. herbicidovorans MH grows on 2,4-D, but neither RdpA nor SdpA catalyzed 2,4-D to a significant extent indicating the existence of a third phenoxyalkanoic acid converting enzyme. However, *tfdA*-like, *tfdA*α-like or *cadAB*-like genes were not detected in strain MH with PCR- and hybridization experiments.

Finally, we modeled the native structure of RdpA and SdpA with TauD as a template and speculated about the active sites of the two enzymes. The overall structures of RdpA and SdpA could be modeled on the TauD structure and showed the typical jellyroll motif. The model confirmed the predicted iron(II)- and α-ketoglutarate-binding residues in both dioxygenases. In both proteins, a cavity was formed by several amino acid residues, which had the potential to bind the aromatic ring of the phenoxypropanoic acids. The most striking difference between RdpA and SdpA was the replacement of the neutral Gly-107 in RdpA by the basic Asn-95 in SdpA at the active site. This indicates an important rote of this residue in interacting with the alkyl- or the carboxy-moiety of the substrates and hence also in determining the stereospecificity of the enzyme. Since these are only model predictions based on an existing template structure, further direct crystallization studies are needed to obtain a more appropriate view on the native fold and the active sites of RdpA and SdpA. The work presented here gives the basis for such experiments.

COR-AAD1-00003405
Bayer EX1008 (Part 7 of 9)

ZUSAMMENFASSUNG

Das Bakterium *Sphingomonas herbicidovorans* MH baut Phenoxyalkansäure-Herbizide wie die chiralen Verbindungen Mecoprop (2-(*R,S*)-2-Methyl-4-chlorophenoxypropionsäure) und Dichlorprop (2-(*R,S*)-2,4-Dichlorophenoxypropionsäure) ab. Der Stamm MH baut Mecoprop und Dichlorprop enantiospezifisch ab, wobei das *(S)* Enantiomer bevorzugt umgewandelt wird. Diese Doktorarbeit wurde ausgeführt um (i) den genetischen Hintergrund des Mecoprop- und Dichlorprop-Abbauweges zu untersuchen und um (ii) die zwei α-Ketoglutarat abhängigen Dioxygenasen zu charakterisieren, die den ersten Abbauschritt katalysieren und um die Eigenschaften dieser enantioselektiven Enzymreaktion zu studieren.

Um den genetischen Hintergrund des Phenoxyalkansäure-Abbauweges in *S. herbicidovorans* MH aufzuklären, wurden PCR- und Hybridisierungsexperimente mit Primern und Sonden, die aus verwandten Genen abgeleitet wurden, durchgeführt. Der Stamm MH exprimiert zwei verschiedene α-Ketoglutarat abhängige Dioxygenasen, *(R)*- und *(S)*-Dichlorprop Dioxygenasen, die Phenoxypropionsäure-Herbizide in die entsprechenden Phenole umwandeln. Es wurde vorgeschlagen, dass die Phenole analog des bekannten 2,4-D (2,4-Dichlorophenoxyessigsäure) Abbauweges von *Ralstonia eutropha* JMP134(pJP4) mittels einer Phenol Hydroxylase, die ein substituiertes Catechol bildet, abgebaut werden und dann durch den modifizierten *ortho*-cleavage Abbauweg metabolisiert werden. Verschiedene Gene dieses Abbauweges wurden aus Stamm MH isoliert: ein mutmassliches Phenol Hydroxylase-Gen (*tfdB*), ein mögliches Regulatorgen (*cadR*), zwei Gene für Dichlorocatechol 1,2-Dioxygenasen ($dccA_{I/II}$), eine vollständige und eine unvollständige Genkopie einer Dienelactone Hydrolase ($dccD_{I/II}$), ein Gen für einen Teil einer Maleylacetat Reduktase (*dccE*) und ein Gen für eine potentielle Phenoxyalkansäure Permease (*tfdK*). Ein Chloromuconat Cycloisomerase-Gen wurde nicht gefunden. Im Gegensatz zu den 2,4-D Abbauwegen in anderen Mikroorganismen sind die *sdp*, *rdp*, und *dcc*-Gene in *S. herbicidovorans* MH nicht in einem Regulon angeordnet und ihre Expression ist nicht streng reguliert. Es wurde weiter auch kein einheitliches Bild über den möglichen Ursprung der *sdp*, *rdp*, und *dcc*-Gene erhalten. *rdpA* vom *Alphaproteobakterium S. herbicidovorans* MH war 99% identisch zu *rdpA* vom *Betaproteobakterium Delftia acidovorans* MC1. Eine solche Ähnlichkeit deutet an, dass kürzlich ein Genaustausch zwischen *Alpha-* und *Betaproteobakterien* stattgefunden hat.

Im Gegensatz dazu können $DccA_I$ und $DccA_{II}$ nicht mit den bekannten Chlorocatechol 1,2-Dioxygenasen von *Beta-* und *Gammaproteobakterien* gruppiert werden, sondern bilden einen eigenen Ast in einer Klusteranalyse. Daher wird vorgeschlagen, dass verschiedene Reservoirs von Genen des modifizierten *ortho*-cleavage Abbauweges in *Alphaproteobakterien* und *Beta-* und *Gammaproteobakterien* existieren und dass die Gene zwischen diesen Bakteriengruppen nur begrenzt ausgetauscht werden.

Im weiteren untersuchten wir die zwei α-Ketoglutarat abhängigen Dichlorprop Dioxygenasen, die 30% identisch zueinander sind. Die Aminosäuresequenz von RdpA ist 100% identisch mit derjenigen von RdpA vom Dichlorprop-Abbauer *D. acidovorans* MC1, während die Aminosäuresequenz von SdpA nur 63% identisch ist mit derjenigen von SdpA von Stamm MC1. Die Identität zu TfdA und TauD liegt im Bereich zwischen 30–37%. Ein in α-Ketoglutarat abhängigen Dioxygenasen konserviertes Motiv, $HXDX_{24}TX_{131}HX_{10}R$ in RdpA und $HXDX_{24}TX_{127}HX_{10}R$ in SdpA, wurde in beiden Proteinen gefunden. Für RdpA wurde vorhergesagt, dass His-111, Asp-113 und His-270 die 2-His-1-carboxylate facial triad bilden, die in die Eisen(II)-Bindung involviert ist, und Thr-138 und Arg-281 bilden mögliche α-Ketoglutarat bindende Aminosäuren. In SdpA wurden His-102, Asp-104 und His-257 als Eisen(II)-bindende und Thr-129 und Arg-268 als α-Ketoglutarat bindende Aminosäuren vorhergesagt.

Wir haben beide Enzyme als 6xHis-tagged Fusionsproteine exprimiert, gereinigt und sie hinsichtlich ihrer physikalisch-chemischen Eigenschaften, ihrer Substrat-, Kosubstrat- und Kofaktoren-Spektren und ihrer Enzymkinetik charakterisiert. RdpA war ein Trimer mit einer Untereinheit von 36 kDa, während SdpA ein Monomer mit einer Grösse von 32 kDa war. RdpA wandelte nur die *(R)* Enantiomere von Dichlorprop und Mecoprop um, SdpA war im Gegensatz dazu spezifisch für die *(S)* Enantiomere. Beide Dichlorprop-Dioxygenasen waren nur schwach oder überhaupt nicht aktiv mit Phenoxyessig- und Phenoxybuttersäuren. Die RdpA Aktivität war linear abhängig von der Sauerstoffkonzentration, während SdpA Michaelis-Menten-Kinetik-Verhalten mit Sauerstoff als Substrat zeigte und einen apparenten K_m-Wert von 159 μM aufwies. Beide Dioxygenasen waren ziemlich spezifisch für das Kosubstrat α-Ketoglutarat. Das einzige andere Kosubstrat, das Aktivität unterstützte, war 2-Oxoadipat. Hohe Spezifizität wurde auch für Fe(II) gezeigt, das durch kein anderes divalentes Kation ersetzt werden konnte. Ohne Ascorbat wurde eine verminderte Aktivität von RdpA und SdpA gemessen, was auf eine entkoppelte α-Ketoglutarat-Dekarboxylierung hindeutet.

COR-AAD1-00003408
Bayer EX1008 (Part 7 of 9)

S. herbicidovorans MH wächst auf 2,4-D, aber weder RdpA noch SdpA wandeln 2,4-D mit einer signifikanten Umsatzrate um. Dies deutet darauf hin, dass ein drittes, Phenoxyalkansäure umsetzendes Enzym existiert. Dennoch wurden mit PCR- und Hybridisierungsexperimenten keine *tfdA*-ähnliche, *tfdA*α-ähnliche oder *cadAB*-ähnliche Gene im Stamm MH gefunden.

Schliesslich modellierten wir die Struktur von RdpA und SdpA mit TauD als Vorlage und spekulierten über die aktive Seite der beiden Enzyme. Die Struktur von RdpA und SdpA konnte 'auf' TauD modelliert werden und das typische 'jellyroll' Motiv wurde gefunden. Das Modell bestätigte die vorhergesagten Eisen- und α-Ketoglutarat bindenden Aminosäuren in beiden Dioxygenasen. In beiden Proteinen bildeten einige Aminosäuren eine ‚Höhle', die ein Bindungspotential für den aromatischen Ring der Phenoxyalkansäure hatte. Der erstaunlichste Unterschied zwischen RdpA und SdpA war, dass das neutrale Gly-107 von RdpA in SdpA durch das basische Asn-95 ersetzt wurde. Das deutet darauf hin, dass diese Aminosäuren eine wichtige Rolle in der Interaktion mit der Alkyl- bzw. mit der Carboxygruppe der chiralen Substrate spielen und daher die Enantiospezifität bestimmen könnten. Alle diese Voraussagen beruhen auf einem Model, das auf nur einer Vorlage gemacht wurde. Deshalb sind jetzt Kristallisationsstudien nötig, um eine noch bessere Sicht auf die Struktur und die aktive Seite von RdpA und SdpA zu gewinnen. Die hier präsentierte Arbeit bildet eine Grundlage für solche Experimente.

COR-AAD1-00003409
Bayer EX1008 (Part 7 of 9)

CHAPTER 1

General Introduction

OUTLINE OF THE THESIS

Herbicides are applied in large amounts and are thereby introduced into the environment. Besides the desired effects, they are designed for, they contaminate and may harm ecosystems. Because of their synthetic structure and recalcitrance, it is important to know, if and how herbicides are degraded. In particular, many herbicides (such as mecoprop and dichlorprop) are chiral compounds, which can effect degradability, but is often not taken into account. We propose that the herbicide enantiomers have to be treated as individual molecules and that degradation has to be studied for each of them separately.

Microbial degradation is an important route for mineralization of phenoxyalkanoic acid herbicides. Many pure bacterial cultures have been described that metabolize phenoxyalkanoic acid herbicides, among which *Sphingomonas herbicidovorans* MH. Strain MH grows on mecoprop, dichlorprop and 2,4-dichlorophenoxyacetic acid as sole carbon and energy source. Interestingly, *S. herbicidovorans* MH transforms both enantiomers, but prefers *(S)*-mecoprop and *(S)*-dichlorprop over the *(R)* enantiomers. Enantioselective degradation of such herbicides is due to different uptake systems and two distinct α-ketoglutarate-dependent dioxygenases involved in the initial degradation step of mecoprop and dichlorprop to the achiral phenol. Despite the knowledge on the uptake and dioxygenase activities, the genes for the mecoprop and dichlorprop degradation pathway had not been isolated and studied so far in *S. herbicidovorans* MH.

The first goal of this thesis was to investigate the genetic background of phenoxyalkanoic acid herbicide degradation in *S. herbicidovorans* MH. Specific research questions to be answered were: (i) Which genes are involved in the degradation pathway of the *(R)*- and *(S)*-enantiomer of phenoxypropanoic acid herbicides? (ii) How are the genes organized? (iii) How are they regulated? Secondly, we focused on the biochemical characterization of the two α-ketoglutarate-dependent dioxygenases, which are involved in the initial, enantioselective degradation step of mecoprop and dichlorprop. Our specific

COR-AAD1-00003412
Bayer EX1008 (Part 7 of 9)

interest was to compare the two enzymes to each other and to other dioxygenases of this family in terms of sequence similarity, substrate specificities, and physicochemical characteristics. Furthermore, models of the two dioxygenases were compared to gain insights into the molecular details of chiral catalysis.

The thesis is presented as follows. The introduction (chapter I) consists of two different parts. In the first part, the general problems with chiral substances in the environment and the state of the art on mecoprop and dichlorprop degradation are described. In the second part of the introduction, the family of α-ketoglutarate-dependent dioxygenases is introduced. Chapter II describes an analysis of the genes coding for the enzymes involved in phenoxyalkanoic acid degradation in *S. herbicidovorans* MH. In Chapter III and IV, we focus on the two enantioselective α-ketoglutarate-dependent dioxygenases and their biochemical characterization is presented. Chapter V will discuss the results obtained during this thesis work in a more general perspective and will present structure models of the two dioxygenases. Finally, the appendix contains the data from several growth studies and partial protein purifications of the *(S)*-dichlorprop dioxygenase.

COR-AAD1-00003413
Bayer EX1008 (Part 7 of 9)

General Introduction: Chirality of Pollutants – Effects on Metabolism and Fate

In most cases, enantiomers of chiral compounds behave differently in biochemical processes. Therefore, the effects and the environmental fate of the enantiomers of chiral pollutants need to be investigated separately. In this review, the different fates of the enantiomers of chiral phenoxyalkanoic acid herbicides, acetamides, organochlorines, and linear alkylbenzenesulfonates are discussed. The focus lies on the biological degradation, which may be enantioselective in contrast to non-biotic conversions. The data show that it is difficult to predict which enantiomer may be enriched and that accumulation of an enantiomer is dependent on the environmental system, the species, and the organ. Racemization and enantiomerization processes occur and make the interpretation of the data even more complex. Enantioselective degradation implies that enzymes involved in the conversion of such compounds are able to differentiate between the enantiomers. 'Enzyme pairs' have evolved which exhibit an almost identical overall fold. Only subtle differences in their active site determine their enantioselectivities. On the other extreme, there are examples of non-homologous 'enzyme pairs' that have developed through convergent evolution to enantioselectively turn over the enantiomers of a chiral compound. For a better understanding of enantioselective reactions, more detailed studies of enzymes involved in enantioselective degradation need to be performed.

Published previously in Applied Microbiology and Biotechnology (2004) 64: 300-316 by T. A. Müller and H.-P. E. Kohler.

COR-AAD1-00003415
Bayer EX1008 (Part 7 of 9)

Chapter 1

INTRODUCTION

A chiral (Greek *cheir*, hand) object or molecule is not superimposable on its mirror-image whereas an achiral object can be superimposed on its mirror-image. An alternative definition is the lack of symmetrical elements: a chiral object lacks reflectional symmetry (123). Common known chiral objects are a person's right and left hands, snail shells and clockwise- or counterclockwise-threaded screws. For chiral molecules, a tetrahedral C-atom bound to four different substituents is most common. The carbon atom is the stereogenic center and the two possible structures behave like the image and mirror-image of each other and are not superimposable. These structures are called enantiomers (Greek *enantios*, opposite). Amazingly, chirality is more the rule than the exception in our living world; and the important building blocks of life, such as DNA, RNA, and proteins, are all composed of chiral molecules. Moreover, they are homochiral – proteins consist of L-amino acids, and DNA and RNA consist of the D-enantiomers of deoxyribose and ribose, respectively.

The phenomenon of molecular chirality was first observed in the middle of the nineteenth century. Pasteur prepared sodium ammonium salts of the optically active (+)-tartaric acid and the optically inactive racemic acid. He observed that both crystals comprised hemihedral facets and that the hemihedral facets of the crystals of the optically active (+)-tartaric acid all lay in the same direction, whereas some of the hemihedral facets of the crystals of the optically inactive racemic acid inclined to the left and some to the right. He separated the crystals and found that the solution of crystals with hemihedral facets to the right deviated the plane of polarized light to the right and vice versa. He had discovered that the optical inactivity of racemic tartaric acid is due to the fact that it is a mixture of right- and left-handed tartaric acid. Later, van't Hoff and Le Bel introduced the model of the tetrahedral carbon atom to explain enantiomerism.

Although pure enantiomers of chiral compounds have identical physico-chemical properties – for a more thorough discussion about racemates and their enantiomer compounds, see Eliel and Wilen (26) – their behavior in biochemical

COR-AAD1-00003416
Bayer EX1008 (Part 7 of 9)

processes might be strikingly different. The effects of differently acting stereoisomeric drugs can be categorized basically as follows (5).

a) The stereoisomers of a chiral drug may have similar modes of action, but may differ in their affinity to a receptor or an enzyme resulting in different reaction rates.

b) The inactive stereoisomer may act as a competitive antagonist.

c) Enantiomers may have opposite or different effects as is the case for barbiturates, where the (–)-enantiomer is a sedative and the (+)-enantiomer has convulsive effects.

d) There are many chiral drugs for which one or both enantiomers have the desired effect and only one enantiomer causes unwanted side-effects. Well known is the Contergan tragedy. Contergan was a sedative that contained racemic thalidomide. Both enantiomers had the desired therapeutic effects, whereas only the *(S)*-enantiomer had teratogenic effects and caused severe malformations of human babies (7).

e) Side-effects may be non-stereoselective and both isomers may cause them, but only one isomer may have the desired effect.

f) In contrast to this, the inactive enantiomer may antagonize the side-effects of the active isomer. In such cases, an enantiomerically pure compound is not preferred.

As this list shows, the relationships between the effects of active and inactive stereoisomers in a pharmacological context can get quite complicated and certainly cannot be easily predicted, but needs to be empirically established. Therefore, stereoisomers should be treated as separate drugs and developed accordingly (32).

It is important to note that the dispositions mentioned above not only hold for pharmacologically active compounds but equally apply to all bioactive compounds that are chiral. Chiral pesticides, for instance, are introduced into the environment in large amounts as racemic mixtures. In many cases, the effects of the enantiomers of herbicides on plants have been investigated, but not the fates of

COR-AAD1-00003417
Bayer EX1008 (Part 7 of 9)

the enantiomers after application. Furthermore, not much is known about the degradation potential of the enantiomers. The application of racemic mixtures leads often to 'isomeric ballast', thereby unnecessarily polluting the environment (6, 143).

In the environment, abiotic transformations of chiral compounds are mostly non-enantioselective. This is in contrast to biological processes, which usually proceed with high stereo- or enantioselectivity. Therefore, changes in enantiomeric ratios (ER) and enantiomeric fractions (EF) are good indicators of biological degradation. The ER is defined as the ratio of the concentration of one of the enantiomers of a chiral compound divided by the concentration of the other enantiomer; and the EF is defined as the ratio of ER divided by ER+1 (42, 44, 63, 144, 147).

Table 1: Chiral environmental pollutants discussed in this review

Class	Representatives	Main use	Environmental systems discussed in this review
Phenoxypropanoic acids	Mecoprop, dichlorprop	Herbicide	Soil, aquatic systems, wastewater treatment plants, sewage sludge, landfill leachates, plants
Acetamide pesticides	Acetochlor, metalaxyl, metolachlor, dimethenamid	Pesticide	Soil, aquatic systems, sewage sludge, plants
Organochlorines	α-Hexachlorocyclo-hexane, chlordane	Contaminant of technical lindane (insecticide)	Soil, sediment, aquatic systems, sewage sludge, methanogenic conditions, biota
Linear alkylbenzene-sulfonates (LAS), linear alkylbenzenes (LAB)		Detergent	Soil

Here, we review the literature on the metabolism and environmental fate of chiral pollutants (Table 1). We focus on differences in the environmental fate of the enantiomers, i.e. on enantioselective biotic conversions. We intend to show how important it is to differentiate between enantiomers and stereoisomers and to treat enantiomers as distinct compounds with respect to their degradation potential. Furthermore, we describe enzymes involved in enantioselective processes. We

COR-AAD1-00003418
Bayer EX1008 (Part 7 of 9)

discuss stereoselectivity and the similarities and differences between such enzyme pairs that act on the enantiomers of chiral substrates.

CHIRAL POLLUTANTS AND THEIR FATE IN THE ENVIRONMENT

Phenoxypropanoic acid herbicides. Representatives of phenoxyalkanoic acid herbicides are 2,4-dichlorophenoxyacetic acid (2,4-D), 2-methyl-4-chlorophenoxyacetic acid (MCPA), 2,4,5-trichlorophenoxyacetic acid (2,4,5-T) and the chiral compounds mecoprop (2-(*R,S*)-2-methyl-4-chlorophenoxypropanoic acid) and dichlorprop (2-(*R,S*)-2,4-dichlorophenoxypropanoic acid; Fig. 1). They are systemic and post-emergence herbicides and act as synthetic auxins (1, 2, 77). They were introduced in the1940s and 1950s to control broadleaf weeds in agriculture, lawn pastures and industry. Racemic mecoprop is also used to control growth of weeds in building material such as bituminous seals, insulators for flat roofs and rubber seals (9, 10). Phenoxyalkanoic acid herbicides, often applied in formulation with other herbicides, are among the most widely used herbicides in the world (145). In 1999, 12.7–15.0×10^6 kg active ingredients (a.i.) of 2,4-D were used to control broadleaf weeds in agriculture, 7.7–9.0×10^6 kg a.i. in the industrial/commercial/government market and 3.2–4.1×10^6 kg a.i. in the home and garden sector in the United States (22). Mecoprop was applied in a range of 1.4–2.3×10^6 kg a.i. in the United States (22).

The chiral herbicides mecoprop and dichlorprop each have one stereogenic center and, therefore, two enantiomers exist (Fig. 1). Since 1953, it has been known that only the *(R)* enantiomers show herbicidal activity (83). Nevertheless, the racemic mixtures were and still are applied, thereby introducing large amounts of isomeric ballast into the environment. In many countries, mecoprop and dichlorprop are nowadays also sold as enantiomerically pure compounds (named mecoprop-P and dichlorprop-P, respectively; 143).

COR-AAD1-00003419
Bayer EX1008 (Part 7 of 9)

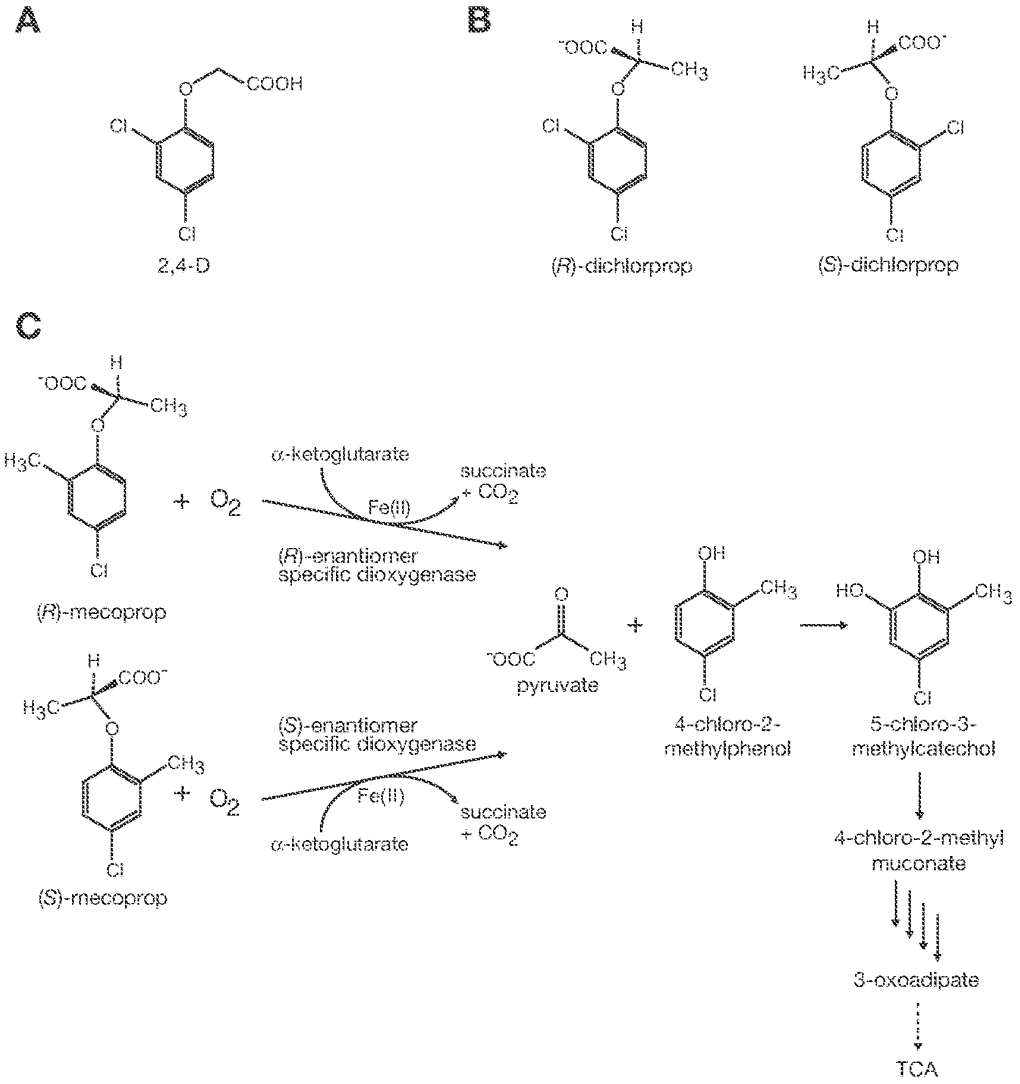


Fig. 1. Chemical structure of the phenoxyalkanoic acid herbicides 2,4-dichlorophenoxyacetic acid (2,4-D, **A**), which is achiral, and the two enantiomers of dichlorprop, which is chiral (**B**). **C** Proposed degradation pathway of *(R)*- and *(S)*-mecoprop by *Alcaligenes denitrificans* and *Sphingomonas herbicidovorans* MH. Note that *A. denitrificans* exclusively degrades (*R*)-mecoprop, whereas *S. herbicidovorans* MH degrades both enantiomers (modified from 105, 134, Chapter 2).

As outlined above, the enantiomers of chiral compounds behave differently in biochemical processes. Therefore, to study the fate of chiral herbicides, it is important to differentiate between the enantiomers and to monitor the different degradation patterns. Today, GC, GC-MS, and HPLC methods are available to

COR-AAD1-00003420
Bayer EX1008 (Part 7 of 9)

separate and quantitate enantiomers and to selectively investigate the environmental fate of the enantiomers of chiral pollutants (90).

The environmental fate of phenoxyalkanoic acid herbicides is determined by their physico-chemical properties and by their biodegradability. They are water soluble (up to 620 mg/l) and are strong acids (145). Since they are mostly present in the dissociated (anionic) form in the environment, they do not adsorb onto soil and have a low tendency to accumulate in organic matter (33, 149). The half-life in soil after application is from one to several weeks (Table 2) and, due to their mobility, there is a risk of contaminating aquatic systems (46). Indeed, phenoxyalkanoic acid herbicides are often found in subsurface and groundwater samples (33, 38). Concentrations in surface soils were in the range of milligrams per kilogram of soil, whereas concentrations were lower in groundwater samples, i.e., 10–250 μg/l downstream of landfills (80, 149) and less than 1 μg/l in groundwater aquifers polluted due to agricultural use (120).

The effect of environmental conditions on the photodecomposition of dichlorprop and mecoprop in soil surfaces was investigated by Romero *et al.* (116). They found that, on dry soil surfaces, photolysis may dominate other transformation pathways. However, in moist soils, photodecomposition played an important role only during the first 2 days of exposure. Afterwards, when microbial degradation became dominant, photodecomposition was much less important. In a study using different types of calcareous soils, mecoprop and dichlorprop dissipation was investigated (117). Generally, degradation was slower in clay loam soils than in silt and sandy loam soils (Table 2). Dissipation was enantioselective indicating biological degradation and was dependent on the soil type. The (*S*) enantiomer persisted for a longer time in silt and sandy loam soils than in clay loam soils. The addition of peat had intriguing effects as the persistence of mecoprop and dichlorprop increased in silt and sandy loam soils, but decreased in clay loam soils. Lewis *et al.* (73) studied the effect of environmental changes on the enantioselective degradation of mecoprop and dichlorprop in Brazilian forest and pasture soils. The pasture samples preferentially degraded (*S*)-dichlorprop, whereas both enantiomers were equally transformed in forest

COR-AAD1-00003421
Bayer EX1008 (Part 7 of 9)

samples. Enrichments in organic nutrients shifted the enantioselectivity for methyl-dichlorprop towards the preferential degradation of the (*S*) enantiomer. Other studies showed, that the (*S*) enantiomer was degraded significantly faster in soil than the herbicidally active (*R*) enantiomer (37, 90). Only two studies reported enantiomerization and/or racemization (13, 90). Both studies showed that enantiomerization was biologically mediated. The authors drew the important conclusion that, due to enantiomerization, the measured enantiomeric composition of residues does not reflect that of the applied products. Additionally, two-phase degradation kinetics with initially slower rates was observed in one of these studies (90). The authors suggested that two or more different enzyme systems are involved in the degradation.

In marine systems polluted with racemic dichlorprop, (*R*)-dichlorprop is preferentially degraded by microorganisms (78, 79). In aerobic aquifer samples incubated with different concentrations of mecoprop in laboratory experiments, mecoprop was degraded within 200 days (46). (*R*)- and (*S*)-mecoprop was found in equal concentrations in the landfill leachate of Kölliken (Switzerland), indicating a racemic mixture of mecoprop in the landfill itself. But in groundwater samples downstream of the landfill, the enantiomeric ratio of mecoprop increased, i.e., (*R*)-mecoprop was in excess. As sorption to organic material was of minor importance and should be non-enantioselective, this finding indicates in-situ biodegradation (149). Williams *et al.* (144) showed in a recent study that degradation of mecoprop in a limestone aquifer downstream of a landfill depended on the redox conditions. Under methanogenic, sulphate-reducing or iron-reducing conditions, mecoprop was not degraded. In nitrate-reducing microcosms, *(R)*-mecoprop was degraded, whereas the *(S)* enantiomer was stable. In contrast, *(S)*-mecoprop degraded faster than *(R)*-mecoprop under aerobic conditions. In a field experiment in Denmark, mecoprop and dichlorprop were degraded in an aerobic aquifer within a distance of 1 m from the source within a period of 120 days. But in contrast to the reports mentioned beforehand, no enantioselective degradation was observed (118).

COR-AAD1-00003422
Bayer EX1008 (Part 7 of 9)

Table 2: Degradation rates for dichlorprop and mecoprop found in environmental samples

Compound	System	Sample	Rate constants ($t_{1/2}$; days)			Degradation time (days)[a], (lag phase; days)	Ref.
			(R,S)-	*(R)*-	*(S)*-		
Dichlorprop	Brazilian soil	Forest	(11)[b,c]				(73)
		Pasture	(16)[b,d]				(73)
	Calcareous soils	Silt loam	55 (13)[e]	77 (9)[e], 155 (5)[f]	41 (17)[e]		(117)
		Sandy loam	53 (13)[e]	59 (12)[e]	47 (15)[e]		
		Clay loam	11 (62)[e]	7 (98)[e], 38 (18)[f]	18 (38)[e]		
	Garden soil	Sandy loam		32 (21.9), 150 (4.6)[e,g]	98 (7.1), 176 (3.9)[e,g]		(90)
	Soil		(6.6)[b]	(8.7)[b]	(4.4)[b]		(37)
	Aquatic system	Aerobic aquifer (in situ)				120 (60)[h]	(118)
	Sewage sludge	Aerobic		213±41, 352±92[i]	225±79, 188±3[i]	(4.33-6.2)	(146)
Mecoprop	Calcareous soils	Silt loam	43 (15)[e]	58 (12)[e], 157 (4)[f]	33 (21)[e]		(117)
		Sandy loam	63 (11)[e]	86 (8)[e], 97 (7)[f]	56 (12)[e]		
		Clay loam	14 (50)[e]	9 (77)[e], 17 (40)[f]	22 (32)[e]		
	Soil	Sandy loam	(9±1)[e]				(126)
		Heavy loam	(8±2)[e]				(126)
		Clay loam	(7±2)[e]				(126)
	Garden soil	Sandy loam		69 (10), 174 (4)[e,g]	102 (6.8), 189 (3.7)[e,g]		(90)
	Aquatic system	Aerobic aquifer (lab)				200 (20-110)[k]	(46)

COR-AAD1-00003423
Bayer EX1008 (Part 7 of 9)

Table 2 (cont.): Degradation rates for dichlorprop and mecoprop found in environmental samples

Compound	System	Sample	Rate constants ($t_{1/2}$; days)			Degradation time (days)[a], (lag phase; days)	Ref.
			(R,S)-	*(R)*-	*(S)*-		
		Aerobic aquifer (in situ)				106-132 (60-80)[k]	(118)
		Limestone aquifer: aerobic		1.32[l]	1.9[l]		(144)
		Limestone aquifer: nitrate-reducing		0.65[l]	not degraded		(144)
		Limestone aquifer: Fe-reducing (NO_3^- added)				225 (21)[m]	(144)
		Limestone aquifer: methanogen/sulphate reducing	not degraded				(144)
	Sewage sludge	Aerobic		176±28, 304±88[j]	174±52, 273±47[j]	(4.33-6.2)	(146)

[a] Degradation time is defined as the time until dichlorprop or mecoprop was degraded to a concentration below the detection limit

[b] First-order kinetic

[c] In 38% of the samples, the *(S)* enantiomer was degraded faster, in 13% the *(R)* enantiomer.

[d] In 93% of the samples, the *(S)* enantiomer was degraded faster, in 6.7% the *(R)* enantiomer.

[e] Data obtained from experiments with the racemate. First-order kinetic, unit of the rate constant: 10^{-3} day^{-1}.

[f] Data obtained from experiments with the single pure enantiomer. First-order kinetic, unit of the rate constant: 10^{-3} day^{-1}.

[g] The two rate constants were determined during two degradation phases: slow phase 0-16 days, fast phase 16-35 days.

[h] Non-enantioselective degradation

[i] Data obtained from experiments with the racemate (first number) and the single enantiomer (second number). Zero-order kinetic (*x* $\mu mol\ h^{-1} g^{-1}$ dry weight)

[k] The concentrations were too low to measure enantioselective degradation. However, a second lag phase after removal of 50% of the initial concentration strongly indicated enantioselective degradation

[l] Data obtained from experiments with the racemate. Zero-order kinetic, units expressed as *x* $\mu mol\ h^{-1}\ g^{-1}$ dry weight

[m] No degradation was observed for 119 days. Nitrate was then added to the microcosm and, after a lag-phase of 21 days, mecoprop degraded suggesting that nitrate acted as an electron-acceptor.

COR-AAD1-00003424
Bayer EX1008 (Part 7 of 9)

Experiments with activated and digested sludge showed that phenoxypropanoic acid herbicides are degraded aerobically but not anaerobically. Mecoprop and dichlorprop (10–40 mg/l) were degraded aerobically within 7 days, the (*S*) enantiomers being preferentially degraded, while degradation was not observed during 49 days of incubation under anaerobic conditions (146). An experiment with 1 mM mecoprop in a simulated wastewater treatment plant showed 100% removal after 40 days (106).

All these studies showed that biological degradation is the most important process by which these herbicides are eliminated from the environment. Furthermore, biological degradation was enantioselective in most cases, emphasizing the importance of investigating the environmental fate of each enantiomer separately. In these cases, the observed changes in enantiomeric fractions or ratios gave conclusive evidence for natural attenuation of the herbicides (144, 149). However, racemization may occur and therefore, careful experiments and measurements are needed for solid interpretations.

In most cases, microorganisms enantioselectively degrade mecoprop and dichlorprop. A particular strain might degrade only one enantiomer or it might sequentially degrade the two enantiomers. Degradation was well investigated for the achiral phenoxyalkanoic acid herbicide 2,4-D in *Ralstonia eutropha* JMP134(pJP4). 2,4-D is degraded by an α-ketoglutarate-dependent dioxygenase (TfdA) by ether-bond cleavage to 2,4-dichlorophenol (35, 36, 130). Then, 2,4-dichlorophenol is hydroxylated to 3,5-dichlorocatechol by a phenol-hydroxylase (TfdB; 31, 76, 111). The catechol undergoes *ortho*-ring fission catalyzed by a chlorocatechol 1,2-dioxygenase (TfdC) yielding 2,4-dichloro-*cis,cis* muconate (8, 111), which then is metabolized to *cis*-2-chlorodienelactone and further to 2-chloromaleylacetate by a muconate cycloisomerase and a dienelactone hydrolase (TfdD and TfdE, respectively; 66, 111). It was suggested that the chiral phenoxyalkanoic acid herbicides are degraded accordingly. Table 3 lists all known bacterial strains in pure culture that are able to grow with mecoprop and dichlorprop as the sole carbon and energy source. The earliest reported investigations were made with *Alcaligenes denitrificans* (Table 3), which was isolated from a consortium and

COR-AAD1-00003425
Bayer EX1008 (Part 7 of 9)

exclusively degrades the (*R*) enantiomer using it as sole carbon and energy source (133, 134). (*R*)-mecoprop degradation was shown to proceed in a manner analogous to 2,4-D degradation, i.e., degradation to the achiral 4-chloro-2-methylphenol and then to 5-chloro-3-methylcatechol (Fig. 1C). Subsequently, 5-chloro-3-methylcatechol is degraded through the modified *ortho*-cleavage pathway, yielding 2-methyllactone, 2-methylmaleylacetate, and finally 5-methyl-3-oxoadipate. In a further study, the question was addressed whether the genes encoding the enzymes involved in mecoprop degradation were similar to those encoding the enzymes for 2,4-D degradation. A fragment of a *tfdA*-like gene was amplified by PCR from *A. denitrificans* and sequenced. It was 86% identical to the corresponding region of *tfdA* from *R. eutropha* JMP134(pJP4) (119). However, the α-ketoglutarate-dependent dioxygenase and the other enzymes involved in degradation have not been further characterized in this strain.

In 1990, *Sphingomonas herbicidovorans* MH (formerly *Flavobacterium* sp.) was isolated from soil samples polluted with dichlorprop (49, 148). In contrast to *A. denitrificans*, *S. herbicidovorans* MH is able to degrade both enantiomers of dichlorprop and mecoprop to completion (148). Growth experiments with either the racemate or single isomers showed that *S. herbicidovorans* MH degraded the substrates enantioselectively. The (*S*) enantiomer was degraded before the (*R*) enantiomer in all growth experiments performed so far. When *S. herbicidovorans* MH was incubated with the single enantiomer, a lag phase of about 3 days for (*S*)- and one of about 7 days for (*R*)-mecoprop was observed. However, when grown on the racemate, degradation is sequential, the (*S*) enantiomer being used first (148). Enantioselectivity was also found for substrate uptake. When *S. herbicidovorans* MH grew on the single enantiomers, only the enantiomer that served as the substrate was taken up. These data and further experiments indicated that *S. herbicidovorans* MH harbors two inducible transport systems involved in enantioselective uptake (105, 147).

COR-AAD1-00003426
Bayer EX1008 (Part 7 of 9)

Table 3: Isolated dichlorprop- and mecoprop degraders

Strain	Phenoxyalkanoic acid substrates	Isolation source	References
Sphingomonas herbicidovorans MH	(*R,S*)-Mecoprop, (*R,S*)-Dichlorprop, 2,4-D, MCPA	Soil (dichlorprop)	(49, 63, 148)
Delftia (formerly *Comamonas*) *acidovorans* MC1	(*R,S*)-Mecoprop, (*R,S*)-Dichlorprop, 2,4-D, MCPA	Herbicide contaminated building rubble (2,4-D)	(93, 94)
Rhodoferax sp. strain P230	(*R,S*)-Mecoprop, (*R,S*)-Dichlorprop, 2,4-D, MCPA	Concrete rubble of a demolished herbicide production plant (2,4-dichlorophenol)	(25)
Alcaligenes denitrificans	(*R*)-Mecoprop	Garden soil	(134)
Alcaligenes sp. CS1	(*R,S*)-Mecoprop, (*R,S*)-Dichlorprop, 2,4-D, MCPA	Agricultural soil (mecoprop)	(125)
Ralstonia sp. CS2	(*R,S*)-Mecoprop, (*R,S*)-Dichlorprop, 2,4-D, MCPA	Agricultural soil (mecoprop)	(125)

COR-AAD1-00003427
Bayer EX1008 (Part 7 of 9)

Two strains, *Alcaligenes* sp. CS1 and *Ralstonia* sp. CS2, were isolated from agricultural soils. They are able to degrade racemic mecoprop and dichlorprop in addition to the achiral herbicides 2,4-D and MCPA (125). The genomes of both isolates were screened under low-stringency conditions with *tfd*-gene probes in hybridization experiments. The experiments demonstrated that both strains harbored *tfdABC*-like genes on plasmids. *Rhodoferax* strain P230, another strain that is able to degrade chiral phenoxyalkanoic acid herbicides was isolated from contaminated building material. According to preliminary PCR experiments, this strain also harbors *tfdA*-like genes (25). *Delftia acidovorans* MC1 (formerly *Comamonas acidovorans* MC1) was isolated from a herbicide-contaminated building site (93, 94). The strain is able to degrade racemic dichlorprop but, unfortunately, enantiospecific degradation was not investigated. To isolate the genes coding for the enzymes, PCR experiments were carried out with primers for *tfdA*, *tfdB,* and *tfdC* (62, 136) revealing the presence of *tfdBC* genes. In contrast to these genes, a *tfdA*-like gene could not be amplified with the applied primers although enzyme activities dependent on ferrous ions and α-ketoglutarate could be detected in cell-free extracts.

Acetamide pesticides. The group of acetamide pesticides comprises a large number of herbicides and fungicides (Fig. 2). The activity is dependent on the acyl moiety. In the case of herbicides, the substituent is often $-CH_2Cl$, whereas in the case of fungicides the substituent is often $-CH_2OCH_3$. Acetamide pesticides are used to control annual grasses and certain broadleaf weeds in corn, soybeans, and peanuts. They are also used to control phytopathogenic fungi, such as *Peronosporales* in potatoes, sugar beets, and other crops (72, 122, 145). Acetamide pesticides act as protein synthesis inhibitors (18) and RNA-polymerase I inhibitors (11). The compounds metolachlor [2-chloro-*N*-(2-ethyl-6-methylphenyl)-*N*-(2-methoxy-1-methylethyl)acetamide], metolachlor-s and alachlor [2-chloro-*N*-(2,6-diethylphenyl)-*N*-(methoxymethyl)acetamide] are among the most commonly used pesticides in the world and in 1999, $11.8–13.6\times10^6$ kg, $7.3–8.6\times10^6$ kg, and $3.2–4.5\times10^6$ kg million a.i., respectively, were applied in the United States (22).

COR-AAD1-00003428
Bayer EX1008 (Part 7 of 9)

Other commonly applied acetamide pesticides are acetochlor [2-chloro-*N*-(2-ethyl-6-methylphenyl)-*N*-(ethoxymethyl)acetamide], metalaxyl [*N*-(2,6-dimethylphenyl)-*N*-(methoxyacetyl)alanine methyl ester] and dimethenamid [2-chloro-*N*-(2,4-dimethylthien-3-yl)-N-(2-methoxyl-1-methylethyl)acetamide]. Alachlor is achiral, acetochlor is axial-chiral and metalaxyl is C-chiral, giving two enantiomers. Dimethenamid and metolachlor are axial and C-chiral and, therefore, four stereoisomers exist. For metolachlor, herbicidal activity is exclusively associated with the 1'(*S*) isomers. In the case of metalaxyl, the (*R*) enantiomer is about 3–10 times more fungicidally active than the (*S*) enantiomer (34).

Degradation of different acetamides in soil and sewage sludge proceeds in the order alachlor > acetochlor > dimethenamid > metolachlor > metalaxyl, with half-lives ranging from 4–32 days in soil and from 10–86 hours in sewage sludge (14, 91). Dimethenamid and metolachlor degradation showed low to moderate enantio- and/or stereoselectivity, whereas metalaxyl was degraded highly enantioselectively. Enantioselectivity was dependent on the environmental system: in soil, 1'(*R*)-(–)-Metalaxyl was degraded faster than the (*S*) enantiomer, whereas reversed enantioselectivity was found in sewage sludge (14, 91). Different rates and opposite enantioselectivity were also found in a study in which the degradation in soil was compared to the one in plants. The (*R*) enantiomer was degraded faster in soil, the (*S*) enantiomer faster in plants (82). In a recent study (16), the faster degradation of the herbicidal active (*R*) enantiomer in soil was confirmed. It was also found, that only 40–50% of metalaxyl was degraded to the chiral intermediate metalaxyl carboxylic acid (MX-acid; 2-[(2,6-dimethylphenyl)methoxyacetyl-amino]propanoic acid). In this step, the configuration of the chiral C-atom was retained. Further degradation of MX-acid is also enantioselective, the *(S)* enantiomer being converted more rapidly. The remaining metalaxyl is metabolized through other pathways. Both enantiomers of metalaxyl and MX-acid are configurationally stable and no indications of biological mediated racemization or enantiomerization have been found (16, 82). Monkiedje and coworkers (89) investigated the degradation and persistence of racemic and enantiopure forms of metalaxyl in temperate and tropical soils. All forms of metalaxyl had lower degra-

COR-AAD1-00003429
Bayer EX1008 (Part 7 of 9)

dation rates in Cameroonian soils than in German soils. Interestingly, an opposite enantioselectivity was observed in the two regions. The (*R*) enantiomer was faster degraded than the *(S)* enantiomer in German soils, but slower than the *(S)* enantiomer in Cameroonian soils. This finding suggests that different microbial populations are involved in the degradation process. In another recent study, the enantioselectivity correlated with the soil pH (12). In aerobic soils with pH>5, the (*R*) enantiomer was faster degraded than the *(S)* enantiomer. In aerobic soils with pH 4–5, both enantiomers were degraded similarly, whereas in aerobic soils with pH<4 and in anaerobic soils, the enantioselectivity was reversed. The authors reevaluated published kinetic data from dichlorprop and mecoprop studies and found indications of similar correlations. However, no correlation between enantioselectivity and soil pH was observed for MX-acid, the chiral intermediate.

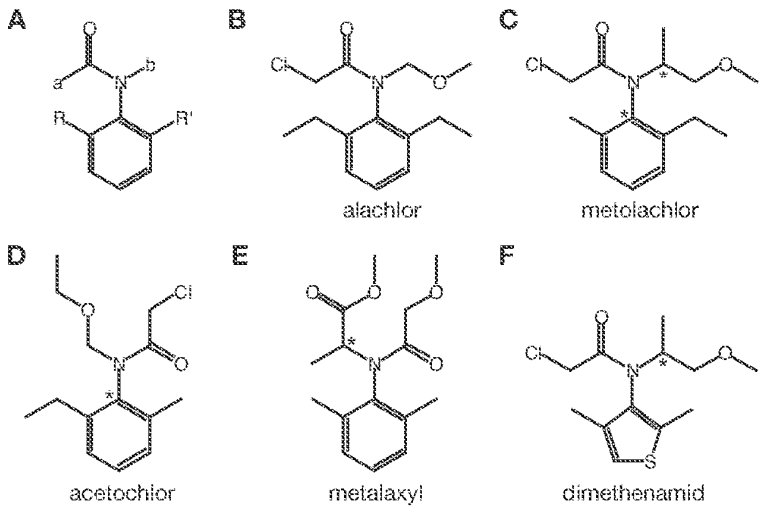


Fig. 2. Chemical structures of acetamide pesticides. **A** General structure. R and R' represent CH_3- and/or C_2H_5-. **B-F** Structures of the five acetamide pesticide alachlor (achiral), metolachlor, acetochlor, metalaxyl, and dimethenamid. The chiral centers and the axial-chiral elements are indicated by asteriks. Note that, in dimethenamid, phenyl is replaced by 2,4-dimethylthien-3-yl.

COR-AAD1-00003430
Bayer EX1008 (Part 7 of 9)

In the case of metolachlor, there is currently a chiral switch from racemic metolachlor to (*S*)-metolachlor, which is highly enriched in the herbicidally active enantiomer. Most likely, this results in lower overall concentrations and a changed enantiomeric ratio in environmental samples. Indeed, in Switzerland, a rapid response in terms of the enantiomeric composition was observed in surface waters after the replacement of the racemic metolachlor by the highly enriched enantiomer (17).

Organochlorines: hexachlorocyclohexane and chlordane. Hexachlorocyclohexane (HCH) belongs to the organochlorine compounds and used to be one of the most widely applied broad-spectrum insecticides. It was introduced during world war II (92) and was used mainly in forestry, agriculture, and as a wood preservative. HCH comprises eight isomers, the chiral α-, and the achiral β-, γ-, δ-, ε-, η–, υ-, and ι–isomers, of which only the γ-HCH has insecticidal properties. Technical grade lindane (Fig. 3A) consists typically of 60–70% α-HCH, 5–12% β-HCH, 10–15% γ-HCH and 6–10% δ-HCH (15, 56), whereas the commercial insecticide marketed today comprises 99% of the γ-isomer. In Europe, the use of technical grade lindane was banned in the 1970s and in 2000, lindane was completely banned for all agricultural and gardening applications. Although the total amount of applied HCH was reduced globally, it is still a contaminant of great concern in many countries (e.g., in India). HCH is semivolatile and has a low tendency to accumulate in soils. It is transported by water and air and, today, HCH has accumulated in regions where HCH never was used, such as the Arctic and the Baltic Sea (see for instance (42, 84, 141). Chlordane is another representative of the organochlorine pesticides and was widely applied in the United States from 1945 until it was banned in 1988 (20, 43). Technical chlordane comprises 140 compounds and was used to control pests in lawn, garden, and crops and as a termiticide (43). The organochlorine representatives *cis*- and *trans*-chlordane (Fig. 3B) and heptachlor epoxide, a metabolite of heptachlor, are chiral and each enantiomer has different biological properties and environmental fate (112, for a review see 44).

COR-AAD1-00003431
Bayer EX1008 (Part 7 of 9)

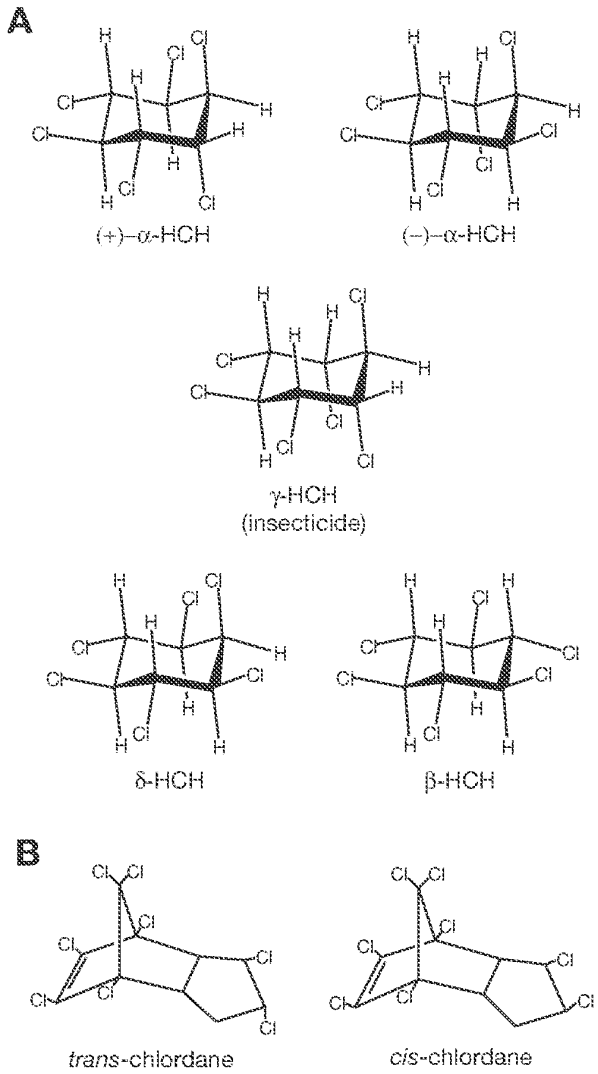


Fig. 3. Chemical structures of organochlorine pesticides. **A** Chemical structure of five hexachlorocyclohexane (HCH) stereoisomers in technial lindane. Note that only α-HCH is chiral and that only γ-HCH has insecticidal properties. **B** Chemical structures of the organochlorine pesticides *cis*- and *trans*-chlordane.

Today, the Arctic Ocean is a source of HCH. HCH is eliminated from the Arctic Ocean by water outflow, volatilization, and degradation (72). A study of the removal of α- and γ-HCH in the eastern Arctic ocean found that the rate constants for microbial degradation were about 3–10 times higher than those for hydrolysis (42). Enantioselective degradation was observed, the (+)-α-HCH being converted

COR-AAD1-00003432
Bayer EX1008 (Part 7 of 9)

preferentially. The calculated half-lives for (+)-α-HCH, (–)-α-HCH, and γ-HCH were 5.9, 23.1, and 18.8 years, respectively. However, reversed enantioselectivity was found in other marine environments, such as the Bering Sea and the Chukchi Seas (57). Enantioselective degradation was also investigated in other aquatic environments. It was found that enantioselective degradation was greatest in small Arctic lakes with enantiomeric ratios between 0.3 and 0.7, although the nutrient availability in such lakes is very low (29, 71). Law *et al.* suggested (71) that this was due to biofilm formation and environmental conditions in which the contact between α-HCH and the microbial population was maximized by either the path length, as in streams, or the long water residence time, as in lakes. In the food web, no preference for the enrichment of one enantiomer in higher trophic levels could be observed. Cetaceans, dolphin species, showed preferential accumulation of (+)-α-HCH (54). (+)-α-HCH was also more abundant than the (–) enantiomer in the blubber of harbor seals, grey seals, and harp seals and in the liver, kidney, and muscle tissues of ducks (54). In contrast to this, an ER of <1 was found in hooded seals (54). In invertebrates, mussels, and fishes, the ratio reflected that of the surrounding water, indicating no preferential accumulation (52, 88). Also, for chlordane compounds, no uniform trend for ER changes and increasing trophic levels could be found (142). These findings suggest that it will be difficult to predict which enantiomer may be enriched and that accumulation is dependent on both the organ and the species.

In soils, organochlorines are also enantioselectively degraded. In soils from the United States corn belt, (+)-*trans* chlordane was preferentially degraded, whereas for *cis*-chlordane, the (–)-enantiomer was converted faster except in four soils, in which non-enantioselective degradation was found (3). α-HCH was enantioselectively degraded in three muck soils, but not in silt loam soils from British Columbia (30). In soils from near a former HCH factory, only low enantioselectivity was found (ER = 1.099; 92). In archived UK soils, statistically significant enantioselective degradation was not observed for *cis*- or *trans*-chlordane, nor for α-HCH (85). The reported half-lives for α-HCH and other organochlorines in soils were ~7 years (α-HCH) to 25 years (dieldrin; 85).

COR-AAD1-00003433
Bayer EX1008 (Part 7 of 9)

In anaerobic sewage sludge, HCH is degraded with half-lives of 20–178 h, in the order of γ-HCH > (+)-α-HCH > (–)-α-HCH > δ-HCH > β-HCH. Indications are given that degradation is 80–95% biologically mediated, although abiotic degradation in sterilized sewage sludge is much higher than hydrolysis in water (15, 104). α-HCH is degraded enantioselectively, whereby the (+)-enantiomer is degraded faster. This leads to enrichment of (–)-α-HCH in sewage sludge (15). Middeldorp *et al.* (87) described a bacterial consortium which was able to degrade β-HCH as well as α-, γ- and δ-HCH under methanogenic conditions.

A microbial community able to degrade HCH was isolated from marine environments (53). It degrades the (+)-α-HCH and the corresponding β-pentachlorocyclohexene (β-PCCH) faster than the respective enantiomers. Another consortium comprising eight bacterial strains and a fungus was isolated from soil and sewage. It preferentially degraded α-HCH, but nothing is reported about enantioselectivity (81). Two *Bacillus* strains, *B. circulans* and *B. brevis*, isolated from contaminated soil, are able to degrade α-, β-, γ- and δ-HCH at high rates (40) and two *Pseudomonas* strains isolated from agricultural soils are able to degrade γ-HCH (102). *S. paucimobilis* UT26 is able to grow on γ-HCH as sole carbon- and energy source (55, 96, 98). The *lin*-genes were sequenced and shown to code for the enzymes involved in HCH-metabolism (97-99).

Linear alkylbenzenesulfonates and linear alkylbenzenes. Linear alkylbenzenesulfonates (LAS) and linear alkyl benzenes (LAB) and their degradation products are environmentally relevant chiral substances (Fig. 4). LAS are used as detergents and LAB are the precursors in LAS synthesis and are found in low amounts in commercial LAS (19, 48). LAS and LAB are biodegradable under aerobic conditions (132). It was suggested that degradation starts with ω-oxidation of the alkyl side chain (108) and chain-shortening proceeds with β-oxidation, which is hindered when the side-chain is cut back to four or five carbon atoms from the point of attachment to the benzene ring (23, 50, 139). *Rhodococcus rhodochrous* PB1 enantioselectively metabolizes the LAB-intermediate 3-phenylbutyric acid. *R. rhodochrous* is able to grow on (*R*)-3-phenylbutyric acid, whereas

COR-AAD1-00003434
Bayer EX1008 (Part 7 of 9)

the (*S*) enantiomer is only cometabolically transformed to presumably (*S*)-3-(2,3-dihydroxyphenyl)butyric acid (124). This compound is then abiotically transformed to reactive and potentially toxic quinones (64, 124). Recently, *D. acidovorans* SPB1 was isolated from an enrichment culture (121) which degrades 2-(4-sulfophenyl)butyrate (SPB) sequentially (Fig. 4B). The (*R*) enantiomer is degraded first and only when it is exhausted does the (*S*) enantiomer start degrading. Metabolism converges at the achiral 4-sulfocatechol. 4-sulfocatechol undergoes *ortho* cleavage via 3-sulfo-*cis,cis*-muconate.

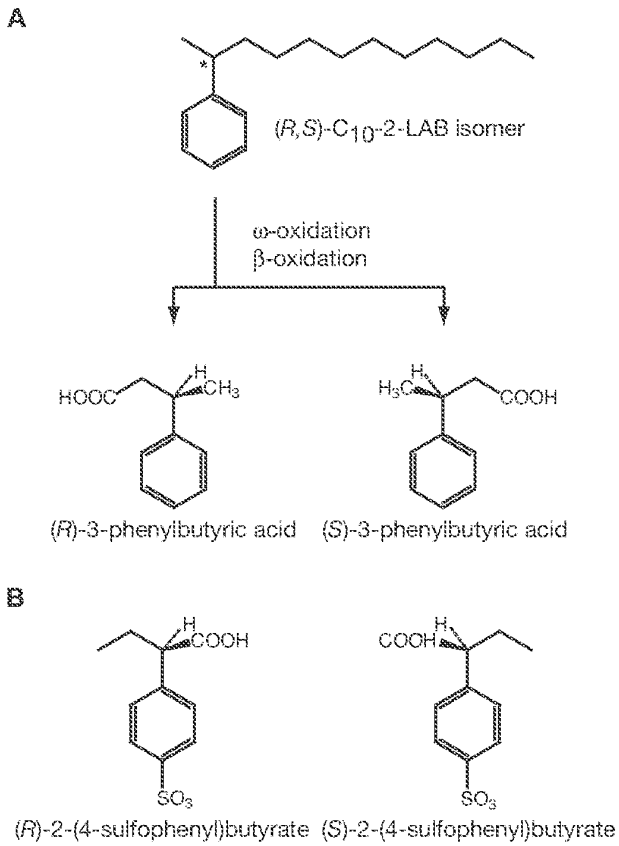


Fig. 4. Linear alkyl benzenes (LAB) and derivatives. **A** Chemical structure of a LAB isomer and the metabolite 3-phenylbutyric acid. Chain shortening is supposed to be non-enantioselective, as the stereogenic center is far away from the reaction point. **B** Chemical structure of 2-(4-sulfophenyl)butyrate.

COR-AAD1-00003435
Bayer EX1008 (Part 7 of 9)

ENANTIOSELECTIVE ENZYMES

Enantioselective degradation of chiral pollutants by microorganisms is rather the rule than the exception. For enantioselective metabolism, one ore more enzyme reactions involved in the uptake or in the different degradation steps must be enantioselective. The three-point model (24, 107) is often used to explain the phenomenon of stereoselectivity in enzymatic reactions. As shown in Fig. 5, the model postulates that the active enantiomer binds more tightly to the active site of the enzyme because the sequence of the three groups around the asymmetric carbon atom, ABC, forms the triangular face of a tetrahedron that matches the complementary triad of the chiral binding site, A'B'C', of the active site. The less active enantiomer binds ineffectively, since it has a mirror-image sequence of the three groups, CBA, which leads to a mismatch with the active site (65). In some cases, this model needs to be expanded to a so-called four-location model (86; Fig. 5, III). When isocitrate dehydrogenase is provided with the substrate racemate, L-isocitrate is exclusively bound to the protein crystals in the absence of Mg^+ but, in the presence of Mg^+, the D-isomer binds. The crystal structure revealed that three of the four groups of the C2-atom of isocitrate bind to the same three residues, but not the fourth group. In other words, the protein needs not three but four locations in the active site to differentiate between the two enantiomers. In general, the three-point model works as long as it is assumed that the binding site can be approached only from one direction. But if the active site is in a cleft or on protruding residues, only binding or direction to the fourth group enables the protein to distinguish between the enantiomers.

COR-AAD1-00003436
Bayer EX1008 (Part 7 of 9)

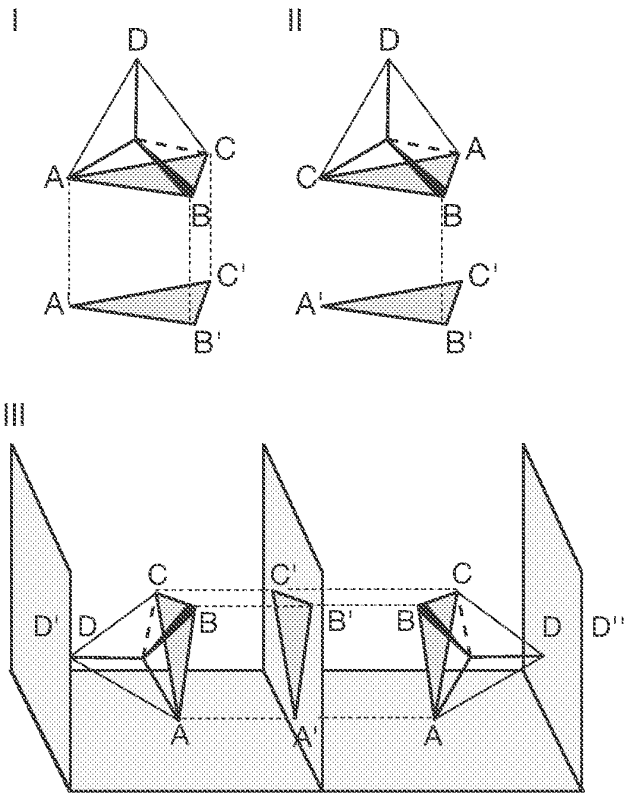


Fig. 5. Three-point attachment model modified from Easson and Stedman and Ogston (24, 107; diagram I and II) and the four-location model by Mesecar and Koshland (86); diagram III). A', B', C' binding sites in the active site of the enzyme. For one enantiomer of the chiral substrate, the three ligands (A, B, C) are oriented counterclockwise and coincide with the binding sites of the enzyme. It can be seen that the ligands of the other enantiomer (diagram II) bind ineffectively to the enzyme. If the active site can be approached from both sides (diagram III), both enantiomer will bind. In such a case, an additional binding site – a fourth location (D' and D'', respectively) – is necessary for selective recognition of an enantiomer.

Degradation of the enantiomers of chiral pollutants may proceed along different avenues:

a) Two enantioselective enzymes exist, each converting only one substrate enantiomer.
b) Both enantiomers are simultaneously converted by one enzyme, but at different rates.
c) Sequential conversion of the substrate enantiomers by one enzyme, i.e., the enzyme preferentially degrades one enantiomer. The other enantiomer is

COR-AAD1-00003437
Bayer EX1008 (Part 7 of 9)

eventually also degraded, but only when the former one has been (completely) degraded.

d) Enantioselective conversion of one enantiomer by one enzyme and isomerization of the other enantiomer by an isomerase.

Not many of the enzymes involved in the degradation of chiral pollutants are well studied in terms of their stereoselectivity. Recently, two genes, *rdpA* and *sdpa*, were isolated and sequenced from *S. herbicidovorans* MH (Chapter 2). The genes encode two distinct α-ketoglutarate-dependent dioxygenases, are involved in enantioselective degradation of dichlorprop and mecoprop in this strain and cleave the ether bond to the corresponding phenol with concomitant release of pyruvate and succinate. α-Ketoglutarate and oxygen are required as cosubstrates, iron(II) as a cofactor, and ascorbate as a reducing agent. It was shown that SdpA is constitutively expressed whereas RdpA is induced during growth on the (*R*) enantiomer or the racemate. Interestingly, SdpA was repressed when *S. herbicidovorans* MH was grown on (*R*)-mecoprop (105). *rdpA* and *sdpA*-genes were also isolated and sequenced from the dichlorprop degrader *D. acidovorans* MC1. RdpA and SdpA were partially purified and it was found that RdpA converts (*R*)-dichlorprop, *(R)*- and *(S)*-mecoprop, but not (*S*)-dichlorprop (137, 138). SdpA from this strain is enantioselective and converts only the *(S)* enantiomer of the two phenoxypropanoic acid herbicides. The amino acid residues, which are involved in substrate- and cofactor-binding, have not yet been determined. However, from alignments with other α-ketoglutarate-dependent dioxygenase and inhibitor studies, it is likely that there are two histidines and one aspartate involved in Fe(II)-binding (the 2-His-1-carboxy-facial triad; 45). At the moment, nothing is known about the stereospecificity of the substrate-binding sites and whether the substrate-binding sites of the two enzymes are similar or not. α-Ketoglutarate-dependent dioxygenases involved in 2,4-D degradation were also able to utilize phenoxypropanoic acids as substrates. Interestingly, they are highly enantioselective and convert only one enantiomer. TfdA from *R. eutropha* JMP134(JP4) and *Burkholderia cepacia* RASC oxidize only (*S*)-dichlorprop, whereas TfdA from *A.*

COR-AAD1-00003438
Bayer EX1008 (Part 7 of 9)

denitrificans exclusively converts the (*R*) enantiomer (119). This indicates that closely related enzymes may exhibit different enantioselectivities.

Another example of an enzyme that enantioselectively catalyzes a key reaction in the degradation of a recalcitrant pollutant is γ-hexachlorocyclohexane (HCH) dehydrochlorinase (LinA) from *S. paucimobilis* UT26 (97, 99). LinA catalyzes two reactions. The first reaction is the dechlorination of γ-HCH to γ-pentachlorocyclohexene (PCCH) and the second reaction is the dechlorination of γ-PCCH to 1,3(*R*),4,6-(*R*)-tetrachlorocyclo-hexa-1,4-diene (CDN), a compound that is presumed to spontaneously rearrange to 1,2,4-trichlorobenzene (TCB). For these reactions, no cofactors are needed. Beside γ-HCH, LinA also converts α– and δ-HCH, but not β-HCH, which indicates that the enzyme requires a biaxial HCl-pair on the substrate molecule. δ-HCH is only converted to δ-PCCH. Interestingly, LinA differentiates between 1,3(*S*),4(*R*),5(*R*),6(*S*)-PCCH and 1,3(*R*),4(*S*),_5(*S*),6(*R*)-PCCH, whereby only the former enantiomer is a metabolite in the degradation of γ-HCH. When provided with the racemate obtained by chemical alkaline dehydrochlorination, LinA converts the former enantiomer to 1,2,4-TCB and the latter one to 1,2,3-TCB. Therefore, the first step in the degradation of γ-HCH is highly enantioselective and gives rise to only one product enantiomer. Site-directed mutagenesis experiments allowed a closer look at the active site and it was found that the catalytic dyad, His-73 and Asp-25, is involved in stereoselectivity. It was suggested that the topological differentiation is caused by this catalytic dyad, whereas the enantiomeric differentiation is due to noncovalent interaction of the double-bond substituents with noncatalytic residues in the active site (135).

Ring-hydroxylating dioxygenases are important enzymes in the degradation of many aromatic pollutants. In most cases, they convert their achiral substrate to chiral products (*cis*-dihydrodiols), a process which is regio- and enantioselective; and many conversions lead to enantiomerically pure products (51). Naphthalene dioxygenase (NDO) belongs to this class of enzymes. Because the structure of NDO was solved (59, 60), it is the model enzyme for studying molecular aspects of enantioselectivity in such reactions. NDO is a multicomponent enzyme and

COR-AAD1-00003439
Bayer EX1008 (Part 7 of 9)

catalyzes a wide range of reactions, such as *cis*-hydroxylations, mono-oxygenations, and desaturations. It consists of three components: an iron-sulfur-flavoprotein reductase, an iron-sulfur-ferredoxin, and the oxygenase itself, which is built of a small α- and a large β-subunit with the overall structure $\alpha_3\beta_3$ (27, 60). NDO is NAD(P)H dependent and the reductase and ferredoxin component transfer the electron from NAD(P)H to the oxygenase (27, 28, 41). Each subunit of the oxygenase component contains a Riesketype [2Fe-2S] center and a mononuclear nonheme iron. Electrons are transferred from the Rieskecenter to the mononuclear iron of an adjacent α-subunit, which is the site of oxygen activation and catalysis. Phenylalanine residue 253 (F253) has been shown to play an important role in controlling regio- and enantioselectivity in phenanthrene, biphenyl and naphthalene oxidation. By site-directed mutagenesis, F352 was altered into different amino acids. NDO variant F352W, in which phenylalanine was replaced by tryptophan, exhibited the most pronounced changes in stereochemistry (109, 110). Other variants of F352 also showed altered regioselectivity with biphenyl and phenanthrene. The combination of a F352V variant of NDO and the enantioselective toluene *cis*-dihydrodiol dehydrogenase from *P. putida* F1 was used to produce the enantiomerically pure (–)-biphenyl *cis*-(*3S,4R*)-dihydrodiol and (–)-phenanthrene *cis*-(*1S,2R*)-dihydrodiol from biphenyl and phenanthrene, respectively (110). The enantioselective oxidation of dihydrodiols was also investigated for chlorobenzene *cis*-dihydrodiol dehydrogenase (TcbB) from *Pseudomonas* sp. strain P51 and it was found that the enantioselectivity of the conversion is highly dependent on the substrate (114). TcbB exclusively oxidizes (+)-*cis*-(*1R,2S*)-indandiol, whereas both enantiomers of *cis*-1,2-dihydroxy-1,2,3,4-tetrahydronaphthalene are converted.

Racemases (isomerases) catalyze racemization of their substrates and are thereby involved in enantioselective degradation pathways. One well studied example is mandelic acid racemase (MR). MR converts D- to L-mandelic acid and vice versa. *P. putida* biotype A degrades both enantiomers of mandelic acid by means of a racemase. L-Mandelic acid is the substrate of a L-(+)-mandelic acid dehydrogenase, which is highly enantioselective. Further metabolism proceeds

COR-AAD1-00003440
Bayer EX1008 (Part 7 of 9)

through the so-called mandelate pathway to benzoic acid (61), which is further metabolized via catechol and through the *ortho*-cleavage pathway. D-Mandelic acid is metabolized by the same enzymes except that it is initially converted to the L-enantiomer by MR. Interestingly, MR itself is nonenantioselective, i.e., D-mandelic acid is converted to the L-enantiomer at the same rate as the L-enantiomer is converted to the D-enantiomer (140). The racemization proceeds by a two-base mechanism (113). This means that two basic amino acid residues, which are juxtaposed on either side of the chiral substrate carbon, are involved. One base abstracts the proton of the substrate whereas the conjugate acid of the other base protonates the intermediate from the other side. For the opposite reaction, the roles are reversed. For MR from *P. putida* F1, the two basic residues were identified as lysine residue 166 (K166) and histidine residue 297 (H297; 58, 69, 70, 103). K166 abstracts the α-proton from the (*S*) enantiomer whereas H297 deprotonates the (*R*) enantiomer.

An interesting example of an enzyme pair which metabolizes the enantiomers of a chiral compound is the paired tropinone reductases (TR-I, TR-II) from *Datura stramonium*. Many plants produce tropane alkaloids and, in this synthesis, the TRs reduce a carbonyl group of an alkaloid intermediate, tropinone, to hydroxygroups with different diastereometric configurations: tropine (3α-hydroxytropane) and P-tropine (3β-hydroxytropane). The crystal structures of both TRs were determined (100). The two enzymes share 64% amino acid identity and the overall folding is almost identical. The binding sites for the cofactor NADH and the positions of the active site residues are well conserved. The active sites are composed mainly of hydrophobic amino acids but differently charged amino acids cause different electrostatic environments. In TR-I, there is a positively charged histidine (H112), whereas in TR-II a polar tyrosine (Y100) occupies this position. In TR-II, the hydrophobic valine residue 168 of TR-I is replaced by the negatively charged glutamate residue 156. These differences are of importance for the positioning of tropinone. The nitrogen atom of tropinone is negatively charged under physiological pH conditions and, thereby, tropinone is oriented in different ways in the active site by the different electrostatic environments.

COR-AAD1-00003441
Bayer EX1008 (Part 7 of 9)

These examples demonstrate how single amino acid residues are responsible for highly enantioselective reactions and enable the enzymes to differentiate between enantiomers. Just by changing a few amino acid residues involved in regio- and enantioselective substrate recognition, the stereoselectivity of an enzymatic reaction can be changed or even reversed.

Convergent evolution is another approach nature has chosen to metabolize enantiomers of chiral compounds. Many enzyme pairs, each turning over one enantiomer of a chiral compound, have evolved independently and are not related to each other. Examples are the D- and L-lactate dehydrogenases (D-LDH, L-LDH), which belong to the D- and L-ketoacid dehydrogenase families, respectively. Sequence comparisons show that these two enzyme families are not related to each other evolutionarily. L- and D-LDH catalyze the reduction of pyruvate to lactate, with the concomitant consumption of NADH, producing enantiomerically pure products. By crystal structure analysis, it was found, that the overall folding of the D-LDH is completely different from that of L-LDH. It was hypothesized that, despite the different folding, the active sites are mirror-images of each other (39, 68). This is true insofar as the same amino acid residues are involved in substrate-binding and catalysis and they are in structurally equivalent positions. However, their exact roles in binding and catalysis may not be the same (129). Convergent evolution was also found for the D-amino acid transferases (D-AAT) and the L-aspartate aminotransferases (L-Asp-AT). D-AAT and L-Asp-AT do not share any identity at the sequence level and their overall folding is different, but the enzymatic mechanism is similar. Both enzymes contain a pyridoxal phosphate (PLP) and catalyze a transamination of the respective amino acid enantiomer. Sugio *et al.* (131) showed that there are striking similarities between the active sites of the two enzymes, especially concerning the binding of the PLP and its intermediates. The α-amino- and α-carboxyl group of the substrate amino acid are bound in the same orientation in relation to the pyridoxal phosphate ring and the protein. The side-chain is therefore, due to the inversed chirality, oriented in the opposite direction.

Other interesting enzymes in terms of their enantioselectivity are the 2-halo-acid dehalogenases (DEXs) which convert chiral 2-haloacids into 2-hydroxyacids.

COR-AAD1-00003442
Bayer EX1008 (Part 7 of 9)

DEXs are involved in the degradation of halogenated organic compounds and are classified into four groups based on their substrate and stereochemical specificities (128). L-DEXs convert L-haloacids into D-hydroxyacids with inversion of the configuration at the C2-carbon atom of the substrate. D-DEX acts specifically on the D-enantiomer to produce L-hydroxyacids. DL-DEX_i dehalogenates both enantiomers with inversion of the configuration at the C2-carbon atom; and DL-DEX_r converts both enantiomers to the corresponding hydroxyacids with retention of the configuration at the C2-carbon atom. L-DEXs are well studied, both in terms of reaction mechanisms and in terms of substrate- and stereo-specificity (67, 74, 75, 127). Additionally, crystal structures of two representative enzymes, L-DEX from *Pseudomonas* sp. YL and L-DEX from *Xanthobacter autotrophicus* GJ10 have been solved (47, 74, 115). The normal reaction mechanism proceeds via an ester intermediate. First, Asp-10 acts as a nucleophile and attacks the C2-carbon atom of the substrate forming an ester-intermediate and a halide ion. A water molecule is activated and hydrolyzes the intermediate from the back giving the D-hydroxyacid. From mutagenesis studies and the crystal structure of L-DEX YL, several amino acid residues (Tyr-12, Leu-45, Phe-60, Trp-179, Gln-44, Lys-151, Asn-177) were identified which built a hydrophobic pocket. While the carboxylic moiety of the substrate is bound to Asp-10, the alkyl group is located in the hydrophobic pocket. This hydrophobic pocket is responsible for the stereo- and substrate-specificity of the enzyme. It is not possible to accommodate an alkyl group at the place of the hydrogen atom due to steric hindrance by the main chain and the side chain atoms of Leu-11, Tyr-12, and their neighbors in this pocket. This determines the enantioselectivity (and substrate specificity) of the enzyme. In contrast to L-DEX, DL-DEX_r converts both enantiomers. DL-DEX from *Pseudomonas* sp. strain 113 (DL-DEX 113) has a significant sequence homology with D-DEXs, e.g. 23% with D-DEX from *P. putida* AJ1, but little with L-DEXs (101). To study the reactive site, several polar and charged amino acid residues conserved among DL- and D-DEX were mutated. When the enzymatic activity was lower than in the wild type, the effect was always equal for both enantiomers. The results suggest that DL-DEX 113 has one single

COR-AAD1-00003443
Bayer EX1008 (Part 7 of 9)

active site for D- and L-2-haloacids. In other words, DL-DEX 113 does not – in contrast to L-DEX – discriminate between the alkyl group and the hydrogen atom at the C2-atom of 2-haloacids (101).

L-DEX are examples of enzymes that discriminate between enantiomers by the spatial arrangement of the active site rather than by specific interactions of single amino acid residues with the substrate. It would be interesting to know, how the substrates are bound to the active sites in D- and DL-DEX in order to compare the mechanism, but crystallographic data are not yet available.

We have described enzymes with overall conserved folding, where just a few amino acid residues determine stereospecificity together with examples of enzymes that express opposite stereospecificity and have completely different folds and surprisingly similar active sites that are mirror-images. Theoretically, two enzymes with identical sequences but built from enantiomeric amino acid monomers, i.e., one built from L-amino acids and the other from D-amino acids, should have opposite stereospecificities for chiral substances. Such an enzyme pair was studied by Milton *et al.* (21). They synthesized the HIV-1 protease completely with D-amino acids. The D-HIV-1 protease indeed showed the opposite substrate specificity. Inversed specificity was also observed with enantiomeric inhibitors. These data imply that the L- and the D-forms of the enzyme are exactly image and mirror-image of each other, resulting in opposite substrate specificity.

CONCLUSION

The environmental fate of the enantiomers of chiral compounds differs not only with regards to unwanted side-effects but also with regard to degradation. As the examples show, there is no rule to decide which enantiomer is preferably degraded. It depends on the specific compounds, the environmental compartment, the environmental conditions, and the microbial community. As other authors have emphasized, it is important to consider both stereochemistry and chirality when studying the effects and degradation potential of chiral compounds (e.g. 4, 5, 64, 65). This is also true when enantiomerically pure compounds are used and therefore, only one enantiomer is introduced into the environment. As was pointed out,

COR-AAD1-00003444
Bayer EX1008 (Part 7 of 9)

enantiomers may undergo racemization or enantiomerization processes and therefore, the environmental fate of each enantiomer always needs to be investigated.

Studies on enantioselective enzymes have helped and will help to broaden our understanding of the effects of chirality on the living world. It will be important to study such enzymes more intensively to learn how nature deals with chiral objects. The following questions need to be addressed. Does an enzyme change its stereospecificity easily? How do enzymes which are evolutionarily not related to each other adapt to convert enantiomers of a chiral compound? Evolution has not preferred one particular mechanism, as far as we know, but further studies need to be carried out to answer such questions in more detail.

COR-AAD1-00003445
Bayer EX1008 (Part 7 of 9)

REFERENCES

1. Åberg, B. 1973. Plant growth regulators. XXXI. Some monochloro-monomethylphenoxyacetic and related optically active propionic acids. Swedish J. agric. Res. 3:49-62.
2. Ahrens, W. H. 1994. Herbicide Handbook (WSSA), 7th ed. Weed Science Society of America, Champaign.
3. Aigner, E. J., A. D. Leone, and R. L. Falconer. 1998. Concentrations and enantiomeric ratios of organochlorine pesticides in soils from the U.S. corn belt. Environ. Sci. Technol. 32:1162-1168.
4. Ariëns, E. J. 1993. Nonchiral, homochiral and composite chiral drugs. Trends Pharmacol. Sci. 14:68-75.
5. Ariëns, E. J. 1989. Racemates - an impediment in the use of drugs and agrochemicals, p. 31-68. *In* A. M. Krstulovic (ed.), Chiral separations by HPLC. Ellis Horwood Ltd., Chichester, Great Britain.
6. Ariëns, E. J. 1983. Stereoselectivity of bioactive agents: General aspects, p. 11-32. *In* E. J. Ariëns, W. Soudijn, and P. B. M. W. M. Timmermans (ed.), Stereochemistry and biological activity of drugs. Blackwell Scientific Publications, Oxford.
7. Bentley, R. 1995. From optical activity in quartz to chiral drugs: Molecular handedness in biology and medicine. Perspect. Biol. Med. 38:188-229.
8. Bhat, M. A., T. Ishida, K. Horiike, C. S. Vaidyanathan, and M. Nozaki. 1993. Purification of 3,5-dichlorocatechol 1,2-dioxygenase, a nonheme iron dioxygenase and a key enzyme in the biodegradation of a herbicide, 2,4-dichlorophenoxyacetic acid (2,4-D), from *Pseudomonas cepacia* CSV90. Arch. Biochem. Biophys. 300:738-746.
9. Bucheli, T. D., S. R. Müller, S. Heberle, and R. P. Schwarzenbach. 1998. Occurrence and behavior of pesticides in rainwater, roof runoff, and artificial stormwater infiltration. Environ. Sci. Technol. 32:3457-3464.
10. Bucheli, T. D., S. R. Müller, A. Voegelin, and R. P. Schwarzenbach. 1998. Bituminous roof sealing membranes as major sources of the herbicide (R,S)-mecoprop in roof runoff waters: potential contamination of groundwater and surface waters. Environ. Sci. Technol. 32:3465-3471.
11. Buchenauer, H. 1990. Phenylamides, p. 234-238. *In* G. Haug and D. Hoffmann (ed.), Chemistry of plant protection, vol. 6. Springer Verlag, New York.
12. Buerge, I. J., T. Poiger, M. D. Müller, and H.-R. Buser. 2003. Enantioselective degradation of metalaxyl in soils: chiral preference changes with soil pH. Environ Sci Technol 37:2668-2674.
13. Buser, H.-R., and M. D. Müller. 1997. Conversion reactions of various phenoxyalkanoic acid herbicides in soil. 2. Elucidation of the enantiomerization process of chiral phenoxy acids from incubation in a D_2O/soil system. Environ. Sci. Technol. 31:1960-1967.
14. Buser, H.-R., and M. D. Müller. 1995. Environmental behavior of acetamide pesticide stereoisomers. 1. Stereo- and enantioselective determination using chiral high-resolution gas chromatography and chiral high-performance liquid chromatography. Environ. Sci. Technol. 29:2023-2030.

COR-AAD1-00003446
Bayer EX1008 (Part 7 of 9)

15. Buser, H.-R., and M. D. Müller. 1995. Isomer and enantioselective degradation of hexachlorocyclohexane isomers in sewage sludge under anaerobic conditions. Environ. Sci. Technol. 29:664-672.

16. Buser, H.-R., M. D. Müller, T. Poiger, and M. E. Balmer. 2002. Environmental behavior of the chiral acetamide pesticide metalaxyl: Enantioselective degradation and chiral stability in soil. Environ. Sci. Technol. 36:221-226.

17. Buser, H.-R., T. Poiger, and M. D. Müller. 2000. Changed enantiomer composition of metalochlor in surface water following the introduction of the enantiomerically enriched product to the market. Environ. Sci. Technol. 34:2690-2696.

18. Chesters, G., G. V. Simsiman, J. Levy, B. J. Alhajjar, R. N. Fathulla, and J. M. Harkin. 1989. Environmental fate of alachlor and metolachlor. Rev. Environ. Contam. Toxicol. 110:1-74.

19. de Almeida, J. L. G., M. Dufaux, Y. Ben Taarit, and C. Naccache. 1994. Linear alkylbenzene. J. Am. Oil Chem. Soc. 71:675-694.

20. Dearth, M. A., and R. A. Hites. 1991. Complete analysis of technical chlordane using negative ionization mass spectrometry. Environ. Sci. Techol . 25: 245- 254.

21. deL Milton, R. C., S. C. Milton, and S. B. H. Kent. 1992. Total chemical synthesis of a D-enzyme: the enantiomers of HIV-1 protease show reciprocal chiral substrate specificity. Science 256:1445-1448.

22. Donaldson, D., T. Kiely, and A. Grube. 2002. Pesticides industry sales and usage. 1998 and 1999 market estimates. U.S. Environmental Protection Agency.

23. Douros, J. D., and J. W. Frankenfeld. 1968. Oxidation of alkylbenzenes by a strain of *Micrococcus cerificans* growing on *n*-paraffins. Appl. Environ. Microbiol. 16:532-533.

24. Easson, L. H., and E. Stedman. 1933. Studies on the relationship between chemical constitution and physiological action. V. Molecular dissymmetry and physiological activity. Biochem. J. 27:1257-1266.

25. Ehrig, A., R. H. Müller, and W. Babel. 1997. Isolation of phenoxy herbicide-degrading *Rhodoferax* species from contaminated building material. Acta Biotechnol. 17:351-356.

26. Eliel, E. L., and S. H. Wilen. 1994. Stereochemistry of organic compounds. John Wiley & Sons, New York.

27. Ensley, B. D., and D. T. Gibson. 1983. Naphthalene dioxygenase: purification and properties of a terminal oxygenase component. J. Bacteriol. 155:505-511.

28. Ensley, B. D., D. T. Gibson, and A. L. Laborde. 1982. Oxidation of naphthalene by a multicomponent enzyme system from *Pseudomonas* sp. strain NCIB 9816. J. Bacteriol. 149:948-954.

29. Falconer, R. L., T. F. Bidleman, D. J. Gregor, R. Semkin, and C. Teixeira. 1995. Enantioselective breakdown of α-hexachlorocyclohexane in a small arctic lake and its watershed. Environ. Sci. Technol. 29:1297-1302.

30. Falconer, R. L., T. F. Bidleman, and S. Y. Szeto. 1997. Chiral pesticides in soils of the Fraser Valley, British Columbia. J. Agric. Food Chem. 45:1946-1951.

31. Farhana, L., and P. B. New. 1997. The 2,4-dichlorophenol hydroxylase of *Alcaligenes eutrophus* JMP134 is a homotetramer. Can. J. Microbiol. 43:202-205.

COR-AAD1-00003447
Bayer EX1008 (Part 7 of 9)

32. FDA. 1992. FDA's policy statement for the development of new stereoisomeric drugs. Chirality 4:338-340.

33. Felding, G. 1995. Leaching of phenoxyalkanoic acid herbicides from farmland. Sci. Total Envir. 168:11-18.

34. Fisher, D. J., and A. L. Hayes. 1985. A comparison of the biochemical and physiological effects of the systemic fungicide cyprofuram with those of the related compounds metalaxyl and metolachlor. Crop Protect. 4:501-510.

35. Fukumori, F., and R. P. Hausinger. 1993. *Alcaligenes eutrophus* JMP134 "2,4-dichlorophenoxyacetate monooxygenase" is a α-ketoglutarate-dependent dioxygenase. J. Bacteriol. 175:2083-2096.

36. Fukumori, F., and R. P. Hausinger. 1993. Purification and characterization of 2,4-dichlorophenoxyacetate/α-ketoglutarate dioxygenase. J. Biol. Chem. 268:24311-24317.

37. Garrison, A. W., P. Schmitt, D. Martens, and A. Kettrup. 1996. Enantiomeric selectivity in the environmental degradation of dichlorprop as determined by High-Performance Capillary Electrophoresis. Environ. Sci. Technol. 30:2249-2455.

38. Gintautas, P. A., S. R. Daniel, and D. L. Macalady. 1992. Phenoxyalkanoic acid herbicides in municipal landfill leachates. Environ. Sci. Technol. 26:517-521.

39. Goldberg, J. D., T. Yoshida, and P. Brick. 1994. Crystal structure of a NAD-dependent D-glycerate dehydrogenase at 2.4 Å resolution. J. Mol. Biol. 236:1123-1140.

40. Gupta, A., C. P. Kaushik, and A. Kaushik. 2001. Degradation of hexachlorocyclohexane isomers by two strains of *Alcaligenes faecalis* isolated from a contaminated site. Bull. Environ. Contam. Toxicol. 66:794-800.

41. Haigler, B. E., and D. T. Gibson. 1990. Purification and properties of ferredoxin$_{NAP}$, a component of naphthalene dioxygenase from *Pseudomonas* sp. strain NCIB 9816. J. Bacteriol. 172:465-468.

42. Harner, T., H. Kylin, T. F. Bidleman, and W. M. Strachan. 1999. Removal of α- and γ-hexachlorocyclohexane in the Eastern Arctic ocean. Environ. Sci. Technol. 33:1157-1164.

43. Hayes, W. J., and E. R. Laws. 1991. Classes of pesticides, vol. 2. Academic Press, San Diego.

44. Hegeman, W. J. M., and R. W. P. M. Laane. 2002. Enantiomeric enrichment of chiral pesticides in the environment. Rev. Environ. Contam. Toxicol. 173:85-116.

45. Hegg, E. L., and L. Que, Jr. 1997. The 2-His-1-carboxylate facial triad--an emerging structural motif in mononuclear non-heme iron(II) enzymes. Eur. J. Biochem. 250:625-629.

46. Heron, G., and T. H. Christensen. 1992. Degradation of the herbicide mecoprop in an aerobic aquifer determined by laboratory batch studies. Chemosphere 24:547-557.

47. Hisano, T., Y. Hata, T. Fujii, J. Q. Liu, T. Kurihara, N. Esaki, and K. Soda. 1996. Crystal structure of L-2-haloacid dehalogenase from *Pseudomonas* sp. YL. An α/β hydrolase structure that is different from the α/β hydrolase fold. J. Biol. Chem. 271:20322-30.

COR-AAD1-00003448
Bayer EX1008 (Part 7 of 9)

48. Holt, M. S., and S. L. Bernstein. 1992. Linear alkylbenzenes in sewage sludges and sludge amended soils. Wat. Res. 26:613-624.

49. Horvath, M., G. Ditzelmüller, M. Loidl, and F. Streichsbier. 1990. Isolation and characterization of a 2-(2,4-dichlorophenoxy)propionic acid degrading soil bacterium. Appl. Microbiol. Biotechnol. 33:213-216.

50. Huddleston, R. L., and R. C. Allred. 1963. Microbial oxidation of sulfonated alkylbenzenes. Dev. Ind. Microbiol. 4:24-38.

51. Hudlicky, T., D. Gonzales, and D. T. Gibson. 1999. Enzymatic dihydroxylation of aromatics in enantioselective synthesis: expanding asymmetric methodology. Aldrichimica acta 32:53-62.

52. Hühnerfuss, H., J. Faller, R. Kallenborn, W. A. König, P. Ludwig, B. Pfaffenberger, M. Oehme, and G. Rimkus. 1993. Enantioselective and nonenantioselective degradation of organic pollutants in the marine ecosystem. Chirality 5:393-399.

53. Hühnerfuss, H., J. Faller, W. A. König, and P. Ludwig. 1992. Gas chromatographic separation of the enantiomers of marine pollutants. 4. Fate of hexachlorocyclohexane isomers in the Baltic and North sea. Environ. Sci. Technol. 26:2127-2133.

54. Hummert, K., W. Vetter, and B. Luckas. 1995. Levels of alpha-HCH, lindane, and enantiomeric ratios of alpha-HCH in marine mammals from the northern hemisphere. Chemosphere 31:3489-500.

55. Imai, R., Y. Nagata, M. Fukuda, M. Takagi, and K. Yano. 1991. Molecular cloning of a *Pseudomonas paucimobilis* gene encoding a 17-kilodalton polypeptide that eliminates HCl molecules from γ-hexachlorocyclohexane. J. Bacteriol. 173:6811-6819.

56. Iwata, H., S. Tanabe, N. Sakal, and R. Tatsukawa. 1993. Distribution of persistent organochlorines in the oceanic air and surface seawater and the role of ocean on their global transport and fate. Environ. Sci. Technol. 27:1080-1098.

57. Jantunen, L. M. M., and T. F. Bidleman. 1998. Organochlorine pesticides and enantiomers of chiral pesticides in Arctic ocean water. Arch. Environ. Contam. Toxicol. 35:218-228.

58. Kallarakal, A. T., B. Mitra, J. W. Kozarich, J. A. Gerlt, J. G. Clifton, G. A. Petsko, and G. L. Kenyon. 1995. Mechanism of the reaction catalyzed by mandelate racemase: structure and mechanistic properties of the K166R mutant. Biochemistry 34:2788-2797.

59. Karlsson, A., J. V. Parales, R. E. Parales, D. T. Gibson, H. Eklund, and S. Ramaswamy. 2003. Crystal structure of naphthalene dioxygenase: side-on binding of dioxygen to iron. Science 299:1039-1042.

60. Kauppi, B., K. Lee, E. Carredano, R. E. Parales, D. T. Gibson, H. Eklund, and S. Ramaswamy. 1998. Structure of an aromatic-ring-hydroxylating dioxygenase-naphthalene 1,2-dioxygenase. Structure 6:571-586.

61. Kenyon, G. L., and G. D. Hegeman. 1979. Mandelate racemase. Adv. Enzymol. Relat. Areas Mol. Biol. 50:325-360.

62. Kleinsteuber, S., D. Hoffmann, R. H. Müller, and W. Babel. 1998. Detection of chlorocatechol 1,2-dioxygenase genes in Proteobacteria by PCR and gene probes. Acta Biotechnol. 18:231-240.

COR-AAD1-00003449
Bayer EX1008 (Part 7 of 9)

63. Kohler, H.-P. E. 1999. *Sphingomonas herbicidovorans* MH: a versatile phenoxyalkanoic herbicide degrader. J. Ind. Microbiol. Biotechnol. 23:336-340.

64. Kohler, H.-P. E., W. Angst, W. Giger, C. Kranz, S. Müller, and M. J.-F. Suter. 1997. Environmental fate of chiral pollutants - the necessity of considering stereochemistry. Chimia 51:947-951.

65. Kohler, H.-P. E., K. Nickel, and C. Zipper. 2000. Effect of chirality on the microbial degradation and the environmental fate of chiral pollutants, p. 201-231. *In* B. Schink (ed.), Advances in microbial ecology, vol. 16. Kluwer Academics/Plenum Publishers, New York.

66. Kuhm, A. E., M. Schlömann, H. J. Knackmuss, and D. H. Pieper. 1990. Purification and characterization of dichloromuconate cycloisomerase from *Alcaligenes eutrophus* JMP 134. Biochem. J. 266:877-883.

67. Kurihara, T., J. Q. Liu, V. Nardi-Dei, H. Koshikawa, N. Esaki, and K. Soda. 1995. Comprehensive site-directed mutagenesis of L-2-halo acid dehalogenase to probe catalytic amino acid residues. J. Biochem. (Tokyo) 117:1317-1322.

68. Lamzin, V. S., Z. Dauter, and K. S. Wilson. 1994. Dehydrogenation through the looking-glass. Nat. Struct. Biol. 1:281-282.

69. Landro, J. A., J. A. Gerlt, J. W. Kozarich, C. W. Koo, V. J. Shah, G. L. Kenyon, D. J. Neidhart, S. Fujita, and G. A. Petsko. 1994. The role of lysine 166 in the mechanism of mandelate racemase from *Pseudomonas putida*: mechanistic and crystallographic evidence for stereospecific alkylation by (*R*)-α-phenylglycidate. Biochemistry 33:635-643.

70. Landro, J. A., A. T. Kallarakal, S. C. Ransom, J. A. Gerlt, J. W. Kozarich, D. J. Neidhart, and G. L. Kenyon. 1991. Mechanism of the reaction catalyzed by mandelate racemase. 3. Asymmetry in reactions catalyzed by the H297N mutant. Biochemistry 30:9274-9281.

71. Law, S. A., M. L. Diamond, P. A. Helm, L. M. Jantunen, and M. Alaee. 2001. Factors affecting the occurrence and enantiomeric degradation of hexachlorocyclohexane isomers in northern and temperate aquatic systems. Environ. Toxicol. Chem. 20:2690-2698.

72. LeBaron, H., J. E. McFarland, B. J. Simoneaux, and E. Ebert. 1988. Metolachlor, p. 335-382. *In* P. C. Kearney and D. D. Kaufman (ed.), Herbicides. Chemistry, degradation and mode of action, vol. 3. Marcel Dekker Inc., New York.

73. Lewis, D. L., A. W. Garrison, K. E. Wommack, A. Whittemore, P. Steudler, and J. Melillo. 1999. Influence of environmental changes on degradation of chiral pollutants in soils. Nature 401:898-901.

74. Li, Y.-F., Y. Hata, T. Fujii, T. Hisano, M. Nishihara, T. Kurihara, and N. Esaki. 1998. Crystal structures of reaction intermediates of L-2-haloacid dehalogenase and implications for the reaction mechanism. J. Biol. Chem. 273:15035-15044.

75. Liu, J.-Q., T. Kurihara, M. Miyagi, N. Esaki, and K. Soda. 1995. Reaction mechanism of L-2-haloacid dehalogenase of *Pseudomonas* sp. YL. Identification of Asp^{10} as the active site nucleophile by ^{18}O incorporation experiments. J. Biol. Chem. 270:18309-18312.

76. Liu, T., and P. J. Chapman. 1984. Purification and properties of a plasmid-encoded 2,4-dichlorophenol hydroxylase. FEBS Lett. 173:314-318.

COR-AAD1-00003450
Bayer EX1008 (Part 7 of 9)

77. Loos, M. A. 1975. Phenoxyalkanoic acids, p. 1-128. *In* P. C. Kearney and D. D. Kaufmann (ed.), Herbicides. Chemistry, degradation and mode of action, 2nd ed, vol. 1. Marcel Dekker, Inc., New York.

78. Ludwig, P., W. Gunkel, and H. Hühnerfuss. 1992. Chromatographic separation of the enantiomers of marine pollutants. Part 5: enantioselective degradation of phenoxycarboxylic acid herbicides by marine microorganisms. Chemosphere 24:1423-1429.

79. Ludwig, P., H. Hühnerfuss, W. A. König, and W. Gunkel. 1992. Gas chromatographic separation of the enantiomers of marine pollutants. Part 3. Enantioselective degradation of α-hexachlorocyclohexane and γ-hexachlorocyclohexane by marine microorganisms. Mar. Chem. 38:13-23.

80. Lyngkilde, J., and T. H. Christensen. 1992. Fate of organic contaminants in the redox zone of a landfill leachate pollution plume. J. Contam. Hydrol. 10:291-307.

81. Manonmani, H. K., D. H. Chandrashekaraiah, N. Sreedhar Reddy, C. D. Elcey, and A. A. M. Kunhi. 2000. Isolation and acclimation of a microbial consortium for improved aerobic degradation of α-hexachlorocyclohexane. J. Agric. Food Chem. 48:4341-4351.

82. Marucchini, C., and C. Zadra. 2002. Stereoselective degradation of metalaxyl and metalaxyl-M in soil and sunflower plants. Chirality 14:32-38.

83. Matell, M. 1953. Stereochemical studies on plant growth regulators. VII. Optically active α-(2-methyl-4-chlorophenoxy)-propionic acid and α-(2,4-dichlorophenoxy)-*n*-butyric acid and their steric relations. Ark. Kemi 6:365-373.

84. Meharg, A. A., J. Wright, G. J. L. Leeks, P. D. Wass, and D. Osborn. 1999. Temporal and spatial patterns in α- and γ-hexachlorocyclohexane concentrations in industrially contaminated rivers. Environ. Sci. Technol. 33:2001-2006.

85. Meijer, S. N., C. J. Halsall, T. Harner, A. J. Peters, W. A. Ockenden, A. E. Johnston, and K. C. Jones. 2001. Organochlorine pesticide residues in archived UK soil. Environ. Sci. Technol. 35:1989-1995.

86. Mesecar, A. D., and D. E. Koshland Jr. 2000. A new model for protein stereospecificity. Nature 403:614-615.

87. Middeldorp, P. J. M., M. Jaspers, A. J. B. Zehnder, and G. Schraa. 1996. Biotransformation of α-, β-, γ-, and δ-hexachlorocyclohexane under methanogenic conditions. Environ. Sci. Technol. 30:2345-2349.

88. Moisey, J., A. T. Fisk, K. A. Hobson, and R. J. Norstrom. 2001. Hexachlorocyclohexane (HCH) isomers and chiral signatures of α-HCH in the Arctic marine food web of the Northwater Polynya. Environ. Sci. Technol. 35:1920-1927.

89. Monkiedje, A., M. Spiteller, and K. Bester. 2003. Degradation of racemic and enantiopure metalaxyl in tropical and temperate soils. Environ. Sci. Technol. 37:707-712.

90. Müller, M. D., and H.-R. Buser. 1997. Conversion reactions of various phenoxyalkanoic acid herbicides in soil. 1. Enantiomerization and enantioselective degradation of the chiral 2-phenoxypropionic acid herbicides. Environ. Sci. Technol. 31:1953-1959.

91. Müller, M. D., and H.-R. Buser. 1995. Environmental behavior of acetamide pesticide stereoisomers. 2. Stereo- and enantioselective degradation in sewage sludge and soil. Environ. Sci. Technol. 29:2031-2037.

COR-AAD1-00003451
Bayer EX1008 (Part 7 of 9)

92. Müller, M. D., M. Schlabach, and M. Oehme. 1992. Fast and precise determination of α-hexachlorocyclohexane enantiomers in environmental samples using chiral high-resolution gas chromatography. Environ. Sci. Technol. 26:566-569.

93. Müller, R. H., S. Jorks, S. Kleinsteuber, and W. Babel. 1999. *Comamonas acidovorans* strain MC1: a new isolate capable of degrading the chiral herbicides dichlorprop and mecoprop and the herbicides 2,4-D and MCPA. Microbiol. Res. 154:241-246.

94. Müller, R. H., S. Kleinsteuber , and W. Babel. 2001. Physiological and genetic characteristics of two bacterial strains utilizing phenoxypropionate and phenoxyacetate herbicides. Microbiol. Res. 156:121-131.

95. Müller, T. A., T. Fleischmann, J. R. van der Meer, and H.-P. E. Kohler. in preparation. Characterization of genes involved in chiral phenoxyalkanoic acid herbicides degradation in *Sphingomonas herbicidovorans* MH.

96. Nagasawa, S., R. Kikuchi, Y. Nagata, M. Takagi, and M. Matsuo. 1993. Aerobic mineralization of γ-HCH by *Pseudomonas paucimobilis* UT26. Chemosphere 26:1719-1728.

97. Nagata, Y., R. Imai, A. Sakai, M. Fukuda, K. Yano, and M. Takagi. 1993. Isolation and characterization of Tn5-induced mutants of *Pseudomonas paucimobilis* UT26 defective in γ-hexachlorocyclohexane dehydrochlorinase (LinA). Biosci. Biotechnol. Biochem. 57:703-709.

98. Nagata, Y., K. Miyauchi, and M. Takagi. 1999. Complete analysis of genes and enzymes for γ-hexachlorocyclohexane degradation in *Sphingomonas paucimobilis* UT26. J. Ind. Biol. Biotechnol. 23:380-390.

99. Nagata, Y., T. Nariya, R. Ohtomo, M. Fukuda, K. Yano, and M. Takagi. 1993. Cloning and sequencing of a dehalogenase gene encoding an enzyme with hydrolase activity involved in the degradation of γ-hexachlorocyclohexane in *Pseudomonas paucimobilis*. J. Bacteriol. 175:6403-6410.

100. Nakajima, K., A. Yamashita, H. Akama, T. Nakatsu, H. Kato, T. Hashimoto, J. Oda, and Y. Yamada. 1998. Crystal structure of two tropinone reductases: different reaction stereospecificities in the same protein fold. Proc. Natl. Acad. Sci. USA 95:4876-4881.

101. Nardi-Dei, V., T. Kurihara, C. Park, N. Esaki, and K. Soda. 1997. Bacterial DL-2-haloacid dehalogenase from *Pseudomonas* sp. strain 113: gene cloning and structural comparison with D- and L-2-haloacid dehalogenases. J. Bacteriol. 179:4232-4238.

102. Nawab, A., A. Aleem, and A. Malik. 2003. Determination of organochlorine pesticides in agricultural soil with special reference to γ-HCH degradation by *Pseudomonas* strains. Bioresour. Technol. 88:41-46.

103. Neidhart, D. J., P. L. Howell, G. A. Petsko, V. M. Powers, R. S. Li, G. L. Kenyon, and J. A. Gerlt. 1991. Mechanism of the reaction catalyzed by mandelate racemase. 2. Crystal structure of mandelate racemase at 2.5-Å resolution: identification of the active site and possible catalytic residues. Biochemistry 30:9264-9273.

104. Ngabe, B., T. F. Bidleman, and R. L. Falconer. 1993. Base hydrolysis of α- and γ-hexachlorocyclohexanes. Environ. Sci. Technol. 27:1930-1933.

COR-AAD1-00003452
Bayer EX1008 (Part 7 of 9)

105. Nickel, K., M. J.-F. Suter, and H.-P. E. Kohler. 1997. Involvement of two α-ketoglutarate-dependent dioxygenases in enantioselective degradation of (*R*)- and (*S*)-mecoprop by *Sphingomonas herbicidovorans* MH. J. Bacteriol. 179:6674-6679.

106. Nitschke, L., A. Wilk, W. Schüsseler, G. Metzner, and G. Lind. 1999. Biodegradation in laboratory activated sludge plants and aquatic toxicity of herbicides. Chemosphere 39:2313-2323.

107. Ogston, A. G. 1948. Interpretation of experiments on metabolic processes, using isotopic tracer elements. Nature 162:963.

108. Painter, H. A. 1992. Anionic surfactants, p. 1-88. *In* N. T. de Oude (ed.), The handbook of environmental chemistry, vol. 3, part F. detergents. Springer Verlag, Berlin.

109. Parales, R. E., K. Lee, S. M. Resnick, H. Jiang, D. J. Lessner, and D. T. Gibson. 2000. Substrate specificity of naphthalene dioxygenase: effect of specific amino acids at the active site of the enzyme. J. Bacteriol. 182:1641-1649.

110. Parales, R. E., S. M. Resnick, C. L. Yu, D. R. Boyd, N. D. Sharma, and D. T. Gibson. 2000. Regioselectivity and enantioselectivity of naphthalene dioxygenase during arene *cis*-dihydroxylation: control by phenylalanine 352 in the α-subunit. J. Bacteriol. 182:5495-5504.

111. Perkins, E. J., M. P. Gordon, O. Caceres, and P. F. Lurquin. 1990. Organization and sequence analysis of the 2,4-dichlorophenol hydroxylase and dichlorocatechol oxidative operons of plasmid pJP4. J. Bacteriol. 172:2351-2359.

112. Pfaffenberger, B., I. Hardt, H. Hühnerfuss, W. A. König, G. Rimkus, A. Glausch, V. Schurig, and J. Hahn. 1994. Enantioselective degradation of alpha-hexachlorocyclohexane and cyclodiene insecticides in roe-deer liver samples from different regions of Germany. Chemosphere 29:1543-1554.

113. Powers, V. M., C. W. Koo, G. L. Kenyon, J. A. Gerlt, and J. W. Kozarich. 1991. Mechanism of the reaction catalyzed by mandelate racemase. 1. Chemical and kinetic evidence for a two-base mechanism. Biochemistry 30:9255-9263.

114. Raschke, H., T. Fleischmann, J. R. van der Meer, and H.-P. E. Kohler. 1999. *cis*-chlorobenzene dihydrodiol dehydrogenase (TcbB) from *Pseudomonas* sp. strain P51, expressed in *Escherichia coli* DH5α(pTCB149), catalyzes enantioselective dehydrogenase reactions. Appl. Environ. Microbiol. 65:5242-5246.

115. Ridder, I. S., H. J. Rozeboom, K. H. Kalk, D. B. Janssen, and B. W. Dijkstra. 1997. Three-dimensional structure of L-2-haloacid dehalogenase from *Xanthobacter autotrophicus* GJ10 complexed with the substrate-analogue formate. J Biol Chem 272:33015-33022.

116. Romero, E., G. Dios, M. B. Mingorance, M. B. Matallo, A. Peña, and F. Sánchez-Rasero. 1998. Photodegradation of mecoprop and dichlorprop on dry, moist and amended soil surfaces exposed to sunlight. Chemosphere 37:577-589.

117. Romero, E., M. B. Matallo, A. Pena, F. Sánchez-Rasero, P. Schmitt-Kopplin, and G. Dios. 2001. Dissipation of racemic mecoprop and dichlorprop and their pure R-enantiomers in three calcareous soils with and without peat addition. Environ. Pollut. 111:209-215.

118. Rügge, K., R. K. Juhler, M. M. Broholm, and P. L. Bjerg. 2002. Degradation of the (*R*)- and (*S*)-enantiomers of the herbicides MCPP and dichlorprop in a continuous field-injection experiment. Water Res. 36:4160-4164.

COR-AAD1-00003453
Bayer EX1008 (Part 7 of 9)

119. Saari, R. E., D. A. Hogan, and R. P. Hausinger. 1999. Stereospecific degradation of the phenoxypropionate herbicide dichlorprop. J. Mol. Catal. B: Enzymatic 6:421-428.

120. Scheidleder, A., J. Grath, G. Winkler, U. Stärk, C. Koreimann, C. Gmeiner, S. Nixon, J. Casillas, P. Gravesen, J. Leonard, and M. Elvira. 1999. Groundwater quality and quantity in Europe. European Environment Agency.

121. Schulz, S., W. Dong, U. Groth, and A. M. Cook. 2000. Enantiomeric degradation of 2-(4-sulfophenyl)butyrate via 4-sulfocatechol in *Delftia acidovorans* SPB1. Appl. Environ. Microbiol. 66:1905-1910.

122. Sharp, D. S. 1988. Alachlor, p. 335-382. *In* P. C. Kearney and D. D. Kaufman (ed.), Herbicides. Chemistry, degradation and mode of action, vol. 3. Marcel Dekker Inc., New York.

123. Sheldon, R. A. 1993. Chirotechnology: Industrial synthesis of optically active compounds. Marcel Dekker.

124. Simoni, S., S. Klinke, C. Zipper, W. Angst, and H.-P. E. Kohler. 1996. Enantioselective metabolism of chiral 3-phenylbutyric acid, an intermediate of linear alkylbenzene degradation, by *Rhodococcus rhodochrous* PB1. Appl. Environ. Microbiol. 62:749-755.

125. Smejkal, C. W., T. Vallaeys, F. A. Seymour, S. K. Burton, and H. M. Lappin-Scott. 2001. Characterization of (*R/S*)-mecoprop [2-(2-methyl-4-chlorophenoxy) propionic acid]-degrading *Alcaligenes* sp.CS1 and *Ralstonia* sp. CS2 isolated from agricultural soils. Environ. Microbiol. 3:288-293.

126. Smith, A. E., and B. J. Hayden. 1981. Relative persistence of MCPA, MCPB and mecoprop in Saskatchewan soils, and the identification of MCPA in MCPB-treated soils. Weed Research 21:179-183.

127. Smith, J. M., K. Harrison, and J. Colby. 1990. Purification and characterization of D-2-haloacid dehalogenase from *Pseudomonas putida* strain AJ1/23. J Gen Microbiol 136 (Pt 5):881-886.

128. Soda, K., T. Kurihara, J.-Q. Liu, V. Nardi-Dei, C. Park, M. Miyagi, S. Tsunasawa, and N. Esaki. 1996. Bacterial 2-haloacid dehalogenases: Structures and catalytic properties. Pure and Appl. Chem. 68:2097-2103.

129. Stoll, V. S., M. S. Kimber, and E. F. Pai. 1996. Insights into substrate binding by D-2-ketoacid dehydrogenases from the structure of *Lactobacillus pentosus* D-lactate dehydrogenase. Structure 4:437-447.

130. Streber, W. R., K. N. Timmis, and M. H. Zenk. 1987. Analysis, cloning, and high-level expression of 2,4-dichlorophenoxyacetate monooxygenase gene *tfdA* of *Alcaligenes eutrophus* JMP134. J. Bacteriol. 169:2950-2955.

131. Sugio, S., G. A. Petsko, J. M. Manning, K. Soda, and D. Ringe. 1995. Crystal structure of a D-amino acid aminotransferase: how the protein controls stereoselectivity. Biochemistry 34:9661-9669.

132. Swisher, R. D. 1987. Surfactant Biodegradation, vol. 18. Marcel Dekker, New York.

133. Tett, V. A., A. J. Willets, and H. M. Lappin-Scott. 1994. Enantioselective degradation of the herbicide mecoprop [2-(2-methyl-4-chlorophenoxy)propionic acid] by mixed and pure bacterial cultures. FEMS Microbiol. Ecol. 14:191-200.

COR-AAD1-00003454
Bayer EX1008 (Part 7 of 9)

134. Tett, V. A., A. J. Willetts, and H. M. Lappin-Scott. 1997. Biodegradation of the chlorophenoxy herbicide (*R*)-(+)-mecoprop by *Alcaligenes denitrificans*. Biodegradation 8:43-52.

135. Trantírek, L., K. Hynková, Y. Nagata, A. Murzin, A. Ansorgová, V. Sklenar, and J. Damborsky. 2001. Reaction mechanism and stereochemistry of γ-hexachlorocyclohexane dehydrochlorinase LinA. J. Biol. Chem. 276:7734-7740.

136. Vallaeys, T., R. R. Fulthorpe, A. M. Wright, and G. Soulas. 1996. The metabolic pathway of 2,4-dichlorophenoxyacetic acid degradation involves different families of *tfdA* and *tfdB* genes according to PCR-RFLP analysis. FEMS Microbiol. Ecol. 20:163-172.

137. Westendorf, A., D. Benndorf, R. H. Müller, and W. Babel. 2002. The two enantiospecific dichlorprop/α-ketoglutarate-dioxygenases from *Delftia acidovorans* MC1 - protein and sequence data of RdpA and SdpA. Microbiol. Res. 157:1-6.

138. Westendorf, A., R. H. Müller, and W. Babel. 2003. Purification and characterisation of the enantiospecific dioxygenases from *Delftia acidovorans* MC1 initiating the degradation of phenoxypropionate and phenoxyacetate herbicides. Acta Biotechnol. 23:3-17.

139. White, G. F., and N. J. Russell. 1994. Biodegradation of anionic surfactants and related molecules, p. 143-177. *In* C. Ratledge (ed.), Biochemistry of microbial degradation. Kluwer Academic Publishers, Dordrecht.

140. Whitman, C. P., G. D. Hegeman, W. W. Cleland, and G. L. Kenyon. 1985. Symmetry and asymmetry in mandelate racemase catalysis. Biochemistry 24:3936-3942.

141. Wiberg, K., E. Brorström-Lundén, I. Wängberg, T. F. Bidleman, and P. Haglund. 2001. Concentrations and fluxes of hexachlorocyclohexanes and chiral composition of α-HCH in environmental samples from the Southern Baltic Sea. Environ. Sci. Technol. 35:4739-4746.

142. Wiberg, K., R. J. Letcher, C. D. Sandau, R. J. Norstrom, M. Tysklind, and T. F. Bidleman. 2000. The enantioselective bioaccumulation of chiral chlordane and α-HCH contaminants in the polar bear food chain. Environ. Sci. Technol. 34:2668-2674.

143. Williams, A. 1996. Opportunities for chiral agrochemicals. Pest. Sci. 46:3-9.

144. Williams, G. M., I. Harrison, C. A. Carlick, and O. Crowley. 2003. Changes in enantiomeric fraction as evidence of natural attenuation of mecoprop in a limestone aquifer. J. Contam. Hydrol. 64:253-267.

145. Worthing, C. R., and R. J. Hance. 1991. The Pesticide Manual - A World Compendium, 9th ed. The British Crop Council, Farnham, Great Britain.

146. Zipper, C., C. Bolliger, T. Fleischmann, M. J.-F. Suter, W. Angst, M. D. Müller, and H.-P. E. Kohler. 1999. Fate of the herbicides mecoprop, dichlorprop, and 2,4-D in aerobic and anaerobic sewage sludge as determined by laboratory batch studies and enantiomer-specific analysis. Biodegradation 10:271-278.

147. Zipper, C., M. Bunk, A. J. B. Zehnder, and H.-P. E. Kohler. 1998. Enantioselective uptake and degradation of the chiral herbicide dichlorprop [(*RS*)-2-(2,4-dichlorophenoxy)propanoic acid] by *Sphingomonas herbicidovorans* MH. J. Bacteriol. 180:3368-3374.

COR-AAD1-00003455
Bayer EX1008 (Part 7 of 9)

148. Zipper, C., K. Nickel, W. Angst, and H.-P. E. Kohler. 1996. Complete microbial degradation of both enantiomers of the chiral herbicide mecoprop [(*RS*)-2-(4-chloro-2-methylphenoxy)propionic acid] in an enantioselective manner by *Sphingomonas herbicidovorans* sp. nov. Appl. Environ. Microbiol. 62:4318-4322.

149. Zipper, C., M. J.-F. Suter, S. B. Haderlein, M. Gruhl, and H.-P. E. Kohler. 1998. Changes in the enantiomeric ratio of (*R*)- to (*S*)-mecoprop indicate in situ biodegradation of this chiral herbicide in a polluted aquifer. Environ. Sci. Technol. 32:2070-2076.

COR-AAD1-00003456
Bayer EX1008 (Part 7 of 9)

General Introduction:

α-Ketoglutarate-Dependent Dioxygenases

α-Ketoglutarate-dependent dioxygenases are a large group of non-heme iron enzymes and have been identified in many organisms ranging from prokaryotes, eukaryotes and even viruses. They catalyze a wide range of oxidative processes such as hydroxylations, epoxidations, desaturations, ring formation, and expansion reactions. These enzymes are involved in the biosynthesis of a variety of important molecules such as antibiotics, plant hormones, carnitine and collagen (4, 14, 24, 34, 43, 53). α-Ketoglutarate-dependent dioxygenases do not show high sequence similarity, but are grouped according to their biochemical features. Besides the prime substrate and oxygen, they require α-ketoglutarate as a cosubstrate, iron(II) as a cofactor and ascorbate as a reducing agent. In the course of the reaction, one oxygen atom is incorporated into the prime substrate and the other one ends up in succinate. Despite their sequence diversity, α-ketoglutarate dependent dioxygenases have in common a 2-His-1-carboxylate motif, which is involved in iron binding (15). This motif is part of a rather conserved region, which has been used to classify the members in three subgroups. Subgroup I members share the motif $HXDX_{50-70}HX_{10}(R/K)XS$, subgroup II members share the motif $HX(D/E)X_{138-207}HX_{10-13}R$ and subgroup III members share the motif $HXDX_{72-101}HX_{10}(R/K)XS$ (18).

Here, I would like to give details on the functioning of a few α-ketoglutarate-dependent dioxygenases, which is indicative of the diversity of the reactions they catalyze, and of biosynthetic pathways they are involved in. In addition, table 1 lists the most important α-ketoglutarate-dependent dioxygenases and Fig. 1 depicts reactions catalyzed by α-ketoglutarate-dependent dioxygenases.

COR-AAD1-00003458
Bayer EX1008 (Part 7 of 9)

Table 1: Overview of representative α-ketoglutarate-dependent dioxygenases

Dioxygenase[a]	Organism	Structure	Involved in	Reaction (Fig. 1)	Reaction type	Crystal structure	Ref.
Prolyl-4-hydroxylase	Mammals, plants, insects, nematodes, virus-1	tetramer ($\alpha_2\beta_2$) dimer monomer	collagen and elastin biosynthesis	1	hydroxylation		(21, 29)
Lysyl-hydroxylase	Humans	dimer	collagen biosynthesis		hydroxylation		(22)
IPNS	*Cephalosporium acremonium*, *Penicillium chrysogenum*	tetramer	penicillin biosynthesis	2	cyclization		(50, 52)
DAOCS/DACS	*Cephalosporium acremonium*, *Streptomyces clavuligerus*[b]	monomer	cephalosporin biosynthesis	3	expansion hydroxylation	yes	(1, 61)
CAS	*Streptomyces clavuligerus*	monomer	clavulanic acid biosynthesis	4	hydroxylation cyclization desaturation	yes	(19, 26)
AlkB	*Escherichia coli*, homologs in human	monomer	DNA and RNA repair	5	demethylation		(60)
γ-Butyrobetaine hydroxylase	*Pseudomonas* sp. AK1, calf liver, humans	heterodimer	L-carnitine biosynthesis (Lipid metabolism)	6	hydroxylation		(25)
ANS	Plants	monomer	anthocyanin biosynthesis	7	desaturation	yes	(56, 66)
TauD	*E. coli*	dimer	use of taurine as alternative sulfur source	8	hydroxylation	yes	(7, 9, 32)
YLL057c	*Saccharomyces cerevisiae*	monomer	use of alternative sulfur sources		hydroxylation		(17)

COR-AAD1-00003459
Bayer EX1008 (Part 7 of 9)

Table 1 (cont.): Overview of representative α-ketoglutarate-dependent dioxygenases

Dioxygenase[a]	Organism	Structure	Involved in	Reaction (Fig. 1)	Reaction type	Crystal structure	Ref.
AtsK	*Pseudomonas putida* S-313	tetramer	use of alternative sulfur sources	9	hydroxylation		(20, 28)
TfdA	*Ralstonia eutropha* JMP134(pJP4)	dimer	2,4-D degradation	10	hydroxylation	model	(11, 12, 18)
RdpA	*Delftia acidovorans* MC1	trimer	(*R*)-dichlorprop degradation	11	hydroxylation		(62, 63)
SdpA	*Delftia acidovorans* MC1	monomer	(*S*)-dichlorprop degradation	12	hydroxylation		(62, 63)
HtxA	*Pseudomonas stutzeri* WM88	dimer	use of hypophosphite as P-source	13	hydroxylation		(64)

[a] See text for explanation of abbreviations.

[b] In *C. acremonium*, one enzyme (DAOC/DACS) catalyzes the two subsequent reactions (from penicillin N to deacetoxycephalosporin and then to deacetylcephalosporin C), in *S. clavuligerus*, , two related enzymes exist (DAOCS and DACS) of which each catalyzes one reaction.

COR-AAD1-00003460
Bayer EX1008 (Part 7 of 9)

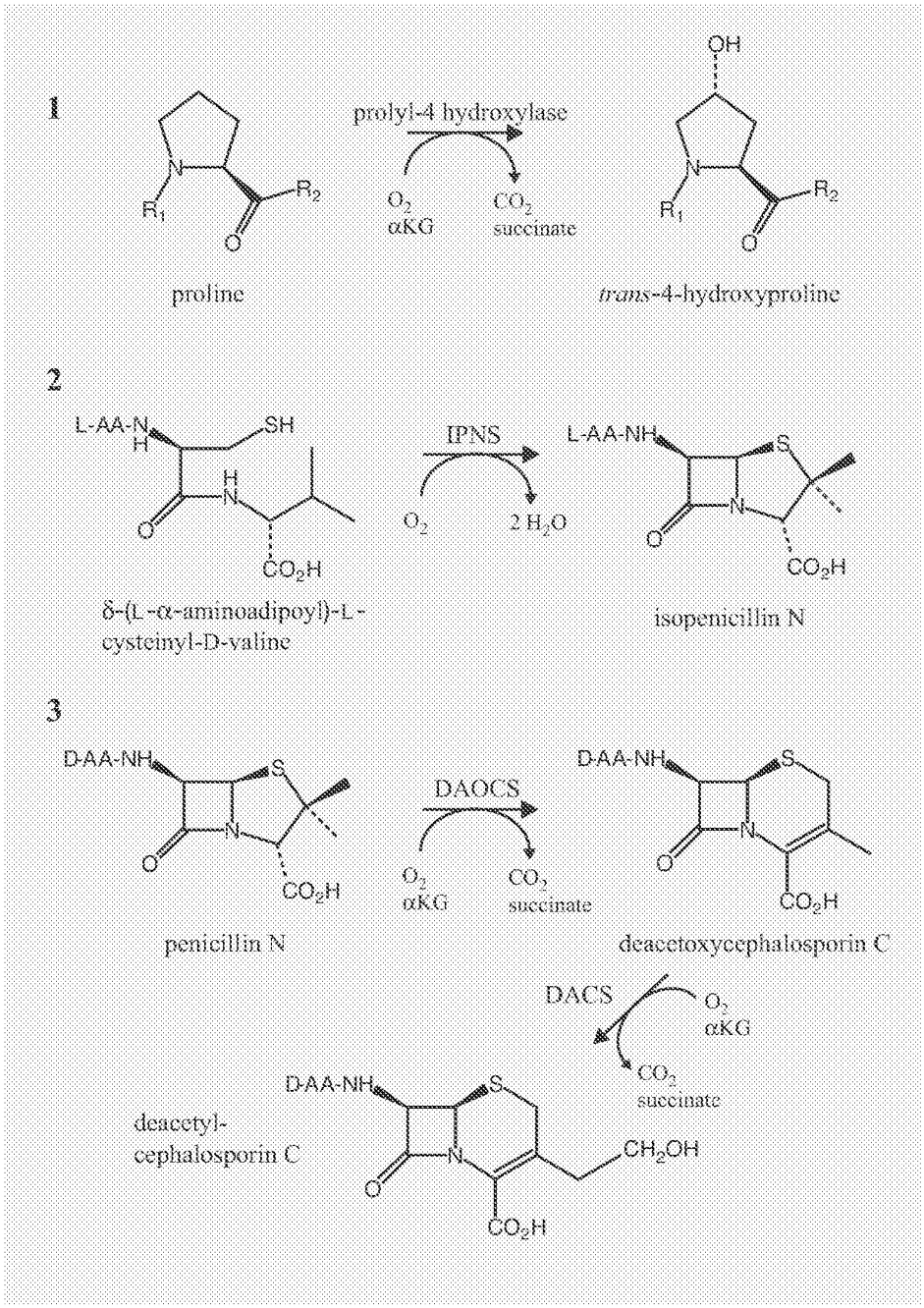


Fig. 1. Reactions catalyzed by α-ketoglutarate-dependent dioxygenases. 1 prolyl 4-hydroxylase. 2 isopenicillin N synthase. 3 Deacetoxycephalosporin C synthase and Deacetylcephalosporin C synthase.

COR-AAD1-00003461
Bayer EX1008 (Part 7 of 9)

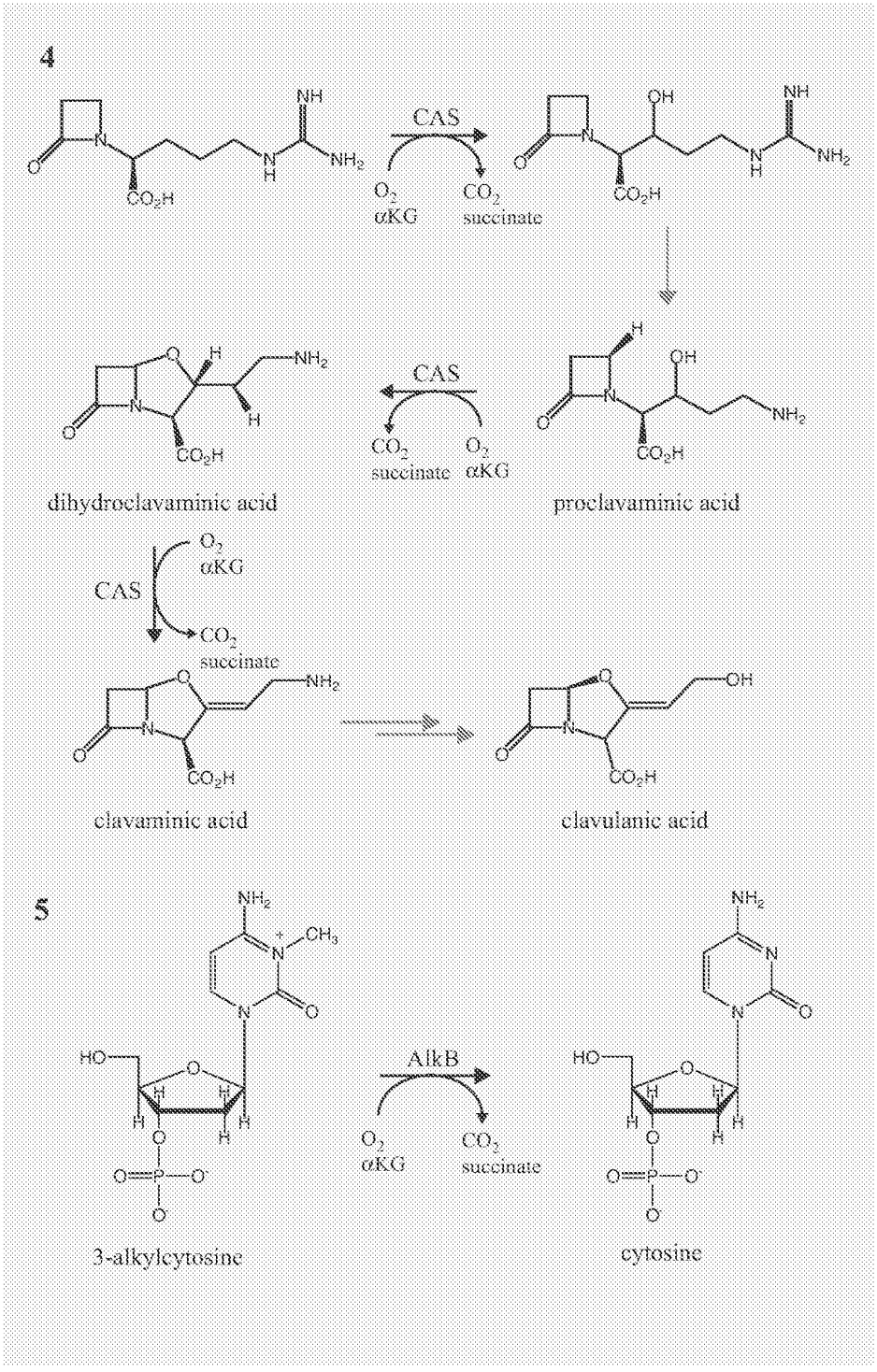


Fig. 1 (cont.) 4 Clavaminate synthase. 5 AlkB.

COR-AAD1-00003462
Bayer EX1008 (Part 7 of 9)

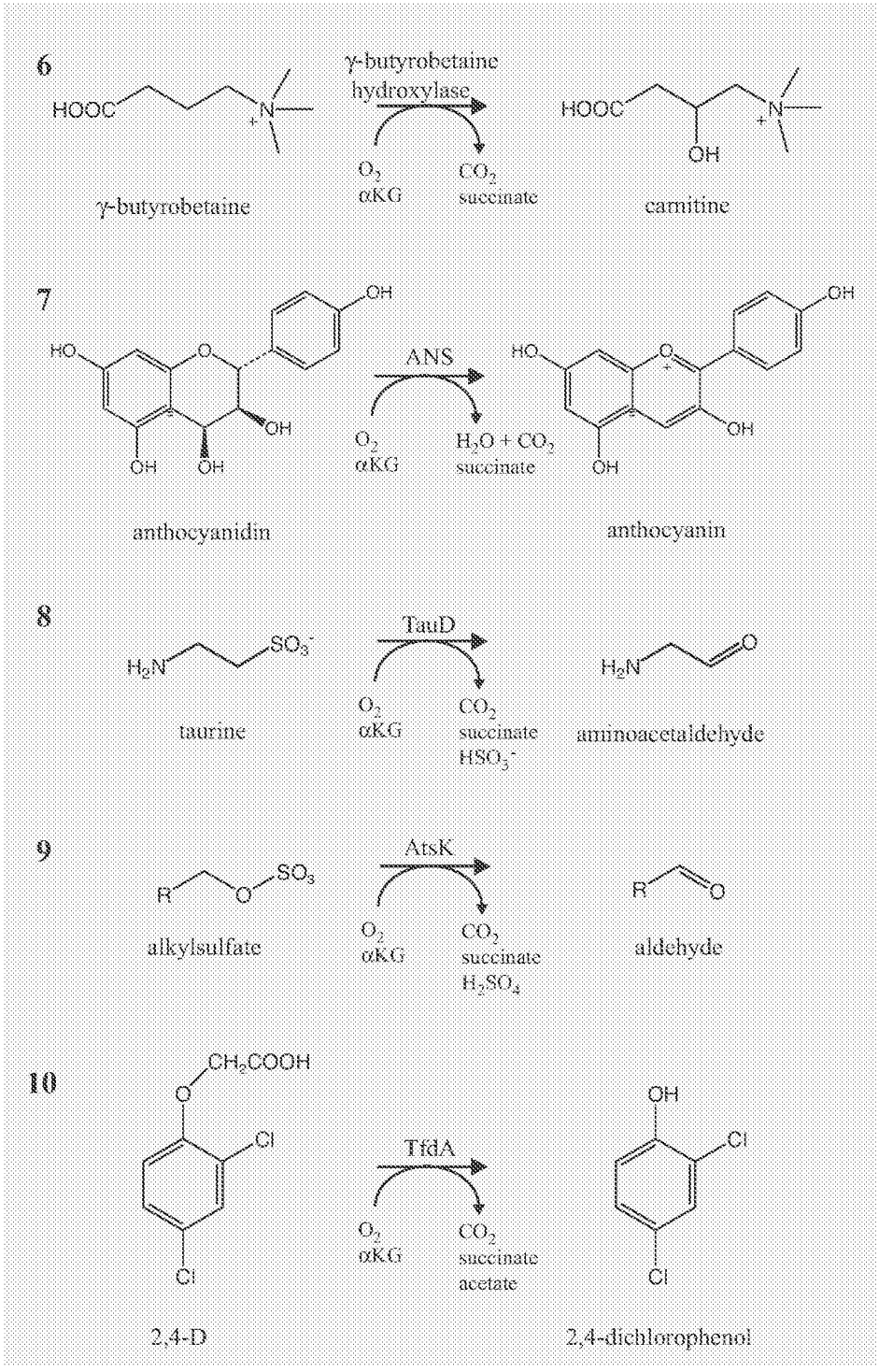


Fig. 1 (cont.) 6 γ-butyrobetaine hydroxylase. 7 anthocyanidin synthase. 8 taurine dioxygenase. 9 alkylsulfonate dioxygenase. 10 2,4-D dioxygenase.

COR-AAD1-00003463
Bayer EX1008 (Part 7 of 9)

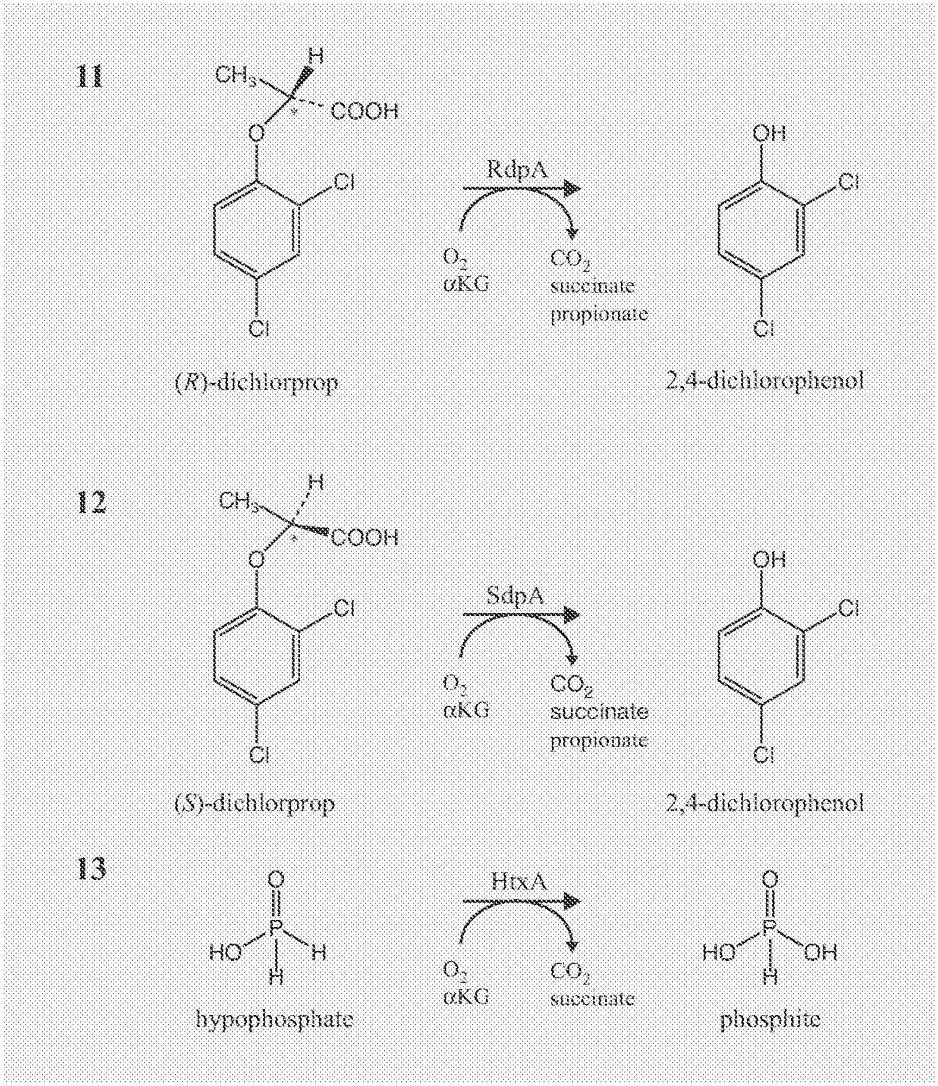


Fig. 1 (cont.) 11 *(R)*-dichlorprop dioxygenase. 12 *(S)*-dichlorprop dioxygenase 13 hypophosphite dioxygenase.

Representative α-ketoglutarate-dependent dioxygenases

Prolyl-4-hydroxylase represents α-ketoglutarate-dependent dioxygenases that are involved in protein modification. It catalyzes the post-translational hydroxylation of proline residues to *trans*-4-hydroxyprolyl in many organisms such as humans, chickens and nematodes (Fig. 1.1) (see reviews 21, 37). In mammals, hydroxylated prolines are essential for the formation of the triple helix

COR-AAD1-00003464
Bayer EX1008 (Part 7 of 9)

structure of collagen and elastin, because they stabilize the structure by forming inter- and intrachain hydrogen bonds (29).

Deacetoxycephalosporin C synthase (DAOCS), deacetylcephalosporin C synthase (DACS), isopenicillin N synthase (IPNS) and clavaminate synthase (CAS) are well known α-ketoglutarate-dependent dioxygenases involved in antibiotic formation. DAOCS and DACS from *Streptomyces clavuligerus* catalyze sequential reactions in the biosynthesis of the antibiotic cephalosporin. DAOCS carries out the ring expansion of penicillin N to deacetoxycephalosporin C whereas DACS hydroxylates deacetoxycephalosporin C to deacetylcephalosporin C (Fig. 1.3) (2). IPNS catalyzes the formation of isopenicillin N from δ-(L-α-aminoadipoyl)-L-cysteinyl-D-valine in cephalosporin biosynthesis (Fig. 1.3). IPNS was the first well characterized α-ketoglutarate-dependent dioxygenase and possesses the conserved motif common to the subgroup I dioxygenases. However, the primary amino acid sequence is only distantly related to this enzyme family, and IPNS does not require α-ketoglutarate as cosubstrate (50, for reviews, see 51, 52, 54). Nevertheless, this enzyme is particularly interesting, because extensive crystallographic data and data of other studies about binding of cofactors and cosubstrates are available. Since IPNS carries a similar native enzyme fold as other α-ketoglutarate-dependent dioxygenases, it serves as an important model for understanding the enzymatic mechanism of this family (23, 27, 40, 41, 52, 58, 59). CAS represents the diversity of α-ketoglutarate-dependent dioxygenases 'par excellence'. It catalyzes three reactions, a hydroxylation, an oxidative cyclization and a desaturation all involved in the biosynthesis of the β-lactamase inhibitor clavulanic acid (Fig. 1.4) (10, 49).

The α-ketoglutarate-dependent dioxygenase AlkB from *E. coli* is involved in DNA and RNA repair. AlkB couples the oxidative decarboxylation of α-ketoglutarate to the hydroxylation of 1-methyladenine and 3-methylcytosine resulting in the release of formaldehyde and the unmodified base (Fig. 1.5) (60).

α-Ketoglutarate-dependent dioxygenases also occur in plants and participate in many biosynthetic pathways such as those for flavonoids, gibbellerins and alkaloids (for a review, see 14). One example is anthocyanidin synthase (ANS)

COR-AAD1-00003465
Bayer EX1008 (Part 7 of 9)

which catalyzes the desaturation of anthocyanidin to anthocyanin in the flavonoid pathway (Fig. 1.7) (56).

Taurine dioxygenase (TauD) oxidizes taurine to sulfite and aminoacetaldehyde in *E. coli* (Fig. 1.8) (7). Another subgroup of α-ketoglutarate-dependent dioxygenases are the phenoxyalkanoic acid herbicide converting enzymes 2,4-D dioxygenase (TfdA), *(R)*-dichlorprop dioxygenase (RdpA) and *(S)*-dichlorprop dioxygenase (SdpA; 11, 12, 33, 48, 57, 62, 63). They catalyze the first step in the degradation of herbicides such as 2,4-D, mecoprop and dichlorprop by oxidative cleavage of the ether-bond of the phenoxyalkanoic acid, a reaction that yields the respective phenol as a product (Fig. 1.10-1.12). Just recently, the first α-ketoglutarate-dependent dioxygenase that acts on an inorganic substrate was isolated. Hypophosphite dioxygenase (HtxA) from *Pseudomonas stutzerii* WM88 converts hypophosphite to hypophosphate, which then can be further metabolized. The reaction enables the bacterium to use hypophosphite as inorganic phosphorus source (Fig. 1.13) (64).

In the past few years, enzyme mechanisms and possible intermediates of α-ketoglutarate-dependent dioxygenases catalyzed reactions were intensively investigated. The crystal structures of IPNS, DAOCS, CAS, TfdA, TauD and AlkB and subsequent biochemical studies revealed how the different substrates, iron(II) and dioxygen are positioned at the active sites (6, 8, 9, 16, 18, 26, 32, 40, 41, 60, 61, 67, 68). Despite their low sequence identity, α-ketoglutarate-dependent dioxygenases possess several common structural and mechanistic characteristics. Results from transient kinetic studies coupled with the structural data have led to a proposal for a common reaction mechanism (4, 35, 36, 38, 42, 46, 53, 55).

Here, I want to focus on subgroup II α-ketoglutarate-dependent dioxygenases and will therefore discuss the enzyme mechanism of TauD and TfdA in more details. Additionally, I want to shortly introduce the phenoxypropanoic acid converting enzymes RdpA and SdpA.

COR-AAD1-00003466
Bayer EX1008 (Part 7 of 9)

α-Ketoglutarate-dependent taurine dioxygenase (TauD)

TauD converts taurine to sulfite and aminoacetaldehyde while decomposing α-ketoglutarate to succinate and CO_2 and enables its host to use taurine as a sulfur source (7). TauD is 30% similar to TfdA and 38% to AtsK, the alkylsulfatase from *Pseudomonas putida* (11, 12, 20). TauD has a relative relaxed substrate specificity with respect to the sulfonic acid but shows stricter specificities for the cosubstrate α-ketoglutarate. This can only be replaced by α-ketoadipate but with a loss up to 4-10% of the original activity (7). Titration studies demonstrated that each TauD subunit binds one ferrous iron molecule, one α-ketoglutarate, and one taurine (46).

The X-ray crystal structure of TauD complexed to Fe(II), α-ketoglutarate and taurine has been solved (9, 32). The native fold of TauD resembles the one of other α-ketoglutarate dependent dioxygenases such as IPNS and is most similar to the one of CAS (40, 61, 68). The jellyroll motif found in all native structures of α-ketoglutarate-dependent dioxygenases so far is formed by the β-strands β5-8 and β14-17. The Fe(II) binding residues were determined to be His-99, Asp-101 and His-255. α-Ketoglutarate is bound to Fe(II) in a bidentate manner through the C1 carboxylate and the C2 oxo-group, whereas the C5 carboxylate forms a salt bridge to Arg-266 and a hydrogen bond with Thr-126 (Fig. 2). The substrate binding residues for the taurine amine group are likely to be Tyr-73, Asn-95, and Ser-158. They form hydrogen bonds with the amine moiety and thereby build a distorted tetrahedral environment. The sulfonate ion interacts with Arg-270, His-70 and the backbone of Val-102. These hydrogen-bonds allow TauD to select for a tetrahedral substrate anion, which is consistent with the finding that His-70 is conserved in alkylsulfonate and alkylsulfate α-ketoglutarate-dependent dioxygenases such as AtsK.

COR-AAD1-00003467
Bayer EX1008 (Part 7 of 9)

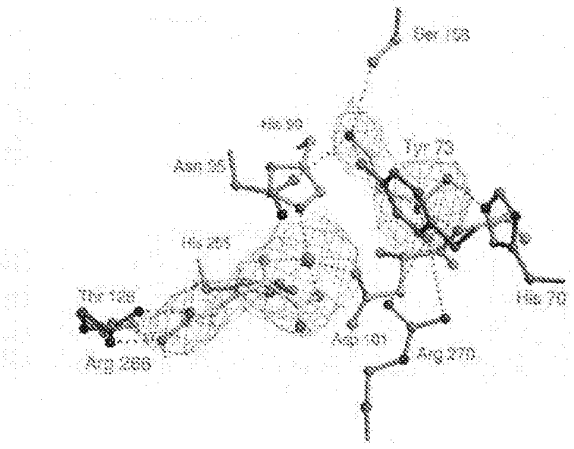


Fig. 2. The active site of TauD according to Elkins *et al.* (9). Shown are the protein ligands, the two substrates (taurine and α-ketoglutarate) and other important protein side chains.

Based on crystallization and spectroscopic studies, an enzyme mechanism for TauD was proposed (9, 32, 35, 36, 46), which significantly contributed to further understanding of the common enzyme mechanism for this class of enzymes (Fig. 3). It was proposed that in the resting enzyme, a sixcoordinate iron is in the centre of the active site and three iron ligands are occupied by water molecules. α-Ketoglutarate binds to Fe(II) in a bidentate manner displacing two water molecules, which restores the sixcoordinate metal center. In general, an ordered binding mechanism was suggested for α-ketoglutarate-dependent dioxygenases, in which the α-ketoglutarate binds prior to either substrate or dioxygen. In taurine dioxygenase, taurine binds prior to oxygen in contrast to other α-ketoglutarate dependent dioxygenases such as prolyl-hydroxylase in which the binding order is reversed (22). The binding of taurine leads to a conformational change from six-coordinate to pentacoordinate Fe(II) by loss of the third water molecule. This conformational change was confirmed by crystallization experiments with apo and holoforms of TauD (32). O_2 then binds opposite of His-255 restoring a sixcoordinate iron again. The oxygen-binding results in the formation of a species with iron(III) superoxide radical anion character. It has further been postulated that the attack of O_2 at the carboxylate moiety of α-ketoglutarate leads to an iron(IV)

COR-AAD1-00003468
Bayer EX1008 (Part 7 of 9)

peroxo species and then an iron(II) peracid product which in turn is transformed by heterolytic cleavage of the O–O bond to an iron(IV)–oxo species. Substrate hydroxylation is supposed to occur in a two step-process involving hydrogen atom abstraction followed by binding of the oxygen at the C1 of taurine. Unfortunately, no experimental evidence was found for any of these intermediates, but an analogous non-heme iron complex that consisted of Fe(IV) and a nonheme macrocyclic ligand has been characterized spectroscopically. This crystal structure revealed that an iron(IV)-oxo species can exist in a nonporphyrin ligand environment (42). Just recently, Price *et al.* (36) characterized a high-spin Fe(IV) complex in TauD. They propose intermediates, which exhibit resonance hybrid characteristics between Fe(III) and Fe(IV). One of these intermediates is the above mentioned ferryl-oxo species, another a peroxyhemiketal complex. However, none of these structures has been known among other inorganic and protein complexes.

α-Ketoglutarate-dependent dioxygenases are inactivated in the absence of a reducing agent because uncoupling of oxidative α-ketoglutarate decomposition from substrate oxidation leads to the oxidation of iron(II) to iron(III) at the active site (30, 31, 39). In the presence of a reducing agent such as ascorbate, this inactivation is reversible. TauD is also inactivated by oxygen in the absence of taurine in a process called self-hydroxylation. Self-hydroxylation leads to a transient tyrosyl radical (Tyr-73), that undergoes hydroxylation to a catechol (44, 45). This modification causes an irreversible inactivation of TauD.

COR-AAD1-00003469
Bayer EX1008 (Part 7 of 9)

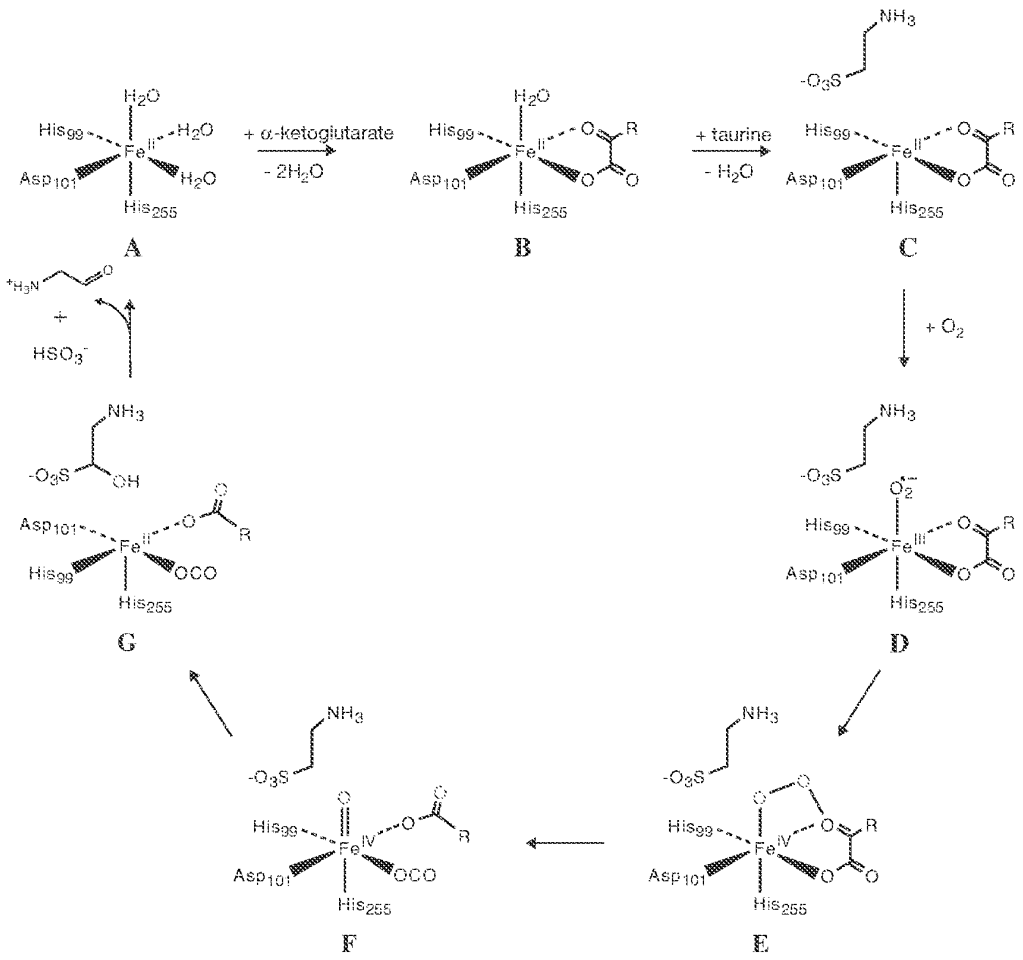


Fig. 3. Proposed reaction mechanism of TauD (9, 14, 32, 35, 36, 46). A. Resting TauD, in which all three ligand places are occupied by water molecules. B. Binary complex with α-ketoglutarate bound in a bidentate manner (complex absorbs at 530 nm). C. Ternary complex upon binding of taurine, i.e. conformational change to an unsaturated Fe(II) center. The complex absorbs at 520 nm. D. Species with iron(III) superoxide radical anion character E. Iron(IV) peroxo species. F. Fe(IV)oxospecies. G. Iron(II) peracid species.

α-Ketoglutarate-dependent 2,4-D dioxygenase (TfdA)

TfdA, the α-ketoglutarate-dependent 2,4-D dioxygenase from *Ralstonia eutropha* JMP134(pJP4) converts 2,4-D and several other phenoxyalkanoic acid to the corresponding phenol and the ketoalkanoic acid (11-13). TfdA exhibits best catalytic efficiency with 2,4-D, but also converts other substituted phenoxyacetic acids, *(S)*-dichlorprop and cinnamic acids (5, 11-13). Ferrous iron at the active site cannot be replaced by another divalent cation such as Co(II), Cu(II), Li(II), Mg(II),

COR-AAD1-00003470
Bayer EX1008 (Part 7 of 9)

Mn(II), Ni(II) and Zn(II); whereas the cosubstrate specificity is more relaxed since α-ketoadipate and pyruvate can substitute α-ketoglutarate, although with the result of a much lower enzymatic rate.

Inactivation as for other α-ketoglutarate-dependent dioxygenases is also observed for TfdA. TfdA is rapidly inactivated in the absence of 2,4-D (5, 47). A charge-transfer to oxygen leads to a Fe(III) in the active center, which can be reactivated by ascorbate. The iron-oxidation of TfdA is not due to uncoupling of α-ketoglutarate decarboxylation and substrate hydroxylation as it is for other α-ketoglutarate dependent dioxygenases (30, 31, 39). The generation of an inactive TfdA species that could not be reversed by ascorbate was observed in the presence of poor substrates such as thiophenoxyacetic acid. This inactivated TfdA arose from an oxidative reaction which is likely to involve hydroxyl radical reactions (47).

The TfdA structure has not been resolved by crystallography, but has been modeled by using the crystal structure of TauD (9). The modeling suggested that the overall fold of the two enzymes must be very similar. The metal ligands are, consistent with spectroscopic and mutagenesis studies (18), His-114, Asp-116 and His-263, whereas Arg-274 forms a salt bridge with C5 of α-ketoglutarate. In contrast to the proposed structural model, the involvement of Thr-141 in a hydrogen bond with the C5 of α-ketoglutarate could not be confirmed by mutagenesis (6). Arg-278, Lys-71, His-214 and the backbone amide of Ser-117 interact with the carobxy group of 2,4-D and Lys-95 was shown to interact with the ether oxygen of 2,4-D. It was further hypothesized that Arg-78 acts as a gate for 2,4-D entry into the active site and that His-213 and His-216 facilitate 2,4-D binding. Since these residues are not conserved among α-ketoglutarate dependent dioxygenases, this reflects differences in the substrate binding sites (18).

In addition to modeling the structure, several studies were directed to obtain more information about the metal-ligand residues. X-ray absorption and electron paramagnetic resonance/electron spin-echo envelop modulation studies with Cu(II)-TfdA suggested that two equatorially oriented histidines interact with the copper and that one histidine is replaced or reoriented upon binding of 2,4-D,

COR-AAD1-00003471
Bayer EX1008 (Part 7 of 9)

α-ketoglutarate and O_2 (3, 65). However, Cu(II)-TfdA does not seem to be identical to Fe(II)-TfdA since α-ketoglutarate is bound in a monodentate manner to the copper center, but in a bidentate manner to the ferrous iron. A significant change in the metal environment upon formation of the Cu(II)- and Fe(II)-NO-TfdA-α-ketoglutarate-2,4-D complex suggested first a reorientation of the active site, i.e., the loss of a His-ligand. This model was not consistent with findings of other α-ketoglutarate-dependent dioxygenases and therefore, the metal environment change may more likely be explained by the following model: α-ketoglutarate binds in a bidentate manner and 2,4-D is located in a pocket near the Fe(II). The 2-His-1-Asp facial triad is maintained upon binding of 2,4-D, but a water molecule is lost. Thereby, the metal environment changes from a six- to a five-coordination, which agrees with the results obtained with TauD.

α-Ketoglutarate-dependent (*R*)- and (*S*)-dichlorprop dioxygenase (RdpA and SdpA) from *Delftia acidovorans* MC1

Two dichlorprop dioxygenase genes *rdpA* and *sdpA* have been isolated from the dichlorprop degrading microorganism *D. acidovorans* MC1 (62). Sequence information showed that RdpA and SdpA must belong to the α-ketoglutarate-dependent dioxygenases. They catalyze the enantioselective conversion of *(R)*- and *(S)*-dichlorprop to the achiral phenol. RdpA and SdpA are strictly specific for the respective enantiomer, but SdpA also converts 2,4-D. Other ketoacids do not support enzymatic activity. Both enzymes were also strictly dependent on ferrous iron and other divalent cations showed an inhibitory effect (63). No further investigations concerning amino acids involved in catalysis have been carried out so far.

COR-AAD1-00003472
Bayer EX1008 (Part 7 of 9)

REFERENCES:

1. Baldwin, J. E., R. M. Adlington, M. J. Crabbe, G. Knight, T. Nomoto, C. J. Schofield, and H.-H. Ting. 1987. The enzymatic ring expansion of penicillins to cephalosporins: side chain specificity. Tetrahedron 43:3009-3014.
2. Baldwin, J. E., R. M. Adlington, N. P. Crouch, C. J. Schofield, N. J. Turner, and R. T. Aplin. 1991. Cephalosporin biosynthesis: a branched pathway sensitive to an isotope effect. Tetrahedron 47:9881-9900.
3. Cosper, N. J., C. M. V. Stalhandske, R. E. Saari, R. P. Hausinger, and R. A. Scott. 1999. X-ray absorption spectroscopic analysis of Fe(II) and Cu(II) forms of a herbicide-degrading α-ketoglutarate dioxygenase. J. Biol. Inorg. Chem. 4:122-129.
4. Costas, M., M. P. Mehn, M. P. Jensen, and L. Que, Jr. 2004. Dioxygen activation at mononuclear nonheme iron active sites: enzymes, models, and intermediates. Chem. Rev. 104:939-986.
5. Dunning Hotopp, J. C., and R. P. Hausinger. 2001. Alternative substrates of 2,4-dichlorophenoxyacetate/α-ketoglutarate dioxygenase. J. Mol. Catal. B: Enzymatic 15:155-162.
6. Dunning Hotopp, J. C., and R. P. Hausinger. 2002. Probing the 2,4-dichlorophenoxyacetate/α-ketoglutarate dioxygenase substrate-binding site by site-directed mutagenesis and mechanism-based inactivation. Biochemistry 41:9787-9794.
7. Eichhorn, E., J. R. van der Ploeg, M. A. Kertesz, and T. Leisinger. 1997. Characterization of α-ketoglutarate-dependent taurine dioxygenase from *Escherichia coli*. J. Biol. Chem. 272:23031-23036.
8. Elkins, J. M., P. J. Rutledge, N. I. Burzlaff, I. J. Clifton, R. M. Adlington, P. L. Roach, and J. E. Baldwin. 2003. Crystallographic studies on the reaction of isopenicillin N synthase with an unsaturated substrate analogue. Org. Biomol. Chem. 1:1455-1460.
9. Elkins, J. M., M. J. Ryle, I. J. Clifton, J. C. Dunning Hotopp, J. S. Lloyd, N. I. Burzlaff, J. E. Baldwin, R. P. Hausinger, and P. L. Roach. 2002. X-ray crystal structure of *Escherichia coli* taurine/α-ketoglutarate dioxygenase complexed to ferrous iron and substrates. Biochemistry 41:5185-5192.
10. Elson, S. W., K. H. Baggaley, J. Gillett, S. Holland, N. H. Nicholson, J. T. Sime, and S. R. Woroniecki. 1987. Isolation of two novel intracellular β-lactams and a novel dioxygenase cyclising enzyme from *Streptomyces clavuligerus*. J. Chem. Soc., Chem. Comm. 22:1736-1738.
11. Fukumori, F., and R. P. Hausinger. 1993. *Alcaligenes eutrophus* JMP134 "2,4-dichlorophenoxyacetate monooxygenase" is a α-ketoglutarate-dependent dioxygenase. J. Bacteriol. 175:2083-2096.
12. Fukumori, F., and R. P. Hausinger. 1993. Purification and characterization of 2,4-dichlorophenoxyacetate/α-ketoglutarate dioxygenase. J. Biol. Chem. 268:24311-24317.
13. Hausinger, R., and F. Fukumori. 1995. Characterization of the first enzyme in 2,4-dichlorophenoxyacetic acid metabolism. Environ. Health Perspectives Suppl. 103:37-39.

COR-AAD1-00003473
Bayer EX1008 (Part 7 of 9)

14. Hausinger, R. P. 2004. Fe(II)/α-ketoglutarate dependent hydroxylases and related enzymes. Crit. Rev. Biochem. Mol. Biol. 39:1-47.

15. Hegg, E. L., and L. Que, Jr. 1997. The 2-His-1-carboxylate facial triad--an emerging structural motif in mononuclear non-heme iron(II) enzymes. Eur. J. Biochem. 250:625-629.

16. Henshaw, T. F., M. Feig, and R. P. Hausinger. in press. Aberrant activity of the DNA repair enzyme AlkB. J. Inorg. Biochem.

17. Hogan, D. A., T. A. Auchtung, and R. P. Hausinger. 1999. Cloning and characterization of a sulfonate/a-ketoglutarate dioxygenase from Saccharaomyces cerevisiae. J. Bacteriol. 181:5876-5879.

18. Hogan, D. A., S. R. Smith, E. A. Saari, J. McCracken, and R. P. Hausinger. 2000. Site-directed mutagenesis of 2,4-dichlorophenoxyacetic acid/α-ketoglutarate dioxygenase. J. Biol. Chem. 275:12400-12409.

19. Janc, J. W., L. A. Egan, and C. A. Townsend. 1995. Purification and characterization of clavaminate synthase from *Streptomyces antibioticus*. A multifunctional enzyme of clavam biosynthesis. J. Biol. Chem. 270:5399-5404.

20. Kahnert, A., and M. A. Kertesz. 2000. Characterization of a sulfur-regulated oxygenative alkylsulfatase from *Pseudomonas putida* S-313. J. Biol. Chem. 275:31661-31667.

21. Kivirikko, K. I., R. Myllylä, and T. Pihlajaniemi. 1989. Protein hydroxylation: prolyl 4-hydroxylase, an enzyme with four cosubstrates and a multifunctional subunit. FASEB J. 3:1609-1617.

22. Kivirikko, K. I., and T. Pihlajaniemi. 1998. Collagen hydroxylases and the protein disulfide isomerase subunit of prolyl 4-hydroxylases. Adv. Enzymol. Relat. Areas Mol. Biol. 72:325-398.

23. Landman, O., I. Borovok, Y. Aharonowitz, and G. Cohen. 1997. The glutamine ligand in the ferrous iron active site of isopenicillin N synthase of *Streptomyces jumonjinensis* is not essential for catalysis. FEBS Lett. 405:172-174.

24. Lange, S. J., and L. Q. Jr. 1998. Oxygen activating nonheme iron enzymes. Curr. Op. Chem. Biol. 2:159-172.

25. Lindstedt, G., S. Lindstedt, and I. Nordin. 1977. Purification and properties of γ-butyrobetaine hydroxylase from *Pseudomonas* sp AK 1. Biochemistry 16:2181-2188.

26. Lloyd, M. D., H. J. Lee, K. Harlos, Z. H. Zhang, J. E. Baldwin, C. J. Schofield, J. M. Charnock, C. D. Garner, T. Hara, A. C. Terwisscha van Scheltinga, K. Valegård, J. A. Viklund, J. Hajdu, I. Andersson, A. Danielsson, and R. Bhikhabhai. 1999. Studies on the active site of deacetoxycephalosporin C synthase. J. Mol. Biol. 287:943-960.

27. Ming, L.-J., L. Que, Jr., A. Kriauciunas, C. A. Frolik, and V. J. Chen. 1991. NMR studies of the active site of isopenicillin N synthase, a non-heme iron(II) enzyme. Biochemistry 30:11653-11659.

28. Müller, I., A. Kahnert, T. Pape, G. M. Sheldrick, W. Meyer-Klaucke, T. Dierks, M. Kertesz, and I. Uson. 2004. Crystal structure of the alkylsulfatase AtsK: insights into the catalytic mechanism of the Fe(II) α-ketoglutarate-dependent dioxygenase superfamily. Biochemistry 43:3075-3088.

COR-AAD1-00003474
Bayer EX1008 (Part 7 of 9)

29. Myllyharju, J. 2003. Prolyl 4-hydroxylases, the key enzymes of collagen biosynthesis. Matrix Biol. 22:15-24.

30. Myllylä, R., E.-R. Kuutti-Savolainen, and K. I. Kivirikko. 1978. The role of ascorbate in the prolyl hydroxylase reaction. Biochem. Biophys. Res. Commun. 83:441-448.

31. Myllylä, R., K. Majamaa, V. Günzler, H. M. Hanauske-Abel, and K. I. Kivirikko. 1984. Ascorbate is consumed stoichiometrically in the uncoupled reactions catalyzed by prolyl 4-hydroxylase and lysyl hydroxylase. J. Biol. Chem. 259:5403-5405.

32. O'Brien, J. R., D. J. Schuller, V. S. Yang, B. D. Dillard, and W. N. Lanzilotta. 2003. Substrate-induced conformational changes in *Escherichia coli* taurine/α-ketoglutarate dioxygenase and insight into the oligomeric structure. Biochemistry 42:5547-5554.

33. Poh, R., X. Xia, I. J. Bruce, and A. R. Smith. 2001. 2,4-dichlorophenoxyacetate/α-ketoglutarate dioxygenases from *Burkholderia cepacia* 2a and *Ralstonia eutropha* JMP134. Microbios 105:43-63.

34. Prescott, A. G., and M. D. Lloyd. 2000. The iron(II) and 2-oxoacid-dependent dioxygenases and their role in metabolism. Nat. Prod. Rep. 17:367-383.

35. Price, J. C., E. W. Barr, T. E. Glass, C. Krebs, and J. M. Bollinger, Jr. 2003. Evidence for hydrogen abstraction from C1 of taurine by the high-spin Fe(IV) intermediate detected during oxygen activation by taurine:α-ketoglutarate dioxygenase (TauD). J. Am. Chem. Soc. 125:13008-13009.

36. Price, J. C., E. W. Barr, B. Tirupati, J. M. Bollinger, Jr., and C. Krebs. 2003. The first direct characterization of a high-valent iron intermediate in the reaction of an α-ketoglutarate-dependent dioxygenase: a high-spin Fe(IV) complex in taurine/α-ketoglutarate dioxygenase (TauD) from *Escherichia coli*. Biochemistry 42:7497-7508.

37. Prockop, D. J., and K. I. Kivirikko. 1995. Collagens: molecular biology, diseases, and potentials for therapy. Annu. Rev. Biochem. 64:403-434.

38. Proshlyakov, D. A., T. F. Henshaw, G. R. Monterosso, M. J. Ryle, and R. P. Hausinger. 2004. Direct detection of oxygen intermediates in the non-heme Fe enzyme taurine/α-ketoglutarate dioxygenase. J. Am. Chem. Soc. 126:1022-1023.

39. Puistola, U., T. M. Turpeenniemi-Hujanen, R. Myllylä, and K. I. Kivirikko. 1980. Studies on the lysyl hydroxylase reaction. I. Initial velocity kinetics and related aspects. Biochim. Biophys. Acta 611:40-50.

40. Roach, P. L., I. J. Clifton, V. Fülöp, K. Harlos, B. G. J., J. Hajdu, I. Andersson, C. J. Schofield, and J. E. Baldwin. 1995. Crystal structure of isopenicillin N synthase is the first from a new structural family of enzymes. Nature 375:700-704.

41. Roach, P. L., I. J. Clifton, C. M. H. Hensgens, N. Shibata, C. J. Schofield, J. Hajdu, and J. E. Baldwin. 1997. Structure of isopenicillin *N* synthase complexed with substrate and the mechanism of penicillin formation. Nature 387:827-830.

42. Rohde, J.-U., J.-H. In, M. H. Lim, W. W. Brennessel, M. R. Bukowski, A. Stubna, E. Munck, W. Nam, and L. Que, Jr. 2003. Crystallographic and spectroscopic characterization of a nonheme Fe(IV)=O complex. Science 299:1037-1039.

43. Ryle, M. J., and R. P. Hausinger. 2002. Non-heme iron oxygenases. Curr. Opin. Chem. Biol. 6:193-201.

COR-AAD1-00003475
Bayer EX1008 (Part 7 of 9)

44. Ryle, M. J., K. D. Koehntop, A. Liu, L. Que, Jr., and R. P. Hausinger. 2003. Interconversion of two oxidized forms of taurine/α-ketoglutarate dioxygenase, a non-heme iron hydroxylase: evidence for bicarbonate binding. Proc. Natl. Acad. Sci. USA 100:3790-3795.

45. Ryle, M. J., A. Liu, R. B. Muthukumaran, R. Y. N. Ho, K. D. Koehntop, J. McCracken, L. Que, Jr., and R. P. Hausinger. 2003. O_2- and α-ketoglutarate-dependent tyrosyl radical formation in TauD, an α-keto acid-dependent non-heme iron dioxygenase. Biochemistry 42:1854-1862.

46. Ryle, M. J., R. Padmakumar, and R. P. Hausinger. 1999. Stopped-flow kinetic analysis of *Escherichia coli* taurine/α-ketoglutarate dioxygenase: interactions with α-ketoglutarate, taurine, and oxygen. Biochemistry 38:15278-86.

47. Saari, R. E., and R. P. Hausinger. 1998. Ascorbic acid-dependent turnover and reactivation of 2,4-dichlorophenoxyacetic acid/α-ketoglutarate dioxygenase using thiophenoxyacetic acid. Biochemistry 37:3035-3042.

48. Saari, R. E., D. A. Hogan, and R. P. Hausinger. 1999. Stereospecific degradation of the phenoxypropionate herbicide dichlorprop. J. Mol. Catal. B: Enzymatic 6:421-428.

49. Salowe, S. P., E. N. Marsh, and C. A. Townsend. 1990. Purification and characterization of clavaminate synthase from *Streptomyces clavuligerus*: an unusual oxidative enzyme in natural product biosynthesis. Biochemistry 29:6499-6508.

50. Samson, S. M., R. Belagaje, D. T. Blankenship, J. L. Chapman, D. Perry, P. L. Skatrud, R. M. VanFrank, E. P. Abraham, J. E. Baldwin, S. W. Queener, and T. D. Ingolia. 1985. Isolation, sequence determination and expression in *Escherichia coli* of the isopenicillin N synthetase gene from *Cephalosporium acremonium*. Nature 318:191-194.

51. Schenk, W. A. 2000. Isopenicillin N synthase: An enzyme at work. Angew. Chem. Int. Ed. 39:3409-4311.

52. Schofield, C. J., J. E. Baldwin, M. F. Byford, I. Clifton, J. Hajdu, C. Hensgens, and P. Roach. 1997. Proteins of the penicillin biosynthesis pathway. Curr. Opin. Struct. Biol. 7:857-864.

53. Schofield, C. J., and Z. Zhang. 1999. Structural and mechanistic studies on 2-oxoglutarate-dependent oxygenases and related enzymes. Curr. Opin. Struct. Biol. 9:722-731.

54. Sim, T. S., and P. Loke. 2000. Molecular studies on isopenicillin N synthases. Appl. Microbiol. Biotechn. 54:1-8.

55. Solomon, E. I. 2001. Geometric and electronic structure contributions to function in bioinorganic chemistry: active sites in non-heme iron enzymes. Inorg. Chem. 40:3656-3669.

56. Springob, K., J. I. Nakajima, M. Yamazaki, and K. Saito. 2003. Recent advances in the biosynthesis and accumulation of anthocyanins. Nat. Prod. Rep. 20:288-303.

57. Suwa, Y., A. D. Wright, F. Fukimori, K. A. Nummy, R. P. Hausinger, W. E. Holben, and L. J. Forney. 1996. Characterization of a chromosomally encoded 2,4-dichlorophenoxyacetic acid/α-ketoglutarate dioxygenase from *Burkholderia* sp. strain RASC. Appl. Environ. Microbiol. 62:2464-2469.

58. Tan, D. S., S. G. Ang, and T. S. Sim. 1998. Involvement of a third histidine in the ferrous active site of isopenicillin N synthase of Cephalosporium acremonium

COR-AAD1-00003476
Bayer EX1008 (Part 7 of 9)

repudiated by recombinant double histidine mutants. Biochem Mol Biol Int 44:333-45.

59. Tan, D. S. H., and T. S. Sim. 1996. Functional analysis of conserved histidine residues in *Cephalosporium acremonium* isopenicillin N synthase by site-directed mutagenesis. J. Biol. Chem. 271:889-894.

60. Trewick, S. C., T. F. Henshaw, R. P. Hausinger, T. Lindahl, and B. Sedgwick. 2002. Oxidative demethylation by *Escherichia coli* AlkB directly reverts DNA base damage. Nature 419:174-178.

61. Valegård, K., A. C. Terwisscha van Scheltinga, M. D. Lloyd, T. Hara, S. Ramaswamy, A. Perrakis, A. Thompson, H. J. Lee, J. E. Baldwin, C. J. Schofield, J. Hajdu, and I. Andersson. 1998. Structure of a cephalosporin synthase. Nature 394:805-809.

62. Westendorf, A., D. Benndorf, R. H. Müller, and W. Babel. 2002. The two enantiospecific dichlorprop/α-ketoglutarate-dioxygenases from *Delftia acidovorans* MC1 - protein and sequence data of RdpA and SdpA. Microbiol. Res. 157:1-6.

63. Westendorf, A., R. H. Müller, and W. Babel. 2003. Purification and characterisation of the enantiospecific dioxygenases from *Delftia acidovorans* MC1 initiating the degradation of phenoxypropionate and phenoxyacetate herbicides. Acta Biotechnol. 23:3-17.

64. White, A. K., and W. W. Metcalf. 2002. Isolation and biochemical characterization of hypophosphite/2-oxoglutarate dioxygenase. A novel phosphorus-oxidizing enzyme from *Pseudomonas stutzeri* WM88. J. Biol. Chem. 277:38262-38271.

65. Whiting, A. K., L. J. Que, R. E. Saari, R. P. Hausinger, M. A. Fredrick, and J. McCracken. 1997. Metal coordination environment of a Cu(II)-substituted α-keto acid-dependent dioxygenase that degrades the herbicide 2,4-D. J. Am. Chem. Soc. 119:3413-3414.

66. Wilmouth, R. C., J. J. Turnbull, R. W. Welford, I. J. Clifton, A. G. Prescott, and C. J. Schofield. 2002. Structure and mechanism of anthocyanidin synthase from *Arabidopsis thaliana*. Structure (Camb) 10:93-103.

67. Zhang, Z., J. Ren, K. Harlos, C. H. McKinnon, I. J. Clifton, and C. J. Schofield. 2002. Crystal structure of a clavaminate synthase-Fe(II)-2-oxoglutarate-substrate-NO complex: evidence for metal centered rearrangements. FEBS Lett. 517:7-12.

68. Zhang, Z., J. Ren, D. K. Stammers, J. E. Baldwin, K. Harlos, and C. J. Schofield. 2000. Structural origins of the selectivity of the trifunctional oxygenase clavaminic acid synthase. Nat. Struct. Biol. 7:127-133.

COR-AAD1-00003477
Bayer EX1008 (Part 7 of 9)

CHAPTER 2

Genetic Analysis of Phenoxyalkanoic Acid Degradation in *Sphingomonas herbicidovorans* MH

Phenoxyalkanoic acid degradation is well studied in *Beta-* and *Gammaproteobacteria*, but the genetic background has not been elucidated so far in *Alphaproteobacteria*. We report the isolation of several genes involved in dichlor- and mecoprop degradation from the Alphaproteobacterium Sphingomonas herbicidovorans MH and propose that the degradation proceeds analogously to that previously reported for 2,4-D. Two genes for α-ketoglutarate-dependent dioxygenases, $sdpA_{MH}$ and $rdpA_{MH}$, were found which both were adjacent to sequences with potential IS-elements. Furthermore, a gene for a dichlorophenol hydroxylase (*tfdB*), a putative regulatory gene (*cadR*), two genes for dichlorocatechol 1,2-dioxygenases ($dccA_{I/II}$), two for dienelactone hydrolases ($dccD_{I/II}$), part of a gene for maleylacetate reductase (*dccE*) and one gene for a potential phenoxyalkanoic acid permease were isolated. In contrast to other 2,4-D degraders, the *sdp*, *rdp*, and *dcc* genes were scattered over the genome and their expression was not tightly regulated. No coherent pattern was derived on the possible origin of the *sdp*, *rdp*, and *dcc* pathway genes. $rdpA_{MH}$ was 99% identical to $rdpA_{MC1}$, a (*R*)-dichlorprop/α-ketoglutarate dioxygenase from *Delftia acidovorans* MC1, which is evidence for a recent gene exchange between *Alpha-* and *Betaproteobacteria*. Conversely, $DccA_I$ and $DccA_{II}$ did not group within the known chlorocatechol 1,2-dioxygenases, but formed a separate branch in clustering analysis. This suggests a different reservoir and reduced transfer for the genes of the modified *ortho*-cleavage pathway in *Alphaproteobacteria* than the ones in *Beta-* and *Gammaproteobacteria*.

The main part of this chapter has been accepted for publication in Applied and Environmental Microbiology (June 2004) by T. A. Müller, S. M. Byrde, C. Werlen, J. R. van der Meer, H.-P. E. Kohler.

COR-AAD1-00003479
Bayer EX1008 (Part 7 of 9)

INTRODUCTION

Phenoxyalkanoic acid herbicides such as 2,4-dichlorophenoxyacetic acid (2,4-D), chiral mecoprop [(*R*,*S*)-2-(4-chloro-2-methyl-phenoxypropanoic acid], and chiral dichlorprop [(*R*,*S*)-2-(2,4-dichlorophenoxypropanoic acid)] (Fig. 1) are widely used against broadleaved weeds in agriculture, lawn pastures and industries. They were introduced in large amounts into the environment in the 1940s and 1950s (1, 10, 55). 2,4-D, mecoprop and dichlorprop are synthetic compounds and have only been applied for some decades. However, microorganisms able to use them as sole carbon and energy source have been isolated from different environments (21, 50, 51, 58, chapter 1). 2,4-D degrading strains from the *Beta-* and *Gammaproteobacteria* groups mostly harbor similar genes for 2,4-D degradation (17, 24, 33, 48, 49), which is supportive that frequent gene exchange has occurred and hence their adaptation and wide distribution (17).

In many cases, the first step in the degradation of phenoxyalkanoic acids is the enzymatic conversion of the acids to the corresponding phenols, then via the catechols and through the modified *ortho*-cleavage pathway (21, 41). The best-studied degradation pathway is that of 2,4-D in the soil bacterium *Ralstonia eutropha* JMP134(pJP4) (Fig. 1). Both the genetic and the enzymatic details of the pathway have been established in this bacterium. *R. eutropha* JMP134(pJP4) degrades 2,4-D by an α-ketoglutarate-dependent dioxygenase that cleaves the ether-bond to produce 2,4-dichlorophenol (15, 16, 43). 2,4-Dichlorophenol in turn is hydroxylated to 3,5-dichlorocatechol by a phenol-hydroxylase ($TfdB_{I/II}$) (13, 29, 38). 3,5-Dichlorocatechol undergoes *ortho*-ring fission to 2,4-dichloro-*cis,cis*-muconate, a reaction catalyzed by chlorocatechol 1,2-dioxygenase ($TfdC_{I/II}$) (29, 37-39). 2,4-Dichloro-*cis,cis*-muconate is then converted to *cis*-2-chlorodiene-lactone and further to 2-chloromaleylacetate by chloromuconate cycloisomerase ($TfdD_{I/II}$) and dienelactone hydrolase activity ($TfdE_{I/II}$), respectively (27, 38). Finally, chloromaleylacetate is reduced to 3-oxoadipate via maleylacetate by maleylacetate reductase ($TfdF_{I/II}$) (38, 39). Tett *et al.* (46) showed that *(R)*-mecoprop degradation in *Alcaligenes denitrificans* proceeds analogously to 2,4-D degradation in *R. eutropha* JMP134(pJP4). Similarly, phenol hydroxylase, chloro-

COR-AAD1-00003480
Bayer EX1008 (Part 7 of 9)

catechol 1,2-dioxygenase and chloromuconate cycloisomerase activities are induced in *Delftia acidovorans* MC1 upon exposure to dichlorprop. This suggests that dichlorprop is also metabolized through a modified *ortho*-cleavage pathway (6).

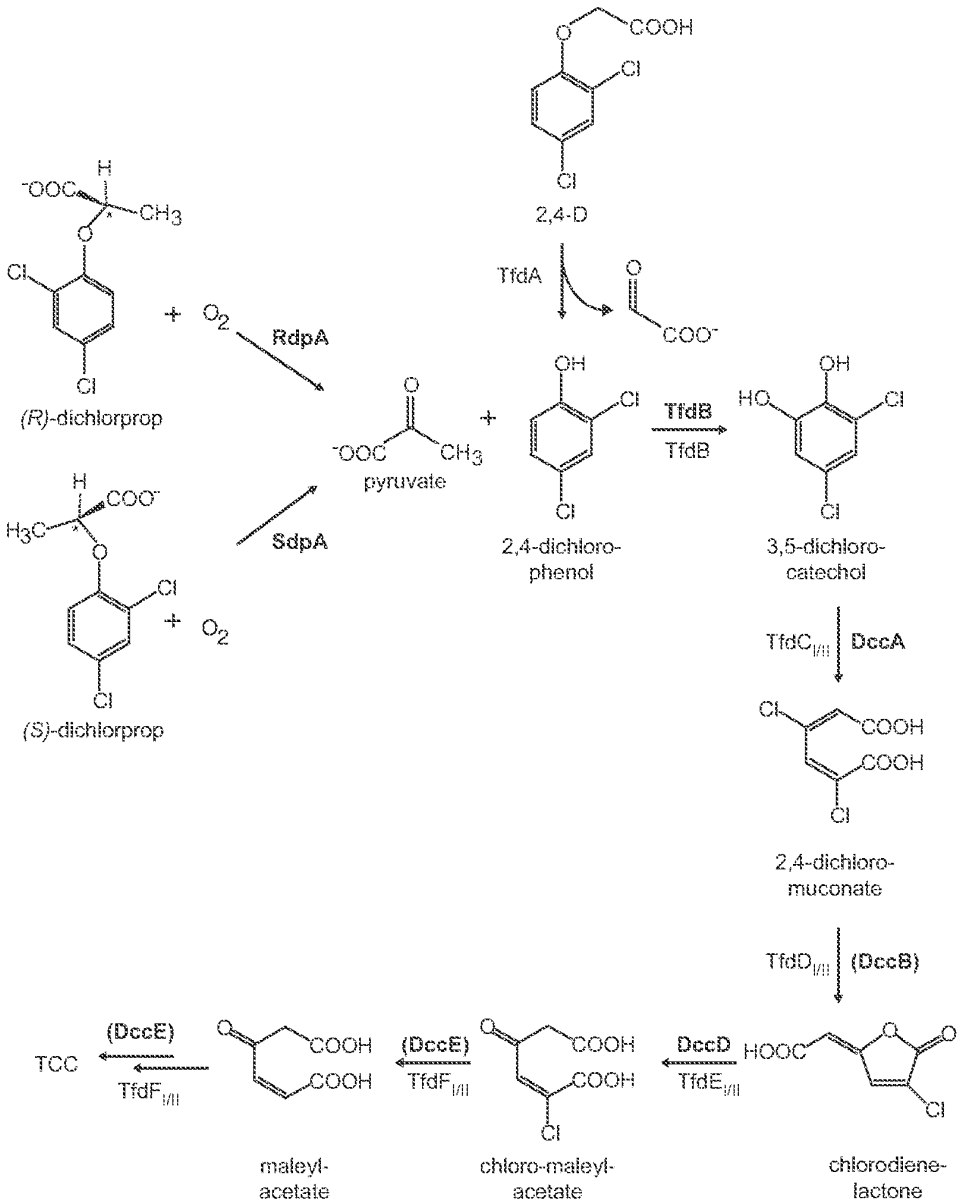


Fig. 1. Pathway proposed for dichlorprop degradation in *S. herbicidovorans* MH and for 2,4-D degradation in *R. eutropha* JMP134(pJP4). The enzymes of the pathway in *S. herbicidovorans* MH are printed in bold. The enzymes of the genes, which have not yet or partially been isolated from *S. herbicidovorans* MH are displayed within brackets.

COR-AAD1-00003481
Bayer EX1008 (Part 7 of 9)

Sphingomonas herbicidovorans MH is a versatile phenoxyalkanoic acid degrader and grows on mecoprop and dichlorprop as sole carbon and energy sources (22, 26, 58). Although strain MH metabolizes both enantiomers, it preferentially uses the *(S)* enantiomer. Nickel *et al.* (36) showed that *S. herbicidovorans* MH harbors two distinct α-ketoglutarate-dependent dioxygenase activities that are involved in the enantioselective degradation of mecoprop and dichlorprop to achiral phenols. However, nothing is known about the genetic background of the mecoprop and dichlorprop degradation pathway in strain MH. *S. herbicidovorans* MH belongs to the *Alphaproteobacteria* whereas other well-studied phenoxyalkanoic acid degraders such as *R. eutropha* JMP134(pJP4) and *D. acidovorans* MC1 belong to the *Betaproteobacteria* and the *Gamma-proteobacteria*. Total DNA from phenoxyalkanoic acid degrading *Alphaproteo-bacteria* did not hybridize to *tfdA* gene probes encoding α-ketoglutarate-dependent 2,4-D dioxygenases (17, 24, 33, 48, 49). PCR-experiments aimed at amplifying DNA fragments from *Sphingomonas* strains with *tfdA*-primers also failed (42, 48). Therefore, the hypothesis was formulated that *Alphaproteobacteria* might harbor different dioxygenases catalyzing the initial step of phenoxyalkanoic acid degradation. Only recently, the first *tfdA*-homologous gene, *tfdA*α, was isolated from a 2,4-D degrading bacterium belonging to the *Bradyrhizobium-Agromyces-Nitrobacter-Afipia* (BANA)-cluster of *Alphaproteobacteria* (23). On the other hand, fragments similar to phenol hydroxylase (e.g., *tfdB*-like) and chlorocatechol 1,2-dioxygenase genes (e.g. *tfdC*-like) have also been amplified from *Sphingo-monas* strains with degenerate primers in the PCR (30, 48). Whereas the *tfdB*-like gene fragments from *Sphingomonas* strains were more than 60% similar to *tfdB* genes from *Beta-* and *Gammaproteobacteria*, *tfdC*-like gene fragments showed little similarity to other known chlorocatechol 1,2-dioxygenase genes and formed a rather coherent group among themselves (48). Hence, *Alphaproteobacteria* might not only harbor different dioxygenases but also different chlorocatechol degradation genes and it was thus proposed that gene flow might be less common between *Alpha-* and *Beta-* or *Gammaproteobacteria* than among *Beta-* and *Gammaproteobacteria* themselves (17, 18).

COR-AAD1-00003482
Bayer EX1008 (Part 7 of 9)

In order to test this hypothesis and to elucidate the phenoxyalkanoic acid degradation pathway, we isolated and characterized several genes from *S. herbicidovorans* MH by PCR amplification with degenerated primers, DNA:DNA hybridization, cosmid library construction and DNA sequencing. We propose that these genes are involved in phenoxyalkanoic acid degradation in strain MH and are equivalent to those known from the 2,4-D degradation pathway of *R. eutropha* JMP134(pJP4). The expression of the characterized genes was analyzed in hybridization experiments with mRNA isolated from *S. herbicidovorans* MH cultures that were induced with mecoprop or 2,4-D. The two chlorocatechol 1,2-dioxygenases were expressed in *Escherichia coli* and characterized in terms of their substrate specificities. Finally, the phylogenetic relationships of the *S. herbicidovorans* MH chlorocatechol pathway genes were compared to those of other phenoxyalkanoic acid degradation pathways.

MATERIALS AND METHODS

Bacterial strains and culture conditions. *S. herbicidovorans* MH was grown in baffled Erlenmeyer flasks shaking at 30°C either in complex medium (57) or in mineral medium supplemented with the appropriate carbon- and energy source. The mineral medium was prepared as described in Nickel *et al.* (36), and was modified by reducing the amount of added peptone to 10 mg/l and by adding 10 mg/l yeast extract. *E. coli* strains were grown either at 30°C or at 37°C in Luria-Bertani (LB) medium (40) with the appropriate antibiotic. Ampicillin and kanamycin were added to final concentrations of 50 μg/ml, chloramphenicol to 25 μg/ml. If necessary, 5-bromo-4-chloro-3-indolyl-β-D-galactoside (Biosynth AG, Staad, Switzerland) was added to a final concentration of 50 μg/ml.

Standard molecular techniques. Cloning and digestions were done according to established procedures (4, 40). Restriction enzymes and other DNA modifying enzymes were purchased from Promega (Wallisellen, Switzerland) and Fermentas (Nunningen, Switzerland). Plasmids and cosmids were isolated by the boiling miniprep method, the alkaline lysis method according to Sambrook *et al.* (40) or with the E.Z.N.A. plasmid miniprep kit II (Peqlab Biotechnologies GmbH, Baden-Dättwil, Switzerland) as suggested by the manufacturer. Gel extraction was carried out with the MinElute Gel extraction Kit (Qiagen AG, Basel, Switzerland) according to the protocol of the supplier.

COR-AAD1-00003483
Bayer EX1008 (Part 7 of 9)

Construction of a cosmid library of *S. herbicidovorans* MH. The SuperCos1 Cosmid Vector Kit (Strategene, Amsterdam, The Netherlands) was used to construct a cosmid library. *S. herbicidovorans* MH was grown in 500 ml mineral medium containing 200 mg/l (*R,S*)-mecoprop until a turbidity of 0.15 (measured at 546 nm) was reached. The culture was harvested by centrifugation for 30 min at 6000 × *g*. The pellet was resuspended in 15 ml lysis buffer (10 mM NaCl, 20 mM Tris-HCl, pH 8, 1 mM EDTA, 100 μg/ml proteinase K and 0.5% (w/v) SDS) and incubated overnight at 50°C. The DNA was isolated by phenol-chloroform extraction (40), precipitated with ethanol and dissolved in 4 ml TE (10 mM Tris-HCl, pH 8, 1 mM EDTA) and stored at 4°C. Partial digestion of the DNA was done with *Sau*3AI using different enzyme concentrations for 15 min at 37°C. The digestion was stopped by adding EDTA to a final concentration of 1 mM. The preparation of the host strain *E. coli* XL-1 BlueMR, the packaging and the titering were carried out according to the protocol of the supplier (Stratagene). Finally, about thousand clones were picked and grown overnight in microtiter plates in LB supplemented with kanamycin at 30°C. Glycerol was added to a final concentration of 15% and the cosmid library was stored at –80°C.

Screening for genes involved in phenoxyalkanoic acid degradation by PCR. To isolate *rdpA*, we amplified a fragment with the PCR-primers RDPin_fG and RDPin_r (53) from chromosomal DNA of *S. herbicidovorans* MH. Oligonucleotides for PCR were obtained from Microsynth GmbH (Balgach, Switzerland). The following conditions were applied: initial denaturation for 5 min at 93.5°C; denaturing for 30 sec at 93.5°C; annealing for 30 sec at 52°C, 49°C, 46°C, 43°C, 41°C, and 39°C; extension for 45 sec at 72°C (5 cycles at each annealing temperature; 10 cycles at 39°C) followed by a final extension for 4 min at 72°C. A chlorophenol hydroxylase gene fragment (*tfdB*) was amplified with the tfdBup and tfdBlow primers from total DNA of *S. herbicidovorans* MH as described by Vallaeys *et al.* (48).

To screen for a chlorocatechol 1,2-dioxygenase gene, the degenerate PCR-primers CCDb and CCDe described by Leander et al. (30) were used. The PCR-protocol was as follows: initial denaturation for 6 min at 93.5°C, 35 cycles denaturation for 1 min at 95°C, annealing for 1 min at 48°C and extension for 1 min at 72°C followed by one extension cycle for 6 min at 72°C. PCR-fragments were cloned in pGEM®-T Easy (Promega) and sequenced to check the insert (Table 1).

Hybridization of the cosmid library and construction of plasmids harboring genes involved in phenoxyalkanoic acid degradation. For colony blotting of the cosmid library, the colonies were grown overnight on LB agar plates at 37°C. Colony material was transferred to Hybond™-XL membrane (Amersham Biosciences, Dübendorf, Switzerland) by direct contact. The colony material on the membrane was lysed twice with a solution of 0.5 M NaOH for 2 min and washed twice with a solution of 1 M Tris-HCl (pH 8). The DNA was fixed on the membrane by UV light (254 nm, 120 mJ/cm^2) in a Stratalinker model 1800 (Stratagene).

COR-AAD1-00003484
Bayer EX1008 (Part 7 of 9)

The cosmid library of *S. herbicidovorans* MH was hybridized with the inserts of pMec1 (*dccA*-fragment) and pMec5 (*rdpA*-fragment). The fragments were radioactively labeled with [α-^{32}P]dATP using the Random Primed DNA Labeling Kit according to the supplier's protocol (Roche Applied Science, Rotkreuz, Switzerland). Positively reacting cosmids were isolated, digested and checked by Southern hybridization. Additionally, all positive reacting cosmids were hybridized in the same way with the insert of pMec23 to screen for the *tfdB*-gene. Suitable fragments were then subcloned in pUC-vectors (5) yielding the plasmids listed in Table 1.

Table 1. Plasmids constructed in this work

plasmid	relevant characteristics	source
pMec1	0.3-kb PCR-fragment obtained with CCDb and CCDe primers cloned into pGEM®-T Easy; contains part of *dccA*	total DNA
pMec2	1.5-kb *Sal*I-fragment in pUC28 (5), contains part of the chlorocatechol degradation cluster II	cosmid 9H11
pMec4	2.3-kb *Sal*I-fragment in pUC28, contains part of the chlorocatechol degradation cluster I	11D11
pMec5	0.3-kb PCR-fragment obtained with RDPin_f and RDPin_r primers; contains part of *rdpA*	total DNA
pMec7	$dccA_I$ in pGEM®-T Easy	pMec4
pMec9	$dccA_I$ in pRSET6α (*Nde*I-*Bam*HI cloned) (44)	pMec7
pMec10	2.8-kb *Nco*I-fragment in pUC28; contains *rdpA* and a transposase	10A12
pMec12	4.5-kb *Bam*HI-fragment in pUC28; contains part of the chlorocatechol degradation cluster II	9H11
pMec14	0.7-kb PCR-fragment in pGEM®-T Easy, contains *rdpA*	pMec10
pMec16	5-kb *Kpn*I-fragment in pUC28; contains *sdpA*	10A12
pMec18	0.7-kb PCR-fragment in pGEM®-T Easy, contains *sdpA*	pMec16
pMec20	$dccA_{II}$ in pGEM®-T Easy	pMec12
pMec21	$dccA_{II}$ in pET8c (44)	pMec20
pMec23	1.1-kb PCR-fragment obtained with primers tfdBup and tfdBlow cloned into pGEM®-T Easy, contains part of *tfdB*	total DNA
pMec25	5.5-kb *Sal*I-fragment in pUC18Not; contains *tfdB*	11D11

Transposon insertion and sequencing. The EZ::TN<KAN-2> Tnp Transposome™ Kit (Epicentre Technologies, Madison, USA) was used for the insertion of a kanamycin resistance marker and sequencing priming sites into the plasmids with cloned *S. herbicidovorans* MH DNA. The insertion reaction was carried out according to the protocol of the supplier. DNA sequencing was performed on double stranded DNA templates with the Thermo Sequenase Primer Cycle Sequencing Kit with 7-deaza-dGTP (Amersham Biosciences) and M13 primers (5) or KAN-2 FP-

COR-AAD1-00003485
Bayer EX1008 (Part 7 of 9)

1/RP-1 primers (Epicentre Technologies). Sequencing reactions were analyzed on an automated DNA sequencer model 4200 IR^2 (LI-COR Inc., Lincoln, USA). Primers for sequencing were labelled at the 5'-end with IRD-700 or IRD-800 and were purchased from MWG Biotech AG (Ebersberg, Germany). Sequencing data were analyzed with DNASTAR software (DNASTAR Inc., Madison, USA) and compared to the databases by BLAST searches (www.ncbi.nlm.nih.gov/Blast; 45). Sequences were deposited in the EMBL database under accession numbers AJ628859-AJ628863.

Construction of expression plasmids pMec9 and pMec21, expression of DccA$_{I/II}$ in *E. coli* and preparation of cell extract. The *dccA$_I$* gene was reamplified from a cosmid fragment by PCR with the primer pair CCD2/CCD3 (5'-GAGAGGTCATATGAGCAATCGT-3', 5'-AACGCGAGGATCCGCAGACCAT-3') thereby introducing a *Nde*I- and a *Bam*HI-restriction site (underlined). The *dccA$_{II}$*-gene was amplified by PCR with the forward primer ClcA2_for (5'-AGGTTCCATGGGCAATCG-3') to introduce a *Nco*I-site and the reverse primer ClcA2_rev (5'-AGGATCCGTGCCTGTCAG-3') to create a *Bam*HI-site. The fragments were first cloned into pGEM®-T Easy and verified by sequencing. They were then digested with the respective enzymes and cloned in the same restriction sites in pRSET6α and pET8c, respectively (44) (Table 1).

To express the proteins, a preculture of *E. coli* BL21 (DE3)(pLysS) harboring pMec9 or pMec21 was grown overnight at 37°C. A volume of 1% (v/v) of the preculture was transferred to fresh medium and grown at 30°C until a turbidity of 0.4 – 0.6 (measured at 546 nm) was reached, after which isopropyl-β-D-thiogalactopyranoside was added to a final concentration of 0.05 mM. The culture was incubated for another 3 hours at 30°C and the cells were harvested by centrifugation. A pellet of approximately 1 g wet weight was resuspended in 2.5 ml of a solution of 40 mM Tris-HCl, pH 7.4 containing 0.3 mM EDTA. The cells were broken by one passage through a French Pressure cell at 1 MPa. The lysate was centrifuged at 16'000 × *g* for 30 min at 4°C, the supernatant recovered and stored at –20°C until use as cell extract in enzyme activity measurements.

Enzyme assay. Enzymatic activity of chlorocatechol 1,2-dioxygenase with all substrates was measured spectrophotometrically at 260 nm in a quartz cuvette for 30 sec except for protocatechuate, which was monitored at 290 nm. To 485 µl buffer (containing 40 mM Tris-HCl, 0.3 mM EDTA and with a pH of 7.4), 10 µl cell-extract of *E. coli* BL21 (DE3)(pLysS) harboring pMec9 or pMec21 containing between 15 and 30 µg total protein was added. The reaction was started by adding the substrate from a 20 mM stock in methanol to a final concentration of 0.4 mM. To calculate activity, extinction coefficients were taken from Broderick and O'Halloran and Dorn *et al.* (7, 11).

Induction experiment. *S. herbicidovorans* MH was grown on mineral medium with 20 mM pyruvate to a turbidity of 0.4–0.6 (measured at 546 nm). The culture was induced by the

COR-AAD1-00003486
Bayer EX1008 (Part 7 of 9)

addition of *(R)*-, *(S)*-mecoprop or 2,4-D dissolved in DMSO (10 g/l) to a final concentration of 100 mg/l and incubated for another 30 min at 30°C. A culture to which only DSMO was added was used as a negative control. To stop induction and prevent RNA degradation, one volume of culture was added to two volumes of RNA-protector immediately after sampling (Qiagen AG). The mixture was incubated at room temperature for 5 min, centrifuged at 13'000 × *g* for 1 min and the supernatant was decanted. The pellets were stored at –20°C.

RNA-extraction. RNA was extracted with the RNeasy® Mini Kit from Qiagen AG according to the supplier's protocol. The RNA, solved in RNase free water, was then stored by adding two volumes of ethanol and 0.1 volume of 5 M sodium acetate (pH 5.2) at –20°C. RNA-concentrations were determined spectrophotometrically at 260 nm.

In vitro synthesis of antisense mRNA. The pGEM®-T Easy plasmids pMec14, 18 and 20 harboring *rdpA*, *sdpA*, and $dccA_{II}$, respectively, were linearized by restriction enzyme digestion in order to allow insert-specific transcription from either the T7 or the SP6 promoter. In vitro transcription reactions were carried out with biotin-16-UTP and T7 or SP6 RNA polymerase with the Riboprobe® in vitro Transcription Systems (Promega) according to the protocol of the supplier. The size and yield of all antisense mRNA probes were checked on 1% agarose gels.

Dot blot hybridization of mRNA. Total RNAs were washed with 70% ethanol and dissolved in 50 µl RNase-free water. Equal volumes of RNA dilutions (0.5 µg/50 µl, 0.1 µg/50 µl, 0.05 µg/50 µl) were blotted onto positively charged nylon membranes (Qiagen GmbH) in a dot-blot manifold (Invitrogen Life Technologies, Basel, Switzerland) containing a 96-well 3 mm gasket. The samples were washed with an equal volume of 1 × SSC (0.15 M NaCl, 15 mM sodium citrate) directly after their application. On each blot, a series of DNA standards were included (not shown). The standards contained 100, 50, 10, 1, 0.1 ng DNA/50 µl of the plasmid pMec14, 18 or 20.

Phylogenetic Analysis. Amino acid sequences were aligned with the software tool CLUSTALX (47). Phylogenetic analysis was done with the maximum likelihood method by using the software Tree-Puzzle (http://www.tree-puzzle.de). The dendrogram was drawn with the program TreeViewPPC (http://taxonomy.zoology.gla.ac.uk/ rod/rod.html).

Chemicals. *(R,S)*-, *(R)*-mecoprop and 2,4-D were purchased at Riedel-de Haën (Buchs, Switzerland; PESTANAL®, 99% purity). *(S)*-mecoprop was synthesized by C. Zipper (1998) (56). Catechol, 4-chloro-, 3,5-dichloro-, 4,5-dichloro-, tetrachloro-, 3-methyl- and 4-nitrocatechol were purchased at Sigma-Aldrich (Buchs, Switzerland; 97-99% purity). 3-Chlorocatechol was bought at Promochem GmbH (Wesel, Germany; 99% purity). All other chemicals were either obtained from Fluka (Buchs, Switzerland) or from Merck AG (Dietikon, Switzerland).

COR-AAD1-00003487
Bayer EX1008 (Part 7 of 9)

RESULTS

Sequence determination of *sdpA*, *rdpA* and *tfdB*. Degradation of phenoxyalkanoic acid herbicides usually begins with an ether cleavage to the corresponding phenol by α-ketoglutarate dependent dioxygenases (15, 16, 43, 53, 54). By using a primer set previously developed for isolating a gene fragment encoding a (*R*)-dichlorprop dioxygenase from *D. acidovorans* MC1 (53), a 0.3-kb fragment was amplified from total DNA of *S. herbicidovorans* MH. This PCR-amplified fragment was cloned (pMec5) and sequenced to confirm its identity to the dichlorprop dioxygenase gene. It was subsequently used to screen a cosmid library of *S. herbicidovorans* MH. Several cosmids were positively hybridizing with the pMec5 insert and a 2.8-kb *Nco*I-fragment was identified from cosmid 10A12 to contain the region of identity to pMec5. This fragment was subcloned (pMec10), sequenced and analyzed in detail (Table 2). The sequence revealed two open reading frames (ORFs), one of which was almost identical to the (*R*)-dichlorprop dioxygenase gene *rdpA* from *D. acidovorans* MC1 ($rdpA_{MC1}$; Table 2 and Fig. 2A). At the nucleotide level, the 888-bp *rdpA* ORF from *S. herbicidovorans* MH contained one neutral mutation compared to $rdpA_{MC1}$ whereas the predicted $RdpA_{MH}$ protein had a 100% identical amino acid sequence to $RdpA_{MC1}$. RdpA belonged to the class of α-ketoglutarate dependent dioxygenases and showed a 35% identical amino acid sequence to TauD from *Pseudomonas aeruginosa*, and percentages of identities below 33% to other members of this enzyme class (Table 3). Upstream of $rdpA_{MH}$, a 1200-bp region was found which was similar to an insertion element from *Ralstonia* sp. strain JS705 (Table 2). The transposase ORF comprised 1149 nucleotides.

COR-AAD1-00003488
Bayer EX1008 (Part 7 of 9)

Table 2. Genes and corresponding products isolated from *S. herbicidovorans* MH

plasmid	ORF[a]	position (nt)[b]	probable function or product	homologous protein[c]	source	reference accession number	% amino acid identity[d]	# amino acids[e]
pMec10	*tnpA*	226-1374	transposase	TnpA	*Ralstonia* sp. JS705	CAD60927	87 (352/403)	403/414
	rdpA	1733-2620	(*R*)-dichlorprop/α-ketoglutarate dioxygenase	RdpA	*D. acidovorans* MC1	AAM90962	100 (295/295)	295/295
pMec16	(*tnpA*)	(1-447)	transposase (C-terminus)	transposase	*Ralstonia* sp. JS705	CAD60927	79 (117/148)	-/414
	sdpA	750-1613	(*S*)-dichlorprop/α-ketoglutarate dioxygenase	SdpA	*D. acidovorans* P4a	AAM90963	58 (171/290)	287/292
pMec25	(*cadR*)	(1-972)	transcriptional regulator	CadR	*Bradyrhizobium* sp. HW13	BAB78520	65 (181/276)	-/336
	ORF2	1062-2627[f]	outer membrane receptor protein	COG1629	*Novosphingobium aromaticivorans*	ZP_00096178	26 (129/488)	521/743
	tfdB	2654-4453	dichlorophenol hydroxylase	TfdB	*D. acidovorans* MC1	AAM76774	57 (334/585)	600/586
pMec4 (cluster I)	(*dccE*)	(1-247)	(partial) maleylacetate reductase	TfdF	*Burkholderia cepacia*	AAK81685	53 (42/78)	-/357
	$dccA_I$	514-1350	chlorocatechol 1,2-dioxygenase	TfdC	*R. eutropha* JMP134(pJP4)	P05403	53 (134/255)	278/255
	$dccD_I$	1293-2015	dienelactone hydrolase	$TfdE_{II}$	*R. eutropha* JMP134(pJP4)	P94136	47 (106/222)	240/235

COR-AAD1-00003489
Bayer EX1008 (Part 7 of 9)

Table 2 (cont.). Genes and corresponding products isolated from *S. herbicidovorans* MH

plasmid	ORF[a]	position (nt)[b]	probable function or product	homologous protein[c]	source	reference accession number	% amino acid identity[d]	# amino acids[e]
pMec2+12 (cluster II)	*tfdK*	595-1968	putative transport protein	TfdK	*R. eutropha* JMP134(pJP4)	AAC44725	36 (159/440)	457/463
	(orfB)	2494-2865[g]	ISC*e3* transposase orfB (C-terminus)	ISC*e3* transposase OrfB	*Caulobacter crescentus* CB15	NP_419441	65 (81/123)	-/326
	dccA$_{II}$	3320-4087	chlorocatechol 1,2-dioxygenase	TfdC	*R. eutropha* JMP134(pJP4)	BAA74530	51 (125/242)	256/251
	(*dccD*$_{II}$)	4100-(4705)	(interrupted dienelactone hydrolase)	TfdE$_{II}$	*R. eutropha* JMP134(pJP4)	P94136	50 (88/173)	-/235
	(*tnpA*)	(5161-4677)	transposase (C-terminus)	TnpA of IS*6100*	*Salmonella enterica* subsp.	AAG03007	100 (156/156)	-/264

[a] Incomplete ORFs are set in parentheses.

[b] The position is given respectively to the nucleotides of the plasmid insert.

[c] Given is the most similar protein identified by BLASTX.

[d] The values in parentheses refer to the number of identical amino acids over the aligned region.

[e] The number of amino acids of the protein in *S. herbicidovorans* MH is given first, the number of the reference protein second.

[f] The exact start position of the ORF could not be determined. Other possible start codons are at nucleotides 969, 1185, and 1290.

[g] The nucleotide region represents the part, which is similar to the C-terminus of outer membrane proteins, since no start codon was found upstream of position 2494 and at nucleotide 2389, a stop codon is encoded.

COR-AAD1-00003490
Bayer EX1008 (Part 7 of 9)

The cosmid 10A12 was subsequently hybridized under low stringency conditions with a 0.7-kb *Eco*RI-fragment of pMec10 containing the $rdpA_{MH}$ gene which revealed a weak signal in addition to the *rdpA* containing fragments itself (not shown). The signal could be located to a 5-kb *Kpn*I-fragment, which was cloned (pMec16) and partially sequenced. An ORF of 864 nucleotides was identified whose predicted amino acid sequence showed significant similarity to the group of α-ketoglutarate dependent dioxygenases and highest similarity to the α-ketoglutarate-dependent *(S)*-dichlorprop dioxygenase from *D. acidovorans* MC1 (Table 2). For this reason, this ORF was designated $sdpA_{MH}$. The predicted amino acid sequence for $SdpA_{MH}$ was 63% identical to SdpA from *D. acidovorans* MC1 ($SdpA_{MC1}$) and 37% to TfdA from *R. eutropha* JMP134(pJP4) (Table 3). Upstream of $sdpA_{MH}$, a similar insertion element was identified as the one in the region upstream of $rdpA_{MH}$. However, the complete ORF of this element was not present on the insert of pMec16.

With the primer pair tfdBup and tfdBlow, a 1.1-kb PCR-fragment was amplified from total DNA of *S. herbicidovorans* MH, cloned (pMec23) and sequenced. The insert was then used to hybridize cosmids 10A12, 9H11 and 11D11, which harbor other genes of phenoxyalkanoic acid degradation. A 5.5-kb *Sal*I fragment from 11D11 was subsequently cloned (pMec25) and partially sequenced. The sequence revealed two complete and one incomplete ORF whose deduced amino acid sequences showed similarity to known proteins in the databank (Table 2). The deduced amino acid sequence of the incomplete ORF at the left end of the insert was similar to CadR from *Bradyrhizobium* sp. HW13 and was therefore tentatively designated *cadR* (25). The ORF downstream showed low similarity (<26%) to the C-terminal region of outer membrane receptor proteins. The ORF starting at nucleotide 2654 and comprising 1800 bp showed similarity to a dichlorophenol hydroxylase gene and was designated *tfdB* (Table 2).

COR-AAD1-00003491
Bayer EX1008 (Part 7 of 9)

Table 3. Identity of RdpA and SdpA to other α-ketoglutarate dependent dioxygenases (determined by BlastP two sequences)

protein	Strain	amino acids	accession number	substrate	RdpA % identity	SdpA % identity
RdpA	*S. herbicidovorans* MH	295	AJ628859	*(R)*-dichlorprop	-	30 (79/262)
	Delftia acidovorans MC1	295	AAM90962	*(R)*-dichlorprop		
SdpA	*S. herbicidovorans* MH	287	AJ628860	*(S)*-dichlorprop	30 (79/262)	-
TauD	*E. coli* K-12	283	AAC73471	taurine	33 (94/281)	29 (82/280)
TauD	*Pseudomonas aeruginosa*	277	NP 252624	taurine	35 (99/282)	32 (91/277)
AtsK	*Pseudomonas putida*	301	AAD31784	alkyl sulfate esters	31 (93/293)	27 (77/277)
TfdA	*Burkholderia cepacia* (pIJB)	288	AAB47567	2,4-D	28 (82/290)	35 (90/252)
TfdA	*Burkholderia* sp. RASC	297	AAB17363	2,4-D	26 (79/293)	37 (107/284)
TfdA	*Ralstonia eutropha* JMP134(pJP4)	287	AAA21983	2,4-D	30 (88/288)	37 (107/287)
RdpA	*Delftia acidovorans* P4a	287	AAM76772	2,4-D	28(81/288)	36 (105/286)
SdpA	*Delftia acidovorans* MC1	292	AAM90963	*(S)*-dichlorprop	27 (75/268)	63 (183/290)
TfdA	strain RD-5-C2 (member of BANA-cluster)	295	BAB92964	2,4-D	28 (83/287)	36 (106/288)
TfdA	*Achromobacter xylosoxidans subsp. Denitrificans*	287	AAF59421	2,4-D	27 (80/288)	37 (106/286)

COR-AAD1-00003492
Bayer EX1008 (Part 7 of 9)

Sequence determination and organization of two chlorocatechol degradation gene clusters. To determine whether genes for chlorocatechol degradation through an *ortho*-cleavage pathway were present in the genome of strain MH, a PCR was carried out with the conserved primer set CCDb and CCDe (30). Amplified fragments were cloned and sequenced to determine the nature of the insert. One clone (pMec1) was found to contain a part of a putative chlorocatechol 1,2-dioxygenase gene (Table 1). The cosmid library was then hybridized with the pMec1 insert to retrieve the complete gene for chlorocatechol 1,2-dioxygenase. Interestingly, two different fragments of cosmids 9H11 and 11D11 were hybridizing, which were both subcloned and sequenced (pMec2 and pMec4). The insert of pMec4 revealed three ORFs, the deduced amino acid of one of which sequence had significant similarity to chlorocatechol 1,2-dioxygenases (Table 2). This ORF was tentatively designated $dccA_I$ for dichlorocatechol 1,2-dioxygenase. The exact start of $dccA_I$ could not be determined completely, since several alternative possible start codons occurred in sequential position (i.e., at positions 265, 367, 400, 472 and 514). However, on the basis of the position of a putative Shine-Dalgarno sequence (AGGAGA at position 500), we propose the $dccA_I$ gene start at position 514. Interestingly, flanking the $dccA_I$ gene were ORFs putatively encoding a dienelactone hydrolase (designated $dccD_I$) (Fig. 2A, Table 2) and a maleylacetate reductase. The maleylacetate reductase ORF was not completely recovered on the insert of pMec4.

The left end of the insert of pMec2 contained a part of a chlorocatechol 1,2-dioxygenase gene. To retrieve the complete ORF, a 4.5-kb *Bam*HI-fragment from cosmid 9H11, which was partially overlapping to the insert of pMec2, was cloned (pMec12) and sequenced. The whole ORF encoding the putative chlorocatechol 1,2-dioxygenase was obtained and tentatively designated $dccA_{II}$ since it was not identical to $dccA_I$. Flanking the $dccA_{II}$ on the inserts of pMec2 and pMec12 were ORFs for another dienelactone hydrolase and a putative transport facilitator protein (Table 2, Fig. 2A). However, the second possible ORF for dienelactone hydrolase ($dccD_{II}$) was interrupted by a part of an insertion element identical to IS*6100*. The ORF upstream of $dccA_{II}$ most likely codes for a transporter protein similar to the

COR-AAD1-00003493
Bayer EX1008 (Part 7 of 9)

TfdK 2,4-D transporter. Between $dccA_{II}$ and *tfdK*, the sequence revealed part of another insertion element (IS*Cc3*). The sequence information thus indicated that *S. herbicidovorans* MH harbored at least two complete genes for a chlorocatechol 1,2-dioxygenase, which both were located upstream of a (partial) dienelactone hydrolase gene. Evidence was also found for a chloromaleylacetate reductase upstream of $dccA_I$. Except for a gene for chloromuconate cycloisomerase, this would provide an almost complete modified *ortho* cleavage pathway to strain MH.

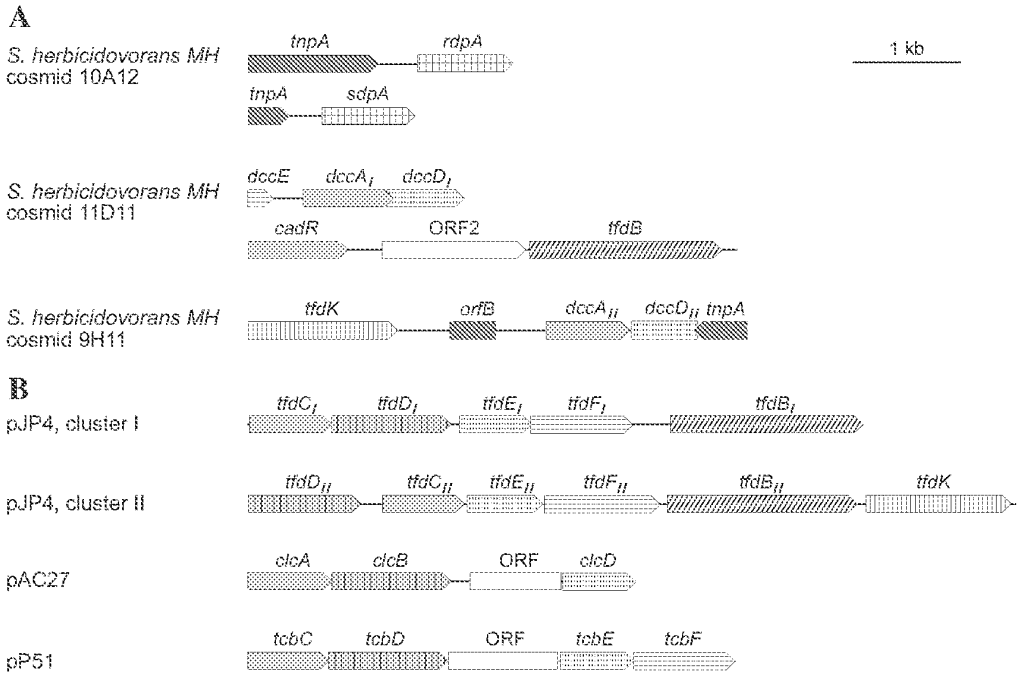


Fig. 2. (A) Configuration of phenoxyalkanoic acid degradation genes in *S. herbicidovorans* MH, (B) Comparison of the gene clusters for the modified *ortho*-cleavage degradation pathway in different bacteria. pJP4, *R. eutropha* JMP134 (M35097, U16782); pAC27, *P. putida* (M16964); pP51, *Pseudomonas* sp. (M57629). The arrows indicate the localization, the size and the direction of the transcription of the genes. Dashed lines around boxes represent incompletely sequenced open reading frames. Similar patterns of hatching and shading between genes indicate DNA homology or amino acid similarity of the translated gene products. α-ketoglutarate dependent dioxygenases, 2,4-D transport protein, (chloro)phenol hydroxylases, chlorocatechol 1,2-dioxygenases, chloromuconate cycloisomerases, dienelactone hydrolases, maleylacetate reductases, transposases.

COR-AAD1-00003494
Bayer EX1008 (Part 7 of 9)

Expression of $DccA_I$ and $DccA_{II}$ in *E. coli* BL21(DE3)(pLysS). The $dccA_I$ and $dccA_{II}$ ORFs were expressed in *E. coli* BL21(DE3)(pLysS) harboring pMec9 and pMec21. In both cell extracts, bands of the expected sizes 30.9 and 27.9 kDa, respectively, were seen on SDS-PAGE gels (not shown), which verified the translation of both genes in *E. coli*. Incubation of the cell extracts with 4-methylcatechol clearly showed the appearance of 4-methylmuconate with a maximal absorption at 255 nm (Fig. 3). The substrate range for both enzymes was determined in cell extracts from *E. coli* BL21(DE3)(pLysS) by incubation with different substituted catechols (Table 4). $DccA_I$ and $DccA_{II}$ exhibited essentially the same substrate range (Table 4). Both enzymes converted chloro- and methyl-substituted catechols; the highest activity was detected with 4-methylcatechol whereas 3,5-dichlorocatechol was preferred to monosubstituted catechols and catechol. 4,5-Dichlorocatechol was also converted, although at very low rates. No activity was measured with tetrachlorocatechol, *p*-nitrocatechol, protocatechuate, and hydroquinone.

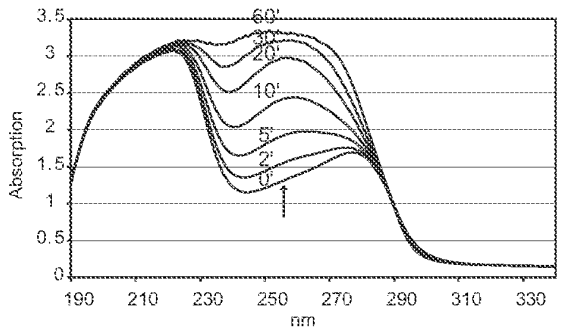


Fig. 3. UV-spectrum of 4-methylcatechol turnover by cell-extracts of *E. coli* BL21(DE3)(pLysS) harboring pMec9 induced with isopropyl-β-D-thiogalacto-pyranoside. The different lines represent different incubation times in min. The arrow points to the increase in absorption at 255 nm (λ_{max} of 3-methylmuconate).

COR-AAD1-00003495
Bayer EX1008 (Part 7 of 9)

Table 4. $DccA_I$ and $DccA_{II}$ activities with different substrates measured in cell-extract of *E. coli* BL21(DE3)(pLysS) harboring pMec9 or pMec21

Substrate	Activity $DccA_I$	$DccA_{II}$
Catechol	22.66[a] (±1.59)[b]	18.86[a] (±3.23)[b]
3-Chlorocatechol	41.02 (±1.93)	34.43 (±2.01)
4-Chlorocatechol	24.59 (±1.55)	22.13 (±0.69)
3-Methylcatechol	61.69 (±3.05)	47.16 (±3.40)
4-Methylcatechol	100 [1.48-2.59][c]	100 [1.12-2.15][c]
3,5-Dichlorocatechol	56.52 (±3.91)	49.11 (±2.88)
4,5-Dichlorocatechol	0.66 (±0.34)	0.64 (±0.31)
Tetrachlorocatechol	0	0
p-Nitrocatechol	0	0
Protocatechuate	0	0
Hydroquinone	0	0

[a] Enzyme activities in % compared to the value obtained with 4-methylcatechol. The data represent means of three independent cell-extracts of which each was measured three times with all substrates except for tetrachloro- and *p*-nitrocatechol, protocatechuate and hydroquinone, which represent means of two independent cell-extracts.

[b] Standard deviations

[c] The values in square brackets represent the range of specific activity in the cell extracts (in U/mg protein).

Expression of *rdpA*, *sdpA*, *dccA$_I$* and *dccA$_{II}$*. To investigate whether *rdpA*, *sdpA* and *dccA$_{I/II}$* were involved in phenoxyalkanoic acid degradation in *S. herbicidovorans* MH, we grew the strain in batch cultures with pyruvate and pulsed the culture with (*R*)-, (*S*)-mecoprop or 2,4-D. The formation of specific mRNAs was then determined by dotblot hybridizations (Fig. 4). Unexpectedly, mRNAs for *sdpA* and *rdpA* were always present, irrespective of the addition of mecoprop and 2,4-D, but mRNA for *dccA$_{I/II}$* appeared specifically after exposure to both mecoprop and 2,4-D (Fig. 4). It has to be noted, however, that the hybridization experiments cannot distinguish between *dccA$_I$* and *dccA$_{II}$* because of their high similarity. These results strongly suggest that mecoprop and 2,4-D induce a modified *ortho* cleavage pathway involving *dccA$_I$* and/or *dccA$_{II}$*.

COR-AAD1-00003496
Bayer EX1008 (Part 7 of 9)

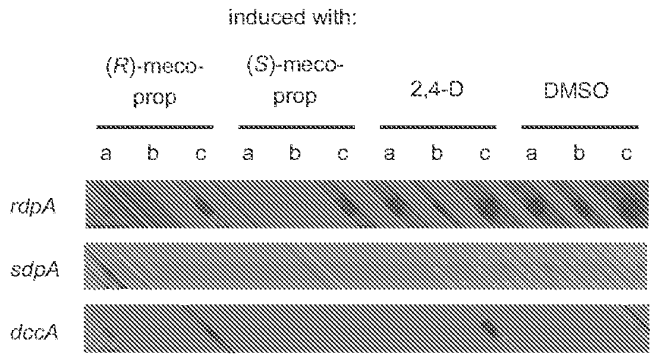


Fig. 4. Dot blot hybridization of total RNA isolated from batch cultures of *S. herbicidovorans* MH after induction with *(R)*-, *(S)*-mecoprop or 2,4-D. Antisense mRNA probes used for hybridization are indicated on the left. *(R)*-, *(S)*-mecoprop and 2,4-D on the top show the induction substrate; DMSO represents the uninduced state. a, b, c stand for individual replicates.

DISCUSSION

Phenoxyalkanoic acid degradation in *S. herbicidovorans* MH. Here we studied the genetic background of phenoxyalkanoic acid degradation in *S. herbicidovorans* strain MH. Several candidate genes were isolated, which showed similarity on amino acid level to other proteins involved in phenoxyalkanoic acid and chlorocatechol degradation. Strain MH harbors two genes encoding two α-ketoglutarate dependent dioxygenases (named $RdpA_{MH}$ and $SdpA_{MH}$), which were rather different to the archetypal TfdA enzyme (Table 3) but very similar to two dioxygenases from *D. acidovorans* MC1. Enzymes from *D. acidovorans* MC1 catalyze the enantioselective reaction of dichlorprop to dichlorophenol (53). $RdpA_{MH}$ and $SdpA_{MH}$ have been expressed in *E. coli* and indeed catalyze the enantioselective conversion of mecoprop and dichlorprop (Chapters 3 and 4). This strongly suggests that $RdpA_{MH}$ and $SdpA_{MH}$ catalyze the first step in the degradation pathway of mecoprop and dichlorprop in strain MH (Fig. 1). Both genes were constitutively expressed and not specifically induced upon exposure to mecoprop or 2,4-D. Previously, however, it was observed that the *(R)*-specific enzyme is only present when strain MH is grown on *(R)*-mecoprop, *(R)*-

COR-AAD1-00003497
Bayer EX1008 (Part 7 of 9)

dichlorprop or the racemate whereas *(S)*-activity is always present except when the strain is grown on the *(R)*-enantiomer (36). Therefore, it might be that expression of $rdpA_{MH}$ and $sdpA_{MH}$ is further regulated on the translational or posttranslational level.

S. herbicidovorans MH was shown to harbor two distinct chlorocatechol 1,2-dioxygenases genes, designated $dccA_I$ and $dccA_{II}$. Both genes were induced when strain MH was exposed to mecoprop or 2,4-D. When expressed in *E. coli*, $DccA_I$ and $DccA_{II}$ showed activity towards different substituted catechols but preferred 3,5-dichlorocatechol to monosubstituted catechols. Both enzymes showed essentially the same substrate specificities. From these results we conclude that $DccA_I$, $DccA_{II}$ or both are involved in dichlorprop, mecoprop and 2,4-D degradation in *S. herbicidovorans* MH. However, we do not know whether the two dichlorocatechol 1,2-dioxygenases have different roles.

We hypothesize that also the *tfdB*-like gene is involved in mecoprop and dichlorprop degradation in strain MH, although this was not specifically tested here. The finding of other genes from the modified *ortho*-cleavage pathway (i.e., dienelactone hydrolase and maleylacetate reductase) is further evidence to propose that 3,5-dichlorocatechol and 3-methyl-5-chlorocatechol are processed through a metabolic pathway similar to the one for 2,4-D degradation in *R. eutropha* JMP134 (pJP4) (Fig. 1). Currently, no information is available concerning the location of a chloromuconate cycloisomerase gene, the product of which would be needed to complete the pathway.

Genetic organization of phenoxyalkanoic degradation. The genes for phenoxyalkanoic acids degradation in *S. herbicidovorans* MH were not organized in one or two operons but scattered over the genome. The $rdpA_{MH}$ and $sdpA_{MH}$ gene were located on the same cosmid but separated by at least 10 kb. The genes for chlorophenol and chlorocatechol degradation were organized in three clusters, which were located on different cosmids. Such a gene organization is in contrast to that of the *tfd* genes for 2,4-D degradation in *R. eutropha* JMP134(pJP4), which are present in one compact region of 22 kb (29). A dispersed gene organization seems to be common for *Sphingomonas* strains. For instance, the *pcp* genes coding

COR-AAD1-00003498
Bayer EX1008 (Part 7 of 9)

for pentachlorophenol degradation in *Sphingobium chlorophenolicum* ATCC 39723 are organized on non-contigueous parts of the DNA (8). A scattered gene organization was also found for the dioxin-degradative genes in *Sphingomonas* sp. strain RW1 (2). The *lin* genes for lindane degradation in *Sphingomonas paucimobilis* are present in five different operons and unlinked clusters (28). This contrasting gene organization in sphingomonads may have consequences for regulation of pathway expression. Expression of $rdpA_{MH}$ and $sdpA_{MH}$ in strain MH was constitutive whereas $dccA_{I/II}$ were inducibly expressed. This scheme is similar to the one for expression of the lindane pathway in *S. paucimobilis*, where the first three genes are constitutively expressed and only the genes for chlorohydroquinone conversion are inducible (34). In contrast, the 2,4-D pathway in *R. eutropha* JMP134 (pJP4) is very tightly regulated (31, 32). It might be that the organization observed in *Sphingomonas herbicidovorans* MH is not optimized yet and that regulatory networks controlling *rdpA* and *sdpA* expression will evolve when the strain remains being exposed to phenoxyalkanoic acid containing environments. On the other hand, the absence of inducible expression might just be a different strategy found in sphingomonads compared to pseudomonads, which nonetheless results in functional catabolic pathways. When considering that inducible catabolic pathways often seem to need a threshold concentration before induction takes place, it may even be an advantageous strategy to continously produce the first enzymes necessary for the pathway.

Potentially two clusters might be involved in chlorocatechol degradation in strain MH. Both clusters clearly have a different gene order than the typical operons for chlorocatechol such as the *clcABD* genes from *P. putida* (pAC27) (14), the *tfdCDEF* genes in *R. eutropha* JMP134(pJP4) (9, 19, 20, 38) and the *tcbCDEF* genes in *Pseudomonas* sp. P51 (52) (Fig. 2B). It was noteworthy, that a gene for a chloromuconate cycloisomerase was not present within the regions sequenced from strain MH. Furthermore, cluster II was flanked by sequences with clear homology to (parts of) IS-elements that even interrupted $dccD_{II}$; this points at (recent) genetic rearrangements.

COR-AAD1-00003499
Bayer EX1008 (Part 7 of 9)

Evolutionary aspects of the phenoxyalkanoic acid degradation pathway in *S. herbicidovorans* MH. It has been proposed that phenoxyalkanoic acid degradation genes are highly mobile and thus are easily transferred among bacteria (17, 24, 33, 48, 49). On the other hand, gene flow is assumed to be less frequent between *Alphaproteobacteria* and *Beta-* and *Gammaproteobacteria* than among *Beta-* and *Gammaproteobacteria* (17). The unique combination and organization of the phenoxyalkanoic acid degradation genes in *S. herbicidovorans* MH indicate that a recent gene exchange between *Alpha-* and *Betaproteobacteria* must have taken place. This can be concluded from the finding that $RdpA_{MH}$ is 100% identical to $RdpA_{MC1}$ from *D. acidovorans* MC1, a member of the *Betaproteobacteria*. The transposase genes located next to $rdpA_{MH}$ and $sdpA_{MH}$ also support the hypothesis of gene mobilization. The transposase gene located nearby $rdpA_{MH}$ is very similar to a presumably promiscuous IS element which was implicated in transferring the toluene dioxygenase from *Ralstonia* sp. strain JS745 to *Ralstonia* sp. strain JS705 (35).

$RdpA_{MH}$ and $SdpA_{MH}$ are only modestly similar to TfdAα, the *tfdA*-like representatives of other *Alphaproteobacteria*, but more similar to the respective genes in the *Betaproteobacteria D. acidovorans* MC1. This contradicts the hypothesis that the *tfdA*-like representatives of *Alphaproteobacteria* and *Beta-* and *Gammaproteobacteria* have arisen by divergent evolution (23). However, all known *Alphaproteobacteria* harboring tfdAα have been isolated from pristine environments whereas *S. herbicidovorans* MH was isolated from a soil column percolated with dichlorprop (22). These conditions might have been more favorable for selection of *S. herbicidovorans* MH transconjugants which harbor a *rdp* gene than those carrying a *tfdAα* gene.

COR-AAD1-00003500
Bayer EX1008 (Part 7 of 9)

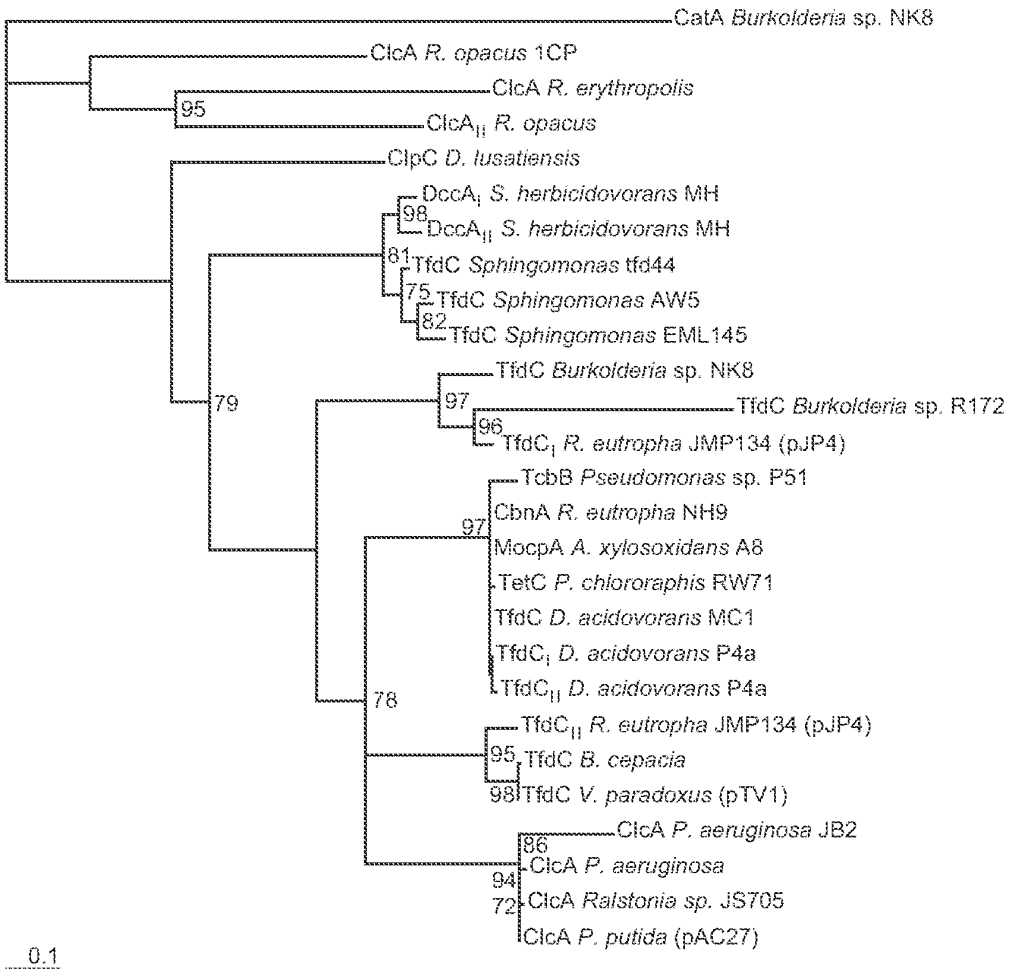


Fig. 5. Dendrogram illustrating sequence similarities of chlorocatechol 1,2-dioxygenases. The dendrogram was constructed as described in the material and methods section. CatA from *Burkholderia* sp. NK8 was used as an outgroup. The *dccA$_{I/II}$*-genes from *S. herbicidovorans* MH are the only completely sequenced chlorocatechol 1,2-dioxygenases from a *Sphingomonas* strain. The partial PCR-sequences deposited in the database and their conceptual translations for other *Sphingomonas* strains were used to perform the dendrogram since the classification was not affected by the shortened sequences. The numbers at the branches stand for quartet puzzling (QP) reliability. Branches with values in the range of 90-100% are very strongly supported and with values >70% are principally reliable. Accession numbers for the sequences: TfdC *R. eutropha* JMP134(pJP4) P05403; TfdC$_{II}$ *R. eutropha* JMP134(pJP4) AAC44730; TfdC *D. acidovorans* P4a AAC35836, TfdC$_{II}$ *D. acidovorans* P4a AAM76776; TfdC *Burkholderia* sp. NK8 BAB56009; TfdC *Variovorax paradoxus* (pTV1) AAC01745; TfdC *Burkholderia cepacia* AAK81678; CbnA *R. eutropha* NH9 BAA74530; TetC *Pseudomonas chlororaphis* RW71 CAB89821; MocpA *Achromobacter xylosoxidans* A8 CAD56206; TcbB *Pseudomonas* sp. P51 P27098; ClcA *Pseudomonas aeruginosa* AAF00195; ClcA *P. putida* (pAC27) P11451; ClcA *Ralstonia* sp. JS705 CAA06968; ClcA *P. aeruginosa* JB2 AAC69474;

COR-AAD1-00003501
Bayer EX1008 (Part 7 of 9)

In contrast to the α-ketoglutarate dependent dioxygenase genes, chlorocatechol 1,2-dioxygenases from *Beta-* and *Gammaproteobacteria* present in the database are less related to $DccA_{I/II}$ than they are among themselves. The phylogenetic relationships of strain MH chlorocatechol 1,2-dioxygenases became apparent in a dendrogram that includes several (chloro)catechol 1,2-dioxygenase and places the one from *Burkholderia* sp. NK8 as an outgroup (Fig. 5). The chlorocatechol 1,2-dioxygenases from Gram-positive bacteria clearly grouped together and formed a separate branch, which is in agreement with the results obtained by Eulberg et al. (12). Six different groups of chlorocatechol 1,2-dioxygenase could be defined: (i) ClpC, (ii) *Sphingomonas* homologs, (iii) TfdC_pJP4 homologs, (iv) the TcbC-TetC-group, (v) $TfdC_{II}$_pJP4 homologs and (vi) the ClcA homologs. Subgroups (i) and (ii) build new branches whereas the classification of subgroups (iii) to (vi) agrees with the one described by Armengaud et al. (3). The two novel groups comprise sequences from *Alphaproteobacteria*, which were included for the first time in a dendrogram. The analysis shows a separate cluster of *Sphingomonas* chlorocatechol 1,2-dioxygenases and supports our hypothesis that *Sphingomonas* strains have not exchanged their different chlorocatechol 1,2-dioxygenase genes recently with those from *Beta-* and *Gammaproteobacteria*. The phenoxyalkanoic acid degradation pathway of strain MH turned out to be unique in its composition, genetic organization and regulation and it will be important to further study its characteristics in order to broaden our understanding of pathways different to the canonical 2,4-D degradation pathways in *Beta-* and *Gammaproteobacteria*.

Fig. 5 (cont.) ClpC *Defluvibacter lusatiensis* CAD60254; TfdC *Burkholderia* sp. R172 AAP92136; ClcA *Rhodococcus erythropolis* JC6206; ClcA *Rhodococcus opacus* 1CP AAC38251; CatA *Burkholderia* sp. NK8 BAB21462. For the partial sequences, the conceptual translation supplied by the authors was used and the accession numbers refer to the protein databases. *tfdC Sphingomonas* sp. tfd44 AAC23513; *tfdC D. acidovorans* MC1 AAD55082; *tfdC Sphingomonas* sp. EML 146 AAC23511; *tfdC Sphingomonas* sp. AW5 AAC23512.

COR-AAD1-00003502
Bayer EX1008 (Part 7 of 9)

REFERENCES

1. Ahrens, W. H. 1994. Herbicide Handbook (WSSA), 7th ed. Weed Science Society of America, Champaign.
2. Armengaud, J., B. Happe, and K. N. Timmis. 1998. Genetic analysis of dioxin dioxygenase of *Sphingomonas* sp. strain RW1: catabolic genes dispersed on the genome. J. Bacteriol. 180:3954-3966.
3. Armengaud, J., K. N. Timmis, and R. M. Wittich. 1999. A functional 4-hydroxysalicylate/hydroxyquinol degradative pathway gene cluster is linked to the initial dibenzo-*p*-dioxin pathway genes in *Sphingomonas* sp. strain RW1. J. Bacteriol. 181:3452-3461.
4. Ausubel, F. M., R. Brent, R. E. Kingston, D. D. Moore, J. G. Seidman, J. A. Smith, and K. Struhl (ed.). 2002. Current protocols in molecular biology. John Wiley & Sons, Inc., New York, N. Y.
5. Benes, V., Z. Hostomosky, L. Arnold, and V. Paces. 1993. M13 and pUC vectors with new unique restriction sites for cloning. Gene 130:151-152.
6. Benndorf, D., and W. Babel. 2002. Assimilatory detoxification of herbicides by *Delftia acidovorans* MC1: induction of two chlorocatechol 1,2-dioxygenases as a response to chemostress. Microbiology 148:2883-2888.
7. Broderick, J. B., and T. V. O'Halloran. 1991. Overproduction, purification, and characterization of chlorocatechol dioxygenase, a non-heme iron dioxygenase with broad substrate tolerance. Biochemistry 30:7349-7358.
8. Cai, M., and L. Xun. 2002. Organization and regulation of pentachlorophenol-degrading genes in *Sphingobium chlorophenolicum* ATCC 39723. J. Bacteriol. 184:4672-4680.
9. Don, R. H., A. J. Weightman, H.-J. Knackmuss, and K. N. Timmis. 1985. Transposon mutagenesis and cloning analysis of the pathways for degradation of 2,4-dichlorophenoxyacetic acid and 3-chlorobenzoate in *Alcaligenes eutrophus* JMP134(pJP4). J. Bacteriol. 161:85-90.
10. Donaldson, D., T. Kiely, and A. Grube. 2002. Pesticides industry sales and usage. 1998 and 1999 market estimates. U.S. Environmental Protection Agency.
11. Dorn, E., and H. J. Knackmuss. 1978. Chemical structure and biodegradability of halogenated aromatic compounds. Two catechol 1,2-dioxygenases from a 3-chlorobenzoate-grown pseudomonad. Biochem. J. 174:73-84.
12. Eulberg, D., L. A. Golovleva, and M. Schlömann. 1997. Characterization of catechol catabolic genes from *Rhodococcus erythropolis* 1CP. J. Bacteriol. 179:370-381.
13. Farhana, L., and P. B. New. 1997. The 2,4-dichlorophenol hydroxylase of *Alcaligenes eutrophus* JMP134 is a homotetramer. Can. J. Microbiol. 43:202-205.
14. Frantz, B., and A. M. Chakrabarty. 1987. Organization and nucleotide sequence determination of a gene cluster involved in 3-chlorocatechol degradation. Proc. Natl. Acad. Sci. USA 84:4460-4464.
15. Fukumori, F., and R. P. Hausinger. 1993. *Alcaligenes eutrophus* JMP134 "2,4-dichlorophenoxyacetate monooxygenase" is a α-ketoglutarate-dependent dioxygenase. J. Bacteriol. 175:2083-2096.

COR-AAD1-00003503
Bayer EX1008 (Part 7 of 9)

16. Fukumori, F., and R. P. Hausinger. 1993. Purification and characterization of 2,4-dichlorophenoxyacetate/α-ketoglutarate dioxygenase. J. Biol. Chem. 268:24311-24317.

17. Fulthorpe, R. R., C. McGowan, O. V. Maltseva, W. E. Holben, and J. M. Tiedje. 1995. 2,4-Dichlorophenoxyacetic acid-degrading bacteria contain mosaics of catabolic genes. Appl. Environ. Microbiol. 61:3274-3281.

18. Fulthorpe, R. R., A. N. Rhodes, and J. M. Tiedje. 1996. Pristine soils mineralize 3-chlorobenzoate and 2,4-dichlorophenoxyacetate via different microbial populations. Appl. Environ. Microbiol. 62:1159-1166.

19. Ghosal, D., and I.-S. You. 1988. Nucleotide homology and organization of chlorocatechol oxidation genes of plasmids pJP4 and pAC27. Mol. Gen. Genet. 211:113-120.

20. Ghosal, D., and I. S. You. 1989. Operon structure and nucleotide homology of the chlorocatechol oxidation genes of plasmids pJP4 and pAC27. Gene 83:225-232.

21. Häggblom, M. M. 1992. Microbial breakdown of halogenated aromatic pesticides and related compounds. FEMS Microbiol. Rev. 103:29-72.

22. Horvath, M., G. Ditzelmüller, M. Loidl, and F. Streichsbier. 1990. Isolation and characterization of a 2-(2,4-dichlorophenoxy)propionic acid degrading soil bacterium. Appl. Microbiol. Biotechnol. 33:213-216.

23. Itoh, K., R. Kanda, Y. Sumita, H. Kim, Y. Kamagata, K. Suyama, H. Yamamoto, R. P. Hausinger, and J. M. Tiedje. 2002. *tfdA*-Like genes in 2,4-dichlorophenoxyacetic acid-degrading bacteria belonging to the *Bradyrhizobium-Agromonas-Nitrobacter-Afipia* cluster in α-*proteobacteria.* Appl. Environ. Microbiol. 68:3449-3454.

24. Ka, J. O., W. E. Holben, and J. M. Tiedje. 1994. Genetic and phenotypic diversity of 2,4-dichlorophenoxyacetic acid (2,4-D)-degrading bacteria isolated from 2,4-D-treated field soils. Appl. Environ. Microbiol. 60:1106-1115.

25. Kitagawa, W., S. Takami, K. Miyauchi, E. Masai, Y. Kamagata, J. M. Tiedje, and M. Fukuda. 2002. Novel 2,4-dichlorophenoxyacetic acid degradation genes from oligotrophic *Bradyrhizobium* sp. strain HW13 isolated from a pristine environment. J. Bacteriol. 184:509-518.

26. Kohler, H.-P. E. 1999. *Sphingomonas herbicidovorans* MH: a versatile phenoxyalkanoic herbicide degrader. J. Ind. Microbiol. Biotechnol. 23:336-340.

27. Kuhm, A. E., M. Schlömann, H. J. Knackmuss, and D. H. Pieper. 1990. Purification and characterization of dichloromuconate cycloisomerase from *Alcaligenes eutrophus* JMP 134. Biochem. J. 266:877-883.

28. Kumari, R., S. Subudhi, M. Suar, G. Dhingra, V. Raina, C. Dogra, S. Lal, J. R. van der Meer, C. Holliger, and R. Lal. 2002. Cloning and characterization of *lin* genes responsible for the degradation of hexachlorocyclohexane isomers by *Sphingomonas paucimobilis* strain B90. Appl. Environ. Microbiol. 68:6021-6028.

29. Laemmli, C. M., J. H. J. Leveau, A. J. B. Zehnder, and J. R. van der Meer. 2000. Characterization of a second *tfd* gene cluster for chlorophenol and chlorocatechol metabolism on plasmid pJP4 in *Ralstonia eutropha* JMP134(pJP4). J. Bacteriol. 182:4165-4172.

30. Leander, M., T. Vallaeys, and R. Fulthorpe. 1998. Amplification of putative chlorocatechol dioxygenase gene fragments from α- and *β-proteobacteria.* Can. J. Microbiol. 44:482-486.

COR-AAD1-00003504
Bayer EX1008 (Part 7 of 9)

31. Leveau, J. H. J., F. König, H. Füchslin, C. Werlen, and J. R. van der Meer. 1999. Dynamics of multigene expression during catabolic adaptation of *Ralstonia eutropha* JMP134(pJP4) to the herbicide 2,4-dichlorophenoxyacetate. Mol. Microbiol. 33:396-406.

32. Leveau, J. H. J., and J. R. van der Meer. 1996. The *tfdR* gene product can successfully take over the role of the insertion element-inactivated TfdT protein as a transcriptional activator of the *tfdCDEF* gene cluster, which encodes chlorocatechol degradation in *Ralstonia eutropha* JMP134(pJP4). J. Bacteriol. 178:6824-6832.

33. McGowan, C., R. Fulthorpe, A. Wright, and J. M. Tiedje. 1998. Evidence for interspecies gene transfer in the evolution of 2,4-dichlorophenoxyacetic acid degraders. Appl. Environ. Microbiol. 64:4089-4092.

34. Miyauchi, K., H.-S. Lee, M. Fukuda, M. Takagi, and Y. Nagata. 2002. Cloning and characterization of *linR*, involved in regulation of the downstream pathway for γ-hexachlorocyclohexane degradation in *Sphingomonas paucimobilis* UT26. Appl. Environ. Microbiol. 68:1803-1807.

35. Müller, T. A., C. Werlen, J. Spain, and J. R. van der Meer. 2003. Evolution of a chlorobenzene degradative pathway among bacteria in a contaminated groundwater mediated by a genomic island in *Ralstonia*. Environ. Microbiol. 5:163-173.

36. Nickel, K., M. J.-F. Suter, and H.-P. E. Kohler. 1997. Involvement of two α-ketoglutarate-dependent dioxygenases in enantioselective degradation of (*R*)- and (*S*)-mecoprop by *Sphingomonas herbicidovorans* MH. J. Bacteriol. 179:6674-6679.

37. Pérez-Pantoja, D., L. Guzmán, M. Manzano, D. H. Pieper, and B. González. 2000. Role of $tfdC_ID_IE_IF_I$ and $tfdD_{II}C_{II}E_{II}F_{II}$ gene modules in catabolism of 3-chlorobenzoate by *Ralstonia eutropha* JMP134(pJP4). Appl. Environ. Microbiol. 66:1602-1608.

38. Perkins, E. J., M. P. Gordon, O. Caceres, and P. F. Lurquin. 1990. Organization and sequence analysis of the 2,4-dichlorophenol hydroxylase and dichlorocatechol oxidative operons of plasmid pJP4. J. Bacteriol. 172:2351-2359.

39. Plumeier, I., D. Pérez-Pantoja, S. Heim, B. González, and D. H. Pieper. 2002. Importance of different *tfd* genes for degradation of chloroaromatics by *Ralstonia eutropha* JMP134. J. Bacteriol. 184:4054-4064.

40. Sambrook, J., E. F. Fritsch, and T. Maniatis. 1989. Molecular Cloning: a laboratory manual. Cold Spring Harbor Laboratory, Cold Spring Harbor, N.Y.

41. Schlömann, M. 1994. Evolution of chlorocatechol catabolic pathways. Biodegradation 5:301-321.

42. Smejkal, C. W., T. Vallaeys, S. K. Burton, and H. M. Lappin-Scott. 2001. Substrate specificity of chlorophenoxyalkanoic acid-degrading bacteria is not dependent upon phylogenetically related *tfdA* gene types. Biol. Fertil. Soils 33:507-513.

43. Streber, W. R., K. N. Timmis, and M. H. Zenk. 1987. Analysis, cloning, and high-level expression of 2,4-dichlorophenoxyacetate monooxygenase gene *tfdA* of *Alcaligenes eutrophus* JMP134. J. Bacteriol. 169:2950-2955.

COR-AAD1-00003505
Bayer EX1008 (Part 7 of 9)

44. Studier, F. W., and B. A. Moffatt. 1986. Use of bacteriophage T7 RNA polymerase to direct selective high-level expression of cloned genes. J. Mol. Biol. 189:113-130.

45. Tatusova, T. A., and T. L. Madden. 1999. BLAST 2 sequences, a new tool for comparing protein and nucleotide sequences. FEMS Microbiol. Lett. 174:247-250.

46. Tett, V. A., A. J. Willetts, and H. M. Lappin-Scott. 1997. Biodegradation of the chlorophenoxy herbicide (*R*)-(+)-mecoprop by *Alcaligenes denitrificans*. Biodegradation 8:43-52.

47. Thompson, J. D., T. J. Gibson, F. Plewniak, F. Jeanmougin, and D. G. Higgins. 1997. The CLUSTAL_X windows interface: flexible strategies for multiple sequence alignment aided by quality analysis tools. Nucl. Acids Res. 25:4876-4882.

48. Vallaeys, T., L. Courde, C. McGowan, A. D. Wright, and R. R. Fulthorpe. 1999. Phylogenetic analyses indicate independent recruitment of diverse gene cassettes during assemblage of the 2,4-D catabolic pathway. FEMS Microbiol. Ecol. 28:373-382.

49. Vallaeys, T., R. R. Fulthorpe, A. M. Wright, and G. Soulas. 1996. The metabolic pathway of 2,4-dichlorophenoxyacetic acid degradation involves different families of *tfdA* and *tfdB* genes according to PCR-RFLP analysis. FEMS Microbiol. Ecol. 20:163-172.

50. van der Meer, J. R. 1997. Evolution of novel metabolic pathways for the degradation of chloroaromatic compounds. Antonie van Leeuwenhoek 71:159-178.

51. van der Meer, J. R., W. M. de Vos, S. Harayama, and A. J. B. Zehnder. 1992. Molecular mechanisms of genetic adapation to xenobiotic compounds. Microbiol. Rev. 56:677-694.

52. van der Meer, J. R., R. I. L. Eggen, A. J. B. Zehnder, and W. M. de Vos. 1991. Sequence analysis of the *Pseudomonas* sp. strain P51 *tcb* gene cluster, which encodes metabolism of chlorinated catechols: evidence for specialization of catechol 1,2-dioxygenases for chlorinated substrates. J. Bacteriol. 173:2425-2434.

53. Westendorf, A., D. Benndorf, R. H. Müller, and W. Babel. 2002. The two enantiospecific dichlorprop/α-ketoglutarate-dioxygenases from *Delftia acidovorans* MC1 - protein and sequence data of RdpA and SdpA. Microbiol. Res. 157:1-6.

54. Westendorf, A., R. H. Müller, and W. Babel. 2003. Purification and characterisation of the enantiospecific dioxygenases from *Delftia acidovorans* MC1 initiating the degradation of phenoxypropionate and phenoxyacetate herbicides. Acta Biotechnol. 23:3-17.

55. Worthing, C. R., and R. J. Hance. 1991. The Pesticide Manual - A World Compendium, 9th ed. The British Crop Council, Farnham, Great Britain.

56. Zipper, C. 1998. Microbial degradation and environmental fate of chiral phenoxyalkanoic acid herbicides. Ph. D. thesis. ETH Zürich, Zürich.

57. Zipper, C., M. Bunk, A. J. B. Zehnder, and H.-P. E. Kohler. 1998. Enantioselective uptake and degradation of the chiral herbicide dichlorprop [(*RS*)-2-(2,4-dichlorophenoxy)propanoic acid] by *Sphingomonas herbicidovorans* MH. J. Bacteriol. 180:3368-3374.

COR-AAD1-00003506
Bayer EX1008 (Part 7 of 9)

58. Zipper, C., K. Nickel, W. Angst, and H.-P. E. Kohler. 1996. Complete microbial degradation of both enantiomers of the chiral herbicide mecoprop [(*RS*)-2-(4-chloro-2-methylphenoxy)propionic acid] in an enantioselective manner by *Sphingomonas herbicidovorans* sp. nov. Appl. Environ. Microbiol. 62:4318-4322.

COR-AAD1-00003507
Bayer EX1008 (Part 7 of 9)

CHAPTER 3

Purification and Characterization of α-Ketoglutarate-dependent *(R)*-Dichlorprop Dioxygenase RdpA from *Sphingomonas herbicidovorans* MH

Sphingomonas herbicidovorans MH harbors two distinct α-ketoglutarate-dependent dichlorprop dioxygenases involved in phenoxyalkanoic acid herbicide degradation. Here, we report the purification and biochemical characterization of the *(R)*-dichlorprop dioxygenase (RdpA). RdpA was expressed and purified as a 6xHis-tagged fusion protein from *E. coli* BL21(DE3)(pLysS). RdpA belongs to subgroup II of α-ketoglutarate-dependent dioxygenases and has the specific common motif $HXDX_{24}TX_{131}HX_{10}R$. His-111, Asp-113 and His-270 build the 2-His-1-carboxylate facial triad and are predicted to be involved in iron binding. RdpA enantiospecifically transformed only the (*R*) enantiomers of mecoprop and dichlorprop with α-ketoglutarate as cosubstrate to the achiral phenols under concomitant release of succinate and pyruvate. Kinetic investigations showed highest affinity to *(R)*-mecoprop [2-(*R*)-2-methyl-4-chlorophenoxypropanoic acid] (K_m-value = 98.8 μM) and highest turnover rates for *(R)*-4-chlorophenoxypropanoic acid (k_{cat} = 241.9 min^{-1}). RdpA preferred phenoxypropanoic acids to other phenoxyalkanoic acids indicating that the alkyl moiety attached to α-carbon atom plays an important role for optimal orientation of the substrate at the active site. The apparent K_m-value for α-ketoglutarate was 2.8 μM. RdpA did not exhibit Michaelis-Menten kinetics with oxygen as a substrate, but was linearly dependent on O_2 in the measured range of air-saturated water (0-0.23 mM). Only 2-oxoadipate could replace α-ketoglutarate as cosubstrate, but activity was reduced to 2% of the activity on mecoprop with α-ketoglutarate. Ferrous iron was necessary for full activity of the enzyme and other divalent cations could not replace it.

Submitted to the Journal of Bacteriology (July 2004) by T. A. Müller, T. Fleischmann, J. R. van der Meer, H.-P. E. Kohler.

COR-AAD1-00003509
Bayer EX1008 (Part 7 of 9)

INTRODUCTION

Phenoxyalkanoic acid herbicides are widely used to control broadleaf weeds in agriculture, lawn pastures and industries. They are systemic and post emergence herbicides and act as synthetic auxins (1, 2, 26). Representatives are mecoprop (2-(*R,S*)-2-methyl-4-chlorophenoxypropanoic acid), dichlorprop (2-(*R,S*)-2,4-dichloro-phenoxypropanoic acid) and 2,4-D (2,4-dichlorophenoxyacetic acid). Mecoprop and dichlorprop are chiral, have one stereogenic center and therefore, exist as two enantiomers. Already in the fifties, it was shown that only the (*R*) enantiomers have herbicidal effects (27). However, both enantiomers were and still are applied and thereby, large amounts of isomeric ballast are introduced into the environment (11, 46, 47). *Sphingomonas herbicidovorans* MH, an *Alphaproteo-bacterium*, is able to grow on both enantiomers of mecoprop and dichlorprop and on 2,4-D as sole carbon and energy source (20, 22, 49). In batch cultures, it degrades the two enantiomers sequentially, the *(S)* enantiomer being used first. (23, Chapter 1).

In *S. herbicidovorans* MH, the chiral mecoprop or dichlorprop is converted to the achiral phenol in an enantioselective reaction (Fig. 1). Nickel *et al.* (33) showed in experiments with cell-extracts, that two distinct enzymes are involved, which are highly specific for the respective enantiomer and that both enzymes belong to the enzyme family of α-ketoglutarate-dependent dioxygenases. α-Ketoglutarate-dependent dioxygenases build a heterologous group of enzymes, which are classified according to their biochemical characteristics. They are non-heme iron dioxygenases and require oxygen and α-ketoglutarate as cosubstrates, ferrous ion as cofactor and ascorbate as a reducing agent. They catalyze a wide range of oxidative processes such as hydroxylations, epoxidations, desaturations, ring formation and expansion reactions (for reviews, see 8, 17, 25, 36, 41). Despite the diversity of their primary sequence, all of these dioxygenases have a 2-His-1-carboxylate facial triad (for a review, see 18) at the catalytic center. Furthermore, they have a motif in common according to which they are grouped into three sub-groups (19). Important here is subgroup II, of which the representatives have the motif $HX(D/E)X_{23\text{-}26}(T/S)X_{114\text{-}183}HX_{10\text{-}13}R$. Well known members are the α-

COR-AAD1-00003510
Bayer EX1008 (Part 7 of 9)

ketoglutarate-dependent taurine dioxygenase (TauD) from *Escherichia coli* involved in taurine utilization (12) and 2,4-D dioxygenase (TfdA) from *R. eutropha* JMP134(pJP4) involved in 2,4-D degradation (14-16). TfdA catalyzes the oxidative cleavage of the ether-bond in 2,4-D to 2,4-dichlorophenol.

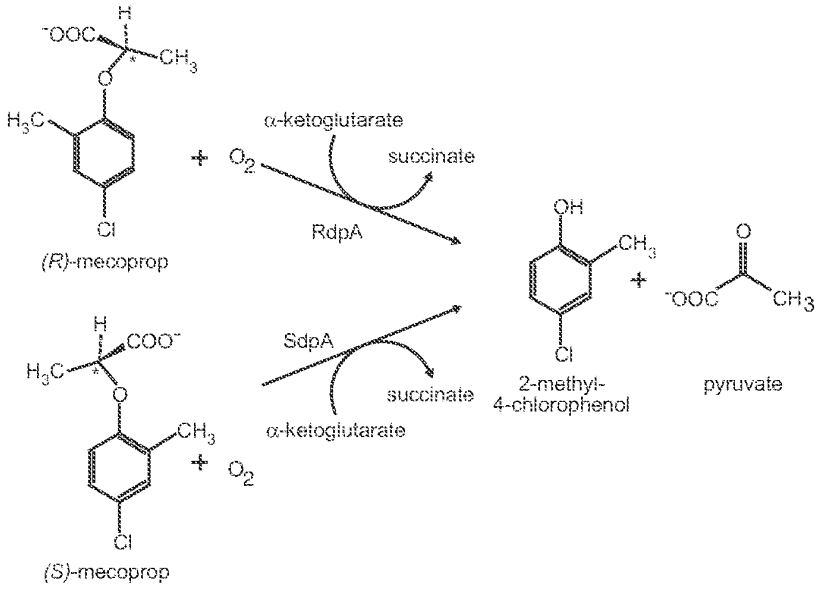


Fig. 1. Initial degradation step of chiral phenoxypropanoic acids *in S. herbicidovorans* MH catalyzed by the α-ketoglutarate-dependent *(R)*-dichlorprop dioxygenases (RdpA) and α-ketoglutarate-dependent *(S)*-dichlorprop dioxygenases (SdpA).

Recently, the genes coding for the enzymes involved in phenoxypropanoic acid degradation in *S. herbicidovorans* MH have been identified and isolated (Chapter 2). The genes for two α-ketoglutarate-dependent dioxygenases named RdpA and SdpA were discovered and are likely to be responsible for the initial degradation steps of mecoprop and dichlorprop. At amino acid level, RdpA is 30% identical to TfdA but 100% to RdpA from *Delftia acidovorans* MC1, another phenoxypropanoic acid degrader (28, 44). The primary sequence of SdpA, on the other hand, only showed 30% amino acid identity with RdpA.

In this study, we expressed and purified RdpA as a 6xHis-tagged fusion protein. Enzyme activity measurements with the purified protein verified the

COR-AAD1-00003511
Bayer EX1008 (Part 7 of 9)

classification as an α-ketoglutarate-dependent dioxygenase and primary sequence alignment showed that RdpA belonged to subgroup II. We further characterized RdpA in terms of kinetic behavior for different substrates and cosubstrates, determined the (co)substrate specificities, and provided evidence that RdpA exclusively converts the *(R)* enantiomer of phenoxypropanoic acid herbicides.

MATERIALS AND METHODS

Bacterial strains and culture conditions. *Escherichia coli* DH5α was used as a host for cloning experiments and *E. coli* BL21(DE3)(pLysS) as a host for expression studies with constructs in pET-15b (Novagen, Darmstadt, Germany). *E. coli* strains were grown at 30°C or 37°C in Luria-Bertani (LB) medium (40). When appropriate, ampicillin and chloramphenicol were added at 50 μg/ml and 25 μg/ml final concentrations, respectively. Solid media were prepared by the addition of 1.5% (w/v) agar.

Standard molecular techniques. Cloning and digestions were done according to established procedures (4, 40). Restriction enzymes and other DNA modifying enzymes were purchased from Promega (Wallisellen, Switzerland) and Fermentas (Nunningen, Switzerland). Plasmids and cosmids were isolated by the boiling miniprep method, the alkaline lysis method according to Sambrook *et al.* (40) or with the E.Z.N.A. plasmid miniprep kit II (Peqlab Biotechnologies GmbH, Baden-Dättwil, Switzerland) as suggested by the manufacturer. Gel extraction was carried out with the MinElute Gel Extraction Kit (Qiagen AG, Basel, Switzerland) according to the protocol of the supplier.

Construction of N-terminal His-tagged recombinant RdpA expression plasmid. Expression plasmid pMec15 was constructed in the PCR by reamplification of the *rdpA* gene from pMec10 (Chapter 2) with the following primers: 5'-CGC TCA TAT GCA TGC TGC ACT-3' and 5'-AGC GGG GAT CCG CGT CGC C-3'. Thereby, a *Nde*I restriction site at the translational start and a *Bam*HI restriction site just past the stop codon were introduced (underlined nucleotides). The fragment was first cloned into pGEM®-T Easy (Promega) generating pMec14 and verified by sequencing. The plasmid was then digested with *Nde*I and *Bam*HI and ligated into the same sites of vector pET-15b yielding pMec15.

Expression and purification of recombinant RdpA. *E. coli* BL21(DE3)(pLysS) harboring pMec15 was grown in Erlenmeyer flasks containing LB-medium complemented with ampicillin and chloramphenicol at 30°C with constant shaking. To express the proteins, a preculture of *E. coli* BL21(DE3)(pLysS) harboring pMec15 was grown overnight at 37°C. A volume of 1% (v/v) of the preculture was transferred to fresh medium and grown at 30°C until an optical density of 0.4–0.6 (measured at 546 nm) was reached, after which isopropyl-β-D-

COR-AAD1-00003512
Bayer EX1008 (Part 7 of 9)

thiogalactopyranoside was added to a final concentration of 1 mM. The culture was incubated for another 3 hours at 30°C and the cells were harvested by centrifugation at 7'500 × *g* for 30 min at 4°C and the pellet was stored at –20°C until further use. For the preparation of cell extracts, 1 g of cells (wet weight) was resuspended in 3 ml of lysis buffer (50 mM NaH_2PO_4, 300 mM NaCl, 10 mM imidazole, pH adjusted to 8) and the cells were broken by one passage through a French press at 1 MPa. The lysate was centrifuged for 45 min at 16'000 × *g* at 4°C and aliquots were stored at –20°C.

RdpA was purified in a one-step procedure. Up to one mg of protein was loaded on a 2-ml Ni-NTA superflow-agarose column (Qiagen) at a flow rate of 0.5 ml/min. Unbound protein was removed stepwise with three times five column volumes of wash-buffer (50 mM NaH_2PO_4, 300 mM NaCl) containing 20 mM, 50 mM, and 100 mM imidazole (pH adjusted to 8), respectively, at the same flow rate. RdpA was then eluted in 1-ml fractions with elution buffer (50 mM NaH_2PO_4, 300 mM NaCl, 250 mM imidazole, pH adjusted to 8) at a flow rate of 0.8 ml/min. The active fractions were pooled and desalted into 20 mM Tris-HCl, pH 7.5, using PD-10 columns (Amersham Biosciences, Dübendorf, Switzerland) and stored at 4°C. Thrombin protease (Amersham Biosciences) was used to cleave the N-terminal His-tag. The N-terminal His-tag of approximately 10 μg of RdpA was completely cleaved by 0.5 U of thrombin protease within 2 h at room temperature.

Enzyme Activity Assays. *Coupled continuous assay.* For purification and kinetic measurements of phenoxypropanoic acids, a coupled continuous assay using L-lactate dehydrogenase from rabbit muscle (Sigma-Aldrich, Buchs, Switzerland) as a reporter enzyme was developed. RdpA converts (substituted) phenoxypropanoic acids stoichiometrically to the corresponding phenol and pyruvate. Pyruvate is converted by L-lactate dehydrogenase to lactate with concomitant consumption of NADH. NADH-consumption was monitored spectrophotometrically by the decrease of absorbance at 340 nm. The extinction coefficient of 6.3 $\mu Mol^{-1} \times ml \times cm^{-1}$ was used to calculate specific activity. The standard assay mixture contained 50 mM imidazole, pH 6.75, 1 mM substrate, 1 mM α-ketoglutarate, 100 μM $(NH_4)_2Fe(SO_4)_2$, 1 mM ascorbic acid, 0.32 mM NADH, 1.2 U L-lactate dehydrogenase and 0.05 μg of purified RdpA in a volume of 0.5 ml. Activity assays were done at 30°C if not stated otherwise and started by the addition of the substrate. NADH-consumption was monitored for 30 sec and the linear portion of the curve was used to calculate activity. The substrate specific oxidation rates were corrected for nonspecific NADH oxidation in the absence of substrate (endogenous rate). Specific activities are given in standard enzyme units (μmol of NADH consumed per min which is equal to μmol of mecoprop consumed per min) per mg of protein.

End-point assay. Analysis of alternative substrate use was done in an end-point assay by measuring the formation of the product by HPLC. The standard assay mixture contained 50 mM

COR-AAD1-00003513
Bayer EX1008 (Part 7 of 9)

imidazole, pH 6.75, 1 mM substrate, 1 mM α-ketoglutarate, 100 μM $(NH_4)_2Fe(SO_4)_2$ and 1 mM ascorbic acid. The assay mixtures were incubated at 30°C for 1 min and inactivated in a boiling waterbath for 2 min. Negative controls without RdpA were treated in the same manner. The products were analyzed on a Nucleodex α-PM column (200 by 4 mm, Macherey-Nagel, Düren, Germany) as described previously (33). Specific activity was defined as the amount of phenol (μmol) which was formed per min and per mg of protein in the presence of the phenoxalkanoic acids. Oxidation rates were corrected for non-specific formation of the product in the absence of the enzyme.

Oxygen electrode measurements. Kinetic measurements with oxygen were done in a Rank brothers oxygen electrode at 30°C. The standard assay mixture contained 50 mM imidazole, pH 6.75, 2 mM substrate, 2 mM α-ketoglutarate, 100 μM $(NH_4)_2Fe(SO_4)_2$ and 1 mM ascorbic acid in a 1-ml volume. The assays were started by the addition of the substrate and O_2-concentration was monitored in 2 sec intervals for 15 min. An assay without substrate showed that inherent O_2-consumption was small and could be neglected for the calculation of specific activities. Specific activity was defined as the amount of oxygen (μmol) that the enzyme oxidized per min and per mg of protein in the presence of all substrates.

Kinetic Measurements. The kinetic parameters K_m and k_{cat} were calculated with a computer program (IgorPro, WaveMetrics Inc., Lake Oswego, OR). The calculation was based on weighted nonlinear regression analysis of the Michaelis-Menten model. To calculate K_m and k_{cat} of RdpA with respect to oxygen, we used the first derivative, i.e. the velocity (μmol × min^{-1}), of the monitored oxygen concentration in dependence of time.

Protein concentration determination and SDS-PAGE. Protein concentrations were measured using the Bradford-method (7) with the Bio-Rad reagent dye concentrate reagens following the instructions of the manufacturer (Bio-Rad, Reinach, Switzerland). Bovine serum albumin fraction V (Sigma-Aldrich) was used as a reference protein. Sodium dodecyl sulfate-polyacrylamide gel electrophoresis (SDS-PAGE) was carried out with 12% acrylamide slab gels according to established procedures (24).

Native size determination of RdpA. Molecular weight analysis of purified RdpA was determined on a Superdex 200 preparation grade HiLoad 16/60 size exclusion column (Amersham Biosciences). Approximately 0.25 mg of protein were loaded on the HiLoad column and eluted at a flow rate of 0.2 ml/min in 50 mM Na_2HPO_4-KH_2PO_4-buffer (pH 7) containing 150 mM NaCl. The calibration curve was done with the gel filtration standard from Bio-Rad containing thyroglobulin (bovine, 670 kDa), Gamma globulin (bovine, 158 kDa), Ovalbumin (chicken, 44 kDa), Myoglobulin (horse, 17 kDa) and Vitamin B-12 (1.35 kDa). Blue dextran was used to determine the void volume.

COR-AAD1-00003514
Bayer EX1008 (Part 7 of 9)

Sequencing. DNA sequencing was performed on double stranded DNA templates with the Thermo Sequenase Primer Cycle Sequencing Kit with 7-deaza-dGTP (Amersham Biosciences) and M13 primers (5). Sequencing reactions were analyzed on an automated DNA sequencer model 4200 IR^2 (LI-COR Inc., Lincoln, USA). Primers for sequencing were labelled at the 5'-end with IRD-700 or IRD-800 and were purchased from MWG Biotech AG (Ebersberg, Germany). Sequencing data were analyzed with DNASTAR software (DNASTAR Inc., Madison, USA) and compared to the databases by BLAST searches (www.ncbi.nlm.nih.gov/BLAST, (42)).

Chemicals. Phenoxyalkanoic acids were purchased at Riedel-de Haën (Buchs, Switzerland; PESTANAL®, 99% purity) or Sigma-Aldrich (97-99% purity). *(S)*-mecoprop and *(S)*-dichlorprop were synthesized by C. Zipper (48). α-Ketoglutarate and other (di)carboxyacids were bought from Sigma-Aldrich. All other chemicals were obtained from Fluka (Buchs, Switzerland) or from Merck AG (Dietikon, Switzerland).

RESULTS

Expression and purification of recombinant RdpA. The *rdpA* gene was expressed in *E. coli* BL21 (DE3)(pLysS) harboring pMec15 as a N-terminal His-tag fusion protein. The expression produced a moderate level of recombinant RdpA in the soluble fraction amounting to approximately 16% of total protein. Decrease of incubation temperature during expression in *E. coli* did not increase the amount of the 6xhis-tagged RdpA in cell-free extract. 6xHis-tagged RdpA was purified about 16-fold in a single step procedure to apparent homogeneity by Ni-NTA-affinity chromatography (Table 1 and Fig. 2). The calculated mass of RdpA was 33.2 kDa and that of the 6xHis-tagged RdpA fusion protein 34.9 kDa, which was consistent with the size estimated by SDS-PAGE of approximately 36 kDa. The recombinant RdpA was treated with thrombin protease to cleave the 6xHis-tag and enzyme activity of the native and the recombinant protein was measured. Both enzymes were equally active towards (*R*)-mecoprop suggesting that the 6xHis-tag had no influence on the activity. Therefore, all experiments were carried out with the recombinant protein, if not stated otherwise.

COR-AAD1-00003515
Bayer EX1008 (Part 7 of 9)

Table 1: Representative purification table of α-ketoglutarate-dependent *(R)*-di-chlorprop dioxygenase

	volume (ml)	total protein (mg)	total activity (U)	specific activity (U/mg protein)	recovery %	purification -fold
cell extract	10	133.1	30.9	0.2	100	1
Ni-NTA superflow	7	1.8	7	3.8	22.7	16.5

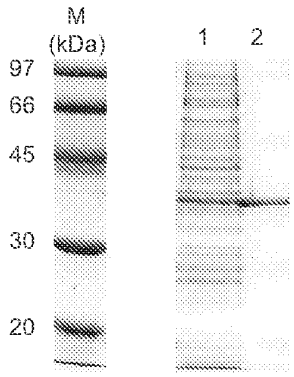


Fig. 2. Purification of α-ketoglutarate-dependent *(R)*-dichlorprop dioxygenase from *S. herbicidovorans* MH expressed in *E. coli* BL21(DE3)(pLysS)(pMec15) as a 6xHis-tagged fusion protein. Protein samples were analyzed on denaturing gel electrophoresis on a 12% polyacrylamide gel and stained with Coomassie Brilliant Blue. Lane M, molecular weight markers (indicated in kDa), lane 1, extract of induced cells, lane 2, apparently pure RdpA (obtained after Ni-NTA-superflow chromatography).

The native structure of the protein was determined by size exclusion chromatography after cleaving the 6xHis-tag by thrombin treatment. A native weight of 104±7 kDa was found which was consistent with a homotrimeric structure assuming a subunit weight of 33.2 kDa.

RdpA is an α-ketoglutarate-dependent dioxygenase catalyzing an enantioselective reaction. (*R*)-dichlorprop dioxygenase was classified as an α-ketoglutarate-dependent dioxygenase according to its amino acid sequence (Chapter 2). This finding was verified by enzyme assays. RdpA activity was completely abolished in the absence of α-ketoglutarate, strongly reduced in assays without ferrous iron and slightly reduced in the absence of ascorbate (Table 2).

COR-AAD1-00003516
Bayer EX1008 (Part 7 of 9)

Table 2: Dependence of α-ketoglutarate-dependent *(R)*-dichlorprop dioxygenase activity on substrate, cosubstrate and cofactors.

	specific activity (U/mg protein)	% activity
complete assay	3.4	100
– *(R)*-mecoprop[a]	0	0
– α-ketoglutarate[a]	0	0
– Fe(II)[a]	0.6	12.7
– ascorbate[a]	2.9	85.3

[a] Complete assay without the specified component.

Enzymatic activity of RdpA was measured with three different assays: (i) the coupled continuous assay, (ii) the end-point assay and (iii) O_2-measurements. In all these assays, different substrate or product concentrations of the enzymatic reaction were measured. Hence, the specific activity was calculated upon the production of pyruvate in the coupled continuous assay, the formation of the phenolic compound in the end-point assay and the consumption of oxygen with the oxygen electrode. All calculations resulted in similar specific activities demonstrating that oxygen consumption, pyruvate and phenol production had a 1:1 stoichiometry as expected for this reaction (Fig. 1). It has to be noted that specific activity was reproducible for a single purified RdpA batch, but that between replicates, i.e., RdpA purified from independently induced *E. coli* cultures, varied by a factor of 2 and ranged between 2 – 4 U/mg protein.

We measured enzyme activity of RdpA with the racemate and the single enantiomers of mecoprop and dichlorprop. RdpA only converted the (*R*) enantiomer of both compounds but not the (*S*) enantiomers. When incubated with the racemate, no inhibition of the enzyme by the (*S*) enantiomer was observed (not shown).

COR-AAD1-00003517
Bayer EX1008 (Part 7 of 9)

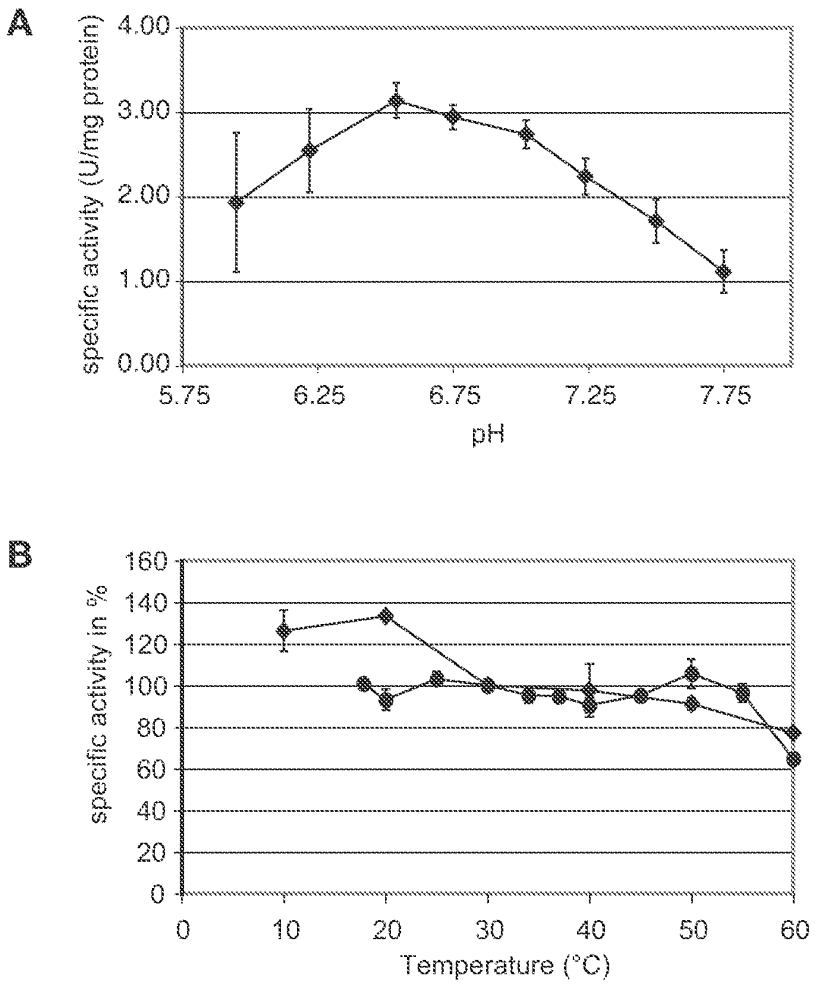


Fig. 3. Temperature (panel A) and pH (panel B) dependence of α-ketoglutarate-dependent *(R)*-dichlorprop dioxygenase. (A) The black diamonds represent data obtained with the end-point assay, the black circles data obtained with the coupled continuous assay. The measurements were carried out with two independently purified *(R)*-dichlorprop dioxygenase samples. (B) The diamonds show the mean value of six measurements of two independent experiments. Enzyme activity was determined with the coupled continuous assay.

Physicochemical characterization. RdpA was stable at 4°C for up to eight weeks and at room temperature for up to seven days, but was inactivated by several freezing and thawing cycles. Therefore, RdpA was stored at 4°C. The pH-optimum was investigated in 50 mM imidazole in a range from pH 6 to 7.75 and the optimum was found to be between 6.5-6.75 (Fig. 3A). Temperature dependence

COR-AAD1-00003518
Bayer EX1008 (Part 7 of 9)

was also studied, but no optimum could be determined (Fig. 3B). The measurements were carried out with two independently purified RdpA batchs and specific activity was measured once with the coupled continuous assay, and then repeated with the end-point assay in order to avoid misleading results due to inactivation of the reporter enzyme L-lactate dehydrogenase in the coupled-continuous assay. RdpA-activity was stable over a wide range of 20 to 55°C. A slightly higher activity was observed at 10°C and 20°C, but only in the end-point assay. However, the general trend for both enzyme activity measurements agreed and showed no Arrhenius-like behaviour.

Substrate, cosubstrate and cofactor specificities. Substrate specificities of RdpA were determined using the coupled-continuous assay for phenoxypropanoic acids and using the end-point assay for all other substrates. On one hand, we examined the influence of the alkanoic acid group attached by an ether bond to the phenoxyring by testing activities with phenoxyacetic, phenoxypropanoic, and phenoxybutyric acids as substrates. On the other hand, the effect of different substituents such as hydroxy-, methyl- and chloride groups at the aromatic ring was investigated. The phenoxypropanoic acids are chiral and as mentioned earlier, $RdpA_H$ only converted *(R)*-dichlorprop and *(R)*-mecoprop. RdpA exclusively converted phenoxypropanoic acids and none of the phenoxyacetic or –butyric acids, with the exception of 3-methyl-5-chlorophenoxyacetic acid (MCPA), which was oxidized at 10% of the highest activity. 2-(*R,S*)-4-chlorophenoxypropanoic acid was turned over with the highest rate followed by dichlorprop and mecoprop. Interestingly, also the hydroxylated and the unsubstituted phenoxypropanoic acids were converted (Table 3).

COR-AAD1-00003519
Bayer EX1008 (Part 7 of 9)

Table 3: Substrate specificities of α-ketoglutarate-dependent *(R)*-dichlorprop dioxygenase[a]

Substrate	Activity[b] (% ± std. dev.)	Activity (U/mg protein)
(*R,S*)-Mecoprop	100	3.1 / 4.2[c]
(*R,S*)-Dichlorprop	115.5±3.6	3.6
2-(*R,S*)-Phenoxypropanoic acid	39.7±7.6	1.2
2-(*R,S*)-3-Chlorophenoxypropanoic acid	14.8±2.0	0.5
2-(*R,S*)-4-Chlorophenoxypropanoic acid	152.1±9.0	4.9
2-(*R,S*)-2,4,5-Trichlorophenoxypropanoic acid	49.4±4.3	1.6
2-(*R,S*)-4-Hydroxyphenoxypropanoic acid	51.3±7.3	1.6
2,4-D[d]	<1	<0.1
MCPA[d]	7.7±4.3	0.3
2,4-Dichlorophenoxybutyric acid[d,e]	<1	<0.1
4-Chloro-2-methylphenoxybutyric acid[d]	<1	<0.1

[a] The substrate range was determined with $RdpA_H$ purified from two independent batchs and enzyme activity of each batch was measured three times with all substrates.
[b] The standard deviation is given in %.
[c] The first number is the activity determined in the coupled continuous assay, the second in the end-point-assay.
[d] Enzyme activity was determined with the end-point-assay.
[e] In one measurement, very low activity could be determined. However, the measured 2,4-dichloro-phenol concentration was below the detection limit of 1 μM and no increase of the amount of 2,4-dichlorophenol converted per time was observed when the amount of $RdpA_H$ in the assay was increased. Therefore, the activity was set to <1%

We also tested whether several carboxylic- and dicarboxylic acids could replace α-ketoglutarate as a cofactor. Since the reporter enzyme in the coupled continuous assay, L-lactate dehydrogenase, showed activity with some co-substrates, RdpA activity was determined with the end-point assay. RdpA exhibited a quite narrow cosubstrate range (Table 4). Only with 2-oxoadipate, the C_6-dicarboxylic acid, slight activity was observed whereas the other tested co-substrates, oxaloacetate, 2-oxobutyrate and 2-oxovalerate, could not replace α-ketoglutarate.

COR-AAD1-00003520
Bayer EX1008 (Part 7 of 9)

Table 4: Cosubstrate specificities of α-ketoglutarate-dependent *(R)*-dichlorprop dioxygenase

Cosubstrate	% Activity	Specific activity (U/mg protein)
α-Ketoglutarate	100	3.8
Oxaloacetate	0	0
2-Oxobutyrate	0	0
2-Oxovalerate	0	0
2-Oxoadipate	1.9	0.1

In the absence of ferrous iron, RdpA activity was reduced to 12% of its maximal activity. Activity was independent of the iron-salt, but other divalent cations could not support activity in the same range as Fe(II) (Table 5). Activity was diminished with $CaCl_2$ and $MgCl_2$ to about the same level as in the absence of ferrous ion and was totally abolished with Co(II), Mn(II), and Ni(II), indicating an inhibition of the enzyme by these cations.

Table 5: Cofactor specificities of α-ketoglutarate-dependent *(R)*-dichlorprop dioxygenase

Cofactor	% Activity	Specific activity (U/mg protein)
$Fe(NH_4)_2(SO_4)_2$	100	2.8
$Fe(SO_4)$	97.5	2.7
$CaCl_2$	15.9	0.4
$CoCl_2$	0	0
$MgCl_2$	9.4	0.3
$MnCl_2$	0	0
$NiCl_2$	0	0

Kinetic analysis. We determined the kinetic parameters for the *(R)* enantiomers of mecoprop, dichlorprop, and 2-(*R,S*)-4-chlorophenoxypropanoic acid, the cosubstrates α-ketoglutarate and oxygen. For the phenoxypropanoic acids and α-ketoglutarate, the coupled continuous assay was used whereas the O_2-consumption was measured in an oxygen electrode. Michaelis-Menten kinetic was observed for the *(R)*-phenoxypropanoic acids and α-ketoglutarate. RdpA exhibited the lowest K_m-value and highest efficiency for *(R)*-mecoprop, whereas k_{cat} was

COR-AAD1-00003521
Bayer EX1008 (Part 7 of 9)

highest for (*R,S*)-4-chlorophenoxypropanoic acid (Table 6). The apparent K_m-value for α-ketoglutarate was 2.8 μM which was below the lowest tested α-ketoglutarate concentration, but the obtained data fitted well to a Michaelis-Menten curve and the value seems reliable.

Table 6: Kinetic parameters of α-ketoglutarate-dependent *(R)*-dichlorprop dioxygenase

Substrate	K_m (μM)	k_{cat} (min^{-1})	k_{cat}/K_m ($\mu M^{-1} \times min^{-1}$)
(*R*)-Mecoprop (10 – 2000 μM)	98.8±6.4	114.2	1.16
(*R*)-Dichlorprop (50 – 2000 μM)	163.7±13.5	170.1	1.04
(R)-4-Chlorophenoxypropanoic acid (120 – 2000 μM)	262.4±10.1	241.9	0.92
α-Ketoglutarate (7-1900 μM)	2.8±0.8	135.6	48.82

Oxygen kinetic parameters were measured by monitoring the O_2-consumption in an oxygen electrode. The reaction rate at the different O_2-concentrations was then calculated by taking the first derivative of the O_2-consumption curve. The dependence on oxygen kinetic did not follow Michaelis-Menten kinetics in the oxygen concentration range of air-saturated water at 30°C (Fig. 4) and therefore, a K_m-value could not be calculated.

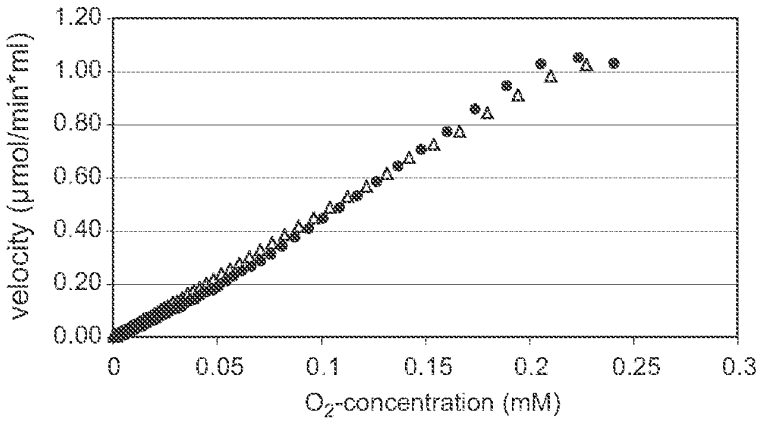


Fig. 4. Kinetics of α-ketoglutarate-dependent *(R)*-dichlorprop dioxygenase towards oxygen. The open triangles and black circles represent two independent experiments.

COR-AAD1-00003522
Bayer EX1008 (Part 7 of 9)

DISCUSSION

RdpA is an α-ketoglutarate-dependent dioxygenase. α-Ketoglutarate-dependent dioxygenases are grouped according to their cosubstrate and cofactor requirement. Enzyme activity measurements demonstrated that RdpA belonged to the heterologous enzyme family of α-ketoglutarate-dependent dioxygenases, since its activity was strictly dependent on oxygen and α-ketoglutarate. Initial activity was reduced without ascorbate to about 85% of the highest activity. Ascorbate is formally not needed in the reaction and it is generally thought that it keeps Fe(II) in the reduced state. Two other α-ketoglutarate-dependent dioxygenases, prolyl 4-hydroxylase and lysyl hydroxylase, are almost completely inactivated within one minute in the absence of ascorbate (10, 30, 31, 37). The inactivation is thought to involve a side reaction in which α-ketoglutarate is decarboxylated. This reaction is coupled to the oxidation of Fe(II) to Fe(III). Ascorbate reduces the ferryl iron thereby reactivating the enzyme. TfdA, on the other hand, is not as sensitive to the absence of ascorbate and is only inactivated after 30-40 minutes (15). However, the reduced activity of RdpA when ascorbate was absent indicates that the side-reaction of α-ketoglutarate decarboxylation takes place although inactivation is not as fast as it is for the peptide hydroxylases.

An alignment of α-ketoglutarate-dependent dioxygenases with sequence homology to RdpA revealed the 2-His-1-carboxylate facial triad and several other conserved amino acid residues (Fig. 5). RdpA possesses the motif of subgroup II of the α-ketoglutarate-dependent dioxygenase family, which is $HXDX_{24}TX_{131}HX_{10}R$. Based on the crystal structure of TauD and on the structure model of TfdA and on mutagenesis studies, the role of some conserved amino acid residues in RdpA were predicted (13, 34, 38). His-111, Asp-113 and His-270 wre recognized to build the facial triad and are likely to ligands for iron-binding, whereas Thr-138 and Arg-281 are putative α-ketoglutarate binding sites.

The *(R)*-dichlorprop dioxygenases from *S. herbicidovorans* MH and *D. acidovorans* MC1 are, to our knowledge, the only representatives of the class of α-ketoglutarate-dependent dioxygenases with a homotrimeric structure (43). Most

COR-AAD1-00003523
Bayer EX1008 (Part 7 of 9)

enzymes of this class are mono- or homodimers such as SdpA from *D. acidovorans* MC1 and TfdA, tetramers such as the alkylsulfatase from *Pseudomonas putida* are also known (12, 15, 43).

RdpA is surprisingly insensitive to temperature. No Arrhenius-like activity increase was observed and $RdpA_H$ was stable up to 55°C. This findings partially agree with those for an α-ketoglutarate-dependent 2,4-D dioxygenase from *Burkholderia cepacia* 2a, which also showed an unexpectedly low activity increase with increasing temperature and at 10°C, still showed 77% activity of the one obtained at 25°C (35). In contrast, TfdA from *R. eutropha* JMP134(pJP4), exhibits a more typical activity increase with higher temperature, is only stable up to 30°C, and is completely inactivated at 40°C within 5 min (15).

RdpA catalyzes the enantioselective reaction from (*R*)-phenoxypropanoic acids to the achiral phenol. RdpA converts only the (*R*)-enantiomer of phenoxypropanoic acid herbicides, but not the (*S*) enantiomer. Also after prolonged incubation, we could not find any activity with the (*S*)-enantiomer of either dichlorprop or mecoprop. We propose therefore that RdpA from *S. herbicidovorans* MH catalyzes an enantioselective reaction. This result agrees with the results obtained with the identical *(R)*-dichlorprop dioxygenase RdpA from *D. acidovorans* MC1 which did not convert (*S*) enantiomers of phenoxypropanoic acids to a significant extent (44). α-Ketoglutarate-dependent 2,4-D dioxygenases are also able to oxidize mecoprop and dichlorprop and they also convert only one enantiomer. Surprisingly, they differ in the preference of the enantiomer despite their high nucleotide sequence similarity. TfdA from *R. eutropha* JMP134(pJP4) and *Burkholderia cepacia* RASC cleave the ether-bond of only (*S*)-dichlorprop, whereas TfdA from *A. denitrificans* exclusively converts the (*R*) enantiomer (39). It can be concluded that none of these α-ketoglutarate-dependent dioxygenases is able to convert both enantiomers of phenoxypropanoic acids with a significant catalytic rate. To oxidize both enantiomers, two distinct dioxygenases are required in strains such as *S. herbicidovorans* MH or *D. acidovorans* MC1 (33, 43, 44, Chapters 2 and 4).

COR-AAD1-00003524
Bayer EX1008 (Part 7 of 9)

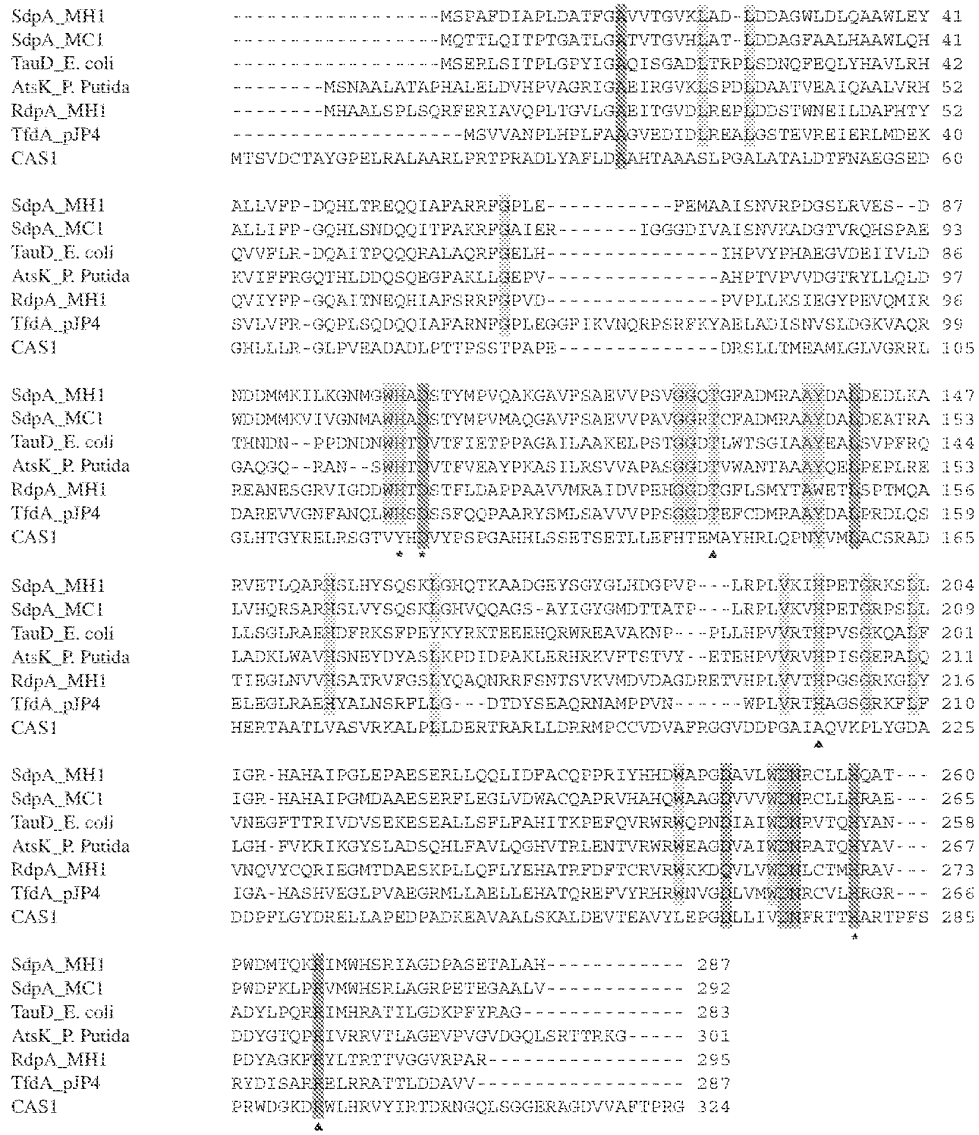


Fig. 5. Alignment of amino acid sequences of RdpA from strain MH and other group II α-ketoglutarate-dependent dioxygenases. The sequence names and accession numbers are shown in parentheses: 2,4-D dioxygenase from *R. eutropha* JMP134(pJP4) (TfdA_pJP4, AAA21983), *(R)*-dichlorprop dioxygenase from *S. herbicidovorans* MH (RdpA_MH, CAF32811), *(S)*-dichlorprop dioxygenase from *S. herbicidovorans* MH (SdpA_MH, CAF32813), *(S)*-dichlorprop dioxygenase from *D. acidovorans* MC1 (SdpA_MC1, AAM90963), taurine dioxygenase from *E. coli* (TauD, AAC73471), alkylsulfate dioxygenase from *Pseudomonas putida* (AtsK, AAD31784); clavaminate synthase from *Streptomyces clavuligeres* (CAS1, A44241). Highly conserved residues (dark grey boxes) and residues conserved in six out of the seven sequences (light grey boxes) are highlighted. Asterisks mark the (conserved) Fe(II)-binding residues, triangles the α-ketoglutarate binding residues of TauD and TfdA (13, 34). They are aligned to the proposed residues of RdpA_MH. Amino acid numbers for each sequence are indicated at the right of each line.

COR-AAD1-00003525
Bayer EX1008 (Part 7 of 9)

Substrate and cosubstrate specificities of RdpA. RdpA exhibited narrow substrate specificities with respect to the alkyl moiety at the alkanoic acid side chain since only phenoxypropanoic acids were converted, but not 2,4-D and phenoxybutyric acids. This is in contrast to RdpA from *D. acidovorans* MC1, which reacted with 2,4-D at 14% activity of the activity obtained with *(R)*-dichlorprop (44). Also TfdA from *R. eutropha* JMP134(pJP4) exhibited a broader substrate range and converts, besides phenoxyacetic acids, also *(S)*-phenoxypropanoic acids. However, neither RdpA nor TfdA react with phenoxybutyric acids (15, 44). All these results indicate that the active sites of RdpA and of TfdA might be specific with regard to the alkanoic acid substituent and are indifferent with regard to the substituents of the aromatic ring. Additionally, RdpA is not inhibited by the *(S)* enantiomers of phenoxypropanoic acids, which indicates no binding of these enantiomers at the active site. It can therefore be proposed that only the *(R)* enantiomers fit into the active site and that the other substrates are excluded either by steric hindrance or due to repulsion of charged amino acid residues.

α-Ketoglutarate-dependent dioxygenases show different cosubstrate specificities. AtsK, an alkylsulfatase from *Pseudomonas putida* S-313, and TfdA, for instance, exhibit a broad cosubstrate range and many oxoacids substitute for α-ketoglutarate (15, 21). TauD and the inorganic α-ketoglutarate-dependent hypophosphite dioxygenase HtxA exhibited stricter specificities and besides α-ketoglutarate, only 2-oxoadipate supported (reduced) activity in the range of 4 – 23% (12, 15, 45). RdpA showed the same cosubstrate specificities as the latter group, but the remaining activity with 2-oxoadipate was only 2%. Many α-ketoglutarate-dependent dioxygenases including RdpA are well adapted to α-ketoglutarate and have high affinity to α-ketoglutarate with apparent K_m-values in the range of 3 – 20 μM.

Activity linearly dependent on oxygen. The oxygen kinetics for RdpA did not follow the Michaelis-Menten model. Initial velocities were determined in the range of 0 – 0.23 mM O_2, of which the upper value represents maximum oxygen solubility of air-saturated water at 30°C. A linear relationship between O_2-concen-

COR-AAD1-00003526
Bayer EX1008 (Part 7 of 9)

tration and V_{max} was observed and hence, a K_m-value could not be calculated. The linear dependence can be explained by the fact, that the enzyme is only fully saturated at concentrations above 0.23 mM O_2 as it was determined for the 3,5-dichlorocatechol dioxygenase from *Pseudomonas cepacia* CSV90 with a K_m-value of 652 μM O_2 (6). To observe Michaelis-Menten kinetics, it would be necessary to carry out enzyme activity measurements with pure oxygen dissolved in water. In contrast to the low oxygen affinity of RdpA, apparent K_m-values of 40 – 50 μM O_2 were observed for lysyl hydroxylase and an α-ketoglutarate-dependent 4-hydroxylase from *Catharanthus roseus* which is involved in vindoline biosynthesis (9, 37). Flavonol dioxygenase exhibits even higher affinity and a K_m-value of 5.26 μM O_2 was determined (3). This indicates that, in comparison to other α-ketoglutarate-dependent dioxygenases, RdpA exhibits unusual low affinity to oxygen and that its activity is highly dependent on oxygen concentration under natural conditions. Furthermore, it has to be noted that oxygen concentrations in 'normal' laboratory enzymatic measurements are not saturating for this enzyme.

We presented here the characteristics of the α-ketoglutarate-dependent *(R)*-dichlorprop dioxygenase from *S. herbicidovorans* MH that catalyzes the enantioselective reaction from *(R)*-phenoxypropanoic acids to the achiral phenol. Interestingly, *S. herbicidovorans* MH harbors a second dioxygenase which is specific for the *(S)* enantiomers (32, Chapter 4). These two dioxygenases are a good example of an enzyme pair of which each enzyme converts one enantiomers of a chiral substrate. It will be important to further elucidate the enzyme mechanisms, how they discriminate between the enantiomers, and how they evolved in one strain.

COR-AAD1-00003527
Bayer EX1008 (Part 7 of 9)

REFERENCES

1. Åberg, B. 1973. Plant growth regulators. XXXI. Some monochloro-monomethylphenoxy-acetic and related optically active propionic acids. Swedish J. agric. Res. 3:49-62.
2. Ahrens, W. H. 1994. Herbicide Handbook (WSSA), 7th ed. Weed Science Society of America, Champaign.
3. Anzellotti, D., and R. K. Ibrahim. 2000. Novel flavonol 2-oxoglutarate dependent dioxygenase: affinity purification, characterization, and kinetic properties. Arch. Biochem. Biophys. 382:161-72.
4. Ausubel, F. M., R. Brent, R. E. Kingston, D. D. Moore, J. G. Seidman, J. A. Smith, and K. Struhl (ed.). 2002. Current protocols in molecular biology. John Wiley & Sons, Inc., New York, N. Y.
5. Benes, V., Z. Hostomosky, L. Arnold, and V. Paces. 1993. M13 and pUC vectors with new unique restriction sites for cloning. Gene 130:151-152.
6. Bhat, M. A., T. Ishida, K. Horiike, C. S. Vaidyanathan, and M. Nozaki. 1993. Purification of 3,5-dichlorocatechol 1,2-dioxygenase, a nonheme iron dioxygenase and a key enzyme in the biodegradation of a herbicide, 2,4-dichlorophenoxyacetic acid (2,4-D), from *Pseudomonas cepacia* CSV90. Arch. Biochem. Biophys. 300:738-746.
7. Bradford, M. M. 1976. A rapid and sensitive method for the determination of microgram quantities of protein utilizing the principle of protein-dye binding. Anal. Biochem. 72:248-254.
8. Costas, M., M. P. Mehn, M. P. Jensen, and L. Que, Jr. 2004. Dioxygen activation at mononuclear nonheme iron active sites: enzymes, models, and intermediates. Chem. Rev. 104:939-986.
9. de Carolis, E., and V. de Luca. 1993. Purification, characterization, and kinetic analysis of a 2-oxoglutarate-dependent dioxygenase involved in vindoline biosynthesis from *Catharanthus roseus*. J. Biol. Chem. 268:5504-5511.
10. de Jong, L., S. P. J. Albracht, and A. Kemp. 1982. Prolyl 4-hydroxylase activity in relation to the oxidation state of enzyme-bound iron. The role of ascorbate in peptidyl proline hydroxylation. Biochim. Biophys. Acta 704:326-332.
11. Donaldson, D., T. Kiely, and A. Grube. 2002. Pesticides industry sales and usage. 1998 and 1999 market estimates. U.S. Environmental Protection Agency.
12. Eichhorn, E., J. R. van der Ploeg, M. A. Kertesz, and T. Leisinger. 1997. Characterization of α-ketoglutarate-dependent taurine dioxygenase from *Escherichia coli*. J. Biol. Chem. 272:23031-23036.
13. Elkins, J. M., M. J. Ryle, I. J. Clifton, J. C. Dunning Hotopp, J. S. Lloyd, N. I. Burzlaff, J. E. Baldwin, R. P. Hausinger, and P. L. Roach. 2002. X-ray crystal structure of *Escherichia coli* taurine/α-ketoglutarate dioxygenase complexed to ferrous iron and substrates. Biochemistry 41:5185-5192.
14. Fukumori, F., and R. P. Hausinger. 1993. *Alcaligenes eutrophus* JMP134 "2,4-dichlorophenoxyacetate monooxygenase" is a α-ketoglutarate-dependent dioxygenase. J. Bacteriol. 175:2083-2096.
15. Fukumori, F., and R. P. Hausinger. 1993. Purification and characterization of 2,4-dichlorophenoxyacetate/α-ketoglutarate dioxygenase. J. Biol. Chem. 268:24311-24317.

COR-AAD1-00003528
Bayer EX1008 (Part 7 of 9)

16. Hausinger, R., and F. Fukumori. 1995. Characterization of the first enzyme in 2,4-dichlorophenoxyacetic acid metabolism. Environ. Health Perspectives Suppl. 103:37-39.

17. Hausinger, R. P. 2004. Fe(II)/α-ketoglutarate dependent hydroxylases and related enzymes. Crit. Rev. Biochem. Mol. Biol. 39:1-47.

18. Hegg, E. L., and L. Que, Jr. 1997. The 2-His-1-carboxylate facial triad--an emerging structural motif in mononuclear non-heme iron(II) enzymes. Eur. J. Biochem. 250:625-629.

19. Hogan, D. A., S. R. Smith, E. A. Saari, J. McCracken, and R. P. Hausinger. 2000. Site-directed mutagenesis of 2,4-dichlorophenoxyacetic acid/α-ketoglutarate dioxygenase. J. Biol. Chem. 275:12400-12409.

20. Horvath, M., G. Ditzelmüller, M. Loidl, and F. Streichsbier. 1990. Isolation and characterization of a 2-(2,4-dichlorophenoxy)propionic acid degrading soil bacterium. Appl. Microbiol. Biotechnol. 33:213-216.

21. Kahnert, A., and M. A. Kertesz. 2000. Characterization of a sulfur-regulated oxygenative alkylsulfatase from *Pseudomonas putida* S-313. J. Biol. Chem. 275:31661-31667.

22. Kohler, H.-P. E. 1999. *Sphingomonas herbicidovorans* MH: a versatile phenoxyalkanoic herbicide degrader. J. Ind. Microbiol. Biotechnol. 23:336-340.

23. Kohler, H.-P. E., W. Angst, W. Giger, C. Kranz, S. Müller, and M. J.-F. Suter. 1997. Environmental fate of chiral pollutants - the necessity of considering stereochemistry. Chimia 51:947-951.

24. Laemmli, U. K. 1970. Cleavage of structural proteins during the assembly of the head of bacteriophage T4. Nature 227:680-685.

25. Lange, S. J., and L. Que. 1998. Oxygen activating nonheme iron enzymes. Curr. Op. Chem. Biol. 2:159-172.

26. Loos, M. A. 1975. Phenoxyalkanoic acids, p. 1-128. *In* P. C. Kearney and D. D. Kaufmann (ed.), Herbicides. Chemistry, degradation and mode of action, 2nd ed, vol. 1. Marcel Dekker, Inc., New York.

27. Matell, M. 1953. Stereochemical studies on plant growth regulators. VII. Optically active α-(2-methyl-4-chlorophenoxy)-propionic acid and α-(2,4-dichlorophenoxy)-*n*-butyric acid and their steric relations. Ark. Kemi 6:365-373.

28. Müller, R. H., S. Jorks, S. Kleinsteuber, and W. Babel. 1999. *Comamonas acidovorans* strain MC1: a new isolate capable of degrading the chiral herbicides dichlorprop and mecoprop and the herbicides 2,4-D and MCPA. Microbiol. Res. 154:241-246.

29. Müller, T. A., and H.-P. E. Kohler. 2004. Chirality of pollutants - effects on metabolism and fate. Appl. Microbiol. Biotechnol. 64:300-316.

30. Myllylä, R., E.-R. Kuutti-Savolainen, and K. I. Kivirikko. 1978. The role of ascorbate in the prolyl hydroxylase reaction. Biochem. Biophys. Res. Commun. 83:441-448.

31. Myllylä, R., K. Majamaa, V. Günzler, H. M. Hanauske-Abel, and K. I. Kivirikko. 1984. Ascorbate is consumed stoichiometrically in the uncoupled reactions catalyzed by prolyl 4-hydroxylase and lysyl hydroxylase. J. Biol. Chem. 259:5403-5405.

COR-AAD1-00003529
Bayer EX1008 (Part 7 of 9)

32. Nickel, K. 1995. Enantioselective degradation of the herbicide mecoprop by *Flavobacterium* sp. MH. Diploma thesis. EAWAG.

33. Nickel, K., M. J.-F. Suter, and H.-P. E. Kohler. 1997. Involvement of two α-ketoglutarate-dependent dioxygenases in enantioselective degradation of (*R*)- and (*S*)-mecoprop by *Sphingomonas herbicidovorans* MH. J. Bacteriol. 179:6674-6679.

34. O'Brien, J. R., D. J. Schuller, V. S. Yang, B. D. Dillard, and W. N. Lanzilotta. 2003. Substrate-induced conformational changes in *Escherichia coli* taurine/α-ketoglutarate dioxygenase and insight into the oligomeric structure. Biochemistry 42:5547-5554.

35. Poh, R., X. Xia, I. J. Bruce, and A. R. Smith. 2001. 2,4-dichlorophenoxyacetate/alpha-ketoglutarate dioxygenases from *Burkholderia cepacia* 2a and *Ralstonia eutropha* JMP134. Microbios 105:43-63.

36. Prescott, A. G., and M. D. Lloyd. 2000. The iron(II) and 2-oxoacid-dependent dioxygenases and their role in metabolism. Nat. Prod. Rep. 17:367-383.

37. Puistola, U., T. M. Turpeenniemi-Hujanen, R. Myllylä, and K. I. Kivirikko. 1980. Studies on the lysyl hydroxylase reaction. I. Initial velocity kinetics and related aspects. Biochim. Biophys. Acta 611:40-50.

38. Romantschuk, M. L., G. Y. Richter, P. Mukhopadhyay, and D. Mills. 1991. IS*801*, an insertion sequence element isolated from *Pseudomonas syringae* pathovar *phaseolica*. Mol. Microbiol. 5:617-622.

39. Saari, R. E., D. A. Hogan, and R. P. Hausinger. 1999. Stereospecific degradation of the phenoxypropionate herbicide dichlorprop. J. Mol. Catal. B: Enzymatic 6:421-428.

40. Sambrook, J., E. F. Fritsch, and T. Maniatis. 1989. Molecular Cloning: a laboratory manual. Cold Spring Harbor Laboratory, Cold Spring Harbor, N.Y.

41. Schofield, C. J., and Z. Zhang. 1999. Structural and mechanistic studies on 2-oxoglutarate-dependent oxygenases and related enzymes. Curr. Opin. Struct. Biol. 9:722-731.

42. Tatusova, T. A., and T. L. Madden. 1999. BLAST 2 sequences, a new tool for comparing protein and nucleotide sequences. FEMS Microbiol. Lett. 174:247-250.

43. Westendorf, A., D. Benndorf, R. H. Müller, and W. Babel. 2002. The two enantiospecific dichlorprop/α-ketoglutarate-dioxygenases from *Delftia acidovorans* MC1 - protein and sequence data of RdpA and SdpA. Microbiol. Res. 157:1-6.

44. Westendorf, A., R. H. Müller, and W. Babel. 2003. Purification and characterisation of the enantiospecific dioxygenases from *Delftia acidovorans* MC1 initiating the degradation of phenoxypropionate and phenoxyacetate herbicides. Acta Biotechnol. 23:3-17.

45. White, A. K., and W. W. Metcalf. 2002. Isolation and biochemical characterization of hypophosphite/2-oxoglutarate dioxygenase. A novel phosphorus-oxidizing enzyme from *Pseudomonas stutzeri* WM88. J. Biol. Chem. 277:38262-38271.

46. Williams, A. 1996. Opportunities for chiral agrochemicals. Pest. Sci. 46:3-9.

47. Worthing, C. R., and R. J. Hance. 1991. The Pesticide Manual - A World Compendium, 9th ed. The British Crop Council, Farnham, Great Britain.

COR-AAD1-00003530
Bayer EX1008 (Part 7 of 9)

48. Zipper, C. 1998. Microbial degradation and environmental fate of chiral phenoxyalkanoic acid herbicides. Ph. D. thesis. ETH Zürich, Zürich.

49. Zipper, C., K. Nickel, W. Angst, and H.-P. E. Kohler. 1996. Complete microbial degradation of both enantiomers of the chiral herbicide mecoprop [(*RS*)-2-(4-chloro-2-methylphenoxy)propionic acid] in an enantioselective manner by *Sphingomonas herbicidovorans* sp. nov. Appl. Environ. Microbiol. 62:4318-4322.

COR-AAD1-00003531
Bayer EX1008 (Part 7 of 9)

Chapter 4

α-Ketoglutarate Dependent *(S)*-Dichlorprop Dioxygenase (SdpA) from *Sphingomonas herbicidovorans* MH: Purification and Characterization of an Enantiospecific Enzyme

Sphingomonas herbicidovorans MH harbors two enantiospecific α-ketoglutarate-dependent dichlorprop dioxygenases involved in phenoxyalkanoic acid degradation. Here, we characterize *(S)*-dichlorprop dioxygenase (SdpA), which was expressed and purified as a 6xHis-tagged fusion protein from *E. coli* BL21(DE3)(pLysS). SdpA belongs to sub-group II of α-ketoglutarate-dependent dioxygenases. It enantiospecifically transformed the *(S)* enantiomers of phenoxypropanoic acids and was slightly inhibited in the presence of the *(R)* enantiomer. It showed highest activity for (*R,S*)-mecoprop [2-(*R,S*)-2-methyl-4-chlorophenoxypropanoic acid] and preferred substituted phenoxy-propanoic acids to substituted phenoxybutyric acids and –acetic acids. Kinetic investigations showed Michaelis-Menten kinetics with all substrates and cosubstrates. SdpA had the highest affinity and the highest turnover rate for (*S*)-mecoprop (K_m-value = 132 μM, k_{cat} = 304 min^{-1}). For oxygen and α-ketoglutarate, the apparent K_m-values were 159 μM and 19.6 μM, respectively. Cosubstrate specificity was narrow since only with 2-oxoadipate, apart from α-ketoglutarate, slight activity was measured. In the absence of ferrous iron, enzyme activity was strongly decreased and other divalent cation could not replace Fe(II). Although results from growth experiments suggest that strain MH should harbor another more specific 2,4-D converting enzyme, *tfdA*-like, a *tfdA*α-like or *cadAB*-like genes were not discovered in a screening by heterologous hybridization and PCR.

INTRODUCTION

Phenoxyalkanoic acid herbicides such as 2,4-dichlorophenoxyacetic acid (2,4-D), chiral mecoprop (2-(*R,S*)-2-methyl-4-chlorophenoxypropanoic acid) and chiral dichlorprop (2-(*R,S*)-2,4-dichlorophenoxy-propanoic acid) have been widely used against broadleaf weeds in agriculture, industries and lawn pastures since the 1940ies (1, 10). A number of bacteria was isolated from the environment which are able to degrade these herbicides. One representative is the *Alphaproteobacterium Sphingomonas herbicidovorans* MH, which is able to grow on several phenoxy-alkanoic acid herbicides as sole carbon and energy source (20, 25, 46). *S. herbicidovorans* MH degrades mecoprop and dichlorprop enantioselectively, the *(S)*-enantiomer being used first (47). The chiral substrates are converted to the achiral phenols, which are then transformed to the respective catechols (Chapter 2). The catechols are metabolized through the modified *ortho*-cleavage pathway to intermediates of the tricarboxylic acid cycle. This pathway is analogous to the well-studied degradation pathway of 2,4-D in *Ralstonia eutropha* JMP134(pJP4). However, the genetic background of the pathway differs in these two strains despite the analogy of the reactions (9, 13, 14, 32, 39, Chapter 2).

α-Ketoglutarate-dependent dioxygenases are non-heme iron enzymes, which are involved in various reactions such as hydroxylations, epoxidations, ring formations, and expansion reactions (17, 33). They are grouped according to their cosubstrate requirement since most members need dioxygen and α-ketoglutarate as cosubstrates, ferrous iron as cofactor and ascorbate as a reducing agent. α-Keto-glutarate dependent-dioxygenases exhibit low amino acid sequence similarity, but they share a 2-His-1-carboxylate facial triad (18). Phenoxyalkanoic acid herbicide degraders such as *R. eutropha* JMP134(pJP4) and the *(R)*-mecoprop degrader *Alcaligenes denitrificans* harbor an α-ketoglutarate-dependent 2,4-D dioxygenase, called TfdA (13, 14, 36). Two distinct dioxygenases, named *(R)*- and *(S)*-dichlor-prop dioxygenases (RdpA and SdpA, respectively), were isolated from *S. herbicidovorans* MH. They are thought to catalyze the oxidative ether-cleavage of the respective enantiomer of phenoxypropanoic acids to the achiral phenol (Fig. 1) (30, Chapter 3). RdpA and SdpA share 30% and 37% amino acid identity with

COR-AAD1-00003534
Bayer EX1008 (Part 7 of 9)

TfdA from *R. eutropha* JMP134(pJP4), respectively (13, 14, Chapter 2). Sequence comparisons of RdpA and SdpA to other α-ketoglutarate-dependent dioxygenases showed, that RdpA is identical to *(R)*-dichlorprop dioxygenase from the dichlorprop degrader *Delftia acidovorans* MC1 (here designated $RdpA_{MC1}$), whereas SdpA is 60% identical to *(S)*-dichlorprop dioxygenase (here designated $SdpA_{MC1}$) from the same strain (43). $RdpA_{MC1}$ and $SdpA_{MC1}$ were enantiospecific and converted only the respective enantiomer of phenoxypropanoic acids (44).

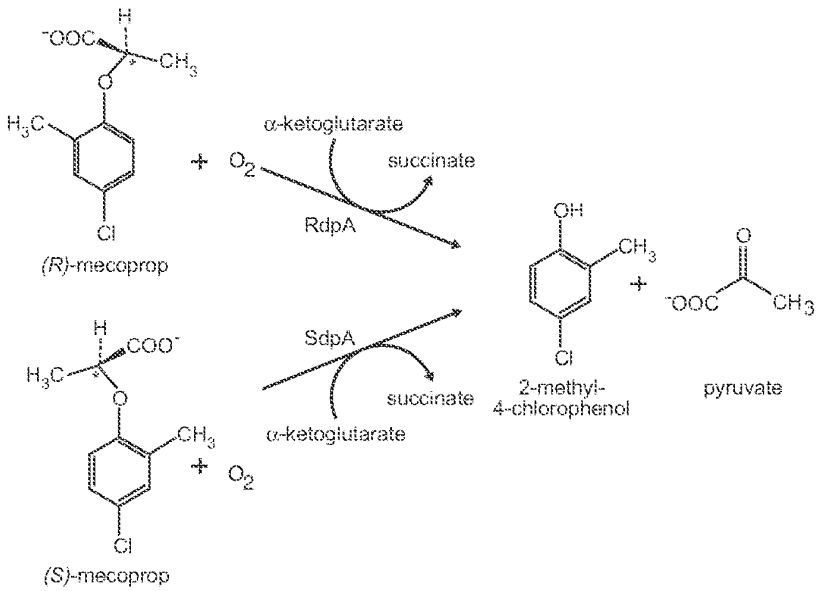


Fig. 1. Initial degradation step of chiral phenoxypropanoic acids in *S. herbicidovorans* MH catalyzed by the α-ketoglutarate-dependent *(R)*-dichlorprop dioxygenases (RdpA) and α-ketoglutarate-dependent *(S)*-dichlorprop dioxygenases (SdpA).

Phenoxyalkanoic acid degraders have been classified in three groups according to their genetic background (15, 23). Group I comprises 2,4-D degrading *Beta-* and *Gammaproteobacteria* which harbor *tfd*-gene homologs and were isolated from contaminated sites. Fast growing *Alphaproteobacteria,* mostly *Sphingomonas* strains, build group II and it was postulated that they do not possess *tfdA*-homologs. The third group is composed of slow-growing *Alphaproteobacteria*, which are associated with members of the *Bradyrhizobium-Agromonas-Nitrobacter-Afipia* (BANA)-cluster isolated from pristine environements. These

COR-AAD1-00003535
Bayer EX1008 (Part 7 of 9)

strains harbor a distinct group of 2,4-D degrading genes, the *cad*-genes. The *cadAB*-genes code for the large and small subunit of a 2,4-D oxygenase and share homology to the 2,4,5-trichlorophenoxyacetic acid oxygenase *tftAB*-genes from *Burkholderia cepacia* AC1100, but not to *tfdA* (21, 22, 24). It was hypothesized that members of group II and III do not possess *tfdA*-homologs but recently, such gene homologs were detected in several *Alphaproteobacteria*. The *tfdA*α-genes, as they were named, showed 56-60% nucleotide identity to *tfdA* (21, 22).

Here, we report the characterization of the α-ketoglutarate-dependent *(S)*-dichlorprop dioxygenase from *S. herbicidovorans* MH. We have expressed SdpA as a 6xHis-tagged fusion protein and determined physicochemical parameters, the substrate, cosubstrate and cofactor specificities and verified its classification. Additionally, we screened for another phenoxyalkanoic acid converting enzyme specific for 2,4-D but no *tfdA*-like, *tfdA*α-like or a *cadAB*-like gene was detected.

MATERIALS AND METHODS

Bacterial strains and culture conditions. *Escherichia coli* DH5α was used as a host for cloning experiments and *E. coli* BL21(DE3)(pLysS) as a host for expression vector pET-15b (Novagen, Darmstadt, Germany). *E. coli* strains were grown at 30°C or 37°C in Luria-Bertani (LB) medium (37). When appropriate, ampicillin and chloramphenicol were added at 50 μg/ml and 25 μg/ml final concentrations, respectively. Solid media were prepared by the addition of 1.5% (w/v) agar.

Standard molecular techniques. Cloning and digestions were done according to established procedures (3, 37). Restriction enzymes and other DNA modifying enzymes were purchased from Promega (Wallisellen, Switzerland) and Fermentas (Nunningen, Switzerland). Plasmids and cosmids were isolated by the boiling miniprep method, the alkaline lysis method according to Sambrook *et al.* (37) or with the E.Z.N.A. plasmid miniprep kit II (Peqlab Biotechnologies GmbH, Baden-Dättwil, Switzerland) as suggested by the manufacturer. Gel extraction was carried out with the MinElute Gel extraction Kit (Qiagen AG, Basel, Switzerland) according to the protocol of the supplier.

Sequencing. DNA sequencing was performed on double stranded DNA templates with the Thermo Sequenase Primer Cycle Sequencing Kit with 7-deaza-dGTP (Amersham Bio-sciences) and M13 primers (4). Sequencing reactions were analyzed on an automated DNA sequencer model 4200 IR^2 (LI-COR Inc., Lincoln, USA). Primers for sequencing were labelled at

COR-AAD1-00003536
Bayer EX1008 (Part 7 of 9)

the 5'-end with IRD-700 or IRD-800 and were purchased from MWG Biotech AG (Ebersberg, Germany). Sequencing data were analyzed with DNASTAR software (DNASTAR Inc., Madison, USA) and compared to the databases by BLAST searches (www.ncbi.nlm.nih.gov/BLAST, 40).

Screening for other α-ketoglutarate-dependent phenoxyalkanoic acid dioxygenases. To screen for *tfdA*- and *tfdA*α-like genes, we carried out the PCR with the *tfdA*-derived primers tfdAfor 5'-TGG CAI AGC GAC AGI TCC TTT-3', tfdArev 5'-CIG CGG TTG TCC CAI ATC IC-3', tfdAfor2 5'-ACG GAG TTC TG(C/T) GA(C/T) AT-3' and tfdArev2 5'-AAC GCA GCG (G/A)T(G/T) ATC CCA-3' (42) in all possible combinations with chromosomal DNA of *S. herbicidovorans* MH. Oligonucleotides for PCR were obtained from Microsynth GmbH (Balgach, Switzerland). The following conditions were applied: initial denaturation for 2 min at 93.5°C; denaturing for 30 sec at 93.5°C; annealing for 30 sec at 63°C, 59°C, 56°C, 53°C, 50°C, and 46°C; extension for 45 sec at 72°C (5 cycles at each annealing temperature) or as an alternative, 35 cycles at an annealing temperature of 35°C; followed by a final extension for 4 min at 72°C. As a positive control, total DNA of *R. eutropha* JMP134(pJP4) was used.

For southern hybridization, total DNA of *S. herbicidovorans* MH fractionated on agarose gel was blotted on a Hybond™-XL membrane (Amersham Biosciences, Dübendorf, Switzerland) with a vacuum blotter (VacuGene XL, Amersham Biosciences) by the procedure described by Ravatn et al. (35). Total DNA was hybridized with a 0.7-kb *Eco*RI-fragment from pCBA101 (0.7-kb *Eco*RI-fragment with *tfdA* in pGEM7, J. R. van der Meer, unpublished) and with a 1.1-kb *Sal*I-fragment of pBHS1 harboring a part of *cadAB* (24). The fragments were radioactively labeled with [α-^{32}P]dATP using the Random Primed DNA Labeling Kit or with digoxigenin-dUTP using the DIG High Prime DNA labeling and Detection Starter Kit II according to the protocol of the manufacturer (Roche Applied Science, Rotkreuz, Switzerland). Hybridization experiments were performed in SDS/BSA hybridization buffers (0.5 M sodium-phosphate [pH7], 7% sodium dodecyl sulfate, 1% bovine serum albumin) at 55°C for 16 hours. The membranes were washed twice with a solution of 5 × SSC containing 1 mM EDTA for 2 min at room temperature and twice with a solution of 2 × SSC plus 0.1% SDS for 30 min at 55°C. Binding of digoxigenin-labeled probes was immunologically detected according to the supplier's protocol (Roche Applied Science).

Construction of N-terminal 6xHis-tagged recombinant SdpA expression plasmid. Expression plasmid pMec19 was constructed in the PCR by reamplification of the *SdpA* gene from pMec16 (Chapter 2) with the following primers: 5'-CAG GAG GAT TCA TAT GTC A-3' and 5'-GCC AGC TGG ATC CGC CGA TGA-3'. Thereby, a *Nde*I restriction site at the translational start codon and a *Bam*HI restriction site just past the translational stop codon were introduced (underlined nucleotides). The fragment was first cloned into pGEM®-T Easy

COR-AAD1-00003537
Bayer EX1008 (Part 7 of 9)

(Promega), generating pMec18, and verified by sequencing. The plasmid was then digested with *Nde*I and *Bam*HI and ligated into the same sites of vector pET-15b yielding pMec19.

Expression and purification of recombinant SdpA. *E. coli* BL21(DE3)(pLysS) harboring pMec19 was grown in Erlenmeyer flasks containing LB-medium complemented with ampicillin and chloramphenicol at 30°C with constant shaking. To express the protein, a preculture of *E. coli* BL21 (DE3)(pLysS) harboring pMec19 was grown overnight at 37°C. A volume of 1% (v/v) of the preculture was transferred to fresh medium and grown at 30°C until an optical density of 0.4–0.6 (measured at 546 nm) was reached, after which isopropyl-β-D-thiogalactopyranoside was added to a final concentration of 1 mM. The culture was incubated for another 3 hours at 30°C and the cells were harvested by centrifugation at 7'500 × *g* for 30 min at 4°C and the pellet was stored at –20°C until further use. For the preparation of cell extracts, 1 g cells (wet weight) was resuspended in 3 ml lysis buffer (50 mM NaH_2PO_4, 300 mM NaCl, 10 mM imidazole, pH adjusted to 8) and the cells were broken by one passage through a French press (Hypramag, Zurich, Switzerland) at 1 MPa. The lysate was centrifuged for 45 min at 16'000 × *g* at 4°C and aliquots were stored at –20°C.

6xHis-tagged SdpA was purified in a two-step procedure. Unless stated otherwise, all steps were carried out at 4°C. Up to one mg protein was loaded on a 5-ml Ni-NTA superflow-agarose column (Qiagen) at a flow rate of 0.3 ml/min. Unbound protein was removed stepwise with five column volumes of wash-buffer (50 mM NaH_2PO_4, 300 mM NaCl) containing 20 mM imidazole (pH adjusted to 8) and five column volumes of wash buffer containing 50 mM imidazole (pH adjusted to 8). $SdpA_H$ was then eluted in 1-ml fractions with elution buffer (50 mM NaH_2PO_4, 300 mM NaCl, 200 mM imidazole, pH adjusted to 8) at a flow rate of 0.6 ml/min. The active fractions were pooled and desalted into 20 mM Tris-HCl (pH 7.5) using PD-10 columns (Amersham Biosciences, Dübendorf, Switzerland) at room temperature and loaded on a Q2 Bio-Scale column (BioRad) equilibrated in the same buffer. The enzyme was eluted with a linear concentration gradient from 20 mM Tris-HCl (pH 7.5) to 20 mM Tris-HCl (pH 7.5) plus 600 mM NaCl in six column volumes. SdpA was found to elute at approximately 200-250 mM NaCl. The active fractions were pooled again and stored at 4°C. Thrombin protease (Amersham Biosciences) was used to cleave the N-terminal His-tag. The N-terminal His-tag of approximately 10 μg SdpA was completely cleaved by 0.5 U thrombin protease within 2 hrs at room temperature.

Enzyme Activity Assays. Enzyme activity measurements were carried out using the three following different assays (Chapter 3): (i) coupled continuous assay, (ii) end-point assay and measuring of product formation by HPLC, and (iii) oxygen electrode measurements. The coupled continuous assay was used to determine specific activities of SdpA towards phenoxypropanoic acids, the end-point assay for all other substrates. In all assays, 50 mM imidazole (pH 6.75), 1

COR-AAD1-00003538
Bayer EX1008 (Part 7 of 9)

mM substrate, 1 mM α-ketoglutarate, 100 μM $(NH_4)_2Fe(SO_4)_2$ and 1 mM ascorbic acid were used and the reaction was started by the addition of the enzyme.

Protein concentration determination and SDS-PAGE. Protein concentrations were measured using the Bradford-method (6) with the Bio-Rad reagent dye concentrate reagens following the instructions of the manufacturer (Bio-Rad, Reinach, Switzerland). Bovine serum albumin fraction V (Sigma-Aldrich) was used as a reference protein. Sodium dodecyl sulfate-polyacrylamide gel electrophoresis (SDS-PAGE) was carried out with 12% acrylamide slab gels according to established procedures (26).

Native size determination of SdpA. Molecular weight analysis of purified 6xHis tagged SdpA was determined on a Superdex 200 preparation grade HiLoad 16/60 size exclusion column (Amersham Biosciences). Approximately 0.25 mg protein were loaded on the HiLoad column and eluted at a flow rate of 0.2 ml/min in 50 mM Na_2HPO_4-KH_2PO_4-buffer (pH 7) containing 150 mM NaCl. The calibration curve was done with the gel filtration standard from Bio-Rad containing thyroglobulin (bovine, 670 kDa), Gamma globulin (bovine, 158 kDa), Ovalbumin (chicken, 44 kDa), Myoglobulin (horse, 17 kDa) and Vitamin B-12 (1.35 kDa). Blue dextran was used to determine the void volume.

Chemicals. Phenoxyalkanoic acids were purchased at Riedel-de Haën (Buchs, Switzerland; PESTANAL®, 99% purity) or Sigma-Aldrich (97-99% purity). *(S)*-mecoprop and *(S)*-dichlorprop were synthesized by C. Zipper (45). α-Ketoglutarate and other (di)carboxyacids were purchased from Sigma-Aldrich. All other chemicals were obtained from Fluka (Buchs, Switzerland) or from Merck AG (Dietikon, Switzerland).

RESULTS

Expression and purification of recombinant SdpA. The *sdpA* gene was expressed in *E. coli* BL21 (DE3)(pLysS) harboring pMec19. The expression produced low levels of 6xHis-tagged SdpA amounting to less than 10% of total protein concentration in the soluble fraction of the cell-extract as determined on SDS-PAGE. Reduction of the expression temperature did not increase the amount of soluble SdpA and therefore, all expression experiments were carried out at 30°C. Recombinant SdpA was purified in a two-step procedure to apparent homogeneity as summarized in Table 1 and Fig. 2. The calculated subunit size of the 6xHis-tagged SdpA was 33.7 kDa, which was consisted with a size of approximately 32 kDa determined by SDS-PAGE. Gel filtration chromatography was used to estimate a native size of approximately 32 kDa suggesting a

COR-AAD1-00003539
Bayer EX1008 (Part 7 of 9)

monomeric structure. The 6xHis-tag was cleaved by thrombin protease treatment from the recombinant SdpA. The native and the recombinant protein were equally active in enzyme activity measurements, Hence, the 6xHis-tagged α-ketoglutarate-dependent *(S)*-dichlorprop dioxygenase was used in all further experiments.

Table 1: Representative purification table of α-ketoglutarate-dependent *(S)*-dichlorprop dioxygenase

	volume (ml)	total protein (mg)	total activity (U)	specific activity (U/mg protein)	recovery %	purification -fold
cell extract	3.5	42.6	18.5	0.4	100	1
Ni-NTA superflow	5	1.0	7.7	7.4	41.7	17.0
Bio-Scale Q2	3	0.7	6.3	8.9	34.3	20.5

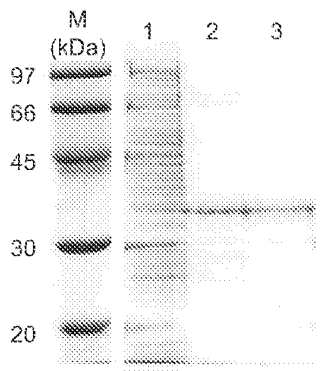


Fig. 2. Purification of *Sphingomonas herbicidovorans* MH 6xHis tagged recombinant α-ketoglutarate-dependent *(S)*-dichlorprop dioxygenase from *E. coli* BL21(DE3)(pLysS) harboring (pMec19). Protein samples were analyzed on denaturing gel electrophoresis on a 12% polyacrylamide gel and stained with Coomassie Brilliant Blue. Lane M, molecular weight markers (indicated in kDa), lane 1, extract of induced cells, lane 2, partially purified SdpA (obtained after Ni-NTA-superflow chromatography), lane 3, apparently pure SdpA (obtained after anion-exchange chromatography).

SdpA is an α-ketoglutarate-dependent dioxygenase catalyzing an enantioselective reaction. SdpA had been grouped into the family of α-ketoglutarate-dependent dioxygenases according to its amino acid sequence (Chapter 2). Enzyme activity measurements confirmed this classification. SdpA

COR-AAD1-00003540
Bayer EX1008 (Part 7 of 9)

activity was abolished in the absence of α-ketoglutarate and strongly reduced in the absence of Fe(II) (Table 2). Without ascorbate, activity was decreased to less than 40% of the one in the presence of all components. Additionally, the three different activity measurements, the coupled-continuous assay, the end-point assay and oxygen-electrode measurements, demonstrated that SdpA converted mecoprop stoichiometrically to 2-methyl-4-chlorophenol and pyruvate under con-comitant consumption of molecular oxygen (Fig. 1).

SdpA converted only the *(S)* enantiomers of phenoxypropanoic acids and no activity was observed with the *(R)* enantiomers. In the presence of *(R)*-mecoprop, i.e., when the racemate was used, activity reduced to approximately 85% indicating slight inhibition (data not shown).

Table 2: Dependence of α-ketoglutarate-dependent *(S)*-dichlorprop dioxygenase activity on substrate, cosubstrate and cofactor

	Specific activity (U/mg protein)	% Activity
Complete assay	7.0	100
– *(R)*-mecoprop[a]	0	0
– α-ketoglutarate[a]	0	0
– Fe(II)[a]	0.6	8.2
– ascorbate[a]	2.7	37.8

[a] Complete assay without the specified component.

Physicochemical characterization. SdpA did not lose measurable activity at room temperature for several hours and lost less than 10% of its activity when stored at 4°C within 3 days. Storage on ice and freezing-thawing cycles reduced activity to about 80%. It appeared important to prewarm SdpA for several minutes at room temperature prior to activity measurements. The temperature optimum was established to be between 35° and 40°C (Fig. 3A). The pH-optimum was determined in 50 mM imidazole buffer with the respective pH and was found to be between pH 6.5 and 6.75 (Fig. 3B).

COR-AAD1-00003541
Bayer EX1008 (Part 7 of 9)

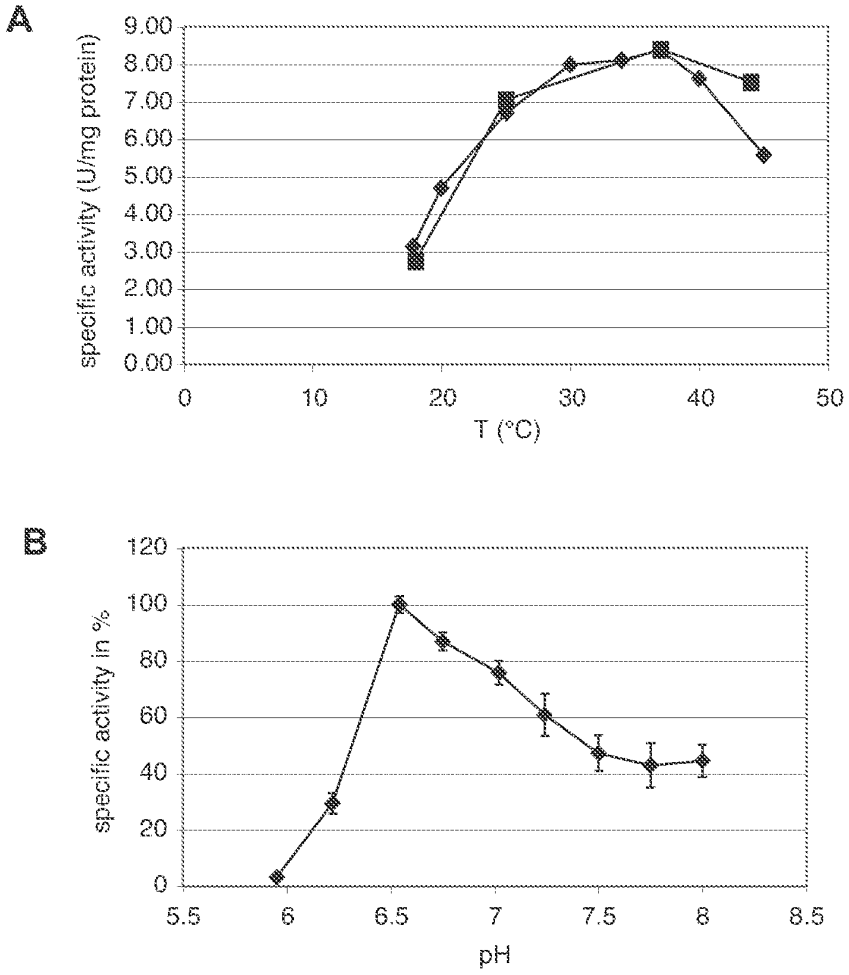


Fig. 3. Temperature (panel A) and pH (panel B) dependence of α-ketoglutarate-dependent *(S)*-dichlorprop dioxygenase. (A) The black squares represent data obtained with the end-point assay, the black diamonds data obtained with the coupled continuous assay. The measurements were carried out with two independently purified *(S)*-dichlorprop dioxygenase samples. (B) The diamonds show the mean value of six measurements of two independent experiments. Enzyme activity was determined with the coupled continuous assay.

Substrate, cosubstrate and cofactor specificities. For several substrates, it was tested whether they support activity of SdpA. In one series including besides the phenoxypropanoic acids the phenoxyacetic and phenoxybutyric acids, the influence of the alkanoic acid attached to the phenoxygroup by an ether-bond was tested. In other experiments, the effects of having different substituents such as methyl-, hydroxy- and chloride groups on the aromatic moiety were studied.

COR-AAD1-00003542
Bayer EX1008 (Part 7 of 9)

Substrate specificities of SdpA for phenoxypropanoic acid were determined by using the continuous-coupled asssay whereas the end-point assay was applied for all other substrates. When single enantiomers of the tested phenoxypropanoic acids were not commercially available, racemic mixtures were used at a final concentration of the *(S)* enantiomers of 1 mM. SdpA showed the highest turnover rate for substituted phenoxypropanoic acids. Of those, mecoprop was transformed at the highest rate (Table 3). Unsubstituted phenoxypropanoic acid was converted at only 11.6% of the activity with mecoprop. 3-Methyl-5-chlorophenoxyacetic acid was oxidized at a rate of 20% of the activity with mecoprop. 2,4-D supported activity only poorly at approximately 5% of the highest activity and phenoxybutyric acids were not converted at considerable rates.

Table 3: Substrate Specificities of α-ketoglutarate-dependent *(S)*-dichlorprop dioxygenase[a]

Substrate	Activity[b] (% ± std. dev.)	Activity (U/mg protein)
(*R,S*)-Mecoprop[c]	100	8.19 / 6.25[d]
(*R,S*)-Dichlorprop[c]	65.3±9.7	5.08
2-(*R,S*)-Phenoxypropanoic acid[c]	11.6±2.6	0.94
2-(*R,S*)-3-Chlorophenoxypropanoic acid	33.2±2.5	2.88
2-(*R,S*)-4-Chlorophenoxypropanoic acid[c]	66.1±3.2	5.92
2-(*R,S*)-2,4,5-Trichlorophenoxypropanoic acid[c]	71.5±6.6	1.39
2-(*R,S*)-4-Hydroxyphenoxypropanoic acid[c]	19.6±3.2	1.80
2,4-D[e, f]	5.6±5.2	0.33
3-Methyl-5-chlorophenoxyacetic acid[e]	20.3±6.2	1.25
2,4-Dichlorophenoxybutyric acid[e]	<1	<0.1
4-Chloro-2-methylphenoxybutyric acid[e]	2.3±1.2	0.14

[a] The substrate range was determined with two independently purified batches of SdpA and enzyme activity of each batch was measured three times with all the substrates.
[b] The standard deviation is given in %.
[c] Enzyme activity was determined with the coupled continuous assay.
[d] The first number is specific activity measured in the coupled continuous assay, the second in the end-point-assay.
[e] Enzyme activity was determined with the end-point-assay.
[f] Only one SdpA sample showed slight activity with 2,4-D. The data represent a mean value and might be overestimated.

COR-AAD1-00003543
Bayer EX1008 (Part 7 of 9)

To investigate, if and which other carbonic acids could substitute α-keto-glutarate, the end-point assay had to be used since the reporter enzyme of the coupled-continuous assay, D-lactate dehydrogenase, showed activity with some of the tested carbonic acids. SdpA appeared to be quite specific for α-ketoglutarate. The only tested cosubstrate able to support activity (slightly) was 2-oxoadipate (Table 4).

We further examined whether divalent cations could substitute Fe^{2+} in the enzyme reaction. The alternative cations Ca^{2+}, Co^{2+}, Mg^{2+}, Mn^{2+}, and Ni^{2+} could not substitute for Fe^{2+} and even completely abolished $SdpA_H$ activity indicating an inhibitory effect (Table 5).

Table 4: Cosubstrate specificities of α-ketoglutarate-dependent *(S)*-dichlorprop dioxygenase

cosubstrate	specific activity (U/mg protein)	% activity
α-ketoglutatarate	6.7	100
oxaloacetate	0	0
2-oxobutyrate	0.03	0
2-oxovalerate	0	0
2-oxoadipate	0.3	5

Table 5: Cofactor specificities of α-ketoglutarate-dependent *(S)*-dichlorprop dioxygenase

Cofactor	Specific activity (U/mg protein)	% Activity
$Fe(NH_4)_2(SO_4)_2$	7.2	100
$Fe(SO_4)$	6.8	92.8
$CaCl_2$	0	0
$CoCl_2$	0	0
$MgCl_2$	0	0
$MnCl_2$	0	0
$NiCl_2$	0	0

COR-AAD1-00003544
Bayer EX1008 (Part 7 of 9)

Kinetic analysis. We examined the kinetic behaviour of SdpA towards phenoxypropanoic acids, α-ketoglutarate and oxygen (Table 6). For the measurements of the prime substrates and α-ketoglutarate, the coupled continuous assay was carried out; O_2-kinetic was determined in the oxygen-electrode. Generally, SdpA exhibited Michaelis-Menten kinetic with all tested substrates and cosubstrates. *(S)*-Mecoprop was the best prime substrate, i.e., the apparent K_m-value was lowest and the catalytic efficiency was the highest. SdpA had high affinity to α-ketoglutarate with an apparent K_m-value of 19.6 μM whereas it had quite low affinities to O_2; a K_m-value of 159 μM was calculated for oxygen.

Table 6: Kinetic parameters of α-ketoglutarate-dependent *(S)*-dichlorprop dioxygenase

substrate	K_m (μM)	k_{cat} (min^{-1})	k_{cat}/K_m ($\mu M^{-1} \times min^{-1}$)
(*S*)-mecoprop (50 – 2000 μM)	132±17.7	303.9	2.3
(*S*)-dichlorprop (120 – 2000 μM)	494.8±43.9	284.6	0.58
O_2 (0.02 – 0.2 mM)	159.32	116[a]	0.754
α-ketoglutarate (8 – 1000 μM)	19.6±2.5	229.7	11.72

[a] The kinetic values for O_2 were determined with material from two different purified SdpA, which both were less active than the ones used for other kinetic experiments. However, the stoichiometry of the reaction was verified with material from a third purification batch (data not shown).

Screening for other 2,4-D degrading genes. We screened total DNA of *S. herbicidovorans* MH for a *tfdA*-like dioxygenase and for the aromatic ring hydroxylating dioxygenase CadAB by hybridization and PCR experiments. The *tfdA*- and the *cadAB*-derived probes did not hybridize to total DNA of *S. herbicidovorans* MH and no *tfdA*-like gene could be amplified with the PCR-primers derived from the conserved regions of *tfdA*- and *tfdA*α-genes.

DISCUSSION

SdpA is an α-ketoglutarate-dependent dioxygenase. A Blast search had already suggested that SdpA belongs to the diverse family of α-ketoglutarate-dependent dioxygenases. These enzymes are classified in three groups according to

COR-AAD1-00003545
Bayer EX1008 (Part 7 of 9)

a conserved motif containing the 2-His-1-carboxylate facial triad. By sequence alignment, the motif of group II α-ketoglutarate-dependent dioxygenases ($HXDX_{24}TX_{127}HX_{10}R$) was detected in the primary sequence as well. According to the crystal structure of α-ketoglutarate-dependent taurine dioxygenase (TauD) from *E. coli* K-12 (12, 31), a structure model and mutagenesis studies of TfdA (12, 19), His-102, Asp-104 and His-257 are predicted to be the iron(II) binding sites and build the 2-His-1-carboxylate facial triad. Thr-129 and Arg-268 are putative α-ketoglutarate binding sites.

Enzyme activity measurements confirmed the classification of SdpA as an α-ketoglutarate-dependent dioxygenase. Enzyme activity was completely abolished in the absence of α-ketoglutarate and strongly reduced in the absence of ferrous iron. Interestingly, SdpA showed only 38% initial activity in the absence of ascorbate, although ascorbate is formally not needed for the conversion of phenoxypropanoic acids. Ascorbate is thought to keep the iron(II) at the catalytic center in the reduced state and also both prolyl-4-hydroxylase and lysyl-hydroxylase were inactivated rapidly in the absence of ascorbate (8, 27, 28, 34). Even more strikingly, AlkB, a DNA base repair enzyme from *E. coli*, did not exhibit any activity at all in the absence of ascorbate (41). The inactivation mechanism was proposed to involve decarboxylation of α-ketoglutarate in a side-reaction, which is coupled to the oxidation of Fe(II) to Fe(III). The inactivation is reversible in the presence of ascorbate, because the iron is reduced again.

Enantioselective conversion of phenoxypropanoic acid herbicides involves the enzyme pair RdpA and SdpA. SdpA exclusively converted *(S)*-dichlorprop and *(S)*-mecoprop but not the *(R)* enantiomers. This confirms previous enzyme activity experiments with cell-free extracts in which the existence of two distinct α-ketoglutarate-dependent dioxygenases in strain MH was proposed. Only recently, the α-ketoglutarate-dependent *(R)*-dichlorprop dioxygenase, specific for the *(R)* enantiomers, was isolated and characterized (30, Chapter 3). Apparently, *S. herbicidovorans* MH harbors two distinct enzymes with opposite enantio-specificities. The existence of two enantiospecific enzymes would make an interesting model for understanding the basis of enantioselectivity. In some cases,

COR-AAD1-00003546
Bayer EX1008 (Part 7 of 9)

like TfdA from *R. eutropha* JMP134(pJP4), from *Burkholderia cepacia* RASC and from *A. denitrificans*, one could assume that only the active site must be different, since $TfdA_{pJP4}$ and $TfdA_{RASC}$ only transform *(S)*-dichlorprop whereas TfdA from *A. denitrificans* cleaves the ether-bond of *(R)*-mecoprop and all three use 2,4-D as substrates as well (36). This was also shown for the enzyme pair tropinone reductase I and II from *Daturam stramonium* involved in the enantioselective biosynthesis of tropane alkaloids. They share 64% amino acid identity and their native structure is almost identical, but their active sites differ (29). Another possibility for differing enantiospecificity is a completely different overall enzyme fold, but a similar active site. This is apparently the case for the enzyme pair L- and D-lactate dehydrogenase which do not share sequence similarity to each other, have a completely different fold, but possess a surprisingly similar active site (16, 38). Since RdpA and SdpA have very little primary sequence identity to TauD, useful predictions on their overall structure about the similarity of their native folds, the substrate binding sites and the active sites cannot be answered by primary sequence alignment alone, but the determination of a crystal structure or appropriate modeling is required.

Substrate, cosubstrate and cofactor specificities of SdpA. SdpA exhibited activity with most tested phenoxyalkanoic acids. High activity was observed for chloro- and methylsubstituted derivatives of phenoxypropanoic acids and the catalytic efficiency was highest for *(S)*-mecoprop. This indicates that SdpA has adapted to methyl- and chlorophenoxyalkanoic acids. This agrees with the results obtained with $SdpA_{MC1}$ but is in contrast to TfdAα, which prefers unsubstituted phenoxyacetic acids to chlorophenoxyacetic acids (21). Furthermore, it indicates that the substituents are important to accommodate the substrate at the catalytic center. Surprisingly, 2,4,5-trichlorophenoxypropanoic acid was the second best substrate of all acids tested and was converted at rates of 71% of highest activity obtained with mecoprop. The third chloride atom seems to also fit into the active site and apparently does not hinder the conversion. Despite their close relatedness, SdpA from *D. acidovorans* MC1 showed no activity at all with 2,4,5-trichlorophenoxypropanoic acid (44). In general, substituted phenoxy-

COR-AAD1-00003547
Bayer EX1008 (Part 7 of 9)

propanoic acids were better substrates than substituted phenoxyacetic and phenoxybutyric acids. This suggests that the alkyl moiety of the alkanoic acid side chain is more important than the substituent at the aromatic ring for activity. Similar observations were made for TfdA, which has 2,4-D as the best substrates, but also hydroxylates propionic acids although with much lower catalytic efficiency (13, 14).

SdpA exhibited Michaelis-Menten kinetics for oxygen, but the calculated apparent K_m-value of 159 μM was high when compared to the ones of other α-ketoglutarate-dependent dioxygenases, but not as high as the one of RdpA, for which even no Michaelis-Menten kinetics could be observed in the range of 0-0.2 mM O_2 (Chapter 3). For example, the α-ketoglutarate-dependent dioxygenases lysyl-hydroxylase and deacetoxycephalosporin C synthase have affinity constants in the range of 40 – 50 μM for O_2 (7, 34) and flavonol dioxygenase has an apparent K_m-value of 5.26 μM O_2 (2). In contrast to these α-ketoglutarate-dependent dioxygenases, 3,5-dichlorocatechol dioxygenase from *Pseudomonas cepacia* CSV90 has a K_m-value of 652 μM for O_2 (5).

SdpA has high affinity for α-ketoglutarate (apparent K_m-value of 19.6 μM). This agrees well with the results obtained for other α-ketoglutarate-dependent dioxygenases such as RdpA, $SdpA_{MC1}$, TfdA and TauD (11, 14, 44, Chapter 3). In contrast to TfdA and TfdAα, but in agreement with RdpA, SdpA had a narrow cosubstrate specificity and only 2-oxoadipate could substitute for α-ketoglutarate at low rates (14, 21, Chapter 3). The cofactor range was limited to ferrous iron and other divalent cations could not substitute. This concurs with the findings from other α-ketoglutarate-dependent dioxygenases (11, 14, 44, Chapter 3).

Existence of another dioxygenase involved in phenoxyalkanoic acid degradation in strain MH. RdpA and SdpA do not convert 2,4-D at a significant rate. Yet previously, it had been shown that *S. herbicidovorans* MH grows on 2,4-D with a higher specific growth rate than on mecoprop and dichlorprop (46). This would suggest, that another phenoxyalkanoic acid converting enzyme, specific for 2,4-D, must exist in *S. herbicidovorans* MH. Despite our attempts to detect genes for other phenoxyalkanoic acid converting enzymes in *S. herbicidovorans* MH by

COR-AAD1-00003548
Bayer EX1008 (Part 7 of 9)

hybridization and PCR-experiments, we found no conclusive evidence for a *tfdA*-like, a *tfdAα*-like, or a *cadAB*-like gene(s). The reason for this failure might be that the unknown gene is too dissimilar to be detected with the known *tfdA*, *tfdAα*- or *cadAB* consensus primers or hybridization probes. Therefore, it still remains unclear what kind of enzyme is responsible for the high growth rates of *S. herbicidovorans* MH with 2,4-D.

Many questions concernings the substrate binding sites, the active site, the protein folding and perhaps even the possibility to change the enantiospecificity of RdA to that of SdpA (or vice versa) remain. The answers to these questions will shed light on the interactions of enzymes and their chiral substrates and may allow us to identify, which features dictate enantiospecificity. Rational mutagenesis studies based on enzyme structures or models are planned to answer such questions in the future.

COR-AAD1-00003549
Bayer EX1008 (Part 7 of 9)

REFERENCES

1. Ahrens, W. H. 1994. Herbicide Handbook (WSSA), 7th ed. Weed Science Society of America, Champaign.
2. Anzellotti, D., and R. K. Ibrahim. 2000. Novel flavonol 2-oxoglutarate dependent dioxygenase: affinity purification, characterization, and kinetic properties. Arch. Biochem. Biophys. 382:161-72.
3. Ausubel, F. M., R. Brent, R. E. Kingston, D. D. Moore, J. G. Seidman, J. A. Smith, and K. Struhl (ed.). 2002. Current protocols in molecular biology. John Wiley & Sons, Inc., New York, N. Y.
4. Benes, V., Z. Hostomosky, L. Arnold, and V. Paces. 1993. M13 and pUC vectors with new unique restriction sites for cloning. Gene 130:151-152.
5. Bhat, M. A., T. Ishida, K. Horiike, C. S. Vaidyanathan, and M. Nozaki. 1993. Purification of 3,5-dichlorocatechol 1,2-dioxygenase, a nonheme iron dioxygenase and a key enzyme in the biodegradation of a herbicide, 2,4-diochlorophenoxyacetic acid (2,4-D), from *Pseudomonas cepacia* CSV90. Arch. Biochem. Biophys. 300:738-746.
6. Bradford, M. M. 1976. A rapid and sensitive method for the determination of microgram quantities of protein utilizing the principle of protein-dye binding. Anal. Biochem. 72:248-254.
7. de Carolis, E., and V. de Luca. 1993. Purification, characterization, and kinetic analysis of a 2-oxoglutarate-dependent dioxygenase involved in vindoline biosynthesis from *Catharanthus roseus*. J. Biol. Chem. 268:5504-5511.
8. de Jong, L., S. P. J. Albracht, and A. Kemp. 1982. Prolyl 4-hydroxylase activity in relation to the oxidation state of enzyme-bound iron. The role of ascorbate in peptidyl proline hydroxylation. Biochim. Biophys. Acta 704:326-332.
9. Don, R. H., A. J. Weightman, H.-J. Knackmuss, and K. N. Timmis. 1985. Transposon mutagenesis and cloning analysis of the pathways for degradation of 2,4-dichlorophenoxyacetic acid and 3-chlorobenzoate in *Alcaligenes eutrophus* JMP134(pJP4). J. Bacteriol. 161:85-90.
10. Donaldson, D., T. Kiely, and A. Grube. 2002. Pesticides industry sales and usage. 1998 and 1999 market estimates. U.S. Environmental Protection Agency.
11. Eichhorn, E., J. R. van der Ploeg, M. A. Kertesz, and T. Leisinger. 1997. Characterization of α-ketoglutarate-dependent taurine dioxygenase from *Escherichia coli*. J. Biol. Chem. 272:23031-23036.
12. Elkins, J. M., M. J. Ryle, I. J. Clifton, J. C. Dunning Hotopp, J. S. Lloyd, N. I. Burzlaff, J. E. Baldwin, R. P. Hausinger, and P. L. Roach. 2002. X-ray crystal structure of *Escherichia coli* taurine/α-ketoglutarate dioxygenase complexed to ferrous iron and substrates. Biochemistry 41:5185-5192.
13. Fukumori, F., and R. P. Hausinger. 1993. *Alcaligenes eutrophus* JMP134 "2,4-dichlorophenoxyacetate monooxygenase" is a α-ketoglutarate-dependent dioxygenase. J. Bacteriol. 175:2083-2096.
14. Fukumori, F., and R. P. Hausinger. 1993. Purification and characterization of 2,4-dichlorophenoxyacetate/α-ketoglutarate dioxygenase. J. Biol. Chem. 268:24311-24317.

COR-AAD1-00003550
Bayer EX1008 (Part 7 of 9)

15. Fulthorpe, R. R., A. N. Rhodes, and J. M. Tiedje. 1996. Pristine soils mineralize 3-chlorobenzoate and 2,4-dichlorophenoxyacetate via different microbial populations. Appl. Environ. Microbiol. 62:1159-1166.

16. Goldberg, J. D., T. Yoshida, and P. Brick. 1994. Crystal structure of a NAD-dependent D-glycerate dehydrogenase at 2.4 Å resolution. J. Mol. Biol. 236:1123-1140.

17. Hausinger, R. P. 2004. Fe(II)/α-ketoglutarate dependent hydroxylases and related enzymes. Crit. Rev. Biochem. Mol. Biol. 39:1-47.

18. Hegg, E. L., and L. Que, Jr. 1997. The 2-His-1-carboxylate facial triad--an emerging structural motif in mononuclear non-heme iron(II) enzymes. Eur. J. Biochem. 250:625-629.

19. Hogan, D. A., S. R. Smith, E. A. Saari, J. McCracken, and R. P. Hausinger. 2000. Site-directed mutagenesis of 2,4-dichlorophenoxyacetic acid/α-ketoglutarate dioxygenase. J. Biol. Chem. 275:12400-12409.

20. Horvath, M., G. Ditzelmüller, M. Loidl, and F. Streichsbier. 1990. Isolation and characterization of a 2-(2,4-dichlorophenoxy)propionic acid degrading soil bacterium. Appl. Microbiol. Biotechnol. 33:213-216.

21. Itoh, K., R. Kanda, Y. Sumita, H. Kim, Y. Kamagata, K. Suyama, H. Yamamoto, R. P. Hausinger, and J. M. Tiedje. 2002. *tfdA*-Like genes in 2,4-dichlorophenoxyacetic acid-degrading bacteria belonging to the *Bradyrhizobium-Agromonas-Nitrobacter-Afipia* cluster in α-*proteobacteria*. Appl. Environ. Microbiol. 68:3449-3454.

22. Itoh, K., Y. Tashiro, K. Uobe, Y. Kamagata, K. Suyama, and H. Yamamoto. 2004. Root nodule *Bradyrhizobium* spp. harbor *tfdA*α and *cadA*, homologous with genes encoding 2,4-dichlorophenoxyacetic acid-degrading proteins. Appl. Environ. Microbiol. 70:2110-2118.

23. Kamagata, Y., R. R. Fulthorpe, K. Tamura, H. Takami, L. J. Forney, and J. M. Tiedje. 1997. Pristine environments harbor a new group of oligotrophic 2,4-dichlorophenoxyacetic acid-degrading bacteria. Appl. Environ. Microbiol. 63:2266-2272.

24. Kitagawa, W., S. Takami, K. Miyauchi, E. Masai, Y. Kamagata, J. M. Tiedje, and M. Fukuda. 2002. Novel 2,4-dichlorophenoxyacetic acid degradation genes from oligotrophic *Bradyrhizobium* sp. strain HW13 isolated from a pristine environment. J. Bacteriol. 184:509-518.

25. Kohler, H.-P. E. 1999. *Sphingomonas herbicidovorans* MH: a versatile phenoxyalkanoic herbicide degrader. J. Ind. Microbiol. Biotechnol. 23:336-340.

26. Laemmli, U. K. 1970. Cleavage of structural proteins during the assembly of the head of bacteriophage T4. Nature 227:680-685.

27. Myllylä, R., E.-R. Kuutti-Savolainen, and K. I. Kivirikko. 1978. The role of ascorbate in the prolyl hydroxylase reaction. Biochem. Biophys. Res. Commun. 83:441-448.

28. Myllylä, R., K. Majamaa, V. Günzler, H. M. Hanauske-Abel, and K. I. Kivirikko. 1984. Ascorbate is consumed stoichiometrically in the uncoupled reactions catalyzed by prolyl 4-hydroxylase and lysyl hydroxylase. J. Biol. Chem. 259:5403-5405.

29. Nakajima, K., A. Yamashita, H. Akama, T. Nakatsu, H. Kato, T. Hashimoto, J. Oda, and Y. Yamada. 1998. Crystal structure of two tropinone reductases:

COR-AAD1-00003551
Bayer EX1008 (Part 7 of 9)

different reaction stereospecificities in the same protein fold. Proc. Natl. Acad. Sci. USA 95:4876-4881.

30. Nickel, K., M. J.-F. Suter, and H.-P. E. Kohler. 1997. Involvement of two α-ketoglutarate-dependent dioxygenases in enantioselective degradation of (*R*)- and (*S*)-mecoprop by *Sphingomonas herbicidovorans* MH. J. Bacteriol. 179:6674-6679.

31. O'Brien, J. R., D. J. Schuller, V. S. Yang, B. D. Dillard, and W. N. Lanzilotta. 2003. Substrate-induced conformational changes in *Escherichia coli* taurine/α-ketoglutarate dioxygenase and insight into the oligomeric structure. Biochemistry 42:5547-5554.

32. Perkins, E. J., M. P. Gordon, O. Caceres, and P. F. Lurquin. 1990. Organization and sequence analysis of the 2,4-dichlorophenol hydroxylase and dichlorocatechol oxidative operons of plasmid pJP4. J. Bacteriol. 172:2351-2359.

33. Prescott, A. G., and M. D. Lloyd. 2000. The iron(II) and 2-oxoacid-dependent dioxygenases and their role in metabolism. Nat. Prod. Rep. 17:367-383.

34. Puistola, U., T. M. Turpeenniemi-Hujanen, R. Myllylä, and K. I. Kivirikko. 1980. Studies on the lysyl hydroxylase reaction. I. Initial velocity kinetics and related aspects. Biochim. Biophys. Acta 611:40-50.

35. Ravatn, R., S. Studer, D. Springael, A. J. B. Zehnder, and J. R. van der Meer. 1998. Chromosomal integration, tandem amplification, and aeamplification in *Pseudomonas putida* F1 of a 105-kilobase genetic element containing the chlorocatechol degradative genes from *Pseudomonas* sp. strain B13. J. Bacteriol. 180:4360-4369.

36. Saari, R. E., D. A. Hogan, and R. P. Hausinger. 1999. Stereospecific degradation of the phenoxypropionate herbicide dichlorprop. J. Mol. Catal. B: Enzymatic 6:421-428.

37. Sambrook, J., E. F. Fritsch, and T. Maniatis. 1989. Molecular Cloning: a laboratory manual. Cold Spring Harbor Laboratory, Cold Spring Harbor, N.Y.

38. Stoll, V. S., M. S. Kimber, and E. F. Pai. 1996. Insights into substrate binding by D-2-ketoacid dehydrogenases from the structure of *Lactobacillus pentosus* D-lactate dehydrogenase. Structure 4:437-447.

39. Streber, W. R., K. N. Timmis, and M. H. Zenk. 1987. Analysis, cloning, and high-level expression of 2,4-dichlorophenoxyacetate monooxygenase gene *tfdA* of *Alcaligenes eutrophus* JMP134. J. Bacteriol. 169:2950-2955.

40. Tatusova, T. A., and T. L. Madden. 1999. BLAST 2 sequences, a new tool for comparing protein and nucleotide sequences. FEMS Microbiol. Lett. 174:247-250.

41. Trewick, S. C., T. F. Henshaw, R. P. Hausinger, T. Lindahl, and B. Sedgwick. 2002. Oxidative demethylation by *Escherichia coli* AlkB directly reverts DNA base damage. Nature 419:174-178.

42. Vallaeys, T., R. R. Fulthorpe, A. M. Wright, and G. Soulas. 1996. The metabolic pathway of 2,4-dichlorophenoxyacetic acid degradation involves different families of *tfdA* and *tfdB* genes according to PCR-RFLP analysis. FEMS Microbiol. Ecol. 20:163-172.

43. Westendorf, A., D. Benndorf, R. H. Müller, and W. Babel. 2002. The two enantiospecific dichlorprop/α-ketoglutarate-dioxygenases from *Delftia acidovorans* MC1 - protein and sequence data of RdpA and SdpA. Microbiol. Res. 157:1-6.

COR-AAD1-00003552
Bayer EX1008 (Part 7 of 9)

44. Westendorf, A., R. H. Müller, and W. Babel. 2003. Purification and characterisation of the enantiospecific dioxygenases from *Delftia acidovorans* MC1 initiating the degradation of phenoxypropionate and phenoxyacetate herbicides. Acta Biotechnol. 23:3-17.

45. Zipper, C. 1998. Microbial degradation and environmental fate of chiral phenoxyalkanoic acid herbicides. Ph. D. thesis. ETH Zürich, Zürich.

46. Zipper, C., M. Bunk, A. J. B. Zehnder, and H.-P. E. Kohler. 1998. Enantioselective uptake and degradation of the chiral herbicide dichlorprop [(*RS*)-2-(2,4-dichlorophenoxy)propanoic acid] by *Sphingomonas herbicidovorans* MH. J. Bacteriol. 180:3368-3374.

47. Zipper, C., K. Nickel, W. Angst, and H.-P. E. Kohler. 1996. Complete microbial degradation of both enantiomers of the chiral herbicide mecoprop [(*RS*)-2-(4-chloro-2-methylphenoxy)propionic acid] in an enantioselective manner by *Sphingomonas herbicidovorans* sp. nov. Appl. Environ. Microbiol. 62:4318-4322.

COR-AAD1-00003553
Bayer EX1008 (Part 7 of 9)

CHAPTER 5

General Discussion & Outlook

This study focused on the genetics of phenoxyalkanoic acid degradation in *Sphingomonas herbicidovorans* MH and on the biochemical characterization of the two α-ketoglutarate-dependent dioxygenases involved in the initial, enantioselective degradation step. In the final chapter of this thesis, I will try to discuss how the results contribute to a broader understanding of phenoxyalkanoic acid degradation and of enantioselective enzymatic reactions.

Degradation pathway of phenoxypropanoic acids in *S. herbicidovorans* MH. One of our aims was to unravel the complete degradation pathway of phenoxyalkanoic acid herbicides in strain MH. In chapter 2, we showed that *S. herbicidovorans* MH degrades mecoprop, dichlorprop and 2,4-D through a modified-*ortho*-cleavage pathway, i.e., a pathway analogous to 2,4-D degradation in *Ralstonia eutropha* JMP134(pJP4). Surprisingly, however, the isolated genes and the genetic organization for the mecoprop pathway from *S. herbicidovorans* MH were not similar to the canonical *tfd*-genes found in typical 2,4-D degraders such as *R. eutropha* JMP134(pJP4) and *Variovorax paradoxus*. *S. herbicidovorans* MH harbored the *rdpA*- and the *sdpA*-gene encoding two α-ketoglutarate-dependent dichlorprop dioxygenases. Further, a phenol-hydroxylase gene (*tfdB*) and most of the genes of chlorocatechol degradation were discovered: two dichlorocatechol 1,2-dioxygenase genes ($dccA_{I/II}$), two dienelactone hydrolase genes $dccD_{I/II}$, one gene *dccE* coding for a maleylacetate reductase, a putative transport gene (*tfdK*) and a putative regulator gene (*cadR*). Four aspects were remarkable for the phenoxypropanoic acid degradation pathway in *S. herbicidovorans* MH: (i) the genes were flanked by IS elements; (ii) the homology of the dichlorprop genes in strain MH to other phenoxyalkanoic acid genes pointed to different evolutionary origins; (iii) the genes were 'scattered' over the genome (i.e., not organized in one or two long polycistronic operons) and for several genes two complete copies were found; (iv) expression of the genes of the dichlorprop pathway was not tightly regulated. These points indicate a different evolutionary background for the dichlorprop pathway genes from the one in

COR-AAD1-00003556
Bayer EX1008 (Part 7 of 9)

Beta- and *Gammaproteobacteria* and suggest that *S. herbicidovorans* MH might be able to acquire DNA from other sources by horizontal gene transfer relatively easily. With regard to the expression of new DNA, our results would point to a strategy employed by the organism to express new genes constitutively and perhaps later in evolutionarly development to control them by inducible expression. Similar results have been found with regard to catabolic pathways in other *Sphingomonas* strains (1-3), and might indicate a more general phenomenon for Sphingomonads to enable them to use new carbon sources and to adapt to new 'ecological niches'. From a scientific point of view, *Sphingomonas* strains are ideal for isolating novel genes and for studying evolutionary processes. It would be interesting to try to determine whether the IS elements in *S. herbicidovorans* MH are sufficiently active to mobilize the gene cassettes and transfer them to a new host. Recently, for example, it was shown that *Sphingomonas paucimobilis* has very active IS elements, which rearrange and delete the genes for the lindane degradation pathway (3). It would also be fascinating to study whether strain MH is carrying vehicles for horizontal gene transfer (e.g., plasmids, phages, or genomic islands) or even might be able to take up DNA by transformation. Many interesting genetic and regulatory questions regarding the dichlorprop pathway still remain unanswered. Does the isolated *cadR*-gene code for a regulatory protein of this pathway? Do other regulatory genes exist for this pathway? Where is the gene for the chloromuconate cycloisomerase? Is the isolated *tfdK*-gene a 2,4-D or perhaps a mecoprop or a dichlorprop transporter protein? Do other transport proteins exist for phenoxypropanoic acids? The results obtained so far indicate that *Sphingomonas* strains either are at a different evolutionary stage than the canoncial 2,4-D degraders or apply other strategies for gene organization and regulation to survive in a 'contaminated' environment.

Phenoxyalkanoic acid converting dioxygenases. In chapter 3 and 4, we studied the two α-ketoglutarate-dependent dioxygenases RdpA and SdpA, which catalyze the enantioselective conversion of *(R)*- and *(S)*-phenoxy-

COR-AAD1-00003557
Bayer EX1008 (Part 7 of 9)

propanoic acids to the achiral phenol. We purified and characterized both enzymes in terms of physicochemical parameters, substrate, cosubstrate, and cofactor specificities and determined the enzyme kinetic parameters. We demonstrated that both enzymes are enantiospecific and that they do not convert 2,4-D at a significant rate. Since *S. herbicidovorans* MH grows on 2,4-D, it would be plausible to presume the existence of a third phenoxyalkanoic acid dioxygenase. Indeed, we screened for a 2,4-D converting enzyme, but no *tfdA*-like, *tfdA*α-like or *cadAB*-like gene could be isolated (Chapter 4). Two possible explanations can be given at the moment: either we did not detect the gene with the chosen methods or *S. herbicidovorans* MH harbors another unknown 2,4-D converting dioxygenase. I suggest that no other *tfdA*-like gene exists in strain MH, since neither hybridization nor PCR-experiments led to positive results. The occurrence of a *tfdA*α or a *cadAB*-like gene is, to my opinion, also unlikely, since in the PCR, no *tfdA*α fragment was amplified and in hybridization experiments with *cadAB*-derived probes, no positive results were obtained. However, I would not totally rule out the possibility that *S. herbicidovorans* MH harbors one of these genes due to the following reasons. *tfdA*α genes have been isolated from many *Sphingomonas* strains and we might just have failed to amplify it in the PCR. The same argument may hold for the *cadAB*-like gene. Furthermore, *S. herbicidovorans* MH harbors a *cadR*-like gene, which may indicate to the existence of other genes from the *cad*-pathway. Unfortunately, we had neither time nor money to sequence additional large regions from our cosmids to screen for other *cad*-genes. Therefore, additional genetic experiments or large scale sequencing will be required to further elucidate the pathway for 2,4-D and phenoxypropanoic acid degradation in strain MH.

The enantiospecific *(R)*- and *(S)*-dichlorprop dioxygenases. Chirality plays an important role in biochemical processes and enantioselective degradation of chiral substances is rather the rule than the exception (Chapter 1). This study about phenoxypropanoic acid degradation in *S. herbicidovorans* MH elucidated one aspect of the biochemical background of enantioselective

COR-AAD1-00003558
Bayer EX1008 (Part 7 of 9)

phenoxypropanoic acid degradation. The two enantiospecific α-ketoglutarate dioxygenases RdpA and SdpA are responsible for the enantioselective degradation of these herbicides in strain MH. We demonstrated that both dioxygenases are strictly enantiospecific. Interestingly, *S. herbicidovorans* MH harbors two enzymes catalyzing the opposite enantioselective reaction and these enzymes are only 30% identical. One hypothesis for enantioselectivity is that the enzymes share similar primary amino acid sequences and have a similar native fold, but differ in their active sites (13). Such a difference might arise in divergent evolution. One example are the 2,4-D dioxygenases, which also convert phenoxypropanoic acids. The amino acid sequences of a PCR-fragment of 2,4-D dioxygenases from *R. eutropha* JMP134(pJP4) and from *Alcaligenes denitrificans* are 86% identical, but the enzymes exhibit opposite enantioselectivity for phenoxypropanoic acid herbicides in cell-free extract (15). Contrasting examples for enantioselectivity exist, in which the enzymes have little primary sequence similarity resulting in a different protein fold. Such enzyme pairs have arisen by convergent evolution (5, 10, 17, 19, chapter 1). The low sequence similarity of SdpA and RdpA is suggestive for this hypothesis, although the results obtained so far do not allow further speculation about the evolution of the two dioxygenases.

Modeling of the structure of RdpA and SdpA. The existence of two enzymes that catalyze opposite enantioselective reactions assures that both enzymes are well adapted to their substrate and convert it with high specificity. What exactly is causing the difference in enantioselectivity? Only a few enzyme pairs have been examined in details, although enantioselective conversions are very important in biocatalysis to produce enantiomerically pure chemicals in the pharma, agro and food industrial sector (11, 18). Many production processes are based on enzymes that have been modified by random techniques such as DNA shuffling, mutagenesis and others (8, 9). For instance, the enantiospecificity of the D-specific hydantoinase from *E. coli* was converted by several mutagenesis steps leading to a L-specific hydantoinase, which is used for the production of L-methionine (12). Unfortunately, the

COR-AAD1-00003559
Bayer EX1008 (Part 7 of 9)

molecular details for the enantiospecificities are not completely understood in many cases. The characterization of additional enzyme pairs with opposite enantiospecificities such as RdpA and SdpA will help to increase our understanding of the structural and mechanistic features dictating enantiospecificity and may be valuable for future engineering of enzymes with tailored chiral synthesis or degradation activities.

To understand at least some of the structural differences between RdpA and SdpA, I tried to model both enzymes' fold on an existing structure of a similar protein. For RdpA and SdpA, it was possible to use the structure of the related α-ketoglutarate-dependent dioxygenase TauD. Modeling was done with the Swiss Model, an automated Comparative Protein Modelling Server, at Expasy (http://swissmodel.expasy.org/) using the so-called 'first approach mode' (6, 14, 16). When SdpA was subsequently modeled on the apo-form of TauD (PDB 1otj), a 'misfolded' active site was the result. RdpA could not be modeled directly without the complexed template. Hence, the TauD sequence complexed to Fe(II), α-ketoglutarate and taurine was entered into the program (database coordinates: PDB 1os7, ExPDB 1os7B).

With this templates, the models of RdpA and SdpA predicted an almost identical overall fold (Fig. 1), which was very similar to the one of TauD. The typical jellyroll motif of α-ketoglutarate-dependent dioxygenase was identified in both proteins. His-111, Asp-113, His-270 in RdpA and His-102, Asp-104 and His-257 in SdpA are positioned well to function in binding of the iron(II) (Fig. 2A and B), which agrees with the prediction of the 2-His-1-carboxylate facial triad made according to the alignment (Fig. 5, chapter 3). The same holds true for Thr-138 and Arg-281 in RdpA and Thr-129 and Arg-268 in SdpA, which are proposed to interact with α-ketoglutarate. The model shows that the iron(II)- and α-ketoglutarate binding sites of RdpA and SdpA were located at almost identical positions in the modeled fold (Fig. 2C). We may also speculate about possible substrate binding residues. In the 'front' of the active sites, Ser-114, Thr-115, Tyr-216, Val-220, Tyr-221 in RdpA and Ser-105, Thr-106, Arg-207, His-208 in SdpA build similar cavities, which seem to leave enough space

COR-AAD1-00003560
Bayer EX1008 (Part 7 of 9)

to position the aromatic ring of phenoxypropanoic acids. One residue, which could be involved in phenoxypropanoic acid binding in SdpA, is His-208. It is located near the active site in the cavity and it corresponds to His-214 of TfdA, which participates in 2,4-D positioning or catalysis (4, 7).

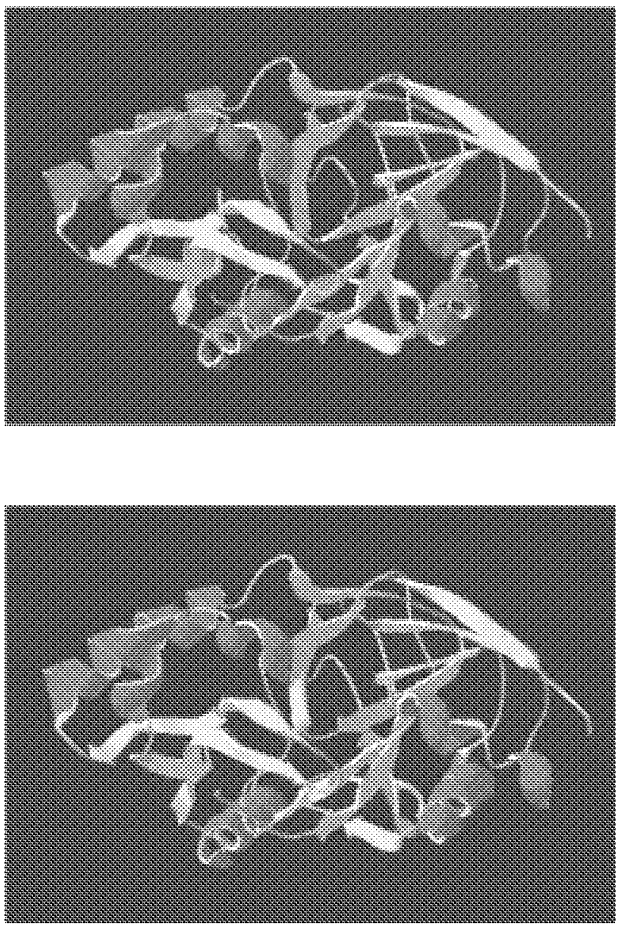


Fig. 1. Models of the native structures of RdpA (on the left) and SdpA (on the right). Helices are shown in red, β-strands in yellow. The β-strands of the conserved jellyroll motif are colored separately in green. The pictures were constructed with the program Swiss-PdbViewer (http://swissmodel.expasy.org/spdbv/).

Another interesting residue is Ser-161 of SdpA of which the amide backbone may also play a role in substrate binding. The corresponding residue in TauD, Ser-158, is involved in binding of the amine of taurine. The most striking difference between RdpA and SdpA is the 'replacement' of the neutral Gly-107

COR-AAD1-00003561
Bayer EX1008 (Part 7 of 9)

in RdpA by the basic Asn-98 in SdpA. In TauD, the corresponding amino acid residue Asn-95 binds to the amine of taurine. This indicates that the two residues may also play an important role in orienting the respective enantiomer of the phenoxypropanoic acid in RdpA and SdpA. Two opposed mechanism of interactions between the substrate propanoic acid moiety and the asparagine are plausible. The side-chain of asparagine is positively charged at a biological pH and hence, hydrogen bonds may be formed with the carboxylic group of the propanoic acid moiety of the substrate. On the contrary, the placement of the carboxylic group of the phenoxypropanoic acid might be sterically hindered due to the 'large' side chain of asparagine, which is bigger than the H-atom of glycine. At the moment, none of these mechanisms can be favored and therefore, we cannot make exact predictions about the placement of the substrate.

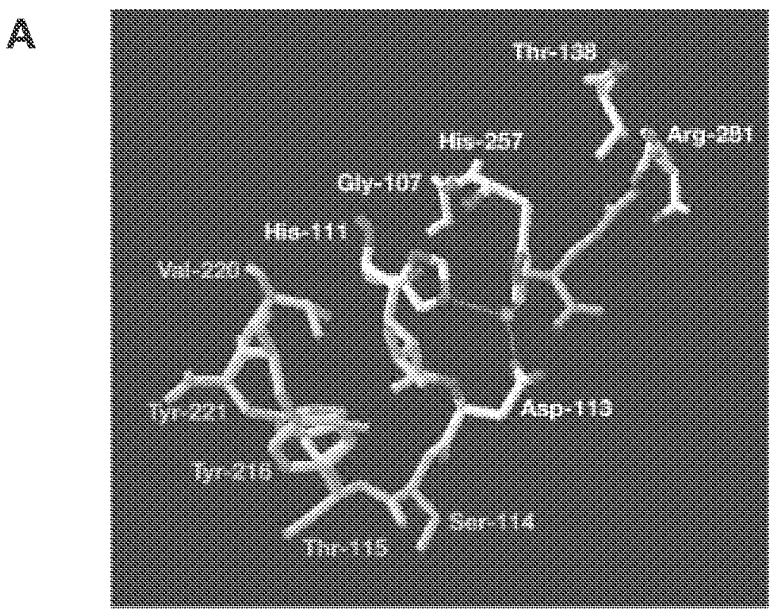


Fig. 2. A. Model of the active site of RdpA. The predicted iron(II)- and α-ketoglutarate binding residues are shown in white-red-blue; the predicted substrate binding residues are in orange. α-Ketoglutarate and iron(II) are in grey. The iron(II)-binding residues of RdpA are shown in yellow, the ones of SdpA in dark blue. The α-ketoglutarate binding residues are in light yellow (RdpA) and light green (SdpA); the substrate binding residues in orange (RdpA) and light blue (SdpA). The pictures were constructed with the program Swiss-PdbViewer.

COR-AAD1-00003562
Bayer EX1008 (Part 7 of 9)

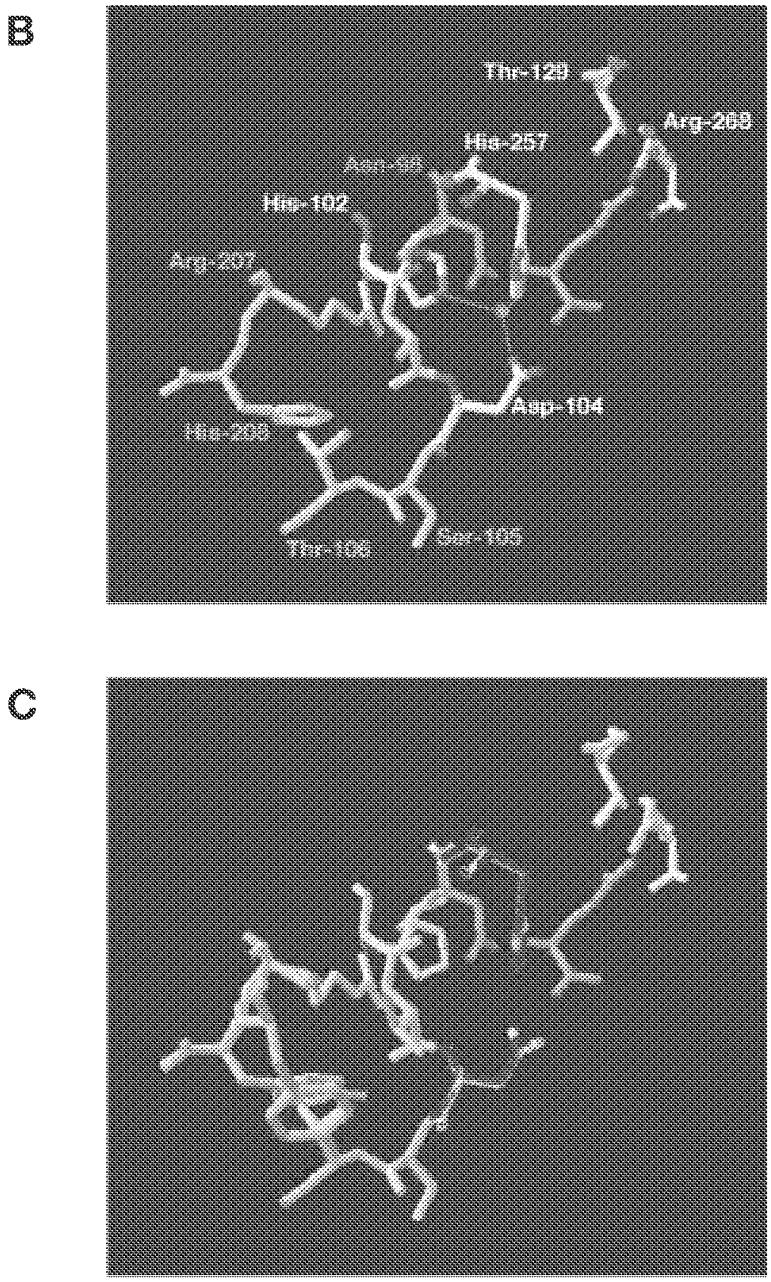


Fig. 2 (cont.) B. Model of the active site of SdpA. The predicted iron(II)- and α-ketoglutarate binding residues are shown in white-red-blue; the predicted substrate binding sites in light blue. α-ketoglutarate and iron(II) are in grey. C. Superposition of the modeled active sites of RdpA and SdpA.

COR-AAD1-00003563
Bayer EX1008 (Part 7 of 9)

Nevertheless, this simple model provides interesting insights into the active sites of the two dioxygenases. One has to be aware though that the applied procedure most likely biases the outcome because both proteins were modeled with the same template. The model might be useful to make reasonable predictions about the enantiospecificity, which could then be tested in mutagenesis and spectroscopic studies. Finally, direct crystallization will be necessary to elucidate the native structure, to fully understand the enzyme features, which dictate enantiospecificity, and to gain more details about the mechanistics of these reactions. The work presented here gives the basis for such experiments.

COR-AAD1-00003564
Bayer EX1008 (Part 7 of 9)

REFERENCES:

1. Armengaud, J., B. Happe, and K. N. Timmis. 1998. Genetic analysis of dioxin dioxygenase of *Sphingomonas* sp. strain RW1: catabolic genes dispersed on the genome. J. Bacteriol. 180:3954-3966.
2. Cai, M., and L. Xun. 2002. Organization and regulation of pentachlorophenol-degrading genes in *Sphingobium chlorophenolicum* ATCC 39723. J. Bacteriol. 184:4672-4680.
3. Dogra, C., V. Raina, R. Pal, M. Suar, S. Lal, K. H. Gartemann, C. Holliger, J. R. van der Meer, and R. Lal. 2004. Organization of *lin* genes and IS*6100* among different strains of hexachlorocyclohexane-degrading *Sphingomonas paucimobilis*: evidence for horizontal gene transfer. J. Bacteriol. 186:2225-2235.
4. Elkins, J. M., M. J. Ryle, I. J. Clifton, J. C. Dunning Hotopp, J. S. Lloyd, N. I. Burzlaff, J. E. Baldwin, R. P. Hausinger, and P. L. Roach. 2002. X-ray crystal structure of *Escherichia coli* taurine/α-ketoglutarate dioxygenase complexed to ferrous iron and substrates. Biochemistry 41:5185-5192.
5. Goldberg, J. D., T. Yoshida, and P. Brick. 1994. Crystal structure of a NAD-dependent D-glycerate dehydrogenase at 2.4 Å resolution. J. Mol. Biol. 236:1123-1140.
6. Guex, N., and M. C. Peitsch. 1997. SWISS-MODEL and the Swiss-PdbViewer: An environment for comparative protein modeling. Electrophoresis 18:2714-2723.
7. Hogan, D. A., S. R. Smith, E. A. Saari, J. McCracken, and R. P. Hausinger. 2000. Site-directed mutagenesis of 2,4-dichlorophenoxyacetic acid/α-ketoglutarate dioxygenase. J. Biol. Chem. 275:12400-12409.
8. Jaeger, K.-E., T. Eggert, A. Eipper, and M. T. Reetz. 2001. Directed evolution and the creation of enantioselective biocatalysts. Appl. Microbiol. Biotechnol. 55:519-530.
9. Jaeger, K.-E., and M. T. Reetz. 2000. Directed evolution of enantioselective enzymes for organic chemistry. Curr. Opin. Chem. Biol. 4:68-73.
10. Lamzin, V. S., Z. Dauter, and K. S. Wilson. 1994. Dehydrogenation through the looking-glass. Nat. Struct. Biol. 1:281-282.
11. Liese, A., K. Seelbach, and C. Wandrey. 2000. Industrial Biotransformations. Wiley-VCH, Weinheim.
12. May, O., P. T. Nguyen, and F. H. Arnold. 2000. Inverting enantioselectivity by directed evolution of hydantoinase for improved production of L-methionine. Nat. Biotechnol. 18:317-320.
13. Nakajima, K., A. Yamashita, H. Akama, T. Nakatsu, H. Kato, T. Hashimoto, J. Oda, and Y. Yamada. 1998. Crystal structure of two tropinone reductases: different reaction stereospecificities in the same protein fold. Proc. Natl. Acad. Sci. USA 95:4876-4881.
14. Peitsch, M. C. 1995. Protein modeling by e-mail. Bio-Technology 13:723.
15. Saari, R. E., D. A. Hogan, and R. P. Hausinger. 1999. Stereospecific degradation of the phenoxypropionate herbicide dichlorprop. J. Mol. Catal. B: Enzymatic 6:421-428.

COR-AAD1-00003565
Bayer EX1008 (Part 7 of 9)

16. Schwede, T., J. Kopp, N. Guex, and M. C. Peitsch. 2003. SWISS-MODEL: An automated protein homology-modeling server. Nucleic Acids Res. 31:3381-3385.

17. Stoll, V. S., M. S. Kimber, and E. F. Pai. 1996. Insights into substrate binding by D-2-ketoacid dehydrogenases from the structure of *Lactobacillus pentosus* D-lactate dehydrogenase. Structure 4:437-447.

18. Straathof, A. J., S. Panke, and A. Schmid. 2002. The production of fine chemicals by biotransformations. Curr. Opin. Biotechnol. 13:548-56.

19. Sugio, S., G. A. Petsko, J. M. Manning, K. Soda, and D. Ringe. 1995. Crystal structure of a D-amino acid aminotransferase: how the protein controls stereoselectivity. Biochemistry 34:9661-9669.

COR-AAD1-00003566
Bayer EX1008 (Part 7 of 9)

CHAPTER 6

Appendix

INTRODUCTION

One aim of this thesis was to isolate and characterize the two α-ketoglutarate-dependent dioxygenases from *Sphingomonas herbicidovorans* MH, which are involved in the initial enantioselective degradation step of phenoxypropanoic acids. Two strategies were applied to reach this goal: a 'genetic one', i.e., isolation of the genes, and a 'biochemical one', i.e., purification of the protein. As described in chapter 2, we isolated the *rdpA*-gene by using PCR-primers devoloped on the basis of the related *rdpA*-gene from *Delftia acidovorans* MC1. At the beginning of this study, both approaches were followed up and we intended to purify the *(S)*-dichlorprop dioxygenase from crude extract and to screen for the gene by applying reverse genetics. For the reverse genetics approach, three 'subgoals' were set:

a) Growth studies to determine optimal growth conditions for obtaining cells with as a high as possible *(S)*-dichlorprop dioxygenase activity
b) Purification of *(S)*-dichlorprop dioxygenase from cell-free extract
c) Screening for the gene by reverse genetics

Although – in the end – we did not succeed completely to purify the *(S)*-dichlorprop dioxygenase from native *S. herbicidovorans* MH cells, I would like to describe some of the results here because a lot of time was spent on this approach. At that moment, the biochemical approach was the most promising, since PCR and hybridization experiments with *tfdA*-derived primers and *tfdA*-probes had not led to positive results (chapter 4).

MATERIALS AND METHODS

Growth experiments. Standard growth experiments were carried out as described in chapter 2. To obtain higher cell mass, glucose, yeast extract and peptone were added to complex medium at the final concentrations of 0.44 g/l, 1.2 g/l and 6 g/l, respectively. To obtain large amounts of cells for the protein purification, *S. herbicidovorans* MH was cultivated on complex medium in a 700-l reactor at ETH Hönggerberg to an OD_{546} of approximately 1.5. Cells were harvested by centrifugation at 7'500 × *g* at 4°C for 15 min.

COR-AAD1-00003568
Bayer EX1008 (Part 7 of 9)

Preparation of cell-free extracts. For the preparation of cell-free extracts, 1 g cells (wet weight) was washed once in 20 mM $NaHPO_4$-KH_2PO_4, pH adjusted to 6.5, centrifuged and resuspended in 3 ml cell-extract buffer (20 mM Tris-HCl, 1 mM dithiothreitol, 0.095 mg/ml AEBSF, pH adjusted to 7.5). The cells were broken by two passages through a French press at 1 MPa, the lysate was centrifuged at 16'000 × *g* at 4°C for 40 min and the aliquots were stored at –20°C.

Partial Purification of *(S)*-dichlorprop dioxygenase. *Anion exchange chromatography.* Approximately 50 mg cell-free extract was loaded on a Q10 Bio-Scale column (Bio-Rad, Reinach, Switzerland) in 20 mM Tris-HCl, pH 7.5. The enzymes were eluted with a linear concentration gradient from 20 mM Tris-HCl (pH 7.5) to 20 mM Tris-HCl (pH 7.5) containing 1 M NaCl in ten column volumes. *(S)*-dichlorprop dioxygenase was found to elute at approximately 200-250 mM NaCl. The active fractions were pooled, concentrated with YM-10 columns according to the instructions of the manufacturer (Amersham Biosciences, Dübendorf, Switzerland) and stored at -20°C until further use.

Hydroxyapatite chromatography. Active anion-exchange fractions were loaded on a hydroxyapatite column (Macro-Prep® Ceramic Hydroxyapatite, Type I, 40 μm, 20 ml column volume, Bio-Rad). The fractions were loaded in 1 mM K_2HPO_4×3 H_2O/PO_4^{3-} buffer (pH adjusted to 6.8) and eluted with a linear concentration gradient to 400 mM K_2HPO_4×3 H_2O/PO_4^{3-} buffer (pH adjusted to 6.8) in ten column volumes. The active fractions eluted at approximately 5-10 mM K_2HPO_4×3 H_2O/PO_4^{3-}. They were again pooled and concentrated as after the anion-exchange chromatography step and stored at –20°C until further use.

It has to be noted that the use of hydrated potassium phosphate (K_2HPO_4×3 H_2O) and PO_4^{3-} was important, because the pyrophosphate, contained in the commercially available anhydrous K_2HPO_4, bound irreversibly to the ceramic hydroxyapatite material and prevented binding of the proteins to the column material.

Gel filtration. Gel filtration was carried out on a Superdex 200 preparation grade HiLoad 16/60 size exclusion column (Amersham Biosciences). Active protein fractions were loaded on the HiLoad column and eluted at a flow rate of 0.2 ml/min in 50 mM Na_2HPO_4-KH_2PO_4-buffer (pH 7) containing 150 mM NaCl. The calibration curve was done with the gel filtration standard from Bio-Rad consisting thyroglobulin (bovine, 670 kDa), Gamma globulin (bovine, 158 kDa), Ovalbumin (chicken, 44 kDa), Myoglobulin (horse, 17 kDa) and Vitamin B-12 (1.35 kDa). Blue dextran was used to determine the void volume.

SDS-PAGE and Electroblotting. SDS-PAGE was carried out as described in chapter 2. Electroblotting of proteins to a PVDF protein sequencing membrane (Bio-Rad) was carried out according to standard procedures (1).

COR-AAD1-00003569
Bayer EX1008 (Part 7 of 9)

Standard molecular procedures and construction of the cosmid library. Cloning, plasmid isolations and sequencing were done according to established procedures (1, 4). The construction of the cosmid library was carried out as described in Chapter 2.

Hybridization experiments. For southern hybridization, total DNA of *S. herbicidovorans* MH fractionated on an agarose gel was blotted on a Hybond™-XL membrane (Amersham Biosciences, Dübendorf, Switzerland) with a vacuum blotter (VacuGene XL, Amersham Biosciences) by the procedure described by Ravatn et al. (3). Colony blotting of the cosmid library was carried out as described in chapter 2. Total DNA and the colony blots were hybridized with oligonucleotides obtained by backtranslation of the N-terminal sequences (table 1). The oligonucleotides were radioactively labeled with [γ-^{32}P]ATP using T4 polynucleotide kinase according to the protocol of the manufacturer (Promega, Wallisellen, Switzerland). For non-radioactive labeling, the oligonucleotides were labeled with biotin 16-ddUTP using terminal dideoxyribonucleotide transferase also according to the manufacturer's instructions (Promega). Hybridization experiments were performed in SDS/BSA hybridization buffers (0.5 M sodium-phosphate [pH7], 7% sodium dodecyl sulfate, 1% bovine serum albumin) at 40, 45, and 48°C for 16 hours. The membranes were washed twice with a solution of 5 × SSC containing 1 mM EDTA for 2 min at room temperature and twice with a solution of 2 × SSC plus 0.1% SDS for 30 min at the hybridization temperature. Chemiluminescent detection of biotinylated DNA-probes was carried out according to the protocol 'Southern-Light™ & Southern *Star*™ Systems' (Applied Biosystems, Rotkreuz, Switzerland).

Enyzme activity measurements. Enzyme activity measurements were done with the end-point assay measuring the product formation by HPLC as described in chapter 3.

RESULTS AND DISCUSSION

Growth of *S. herbicidovorans* MH. *S. herbicidovorans* MH grew exponentially on complex medium to an optical density measured at 546 (OD_{546}) of about 0.8 (Fig. 1A). Further growth was linear. By adding glucose to the culture, exponential growth could be restored until an OD_{546} of about 4 (Fig. 1B). Strain MH grew exponentially again, when peptone and yeast extract were added. The maximal OD_{546} reached with this complex medium and the addition of the components during batch growth was 7 (data not shown). The data indicated that on complex medium, *S. herbicidovorans* MH grows exponentially only in the presence of glucose. A glucose concentration of 0.44 g/l, which was the glucose concentration in the complex medium used, should yield an OD_{546} of about 0.8

COR-AAD1-00003570
Bayer EX1008 (Part 7 of 9)

according to rough medium calculations. *S. herbicidovorans* MH grew exponentially to about this turbidity, and at higher densities, exponential growth was only observed, when glucose was added to the medium. Unfortunately, exponential growth was inhibited at too high glucose concentratons as growth studies with glucose concentration of 0.5% (w/v) in the medium showed (data not shown).

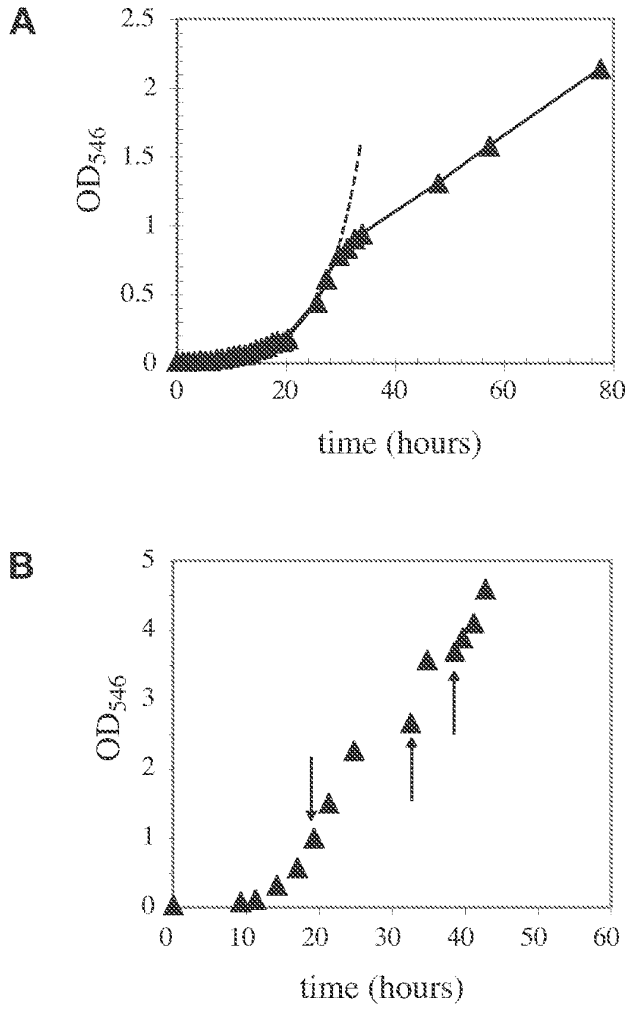


Fig. 1. (A) Growth of *S. herbicidovorans* MH on complex medium. The triangles represent the measured optical density at 546 nm; the dashed line indicates the trendline for exponential growth. (B) Growth of *S. herbicidovorans* MH on complex medium. The arrows indicate the addition of glucose to the medium.

COR-AAD1-00003571
Bayer EX1008 (Part 7 of 9)

***(S)*-dichlorprop dioxygenase activity is 'dependent' on growth phase.** Former experiments by Nickel et al. (2) showed that *(S)*-dichlorprop dioxygenase was expressed when *S. herbicidovorans* MH was grown on complex medium. A closer look at the growth phases revealed, that SdpA was only expressed above an OD_{546} of 0.8 (Fig. 2). Interestingly, highest specific activity in cell-free extract was seen around an OD_{546} of 1.5 whereas above an OD_{546} of 1.7, specific activity decreased significantly. It can be hypothesized that glucose represses the expression of SdpA during the exponential growth phase of *S. herbicidovorans* MH. However, I do not have an explanation for the decreased activity above an OD_{546} of 1.7.

In conclusion, the growth experiments showed that the fastest way to cultivate large quantities of *S. herbicidovorans* MH and to obtain optimal (*S*)-dioxygenase activity would be to grow the strain in a large volume to an OD_{546} of about 1.5.

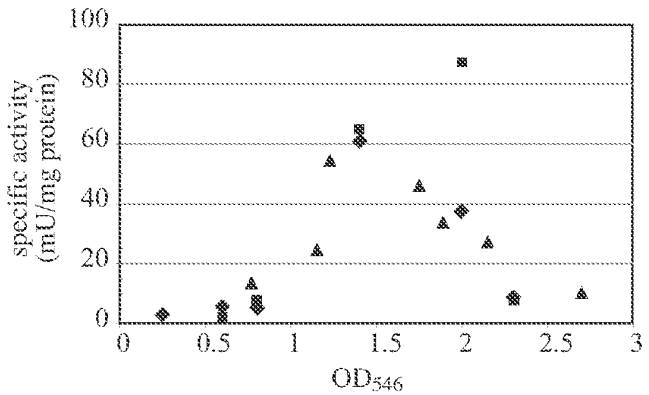


Fig. 2. Specific activity of *(S)*-dichlorprop dioxygenase at the different growth phases (cell densities indicated as OD_{546}). The different markers (triangles, diamonds and circles) represent three independent replicates.

Partial purification of SdpA. SdpA was partially purified with different chromatographic methods and procedures. Here, I describe the one, which led to the most purified proteins fractions according to visual inspection on a SDS-PAGE gel. The following procedure was applied: anion-exchange chromatography,

COR-AAD1-00003572
Bayer EX1008 (Part 7 of 9)

hydroxyapatite chromatography and gel filtration. The most active fractions were loaded on a SDS-PAGE gel (Fig. 3), which was blotted on a PVDF membrane. The N-terminal sequence of the three major protein bands were determined (Table 1) at the Edman-Sequencing facility of ETH Hönggerberg. The N-terminal sequences of band-1 and band-2 showed ambiguous homology whereas the N-terminal sequence of band-3 was similar to an oxidoreductase.

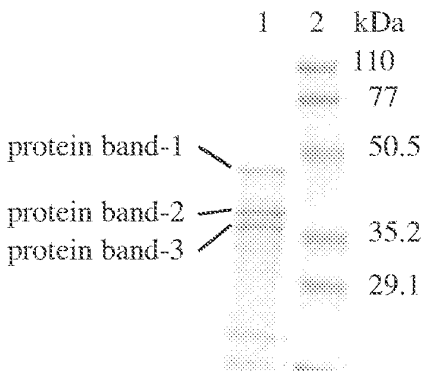


Figure 3. SDS-PAGE of partially purified *(S)*-dichlorprop dioxygenase. Lane 1, partially purified *(S)*-dichlorprop dioxygenase; lane 2, prestained molecular weight marker (Low Range, Bio-Rad) The arrows indicate the three protein bands, which were N-terminally sequenced.

Reverse genetics. All obtained N-terminal amino acid sequences were backtranslated into nucleotide sequences (Table 1) and total chromosomal DNA of *S. herbicidovorans* MH was hybridized with the labeled oligonucleotides. The best hybridization result was obtained with oligonucleotide-2, whereas oligonucleotide-1 hybridized weakly to total DNA and oligonucleotide-3 did not hybridize at all. Due to these results and an assumed subunit size of (*S*)-dichlorprop dioxygenase of 34 kDa, we hybridized the cosmid library of *S. herbicidovorans* MH with oligonucleotide-2. We isolated several positive reacting cosmids, subcloned fragments and sequenced them, but none of the fragments showed any similarity to α-ketoglutarate-dependent dioxygenases genes.

COR-AAD1-00003573
Bayer EX1008 (Part 7 of 9)

Table 1. The N-terminal sequences of the protein bands and the backtranslated oligonucleotide sequences used for hybridization experiments

	amino acids from N-terminal sequencing[a] or oligonucleotides derived by backtranslation																
protein band on SDS-PAGE	1	2	3	4	5	6	7	8	9	10	11	12	13	14	15	16	17
protein band-1	A	N	F	T	G	F	N I										
oligonucleotide-1[b]	gcn	aay	tty	can	ggn	tty	aay ath										
protein band-2	M	N	P	A	F	D	Q G	A	N	I	D	A					
SdpA[c]	M	S	P	S	F	D	I	A	P	P	L	A					
oligonucleotide-2[b]	atg	aay ggn	ccn	gcn	tty	gay	car ggn	gcn	aay	ath	gay	gcn					
sdpA[d]	atg	tca	ccc	gcc	ttc	gac	atc	gcc	ccg	ctc	gac	gcc					
protein band-3	M	N	Y	V	T	L	N	N	L	K	M	P	Q	L	G	F	G
oligonucleotide-3[b]	atg	aay	tay	gtn	can	ctn ttr	aay	aay	ctn ttr	aar	atg	ccn	car	ctn ttr	ggn	tty	ggn

[a] Normal printed amino acid residues could not be identified unambigously in Edman-sequencing.

[b] R = A or G; Y = c or t; H = a, c, or t; N = a, c, g, or t.

[c] The N-terminal amino acid sequence of SdpA (translated from the nucleotide sequencence) is given. Amino acid residues, which do not agree with the residues determined by Edman-sequencing are indicated in normal letters.

[d] Nucleotide sequence of *sdpA* (accession number AJ628860)

COR-AAD1-00003574
Bayer EX1008 (Part 7 of 9)

Now, from a distant point of view, having isolated the *sdpA*-gene and being able to compare the nucleotide sequence as well as the deduced amino acid sequences, we suppose that we partially purified the right protein which corresponded to oligonucleotide-2. It is likely, that with further purification steps and a higher amount of purified protein, we would have been able to purify the (*S*)-dichlorprop dioxygenase, but – luckily – the genetic approach was quicker ☺.

COR-AAD1-00003575
Bayer EX1008 (Part 7 of 9)

REFERENCES

1. Ausubel, F. M., R. Brent, R. E. Kingston, D. D. Moore, J. G. Seidman, J. A. Smith, and K. Struhl (ed.). 2002. Current protocols in molecular biology. John Wiley & Sons, Inc., New York, N. Y.
2. Nickel, K., M. J.-F. Suter, and H.-P. E. Kohler. 1997. Involvement of two α-ketoglutarate-dependent dioxygenases in enantioselective degradation of (*R*)- and (*S*)-mecoprop by *Sphingomonas herbicidovorans* MH. J. Bacteriol. 179:6674-6679.
3. Ravatn, R., S. Studer, D. Springael, A. J. B. Zehnder, and J. R. van der Meer. 1998. Chromosomal integration, tandem amplification, and aeamplification in *Pseudomonas putida* F1 of a 105-kilobase genetic element containing the chlorocatechol degradative genes from *Pseudomonas* sp. strain B13. J. Bacteriol. 180:4360-4369.
4. Sambrook, J., E. F. Fritsch, and T. Maniatis. 1989. Molecular Cloning: a laboratory manual. Cold Spring Harbor Laboratory, Cold Spring Harbor, N.Y.

COR-AAD1-00003576
Bayer EX1008 (Part 7 of 9)

CURRICULUM VITAE

TINA ANDREA MÜLLER
born March 8, 1973 in Winterthur

1980 – 1986	Primary School in Frauenfeld
1986 – 1993	Matura Typus B at the Kantonsschule Frauenfeld
1993 – 1999	Studies in Environmental Sciences at the Swiss Federal Institute of Technology Zurich
1999 – 2004	Doctoral studies at the Swiss Federal Institute for Environmental Technology (EAWAG) in Dübendorf
June 15, 2004	Date of oral examination

COR-AAD1-00003577
Bayer EX1008 (Part 7 of 9)

Enantioselektive Verwertung von Phenoxyalkanoat-Herbiziden durch Bakterien – Eine Charakterisierung der Dioxygenasen des initialen Abbau-Schrittes

Von der Fakultät für Biowissenschaften, Pharmazie und Psychologie

der Universität Leipzig

genehmigte

DISSERTATION

zur Erlangung des akademischen Grades

doctor rerum naturalium

(Dr. rer. nat.)

vorgelegt

von

Diplom-Biochemikerin Anne Westendorf,

geboren am 21.05.1978 im Ostseebad Kühlungsborn

Dekan: Prof. Dr. Kurt Eger

Gutachter: Prof. Dr. Wolfgang Babel

Prof. Dr. Jan R. Andreesen

Prof. Dr. Walter Reinecke

Tag der Verteidigung: 11.03.2005

COR-AAD1-00003578

Bayer EX1008 (Part 7 of 9)

Bibliographische Beschreibung

Anne Westendorf

Enantioselektive Verwertung von Phenoxyalkanoat-Herbiziden durch Bakterien - Biochemische Charakterisierung der Dioxygenasen des initialen Abbau-Schrittes

Universität Leipzig, Dissertation, 37 Abbildungen, 28 Tabellen, 10 Gleichungen, 169 Literaturstellen

Referat

In den letzten Jahren wurde eine Menge über den enzymatischen Hintergrund des Phenoxyalkanoat-Abbaus durch Bakterien bekannt. Es sind sowohl Stämme mit hoher Spezifität für Phenoxyacetate, wie *Ralstonia euthropha* JMP134 (Pieper et al., 1988) und *Delftia acidovorans* P4a (Hoffmann et al., 1996, 2003), oder für Phenoxybutyrate, wie *Aureobacterium* sp. K2-17 und *Rhodococcus erythropolis* K2-3 (Mertingk et al., 1998; Sträuber et al., 2003), als auch solche mit breiterem Herbizidverwertungsspektrum wie *Sphingobium herbicidovorans* MH (Horvath et al., 1990; Zipper et al., 1996), *Rhodoferax* sp. P230 (Ehrig et al., 1998) und *Delftia acidovorans* MC1 (Müller et al., 1999) gefunden und charakterisiert worden. Letztere drei Stämme sind Objekt der vorliegenden Untersuchungen. In diesen Bakterien wurden jeweils zwei enantioselektive Phenoxyalkanoat-spaltende Enzyme gefunden. Es handelt sich um α-Ketoglutarat-abhängige Dioxygenasen, die die Spaltung der Etherbindung der Phenoxyalkanoate in die jeweiligen substituierten Phenole und 2-Oxoalkanoate katalysieren. Die Enzyme sind streng enantioselektiv, die (R)-2-(2,4-Dichlorphenoxy)propionat/α-Ketoglutarat Dioxygenasen (RdpA) spalten die (R)-, nicht aber die (S)-Enantiomeren der 2-Phenoxypropionate, die (S)-2-(2,4-Dichlorphenoxy)propionat/α-Ketoglutarat Dioxygenasen (SdpA) spalten analog dazu die (S)-, nicht aber die (R)-Enantiomeren. Weniger streng ist die Selektivität jedoch hinsichtlich der Alkanoat-Seitenkette und der Substituenten am aromatischen Ring. Das *rdpA*-Gen ist in den drei unterschiedlichen Stämmen identisch. Erstaunlich ist jedoch, dass die Genprodukte unterschiedliche kinetische Eigenschaften aufweisen. Als Ursache dafür konnten multiple Enzymformen nachgewiesen werden, die auf Monomere mit unterschiedlichen pI-Werten zurückgeführt werden können. Die Monomeren unterscheiden sich in ihrem Spektrum in den jeweiligen Stämmen. Wie am Beispiel von $RdpA_{MC1}$ gezeigt, weisen die Enzymformen Unterschiede in ihren kinetischen Konstanten auf. Die *sdpA*-Gene

COR-AAD1-00003579
Bayer EX1008 (Part 7 of 9)

sind im Gegensatz dazu in den einzelnen Stämmen verschieden. Das führt zu grundsätzlich unterschiedlichen Substratverwertungsprofilen bzw. kinetischen Konstanten. Das Enzym aus MC1 zeigt gute Spaltungsaktivitäten für die (S)-Enantiomeren der Phenoxypropionate und die Phenoxyacetat-Derivate; das $SdpA_{P230}$ setzt dagegen die Phenoxyacetate nicht um. Wie für RdpA konnten auch hier multiple Enzymformen nachgewiesen werden, die sich wiederum in ihren kinetischen Eigenschaften unterscheiden.

Die Art der Modifizierungen an den RdpA- und SdpA-Enzymen konnte bislang nicht endgültig geklärt werden. Am $SdpA_{MC1}$ wurden Hydroxylierungen an Trp-Resten gefunden, die in Nähe zum aktiven Zentrum stehen und eher typisch für α-KG-abhängige Enzyme sind. Sie bewirken eine reversible Inaktivierung des Enzyms und sollten daher mit den hier beobachteten kinetischen Effekten weniger in Verbindung gebracht werden. Eher sind Massendifferenzen von Interesse, die auf eine Modifizierung an Cys-Resten hinweisen. Die Spezifizierung dieser Moleküle sollte weiteren Aufschluss geben, bleibt aber weiteren Untersuchungen vorbehalten.

COR-AAD1-00003580
Bayer EX1008 (Part 7 of 9)

Inhaltsverzeichnis

INHALTSVERZEICHNIS IV

ABKÜRZUNGEN VIII

1 EINLEITUNG 1

1.1 Dioxygenasen mit Nicht-Häm-gebundenem Eisen 1

1.2 α-Ketoglutarat-abhängige Dioxygenasen 2

1.2.1 Reaktionsmechanismus 4

1.2.2 Multiple Enzymformen und α-Ketoglutarat-abhängige Dioxygenasen 5

1.3 Optische Aktivität und die Umwelt 6

1.3.1 Stereospezifische Enzyme 7

1.3.2 Mikrobieller Phenoxyalkanoat-Abbau 8

1.4 Problemstellung 10

2 MATERIAL UND METHODEN 11

2.1 Mikroorganismen 11

2.2 Kultivierung 11

2.2.1 Medien 12

2.2.2 Batch-Kultivierung 12

2.2.3 Batch-Kultivierung genetisch veränderter Mikroorganismen 12

2.2.4 Fed-Batch-Kultivierung 13

2.3 Enzymreinigung 13

2.3.1 Zellernte und Zellaufschluss 13

2.3.2 Reinigung der nativen Enzyme 13

2.3.2.1 Protaminsulfat- und Ammoniumsulfat-Fällung 13

2.3.2.2 Ionenaustausch-Chromatographie 14

2.3.2.2.1 an Source30Q 14

2.3.2.2.2 an PBE94 14

2.3.2.3 Hydrophobe Chromatographie 15

2.3.2.4 Präparative Gelelektrophorese 15

2.3.2.4.1 Trennung der $RdpA_{MC1}$-Enzymformen 15

2.3.2.4.2 Trennung der $SdpA_{MC1}$-Enzymformen 16

2.3.3 Reinigung der rekombinanten Enzyme $RdpA_{MC1}$-rec und $SdpA_{MC1}$-rec 16

2.3.3.1 Affinitätschromatographie 16

2.3.3.2 Abspaltung der Strep-tag(II)-Sequenz 17

COR-AAD1-00003581
Bayer EX1008 (Part 7 of 9)

2.4 Aufkonzentrieren, Umpuffern und Entsalzen 17
2.4.1 Säulenchromatographisch mittel Gelfiltration 17
2.4.2 Ultrafiltration 17
2.5 Proteinbiochemische Untersuchungen 17
2.5.1 Säulenchromatographische Bestimmung der Molmasse 17
2.5.2 Bestimmung der Anzahl funktionell aktiver Zentren 18
2.5.3 Gelelektrophoretische Methoden 18
2.5.3.1 SDS-PAGE 18
2.5.3.2 Native Gelelektrophorese 19
2.5.3.2.1 Kontinuierliche Gelelektrophorese 19
2.5.3.2.2 Diskontinuierliche Gelelektrophorese 19
2.5.3.3 Peptid-Gelelektrophorese 19
2.5.3.4 2D-Gelelektrophorese 19
2.5.3.4.1 Erste Dimension: Isoelektrische Fokussierung 20
2.5.3.4.2 Zweite Dimension: SDS-PAGE 20
2.5.3.5 Western-Blot 21
2.5.4 Färben, Scannen und Auswerten 21
2.5.4.1 Silber-Färbung 21
2.5.4.2 Coomassie-Färbung 21
2.5.4.3 Kolloidale Coomassie-Färbung 22
2.5.4.4 Scannen und Auswerten 22
2.5.5 Enzymatischer und chemischer Verdau von Proteinen 22
2.5.6 N-terminale Sequenzierung von Proteinen und Datenbankrecherche 23
2.5.7 Massenspektrometrische Methoden 23
2.5.7.1 Identifizierung von Proteinen 23
2.5.7.2 Untersuchung von Modifizierungen 23
2.5.8 Internet-Links 24
2.6 Enzymkinetische Untersuchungen 24
2.6.1 Bestimmung der Phenoxyalkanoat-Spaltungsaktivität 24
2.6.2 Ermittlung der Extinktionskoeffizienten von DCP und MCP 25
2.6.3 Auswertung der ermittelten Daten 25
2.7 Gentechnische Arbeiten 26
2.7.1 Nährmedien für gentechnische Arbeiten 26
2.7.2 Isolation von Nukleinsäuren 26
2.7.2.1 Präparation von genomischer DNA 26
2.7.2.2 Präparation von plasmidaler DNA 27
2.7.3 Ableitung von Primern für die Gene $rdpA_{MC1}$ und $sdpA_{MC1}$ 27
2.7.4 PCR-Reaktion zur Amplifizierung der $rdpA_{MC1}$- und $sdpA_{MC1}$-Gene 27
2.7.5 Ligation der Gene $rdpA_{MC1}$ und $sdpA_{MC1}$ mit dem pGEMT-Vektor 28

COR-AAD1-00003582
Bayer EX1008 (Part 7 of 9)

2.7.6 Ligation der Gene $rdpA_{MC1}$ und $sdpA_{MC1}$ mit dem pASK-IBA7-Vektor ... 28
2.7.7 Übertragung der DNA durch Transformation ... 28
2.7.7.1 Transformation ... 28
2.7.7.2 Elektrotransformation ... 28
2.7.8 Selektion rekombinanter Klone ... 29
2.7.9 DNA-Sequenzierung ... 29
2.8 Analytik ... 29
2.8.1 Bestimmung der Proteinkonzentration ... 29
2.8.2 Bestimmung der Phenoxyalkanoat-Konzentration ... 30
2.8.3 Bestimmung der α-Ketoglutarat-Konzentration ... 30
2.8.4 Bestimmung der optischen Dichte ... 30
2.8.5 Bestimmung von Leitfähigkeit, Sauerstoffkonzentration und pH-Wert ... 30
3 ERGEBNISSE ... 31
3.1 Enzymreinigung ... 31
3.1.1 Reinigung der Phenoxyalkanoat-spaltenden Enzyme aus *Delftia acidovorans* MC1 ... 31
3.1.1.1 Säulenchromatographische Enzymreinigung ... 31
3.1.1.2 Gelelektrophoretische Trennung von Enzymformen ... 33
3.1.1.2.1 Separation der $SdpA_{MC1}$-Enzymformen ... 33
3.1.1.2.2 Separation der $RdpA_{MC1}$-Enzymformen ... 35
3.1.2 Reinigung der Phenoxypropionat-spaltenden Enzyme aus *Rhodoferax* sp. P230 ... 37
3.1.3 Reinigung der Phenoxyalkanoat-spaltenden Enzyme aus *Sphingobium herbicidovorans* MH ... 39
3.1.4 Reinigung der rekombinanten Enzyme $RdpA_{MC1}$-rec und $SdpA_{MC1}$-rec ... 41
3.2 Proteinbiochemische Charakterisierung ... 43
3.2.1 Primärstruktur ... 43
3.2.1.1 Primärstrukturen der RdpA- und SdpA-Enzyme aus MC1, P230 und MH ... 43
3.2.1.2 Sequenzvergleiche und konservierte Regionen ... 44
3.2.2 Sekundärstruktur ... 45
3.2.3 Physikochemische Eigenschaften und Quartärstruktur ... 47
3.2.3.1 Enzyme aus *Delftia acidovorans* MC1 ... 47
3.2.3.1.1 Gelchromatographische Bestimmung der Molmasse ... 47
3.2.3.1.2 Gelelektrophoretischer Nachweis von Ladungsisomerie, Bestimmung der Molmasse und der isoelektrischen Punkte ... 48
3.2.3.1.3 Quartärstruktur der Enzyme $SdpA_{MC1}$ und $RdpA_{MC1}$ ... 50
3.2.3.2 Enzyme aus *Rhodoferax* sp. P230 und *Sphingobium herbicidovorans* MH ... 53
3.2.3.2.1 Die (R)-spezifischen Enzyme ... 53
3.2.3.3 Die (S)-spezifischen Enzyme ... 53
3.2.3.4 Rekombinante Enzyme ... 56
3.2.4 Posttranslationale Modifikationen ... 57

COR-AAD1-00003583
Bayer EX1008 (Part 7 of 9)

3.2.4.1 Die (R)-spezifischen Enzyme 57
3.2.4.2 Das $SdpA_{MC1}$ 57
3.3 Enzymkinetische Charakterisierung und Reaktionsmechanismus 58
3.3.1 Bestimmung der Anzahl funktionell aktiver Zentren 58
3.3.2 Substratverwertungsspektren 59
3.3.2.1 Die (R)-spezifischen Dioxygenasen 59
3.3.2.2 Die (S)-spezifischen Dioxygenasen 60
3.3.3 Enzymstabilität und Reaktionsordnung 61
3.3.4 Kinetische Kennlinien 64
3.3.4.1 Die Kennlinien der (S)-spezifischen Dioxygenasen 64
3.3.4.1.1 Das $SdpA_{MC1}$ 64
3.3.4.1.2 Die Kennlinien der SdpA-Enzyme aus P230 und MH 67
3.3.4.2 Die Kennlinien der (R)-spezifischen Dioxygenasen 68
3.3.5 Kinetische Konstanten 70
3.3.5.1 Konstanten der (S)-spezifischen Enzyme 70
3.3.5.2 Konstanten der (R)-spezifischen Enzyme 72
3.3.6 Reaktionsmechanismus 74

4 DISKUSSION 77
4.1 Enzymausstattung 77
4.2 Proteinbiochemie 81
4.2.1 Sequenzanalyse 81
4.2.2 Multiple Enzymformen 83
4.3 Klassifizierung der Enzyme 86
4.4 Reaktionsmechanismus und Enzymstabilität 87
4.5 Enzymkinetik 90
4.5.1 Kinetische Kennlinien und Kooperativität 90
4.5.2 Posttranslationale Modifizierung und Enzymkinetik 94

5 ZUSAMMENFASSUNG 97

6 LITERATUR 99

COR-AAD1-00003584
Bayer EX1008 (Part 7 of 9)

Abkürzungen

α-KG	α-Ketoglutarat
Akt.	Aktivität
APS	Ammoniumperoxodisulfat
BNPS	3-Bromo-3-Methyl-2-(2-nitrophenylmercapto)-3H-indol
CAPS	N-Cyclohexyl-3-aminopropanesulfonat
CHAPS	3-[(3-Choramidopropyl)-dimethylammino]-1-propanesulfonate
CHCA	α-Cyano-4-hydroxyzimtsäure
2,4-D	2,4-Dichlorphenoxyacetat
2,4-DB	4-(2,4-Dichlorphenoxy)butyrat
DCP	2,4-Dichlorphenol
DMF	Dimethylformamid
DNA	*desoxyribonucleic acid*
dNTP	Desoynukleosidtriphosphat
(R,S)-DP	(R,S)-2-(2,4-Dichlorphenoxy)propionat
DTT	Dithiotreitol
EDTA	Ethylendiamintetraacetat
f	Funktion
HIC	*hydrophobic interaction chromatography*
HPLC	*high pressure liquid chromatography*
IEF	isoelektrische Fokussierung
IEX	*ion exchange chromatography*
IKA	Inkubationsansatz
IPG	immobilisierter pH-Gradient
IPTG	Isopropyl-β-D-thio galactopyranosid
k_{kat}	Wechselzahl
K_i	Inhibitionskonstante
K_M	Michaelis-Menten-Konstante
k_x	Geschwindigkeitskonstanten
Koeff.	Koeffizient
MALDI	*matrix assisted laser desorbtion ionization*
MC1	*Delftia acidovorans* MC1
MCP	4-Chlor-2-methylphenol

COR-AAD1-00003585
Bayer EX1008 (Part 7 of 9)

MCPA	4-Chlor-2-methylphenoxyacetat
MCPB	4-Chlor-2-methylphenoxybutyrat
(R,S)-MCPP	(R,S)-2-(4-Chlor-2-methylphenoxy)propionat
MH	*Sphingobium herbicidovorans* MH
MM	Molmasse
MS	Massenspektrometrie
OD	optische Dichte
P230	*Rhodoferax sp.* P230
PAGE	Polyacrylamid-Gelelektrophorese
PCR	*polymerase chain reaction*
PVDF	Polyvinylidene Fluoride
PYE	*peptone yeast extract*
R^2	Korrelationskoeffizient
RdpA	(R)-DP/α-KG-Dioxygenase
rel. spez. Akt.	relative spezifische Aktivität
R_f	Wanderungsgeschwindigkeit
rpm	*rounds per minute*
SdpA	(S)-DP/α-KG-Dioxygenase
SDS	*sodium dodecyl sulfate*
TauD	Taurin/α-KG-Dioxygenase
TCA	Trichloracetat
Temed	N´N´N´N´-Tetramethylethylendiamin
TFA	Trifluoressigsäure
TfdA	2,4-D/α-KG-Dioxygenase
TfdB	Dichlorphenol-Hydroxylase
TfdC	Dichlorcatechol-1,2-Dioxygenase
TfdD	Chlormuconatcycloisomerase
TfdK	2,4-D-Transportprotein
Tris	Tri(hydroxymethyl)aminomethan
v/v	*volume per volume*
w/v	*weight per volume*
X-Gal	5-Bromo-4-chloro-3-indolyl-β-D-galactosid

COR-AAD1-00003586
Bayer EX1008 (Part 7 of 9)

1 Einleitung

In der Agrarwirtschaft werden Phenoxyalkanoat-Herbizide zur Bekämpfung von dikotyledonen Unkräutern eingesetzt, womit sie zum Schutz von monocotyledonen Kultur- und Nutzpflanzen beitragen. Phenoxyalkanoate imitieren die Wirkung pflanzlicher Auxine und verursachen auf diese Weise ein unkontrolliertes Wachstum, das zu einer abnormen Entwicklung von zweikeimblättrigen Pflanzen und letztendlich zu deren Absterben führt (Loos, 1975). Wird maßvoll mit diesen Verbindungen umgegangen, ist das Potential zur Entgiftung in biologischen Systemen so groß, dass die Stoffe nicht zum umweltpolitischen Problem werden. Phenoxyalkanoate sind biologisch abbaubar; das latente Potential zum Abbau ist in Mikroorganismen verpackt. Spezifiziert bedeutet dies, dass Enzyme an der Degradation von Phenoxyalkanoaten beteiligt sind. Dafür kommen Mono- und Dioxygenasen in Frage.

1.1 Dioxygenasen mit Nicht-Häm-gebundenem Eisen

Dioxygenasen sind Enzyme, die beide Atome des Sauerstoffmoleküls in das Substrat einbauen. Erscheinen die beiden Sauerstoffatome dabei im selben Produkt, so spricht man von einer intramolekularen Dioxygenase. Analog werden die Sauerstoffatome bei intermolekularen Dioxygenasen in zwei verschiedenen Reaktionsprodukten wiedergefunden. Dioxygenasen lassen sich nicht nur anhand dieses Merkmals unterscheiden, sondern können basierend auf der unterschiedlichen Koordination des Metallions im aktiven Zentrum des Enzyms in drei Gruppen unterteilen werden: 1.) Häm-koordiniertes Metallion, 2.) Nicht-Häm-koordiniertes Metallion und 3.) Eisen-Schwefel-Cluster.

Im folgendem sollen Dioxygenasen mit einem Nicht-Häm-koordiniertem Metallion im aktiven Zentrum näher betrachtet werden. Diese Gruppe der Dioxygenasen ist, wie auch die durch sie katalysierten Reaktionen, sehr vielfältig. Sie spalten aromatische Ringstrukturen, oxidieren ungesättigte Fettsäuren, schließen Ringstrukturen, spalten Ether-Bindungen und vieles mehr. In diese Gruppe gehören sowohl die Lipoxygenase (Nelson et al., 1994), die Isopenicillin-N-Synthase (Baldwin et al., 1991) als auch die α-Ketoglutarat-abhängigen Dioxygenasen (Prescott et al., 1993), die Catechol-Dioxygenasen und die Rieske-Oxygenasen. Innerhalb dieser Gruppe sind die Metallionen wiederum in sehr unterschiedlichen räumlichen Anordnungen koordiniert: bei den intradiolisch spaltenden Catechol-Dioxygenasen (Fe(III)-Ion über 2 Tyr und 2 His, [Ohlendorf et al., 1988/94]) trigonal bipyramidal, im Falle der extradiolisch spaltenden Catechol-Dioxygenasen (Fe(II)-Ion, selten auch Mn(II), [Que et al., 1981; Bold et al., 1995; Whiting et al., 1996] über 2 His, Glu, [Han et al., 1995; Senda et al., 1996]) in Form

COR-AAD1-00003587
Bayer EX1008 (Part 7 of 9)

einer quadratischen Pyramide und in der Anordnung eines verzerrten Oktaeders bei der Lipoxygenase (Fe(III) über 3 His, Ile-CO_2^- und Asn, [Boyington et al. 1990; Minor et al., 1996]) der Isopenicillin-N-synthase (Fe(II) über 2 His und Asp, Gln, [Roach et al., 1995a]) und den α-Ketoglutarat-abhängigen Dioxygenasen (Fe(II) über 2 His und Asp, [Hegg et al., 1999; Elkins et al., 2002]). Bei all diesen Enzymen ist das Metallion im aktiven Zentrum so koordiniert, dass mindestens eine der vier Bindungsstellen frei oder mit Lösungsmittel (H_2O) besetzt ist, also frei verfügbar für die Substratbindung bleibt. Dies ist ein großer Unterschied zu den Häm-Dioxygenasen, bei denen das Eisen über alle vier Bindungsstellen komplexiert ist, und sollte ein entscheidender Grund für die Vielfältigkeit der Reaktionsmechanismen in der Gruppe der α-Ketoglutarat-abhängigen Dioxygenasen darstellen (Que und Ho, 1996). Der Angriff des Sauerstoffs auf das Substrat kann sowohl elektrophil (intradiolische Catechol-Dioxygenasen), nucleophil (extradiolische Catechol-Dioxygenasen) als auch radikalisch erfolgen (Lipoxygenase [de Groot et al., 1973; Egmond et al., 1977]).

1.2 α-Ketoglutarat-abhängige Dioxygenasen

Die α-Ketoglutarat-abhängigen Dioxygenasen bilden die größte Gruppe der Nicht-Häm-Eisen-Dioxygenasen (Hegg et al., 1999). Es handelt sich um intermolekulare Dioxygenasen. Sie katalysieren Reaktionen nach dem in Gleichung 1 dargestellten allgemeinen Mechanismus:

$$\alpha\text{-Ketoglutarat} + O_2 + S \longrightarrow \text{Succinat} + CO_2 + SO$$

Gleichung 1: Allgemeiner Reaktionsmechanismus von durch α-Ketoglutarat-abhängige Dioxygenasen katalysierte Reaktionen, S: Substrat, SO: Produkt

Dioxygenasen dieser Familie sind in vielen Bereichen anzutreffen, sie katalysieren die posttranslationale Hydroxylierung von Aminosäure-Seitenketten während der Collagensynthese (Prolyl-4-Hydroxylase [Hutton et al., 1966; Kivirikko und Prockop, 1967], Lysyl-Hydroxylase [Hausmann, 1967; Kivirikko und Prockop, 1972], Aspartyl-Hydroxylase [Korioth et al., 1994]), die Umsetzung von Thymin zu 5-Hydroxymethyl-uracil im Pyrimidin-Stoffwechsel (Thymin-7-Hydroxylase [Abbot et al., 1967]), den oxidativen Ringschluss von Proclavaminat in der Biosynthese von Clavaminat (Clavaminat-Synthase [Salowe et al., 1990]), die Spaltung der Phenoxyalkanoaten an der Etherbindung (2,4-Dichlorphenoxyacetat-Dioxygenase [Fukomori und Hausinger, 1993b]), die Hydroxylierung von ε-N-Trimethyl-L-Lysin und die Umwandlung von γ-Butyrobetain zu L-Carnitin im Carnitinstoffwechsel (ε-N-Trimethyl-L-Lysin-Hydroxylase [Hulse et al., 1978], γ-Butyrobetain-Hydroxylase [Lindstedt et al., 1970/77]), die Reparatur von DNA durch die oxidative Entgiftung alkylierter Basen (AlkB [Aravind und Koonin, 2001]) und vieles mehr. Aufgrund der katalysierten Reaktionen

COR-AAD1-00003588
Bayer EX1008 (Part 7 of 9)

unterteilten deCarolis und deLuca (1994) die Familie der α-Ketoglutarat-abhängigen Dioxygenasen in die Untergruppen Hydroxylasen, Hydroxylasen/Epoxidasen, Cyclasen, Desaturasen und Ring-Expandasen.

Eine weitere Klassifizierung der α-Ketoglutarat-abhängigen Dioxygenasen nimmt Hogan (1999) vor. Sie unterteilte die Enzyme aufgrund von konservierten Elementen in der Primärstruktur der Proteine in drei Gruppen.

Die **Gruppe(I)**, die Isopenicillin-N-Synthase-ähnlichen Enzyme, bildet dabei die größte Gruppe dieser Dioxygenasen. Ihr gehören unter anderem Enzyme der Collagen-Biosynthese (Prolyl-4-, Aspartyl- und Lysyl-Hydroxylase), Enzyme des Gibberellin- (z.B. Gibberellin-7-Oxidase, Giberellin-13-Oxidase oder Giberellin-2β-Hydroxylase [Hedden, 1997]) und des Flavon-Stoffwechsels an (Flavone-Synthase I [Britsch, 1990], Flavanol-Synthase [Holton et al., 1993], Flavanon-3-Hydroxylase [Saito et al., 1999]). Die Aminosäure-Sequenz H-X-D-X_{55}-H kann in allen diesen Dioxygenasen gefunden werden (Borovok et al., 1996) und ist daher das Charakteristikum dieser Gruppe. Es wurde gezeigt, dass die konservierten Aminosäuren in dieser Folge an der Bildung des Metallbindungs-Zentrums (Roach et al., 1995b; Vålegard et al., 1998) beteiligt sind und in Verbindung mit dem ebenfalls konservierten C-terminal davon gelegenen Sequenzabschnitt R-X-S die Bindung von α-Ketoglutarat vermitteln (Kreisberg-Zakarin et al., 1999; Lukacin und Britsch, 1997).

Die Dioxygenasen der **Gruppe(II)** zeichnen sich durch Sequenz-Ähnlichkeiten zu der 2,4-Dichlorphenoxyacetat/α-KG Dioxygenase (TfdA) aus. Vertreter dieser Gruppe sind unter anderem die Taurin/α-KG Dioxygenase (TauD) (Eichhorn et al., 1997), die Sulfonat/α-KG Dioxygenase (Hogan et al., 1999), die Clavaminat-Synthase (Salowe et al., 1990) und die γ-Butyrobetain-Hydroxylase (Lindstedt et al., 1970/77). Das konservierte Sequenz-Motiv dieser Gruppe lautet H-X-D-$X_{136-205}$-D-N-X_4-H-X_{10}-R. Dieses Motiv enthält unter anderem auch die Sequenz H-X-D, die als Bindungsstelle des Metallzentrums der Gruppe(I)-Dioxygenasen ausgemacht wurde. Diese Aminosäuren sind folglich auch in den TfdA-ähnlichen Enzymen an der Fe(II)-Bindung beteiligt (Hegg et al., 1999; Elkins et al., 2002).

Die **Gruppe(III)** der α-Ketoglutarat-abhängigen Dioxygenasen, die bislang kleinste Gruppe, zeichnet sich durch nur geringe Homologie zu den anderen beiden Gruppen aus. Die Aminosäuren für die Fe(II)-Komplexierung (H-X-D) sind jedoch auch in dieser Gruppe konserviert. Das zuordnende Sequenz-Motiv dieser Dioxygenasen lautet H-X-D-X_{34-38}-P-G-H-X_{36-65}-H-

COR-AAD1-00003589
Bayer EX1008 (Part 7 of 9)

X_4-N-X_5-R. Mitglieder dieser Enzymgruppe sind zum Beispiel die Prolin-4-Hydroxylase (Shibasaki et al., 1999) und die Phytanoyl-CoA-Hydroxylase (Jansen et al., 1998).

Die α-KG-abhängigen Dioxygenasen unterscheiden sich nicht nur in ihrer Primär-Struktur erheblich, sondern auch in ihrer Quartär-Struktur. Man findet sowohl monomere Enzyme, deren Molmassen zwischen 26 kD (Giberellin-2β-Hydroxylase) und 56 kD (Aspartyl-Hydroxylase) liegen, als auch dimere (γ-Butyrobetain-Hydroxylase) und tetramere Proteine (Prolin-4-Hydroxylase). Die di- und tetrameren Enzyme wiederum können aus identischen (4-Hydroxyphenylpyruvat Dioxygenase [Wada et al., 1975]) oder unterschiedlichen Untereinheiten (Prolin-4-Hydroxylase) zusammengesetzt sein. Ebenso verschieden wie das strukturelle Spektrum fallen die kinetischen Konstanten aus, so variiert der K_M-Wert für das Substrat zwischen 0,01 µM (Prolyl-4-Hydoxylase [Kivirikko et al., 1989]) und 720 µM (Cephalosporin-7α-Hydroxylase [Xiao et al., 1991]), also um etwa vier Zehnerpotenzen. Für α-KG, dem zweiten Substrat, ist die Mehrzahl der Dioxygenasen hochspezifisch. Nur wenige Enzyme sind bislang bekannt, die auch andere 2-Oxosäuren als Elektronendonor nutzen können (TfdA, 4-Hydroxypyruvat-Oxidase). Der K_M-Wert für α-KG schwankt innerhalb der α-Ketoglutarat-abhängigen Dioxygenasen um etwa drei Größenordnungen.

1.2.1 Reaktionsmechanismus

In Abbildung 1 ist der postulierte Reaktionsmechanismus für 2,4-Dichlorphenoxyacetat/α-Ketoglutarat Dioxygenase (TfdA) (Hegg et al., 1999) dargestellt. Nach diesem Mechanismus binden die Substrate in der Reihenfolge α-KG, 2,4-Dichlorphenoxyacetat (2,4-D) und Sauerstoff. Als erstes Produkt verlässt CO_2 das aktive Zentrum; in einem weiteren Schritt werden die übrigen Produkte Dichlorphenol (DCP), Glyoxylat und Succinat freigesetzt. Die gleiche Reihenfolge der Bindung der Substrate an das Enzym wurde auch für TauD (Elkins et al., 2002) und für die Thymin-7-Hydroxylase (Holm et al., 1975) beschrieben. Eine zweite in der Literatur beschriebene Bindungsfolge lautet: α-KG, Sauerstoff und Substrat. Diese Folge der Substratbindung wurde für die Prolyl-4-Hydroxylase (Kivirikko et al., 1989), die Lysyl-Hydroxylase (Kivirikko, 1972) und die Deacetoxyvindolin-Hydroxylase (deCarolis und deLuca, 1993) postuliert. Die Ablösung der Substrate ist nicht näher untersucht worden, jedoch konnte für die Enzyme Prolyl-4-Hydroxylase (Kivirikko et al., 1989), Lysyl-Hydroxylase (Puistola et al., 1980), Thymin-7-Hydroxylase (Holme, 1975) und Deacetoxyvindolin-4-Hydroxylase (deCarolis und deLuka, 1993) mit enzymkinetischen Methoden ein *ordered*

COR-AAD1-00003590
Bayer EX1008 (Part 7 of 9)

TerTer-Mechanismus nachgewiesen werden. Die 4-Hydroxyphenylpyruvat Dioxygenase weist dagegen einen *ordered* BiBi-Mechanismus auf (Rundgren, 1977b).

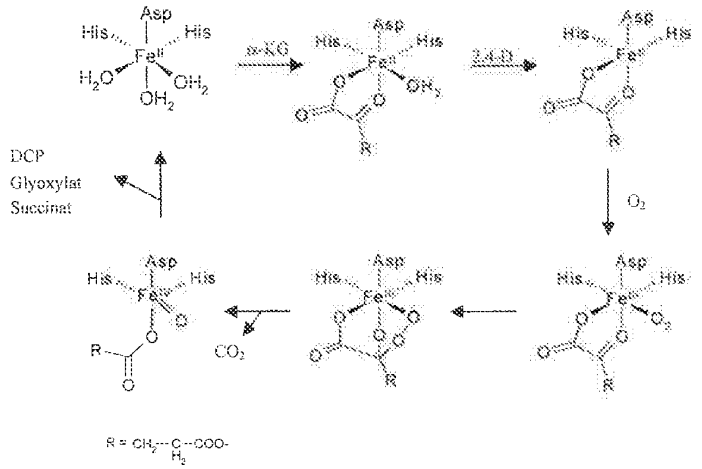


Abbildung 1: Reaktionsmechanismus des 2,4-Dichlorphenoxyacetat/α-Ketoglutarat Dioxygenase (TfdA) nach Hegg et al. (1999)

1.2.2 Multiple Enzymformen und α-Ketoglutarat-abhängige Dioxygenasen

Das Phänomen vom Auftreten multipler Enzymformen ist seit vielen Jahren bekannt und wurde für eine Vielzahl von Mikroorganismen, Pflanzen und Tieren beschrieben (Shaw, 1969). Dem Vorhandensein verschiedener Formen eines Enzyms bzw. analoger Enzymreaktionen können unterschiedliche molekulare Ursachen zu Grunde liegen (Naessens und Vandamme, 2003). Es kann sich dabei um

- voneinander genetisch unabhängige Proteine
- genetische Varianten
- Heteropolymere von mindestens zwei nicht kovalent verknüpften Polypeptidketten
- Polymerisierung von identischen Untereinheiten
- posttranslationale Modifizierungen
- unterschiedliche Konformations-Zustände

handeln. Die Faktoren, die das Auftreten von Enzymformen beeinflussen, können ebenso vielfältig sein (Naessens und Vandamme, 2003):

- Art und Menge der Kohlenstoff- und Stickstoffquelle
- Temperatur
- Aggregatzustand des Mediums
- Redoxverhältnisse
- Wachstumsphasen

COR-AAD1-00003591
Bayer EX1008 (Part 7 of 9)

- Einfluss von Induktoren oder Inhibitoren.

Multiple Enzymformen unterscheiden sich zumeist in ihrer zellulären Lokalisation, ihrer Regulation oder in ihrem kinetischen Verhalten. Sie bieten dem Organismus eine Möglichkeit der Feinregulation des Stoffwechsels.

1.3 Optische Aktivität und die Umwelt

Optisch aktive Moleküle sind asymmetrisch, sie sind mit ihrem Spiegelbild nicht in Deckung zu bringen, d.h. sie verhalten sich, sinnbildlich gesehen, wie die rechte zu der linken Hand. Zwei Moleküle, die sich wie Bild und Spiegelbild verhalten, werden als Enantiomere bezeichnet. Derartige Moleküle zeichnen sich in der Regel durch das Vorhandensein eines Kohlenstoffatoms (asymmetrisches oder chirales Zentrum) mit vier verschiedenen Substituenten unterschiedlicher räumlicher Anordnung aus. Chiralität ist in der Natur eher Regel als Ausnahme, so sind die DNA, RNA und Proteine aus chiralen Verbindungen aufgebaut. Proteine bestehen aus L-Aminosäuren, DNA und RNA aus den D-Enantiomeren der Desoxyribose und Ribose.

Reine Enantiomere chiraler Verbindungen haben identische physikochemische Eigenschaften (diskutiert in Eliel und Wilen, 1994), können sich jedoch in ihrem biochemischen Verhalten unterscheiden. Die möglichen physiologischen Wirkungen wurden vor allem im Zusammenhang mit der Anwendung von Arzneimitteln untersucht und von Ariëns (1989) wie folgt zusammengefasst:

- Stereoisomere weisen den gleichen Reaktionsmechanismus auf, unterscheiden sich aber in ihrer Affinität zum Enzym (Rezeptor)
- das inaktive Enantiomer wirkt als kompetitiver Inhibitor
- die Enantiomere haben entgegen gesetzte Wirkungen (z.B. Barbiturate)
- ein Enantiomer zeigt den gewünschten physiologischen Effekt, das andere einen ungewollten (z.B. Contergan [Bentley, 1995])
- beide Enantiomere zeigen unerwünschte Nebeneffekte, aber nur eins den gewünschten Effekt
- oder, die negativen Wirkungen des aktiven Enantiomers werden durch das inaktive Stereoisomer neutralisiert.

Chiralität spielt nicht nur in der Pharmazie eine entscheidende Rolle, sondern überall dort, wo bioaktive Verbindungen genutzt werden. Chirale Pestizide wurden beispielsweise über viele Jahrzehnte in großen Mengen als Racemate auf die Felder ausgebracht. Heute schränkt man, zumindest in den industrialisierten Ländern, den Einsatz auf das wirksame Enantiomer ein. In

COR-AAD1-00003592
Bayer EX1008 (Part 7 of 9)

vielen Fällen ist die Wirkung der Herbizide auf die Pflanzen enantiospezifisch und gut untersucht (Hassal, 1990; Roberts, 1998), das Schicksal der Enantiomeren im Boden dagegen nicht. Bislang ist wenig über den enantiospezifischen Abbau von Herbiziden und dessen biochemische Hintergründe bekannt. Das Phänomen des Verschwindens eines Enantiomeres oder die Verschiebung des Enantiomeren-Verhältnisses in biologischen Proben wurde jedoch schon häufig beobachtet (Zipper et al., 1998/99; Romero et al., 2000; Schulz et al., 2000; Rügge et al., 2002; Harrison et al., 2003).

1.3.1 Stereospezifische Enzyme

In Korrelation mit dem oben Gesagten schließt der Stoffwechsel von optisch aktiven Verbindungen stereoselektive Schritte, die die Aufnahme und Katalyse umfassen, mit ein. Zur Erklärung der Enantioselektivität von Enzymen wird oft das Drei-Punkte-Modell (Ogston, 1948; Easson und Stedman, 1993) genutzt. Dieses besagt, dass das aktive Enantiomer an das Enzym bindet, da die Anordnung dreier Substituenten am asymmetrischen Zentrum des Substrats komplementär zum aktiven Zentrum ist. Für das andere Enantiomer trifft dies dann nicht zu. Dieses Modell erklärt die Spezifität aber nur solange, wie vorausgesetzt wird, dass das aktive Zentrum nur von einer Seite zugänglich ist. Eine Erweiterung des Drei-Punkte-Modells wird durch die Einführung einer vierten Bindungsstelle erreicht (Mesecar und Koshland, 2000a/b). Wird z.B. das Apoenzym der Isocitrat-Dehydrogenase (in Abwesenheit von Mg^{2+}) mit seinem racemischen Substrat konfrontiert, so bindet ausschließlich L-Isocitrat, in Anwesenheit von Mg^{2+} bindet das D-Isomer. Die Kristall-Struktur des Enzyms zeigte, dass drei der vier Gruppen (das -H vom C_2, das auf das NAD^+ übertragen wird, die β-COO^--Gruppe, die als CO_2 abgespalten wird und das C_3) des Isocitrates sowohl beim L- als auch beim D-Isocitrat an die gleichen Stellen des aktiven Zentrums gebunden werden. Der Bindungsort für die vierte Gruppe, dem OH-, ist im Apoenzym komplett verschieden zu dem Bindungsort im Metall-beladenen Enzym. Mit anderen Worten: es sind vier und nicht drei Punkte zur enantioselektiven Bindung nötig.

Der Abbau der Enantiomeren chiraler Verbindungen kann auf unterschiedlichem Wege erfolgen (Müller und Kohler, 2004):

- es existieren zwei enantioselektive Enzyme für die Interaktion mit der optisch aktiven Substanz
- beide Enantiomere werden vom gleichen Enzym simultan, aber mit unterschiedlichen Umsatzraten verwertet
- beide Enantiomere werden vom gleichen Enzym nacheinander verwertet

COR-AAD1-00003593
Bayer EX1008 (Part 7 of 9)

- ein Enantiomer wird enantioselektiv abgebaut, das andere durch eine Isomerase umgesetzt

1.3.2 Mikrobieller Phenoxyalkanoat-Abbau

Bekannte Vertreter der Phenoxyalkanoat-Herbizide sind die Phenoxyacetate 2,4-Dichlorphenoxyacetat (2,4-D) und 4-Chlor-2-methylphenoxyacetat (MCPA), die optisch aktiven Phenoxypropionate (R,S)-2-(2,4-Dichlorphenoxy)propionat ([R,S]-DP, Dichlorprop) und (R,S)-2-(4-Chlor-2-methylphenoxy)propionat ([R,S]-MCPP, Mecoprop) und die Phenoxybutyrate 4-(2,4-Dichlorphenoxy)butyrat (2,4-DB) und 4-(4-Chlor-2-methylphenoxy)butyrat (MCPB). Diese Herbizide sind die am häufigsten eingesetzten Unkrautbekämpfungsmittel (Worthing und Hance, 1991). Weltweit wurden 1999 allein in der Weizenproduktion etwa $15 \cdot 10^6$ kg 2,4-D verwendet; vom Mecoprop wurden allein in den USA $2{,}3 \cdot 10^6$ kg ausgebracht (Donaldson et al., 2002). Die Phenoxypropionate besitzen ein asymmetrisches Zentrum, d.h. sie sind chiral und es existieren je zwei Enantiomere, von denen nur die (R)-Enantiomere biologisch aktiv sind (Matell, 1953). Trotzdem werden in einigen Ländern der Welt immer noch die Racemate dieser Herbizide in der Landwirtschaft eingesetzt.

Der mikrobielle Abbau der achiralen Phenoxyacetate (2,4-D und MCPA) ist in *Ralstonia eutropha* JMP134 (pJP4) gut untersucht. Zunächst werden die Phenoxyacetate von einer α-KG-abhängigen Dioxygenase (TfdA) an der Etherbindung in das substituierte Phenol (2,4-Dichlorphenol [DCP] oder 4-Chlor-2-methylphenol [MCP]) und Glyoxylat gespalten (Streber et al., 1987; Fukumori und Hausinger, 1993a/b). Im Anschluss wird das Phenol-Derivat von der Phenolhydroxylase (TfdB) zum korrespondierenden Catechol (3,5-Dichlorcatechol, 5-Chlor-3-methylcatechol) hydroxyliert (Liu und Chapman, 1984), welches dann über den modifizierten *ortho*-Weg (Reineke, 1986; Reineke und Knackmuss, 1988) weiter metabolisiert wird: Aus der Ringspaltung (Chlorcatechol-1,2-Dioxygenase [TfdC], Bath et al., 1993) resultiert das Muconat (2,4-Dichlor-*cis,cis*-muconat, 4-Chlor-3-methyl-*cis,cis*-muconat), welches dechloriert und cycloisomerisiert wird (TfdD und TfdE, Kuhm et al., 1990). Im weiteren Verlauf wird der zweite Substituent abgespalten und das Kohlenstoffgerüst über 3-Ketoadipat zu Succinat und Acetyl-CoA abgebaut.

Variationen dieses Abbauweges betreffen meist die Dehalogenierungsreaktionen (Evans et al., 1971a/b). Neben α-Ketoglutarat-abhängigen Dioxygenasen wurden in seltenen Fällen noch andere Enzyme gefunden, die die Spaltung der Etherbindung der Phenoxyalkansäuren katalysieren. Im Stamm *Pseudomonas cepacia* AC1100 wurde eine Monooxygenase identifiziert,

COR-AAD1-00003594
Bayer EX1008 (Part 7 of 9)

die die Spaltung von 2,4,5-Trichlorphenoxyacetat katalysiert (Xun und Wagnon, 1995). Für die Spaltung des 2,4-DB wurde in *Rhodococcus erythropolis* K2-3 ein Cytochrom P450 (Sträuber et al., 2003) gefunden.

Für die chiralen Phenoxypropionate wird ein gleicher oder zumindest sehr ähnlicher mikrobieller Abbauweg postuliert. So konnten nach der Etherspaltung zu den Phenoxyacetaten identische substituierte Phenole (DCP, MCP) nachgewiesen werden. Ebenfalls wurden die Gene (*tfdB*, *tfdC*, *tfdD*) für die Enzyme des modifizierten *ortho*-Weges in den Phenoxypropionat-spaltenden Stämmen gefunden (Zipper et al., 1996; Müller et al., 2001; Smejkal et al., 2001). Versuche mit Rohextrakten haben bereits gezeigt, dass analog zum TfdA eine Stimulierung der Reaktion durch α-KG, Fe^{2+} und Ascorbat erfolgt (Müller et al., 2001), was nahe legt, dass der Reaktionsmechanismus zur Spaltung der Phenoxypropionate dem der Phenoxyacetate entspricht.

Erste Hinweise auf eine enantiospezifische Spaltung der Phenoxypropionate folgen aus Substratverwertungsprofilen und Induktionsversuchen. So wurde für *Alcaligenes denitrificans* gezeigt, dass er in der Lage ist, prototroph auf dem (R)-Enantiomer des MCPP zu wachsen, (S)-MCPP wird hingegen nicht verwertet (Tett et al., 1994/97). Im Falle von *Rhodoferax* sp. P230 (P230) konnte gezeigt werden, dass für die Verwertung der (R)-Enantiomere ein konstitutives Enzym verantwortlich ist. Das Enzym der (S)-Enantiomeren-Spaltung ist induzierbar (Müller et al., 2001). *Sphingobium herbicidovorans* MH (MH) ist in der Lage, beide Enantiomere der Phenoxypropionate komplett zu verwerten (Horvath et al., 1990). Induktionsversuche haben gezeigt, dass Enantiospezifität für den ersten Spaltungsschritt vorliegt, das (S)-spezifische Enzym in MH ist konstitutiv, das (R)-spezifische induzierbar (Nickel et al., 1993). Ebenso konnte eine enantiospezifische Aufnahme der Herbizide nachgewiesen werden (Zipper et al., 1998). Für *Delftia acidovorans* MC1 (MC1) konnte erstmals der Beweis für die Existenz von zwei Enzymen erbracht werden. Durch die Aufreinigung des Rohextraktes am Anionenaustauscher (*Source30Q*) konnten enantioselektive Enzyme voneinander getrennt werden, kinetische Eigenschaften blieben weitgehend offen (Müller und Babel, 1999).

COR-AAD1-00003595
Bayer EX1008 (Part 7 of 9)

1.4 Problemstellung

Es sind bislang nur wenige Stämme bekannt, die über ein breites Substratverwertungsspektrum für Phenoxyalkanoate verfügen. Viele Bakterien-Stämme sind dazu in der Lage, die Phenoxyacetate zu verwerten, spalten aber die Phenoxypropionate und -butyrate nicht oder nur in sehr geringem Umfang. Anders ist dies bei *Delftia acidovorans* MC1, *Rhodoferax* sp. P230 und *Sphingobium herbicidovorans* MH, sie spalten sowohl die Phenoxyacetate als auch die Enantiomere der Phenoxypropionate (z.T. auch die Phenoxybutyrate).

Ziel dieser Arbeit ist es, den initialen Schritt der bakteriellen Spaltung substituierter Phenoxyalkanoate biochemisch zu beschreiben. Hierzu sollen die initialen Enzyme gereinigt und proteinbiochemisch hinsichtlich ihrer physikochemischen Eigenschaften, ihrer Primär- und Quartär-Struktur sowie eventueller Modifikationen untersucht werden. Die enzymkinetische Beschreibung der Enzyme soll die Aufnahme und Diskussion von Substratverwertungsspektren, kinetischer Kennlinien und Konstanten umfassen. Auf enantioselektive Eigenschaften soll eingegangen und die erhaltenen Ergebnisse sollen über die Spezies-Grenzen hinaus verglichen werden.

COR-AAD1-00003596
Bayer EX1008 (Part 7 of 9)

2 Material und Methoden

2.1 Mikroorganismen

Als Quelle zur Isolierung von *Delftia acidovorans* MC1 (Müller et al., 1999a) und *Rhodoferax* sp. P230 (Ehrig et al., 1997) diente Herbizid-kontaminierter Bauschutt. *Sphingobium* (*Sphingomonas*) *herbicidovorans* MH (Zipper et al., 1996; Takeuchi et al., 2001) (früher *Flavobacterium*) wurde aus einer Bodenprobe isoliert (Horvath et al., 1990).

***Delftia acidovorans* MC1** (MC1) ist ein bewegliches, gramnegatives Stäbchen mit einer Länge von 3-12 µm und einem Durchmesser von 0,7-1 µm. Es ist in der Lage, die Herbizide (R,S)-DP und (R,S)-MCPP produktiv zu verwerten; er wächst prototroph auf den Herbiziden und zeigt zudem einen signifikanten MCPA- und 2,4-D-Umsatz. Im Genom von MC1 konnten die codierenden Gene (*tfdB, tfdC, tfdD*) für die Enzyme des modifizierten *ortho*-Weges nachgewiesen werden, welche plasmidal codiert sind. Untersuchungen mit *tfdA*-spezifischen Sonden zeigten dagegen kein Signal (Müller et al., 2001).

Bei ***Rhodoferax* sp. P230** (P230) handelt es sich um einen gramnegatives, bewegliches, stäbchenförmiges Bakterium. Der Stamm P230 ist in der Lage, sowohl (R,S)-DP und (R,S)-MCPP als auch 2,4-D und MCPA zu verwerten. Prototrophes Wachstum mit Phenoxyalkanoaten als einzige Kohlenstoff und Energiequelle ist dagegen nicht möglich. Es werden unterschiedliche Vitamine (Thiamin, Biotin), besser noch Hefeextrakt für ein optimales Wachstum benötigt. Im Genom von P230 konnten die Gene (*tfdA, tfdB, tfdC, tfdD*) der degradativen Enzyme des *ortho*-Weges nachgewiesen werden (Müller et al., 2001).

***Sphingobium herbicidovorans* MH** (MH) weist ebenfalls eine Stäbchenform auf (Länge 1,0-2,1 µm; Durchmesser 0,4-0,7 µm) und ist in der Gram-Färbung negativ. Es ist ein unbewegliches, gelb pigmentiertes Bakterium. Der Stamm ist in der Lage, auf den Phenoxypropionaten und -acetaten zu wachsen, kann aber auch Phenoxybutyrate verwerten (Horvath et al., 1990). Auch im Genom von MH konnten die Gene *tfdB, tfdC* und *tfdD* nachgewiesen werden (Zipper et al., 1996).

2.2 Kultivierung

Alle mikrobiologischen Arbeiten wurden unter sterilen Bedingungen durchgeführt. Die Geräte zur Kultivierung inklusive Zubehör und alle Nährmedien wurden 20 Minuten im Autoklav bei 121°C und 1,1 kPa sterilisiert. Herbizide wurden steril filtriert (Porenweite der Filter: 0,2 µm).

COR-AAD1-00003597
Bayer EX1008 (Part 7 of 9)

2.2.1 Medien

- **Spurensalzlösung:** 71,2 mg/l $MgSO_4 \cdot 7\ H_2O$; 0,615 mg/l $MnSO_4 \cdot 1\ H_2O$; 0,44 mg/l $ZnSO_4 \cdot 7\ H_2O$; 0,785 mg/l $CuSO_4 \cdot 5\ H_2O$; 49,8 mg/l $FeSO_4 \cdot 7\ H_2O$; 0,252 mg/l $Na_2MoO_4 \cdot 2\ H_2O$; pH-Wert mit 1N H_2SO_4 auf $\leq 1,5$ einstellen
- **Mineralsalzmedium:** 1/10 Spurenelementlösung (v/v); 1,523 g/l NH_4Cl; 0,6805 g/l KH_2PO_4; 0,8709 g/l K_2HPO_4; 0,011 g/l $CaCl_2 \cdot 6\ H_2O$; pH 8
- **Selektivagar:** 2 g/l OXOID®-Agar; 50 % Mineralsalzmedium in Wasser; 0,4 g/l (R,S)-DP; pH 8,5
- **PYE-Medium:** 3 g/l Bacto®-Pepton; 3 g/l Hefeextrakt; 1,802 g/l Fructose; pH 8,5
- **PYE-Agar:** PYE-Medium; 1,8 g/l Bacto®-Agar; pH 8,5
- **Substrat:** 20 g/l (R,S)-DP in 0,1 M NaOH
- **LB-Medium:** 5 g/l Hefeextrakt; 10 g/l Trypton; 5 g/l NaCl; pH 7,0

2.2.2 Batch-Kultivierung

Die Bakterienstämme MC1, P230 und MH wurden im Batch-Verfahren in 0,5 l Kulturen in 1 l Erlenmeyerkolben rangezogen. Angeimpft wurden die Kolben jeweils mit etwa zehn Bakterienkolonien, die zuvor auf Selektivagar mit (R,S)-DP als einziger Kohlenstoff- und Energiequelle angezogen wurden. Kultiviert wurde über Nacht in PYE-Medium, bei 30°C unter aeroben Bedingungen auf einer Schüttelbank (Swip SM 25 DIGI, Edmund Bühler, BRD) mit einer Frequenz von 155 rpm. Anschließend wurden zur Induktion von Enzymen des (R,S)-DP-Abbauweges 100 mg/l (R,S)-DP zugegeben. Der Abbau des Herbizides wurde mittels HPLC-Analyse (siehe Abschnitt 2.8.2) kontrolliert und die Kultur nach vollständigem Abbau der Herbizide geerntet oder im Falle von MC1 als Inokulum für eine anschließende Fed-Batch-Kultivierung eingesetzt. Die Reinheit der Kultur wurde durch Ausstriche auf PYE-Agar-Platten geprüft.

2.2.3 Batch-Kultivierung genetisch veränderter Mikroorganismen

Die Vorkultur genetisch veränderter Mikroorganismen wurde über Nacht in LB-Medium (0,05 g/l Ampicillin) (30°C, 180 rpm) im 300 ml-Maßstab angezogen. Mit diesen Bakterien wurde die Hauptkultur (LB-Medium + 0,1 g/l Ampicillin) mit einer $OD_{700} = 0,1$ angeimpft und bei 27°C und 220 rpm inkubiert. Das Wachstum der Kultur wurde fortwährend über die optische Dichte verfolgt. Bei einer $OD_{700} = 0,5$ wurden zur Induktion der Proteinsynthese des zu überexprimierenden Enzyms 2 ng/l Anhydrotetracyclinhydrochlorid zugesetzt. Nach drei Stunden wurden die Zellen geerntet.

COR-AAD1-00003598
Bayer EX1008 (Part 7 of 9)

2.2.4 Fed-Batch-Kultivierung

Die Fed-Batch-Kultivierung der Hauptkultur erfolgte in einem Fermenter (INFORS AG, Bottmingen, Schweiz, Typ ALGU 503) im 17 l Maßstab unter sterilen Bedingungen. Angeimpft wurde mit 2 l der Vorkultur in 15 l Mineralsalzmedium. Die Kultivierung erfolgte bei 30°C, pH 8 und 800 rpm. Die Bakterienkultur wurde mit 1,5 l/h Luft belüftet. Die Spurenelementlösung wurde ständig mit einer Flussrate von 0,77 ml/h zugegeben. Die Schaumbildung wurde bei Bedarf durch Zugabe von Entschäumer (5%ige Silikon-Antischaum-Emulsion) unterdrückt. Der Biomassezuwachs sowie der Substratverbrauch wurden verfolgt, so dass der Zufluss des Substrates fortwährend dem Wachstum der Bakterien angepasst werden konnte. Ab dem vierten Tag der Kultivierung wurden täglich 8 l Bakteriensuspension geerntet und der Fermenter anschließend mit Mineralsalzmedium wieder auf 17 l aufgefüllt. Die Reinheit der Kultur wurde täglich durch Ausstriche auf PYE-Agar-Platten kontrolliert.

2.3 Enzymreinigung

2.3.1 Zellernte und Zellaufschluss

Die Ernte der Zellen erfolgte durch 15-minütige Zentrifugation (Hettich Sepatech Varifuge 20RS, BRD) der Zellsuspension bei 4°C und 8875×g. Die Zellen wurden dreimal mit Tris/HCl-Puffer (10 mM, pH 7,5) gewaschen und anschließend zur Lagerung bei -20°C im gleichen Puffer aliquotiert eingefroren.

Der Zellaufschluss erfolgte mit Hilfe der French-Pressure Cell Press Technik (American Instrument Company, Silver Spring, Maryland, USA) in Tris/HCl Puffer (10 mM, pH 7,5). Die optische Dichte der Zellsuspension bei 700 nm betrug zwischen 80 und 140. Die Desintegration erfolgte über drei Passagen bei einem angelegten Druck von 20000 psi (1379 bar). Anschließend wurde der Extrakt 25 min bei 4°C und 20000×g zentrifugiert (ZK 380, Berthold Hermle GmbH & Co--Zentrifugen, Gosheim, BRD). Der Überstand stellt den Rohextrakt dar.

2.3.2 Reinigung der nativen Enzyme

2.3.2.1 Protaminsulfat- und Ammoniumsulfat-Fällung

Dem aus dem Zellaufschluss gewonnenen Rohextrakt wurde 1%ige Protaminsulfatlösung (pH 7) bis zu einer Konzentration von 0,15% zugesetzt und unter ständigem Rühren 20 min bei 4°C inkubiert. Anschließend wurden die gefällten Bestandteile durch Zentrifugation (4°C, 20 min, 20000×g, ZK 380, Hermle, Gosheim, BRD) von der löslichen Fraktion abgetrennt. Das Pellet wurde verworfen und der Überstand einer fraktionierten Ammoniumsulfatfällung unterzogen. Dazu wurde unter ständigem Rühren bei 4°C festes Ammoniumsulfat bis zu einer

COR-AAD1-00003599
Bayer EX1008 (Part 7 of 9)

Konzentration von 1,25 M zugegeben. Nach 20 min wurde das ausgefallene Protein abzentrifugiert (4°C, 20 min, 20000×g, ZK 380, Hermle, Gosheim, BRD) und verworfen. Dem Überstand wurde wiederum festes Ammoniumsulfat zugesetzt, bis eine Konzentration von 2,5 M erreicht wurde. Das nach Zentrifugation erhaltene Pellet wurde in konzentrierter Form in Tris/HCl-Puffer (10 mM, pH 7,5) aufgenommen und einer Entsalzung unterzogen (siehe 2.4.1).

2.3.2.2 Ionenaustausch-Chromatographie

Die säulenchromatographischen Reinigungen erfolgten an dem GradiFrac System (Amersham Pharmacia Biotech, Schweden) mit der Pumpe P1 (LKB-Pumpe P-1, Pharmacia LKB, Uppsala, Schweden), dem Fraktionssammler (Gradi-Frac-Fraktionssammler, Pharmacia LKB, Uppsala, Schweden) und dem UV-Detektor UV-1. Alle Reinigungsschritte wurden bei 4°C durchgeführt.

2.3.2.2.1 an Source30Q

Die Ionenaustauschchromatographie erfolgte an einer *Source30Q* Säule (∅ 2,5 cm, Länge 14 cm, Amersham Biosciences Europe GmbH, Freiburg, BRD). Die Säule wurde mit Tris/HCl-Puffer (10 mM, pH 7,5) equilibriert. Nach dem Probenauftrag wurde das nicht gebundene Protein mit dem gleichen Puffer abgewaschen. Eluiert wurde das $SdpA_{MCI}$ mit einem linearen Gradienten von 0–0,15 M NaCl in Tris/HCl-Puffer (10 mM, pH 7,5) in einem Gesamtvolumen von 240 ml. Es wurden Fraktionen zu 8 ml gesammelt. Das $RdpA_{MCI}$ wurde mit einem Gradienten von 0,15–0,4 M NaCl in Tris/HCl (10 mM, pH 7,5) in einem Gesamtvolumen von 320 ml eluiert. Auch hier betrug die Fraktionsgröße 8 ml. Der Gradient wurde mit Hilfe eines Gradientenmischers generiert. Als Puffer kamen Tris/HCl-Puffer (10 mM, pH 7,5) und 1 M NaCl in Tris/HCl-Puffer (10 mM, pH 7,5) zum Einsatz. Die Flussrate betrug 1 ml/min. Die Fraktionen wurden auf Enzymaktivität und Proteingehalt untersucht. Regeneriert wurde die Säule durch Waschen mit 1 M NaCl in Tris/HCl (10 mM, pH 7,5) und Equilibrierung mit Tris/HCl-Puffer (10 mM, pH 7,5).

2.3.2.2.2 an PBE94

Die Enzyme aus MH und P230 wurden einer Aufreinigung an dem Anionenaustauscher *PBE94* (80 ml Bettvolumen, Amersham Biosciences Europe GmbH, Freiburg, BRD) unterzogen. Das Säulenmaterial wurde zunächst mit Tris/HCl-Puffer (10 mM, pH 7,5) equilibriert und nach Probenauftrag mit 0,1 M NaCl in Tris/HCl (10 mM, pH 7,5) gewaschen. Das Protein wurde mit einem NaCl-Gradienten von 0,10-0,35 M NaCl in Tris/HCl-Puffer (10 mM,

COR-AAD1-00003600
Bayer EX1008 (Part 7 of 9)

pH 7,5) in einem Gesamtvolumen von 800 ml eluiert. Die Flussrate betrug 1 ml/min, es wurden 8 ml-Fraktionen gesammelt.

2.3.2.3 Hydrophobe Chromatographie

Die hydrophobe Chromatographie erfolgte an einer Butyl-Sepharose-Säule (Amersham Biosciences Europe GmbH, Freiburg, BRD) mit einem Bettvolumen von 20 ml. Die Säule wurde für die Reinigung der Enzyme mit der jeweiligen Konzentration Ammoniumsulfat in Tris/HCl-Puffer (10 mM, pH 7,5) equilibriert. Eluiert wurde das Protein mit den in Tabelle 1 aufgeführten Gradienten. Der Gradient wurde aus den Puffern 1,5 M $(NH_4)_2SO_4$ in Tris/HCl (10 mM, pH 7,5) und Tris/HCl (10 mM, pH 7,5) gemischt. Es wurden 8 ml-Fraktionen gesammelt, die auf Enzymaktivität und Proteingehalt untersucht wurden. Die Flussrate betrug 1 ml/min.

Tabelle 1: Elutionsbedingungen für die (S)- und (R)-spezifischen Enzyme der Stämme MC1, MH und P230 an Butyl-Sepharose

Enzym	Ammoniumsulfatgradient
$RdpA_{MC1}$	1,07-0,35 M in 480 ml
$RdpA_{MH}$	1,125-0,45 M in 480 ml
$RdpA_{P230}$	1,07-0,3 M in 240 ml
$SdpA_{MC1}$	0,3-0 M in 300 ml
$SdpA_{MH}$	1,125-0,45 M in 480 ml
$SdpA_{P230}$-1	0,975-0 M in 360 ml
$SdpA_{P230}$-2	0,975-0 in 360 ml

2.3.2.4 Präparative Gelelektrophorese

Die Separation der isomeren Enzymformen des $SdpA_{MC1}$ und des $RdpA_{MC1}$ erfolgte mittels präparativer Elektrophorese mit der Prep Cell (Modell 491) von Bio-Rad (München, BRD). Kombiniert wurde das Gerät mit einem UV-Detektor (Modell EM-1), einem Fraktionssammler (Modell 2110), einem Flachbettschreiber (Model 1327) und einer Econo-Pumpe (Modell EP-1), ebenfalls von der Firma Bio-Rad (München, BRD).

2.3.2.4.1 Trennung der $RdpA_{MC1}$-Enzymformen

Die Auftrennung der nativen $RdpA_{MC1}$-Enzymformen erfolgte im kontinuierlichen nativen Elektrophoresesystem. Bei dieser Methode muss auf die Vorteile eines Sammelgels verzichtet werden, daher ist es wichtig, die Proteinprobe so konzentriert wie möglich auf das Gel aufzubringen. Es wurde das Imidazol/HEPES-Puffersystem (pH 7,4) genutzt. In Tabelle 2 ist die Zusammensetzung der Puffer und des Gels dargestellt. Die Abmessungen des Gels sowie die Laufbedingungen sind der Tabelle 3 zu entnehmen. Die Elution der Enzyme erfolgte mit Tris/HCl-Puffer (10 mM, pH 7,5) und einer Geschwindigkeit von 0,5 ml/min. Es wurden 3 ml-Fraktionen gesammelt.

COR-AAD1-00003601
Bayer EX1008 (Part 7 of 9)

Tabelle 2: Zusammensetzung der Gele und Puffer der kontinuierlichen Elektrophorese

Gel	5% T / 2,6% C 8,6 mM Imidazol, 7 mM HEPES, pH 7,4	
Puffer	**Laufpuffer**	**Probenpuffer**
	43 mM Imidazol 35 mM HEPES pH 7,4	4,3 mM Imidazol 3,5 mM HEPES pH 7,4 40% Glycerin (v/v) 0,02% Bromphenolblau (w/v)

2.3.2.4.2 Trennung der $SdpA_{MC1}$-Enzymformen

Die präparative Trennung der $SdpA_{MC1}$-Enzymformen erfolgte in einem diskontinuierlichem nativen Acrylamidgel unter Verwendung des Tris/Glycin-Puffersystems nach Laemmli et al. (1970). Es wurde der native Probenpuffer der Firma Invitrogen genutzt. Das Protein wurde mit Tris/HCl (10 mM, pH 7,5) und einer Geschwindigkeit von 0,5 ml/min eluiert und in 3 ml Fraktionen aufgefangen. Die gesamte Präparation erfolgte bei einer Temperatur von 4°C.

Tabelle 3: Trennbedingungen der $SdpA_{MC1}$-Enzymformen mittels präparativer Elektrophorese

Sammelgel	4% T / 2% C
Sammelgelhöhe	1,5 cm
Trenngel	6% T / 2% C
Trenngelhöhe	10,3 cm
Gelröhrengröße	37 mm ID
Probenmenge	18,5 mg $SdpA_{MC1}$ HIC
Laufbedingungen	200 V konstant
Laufzeit	ca. 48 h

2.3.3 Reinigung der rekombinanten Enzyme $RdpA_{MC1}$-rec und $SdpA_{MC1}$-rec

2.3.3.1 Affinitätschromatographie

Mittels der Affinitätschromatographie ist es möglich, markierte Proteine in einer Einschritt-reinigungsprozedur in hochreiner Form darzustellen. Diese Methode wurde in der vorliegenden Arbeit dazu verwendet, die überexprimierten Enzyme $SdpA_{MC1}$-rec und $RdpA_{MC1}$-rec, welche N-terminal um eine Strep-tag(II) Sequenz (NH_2-WSHPQFEK-COOH, Schmidt et al., 1996) verlängert wurden, aufzureinigen. Als Säulenmaterial wurde Strep-Tactin Superflow (10 ml) (Voss und Skerra, 1997) der Firma IBA (Göttingen, BRD) genutzt. Das Chromatographiematerial wurde zunächst mit Tris/HCl (100 mM, pH 8,0) equilibriert. Nach dem Probenauftrag wurde das nicht spezifisch gebundene Protein mit dem gleichen Puffer mit einer Flussrate von 1 ml/min eluiert. Anschließend wurde die Säule mit Tris/HCl-Puffer (100 mM, pH 8,0) + 500 mM NaCl gewaschen. Die Elution der rekombinanten Proteine erfolgte mit 2,5 mM Desthiobiotin in Tris/HCl (100 mM, pH 8,0). Es wurden Fraktionen zu

COR-AAD1-00003602
Bayer EX1008 (Part 7 of 9)

10 ml gesammelt. Zur Regeneration des Säulenmaterials wurde 1 mM HABA in Tris/HCl (100 mM, pH 8,0) verwendet.

2.3.3.2 Abspaltung der Strep-tag(II)-Sequenz

Zur Abspaltung der Strep-tag(II)-Sequenz wurde das Eluat der Affinitätsreinigung mittels Vivaspin 20 (MWCO 30000) in Tris/HCl-Puffer (50 mM, pH 8,0) + 100 mM NaCl + 1 mM CaCl umgepuffert (siehe 2.4.2). Pro mg Fusionsprotein wurden 50 µg des proteolytischen Enzyms Faktor Xa (Amersham Biosciences Europe GmbH, Freiburg, BRD) zugesetzt. Die Spaltung erfolgte über 18 h bei 13°C. Nicht gespaltenes Protein sowie die abgespaltenen Strep-tag(II)-Sequenzen wurden durch eine Passage über die Affinitätssäule mit Strep-Tactin abgetrennt.

2.4 Aufkonzentrieren, Umpuffern und Entsalzen

2.4.1 Säulenchromatographisch mittel Gelfiltration

Die Entsalzung der Proteinlösung erfolgte mit Hilfe der Größenausschlusschromatographie an einer *HiPrep™*26/10 *Desalting*-Säule (Sephadex® G-25 Fine, Amersham Biosciences Europe GmbH, Freiburg, BRD). Equilibriert wurde die Säule mit dem Laufpuffer Tris/HCl (10 mM, pH 7,5). Die Probe wurde mit einer Geschwindigkeit von 3 ml/min aufgetragen und mit dem Laufpuffer in gleicher Geschwindigkeit eluiert. Es wurden Fraktionen von 10 ml Größe gesammelt. Die Fraktionen wurden auf Leitfähigkeit (2.8.5) und Proteingehalt (2.8.1) geprüft.

2.4.2 Ultrafiltration

Die Entsalzung, Aufkonzentrierung und Umpufferung von Proteinlösungen wurde bei geringen Proteinmengen mittels Ultrafiltration erreicht. Hierzu wurden Vivaspineinheiten der Firma Vivascience (Hannover, BRD) unterschiedlichen Fassungsvermögens und einer Ausschlussgröße von 10 oder 30 kD verwendet. Die Ultrafiltration erfolgte mittels Zentrifugation im Swingout-Rotor bei 3000×g und 10°C (ZK 380, Hermle, Gosheim, BRD). Das Protein wurde mit reichlichen Mengen des jeweilig benötigten Puffers gewaschen.

2.5 Proteinbiochemische Untersuchungen

2.5.1 Säulenchromatographische Bestimmung der Molmasse

Die Molmasse (MM) der nativen Enzyme wurde mittels Größenausschlusschromatographie an der Bio-Sil™ SEC-250 Säule (300 mm×7,8 mm von Bio-Rad, München, BRD) bestimmt. Die Erstellung der Eichkurve erfolgte mit einem Standard, der fünf Komponenten enthielt: *Thyroglobin 670 kD, Bovin gamma globin 158 kD, Chicken ovalbumin 44 kD, Equine my-*

COR-AAD1-00003603
Bayer EX1008 (Part 7 of 9)

oglobin 17 kD, Vitamin B12 1,35 kD. Als Laufpuffer wurde 0,05 M NaH_2PO_4/Na_2HPO_4 (pH 6,8) mit 0,15 M NaCl verwendet. Die Gelfiltration erfolgte an einer HPLC-Anlage (Shimadzu, Kyoto, Japan) bei 23°C, einem Druck von 70 bar und einer Flussrate von 1 ml/min. Es wurden 20 µl Probe auf die Säule aufgetragen. Die Detektion erfolgte bei 280 nm.

Die Bestimmung der MM von Monomeren der untersuchten Enzyme erfolgte nach Denaturierung der Proteine. Dazu wurde 1% SDS (w/v) zum Protein gegeben und der Ansatz einer 10-minütigen Inkubation bei 95°C unterzogen. Dem Laufpuffer wurde 0,5% SDS (w/v) zugesetzt.

2.5.2 Bestimmung der Anzahl funktionell aktiver Zentren

Die Fraktion des funktionell aktiven Enzyms in den einzelnen Enzympräparaten wurde über die Bindung von α-KG ermittelt. Dabei wurde angenommen, dass die Bindung hoch spezifisch am aktiven Zentrum erfolgt. Dazu wurde das Enzym mit einer adäquaten Menge von α-Ketoglutarat in entgastem Tris/HCl (10 mM, pH 7,5) für 15 min bei 30°C unter Stickstoff-Atmosphäre und ständigem Schütteln im Thermomixer (Eppendorf, Hamburg, BRD) inkubiert. Anschließend wurde das Protein durch Ultrafiltration mittels Vivaspin 2 (Polyethersulfon, MWCO 30000, Vivascience, Hannover, BRD) bei 10°C und 3000×g (Hermle Tischzentrifuge) von der α-Ketoglutaratlösung getrennt. Nicht gebundenes α-Ketoglutarat wurde chromatographisch bestimmt (siehe 2.5.2).

2.5.3 Gelelektrophoretische Methoden

2.5.3.1 SDS-PAGE

Die SDS-gelelektrophoretische Auftrennung der Proteine zur Reinheitskontrolle erfolgte unter nicht reduzierenden Bedingungen in einem 12%ige Acrylamidgel. Es wurden pro Spur 1-2 µg Protein in Probenpuffer aufgetragen. Die Stromstärke betrug 10 mA/Gel.

Tabelle 4: Zusammensetzung der Gele und Puffer der SDS-Gelelektrophorese

Gel	Trenngel	Sammelgel
	12% T/2,67% C Tris/HCL (0,375 M, pH 8,8) 0,1% SDS (w/v) 0,05% APS (w/v) 10 µl Temed	4% T/2,67% C Tris/HCl (0,125 M, pH 6,8) 0,1% SDS (w/v) 0,05% APS (w/v) 10 µl Temed
Puffer	**Laufpuffer**	**Probenpuffer**
	2,9 g/l Tris 14,4 g/l Glycin 1,0 g/l SDS	2,0 ml Glycerol 0,5 ml 1% Bromphenolblau (w/v) 2,5 ml 0,5 M Tris/HCl pH 6,8 4,0 ml 10% SDS (w/v) mit Wasser auf 10 ml auffüllen

Standard: *Mark 12™ Wide Range* Protein Standard (Novex, San Diego, USA) Myosin 200 kD; β-Galactosidase 116,3 kD; Phosphorylase B 97,4 kD; Rinderserumalbumin 66,3 kD; Glutamatdehydrogenase

COR-AAD1-00003604
Bayer EX1008 (Part 7 of 9)

55,4 kD; Laktatdehydrogenase 36,5 kD; Carboanhydrase 31 kD; Trypsininhibitor 21,5 kD; Lysozym 14,4 kD; Aprotinin 6 kD; Insulin-β-Kette 3,5 kD; Insulin-α-Kette 2,5 kD

2.5.3.2 Native Gelelektrophorese

2.5.3.2.1 Kontinuierliche Gelelektrophorese

Die Auftrennung der nativen RdpA-Enzymformen erfolgte im Minigel, wie in 2.3.2.4.1 beschrieben.

2.5.3.2.2 Diskontinuierliche Gelelektrophorese

Um das SdpA nativ aufzutrennen, wurde das Tris/Glycin-Puffersystem benutzt. Es wurden 6% T/2% C-ige Gele verwendet. Die Zusammensetzung der Gele und Puffer ist in Tabelle 4 dargestellt. SDS wurde in diesem Fall weggelassen. Die Laufbedingungen wurden nicht verändert.

Standard: *High molecular weight calibration kit* (Amersham Pharmacia, Freiburg, BRD), Thyroglobin 667 kD; Ferritin 440 kD; Katalase 232 kD; Laktatdehydrogenase 66 kD

2.5.3.3 Peptid-Gelelektrophorese

Die Peptid-Gelelektrophorese wurde, wie von Schägger und Jagow (1987) beschrieben im Tris/Tricin-Puffer durchgeführt (Tabelle 5). Die Stromstärke betrug für 0,5 h zunächst 10 mA/Gel und wurde dann für 4 h auf 20 mA/Gel erhöht.

Tabelle 5: Zusammensetzung des Gels und der Puffer für die Peptidelektrophorese

Gel	Sammelgel	„Spacer"-Gel	Trenngel
	4% T / 3% C 0,75 M Tris/HCl, pH 8,45 0,25% SDS (w/v) 0,01% APS (w/v) 0,001% TEMED (v/v)	9,6% T/3% C 1 M Tris/HCl, pH 8,45 1% SDS (w/v) 0,01% APS (w/v) 0,001% TEMED (v/v)	13% T/3% C 0,82 M Tris/HCl, pH 8,45 27% Glycerin (v/v) 0,8% SDS (w/v) 0,01% APS (w/v) 0.001% TEMED (v/v)
Puffer	**Anoden-Puffer**	**Kathodenpuffer**	**Proben-Puffer**
	0,2 M Tris/HCl, pH 8,9	0,1 M Tris 0,1 M Tricine 0,1% SDS (w/v)	0,05 M Tris/HCl, pH 6,8 0,3 M Mercaptoethanol 12% Glycerol (v/v) 4% SDS (w/v) 0,1% Coomassie-Brillant-blauG250 (w/v)

Standard: *Ultra low range standard* (Sigma, BRD), Triosephosphatisomerase 26,6 kD; Myoglobin 17 kD; α-Lactalbumin 14,2 kD; Aprotinin 6,5 kD; Insulin-β-Kette 3,5 kD; Bradykinin 1,06 kD

2.5.3.4 2D-Gelelektrophorese

Die isoelektrische Fokussierung wurde in der *IPG Phore Electrophorese-Einheit* von Pharmacia (Uppsala, Schweden) durchgeführt, die anschließende SDS-PAGE in der Hoefer *Dalt Elektrophorese-Einheit* (Pharmacia, Uppsala, Schweden). Die Gele wurden im *GelAir Dryer* (Bio-Rad, München, BRD) getrocknet.

COR-AAD1-00003605
Bayer EX1008 (Part 7 of 9)

2.5.3.4.1 Erste Dimension: Isoelektrische Fokussierung

Die entsalzten Proben für die 2D-Gelelktrophorese wurden zunächst mit 10% TCA behandelt und das gefällte Protein 3mal mit Aceton gewaschen. Anschließend wurde das Protein in 80 µl Probenpuffer aufgenommen und 10 min unter ständigem Schütteln inkubiert (1400 rpm). Nach Zugabe von 320 ml IEF-Puffer (Tabelle 6) und 5 min Inkubation wurden die unlöslichen Bestandteile abzentrifugiert (30 min, 10000×g, 20°C). Es wurden 350 µl des Überstandes pro *DryStrip* aufgetragen und anschließend mit 2 ml *DryStrip Cover Fluid* überschichtet.

Tabelle 6: Pufferzusammensetzung und Laufbedingungen für die IEF

Puffer	**Probenpuffer**		**IEF-Puffer**	
	250 µl IEF-Puffer 5 mg CHAPS 2,5 µl Bromphenolblau (1mg/ml)		600 mg Harnstoff 800 µl dest. Wasser 25 µl Triton X-100 6,5 µl IPG-Puffer pH 3-10 (Pharmacia) 3,5 mg DTT	
Laufbedingungen	**Schritt**	**U [V]**	**t [h]**	**Vh**
analytisch	Rehydratisierung	0	10	0
	1	500	0,01	2,5
	2	500	1	500
	3	8000	5	21250
	4	8000	10	80000
präparativ	Rehydratisierung	0	10	0
	1	500	0,01	2,5
	2	500	10	5000
	3	8000	5	21250
	4	8000	25	200000

Nach der isoelektrischen Fokussierung wurden die *DryStrips* mit Wasser gespült und dann 15 min in 2 ml Reduktionspuffer (50 mM Tris/HCl, pH 8,8, 6M Harnstoff, 30% Glycerol (v/v), 4% SDS (w/v), 2% DTE (w/v)) equilibriert. Im Anschluss wurden die *DryStrips* 15 min in 2 ml Modifizierungspuffer (50 mM Tris/HCl, pH 8,8, 6M Harnstoff, 30% Glycerol (v/v), 4% SDS (w/v), 2,5% Iodacetamid (w/v), eine Spatelspitze Bromphenolblau) inkubiert.

2.5.3.4.2 Zweite Dimension: SDS-PAGE

Die Auftrennung der Proteine in der zweiten Dimension erfolgte in einem großen 12%igen SDS-Gel. Die Zusammensetzung des Gels und der Puffer entspricht den Angaben in Tabelle 4. Der Lauf erfolgte bei 100 V (16-20 h) unter ständiger Kühlung durch einen externen Thermostaten bei 12°C.

COR-AAD1-00003606
Bayer EX1008 (Part 7 of 9)

2.5.3.5 Western-Blot

Nach der Gelelektrophorese wurde das Gel 5 min in Wasser gewaschen und anschließend 10-15 min in 10 mM CAPS/NaOH-Puffer (pH 11) equilibriert. Die PVDF-Membran (Bio-Rad, USA) wurde zunächst in reinem Methanol gut befeuchtet, durch Wasserzugabe wurde der Methanolgehalt langsam verringert und anschließend wurde die Membran in CAPS/NaOH-Puffer mit 20% Methanol (v/v) equilibriert. Ebenso wurde ein Stück Filterpapier behandelt. Ein weiteres Stück Filterpapier wurde in CAPS/NaOH mit 5% Methanol (v/v) getränkt. Anschließend wurden die Komponenten sandwichartig von der Anode zur Kathode wie folgt geschichtet: Filterpapier (5% Methanol (v/v)), Gel, PVDF-Membran, Filterpapier (20% Methanol (v/v). Der Proteintransfer erfolgte als sogenannter *semidry-blot* in einer *Trans Blot Semi-Dry Cell* (Bio-Rad, USA) für 2 h bei 2 mA/cm^2. Im Anschluss wurde die Membran mit Coomassie gefärbt (siehe 2.5.4.2) und getrocknet.

2.5.4 Färben, Scannen und Auswerten

2.5.4.1 Silber-Färbung

Tabelle 7: Protokoll zur Herstellung und Durchführung der modifizierten Silberfärbung nach Blum et al. (1987)

Lösung	Herstellung	Färbezeit
Fixierer	50% Methanol (v/v), 10% Essigsäure (v/v) in Wasser	1 h
Waschlösung I	30% Ethanol (v/v) in Wasser	3 × 20 min
Thiosulfatlösung	2,5 ml 1%ige Natriumthiosulfatlösung mit Wasser auf 250 ml auffüllen	1 min
Wasser	-	3×20 s
Imprägnierer	25 ml 2%ige Silbernitratlösung und 100 µl 37%ige Formaldehydlösung mit Wasser auf 250 ml auffüllen	20 min
Wasser	-	2×2 min
Entwickler	15 g Na_2CO_3 in Wasser lösen, 60 µl 37%ige Formaldehydlösung, 100 µl 1%ige Thiosulfatlösung zugeben und mit Wasser auf 250 ml auffüllen (erst kurz vor der Verwendung herstellen)	5--20 min
Wasser	-	1,5 min
Stopper	50% Methanol (v/v), 10% Essigsäure (v/v) in Wasser	10 min
Preservelösung	12% Glycerin (v/v) in Wasser	20 min

2.5.4.2 Coomassie-Färbung

Die Gele wurden für 15 min in der Färbelösung (9% Eisessig (v/v), 45% Methanol (v/v), 0,2% Coomassie-Brillantblau G250 (w/v) in Wasser) inkubiert und anschließend durch Schütteln in der Entfärbelösung (7,5% Eisessig (v/v), 5% Methanol (v/v) in Wasser) aufbereitet. Die Entfärbelösung wurde dabei mehrmals gewechselt.

COR-AAD1-00003607
Bayer EX1008 (Part 7 of 9)

2.5.4.3 Kolloidale Coomassie-Färbung

Die Gele wurden über Nacht in der Färbelösung (1,6% *ortho*-Phosphorsäure (v/v), 20% Methanol (v/v), 0,6 M Ammoniumsulfat, 0,08% Coomassie Brilliantblau G250) (w/v) in Wasser) geschwenkt. Anschließend wurde der Hintergrund durch mehrmaliges Waschen mit Wasser wieder entfärbt.

2.5.4.4 Scannen und Auswerten

Getrocknete Gele und Blot-Membranen wurden mit einem Flachbettscanner (Powerlook 2000, Umax) eingescannt. Die erhaltenen Bitmap-Dateien wurden für die weitere Verarbeitung mit Bildauswertungssoftware im TIF-Dateiformat gespeichert. Die in der Software MagicScan 4.1 genutzten Einstellungen sind in Tabelle 8 aufgeführt.

Tabelle 8: Einstellungen der Software MagicScan 4.1 bei der Bildaufnahme mit dem Flachbettscanner (Powerlook 2000, Umax)

Einstellung	Silber-/Coomassie-Färbung	Western Blots
Vorlage	Durchsicht	Aufsicht
Betriebsart	Graustufen/ Echtfarben	Graustufen
Auflösung	200 dpi	200 dpi
Entrastern	aus	aus
Filter	ohne Filter	ohne Filter
Lichter	0	Auto
Schatten	255	Auto
Gamma	1	Auto

2.5.5 Enzymatischer und chemischer Verdau von Proteinen

Die proteolytische Spaltung der Proteine erfolgte nach dem Protokoll von Shevchenko et al. (1996), modifiziert nach Kinter und Sherman (2000).

Tabelle 9: Arbeitsschritte zur Durchführung der enzymatischen und chemischen Spaltung von Proteinen im Gel

Schritt	Durchführung	Zeit
1	200 µl 50% Methanol (v/v), 5% Essigsäure (v/v), 45% dest. Wasser (v/v), schütteln, Überstand verwerfen	3 x 3 h
2	200 µl Acetonitril, schütteln, Überstand verwerfen	5 min
3	Vakuumzentrifugation	5 min
4	30 µl 10 mM 1,4-Dithioerythritol in 100 mM Ammoniumhydrogencarbonat, schütteln, Überstand verwerfen	30 min
5	30 µl 100 mM Iodacetamid in 100 mM Ammoniumhydrogencarbonat, schütteln, Überstand verwerfen	30 min
6	200 µl Acetonitril, schütteln, Überstand verwerfen	5 min
7	200 µl 100 mM Ammoniumhydrogencarbonat, schütteln, Überstand verwerfen	10 min
8	200 µl Acetonitril, schütteln, Überstand verwerfen	5 min
9	Vakuumzentrifugation	5 min
10 a	Gelstück mit Enzymlösung*[1-3] überschichten, 37°C	über Nacht
10 b	30 µl BNPS-Skatollösung (500 µg in 500 µl 75%ige Essigsäure), 47°C	1 h
11	+ 30 µl 50 mM Ammoniumhydrogencarbonat, schütteln, Überstand sammeln	10 min

COR-AAD1-00003608
Bayer EX1008 (Part 7 of 9)

12	30 µl Extraktionspuffer, schütteln, Überstand sammeln	2 x 10 min
13	Vakuumzentrifugation bis zur Trockene	

*[1]N-terminale Sequenzierung: 2,5 µg LysC/50 µl 25 mM Tris/HCl pH 8,5; 1 mM EDTA; 0,05% SDS
*[2]MS-Analyse: 0,1 µg Trypsin/µl Ammoniumcarbonatlösung (100 mM)
*[3]MS-Analyse: 0,05 µg AspN/µl Ammoniumcarbonatlösung (100 mM)
N-terminale Sequenzierung: BNPS: 3-Bromo-3-methyl-2-(2-nitrophenylmercapto)-3H-indol (Sigma, BRD)
Extraktionspuffer: 10 ml Acetonitril, 5 ml dest. Wasser, 1,176 ml 85%ige Ameisensäure

2.5.6 N-terminale Sequenzierung von Proteinen und Datenbankrecherche

Die N-terminale Sequenzierung von Proteinen erfolgte instrumentalisiert nach dem Prinzip des Edman-Abbaus. Nach dem Blotten der Proteine auf eine PVDF-Membran wurden diese ausgeschnitten und direkt auf der Membran fixiert im Proteinsequenzer (Applied Biosystems Procise 491 cLC) analysiert.

Zur Einordnung der Proteine in bestehende Enzymklassen wurde eine Datenbanksuche mit NCBI (http://www.ncbi.nlm.nih.gov/BLAST/), die auf bakterielle Proteine beschränkt wurde, durchgeführt. Zur Suche wurde die Matrix Blosum62 verwendet.

Zum direkten Vergleich von Proteinen wurde das Programm MultAlign (http://prodes.toulouse.inra.fr/multalin/multalin.html), das auf der Basis des *multiple sequence hierarchical clustering* (Corpet, 1988) basiert, genutzt.

2.5.7 Massenspektrometrische Methoden

2.5.7.1 Identifizierung von Proteinen

Zur Identifizierung von Proteinen wurden diese zunächst im Gel tryptisch verdaut (2.5.5). Anschließend wurden die Peptidgemische mittels Ziptip (Millipore, Billerica, USA) entsalzt. Das Auftragen auf die MALDI-Matrize/Target/Platte erfolgte durch Elution der Peptide aus der Gel-Matrix mit 2 µl einer Lösung aus Acetonitril (60% (v/v)), TFA (0,1% (v/v)) und CHCA (10 mg/ml) in Wasser. Die Proteinidentifizierung wurde mittels des „AP (atmospheric pressure)-MALDI/TRAP XCT™ von *Agilent Technologies* durchgeführt. Mit diesem Gerät ist es unter Einsatz einer Ionenfalle auch möglich, MS-MS-Spektren aufzunehmen. Die Auswertung erfolgte mit der Trap Software 4.2 SR1 Data Analysis v2.2 (Bruker Daltonik GmbH, Leipzig, BRD). Mit den erhaltenen Daten wurde dann zur Zuordnung von Peptiden eine Datenbanksuche mit MASCOT (www.matrixscience.com, (Perkins et al., 1999) durchgeführt.

2.5.7.2 Untersuchung von Modifizierungen

Die Untersuchungen zu posttranskriptionalen Modifizierungen erfolgten nach tryptischer In-Gel-Spaltung der Monomere mittels MALDI-TOF-TOF (MS/MS) Analysen mit dem 4700

COR-AAD1-00003609
Bayer EX1008 (Part 7 of 9)

Proteomics Analyzer (Applied Biosystems) und ESI-qQ-TOF (MS/MS)-Analysen am Gerät QStar Pulsar von PE Sciex (Applied Biosystems).

2.5.8 Internet-Links

http://www.expasy.org/cgi-bin/protparam	Ermittlung physikochemischer Eigenschaften aus der Primärstruktur
http://prodes.toulouse.inra.fr/multalin/multalin.html	Alignment von Primärstrukturen auf der Basis von Aminosäure-Ähnlichkeiten
http://i.moltalk.org/	Alignment von Primärstrukturen auf der Basis bekannter Sekundärstrukturen
http://www.ncbi.nlm.nih.gov/BLAST/	Datenbank zur Suche nach Sequenzhomologien zu bekannten Proteinen und Genen
http://www.matrixscience.com/search_form_select.html	Datenbank zur Suche nach bekannten Peptidmassen-Fingerprints von Proteinen und MS/MS-Ionen

2.6 Enzymkinetische Untersuchungen

2.6.1 Bestimmung der Phenoxyalkanoat-Spaltungsaktivität

Der Enzymtest umfasst zwei Schritte, erstens die Spaltungsreaktion und zweitens die Indikatorreaktion. Bei der Spaltung läuft folgende Reaktion ab:

2,4-DP + α-Ketoglutarat + O_2 ⟶ DCP + CO_2 + Succinat + Pyruvat

In der Indikatorreaktion wird das entstandene DCP durch die Reduktion von 4-Aminoantipyrin (Emerson, 1943 und 1948) im Alkalischen und der daraus folgenden Bildung eines roten Antipyrin-Farbstoffes nachgewiesen. Die Aktivität des Enzyms wurde mit dem Spektrophotometer (U-2000 Spektrophotometer, Hitachi Ltd., Tokyo, Japan) durch Messung der 4-Aminoantipyrin-Reduktion bei einer Wellenlänge von λ = 510 nm bestimmt (Fukumori und Hausinger, 1993b).

Inkubationsansatz (IKA):

10 mM Imidazol/ HCl (pH 6,0)
1 mM Substrat
1 mM α-Ketoglutarat
200 µM Ascorbinsäure
200 µM Ammoniumeisen-(II)-sulfat
x µl Enzymlösung

COR-AAD1-00003610
Bayer EX1008 (Part 7 of 9)

Die Inkubation erfolgte für 5 min bei 30°C (RdpA) oder bei 25°C (SdpA) unter ständigem Schütteln in einem Thermomixer (Thermomixer Comfort 5355, Eppendorf-Netheler-Hinz GmbH, Hamburg, BRD). Die Reaktion wurde durch Zugabe von 50 µl 20 mM EDTA-Lösung abgestoppt. Die Farbreaktion erfolgte im Testansatz nach der Modifikation von Fukumori und Hausinger (1993a).

Testansatz:
1 ml IKA
100 µl Borsäure-KCl-NaOH-Puffer (pH10)
10 µl 2%iges 4-Aminoantipyrin
10 µl 8%iges Kaliumhexacyanoferrat-(III)

Nach 5 min Reaktion wurde die Extinktion bei λ = 510 nm (U-2000 Spektrophotometer, Hitachi Ltd., Tokyo, Japan) bestimmt.

Zur Ermittlung kinetischer Daten wurde der zeitliche Verlauf der Produktbildung durch das Abstoppen von vier IKA innerhalb von zwei Minuten ermittelt. Es wurden Enzymaktivitäten zwischen 2 und 5 mU eingesetzt. Die Enzymkonzentration wurde so gewählt, dass die ermittelten Umsatzraten zwischen 1 und 14 nmol/min lagen. In diesem Geschwindigkeitsbereich und dem Zeitfenster von zwei Minuten konnte eine *steady state*-Kinetik gewährleistet werden. Es wurden lineare Kurvenzüge mit einem $R^2 \geq 0{,}99$ erhalten.

2.6.2 Ermittlung der Extinktionskoeffizienten von DCP und MCP

Die Ermittlung der Extinktionskoeffizienten erfolgte durch die Variation der DCP- und MCP-Konzentrationen im Inkubationsansatz der Enzymbestimmungsmethode. Dieser enthielt bis auf das Enzym alle Komponenten des Inkubationsansatzes (siehe 2.6.1). Die Extinktion wurde bei 510 nm gemessen und der Extinktionskoeffizient aus dem Anstieg der Geraden E_{510} = f(cDCP bzw. MCP) bestimmt.

2.6.3 Auswertung der ermittelten Daten

Die kinetische Auswertung erfolgte über die linearisierenden Verfahren nach Lineweaver und Burk, Hanes sowie Eadie und Hofstee. Da es bei diesen Verfahren zu einer Messfehlerverzerrung kommt, wurden die Messwerte nach folgenden Kriterien gewichtet:

Lineweaver-Burk:	$x_i = 1/c_{Substrat_i}$	$y_i = 1/v_i$	$w_i = v_i^4$
Hanes:	$x_i = c_{Substrat_i}$	$y_i = c_{Substrat}/v_i$	$w_i = v_i^4/c_{Substrat}^2$
Eadie-Hofstee :	$x_i = v_i/c_{Substrat_i}$	$y_i = v_i$	$w_i = v_i^4 + c_{Substrat}^2$

COR-AAD1-00003611
Bayer EX1008 (Part 7 of 9)

$$Anstieg = \frac{\sum(w_i x_i y_i) * \sum w_i - \sum(w_i y_i) * \sum(w_i x_i)}{\sum(w_i x_i^2) * \sum w_i - (\sum w_i x_i)^2}$$

Gleichung 2: Gleichung zur Berechnung des gewichteten Anstiegs der Regressionsgeraden

$$Abschnitt = \frac{\sum(w_i y_i)}{\sum w_i} - Anstieg * \frac{\sum(w_i x_i)}{\sum w_i}$$

Gleichung 3: Gleichung zur Berechnung des gewichteten Abschnitts der Regressionsgeraden

Ebenfalls wurde eine Auswertung der Daten über nichtlineare Regression durchgeführt. Dabei wurden die Messwerte mit Hilfe von SigmaPlot 8 zum einen in die Michaelis-Menten-Gleichung (4) und zum anderen in die Hill-Gleichung (5) gefittet.

a) $$v = \frac{v_{max} * [S]}{K_M + [S]}$$ b) $$v = \frac{v_{max} * [S]}{K_M + \left(1 + \frac{[S]}{K_i}\right) * [S]}$$

Gleichung 4: Michaelis-Menten-Gleichung a) ohne und b) mit Substratüberschusshemmung

a) $$v = \frac{v_{max} * [S]^n}{K_M + [S]^n}$$ b) $$v = \frac{v_{max} * [S]^n}{K_M + \left(1 + \frac{[S]}{K_i}\right) * [S]^n}$$

Gleichung 5: Hill-Gleichung a) ohne und b) mit Substratüberschusshemmung

2.7 Gentechnische Arbeiten

2.7.1 Nährmedien für gentechnische Arbeiten

- **LB-Medium**: 5 g/l Hefeextrakt; 10 g/l Trypton; 5 g/l NaCl; pH auf 7,0 einstellen
- **Selektivagar**: LB-Medium; 15 g/l Agar; 0,1 g/l Ampicillin; 0,004% X-Gal in DMF; 0,2 g/l IPTG
- **SOC-Medium**: 5 g/l Hefeextrakt; 20 g/l Trypton; 0,6 g/l NaCl; 0,2 g/l KCl; 0,203 g/l $MgCl_2 \cdot 6\ H_2O$; 0,246 g/l $MgSO_4 \cdot 7\ H_2O$; 0,02 M Glucose; pH auf 7,0 einstellen

2.7.2 Isolation von Nukleinsäuren

2.7.2.1 Präparation von genomischer DNA

Die genomische DNA von Bakterien wurde durch Hitze-Desintegration der Zellen erhalten. Dazu wurden die Zellen in sterilem Wasser suspendiert und 10 min in einem 100°C Wasserbad belassen. Die Zellfragmente wurden abzentrifugiert (15 min, 15000×g, 4°C). Im Überstand ist sowohl die genomische als auch die plasmidale DNA enthalten.

COR-AAD1-00003612
Bayer EX1008 (Part 7 of 9)

2.7.2.2 Präparation von plasmidaler DNA

Zur Isolation der Plasmide wurden das Invisorb® Spin Plasmid Mini Kit (Invitek GmbH, Berlin) und das Quiagen Midi-Präparation Kit (Qiagen, Hilden) eingesetzt. Die Präparation erfolgte entsprechend den Angaben des Herstellers.

2.7.3 Ableitung von Primern für die Gene *rdpA*$_{MC1}$ und *sdpA*$_{MC1}$

Die spezifischen Primerpaare für die Gene *sdpA* und *rdpA* wurden aus ihren Nukleinsäure-Sequenzen (Schleinitz et al., 2004) abgeleitet. Die Primerpaare wurden so generiert, dass die kompletten Gene amplifiziert werden. Gleichzeitig wurden den Primern Sequenzen für die Schnittstellen der Restriktionsendonukleasen *Eco*31I (GGTCTC) und *Bpi*I (GAAGAC) zugefügt. Die verwendeten Primer sind in Tabelle 10 dargestellt.

Tabelle 10: Primersequenzen der Gene *rdpA*$_{MC1}$ und *sdpA*$_{MC1}$

Primer-Bezeichnung	Sequenz
IBA7Rf, rdpA forward	5´-ATGGTAGGTCTCAGCGCATGCATGCTGCACTGTCCCCC-3´
IBA7Rr, rdpA reverse	5´-ATGGTAGGTCTCATATCAGCGCGCCGGGCGCACGCC-3´
IBA7Sf, sdpA forward	5´-ATGGTAGAAGACAAGCGCATGCAGACGACGCTGCAGATC-3´
IBA7Sr, sdpA reverse	5´-ATGGTAGAAGACAATATCACACCAGGGCGGCGCCCTCG-3´

Die über die Primer eingeführten Erkennungsstellen für die Restriktionsendonukleasen Eco31I bzw. BpiI sind markiert.

2.7.4 PCR-Reaktion zur Amplifizierung der *rdpA*$_{MC1}$- und *sdpA*$_{MC1}$-Gene

Die Gene *rdpA*$_{MC1}$ und *sdpA*$_{MC1}$ wurden mit speziellen Primern (siehe 2.7.3) durch PCR aus dem Genom von *Delftia acidovorans* MC1 amplifiziert. Um eine geringe Fehlerrate bei der DNA-Synthese zu gewährleisten und eine TA-Klonierung der Produkte zu ermöglichten, wurden das *Expand Long Template* PCR-System (Roche Diagnostics GmbH, Mannheim) mit einer *Proof-reading*-DNA-Polymerase eingesetzt.

Die PCR-Reaktion wurde im 20 µl-Ansatz mit dem Multicycler PTC-200 (Biozym Diagnostik GmbH, Hess. Oldendorf) durchgeführt. Als *template* wurde 4 µl genomische oder plasmidale DNA, je 10 pmol Primer, 0,175 µM dNTP-Mix, 1 U Polymerase in 1×PCR-Puffer eingesetzt. Die PCR wurde unter den in Tabelle 11 spezifizierten Bedingungen durchgeführt.

Tabelle 11: PCR-Programm zur Amplifizierung der Gene *rdpA*$_{MC1}$ und *sdpA*$_{MC1}$, es wurden 14 Zyklen unter Nutzung des Programmschrittes Elongation 1 und 16 Zyklen unter Verwendung von Elongation 2 durchgeführt

Programmschritt	Temperatur	Zeit
Denaturierung	96°C	3 min
Denaturierung	94°C	10 s
Anlagerung der Primer	55°C	30 s
Elongation 1	68°C	45 s
Elongation 2	68°C	45 s + 5 s/Zyklus

COR-AAD1-00003613
Bayer EX1008 (Part 7 of 9)

Die Kontrolle der PCR-Amplifikate erfolgte durch elektrophoretische Auftrennung im Agarosegel (1,5% in TAE: 0,02 M TrisBase, 0,01 M Eisessig, 0,5 mM EDTA) bei einer Spannung von 100 V.

2.7.5 Ligation der Gene *rdpA*$_{MC1}$ und *sdpA*$_{MC1}$ mit dem pGEMT-Vektor

Die erhaltenen PCR-Produkte wurden direkt unter Nutzung der überhängenden 3´-A-Enden mit dem pGEMT®-Vektor-System (Promega, Madison, USA) entsprechend den Angaben des Herstellers kloniert. Die Ligation von Vektor- und Insert-DNA erfolgte bei 14°C über Nacht in einem 10 µl Ansatz. Der Ansatz enthielt Insert-DNA und Vektor-DNA im Verhältnis 1:2, sowie 1 U T4-DNA-Ligase (New England Biolabs GmbH, Schwalbach) in 1×Ligasepuffer.

2.7.6 Ligation der Gene *rdpA*$_{MC1}$ und *sdpA*$_{MC1}$ mit dem pASK-IBA7-Vektor

Zur Expression der Gene wurde das Plasmid pASK-IBA7 (IBA GmbH, Göttingen) benutzt. In diesem Vektor stehen die Gene unter Kontrolle des starken *tetA*-Promotors (Skerra, 1994), der eine effizient regulierbare Expression durch Induktion mittels Anhydrotetracyclin ermöglicht. Durch die Verwendung von pASK-IBA7 wird eine Strep-tag(II)-Sequenz, welche durch die Spaltung mit der Protease Faktor Xa nach Reinigung des Proteins wieder entfernt werden kann, N-terminal an das Protein synthetisiert.

Die Ligation erfolgte mit dem *Eco*31I-geschnittenen Vektor pASK-IBA7 und dem mittels *Bpi*I aus dem Vektor pGEMT geschnittenen Gen nach der Vorschrift siehe 2.7.5.

2.7.7 Übertragung der DNA durch Transformation

2.7.7.1 Transformation

Zur Transformation wurden 100 µl einer Suspension des Stammes *E. coli* (Top10F-Zellen, Quiagen) mit 2 µl der ligierten Plasmid-DNA (siehe 2.7.6) vermischt. Die Probe wurde 30 min auf Eis gelagert, der Hitzeschock zur Aufnahme der DNA erfolgte für 2 min bei 42°C. Im Anschluss wurden die Zellen zur Ausprägung der vektorcodierten Antibiotika-Resistenz 60 min bei 37°C in LB-Medium inkubiert, bevor sie auf Selektivagar ausplattiert und über Nacht bei 37°C inkubiert wurden.

2.7.7.2 Elektrotransformation

Die Elektroporation wurde mit dem Easyject Plus Elektroporator (peqlab Biotechnologie GmbH, Erlangen) durchgeführt. Die Anwendung erfolgte entsprechend den Informationen des Herstellers. Es wurde der Stamm Rosetta™(DE3)pLysS (Novagene, Madison, USA) verwendet.

COR-AAD1-00003614
Bayer EX1008 (Part 7 of 9)

Die zur Elektroporation eingesetzte ligierte DNA wurde zunächst nach Marusyk und Sergeant (1980) über Mikrodialyse entsalzt, die Herstellung elektrokompetenter Zellen erfolgte nach Nickoloff (1995).

Für die Elektroporation wurden 40 µl der elektrokompetenten Zellen und 1 µl DNA eingesetzt. Die Elektroporation erfolgte in einer 2 mm-Küvette (peqlab Biotechnologie GmbH) entsprechend dem Elektroporationsbericht (Eurogentec, 1995) bei einer Spannung von 2500 V, einer Kapazität von 40 µF, einem Widerstand von 125 Ω und einem Impuls von 5 ms. Sofort nach der Transformation erfolgte die Zugabe von 1 ml SOC-Medium (2.7.1) zur Suspension. Danach wurde das Zellmaterial für 60 min bei 37°C unter Schütteln inkubiert.

2.7.8 Selektion rekombinanter Klone

Nach der Transformation wurden die Zellen auf Selektivagar ausplattiert und über Nacht bei 37°C inkubiert. Die rekombinanten Klone wurden über blau/weiß-Selektion erfasst.

2.7.9 DNA-Sequenzierung

Die Kontroll-Sequenzierung erfolgte nach Sanger et al. (1977) und wurde unter Verwendung des *ABI Prism BigDye™ Terminator Cycle Sequencing Ready reaction Kits* (PE Applied Biosystems) durchgeführt.

Tabelle 12: PCR-Programm (25 Zyklen) und Primersequenzen zur Sequenzierung

Programmschritt	Temperatur	Zeit
Denaturierung	96 °C	30 s
Anlagerung der Primer	55 °C	15 s
Elongation	60 °C	4 min
Primer	**Sequenz**	
M13 *forward*	5´-GACCGGCAGCAAAAT-3´	
M13 *reverse*	5´-GTCCTTTGTCGATACTG-3´	

Die Sequenzierungsreaktion erfolgte in einem 10 µl-Ansatz, der 2 µl *BigDye™ Terminator Ready Reaction Mix* (PE Applied Biosystems), 4 µl denaturierte DNA (5 min bei 98°C), 10 pmol Primer, 2 µl 5×Puffer und 1 µl DMSO enthielt. Die Reaktion erfolgte im Multicycler PTC 200 (Biozym Diagnostik GmbH) nach dem in Tabelle 12 aufgeführten Programm.

2.8 Analytik

2.8.1 Bestimmung der Proteinkonzentration

Die Proteinbestimmung erfolgte nach Bradford (1976) anhand einer Eichkurve mit Rinderserumalbumin als Referenzprotein. Die Proben wurden entsprechend mit Wasser verdünnt und dann im Verhältnis 1:10 mit Bradfordreagenz versetzt. Nach genau 5 min Inkubation wurde die E_{595} gemessen und anhand der Eichkurve die Proteinkonzentration errechnet.

COR-AAD1-00003615
Bayer EX1008 (Part 7 of 9)

2.8.2 Bestimmung der Phenoxyalkanoat-Konzentration

Die Phenoxyalkanoate wurden mit HPLC-Analyse detektiert und mit Hilfe eines Standards quantifiziert. Dazu wurden 20 µl der zu analysierenden Lösung an einer Nucleosil-100-C18-Chromatographie-Säule (250 mm × 4 mm, 5 µm Korngröße (Knauer-Säulentechnik, Berlin, BRD)) aufgetrennt. Als Laufpuffer wurde ein 40% (v/v) Acetonitril enthaltender Phosphatpuffer (131,5 mM, pH 2,8) verwendet, mit dem die Probe mit einer Flussrate von 1 ml/min kontinuierlich eluiert wurde. Detektiert wurden die Phenoxyalkansäuren bei λ = 283 nm mit einem Diodenarray-Detektor (Shimadzu, Duisburg, BRD).

2.8.3 Bestimmung der α-Ketoglutarat-Konzentration

Die α-Ketoglutaratkonzentration wurde in einer proteinfreien Lösung mittels Ionenchromatograph (DX-100) unter Verwendung der Supressor-Technik bestimmt. Die Ionen wurden am Anionenaustauscher IonPacAS14 (Dionex) getrennt. Als Laufpuffer diente Na_2CO_3/$NaHCO_3$-Puffer (5,2 mM, pH10), die Laufgeschwindigkeit betrug 2,5 ml/min. Die Ionen wurden anhand ihrer Leitfähigkeit detektiert.

2.8.4 Bestimmung der optischen Dichte

Die optische Dichte (OD_{700}) der Zellsuspension wurde am Spektrometer (U-2000 Spektrometer, Hitachi Ltd., Tokyo, Japan) bei einer Wellenlänge von λ = 700 nm gemessen. Die Biomasse wurde nach folgender Formel berechnet: $Biomasse(g/l) \approx \frac{OD_{700}}{2}$.

Diese Gleichung gilt dabei nur für die Vorraussetzung, dass $OD_{700} \leq 0{,}3$. Bei Bedarf wurde die Zellsuspension entsprechend mit Wasser verdünnt.

2.8.5 Bestimmung von Leitfähigkeit, Sauerstoffkonzentration und pH-Wert

Die Leitfähigkeit von Lösungen wurde mit Hilfe des Leitfähigkeitsmessgerätes LF 96 (WTW Microprocessor Conductivity Meter LF 96, 82362 Weilheim) gemessen. Anhand von Eichkurven konnte dann die Salzkonzentration in den wässrigen Lösungen ermittelt werden.

Die Sauerstoffkonzentration wurde mit dem Messgerät Multi line P4 mit der Elektrode Oxi-Cal®-SL (WTW, 82362 Weilheim) bestimmt.

Mittels des pH-Meters 765 Calimatic Knick (WTW, 82362 Weilheim) wurden die Protonenkonzentrationen in den Puffern eingestellt.

COR-AAD1-00003616
Bayer EX1008 (Part 7 of 9)

3 Ergebnisse

3.1 Enzymreinigung

3.1.1 Reinigung der Phenoxyalkanoat-spaltenden Enzyme aus *Delftia acidovorans* MC1

3.1.1.1 Säulenchromatographische Enzymreinigung

Vor dem Einsatz der chromatographischen Trennmethoden wurden die Nukleinsäuren mittels 0,15%ger Protaminsulfat-Fällung aus dem Rohextrakt entfernt. Anschließend konnte mit einer Ammoniumsulfat-Fällung ein Anreicherungsfaktor von 1,5 für die Herbizidspaltsaktivität erreicht werden. Dabei präzipitierten die Enzyme für die Spaltung von (R,S)-DP, (R,S)-MCPP und 2,4-D in dem Konzentrationsbereich zwischen 1,0 und 2,5 M Ammoniumsulfat fast vollständig (Tabelle 13). Die Auftrennung des aus der Ammoniumsulfat-Fällung resultierenden Proteingemisches am Anionenaustauscher *Source30Q* führte zum Vorliegen von zwei Phenoxyalkanoat-spaltenden Fraktionen mit enantioselektiven Eigenschaften bezüglich der Phenoxypropionate (Abbildung 2).

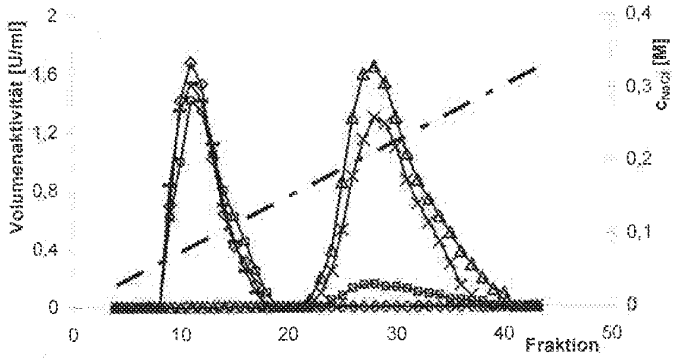


Abbildung 2: Elutionsprofil der Phenoxyalkanoat-spaltenden Enzyme aus *Delftia acidovorans* MC1 an *Source30Q*. (S)-DP (◊), (S)-MCPP (—), 2,4-D (□), (R)-DP (Δ), (R)-MCPP (x), NaCl (gestrichelt)

Die Proteinfraktion, die bei 0,1 M NaCl von der Säule eluiert ($SdpA_{MC1}$), enthält die Spaltungsaktivität für die (S)-Enantiomeren der Phenoxypropionate sowie etwa 90% der 2,4-D-Spaltungsaktivität. Bei einer Salzkonzentration von 0,2 M NaCl wird die zweite Enzymfraktion ($RdpA_{MC1}$) von der Säule gewaschen. Sie enthält das Enzym zur Metabolisierung der (R)-Enantiomeren der Phenoxypropionate und daneben noch etwa 10% der Spaltungsaktivität für 2,4-D. An dem Ionenaustauscher *Source30Q* konnte eine Anreicherung von rund 2,5 für die Spaltungsaktivitäten des $RdpA_{MC1}$ und von 7,5 für das $SdpA_{MC1}$ erreicht werden. Bei diesem Reinigungsschritt gingen 40% bzw. 45% der Enzymaktivitäten verloren.

COR-AAD1-00003617
Bayer EX1008 (Part 7 of 9)

Mittels hydrophober Chromatographie an Butyl-Sepharose konnte das Enzym $SdpA_{MCI}$ (Elution zwischen 0,43 und 0,38 M $(NH_4)_2SO_4$; Abbildung 3A) auf das 38-fache und das Enzym $RdpA_{MCI}$ (Elution zwischen 0,85 und 0,8 M $(NH_4)_2SO_4$, Abbildung 3B) auf das 5,6-fache der ursprünglichen spezifischen Aktivität angereichert werden. Die Enzymausbeute lag für beide Dioxygenasen bei 40% (Tabelle 13).

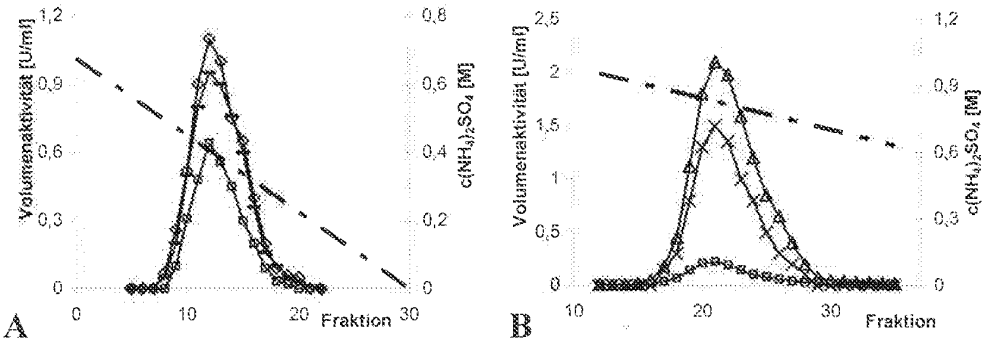


Abbildung 3: Elutionsprofil des $SdpA_{MCI}$ (A) und $RdpA_{MCI}$ (B) an Butyl-Sepharose (S)-DP (◊), (S)-MCPP (—), 2,4-D (□), (R)-DP (Δ), (R)-MCPP (x), $(NH_4)_2SO_4$ (gestrichelt)

Im Anschluss an die hydrophobe Chromatographie wurde das $RdpA_{MCI}$ mittels Größenausschluss-Chromatographie entsalzt und an dem Anionenaustauscher *PBE94* gereinigt. Bei diesem Reinigungsschritt konnte nochmals eine Anreicherung des Enzyms um den Faktor 2 erreicht werden. Enzymaktivität ging nicht verloren.

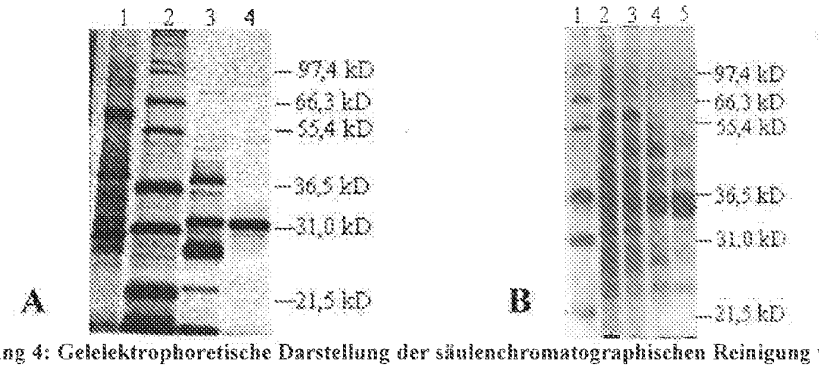


Abbildung 4: Gelelektrophoretische Darstellung der säulenchromatographischen Reinigung von $SdpA_{MCI}$ und $RdpA_{MCI}$. A: $SdpA_{MCI}$ 1: Rohextrakt, 2: Standard, 3: IEX (*Source30Q*), 4: HIC, **B: $RdpA_{MCI}$** 1: Standard, 2: Rohextrakt, 3: IEX (*Source30Q*), 4: HIC, 5: IEX (*PBE94*)

In Abbildungen 4A+B sind die Anreicherungen der Dioxygenasen anhand der Auftrennung der Präparate im Acrylamidgel dargestellt. Es ist deutlich zu erkennen, dass das $SdpA_{MCI}$ nach der hydrophoben Chromatographie nahezu 100%ig rein ist. Für das $RdpA_{MCI}$ konnte nach der Anionenaustausch-Chromatographie an *PBE94* eine ausreichende Reinheit erzielt werden.

COR-AAD1-00003618
Bayer EX1008 (Part 7 of 9)

Tabelle 13: Dokumentation der Reinigung des $SdpA_{MC1}$ und $RdpA_{MC1}$ aus *Delftia acidovorans* MC1, die Ermittlung der spezifischen Aktivitäten erfolgte unter Einsatz von 1 mM (R)-DP, (R)-MCPP, MCPA bzw. 2,4-D oder 0,5 mM (S)-DP bzw. (S)-MCPP

Reinigungsschritt	Substrat	rel. Protein-gehalt [%]	spez. Aktivität [U/mg]	Gesamtaktivität [U]	Anreicherung [-fach]	Ausbeute [%]
Rohextrakt	*(R)-DP*	100	0,238	156	1	100
	(R)-MCPP		0,166	109	1	100
	2,4-D		0,09	59	1	100
	MCPA		0,128	83	1	100
	(S)-DP		0,158	103	1	100
	(S)-MCPP		0,129	85	1	100
Ammoniumsulfat-Fällung	*(R)-DP*	88	0,347	151	1,5	97
	2,4-D		0,133	57	1,5	97
	(S)-DP		0,221	100	1,4	97
IEX $RdpA_{MC1}$ (*Source30Q*)	*(R)-DP*	24	0,584	91	2,5	58
	2,4-D		0,067	10	0,7	18
	(S)-DP		-	-	-	-
HIC $RdpA_{MC1}$	*(R)-DP*	8	1,333	67	5,6	43
	2,4-D		0,072	2	0,8	4
	(S)-DP		-	-	-	-
IEX $RdpA_{MC1}$ (*PBE94*)	*(R)-DP*	3	2,803	62,4	11,8	40
	2,4-D		0,421	1,8	4,7	3
	(S)-DP		-	-	-	-
IEX $SdpA_{MC1}$ (*Source30Q*)	*(R)-DP*	6	-	-	-	-
	2,4-D		0,586	24	6,5	41
	(S)-DP		1,169	48	7,4	46
HIC $SdpA_{MC1}$	*(R)-DP*	1	-	-	-	-
	2,4-D		2,76	17	31	28
	(S)-DP		6,064	41	39	40

3.1.1.2 Gelelektrophoretische Trennung von Enzymformen

3.1.1.2.1 Separation der $SdpA_{MC1}$-Enzymformen

Durch die säulenchromatographische Reinigung des $SdpA_{MC1}$ erhält man bei hoher Anreicherung ein offensichtlich reines Präparat (Abbildung 4A). Ergebnisse aus weiteren analytischen Verfahren (2D-, native Gelelektrophorese) zeigen aber, dass eine Auftrennung in multiple Enzymformen möglich ist. So konnten im $SdpA_{MC1}$-Präparat nach HIC bis zu drei Formen der (S)-spezifischen Dioxygenase nachgewiesen werden (Abbildung 6A). Zwei der drei Enzymformen konnten mit Hilfe der präparativen Gelelektrophorese voneinander separiert werden. In Abbildung 5 ist die Elution sowohl des Proteins als auch der Enzymaktivität zu sehen. Man kann deutlich die Auftrennung des HIC-Präparates in einen Proteinpeak mit Ausbildung einer Schulter erkennen. Nach Analyse der gesammelten Fraktionen im analytischen nativen Gel wurden die Fraktionen so vereinigt, dass zwei Präparate, in denen jeweils eines der nativen Proteine stark angereichert vorliegt, gewonnen wurden (Abbildung 6A). Unter denaturieren-

COR-AAD1-00003619
Bayer EX1008 (Part 7 of 9)

den Bedingungen erscheinen beide Präparate wieder als homogene Proteinbande bei 32 kD (Abbildung 6B).

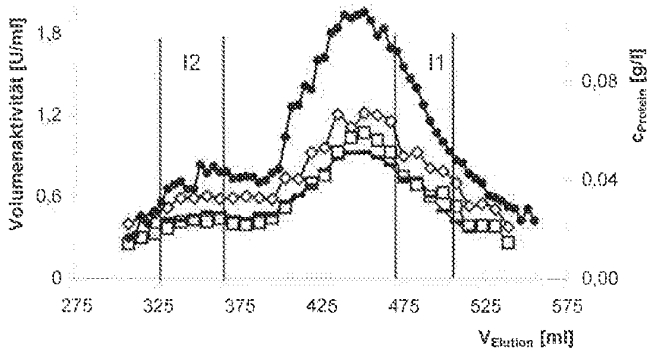


Abbildung 5: Elutionsprofil der $SdpA_{MCI}$-Enzymformen aus dem präparativen Gel (S)-DP (◊), (S)-MCPP (--), 2,4-D multipliziert mit 2 (□), Protein (●), die Bereiche I1 und I2 kennzeichnen die vereinigten Fraktionen

Nach diesem Reinigungsschritt konnten nur noch 50% des eingesetzten Proteins wiedergefunden werden, von dem etwa 18% der gereinigten Enzymform $SdpA_{MCI}$-I2 und 35% der gereinigten Enzymform $SdpA_{MCI}$-I1 zugeordnet werden konnten. Damit liegt das Verhältnis von I2 zu I1 bei etwa 1:2. Von der Gesamtenzymaktivität konnten ebenfalls nur 50% wiedergefunden werden (Tabelle 14).

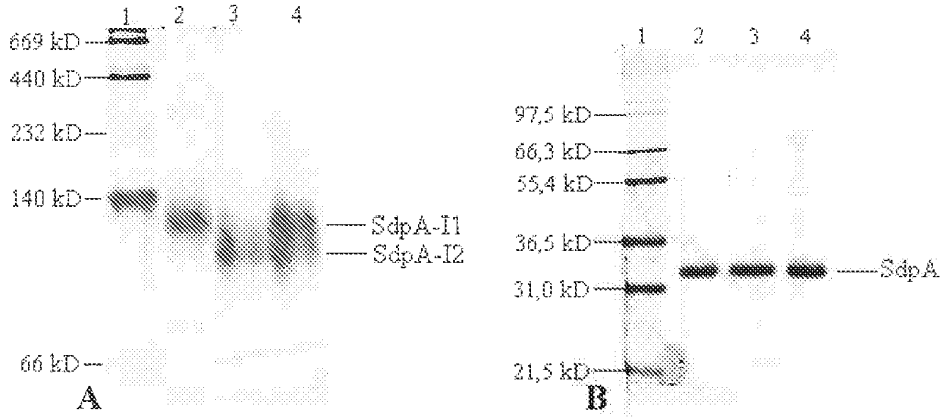


Abbildung 6: Kontrollgele der Separation der $SdpA_{MCI}$-Enzymformen A: nativ 1: Standard, 2: $SdpA_{MCI}$-I2, 3: $SdpA_{MCI}$-I1, 4: $SdpA_{MCI}$ (HIC), **B: denaturierend** 1: Standard, 2: $SdpA_{MCI}$-I1, 3: $SdpA_{MCI}$-I2, 4: $SdpA_{MCI}$ (HIC)

Dabei ist die Spaltungsaktivität für die untersuchten Herbizide gleichermaßen verloren gegangen. Eine weitere Anreicherung der Enzymaktivität war durch diesen Reinigungsschritt nicht mehr möglich. Die gereinigten Präparate wurden im Folgenden sowohl kinetisch als auch proteinbiochemisch charakterisiert.

COR-AAD1-00003620
Bayer EX1008 (Part 7 of 9)

Tabelle 14: Reinigungsprotokoll der $SdpA_{MC1}$-Enzymformen an der präparativen Elektrophorese, die Ermittlung der spezifischen Aktivitäten erfolgte unter Einsatz von 1 mM MCPA bzw. 2,4-D oder 0,5 mM (S)-DP bzw. (S)-MCPP

Enzympräparat	Herbizid	Spezifische Aktivität [U/mg]	Anreicherung [fach]	Gesamtaktivität [%]
		HIC		
$SdpA_{MC1}$	*(S)-DP*	7,96	1	100
	(S)-MCPP	7,13	1	100
	2,4-D	4,45	1	100
	MCPA	6,81	1	100
		Präparative Elektrophorese		
$SdpA_{MC1}$-I1	*(S)-DP*	10,76	1,35	15,7
	(S)-MCPP	9,85	1,38	13,5
	2,4-D	4,49	1,01	14,6
	MCPA	8,04	1,18	14,3
$SdpA_{MC1}$-I2	*(S)-DP*	6,60	0,83	7,4
	(S)-MCPP	6,61	0,93	5,0
	2,4-D	3,93	0,88	7,7
	MCPA	5,99	0,88	7,9

3.1.1.2.2 Separation der $RdpA_{MC1}$-Enzymformen

Nach der klassischen Reinigung des $RdpA_{MC1}$ mittels säulenchromatographischer Techniken erhält man ein Enzympräparat, welches drei native Enzymformen der Dioxygenase enthält (Abbildung 8A). Wie beim $SdpA_{MC1}$ wurde versucht, diese Enzymformen mittels präparativer Elektrophorese voneinander zu trennen. Abbildung 7 zeigt das Elutionsprofil der Enzymaktivität und des Proteins aus dem Acrylamidgel.

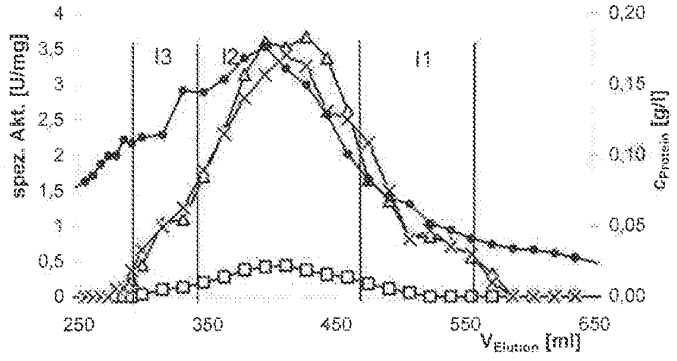


Abbildung 7: Elutionsprofil der $RdpA_{MC1}$-Enzymformen aus dem präparativen Gel (R)-DP (Δ), (R)-MCPP (x), 2,4-D (□), Protein (●), die Bereich I1, I2 und I3 markieren die vereinigten Fraktionen

Es ist ein mehrphasiger Verlauf in der Elution der Enzymaktivität zu erkennen, der als Anhaltspunkt für die Vereinigung der Fraktionen zur Gewinnung der einzelnen Enzymformen genutzt wurde. In Abbildung 8A sind die jeweiligen $RdpA_{MC1}$-Präparate, die unter nativen Bedingungen im Gel elektrophoretisch aufgetrennt wurden, zu sehen. Es wird deutlich, dass es gelungen ist, die Enzymformen $RdpA_{MC1}$-I1 und -I3 zumindest in angereicherter Form dar-

COR-AAD1-00003621
Bayer EX1008 (Part 7 of 9)

zustellen, denn es sind immer noch Anteile der Enzymform I2 in beiden Präparaten vorhanden. Bei der zweiten Proteinbande in der Spur 2 (Präparat $RdpA_{MC1}$-I3) handelt es sich um die 1,2-Catechol-Dioxygenase (Identifizierung mittels MS-Fingerprint), die unter den gewählten Bedingungen nicht quantitativ vom $RdpA_{MC1}$ zu trennen war. Ein Anreicherungspräparat $RdpA_{MC1}$-I2 konnte nicht gewonnen werden.

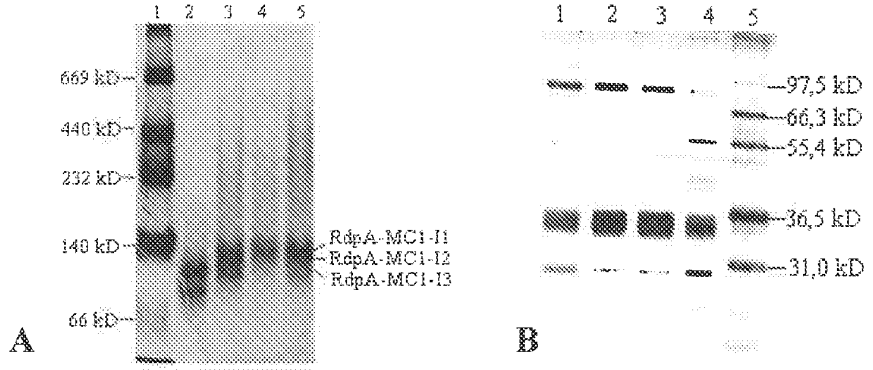


Abbildung 8: Gelelektrophoretische Auftrennung der RdpA-Enzymformen im Acrylamidgel A: native Bedingungen 1: Standard, 2: $RdpA_{MC1}$-I3, 3: $RdpA_{MC1}$-I2, 4: $RdpA_{MC1}$-I1, 5: $RdpA_{MC1}$-IEX (*PBE94*) **B: denaturierend** 1: $RdpA_{MC1}$-I3, 2: $RdpA_{MC1}$-I2, 3: $RdpA_{MC1}$-I1, 4: $RdpA_{MC1}$-IEX (*PBE94*), 5: Standard

Bei den $RdpA_{MC1}$-Präparaten handelt es sich nicht um reine Enzyme. Neben den verschiedenen Enzymformen sind noch weitere Fremdproteine in den Fraktionen enthalten, wie die Auftrennung im SDS-Gel (Abbildung 8B) zeigt. Die präparative Elektrophorese brachte keine weitere Anreicherung der RdpA-Spaltungsaktivitäten (Tabelle 15). Es konnten 69% der Enzymaktivität und des Proteins wiedergefunden werden, von denen 50% in den Präparaten $RdpA_{MC1}$-I1 und -I3 vereinigt wurden.

Tabelle 15: Reinigungsprotokoll der $RdpA_{MC1}$-Enzymformen an der präparativen Elektrophorese

Enzympräparat	Herbizid	Spezifische Aktivität [U/mg]	Anreicherung [-fach]	Gesamtaktivität [%]
		IEX (*PBE94*)		
$RdpA_{MC1}$	*(R)-DP*	2,80	1	100
	(R)-MCPP	2,02	1	100
	2,4-D	0,42	1	100
	MCPA	0,32	1	100
		Präparative Elektrophorese		
$RdpA_{MC1}$-I1	*(R)-DP*	2,99	1,01	21,4
	(R)-MCPP	1,345	0,67	14,2
	2,4-D	0,51	1,21	25,8
	MCPA	0,40	1,25	26,5
$RdpA_{MC1}$-I3	*(R)-DP*	2,09	0,75	9,1
	(R)-MCPP	1,54	0,77	9,3
	2,4-D	0,42	1	12,1
	MCPA	0,34	1,2	14,5

COR-AAD1-00003622
Bayer EX1008 (Part 7 of 9)

3.1.2 Reinigung der Phenoxypropionat-spaltenden Enzyme aus *Rhodoferax* sp. P230

Die Biomasse, die zur Gewinnung der Phenoxyalkanoat-spaltenden Enzyme aus *Rhodoferax* sp. P230 (P230) eingesetzt wurde, wurde durch Batch-Kultivierung erzeugt. Auf die Behandlung des Rohextraktes mit Protaminsulfat-Fällung sowie auf eine Ammoniumsulfat-Fällung wurde in diesem Fall verzichtet, da durch diese beiden Schritte bereits bis zu 60% der (S)-spezifischen Enzymaktivität verloren gehen (Ruhland, 2003).

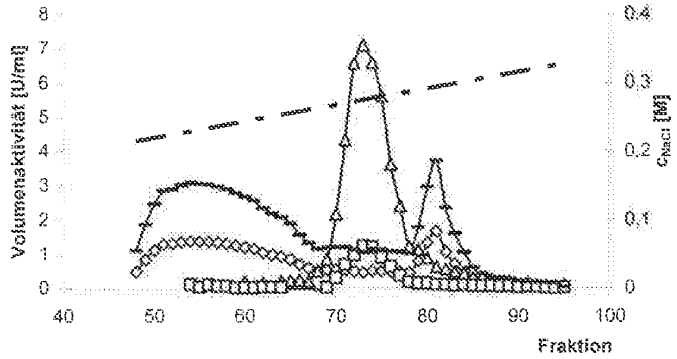


Abbildung 9: Elutionsprofil der Phenoxyalkanoat-spaltenden Enzyme aus P230 an *PBE94* (S)-DP*10 (◊), (S)-MCPP*10 (—), 2,4-D (□), (R)-DP (Δ), NaCl (gestrichelt)

Nach der Passage des Rohextraktes über den Ionenaustauscher *PBE94* lagen drei Phenoxyalkanoat-spaltende Fraktionen vor (Ruhland, 2003), eine mit hoher (R)-spezifischer Aktivität ($RdpA_{P230}$), die bei einer NaCl-Konzentration von 0,28 M von der Säule eluiert, und in der Lage ist, sowohl die (R)-Enantiomere der Phenoxypropionate, als auch die Phenoxyacetate zu spalten, und zwei Fraktionen mit (S)-spezifischer Aktivität, von denen eine bei 0,23 M ($SdpA_{P230}$-1) und die andere bei einer NaCl-Konzentration von 0,29 M ($SdpA_{P230}$-2) eluiert (Abbildung 9). Die (S)-spezifischen Fraktionen enthalten die Spaltungsaktivitäten für die (S)-Enantiomere der substituierten 2-Phenoxypropionate und, durch eine offensichtliche Überlagerung mit dem $RdpA_{P230}$ im Elutionsprofil, gewisse Anteile der Spaltungsaktivität für die Phenoxyacetate und (R)-Enantiomere der Phenoxypropionate (Tabelle 16, Abbildung 11A). Die Trennung der Proteine am Ionenaustauscher ging mit einem Verlust von (R)-spezifischer Spaltungsaktivität von etwa 20% und von (S)-spezifischer Spaltungsaktivität von 30% einher. Es konnte eine Anreicherung des $RdpA_{P230}$ um das 17-fache und der (S)-spezifischen Dioxygenasen um das 9-fache erreicht werden. Mit der sich anschließenden Reinigung an Butyl-Sepharose wurde eine weitere Anreicherung der Dioxygenasen aus P230 möglich. Das $RdpA_{P230}$ eluiert bei einer Salzkonzentration von 0,73 M Ammoniumsulfat.

COR-AAD1-00003623
Bayer EX1008 (Part 7 of 9)

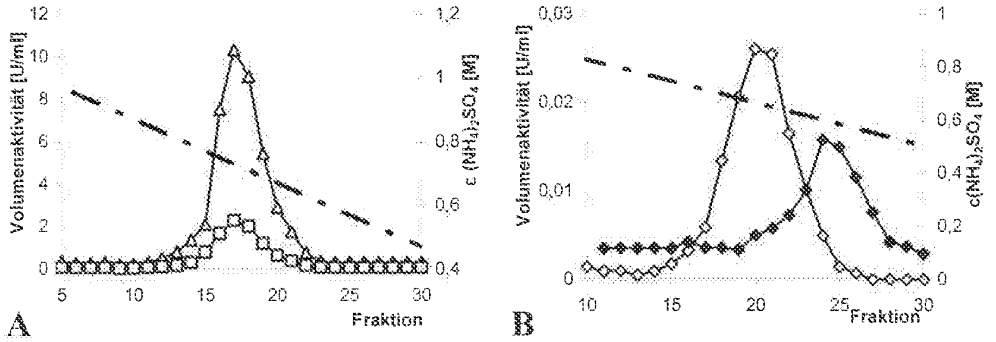


Abbildung 10: Elutionsprofile der Enzyme aus P230 an Butyl-Sepharose A: $RdpA_{P230}$, B: (S)-spezifische Enzyme, Substrat: (S)-DP 2,4-D (□), (R)-DP (Δ), $SdpA_{P230}$-1 (◊), $SdpA_{P230}$-2 (♦) $(NH_4)_2SO_4$ (gestrichelt)

Es wurde - bei einem Aktivitätsverlust von ca. 40% - auf das 50-fache der Aktivität des Rohextraktes angereichert. Von der (S)-spezifischen Spaltungsaktivität gehen an der hydrophoben Chromatographiesäule 83% der aufgetragenen Aktivität verloren. Dennoch ist bei diesem

Tabelle 16: Dokumentation der Reinigung der (S)- und (R)-spezifischen Dioxygenasen *aus Rhodoferax* sp. P230 Die Ermittlung der spezifischen Aktivitäten erfolgte unter Einsatz von 1 mM (R)-DP, (R)-MCPP, MCPA bzw. 2,4-D oder 0,5 mM (S)-DP bzw. (S)-MCPP

Reinigungsschritt	Substrat	rel. Proteingehalt [%]	spez. Aktivität [U/mg]	Gesamtaktivität [U]	Anreicherung [-fach]	Ausbeute [%]
Rohextrakt	*(R)-DP*	100	0,161	136,5	1	100
	(R)-MCPP		0,12	101,2	1	100
	2,4-D		0,034	31,5	1	100
	MCPA		0,036	33,4	1	100
	(S)-DP		0,03	21,2	1	100
	(S)-MCPP		0,05	41,5	1	100
IEX $RdpA_{P230}$ (*PBE94*)	*(R)-DP*	5	2,843	111,3	17,6	82
	2,4-D		0,6	23,4	16,1	75
	(S)-DP		0,027	1,1	1,1	5
HIC $RdpA_{P230}$	*(R)-DP*	1,2	8,369	82,5	52	60
	2,4-D		1,856	18,3	50	58
	(S)-DP		-	-	-	-
IEX $SdpA_{P230}$-1 (*PBE94*)	*(R)-DP*	5	-	-	-	-
	2,4-D		-	-	-	-
	(S)-DP		0,467	17,6	9,5	43
HIC $SdpA_{P230}$-1	*(R)-DP*	0,4	-	-	-	-
	2,4-D		-	-	-	-
	(S)-DP		0,463	1,6	18,5	8
IEX $SdpA_{P230}$-2 (*PBE94*)	*(R)-DP*	3	1,676	36	10,4	26
	2,4-D		0,339	7,3	9,1	23
	(S)-DP		0,252	5,4	10,1	26
HIC $SdpA_{P230}$-2	*(R)-DP*	0,3	-	-	-	-
	2,4-D		-	-	-	-
	(S)-DP		0,438	1	17,5	5

COR-AAD1-00003624
Bayer EX1008 (Part 7 of 9)

Schritt noch eine Anreicherung erreicht worden; das $SdpA_{P230}$-1 wurde auf das 19-fache und das $SdpA_{P230}$-2 auf das 25-fache des Rohextraktes angereichert. Die Enzympräparate enthalten in dieser Reinigungsstufe noch erhebliche Mengen Fremdprotein, dennoch wurden keine Reinigungsschritte durchgeführt, da ansonsten die Enzymausbeute für weiterführende Untersuchungen zu klein geworden wäre. Abbildung 11A und Tabelle 16 dokumentieren den Reinigungserfolg.

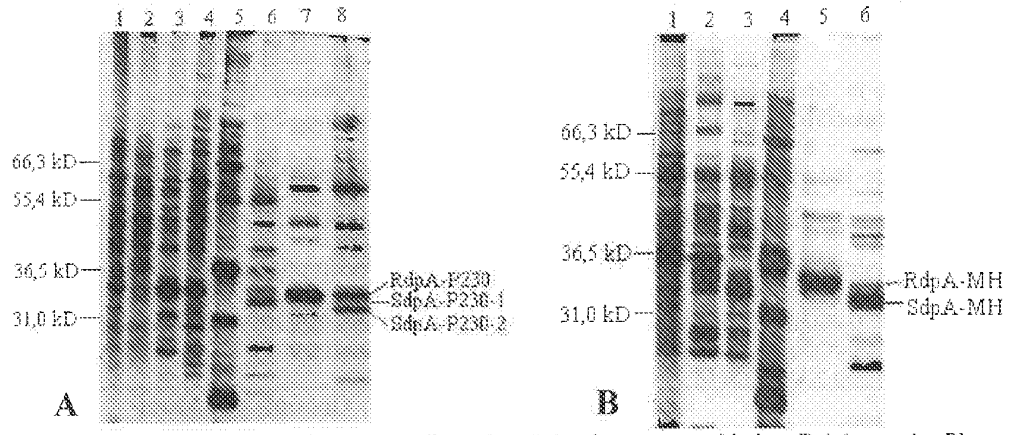


Abbildung 11: Gelelektrophoretische Darstellung der säulenchromatographischen Reinigung der Phenoxyalkanoat-spaltenden Enzyme aus A: P230 1: Rohextrakt, 2:IEX-$SdpA_{P230}$-1, 3: IEX-$RdpA_{P230}$, 4: IEX-$SdpA_{P230}$-2, 5 : Standard, 6: HIC-$SdpA_{P230}$-1, 7: HIC-$RdpA_{P230}$, 8: HIC-$SdpA_{P230}$-2 **B: MH (R,S)-DP-induziert** 1: Rohextrakt, 2: IEX-$RdpA_{MH}$, 3: IEX-$SdpA_{MH}$, 4: Standard, 5: HIC-$RdpA_{MH}$, 6: HIC-$SdpA_{MH}$

Aus P230 konnten drei Phenoxyalkanoat-spaltende Enzyme gereinigt werden, ein (R)-spezifisches Enzym mit Spaltungsaktivitäten für die (R)-Enantiomeren der Phenoxypropionate und für die Phenoxyacetate sowie zwei (S)-spezifische Enzyme, die jeweils nur die (S)-Enantiomere des Dichlorprop und Mecoprop spalten.

3.1.3 Reinigung der Phenoxyalkanoat-spaltenden Enzyme aus *Sphingobium herbicidovorans* MH

Biomasse von *Sphingobium herbicidovorans* MH (MH), die mit unterschiedlichen Herbiziden induziert wurde, zeigt beim Reinigungsschritt an *PBE94* unterschiedliche Elutionsprofile für die Phenoxyalkanoat-spaltenden Enzyme. Werden die Herbizid-spaltenden Enzyme nach Wachstum der MH-Zellen auf PYE (über Nacht) mit einem Gemisch aus (R,S)-DP/2,4-DB (5:1) induziert, so erhält man nach Auftrennung des Rohextraktes am Ionenaustauscher drei Proteinfraktionen, die sich durch unterschiedliche Substratverwertungsspektren auszeichnen (Abbildung 12A). Bei einer Salzkonzentration von 0,27 M NaCl eluiert zuerst eine Enzymfraktion vom Säulenmaterial, die sowohl die (S)-Enantiomere der 2-Phenoxypropionate, die

COR-AAD1-00003625
Bayer EX1008 (Part 7 of 9)

Phenoxyacetate, als auch die Phenoxybutyrate spaltet. Dieses Enzym wird vom zweiten Aktivitätspeak des Profils stark überlagert. Als zweites eluiert ein Enzym von der Säule (0,28 M NaCl), das neben den (R)-Enantiomeren der 2-Phenoxypropionate auch Phenoxyacetate als Substrate akzeptiert: das $RdpA_{MH}$. Nach dem $RdpA_{MH}$ eluiert (0,3 M NaCl) wiederum ein (S)-spezifisches Enzym ($SdpA_{MH}$), welches die Herbizide (S)-DP und (S)-MCPP, aber auch 2,4-D und MCPA spaltet. Phenoxybutyrat wird von diesem Enzym nicht umgesetzt.

Konfrontiert man die MH-Zellen nur mit dem Herbizid (R,S)-DP, so können am Ionenaustauscher nur noch zwei Proteinspezies separiert werden. Die Proteinfraktion, welche unter

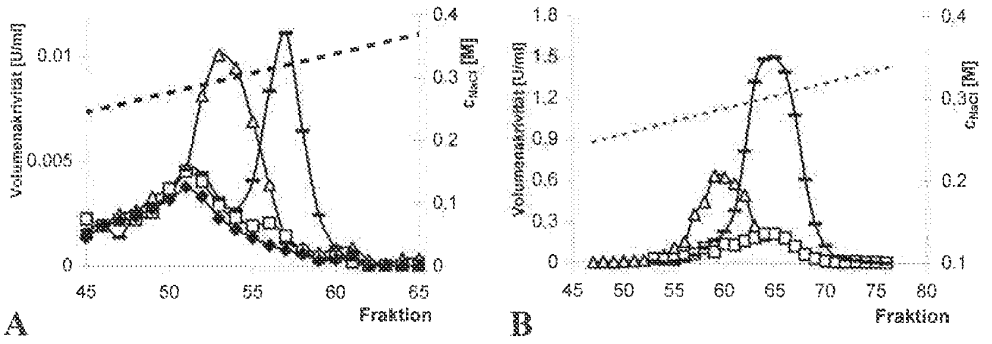


Abbildung 12: Elutionsprofil der Phenoxyalkanoat-Spaltungsaktivitäten aus MH an *PBE94* A: (R,S)-DP/2,4-DB-konfrontierte Zellen, B: (R,S)-DP-konfrontierte Zellen. (S)-DP (◊), (S)-MCPP (—), 2,4-D (□), (R)-DP (Δ), 2,4-DB (♦), NaCl (gestrichelt)

anderem die Spaltungsaktivität für das 2,4-DB enthält, kann in diesen Zellen nicht nachgewiesen werden. Da die Enzymaktivitäten bei nur mit (R,S)-DP induzierten Proteinen deutlich über denen von (R,S)-DP/2,4-DB induzierten liegen (Faktor 100) und aus den mit 2,4-DB-konfrontierten Zellen nicht genügend Enzym für kinetische und proteinbiochemische Untersuchungen gewonnen werden kann, wurde im folgenden nur mit den (R,S)-DP-induzierten Proteinen weitergearbeitet.

An Butyl-Sepharose konnte hier eine weitere Anreicherung der (S)-und (R)-spezifischen Enzyme erreicht werden. So konnte das $RdpA_{MH}$ in diesem Reinigungsschritt auf das 44-fache des Rohextraktes angereichert werden. Bei der Reinigung gingen allerdings etwa 85% der Enzymaktivität verloren. Das (S)-spezifische Enzym wurde 11-fach angereichert; es gingen über 90% der Spaltungsaktivität verloren. Abbildung 11B zeigt die elektrophoretische Auftrennung der einzelnen Reinigungsschritte und veranschaulicht so den Reinigungserfolg. Das Reinigungsprotokoll dieses Schrittes ist der Tabelle 17 zu entnehmen.

COR-AAD1-00003626
Bayer EX1008 (Part 7 of 9)

Tabelle 17: Dokumentation der Reinigung der (S)- und (R)-spezifischen Dioxygenasen aus *Sphingobium herbicidovorans* MH, die Ermittlung der spezifischen Aktivitäten erfolgte unter Einsatz von 1 mM (R)-DP, (R)-MCPP, MCPA bzw. 2,4-D oder 0,5 mM (S)-DP bzw. (S)-MCPP

Reinigungs-schritt	Substrat	rel. Protein-gehalt [%]	spez. Aktivität [U/mg]	Gesamt-aktivität [U]	Anrei-cherung [-fach]	Ausbeute [%]
Rohextrakt	*(R)-DP*	100	0,04	33,99	1	100
	(R)-MCPP		0,038	31,34	1	100
	2,4-D		0,016	13,2	1	100
	MCPA		0,034	28,04	1	100
	(S)-DP		0,135	111,34	1	100
	(S)-MCPP		0,231	190,51	1	100
IEX $RdpA_{MH}$ (*PBE94*)	*(R)-DP*	3	0,87	24,57	22	75
	2,4-D		0,851	2,40	5,3	18
	(S)-DP		0,313	8,84	2,3	8
HIC $RdpA_{MH}$	*(R)-DP*	0,3	1,757	4,5	44	14
	2,4-D		0,201	0,515	13	4
	(S)-DP		-	-	-	-
IEX $SdpA_{MH}$ (*PBE94*)	*(R)-DP*	4	0,163	5,97	4	18
	2,4-D		0,112	4,10	7	31
	(S)-DP		1,76	64,47	13	58
HIC $SdpA_{MH}$	*(R)-DP*	0,7	-	-	-	-
	2,4-D		0,085	0,49	5,3	3,74
	(S)-DP		1,532	8,89	11,4	8

3.1.4 Reinigung der rekombinanten Enzyme $RdpA_{MC1}$-rec und $SdpA_{MC1}$-rec

Die Reinigung der recombinanten Enzyme erfolgte an Strep-Tactin, einer Affinitätsmatrix. Die Enzyme konnten auf diese Weise in einer Einschrittprozedur bis zur Homogenität angereichert werden (Abbildung 13). Das $RdpA_{MC1}$-rec wurde 117-fach angereichert, das $SdpA_{MC1}$-rec 46-fach (Tabelle 18); bis zu 35% der eingesetzten Enzymaktivität gingen

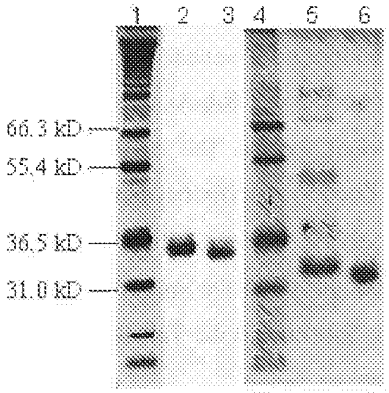


Abbildung 13: Elektrophoretische Auftrennung der gereinigten rekombinanten Enzyme $RdpA_{MC1}$-rec und $SdpA_{MC1}$-rec unter denaturierenden Bedingungen. 1+4: Standard, 2: $RdpA_{MC1}$-rec-tag, 3: $RdpA_{MC1}$-rec, 5: $SdpA_{MC1}$-rec-tag, 6: $SdpA_{MC1}$-rec

COR-AAD1-00003627
Bayer EX1008 (Part 7 of 9)

verloren. Bei beiden Enzymen wurde eine Aktivitätssteigerung durch die Abspaltung des Strep-tag(II) beobachtet. Die Ausbeute der überexprimierten Proteine $RdpA_{MC1}$-rec und $SdpA_{MC1}$-rec war allerdings nur gering. Im Falle des $RdpA_{MC1}$-rec konnte im Rohextrakt des Überexpressionsstammes nur etwa die Hälfte der im Rohextrakt von MC1 gefundenen Enzymaktivität nachgewiesen werden. Für das $SdpA_{MC1}$-rec war sie doppelt so hoch wie im Wildtyp.

Tabelle 18: Reinigungsprotokoll für die Gewinnung der recombinanten Enzyme $RdpA_{MC1}$-rec und $SdpA_{MC1}$-rec

Fraktion	Substrat	spez. Akt. [U/mg]	Anreicherung [-fold]	Ausbeute [%]
Rohextrakt	*(R)-DP*	0,1061	1	100
	2,4-D	0,011	1	100
$RdpA_{MC1}$-rec-tag	*(R)-DP*	9,868	93	51
	2,4-D	1,015	92	50
$RdpA_{MC1}$-rec	*(S)-DP*	11,66	110	65
	2,4-D	1,287	117	65
Rohextrakt	*(S)-DP*	0,527	1	100
	2,4-D	0,164	1	100
$SdpA_{MC1}$-rec-tag	*(S)-DP*	17,03	33	53
	2,4-D	6,1	37	55
$SdpA_{MC1}$-rec	*(S)-DP*	21,97	42	67
	2,4-D	7,591	46	64

COR-AAD1-00003628
Bayer EX1008 (Part 7 of 9)

3.2 Proteinbiochemische Charakterisierung

3.2.1 Primärstruktur

3.2.1.1 Primärstrukturen der RdpA- und SdpA-Enzyme aus MC1, P230 und MH

Die Primärstrukturen der RdpA- und SdpA-Enzyme aus *Delftia acidovorans* MC1, *Rhodoferax* sp. P230 und *Sphingobium herbicidovorans* MH wurden aus den Sequenzdaten der betreffenden Gene hergeleitet. Um die Gene fassen zu können, wurden Primer aus den mittels Edman-Abbau gewonnenen N-terminalen bzw. internen Aminosäuresequenzen (Tabelle 19) abgeleitet[1]. Mit Hilfe der von den $RdpA_{MC1}$-Aminosäuresequenzen abgeleiteten Primern war es möglich, das *rdpA*-Gen in *Delftia acidovorans* MC1 zu finden und zu sequenzieren.

Tabelle 19: Sequenzdaten des RdpA- und des SdpA-Enzyme (ermittelt mittels Edman-Abbau), die N-Termini sind kursiv, unsichere Aminosäuren in Klammern dargestellt. Unterstrichene Aminosäuren wurden zur Primer-Herleitung genutzt

Protein	Sequenz	Primer
$RdpA_{MC1}$	*MHAALSPLSQRFERIAVQPLTGV*	
	SIEGYPEVQMIRREANESGRVIGDDXHTXIIX	
	ETLSPTMQATIEGLN	3´-ACGTYCGNTGNTAICTYCC-5´
	NEILDAFHTYQVIYFPGQAITNEQHIAFSR	5´-GCITTYCAYACNTAYCAGGT-3´
$SdpA_{MC1}$	*MQTTLQITPTGATLGATVTGVHLAT*	5´-ATGCARACIACICTGCARATYC-3´
	LGHVQQAGSAYT	3´-GTACANGTYGTYCGNCC-5´
$SdpA_{P230}$-1	*TIRRIR(Q)SPAFSIAPLNATFGAVVTGVXLA*	5´-GGNGCNGTNGTNACNGG-3´
	TMALPLVVEAS	
	KSLLIG(N)(S)AHAIPG	5´-GCNCAYGCNATHCCNGG-3´
	DAVLWNDR	5´-GAYGCNGTNYTNTGGGAYAA-3´

Identische *rdpA*-Gene konnten auf dieser Basis auch in den Stämmen *Rhodoferax* sp. P230 und *Sphingobium herbicidovorans* MH nachgewiesen werden. Für das $RdpA_{P230}$ konnte die Übereinstimmung der Primärstruktur des Enzyms mit dem $RdpA_{MC1}$ auch auf Proteinebene mittels Spaltmustervergleichs nach tryptischem Verdau erbracht werden (Ruhland, 2003). Die abgeleiteten Primer des $SdpA_{MC1}$ ermöglichten gleichermaßen die Sequenzierung des *sdpA*-Gens in MC1. In MH und P230 konnten dagegen, anders als beim RdpA, keine identischen *sdpA*-Gene gefunden werden. Das $sdpA_{MH}$ konnte unter Nutzung von Sequenzdaten von MC1 gefasst und sequenziert werden. Für P230 stehen der Nachweis und die Identifizierung der Gene für die (S)-spezifischen Enzyme bislang noch aus (A. Götz, persönliche Mitteilung).

[1] Aminosäuresequenzierung, 2D-Gelelektrophorese und Proteinidentifizierung mittels Massenspektrometrie erfolgte in enger Zusammenarbeit mit Dr. D. Benndorf (UFZ, Leipzig). Das Enzympräparat $SdpA_{P230}$-1 wurde im Rahmen der Diplomarbeit von A. Götz (UFZ, Leipzig) gewonnen. Die Primer sowie die Nukleinsäuresequenzen für die Enzyme aus MC1 wurden von K.M. Schleinitz (UFZ, Leipzig) im Rahmen einer Promotion erarbeitet. Die Primer des $SdpA_{P230}$-1 wurden von Dr. S. Kleinsteuber (UFZ, Leipzig) entwickelt. Die Nukleinsäuresequenzen der Dioxygenasen aus MH wurden von T.A. Müller (EAWAG, Dübendorf) im Rahmen einer Promotion ermittelt.

COR-AAD1-00003629
Bayer EX1008 (Part 7 of 9)

Die Tabelle 20 fasst die aus den Nukleinsäuresequenzen abgeleiteten Primärstrukturen der α-KG-abhängigen Phenoxypropionat-spaltenden Dioxygenasen zusammen.

Tabelle 20: Aminosäuresequenzen der Phenoxypropionat-spaltenden Dioxygenasen[1] aus MC1, MH, P230

Protein	Aminosäuresequenz
$RdpA_{MC1}$ (Q8KSD1) **$RdpA_{P230}$** (Q8KSC9) **$RdpA_{MH}$** (Q8KSC8)	MHAALSPLSQ RFERIAVQPL TGVLGAEITG VDLREPLDDS TWNEILDAFH TYQVIYFPGQ AITNEQHIAF SRRFGPVDPV PLLKSIEGYP EVQMIRREAN ESGRVIGDDW HTDSTFLDAP PAAVVMRAID VPEHGGDTGF LSMYTAWETL SPTMQATIEG LNVVHSATRV FGSLYQAQNR RFSNTSVKVM DVDAGDRETV HPLVVTHPGS GRKGLYVNQV YCQRIEGMTD AESKPLLQFL YEHATRFDFT CRVRWKKDQV LVWDNLCTMH RAVPDYAGKF RYLTRTTVGG VRPAR
$SdpA_{MC1}$ (Q8KSD0)	MQTTLQITPT GATLGATVTG VHLATLDDAG FAALHAAWLQ HALLIFPGQH LSNDQQITFA KRFGAIERIG GGDIVAISNV KADGTVRQHS PAEWDDMMKV IVGNMAWHAD STYMPVMAQG AVFSAEVVPA VGGRTCFADM RAAYDALDEA TRALVHQRSA RHSLVYSQSK LGHVQQAGSA YIGYGMDTTA TPLRPLVKVH PETGRPSLLI GRHAHAIPGM DAAESERFLE GLVDWACQAP RVHAHQWAAG DVVVWDNRCL LHRAEPWDFK LPRVMWHSRL AGRPETEGAA LV
$SdpA_{MH}$ (Q700X4)	MSPAFDIAPL DATFGAVVTG VKLADLDDAG WLDLQAAWLE YALLVFPDQH LTREQQIAFA RRFGPLEFEM AAISNVRPDG SLRVESDNDD MMKILKGNMG WHADSTYMPV QAKGAVFSAE VVPSVGGQTG FADMRAAYDA LDEDLKARVE TLQARHSLHY SQSKLGHQTK AADGEYSGYG LHDGPVPLRP LVKIHPETGR KSLLIGRHAH AIPGLEPAES ERLLQQLIDF ACQPPRIYHH DWAPGDAVLW DNRCLLHQAT PWDMTQKRIM WHSRIAGDPA SETALAH
$SdpA_{P230}$-1 **$SdpA_{P230}$-2**	*TIRRIR(Q)SPA FSIAPLNATF GAVVTGVXL A* GNMGWHADST YMPVQAK AAYDALDEDL KAR TMALPLVVEA S KSLLIG(N)HAH AIPGLEPAES ERLLQQLID FACQPPRIY HHDWAPGDAV LWDNR

3.2.1.2 Sequenzvergleiche und konservierte Regionen

Der Vergleich der Aminosäuresequenzen der Phenoxypropionat-spaltenden Enzyme mit bereits bekannten Sequenzen anderer α-Ketoglutarat-abhängiger Dioxygenasen zeigt eine hohe Ähnlichkeiten zu bekannten 2,4-Dichlorphenoxyacetat- (TfdA) und Taurin-Dioxygenasen (TauD). So weist das RdpA eine Sequenzidentität von 39% (55% Ähnlichkeit) mit TauD und von 32% (47% Ähnlichkeit) mit TfdA aus *Ralstonia eutropha* JMP134 auf. Sequenzvergleiche mit dem $SdpA_{MC1}$ zeigen eine 29%ige Identität (47% Ähnlichkeit) zum TauD und eine 35%ge Identität (50% Ähnlichkeit) zum TfdA aus dem Stamm JMP134. Die (S)-spezifische Dioxygenase aus MH zeigt sowohl zum TauD als auch zum TfdA aus JMP134 eine 40%ige Identität (56% Ähnlichkeit). Ein Vergleich der bekannten Sequenzen der Phenoxypropionat-spaltenden Dioxygenasen zueinander und zum TauD ist in Abbildung 15 zu sehen. RdpA ist in seiner Primärstruktur zu nur etwa 28% identisch und zu nur 47% ähnlich mit den beiden (S)-spezifischen Dioxygenasen aus MC1 und MH, die zueinander wiederum nur zu 60% identisch und zu 70% ähnlich sind. Allen untersuchten Enzymen ist allerdings das Motiv H-X-D-$X_{136-205}$-D-N-X_4-H-X_{10}-R gemeinsam, das Merkmal der Gruppe(II) der α-KG-abhängigen

COR-AAD1-00003630
Bayer EX1008 (Part 7 of 9)

Dioxygenasen. Alle Aminosäuren, die in TfdA und TauD zur Bindung des Fe(II) und des α-KG identifiziert wurden, finden sich auch in den RdpA- und SdpA-Proteinen aus MC1 und MH als konservierte Regionen wieder. Die Aminosäuren, die zur Substratbindung in TauD identifiziert wurden, sind dagegen in den bekannten RdpA- und SdpA-Sequenzen wenig bis nicht konserviert. Die Primärstruktur des $SdpA_{P230}$ ist bislang nicht vollständig bekannt, so dass zu diesem Enzym keine Aussage gemacht werden kann.

3.2.2 Sekundärstruktur

Die Erkenntnisse zur Sekundärstruktur der untersuchten Enzyme beruhen auf dem Vergleich der Primärstrukturen mit der Aminosäuresequenz des TauD unter Einbeziehung der 3D-Struktur dieses Proteins. Für dieses Enzym ist die 3D-Struktur aus Röntgenkristallstrukturanalysen bekannt. Dies steht für die Enzyme RdpA und SdpA noch aus. Es ist jedoch bereits gelungen das $RdpA_{rec}$ zu kristallisieren (in Kooperation mit Prof. N. Sträter, BBZ, Leipzig) (Abbildung 14).

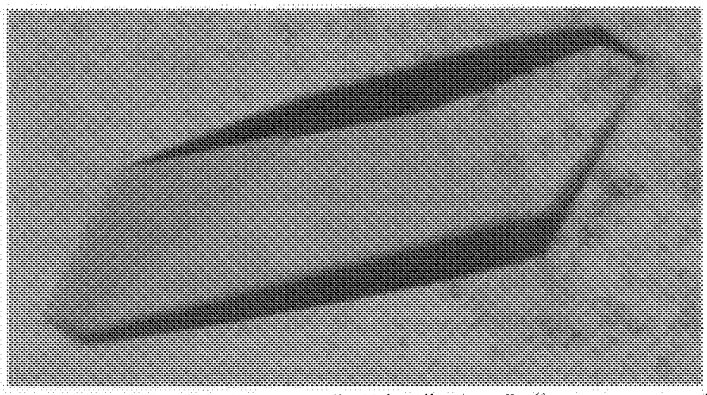


Abbildung 14: Proteinkristall des $RdpA_{MC1}$-rec, die Kristallisations-Bedingungen waren: Einsatz von 12% Polyethylenglycol 3350 als Fällungsreagenz, pH 7.0, 19°C

In Abbildung 15 ist das Sekundärstruktur-basierende Alignment der RdpA- und SdpA-Enzyme der drei Stämme mit dem TauD aus *E. coli* zu sehen. Es ist zu entnehmen, dass sich die Aminosäuresequenzen der Phenoxypropionat-spaltenden Enzyme gut mit der Primär- und Sekundärstruktur des TauD decken. Viele der konservierten und fast alle der hoch konservierten Aminosäuren der Proteine sind in den periodischen Elementen wie α-Helices und β-Faltblättern zu finden. Die Aminosäureabschnitte mit geringerer Übereinstimmung der Primärstrukturen, wo zur besseren Anpassung der Aminosäuresequenz an die Sekundärstruktur des TauD Lücken in diese eingeführt werden mussten, sind zumeist in den nichtperiodischen Sekundärstruktur-Elementen (*coils, turns*) zu finden. Durch Modellierung der Aminosäure-

COR-AAD1-00003631
Bayer EX1008 (Part 7 of 9)

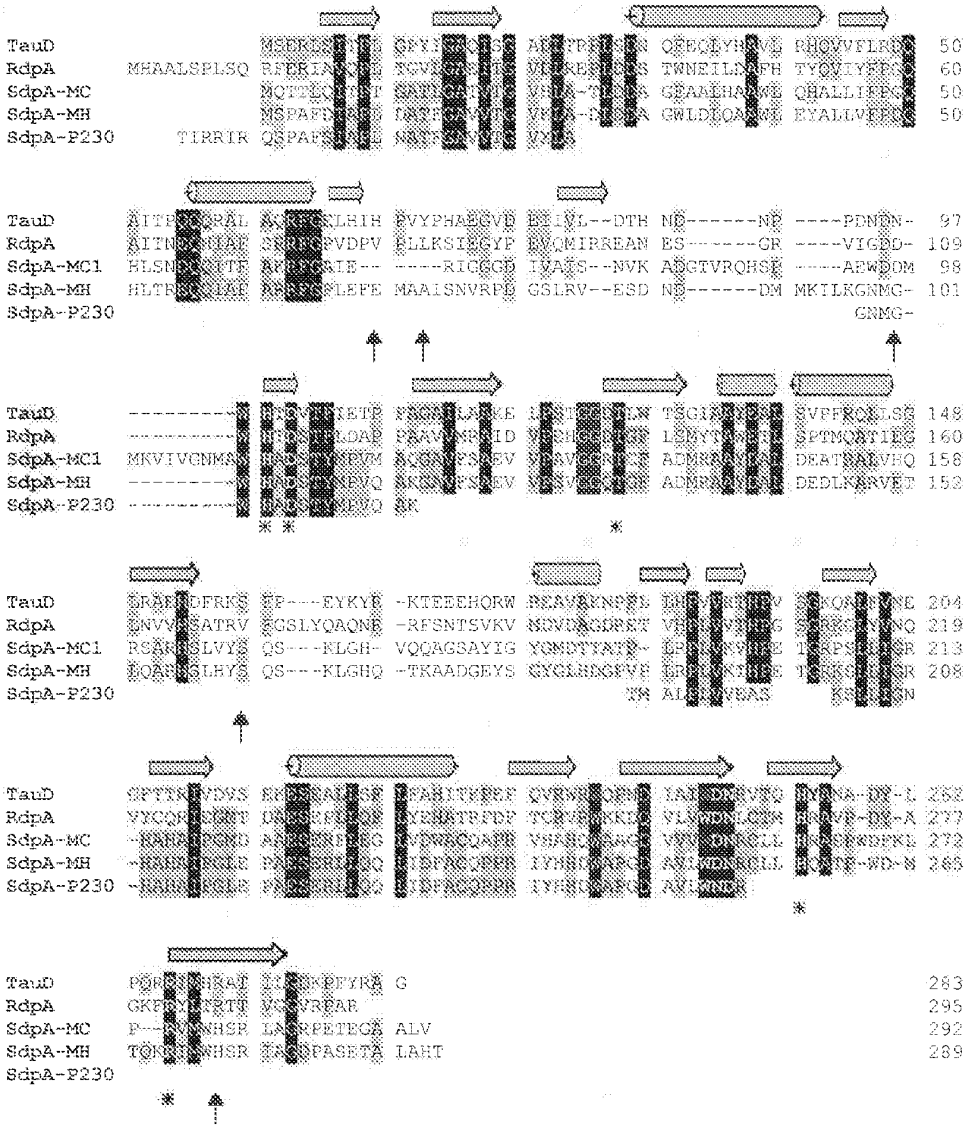


Abbildung 15: Sekundärstruktur-basierendes Alignment der Primärstrukturen vom RdpA, $SdpA_{MC1}$, $SdpA_{MH}$ und $SdpA_{P230}$-1 in Relation zur bekannten Sekundärstruktur des TauD, α-Helices sind als waagerecht liegende, graue Zylinder, β-Faltblätter als graue Pfeile dargestellt. Hochkonservierte Aminosäuren (100-80%) sind schwarz, konservierte Aminosäuren (60-80%) grau unterlegt. Das Sequenzmotiv der Gruppe(II) Dioxygenasen ist gelb hervorgehoben. Mit Sternchen markierte Aminosäuren sind im TauD an der Fe(II)- und α-KG-Bindung, mit Pfeil markierte Reste an der Taurinbindung (Substrat) beteiligt. Für die roten Tryptophanreste sind Oxydationen gefunden worden; für die blauen Aminosäurereste wurden Modifikationen nachgewiesen.

COR-AAD1-00003632
Bayer EX1008 (Part 7 of 9)

sequenzen des RdpA und des $SdpA_{MC1}$ in die 3D-Struktur des TfdA und TauD konnte eine sehr gute Übereinstimmung der Sekundärstrukturen der Enzyme gezeigt werden (K.M. Schleinitz, persönliche Mitteilung). Das Protein besteht danach aus 17 β-Faltblättern, von denen 8 das *jellyroll*-Motiv bilden, und aus 6 α-Helices. Der Aminosäuresequenz-Abschnitt Glu66-Val79 wurde im TauD als Substratbindetasche identifiziert. In diesem Bereich sind wenige bis keine Homologien zu den Phenoxypropionat-spaltenden Enzymen zu finden.

3.2.3 Physikochemische Eigenschaften und Quartärstruktur

3.2.3.1 Enzyme aus *Delftia acidovorans* MC1

Das $RdpA_{MC1}$ besteht aus 295 Aminosäuren, die aus der Primärstruktur errechnete Molmasse des Enzyms beträgt 33,2 kD, der pI des Proteins ergibt sich zu 6,06. Die Molmasse des 292 Aminosäuren umfassenden $SdpA_{MC1}$ ist 32,7 kD, der pI wurde mit 6,45 berechnet.

3.2.3.1.1 Gelchromatographische Bestimmung der Molmasse

Die säulenchromatographische Auftrennung des $SdpA_{MC1}$-Präparates (HIC) an BioSil™ ist in Abbildung 16 zu sehen. Unter nativen Bedingungen wird das im SDS-PAGE homogen erscheinende Enzympräparat in drei Proteinpeaks (63 kD, 23,7 kD, 4,5 kD) fraktioniert. Für das 23,7 kD-Protein konnte enzymatische Aktivität nachgewiesen werden. Die Proteine der Peaks 1 und 3 lagen nur in sehr geringen Konzentrationen vor; für sie konnte keine katalytische Aktivität gezeigt werden. Die Auftrennung der gleichen Enzymprobe unter denaturierenden Bedingungen zeigt ein ähnliches Bild. Wieder sind drei Proteinpeaks zu erkennen, deren Massen sich jedoch aufgrund der veränderten Trennbedingungen leicht zu höheren Massen verschoben haben. Am Elutionsprofil ändert die Anwesenheit von SDS jedoch nichts Grundsätzliches. Als Ergebnis der Gelfiltration bleibt also festzuhalten: das $SdpA_{MC1}$ erscheint unter den gewählten Bedingungen zum überwiegenden Teil als monomeres Protein der Masse 23,7 kD. Eine definitive Aussage über das Vorhandensein eines geringen Anteils eines Homodimers der Masse 63 kD kann wegen der fehlenden Zuordnung von Enzymaktivität zu diesem Proteinpeak nicht gemacht werden. Da Fremd-Proteine in der SDS-gelelektrophoretischen Auftrennung dieser Proteinpräparation nicht vorhanden waren (Abbildung 4A), ist die Zuordnung des 63 kD-Peaks zu einem Dimer jedoch eher wahrscheinlich. Durch die gelchromatographische Trennung der Proteine des $RdpA_{MC1}$-Präparates unter nativen Bedingungen konnten drei Peaks voneinander separiert werden, von denen nur dem Protein mit der Masse 108 kD katalytische Aktivität zugeordnet werden konnte. Die Proteine der Massen 162 kD und 5,9 kD

COR-AAD1-00003633
Bayer EX1008 (Part 7 of 9)

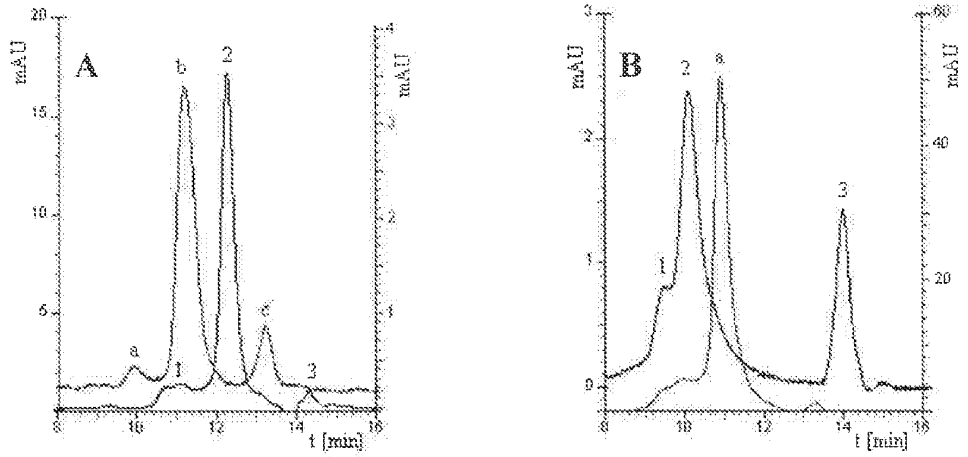


Abbildung 16: Elutionsprofile des (S)- und (R)-spezifischen Präparates an BioSilTM (Gelfiltration) unter nativen sowie denaturierenden (1% SDS) und reduzierenden (1% Mercaptoethanol) Bedingungen **A: $SdpA_{MCI}$**, nativ: 1: 63 kD; 2: 23,7 kD; 3: 4,5 kD; denaturierend: a: 72 kD; b: 33 kD; c: 5,6 kD; **B: $RdpA_{MCI}$** nativ: 1: 161,7 kD; 2: 108,2 kD; 3: 5,9 kD; denaturierend: a: 37 kD

weisen keine Spaltungsaktivität auf. Hier sollte es sich um die Verunreinigungen des (R)-spezifischen Präparates mit anderen Proteinen handeln, die in Abbildung 4B zusehen sind. Bei der Auftrennung unter denaturierenden Bedingungen verschwindet das Protein der Masse 108 kD und ein neuer Proteinpeak mit der Masse 37 kD erscheint. Dieses Resultat lässt auf eine homotrimere Erscheinungsform des $RdpA_{MCI}$ schließen.

3.2.3.1.2 Gelelektrophoretischer Nachweis von Ladungsisomerie, Bestimmung der Molmasse und der isoelektrischen Punkte

Die Auftrennungen der (R)- und (S)-spezifischen Präparate unter denaturierenden Bedingungen sind bereits in den Abbildungen 4A+B dargestellt. Unter Verwendung des Standards und der R_f-Werte der Proteine wurden die Molmassen der monomeren Enzyme von 32,1 kD für das $SdpA_{MCI}$ und von 34,7 kD für das $RdpA_{MCI}$ ermittelt.

Die elektrophoretischen Auftrennungen der $RdpA_{MCI}$- und $SdpA_{MCI}$-Präparate nach der hydrophoben Chromatographie unter nativen Bedingungen zeigen nicht wie erwartet eine homogene Bande im Acrylamidgel. Vielmehr können sowohl für $SdpA_{MCI}$ als auch für $RdpA_{MCI}$ drei Proteinbanden (I1, I2, I3) aufgelöst werden. Mittels massenspektrometrischer Analyse sind diese jeweils eindeutig den betreffenden Enzymen zuzuordnen. Zur Ermittlung der Molmasse der nativen Enzymformen und zur Charakterisierung der Art der Beziehung zwischen den Enzymformen wurden Gele mit unterschiedlicher Acrylamidkonzentration eingesetzt und der Trennverlauf graphisch ausgewertet.

COR-AAD1-00003634
Bayer EX1008 (Part 7 of 9)

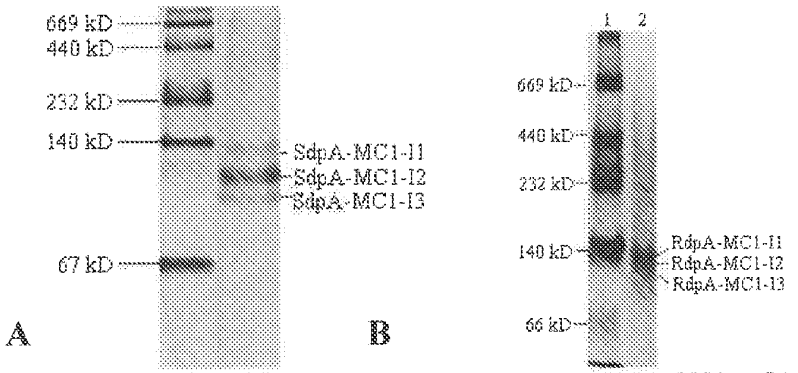


Abbildung 17: Native gelelektrophoretische Auftrennung der Enzympräparate aus MC1 A: $SdpA_{MC1}$, B: $RdpA_{MC1}$

Abbildung 18 zeigt die Auftragung $lg(100*R_f) = f(c_{Acrylamid})$. Erscheinen die Plots unterschiedlicher Proteine in dieser Darstellungsform als zueinander parallele Geraden, so handelt es sich bei diesen Proteinen um Ladungsisomere. Die Parallelität der Geraden ist sowohl für das $SdpA_{MC1}$ als auch für das $RdpA_{MC1}$ gezeigt, wodurch bewiesen wurde, dass es sich bei den Enzymformen um Ladungsisomere handelt. Die Molmassen wurden unter diesen Bedingungen für das $SdpA_{MC1}$ mit 63 kD und für das $RdpA_{MC1}$ mit 113 kD bestimmt. Für das $RdpA_{MC1}$ stimmen die gelelektrophoretisch und säulenchromatographisch ermittelten Molmassen des nativen Proteins überein. Für $SdpA_{MC1}$ ist dies nicht der Fall: das Vorliegen unterschiedlicher Ionenstärken bei den unterschiedlichen Auftrennungen könnte ein Grund dafür

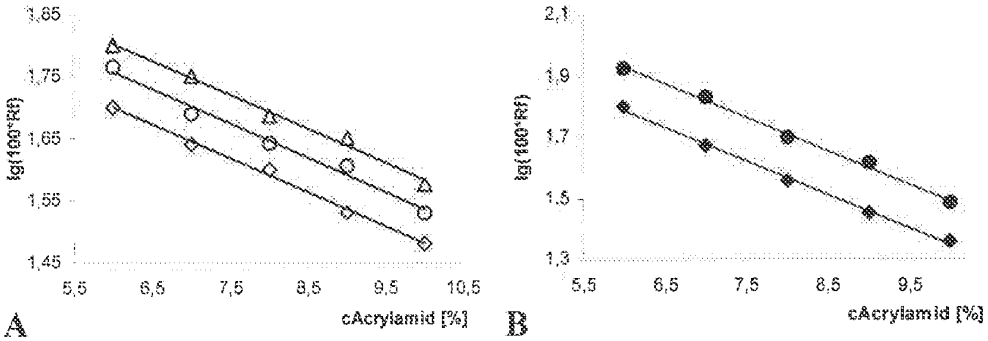


Abbildung 18: Graphische Auswertung der Proteinlaufstrecken im Acrylamidgel unter nativen Bedingungen A: $SdpA_{MC1}$-I1 (◊), $SdpA_{MC1}$-I2 (○), $SdpA_{MC1}$-I3 (Δ), **B:** $RdpA_{MC1}$-I1 (♦), $RdpA_{MC1}$-I2 (●)

sein. Zur Ermittlung der isoelektrischen Punkte der Enzyme wurden die Proteinpräparate 2D-gelelektrophoretisch aufgetrennt (Abbildung 19). Im 2D-Gel erscheint das $SdpA_{MC1}$ wiederum nicht als homogener Spot. Vielmehr erscheinen drei Spots, die nach massenspektrometrischer Analyse dem (S)-spezifischen Enzym zugeordnet werden können. Wie schon bei den nativen Enzymformen handelt es sich auch bei den Monomeren (S1, S2, S3) um Ladungsisomere gleicher Masse. Die Molmassen der Monomere wurden auf 32,5 kD bestimmt, die pI-

COR-AAD1-00003635
Bayer EX1008 (Part 7 of 9)

Werte liegen zwischen 6,16 und 6,35. Analog zum $SdpA_{MC1}$ ergibt sich das Bild für das $RdpA_{MC1}$: es konnten mindestens drei ladungsisomere Monomere (R1, R2, R3) mit einer Molmasse von 35,8 kD nachgewiesen werden. Die isoelektrischen Punkte der Proteine liegen zwischen 5,8 und 5,9.

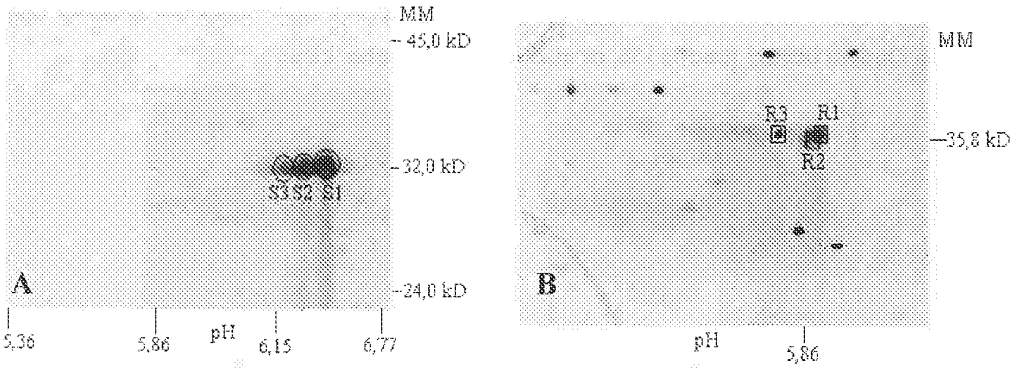


Abbildung 19: 2D-Gelelektrophoretische Auftrennung der $SdpA_{MC1}$- (A) und $RdpA_{MC1}$-Präparate (B)

3.2.3.1.3 Quartärstruktur der Enzyme $SdpA_{MC1}$ und $RdpA_{MC1}$

Anhand der oben ausgeführten Untersuchungen deutet sich schon eine Menge zur Quartärstruktur der α-Ketoglutarat-abhängigen Dioxygenasen aus MC1 an. Vom $SdpA_{MC1}$ wissen wir, dass es sich um ein dimeres Protein mit einer Molmasse von 63 kD handelt. Es konnten drei native Enzyme ($SdpA_{MC1}$-I1, -I2, -I3) nachgewiesen werden, die sich wiederum aus Kombinationen von drei ladungsisomeren Monomeren (S1, S2, S3) zusammensetzen. Das $RdpA_{MC1}$ stellt ein trimeres Protein der Molmasse 108 kD dar. Von diesem Enzym wurden ebenfalls verschiedene native Enzymformen ($RdpA_{MC1}$-I1, -I2, -I3) nachgewiesen, die sich wiederum aus mindestens drei ladungsisomeren monomeren Proteinen (R1, R2, R3) zusammensetzen.

Das Auffinden von drei unterschiedlichen Monomeren ergibt für ein dimeres Protein ($SdpA_{MC1}$) sechs Kombinationsmöglichkeiten und damit sechs theoretische native Enzymformen (S1S1, S1S2, S1S3, S2S2, S2S3, S3S3). Tatsächlich konnten aber nur drei Enzymformen für das $SdpA_{MC1}$ gefunden werden. Die theoretische Anzahl für ein trimeres Protein ($RdpA_{MC1}$) liegt sogar bei zehn, eindeutig nachgewiesen werden konnten jedoch ebenfalls nur drei native $RdpA_{MC1}$-Formen. Um Aussagen zur tatsächlichen Kombination von Monomeren im oligomeren Protein machen zu können, mussten die Enzymformen voneinander getrennt (3.1.1.2) und anschließend separat analysiert werden.

Für das $SdpA_{MC1}$ ist es gelungen, zwei der drei nativen Enzymformen mittels präparativer Gelelektrophorese (3.1.1.2.1) voneinander zu trennen. Diese Enzympräparate wurden 2D-

COR-AAD1-00003636
Bayer EX1008 (Part 7 of 9)

gelelektrophoretisch aufgetrennt (Abbildung 20) und anschließend densiometrisch ausgewertet. Das Enzympräparat $SdpA_{MCI}$-I1 besteht zu 86% aus dem Monomer S1, zu 12% aus S2 und zur 2% aus S3. Rein rechnerisch (siehe unten) ergibt sich aus diesen Daten und den theoretisch möglichen Monomeren-Kombinationen ein Enzymgemisch bestehend aus 76% des Dimers S1S1 und 20% des Dimers S1S2 (Abbildung 21). Der Anteil der anderen theoretischen Dimere beträgt jeweils 1%, ist also vernachlässigbar klein.

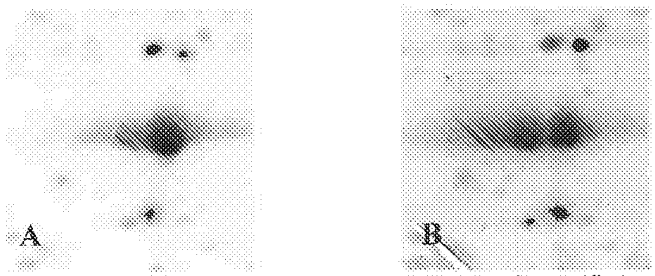


Abbildung 20: Ausschnitte aus den 2D-Gelen zur Auftrennung der (S)-spezifischen Enzymformen A: $SdpA_{MCI}$-I1, B: $SdpA_{MCI}$-I2

Im Enzympräparat $SdpA_{MCI}$-I2 stellt sich die Situation folgendermaßen dar: entsprechend der Analyse besteht das Präparat zu 48% aus dem Monomer S1, zu 37% aus S2 und zu 15% aus S3. Für dieses Präparat ergibt sich demnach eine Zusammensetzung von 74% S1S2 und 22% S1S3. Wiederum liegen die anderen theoretisch abgeleiteten dimeren Proteine nur in vernachlässigbar kleinen Anteilen im Gemisch vor. Nach dieser Auswertung wird offensichtlich, dass mit der präparativen Elektrophorese keine Trennung der Enzymformen, sondern lediglich eine Anreicherung erreicht werden konnte.

Die dritte native Enzymform des $SdpA_{MCI}$ ist bei der Reinigung verlorengegangen, sollte aber nach den vorliegenden Ergebnissen aus den Monomeren S1 und S3 zusammengesetzt sein.

Berechnung der Dimeren-Zusammensetzung: Die $SdpA_{MCI}$-Proteine, die nach Auftrennung im Acrylamidgel unter nativen Bedingungen in einer Proteinbande vorliegen, zeichnen sich durch identische Trenneigenschaften aus. In einer Bande können also nicht gleichzeitig die basischste und sauerste Variante des nativen Proteins vorliegen. Basische Proteine sind während der Elektrophorese weniger geladen als saure (pH 8,8), zeichnen sich also bei identischer Masse durch ein langsameres Laufverhalten aus. Aus diesem Grund sollten im Präparat $SdpA_{MCI}$-I2 überwiegend saure Dimere vorhanden sein, das Vorhandensein von signifikanten Mengen des sauren Dimers S1S1 ist damit ausgeschlossen. Das Präparat-I2 setzt sich also wie folgt zusammen:

$$b(S1+S2) + c(S1+S3) + d(S2+S2) + e(S2+S3) + f(S3+S3) = 50\%$$

$$S1 + S2 + S3 = 100\%$$

COR-AAD1-00003637
Bayer EX1008 (Part 7 of 9)

womit sich für die Monomere im Zusammenhang mit dem ermittelten Monomerenverhältnis folgende Beziehungen ergeben:

(1) S1 = 48% = b + c

(2) S2 = 37% = b + 2d + e

(3) S3 = 15% = c + e + 2f

Durch Einsetzten der Gleichung (1) in (2) und anschließende Subtraktion von der Gleichung (3) ergibt sich:

(4) 2% = d + e + f

Damit ist die Summe der Anteile der dimeren Proteine S2S2, S2S3 und S3S3 kleiner als 2% und kann vernachlässigt werden. Aus den nun stark vereinfachten Gleichungen (1), (2) und (3) kann nun auf das Vorhandensein von 74 ± 2% des Dimers S1S2 und 22 ± 2% des Dimers S1S3 geschlossen werden.

In analoger Weise lässt sich auch die Zusammensetzung anderer Präparate berechnen.

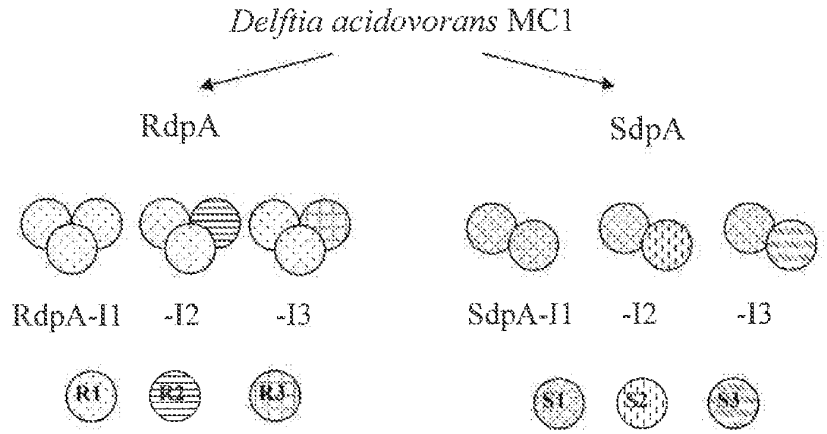


Abbildung 21: Schematische Darstellung der Enzymausstattung von *Delftia acidovorans* MC1

Für das $RdpA_{MC1}$ ist es nicht gelungen, die nativen Enzymformen so voneinander zu trennen (3.1.1.2.2), dass eine sichere Aussage zu den Kombinationen der Untereinheiten im trimeren Protein gemacht werden kann. Sicher ist jedoch, dass das Monomer R1, wie beim $SdpA_{MC1}$, die dominierende Form ist; die Proteine R2 und R3 kommen in wesentlich geringeren Konzentrationen vor. Aus diesem Grund liegt die Annahme nahe, dass das $RdpA_{MC1}$ die Zusammensetzung wie in Abbildung 21 dargestellt aufweist. Eine solche Kombination würde auch die im Gegensatz zum $SdpA_{MC1}$ relativ schlechtere Trennbarkeit der Enzymformen erklären, da der Einfluss der dritten Untereinheit mit deren leicht niedrigeren pI ziemlich gering ist.

COR-AAD1-00003638
Bayer EX1008 (Part 7 of 9)

3.2.3.2 Enzyme aus *Rhodoferax* sp. P230 und *Sphingobium herbicidovorans* MH

3.2.3.2.1 Die (R)-spezifischen Enzyme

Wie bereits oben erwähnt wurde, konnte in allen drei untersuchten Stämmen eine identische Primärstruktur für das RdpA nachgewiesen werden. Physikochemische Eigenschaften wie Molmasse und isoelektrischer Punkt sollten sich für das RdpA der verschiedenen Stämme also nicht unterscheiden. Die Molmasse der (R)-spezifischen monomeren Enzyme konnte für alle drei Stämme im SDS-Gel mit 34,7 kD bestimmt werden. Mit Hilfe der Größenausschluss-Chromatographie wurde eine Molmasse des nativen $RdpA_{P230}$ von 106 kD und des denaturierten Proteins von 39,7 kD bestimmt. Es handelt sich also wie beim $RdpA_{MC1}$ um ein trimeres Protein (Ruhland, 2003). Eine 2D-gelelektrophoretische Auftrennung des $RdpA_{P230}$ ist in Abbildung 22 zu sehen. Man kann deutlich das Vorhandensein verschiedener Spots erkennen, von denen die markanten über MS-Fingerprintanalyse eindeutig dem RdpA zugeordnet werden konnten. Das Erscheinungsbild des $RdpA_{P230}$ im 2D-Gel weicht, trotz der gleichen Primärstruktur, von dem des $RdpA_{MC1}$ stark ab. Konnten für das $RdpA_{MC1}$ eine Hauptform (R1) und mehrere mengenmäßig weniger stark vertretene monomere Nebenformen (R2, R3) nachgewiesen werden, so sind es für das $RdpA_{P230}$ drei Hauptformen und eine zahlenmäßig nicht eindeutig bestimmte Anzahl von Nebenformen. Auch in der elektrophoretischen Auftrennung

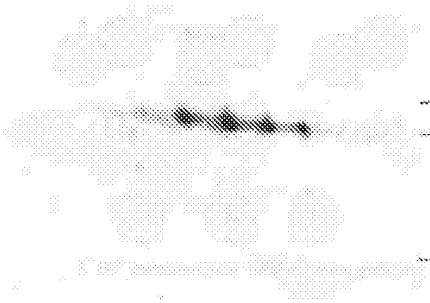


Tabelle 21: Rf-Werte der RdpA- Enzyme nativ: 5% T/2,67% C, denaturierend: 12% T/2,67% C, es wurde die stärkste Bande zugrunde gelegt

Enzym	nativ	denaturierend
RdpA-rec	0,690	0,538
$RdpA_{MC1}$	0,685	0,531
$RdpA_{P230}$	0,655	0,533
$RdpA_{MH}$	0,687	0,535

Abbildung 22: 2D-gelelektrophoretische Auftrennung des $RdpA_{P230}$ (Ausschnitt)

unter nativen Bedingungen unterscheiden sich die RdpA-Enzyme aus P230 und MC1, die Hauptform des P230 besitzt einen signifikant niedrigeren Rf-Wert als die des $RdpA_{MC1}$ (Tabelle 21). Für das native $RdpA_{MH}$ wurde der gleiche R_f-Wert im 5%igen Acrylamidgel bestimmt wie für das Enzym aus MC1. 2D-Gelelektrophoretische Auftrennungen liegen hier nicht vor.

3.2.3.3 Die (S)-spezifischen Enzyme

Die SdpA-Enzyme der drei Stämme MC1, P230 und MH unterscheiden sich in ihrer Primärstruktur erheblich (3.2.1.2), es handelt sich also um komplett unterschiedliche Proteine.

COR-AAD1-00003639
Bayer EX1008 (Part 7 of 9)

Aus dem Stamm *Rhodoferax* sp. P230 konnten zwei (S)-spezifische Enzyme gereinigt werden. Mittels SDS-PAGE wurde die Molmasse des $SdpA_{P230}$-1-Monomers auf 33,3 kD und die des $SdpA_{P230}$-2 auf 32,4 kD bestimmt. Die Molmasse der nativen Enzyme konnte nicht ermittelt werden, da keine reinen Enzympräparate vorlagen. In der 2D-gelelektrophoretischen Auftrennung werden die im SDS-Gel homogenen Proteinbanden beider (S)-spezifischer Enzyme aus P230 in mehrere Proteinfraktionen getrennt (Abbildung 23).

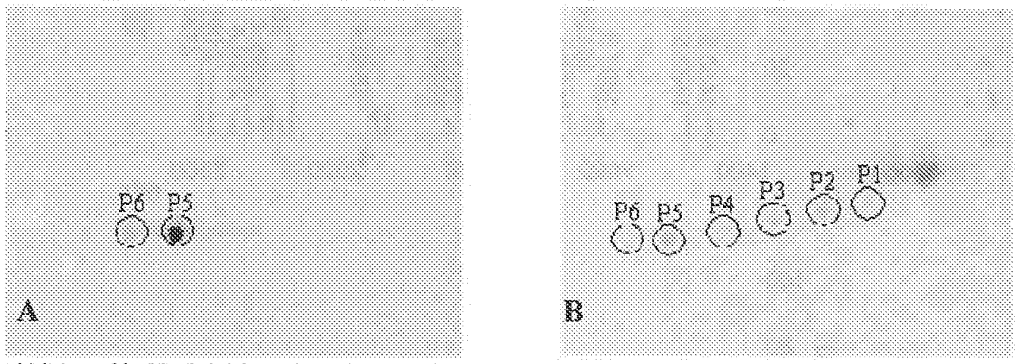


Abbildung 23: 2D-Gelelektrophoretische Auftrennung des $SdpA_{P230}$-1 (A) und $SdpA_{P230}$-2 (B) (Ausschnitte)

Das $SdpA_{P230}$-1 ist ein oligomeres Enzym, das sich aus Kombinationen von zwei Untereinheiten (P5, P6) zusammensetzt. Das Monomer P5 dominiert in dem untersuchten Enzympräparat. Das Enzym $SdpA_{P230}$-2 ist ebenfalls ein oligomeres Enzym, es besteht aus Kombinationen der monomeren Formen P1-6, die Anzahl der Untereinheiten des nativen Enzyms ist nicht bekannt. Auch in diesem Präparat dominiert das Monomer P5. Der Massenunterschied zwischen P1 (32,4 kD; pI 5,8) und P6 (32,2 kD; pI 5,3) beträgt 0,2 kD, die isoelektrischen Punkte der Monomere liegen innerhalb von 0,5 pH-Einheiten. Alle sechs Untereinheiten der (S)-spezifischen Enzyme des P230 zeigen nach tryptischem Verdau und MS-Analyse das gleiche Peptidspaltungsmuster (Abbildungen 24A+B), ebenso identisch sind die Fragmentierungsmuster der Peptide (Abbildungen 24C+D). Die Monomere (P1-6) des $SdpA_{P230}$ sollten sich also durch identische Primärstrukturen auszeichnen. Durch Datenbankrecherche konnte aufgrund des Peptidmustervergleiches mit bereits bekannten Proteinen eine hohe Ähnlichkeit zum $SdpA_{MH}$ festgestellt werden. Peptide, die den Aninosäuresequenzen von 97-113, 136-148, 208-222, 223-236 und 237-253 des SdpA aus MH entsprechen, konnten ebenfalls im tryptischen Verdau der P230-Enzyme gefunden. Trotzdem sind die SdpA-Enzyme aus MH und P230 nicht identisch, wie aus den mittels Edman-Abbau gewonnenen Sequenzen deutlich wird (Tabelle 20).

Das denaturierte Protein $SdpA_{MH}$ besitzt eine Molmasse von 32,2 kD (SDS-PAGE).

COR-AAD1-00003640
Bayer EX1008 (Part 7 of 9)

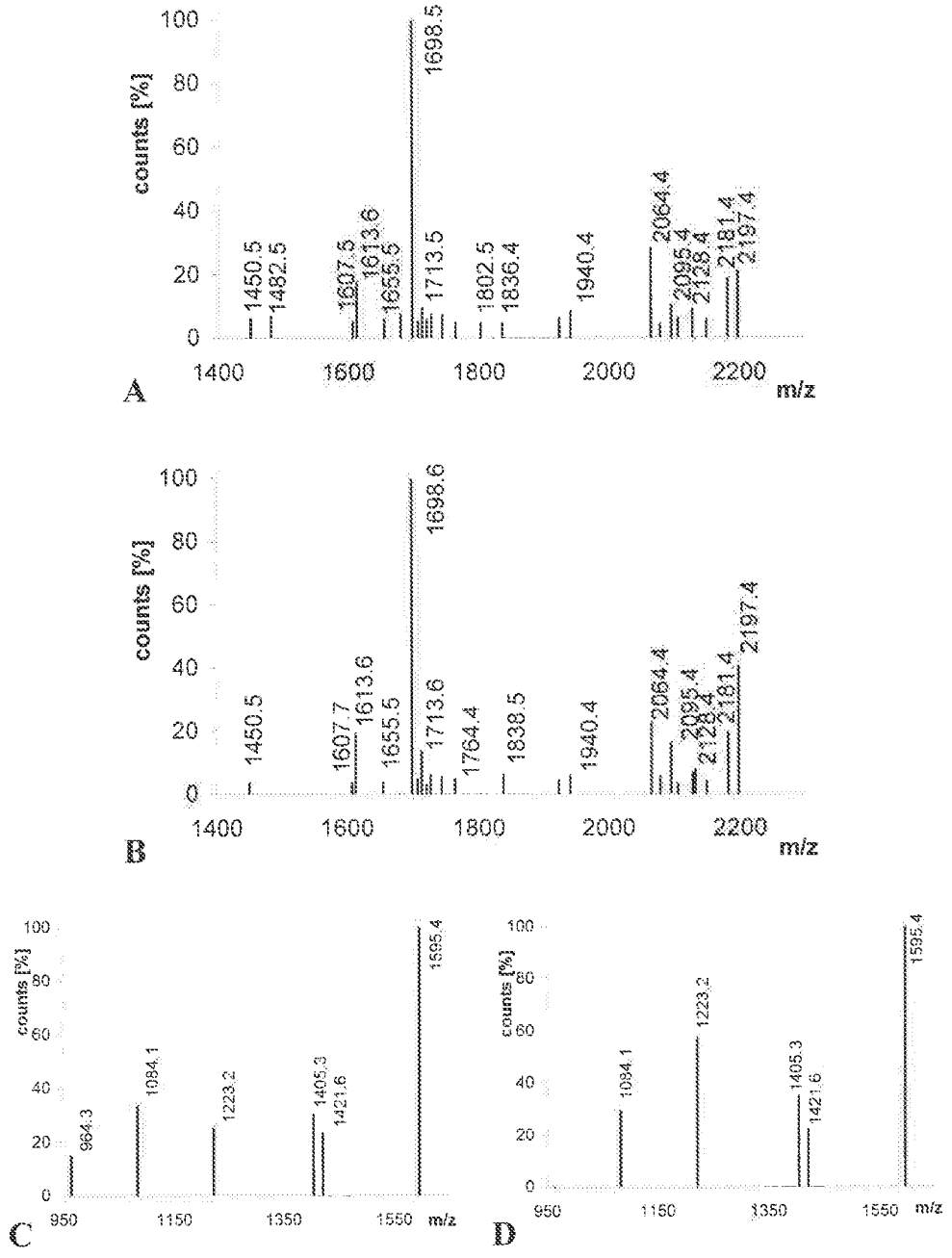


Abbildung 24: Massenspektrometrische Analysen der $SdpA_{P230}$-Monomere (tryptischer Verdau). A: Peptidspaltmuster vom $SdpA_{P230}$-P1 (MS-1), B: Peptidspaltmuster vom $SdpA_{P230}$-P6 (MS-1) C: Fragmentierungsmuster des 1613,6 Peptides des SdpAP230-P1 (MS-2), D: Fragmentierungsmuster des 1613,6 Peptides des $SdpA_{P230}$-P6 (MS-2) werden.

COR-AAD1-00003641
Bayer EX1008 (Part 7 of 9)

3.2.3.4 Rekombinante Enzyme

Die überexprimierten Proteine $RdpA_{MC1}$-rec und $SdpA_{MC1}$-rec zeigen nach Auftrennung im Acrylamidgel sowohl unter nativen als auch denaturierenden Bedingungen jeweils nur eine Proteinbande, was auf das Vorhandensein nur einer Enzymform schließen lässt. Das $SdpA_{MC1}$-rec entspricht dabei dem $SdpA_{MC1}$-I1 (Abbildung 25B), die Enzymform $SdpA_{MC1}$-I2 ist in diesem Präparat nicht detektierbar. Das rekombinante RdpA besitzt den gleichen R_f-Wert wie die Hauptbande des $RdpA_{MC1}$ (Abbildung 25A).

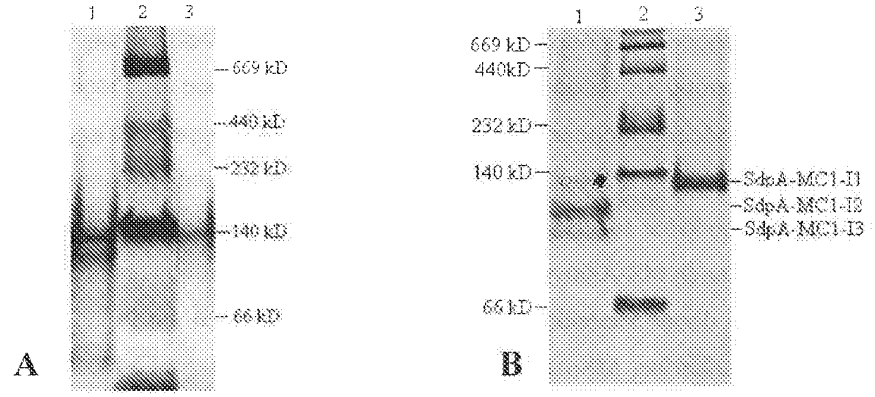


Abbildung 25: Native gelelektrophoretische Auftrennung A: des nativen (Spur 1) und des rekombinanten $RdpA_{MC1}$ (Spur 3), B: des nativen (Spur 1) und rekombinanten $SdpA_{MC1}$ (Spur 3)

Mittels 2D-Gelelektrophorese lassen sich die rekombinanten Enzympräparate im mehrere Spots auftrennen Abbildung 26. Das rekombinante RdpA liefert das gleiche Bild, wie das native Enzym, drei monomere Formen konnten nachgewiesen werden. Auch für das $SdpA_{MC1}$-rec wurden die drei Monomeren S1, S2 und S3 gefunden. Das Monomerenverhältnis des Enzyms entspricht dem des $SdpA_{MC1}$-I2, dementsprechend sollte das rekombinante $SdpA_{MC1}$ zu 74% aus dem Dimer S1S2 und zu 22% des Dimers S1S3 zusammengesetzt sein. Dies widerspricht jedoch den Ergebnissen aus der nativen Gelelektrophorese, wonach die Zusammensetzung analog dem $SdpA_{MC1}$-I1 sein müsste, also dem Dimer S1S1 entspräche.

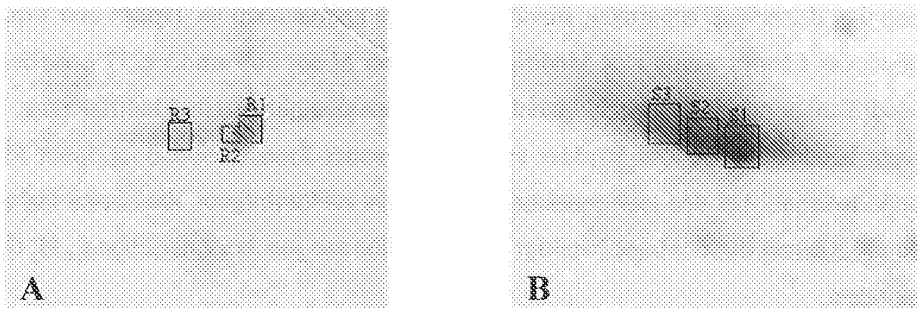


Abbildung 26: 2D-gelelektrophoretische Auftrennung der rekombinanten Enzyme $RdpA_{MC1}$-rec (A) und $SdpA_{MC1}$-rec (B)

COR-AAD1-00003642
Bayer EX1008 (Part 7 of 9)

3.2.4 Posttranslationale Modifikationen

Sowohl für die RdpA- als auch für die SdpA-Enzyme der Bakterienstämme MC1, P230 und MH konnten unterschiedliche Enzymformen mit identischen Aminosäuresequenzen gezeigt werden. Der Unterschied zwischen den Enzymformen ist also in einer posttranslationalen Modifizierung zu suchen.

3.2.4.1 Die (R)-spezifischen Enzyme

Für die drei RdpA-Proteine der untersuchten Stämme konnten ladungsisomere Monomere mit gleicher Masse nachgewiesen werden. Eine posttranslationale Modifizierung der Primärsequenz hat eine Änderung der Gesamtladung, nicht aber der Molmasse des Enzyms bewirkt, ist also eine kleine geladene Gruppe oder bindet an eine geladene Gruppe des Enzyms. Die Aminosäurebereiche 1-24, 43-72, 85-109 und 147-162 wurden per Edman-Abbau eindeutig sequenziert. Es wurden keine zweifelhaften Aminosäure-Peaks und damit potentielle Modifizierungen gefunden. Durch MS-Analysen konnte eine Sequenzabdeckung von 73% erreicht werden, aber auch mit dieser Methode wurden keine Modifizierungen am Protein identifiziert. Nicht gefunden wurden bei MS-Analysen die Aminosäuresequenzen 12-14, 35-72, 96-104, 253-256, und 272-295.

3.2.4.2 Das $SdpA_{MC1}$

Vom $SdpA_{MC1}$ wurden ebenfalls ladungsisomere Monomere mit gleicher Masse nachgewiesen, die das Produkt einer posttranslationalen Modifizierung sein müssen, da nur ein *sdpA*-Gen in MC1 gefunden wurde. Mittels Aminosäuresequenzierung durch Edman-Abbau konnte eine Modifizierung an den Peptiden 1-24 und 170-182 ausgeschlossen werden. Durch MS-Analyse des tryptischen Verdaus ist es gelungen, eine 92%ige Sequenzabdeckung des Proteins zu erreichen. Die Sequenzbereiche 82-87, 135-141, 213-227 und 274-279 wurden nicht gefunden. Bei der Analyse der Peptid-Massen (1677,73 D; 1813,72 D und 1975,85 D), die von den theoretisch erwarteten abwichen, wurden Oxidationen an Trp235 und Trp255 nachgewiesen. Ebenso wurde eine Modifikation mit der Masse 209 am Cys237 gefunden. Bei der Modifikation mit der Masse 209 handelt es sich um eine untypische Modifizierung, die bisher nicht beschrieben ist. Die Struktur und die Elementar-Zusammensetzung dieser Masse sind nicht bekannt. Aus den Isotopenmustern kann man schlussfolgern, dass keine Halogenatome an der Bildung dieser Masse beteiligt sind, sie sollte nur aus den Elementen C, H, O, N und S bestehen.

Die massenspektrometrischen Untersuchungen zur Identifizierung von posttranslationalen Modifikationen wurden von der Arbeitsgruppe von Prof. R. Hoffmann (BBZ, Leipzig) durchgeführt.

COR-AAD1-00003643
Bayer EX1008 (Part 7 of 9)

3.3 Enzymkinetische Charakterisierung und Reaktionsmechanismus

3.3.1 Bestimmung der Anzahl funktionell aktiver Zentren

Die Anzahl funktionell aktiver Zentren wurde über deren α-KG-Bindevermögen ermittelt. Dabei wurde angenommen, dass pro funktionell aktivem Zentrum genau ein α-KG-Molekül bindet. Zentren, die nicht zur Katalyse der Reaktion beitragen, binden kein α-KG.

Tabelle 22: Spezifische Aktivität [U/mg] vom rekombinanten RdpA und des systematisch inaktivierten Enzyms, RdpA (0.797 µM) wurde zum einen durch Inkubation mit unterschiedlichen Mengen DEPC (DEPC-1 = 0.266 µM, DEPC-2 = 0.531µM) und zum anderen durch Temperatureinwirkung inaktiviert

Substrat	RdpA	RdpA + DEPC-1	RdpA + DEPC-2	RdpA + 10 min 35°C
(R)-DP	11,66	4,62	0,715	3,83
(R)-MCPP	8,62	3,74	0,464	2,93
2,4-D	1,29	0,55	0,048	0,45
MCPA	1,1	0,46	0,069	0,41

Zum Nachweis einer direkten Korrelation zwischen der Anzahl von funktionell aktiven Zentren, also der spezifischen Aktivität, und dem Vermögen, α-KG zu binden, wurden Enzympräparate systematisch durch die Zugabe von Diethylpyrocarbonat (DEPC), einem Reagenz, das spezifisch His-Reste modifiziert, inaktiviert (Tabelle 22). Die Zugabe von 33% DEPC der Molarität des RdpA zum Enzym resultiert im Verlust von 60% der spezifischen Aktivität, d.h. nur 40% der aktiven Zentren sollten den enzymatischen Umsatz noch katalysieren. Verdoppelt man die Menge des zugegebenen DEPC (67% der Molarität des RdpA), so wird ein Aktivitätsverlust von 94% beobachtet. Der Aktivitätsverlust durch die Zugabe von DEPC ist nicht stöchiometrisch. Es wird mehr Enzym inaktiviert als erwartet, d.h., allein durch die Einwirkung der Inkubationsbedingungen auf das Enzym muss bereits 30% der Spaltungsaktivität verlorengehen.

In Abbildung 27 konnte gezeigt werden, dass sich ein Verlust von Enzymaktivität direkt proportional zur Verringerung der α-KG-Bindekapazität verhält. Völlig aktives Enzym zeigt im linearen Plot einen Anstieg von 1,03; bei Einsatz des zu 60% inaktivierten RdpA-Präparates beträgt der Anstieg der Geraden 0,46, etwa 43% des völlig aktiven Enzyms. Eine ähnlich hohe Korrelation wurde bei Inaktivierung durch Temperatur beobachtet: eine Inaktivierung um 67% hatte eine Verminderung der α-KG-Bindung von 66% zur Folge. Beim vergleichsweisen Einsatz von Rinderserumalbumin konnte keine α-KG-Bindung nachgewiesen werden. Die direkte Korrelation zwischen α-KG-Bindung und Enzymaktivität wurde genutzt, um Anteile

COR-AAD1-00003644
Bayer EX1008 (Part 7 of 9)

von aktivem Enzym in den jeweiligen Präparaten zu ermitteln. Dies ist ein wichtiges Kriterium, um die Wechselzahl exakt bestimmen zu können.

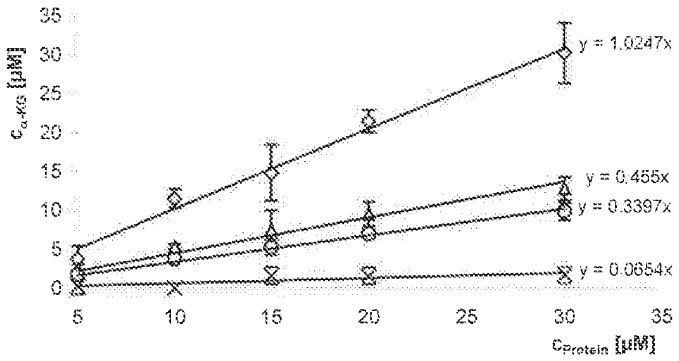


Abbildung 27: Beziehung zwischen α-KG-Bindung und eingesetzter Proteinmenge, Enzymaktivität für Enzympräparate mit unterschiedlicher spezifischer Aktivität RdpA (◊), RdpA + DEPC-1 (Δ), RdpA + DEPC-2 (x) und RdpA + Temperatur (○)

In Tabelle 23 sind die über die α-KG-Bindung ermittelten Anteile von aktivem Enzym in den Enzympräparaten zusammengefasst.

Tabelle 23: Prozentuale Anteile an aktivem Enzym in verschiedenen Enzympräparaten von RdpA und SdpA

Enzym	[%]	Enzym	[%]	Enzym	[%]
$RdpA_{MC1}$-rec	98	$SdpA_{MC1}$-rec	89	$SdpA_{P230}$-1	5
$RdpA_{MC1}$	21	$SdpA_{MC1}$	70	$SdpA_{P230}$-1	8
$RdpA_{P230}$	55	$SdpA_{MC1}$-I1	40	$SdpA_{MH}$	11
$RdpA_{MH}$	9	$SdpA_{MC1}$-I2	35		

3.3.2 Substratverwertungsspektren

Bei der Reinigung der Phenoxypropionat-spaltenden Enzyme aus den Stämmen *Delftia acidovorans* MC1, *Rhodoferax* sp. P230 und *Sphingobium herbicidovorans* MH konnten Enzyme mit unterschiedlichen Substrat- und Enantiospezifitäten voneinander getrennt werden. Alle drei Stämme besitzen sowohl ein (R)- als auch ein (S)-spezifisches Enzym.

3.3.2.1 Die (R)-spezifischen Dioxygenasen

Die (R)-spezifischen Enzyme aller drei Stämme, einschließlich des rekombinanten $RdpA_{MC1}$-rec sind hochspezifisch für die (R)-Enantiomere der 2-Phenoxypropionate; (S)-Enantiomere werden nicht umgesetzt. Die betreffenden Enzyme spalten zu einem gewissen Maße aber auch Phenoxyacetate; Phenoxybutyrate werden nicht gespalten (Tabelle 24). Die höheren Umsatzraten für die 2-Phenoxypropionate im Vergleich zu den Phenoxyacetaten, wobei die 2,4-Dichlor-substituierten Verbindungen wiederum schneller gespalten werden als die 4-Chlor-2-methyl-Verbindungen, sind ebenfalls allen RdpA-Enzymen gemeinsam. Unabhän-

COR-AAD1-00003645
Bayer EX1008 (Part 7 of 9)

gig von diesen grundsätzlichen Aktivitätskriterien wird die Aktivität von den Substituenten beeinflusst. 2,4-dichlorierte Derivate werden mit höherer Rate gespalten als 4-Chlor-2-methyl-Derivate. Unsubstituierte Phenoxyalkanoate sind schlechte Substrate, so werden Substrate ohne Substituenten nicht oder nur sehr schlecht (Phenoxyacetat) umgesetzt, Substrate ohne Chlor an Position 4 des aromatischen Ringes werden ebenfalls nur sehr schlecht verwertet. Die Abwesenheit eines Substituenten an der Position 2 hat dagegen nur einen geringen Einfluss auf die Spaltbarkeit der Verbindung. 3-Phenoxypropionat wird nicht umgesetzt.

Tabelle 24: Relative spezifische Aktivitäten der RdpA-Enzyme (nach HIC) aus MC1, P230 und MH sowie des $RdpA_{MC1}$-rec für verschiedene Phenoxyalkanoate Alle Herbizide außer den (S)-Enantiomeren wurden in einer Konzentration von 1 mM eingesetzt, (S)-Enantiomere lagen in einer Konzentration von 0,5 mM, α-KG von 1 mM im Reaktionsansatz vor. Die Aktivität für (R)-DP wurde eins gesetzt.

Substrat	$RdpA_{MC1}$	$RdpA_{P230}$	$RdpA_{MH}$	$RdpA_{MC1}$-rec
(R)-DP	1,00	1,00	1,00	1,00
(R)-MCPP	0,72	0,73	0,73	0,73
(S)-DP	-	-	-	-
(S)-MCPP	-	-	-	-
2,4-D	0,15	0,27	0,12	0,11
MCPA	0,11	0,23	0,08	0,09
2,4-DB	-	-	-	-
MCPB	-	-	-	-
Phenoxyacetat	0,02	0,01	0,01	0,01
3-Phenoxypropionat	-	-	-	-
(R,S)-2-(4-Chlorphenoxy)propionat	0,51	0,50	0,48	0,50
(R,S)-2-(m-Chlorphenoxy)propionat	0,06	0,09	0,06	0,07

Obwohl sich die Enzyme der drei Stämme in ihrer Primärstruktur nicht unterscheiden, zeigen sie signifikante Unterschiede in den Aktivitäten zur Spaltung der Phenoxyacetate. Die RdpA-Enzyme aus MC1, MH und das rekombinante RdpA spalten die Phenoxyacetate mit 10-15% der Aktivität für (R)-DP. Das $RdpA_{P230}$ weist unter Substratsättigung jedoch die doppelte Umsatzrate, nämlich etwa 25% auf.

Für das zweite Substrat, das α-KG, zeigen alle RdpA-Enzyme eine hohe Spezifität, andere α-Ketosäuren, z.B. Pyruvat, α-Ketobutyrat oder α-Ketovaleriat, dienen nicht als Substrate.

3.3.2.2 Die (S)-spezifischen Dioxygenasen

Die Substratverwertungsspektren der (S)-spezifischen Enzyme sind sehr unterschiedlich. Allen untersuchten SdpA-Enzymen gemeinsam ist, dass sie bevorzugt (S)-Enantiomere der 2-Phenoxypropionate, nicht aber 3-Phenoxypropionate spalten (Tabelle 25). $SdpA_{MC1}$ spaltet (S)-DP bei Substratsättigung mit einer höheren Umsatzrate als (S)-MCPP, bei den SdpA-Enzymen aus P230 und MH ist es genau umgekehrt. Das $SdpA_{MC1}$ spaltet auch Phenoxyace-

COR-AAD1-00003646
Bayer EX1008 (Part 7 of 9)

tat-Derivate mit hoher Rate: 2,4-D wird mit 35% und MCPA sogar mit 45% der Spaltaktivität für (S)-DP umgesetzt. Auch das SdpA-Enzym aus MH ist in der Lage, die Phenoxyacetate als Substrate zu verwerten, die relativen Spaltungsaktivitäten liegen zwischen 17 und 28%. Im Gegensatz zu den RdpA-Enzymen werden im Falle der Phenoxyacetate die 4-Chlor-2-methyl-substituierten Herbizide besser umgesetzt als die 2,4-dichlorierten Substrate. Die Phenoxyacetate werden im Gegensatz zu $SdpA_{MC1}$ und $SdpA_{P230}$ von den SdpA-Enzymen aus P230 nicht gespalten. Unsubstituierte Herbizide werden von allen betrachteten SdpA-Enzymen nur in sehr geringem Umfang umgesetzt.

Tabelle 25: Relative Spaltaktivitäten der SdpA-Enzyme (HIC) aus MC1, P230 und MH sowie des $SdpA_{MC1}$-rec bezüglich des Phenoxyalkanoats Alle Herbizide außer den (S)-Enantiomeren wurden in einer Konzentration von 1 mM eingesetzt, (S)-Enantiomere lagen in einer Konzentration von 0,5 mM, α-KG von 1 mM im Reaktionsansatz vor. *p*-CPP = (R,S)-2-(4-Chlorphenoxy)propionat; *m*-CPP = (R,S)-2-(*m*-Chlorphenoxy)-propionat, 3-PP = 3-Phenoxypropionat. Die Aktivität für (S)-DP wurde 1 gesetzt.

Substrat	$SdpA_{MC1}$	$SdpA_{P230}$-1	$SdpA_{P230}$-2	$SdpA_{MH}$	$SdpA_{MC1}$-rec
(R)-DP	-	-	-	-	-
(R)-MCPP	-	-	-	-	-
(S)-DP	1,00	1,00	1,00	1,00	1,00
(S)-MCPP	0,52	2,60	2,26	2,31	0,50
2,4-D	0,35	-	-	0,17	0,35
MCPA	0,45	-	-	0,28	0,48
2,4-DB	-	-	-	-	-
MCPB	-	-	-	-	-
Phenoxyacetat	0,04	-	-	0,01	0,04
3-PP	-	-	-	-	-
p-CPP	0,53	0,29	0,25	0,17	0,54
m-CPP	0,28	0,67	0,65	-	0,30

Auffällig ist, dass die SdpA-Enzyme aus P230 im Gegensatz zu den SdpA-Enzymen aus MC1, MH und den RdpA-Enzymen, monosubstituierte Substrate mit Chlor in *meta*-Position am aromatischen Ring besser spalten können, als solche mit Chlor-Substituenten in *para*-Position. Andere α-Ketosäuren als α-Ketoglutarat dienen in allen untersuchten SdpA-Enzymen wiederum nicht als Substrat.

3.3.3 Enzymstabilität und Reaktionsordnung

Bei der untersuchten Enzymreaktion handelt es sich um eine Mehrsubstratreaktion vom Typ:

$$A + B + C \underset{k_2}{\overset{k_1}{\rightleftharpoons}} P + Q + R + S$$

Gleichung 6: Allgemeine Reaktionsgleichung Phenoxypropionat-spaltender Enzyme A: Phenoxyalkanoat, B: α-Ketoglutarat, C: O_2, P: 2,4-Dichlorphenol (DCP) bzw. 2-Methyl-4-chlorphenol (MCP), Q: 2-Oxoalkanoat, R: CO_2, S: Succinat

COR-AAD1-00003647
Bayer EX1008 (Part 7 of 9)

Es konnten für die untersuchten Enzyme nur die Hin-, nicht aber die Rückreaktionen nachgewiesen werden; k_2 ist also für diesen enzymatischen Umsatz sehr klein. Die Größen der Geschwindigkeitskonstanten sind bei Mehrsubstratreaktionen zumeist von der Änderung der Konzentrationen aller Ausgangsstoffe oder Produkte abhängig. Die Geschwindigkeitsgleichung für die Hinreaktion ist in Gleichung 7 dargestellt.

$$v = -\frac{d[A]}{dt} = -\frac{d[B]}{dt} = -\frac{d[C]}{dt} = \frac{d[P]}{dt} = \frac{d[Q]}{dt} = \frac{d[R]}{dt} = \frac{d[S]}{dt} = k_1[A][B][C] = k_1[A]^3 = k_1[B]^3 = k_1[C]^3$$

Gleichung 7: Geschwindigkeitsgleichung für die Hinreaktion Phenoxyalkanoat-spaltender Enzyme A: Phenoxyalkanoat B: α-Ketoglutarat, C: O_2, P: DCP bzw. MCP, Q: 2-Oxoalkanoat, R: CO_2, S: Succinat

Die Hinreaktion ist eine Reaktion dritter Ordnung, bei der die Geschwindigkeitskonstante bestimmt werden kann, wenn die Umsatzgeschwindigkeit v und die zeitlichen Änderungen der Konzentration aller drei Ausgangsstoffe (A, B, C) bekannt sind. Da die Ausgangsstoffe in einem stöchiometrischen Verhältnis von eins umgesetzt werden, ist der Betrag der zeitlichen Abnahme der Konzentrationen für alle drei Ausgangsstoffe identisch, es muss also nur der Umsatz eines Stoffes verfolgt werden.

Für die Ermittlung von kinetischen Konstanten unter Verwendung der Gesetzmäßigkeiten von Einsubstratreaktionen ist es notwendig, eine Reaktion erster Ordnung vorliegen zu haben, d.h. die Umsatzrate muss und darf nur von der Konzentration eines Ausgangsstoffes abhängig sein. Um dies in Näherung zu erreichen, wurden die Konzentrationen von zwei Reaktionspartnern so gewählt, dass sie sich während der Reaktion praktisch nicht ändern. Sie wurden deshalb so gewählt, dass im Reaktionsansatz, je nach Experiment, ein großer Überschuss von zwei Reaktanten vorlag, so dass sich während des Umsatzes nur die Konzentration eines Ausgangsstoffes merklich ändert. Unter diesen Vorraussetzungen ergibt sich eine stark vereinfachte Geschwindigkeitsgleichung, die *pseudo-erster* Ordnung ist (Gleichung 8).

$$v = k_1[A][B]_0[C]_0 = k_1'[A]$$

Gleichung 8: Geschwindigkeitsgleichung *pseudo-erster* Ordnung für die Reaktion Phenoxypropionat-spaltender Enzyme A: Phenoxyalkanoat, B: α-Ketoglutarat, C: O_2, P: DCP bzw. MCP, Q: 2-Oxoalkanoat, R: CO_2, S: Succinat

Eine Reaktionskinetik nach Gleichung 8 lässt sich durch halblogarithmische Auftragung linearisieren (Gleichung 9).

$$-\int_{A_0}^{A}\frac{d[A]}{[A]} = \int_{t_0}^{t} k_1' dt \qquad \ln[A] = \ln[A]_0 - k_1' t$$

Gleichung 9: Herleitung der integrierten Form der vereinfachten Geschwindigkeitsgleichung

In Abbildung 28A ist der zeitliche Verlauf der DCP-Bildung bei der Spaltung der Enantiomeren des Dichlorprop durch die Enzyme $RdpA_{MC1}$ und $SdpA_{MC1}$ dargestellt. In den ersten Mi-

COR-AAD1-00003648
Bayer EX1008 (Part 7 of 9)

nuten nimmt die DCP-Konzentration zunächst bei beiden Enzymen linear zu, dann wird die Umsatzgeschwindigkeit der Enzyme kleiner und sinkt schließlich fast auf Null ab. Ein vollständiger Umsatz des Substrates wurde nicht erreicht. Dieser Verlauf der Produktbildung ist für alle eingesetzten Substratkonzentrationen zu beobachten. Nach 2000-4000 Umsätzen am aktiven Zentrum verliert das Enzym komplett seine Aktivität. Ein Inaktivierungseffekt durch Verdünnung als Grund für den Verlust von Enzymaktivität kann ausgeschlossen werden, da der Kurvenverlauf unabhängig von der eingesetzten Enzymkonzentration auftrat. Ebenso konnte eine Verknappung von Substraten wie Sauerstoff und α-KG als Inaktivierungsgrund ausgeschlossen werden. Eine Erhöhung der Substratkonzentration führt zu einer Kurve mit analogem Verlauf; wieder nimmt die DCP-Konzentration zunächst linear zu und bleibt dann nach etwa 2000-4000 Umsätzen pro aktivem Zentrum im Ansatz konstant. Eine Verknappung an Ascorbat kann aufgrund dieser Erkenntnis ausgeschlossen werden, da erstens Ascorbat im Überschuss (200 µM) im Reaktionsansatz vorlag, und zweitens eine Ascorbat-Oxidation zeitabhängig und unabhängig von der Substratkonzentration sein sollte. Der Einsatz von einer höheren Substratkonzentration führt jedoch zu einem schnelleren Umsatz und damit zu einer kürzeren Zeit bis zum Erreichen der Inaktivierung des Enzyms.

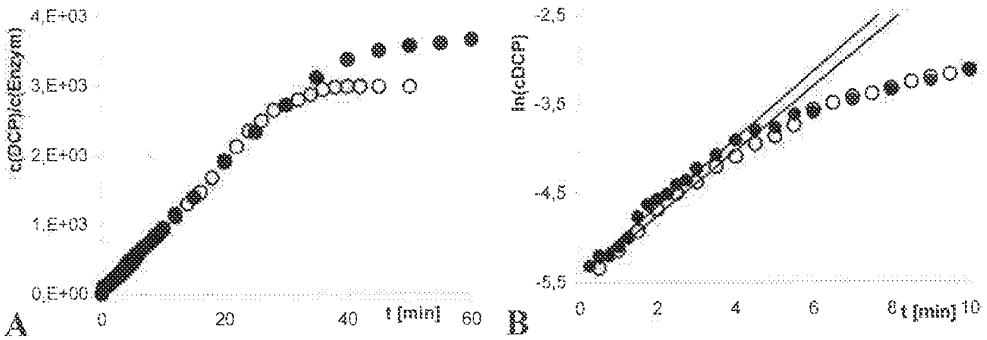


Abbildung 28: Zeitlicher Verlauf der Produktbildung (DCP) beim enzymatischen Umsatz von (R)-DP durch $RdpA_{MC1}$ (o) und von (S)-DP durch SdpA (•). A: c(DCP) = f(t), B: ln(cDCP) = f(t) es wurden 10 µM Dichlorprop, 1 mM α-KG, 200 µM Fe(II) und 200 µM Ascorbat eingesetzt, die eingesetzten Enzyme entsprachen dem Reinheitsgrad nach HIC, 1,7 mg/l $RdpA_{MC1}$, 1,5 mg/l $SdpA_{MC1}$ (die Enzymmenge wurde durch ihr α-KG-Bindevermögen bestimmt), die Sauerstoffkonzentration nahm während der Reaktion von 1 mM auf 0,8 mM ab.

Die lineare Abhängigkeit der Produktbildung von der Zeit in den ersten Minuten deutet eigentlich auf eine Reaktion nullter Ordnung hin, die Umsatzrate des Enzyms scheint unabhängig von der Substratkonzentration. Dies ist jedoch nicht der Fall. Eine Erhöhung der Substratkonzentration im Testansatz führt auch zur Erhöhung der Umsatzraten. Der Anstieg der Kurve kann somit also nicht wirklich linearer Natur sein, vielmehr handelt es sich, da lediglich 1%

COR-AAD1-00003649
Bayer EX1008 (Part 7 of 9)

des Substrates umgesetzt wurde, um einen kleinen Ausschnitt einer hyperbolen Produktbildungskurve erster Ordnung.

Für die Reaktionen des $RdpA_{MCI}$ und des $SdpA_{MCI}$ konnte die Reaktion *pseudo-erster* Ordnung nur wenige Minuten gewährleistet werden (Abbildung 28B). Bereits nach vier Minuten blieb die Geschwindigkeitskonstante nicht mehr konstant, sondern nahm für beide Enzyme über die Zeit stark ab, bis die Reaktion zum Erliegen kam. Die Geschwindigkeitskonstante der Hinreaktion (k_1) konnte in den ersten vier Minuten der Reaktion für das $RdpA_{MCI}$ auf 0,36 min^{-1} und für das $SdpA_{MCI}$ auf 0,38 min^{-1} bestimmt werden.

3.3.4 Kinetische Kennlinien

3.3.4.1 Die Kennlinien der (S)-spezifischen Dioxygenasen

3.3.4.1.1 Das $SdpA_{MCI}$

Das säulenchromatographisch gereinigte $SdpA_{MCI}$ (HIC) zeichnet sich hinsichtlich der eingesetzten Herbizide (S)-(DP), S)-MCPP, 2,4-D und MCPA durch komplexe kinetische Kennlinien aus (Abbildung 29). Die Zunahme der Enzymaktivität in Abhängigkeit von der Substratkonzentration erfolgt deutlich zweiphasig und zeigt im Falle der Phenoxypropionate eine ausgeprägte Substratüberschusshemmung. Bei dem Einsatz von Phenoxyacetaten als Substrat konnten im untersuchten Konzentrationsbereich dagegen keine derartigen Hemmungseffekte beobachtet werden. Die Ursache der komplexen Kinetik eines solchen Enzympräparates ist im Vorhandensein von multiplen Enzymformen begründet, die sich in ihren kinetischen Parametern unterscheiden.

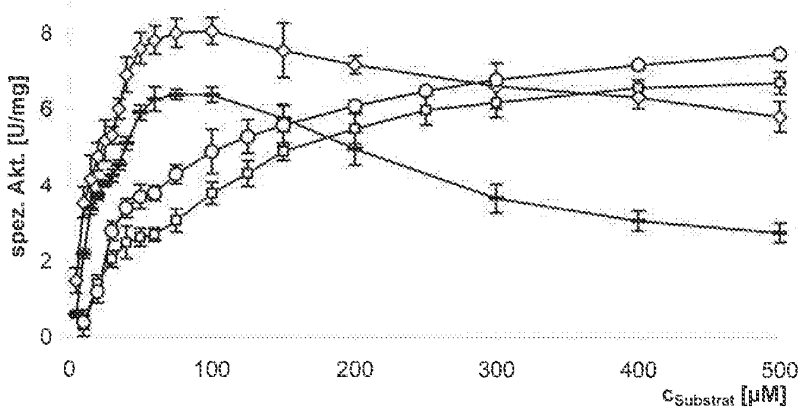


Abbildung 29: Kinetische Kennlinien des $SdpA_{MCI}$ für die Substrate (S)-DP(◊), (S)-MCPP (—), 2,4-D (□) und MCPA (○)

COR-AAD1-00003650
Bayer EX1008 (Part 7 of 9)

Die Abbildungen 30A und B zeigen die kinetischen Kennlinien der voneinander getrennten Enzymformen des $SdpA_{MCI}$ am Beispiel der Phenoxypropionate (Phenoxyacetate sind hier nicht dargestellt, zeigen aber das gleiche Bild). Es ist deutlich zu erkennen, dass sich die Kinetiken der beiden Enzympräparate sowohl in ihrem Anstieg als auch in ihrer Umsatzgeschwindigkeit signifikant voneinander unterscheiden. Die Zunahme der Enzymaktivität in Abhängigkeit von der Substratkonzentration erfolgt in beiden Fällen stetig, eine Zweiphasigkeit kann nicht beobachtet werden. Wiederum zeigt sich für die Phenoxypropionate eine Substratüberschusshemmung. Die Kennlinien des rekombinanten $SdpA_{MCI}$, die zum Vergleich angeführt wurden, decken sich für alle Herbizide gut mit denen der Enzymform $SdpA_{MCI}$-II.
Linearisierende Verfahren zur Auswertung der Kennlinien sind in den Abbildungen 30C und D exemplarisch für das rekombinante $SdpA_{MCI}$ dargestellt. Die kinetischen Kennlinien zeigen in beiden Darstellungsformen, sowohl im Lineweaver-Burk- als auch im Hill-Plot, keine durchgängigen Geraden über den Konzentrationsbereich, was auf ein Abweichen von der Michaelis-Menten-Kinetik hindeutet. In der Lineweaver-Burk-Darstellung (Abbildung 30C) ist ein vierphasiges Verhalten für den (S)-DP Umsatz zu erkennen. Bei kleinen Substratkonzentrationen fällt die Kurve zunächst mit einem geringen Anstieg ab, gefolgt wird diese Phase von einem steileren Abfall der Kurve. Anschließend, bei relativ hohen Substratkonzentrationen flacht die Kurve ab, so dass kaum noch ein Anstieg zu verzeichnen ist. Durch die einsetzende Substratüberschusshemmung steigt die Kurve dann bei sehr hohen Substratkonzentrationen wieder steil an. Der Hill-Plot ist gleichermaßen komplex. Linearität, wie für eine Michaelis-Menten-Kinetik relevant, ist hier nicht erfüllt (Abbildung 30D). Vielmehr zeigt sich das Bild eines kooperativen Enzyms mit sigmoidaler Kinetik. Einen ähnlichen Kurvenverlauf kann man auch bei entsprechender Darstellung der kinetischen Daten der $SdpA_{MCI}$-Enzymformen für alle entsprechenden Herbizide feststellen. Der Tatsache einer offensichtlichen Kooperativität der Enzymreaktion folgend, erhält man eine bessere Angleichung der Daten, wenn man den Formalismus für eine sigmoidale Kinetik zugrunde legt anstatt den für einen hyperbolen Kurvenzug (Abbildung 30E).
Betrachtet man die Abhängigkeit der Umsatzgeschwindigkeit des $SdpA_{MCI}$ von den anderen an der Reaktion beteiligten Substraten bzw. Reaktionskomponenten (Abbildung 30F), so ist festzustellen, dass der Kurvenverlauf auch bei Einsatz des HIC-Präparates, d.h. des Enzymformen-Gemisches, stetig und ohne die Ausprägung von Plateaus verläuft. Für Sauerstoff beobachtet man eine leichte Substratüberschuss-Hemmung. Dieser Effekt wurde im Falle von α-KG bzw. Fe(II) nicht festgestellt. Eine Behandlung der Daten mit verschiedenen Modellen zeigt wiederum, dass die Abhängigkeit von der Konzentration eher sigmoidal als hyperbol ist.

COR-AAD1-00003651
Bayer EX1008 (Part 7 of 9)

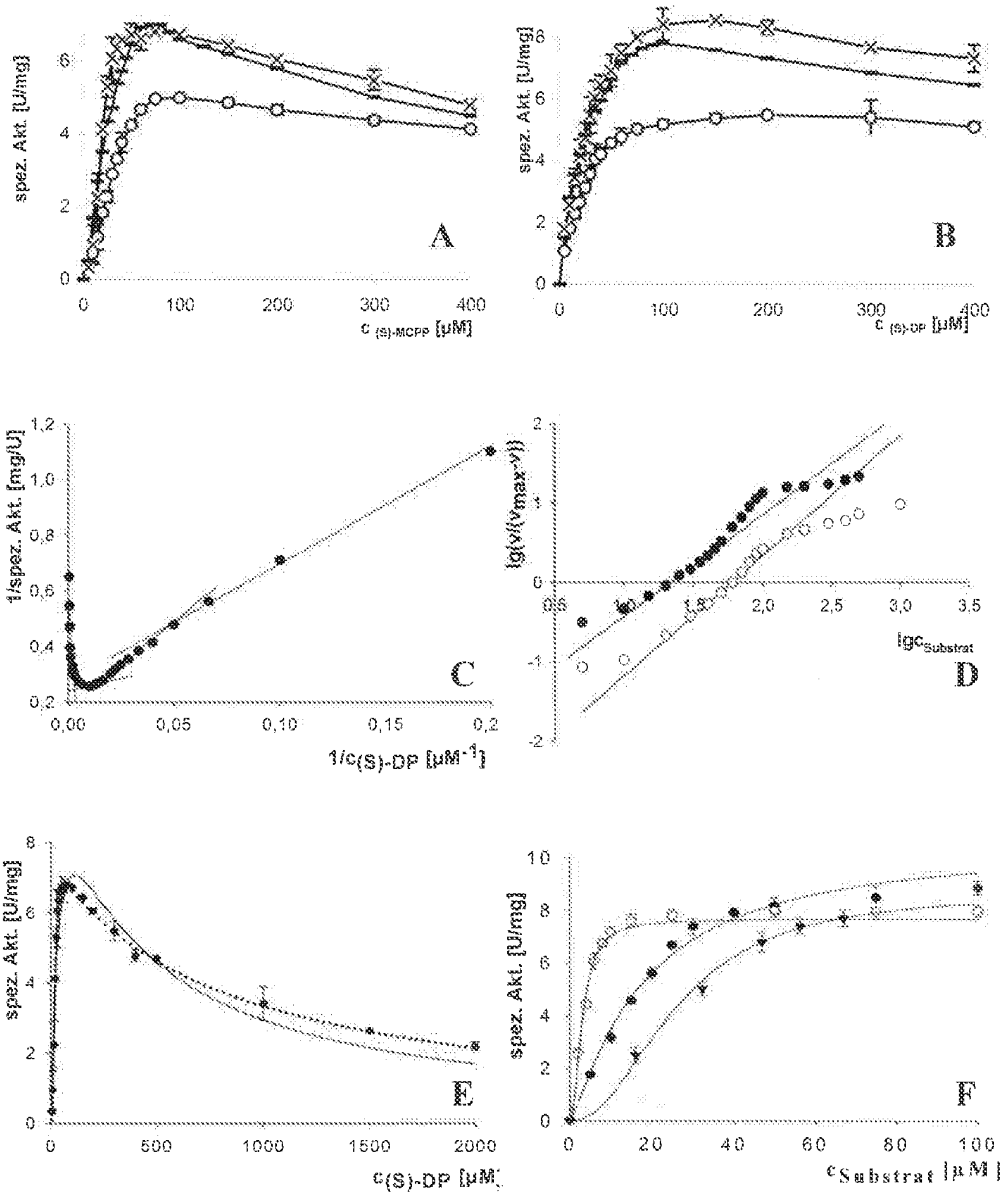


Abbildung 30: Kinetische Darstellungsformen von Messdaten A: Kinetische Kennlinien der $SdpA_{MCI}$-I1 (x), –I2 (o) und $SdpA_{MCI}$-rec (---) in Abhängigkeit von der (S)-MCPP-Konzentration, **B:** Kinetische Kennlinien der $SdpA_{MCI}$-I1 (x), –I2 (o) und $SdpA_{MCI}$-rec (---) in Abhängigkeit von der (S)-DP-Konzentration, **C:** Lineweaver-Burk-Darstellung der Kennlinien des $SdpA_{MCI}$-rec (•), **D:** Hill-Diagramm der Kennlinien des $SdpA_{MCI}$-rec (•) und $RdpA_{MCI}$-rec (o), **E:** Abhängigkeiten der Enzymaktivität des $SdpA_{MCI}$-rec von der (S)-DP-Konzentration, gestrichelt: sigmoidaler Plot, durchgezogene Linie: hyperboler Plot, **F:** Abhängigkeiten der Enzymaktivität des $SdpA_{MCI}$-rec von der Sauerstoff-(○), α-KG- (●) und Fe(II)-Konzentration (▼).

COR-AAD1-00003652
Bayer EX1008 (Part 7 of 9)

3.3.4.1.2 Die Kennlinien der SdpA-Enzyme aus P230 und MH

Für (S)-DP als Substrat weisen die kinetischen Kennlinien der beiden (S)-spezifischen Enzyme aus *Rhodoferax* sp. P230 im Gegensatz zu dem entsprechenden Enzym aus *Delftia acidovorans* MC1 ($SdpA_{MC1}$) keine Plateaubildung auf. Die Umsatzgeschwindigkeiten steigen stetig und zeichnen sich bei erhöhten Substratkonzentrationen durch eine Überschusshemmung aus (Abbildung 31A). Im Verlauf der Kennlinien ist deutlich zu erkennen, dass sich die beiden Enzyme durch unterschiedliche kinetische Parameter auszeichnen. Mit (S)-DP als Substrat wurde für beide Enzyme eine sigmoidale Abhängigkeit gefunden.

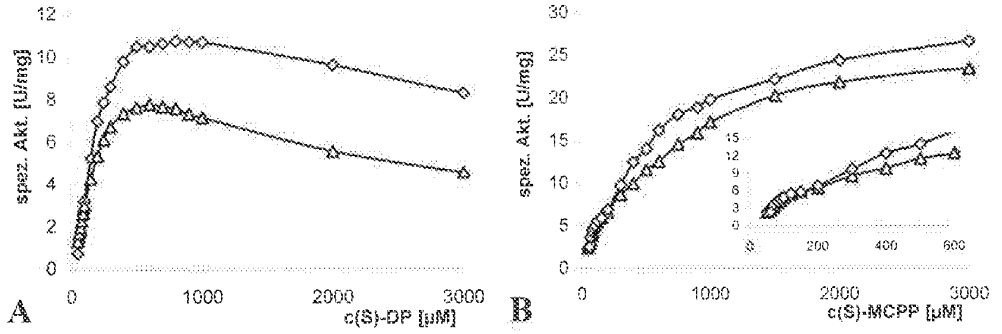


Abbildung 31: Kinetische Kennlinien der (S)-spezifischen Enzyme aus Rhodoferax sp. P230 A: (S)-DP, B: (S)-MCPP, $SdpA_{P230}$-1 (◊).$SdpA_{P230}$-2 (Δ) multipliziert mit 2

Beim Umsatz von (S)-MCPP deutet sich dagegen ein zweiphasiger Verlauf in den kinetischen Kennlinien an, wie aus der größeren Auflösung deutlich wird (Abbildung 31B). Bei einer Substratkonzentration von 90-150 µM ist hier ein ausgeprägtes Plateau zu erkennen. Im Falle des Methyl-Chlor-Derivates der Phenoxypropionate kommt es im untersuchten Bereich zu keiner Substratüberschusshemmung. Für beide Phenoxypropionate weist das $SdpA_{P230}$-1 im Vergleich zum $SdpA_{P230}$-2 die höheren Umsatzraten auf.

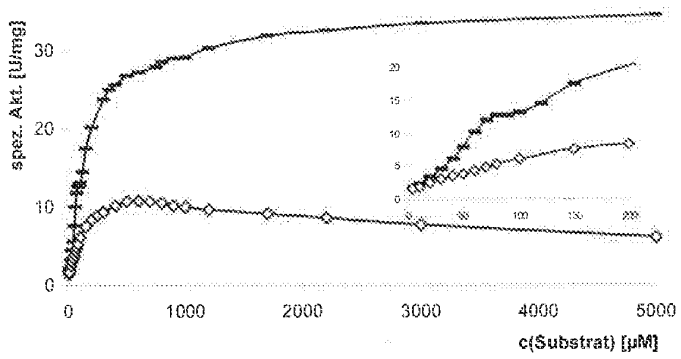


Abbildung 32: Kinetische Kennlinien des SdpA aus *Sphingobium herbicidovorans* MH (S)-DP (◊), (S)-MCPP (—)

COR-AAD1-00003653
Bayer EX1008 (Part 7 of 9)

Die Kennlinien des $SdpA_{MH}$ verhalten sich sehr ähnlich zu denen aus P230. Im Falle von (S)-DP ist ein stetiger Anstieg gefolgt von einem Abfall der Reaktionsgeschwindigkeit zu beobachten. Mit (S)-MCPP als Substrat ist der Anstieg der Umsatzraten von einem Plateau unterbrochen, dies wird wiederum durch eine erhöhte Auflösung deutlich (Abbildung 32), Substratüberschusshemmung wurde nicht beobachtet. Für keines der Herbizide war ein sigmoidaler Kurvenverlauf eindeutig nachzuweisen.

3.3.4.2 Die Kennlinien der (R)-spezifischen Dioxygenasen

In Abbildung 33A sind die Kennlinien der RdpA-Enzyme bezüglich des (R)-DP dargestellt. Die nativen Enzyme aus MC1, P230 und MH zeichnen sich allesamt durch einen zweiphasigen Anstieg aus. Bei einer (R)-DP-Konzentration zwischen 25-60 µM kommt es zu einer Plateau-Bildung. Die Kennlinien des $RdpA_{MC1}$ stimmen sehr gut mit der des $RdpA_{MH}$ überein. Die Umsatzraten des rekombinanten Proteins steigen im Gegensatz zu den nativen Enzymen stetig an. Die Kennlinien bezüglich des (R)-MCPP (Daten nicht dargestellt) verhalten sich analog zu dem für (R)-DP dargestellten Bild. Für keines der Herbizide konnte im untersuchten Bereich eine Substratüberschusshemmung nachgewiesen werden.

Wie für die SdpA-Enzyme konnte auch für die RdpA-Enzyme ein sigmoidaler Kurvenverlauf nachgewiesen werden, was in den Abbildungen 30D-F exemplarisch für das $RdpA_{MC1}$-rec dargestellt wurde. Die (R)-spezifischen Enzymformen aus MC1 konnten zwar nicht komplett voneinander getrennt und in reiner Form dargestellt werden, aber es ist gelungen, Anreicherungspräparate von den $RdpA_{MC1}$-Enzymformen I1 und I3 zu erhalten. Die kinetischen Kennlinien dieser Formen bezüglich des (R)-DP und des 2,4-D sind in den Abbildungen 33C und D zu sehen. Es ist zu bemerken, dass die Kennlinien nicht stetig, sondern unter Ausbildung eines Plateaus ansteigen. Wie bei dem $RdpA_{MC1}$-Präparat nach HIC kann auch für die Enzymformen keine Substratüberschusshemmung nachgewiesen werden.

In Abbildung 33B sind die Abhängigkeiten der Umsatzraten der RdpA-Enzyme aus MC1, P230, MH und des rekombinanten RdpA von der 2,4-D-Konzentration dargestellt. Sowohl für das $RdpA_{P230}$ als auch für das rekombinante RdpA kann deutlich eine stetige Zunahme der Umsatzgeschwindigkeit mit steigender 2,4-D-Konzentration konstatiert werden. Die Kinetiken der Enzyme aus MC1 und MH weisen im Gegensatz dazu im Bereich von 250–400 µM 2,4-D ein deutlich ausgeprägtes Plateau auf, die Kennlinien der beiden Enzyme sind fast identisch. Die Kinetiken des MCPA-Umsatzes (nicht dargestellt) zeigen ein ähnliches Bild wie die der 2,4-D-Spaltung. Für Sauerstoff, α-KG und Fe(II) wurden ebenso wie bei den SdpA-Enzymen stetige sigmoidale Kurvenverläufe gefunden (nicht dargestellt).

COR-AAD1-00003654
Bayer EX1008 (Part 7 of 9)

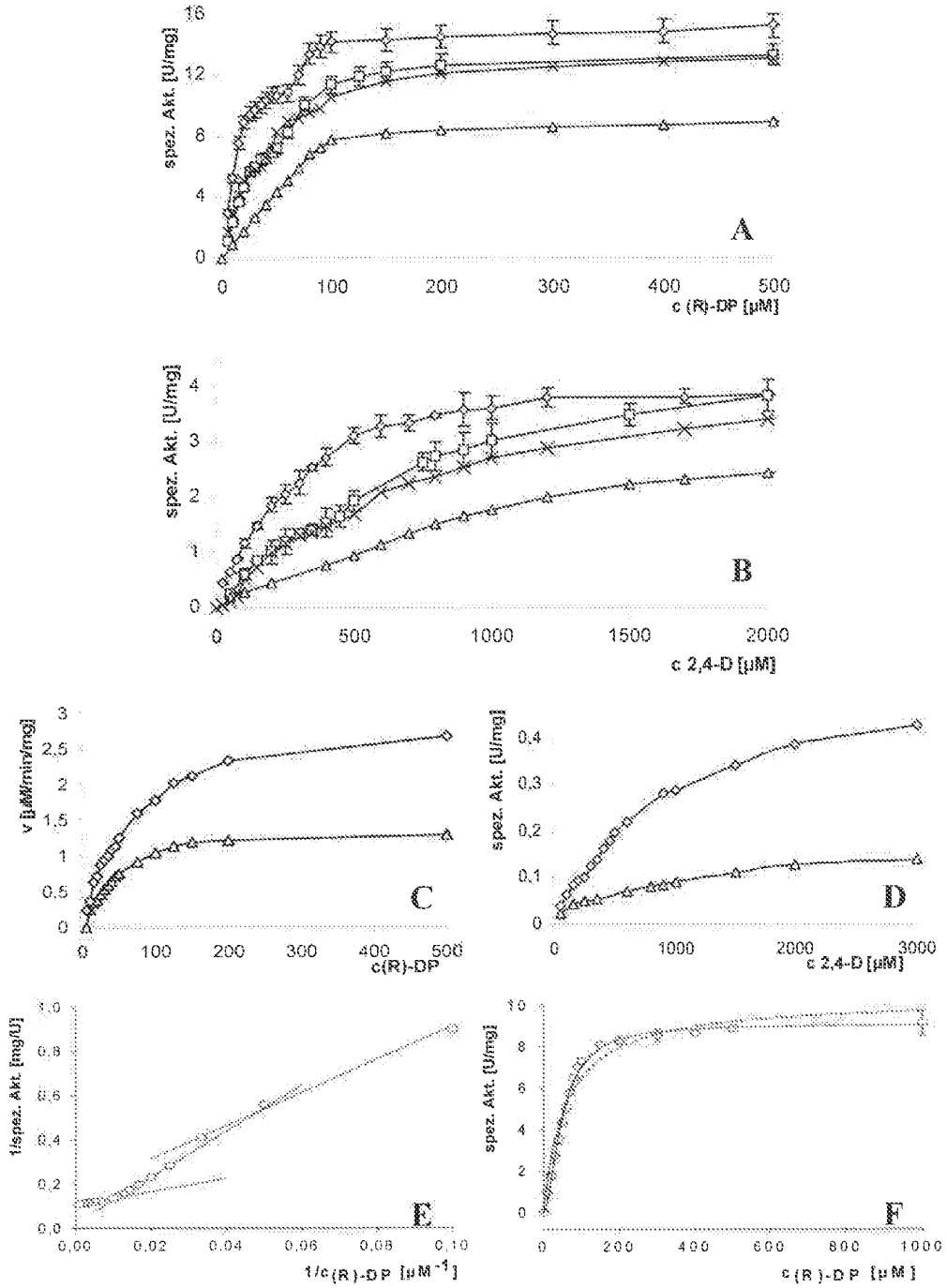


Abbildung 33: Kinetische Kennlinien der $RdpA_{MCI}$- (□), $RdpA_{P230}$- (◇) und $RdpA_{MH}$-Enzymformgemische (x) sowie des $RdpA_{MCI}$-rec (Δ) für (R)-DP (A) und (2,4-D (B) (Umsatzgeschwindigkeiten mal zwei für MCI, MH und rec); Kinetische Kennlinien der RdpA-Enzymformen I1 (◇) und I2 (Δ) bezüglich (R)-DP (C) und 2,4-D (D), E: Lineweaver-Burk-Darstellung der kinetischen Daten des $RdpA_{MCI}$-rec (○), F: kinetische Kennlinie des $RdpA_{MCI}$-rec (○) mit hyperbolem Plot (gepunktete Linie) und sigmoidalem Plot (durchgezogene Linie)

COR-AAD1-00003655
Bayer EX1008 (Part 7 of 9)

3.3.5 Kinetische Konstanten

Der K_M-Wert charakterisiert die Substratkonzentration, bei der das Enzym die halbmaximale Reaktionsgeschwindigkeit erreicht. Er ist ein Maß für die Affinität des Enzyms zu einem Substrat. Je kleiner der K_M-Wert ist, desto affiner ist das Enzym für den Reaktionspartner. k_{kat} gibt die Anzahl der Substratumsätze pro aktiven Zentrums im Enzym in einer bestimmten Zeiteinheit an. Je größer k_{kat} ist, desto schneller wird ein Stoff von dem Protein umgesetzt. Der Quotient aus k_{kat} und K_M wird als katalytische Effizienz bezeichnet und gilt als Maß der Substratspezifität. Hohe Werte sind ein Hinweis auf eine hohe Substratspezifität des Enzyms.

3.3.5.1 Konstanten der (S)-spezifischen Enzyme

In Tabelle 26 wurden die kinetischen Konstanten der SdpA-Proteine zusammengefasst. Die Konstanten sind hierbei als apparente Werte zu verstehen; sie wurden wegen der teilweise unsteten Zunahme der Reaktionsgeschwindigkeit (3.3.4.1) mit steigender Substratkonzentration, d.h. wegen des Auftretens von Plateaus, als *„Overall Kinetik"* bestimmt und spiegeln daher die Summe der Eigenschaften der Enzymformen im Gemisch wider.

So unterschiedlich die SdpA-Enzyme in ihren Substratverwertungsspektren (3.3.2.2) und kinetischen Kennlinien (3.3.4.1) sind, so verschieden stellen sich auch ihre kinetischen Konstanten dar. Die Herbizide (S)-DP und (S)-MCPP werden von den Enzymen aus MC1 und MH mit jeweils in etwa identischen K_M-Werten gebunden. Die K_M-Werte des Enzyms aus MH sind allerdings etwa 5mal so hoch, wie die des Stammes MC1. Im Gegensatz dazu werden diese beiden Herbizide von den (S)-spezifischen Enzymen des P230 mit stark unterschiedlichen Affinitäten gebunden, der K_M-Wert für (S)-DP ist mit 200 µM etwa 3,6mal kleiner als der für (S)-MCPP. Die Phenoxyacetat-Derivate werden von den SdpA-Enzymen aus MC1 und MH ebenfalls gespalten, dabei sind die K_M-Werte des $SdpA_{MC1}$ wie schon für die Phenoxypropionate gesehen, etwa 5mal niedriger als beim $SdpA_{MH}$. Bemerkenswert ist, dass die Enzyme aus dem Stamm P230 Phenoxyacetate nicht umsetzen können. Nach dieser Übersicht zeigt das $SdpA_{MC1}$ für alle Herbizide die höchsten Affinitäten. Die beiden (S)-spezifischen Enzyme aus P230 unterscheiden sich in ihren Affinitäten zu den Herbiziden kaum. Bei den Wechselzahlen zeigt sich ein anderes Bild. Sind die Affinitäten der $SdpA_{P230}$-Enzyme zu den jeweiligen Herbiziden noch nahezu identisch, so unterscheiden sich ihre Wechselzahlen signifikant voneinander. Das $SdpA_{P230}$-1 setzt die beiden Phenoxypropionat-Herbizide mit der doppelten Geschwindigkeit um wie das $SdpA_{P230}$-2. Während die SdpA-Enzyme aus P230 und MH das (S)-MCPP mit etwa 2,5fach höheren Wechselzahlen umsetzen als das (S)-DP, ist dies beim $SdpA_{MC1}$ genau umgekehrt. Die höchsten Umsatzraten für das

COR-AAD1-00003656
Bayer EX1008 (Part 7 of 9)

(S)-Enantiomer des 2,4-Dichlorphenoxypropionates werden vom $SdpA_{MC1}$ erreicht, für das (S)-MCPP jedoch von den Enzymen aus P230 und MH. Die Phenoxyacetate werden vom $SdpA_{MC1}$ mit höheren Wechselzahlen gespalten als vom $SdpA_{MH}$.

Des Weiteren unterscheiden sich die (S)-spezifischen Enzyme der drei Stämme durch ein unterschiedliches Verhalten bei hohen Substratkonzentrationen. Im Falle vom (S)-MCPP ist das Enzym aus MC1 das einzige, das sich im untersuchten Konzentrationsbereich durch Hemmkinetiken auszeichnet. Für (S)-DP zeigen dagegen alle untersuchten Enzyme eine Hemmkinetik, wobei das $SdpA_{MC1}$ den niedrigsten K_i für dieses Herbizid aufweist. Die Hemmkonstanten der anderen Enzyme liegen über denen des $SdpA_{MC1}$.

Die Affinitäten gegenüber dem zweiten Substrat, dem α-KG, sind bei den verschiedenen Enzymen nahezu identisch und liegen bei 18 µM. Der K_M-Wert für den Sauerstoff wurde nur für das $SdpA_{MC1}$ bestimmt, dieser liegt bei 29 µM, hier beobachtet man eine Überschusshemmung mit einem K_i-Wert von etwa 4500 µM. Dies sollte aber keine Rolle spielen, da wässrige Lösungen bei 30°C bereits bei einem Sauerstoffgehalt von 2000 µM gesättigt sind.

Für das $SdpA_{MC1}$ ist es gelungen, das Enzymformengemisch aufzulösen und einzelne Enzymformen voneinander zu trennen und zu analysieren. Diese zeigen kinetische Kennlinien mit signifikant unterschiedlichem Verlauf (3.3.4.1.1), und folglich unterscheiden sich die kinetischen Konstanten. Generell ist zu bemerken, dass sich dabei Unterschiede in den Affinitäten der Enzyme zu den Substraten geringer bemerkbar machen, als dies für die Umsatzraten festgestellt wird. Die Enzymform $SdpA_{MC1}$-f1 zeichnet sich für alle Substrate durch niedrigere K_M-Werte aus als die Form-f2. Die Unterschiede zwischen den Affinitäten liegen bei 25% für die Phenoxyacetate und bei 40% für das (S)-MCPP (Tabelle 26). Die Affinität zu den Substraten sinkt für beide Enzymformen in der Reihenfolge (S)-MCPP > (S)-DP > MCPA > 2,4-D. Damit binden 1.) die Phenoxypropionate affiner an das aktive Zentrum als die Phenoxyacetate und 2.) die 4-Chlor-2-methyl-Derivate besser als die 2,4-Dichlor-substituierten Verbindungen.

Die Umsatzraten des $SdpA_{MC1}$-f1 liegen ebenso wie die Affinitäten allesamt über denen der Form-f2, wobei die Unterschiede zwischen 20 und 100% liegen. Obwohl die Enzyme für (S)-DP einen höheren K_M-Wert als für (S)-MCPP aufweisen, wird dieses Substrat von beiden Enzymen mit der größten Umsatzrate gespalten, gefolgt von (S)-MCPP, MCPA und 2,4-D. Ein wesentlicher Unterschied zwischen den Enzymformen des MC1 zeigt sich beim Vergleich der k_{kat}/K_M-Werte. Dabei erkennt man, dass die Form f1 das Substrat (S)-MCPP nur mit 66% der relativen katalytischen Effizienz wie für das (S)-DP umsetzt. Für f2 sind dagegen die kata-

COR-AAD1-00003657
Bayer EX1008 (Part 7 of 9)

lytischen Effizienzen für beide Herbizide identisch; damit ist das (S)-Mecoprop für das $SdpA_{MC1}$-I2 ein kinetisch besseres Substrat als für I1. Ein ähnliches Profil ergibt sich für die Substrate 2,4-D und MCPA. Zusammenfassend ist zu bemerken, dass die Enzymform I1 sich also durch eine hohe Spezifität für das (S)-DP auszeichnet, die Form I2 weist eher ein breites Substratverwertungsspektrum auf.

Unterschiede in den beiden Enzymformen zeigen sich auch bei der Substratüberschusshemmung, die im Falle von I2 ausgeprägter ist (Tabelle 26). Für das (S)-MCPP unterscheiden sich die Substrathemmkonstanten kaum und für die Phenoxyacetate konnten keine nachgewiesen werden.

Vergleicht man die Ergebnisse in den Enzymformen von $SdpA_{MC1}$ mit denen des rekombinanten $SdpA_{MC1}$-rec, so zeigt sich, dass diese für I1 sowohl hinsichtlich der kinetischen Kennlinien als auch Konstanten mit dem überexprimierten Enzym am ähnlichsten sind.

3.3.5.2 Konstanten der (R)-spezifischen Enzyme

Die RdpA-Proteine der drei untersuchten Stämme, einschließlich des rekombinanten RdpA zeichnen sich durch eine identische Primärstruktur aus, was die Annahme nahelegt, dass sich die Enzyme aus kinetischer Sicht ebenfalls identisch verhalten sollten. Dies ist jedoch nicht durchgängig der Fall. Zwar erwiesen sich die RdpA-Enzyme aus MC1 und MH als kinetisch identisch, die kinetischen Parameter des Enzyms aus P230 und des rekombinanten RdpA weichen jedoch von denen des $RdpA_{MC1}$ und $RdpA_{MH}$ signifikant ab (Tabelle 27). Das $RdpA_{P230}$ zeichnet sich für alle getesteten Herbizide durch höhere Affinitäten und auch höhere Wechselzahlen aus. Die K_M-Werte sind dabei zwischen 30 und 60% niedriger als die korrespondierenden des $RdpA_{MC1}$, die Wechselzahlen übersteigen die des $RdpA_{MC1}$ um das 1,4-3fache. Der Vergleich zum rekombinanten RdpA zeigt, dass das Enzym aus P230 auch hier hinsichtlich K_M als auch k_{kat} besser ist.

Allen untersuchten RdpA-Enzymen ist gemeinsam, dass die Affinitäten zu den Herbiziden und die Wechselzahlen der Spaltung in der Reihenfolge (R)-DP > (R)-MCPP > MCPA > 2,4-D sinken. Bei Betrachtung der katalytischen Effizienz zeigt sich ein homogenes Bild für die Phenoxypropionate derart, dass (R)-MCPP durch die RdpA aller drei Stämme nur etwa 0,4mal so effizient gespalten wie (R)-DP. Letztere Enzyme spalten die Phenoxyacetate nur mit etwa 1% der Effizienz für (R)-DP, das $RdpA_{P230}$ noch mit 2,5%. Schaut man auf die

COR-AAD1-00003658
Bayer EX1008 (Part 7 of 9)

Tabelle 26: Kinetische Konstanten der (S)-spezifischen Enzyme aus MC1, P230 und MH Die Konstanten wurden aus dem sigmoidalem Plot berechnet. - = nicht aufgetreten

Enzym	*Substrat*	spez. Akt. [U/mg]	rel. spez. Akt.	K_M [µM]	k_{kat} [min^{-1}]	k_{kat}/K_M [$µM^{-1} \cdot min^{-1}$]	rel. K_M/k_{kat}	Hill-Koeff.	K_i [µM]
$SdpA_{MC1}$-rec	*(S)-DP*	22 ± 1	1	21 ± 2	704 ± 32	33,5	1	1,28	1250 ± 126
	(S)-MCPP	11 ± 2	0,5	18 ± 4	352 ± 64	19,6	0,59	2,88	782 ± 40
	2,4-D	7,6 ± 0,7	0,35	85 ± 8	243 ± 23	2,9	0,09	1,36	-
	MCPA	11,1 ± 1,9	0,48	47 ± 5	355 ± 61	7,6	0,23	1,66	-
$SdpA_{MC1}$	*(S)-DP*	19 ± 2	1	33 ± 3	607 ± 64	18,4	1	1,27	867 ± 130
	(S)-MCPP	9,9 ± 1,5	0,52	25 ± 5	316 ± 48	12,6	0,68	1,22	1145 ± 54
	2,4-D	6,7 ± 1,8	0,35	107 ± 12	213 ± 58	2	0,11	1,01	-
	MCPA	8,6 ± 3	0,45	47 ± 5	276 ± 96	5,9	0,32	1,05	-
$SdpA_{MC1}$-I1	*(S)-DP*	23,9 ± 3,1	1	26 ± 2	765 ± 99	29,4	1	1,25	1290 ± 94
	(S)-MCPP	10,8 ± 2,4	0,45	18 ± 2,5	347 ± 77	19,3	0,66	3,49	1064 ± 130
	2,4-D	7,7 ± 0,4	0,32	94 ± 15	245 ± 13	2,6	0,09	1,28	-
	MCPA	10,7 ± 1,5	0,45	39 ± 5	341 ± 48	8,7	0,3	1,4	-
$SdpA_{MC1}$-I2	*(S)-DP*	11,6 ± 1	1	36 ± 5	371 ± 32	10,3	1	1,31	802 ± 60
	(S)-MCPP	8,6 ± 1,6	0,74	29 ± 2	275 ± 51	9,5	0,92	2,13	1103 ± 131
	2,4-D	5,1 ± 0,5	0,44	125 ± 6	164 ± 16	1,3	0,13	1,29	-
	MCPA	5,9 ± 1,4	0,51	51 ± 7	188 ± 45	3,7	0,36	1,31	-
$SdpA_{P230}$-1	*(S)-DP*	13,2 ± 3	1	192 ± 6	440 ± 100	2,3	1	1,85	4950 ± 344
	(S)-MCPP	34,4 ± 8	2,6	735 ± 47	1146 ± 266	1,6	0,7	1	-
	2,4-D	-	-	-	-	-	-	-	-
	MCPA	-	-	-	-	-	-	-	-
$SdpA_{P230}$-2	*(S)-DP*	6,3 ± 1,1	1	230 ± 60	204 ± 36	0,89	1	1,42	1644 ± 66
	(S)-MCPP	14,2 ± 2,3	2,26	712 ± 89	454 ± 75	0,64	0,72	1	-
	2,4-D	-	-	-	-	-	-	-	-
	MCPA	-	-	-	-	-	-	-	-
$SdpA_{MH}$	*(S)-DP*	15 ± 1,7	1	151 ± 28	480 ± 54	3,18	1	1	3055 ± 479
	(S)-MCPP	34,6 ± 5,6	2,31	154 ± 8	1107 ± 179	7,19	2,26	1	-
	2,4-D	2,9 ± 0,4	0,17	570 ± 64	93 ± 13	0,16	0,05	1	-
	MCPA	4,2 ± 1	0,28	302 ± 39	134 ± 32	0,44	0,14	1	-

COR-AAD1-00003659

Bayer EX1008 (Part 7 of 9)

absoluten Werte, so wird offensichtlich, dass die Phenoxypropionate von $RdpA_{P230}$ etwa doppelt, die Phenoxyacetate sogar 8mal so effizient gespalten werden wie durch die RdpA-Enzyme aus MC1 und MH. Die Affinitäten der RdpA-Enzyme zu dem zweiten Substrat, dem α-KG, sind in allen drei Stämmen wiederum gleich; der K_M-Wert beträgt auch hier etwa 18 µM. Die Abhängigkeit von der Sauerstoffkonzentration wurde nur für das $RdpA_{MC1}$ untersucht, der K_M-Wert liegt bei 400 µM.

Die angereicherten Enzymformen I1 und I3 des $RdpA_{MC1}$ zeichnen sich durch identische K_M-Werte aus. Auch die relativen katalytischen Effizienzen verhalten sich zueinander sehr ähnlich. Absolute Wechselzahlen konnten aufgrund von zu geringen Proteinmengen nicht ermittelt werden.

3.3.6 Reaktionsmechanismus

Zur Ermittlung der Reaktionsmechanismen der Enzyme $SdpA_{MC1}$ und $RdpA_{MC1}$ wurden Zweisubstratkinetiken unter Variation der Substrate α-KG und Herbizid durchgeführt.

Die Primärauftragung der gewichteten Messdaten des Umsatzes von (S)-DP durch $SdpA_{MC1}$ bei Anwesenheit verschiedener α-KG-Konzentrationen ist in Abbildung 34 dargestellt. Diese zeigt, dass sowohl mit steigender (S)-DP- als auch α-KG-Konzentration die Umsatzgeschwindigkeit zunimmt.

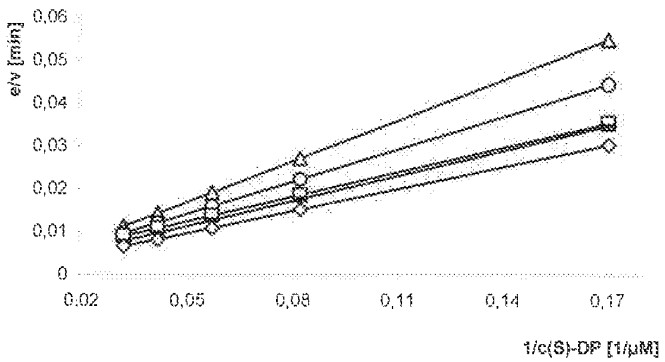


Abbildung 34: Primärauftragung des Umsatzes von (S)-DP durch $SdpA_{MC1}$ bei Anwesenheit verschiedener α-KG-Konzentrationen (1µM (◊), 2,5 µM (—), 5 µM (□), 7,5 µM (○) und 10 µM (Δ)) **nach Lineweaver-Burk** (gewichtete Werte)

Die aus der Primärdarstellung ($\frac{e}{v} = m\frac{1}{c_{Substrat}} + n$) gewonnenen Anstiege ($m$) und Abschnitte ($n$) wurden dann in Abhängigkeit zur Konzentration des α-KG dargestellt (Abbildung 35A und B). Aus den Anstiegen und Abschnitten der so entstandenen Kurvenzüge konnten die so genannten Dalziel-Koeffizienten Φ_0, Φ_1, Φ_2 und Φ_{12} ermittelt werden (Tabelle 28).

COR-AAD1-00003660
Bayer EX1008 (Part 7 of 9)

Tabelle 27 Kinetische Konstanten der (R)-spezifischen Enzyme aus MC1, P230 und MH Die Konstanten wurden aus dem sigmoidalem Plot berechnet.

Enzym	*Substrat*	spez. Akt. [U/mg]	rel. spez. Akt.	K_M [µM]	k_{kat} [min^{-1}]	k_{kat}/K_M [$µM^{-1} \cdot min^{-1}$]	rel. K_M/k_{kat}	Hill-Koeff.
$RdpA_{MC1-rec}$	*(R)-DP*	11,7 ± 2,1	1	49 ± 3	410 ± 73	8,4	1	1,7
	(R)-MCPP	8,6 ± 1,8	0,73	59 ± 2	301 ± 63	5,1	0,61	1,7
	2,4-D	1,3 ± 0,2	0,11	904 ± 40	46 ± 7	0,05	0,006	1,34
	MCPA	1,1 ± 0,3	0,09	510 ± 50	39 ± 10	0,08	0,009	1
$RdpA_{MC1}$	*(R)-DP*	13,9 ± 1,7	1	37 ± 5	487 ± 60	13,16	1	1,7
	(R)-MCPP	10 ± 1,3	0,72	64 ± 7	350 ± 46	5,47	0,42	1,6
	2,4-D	2,1 ± 0,2	0,15	900 ± 86	74 ± 7	0,08	0,006	1,2
	MCPA	1,6 ± 0,2	0,11	540 ± 63	56 ± 7	0,1	0,008	0,98
$RdpA_{MC1-II}$	*(R)-DP*	n.b.	1	60 ± 12	n.b.	n.b.	1	n.b.
	(R)-MCPP	n.b.	0,69	78 ± 15	n.b.	n.b.	0,53	n.b.
	2,4-D	n.b.	0,15	935 ± 123	n.b.	n.b.	1,2	n.b.
	MCPA	n.b.	n.b.	n.b.	n.b.	n.b.	n.b.	n.b.
$RdpA_{MC1-I3}$	*(R)-DP*	n.b.	1	63 ± 18	n.b.	n.b.	1	n.b.
	(R)-MCPP	n.b.	0,45	81 ± 21	n.b.	n.b.	0,45	n.b.
	2,4-D	n.b.	0,1	935 ± 80	n.b.	n.b.	1,3	n.b.
	MCPA	n.b.	n.b.	n.b.	n.b.	n.b.	n.b.	n.b.
$RdpA_{P230}$	*(R)-DP*	15,9 ± 1,3	1	19 ± 3	557 ± 46	29,32	1	1,55
	(R)-MCPP	11,7 ± 1,0	0,73	35 ± 2	410 ± 35	11,7	0,4	1,8
	2,4-D	4,2 ± 0,5	0,27	237 ± 15	147 ± 17	0,62	0,021	1,38
	MCPA	3,7 ± 0,3	0,23	164 ± 11	130 ± 11	0,79	0,025	1,04
$RdpA_{MH}$	*(R)-DP*	13,8 ± 2,1	1	39 ± 3	483 ± 74	12,71	1	1,6
	(R)-MCPP	10,1 ± 1,5	0,73	58 ± 9	354 ± 53	5,8	0,46	1,3
	2,4-D	2,2 ± 0,8	0,12	634 ± 27	77 ± 28	0,12	0,009	1,2
	MCPA	1,8 ± 0,6	0,08	480 ± 25	63 ± 21	0,13	0,01	0,99

n.b.: nicht bestimmt

COR-AAD1-00003661

Bayer EX1008 (Part 7 of 9)

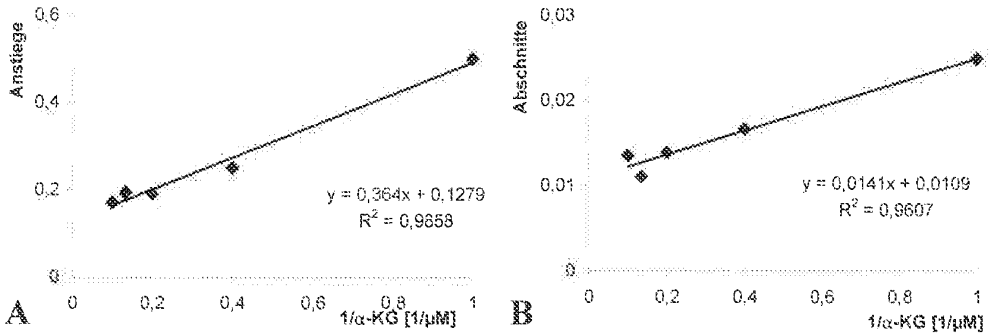


Abbildung 35: Sekundärauftragungen: Anstiege (A) und Abschnitte (B) der Primärauftragung gegen die reziproke α-KG-Konzentration

Mit Hilfe der Dalziel-Koeffizienten und der Gleichung 10 lässt sich dann der Reaktionsmechanismus berechnen:

$$\frac{\Phi_1 \cdot \Phi_2}{\Phi_{12} \cdot \Phi_0} \leq 1$$

Gleichung 10: Term zur Ermittlung des Reaktionsmechanismus bei Mehrsubstratreaktionen

Tabelle 28: Dalziel-Koeffizienten der Phenoxypropionat-spaltenden Enzyme aus *Delftia acidovorans* MC1

	Φ_0 [min^{-1}]	Φ_1 [µM·min]	Φ_2 [µM·min]	Φ_{12} [$µM^2$·min]
$RdpA_{MC1}$	0,020	0,526	0,021	0,712
$SdpA_{MC1}$	0,011	0,128	0,014	0,364

Das Ergebnis der Gleichung 10 ist sowohl für das $RdpA_{MC1}$ als auch das $SdpA_{MC1}$ kleiner als 1, was ein starker Hinweis auf das Vorliegen eines *ordered* BiBi-Mechanismus in Bezug auf die Bindung der Herbizide und α-KG ist. Ein *ordered* BiBi-Mechanismus bedeutet, dass Substratbindung und Produktablösung am aktiven Zentrum in einer definierten Reihenfolge ablaufen, Variationen sind nicht möglich. Weitere Beweise für diesen Mechanismus konnten nicht erbracht werden, da keine Produkthemmung auftrat, womit ausschließlich für die Bindung der Substrate, nicht aber für die Ablösung der Produkte ein *ordered*-Mechanismus nachgewiesen wurde. Eine experimentelle Einbeziehung der Sauerstoffkonzentration, dem dritten Substrat der Enzyme aus MC1, hat nicht stattgefunden. Aber auch dieses Substrat sollte in einem *ordered*-Mechanismus gebunden werden, so dass von einem *ordered* TerTer-Mechanismus für die Substratbindung wahrscheinlich ist.

COR-AAD1-00003662
Bayer EX1008 (Part 7 of 9)

4 Diskussion

Im Rahmen der vorliegenden Arbeit wurden die initialen Enzyme des Phenoxyalkanoat-Abbaus der Bakterienstämme *Delftia acidovorans* MC1, *Rhodoferax* sp. P230 und *Sphingobium herbicidovorans* MH sowohl proteinbiochemisch als auch enzymkinetisch charakterisiert. Es konnten Erkenntnisse über den enantioselektiven Abbau der 2-Phenoxypropionate und ein erster Einblick in die Struktur-Funktionsbeziehungen dieser Proteine gewonnen werden.

4.1 Enzymausstattung

Bei der Suche nach Phenoxyalkanoat-spaltenden Enzymen in den Stämmen MC1, P230 und MH wurde sich auf α-Ketoglutarat-abhängige Dioxygenasen konzentriert, da Hinweise auf solche Enzymaktivitäten schon vorlagen (Nickel et al., 1997; Müller et al., 2001). Nach Monooxygenase-Aktivität, wie sie z.B. für die Phenoxybutyrat- (Sträuber et al., 2003) und 2,4,5-Trichlorophenoxyacetatspaltung (Xun und Wagnon, 1995) beschrieben wurden, wurde nicht gesucht. Alle drei untersuchten Stämme sind zur kompletten Spaltung der (R,S)-Enantiomere der Phenoxypropionate (R,S)-2-(2,4-Dichlorphenoxy)propionat (2,4-DP) und (R,S)-2-(4-Chlor-2-methylphenoxy)propionat (MCPP) als auch zur Spaltung der Phenoxyacetate 2,4-Dichlorphenoxyacetat (2,4-D) und 4-Chlor-2-methylphenoxyacetat (MCPA) (Ehrig et al., 1997, Müller et al., 1999a) in der Lage. Der Stamm MH kann zusätzlich noch die Phenoxybutyrate verwerten (Horvath et al., 1990).

Trotz Verwertung derselben Herbizide unterscheiden sich die drei Stämme doch erheblich in ihren jeweiligen Abbauraten. So wird das (R,S)-DP vom Stamm MC1 mit der dreifachen Geschwindigkeit wie vom Stamm P230 abgebaut (Müller et al., 2001). Besonders deutliche Unterschiede sind auch in der Verwertung der Phenoxyacetate zu erkennen. MH spaltet das 2,4-D mit der gleichen Geschwindigkeit wie das (R,S)-DP (Horvath et al., 1990), während MC1 dieses Herbizid nur mit 1/5, P230 sogar nur mit 1/7 der Geschwindigkeit der (R,S)-DP-Spaltung umsetzt (Müller et al., 2001). Auch für den Abbau der anderen Herbizide wurden signifikante Unterschiede gefunden. Die Ursache für das unterschiedliche Abbauverhalten der Stämme sollte das Resultat unterschiedlicher Enzyme für die Verwertung der Phenoxyalkanoate sein. Da im Genom aller drei Stämme die Gene des kompletten modifizierten *ortho*-Weges sowie zu einem Teil die Enzyme selbst nachgewiesen werden konnten (Zipper et al., 1996; Müller et al., 2001; Smejkal et al., 2001), sollte der Unterschied vor allem im ersten Schritt der Phenoxyalkanoat-Verwertung zu finden sein.

COR-AAD1-00003663
Bayer EX1008 (Part 7 of 9)

Wie aus Induktionsversuchen, insbesondere mit den Stämmen P230 und MH, bekannt ist, erfolgt die Spaltung der Phenoxypropionate in den drei untersuchten Stämmen enantiospezifisch. Das heißt, es gibt je ein Enzym für die Spaltung der (R)-Enantiomere und eins für die der (S)-Enantiomere (Nickel et al., 1993; Zipper et al., 1998; Müller und Babel, 1999b; Müller et al., 2001). Tatsächlich ist es gelungen, diese enantioselektiven Enzyme aus allen Stämmen zu reinigen und zu charakterisieren.

Die (R)-2-(2,4-Dichlorphenoxy)propionat/α-Ketoglutarat Dioxygenasen aus MC1($RdpA_{MC1}$), P230 ($RdpA_{P230}$) und MH ($RdpA_{MH}$) sind einander sehr ähnlich. Sie sind hoch affin für (R)-Enantiomere der Phenoxypropionate und spalten diese mit hohen Umsatzraten. Phenoxyacetate stellen dagegen wesentlich schlechtere Substrate dar. Sie werden lediglich mit 10-20% der Spaltungsaktivität des (R)-DP umgesetzt, die K_M-Werte sind hoch.

Die (S)-2-(2,4-Dichlorphenoxy)propionat/α-Ketoglutarat Dioxygenasen (SdpA) dieser Stämme unterscheiden sich dagegen stark. Aus *Delftia acidovorans* MC1 konnte mit säulenchromatographischen Techniken eine zur Spaltung der (S)-Phenoxypropionaten befähigte Dioxygenase gereinigt werden: das $SdpA_{MC1}$. Dieses Enzym ist in der Lage, neben dem (S)-DP und (S)-MCPP auch die Phenoxyacetate 2,4-D und MCPA in erheblichem Umfang (35-45% der (S)-DP-Spaltungsaktivität) umzusetzen. Im Gegensatz dazu wurden aus *Rhodoferax* sp. P230 zwei (S)-spezifische Enzyme ($SdpA_{P230}$-1, $SdpA_{P230}$-2) gereinigt, die den Umsatz der (S)-Phenoxypropionate, nicht aber den der Phenoxyacetate katalysieren. Die beiden SdpA-Enzyme aus P230 sind in ihren Substratverwertungsspektren identisch, unterscheiden sich aber in ihren Umsatzraten. *Sphingobium herbicidovorans* MH exprimiert ebenfalls zwei (S)-spezifische Enzyme, die sich im Gegensatz zu den Enzymen aus P230 im Substratverwertungsspektrum unterscheiden. Eines der Proteine setzt die (S)-Phenoxypropionate und die Phenoxyacetate (17-28% der (S)-DP-Spaltungsaktivität) um, und das andere verwertet neben den genannten Substraten zusätzlich die Phenoxybutyrate. Allen (S)-spezifischen Enzymen ist gemeinsam, dass sie die (S)-Phenoxypropionate 2,4-DP und MCPP spalten. Sie unterscheiden sich jedoch in ihrem bevorzugten Substrat. Wird das (S)-DP vom $SdpA_{MC1}$ mit der höchsten Rate umgesetzt, so spalten die (S)-spezifischen Enzyme aus P230 und MH dieses Substrat mit wesentlich kleineren Raten als das (S)-MCPP.

Die gemessenen Enzymaktivitäten erklären jedoch keineswegs die beschriebenen Abbauraten der Bakterienkulturen. Für MH wurde in Abbauversuchen gefunden, dass die Herbizide (R,S)-DP und 2,4-D mit ähnlichen Geschwindigkeiten umgesetzt werden (Horvath et al., 1990). Im Rohextrakt dieser Zellen wurde aber 10mal mehr Spaltungsaktivität für die Pheno-

COR-AAD1-00003664
Bayer EX1008 (Part 7 of 9)

xypropionate als für das 2,4-D nachgewiesen. Eine ähnliche Diskrepanz wurde für den (R,S)-DP- und (R,S)-MCPP-Abbau entdeckt, obwohl die MH-Zellen das Mecoprop mit nur 80% der Umsatzrate des Dichlorprop spalten, weist der Rohextrakt der Zellen 1,5mal mehr Spaltungsaktivität für das Mecoprop als für das Dichlorprop auf (3.1.3). Auch für *Delftia acidovorans* MC1 und *Rhodoferax* sp. P230 geben die im Rohextrakt gefundenen Enzymaktivitäten die Abbauraten der intakten Zellen (Müller et al., 2001) nicht wider. Das Verhältnis der Spaltungsaktivitäten der (R)- zu den (S)-Enantiomeren ist in den intakten MC1-Zellen mit 4 etwa 2,7mal so hoch wie im Rohextrakt. Eine Bakterienkultur von P230 spaltet die (R)-Enantiomeren des 2,4-DP mit wesentlich höheren Raten als das (S)-DP. Im Rohextrakt der Zellen wurde jedoch signifikant mehr Spaltungsaktivität für das (S)-Enantiomer des Dichlorprop gefunden. Die Gründe für die Unterschiede zwischen den Abbaupotenzialen der intakten Zellen und der Rohextrakte können vielfältig sein, als Hauptursache werden jedoch die Aktivitätsverluste angesehen. Das TfdA aus *Delftia acidovorans* P4a zeigt ohne Zusatz von Ascorbat, Eisen(II) und 2,4-D im Aufschlusspuffer hohe Aktivitätsverluste (Reinhold, 1998). Aufgrund der Instabilität des TfdA aus *Ralstonia eutropha* JMP 134 wurden Aktivitätsbestimmungen nur mit ganzen Zellen vorgenommen (Pieper et al., 1988). Für überexprimiertes TfdA aus *Ralstonia eutropha* JMP134 wurde eine hohe Instabilität aufgrund von Proteolyse beschrieben (Fukumori und Hausinger, 1993b). Proteolytische Prozesse können jedoch für die Enzyme aus P230 (Ruhland, 2003) und MC1 (Westendorf et al., 2003) als Grund für Aktivitätsverluste ausgeschlossen werden, da die Zugabe von Proteaseinhibitoren nicht zu erhöhten Enzymaktivitäten führte. Die von der Substratspaltung entkoppelte oxidative Decarboxylierung des α-KG führt beim TfdA und TauD zu einem starken aber reversiblen Aktivitätsverlust (Liu et al., 2001; Ryle et al., 2003a). Ein solcher Effekt könnte beim Zellaufschluss auftreten und Einfluss auf die Spaltungsaktivitäten nehmen. Auch anderweitige Gründe wie kurze Halbwertszeiten der Proteine in der Zelle, irreversible Schädigungen des Proteins usw. können extreme Aktivitätsverluste verursachen, ja sogar die Gefahr des totalen Verlustes von Enzymaktivitäten bergen. So legen die Abbauraten der MH-Zellen das Vorhandensein eines weiteren Enzyms mit hoher Spaltungsaktivität für das 2,4-D - ähnlich dem TfdA - nahe. Ein TfdA-Protein konnte aber nicht gereinigt werden, auch im Genom konnte ein *tfdA*-Gen nicht nachgewiesen werden (Zipper et al., 1996). Im Gegensatz zum MH wurde mit Primern von konservierten Regionen des *tfdA* in P230 ein Amplifikat erhalten (Ehrig et al, 1997), aber auch aus diesem Stamm konnte ein solches Enzym nicht gereinigt werden. Weitere Gründe

COR-AAD1-00003665
Bayer EX1008 (Part 7 of 9)

für Unterschiede in dem Spaltvermögen ganzer Zellen und dem Rohextrakt können unterschiedliche Reaktionsbedingungen sein. In der Zelle liegen die Substrate nicht in sättigenden Konzentrationen vor. Die Enzyme konkurrieren miteinander und mit dem weiteren Stoffwechsel um die Substrate (O`Brien et al., 2003). Hier spielen vor allem Effekte im Zusammenhang mit der Bereitstellung und Regeneration von α-Ketoglutarat (α-KG) eine Rolle (Müller und Babel, 2000). Aber auch die Enzyme selbst unterliegen regulatorischen Einflüssen. So konnte für MC1 gezeigt werden, dass bei hohen stationären (R,S)-DP-Konzentrationen der Gehalt des SdpA in der Zelle abnimmt (Benndorf et al., 2004). Als einen weiteren Grund für die unterschiedlichen Substratverwertungspotenziale intakter Zellen und deren Rohextrakte seien hier Induktionsphänomene angeführt; nicht alle Enzyme sind konstitutiv wie die RdpA-Proteine aus P230 und MC1 sowie die SdpA-Enzyme aus MC1 und MH, vielmehr wurde für die (S)-spezifischen Enzyme aus P230 und dem $RdpA_{MH}$ eine Induzierbarkeit nachgewiesen (Nickel et al., 1997; Müller et al., 2001). Ebenso konnte in dieser Arbeit gezeigt werden, dass es auch im Stamm MH ein induzierbares (S)-spezifisches Enzym gibt.

Die Unterschiede der Verwertungseigenschaften der Stämme und der Enzymaktivitäten im Rohextrakt müssen nicht zwangsläufig auf Aktivitätsverluste zurückzuführen sein. Das Problem der Substrataufnahme darf ebenfalls nicht unberücksichtigt bleiben. Für 2,4-D ist bei *Ralstonia eutropha* JMP134 gezeigt worden, dass ein Transportprotein, TfdK, im Operon der 2,4-D-Degradation integriert ist. Dieses Gen gehört in die Superfamilie der MFS (*major facilitator superfamily*)-Transporter, es ordnet sich in die Untergruppe der aromatischen Säure/H^+ Symporter ein (Pao et al., 1998). Eine Eliminierung dieses Gens führt im obigen Stamm zu einer Beeinträchtigung der 2,4-D-Aufnahme bei kleinen Konzentrationen, bei höheren spielt dies offensichtlich keine Rolle mehr (Leveau et al., 1998). Zur Ergänzung dazu wurden Phänomene aktiven Transports auch für MH beschrieben, hier mit deutlich enantioselektiven Eigenschaften unterlegt. Bemerkenswert ist die Tatsache, dass die Anwesenheit von 2,4-D beispielsweise die Induktion dieser Proteine und damit eine Aufnahme unterdrückt wird (Zipper et al., 1998). Versuche mit ^{14}C-markiertem 2,4-D zeigen auch für MC1 eine aktive Aufnahme und Aufnahmekinetiken, die in Abhängigkeit von den Wachstumssubstraten (2,4-DP, 2,4-D) und anderen Kultivierungsbedingungen (pH) sehr unterschiedlich verlaufen, d.h. stark auf eine Rolle solcher Prozesse für die Herbizidverwertung hinweisen (D. Hoffmann und R.H. Müller, persönliche Mitteilung).

COR-AAD1-00003666
Bayer EX1008 (Part 7 of 9)

4.2 Proteinbiochemie

Die RdpA-Proteine der Stämme MC1, P230 und MH sind Produkte ein und desselben Gens, dem *rdpA* (Schleinitz et al., 2004). Die Molmasse des nativen Proteins wurde mit 113 kD bestimmt, die des denaturierten mit 35,8 kD, was für eine trimere Struktur des Proteins spricht. Ein trimeres Protein ist in der Natur selten, da es unsymmetrisch ist, und wurde bislang in der Gruppe der α-KG-abhängigen Dioxygenasen nicht beschrieben, obwohl die Gruppe ansonsten sehr heterogen in ihrer Quartär-Struktur ist (1.2). Bei dem $SdpA_{MC1}$ handelt es sich im Gegensatz zum RdpA um ein dimeres Protein, die Molmasse eines Monomers beträgt 32,5 kD. Die Quartär-Strukturen der (S)-spezifischen Enzyme aus P230 (MM eines Monomers: 32,2-32,4 kD) und MH (MM eines Monomeres: 32,2 kD) konnten bislang nicht aufgeklärt werden, da keine reinen Präparate gewonnen werden konnten.

4.2.1 Sequenzanalyse

Die Sequenzanalyse der RdpA- und SdpA-Proteine aus MC1 und MH zeigen nur wenig Sequenzidentitäten (30-40%) und –ähnlichkeiten (etwa 50%) zu TfdA- und TauD-Enzymen. Der Vergleich der RdpA und SdpA-Aminosäuresequenzen ergibt etwa das gleiche Bild (28% Identität, 47% Ähnlichkeit). Untereinander sind die (S)-spezifischen Enzyme jedoch zu 60% identisch und zu 70% ähnlich. Die Verwandtschaftsverhältnisse einiger Phenoxyalkanoat-spaltender Enzyme sind in Abbildung 36 dargestellt. Aus dieser Abbildung wird deutlich, dass die RdpA- und SdpA-Enzyme der drei Stämme phylogenetisch verschiedene Zweige innerhalb der Gruppe(II) der α-KG-abhängigen Dioxygenasen bilden, die Verwandtschaft ist eher entfernt. Die RdpA-Enzyme bilden einen Zweig mit dem TauD aus *E. coli*, während die (S)-spezifischen Enzyme aus MC1 und MH verwandtschaftlich den TfdA-Proteinen näher stehen, aber trotzdem doch so verschieden von den 2,4-D-spaltenden Enzymen sind, dass diese einen eigenen Tochterstrang bilden. Die Zuordnung in einen gemeinsamen Strang legt einen gemeinsamen genetischen Ursprung nahe, wie er zu einem für die Isoenzyme der Clavaminat-Synthase und zum anderen für die Enzyme Deacetoxycephalosporin-C-Synthase und Deacetylcephalosporin-C-Synthase beschrieben wurde (Marsh et al., 1992). Demnach sollten die SdpA-Proteine aus MC1 und MH einst identisch gewesen sein und hätten sich dann durch unterschiedliche Evolutionsbedingungen voneinander entfernt. Die Zuordnung zu einem separaten Strang ist jedoch nicht eindeutig. Die Nutzung anderer Programme zur Erstellung von Verwandtschaftsbäumen ordnen TfdA- und SdpA-Proteine in den gleichen Zweig. Aufgrund von zu wenig Sequenzdaten derartiger Enzyme kann zur Zeit keine eindeutige Zuordnung zu Enzymfamilien vorgenommen werden (Schleinitz et al., 2004). Die Ähnlichkeit zwischen den

COR-AAD1-00003667
Bayer EX1008 (Part 7 of 9)

TfdA- und SdpA-Proteinen wird auch auf enzymkinetischer Ebene deutlich. Beide Enzyme spalten Phenoxyacetate sowie die (S)-Enantiomere der Phenoxypropionate, die (R)-Enantiomere dienen nicht als Substrat (Nickel et al., 1997; Saari et al., 1998; Müller und Babel, 1999).

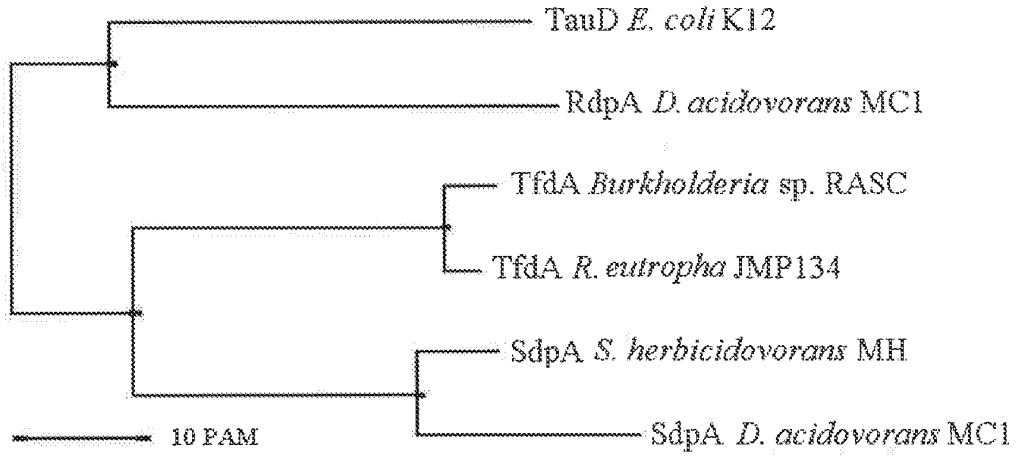


Abbildung 36: Verwandtschaftsbaum ausgesuchter Phenoxyalkanoat-spaltender Enzyme TauD: *E. coli* K12-NP_414902; TfdA: *R. eutropha* JMP134-P10088; *Burkholderia* sp. RASC-Q45423; SdpA: *S. herbicidovorans* MH-Q700X4; *D. acidovorans* MC1-Q8KSD0; RdpA: *D. acidovorans* MC1-Q8KSD1

Die Primärstrukturen der RdpA- und SdpA-Enzyme enthalten wichtige Strukturelemente von α-KG-abhängigen Dioxygenasen. So konnte das Motiv der Gruppe(II)-Dioxygenasen, H-X-D-$X_{136-205}$-D-N-X_4-H-X_{10}-R, in allen Aminosäuresequenzen gefunden werden. Alle Aminosäuren, die im TauD für die Fe(II)-Koordination und Bindung des α-KG identifiziert wurden (Abbildung 15), wurden ebenfalls in den Phenoxyalkanoat-spaltenden Enzymen aus MC1, P230 und MH nachgewiesen; sie gehören zu den hochkonservierten Regionen in den Primärstrukturen aller Enzyme der Gruppe 1.14.11.- (Roach et al., 1995a; Hogan et al., 2000; Aravind und Koonin, 2001; Clifton et al., 2001; Elkins et al., 2002). Die Aminosäuren, die das eigentliche Substrat am aktiven Zentrum binden, sind dagegen sehr unterschiedlich. Im TfdA wurden Arg278, His214, Ser117, Lys95 und Lys71 durch spezifische Mutagenese als 2,4-D-bindende Reste identifiziert (Dunning-Hotopp und Hausinger, 2002; Elkins et al., 2002). Von diesen ist lediglich Ser117 in den RdpA- und SdpA-Enzymen konserviert. Das Prolin wird von der Prolin-3-Hydroxylase mit den Resten Arg95, Arg97, Arg122 und His43 gebunden (Clifton et al., 2002). Keine dieser Aminosäuren ist in den untersuchten Sequenzen zu finden. Taurin wird von TauD über die Reste Tyr73, Asn95 Ser158, Arg270 und His70 im aktiven Zentrum ausgerichtet (Elkins et al., 2002). Von diesen Aminosäuren sind Arg270 im RdpA und Ser158 in den (S)-spezifischen Enzymen aus M1 und MH konserviert.

COR-AAD1-00003668
Bayer EX1008 (Part 7 of 9)

Aus der Primärstruktur können mit Hilfe von Modellierungs-Programmen erste Hinweise für die Sekundärstruktur der Proteine abgeleitet werden, indem versucht wird, die Aminosäuresequenz mit einer bereits bekannten Sekundärstruktur eines verwandten Proteins abzugleichen. Mit Hilfe dieser Methode ist es bereits gelungen, die Sekundärstruktur des TauD vorherzusagen. Hierzu wurde die Aminosäuresequenz, die nur zu etwa 8% mit der der Clavaminat-Synthase übereinstimmt, in die Sekundärstruktur der Clavaminat-Synthase gefittet. Die so erhaltene 3D-Struktur stimmt zu 84% mit der der Clacaminat-Synthase überein (O'Brien et al., 2003) und entspricht zu über 90% der Realität, wie nach Röntgenkristall-Strukturuntersuchungen deutlich wurde (Elkins et al., 2002). Auf die gleiche Art und Weise konnte die Sekundärstruktur der Phenoxyalkanoat-spaltenden Enzyme aus MC1, P230 und MH vorhergesagt werden. Es wurde das für α-KG-abhängige Dioxygenasen typische *jelly-roll*-Motiv erhalten. Die für die Katalyse essentiellen Reste in den gleichen Strukturelementen wie im TauD.

4.2.2 Multiple Enzymformen

Proteom-Untersuchungen an *Delftia acidovorans* MC1 nach Wachstum auf (R,S)-DP als einzige Kohlenstoff- und Energiequelle zeigen das Vorhandensein von multiplen Enzymformen für eine Vielzahl von Proteinen (Benndorf et al, 2004). Bei vielen handelt es sich dabei um Ladungsisomere mit gleicher Masse. So wurden vom TfdB drei Formen, vom TfdD vier Formen und vom Ef Tu (Elongationsfaktor Tu) drei Formen nachgewiesen. Es konnten auch Enzymformen gefunden werden, die sich nur in ihrer Masse, nicht aber im pI unterscheiden. Ein Beispiel hierfür ist das $TfdC_{II}$. Auch echte Isoenzyme, Produkte unterschiedlicher Gene, wurden nachgewiesen ($TfdC_I$ und $TfdC_{II}$). Es ist auffällig, dass von fast allen Enzymen des modifizierten *ortho*-Weges mehrere Enzymformen gefunden wurden. Und so überrascht es nicht, dass auch vom $RdpA_{MC1}$ und vom $SdpA_{MC1}$ nach Auftrennung im 2D-Gel multiple Enzymformen nachgewiesen werden konnten. Gründe für das Auftreten von Enzymformen sind in der Einleitung beschrieben. Da in MC1 jeweils nur ein Gen für das SdpA und RdpA nachgewiesen werden konnte (Schleinitz et al., 2004), handelt es sich bei den Enzymformen nicht um echte Isoenzyme, vielmehr zeichnen sie sich durch eine identische Primärstruktur aus. Unterschiede sind in einer posttranslationalen Modifizierung zu suchen. Als typische Modifizierungen an α-KG-abhängigen Dioxygenasen wurden Hydroxylierungen an Tryptophanresten beschrieben (Liu et al., 2001; Ryle et al., 2003a). An den Tryptophanen 235 und 255 des $SdpA_{MC1}$ konnten Massen-shifts von +16 nachgewiesen werden. Eine solche Massenzunahme korrespondiert mit einer Oxidation des Aminosäurerestes zum Oxindolylalanin (An-

COR-AAD1-00003669
Bayer EX1008 (Part 7 of 9)

derson et al., 2002) oder einer Hydroxylierung am Benzolring des Trp, nicht aber mit einer Hydroxylierung zum 3-Hydroxyindolylalanin. Diese Modifizierung hätte eine Massenzunahme von 18 zur Folge. Eine genauere Analyse der Modifikation an den Tryptophanen im $SdpA_{MC1}$ wurde nicht durchgeführt, so dass eine eindeutige Zuordnung der Massenzunahme zu einer Struktur nicht vorgenommen werden kann. Die Modifikationen an Trp235 und Trp255 sind in keinem Fall die Ursache für das Auftreten verschiedener Spots im 2D-Gel, da erstens eine Hydroxylierung oder Oxidation von Trp-Resten nicht zur Veränderung von Nettoladungen führt und zweitens die Modifikationen in den Proteinen aller Spots nachgewiesen werden konnten. Für TauD wurde eine Hydroxylierung des Tyr73 im TauD beschrieben. Diese Aminosäure liegt komplexiert mit dem Eisen(III) als Catecholderivat im aktiven Zentrum des Enzyms vor (Ryle et al., 2003a/b). Solche Art Modifikation wurde in den untersuchten RdpA- und SdpA-Enzymen nicht nachgewiesen, würde aber auch nicht zu einer Auftrennung der Proteinspezies in der isoelektrischen Fokussierung führen. Der Verlust einer Aminosäure am C- oder N-Terminus könnte ebenfalls zu einem veränderten pI-Wert führen, konnte aber durch massenspektrometrische Analyse der Proteinspots im vorliegenden Falle ausgeschlossen werden. Im $SdpA_{MC1}$ konnte aber eine Modifikation mit der Masse 209 am Cys237 nachgewiesen werden. Die chemische Struktur dieses Derivates konnte bislang nicht ermittelt werden; diese Massendifferenz kann bekannten Strukturen nicht zugeordnet werden. Aus den Isotopenmustern des betreffenden Peptides wird jedoch ersichtlich, dass Halogene kein Bestandteil der Modifizierung sind, also dass unmittelbare Reaktionsprodukte nicht involviert wurden. Ein weiterer Grund, der gegen eine von Metaboliten des Phenoxyalkanoat-Abbaus abgeleitete Modifizierung spricht, ist die Tatsache, dass die rekombinanten Enzyme bei Auftrennung im 2D-Gel ebenfalls in mehrere Spots separiert wurden und die überexpremierenden Zellen jedoch nie mit den Herbiziden in Berührung gekommen sind. Auch findet man die verschiedenen $SdpA_{MC1}$- und $RdpA_{MC1}$-Monomere nach Wachstum von MC1 auf Komplexmedium (Benndorf et al., 2004). Aufgrund der ungeraden Masse von 209 wird wahrscheinlich, dass z.B. eine ungerade Anzahl von Stickstoffatomen Bestandteil der gesuchten Verbindung ist. Doch selbst die Modifikation am Cys237 sollte nicht der Grund für das Auftreten von isomeren Monomeren im 2D-Gel sein, da ein Peptid mit diesem Charakteristikum nach isoelektrischer Fokussierung in keinem der Proteinspots, sondern nur nach im Lösungsverdau mit Trypsin nachgewiesen werden konnte. Proteine liegen im 2D-Gel komplett reduziert vor. Da dies im tryptischen Verdau in Lösung durch das Vorhandensein von 50mal mehr Protein in der Ausgangslösung nicht hundertprozentig gewährleistet werden kann, liegt die Annahme nahe, dass das 209er Molekül durch eine Disulfidbrücke an das Cystein gebunden ist. Weitere

COR-AAD1-00003670
Bayer EX1008 (Part 7 of 9)

Untersuchungen sind dazu aber noch nötig. Ein weiterer Hinweis für die Bindung des Derivates über eine Disulfidbrücke ist die Nicht-Auffindbarkeit einer solchen Modifikation am $RdpA_{MC1}$. Dieses Protein konnte mit einer Sequenzabdeckung von über 85% analysiert werden. Ein Unterschied zwischen den im 2D-Gel auftretenden Proteinformen wurde jedoch nicht gefunden. Untersuchungen unter nicht reduzierenden Bedingungen wurden bislang nicht vorgenommen.

Das Vorliegen von isomeren Monomeren sowohl bei den in *E. coli* überexprimierten als auch bei den nativen Phenoxyalkanoat-spaltenden Enzymen aus MC1 legt die Vermutung nahe, dass es sich bei den Modifikationen um einen generellen Mechanismus für α-KG-abhängige Enzyme handelt. So konnte für die Thymin-7-Hydroxylase eine Reaktionsmechanismusbedingte Modifizierung nachgewiesen werden, Substratanaloga werden zu Verbindungen oxidiert, die irreversibel am aktiven Zentrum des Enzyms binden (Thornburg, 1989; Thornburg und Stubbe, 1993; Lai et al., 1995). *E. coli* ist der Träger von *tauD*, einem Gen, dass die α-KG-abhängige Taurin-Dioxygenase codiert, und sollte bei Vorliegen eines allgemeinen Modifizierungsmechanismus für solche Enzyme auch in der Lage sein, die Phenoxyalkanoat-spaltenden Enzyme zu modifizieren. Bei einer MC1 spezifischen Modifizierung wäre dies nicht der Fall. Führt man diese Überlegung zu Ende, dann sollten alle α-KG-abhängigen Dioxygenasen modifiziert vorliegen, für die RdpA-Proteine aus P230 und MH ist dies auch der Fall. Ebenso wurden bereits von den SdpA-Proteinen aus P230 isomere Monomere gefunden. Auch von der γ-Butyrobetain-Hydroxylase konnten ladungsisomere Monomere nachgewiesen werden. Für eine Vielzahl von α-KG-abhängigen Dioxygenasen wurde jedoch keine isoelektrische Fokussierung durchgeführt, weshalb eine zu frühe Generalisierung nicht gerechtfertigt ist.

Auch für das RdpA-Enzym aus P230 wurden multiple Enzymformen nachgewiesen. Diese weichen trotz der gleichen Nukleinsäuresequenz im Gen von denen des $RdpA_{MC1}$ ab. Gründe hierfür sind nicht bekannt.

Die beiden SdpA-Enzymfraktionen, die aus dem Stamm P230 voneinander getrennt werden konnten, sind nicht Isoenzyme im Sinne der Definition, sondern erwiesen sich ebenfalls als multiple Enzymformen. Da sie die gleichen Peptidspaltungsmuster aufweisen, kann angenommen werden, dass sie sich durch identische Primärstrukturen auszeichnen. Die Auftrennung der beiden $SdpA_{P230}$-Enzyme im 2D-Gel zeigt mehrere, zum Teil identische Spots (Abbildung 23), aus denen nochmals deutlich wird, dass die Zusammensetzung der Oligomere zum Teil aus den gleichen Untereinheiten resultiert. Die verschiedenen monomeren For-

COR-AAD1-00003671
Bayer EX1008 (Part 7 of 9)

men der Enzyme unterscheiden sich wieder signifikant in ihren isoelektrischen Punkten, in ihren Molmassen jedoch nur unwesentlich. Auch für diese Proteine konnte die Art der Modifizierung bislang nicht aufgeklärt werden. In der Literatur wurden bisher keine derartigen Phänomene im Zusammenhang mit Phenoxyalkanoat-spaltenden oder α-KG-abhängigen Dioxygenasen beschrieben. Es können also keine Analogien zu bereits Bekanntem gezogen werden.

Detailierte Untersuchungen zur Verschiebung des Enzymformen-Verhältnisses liegen nicht vor. Bekannt ist aber, dass die Verhältnisse der Enzymformen des TfdD und Ef Tu nicht konstant, sondern variabel sind und mit sich ändernden Wachstumsbedingungen variieren (Benndorf et al., 2004).

4.3 Klassifizierung der Enzyme

Die untersuchten Enzyme katalysieren Reaktionen, die nach dem Schema in Abbildung 37 verlaufen. Es handelt sich somit um Oxidoreduktasen, da der Carbonylkohlenstoff des α-KG sowie der über die Etherbindung an den Aromaten gebundene Kohlenstoff der Seitenkette des Phenoxyalkanoates oxidiert werden, während der molekulare Sauerstoff reduziert wird (Fukumori und Hausinger, 1993b).

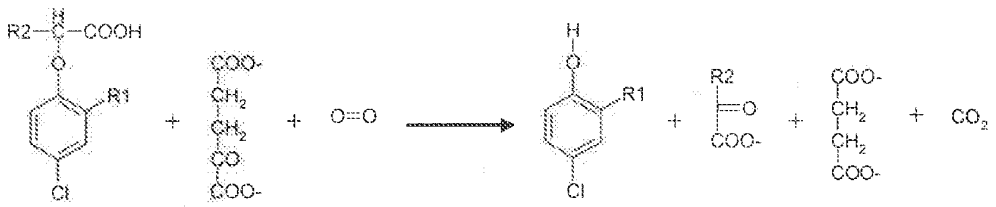


Abbildung 37: Reaktionsgleichung der Phenoxyalkanoat-spaltenden Enzyme aus MC1, P230 und MH R1: -Cl oder $-CH_3$, R2: -H oder $-CH_3$,

Des Weiteren sind die Enzyme in die Subklasse 14 einzuordnen, da für die Reaktion zwei Elektronendonoren notwendig sind: α-KG und Phenoxyalkanoat. Die weitere Unterteilung führt zur Sub-Subklasse 11, charakterisiert durch den Einsatz von α-KG als einer der Elektronendonoren sowie durch den Einbau von je einem Atom Sauerstoff in jeden der Donoren. Diese Charakteristika treffen für die hier behandelte Reaktion zu: α-KG ist für die Enzymreaktion essentiell (Nickel et al., 1997; Müller et al., 2001) und der Sauerstoff ist sowohl im substituierten Phenol als auch im Succinat wiederzufinden (Que und Ho, 1996). Die EC-Nummer lautet also für die untersuchten Enzyme 1.14.11.-. Seriennummern wurden noch nicht vergeben. Andere Enzyme, die dieser Enzymklasse zuzuordnen sind, wären z.B. die γ-Butyrobetain-Hydroxylase (EC 1.14.11.1), die Taurin-Dioxygenase (EC 1.14.11.17) und die

COR-AAD1-00003672
Bayer EX1008 (Part 7 of 9)

Clavaminat-Synthase (EC 1.14.11.21). Allen Enzymen dieser Klasse ist gemeinsam, dass neben den beiden Substraten auch Eisen(II) essentiell für die Reaktion ist und dass Ascorbat den enzymatischen Umsatz stimuliert.

α-KG-abhängige Dioxygenasen sind Enzyme mit Nicht-Häm-gebundenem Eisen und wurden von deCarolis und deLuca (1994) aufgrund ihrer katalysierten Reaktionen in die Untergruppen Hydroxylasen, Hydroxylasen/Epoxidasen, Cyclasen, Desaturasen und Ring-Expandasen unterteilt. Mechanistisch ähnelt die von Phenoxyalkanoat-spaltenden Enzymen katalysierte Reaktion der der Hydroxylasen, die Enzyme koppeln die oxidative Decarboxylierung des α-KG mit der Hydroxylierung des Seitenkettenkohlenstoffatoms, das über die Etherbindung mit dem Aromaten verbunden ist. Das entstandene Hemiacetal zerfällt dann spontan in Dichlorphenol und im Falle der Phenoxyacetate in Glyoxylat (Fukumori und Hausinger, 1993b) bzw. im Falle von Phenoxypropionaten in Pyruvat.

Die Phenoxyalkanoat-spaltenden Enzyme aus den drei Stämmen können aufgrund vom konservierten Sequenzmotiv H-X-D-$X_{136-205}$-D-N-X_4-H-X_{10}-R (Hogan, 1999), das in allen gereinigten und charakterisierten Enzymen aus MC1, P230 und MH gefunden werden konnte, der Gruppe(II) der α-KG-abhängigen Dioxygenasen zugeordnet werden. Ihr Reaktionsmechanismus ist denen der Hydroxylasen sehr ähnlich.

4.4 Reaktionsmechanismus und Enzymstabilität

Die Enzymreaktionen, die von α-KG-abhängigen Enzymen katalysiert werden, sind sehr vielfältig, trotzdem zeichnen sie sich alle durch einen sehr ähnlichen Reaktionsmechanismus aus. Eisen(II)-Ionen sind für die katalytische Aktivität essentiell. Diese werden im aktiven Zentrum von zwei Histidin-Resten und einer Carboxygruppe, entweder vom Glutamat oder vom Aspartat (Hegg et al., 1999; Clifton et al., 2001; Aravind und Koonin, 2001; Elkins et al., 2002), koordiniert. Daran beteiligt sind Aminosäuren, die sich in dem hochkonservierten Sequenzmotiv H-X-D-$X_{136-205}$-D-N-X_4-H-X_{10}-R wiederfinden (Hogan et al., 1999). Dieses Motiv findet sich auch bei den RdpA- und SdpA-Enzymen aus MC1, P230 und MH (3.2.1.2). Für die Aminosäuren H-X-D konnte für andere Enzyme dieser Gruppe eine direkte Beteiligung an der Bildung des Eisen(II)-Zentrums gezeigt werden (Hegg et al., 1999; Elkins et al., 2002). Im Zusammenhang der Sequenzdaten der Proteine mit kinetischen Eigenschaften kann eine analoge Organisation der aktiven Zentren der Phenoxyalkanoat-spaltenden Enzyme aller untersuchten Stämme zu den TauD- und TfdA-Proteinen nahegelegt werden. Wie alle α-KG-abhängigen Dioxygenasen benötigen auch die untersuchten RdpA- und SdpA-Enzyme Eisen(II)-Ionen für ihre katalytische Aktivität. Für die enantioselektiven Enzyme aus MC1

COR-AAD1-00003673
Bayer EX1008 (Part 7 of 9)

konnte eine hemmende Wirkung durch Diethylpyrocarbonat (DEPC), einem spezifischen His-Modifizierungsreagenz, nachgewiesen werden (Westendorf et al., 2003). Ebenso konnte in der vorliegenden Arbeit gezeigt werden, dass sich bei einem mit DEPC behandelten Enzym dessen α-KG-Bindekapazität verringert (3.3.1), womit ein direkter Zusammenhang zwischen den His-Resten, der Enzymaktivität, der α-KG-Bindung und somit dem aktiven Zentrum des Enzyms hergestellt werden konnte. Einen weiteren wichtigen Hinweis auf einen TfdA- und TauD-ähnlichen Reaktionsmechanismus liefert eine Nebenreaktion des Enzyms, die Selbsthydroxylierung. Werden α-KG-abhängige Enzyme mit α-KG und Sauerstoff inkubiert, kommt es zu einer Verschiebung der Absorptionsmaxima der Proteine. Ursache für diesen Effekt ist die Hydroxylierung von Aminosäureseitenketten nahe der aktiven Zentren. So wurde im TfdA Trp112 hydroxyliert (Liu et al., 2001), im TauD wurden Hydroxylgruppen an den Trp128, Trp240 und Trp248 nachgewiesen. Ebenfalls findet man in diesem Enzym Tyr256 hydroxyliert vorliegend (Elkins et al., 2002; Ryle et al., 2003). Für das $SdpA_{MC1}$ wurde das gleichermaßen beobachtet; hier finden sich Hydroxylierungen an Trp235 und Trp255, abgeleitet aus MS-MS-Spektren mit Massenshift von +16.

Enzymkinetische Untersuchungen an α-KG-abhängigen Enzymen zeigen einen *ordered* Mechanismus für den Substratumsatz (Holme, 1975; Rundgren, 1977b; Myllylä et al., 1977; Puistola et al., 1980; Kivirikko et al., 1989; de Carolis und de Luka, 1993). In dieser Arbeit konnte ein solcher Mechanismus auch für die Phenoxyalkanoat-spaltenden Enzyme aus MC1 (zumindest für die Substratanlagerung) gezeigt werden. Die Bindung der Substrate und die Ablösung der Produkte erfolgt in einer festgelegten Reihenfolge. Wie bereits in der Einleitung erläutert (1.2.1), existieren zwei grundsätzliche Vorstellungen über die Reihenfolge der Anlagerung der Substrate. Entweder binden sie in der Folge: α-KG, O_2, Substrat (Kivirikko, 1972; Kivirikko et al., 1989; deCarolis und deLuca, 1993) oder in der Folge: α-KG, Substrat, O_2 (Holm et al., 1975; Hegg et al., 1999; Elkins et al., 2002; Price et al., 2003). Anhand der vorliegenden Daten kann keine definitive Aussage zur Abfolge der Substratbindung am aktiven Zentrum gemacht werden. Das würde detalliertere Studien erfordern. Wegen der sehr ähnlichen Reaktion zum TfdA ist eine Bindung in der Reihe: α-KG, Phenoxyalkanoat und Sauerstoff als wahrscheinlich anzunehmen. Aufgrund der kinetischen Konstanten ist auch die zweite Bindungsreihenfolge nicht auszuschließen. Die multiplen Enzymformen des $SdpA_{MC1}$ zeichnen sich durch identische K_M-Werte bezüglich der Substrate α-KG und Sauerstoff aus, die Affinitätskonstanten bezüglich der Phenoxyalkanoate sind jedoch deutlich verschieden

COR-AAD1-00003674
Bayer EX1008 (Part 7 of 9)

(3.3.5.1). Außerdem unterscheiden sich die Enzymformen in der Modifizierung der Primärstruktur (3.2.3.1). Diese Modifizierung macht sich in ihrem Einfluss auf die kinetischen Konstanten hinsichtlich der Herbizid-Substrate bemerkbar, nicht aber auf die von Sauerstoff und α-KG. Unterstellt man eine Konformationsänderung des Enzyms während der Reaktion (Sami et al., 1997; Vålegard et al., 1998; Zhang et al., 2000; Clifton et al., 2001; O'Brien et al., 2003) und korreliert das mit dem kinetischen Verhalten der Enzymformen, so legt das die Bindung der Substrate α-KG und Sauerstoff vor dem Herbizid nahe. Mechanistisch wäre das so zu verstehen, dass erst die Herbizid-Bindung zu solchen Änderungen im aktiven Zentrum führt, dass die Reaktion durch die Modifizierung moduliert wird. Zur endgültigen Klärung der Bindungsreihenfolge der Substrate und des Reaktionsmechanismus bedarf es noch einiger Untersuchungen. Für TauD jedoch konnte eine Taurin-induzierte Konformationsänderung bereits nachgewiesen werden (O'Brien et al., 2003).

Für α-KG-abhängige Dioxygenasen konnte eine hohe, eng mit dem Reaktionsmechanismus verknüpfte Inaktivierungsrate gezeigt werden. Diese Inaktivierungen können sowohl reversibel als auch irreversibel sein. So wurde für TfdA gezeigt, dass die Inaktivierung des Enzyms durch die Anwesenheit von Ascorbat stark verlangsamt wird. Ascorbat übernimmt wahrscheinlich die Rolle eines Antioxidants und reduziert bereits oxidierte Eisen-Zentren (Saari und Hausinger, 1998). Ein solcher Inaktivierungsschutz konnte auch für andere Enzyme dieser Gruppe nachgewiesen werden. So verlangsamte sich der Aktivitätsverlust des TauD durch Zugabe von Ascorbat um 35% (Ryle et al., 2003a) und bei der Clavaminat-Synthase um 40% (Salowe et al., 1990). Es wurden aktive Sauerstoffspezies postuliert (Siegel, 1983), um die Inaktivierung der Enzyme zu erklären. Entsprechend bestätigt werden konnte dies durch Stabilisierung der Aktivität nach Zugabe von Katalase (Salowe et al., 1990). Auch die Selbsthydroxylierung kann zu einer reversible Inaktivierung des Enzyms führen, durch den Einsatz starker Reduktionsmittel (Dithionit) kann bis zu 60% der Enzymaktivität von TfdA, die so vermindert war, zurück gewonnen werden (Liu et al., 2001). In dieser Selbsthydroxylierung wird ein Schutzmechanismus des Proteins gesehen, der das Enzym vor irreversiblen Inaktivierungen wie z.B. einem Bruch der Peptidkette schützen soll (Liu et al., 2001; Ryle et al., 2003a/b). Von irreversiblen Inaktivierungen α-KG-abhängiger Dioxygenasen wurde bereits berichtet (Que und Ho, 1996; Solomon et al., 2000), molekulare Details sind jedoch nicht bekannt. Ein Erklärungsversuch geht von der Reaktion des Enzyms mit Substratanaloga aus, die durch ihren enzymatischen Umsatz irreversibel an das aktive Zentrum binden. So konnte

COR-AAD1-00003675
Bayer EX1008 (Part 7 of 9)

dem 5-Ethynyluracil eine solche Rolle beim Umsatz durch die Thymin-7-Hydroxylase zugewiesen werden (Thornburg, 1989; Thornburg und Stubbe, 1993; Lai et al., 1995), analoges konnte für das Phenylpropioylat beim Umsatz durch TfdA gezeigt werden (Dunning-Hotopp und Hausinger, 2002).

Starke Aktivitätsverluste während der Reaktion konnten auch für die Phenoxyalkanoat-spaltenden Enzyme aus MC1, P230 und MH nachgewiesen werden. Bei Lagerung der Enzympräparate über einen langen Zeitraum hinweg wurden keine oder nur geringe Aktivitätsverluste festgestellt (Westendorf et al., 2003; Ruhland 2003). Erst im Verlauf des enzymatischen Umsatzes wurden z.T. dramatische Inaktivierungskinetiken verzeichnet. Die Auswertung solcher Inaktivierungsprofile zeigt, dass es nach 2000-4000 Umsätzen am katalytischen Zentrum zum kompletten Verlust der enzymatischen Aktivität kommt. Diese Inaktivierung ist nicht durch den Einsatz von Ascorbat zu verhindern; stärkere Reduktionsmittel sowie der Einsatz von Katalase wurden nicht getestet. Möglicherweise ist dies auch Ausdruck der oben genannten Selbsthydroxylierung, die in Anwesenheit von α-KG und Sauerstoff innerhalb von einigen Minuten (30 min laut Liu et al., 2001) stattfindet. Auch für das $SdpA_{MC1}$ konnten hydroxylierte Proteinspezies nachgewiesen werden (3.2.4.2). Da kinetische Messungen jedoch innerhalb von zwei Minuten durchgeführt werden, bleibt der Einfluss dieses Effektes auf die kinetischen Kennlinien und Konstanten klein.

4.5 Enzymkinetik

4.5.1 Kinetische Kennlinien und Kooperativität

Für alle in dieser Arbeit untersuchten Phenoxyalkanoat-spaltenden Enzyme ($RdpA_{MC1}$, $RdpA_{MC1}$-rec, $RdpA_{P230}$, $RdpA_{MH}$, $SdpA_{MC1}$, $SdpA_{MC1}$-rec, $SdpA_{P230}$-1, $SdpA_{P230}$-2, $SdpA_{MH}$) wurden Abweichungen der Enzymkinetiken vom Michaelis-Menten-Verhalten nachgewiesen. Die Enzympräparate zeigten zum Teil eine Plateaubildung (Reinigungsstufe HIC) und alle zeichneten sich durch einen sigmoidalen Kurvenverlauf aus. Gründe für das Auftreten von Michaelis-Menten-Verhalten-abweichenden Kennlinien können sein:

- die Enzympräparation besteht aus Isoenzymen
- es existieren alternative Reaktionswege
- das Substrat verändert seine Eigenschaften (z.B. durch Micellenbildung)
- es sind Metallionen-Substrat-Komplexe an der Reaktion beteiligt
- es kommt zur Isomerisierung oder Inaktivierung des Enzyms
- die Enzympräparation enthält verschiedene aktive Spezies, die z.B. durch Proteolyse oder Modifikation entstanden sind

COR-AAD1-00003676
Bayer EX1008 (Part 7 of 9)

- das vorliegende Enzym verhält sich kooperativ

Einige der hier aufgeführten Faktoren konnten für die untersuchten Enzyme ausgeschlossen werden. Die Anwesenheit von echten Isoenzymen kann als Ursache für die abweichenden Kinetiken ausgeschlossen werden, da zumindest bei MC1 jeweils nur ein Gen für RdpA und SdpA gefunden werden konnte (Schleinitz et al., 2004). Alternative Reaktionswege wurden bei Phenoxyalkanoat-spaltenden Enzymen als auch bei anderen α-KG-abhängigen Dioxygenasen bisher nicht beschrieben und sind aufgrund von Untersuchungen zur Reaktions-Stöchiometrie auch nicht zu vermuten (Salowe et al., 1990; Eichhorn et al., 1997; Fukumori und Hausinger, 1993b; Müller et al., 2001; Poh et al., 2001). Bis zum heutigen Tag wurden viele enzymkinetische Untersuchungen mit den Substraten 2,4-D, MCPA, den Enantiomeren des 2,4-DP und des MCPP sowie 2,4-DB und MCPB durchgeführt. Die erhaltenen Kennlinien entsprachen dabei immer einer Michaelis-Menten-Kinetik (Fukumori und Hausinger, 1993b; Suwa et al., 1996; Saari et al., 1998; Hogan, 1999; Poh et al., 2001); über davon abweichende Enzymkinetiken wurde nichts berichtet. Daraus kann geschlossen werden, dass die Substrateigenschaften während der Reaktion konstant bleiben und somit nicht der Grund für die beobachteten sigmoidalen Kurvenverläufe sind. Für Enzymreaktionen, bei denen Metallionen-Substrat-Komplexe an der Reaktion beteiligt sind, wurden des öfteren sigmoidale Kurvenverläufe beobachtet. Ein bekanntes Beispiel hierfür ist das ATP, das nur in komplexierter Form mit einem Metall(II)-Ion ($MeATP^{2-}$-Komplex) von Kinasen als Substrat verwendet wird. Hierbei liefert die Abhängigkeit der Reaktionsgeschwindigkeit von der ATP-Konzentration einen sigmoidalen Kurvenzug (Sabater und Delafuente, 1975; Koland und Hammes, 1986; Porter et al., 1988; Podesta und Plaxton, 1991; Onozuka und Nosaka, 2003). Auch für die Spaltung von Phenoxyalkanoaten sind zweiwertige Metallionen, nämlich das Eisen(II), unerlässlich. Den sigmoidalen Kurvenverlauf bedingen sie jedoch nicht, da offensichtlich keine Substrat/Eisen(II)-Komplexe gebildet werden, Eisen(II) liegt im Enzym koordiniert gebunden vor.

Während des enzymatischen Umsatzes kommt es bei den untersuchten Enzymen zu einem starken Aktivitätsverlust. Nach durchschnittlich 2000 bis 4000 Umsätzen verliert ein aktives Zentrum seine katalytische Aktivität (3.3.3). Da während der Aufnahme der kinetischen Kennlinien nicht mehr als 600 Umsätze pro aktivem Zentrums vermessen wurden, ist der Einfluss der Enzyminaktivierung auf den Kurvenverlauf zwar gering, aber nicht total zu vernachlässigen.

Ein weiterer Grund für das Abweichen von einer Michaelis-Menten-Kinetik ist die Anwesenheit verschieden aktiver Enzymspezies. Multiple Enzymformen konnten für die beiden Enzy-

COR-AAD1-00003677
Bayer EX1008 (Part 7 of 9)

me aus MC1 eindeutig nachgewiesen werden. Das Gemisch aus diesen Enzymformen liefert eine Kennlinie, deren Anstieg durch ein Plateau unterbrochen ist. Nach Trennung der Enzymformen löst sich die komplexe Kinetik auf und die Kennlinien verlaufen stetig, folgen aber nicht der Michaelis-Menten-Gleichung. Enzymkinetische Untersuchungen zeigten tatsächlich unterschiedliche kinetische Konstanten für die einzelnen Enzymformen. Die Anwesenheit von multiplen Enzymformen mit verschiedenen Aktivitäten äußert sich also im Auftreten von Plateaus in der kinetischen Kennlinie, bedingt aber nicht den sigmoidalen Kurvenverlauf. Proteolytische Prozesse als Ursache für das Auftreten von multiplen Enzymformen konnten durch Einsatz von Proteaseinhibitoren ausgeschlossen werden. Die Formen sollten also aufgrund des Vorhandenseins von jeweils nur einem Gen das Produkt einer posttranslationalen Modifizierung sein.

Kooperativität ist die häufigste Ursache für das Auftreten von Kurvenverläufen, die verschieden von den hyperbolen Kurvenzügen nach Michaelis-Menten sind. Zur Erklärung des Phänomens der Kooperativität wurden zwei Modelle entwickelt: das Symmetrie-Modell (Monod et al., 1965) und das sequenzielle Modell (Koshland et al., 1966). Beiden Modellen ist gemeinsam, dass sie ein oligomeres, zumindest jedoch ein dimeres Protein voraussetzen. Die Monomere dieses Proteins können in zwei Konformationszuständen existieren: einer R- und einer T-Form, die sich in ihren kinetischen Eigenschaften unterscheiden. Die R-Form kann sich in die T-Form umwandeln. Beim Symmetrie-Modell passiert die Umwandlung mit allen Monomeren gleichzeitig, die Symmetrie des Moleküls bleibt erhalten. Beim sequenziellen Modell geschieht die Umwandlung der Monomeren nacheinander. Es sind sowohl positive als auch negative Kooperationen denkbar. Nach neueren Untersuchungen bleibt die Kooperativität jedoch nicht mehr nur oligomeren Proteinen vorbehalten, auch für monomere Proteine wurde sie jüngst nachgewiesen (Kamata et al., 2004). Die kinetischen Kennlinien von kooperativen Enzymen sind sigmoidal. Es kann aber auch zur Ausbildung von Plateaus kommen, wenn es sich z.B. um negative Kooperation handelt (Conway und Koshland, 1968), oder es aber nach dem sequenziellen-Modell von Koshland et al. (1966) zu Stabilisierung von intermediären Konformationszuständen kommt. Beide Fälle der Plateaubildung wurden bereits beobachtet. So binden die Substrate der Glycerol-3-Phosphat-Cytidyltransferase durch das Auftreten von negativer Kooperativität an die erste Untereinheit mit einer 150fach höheren Affinität als an die zweite, die Bindungskurven der Substrate sind biphasisch (Sanker et al., 2001). Die Kennlinie der Phosphoenolpyruvat-Carboxylase weist für das Phosphoenolpyruvat ein Plateau bei halbmaximaler Umsatzrate auf, welches mit der Stabilisierung der Konformation erklärt wird, bei der sich die eine Hälfte der Untereinheiten in der R-, die andere in der T-

COR-AAD1-00003678
Bayer EX1008 (Part 7 of 9)

Form befindet (Corwin und Fanning, 1968). Sigmoide Kennlinien sowohl mit als auch ohne Plateaubildung wurden für die Phenoxyalkanoat-spaltenden Enzyme aus MC1, P230 und MH nachgewiesen. Die Plateaus werden in diesen Fällen nicht durch Kooperativität verursacht, da nach Separation der multiplen Enzymformen des Enzympräparates die Kennlinien stetig verlaufen. Das Auftreten des sigmoiden Verlaufs kommt dagegen mit großer Wahrscheinlichkeit durch kooperative Interaktionen zustande. Bislang wurde ein solches Phänomen für diese und auch andere α-KG-abhängigen Enzyme nicht definitiv beschrieben. Betrachtet man aber bereits veröffentlichte Kennlinien unter dem Aspekt der Sigmoidität, so zeigt sich, dass z.B. die kinetischen Daten der Sulfonat/α-KG-Dioxygenase (Hogan, 1999) bezüglich des Substrates Taurocholat besser einen sigmoidalen als einen hyperbolen Kurvenzug beschreiben. Der Hill-Koeffizient beträgt etwa 1,5. Ebenso kann ein sigmoidaler Kurvenverlauf aus den Daten für die Spaltung von (R)-DP durch den Rohextrakt von *Alcaligenes denitrificans* (Saari et al., 1999) abgeleitet werden. Für verschiedene α-KG-abhängige Dioxygenasen sind Substrat-induzierte Konformationsänderungen bekannt (Sami et al., 1997; Vålegard et al., 1998; Zhang et al., 2000; Clifton et al., 2001; O'Brien et al., 2003). So wurde gefunden, dass der C-Terminus während der Reaktion über den aktiven Spalt klappt und diesen so vor Lösungsmittelmolekülen abschirmt. TauD wurde als Tetramer kristallisiert und es konnte gezeigt werden, dass in einer solchen Anordnung nur drei der Monomere in der Lage sind, das Taurin zu binden. Ob ein direkter Zusammenhang zwischen den Konformationsänderungen der Proteine und den kinetischen Kennlinien besteht, ist nicht geklärt.

Bei den in dieser Arbeit untersuchten Phenoxyalkanoat-spaltenden Enzymen handelt es sich um di- und trimere Proteine, und trotz dieser Tatsache tritt Kooperativität auf. Für höher aggregierte symmetrische Proteine wurde ein solches Verhalten oft nachgewiesen (Hämoglobin-Homotetramer [Perutz, 1970], Aspartat-Transcarbamylase-Homohexamer [Van Vliet et al., 1991], Aspartokinase-Homotetramer [Janin und Cohen, 1969], Homoserindehydrogenase-Homotetramer [Janin und Cohen, 1969], Phosphofruktokinase-Homotetramer [Badul, 1979]). Bei kleineren Proteinen kommt kooperatives Verhalten eher selten vor, wurde aber auch schon beschrieben (Glucokinase–Monomer [Kamata et al., 2004], Catechol-1,2-Dioxygenase-Homodimer, Homotrimer [Briganti et al., 2000]). Interessanterweise handelt es sich bei den $SdpA_{MC1}$-Enzymformen I2 und I3 nicht um Homodimere, sondern um Heterodimere. Für solche Proteine wurde nach meiner Literaturrecherche noch keine Kooperativität nachgewiesen.

Für die untersuchten Enzyme der drei Stämme konnte positive homotrope Kooperativität gezeigt werden. Das kooperative Verhalten der Phenoxyalkanoat-spaltenden Enzyme ist im Ge-

COR-AAD1-00003679
Bayer EX1008 (Part 7 of 9)

gensatz zu anderen kooperativen Enzymen nicht sehr ausgeprägt. Die Hill-Koeffizienten liegen für alle getesteten Herbizide im Bereich zwischen 1 und 1,8, die einzige Ausnahme bilden hierbei die $SdpA_{MC1}$-Enzyme bezüglich des (S)-MCPP. Für dieses Substrat ist der Hill-Koeffizient bei der Enzymform I2 2 und bei I1 sogar 3,5.

4.5.2 Posttranslationale Modifizierung und Enzymkinetik

Die RdpA- und SdpA-Enzyme reagieren sehr empfindlich auf Änderungen im pH-Wert (Westendorf, 2001), bereits kleine Änderungen in der Protonen-Konzentration haben eine signifikante Änderung der Umsatzraten zur Folge. Nur durch exakte Einstellungen des pH-Wertes war es möglich, reproduzierbare Messdaten zu bekommen. Um die kinetischen Konstanten genau bestimmen zu können, wurden die Enzymkonzentrationen so gewählt, dass die Umsatzraten zwischen 1 und 14 nmol/min lagen. Auf diese Weise wurden über die ersten 2 Minuten lineare Produktbildungskurven mit einem Regressionskoeffizient von >0,99 erhalten. Die kinetischen Daten der Herbizid-spaltenden Enzyme dieser Arbeit wurden auf zwei voneinander unabhängigen Wegen ausgewertet: Zum einen mit linearisierenden Verfahren inklusive der manuellen Wichtung der Werte, zum anderen durch eine Computer-gestützte Auswertung der nicht linearisierten kinetischen Kennlinien. Beide Verfahren liefern sehr ähnliche kinetische Konstanten, deren Standardabweichung etwa 15% beträgt.

Alle Phenoxyalkanoat-spaltenden Enzyme der Stämme MC1 (Westendorf et al., 2003), P230 (Ruhland, 2003) und MH sind enantiospezifisch, sie spalten entweder die (R)- oder die (S)-Enantiomeren der Phenoxypropionate. Die (R)-spezifischen Enzyme der drei Stämme und des rekombinanten RdpA zeichnen sich durch identische Primärstrukturen aus (Schleinitz et al., 2004), trotzdem unterscheiden sich die Proteine in ihren kinetischen Kennlinien und Konstanten signifikant (Tabelle 27). Die RdpA-Enzyme aus MC1 und MH sind einander sehr ähnlich. Sie zeigen fast identische Kennlinien bezüglich der Phenoxyalkanoate, ihre kinetischen Konstanten stimmen überein und sie zeigen das gleiche Laufverhalten im nativen Gel. Dem gegenüber steht das $RdpA_{MC1}$-rec. Dieses Enzym zeigt trotz einer identischen Primärstruktur, den gleichen R_f-Werten und demselben Spotmuster nach Auftrennung im 2D-Gel wie das $RdpA_{MC1}$ von diesem Enzym abweichende Kennlinien und Wechselzahlen. Die Kennlinien sind stetig und nicht, wie bei MC1 und MH durch ein Plateau unterbrochen, was auf das Vorhandensein einer dominanten nativen Enzymform hindeutet. Ein weiteres Indiz hierfür ist das Auftreten nur einer RdpA-Proteinbande nach nativer Auftrennung im Acrylamidgel. Die K_M-Werte des $RdpA_{MC1}$ sind mit denen des rekombinanten Enzyms identisch, die Wechselzahlen

COR-AAD1-00003680
Bayer EX1008 (Part 7 of 9)

liegen jedoch deutlich darüber. All dies lässt den Schluss zu, dass die Modifizierungen, die die Auftrennung der Monomere im 2D-Gel bedingen, nicht mit den Eigenschaften, die zur Trennung im nativen Acrylamidgel führen, korrelieren und keinen Einfluss auf die kinetischen Konstanten und Kennlinien haben, da diese sowohl im rekombinanten als auch nativen RdpA nachgewiesen wurden.

Das RdpA aus P230 weist ebenfalls eine identische Primärstruktur zum $RdpA_{MC1}$ auf, zeichnet sich jedoch durch einen signifikant kleineren R_f-Wert aus. Verschieden ist auch das Spotmuster nach der Auftrennung im 2D-Gel. Dieses Enzym muss demnach eine andere posttranslationale Modifizierung aufweisen als das $RdpA_{MC1}$. Dieses zeigt sich auch in den kinetischen Parametern. Die Kennlinien bei variabler Phenoxyacetat-Konzentration sind stetig, und für alle Herbizide ergeben sich deutlich niedrigere K_M-Werte sowie höhere Wechselzahlen als für $RdpA_{MC1}$. Diese Art der Modifizierung führt also zu gesteigerten katalytischen Eigenschaften des Enzyms, der Effizienzkoeffizient ist für die (R)-Enantiomere der Phenoxypropionate etwa zwei- bis dreimal so hoch wie für $RdpA_{MC1}$, für die Phenoxyacetate sogar 8mal so hoch. Zusammengefasst ist festzustellen: die Modifikationen am *rdpA*-Genprodukt steigern die Umsatzraten der Enzyme bezüglich aller Herbizid-Substrate, die Affinität aber erhöht sich nur für die Phenoxyacetate. Das führt zu einer Verschiebung des Substratverwertungsspektrums. Der Rohextrakt von P230 enthält etwa doppelt soviel 2,4-D-Spaltungsaktivität bezüglich der (R)-DP-Spaltung wie der von MC1. Im Gegensatz zum MC1-Rohextrakt sind in diesem aber keine 2,4-D-spaltenden (S)-spezifischen Enzyme enthalten. Ebenso konnten keine TfdA-Proteine nachgewiesen werden. P230 muss also das gesamte 2,4-D über $RdpA_{P230}$ umsetzen.

Die nativen Enzymformen des $SdpA_{MC1}$ gehen ebenfalls auf posttranslationale modifizierte Monomere mit identischen Aminosäuresequenzen zurück. Diese Enzymformen unterscheiden sich sowohl im Verhältnis der Monomere zueinander als auch in ihren kinetischen Kennlinien und Parametern. Interessanterweise wurden auch für das rekombinante $SdpA_{MC1}$ unterschiedliche Monomere nachgewiesen, die in ihren Eigenschaften mit denen der nativen Proteine übereinstimmen. Das Verhältnis der Monomere im rekombinanten Protein ist identisch mit dem der nativen Enzymform $SdpA_{MC1}$-I2, das kinetische Verhalten bezüglich der Herbizide und das Laufverhalten im nativen Acrylamidgel entspricht aber dem des Proteins $SdpA_{MC1}$-I1. Damit zeigt sich analog wie für RdpA, dass aus den verschiedenen Trenneigenschaften im 2D-Gel nicht auf das kinetische Verhalten der Proteine geschlossen werden kann. Für die Eigenschaften, die zur Trennung der Proteinformen im nativen Acrylamidgel führen, trifft dies eher zu. Die Modifizierung am $SdpA_{MC1}$ führt wiederum zu deutlichen Veränderungen der

COR-AAD1-00003681
Bayer EX1008 (Part 7 of 9)

Substratverwertungseigenschaften, d.h. letztlich ändert sich das Substratverwertungsspektrum (Tabelle 26).

Die in dieser Arbeit gewonnenen Ergebnisse stellen einen ersten Beitrag zum Verständnis der enantioselektiven Spaltung von Phenoxyalkansäuren dar. Durch die Aufklärung der 3D-Struktur der (S)- und (R)-spezifischen Enzyme sollte es möglich sein, einen tiefen Einblick in Struktur-Funktions-Beziehungen zu erlangen. Der molekulare Hintergrund der Enantioselektivität der Enzyme sollte sich offenbaren. Ebenso sollte der Vergleich der 3D-Strukturen der RdpA- und SdpA-Enzyme sowohl der multiplen Enzymformen als auch der einzelnen Stämme untereinander einerseits zum Verständnis der molekularen Ursachen verschiedener Substratverwertungsprofile beitragen und andererseits Einblicke in Möglichkeiten der Regulation der Enzymaktivitäten liefern.

COR-AAD1-00003682
Bayer EX1008 (Part 7 of 9)

5 Zusammenfassung

In der vorliegenden Arbeit wurden die initialen Enzyme des Phenoxyalkanoat-Abbaus, die α-Ketoglutarat-abhängige Dioxygenasen darstellen, aus den Bakterienstämmen *Delftia acidovorans* MC1, *Rhodoferax* sp. P230 und *Sphingobium herbicidovorans* MH gereinigt und sowohl proteinbiochemisch als auch enzymkinetisch charakterisiert.

Alle drei untersuchten Stämme sind zur kompletten Spaltung der (R,S)-Enantiomere der 2-Phenoxypropionate (R,S)-2-(2,4-Dichlorphenoxy)propionat (2,4-DP) und (R,S)-2-(4-Chlor-2-methylphenoxy)propionat (MCPP) sowie zur Spaltung der Phenoxyacetate 2,4-Dichlorphenoxyacetat (2,4-D) und 4-Chlor-2-methylphenoxyacetat (MCPA) (Ebrig et al., 1997, Müller et al., 1999a) in der Lage. Der Stamm MH kann zusätzlich noch die Phenoxybutyrate 2,4-Dichlorphenoxybutyrat (2,4-DB) und 4-Chlor-2-methylphenoxybutyrat (MCPB) verwerten (Zipper et al., 1996).

Die Spaltung der 2-Phenoxypropionate erfolgt in den drei untersuchten Stämmen enantioselektiv, das heißt, es gibt je ein Enzym für die Spaltung der (R)-Enantiomere und für die der (S)-Enantiomere. Die (R)-DP/α-Ketoglutarat Dioxygenase (RdpA) katalysiert die Spaltung der (R)-Enantiomere der 2-Phenoxypropionate und setzt mit geringerer Aktivität auch die Phenoxyacetate um. Dieses Enzym ist in allen drei Stämmen auf das gleiche Gen zurückzuführen (Schleinitz et al., 2004).

Das (S)-spezifische Enzym, (S)-DP/α-KG Dioxygenase (SdpA), setzt prinzipiell die (S)-Enantiomere der 2-Phenoxypropionate um. Es unterscheidet sich jedoch in den einzelnen Stämmen deutlich, insofern es sich hier um unterschiedliche Proteine handelt, die von verschieden Genen codiert werden. Das Enzym aus MC1 setzt neben (S)-DP und (S)-MCPP auch die entsprechenden Phenoxyacetat-Derivate mit deutlicher Aktivität um. Im Stamm MH konnten sogar zwei verschiedene SdpA-Enzyme nachgewiesen werden, die neben den (S)-2-Phenoxypropionaten ebenfalls Phenoxyacetate und in einem Fall sogar noch die entsprechenden Phenoxybutyrat-Derivate umsetzen können. Im Gegensatz dazu beschränkt sich die SdpA-Aktivität im Stamm P230 allein auf die Spaltung der (S)-2-Phenoxypropionate.

Die (R)-spezifischen Enzyme sind oligomere Proteine, die sich aus Monomere mit einer Molmasse von etwa 35,8 kD zusammensetzen. Für die RdpA-Proteine aus MC1 und P230 zeigt sich eine trimere Struktur. Darüber hinaus konnten für die Monomeren ladungsisomere Formen nachgewiesen werden. Diese sind offensichtlich das Produkt einer posttranslationalen Modifizierung; die Art der Modifikation ist noch unbekannt. Das native Enzym aus MC1 setzt

COR-AAD1-00003683
Bayer EX1008 (Part 7 of 9)

sich aus unterschiedlichen Monomeren zusammen. Unter nativen Bedingungen können drei Enzymformen, die sich in ihren pI-Werten unterscheiden, nachgewiesen und teilweise voneinander getrennt werden.

Das $SdpA_{MC1}$ ist ein dimeres Protein mit einer Molmasse von 64 kD. Es wurden drei native ladungsisomere Proteinformen (I1, I2, I3) dieses Enzyms nachgewiesen, die sich aus drei ladungsisomeren Monomeren (S1, S2, S3) zusammensetzen. Der Nachweis der Existenz der Dimere S1S1 (I1), S1S2 (I2) und S1S3 (I3) konnte erbracht werden. Am $SdpA_{MC1}$ wurden Hydroxylierungen an Trp235 und Trp255 sowie eine zusätzliche Masse von 209 am Cys237 nachgewiesen.
Das (S)-spezifische Enzym aus P230 ist ein oligomeres Protein, das sich aus Monomeren von etwa 32,3 kD ableitet. Es konnten zwei native Enzymformen mit gleicher Primärstruktur und sechs ladungsisomere Monomere nachgewiesen werden.
Die Molmasse eines Monomers des $SdpA_{MH}$ beträgt 32,2 kD. Auch bei diesem Enzym handelt es sich um ein oligomeres Protein. Der endgültige Nachweis von multiplen Enzymformen steht noch aus.

Durch kinetische und proteinbiochemische Untersuchungen sowohl an den nativen als auch an rekombinanten Enzymen konnte der Einfluss der Modifizierung auf die kinetischen Konstanten gezeigt werden. Diese führt zu veränderten kinetischen Eigenschaften, wobei unterschiedliche Modifizierungen auch unterschiedliche Effekte bewirken, wie in den einzelnen Stämmen deutlich wird. Die (R)-spezifischen Dioxygenasen zeichnen sich durch identische Primärstrukturen aus, trotzdem unterscheiden sich die einzelnen Proteine deutlich in ihrem kinetischen Verhalten. Dies zeigt sich besonders klar bei der Spaltung der Phenoxyacetate: 2,4-D und das MCPA werden durch $RdpA_{P230}$ mit einem bis zu 8mal höheren k_{kat}/K_M-Quotienten umgesetzt als durch $RdpA_{MC1}$.
Auch die $SdpA_{MC1}$-Enzymformen besitzen die gleiche Aminosäuresequenz. Proteinchemisch unterscheiden sie sich lediglich durch eine bislang nicht identifizierte Modifizierung. Diese hat kinetische Effekte zur Folge: Die Enzymformen unterscheiden sich signifikant in ihren Wechselzahlen bezüglich der Herbizid-Substrate. Ähnliches zeigt sich auch für die Enzymformen des $SdpA_{P230}$.

COR-AAD1-00003684
Bayer EX1008 (Part 7 of 9)

6 Literatur

Abbott M.T., Schandl E.K., Lee R.F., Parker T.S., Midgett R.J.: Cofactor requirements of thymine 7-hydroxylase. Biochim Biophys Acta 132 (1967), 525-528

Anderson L.B., Maderia M., Ouellette A.J.A., Putman-Evans C., Higgins L.A., Krick T., MacCoss M.J., Lim H., Yates III J.R., Barry B.A.: Posttranslational modifications in the CP43 subunit of photosystem II. Proc. Nat. Acad. Sci. 99 (2002), 14676-14681

Aravind L., Koonin E.V.: The DNA-repair protein AlkB, EGL-9, and leprecan define new families of 2-oxoglutarate- and iron-dependent dioxygenases. Genome Biol. 2 (2001), 1-8

Ariëns E.J.: Racemates - an impediment in the use of drugs and agrochemicals. Krstulovic Am. Chiral separations by HPLC. Ellis Horwood, Chichester (1989), 31-68

Babul J.: Significance of phosphofructokinase allostery: The *Escherichia coli* isozymes. Arch. Biol. Med. Exp. (Santiago) 12 (1979), 611-616

Baldwin J.E., Bradley M., Abbott S.D., Adlington R.M.: New penicillins from isopenicillin N synthase. Tetrahedron 47 (1991), 5309-5328

Bath M.A., Ishida T., Horiike K., Vaidyanathan C.S., Nozaki M.: Purification of 3,5-dichlorocatechol-1,2-dioxygenase, a nonheme iron dioxygenase and a key enzyme in the biodegradation of a herbicide, 2,4-dochlorophenoxyacetic acid (2,4-D), from *Pseudomonas cepacia* CSV90. Arch. Biochem. Biophy. 300 (1993), 738-746

Benndorf D., Davidson I., Babel W.: Regulation of catabolic enzymes during long-term exposure of *Delftia acidovorans* MC1 to chlorophenoxy herbicides. Microbiology 150 (2004), 1005-1014

Bentley R.: From optical activity in quartz to chiral drugs: molecular handedness in biology and medicine. Perspect. Biol. Med. 38 (1995), 188-229

Blum, H., Beier, H., Gross, H.J.: Improved silver staining of plant proteins, RNA and DNA in polyacrylamide gels. Electrophoresis 8 (1987), 93-99

Boldt Y.R., Sadowsky M.J., Ellis L.B., Que L. Jr, Wackett L.P.: A manganese-dependent dioxygenase from *Arthrobacter globiformis* CM-2 belongs to the major extradiol dioxygenase family. J. Bacteriol. 177 (1995), 1225-1232

Borovok I., Landman O., Kreisberg-Zakarin R., Aharonowitz Y., Cohen G.: Ferrous active site of isopenicillin-N-synthase: genetic sequence analysis of the endogenous ligands. Biochemistry 35 (1996), 1981-1987

Boyington J.C., Gaffney B.J., Amzel L.M.: Crystallization and preliminary x-ray analysis of soybean lipoxygenase-1, a non-heme iron-containing dioxygenase. J. Biol. Chem. 265 (1990), 12771-12773

Briganti F., Pessione E., Giunta C., Mazzoli R., Scozzafava A.: Purification and catalytic properties of two catechol 1,2-dioxygenase isozymes from benzoate-grown cells of *Acinetobacter radioresistens*. J. Protein Chem. 19 (2000), 709-716

COR-AAD1-00003685
Bayer EX1008 (Part 7 of 9)

Britsch L.: Purification and charcterization of flavone synthase I, a 2-oxoglutarate-dependent desaturase. Arch. Biochem. Biophys. 282 (1990), 152-160

Clifton I.J., Hsueh L.C., Baldwin J.E., Harlos K., Schofield C.J.: Structure of prolin 3-hydroxylase. Eur. J. Biochem. 268 (2001), 6625-6636

deCarolis E., deLuca V.: Purification, characterization, and kinetic analysis of a 2-oxoglutarate-dependent dioxygenase involved in vindoline biosynthesis from *Catharanthus roseus*. J. Biol. Chem. 268 (1993), 5504-5511

deCarolis E., deLuca V.: 2-oxoglutarate-dependent dioxygenase and related enzymes: biochemical characterization. Phytochemistry 36 (1994), 1093-1107

Conway A., Koshland D.E. Jr.: Negative cooperativity in enzyme action. The binding of diphosphopyridine nucleotide to glyceraldehyde 3-phosphate dehydrogenase. Biochemistry 7 (1968), 4011-4023

Corpet F.: Multiple sequence alignment with hierarchical clustering. Nucleic Acids Res. 25 (1988) 10881-10890

Corwin L.M., Fanning G.R.: Studies of parameters affecting the allosteric nature of phosphoenolpyruvate carboxylase of *Escherichia coli*. J. Biol. Chem. 243 (1968), 3517-3525

Cosper N.J., Stalhandske C.M.V., Saari R.E., Hausinger R.P., Scott R.A.: X-ray absorbtion spectroscopic analysis of Fe(II) and Cu(II) forms of a herbicide-degrading α-ketoglutarate dioxygenase. J. Biol. Inorg. Chem. 4 (1999), 122-129

Donaldson D., Kiely T., Grube A.: 1998 and 1999 market estimates. EPA Pesticides industry sales and usage. EPA, Washington, D.C. (2002), 1-32

Dunning Hotopp J.C., Hausinger R.P.: Probing the 2,4-dichlorophenoxyacetate/α-ketoglutarate dioxygenase substrate-binding site by site-directed mutagenasis and mechanism-based inactivation. Biochemistry 41 (2002), 9787-9794

Easson L.H., Stedman E.: Studies on the relationship between chemical constitution and physiological action. V. Molecular dissymmetry and physiological activity. Biochem. J. 27 (1933), 1257-1266

Egmond MR., Fasella PM., Veldink GA., Vliegenthart JF., Boldingh J.: On the mechanism of action of soybean lipoxygenase-1. A stopped-flow kinetic study of the formation and conversion of yellow and purple enzyme species. Eur. J. Biochem. 76 (1977), 469-479

Ehrig A., Müller R.H., Babel W.: Isolation of phenoxy herbicide-degrading *Rhodoferax* species from contaminated building material. Acta Biotechnol. 17 (1997), 351-356

Eliel E.L., Wilen S.H.: Stereochemistry of organic compounds. Wiley, New York (1994)

Elkins J.M., Ryle M.J., Clifton I.J., Dunning Hotopp J.C., Lloyd J.S., Burzlaff N.I., Baldwin J.E., Hausinger R.P., Roach P.L.: X-ray structure of *Escherichia coli* Taurine/α-ketoglutarate dioxygenase complexed to ferrous iron and substrates. Biochemistry 41 (2002), 5185-5192

COR-AAD1-00003686
Bayer EX1008 (Part 7 of 9)

Emerson, E.J.: The condensation of aminoantipyrine. II. A new color test for phenolic compounds. Org. Chem., 8 (1943), 417-419

Emerson, E.J., Kenneth, K.: The condensation of aminoantipyrine VI. A study of the effect of excess base on the reaction of aminoantipyrine with phenolic compounds in the presence of oxidizing agents. Org. Chem., 13 (1948), 532-534

Evans W.C., Smith B.S.W., Moss P., Fernley H.N.: Bacterial metabolism of 4-chlorophenoxyacetate. Biochem. J. 122 (1971a), 509-517

Evans W.C., Smith B.S.W., Farnley H.N., Davies J.I.: Bacterial metabolism of 2,4-dichlorophenoxyacetate. Biochem. J. 122 (1971b), 543-551

Fukumori F., Hausinger R.P.: *Alcaligenes eutrophus* JMP 134 "2,4-dichlorophenoxyacetate monooxygenase" is an α-ketoglutarate-dependent dioxygenase. J. Bacteriol. 175 (1993a), 2083-2086

Fukumori F., Hausinger R.P.: Purification and characterization of 2,4-dichlorophenoxyacetate/α-ketoglutarate dioxygenase. J. Biol. Chem. 268 (1993b), 24311-24317

deGroot J.J., Garssen G.J., Vliegenthart J.F., Boldingh J.: The detection of linoleic acid radicals in the anaerobic reaction of lipoxygenase. Biochim. Biophys. Acta 326 (1973), 279-284

Griggs D.L., Hedden P., Lazarus C.M.: Partial purification of two gibberellin 2β-hydroxylases from cotyledons of *Phaseolus vulgaris*. Phytochemistry 30 (1991), 2507-2512

Han S., Eltis L.D., Timmis K.N., Muchmore S.W., Bolin J.T.: Crystal structure of the biphenyl-cleaving extradiol dioxygenase from a PCB-degrading *pseudomonad*. Science 270 (1995), 976-980

Harrison I., Williams G.M., Carlick C.A.: Enantioselective biodegradation of mecoprop in aerobic and anaerabic microcosms. Chemosphere 53 (2003), 539-549

Hassal K.A.: The biochemistry and uses of pesticides. VHC Weinheim (1990)

Hausmann E.: Cofactor requirements for the enzymatic hydroxylation of lysine in a polypeptide precursor of collagen. Biochim. Biophys. Acta 133 (1967), 591-593

Hedden P.: The oxidases of gibberellin biosynthesis: Their function and mechanism. Physiol. Planta 101 (1997), 709-719

Hegg E.L., Whiting A.K., Saari R.E., McCracken J., Hausinger R.P., Que L. Jr.: Herbicide-degrading alpha-keto acid-dependent enzyme TfdA: metal coordination environment and mechanistic insights. Biochemistry 38 (1999), 16714-16726

Hoffmann D., Müller R.H., Kiesel B., Babel W.: Isolation and characterization of an alcaliphilic bacterium capable of growing on 2,4-dichlorophenoxyacetic acid and 4-chloro-2-methylphenoxyacetic acid. Acta Biotechnol. 16 (1996), 121-131

COR-AAD1-00003687
Bayer EX1008 (Part 7 of 9)

Hoffmann D., Kleinsteuber S., Müller R.H., Babel W.: A transposon encoding the complete 2,4-dichloro-phenoxyacetic acid degrading pathway in the alkalitolerant strain *Delftia acidovorans* P4a. Microbiol. 149 (2003), 2545-2556

Hogan D.A.: Characterization and function of 2,4-dichlorophenoxyacetic acid/α-ketoglutarate dioxygenase and related enzymes. Ph.D. thesis, Michigan State University, East Lansing, MI (1999)

Hogan D.A., Smith S.R., Saari E.A., McCracken J., Hausinger R.P.: Site-directed mutagenesis of 2,4-dichlorophenoxyacetic acid/α-ketoglutarate dioxygenase. J. Biol. Chem. 275 (2000), 12400-12409

Holme E.: A kinetic study of thymine 7-hydroxylase from neurospora crassa. Biochemistry 14 (1975), 4999-5003

Holton T.A., Brugliera F., Tanaka Y.: Cloning and expression of flovonol sythase from *Petunia hybrida*. Plant J. 4 (1993), 1003-1010

Horvath M., Ditzelmüller G., Loidl M., Streichbier F.: Isolation and characterization of a 2-(2,4-dichlorophenoxy)propionic acid-degrading soil bacterium. Appl. Microbiol. Biotechnol. 33 (1990), 213-216

Hulse J.D., Ellis S.R., Henderson L.M.: Carnitine biosynthesis. beta-Hydroxylation of trimethyllysine by an alpha-ketoglutarate-dependent mitochondrial dioxygenase. J. Biol. Chem. 253 (1978), 1654-1659

Hutton J.J. Jr., Trappel A.L., Udenfriend S.: Requirements for alpha-ketoglutarate, ferrous ion and ascorbate by collagen proline hydroxylase. Biochem. Biophys. Res. Commun. 24 (1966), 179-184

Janin J., Cohen G.N.: The threonine-sensitive homoserine dehydrogenase and aspartokinase activities of *Escherichia coli* K 12. A study of the allosteric equilibrium. Eur. J. Biochem. 11 (1969), 520-529

Jansen G.A., Mihalik S.J., Watkins P.A., Jakobs C., Moser H.W., Wanders R.J.: Characterization of Phytanoyl-coenzym A hydroxylase in human liver and activity measurements in patient with peroxisomal disorders. Clin. Chim. Acta 271 (1998), 203-211

Kamata K., Mitsuya M., Nishimura T., Eiki J., Nagata Y.: Structural basis for allosteric regulation of the monomeric allosteric enzyme human glucokinase. Structure (Camb). 12 (2004), 429-438

Kinter M., Sherman N.E.: Protein sequenzing and identification using tandem mass spectrometry. Wiley- Interscience, New York (2000)

Kivirikko K.I., Prockop D.J.: Hydroxylation of proline in synthetic polypeptides with purified protocollagen hydroxylase. J. Biol. Chem. 242 (1967), 4007-4012

Kivirikko K.I., Prockop D.J.: Partial purification and characterization of protocollagen lysine hydroxylase from chick embryos. Biochim. Biophys. Acta 258 (1972), 366-379

COR-AAD1-00003688
Bayer EX1008 (Part 7 of 9)

Kivirikko K.I., Myllyla R., Pihlajaniemi T.: Protein hydroxylation: prolyl 4-hydroxylase, an enzyme with four cosubstrates and a multifunctional subunit. FASEB J. 3 (1989), 1609-1617

Koland J.G., Hammes G.G.: Steady state kinetic studies of purified yeast plasma membrane proton-translocating ATPase. J. Biol. Chem. 261 (1986), 5936-5942

Korioth F., Gieffers C., Frey J.: Cloning and characterization of the human gene encoding aspartyl-β-hydroxylase. Gene 150 (1994), 395-399

Koshland D.E. Jr., Nemethy G., Filmer D.: Comparison of experimental binding data and theoretical models in proteins containing subunits. Biochemistry 5 (1966), 365-85

Kreisberg-Zakarin R., Borovok I., Yanko M., Aharonowitz Y., Cohen G.: Recent advances in the structure and function of isopenicillin N synthase. Antonie Van Leewenhoek 75 (1999), 33-39

Kuhm A.E., Schlömann M, Knackmuss H.J., Pieper D.H.: Purification and characterization of dichloromuconate cycloisomerase from *Alcaligenes eutrophus* JMP134. Biochem. J. 266 (1990), 877-883

Laemmli, U.K.: Cleavage of structural proteins during the assembly of the head of bacteriophage T4. Nature (London) 227 (1970), 679-690

Lai M., Wu W., Stubbe J.A.: Characterization of a novel, stable norcaradiene adduct resulting from inactivation of thymine hydroxylase by 5-ethynyluracil. J. Am. Chem. Soc. 117 (1995), 5023-5030

Leveau J.H., Zehnder A.J., van der Meer J.R.: The *tfdK* gene product facilitates uptake of 2,4-dichlorophenoxyacetate by *Ralstonia eutropha* JMP134(pJP4). J. Bacteriol. 180 (1998), 2237-2243

Lindblad B., Lindstedt G., Lindstedt S., Rundgren M.: Purification and some properties of human 4-hydroxyphenylpyruvate dioxygenase (I). J. Biol. Chem. 252 (1977), 5073-84

Lindstedt G., Lindstedt S.: Cofactor requirements of γ-butyrobetaine hydroxylase from rat liver. J. Biol. Chem. 245 (1970), 4178-4180

Lindstedt G., Lindstedt S., Nordin I.: Purification and properties of gamma-butyrobetaine hydroxylase from *Pseudomonas* sp AK 1. Biochemistry 16 (1977), 2181-2188

Lindstedt S., Nordin I.: Multiple forms of gamma-butyrobetaine hydroxylase (EC 1.14.11.1). Biochem. J. 223 (1984), 119-127

Liu T., Chapman P.J.: Purification and properties of a plasmidal-encoded 2,4-dichlorophenol hydroxylase. FEBS Lett. 173 (1984), 314-318

Liu A., Ho R.Y., Que L. Jr., Ryle M.J., Phinney B.S., Hausinger R.P.: Alternative reactivity of an alpha-ketoglutarate-dependent iron(II) oxygenase: enzyme self-hydroxylation. J. Am. Chem. Soc. 123 (2001), 5126-5127

COR-AAD1-00003689
Bayer EX1008 (Part 7 of 9)

Loos M.A.: Phenoxyalkanoic acids. Herbicides: chemistry, degradation and mode of action. (Eds.: Kearney P.C., Kaufman D.D.), 1, Marcel Dekker, New York (1975), 2-101

Lukacin R., Britsch L.: Identification of strictly conserved histidin and arginine residues a part of the active site in *Petunia hybrida* flovanone 3β-hydroxylase. Eur. J. Biochem. 249 (1997), 748-757

Marsh E.N., Chang M.D., Townsend C.A.: Two isozymes of clavaminate synthase central to clavulanic acid formation: cloning and sequencing of both genes from *Streptomyces clavuligerus*. Biochemistry 31 (1992), 12648-12657

Marusyk R., Sergeant A.: A simple method for dialysis of small-volume samples. Anal. Biochem. 105 (1980), 403-404

Matell M.: Stereochemicals studies on plant growth regulators. VII Optically active α-(2-methyl-4-chlorophenoxy)-propionic acid and α-(2,4-dichlorophenoxy)-*n*-butyric acid and their steric relations. Ark Kemi 6 (1953), 365-373

Mertingk H., Müller R.H., Babel W.: Etherolytic cleavage of 4-(2,4-dichlorophenoxy)butyric acid and 4-(4-chloro-2-methylphenoxy)butyric acid by species of *Rhodococcus* and *Aureobacterium* isolated from an alkaline environment. J Basic Microbiol. 38 (1998), 257-267

Mesecar A.D., Koshland D.E. Jr.: A new model for protein stereospecificity. Nature 403 (2000a), 614-615

Mesecar A.D., Koshland D.E. Jr.: Sites of binding and orientation in a four-location model for protein stereospecificity. IUBMB Life 49 (2000b), 457-466

Minor W., Steczko J., Stec B., Otwinowski Z., Bolin J.T., Walter R., Axelrod B.: Crystal structure of soybean lipoxygenase L-1 at 1.4 Å resolution. Biochemistry 35 (1996), 10687-10701

Monod J., Wyman J., Changeux J.P.: On the nature of allosteric transitions: a plausible model. J. Mol. Biol. 12 (1965), 88-118

Morillo E., Perez-Martinez J.I., Gines J.M.: Leaching of 2,4-D from a soil in the presence of β-cyclodextrin: laboratory columns experiments. Chemosphere 44 (2001), 1065-1069

Müller R.H., Simon D., Große H.J., and Babel W.: Substrate inhibition under stationary growth conditions-nutristat experiments with *Ralstonia eutropha* JMP 134 during growth on phenol and 2,4-dichlorophenoxyacetate. Appl. Microbiol. Biotechnol. 48 (1997), 648-655

Müller R.H., Jorks S., Kleinsteuber S., Babel W.: *Comamonas acidovorans* strain MC1: a new isolate capable of degrading the chiral herbicides dichlorprop and mecoprop and the herbicides 2,4-D and MCPA. Microbiol. Res. 154 (1999), 241-246

Müller R.H., Babel W.: Separation of two dichlorprop/α-ketoglutarate dioxygenases with enantiospecific properties from *Comamonas acidovorans* MC1. Acta Biotechnol. 19 (1999), 349-355

COR-AAD1-00003690
Bayer EX1008 (Part 7 of 9)

Müller R.H., Babel W.: A theoretical study on the metabolic requirements resulting from α-ketoglutarate-dependent cleavage of phenoxyalkanoates. Appl. Environ. Microbiol. 66 (2000), 339-344

Müller R.H., Kleinsteuber S., Babel W.: Physiological and genetic characterization of two bacterial strains utilizing phenoxypropionate and phenoxyacetate herbicides. Microbiol. Res. 156 (2001), 121-131

Müller T.A., Kohler H.P.E.: Chirality of pollutants-effects on metabolism and fate. Applied Microbiol. Biotechnol. 64 (2004), 300-316

Myllyla R., Tuderman L., Kivirikko K.I.: Mechanism of the prolyl hydroxylase reaction. 2. Kinetic analysis of the reaction sequence. Eur. J. Biochem. 80 (1977), 349-357

Naessens M., Vandamme E.J.: Multiple forms of microbial enzymes. Biotech. Lett. 25 (2003), 1119-1124

Nelson M.J., Cowling R.A., Seitz S.P.: Structural characterization of alkyl and peroxyl radicals in solutions of purple lipoxygenase. Biochemistry 33 (1994), 4966-4973

Nickel K., Suter M.J.F., Kohler H.P.E.: Involvement of two α-ketoglutarate-dependent dioxygenase in enantioselective degradation of (R)- and (S)-mecoprop by *Sphingomonas herbicidovorans* MH. J. Bacteriol. 179 (1997), 6674-6679

Nickoloff J.A.: Electroporation Protocols for Microorganisms. Humana Press. Totowa, New Jersey (1995)

O'Brien J.R., Schuller D.J., Yang V.S., Dillard B.D., Lanzilotta W.N.: Substrate-induced conformational changes in *Escherichia coli* taurine/alpha-ketoglutarate dioxygenase and insight into the oligomeric structure. Biochemistry 42 (2003), 5547-5554

Ogston A.G.: Interpretation of experiments on metabolic processes, using isotopic tracer elements. Nature 162 (1948), 963

Ohlendorf D.H., Lipscomb J.D., Weber P.C.: Structure and assembly of protocatechuate 3,4-dioxygenase. Nature 336 (1988), 403-405

Ohlendorf D.H., Orville A.M., Lipscomb J.D.: Structure of protocatechuate 3,4-dioxygenase from *Pseudomonas aeruginosa* at 2.15 Å resolution. J Mol Biol. 244 (1994), 586-608

Onozuka M., Nosaka K.: Steady-state kinetics and mutational studies of recombinant human thiamin pyrophosphokinase. J. Nutr. Sci. Vitaminol. (Tokyo) 49 (2003), 156-62

Pao S.S., Paulsen I.T., Saier M.H. Jr.: Major facilitator superfamily. Microbiol. Mol. Biol. Rev. 62 (1998), 1-34

Perkins D.N., Pappin D.J., Creasy D.M., Cottrell J.S.: Probability-based protein identification by searching sequence databases using mass spectrometry data. Electrophoresis 20 (1999), 3551-3567

COR-AAD1-00003691
Bayer EX1008 (Part 7 of 9)

Perutz M.: Stereochemistry of cooperative effects in haemoglobin. Nature 228 (1970), 726-739

Pieper D.H., Reineke W., Engesser K.H., Knackmuss H.J.: Metabolism of 2,4-dichlorophenoxyacetic acid, 4-chloro-2-methylphenoxyacetic acid, and 2-methylphenoxyacetic acid by *Alcaligenes eutrophus* JMP 134. Arch. Microbiol. 151 (1988), 365-371

Podesta F.E, Plaxton W.C.: Kinetic and regulatory properties of cytosolic pyruvate kinase from germinating castor oil seeds. Biochem. J. 279 (1991), 495-501

Poh R., Xia X., Bruce I.J., Smith A.R.W.: 2,4-dichlorophenoxyacetate/alpha-ketoglutarate dioxygenases from *Burkholderia cepacia* 2a and *Ralstonia eutropha* JMP134. Microbios 105, (2001), 43-63

Porter F.D., Li Y.S., Deuel T.F.: Purification and characterization of a phosphatidylinositol-4-kinase from bovine uteri. J. Biol. Chem. 263 (1988), 8989-8995

Prescott A.G.: A dilemma of dioxyganases (or where biochemistry and molecular biology fail to meet). J. Exp. Bot. 44 (1993), 849-861

Price J.C., Barr E.W., Tirupati B., Bollinger J.M. Jr., Krebs C.: The first direct characterization of a high-valent iron intermediate in the reaction of an alpha-ketoglutarate-dependent dioxygenase: a high-spin Fe(IV) complex in taurine/alpha-ketoglutarate dioxygenase (TauD) from *Escherichia coli*. Biochemistry 42 (2003), 7497-7508

Proda A.G., Airoldi C.: Adsorbtion and preconcentration of 2,4-dichlorophenoxyacetic acid on chemically modified silica gel surface. Fresenius J. Anal. Chem. 371 (2001), 1028-1030

Puistola U., Turpeenniemi-Hujanen T.M., Myllylä R., Kivirikko K.I.: Studies on the lysyl hydroxylase reaction. II. Inhibition kinetics and the reaction mechanism. Biochimica et Biophysica Acta (BBA) - Enzymology, 611 (1980), 51-60

Que L. Jr., Widom J., Crawford R.L.: 3,4-Dihydroxyphenylacetate 2,3-dioxygenase. A manganese(II) dioxygenase from *Bacillus brevis*. J. Biol. Chem. 256 (1981), 10941-10944

Que L. Jr., Ho R.Y.N.: Dioxygen activation by enzymes with mononuclear non-heme iron active sites. Chem. Rev. 96 (1996), 2607-2624

Reinhold P.: Biologische Charakterisierung der Substratspezifität der 2,4-Dichlorphenoxyalkansäure-spaltenden Dioxygenasen alkaliphiler Bakterien. Diplomarbeit an der Universität Leipzig (1998)

Roach P.L., Clifton I.J., Fulop V., Harlos K., Barton G.J., Hajdu J., Andersson I., Schofield C.J., Baldwin J.E.: Crystal structure of isopenicillin-N-synthase is the first from a new structural family of enzymes. Nature 375 (6533) (1995a), 700-704

Roach P.L., Clifton I.J., Hensgens C.M.H., Shibata N., Schofield C.J., Hajdu J., Baldwin J.E.: Structure of isopenicillin N synthase complexed with substrate and the mechanism of penicillin formation. Nature 387 (1995b), 827-830

COR-AAD1-00003692
Bayer EX1008 (Part 7 of 9)

Roberts T.: Metabolic pathway of agrochemicals. Part!: Herbicides and plant growth regulators. The Royal Society of Chemistry, Cambridge, UK (1998), 75-77

Romero E., Matallo M.B., Pena A., Sanchez-Rasero F., Schmitt-Kopplin Ph., Dios G.: Dissipation of racemic mecoprop and dichlorprop and their pure R-enantiomers in three calcareous soils with and without peat addition. Environ. Pollution 111 (2001), 209-215

Reineke W.: Construction of bacterial strains with novel degradativ capabilities for chloroaromatics. J. Basic Microbiol. 26 (1986), 551-567

Reineke W., Knackmuss H-J.: Microbial degradation of haloaromatics. Ann. Rev. Microbiol. 42 (1988), 263-287

Rundgren M.: Multiple forms of human 4-hydroxyphenylpyruvate dioxygenase (II). J. Biol. Chem. 252 (1977a), 5085-5093

Rundgren M.: Steady-state kinetics of 4-hydroxyphenylpyruvate dioxygenase from human liver (III). J Biol Chem. 252 (1977b), 5094-5099.

Ruhland S.: Reinigung und Charakterisierung von Dioxygenasen mit enantioselektiven Eigenschaften zur etherolytischen Spaltung racemischer Phenoxyalkanoatherbizide. Diplomarbeit, Universität Jena (2003)

Rügge K., Juhler R.K., Broholm M.M., Bjerg P.L.: Degradation of the (R)- and (S)-enantiomers of the herbicides MCPP and dichlorprop in a continuous field-injection experiment. Water Research 36 (2002), 4160-4164

Ryle M.J., Liu A., Muthukumaran R.B., Ho R.Y., Koehntop K.D., McCracken J., Que L. Jr., Hausinger R.P.: O_2- and alpha-ketoglutarate-dependent tyrosyl radical formation in TauD, an alpha-keto acid-dependent non-heme iron dioxygenase. Biochemistry 42 (2003a), 1854-1862

Ryle M.J., Koehntop K.D., Liu A., Que Jr. L., Hausinger R.P.: Interconversion of two oxidized forms of Taurine/α-ketoglutarate dioxygenase, a non-heme iron hydroxylase: Evidence for bicarbonate binding. Proc. Nat. Acad. Sci. 100 (2003b), 3790-3795

Saari RE., Hausinger RP.: Ascorbic acid-dependent turnover and reactivation of 2,4-dichlorophenoxyacetic acid/alpha-ketoglutarate dioxygenase using thiophenoxyacetic acid. Biochemistry 37 (1998), 3035-3042

Saari R.E., Hogan D.A., Hausinger R.P.: Stereospecific degradation of the herbicide dichlorprop. J. Molec. Catalysis B Enzymatic 6 (1999), 421-428

Sabater B, Delafuente G.: Kinetic properties and related changes of molecular weight in a fructokinase from *Streptomyces violaceoruber*. Biochim. Biophys. Acta. 377 (1975), 258-270

Saito K., Kobayashi M., Gong Z., Tanaka Y., Yamazaki M.: Direct evidence for anthocyanidin synthase as a 2-oxoglutarate-dependent oxygenase: moleculare cloning and functional expression of cDNA from a red forma of *Perilla frutescens*. Plant J. 17 (1999), 181-189

COR-AAD1-00003693
Bayer EX1008 (Part 7 of 9)

Salowe S.P., Marsh E.N., Townsend C.A.: Purification and characterization of clavaminate synthase from *Streptomyces clavuligerus*: an unusual oxidative enzyme in natural product biosynthesis. Biochemistry 29 (1990), 6499-6508

Sami M., Brown T.J., Roach P.L., Schofield C.J., Baldwin J.E.: Glutamine-330 is not essential for activity in isopenicillin N synthase from *Aspergillus nidulans*. FEBS Lett. 405 (1997), 191-194

Sanger F., Nicklen S., Coulson A.R.: DNA sequencing with chain terminating inhibitors. Proc. Nat. Acad. Sci. USA 74 (1977), 5463-5467

Sanker S., Campbell H.A., Kent C.: Negative cooperativity of substrate binding but not enzyme activity in wild-type and mutant forms of CTP: glycerol-3-phosphate-cytidylyltransferase. J. Biol. Chem. 276 (2001), 37922-37928

Schägger H., von Jagow G.: Tricine-sodium dodecyl sulfate-polyacrylamide gel electrophoresis for the separation of proteins in the range from 1 to 100 kDa. Anal. Biochem. 166 (1987), 368-379

Schleinitz K.M., Kleinsteuber S., Vallaeys T., Babel W.: The genetic backround of 2,4-dichlorophenoxypropionate cleavage in *Delftia acidovorans* MC1. Appl. Environ. Microbiol. 70 (2004), 5357-5365

Schmidt T.G.M., Koepke J., Frank R., Skerra A.: Molecular interaction between the Strep-tag affinity peptide and its cognate target streptavidin. J. Mol. Biol. 255 (1996), 753-766

Schulz S., Dong W., Groth U., Cook A.M.: Enantiomeric degradation of 2-(4-sulfophenyl)butyrate via 4-sulfocatechol in *Delftia acidovorans* SPB1. Applied Environ. Microbiol. 66 (2000), 1905-1910

Senda T., Sugiyama K., Narita H., Yamamoto T., Kimbara K., Fukuda M., Sato M., Yano K., Mitsui Y.: Three-dimensional structures of free form and two substrate complexes of an extradiol ring-cleavage type dioxygenase, the BphC enzyme from *Pseudomonas* sp. strain KKS102. J Mol Biol. 255 (1996), 735-752

Shaw C.R.: Isoenzymes: classification, frequency, and significance. Int.Rev. Cytol. 25 (1969), 297-332

Shibasaki T., Mori H., Chiba S., Ozaki A.: Microbial prolin-4-hydroxylase screening and gene cloning. Appl. Environ. Microbiol. 65 (1999), 4025-4031

Shevchenko A., Wilm M., Vorm O., Mann M.: Mass spectrometric sequencing of proteins silver-stained polyacrylamide gels. Anal. Chem. 68 (1996), 850-858

Siegel B.: α-Ketoglutarate dependent dioxygenases: A mechanism for prolyl hydroxylase action. Bioorganic Chemistry 8 (1979), 219-226

Skerra A.: Use of the tetracycline promotor for the tightly regulated production of a murine antibody fragment in *Escherichia coli*. Gene 151 (1994), 131-135

COR-AAD1-00003694
Bayer EX1008 (Part 7 of 9)

Smejkal C.W., Vallaeys T., Seymour F.A., Burton S.K., Lappin-Scott H.M.: Characterization of (R/S)-mecoprop [2-(2-methyl-4-chlorophenoxy)propionic acid]-degrading *Alkaligenes* sp. CS1 and *Ralstonia* sp. CS2 from agricultural soils. Environ. Microbiol. 3 (2001), 288-293

Solomon E.I., Brunold T.C., Davis M.I., Kemsley J.N., Lee S.K., Lehnert N., Neese F., Skulan A.J., Yang Y.S., Zhou J.: Geometric and electronic structure/function correlations in non-heme iron enzymes. Chem. Rev. 100 (2000), 235-350

Sträuber H., Müller R.H., Babel W.: Evidence of cytochrome P450-catalyzed cleavage of the ether bond of phenoxybutyrate herbicides in *Rhodococcus erythropolis* K2-3. Biodegradation. 14 (2003), 41-50

Streber W.R., Timmis K.N., Zenk M.H.: Analysis, cloning, and high-level expression of 2,4-dichlorophenoxyacetate monooxygenase gene *tfdA* of *Alkaligenes eutrophus* JMP134. J. Bacteriol. 169 (1987), 2950-2955

Takeuchi M., Hamana K., Hiraishi A.: Proposal of the genus *Sphingomonas* sensu stricto and three new genera, *Sphingobium*, *Novosphingobium* and *Sphingopyxis*, on the basis of phylogenetic and chemotaxonomic analyses. Int. J. Syst. Evol. Microbiol. 51 (2001), 1405-1417

Tett V.A., Willetts A.J., Lappin-Scott H.M.: Enantioselective degradation of the herbicide mecoprop [2-(2-methyl-4-chlorophenoxy)propionic acid] by mixed and pure bacterial cultures. FEMS Microbiol. Ecol. 14 (1994), 191-200

Tett V.A., Willetts A.J., Lappin-Scott H.M.: Biodegradation of the chlorophenoxy herbicide (R)-(+)-mecoprop by *Alcaligenes denitrificans*. Biodegradation 8 (1997), 43-52

Thornburg L.D.: Mechanism-based inhibition of thymine hydroxylase. J. Am. Chem. Soc. 111 (1989), 7632-7633

Thornburg L.D., Stubbe J.: Mechanism-based inactivation of thymine hydroxylase, an alpha-ketoglutarate-dependent dioxygenase, by 5-ethynyluracil. Biochemistry 32 (1993), 14034-14042

Van Vliet F., Xi X.G., De Staercke C., de Wannemaeker B., Jacobs A., Cherfils J., Ladjimi M.M., Herve G., Cunin R.: Heterotropic interactions in aspartate transcarbamoylase: turning allosteric ATP activation into inhibition as a consequence of a single tyrosine to phenylalanine mutation. Proc. Natl. Acad. Sci. USA 88 (1991), 9180-9183

Vålegard K., van Scheltinga A.C.Z., Lloyd M.D., Hara T., Ramaswamy S., Perrakis A., Thompson A., Lee H.J., Baldwin J.E., Schofield C.J., Hajdu J., Andersson I.: Structure of a cephalosporin synthase. Nature 394 (1998), 805-809

Voss S., Skerra A.: Mutagenesis of a flexible loop in streptavidin leads to higher affinity for the Strep-tag II peptide and improved performance in recombinant protein purification. Protein Eng. 10 (1997), 975-982

Wada G.H., Fellman J.H., Fujita T.S., Roth E.S.: Purification and properties of avian liver *p*-hydroxyphenylpyruvate hydroxylase. J. Biol. Chem. 250 (1975), 6720-6726

COR-AAD1-00003695
Bayer EX1008 (Part 7 of 9)

Westendorf A.: Reinigung und Charakterisierung der Phenoxyalkanoat [Dichlorprop]/α-Ketoglutarat-Dioxygenase aus *Delftia acidovorans* MC1 unter Berücksichtigung enantioselektiver Eigenschaften. Diplomarbeit, Universität Leipzig (2001)

Westendorf A., Benndorf D., Müller R.H., Babel W.: The two enantiospecific dichlorprop/α-ketoglutarate-dioxygenases from *Delftia acidovorans* MC1 – protein and sequence data of RdpA and SdpA. Microbiol. Res. 157 (2002), 331-336

Westendorf, A., Müller, R.H., Babel, W.: Purification and characterization of the enantiospecific dioxygenases from *Delftia acidovorans* MC1 initiating the degradation of phenoxypropionate and phenoxyacetate herbicides. Acta Biotechnol. 23 (2003), 3-17

Whiting A.K., Boldt Y.R., Hendrich M.P., Wackett L.P., Que L. Jr.: Manganese(II)-dependent extradiol-cleaving catechol dioxygenase from *Arthrobacter globiformis* CM-2. Biochemistry 35 (1996), 160-170

Whiting A.K., Que, L: Metal Coordination Enviroment of a Cu(II)-Substituted α-Ketoacid-dependent Dioxygenase that degrades the Herbicide 2,4-D. J. Am. Chem. Soc., 119 (1997), 3413-3414

Worthing G.M., Hance R.J.: The pesticide manual - a world compendium, 9th edn. The British Crop Council, Farnham (1991)

Xiao X.F., Wolfe S., Demain A.L.: Purification and characterization of cephalosporin-7-alpha-hydroxylase from *Streptomyces clavuligerus*. Biochem. J. 280 (1991), 471-474

Xun L., Wagnon K.B.: Purification and properties of component B of 2,4,5-Trichlorophenoxyacatate oxygenase from *Pseudomonas cepacia* AC1110. Appl. Environ. Microbiol. 61 (1995), 3499-3502

Zhang Z., Ren J., Stammers D.K., Baldwin J.E., Harlos K., Schofield C.J.: Structural origins of the selectivity of the trifunctional oxygenase clavaminic acid synthase. Nat. Struct. Biol. 7 (2000), 127-33

Zipper C., Nickel K., Angst W., Kohler H.P.E.: Complete microbial degradation of both enantiomeres of the chiral herbicide mecoprop [(R,S)-2-(4-chloro-2-methylphenoxy)propionic acid] in an enantioselective manner by *Sphingomonas herbicidovorans* sp. nov. Appl. Environ. Microbiol. 62 (1996), 4318-4322

Zipper C., Bunk M., Zehnder A.J.B., Kohler H.P.E.: Enantioselektive Uptake and Degradation of the Chiral Herbicide Dichlorprop [(R,S)-2-(2,4-Dichlorophenoxy)propionic acid] by *Sphingomonas herbicidovorans* MH. J. Bacteriol. 180 (1998), 3368-3374

Zipper C., Bollinger C., Fleischmann T., Suter M.J.F., Angst W., Müller M.D., Kohler H.P.E.: Fate of the herbicides mecoprop, dichlorprop, and 2,4-D in aerobic and anaerobic sewage sludge as determined by laboratory batch studies and enantiomer-specific analysis. Biodegradation 10 (1999), 271-278

COR-AAD1-00003696
Bayer EX1008 (Part 7 of 9)

Danksagung

An dieser Stelle möchte ich mich bei Professor Dr. W. Babel ganz herzlich für die Möglichkeit zur Anfertigung dieser Arbeit in seinem Department und die lehrreichen Diskussionen bedanken.

Ein ganz besonders großer Dank gebührt Dr. R. H. Müller für seine exzellente Betreuung. Die ständige Hinterfragung von Ergebnissen, die Formulierung von Thesen, die Diskussion von Problemen und die ständige Motivierung führten zu einem schnellen Fortschreiten der Arbeiten. Danke auch für die Möglichkeit zur selbstständigen Arbeitsweise.

Dr. D. Benndorf möchte ich für seine unkomplizierte und kompetente Hilfe bei den proteinbiochemischen Methoden und seine unendlichen Fragen zu den Hintergründen danken und Frau Chr. Schumann danke ich für die experimentelle Durchführung der 2D-Gelelektrophoresen.

Für die massenspektrometrischen Analysen, ohne die die Ergebnisse zu posttranslationalen Modifizierung nicht vorlägen, danke ich Prof. R. Hoffmann und Dipl. Chem. T. Langrock.

Ein großes Dankeschön geht an Dipl.-Ing. H. J. Große, Dr. D Hoffmann, M. Neytschev, Dr. T. Pribyl, C. Schumann und Dr. H. Sträuber, ohne die das Arbeiten bestimmt nur halb soviel Spaß gemacht hätte, danke für die Ratschläge, Tipps und Tricks, die meine Forschung voranbrachten, für das tolle Arbeitsklima usw..

Den zahlreichen Praktikanten und Diplomanden, die an dieser Arbeit mitgewirkt haben sei hiermit auch gedankt.

Des Weiteren danke ich allen Mitarbeitern de UMB und des UBZ für alle gewährten Hilfen und Diskussionen.

COR-AAD1-00003697
Bayer EX1008 (Part 7 of 9)

Eidesstattliche Erklärung

Hiermit versichere ich an Eides statt, dass ich die vorliegende Arbeit „Enantioselektive Verwertung von Phenoxyalkanoat-Herbiziden durch Bakterien - Biochemische Charakterisierung der Dioxygenasen des initialen Abbau-Schrittes" selbstständig und nur unter Verwendung der angegebenen Hilfsmittel und Literatur angefertigt habe. Die aus den Werken sinngemäß oder wörtlich entnommenen Stellen sind als solche kenntlich gemacht.

Leipzig, Oktober 2004 Anne Westendorf

COR-AAD1-00003698
Bayer EX1008 (Part 7 of 9)

Lebenslauf

Persönliche Daten

Name:	Anne Westendorf
Wohnort:	Strasse des 18. Okt. 29/809, 04103 Leipzig
Familienstand:	ledig

Schulbildung

1984-1990	Fritz-Reuter-POS, Ostseebad Kühlungsborn
1990-1996	Fritz-Reuter-Gymnasium, **Abitur**, Ostseebad Kühlungsborn

Studium

Okt. 1996-Sept. 1998	Grundstudium der Fachrichtung Biochemie an der Universität Potsdam, **Vordiplom**
Okt. 1998-März 2001	Hauptstudium der Fachrichtung Biochemie an der Universität Leipzig, **Diplom**
Sep. 2000-März 2001	Anfertigung der Diplomarbeit zum Thema: „Reinigung und Charakterisierung der Phenoxyalkanoat [Dichlorprop]/α-Ketoglutarat-Dioxygenase aus *Delftia acidovorans* MC1 unter Berücksichtigung enantioselektiver Eigenschaften“ am Umweltforschungszentrum Leipzig-Halle GmbH

Promotion

Juni 2001-Mai 2004	Doktorandin im Department Umweltmikrobiologie, Umweltforschungszentrum Leipzig-Halle GmbH. Anfertigung einer wissenschaftlichen Arbeit zum Thema: „Enantioselektive Verwertung von Phenoxyalkanoat-Herbiziden durch Bakterien - Biochemische Charakterisierung der Dioxygenasen des initialen Abbau-Schrittes“ unter Anleitung von Prof. Dr. Wolfgang Babel.

COR-AAD1-00003699
Bayer EX1008 (Part 7 of 9)

Supplemental material for the paper " Comparison of 16S rRNA gene phylogeny and functional *tfdA* gene distribution in thirty-one different 2,4-dichlorophenoxyacetic acid and 4-chloro-2-methylphenoxyacetic acid degraders" by the authors Jacob Bælum, Carsten S. Jacobsen and William E. Holben.

The supplemental material includes the following information:

S1: Materials and methods

S2: Phylogenetic tree of *tfdA* genes

S3: Phylogenetic tree of 16S rRNA genes

S4: Alignment of the different *tfdA* genes based on nucleic acids

S5: Alignment of the different *tfdA* genes based on amino acids

COR-AAD1-00003700
Bayer EX1008 (Part 7 of 9)

Materials and Methods

Bacterial strains

Four 2,4-D degrading bacteria were isolated from Danish agricultural soil from Sj. Odde using the method described by Ka et al. [13], and were further characterized together with 46 earlier described bacterial 2,4-D degraders. Those were isolated from the Kellogg Biological Station, Hickory Comers, Michigan, USA, [14] or the Experimental Farm, Indian Head, Saskatchewan, Canada, or from wastewater or sludge samples in Oregon, USA [not published] using the same method. Initially the strains were checked for uniqueness using repetitive extragenic palindromic PCR (REP–PCR), and 29 were confirmedly unique strains (data not shown), and those were carried forward for further investigation (Table 1). The well known 2,4-D degraders *Cupriavidus necator* JMP134 (1) and *Burkholderia* sp. RASC (2) were included as reference strains in these culture-based comparisons.

Mineralization experiment

To investigate any potential correlation between the class of *tfdA* gene and bacterial substrate specificity for the 31 bacterial isolates (including the two reference strains) towards 2,4-D and MCPA, ~$1.2 \cdot 10^5$ cells of each strain were inoculated individually into 10 ml of mineral salt (MS) medium (3) containing 2.3 mM of 2,4-D or MCPA and 100 mg/L casamino acids. ~50000 DPM U-ring ^{14}C-labeled 2,4-D or MCPA (radiochemical purity >95%; Izotop, Budapest, Hungary) was added to monitor mineralization as $^{14}CO_2$ trapped in 0.5 M NaOH as described elsewhere (4). Microcosms were incubated at 10 °C on a rotary shaker set to 150 rpm at room temperature. The NaOH was removed, counted by liquid scintillation and replaced at days 2, 5, 7, 12, and 35. After mineralization (scored as ≥40% cumulative recovery of $^{14}CO_2$) had occurred, 2 ml of cell culture was removed and stored frozen (-20°C) for nucleic acid extraction.

COR-AAD1-00003701
Bayer EX1008 (Part 7 of 9)

Molecular experiments

Total genomic DNA was extracted from 2 ml of cell culture from each of the strains using the UltraClean microbial DNA isolation kit (Mobio Laboratories, Carlsbad, CA) following the manufacturer's recommendations. ~30 ng of the recovered DNA was used as template in PCR reactions using illustra™ puReTaq Ready-to-go PCR beads (GE Healthcare, Buckinghamshire, UK), with a concentration of each primer (refer to Table 2) of 0.5 µM. The PCR reaction conditions were as follows: 95 °C for 10 min; followed by 25 cycles of 95 °C for 45 sec, primer-pair optimal annealing temperature (refer to Table 2) for 45 sec, and 72 °C for 90 sec. To ensure complete elongation, a final step of 72 °C for 7 min was performed. The PCR products were purified using the UltraClean PCR clean up kit (Mobio Laboratories, Carlsbad, CA) following the manufacturer's recommendations. To minimize the possibility of sequencing errors, the PCR products were sequenced bidirectionally at the MWG facilities (Ebersberg, Germany) using the primers given in Table 2, resulting in sequence lengths of 1329-1405 bp for the 16S rRNA genes, 856 bp for class I and class III *tfdA* genes and 882 bp for class II *tfdA* genes.

Phylogenetic analyses

All of the sequence chromatograms were individually viewed and confirmed manually using the FinchTV software (Geospiza, Seattle, WA, US). The nearest relative of each strain was found using the individual 16S rRNA gene sequences as query and the Basic Local Alignment Search Tool (BLAST) (5) in the GenBank database (http://www.ncbi.nlm.nih.gov/). The 16S rRNA gene sequence set including reference sequences was aligned using the web based RDPX-Bacteria alignment model and the tree was built using the "Weighbor" weighted neighbor-joining tree building algorithm both available through the Ribosomal Database Project 10 (RDP 10) website

COR-AAD1-00003702
Bayer EX1008 (Part 7 of 9)

(http://rdp.cme.msu.edu/)(6, 7). Furthermore, the *tfdA* sequence set was aligned (separately) using the CLUSTALW program package (8). Phylogenetic analysis was performed with the MEGA 4.0 program package (9) using the neighbour-joining (NJ) method (10). Evolutionary distances were computed using the Maximum Composite Likelihood method (11) and bootstrap analysis based on 1,000 replicates (12) was used to place confidence estimates on the trees. All positions containing gaps and missing data were eliminated from the datasets giving a total of 1271 bp in the final dataset for 16S rRNA genes and 855 bp for the *tfdA* genes. For phylogenetic analysis of *tfdA* genes, one reference sequence retrieved from Genbank was included for each of the *tfdA* classes. For class I *C. necator* JMP134 *tfdA* gene with accession number (acc. #) M16730 was chosen, for class II *Burholderia* sp. RASC *tfdA* gene with acc. # U25717 was chosen, and for class III *B. cepacia* 2a *tfdA* gene with acc. # DQ065837 was chosen.

Reference List

1. **Don, R. H. and J. M. Pemberton**. 1981. Properties of 6 pesticide degradation plasmids isolated from *Alcaligenes paradoxus* and *Alcaligenes eutrophus*. J. Bacteriol. **145**:681-686.

2. **Suwa, Y., A. D. Wright, F. Fukimori, K. A. Nummy, R. P. Hausinger, W. E. Holben, and L. J. Forney**. 1996. Characterization of a chromosomally encoded 2,4-dichlorophenoxyacetic acid α-ketoglutarate dioxygenase from *Burkholderia* sp strain RASC. Appl. Environ. Microbiol. **62**:2464-2469.

3. **Sorensen, S. R. and J. Aamand**. 2003. Rapid mineralisation of the herbicide isoproturon in soil from a previously treated Danish agricultural field. Pest Manag. Sci. **59**:1118-1124.

4. **Mortensen, S. K. and C. S. Jacobsen**. 2004. Influence of frozen storage on herbicide degradation capacity in surface and subsurface sandy soils. Environ. Sci. Technol. **38**:6625-6632.

5. **Altschul, S. F., W. Gish, W. Miller, E. W. Myers, and D. J. Lipman**. 1990. Basic local alignment search tool. J. Mol. Biol. **215**:403-410.

6. **Cole, J. R., B. Chai, R. J. Farris, Q. Wang, A. S. Kulam-Syed-Mohideen, D. M. McGarrell, A. M. Bandela, E. Cardenas, G. M. Garrity, and J. M. Tiedje**. 2007. The ribosomal database project (RDP-II): introducing myRDP space and quality controlled public data. Nucleic Acids Res. **35**:D169-D172.

COR-AAD1-00003703
Bayer EX1008 (Part 7 of 9)

7. **Cole, J. R., Q. Wang, E. Cardenas, J. Fish, B. Chai, R. J. Farris, A. S. Kulam-Syed-Mohideen, D. M. McGarrell, T. Marsh, G. M. Garrity, and J. M. Tiedje**. 2009. The Ribosomal Database Project: improved alignments and new tools for rRNA analysis. Nucleic Acids Res. **37**:D141-D145.

8. **Thompson, J. D., D. G. Higgins, and T. J. Gibson**. 1994. CLUSTAL-W - improving the sensitivity of progressive multiple sequence alignment through sequence weighting, position-specific gap penalties and weight matrix choice. Nucleic Acids Res. **22**:4673-4680.

9. **Tamura, K., J. Dudley, M. NEI, and S. Kumar**. 2007. MEGA4: Molecular evolutionary genetics analysis (MEGA) software version 4.0. Mol. Biol. Evol. **24**:1596-1599.

10. **Saitou, N. and M. Nei**. 1987. The Neighbor-Joining method - a new method for reconstructing phylogenetic trees. Mol. Biol. Evol. **4**:406-425.

11. **Tamura, K., M. NEI, and S. Kumar**. 2004. Prospects for inferring very large phylogenies by using the neighbor-joining method. Proc. Natl. Acad. Sci. U. S. A. **101**:11030-11035.

12. **Felsenstein, J.** 1985. Confidence-Limits on Phylogenies - An Approach Using the Bootstrap. Evolution **39**:783-791.

13. **Ka, J.O., Holben, W. E., Tiedje, J. M.,** 1994. Genetic and phenotypic diversity of 2,4-dichlorophenoxyacetic acid (2,4-D)-degrading bacteria isolated from 2,4-D-treated field soils. Appl. Environ. Microbiol. **60**: 1106-1115.

14. **Tonso, N.L., Matheson, V. G., Holben, W. E.,** Polyphasic characterization of a suite of bacterial isolates capable of degrading 2,4-D. Microb. Ecol. **30**: 3-24.

COR-AAD1-00003704
Bayer EX1008 (Part 7 of 9)

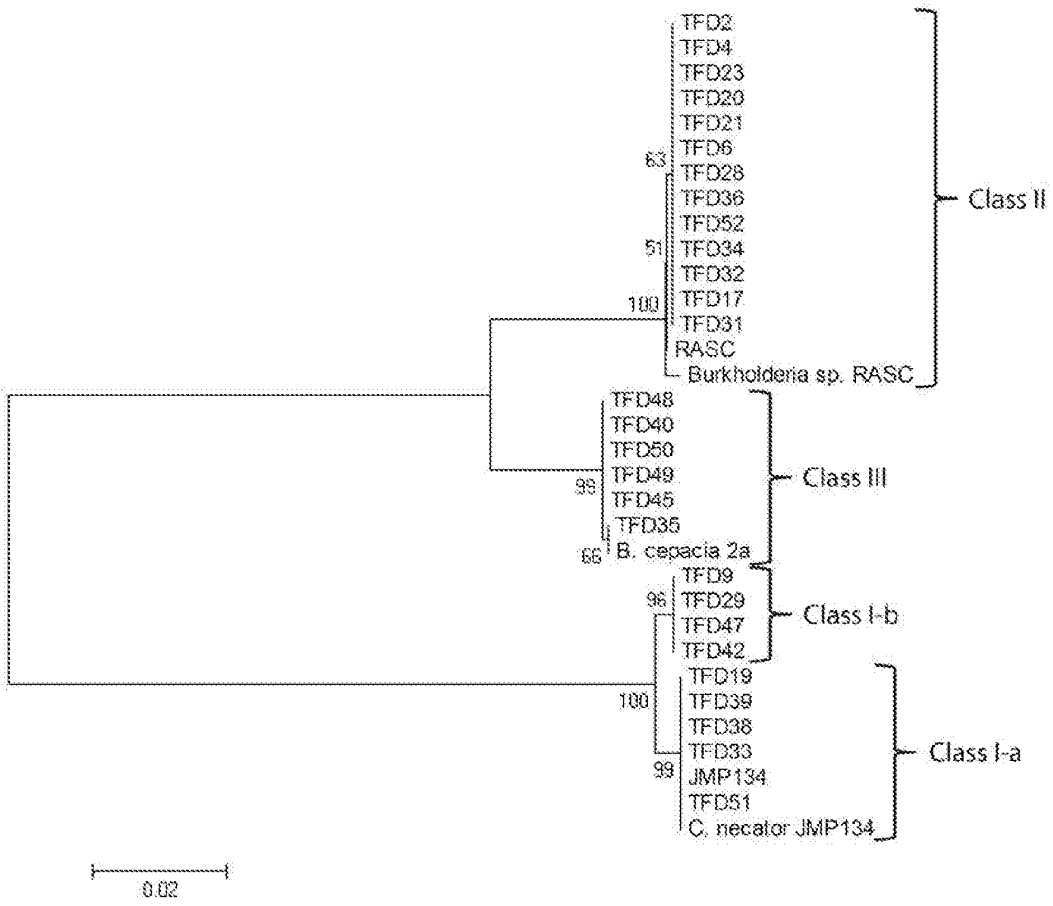


Figure S2. Phylogenetic tree of *tfdA* gene sequences from thirty 2,4-D degrading strains and three reference *tfdA* sequences from *C. necator* JMP134 acc. # M16730, *Burholderia* sp. RASC acc. # U25717 and *B. cepacia* 2a acc. # DQ065837. Note that the additional 'JMP134' and 'RASC' refer to the reference isolates included in the microbiological analyses. The phylogenetic tree was constructed based on essentially full-length CDS (855 bp) using the Neighbor Joining method. Bootstrap values above 50% are shown at nodes. The scale bar indicates substitutions per site.

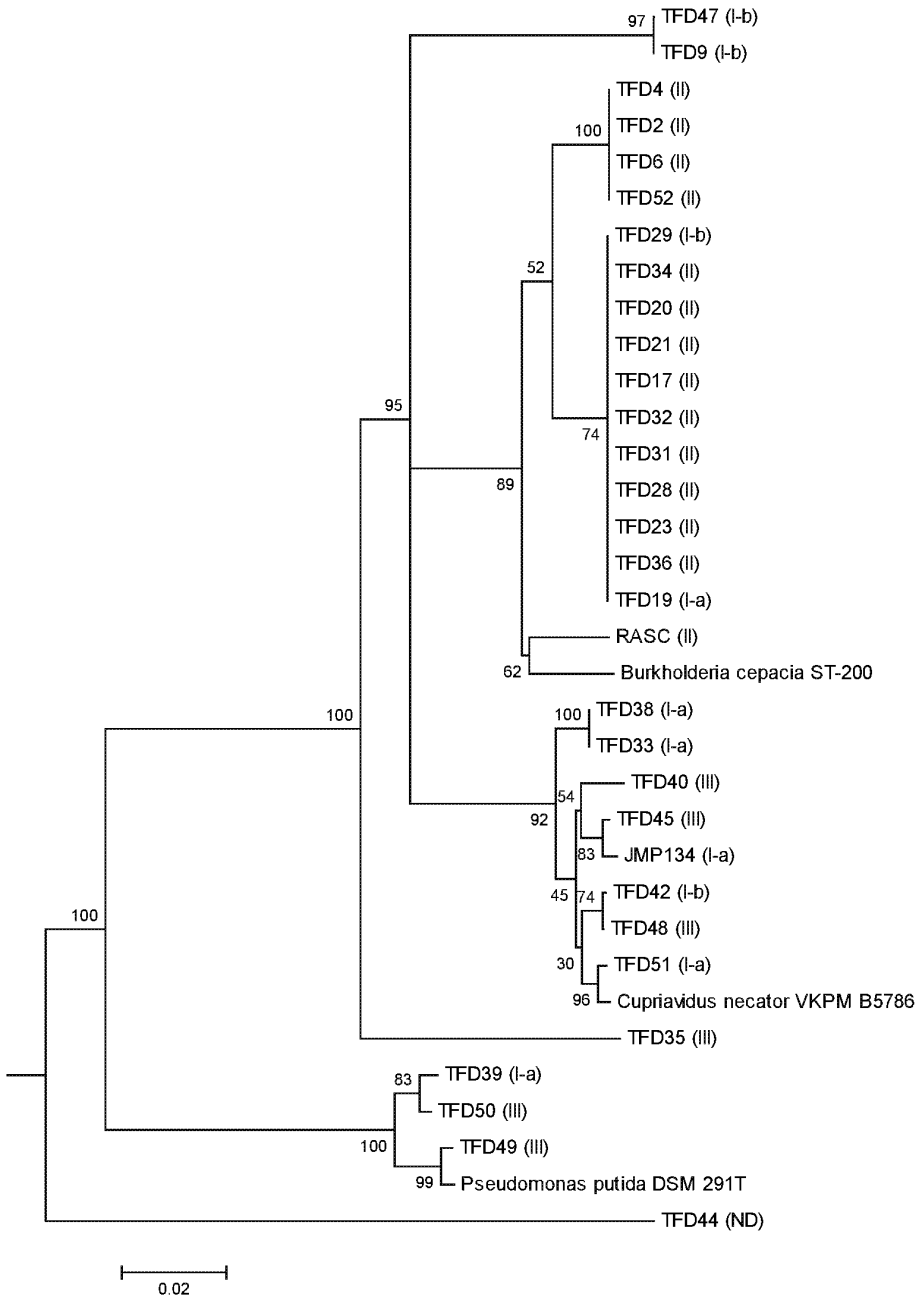
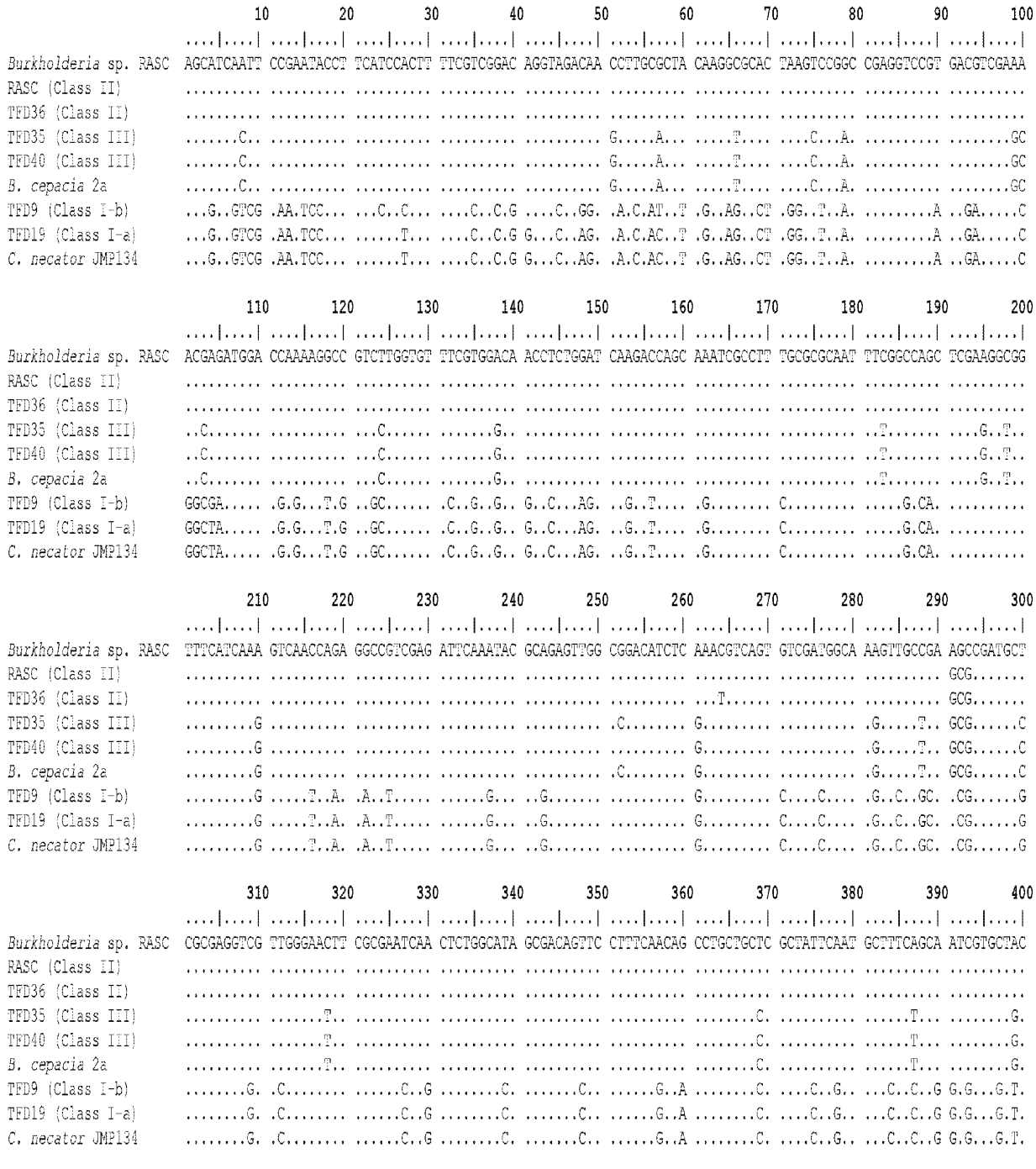
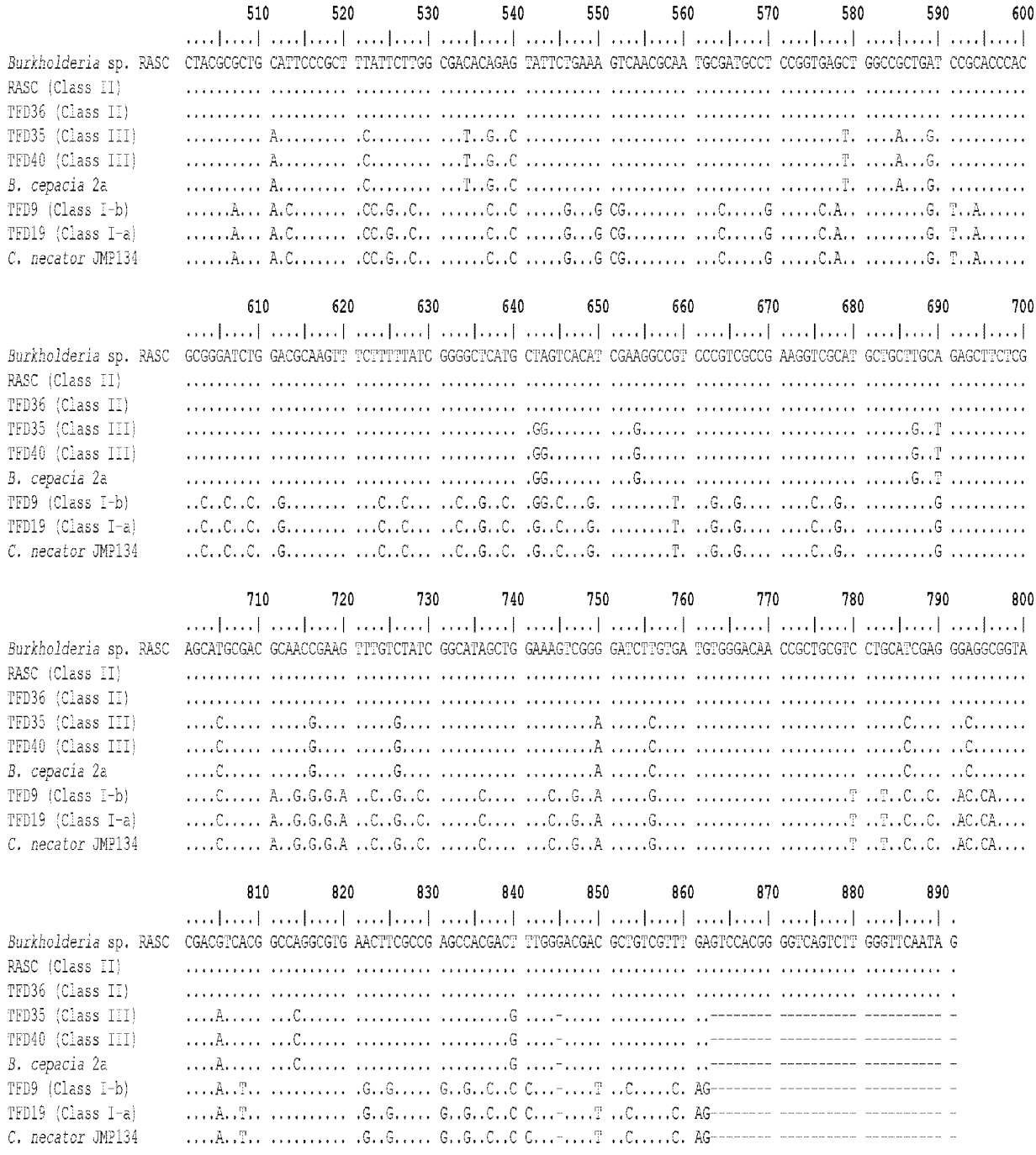
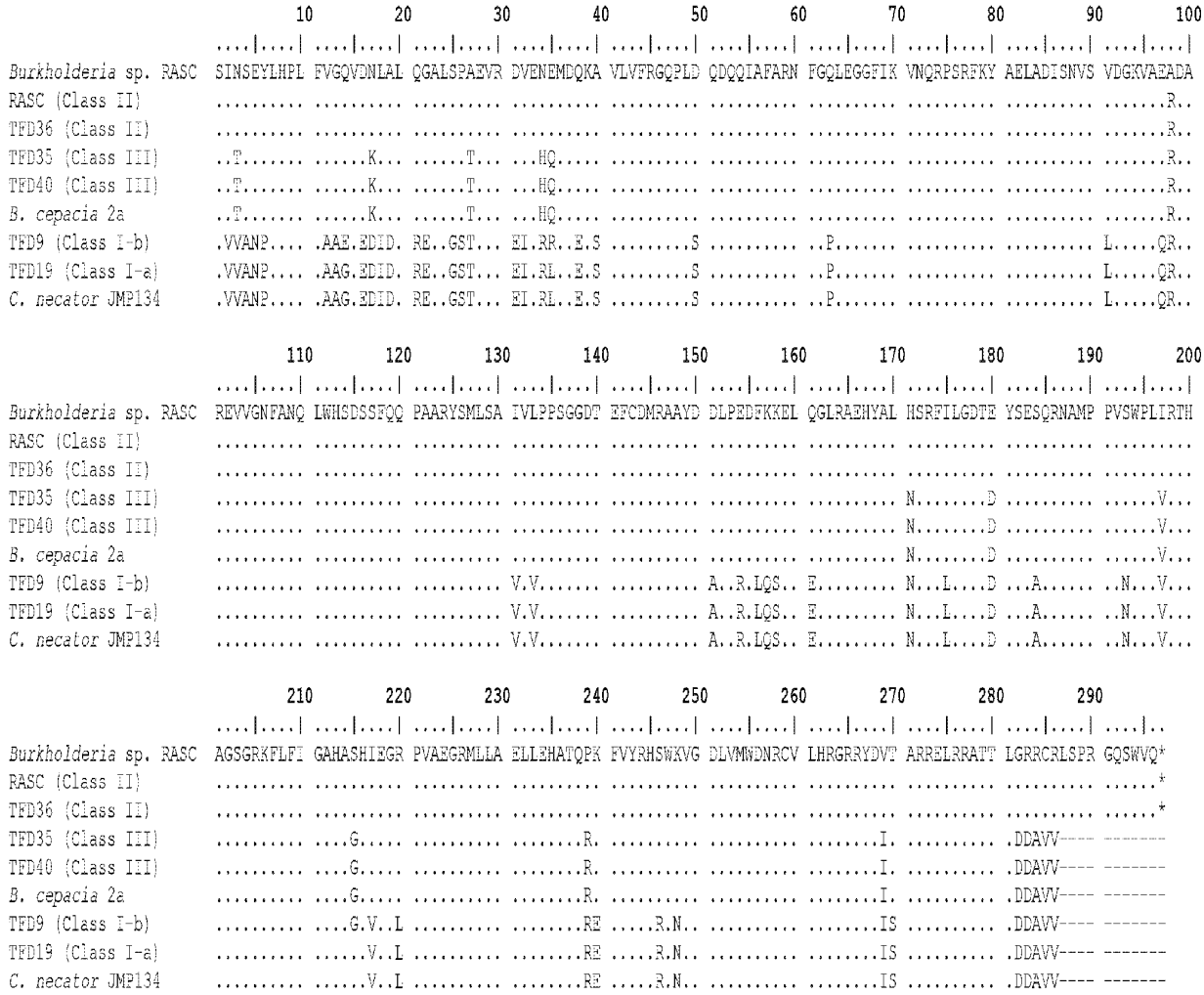


Figure 2. Phylogenetic tree of thirty-one 2,4-D degraders based on 16S rRNA genes and their *tfdA* gene classification. Roman numerals in brackets refer to the class of *tfdA* gene found in that strain. ND indicates that a *tfdA* gene was not detected in that specific strain. Reference sequences obtained through the Browser function at the RDP-10 web page is also included.


10 20 30 40 50 60 70 80 90 100
Burkholderia sp. RASC AGCATCAATT CCGAATACCT TCATCCACTT TTCGTCGGAC AGGTAGACAA CCTTGCGCTA CAAGGCGCAC TAAGTCCGGC CGAGGTCCGT GACGTCGAAA
RASC (Class II)
TFD36 (Class II)
TFD35 (Class III)
TFD40 (Class III)
B. cepacia 2a
TFD9 (Class I-b)
TFD19 (Class I-a)
C. necator JMP134
110 120 130 140 150 160 170 180 190 200
Burkholderia sp. RASC ACGAGATGGA CCAAAAGGCC GTCTTGGTGT TTCGTGGACA ACCTCTGGAT CAAGACCAGC AAATCGCCTT TGCGCGCAAT TTCGGCCAGC TCGAAGGCGG
RASC (Class II)
TFD36 (Class II)
TFD35 (Class III)
TFD40 (Class III)
B. cepacia 2a
TFD9 (Class I-b)
TFD19 (Class I-a)
C. necator JMP134
210 220 230 240 250 260 270 280 290 300
Burkholderia sp. RASC TTTCATCAAA GTCAACCAGA GGCCGTCGAG ATTCAAATAC GCAGAGTTGG CGGACATCTC AAACGTCAGT GTCGATGGCA AAGTTGCCGA AGCCGATGCT
RASC (Class II)
TFD36 (Class II)
TFD35 (Class III)
TFD40 (Class III)
B. cepacia 2a
TFD9 (Class I-b)
TFD19 (Class I-a)
C. necator JMP134
310 320 330 340 350 360 370 380 390 400
Burkholderia sp. RASC CGCGAGGTCG TTGGGAACTT CGCGAATCAA CTCTGGCATA GCGACAGTTC CTTTCAACAG CCTGCTGCTC GCTATTCAAT GCTTTCAGCA ATCGTGCTAC
RASC (Class II)
TFD36 (Class II)
TFD35 (Class III)
TFD40 (Class III)
B. cepacia 2a
TFD9 (Class I-b)
TFD19 (Class I-a)
C. necator JMP134
410 420 430 440 450 460 470 480 490 500
Burkholderia sp. RASC CACCGTCAGG CGGCGATACG GAGTTCTGCG ACATGCGCGC AGCGTACGAC GATCTTCCCG AGGATTTCAA GAAGGAACTG CAGGGATTGC GTGCAGAGCA
RASC (Class II)
TFD36 (Class II)
TFD35 (Class III)
TFD40 (Class III)
B. cepacia 2a
TFD9 (Class I-b)
TFD19 (Class I-a)
C. necator JMP134



S4:Nucleotide sequence alignment showing sequences representing the entire range of diversity in the dataset. Sequences are related to that of *Burkholderia* sp. RASC retrieved from GenBank. The two other reference sequences *B. cepacia* 2a and *C. necator* JMP134 are given as well. Sequences are given in the 5'-3' direction. Numbers above the alignment are the consecutive numbers of the nucleotides. Dots represent nucleotides identical to the *Burkholderia* sp. RASC sequence, while hyphen represents a gap compared to the *Burkholderia* sp. RASC sequence. The RASC sequence is included because we observed a three base pair difference (bp 291-293) compared to the reference sequence of *Burkholderia* sp. RASC. We have done bi-directional resequencing in order to confirm our result.



S5: Amino acid sequence alignment showing the diversity expressed in amino acid sequences representing the entire range of diversity in the dataset. Amino acid sequences are related to that of *Burkholderia* sp. RASC retrieved from GenBank. The amino acid sequence of the two other reference strains *B. cepacia* 2a and *C. necator* JMP134 are given as well. Numbers above the alignment are the consecutive numbers of the amino acids. Dots represent amino acids identical to the *Burkholderia* sp. RASC sequence, while hyphen represents a gap compared to the *Burkholderia* sp. RASC amino acid sequence. The RASC sequence is included because we observed a three base pair difference, resulting in one amino acid difference (in #98) compared to the reference sequence of *Burkholderia* sp. RASC. We have done bi-directional resequencing in order to confirm our result.

JOURNAL OF AGRICULTURAL AND FOOD CHEMISTRY

Cite This: J. Agric. Food Chem. 2018, 66, 12217−12226

pubs.acs.org/JAFC

Two *dcm* Gene Clusters Essential for the Degradation of Diclofop-methyl in a Microbial Consortium of *Rhodococcus* sp. JT-3 and *Brevundimonas* sp. JT-9

Hui Zhang,[†] Ting Yu,[†] Jie Li,[†] Yi-Ran Wang,[†] Guang-Li Wang,*[,†] Feng Li,*[,†] Yuan Liu,[†] Ming-Hua Xiong,[†] and Ying-Qun Ma[‡]

[†]College of Life Sciences, Huaibei Normal University, Huaibei 235000, China

[‡]Advanced Environmental Biotechnology Centre, Nanyang Environment & Water Research Institute, Nanyang Technological University, 1 Cleantech Loop, Singapore 637141, Singapore

Supporting Information

ABSTRACT: The metabolism of widely used aryloxyphenoxypropionate herbicides has been extensively studied in microbes. However, the information on the degradation of diclofop-methyl (DCM) is limited, with no genetic and biochemical investigation reported. The consortium L1 of *Rhodococcus* sp. JT-3 and *Brevundimonas* sp. JT-9 was able to degrade DCM through a synergistic metabolism. To elaborate the molecular mechanism of DCM degradation, the metabolic pathway for DCM was first investigated. DCM was initially transformed by strain JT-3 to diclofop acid and then by strain JT-9 to 2-(4-hydroxyphenoxy) propionic acid as well as 2,4-dichlorophenol. Subsequently, the two *dcm* gene clusters, *dcmAE* and *dcmB1B2CD*, involved in further degradation of 2,4-dichlorophenol, were successfully cloned from strain JT-3, and the functions of each gene product were identified. DcmA, a glutathione-dependent dehalogenase, was responsible for catalyzing the reductive dehalogenation of 2,4-dichlorophenol to 4-chlorophenol, which was then converted by the two-component monooxygenase DcmB1B2 to 4-chlorocatechol as the ring cleavage substrate of the dioxygenase DcmC. In this study, the overall DCM degradation pathway of the consortium L1 was proposed and, particularly, the lower part on the DCP degradation was characterized at the genetic and biochemical levels.

KEYWORDS: *diclofop-methyl, microbial consortium, microbial degradation, molecular mechanism*

Downloaded via CORTEVA AGRISCIENCE on September 11, 2020 at 01:26:59 (UTC).
See https://pubs.acs.org/sharingguidelines for options on how to legitimately share published articles.

1. INTRODUCTION

As one of the representative aryloxyphenoxypropionate (AOPP) herbicides, diclofop-methyl (DCM, (*R,S*)-methyl-2-[4-(2,4-dichlorophenoxy) phenoxy] propionate), with potent inhibition of acetyl-CoA carboxylase as well as photosynthesis and meristem activity, is widely used for the control of annual and perennial grass weeds in broadleaf crop fields such as wheat, barley, and legumes.[1,2] The US Environment Protection Agency reported that the total annual domestic usage of DCM is approximately 750 000 pounds of as an active major ingredient.[3] Due to its widespread application, DCM and its transformation products can be transported to surface waters and shallow groundwater, leading to a high environmental pollution risk.[4−6] In addition, long-term exposure to high concentrations of DCM has been shown to cause lung injury, such as pneumoconiosis,[7] and chromosomal aberration of mammalian lymphocytes both in vivo and in vitro.[8] Thus, the environmental removal and degradation mechanisms of DCM have attracted considerable attention.

Compared to the available physical and chemical removal methods, microbial degradation is thought to be a more effective and thorough strategy to eliminate DCM from a contaminated environment. To date, several strains capable of degrading AOPP herbicides, including the fluazifop-*P*-butyl-degrading strain *Aquamicrobium* sp. FPB-1,[9] the fenoxaprop-P-ethyl (FE)-degrading strain *Acinetobacter* sp. DL-2,[10] the cyhalofop-butyl-degrading strain *Pseudomonas azotoformans* QDZ-1,[11] and the quizalofop-*P*-ethyl (QE)-degrading strain *Ochrobactrum* sp. QE-9,[12] have been isolated based on their ability to utilize AOPP herbicide as a sole carbon and energy source. However, these strains transform the AOPP herbicides into the corresponding acids by a specific carboxylesterase, but show no further degradation, resulting in incomplete degradation. Recently, an FE-mineralizing bacterial consortium W1 was isolated by soil-enrichment culture and the FE degradation mechanism was extensively investigated. Through this, fenoxaprop acid, 6-chloro-2,3-dihydrobenzoxazol-2-one (CDHB), 2-(4-hydroxyphenoxy) propionic acid (HPP), and 2-amino-5-chlorophenol were identified as intermediate metabolites by HPLC/MS.[13,14] *Acinetobacter* sp. DL-2, which is responsible for the transformation of FE to fenoxaprop acid, and *Pigmentiphaga* sp. DL-8, which is involved in the degradation of CDHB and HPP, were successfully isolated from the bacterial consortium W1. However, a single bacterial strain with the ability of converting fenoxaprop acid to CDHB and HPP, which is considered the critical step in the degradation process of FE, has not been isolated.[15] Similarly, the degradation of [^{14}C]DCM to [^{14}C]CO_2 by a biofilm consortium comprising nine bacterial strains and one alga,

Received: October 1, 2018
Revised: October 25, 2018
Accepted: October 30, 2018
Published: October 30, 2018

ACS Publications © 2018 American Chemical Society

DOI: 10.1021/acs.jafc.8b05382
J. Agric. Food Chem. 2018, 66, 12217−12226

COR-AAD1-00003710
Bayer EX1008 (Part 7 of 9)

demonstrated that environmental metabolism of DCM required microbial synergetic degradation.[15] In 1996, a DCM-degrading bacterial consortium consisting of *Chryseomonas luteola* and *Sphingomonas paucimobilis* was isolated from herbicide-polluted soil in Canada.[16] The *Sphingomonas* strain was able to degrade the initial hydrolyzing product of DCM, diclofop acid (DC), to 4-(2,4-dichlorophenoxy) phenol, 2,4-dichlorophenol (DCP) and phenol, yet, accumulation of DCP in the growth medium was observed, suggesting that this strain alone was unable to completely degrade DC as well as DCM.[17]

The information on the microbial degradation of DCM is limited, with no genetic and biochemical investigations reported. This study aims to investigate the molecular mechanism of DCM degradation by the consortium L1, which was isolated from QE-contaminated soil using QE as a sole carbon source.[18] Interestingly, the consortium L1 was proven to be able to degrade DCM by co-operation between strains JT-3 and JT-9. In this study, the overall DCM degradation pathway was elucidated through the degradation tests using the two consortium members JT-3 and JT-9 and the chemical analyses of the DCM intermediates. In addition, the two gene clusters involved in the lower pathway of DCM degradation were cloned from strain JT-3 and the functions of each gene product were characterized. These results suggest a novel DCM degradation pathway by the bacterial consortium.

2. MATERIALS AND METHODS

2.1. Chemicals, Media, and Strains. DCM (purity, 99.5%), DC (purity, 99.2%), HPP (purity, 95%), DCP (purity, 99%), 4-chlorophenol (4-CP) (purity, 99%), and 4-chlorocatechol (4-CC) (purity, 98%) were purchased from J&K Chemical Co., Ltd., China. All other chemicals and reagents were of analytical or high-performance liquid chromatography (HPLC) grade and are commercially available. The primers used in this study were synthesized from Takara Biomedical Technology (Dalian) Co., Ltd., China (Supporting Information, SI, Table S1). Luria–Bertani (LB) medium and mineral salts medium (MM) were used for bacterial cultivation.[12] When necessary, kanamycin (50 μg mL^{-1}) or chloramphenicol (*Cm*, 34 μg mL^{-1}) were added.

2.2. Synergistic Degradation and Growth of the Consortium L1. Strains JT-3 and JT-9 were grown in LB medium for approximately 24 h at 30 °C and 180 rpm. The cells were harvested by centrifugation (5000*g*, 10 min) and washed twice with fresh MM. Cell density was then adjusted to approximately 1.0×10^8 CFU mL^{-1}, and an aliquot (2%, v/v) was inoculated into 100 mL of MM supplemented with 100 mg L^{-1} of DCM or its intermediates as the sole carbon and energy source. All cultures were incubated at 30 °C and 160 rpm on a rotary shaker. At regular intervals, 5 mL of samples were withdrawn from the cultures for analysis. In order to identify the intermediates of DCP prior to ring cleavage, 1 mM 2,2′-dipyridyl was used as an inhibitor of aromatic ring dioxygenases in the MM.[19] The concentrations of DCM and its metabolic intermediates were determined by HPLC analysis based on a peak area from the calibration curve. The amount of cells of each strain was calculated by a dilution and plate counting method.[13] Of note, the individual degradation of each strain was detected under the same conditions as the synergistic degradation of both strains.

2.3. Chemical Analysis. For HPLC analysis, each sample was extracted twice with an equal volume of dichloromethane. The extracts were pooled and dried with anhydrous sodium sulfate. After rotary evaporation, the residues were dissolved in 1 mL of methanol. HPLC analysis was performed as described previously with minor modifications.[12] To identify the metabolic intermediates of DCM transformed by the consortium L1 or by each strain, the samples were subjected to LC ion-trap mass spectrometry (LC–ITMS) analysis.[19] Electrospray ionization (ESI) was performed in negative ion mode and full scan in the range 100–500 *m*/*z*.

Due to the poor ionization efficiency for DCP metabolites in the LC–ITMS analysis, gas chromatography–mass spectrometry (GC–MS) analysis was further conducted to determine the identity of the metabolites. The supernatant from each sample was acidified prior to extraction with ether, as previously described.[20] The resulting organic phases were concentrated and analyzed using a Thermo Fisher Trace GC Ultra gas chromatograph equipped with an HP-5MS capillary column (30 m × 0.25 mm × 0.25 μm) and coupled to a Thermo Fisher ITQ 900 ion trap mass spectrometer. Helium was used as the carrier gas at a flow rate of 1 mL min^{-1}. The oven was initially held at 40 °C for 1 min, ramped to 240 °C at a rate of 5 °C min^{-1}, and held for 3 min. Mass spectra were recorded in the range 40–200 *m*/*z*. The intermediates were identified through comparing the GC retention times and mass spectra of those authentic compounds available in NIST98 mass spectra data library.

2.4. Real-Time Quantitative PCR (RT-qPCR). The genomic DNA from strain JT-3 was isolated using the high salt precipitation method[12] and submitted to BGI Technology Service Co., Ltd. (Shenzhen, China) for whole-genome sequencing and annotation. Target gene primers were designed and used to investigate the transcriptional levels of the gene clusters *dcmAE* and *dcmB1B2CD* in response to the various substrates. Strains JT-3 and JT-9 were grown in LB medium at 30 °C. Cells were harvested, washed twice, and diluted to approximately 1.0×10^8 CFU mL^{-1} with fresh MM. An aliquot (2%, v/v) was inoculated into 100 mL of MM containing 100 mg L^{-1} DCM and incubated at 30 °C and 160 rpm for 54 h. For DCP degradation induction, only strain JT-3 was inoculated into MM containing 100 mg L^{-1} DCP and cultured under the same conditions. In control experiments, yeast extract (0.2%, w/v) was added instead of DCM and DCP. Total RNA was extracted with the RNAiso Plus (Takara) and reverse transcription PCR was performed with the PrimeScript RT reagent kit (Takara) in a 20-μL reaction mixture to obtain cDNA. RT-qPCR was performed with a 7300 Fast Real-Time PCR System (Applied Biosystems) in a 25-μL reaction mixture using SYBR Premix Ex *Taq*II (Takara). All samples were run in triplicate, in three independent experiments. The relative transcriptional levels of the target genes were evaluated according to the $2^{-\Delta\Delta CT}$ method using the 16S rRNA gene as a reference.[21]

2.5. Protein Expression and Purification. The genes *dcmA*, *dcmB1*, *dcmB2* and *dcmC* were amplified from the genomic DNA of strain JT-3 by PCR. The resulting PCR products were respectively digested and cloned into the corresponding sites of pET-29a(+) to generate the expression plasmids. The plasmids were subsequently transformed into *E. coli* (DE3) for protein expression. N-terminal 6× histidine-tagged (H_6) recombinant proteins were purified using a Ni-NTA affinity chromatography column (Sangon Biotech, Shanghai, China).[12] The protein concentrations were determined by the Bradford assay using bovine serum albumin as the standard.

2.6. Enzyme Assays. The dehalogenase activity of DcmA against DCP was measured under anaerobic conditions by adding a reduced form of glutathione (GSH) to remove residual oxygen from the solution. The reaction mixture contained 1 mM GSH, 1–100 μg of purified H_6-DcmA, and 50 μM DCP in 10 mL of phosphate buffer (50 mM, pH7.5). The reaction was initiated with addition of the substrate. The reaction mixture was extracted with ethyl acetate after acidification and subjected to GC–MS analysis to determine the substrate concentration. For kinetic assays, DCP was appropriately diluted into at least six different concentrations in the range 0–150 μM. Data from three independent experiments were fit into the Lineweaver–Burk transformation of the Michaelis–Menten equation with OriginPro 8 software (OriginLab, U.S.A.). One unit (U) of activity was defined as the amount of enzyme consuming 1 μmol of substrate per min at 30 °C.

The nicotinamide adenine dinucleotide (NADH) oxidizing activity of DcmB2 was assayed by measuring the decrease in absorbance of NADH at 320 nm (ε = 6220 M^{-1} cm^{-1}) in 1 mL of phosphate buffer (50 mM, pH7.5) containing 200 μM NADH and 25 μM flavin adenine dinucleotide (FAD) at 25 °C. The reaction was initiated by addition of purified H_6-DcmB2 (0.8 μg). The enzyme activity of 4-CP monooxygenase (DcmB1) was assayed in 50 mM phosphate buffer

DOI: 10.1021/acs.jafc.8b05382
J. Agric. Food Chem. 2018, 66, 12217–12226

COR-AAD1-00003711
Bayer EX1008 (Part 7 of 9)

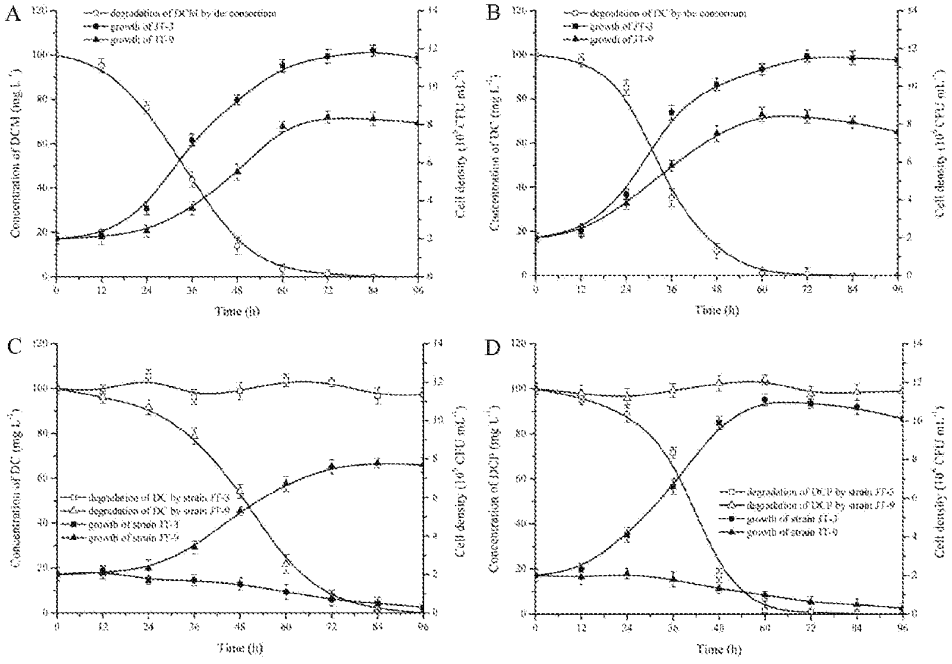


Figure 1. Degradation dynamics of DCM and its intermediates by strains JT-3 and JT-9. (A) Synergistic degradation of DCM by strains JT-3 and JT-9; (B) synergistic degradation of DC by strains JT-3 and JT-9; (C) individual degradation of DC by strain JT-3 and strain JT-9; and (D) individual degradation of DCP by strain JT-3 and strain JT-9.

(pH 7.5), as previously described,[20] with several modifications. The reaction mixture contained 200 μM NADH, 25 μM FAD, purified H_6-DcmB2 (0.1−1 μg), and purified H_6-DcmB1 (10−100 μg) in a final volume of 1 mL. The assay was initiated by addition of substrate 4-CP. One unit (U) of activity was defined as the amount of enzyme required for oxidization of 1 μmol of NADH for reductase DcmB2 or 1 μmol of 4-CP for 4-CP monooxygenase DcmB1 per min. The products of the reaction catalyzed by purified H_6-DcmB1 and H_6-DcmB2 were detected by GC−MS analysis. The detection of activities of the enzymes involved in the sequential transformation of 4-CC was performed as follows. The ring cleavage activity of 4-CC dioxygenase (DcmC) was assessed by monitoring the change in absorption at 260 nm due to the formation of 3-chloro-*cis*,*cis*-muconate (3-CM) from 4-CC.[22] Further, the release of chloride ions was detected and quantified by the measurement of absorbance at 460 nm according to the standard curve for chloride ions from known various concentrations of NaCl solutions, as previously described.[23]

2.7. Gene Knockout and Complementation of *dcmA*. The gene knockout plasmid pK18*mobsacB*-*dcmA* was constructed by fusing the upstream (553 bp) and downstream (499 bp) fragments of the *dcmA* gene and chloramphenicol resistance gene (1075 bp) from plasmid pXMJ19[20] to *Eco*RI/*Hind*III-digested vector pK18*mobsacB*[24] using in-fusion HD cloning kit (Takara). The resulting plasmid was then introducted into strain JT-3 by electrotransformation.[20] The single-crossover colonies were screened on LB plates containing *Cm* and then replica plated on LB plates supplemented with 10% (w/v) sucrose. The *Cm*-resistant but kanamycin-sensitive double-crossover recombinants were selected for PCR analysis.[20] Plasmid pRESQ-*dcmA* for gene complementation was generated by fusion of the *dcmA* gene and its native promoter into *Bgl*II-digested vector pRESQ.[25] Thereafter, the construct was introduced into the mutant strain JT-3Δ*dcmA* by electrotransformation to obtain the *dcmA*-complemented strain JT-3Δ*dcmA*(*dcmA*), regaining the ability of utilizing DCP as the sole carbon source for growth. The gene disruption and gene complementation in these mutants were confirmed by PCR and sequencing.

2.8. Nucleotide Sequence Accession Numbers. The nucleotide sequences of approximately 4.9-kb and 8.4-kb DNA fragments harboring *dcmAE* and *dcmB1B2CD*, respectively, from *Rhodococcus* sp. strain JT-3 described in this study were deposited in the GenBank database under accession numbers MH579712 and MH579713.

3. RESULTS AND DISCUSSION

3.1. Synergistic Degradation and Growth of the Consortium L1. DCM degradation by the consortium L1 was assessed using it as the sole carbon source. When strains JT-3 and JT-9 were simultaneously inoculated into MM containing 100 mg L^{-1} of DCM, DCM was degraded within 72 h (Figure 1A). The amount of cells of strain JT-3 increased from 2.0 × 10^6 CFU mL^{-1} to 11.9 × 10^6 CFU mL^{-1} in 84 h. For strain JT-9, the cells rapidly increased after approximately 24-h lag time, reaching 8.4 × 10^6 CFU mL^{-1} from 2.0 × 10^6 CFU mL^{-1} at 72 h. In our previous study, an esterase, named EstS-JT, catalyzing the initial hydrolysis of DCM to DC was found from strain JT-3 and the function was confirmed by chemical analysis of the enzymatic reaction using LC−MS.[18] Thus, to investigate the degradation pathway lower than DC, the degradation dynamics of DC by both strains JT-3 and JT-9 was examined in MM using DC as the sole carbon source. The two strains exhibited similar degradation and growth curves when inoculated into DCM-containing MM except for the shorter lag phase (12 h) (Figure 1B). These observations indicate that strains JT-3 and JT-9, inoculated as a consortium, are capable of utilizing DCM or DC as the sole carbon source for growth.

In order to estimate the roles of each strain during the DCM degradation, each strain was inoculated to MM supplemented with DC. When strain JT-9 was inoculated alone in DC-containing MM, it was able to degrade 100 mg L^{-1} of DC in 84 h, reaching a cell density of 7.8 × 10^6 CFU mL^{-1} at 84 h (Figure 1C), suggesting that strain JT-9 could utilize DC as its

DOI: 10.1021/acs.jafc.8b05382
J. Agric. Food Chem. 2018, 66, 12217−12226

COR-AAD1-00003712
Bayer EX1008 (Part 7 of 9)

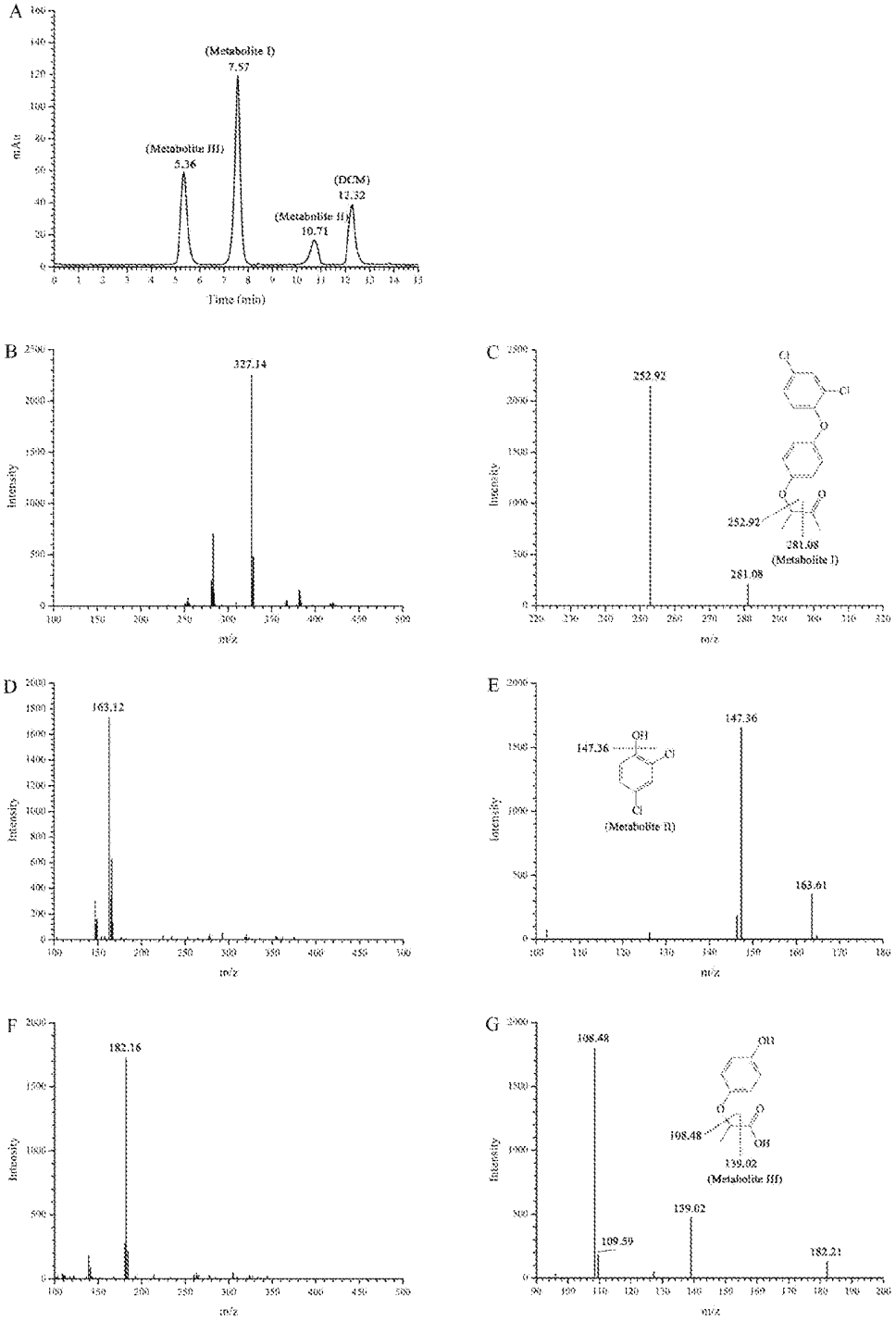


Figure 2. HPLC and LC−ITMS analyses of the DCM metabolites in the DCM degradation by the consortium L1. (A) HPLC chromatogram of the 5-d incubation sample; (B, D, F) mass spectrum of the DCM metabolites I, II and III, respectively; and (C, E, G) second-order mass spectrum of the DCM metabolites I, II and III, respectively.

sole carbon source for growth. In contrast, a negligible change in DC concentration was observed in MM inoculated with strain JT-3 (Figure 1C), indicating that strain JT-3 was incapable of degrading DC. Interestingly, though strain JT-9 could utilize DC as the sole carbon source for growth, an accumulation of DCP was observed during the degradation of DC by strain JT-9 alone, suggesting that the degradation of DC requires the cooperative metabolism of strains JT-9 and

DOI: 10.1021/acs.jafc.8b05382
J. Agric. Food Chem. 2018, 66, 12217−12226

COR-AAD1-00003713
Bayer EX1008 (Part 7 of 9)

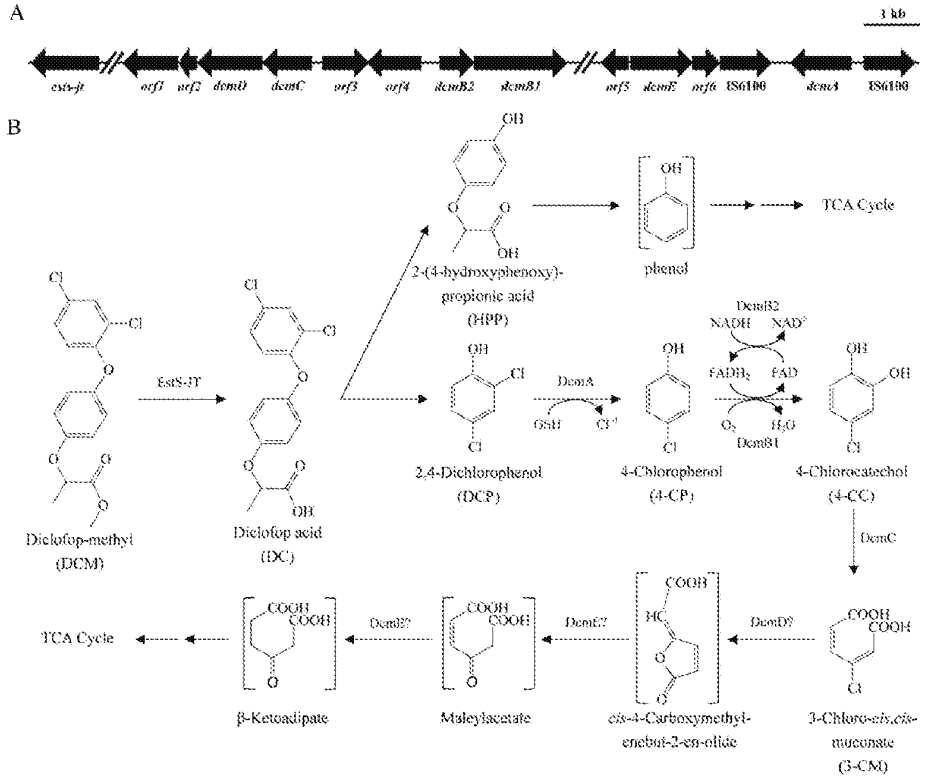


Figure 3. (A) Organization of the *dcm* gene cluster of *Rhodococcus* sp. strain JT-3. The sizes and transcriptional directions of each gene and ORF were indicated by the black arrows. (B) Proposed degradation pathway of DCM by the consortium L1, together with the conversion reaction catalyzed by the *dcm* gene products. TCA, tricarboxylic acid.

JT-3. Thus, DCP degradation by each individual strain was performed in MM; as expected, 100 mg L^{-1} of DCP was degraded by strain JT-3 in 60 h (Figure 1D). The cell density quickly increased to 11.1 × 10^5 CFU mL^{-1} at 60 h and remained stable for 12 h. Conversely, inoculation with strain JT-9 led to no significant change in DCP concentration, with a gradual decrease in the growth curve. These results clearly demonstrate that strain JT-3 initiated the conversion of DCM to DC, which was used as the carbon source by strain JT-9 for further degradation. Subsequently, DCP, as a metabolite of DC, was degraded by strain JT-3. Thus, a synergistic metabolism in the consortium L1 occurs during DCM degradation, with mutual assistance to achieve cell growth and degradation of DCM. Several bacterial consortia have been described to synergistically degrade a variety of environmental contaminants, such as FE[13] and bromoxynil octanoate.[26] Indeed, bromoxynil octanoate was shown to be degraded by the consortium consisting of two bacterial strains (*Sphingopyxis* sp. OB-3 and *Comamonas* sp. 7D-2) through a similar synergistic mechanism.[26] The two members of the consortium facilitated the growth of each other through cross-feeding with metabolites from the degradation pathway.

3.2. Identification of Metabolic Intermediates. In order to determine the metabolic intermediates of DCM degradation by the consortium L1, all samples were analyzed at 5 days after inoculation by HPLC and LC−ITMS. Three metabolites were detected, with retention times of 7.57, 5.36, and 10.71 min, respectively (Figure 2A). Metabolite I was identified as DC, with a protonated molecular parent ion peak at m/z 327.14 (Figure 2B) and characteristic second-order fragment ion peaks at m/z 281.08 (loss of −COOH) and at m/z 252.92 (loss of $-CH_3CH_2$) (Figure 2C). Metabolite II displayed a protonated parent ion peak at m/z 163.12 (Figure 2D) and characteristic second-order fragment ion peak at m/z 147.36 (loss of −OH) (Figure 2E), and was identified as DCP. Metabolite III had a protonated parent ion peak at m/z 182.16 (Figure 2F) and characteristic second-order fragment ion peaks at m/z 139.02 (loss of −COOH) and at m/z 108.48 (loss of $-CH_3CH_2$) (Figure 2G). Thus, it was assigned to HPP, a major intermediate that has been shown to be present in the microbial metabolism of another AOPP herbicide, FE.[10]

On the basis of the identification of DCM metabolites, a plausible DCM degradation pathway by both strains JT-3 and JT-9 was proposed (Figure 3B). Nevertheless, the DCM degradation presented herein was significantly different from the previously reported metabolisms of clodinafop[27] and DCM,[17] in which the corresponding acid, DC, produced by the breakdown of the ester bond of DCM, was transformed to DCP and HPP by hydrolyzing the C−O bond between two benzene rings rather than directly by removal of propionic acid to form phenoxy-phenol. Unfortunately, the gene responsible for the conversion of DC to HPP and DCP is yet not found in strain JT-9.

To further determine how DCP was degraded by strain JT-3 in the consortium L1, strain JT-3 was inoculated in MM containing 100 mg L^{-1} DCP and 1 mM 2,2′-dipyridyl. At 48 h after inoculation, two metabolites with GC retention times of 11.28 and 14.52 min, respectively, were accumulated with

DOI: 10.1021/acs.jafc.8b05382
J. Agric. Food Chem. 2018, 66, 12217−12226

COR-AAD1-00003714
Bayer EX1008 (Part 7 of 9)

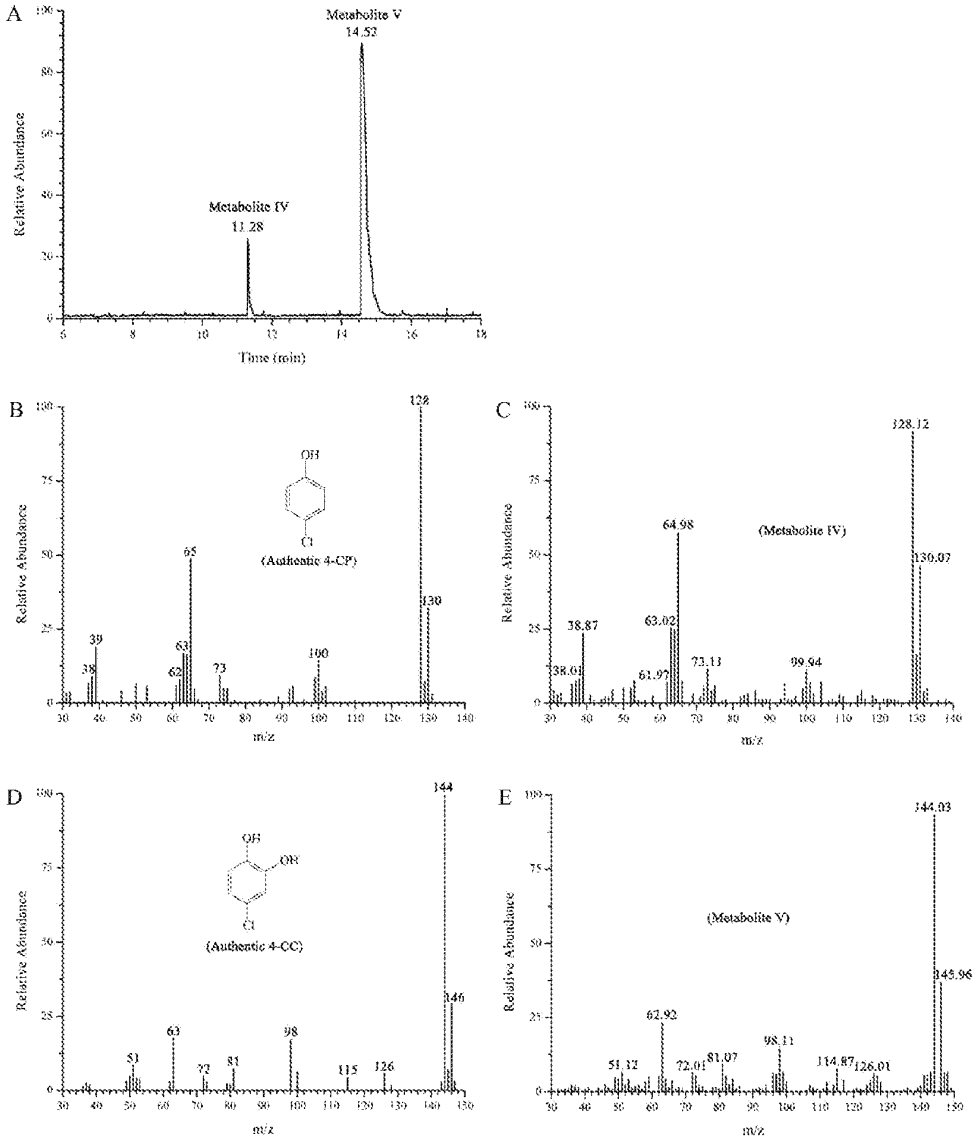


Figure 4. GC−MS analysis of the DCP metabolites in the DCP degradation by *Rhodococcus* sp. strain JT-3. (A) The gas chromatogram is the extracted ion current chromatogram at m/z 128.00 ± 0.50 and 144.00 ± 0.50 from the total ion current chromatogram; (B) mass spectrum of authentic 4-chlorophenol (4-CP); (C) mass spectrum of the GC peak at 11.28 min, identical to that of authentic 4-CP; (D) mass spectrum of authentic 4-chlorocatechol (4-CC); and (E) mass spectrum of the GC peak at 14.52 min, identical to that of authentic 4-CC.

DCP consumption (Figure 4A). Compared to the mass spectra of the authentic compounds, these two metabolites, IV and V, were identified as 4-CP and 4-CC by GC−MS analysis, respectively (Figure 4B−E). Additionally, quantitative analysis of the intermediates indicated that the stoichiometric amount of DCP consumption (482 μM) was nearly equal to the total yield of both 4-CP (411 μM) and 4-CC (28 μM). Furthermore, with the increase in degradation time, a gradual accumulation of 4-CC, coupled with the continuous consumption of 4-CP, was observed (data not shown), demonstrating that strain JT-3 degraded DCP to 4-CP and then 4-CC. In the absence of 2,2′-dipyridyl, 4-CC was not detected, suggesting further degradation of 4-CC by the ring-cleavage (the data were shown later) (Figure 3B). DCP has also been found to be the first intermediate during the degradation of herbicide 2,4-dichlorophenoxyacetic acid (2,4-D),[28,29] wherein 2,4-D was converted into 3,5-dichlorocatechol by hydroxylase and subsequently used as the ring cleavage substrate for further degradation. In the case of DCP degradation by strain JT-3, 4-CP, as the initial intermediate of DCP degradation by the dehalogenation reaction, was detected for the first time herein. Recently, Pandey et al.[30] described a degradation pathway of 2-chloro-4-nitrophenol (2C4NP) in *Burkholderia* sp. strain SJ98 by a similar dehalogenation under aerobic condition. The first step of 2C4NP degradation by strain SJ98 was the reductive dehalogenation, resulting in the formation of 4-nitrophenol.

DOI: 10.1021/acs.jafc.8b05382
J. Agric. Food Chem. 2018, 66, 12217−12226

COR-AAD1-00003715
Bayer EX1008 (Part 7 of 9)

3.3. Sequence Analyses of the DCM Metabolic Gene Clusters. According to the proposed DCM degradation pathway based on the identified intermediates during DCM and DCP degradation, two gene clusters likely involved in DCP degradation were found on contigs 3 and 7 of the draft genome sequence of strain JT-3 and designated *dcmAE* and *dcmB1B2CD*, respectively (Figure 3A). Among *dcmAE*, *dcmA* encodes a protein (DcmA) of 351 amino acid residues, which exhibits 55% and 30% similarity with 2,5-dichlorohydroquinone reductive dechlorinase (AAN64243) from *Sphingomonas paucimobilis* B90 and glutathione *S*-transferase family protein (AGI68666) from *Octadecabacter antarcticus* 307, respectively, suggesting that it appeared to belong to the glutathione *S*-transferase family and was involved in the reductive dechlorination of DCP during DCM degradation. On both the 5′- and 3′-flanking regions of *dcmA*, two complete IS6100 transposable element including inverted repeats were found, in which gene *tnpA* encoding proteins had 99% identity to the IS6100 transposase. Such gene organization flanked by insertion elements was reported to exist in the 2,4-D degradation gene cluster of *Delftia acidovorans* strain P4a, isolated from heavily organochlorine-contaminated soil.[31] The *dcmE* gene encodes a protein (DcmE) of 354 amino acid residues, which displays 58% homology with the maleylacetate reductase MacA (AAC38802) from *Rhodococcus opacus* 1CP. Similar phenomenon is found that the gene (*macA*) encoding MacA was relatively distant from the major counterparts responsible for phenol metabolism, suggesting that the *dcmE* and *macA* genes are not members of the specialized aromatic compound metabolic genes.[32] For another gene cluster, *dcmB1B2CD*, DcmB1, and DcmB2 showed 79% and 56% similarity to the oxygenase and reductase components, respectively, of the 4-nitrophenol hydroxylase (Q8RQQ0) from *Rhodococcus* sp. PN1, suggesting that DcmB1B2 probably belongs to the two-component flavin-diffusible monooxygenase (TC-FDM) family. DcmC and DcmD shared moderate similarity to chlorocatechol 1,2-dioxygenase (AAC38249, 41%) and chloromuconate cycloisomerase (AAC38251, 40%), respectively, from *Rhodococcus opacus* 1CP.

3.4. Transcriptional Analyses of the Gene Cluster *dcmAE* and *dcmB1B2CD*. To estimate whether the gene clusters *dcmAE* and *dcmB1B2CD* are involved in DCM degradation, the transcriptional levels of these two gene clusters in response to substrates DCM and DCP were investigated. At 54 h after inoculation by both JT-3 and JT-9 in MM with or without the substrate DCM, total RNA was extracted from strain JT-3 and utilized as the template for RT-qPCR. RT-qPCR results revealed that the transcriptional levels of *dcmA*, *dcmB1B2*, *dcmC*, *dcmD*, and *dcmE* were dramatically increased compared to those from the samples without the addition of DCM, with a 345-, 271-, 57-, 49-, and 82-fold increase, respectively (Figure 5). The significant diversity in transcription levels of *dcmA*, *dcmE*, *dcmB1B2*, and *dcmC* was probably the reason that each gene was controlled by the respective independent transcriptional operons. Conversely, the approximate equivalence of transcriptional levels between *dcmC* and *dcmD* was suggested to be located in a single transcriptional operon. Likewise, for the samples from MM containing DCP inoculated by strain JT-3, the transcriptional levels of these genes were also obviously up-regulated. Thus, the results indicated that these tested genes were likely involved in DCM degradation by the consortium L1.

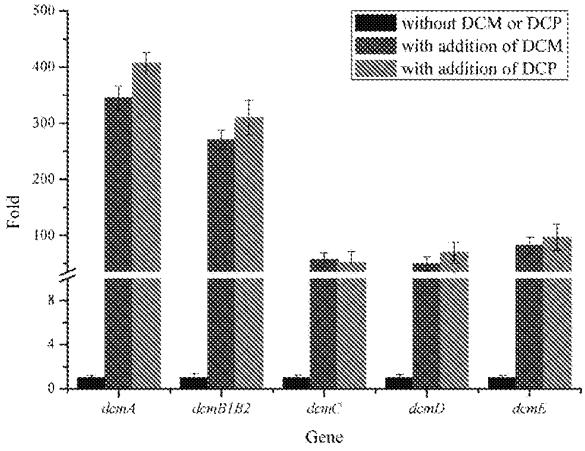


Figure 5. Transcriptional analyses of the gene cluster *dcmAE* and *dcmB1B2CD* of strain JT-3 with or without addition of DCM or DCP by RT-qPCR. DCM-containing MM was inoculated by both strains JT-3 and JT-9 and DCP-containing MM was inoculated by strain JT-3. All experiments were performed in triplicate, and error bars indicate standard deviations.

3.5. DcmA Catalyzes the Reductive Dechlorination of DCP to form 4-CP. Recombinant H_6-DcmA was expressed in *E. coli* BL21 (DE3) by induction of 0.1 mM isopropyl β-D-thiogalactopyranoside (IPTG) at 16 °C overnight. Following purification and concentration, SDS-PAGE analysis only displayed a slight single protein band of approximately 44 kDa (SI Figure S1), matching the calculated molecular mass of the recombinant H_6-DcmA. Conversion of DCP by the purified protein was performed in the reaction mixture containing GSH, and the metabolites from DCP were analyzed by GC−MS. One metabolite was detected at 11.28 min in the chromatogram and it showed a similar mass spectrum to that of authentic 4-CP (SI Figure S2A). The dechlorination activity assay revealed that the catalytic velocity of H_6-DcmA against DCP was strictly dependent on the presence of GSH (SI Figure S3). These results suggest that DcmA catalyzes DCP to 4-CP in the presence of GSH through a mechanism analogous to that for tetrachlorohydroquinone dehalogenation by the GSH-dependent dehalogenase of *Sphingobium chlorophenolicum*,[33] in which the enzyme activated GSH as a nucleophilic group to form a complex between GSH and DCP, leading to the displacement of chlorine in DCP with GSH. The K_m value for GSH of H_6-DcmA was 98 μM and maximal activity (3.2 U mg^{-1}) was achieved in the presence of 1 mM GSH, nearly equivalent to the value of dechlorinase BphK from *Burkholderia xenovorans* strain LB400.[34] When the concentration of GSH added in the reaction mixture was far in excess of the amount required, the concentration of the DCP substrate varied from 0 to 150 μM. The kinetic analysis indicated the K_m value of H_6-DcmA was 26.7 ± 3.1 μM, the catalytic efficiency k_{cat}/K_m and V_{max} values were 0.11 ± 0.02 μM^{-1} S^{1-} and 3.86 ± 0.43 μmol min^{-1} mg^{-1}, respectively.

3.6. DcmB1B2 Catalyzes the Hydroxylation of 4-CP to Form 4-CC. Recombinant H_6-DcmB1 and H_6-DcmB2 were individually expressed in *E. coli* BL21 (DE3) and purified by Ni-NTA affinity chromatography. SDS-PAGE analysis showed that the molecular masses of the purified H_6-DcmB1 and H_6-DcmB2 were approximately 65 and 26 kDa, respectively (SI Figure S1), corresponding to their molecular weights based on

DOI: 10.1021/acs.jafc.8b05382
J. Agric. Food Chem. 2018, 66, 12217−12226

COR-AAD1-00003716
Bayer EX1008 (Part 7 of 9)

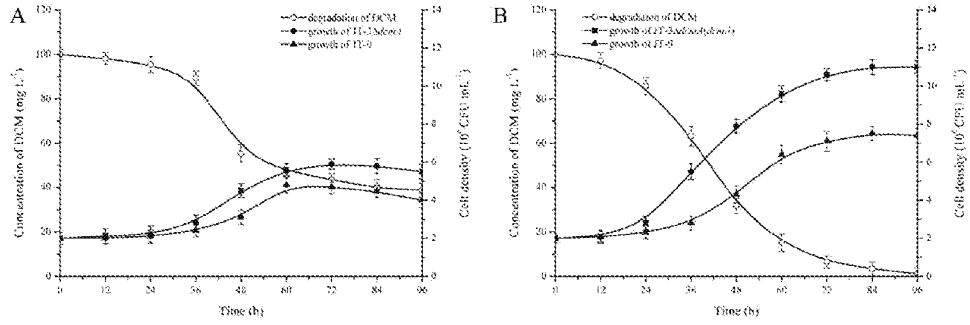


Figure 6. Degradation dynamics of DCM by (A) the mutant strain JT-3Δ*dcmA* and strain JT-9 or (B) by the *dcmA*-complemented mutant strain JT-3Δ*dcmA*(*dcmA*) and strain JT-9.

the deduced amino acid sequences. As the reductase component of 4-CP 4-monooxygenase, the maximal NADH-oxidizing activity of DcmB2 was 1.4 U mg^{-1} in the presence of FAD. The reaction was performed in the excess amount of FAD (25 μM) to determine the kinetic parameters of DcmB2 for NADH, the K_m values of H_6-DcmB2 for NADH was 31.7 ± 3.5 μM, the catalytic efficiency k_{cat}/K_m and V_{max} values were 0.29 ± 0.03 μM^{-1} S^{1-} and 21.4 ± 2.2 μmol min^{-1} mg^{-1}, respectively. When the amount of NADH in the reaction mixture was in excess (200 μM), the K_m values of H_6-DcmB2 for FAD was 4.11 ± 0.37 μM, the catalytic efficiency k_{cat}/K_m and V_{max} values were 2.34 ± 0.31 μM^{-1} S^{1-} and 22.2 ± 2.7 μmol min^{-1} mg^{-1}, respectively. As the function of DcmB2 was confirmed as an NADH/FAD oxidoreductase, conversion of 4-CP by the purified H_6-DcmB1 was performed in the presence of NADH, FAD, and the purified H_6-DcmB2. By the GC−MS analysis of the reaction mixture, 4-CC was identified as the product of the 4-CP conversion; the mass spectrum of the product was almost similar to that for authentic 4-CC (SI Figure S2B). The oxidation activity assay of purified H_6-DcmB1 and H_6-DcmB2 demonstrated that the catalytic activity was closely related to the ratio of the two enzymes in the reaction mixture. A higher hydroxylation activity was clearly observed with an increase in H_6-DcmB1 concentration in the reaction mixture (SI Figure S4). Similar phenomena were observed in the cases of phenol hydroxylase PheA1A2 from *Rhodococcus erythropolis* UPV-1[38] and 4-nitrophenol monooxygenase from *Rhodococcus imtechensis* RKJ300.[20] Maximal activity (0.12 U mg^{-1}) was achieved when the molar ratio of H_6-DcmB2 to H_6-DcmB1 was approximately 1:35. The enzymatic kinetic assays led to the K_m value of H_6-DcmB1 for 4-CP of 14.1 ± 1.7 μM, the k_{cat}/K_m value of 0.21 ± 0.01 μM^{-1} S^{1-}, and the V_{max} value of 2.73 ± 0.29 μmol min^{-1} mg^{-1}.

3.7. DcmC, DcmD, and DcmE are Likely Responsible for the Sequential Conversion of 4-CC. The purified recombinant H_6-DcmC was approximately 35 kDa, consistent with its deduced molecular mass (SI Figure S1). The 4-CC dioxygenase activity assay of the purified H_6-DcmC revealed that the addition of the enzyme in the reaction mixture resulted in an increase of absorbance at 260 nm (SI Figure S5), corresponding to the production of 3-CM.[22] However, no specific absorbance change was observed upon H_6-DcmC omission from the reaction mixture. Moreover, *dcmC* was evidently up-regulated when strain JT-3 was grown in MM using DCM or DCP as the sole carbon source. Due to the negligible increase in absorbance at 375 nm (corresponding to the formation of 5-chloro-2-hydroxymuconic semialdehyde), it was concluded that DcmC in strain JT-3, as a single subunit dioxygenase, might be responsible for the *ortho*-ring cleavage of 4-CC to form 3-CM, rather than its *meta*-cleavage, during the DCP degradation. The enzyme assays of DcmD and DcmE were not performed since their substrates were commercially unavailable. However, considering that DcmD and DcmE exhibited moderate identity with the chloromuconate cycloisomerase (AAC38251) and the maleylacetate reductase (AAC44727) of *R. opacus* 1CP, respectively, and their coding genes were significantly up-regulated in MM containing DCM or DCP, thus, it was speculated that DcmD and DcmE were likely involved in the further conversion of 3-CM.

3.8. DcmA was Crucial for DCM Metabolism of by the Consortium L1. To evaluate the role of DcmA during DCM metabolism by the consortium L1, a mutant strain JT-3Δ*dcmA*, with a replacement of *dcmA* by a *Cm*-resistant gene, was constructed through double crossover recombination. Although the consortium comprising the mutant strain JT-3Δ*dcmA* and strain JT-9 was able to grow with DCM as the sole carbon source, the two strains grew slowly and the maximum cell number was remarkably decreased compared to those of wild-type strains JT-3 and JT-9 (Figure 6A). Additionally, an accumulation of DCP was observed in MM inoculated with both the mutant strain JT-3Δ*dcmA* and strain JT-9, and the consortium of these two strains was no longer able to rapidly degrade DCM, resulting in the poor growth on DCM (Figure 6A). Instead, the *dcmA*-complemented mutant strain JT-3Δ*dcmA*(*dcmA*), together with strain JT-9, regained the ability to efficiently degrade DCM, although they exhibited slower growth and DCM degradation in comparison with the wild-type strains (Figure 6B). The above findings demonstrate that *dcmA* is necessary for the consortium L1 to efficiently degrade DCM.

ASSOCIATED CONTENT

Supporting Information

The Supporting Information is available free of charge on the ACS Publications website at DOI: 10.1021/acs.jafc.8b05382.

Figure S1, SDS-PAGE analysis of the purified recombinant dcm proteins; Figure S2, GC−MS analysis of the products in enzyme catalytic reaction; Figure S3, relationship between initial velocity and various concentrations of GSH; Figure S4, relationship between 4-CP monooxygenase activity and various concentrations of H_6-DcmB1; Figure S5, spectral changes during the conversion of 4-CC catalyzed by the purified H_6-DcmC; and Table S1, primers used in this study (PDF)

DOI: 10.1021/acs.jafc.8b05382
J. Agric. Food Chem. 2018, 66, 12217−12226

COR-AAD1-00003717
Bayer EX1008 (Part 7 of 9)

AUTHOR INFORMATION

Corresponding Authors

*E-mail: guangliwang@aliyun.com (G.-L.W.).
*E-mail: rx2500@163.com (F.L.).

ORCID

Hui Zhang: 0000-0001-6410-4085

Funding

This work was financed by grants from Provincial Natural Science Foundation of Anhui (1808085MC56), Major Program of Natural Science Research in Colleges and Universities in Anhui Province (KJ2018ZD039), Project of Outstanding Young Talents Supporting Plan in Universities of Anhui Province (gxyq2018020), and Construction Project from College Scientific Research Innovation Team of Anhui Province—Ecological Restoration and Utilization of Coal Mining Subsidence Area.

Notes

The authors declare no competing financial interest.

ACKNOWLEDGMENTS

We are also grateful to Dr. Ma of Nanyang Technological University for assistance in the revision of manuscript.

REFERENCES

(1) De Prado, J. L.; Osuna, M. D.; Heredia, A.; De Prado, R. Lolium rigidum, a pool of resistance mechanisms to ACCase inhibitor herbicides. *J. Agric. Food Chem.* **2005**, *53*, 2185−2191.

(2) Diao, J.; Xu, P.; Wang, P.; Lu, Y.; Lu, D.; Zhou, Z. Environmental behavior of the chiral aryloxyphenoxypropionate herbicide diclofop-methyl and diclofop: enantiomerization and enantioselective degradation in soil. *Environ. Sci. Technol.* **2010**, *44*, 2042−2047.

(3) Abdalrahman, S. H.; Elhalwagy, M. E.; Kotb, G. A.; Farid, H.; Farag, A. A.; Draz, H. M.; Isa, A. M.; Sabico, S. Exposure to difenoconazole, diclofop-methyl alone and combination alters oxidative stress and biochemical parameters in albino rats. *Int. J. Clin. Exp. Med.* **2014**, *7*, 3637−3646.

(4) Waite, D. T.; Cessna, A. J.; Grover, R.; Kerr, L. A.; Snihura, A. D. Environmental concentrations of agricultural herbicides in Saskatchewan, Canada: bromoxynil, dicamba, diclofop, MCPA, and trifluralin. *J. Environ. Qual.* **2004**, *33*, 1616−1628.

(5) Cai, X.; Liu, W.; Jin, M.; Lin, K. Relation of diclofop-methyl toxicity and degradation in algae cultures. *Environ. Toxicol. Chem.* **2007**, *26*, 970−975.

(6) Cessna, A. J.; Elliott, J. A. Seasonal variation of herbicide concentrations in prairie farm dugouts. *J. Environ. Qual.* **2004**, *33*, 302−315.

(7) Palut, D.; Ludwicki, J. K.; Kostka, G.; Kopeć-Szlęzak, J.; Wiadrowska, B.; Lembowicz, K. Studies of early hepatocellular proliferation and peroxisomal proliferation in Wistar rats treated with herbicide diclofop. *Toxicology* **2001**, *158*, 119−126.

(8) Unal, F.; Yüzbaşıoğlu, D.; Yilmaz, S.; Akinci, N.; Aksoy, H. Genotoxic effects of chlorophenoxy herbicide diclofop-methyl in mice in *vivo* and in human lymphocytes in *vitro*. *Drug Chem. Toxicol.* **2011**, *34*, 390−395.

(9) Wang, C.; Qiu, J.; Yang, Y.; Zheng, J.; He, J.; Li, S. Identification and characterization of a novel carboxylesterase (FpbH) that hydrolyzes aryloxyphenoxypropionate herbicides. *Biotechnol. Lett.* **2017**, *39*, 553−560.

(10) Dong, W.; Jiang, S.; Shi, K.; Wang, F.; Li, S.; Zhou, J.; Huang, F.; Wang, Y.; Zheng, Y.; Hou, Y.; et al. Biodegradation of fenoxaprop-P-ethyl (FE) by *Acinetobacter* sp. strain DL-2 and cloning of FE hydrolase gene *afeH*. *Bioresour. Technol.* **2015**, *186*, 114−121.

(11) Nie, Z. J.; Hang, B. J.; Cai, S.; Xie, X. T.; He, J.; Li, S. P. Degradation of cyhalofop-butyl (CyB) by *Pseudomonas azotoformans* strain QDZ-1 and cloning of a novel gene encoding CyB-hydrolyzing esterase. *J. Agric. Food Chem.* **2011**, *59*, 6040−6046.

(12) Zhang, H.; Li, M.; Dai, C.; Wang, G.; Xiong, M.; Li, F.; Liu, Y.; Xu, D. Characterization of EstQE, a new member of esterase family VIII from the quizalofop-P-ethyl-degrading bacterium *Ochrobactrum* sp. QE-9. *J. Mol. Catal. B: Enzym.* **2016**, *133*, 167−175.

(13) Dong, W.; Hou, Y.; Xi, X.; Wang, F.; Li, Z.; Ye, X.; Huang, Y.; Cui, Z. Biodegradation of fenoxaprop-ethyl by an enriched consortium and its proposed metabolic pathway. *Int. Biodeterior. Biodegrad.* **2015**, *97*, 159−167.

(14) Hou, Y.; Tao, J.; Shen, W.; Liu, J.; Li, J.; Li, Y.; Cao, H.; Cui, Z. Isolation of the fenoxaprop-ethyl (FE)-degrading bacterium *Rhodococcus* sp. T1, and cloning of FE hydrolase gene *feh*. *FEMS Microbiol. Lett.* **2011**, *323*, 196−203.

(15) Wolfaardt, G. M.; Lawrence, J. R.; Robarts, R. D.; Caldwell, D. E. Bioaccumulation of the herbicide diclofop in extracellular polymers and its utilization by a biofilm community during starvation. *Appl. Environ. Microbiol.* **1995**, *61*, 152−158.

(16) Smithgrenier, L. L.; Adkins, A. Isolation and characterization of soil microorganisms capable of utilizing the herbicide diclofop-methyl as a sole source of carbon and energy. *Can. J. Microbiol.* **1996**, *42*, 221−226.

(17) Adkins, A. Degradation of the phenoxy acid herbicide diclofop-methyl by *Sphingomonas paucimobilis* isolated from a Canadian prairie soil. *J. Ind. Microbiol. Biotechnol.* **1999**, *23*, 332−335.

(18) Zhang, H.; Li, M.; Li, J.; Wang, G.; Li, F.; Xu, D.; Liu, Y.; Xiong, M. A key esterase required for the mineralization of quizalofop-p-ethyl by a natural consortium of *Rhodococcus* sp. JT-3 and *Brevundimonas* sp. JT-9. *J. Hazard. Mater.* **2017**, *327*, 1−10.

(19) Ferreira, M. I. M.; Marchesi, J. R.; Janssen, D. B. Degradation of 4-fluorophenol by *Arthrobacter* sp. strain IF1. *Appl. Microbiol. Biotechnol.* **2008**, *78*, 709−717.

(20) Min, J.; Zhang, J. J.; Zhou, N. Y. A two-component para-nitrophenol monooxygenase initiates a novel 2-chloro-4-nitrophenol catabolism pathway in *Rhodococcus imtechensis* RKJ300. *Appl. Environ. Microbiol.* **2016**, *82*, 714−723.

(21) Livak, K. J.; Schmittgen, T. D. Analysis of relative gene expression data using real-time quantitative PCR and the $2^{-\Delta\Delta CT}$ Method. *Methods* **2001**, *25*, 402−408.

(22) Maltseva, O. V.; Solyanikova, I. P.; Golovleva, L. A. Chlorocatechol 1,2-dioxygenase from *Rhodococcus erythropolis* 1CP. Kinetic and immunochemical comparison with analogous enzymes from gram-negative strains. *Eur. J. Biochem.* **1994**, *226*, 1053−1061.

(23) Ghosh, A.; Khurana, M.; Chauhan, A.; Takeo, M.; Chakraborti, A. K.; Jain, R. K. Degradation of 4-nitrophenol, 2-chloro-4-nitrophenol, and 2,4-dinitrophenol by *Rhodococcus imtechensis* strain RKJ300. *Environ. Sci. Technol.* **2010**, *44*, 1069−1077.

(24) Schäfer, A.; Tauch, A.; Jäger, W.; Kalinowski, J.; Thierbach, G.; Pühler, A. Small mobilizable multi-purpose cloning vectors derived from the *Escherichia coli* plasmids pK18 and pK19: selection of defined deletions in the chromosome of *Corynebacterium glutamicum*. *Gene* **1994**, *145*, 69−73.

(25) van der Geize, R.; Hessels, G. I.; van Gerwen, G. R.; van der Meijden, P.; Dijkhuizen, L. Molecular and functional characterization of *kshA* and *kshB*, encoding two components of 3-ketosteroid 9alpha-hydroxylase, a class IA monooxygenase, in *Rhodococcus erythropolis* strain SQ1. *Mol. Microbiol.* **2002**, *45*, 1007−1018.

(26) Chen, K.; Liu, Y.; Mao, D.; Liu, X.; Li, S.; Jiang, J. An essential esterase (BroH) for the mineralization of bromoxynil octanoate by a natural consortium of *Sphingopyxis* sp. strain OB-3 and *Comamonas* sp. strain 7D-2. *J. Agric. Food Chem.* **2013**, *61*, 11550−11559.

(27) Singh, B. Degradation of clodinafop propargyl by *Pseudomonas* sp. strain B2. *Bull. Environ. Contam. Toxicol.* **2013**, *91*, 730−733.

(28) Wu, X.; Wang, W.; Liu, J.; Pan, D.; Tu, X.; Lv, P.; Yi, W.; Cao, H.; Wang, Y.; Hua, R. Rapid biodegradation of the herbicide 2,4-dichlorophenoxyacetic acid by *Cupriavidus gilardii* T-1. *J. Agric. Food Chem.* **2017**, *65*, 3711−3720.

(29) Xia, Z. Y.; Zhang, L.; Zhao, Y.; Yan, X.; Li, S. P.; Gu, T.; Jiang, J. D. Biodegradation of the herbicide 2,4-dichlorophenoxyacetic acid

DOI: 10.1021/acs.jafc.8b05382
J. Agric. Food Chem. 2018, 66, 12217−12226

COR-AAD1-00003718
Bayer EX1008 (Part 7 of 9)

by a new isolated strain of *Achromobacter* sp. LZ35. *Curr. Microbiol.* **2017**, *74*, 193−202.
(30) Pandey, J.; Heipieper, H. J.; Chauhan, A.; Arora, P. K.; Prakash, D.; Takeo, M.; Jain, R. K. Reductive dehalogenation mediated initiation of aerobic degradation of 2-chloro-4-nitrophenol (2C4NP) by *Burkholderia* sp. strain SJ98. *Appl. Microbiol. Biotechnol.* **2011**, *92*, 597−607.
(31) Hoffmann, D.; Kleinsteuber, S.; Müller, R. H.; Babel, W. A transposon encoding the complete 2,4-dichlorophenoxyacetic acid degradation pathway in the alkalitolerant strain *Delftia acidovorans* P4a. *Microbiology* **2003**, *149*, 2545−2556.
(32) Seibert, V.; Kourbatova, E. M.; Golovleva, L. A.; Schlömann, M. Characterization of the maleylacetate reductase MacA of *Rhodococcus opacus* 1CP and evidence for the presence of an isofunctional enzyme. *J. Bacteriol.* **1998**, *180*, 3503−3508.
(33) Warner, J. R.; Copley, S. D. Pre-steady-state kinetic studies of the reductive dehalogenation catalyzed by tetrachlorohydroquinone dehalogenase. *Biochemistry* **2007**, *46*, 13211−13222.
(34) Fortin, P. D.; Horsman, G. P.; Yang, H. M.; Eltis, L. D. A glutathione S-transferase catalyzes the dehalogenation of inhibitory metabolites of polychlorinated biphenyls. *J. Bacteriol.* **2006**, *188*, 4424−4430.
(35) Saa, L.; Jaureguibeitia, A.; Largo, E.; Llama, M. J.; Serra, J. L. Cloning, purification and characterization of two components of phenol hydroxylase from *Rhodococcus erythropolis* UPV-1. *Appl. Microbiol. Biotechnol.* **2010**, *86*, 201−211.

DOI: 10.1021/acs.jafc.8b05382
J. Agric. Food Chem. 2018, 66, 12217−12226

COR-AAD1-00003719
Bayer EX1008 (Part 7 of 9)

Ecological Indicators 75 (2017) 126–133

Contents lists available at ScienceDirect

Ecological Indicators

journal homepage: www.elsevier.com/locate/ecolind

Enantioselective toxicity and degradation of chiral herbicide fenoxaprop-ethyl in earthworm *Eisenia fetida*

Xu Jing, Guojun Yao, Donghui Liu, Han Qu, Qian Zhou, Zhiqiang Zhou, Peng Wang *

Beijing Advanced Innovation Center for Food Nutrition and Human Health, Department of Applied Chemistry, China Agricultural University, Beijing, 100193, PR China

ARTICLE INFO

Article history:
Received 26 August 2016
Received in revised form 3 December 2016
Accepted 4 December 2016
Available online 27 December 2016

Keywords:
Fenoxaprop-ethyl
Earthworm
Toxicity
Degradation
Chiral

ABSTRACT

The enantioselective degradation of fenoxaprop-ethyl in ecological indicator earthworm was studied and the main metabolites (fenoxaprop, 6-chloro-2,3-dihydrobenzoxazol-2-one, ethyl-2-(4-hydroxyphenoxy)propanoate, 2-(4-hydroxyphenoxy)propanoic acid) were also monitored on an enantiomeric level. The individual enantiomers of fenoxaprop-ethyl and its three chiral metabolites were prepared to study the acute toxicity to earthworm. Chiral analysis methods were set up based on HPLC–MS/MS with chiralpak IC chiral column. Fenoxaprop-ethyl was not found in earthworms, while the primary metabolite fenoxaprop was in relatively high levels indicating a quick hydrolysis degradation. Fenoxaprop was accumulated almost exclusively with R-enantiomer in earthworms and the bio-concentration factors of R-fenoxaprop and S-fenoxaprop were 1.39 and 0.17 respectively with the enantiomer fraction (EF) values about 0.99. The degradation of R-fenoxaprop in earthworms followed first-order kinetics with half-life of 1.82 day. The other metabolites could not be detected in earthworms. The calculated LC_{50} values showed ecological indicator earthworm was more sensitive to the four metabolites than fenoxaprop-ethyl. Furthermore, earthworm was more sensitive to the R-form of the chiral metabolites than the S-form and rac-form. The results suggested metabolites and enantioselectivity should be taken into consideration to better predict the exposure concentration and apply ecological indicators in toxicological studies.

© 2016 Elsevier Ltd. All rights reserved.

1. Introduction

In 2009, almost 30 percent of the registered pesticides have stereogenic center and at least two mirror image enantiomers, and more than 40% of used pesticides in China were chiral (Qu et al., 2014; Ying et al., 2009). The physical and chemical properties of the enantiomers in non-chiral environment are identical. Despite of the differences in bioactivity, toxicity and metabolism, a majority of chiral pesticides have been produced and used as racemate (Cai et al., 2008; Liu et al., 2009). Only concerning the difference between the chiral enantiomers can the environmental risk assessment be credible.

Earthworm (*Eisenia fetida*) is an important soil organism which comprises the largest part of the soil fauna biomass and plays a significant role in soil ecology. Earthworm living in topsoil has a thin and permeable cuticle, which processes a large amount of soil through their feeding and burrowing activities and acts as an early-warning system for emerging soil ecological environment deteriorating (Jager et al., 2005; Lavelle et al., 1997; Shan et al., 2010). Because earthworm can accumulate various contaminants (Šmídová and Hofman, 2014; Wen et al., 2015; Zhang et al., 2014), they are excellent indicators for evaluating the bioaccumulation potential of chemicals (Aly and Schröder, 2007; Armitage and Gobas, 2007). Some terrestrial vertebrate species like birds and small mammals are common predators of earthworm, therefore earthworm is important to the biomagnification of soil contamination. US Environmental Protection Agency (EPA), Ministry of Agriculture of China and Organization for Economic Cooperation and Development (OECD) had used earthworm (*Eisenia fetida*) as a model organism for assessing the potential biological effect of the chemicals released into the environment. In order to evaluate the impacts of pollutants on earthworms, mortality is most frequently checked. Furthermore, growth and reproductive parameters are also often invested.

Fenoxaprop-ethyl (FE, Fig. 1), (±)-ethyl 2-[4-[(6-chloro-2-benzoxazolyl)oxy]phenoxy]propanoate, as a kind of aryloxyphenoxypropionate herbicides, can inhibit acetyl-CoA carboxylase in

* Corresponding author at: Department of Applied Chemistry, China Agricultural University, No.2 Yuanmingyuan West Road, Beijing 100193, PR China.
E-mail address: wangpeng@cau.edu.cn (P. Wang).

http://dx.doi.org/10.1016/j.ecolind.2016.12.006
1470-160X/© 2016 Elsevier Ltd. All rights reserved.

COR-AAD1-00003720
Bayer EX1008 (Part 7 of 9)

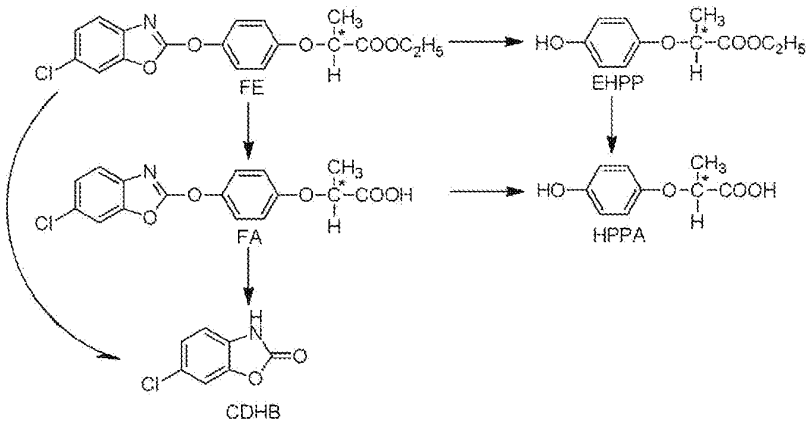


Fig. 1. Chemical structures of FE and its metabolites. Asterisk (*) denotes chiral center.

grasses (Pornprom et al., 2006). It has been widely used in many counties with annual sales of more than 200 million US dollars. With respect to its environmental fate, the primary degradation pathway of FE was hydrolysis and the main degradation product was fenoxaprop (FA, Fig. 1), which also has herbicidal activity as much as one hundred times more effective than fenoxaprop-ethyl in inhibiting grass chloroplasts ACCase (Liu et al., 2007). The metabolite FA can also inhibit seed germination of various grass weeds (Hoagland and Zablotowicz, 1998). Broad leaf herbicides such as 2,4-dicholrophenoxyacetic acid and 2-methyl-4-chlorophenoxy acetic acid can be mixed with FA to better ensure the safety of crops (Singh et al., 2013). It has been reported that FA was generated in microorganisms, soil, rice, wheat, barley, crabgrass, soybean, and so on (Chen et al., 2011; Hoagland and Zablotowicz, 1998; Lucini and Pietro Molinari, 2010; Tal et al., 1993). Forty days after field application, FA was still detectable in soil. Although the degradation of FE in soils, plants and animals has been reported (Chen et al., 2011; Lucini and Pietro Molinari, 2010), a little attention has been devoted to their enantioselective degradation. Enantioselective behavior of FE and FA in soils and rabbits has been studied with S-form being degraded faster than R-form (Zhang et al., 2011; Zhang et al., 2010). Stereoselective environmental behavior of FE and its chiral metabolites deserves enough attentions.

Because of the fast dissipation of FE (Chen et al., 2011; Zhang et al., 2011; Zhang et al., 2010), metabolites are important to consider as well during the process of environmental risk assessment. At present, studies on the metabolites of FE mainly focus on chiral FA and achiral 6-chloro-2,3-dihydrobenzoxazol-2-one (CDHB, Fig. 1), whereas information regarding chiral ethyl-2-(4-hydroxyphenoxy)propanoate (EHPP, Fig. 1) and 2-(4-hydroxyphenoxy)propanoic acid (HPPA, Fig. 1) is relatively much less (Chen et al., 2011; Lucini and Pietro Molinari, 2010; Zhang et al., 2010). It is worth noticing that very little information about enantioselective toxicity of FE and its three chiral metabolites has been known (Zhang et al., 2008). FE is one of the most commonly used post-emergence herbicides and large amounts of FE residues in soil, resulting in potential damage to the soil ecosystem such as the non-target organism earthworm. To our knowledge, it has not been reported that the enantioselective toxicity and degradation of FE and its metabolites in the ecological indicator earthworm. In recent years, the enantioselective fate and toxicity of chiral pesticides in earthworm has been studied to develop optically pure pesticides with high efficiency and low toxicity (Katagi and Ose, 2015), such as insecticides (fipronil, alpha-hexachlorocyclohexane, alpha-cypermethrin, fenvalerate, bifenthrin, lambad-cyhalothrin, methamidophos and cycloxaprid), fungicides (metalaxyl, benalaxyl, furalaxyl, diniconazole, tebuconazole, myclobutanil, hexaconazole, epoxiconazole and tetraconazole) and herbicides (metolachlor and quizalofop-ethyl). Results indicated that chiral pesticide such as fungicide R-metalaxyl not only was more active than the S-metalaxyl but also exhibited lower toxicity and bioaccumulation to earthworm. To evaluate the impacts of chiral pesticides on soil animals, enantioselectivity and metabolites should be considered for accurate environmental risk assessment.

FA is a primary metabolite of FE, CDHB, EHPP and HPPA are also reported metabolites of FE, in which FA, EHPP and HPPA are chiral. In the study, the earthworm was exposed to FE under laboratory condition in natural soil to invest the degradation in earthworm. FE and its four metabolites were measured and the stereoselective behavior of FE and FA was also determined. Enantiomer-specific acute toxicity of FE and its metabolites were measured by the filter paper contact assay.

2. Materials and methods

2.1. Chemicals and materials

Racemic FE (>98.0% purity) was obtained from Institute for Control of Agrichemicals, China Ministry of Agriculture (Beijing, China). Racemic FA, EHPP and HPPA, the two enantiomers of FE, FA, EHPP and HPPA (>98.0% purity) were synthesized according to the reported methods (Anabilino et al., 1998; Kato et al., 2004; Moon et al., 2007). CDHB (>98.0% purity) was obtained from TCI Development Company Limited (Shanghai, China). Standard solutions were prepared in acetone at 1000 μg mL^{-1} and kept in darkness at 4 °C. Water was purified by a Milli-Q system. Methanol (HPLC grade) was bought from Fisher Scientific (Fair Lawn, NJ, USA). All other chemicals and solvents were bought from Beijing Chemical Reagent Company Limited (Beijing, China) and were of analytical grade.

Mature earthworms (*Eisenia fetida*) were obtained from a farm on the outskirts of Beijing and 7-days preculture was conducted to make earthworms to adapt to the experimental conditions. The earthworms were healthy and active before introduced to the experiment. The weights of earthworms were 0.35 ± 0.03 g and the lengths were 5.0 ± 0.5 cm.

The soil was sampled at Baiwang Mountain Forest Park (Beijing, China). The soil was sieved, air-dried at room temperature. The soil composed by clay, 3.4%; silt, 36.2%; sand, 60.4%; organic matter, 4.7%, and the pH value was 7.6. FE and its metabolites were not detected in earthworm or soil.

COR-AAD1-00003721
Bayer EX1008 (Part 7 of 9)

2.2. Acute toxicity test

Based on OECD guideline 207, the acute toxicity in earthworm was investigated by a paper contact toxicity assay. FE and metabolites acetone solution was prepared. Based on a pre-test with five concentrations (0.1, 1, 10, 100, 1000 $\mu g\,cm^{-2}$), the highest dose tested was 2000 $\mu g\,cm^{-2}$ (Table 1). FE and metabolites acetone solution (1 mL) was transferred evenly on the filter paper. After the solution has evaporated, deionized water (1 mL) and earthworm were transferred to the beaker. Each beaker with one earthworm was sealed with plastic film with holes to allow ventilation and oxygen supply, and placed in darkness at 20 °C. Each concentration had ten beakers and the 48 h mortalities (the number of earthworms which do not respond to mechanical stimulus) were recorded.

2.3. Enantioselective degradation

Based on OECD guideline 317, the degradation in earthworm was investigated in the natural soil. An aliquot of 250 g of soil in a 500-mL beaker was spiked with 1 mL of rac-FE (250 $mg\,L^{-1}$). The soil moisture content was adjusted to 30% by adding the deionized water. Earthworms (10 g) after colon cleansing were added to the beaker. The beakers with soil and earthworm were incubated under 20 °C. The deionized water was used to remedy the water evaporation daily.

In the first stage of degradation, soil and earthworms were collected at exposure times of 1, 3, 5, 7, 10, 14 and 17 days and frozen at −20 °C. In the second stage of degradation, earthworms in contaminated soil were shifted to uncontaminated soil after 17 days to investigate the elimination. During the period, worms were recollected at day 0.25, 0.5, 1, 1.5, 2, 3, 5, 7, 10 and 14 and frozen at −20 °C. Each sample point had three repetitions.

2.4. Chemical analysis

HPLC–MS/MS (Thermo Scientific, TSQ Quantum Access Max) equipped with chiralpak IC (250 × 4.6 mm, Daicel Chemical Industries) chiral column was used for enantiomeric analysis of FE enantiomers, FA enantiomers and metabolites EHPP, HPPA and CDHB in soil and earthworm. The mobile phase was methanol + water + formic acid (75 + 25 + 0.1 by volume) with the flow rate of 0.5 $mL\,min^{-1}$ at 20 °C. These compounds were eluted in the order (Fig. 2): HPPA (6.5 min), EHPP (8.4 min), CDHB (11.4 min), R-FA (16.8 min), S-FA (18.3 min), R-FE (77.3 min) and S-FE (85.3 min). Although EHPP and HPPA were chiral, the concentrations of them were below limits of detection (LODs) in the study, thus the quantitative analysis of the single enantiomers was not performed. The HPLC–MS/MS fragmentation information of FE, FA, EHPP, HPPA and CDHB was 362.1/288.1 and 362.1/244.0, 332.0/260.0 and 332.0/152.0, 211.1/137.1 and 211.1/81.2, 181.0/109.1 and 181.0/108.1, 168.0/132.1 and 168.0/76.2, respectively.

For the extraction of soil, 10 g was transferred to a 50-mL polypropylene centrifuge tube, and then ethyl acetate (20 mL) and 1.0 $mmol\,mL^{-1}$ hydrochloric acid (0.1 mL) were added. The tube was vortexed for 5 min, ultrasonically extracted for 30 min, and centrifuged at 3500 rpm for 3 min. The extraction process was repeated and combined solvent was dehydrated by anhydrous sodium sulfate (5 g), evaporated by a rotary evaporator and dissolved in methanol (0.5 mL). For the extraction of earthworm, earthworms (0.5 g) were transferred into a 3-mL plastic centrifuge tube and homogenized by Mixer Mill MM400 (Retsch, Haan, Germany) with oscillation frequency of 30 r/sec for 180 s. After adding ethyl acetate (1 mL), earthworms were extracted by the mixer mill with the same frequency and time, and centrifuged at 10000 rpm for 3 min. The extraction process was repeated three times. The combined solvent was concentrated to dryness under nitrogen and then dissolved in methanol (0.5 mL) for analysis. The methanol solution was passed through a 0.22 μm filter film.

A series of blank soil and earthworms fortified with rac-FE, rac-FA, CDHB, rac-EHPP and rac-HPPA were determined. Recoveries of rac-FE (0.01–0.5 $\mu g\,g^{-1}$ in soil and earthworms), rac-FA (0.04–1.2 $\mu g\,g^{-1}$ in soil; 0.02–1.8 $\mu g\,g^{-1}$ in earthworms), CDHB (0.01–0.5 $\mu g\,g^{-1}$ in soil; 0.03–0.5 $\mu g\,g^{-1}$ in earthworms), rac-EHPP (0.02–1 $\mu g\,g^{-1}$ in soil; 0.2–1 $\mu g\,g^{-1}$ in earthworms) and rac-HPPA (0.02–1 $\mu g\,g^{-1}$ in soil and 0.2–1 $\mu g\,g^{-1}$ in earthworms) ranged between 83 and 114% based on an RSD of 4–19%. The limits of detection (LODs) of rac-FE, rac-FA, CDHB, rac-EHPP and rac-HPPA, the concentration produced a signal-to-noise ratio of 3, were 0.0002, 0.0004, 0.0013, 0.0045 and 0.0033 $\mu g\,g^{-1}$ in soil and 0.0009, 0.0033, 0.0080, 0.0254 and 0.0363 $\mu g\,g^{-1}$ in earthworms, respectively.

3. Results and discussion

3.1. Acute toxicity test

The toxic effects of the individual enantiomers and racemates of FE and the metabolites to earthworm (*Eisenia fetida*) were studied by the filter paper contact test. The calculated LC_{50} values at 48 h with their confidence intervals were shown in Table 1 together with the Pearson's correlation coefficient values (R^2). Based on the LC_{50} values, chemicals could be classified as very toxic (10–100 $\mu g\ cm^{-2}$), moderately toxic (100–1000 $\mu g\,cm^{-2}$) and relatively nontoxic (>1000 $\mu g\,cm^{-2}$) (Roberts and Dorough, 1984). The mortality in the negative controls never exceeded 10% at the end of each test showing the earthworms were active. In general, based on the LC_{50} values, the sequence of the toxicity was CDHB > FA > EHPP > HPPA > FE. The toxicity of the four possible metabolites was all higher than that of FE. Besides, EHPP and HPPA caused behavioural and pathological symptoms of earthworms within minutes, such as twists and exudation of yellow coelomic fluid. Because acute toxicity actually dramatically increased with the cleavage of ester or ether bond, it is difficult to neglect the negative effect of FE to earthworm despite FE has the low toxicity. Furthermore, the most hazardous product CDHB demonstrated high detection rate in the process of FE degradation in literatures (Lu et al., 2007; Zhang et al., 2010). Taking into account the three chiral metabolites, the acute toxicity of racemate and single enantiomers were slightly enantioselective, with R-form more toxic to earthworm than S-form and rac-form. For instance, the LC_{50} values of R-FA, S-FA and rac-FA for earthworm were 265, 469 and 412 $\mu g\ cm^{-2}$, respectively. Previous study showed the degradation of rac-FA in three soils was enantioselective with relative enrichment of R-FA (Zhang et al., 2010). Thus, the abundance of higher toxic R-FA should be regarded. Based on the enantioselective toxicity data, it is necessary to estimate ecological risk on an enantiomeric level.

3.2. Enantioselective degradation

FE rapidly decreased in the soil, while the main metabolite FA and the most hazardous metabolite CDHB were detected (Fig. 3A). The fast hydrolysis of FE in soil was consistent with literatures. The half-lives of FE in different soils were less than 3 days (Chen et al., 2011; Singh et al., 2013; Wink and Luley, 1988). Factors such as microorganisms, water contents and nature components in soil affected the degradation of FE (Jing et al., 2016; Pusino et al., 1996). Although EHPP and HPPA were measured, the concentrations of them were below LODs in soil. Because CDHB, EHPP and EPPA were generated with the cleavage of the ether linkage, so the low level of them indicated that FE was less likely to be degraded by cleavage of ether bond in soil. Microbial species and nutritional

COR-AAD1-00003722
Bayer EX1008 (Part 7 of 9)

Table 1
Acute toxicity of the enantiomers of FE and its metabolites to earthworm.

Chemical		Concentrations tested ($\mu g\,cm^{-2}$)	LC_{50} (95% CI) ($\mu g\,cm^{-2}$)	R^2	P	Classification
FE	rac-form	0,2000	>2000	--	--	relatively nontoxic
	R-form	0,2000	>2000	--	--	relatively nontoxic
	S-form	0,2000	>2000	--	--	relatively nontoxic
HPPA	rac-form	0,800,1000,1200,1400,1600,1800,2000	1961(1718–2717)	0.972	0.001	relatively nontoxic
	R-form	0,800,1000,1200,1400,1600,1800,2000	1659(1561 –1761)	0.850	0.003	relatively nontoxic
	S-form	0,800,1000,1200,1400,1600,1800,2000	1700 (1614–1799)	0.807	0.006	relatively nontoxic
EHPP	rac-form	0,400,800,900,1000,1200,1500,2000	1123(748–1577)	0.787	0.008	relatively nontoxic
	R-form	0,400,800,900,1000,1200,1500,2000	959(795–1101)	0.795	0.007	moderately toxic
	S-form	0,400,800,900,1000,1200,1500,2000	1175(1052–1341)	0.925	0.001	relatively nontoxic
FA	rac-form	0,50,100,200,300,400,500,1000	412(309–557)	0.848	0.003	moderately toxic
	R-form	0,50,100,200,300,400,500,1000	265(213–318)	0.954	0.001	moderately toxic
	S-form	0,50,100,200,300,400,500,1000	469 (345–654)	0.806	0.006	moderately toxic
CDHB	--	0,1,5,10,20,30,40,50	32 (27–39)	0.946	0.001	very toxic

Note: The results were expressed as medium lethal concentration (LC_{50}) values with 95% confidence interval, CI (in parentheses). All derived toxicity values were significant ($P < 0.01$).

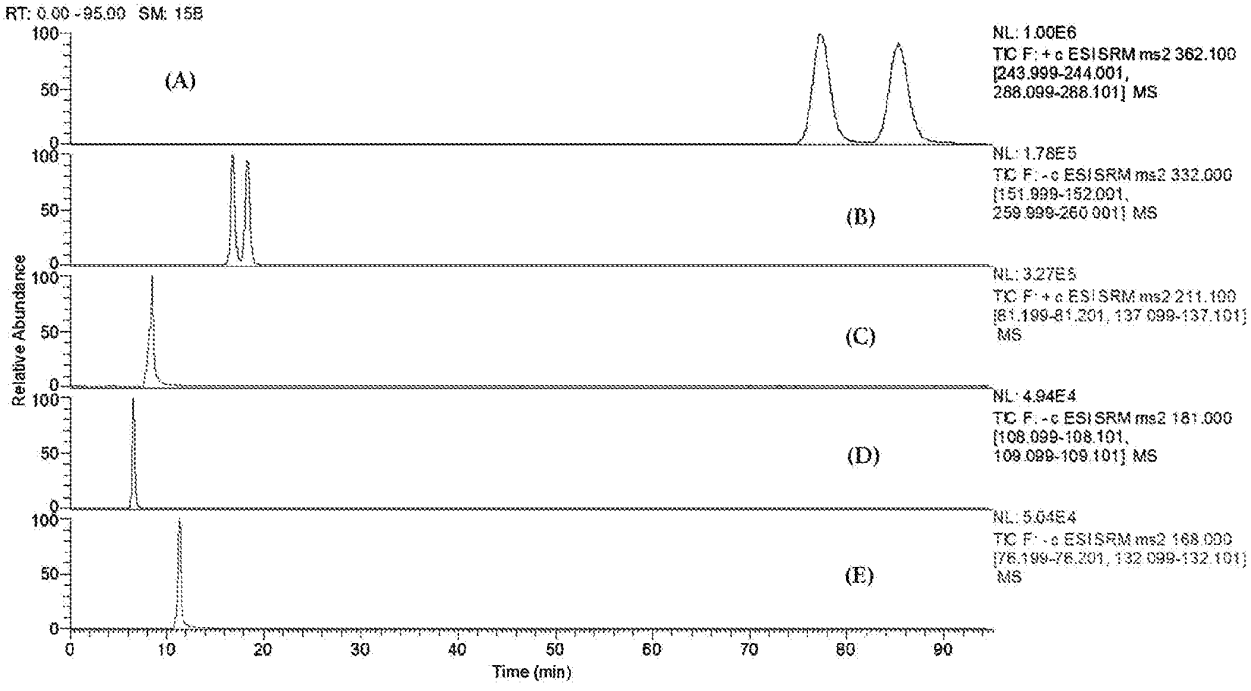


Fig. 2. HPLC/MS–MS chromatograms of FE and its four metabolites. (A) FE; (B) FA; (C) EHPP; (D) HPPA; (E) CDHB.

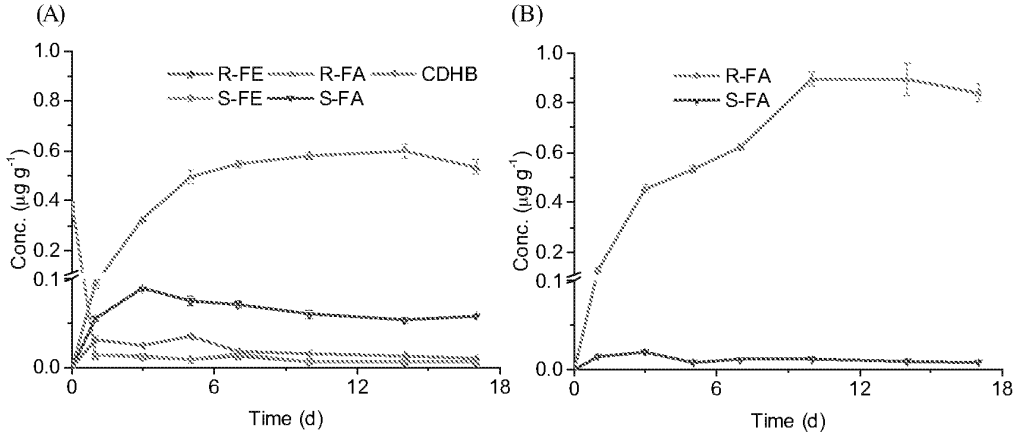


Fig. 3. Concentration-time curves of FE, FA and CDHB in (A) soil and (B) earthworm during the first degradation stage.

COR-AAD1-00003723
Bayer EX1008 (Part 7 of 9)

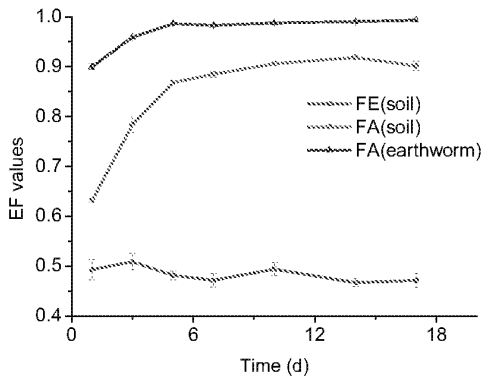


Fig. 4. EF values–time curves of FE in soil, FA in soil and FA in earthworm during the first degradation stage.

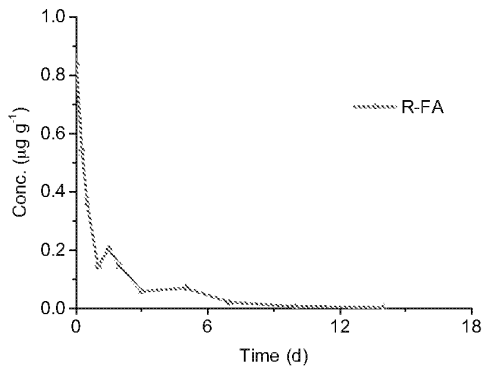


Fig. 5. Concentration-time curves of R-FA in earthworm during the second degradation stage.

status play an important role in ether bond cleavage (Hoagland and Zablotowicz, 1998). In addition to the rapid hydrolysis of FE, soil pH may also suppress the cleavage of ether band. According to the literature, metabolites generated with the cleavage of the ether linkage increased with the increasing acidity (Lin et al., 2007), however the soil pH was weakly alkaline in the study. EHPP and HPPA may be detectable in other soils and pose a potential risk (Toole and Crosby, 1986). The main product FA remained steady at a high level at day 5, which did not change very much until day 17 (Fig. 3A). The EF values of FE and FA were calculated to investigate the enantioselectivity in soil (Fig. 4). The EF values of FE remained around 0.5. R-FA was preferentially formed (Fig. 3A) and the EF values increased from the initial 0.63–0.91 at 10 d, and then remained unchanged. Therefore, the degradation of FE enantiomers was not enantioselective, while the formation of FA enantiomers in the soil was found to be significantly enantioselective. It has been reported that S-FA may convert into R-FA in different soils while FE was configurationally stable (Zhang et al., 2010). The enantioselectivity of FA was probably from the inversion of S-FA to R-FA during the incubation.

In earthworms, in the first stage of degradation (the first 17 days), the concentrations of FE, CDHB, EHPP and HPPA were all below LODs except FA. Although there were FE and CDHB in the soil, the content was low and they may further degrade in earthworms. Only FA was detected and the concentration increased to a maximum level of 0.90 $\mu g\,g^{-1}$ at day 10 in earthworms (Fig. 3B). Earthworms may uptake organic chemicals from skin and gut exposure route. For the chemical compounds with log *Kow* < 5, the major exposure route was skin. The importance of gut exposure route increases with hydrophobicity, and very hydrophobic chemicals (log *Kow* > 6) were absorbed mainly from the gut exposure route (Jager et al., 2003; Xu et al., 2014). Pesticide Properties Data Base (PPDB, 2016) displayed log K_{OW} of FA was 1.04, indicating FA was absorbed mainly through the skin. The bio-concentration factors (BCFs, calculated as the ratio of the concentration ($\mu g\,g^{-1}$) of chemical in the earthworm to the concentration ($\mu g\,g^{-1}$) in the surrounding soil at equilibrium) of R-FA and S-FA were 1.39 and 0.17, respectively. The significant difference of BCFs between the enantiomers revealed that the R-enantiomer was preferentially accumulated over the S-enantiomer in earthworm tissues. Because the concentration of R-FA in soil and the BCF of R-FA were higher than them of S-FA, bioaccumulation of FA in earthworms was enantioselective with almost exclusive accumulation of R-form and the EF values were about 0.99 (Fig. 3B and Fig. 4). According to the previously published results, the bioaccumulation of chiral pesticides in earthworms was not enantioselective with the EF values of 0.5 (Qu et al., 2014; Xu et al., 2014), or just weakly enantioselective with the EF values between 0.37 and 0.61 (Diao et al., 2011; Wang et al., 2014; Xu et al., 2009; Zhou et al., 2012).

In the second degradation stage, R-FA in the earthworms followed first-order kinetics (equation: $C = 0.3878\,e^{-0.403\,t}$, $R^2 = 0.9335$) and the degradation curve was shown in Fig. 5. The half-life of R-FA in the earthworms was 1.82 days. Because of almost exclusive accumulation of R-form in earthworms in the first degradation stage, the concentration of S-FA in earthworms was below LOD in the second degradation stage. Above all, such as the higher toxicity and bio-enrichment ability of R-FA, the data associated with the enantioselective toxicity and degradation of chiral pesticides is beneficial to understand more fully the security of pesticides.

4. Conclusion

In the study, enantioselective acute toxicity of fenoxaprop-ethyl and its metabolites was assayed by filter paper contact test. Compared with the parent compound, the four metabolites were more toxic. Acute toxicity were in the order of 6-chloro-2,3-dihydrobenzoxazol-2-one > fenoxaprop > ethyl-2-(4-hydroxyphenoxy)propanoate >2-(4-hydroxyphenoxy)propanoic acid > fenoxaprop-ethyl. The different acute toxicity of enantiomers of fenoxaprop-ethyl and chiral metabolites existed because earthworm was more sensitive to the R-enantiomer than the S-enantiomer. The degradation of fenoxaprop-ethyl in earthworm was determined by HPLC–MS/MS equipped with chiralpak IC chiral column. Fenoxaprop-ethyl decreased rapidly in soil with earthworms and it was hardly accumulated in earthworm. R-fenoxaprop enantioselectively remained in earthworms with the enantiomer fraction values about 0.99. The degradation of fenoxaprop in earthworm followed first-order kinetics with half-life of 1.82 days. The very toxic metabolite 6-chloro-2,3-dihydrobenzoxazol-2-one, relatively nontoxic metabolites ethyl-2-(4-hydroxyphenoxy)propanoate and 2-(4-hydroxyphenoxy)propanoic acid were not detected in earthworms, it may be due to a low tendency to cleave ether linkage under weakly alkaline soil. Further researches should be conducted to fully evaluate the mechanism of the degradation of these metabolites in ecological indicator earthworm. It is suggested to use optically pure pesticide fenoxaprop-P-ethyl (the active R-enantiomer) instead of fenoxaprop-ethyl (racemate) thus reducing residues in soil and toxicity to earthworms.

Acknowledgement

This work was supported by the National Natural Science Foundation of China (Contract Grants: 21337005, 21277171), supported

COR-AAD1-00003724
Bayer EX1008 (Part 7 of 9)

by Program for Changjiang Scholars and Innovative Research Team in University, supported by the New-Star of Science and Technology and by Beijing Nova program YETP0323, supported by Chinese Universities Scientific Fund 2015LX005, supported by Beijing Advanced Innovation Center for Food Nutrition and Human Health.

References

Šmídová, K., Hofman, J., 2014. Uptake kinetics of five hydrophobic organic pollutants in the earthworm Eisenia fetida in six different soils. J. Hazard. Mater. 267, 175–182.

Aly, M.A.S., Schröder, P., 2007. Effect of herbicides on glutathione S-transferases in the earthworm, Eisenia fetida. Environ. Sci. Pollut. Res. 15, 143–148.

Amabilino, D.B., Ramos, E., Serrano, J.-L., Sierra, T., Veciana, J., 1998. Long-range chiral induction in chemical system: with helical organization, promerogenic monomers in the formation of poly(isocyanide)s and in the organization of liquid crystals. J. Am. Chem. Soc. 120, 9126–9134.

Armitage, J.M., Gobas, F.A.P.C., 2007. A terrestrial food-chain bioaccumulation model for POPs. Environ. Sci. Technol. 41, 4019–4025.

Cai, X., Liu, W., Sheng, G., 2008. Enantioselective degradation and ecotoxicity of the chiral herbicide diclofop in three freshwater alga cultures. J. Agric. Food Chem. 56, 2139–2146.

Chen, X., Yu, S., Han, L., Sun, S., Zhi, Y., Li, W., 2011. Residues and dissipation of the herbicide fenoxaprop-P-ethyl and its metabolite in wheat and soil. Bull. Environ. Contam. Toxicol. 87, 50–53.

Diao, J., Xu, P., Liu, D., Lu, Y., Zhou, Z., 2011. Enantiomer-specific toxicity and bioaccumulation of alpha-cypermethrin to earthworm Eisenia fetida. J. Hazard. Mater. 192, 1072–1078.

Hoagland, R.E., Zablotowicz, R.M., 1998. Biotransformation of fenoxaprop-ethyl by fluorescent pseudomonas strains. J. Agric. Food Chem. 46, 4759–4765.

Jager, T., Fleuren, R.H.L.J., Hogendoorn, E.A., de Korte, G., 2003. Elucidating the routes of exposure for organic chemicals in the earthworm, eisenia andrei (Oligochaeta). Environ. Sci. Technol. 37, 3399–3404.

Jager, T., van der Wal, L., Fleuren, R.H.L.J., Barendregt, A., Hermens, J.L.M., 2005. Bioaccumulation of organic chemicals in contaminated soils: evaluation of bioassays with earthworms. Environ. Sci. Technol. 39, 293–298.

Jing, X., Yao, G., Liu, D., Liu, M., Wang, P., Zhou, Z., 2016. Environmental fate of chiral herbicide fenoxaprop-ethyl in water-sediment microcosms. Sci. Rep. 6, 26797.

Katagi, T., Ose, K., 2015. Toxicity, bioaccumulation and metabolism of pesticides in the earthworm. J. Pestic. Sci. 40, 69–81.

Kato, D.-i., Mitsuda, S., Ohta, H., 2004. Microbial deracemization of α-Substituted carboxylic acids: substrate specificity and mechanistic investigation. Chemistry 35, no-no.

Lavelle, P., Bignell, D., Lepage, M., Wolters, V., Roger, P., Ineson, P., Heal, O.W., Dhillion, S., 1997. Soil function in a changing world: the role of invertebrate ecosystem engineers. Eur. J. Soil Biol. 33, 159–193.

Lin, J., Chen, J., Cai, X., Qiao, X., Huang, L., Wang, D., Wang, Z., 2007. Evolution of toxicity upon hydrolysis of fenoxaprop-p-ethyl. J. Agric. Food Chem. 55, 7626–7629.

Liu, Y., Zhao, E., Zhu, W., Gao, H., Zhou, Z., 2009. Determination of four heterocyclic insecticides by ionic liquid dispersive liquid–liquid microextraction in water samples. J. Chromatogr. A 1216, 885–891.

Lucini, L., Pietro Molinari, G., 2010. Residues of the herbicide fenoxaprop-P-ethyl, its agronomic safener isoxadifen-ethyl and their metabolites in rice after field application. Pest Manag. Sci. 66, 621–626.

Moon, J.-K., Keum, Y.-S., Hwang, E.-C., Park, B.-S., Chang, H.-R., Li, Q.X., Kim, J.-H., 2007. Hapten syntheses and antibody generation for a new herbicide, metamifop. J. Agric. Food Chem. 55, 3416–3422.

PPDB, 2016. Agriculture and Environment Research Unit (AERU). http://sitem.herts.ac.uk/aeru/iupac/Reports/1066.htm.

Pornprom, T., Mahatamnuchoke, P., Usui, K., 2006. The role of altered acetyl-CoA carboxylase in conferring resistance to fenoxaprop-P-ethyl in Chinese sprangletop (Leptochloa chinensis (L.) Nees). Pest Manag. Sci. 62, 1109–1115.

Pusino, A., Petretto, S., Gessa, C., 1996. Montmorillonite surface-catalyzed hydrolysis of fenoxaprop-ethyl. J. Agric. Food Chem. 44, 1150–1154.

Qu, H., Wang, P., Ma, R.-x., Qiu, X.-x., Xu, P., Zhou, Z.-q., Liu, D.-h., 2014. Enantioselective toxicity, bioaccumulation and degradation of the chiral insecticide fipronil in earthworms (Eisenia fetida). Sci. Total Environ. 485–486, 415–420.

Roberts, B.L., Dorough, H.W., 1984. Relative toxicities of chemicals to the earthworm Eisenia fetida. Environ. Toxicol. Chem. 3, 67–78.

Shan, J., Wang, T., Li, C., Klumpp, E., Ji, R., 2010. Bioaccumulation and bound-residue formation of a branched 4-Nonylphenol isomer in the geophagous earthworm metaphire guillelmi in a rice paddy soil. Environ. Sci Technol. 44, 4558–4563.

Singh, S.B., Das, T.K., Kulshrestha, G., 2013. Persistence of herbicide fenoxaprop ethyl and its acid metabolite in soil and wheat crop under indian tropical conditions. J. Environ. Sci. Health Part B 48, 324–330.

Tal, A., Romano, M.L., Stephenson, G.R., Schwan, A.L., Hall, J.C., 1993. Glutathione conjugation: a detoxification pathway for fenoxaprop-ethyl in barley, crabgrass, oat, and wheat. Pestic. Biochem. Physiol. 46, 190–199.

Toole, A.P., Crosby, D.G., 1989. Environmental persistence and fate of fenoxaprop-ethyl. Environ. Toxicol. Chem. 8, 1171–1176.

Wang, H., Chen, J., Guo, B.-Y., Li, J., 2014. Enantioselective bioaccumulation and metabolization of diniconazole in earthworms (Eiseniafetida) in an artificial soil. Ecotoxicol. Environ. Saf. 99, 98–104.

Wen, B., Zhang, H., Li, L., Hu, X., Liu, Y., Shan, X.-q., Zhang, S., 2015. Bioavailability of perfluorooctane sulfonate (PFOS) and perfluorooctanoic acid (PFOA) in biosolids-amended soils to earthworms (Eisenia fetida). Chemosphere 118, 361–366.

Wink, O., Luley, U., 1988. Enantioselective transformation of the herbicides diclofop-methyl and fenoxaprop-ethyl in soil. Pestic. Sci. 22, 31–40.

Xu, P., Liu, D., Diao, J., Lu, D., Zhou, Z., 2009. Enantioselective acute toxicity and bioaccumulation of benalaxyl in earthworm (Eisenia fetida). J. Agric. Food Chem. 57, 8545–8549.

Xu, P., Wang, Y., Zhang, Y., Li, J., Wang, H., 2014. Toxicity and bioaccumulation of ethofumesate enantiomers in earthworm Eisenia fetida. Chemosphere 112, 163–169.

Ying, Z., Ling, L., Kunde, L., Xinping, Z., Weiping, L., 2009. Enantiomer separation of triazole fungicides by high-performance liquid chromatography. Chirality 21, 421–427.

Zhang, A., Xu, C., Liu, W., 2008. Influence of humicity and dissipation of racemic fenoxaprop and its R-enantiomer in Scenedesmus obliquus suspension by cyclodextrins. J. Environ. Sci. Health Part B 43, 231–236.

Zhang, Y., Liu, D., Diao, J., He, Z., Zhou, Z., Wang, P., Li, X., 2010. Enantioselective environmental behavior of the chiral herbicide fenoxaprop-ethyl and its chiral metabolite fenoxaprop in soil. J. Agric. Food Chem. 58, 12878–12884.

Zhang, Y., Li, X., Shen, Z., Xu, X., Zhang, P., Wang, P., Zhou, Z., 2011. Stereoselective metabolism of fenoxaprop-ethyl and its chiral metabolite fenoxaprop in rabbits. Chirality 23, 897–903.

Zhang, W., Chen, L., Liu, K., Chen, L., Lin, K., Chen, Y., Yan, Z., 2014. Bioaccumulation of decabromodiphenyl ether (BDE209) in earthworms in the presence of lead (Pb). Chemosphere 106, 57–64.

Zhou, G., Liu, D., Ma, R., Li, J., Sun, M., Zhou, Z., Wang, P., 2012. Enantioselective kinetics of α-Hexachlorocyclohexane in earthworm (Eisenia fedtia) and forest soil. Chirality 24, 615–620.

COR-AAD1-00003725
Bayer EX1008 (Part 7 of 9)

World J Microbiol Biotechnol (2014) 30:2567–2576
DOI 10.1007/s11274-014-1680-6

ORIGINAL PAPER

16S rRNA gene phylogeny and *tfdA* gene analysis of 2,4-D-degrading bacteria isolated in China

Lizhen Han · Yanbo Liu · Aigong He · Degang Zhao

Received: 7 January 2014 / Accepted: 27 May 2014 / Published online: 5 June 2014
© Springer Science+Business Media Dordrecht 2014

Abstract Twenty-two 2,4-dichlorophenoxyacetic acid (2,4-D)-degrading bacterial isolates were collected from agricultural soils at three sites in China. Sequence analysis of the 16S rRNA genes indicated that the isolates were phylogenetically grouped into four categories: *Ochrobactrum anthropi*, in the *Alpha-* class of the phylum *Proteobacteria* (3 out of 22 isolates), *Cupriavidus* sp., of the *Betaproteobacteria* (3 out of 22), *Pseudomonas* sp. and *Stenotrophomonas* sp., which are *Gammaproteobacteria* (7 out of 22), and *Bacillus* sp., of the phylum *Firmicutes* (9 out of 22). Primers were designed to amplify the conserved domain of *tfdA*, which is known to be involved in the degradation of 2,4-D. Results showed that the *tfdA* genes of all 22 strains were most similar to that of *Cupriavidus necator* JMP134, which belongs to the 2,4-D/α-ketoglutarate dioxygenase TfdA protein family, indicating that the JMP134-type *tfdA* gene is likely to be almost universal among the 2,4-D-degrading bacteria isolated from China. Degradation abilities of these 22 strains were investigated in assays using 2,4-D as the sole source of carbon and energy. Thirteen strains degraded >60 % of the available 2,4-D (500 mg l^{-1}) over a 1-week incubation period, while a further nine *Bacillus* sp. strains degraded 50–81 % of the available 2,4-D. None of these nine strains degraded other selected herbicides, such as mecoprop, 2-methyl-4-chlorophenoxyacetic acid, quizalofop, and fluroxypyr. This is the first report of 2,4-D-degradation by *Bacilli*.

Keywords 2,4-D-degrading bacteria · 16S rRNA gene · *tfdA* gene · Degrading capacity

L. Han · Y. Liu · D. Zhao (✉)
Key Laboratory of Green Pesticide and Agricultural Bioengineering, Ministry of Education, Guizhou University, Guiyang 550025, Guizhou, China
e-mail: dgzhao@gzu.edu.cn

L. Han
e-mail: hanlizhen11@163.com

L. Han · D. Zhao
College of Life Science, Guizhou University, Guiyang 550025, Guizhou, China

Y. Liu · D. Zhao
Guizhou Key Laboratory of Agro-Bioengineering, Guizhou University, Guiyang 550025, Guizhou, China

A. He
College of Foreign Language, Guizhou University, Guiyang 550025, Guizhou, China

Introduction

The phenoxyalkanoic acid herbicide 2,4-dichlorophenoxyacetic acid (2,4-D) has been widely used over the past 60 years to control a broad range of leaf weeds in alfalfa, maize, peanut, soybean, and other crop fields and pastures. Despite recommended foliar application of 2,4-D, a significant amount of the herbicide reaches the ground and interacts with soil microbes. As a result, several 2,4-D-degrading bacterial strains have been isolated from a variety of environments, including agricultural soils, sediments, and waste treatment facilities (Ka et al. 1994; Laemmli et al. 2000; Vallaeys et al. 1998). These bacteria are categorized into three groups on an evolutionary and physiological basis (Itoh et al. 2002; McGowan et al. 1998). Group 1 consists of species belonging to the *Betaproteobacteria* and *Gammaproteobacteria*, and harbor *tfdA* genes homologous to that found in *Cupriavidus necator* JMP134 (formerly *Alcaligenes eutrophus*, *Wautersia eutropha*, or *Ralstonia eutropha*), a well-studied 2,4-D

COR-AAD1-00003726
Bayer EX1008 (Part 7 of 9)

degrader (Streber et al. 1987). Groups 2 and 3 consist of alphaproteobacterial *Bradyrhizobium*- and *Sphingomonas*-related organisms, respectively, and contain the *tfdA*-like gene *tfdAα* (Fulthorpe et al. 1995; Itoh et al. 2000; Kamagata et al. 1997). However, to date, only group 1 *tfdA* genes are associated with 2,4-D degradation in soil (Bælum et al. 2006, 2008; Bælum and Jacobsen 2009; Rodriguez-Cruz et al. 2010). *tfdA* encodes an Fe(II) and α-ketoglutarate (α-KG)-dependent 2,4-D dioxygenase protein, TfdA, which converts 2,4-D into 2,4-dichlorophenol and glyoxylate, while oxidizing α-KG to CO_2 and succinate as an initial step of 2,4-D mineralization (Fukumori and Hausinger 1993a, b; Vedler et al. 2000). TfdA belongs to the group II α-ketoglutarate-dependent dioxygenases, showing a clear homology to the *Escherichia coli* taurine/α-ketoglutarate dioxygenase TauD (Knauer et al. 2012). In group 2 and 3 microorganisms, *cadAB* was predicted to encode an alternative 2,4-D oxygenase, and *cadA* is essential for 2,4-D conversion in pure cultures of species belonging to the *Alphaproteobacteria* (Kitagawa et al. 2002; Itoh et al. 2004; Shimojo et al. 2009). On the basis of *tfdA* gene localization and sequence identity, group 1 bacteria are further categorized into three classes. The class I *tfdA* genes are usually located on broad host-range, self-transmissible plasmids, represented by pJP4 derived from *R. eutropha* JMP134 (Ka and Tiedje 1994; Top et al. 1995). The class II *tfdA* gene, which is only found in the chromosome of *Burkholderia* sp. strain RASC, is 76 % identical to the class I *tfdA* genes. The class III *tfdA* genes are 77 and 80 % identical to the class I and class II *tfdA* genes respectively, and were linked to degradation of 2-methyl-4-chlorophenoxyacetic acid (MCPA) (McGowan et al. 1998; Bælum et al. 2006, 2008).

Although 2,4-D has long been used as a herbicide in wheat and corn fields in China, only a few documented 2,4-D-degrading bacterial strains have been isolated. In this paper, we report the presence of JMP134-type *tfdA* genes in 22 2,4-D-degrading bacterial isolates from China. Most of the isolated strains had strong 2,4-D-degrading activity, and surprisingly, nine of the isolates were identified as *Bacillus* species. To the best of our knowledge, this is the first report of 2,4-D-degrading bacteria containing *tfdA* belonging to the phylum *Firmicutes*. Thus, our findings increase our knowledge of the diversity of 2,4-D-degrading bacterial strains, and may assist in the design of bioremediation strategies to clean up 2,4-D-polluted environments.

Materials and methods

Enrichment and isolation of 2,4-D-degrading bacteria

Soils were collected from three wheat fields located in Beijing (N 40°25′40″, E 116°82′79″), Henan Province (N 34°20′34″, E 114°15′07″), and Qinghai Province (N 36°92′15″, E 101°67′20″), China. All three wheat fields had been treated with 2,4-D for several years, and the soil samples were randomly collected from five sites in each field. The top 15 cm of soil was collected and passed through a 2-mm sieve, then stored at 4 °C until use. Enrichment cultures were initiated by mixing an appropriate amount of soil (10 %, w/v) into 100-ml minimal salts medium (MSM) (Smejkal et al. 2001a) containing 500 mg l^{-1} 2,4-D (Sigma-Aldrich, St. Louis, USA) (in 250 ml conical flasks). After shaking (150 rpm) at 30 °C for 7 days, 10 % volumes of the resulting cultures were inoculated into fresh MSM containing 2,4-D to form a new subculture. When four serial subcultures were completed, the final subcultures were spread onto MSM agar plates containing 500 mg l^{-1} 2,4-D. The plates were incubated at 30 °C for 4 days, and single colonies were isolated by repeated streaking on MSM agar containing 2,4-D. Isolates were stored in 15 % glycerol at −80 °C.

Amplification of 16S rRNA gene sequence

Total genomic DNA from each strain was extracted using an E.Z.N.A. Bacterial DNA Kit (Omega Bio-Tek, Norcross, USA) according to the manufacturer's instructions. 16S rRNA genes were amplified from the extracted genomic DNA using the universal primers 27f (5′-AGAGTTT GATCMTGGCTCAG-3′) and 1492r (5′-TACGGYTACC TTGTTACGACTT-3′). Standard PCR reaction mixtures contained 1× Premix *Taq* (Takara Bio, Tokyo, Japan), 0.4 μM of each primer, and ~50 ng of template DNA. The PCR amplification parameters were: 95 °C for 10 min; followed by 35 cycles of 95 °C for 45 s, 55 °C for 45 s, and 72 °C for 90 s. To ensure complete elongation, a final step of 72 °C for 7 min was performed. Reactions were performed in a BioRad MyCycler Thermocycler. The PCR products were sequenced by Takara Biotech Co., Ltd (Dalian, China).

Plasmid extraction and iCODEHOPs PCR

Plasmid DNA from each strain was extracted using an E.Z.N.A. Plasmid Mini Kit (Omega Bio-Tek, Norcross, USA). Primers were developed from highly conserved blocks of 42 multiply-aligned published TfdA sequences (Table 1) using iCODEHOPs (iCOnsensus-DEgenerate Hybrid Oligonucleotide Primers) designer software (https://icodehop.cphi.washington.edu/i-codehop-context/Welcome; Rose et al. 1998, 2003; Boyce et al. 2009). The 42 TfdA sequences were obtained from the GenBank (http://www.ncbi.nlm.nih.gov/genbank/) and were divided into eight groups based on their amino acid differences using Clustalw2 (http://www.ebi.ac.uk/Tools/msa/clustalw2/; Larkin

COR-AAD1-00003727
Bayer EX1008 (Part 7 of 9)

Table 1 Strains and GenBank accession numbers of TfdA proteins used for multiple alignments

Divided groups	Strain	GenBank accession number
I	*Ralstonia eutropha* JMP134	P100088
	Burkholderia sp. TFD19	ACF35489
	Cupriavidus necator	AAA21983
	Cupriavidus sp. TFD33	ACF35490
	Cupriavidus sp. TFD38	ACF35491
	Cupriavidus sp. TFD51	ACF35493
	Pseudomonas sp. TFD39	ACF35492
	Ralstonia eutropha JMP134	AAR31052
	Ralstonia eutropha JMP134	ACF35494
	Ralstonia eutropha JMP134	YP_025400
II	*Achromobacter xylosoxidans* TFD9	ACF35485
	Achromobacter xylosoxidans TFD47	ACF35486
	Burkholderia sp. TFD29	ACF35488
	Cupriavidus sp. TFD42	ACF35487
III	*Burkholderia cepacia* 2a	AAK81681
	Cupriavidus respiraculi TFD48	ACF35482
	Cupriavidus sp. TFD40	ACF35481
	Cupriavidus sp. TFD45	ACF35480
	Pseudomonas putida TFD49	ACF35483
	Pseudomonas sp. TFD50	ACF35484
	Variovorax soli TFD35	ACF35479
IV	*Burkholderia* sp. TFD2	ACF35467
	Burkholderia sp. TFD4	ACF35469
	Burkholderia sp. TFD6	ACF35466
	Burkholderia sp. TFD17	ACF35470
	Burkholderia sp. TFD20	ACF35471
	Burkholderia sp. TFD21	ACF35472
	Burkholderia sp. TFD23	ACF35473
	Burkholderia sp. TFD28	ACF35474
	Burkholderia sp. TFD31	ACF35475
	Burkholderia sp. TFD32	ACF35476
	Burkholderia sp. TFD34	ACF35477
	Burkholderia sp. TFD36	ACF35465
	Burkholderia sp. TFD52	ACF35478
	Burkholderia tropica	ACF35468
V	*Achromobacter denitrificans* EST4002	AAS49436
	Achromobacter denitrificans EST4002	NP_990895
VI	*Burkholderia* sp. RASC	Q45423
	Burkholderia sp. RASC	AAB17363
VII	*Delftia acidovorans* P4a	AAM76772
VIII	*Burkholderia cenocepacia* AU 1054	ABF81256
	Burkholderia cenocepacia HI2424	ABK13356

et al. 2007) from EMBL. The representative TfdA proteins from each of these groups were from *R. eutropha* JMP134 (GenBank accession number P10088), *Achromobacter xylosoxidans* TFD9 (ACF35485), *Burkholderia cepacia* 2a (AAK81681), *Burkholderia* sp. TFD2 (ACF35467), *Achromobacter denitrificans* EST4002 (AAS49436), *Burkholderia* sp. RASC (Q45423), *Delftia acidovorans* P4a (AAM76772), and *Burkholderia cenocepacia* AU 1054 (ABF81256). Two highly conserved amino acid sequence motifs, DTEFC and NRCV, were chosen as targets. The iCODEHOPs *tfdA* F (5′-CGACACCGAGTTCTGC gayatgmgngc-3′) and *tfdA* R (5′-CGCAGCGGTTGtcccan atnac-3′) primers were derived from these motifs. Approximately 10 μg of plasmid DNA was used as the template in 25-l PCR mixtures containing 1× Premix Ex *Taq* (Takara Bio, Tokyo, Japan) and 0.8 μM of each primer. PCR amplifications were performed using a touchdown protocol consisting of an initial denaturation (95 °C, 5 min), followed by 12 touchdown cycles with decreasing annealing temperatures (62–50 °C, 45 s), 25 cycles with a 50 °C annealing temperature, and a final 7 min extension at 72 °C. PCR amplification was carried out using a BioRad Thermocycler. The PCR products (~370 bp) from each selected strain were purified using an E.Z.N.A. Gel Extraction Kit (Omega Bio-Tek, Norcross, USA) and cloned into the pGEM-T Easy vector (Promega, Madison, USA).

Sequencing and phylogenetic analyses of the 16S rRNA and *tfdA* genes

DNA sequencing was carried out by Invitrogen Biotech Co. Ltd (Shanghai, China) and Takara Biotech Co., Ltd (Dalian, China). The identification of phylogenetic neighbors, based on the 16S rRNA gene sequences of the 2,4-D-degrading strains, was initially carried out using the BLASTN program against a database containing type strains with validly-published prokaryotic names, which was acquired from the EzTaxon-e server (http://eztaxon-e.ezbiocloud.net; Kim et al. 2012). *Methanosarcina lacustris*, an archaeon, was used as the outgroup. BLAST analysis (http://blast.ncbi.nlm.nih.gov/) was also used to conduct similarity searches of the *tfdA* partial gene sequences. Multiple sequence alignment of the *tfdA* sequences was performed using the Clustalw2. For phylogenetic analysis of *tfdA* genes, one reference sequence retrieved from GenBank was included for each of the *tfdA* classes and related *tfdA*-like genes. These reference sequences were: class I, *A. eutropha* JMP134 *tfdA* (GenBank accession number M16730); class II, *Burkholderia* sp. RASC *tfdA* (U25717); class III, *B. cepacia* 2a *tfdA* (AF029344); *tfdAα*, *Alphaproteobacterium* sp. HW13 *tfdAα* (AB074492). *E. coli* str. K-12 substr. MG1655 *tauD* (NC_000913), which also belongs to the group II α-ketoglutarate-dependent dioxygenases, was used as the outgroup. Phylogenetic trees were generated using the neighbor-joining method in

COR-AAD1-00003728
Bayer EX1008 (Part 7 of 9)

the MEGA 5.0 program (Tamura et al. 2011). A bootstrap analysis based on 1,000 replicates was employed to place confidence estimates on the tree.

Monitoring and analysis of growth and degradation capacity

Strains were inoculated into 150 ml of MSM supplemented with 500 mg l^{-1} 2,4-D. The cell concentration of the inoculum was adjusted to obtain an OD_{420} of 0.15 in a 250-ml Erlenmeyer flask. Flasks were incubated at 150 rpm in a rotary shaker. Experiments were independently performed in triplicate. Bacterial growth was quantified by measuring the sample absorbance at 420 nm (Smejkal et al. 2001b) in a Beckman DU640 spectrophotometer. The degradation of 2,4-D was determined by measuring the remaining 2,4-D in cultures using a Waters 600 high performance liquid chromatography (HPLC) system equipped with a C18 reverse-phase column, with methanol/H_3PO_4 (0.1 %) (60:40) as an eluent. A decrease in absorbance at A_{230} at an elution time of ~5.5 min indicated 2,4-D metabolism. Cultures were extracted according to the method of Suwa et al. (1996).

Detection of substrate degradation

Substrate degradation was examined as described previously by Smejkal et al. (2001b). Briefly, nine *Bacillus* sp. strains were precultured to an optical density of ≈0.6–1.0 (OD_{420}) and then serially diluted in 1/4 Ringers solution (Oxoid, Hampshire, England). The 10^{-5} dilution of each culture was plated onto modified Loos agar plates (Smejkal et al. 2003). The herbicides 2,4-D, MCPA, mecoprop, quizalofop, and fluroxypyr were added to the medium at concentrations of 3 mmol l^{-1} respectively, to be used as only carbon sources. Plates were set up in triplicate and incubated for 4 days at 25 °C.

Nucleotide sequence accession numbers

The sequences obtained in this study were deposited in the GenBank database under the following accession numbers: 16S rRNA gene sequences, accession numbers KC857468–KC857486, KF997830, KJ028758-KJ028759; *tfdA* partial sequences, accession numbers KC857488–KC857506, KJ028760–KJ028762.

Results

Isolation of 2,4-D-degrading bacteria

We selected 22 morphologically-distinct 2,4-D-degrading bacteria from the 2,4-D plates, with representatives from all three sites. These isolates were numbered with the prefixes BJ, HH, and QH to indicate the collection areas (Beijing, Henan, and Qinghai, respectively).

Phylogeny analysis based on 16S rRNA gene sequences

Total genomic DNA was isolated from all 2,4-D-degrading bacterial isolates and the 16S rRNA genes were amplified and sequenced. Analysis of the 1.5-kb sequences showed that the 22 isolates represented diverse phylogenetic divisions (Fig. 1). Among the collected isolates, 13 belonged to the classes *Alphaproteobacteria*, *Betaproteobacteria*, and *Gammaproteobacteria*. Two isolates were identified as *Pseudomonas* sp. and five were *Stenotrophomonas* species, all of which belong to the class *Gammaproteobacteria*. Three *Cupriavidus* species, of the class *Betaproteobacteria*, were also identified. The remaining three isolates were *Ochrobactrum anthropi*, which is an alphaproteobacterium. Surprisingly, nine isolates were identified as *Bacillus* sp., belonging to the class *Bacilli*. The genetic differences between these 22 morphologically-distinct isolates indicated that they were indeed separate strains.

Phylogenetic analysis based on *tfdA* gene sequences

The iCODEHOPs primer set was designed based on almost all of the available *tfdA*-like sequences in the GenBank database. PCR amplification of the plasmid DNA generated 365-bp fragments from the 22 bacterial strains using the iCODEHOPs *tfdA* primer set. Conserved domain searches indicated that all of the nucleotide sequences were most similar to genes coding for 2,4-D/α-ketoglutarate dioxygenase TfdA family proteins, which possess characteristic residues within the active site of the enzyme (data not shown). All sequences were compared to existing *tfdA* sequences in the GenBank database using FASTA and BLAST, and phylogenetic trees were constructed (Fig. 2). None of the sequences were an exact match to any previously reported *tfdA* sequences. However, the partial *tfdA* sequences obtained in the current study were determined to belong to the class I *tfdA* genes because of their greater similarity to JMP134-type *tfdA* sequences than to the other three *tfdA* subgroups. All *tfdA*-related sequences had very short branch lengths, indicating they are closely related.

The derived amino acid sequences of the 365-bp *tfdA* fragments from all 22 2,4-D-degrading strains were aligned with the TfdA sequence from *C. necator* JMP134. Differences were identified at 19 sites within the 121-aa sequences (Fig. 3).

Growth and degrading abilities of the isolates

The 22 strains were tested for their ability to grow on MSM containing 2,4-D as the only carbon and energy source. In

COR-AAD1-00003729
Bayer EX1008 (Part 7 of 9)

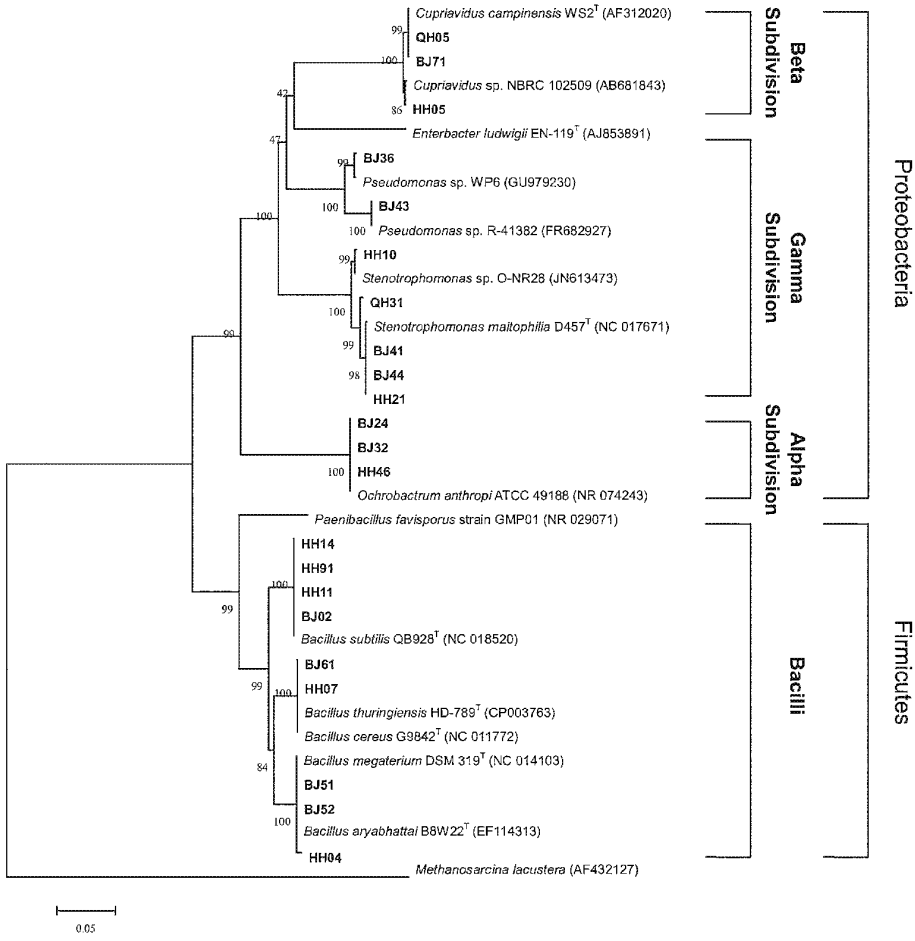


Fig. 1 Phylogenetic tree based on 16S rDNA sequences of 22 2,4-D-degrading bacterial strains isolated from China. GenBank accession numbers are in *parentheses*. The tree is based on 1.5-kb 16S rDNA sequences and was obtained using the neighbor-joining method. Bootstrap values are based on 1,000 resampled datasets. All major branches were conserved in the maximum-parsimony tree. *Methanosarcina lacustris* was used as the outgroup. *The scale bar* indicates the number of nucleotide changes per base position analyzed

all cases, the biomass and degradation percentages of the strains increased in proportion with incubation time. HPLC experiments showed that all strains degraded more than 37 % of the available 2,4-D (500 mg l^{-1}) during the 1-week incubation period at 30 °C. Among them, 13 strains degraded >60 % of the 2,4-D. There were statistically significant differences in amount of biomass and degradation percentages between strain BJ71 and the other strains, with *Cupriavidus campinensis* BJ71 demonstrating more rapid growth and degradation of 2,4-D than the other isolates (Fig. 4). We observed up to 75 % degradation of 2,4-D by this strain over the first 3 days of incubation, whereas 1–2-day lag phases were observed in the other strains (data not shown). Therefore, BJ71 is the most promising candidate for further studies on 2,4-D degradation.

The 2,4-D degradation kinetics of the nine *Bacillus* sp. strains were very similar. 2,4-D levels in the cultures decreased slowly following a lag period of 1 day, and degradation was <30 % over the first 3 days of incubation (Fig. 5). Modified Loos medium indicates microbial dehalogenation of the herbicide compounds, a process that usually follows cleavage of the aromatic ring (Smejkal et al. 2003). The nine *Bacillus* sp. strains were grown on modified Loos medium supplemented with each of the five selected herbicides and examined for their ability to degrade these compounds. After 4 days of incubation, dark violet colonies appeared on the Loos plates containing 2,4-D, indicating that dehalogenation (removal of chlorine atoms) had occurred. All strains showed degradation of 2,4-D, but no activity was found towards mecoprop, MCPA, quizalofop, or fluroxypyr.

Discussion

In the current study, a culture-dependent enrichment approach was used to isolate diverse 2,4-D-degrading bacteria from agricultural soils in China, with 22 indigenous bacterial strains isolated in total. These 2,4-D-degrading bacteria were shown to be phylogenetically distinct from all previously reported strains. A number of studies have reported that most 2,4-D-degrading bacteria

COR-AAD1-00003730
Bayer EX1008 (Part 7 of 9)

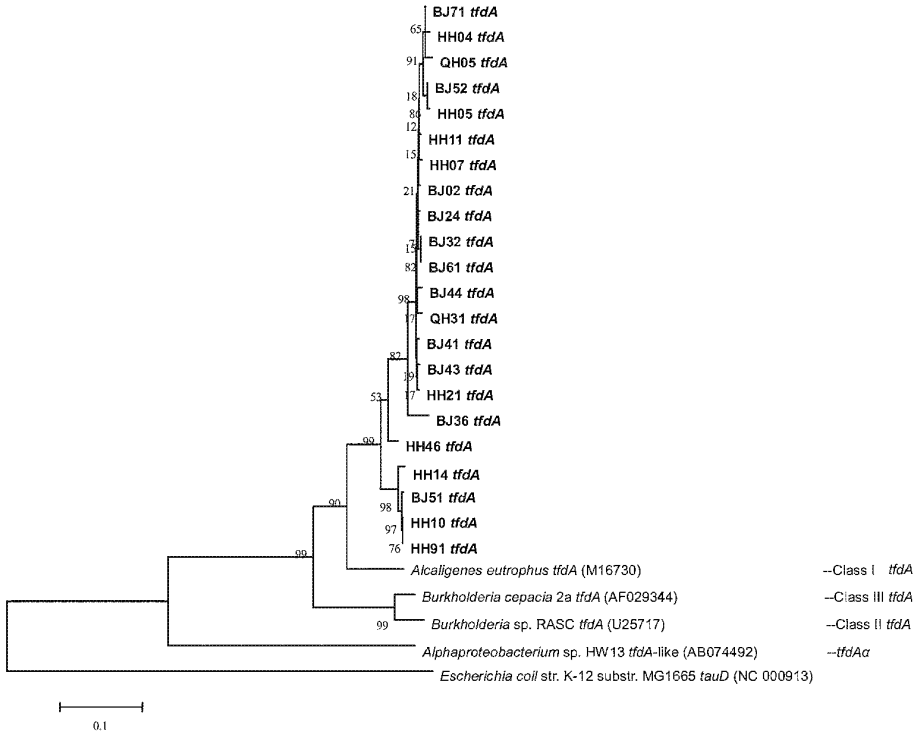


Fig. 2 Phylogenetic tree generated from *tfdA*-like partial gene sequences from 22 2,4-D-degrading bacterial strains isolated from China and reference *tfdA*-like sequences from *C. necator* JMP134 (GenBank accession number M16730), *Burkholderia* sp. RASC (GenBank accession number U25717), *Burkholderia cepacia* 2a (GenBank accession number AF029344), and *Alphaproteobacterium* sp. HW13 (GenBank accession number AB074492). *Escherichia coli* str. K-12 substr. MG1655 *tauD* (GenBank accession number NC_000913) was used as the outgroup. *Scale bar* represents a Jukes-Cantor distance of 0.1. The phylogenetic tree was constructed on the basis of common partial sequences using the neighbor-joining method

containing *tfdA* belong to genera such as *Achromobacter*, *Burkholderia*, *Delftia*, *Halomonas*, *Pseudomonas*, *Ralstonia*, *Rhodoferax*, and *Variovorax*. In contrast to the relatively common occurrence of *tfdA* amongst the *Betaproteobacteria* and *Gammaproteobacteria*, few 2,4-D-degraders belonging to the *Alphaproteobacteria* have been found to contain *tfdA*. It has been reported that 4-(2,4-dichlorophenoxy) butyric acid- and 4-(4-chloro-2-methylphenoxy) butyric acid-degrading bacteria belonging to the genera *Stenotrophomonas* and *Ochrobactrum* could use 2,4-D as a growth substrate, but repeated attempts to amplify putatively conserved *tfd* genes by PCR failed, indicating that *tfd* is not present in these species (Smejkal et al. 2003). However, three *Ochrobactrum* 2,4-D-degrading strains isolated from activated sludge do contain a JMP134 type-*tfdA* gene, but their degradation capacities have not been studied (Lee et al. 2005). We also isolated three strains identified as *O. anthropi* in the current study, further confirming that class I *tfdA* genes are present in *Alphaproteobacteria*. These strains degraded 46–69 % of the available 2,4-D (500 mg l^{-1}) during a 1-week incubation. The genus *Ochrobactrum* is gaining increasing attention in environmental microbiology because of the various xenobiotic-degrading organisms belonging to this group (Müller et al. 1998).

Previous research showed evidence for *tfdA*-like genes in 12 of 27 *Bacillus-Lactobacillus-Streptococcus* subdivision bacterial strains, but none of the isolates were able to degrade 2,4-D (Hogan et al. 1997). Interestingly, in the current study, nine *Bacillus* sp. strains harboring *tfdA* were able to degrade 50–81 % of the available 2,4-D (500 mg l^{-1}) over the 1-week incubation period, though they did not degrade the other selected herbicides. Therefore, we were able to confirm the presence of *tfdA* amongst the *Firmicutes* as well as the *Proteobacteria*. The degradation capacity of the nine *Bacillus* strains was much better than that of *Burkholderia cepacia* DS-1, *Pseudomonas* sp. DS-2, and *Sphingomonas paucimobilis* DS-3 (Cycon et al. 2011), but below that of *C. necator* JMP134, which has the maximum reported degradation rate of about 3 mg l^{-1} h^{-1} after 1 day of incubation (Lerch et al. 2007).

It has been reported that *Cupriavidus* sp. dominate the 2,4-D-degrading community in soil (Macur et al. 2007; Zabaloy and Gómez 2013). However, in the current study, only three *Cupriavidus* strains, BJ71, QH05, and HH05, were found to be effective 2,4-D degraders. With an ability to degrade more than 85 % of the total 2,4-D (500 mg l^{-1}) during the 7-day incubation period, these three strains were superior to the previously identified strain JMP134, which degraded 70 % of the available 2,4-D (250 mg l^{-1}) in the same time period (Lerch et al. 2007).

Several authors have studied *tfdA* sequence diversity using degenerate primers based on ~300 bp of the coding sequences (Gonod et al. 2006; Shaw and Burns 2004;

COR-AAD1-00003731
Bayer EX1008 (Part 7 of 9)

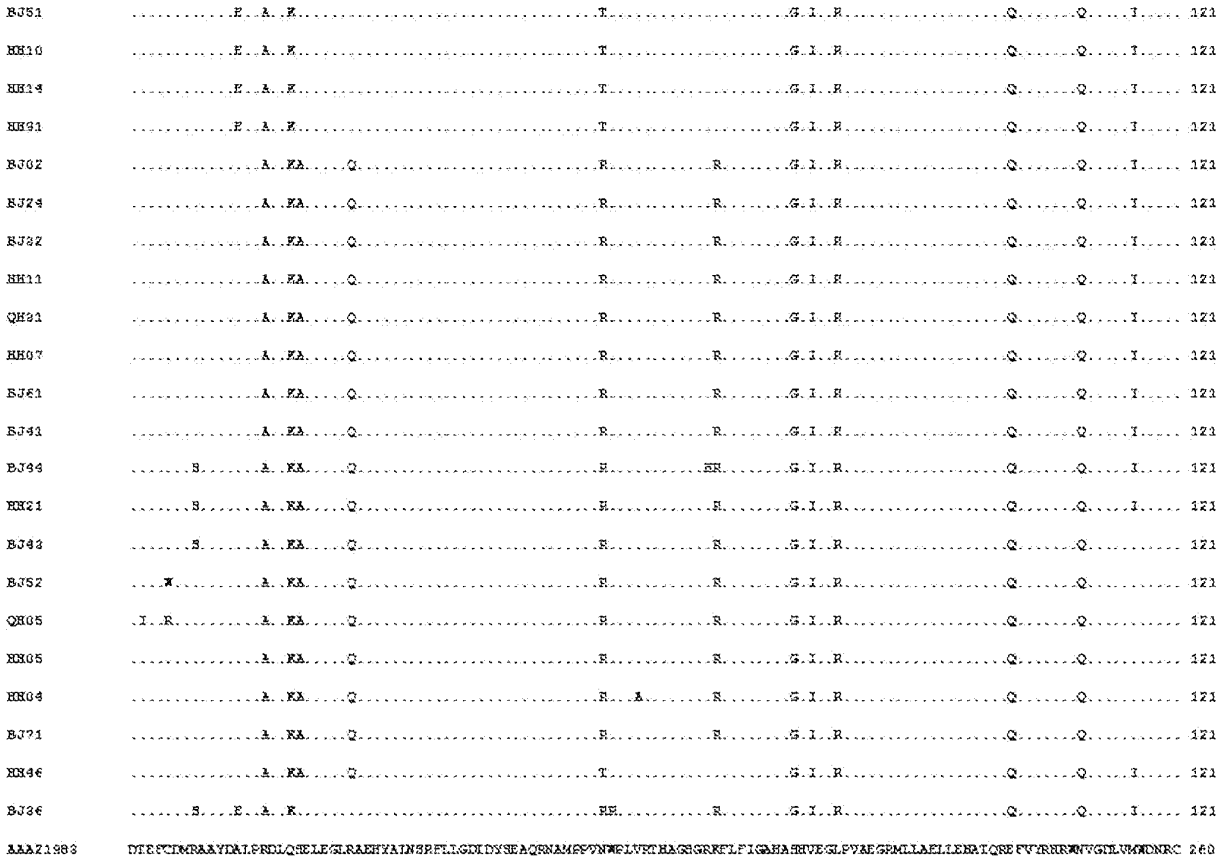


Fig. 3 Alignment of amino acid sequences derived from partial *tfdA*-like sequences from 22 2,4-D-degrading bacterial strains isolated from China compared with the class I TfdA reference sequence (*C. necator* JMP134 *tfdA*-encoded product, GenBank accession number AAA21983) using ClustalW2. Numbers to the *right* of the alignment are the consecutive numbers of the amino acids. *Dots* represent amino acids identical to the *C. necator* JMP134 TfdA sequence

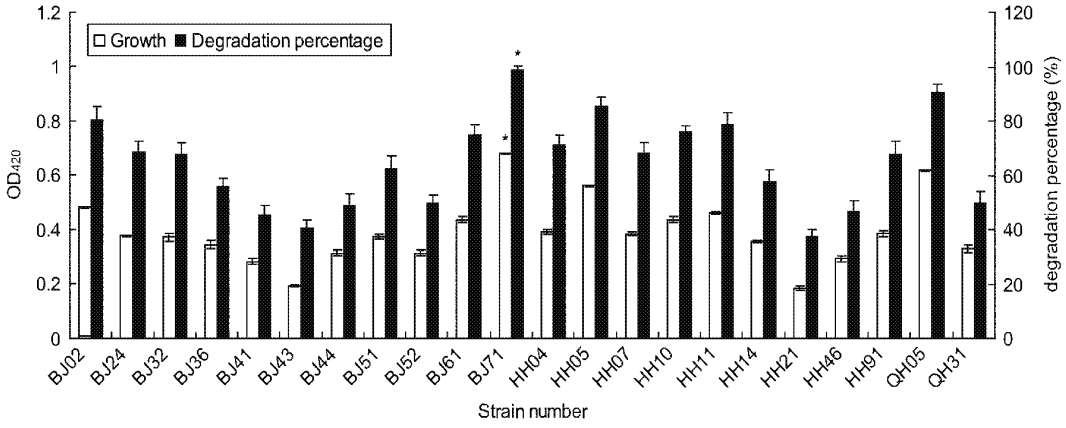


Fig. 4 Biomass and degradation percentages of 22 2,4-D-degrading bacterial strains isolated from China. Cell growth was quantified by measuring the absorbance at 420 nm by spectrophotometer. Degradation percentages were calculated by measuring the remaining 2,4-D in each culture using HPLC. Culture cell density at 420 nm was adjusted to 0.15 and used to inoculate further 150-ml MSM (pH 7.0) broths containing 500 mg l^{-1} 2,4-D in a 250-ml Erlenmeyer flask. Cultures were incubated at 30 °C and 150 rpm in a rotary shaker. All data were obtained after 7 days of incubation, and data represent the mean values of duplicate experiments. *Error bars* indicate standard deviations (SD). *Significant difference at the 5 % significance level according to Duncan's test ($P < 0.05$)

COR-AAD1-00003732
Bayer EX1008 (Part 7 of 9)

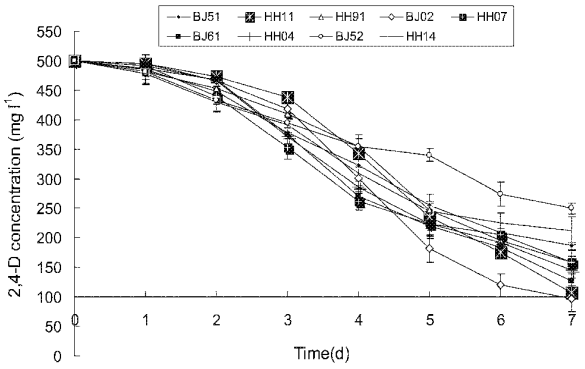


Fig. 5 Degradation of 2,4-D by nine *Bacillus* sp. strains isolated from China during a 1-week incubation. Strains were inoculated into 150 ml of MSM (pH 7.0) containing 500 mg l^{-1} 2,4-D as the sole carbon source in 250 ml flasks and incubated at 30 °C and 150 rpm in a rotary shaker. 2,4-D concentrations in media were measured using HPLC. The standard errors were within 5 % of the mean

Zakaria et al. 2007). An alignment of the *tfdA* genes was used to design iCODEHOPs primer sets for amplifying *tfdA* from the 22 2,4-D-degrading strains isolated in China. The *tfdA* nucleotide sequences from all of the isolates were highly similar to that of *A. eutropha* JMP134. Dunbar et al. (1997) demonstrated that approximately 98 % of their enrichment isolates possessed pJP4-type *tfdA* genes. It was suggested that the competitive fitness of 2,4-D-degrading species may be influenced by one or more of the pJP4-type alleles. Horizontal gene transfer of the 2,4-D-degrading plasmid pJP4 has been shown (McGowan et al. 1998). Plasmid pJP4 contains insertion sequence IS*1071*, which may explain its widespread occurrence in soil bacteria containing catabolic genes (Kim et al. 2013; Sota et al. 2006). In the current study, we assessed the distribution of the 22 isolated strains across the microbial taxa based on 16S rRNA gene sequences. We found that the class I *tfdA* genes isolated from the 22 strains are distributed across multiple taxa, including *Alpha-*, *Beta-*, *Gammaproteobacteria* and *Firmicutes*. This phenomenon is consistent with gene mobility based on horizontal gene transfer. The iCODEHOPs *tfdA* primers were designed based on class I, II, and III *tfdA* genes along with *tfdA*α; however, we did not identify anything other than class I *tfdA* genes. More interestingly, using this iCODEHOPs primer set, a *tauD* partial gene (GenBank accession number KC857507) was amplified from strain QH11, which was isolated from soil that had not been exposed to 2,4-D (data not shown). Therefore, the reason that only JMP134-type *tfdA* genes were identified in the current study may be due to the enrichment method used, which selects for isolation of the predominant strains. A more in-depth analysis of the bacterial community would likely reveal many more taxonomical units that carry *tfdA*-like genes.

Phylogenetic trees were constructed based on the *tfdA* and 16S rRNA gene sequences of the 22 strains isolated in the current study. All *tfdA*-related sequences had short branch lengths and were very closely related to *tfdA* of pJP4. Vallaeys et al. (1996) previously suggested the existence of a fourth class of *tfdA* genes based on PCR-restriction fragment length polymorphism analysis. Class I *tfdA* has been shown to include 313-bp fragments from JMP134 and four other strains that differ from each other by only 2 bp at the most (McGowan et al. 1998). Bælum et al. (2010) suggested that class I *tfdA* genes could be subdivided into two new classes, classes I-a and I-b. The sequences within the subclasses are 100 % identical, while 99 % identity is observed between the subclasses. In the present study, we found small but distinguishable amino acid changes when we analyzed *tfdA* sequences of the 22 strains isolated from China. We found differences at 19 sites within the 121-aa sequences. It is interesting to note that seven of the 19 sites were identical in the 22 *tfdA* partial genes of the 2,4-D-degrading bacteria isolated from China (Fig. 3). This phenomenon supports the suggestion that *tfdA* class I could be divided into two subclasses; however, further differences may exist within the *tfdA* sequences in these strains and these will be investigated in future studies. The *tfdA* genes of the 22 strains isolated from China could be classified as class I-b, while the reference *tfdA* genes from *A. eutrophus* JMP134, and *A. xylosoxidans* TFD9, *Burkholderia* sp. TFD29, and *Cupriavidus* sp. TFD42 (Table 1) were classified as class I-a (data not shown). The sequence data and phylogenetic tree demonstrate that diversity of amino acid sequences does indeed exist in class I *tfdA* genes.

In this work, we isolated dominant 2,4-D-degrading bacteria from wheat fields in three different areas of China that had been routinely treated with the herbicide for several years. We investigated species diversity by 16S rRNA gene sequence analysis, and described physiological and genetic properties of the isolates regarding 2,4-D biodegradation. No relationship between dominant degraders and area characteristics was observed in this study. The results suggested that the 2,4-D-degrading microorganisms containing class I *tfdA* genes are ubiquitous in soils routinely treated with 2,4-D in China. We found that *tfdA* exists in *Alpha-*, *Beta-*, and *Gammaproteobacteria* and *Firmicutes*. This study corroborates prior work suggesting that *tfdA* class I should be divided into two subclasses based on differences in comparison with the pJP4-type *tfdA*. In conclusion, the present work furthers our understanding of 2,4-D-degrading bacterial diversity, and the collection of diverse 2,4-D-degrading strains provides a valuable resource for studies on mechanisms of 2,4-D degradation and bioremediation. Further analysis of these bacteria will allow elucidation of how they adapt to xenobiotic chemicals in the environment.

COR-AAD1-00003733
Bayer EX1008 (Part 7 of 9)

Acknowledgments This work was supported by a Transgenic Major Project (2011ZX08010-003) from China's Ministry of Agriculture and Nature Science Foundation Project J [2013] 2123 of Guizhou Province, China.

References

Bælum J, Jacobsen CS (2009) Taqman probe-based real-time PCR assay for detection and discrimination of class I, II, and III *tfdA* genes in soils treated with phenoxy acid herbicides. Appl Environ Microbiol 75(9):2969–2972

Bælum J, Henriksen T, Hansen HCB, Jacobsen CS (2006) Degradation of 4-chloro-2-methylphenoxyacetic acid in top- and subsoil is quantitatively linked to the class III *tfdA* gene. Appl Environ Microbiol 72(2):1476–1486

Bælum J, Nicolaisen MH, Holben WE, Strobel BW, Sørensen J, Jacobesen CS (2008) Direct analysis of *tfdA* gene expression by indigenous bacteria in phenoxy acid amended agricultural soil. ISME J 2(6):677–687

Bælum J, Jacobsen CS, Holben WE (2010) Comparison of 16S rRNA gene phylogeny and functional *tfdA* gene distribution in thirty-one different 2,4-dichlorophenoxyacetic acid and 4-chloro-2-methylphenoxyacetic acid degraders. Syst Appl Microbiol 33 (2):67–70

Boyce R, Chilana P, Rose TM (2009) iCODEHOP: a new interactive program for designing COnsensus-DEgenerate Hybrid Oligonucleotide Primers from multiply aligned protein sequences. Nucleic Acids Res 1–7. doi: 10.1093/nar/gkp379

Cycoń M, Zmijowska A, Piotrowska-Seget Z (2011) Biodegradation kinetics of 2,4-D by bacterial strains isolated from soil. Cent Eur J Biol 6:188–198

Dunbar J, Wong DCL, Yarus MJ, Forney LJ (1997) Genetic diversity through the looking glass: effect of enrichment bias. Appl Environ Microbiol 63(4):1326–1331

Fukumori F, Hausinger RP (1993a) Purification and characterization of 2,4-dichlorophenoxyacetate/α-ketoglutarate dioxygenase. J Biol Chem 268(32):24311–24317

Fukumori F, Hausinger RP (1993b) *Alcaligenes eutrophus* JMP134 "2,4-dichlorophenoxyacetate monooxygenase" is an α-ketoglutarate-dependent dioxygenase. J Bacteriol 175(7):2083–2086

Fulthorpe RR, McGowan C, Maltseva OV, Holben WE, Tiedje JM (1995) 2,4-Dichlorophenoxyacetic acid-degrading bacteria contain mosaics of catabolic genes. Appl Environ Microbiol 61 (9):3274–3281

Gonod LV, Martin-Laurent F, Chenu C (2006) 2,4-D impact on bacterial communities, and the activity and genetic potential of 2,4-D degrading communities in soil. FEMS Microbiol Ecol 58 (3):529–537

Hogan DA, Buckley DH, Nakatsu CH, Schmidt TM, Hausinger RP (1997) Distribution of the *tfdA* gene in soil bacteria that do not degrade 2,4-dichlorophenoxyacetic acid (2,4-D). Microb Ecol 34 (2):90–96

Itoh K, Kanda R, Momoda Y, Sumita Y, Kamagata Y, Suyama K, Yamamoto H (2000) Presence of 2,4-D-catabolizing bacteria in a Japanese arable soil that belong to BANA (*Bradyrhizobium-Agromonas-Nitrobacter-Afipia*) cluster in α-Proteobacteria. Microbes Environ 15(2):113–117

Itoh K, Kanda R, Sumita Y, Kim H, Kamagata Y, Suyama K, Yamamoto H, Hausinger RP, Tiedje JM (2002) *tfdA*-like genes in 2,4-dichlorophenoxyacetic acid-degrading bacteria belonging to the *Bradyrhizobium-Agromonas-Nitrobacter-Afipia* cluster in α-Proteobacteria. Appl Environ Microbiol 68(7):3449–3454

Itoh K, Tashiro Y, Uobe K, Kamagata Y, Suyama K, Yamamoto H (2004) Root nodule *Bradyrhizobium* spp. harbor *tfdA* alpha and *cadA*, homologous with genes encoding 2,4-dichlorophenoxyacetic acid-degrading proteins. Appl Environ Microbiol 70: 2110–2118

Ka JO, Tiedje JM (1994) Integration and excision of a 2,4-dichlorophenoxyacetic acid-degradative plasmid in *Alcaligenes paradoxus* and evidence of its natural intergenetic transfer. J Bacteriol 176(17):5284–5289

Ka JO, Holben WE, Tiedje JM (1994) Genetic and phenotypic diversity of 2,4-dichlorophenoxyacetic acid (2,4-D)-degrading bacteria isolated from 2,4-D-treated field soils. Appl Environ Microbiol 60(4):1106–1115

Kamagata Y, Fulthorpe RR, Tamura K, Takami H, Formey LJ, Tiedje JM (1997) Pristine environments harbour a new group of oligotrophic 2,4-dichlorophenoxyacetic acid-degrading bacteria. Appl Environ Microbiol 63(6):2266–2272

Kim OS, Cho YJ, Lee K, Yoon SH, Kim M, Na H, Park SC, Jeon YS, Lee JH, Yi H, Won S, Chun J (2012) Introducing EzTaxon-e: a prokaryotic 16S rRNA gene sequence database with phylotypes that represent uncultured species. Int J Syst Evol Microbiol 62 (3):716–721

Kim DU, Kim MS, Lim JS, Ka JO (2013) Widespread occurrence of the *tfd-II* genes in soil bacteria revealed by nucleotide sequence analysis of 2,4-dichlorophenoxyacetic acid degradative plasmids pDB1 and p712. Plasmid 69(3):243–248

Kitagawa W, Takam S, Miyauchi K, Masai E, Kamagata Y, Tiedje JM (2002) Novel 2,4-dichlorophenoxyacetic acid degradation genes from oligotrophic *Bradyrhizobium* sp. strain HW13 isolated from a pristine environment. J Bacteriol 184:509–518

Knauer SH, Hartl-Spiegelhauer O, Schwarzinger S, Hänzelmann P, Dobbek H (2012) The Fe(II)/α-ketoglutarate-dependent taurine dioxygenases from *Pseudomonas putida* and *Escherichia coli* are tetramers. FEBS J 279(5):816–831

Laemmli CM, Leveau JHJ, Zehnder AJB, van der Meer JR (2000) Characterization of a second *tfd* gene cluster for chlorophenol and chlorocatechol metabolism on plasmid pJP4 in *Ralstonia eutropha* JMP134 (pJP4). J Bacteriol 182(15):4165–4172

Larkin MA, Blackshields G, Brown NP, Chenna R, McGettigan PA, McWilliam H, Valentin F, Wallace IM, Wilm A, Lopez R, Thompson JD, Gibson TJ, Higgins DG (2007) Clustal W and clustal X version 2.0. Bioinformatics 23(21):2947–2948

Lee TH, Kurata S, Nakatsu CH, Kamagata Y (2005) Molecular analysis of bacterial community based on 16S rDNA and functional genes in activated sludge enriched with 2,4-dichlorophenoxyacetic acid (2,4-D) under different cultural conditions. Microb Ecol 49(1):151–162

Lerch TZ, Dignac MF, Barriuso E, Bardoux G, Mariotti A (2007) Tracing 2,4-D metabolism in *Cupriavidus necator* JMP134 with ^{13}C-labelling technique and fatty acid profiling. J Microbiol Methods 71:162–174

Macur RE, Wheeler JT, Burr MD, Inskeep WP (2007) Impacts of 2,4-D application on soil microbial community and on populations associated with 2,4-D degradation. Microbiol Res 162(1):37–45

McGowan C, Fulthorpe R, Wright A, Tiedje JM (1998) Evidence for interspecies gene transfer in the evolution of 2,4-dichlorophenoxyacetic acid degraders. Appl Environ Microbiol 64(10): 4089–4092

Müller RH, Jorks S, Kleinsteuber S, Babel W (1998) Degradation of various chlorophenols under alkaline conditions by gram-negative bacteria closely related to *Ochrobactrum anthropi*. J Basic Microb 38(4):269–281

Rodriguez-Cruz MS, Bælum J, Shaw LJ, Sorensen SR, Shi SJ, Aspray TJ, Jacobsen CS, Bending GD (2010) Biodegradation of the herbicide mecoprop-p with soil depth and its relationship with class III *tfdA* genes. Soil Biol Biochem 42(1):32–39

Rose TM, Schultz ER, Henikoff JG, Pietrokovski S, McCallum CM, Henikoff S (1998) Consensus-degenerate hybrid oligonucleotide

COR-AAD1-00003734
Bayer EX1008 (Part 7 of 9)

primers for amplification of distantly related sequences. Nucleic Acids Res 26(7):1628–1635

Rose TM, Henikoff JG, Henikoff S (2003) CODEHOP (COnsensus-DEgenerate Hybrid Oligonucleotide Primer) PCR primer design. Nucleic Acids Res 31(13):3763–3766

Shaw L, Burns RG (2004) Enhanced mineralization of [U-^{14}C]2,4-dichlorophenoxyacetic acid in soil from the rhizosphere of *Trifolium pretense*. Appl Environ Microbiol 70(8):4766–4774

Shimojo M, Kawakami M, Aamda K (2009) Analysis of genes encoding the 2,4-dichlorophenoxyacetic acid-degrading enzyme from *Sphingomonas agrestis* 58-1. J Biosci Bioeng 108: 56–59

Smejkal CW, Vallaeys T, Seymour FA, Burton SK, Lappin-Scott HM (2001a) Characterization of (R/S)-mecoprop [2-(2-methyl-4-chlorophenoxy)propionic acid]-degrading *Alcaligenes* sp. CS1 and *Ralstonia* sp. CS2 isolated from agricultural soils. Environ Microbiol 3(4):288–293

Smejkal CW, Vallaeys T, Burton SK, Lappin-Scott HM (2001b) A rapid method to screen degradation ability in chlorophenoxyalkanoic acid herbicide-degrading bacteria. Lett Appl Microbiol 32(4):273–277

Smejkal CW, Seymour FA, Burton SK, Lappin-Scott HM (2003) Characterisation of bacterial cultures enriched on the chlorophenoxyalkanoic acid herbicides 4-(2,4-dichlorophenoxy) butyric acid and 4-(4-chloro-2-methylphenoxy) butyric acid. J Ind Microbiol Biotechnol 30(9):561–567

Sota M, Yano H, Naqata Y, Ohtsubo Y, Genka H, Kawasaki H, Tsuda M (2006) Functional analysis of unique class II insertion sequence IS*1071*. Appl Environ Microbiol 72(1):291–297

Streber WR, Timmis KN, Zenk MH (1987) Analysis, cloning, and high-level expression of 2,4-dichlorophenoxyacetate monooxygenase gene *tfdA* of *Alcaligenes eutrophus* JMP134. J Bacteriol 169(7):2950–2955

Suwa Y, Wright AD, Fukimori F, Nummy KA, Hausinger RP, Holben WE, Forney LJ (1996) Characterization of a chromosomally encoded 2,4-dichlorophenoxyacetic acid/α-ketoglutarate dioxygenase from *Burkholderia* sp. strain RASC. Appl Environ Microbiol 62(7):2464–2469

Tamura K, Peterson D, Peterson N, Stecher G, Nei M, Kumar S (2011) MEGA5: molecular evolutionary genetics analysis using maximum likelihood, evolutionary distance, and maximum parsimony methods. Mol Biol Evol 28(10):2731–2739

Top EM, Holben WE, Forney LJ (1995) Characterization of diverse 2,4-dichlorophenoxyacetic acid-degradative plasmids isolated from soil by complementation. Appl Environ Microbiol 61(5): 1691–1698

Vallaeys T, Fulthrope RR, Wright AM, Soulas G (1996) The metabolic pathway of 2,4-dichlorophenoxyacetic acid degradation involves different families of *tfdA* and *tfdB* genes according to PCR-RFLP analysis. FEMS Microbiol Ecol 20(3):163–172

Vallaeys T, Albino L, Soulas G, Wright AD, Weightman AJ (1998) Isolation and characterization of a stable 2,4-dichlorophenoxyacetic acid degrading bacterium, *Variovorax paradoxus*, using chemostat culture. Biotechnol Lett 20(11):1073–1076

Vedler E, Kõiv V, Heinaru A (2000) Analysis of the 2,4-dichlorophenoxyacetic acid-degradative plasmid pEST4011 of *Achromobacter xylosoxidans* subsp. *denitrificans* strain EST4002. Gene 255(2): 281–288

Zabaloy MC, Gómez MA (2013) Isolation and characterization of indigenous 2,4-D herbicide degrading bacteria from an agricultural soil in proximity of Sauce Grande River, Argentina. Ann Microbiol. doi:10.1007/s13213-013-0731-9

Zakaria D, Lappin-Scott H, Burton S, Whitby C (2007) Bacterial diversity in soil enrichment cultures amended with 2-(2-methyl-4-chlorophenoxy)propionic acid (mecoprop). Environ Microbiol 9(10):2575–2587

COR-AAD1-00003735
Bayer EX1008 (Part 7 of 9)

12878 J. Agric. Food Chem. 2010, 58, 12878–12884
DOI:10.1021/jf103537a

JOURNAL OF AGRICULTURAL AND FOOD CHEMISTRY
ARTICLE

Enantioselective Environmental Behavior of the Chiral Herbicide Fenoxaprop-ethyl and Its Chiral Metabolite Fenoxaprop in Soil

YANFENG ZHANG, DONGHUI LIU, JINLING DIAO, ZEYING HE, ZHIQIANG ZHOU, PENG WANG,* AND XUEFENG LI*

Department of Applied Chemistry, China Agricultural University, Beijing 100193, China

The enantioselective degradation behavior of fenoxaprop-ethyl (FE) and its chiral metabolite fenoxaprop (FA) in three soils under native conditions was investigated. Two pairs of enantiomers were analyzed by high-performance liquid chromatography (HPLC) with an amylose tri-(3,5-dimethylphenylcarbamate) (ADMPC) chiral column. The degradation of racemic FE in three soils showed the herbicidally inactive *S*-(−)-enantiomer degraded faster than the active *R*-(+)-enantiomer. FE was configurationally stable in soils because no interconversion to the respective antipodes was observed during incubation of the enantiopure *S*-(−)- or *R*-(+)-FE. The main metabolites of FE were confirmed as FA and 6-chloro-2,3-dihydrobenzoxazol-2-one (CDHB), and the formation of the chiral metabolite FA showed enantioselectivity in soils. The degradation of rac-FA was also enantioselective with the *S*-(−)-FA preferentially degraded: the half-life ($t_{1/2}$) of the *S*-form in the three soils ranged from 2.03 to 5.17 days, and that of *R*-form ranged from 2.42 to 20.39 days. The inversion of the *S*-(−)-enantiomer into the *R*-(+)-enantiomer occurred in two of the three soils when the enantiopure *S*-(−)- and *R*-(+)-FA were incubated. The data from sterilized control experiments indicated that the enantioselectivity of FE and FA was attributed to microbially mediated processes.

KEYWORDS: Enantioselectivity; chiral; fenoxaprop-ethyl; fenoxaprop; enantiomer; inversion

Downloaded via CORTEVA AGRISCIENCE on September 11, 2020 at 01:49:21 (UTC).
See https://pubs.acs.org/sharingguidelines for options on how to legitimately share published articles.

INTRODUCTION

Most enantiomers have identical physicochemical properties and abiotic degradation rates, but they may deviate dramatically in biological activity, toxicity, and microbial degradation rates when individual enantiomers interact with other chiral molecules (*1*−*4*). Furthermore, other reports describe that different enantiomers in racemates are enantioselectively metabolized (*4*−*6*). Enantioselectivity plays an important role in the environmental fate and ecological risks of a chiral compound, as many environmental processes are enantioselective (*7*, *8*). As a result, the enantiomeric composition may be changed by enantioselective degradation or enantiomerization over time. So efforts should be made to define the mode of action and elucidate the metabolic pathways of each enantiopure stereoisomer by using enantioselective analysis. Information with respect to differences in stereoselective dissipation kinetics and environmental behavior of individual enantiomers will help us improve our understanding of the pesticide risk to humans, animals, and the environment.

Fenoxaprop-ethyl (FE, **Figure 1**), (±)-ethyl 2-[4-[(6-chloro-2-benzoxazolyl)oxy]phenoxy]propanoate, a selective aryloxyphenoxypropionate (AOPP) herbicide, is registered for postemergence control of various annual and perennial grass weeds in dicotyledonous crops as well as grains (*9*). FE works by blocking acetyl coenzyme A carboxylase (ACCase) found in plant chloroplasts, which effectively inhibits lipid synthesis in target plants (*10*, *11*). This inhibition leads to chlorosis in susceptible weed species, followed by growth suppression and exsiccation. FE is not persistent in the environment and its degradation mainly follows two different mechanisms under different conditions, which may yield new chemicals (*12*). Because of the breakdown of the ester bond of FE, the parent compound is hydrolyzed to its corresponding acid fenoxaprop (FA), 2-[4-(6-chloro-2-benzoxazolyloxy) phenoxy] propionic acid, which is still biologically active (*13*). By another mechanism, FE (and FA) undergoes degradation forming 6-chloro-2,3-dihydrobenzoxazol-2-one (CDHB) by cleavage of the ether linkage of FE (*14*, *15*). Sometimes both pathways are concurrent in neutral conditions (*12*). FE and FA are chiral, but CDHB is achiral.

FE (and FA) has an asymmetrically substituted C-atom and thus consists of a pair of enantiomers with *S*-(−) and *R*-(+) absolute configurations and optical rotations (*16*), but the herbicidal activity mostly originates from the *R*-(+)-enantiomer. Studies showed that enantiomers of α-HCH, metolachlor, metalaxyl, benalaxyl, and lactofen behaved significantly differently during biodegradation and bioaccumulation in a variety of ecosystems (*2*, *5*, *17*−*19*). Moreover, enantiomerization of chiral compounds, such as dichlorprop and mecoprop, was found under certain conditions (*20*). Wink et al. elucidated that no racemization of FE took place, but the inversion of *S*-FA to *R*-FA was observed (*21*). Therefore, information on the environmental fate and ecotoxicological effect of each enantiomer of the parent compound FE or chiral metabolite FA should be reevaluated (*22*).

*To whom correspondence should be addressed. E-mail: wangpeng@cau.edu.cn (P.W.) or lxf1966@263.net (X.L.).

 Published on Web 12/01/2010 © 2010 American Chemical Society

COR-AAD1-00003736
Bayer EX1008 (Part 7 of 9)

Enantioselective dissipation in soils has been observed for various chiral pesticides, and some studies suggested that soil properties that have a major impact on the activity of the soil microbial community could influence chiral signatures (*8*, *19*). Therefore, degradation studies on the stereochemical aspects of FE and its main chiral metabolite FA in three soils were investigated under native and sterilized conditions using enantioselective high-performance liquid chromatography (HPLC). Meanwhile, this paper also monitored the chiral stability of FE and FA in soil with enantiopure compounds.

MATERIALS AND METHODS

Chemicals and Materials. Racemic-fenoxaprop-ethyl (rac-FE, 98.0%) and *R*-(+)-fenoxaprop-ethyl [*R*-FE, optical purity 98.0%] were kindly supplied by Institute for Control of Agrichemicals, Ministry of Agriculture of China. Racemic-fenoxaprop (rac-FA, 97.5%), *R*-(+)-fenoxaprop (*R*-FA, optical purity 97.5%) and 6-chloro-2,3-dihydrobenzoxazol-2-one (CDHB, 98.0%) were obtained from the hydrolysis of their corresponding parent compounds (*23*). *S*-(−)-Fenoxaprop-ethyl (*S*-FE, optical purity 99.0%) and *S*-(−)-fenoxaprop (*S*-FA, optical purity 99.0%) were collected manually from multiple injections (50 μL) of the corresponding racemic mixture by observing the UV-signal on an Agilent HPLC with a chiral column (250 mm × 4.6 mm i.d.). Ethyl ether, *n*-hexane, 2-propanol (analytical grade), and trifluoroacetic acid (TFA) were from Fisher Scientific (Fair Lawn, NJ, U.S.A.). All other chemicals and solvents were purchased from commercial sources and were analytical grade.

Soil Samples. Three soil samples representing diversely physicochemical properties were collected at 0−10 cm plow layer from geographically distinct agriculture regions of China. All samples were air-dried at room temperature, homogenized, passed through a 2-mm sieve, and stored in the dark at 4 °C. More details on soil sites and specific physicochemical characteristics (particle size, texture, pH, and organic carbon) are presented in **Table 1**.

Incubation in Soils under native Conditions. Separate incubation experiments were conducted with the racemate and the pure *S*-(−)- and *R*-(+)-compounds, respectively, using 50-mL polypropylene centrifuge tube covered with aluminum foil. Approximately 5 g of soil (dry weight equivalent) was fortified with 50 μg (50 μL of a 1000 μg/mL stock solution in acetone) of rac-, *S*-(−)-, or *R*-(+)-FE and rac-, *S*-(−)-, or *R*-(+)-FA, respectively, and allowed to air-dry for 5 min before being homogenized thoroughly for 5 min (fortification level of 10 μg/g, experiments SN1-SN6, SY1-SY6, and SC1-SC6, respectively). The soil samples were rehydrated and incubated at 25 °C in the dark, and sample weights were controlled regularly by weighing for water content (about 60% of the field holding capacity (w/w)) in order to compensate for loss of water by addition of deionized water. Three replicate samples were removed from each treatment at different time intervals and immediately transferred into a freezer (−20 °C). Triplicate samples were taken immediately after fortification ($t = 0$) to determine the recovery and reproducibility of extraction in the soil (see below). Blank determinations of the soil prior to fortification revealed no FE, FA, or CDHB present.

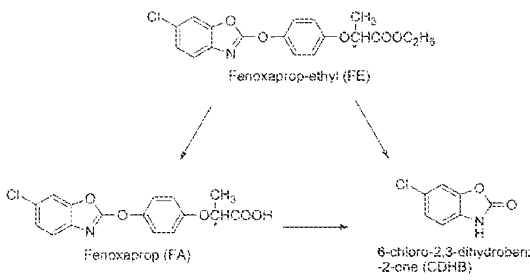


Figure 1. Chemical structures of fenoxaprop-ethyl and its primary metabolites (fenoxaprop and CDHB). Chiral center is denoted by an asterisk (*).

Incubation in Soils under Sterilized Conditions. To determine if the enantioselective dissipation was a result of microbially mediated transformations, a set of soil samples were also prepared and subjected to sterilization treatment, which was achieved by autoclaving the samples twice at 121 °C for 60 min with 24-h intervals to eliminate microbial activity. Portions of 10 g of soil were placed into a separate 50-mL flask and fortified with 100 μg of rac-FE or rac-FA aseptically (spike level, 10 μg/g). Each flask was treated with the nonsterilized samples with addition of sterile water, which was then sealed with film to maintain sterile conditions.

Extraction of Incubated Soil Samples. Samples were thawed at room temperature (half of each sterilized soil sample was removed and placed into 50 mL polypropylene centrifuge tubes, which was equivalent to the native one) and then extracted with ethyl acetate (25 mL) followed by 200 μL of 6 M HCl for efficient extraction of FA. The tube was stirred on a vortex shaker for 3 min, ultrasonically extracted for 10 min, and centrifuged at 4000 rpm for 5 min. Then the organic layer was filtered through anhydrous sodium sulfate for dehydration. The same extraction step was repeated twice with 25 mL of ethyl acetate. The extracts were combined and reduced to near dryness on a vacuum rotary evaporator at 40 °C and then dissolved in 0.5 mL of 2-propanol. An aliquot (20 μL) was analyzed by HPLC.

Enantioselective HPLC Analysis. An Agilent 1200 series HPLC system (Agilent Technology) equipped with a G1322A degasser, a G1311A quat pump, a G1329A automatic liquid sampler, a G1314B variable wavelength UV detector, and Agilent Chemstation software was used. A method for the simultaneous enantiomeric determination of the FE and FA enantiomers and the major metabolite CDHB in soil samples was set up. The baseline separation of these compounds by an amylose tri-(3,5-dimethylphenylcarbamate) (ADMPC) chiral column was obtained with a mobile phase of *n*-hexane/2-propanol/trifluoroacetic acid (TFA) (95.5:0.1, v/v/v) with a flow rate of 1.0 mL/min. TFA was added into the mobile phase for the determination of FA and CDHB as a mobile phase acidic additive. Wavelength for UV detection was 230 nm and temperature for chromatographic separation was 20 °C. These compounds gave five separate peaks, which were as follows: *S*-(−)- and *R*-(+)-FE, CDHB, and *S*-(−)- and *R*-(+)-FA, and the elution order and the identities were established by comparison with the retention time of the enantiopure standards of the FE and FA and the standard of CDHB.

The standard solutions of *S*-(−)-FE, *R*-(+)-FE, *S*-(−)-FA, *R*-(+)-FA, and CDHB (0.5, 1, 5, 10, and 50 μg/mL each compound) for linearity were prepared by diluting the stock standard solution. Calibration curves were generated by plotting peak area of each compound versus their concentration. Recovery estimation was carried out over three concentration levels (adding the standard solutions in 5 g free soil sample to get final concentrations of 0.1, 1.0, 10 μg/g). Recoveries of these compounds were determined immediately after fortification. Experiments showed that the recovery of the above procedure was >90% for FE, FA, and CDHB in soils. The limit of quantification (LOQ) for these compounds in all samples was found to be 0.05 μg/g on the basis of an acceptable RSD of 20%.

Kinetics Analysis. When the degradation fits well to the first-order kinetics, k_S or k_R is the individual degradation rate constant. Corresponding rate constant k is determined from the linear plots

Table 1. Properties and Locations of Tested Soils

	particle-size					
soil site[a]	sand (%)	silt (%)	clay (%)	soil texture	pH (water)[b]	C_{org} (%)
Neimenggu Chifeng (SC)	74.4	21.9	3.7	sandy loam	8.1	1.9
Shandong Yanzhou (SY)	41.9	52.6	5.5	silt loam	6.9	1.1
Jiangxi Nanchang (SN)	30.2	28.1	41.7	clay	5.0	0.7

[a] The sites in China. [b] Suspension of soil in water, 1:2.5 (w/w).

COR-AAD1-00003737
Bayer EX1008 (Part 7 of 9)

of ln[S] or ln[R] versus time t (19):

$$\ln[S] = \ln[S]_{t=0} - k_S \times t \quad (1)$$

$$\ln[R] = \ln[R]_{t=0} - k_R \times t \quad (2)$$

where [S] and [R] are the concentrations at time t, and k_S and k_R are the degradation rate constants of S- and R-enantiomers, respectively.

If degradation is enantioselective ($k_S \neq k_R$), enantiomer composition (ER) of the residues is changing with time, and ER may be expressed as a function of time (t) in the relationship (5)

$$ER_t = [S]/[R] = ER_0 \times e^{(k_R - k_S)} = ER_0 \times e^{\Delta k} \quad (3)$$

where ER_0 is the initial ER value, and Δk is the difference between k_S and k_R, which reflects the rate at which ER deviates from ER_0 over time. The above relationship can be further expressed in a linear form after logarithmic transformation of ER (4):

$$\ln(ER_t) = \ln(ER_0) + \Delta k \quad (4)$$

A plot of ln(ER) versus t can be used to determine the rate difference Δk and enantioselectivity.

RESULTS AND DISCUSSION

Degradation of FE in Soil. The rapid disappearance of both enantiomers of FE with time was observed in experiments SN1-SN3, SY1-SY3, and SC1-SC3 when the racemate, the enantiopure S-(−)- and R-(+)-FE were incubated under nonsterilized conditions. **Figure 2a**−**c** showed the chromatograms of the elution of FE from samples of experiment SN1 (incubation with rac-FE) after 0, 0.5, and 20 days, respectively. An initially racemic composition of FE was confirmed, and a slightly faster decrease of S-(−)-FE in comparison to the R-(+)-FE indicated a preferential dissipation of the S-(−)-enantiomer by the soil's enzymatic systems during the incubation. Enantioselective degradation led to relative enrichment of R-(+)-enantiomer which is active against herbs. Degradation in experiment SN1 thus showed an enantioselectivity in the same sense as in experiments SY1 and SC1.

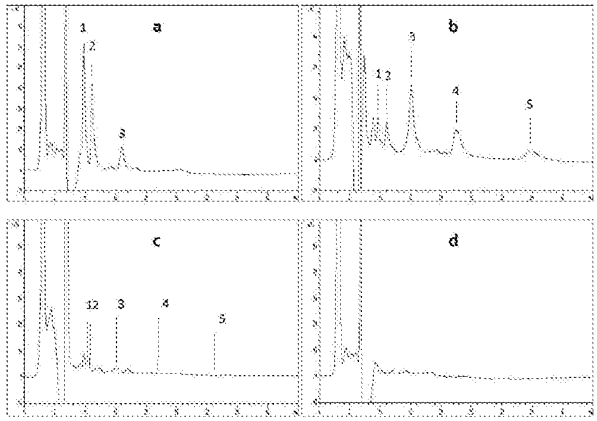


Figure 2. Chromatograms of enantioselective degradation of rac-FE in soil (expt SN1): (**a**) 0 day; (**b**) 0.5 day; (**c**) 20 days; (**d**) blank soil. Peaks: 1, S-(−)-FE; 2, R-(+)-FE; 3, CDHB; 4, S-(−)-FA; 5, R-(+)-FA.

The data of the residual concentrations on two enantiomers were used for estimating the enantiomeric ratio (ER) values (**Table 2**) in these experiments. The ER values of FE from experiment SN1 consistently changed from the initial value of 0.98 (racemic) to 0.42 (concentration [S] < [R], **Figure 3a**). A t test between the means of the ER values of spiked soil and ER = 0.98 yielded a p value of 0.031. Using eq 4, a plot of ln(ER) versus incubation time t was linear for rac-FE (**Figure 3d**). The rate difference Δk calculated from this plot was -0.821 day^{-1}. The ER values of FE from experiment SY1 consistently decreased with time from the initial value of 0.98 to 0.75. A t test between the means of the ER values of spiked soil and ER = 0.98 yielded a p value of 0.012. A plot of ln(ER) versus incubation time t was also linear (R^2 = 0.75) for rac-FE and the rate difference Δk was -0.067 day^{-1}. The ER values of FE from experiment SC1 decreased with time from the initial value of 0.98−0.58. A t test between the means of the ER values of spiked soil and ER = 0.98 yielded a p value of 0.031. A plot of ln(ER) versus incubation time t was linear (R^2 = 0.99) for rac-FE, and the rate difference Δk calculated from this plot was -0.251 day^{-1}. In sum, the degradation of FE in the three soils was enantioselective.

In microbially inhibited experiments (rac-FE) with autoclaved soil samples, ER values also remained close to 1.00, the same as the FE standard. Thus, the enantioselective degradation of FE in native soil samples was predominantly achieved by a biotic pathway.

Chiral Stability of FE in Soil. The incubation experiments group 2 (SN2, SY2, SC2) and group 3 (SN3, SY3, SC3) spiked with enantiopure S-(−)- and R-(+)-FE, respectively. The data documented the high enantiomeric purity of S-(−)- and R-(+)-FE prior to incubation and indicated degradation of

Table 2. Enantiomer Ratio (ER = S/R) of rac-FE and rac-FA metabolite in Experiment SC1, SY1, and SN1

	SC1		SY1		SN1	
time (days)	ER[a] rac-FE	ER rac-FA	ER rac-FE	ER rac-FA	ER rac-FE	ER rac-FA
0	0.98 ± 0.01		0.98 ± 0.01		0.98 ± 0.01	
0.08	0.97 ± 0.01	0.94 ± 0.08	0.93 ± 0.01	0.99 ± 0.08	0.87 ± 0.01	1.96 ± 0.08
0.17	0.93 ± 0.01	0.90 ± 0.08	0.92 ± 0.01	0.76 ± 0.08	0.82 ± 0.01	1.54 ± 0.08
0.33	0.82 ± 0.05	0.88 ± 0.07	0.89 ± 0.05	0.76 ± 0.01	0.73 ± 0.05	1.45 ± 0.07
0.50	0.77 ± 0.05	0.86 ± 0.07	0.82 ± 0.05	0.75 ± 0.07	0.57 ± 0.05	1.21 ± 0.07
1	0.69 ± 0.01	0.76 ± 0.06	0.79 ± 0.01	0.66 ± 0.07	0.42 ± 0.01	0.98 ± 0.06
2	0.58 ± 0.01	0.72 ± 0.10	0.75 ± 0.01	0.61 ± 0.06		0.95 ± 0.08
3		0.62 ± 0.10		0.40 ± 0.10		0.84 ± 0.08
5		0.56 ± 0.08		0.33 ± 0.08		0.81 ± 0.08
7		0.35 ± 0.08		0.17 ± 0.08		0.72 ± 0.07
10		0.31 ± 0.05		0.10 ± 0.07		0.70 ± 0.07
15		0.30 ± 0.07		0.07 ± 0.07		
20		0.29 ± 0.06		0.05 ± 0.06		
25				0.03 ± 0.06		

[a] Values represent the mean ± SD.

COR-AAD1-00003738
Bayer EX1008 (Part 7 of 9)

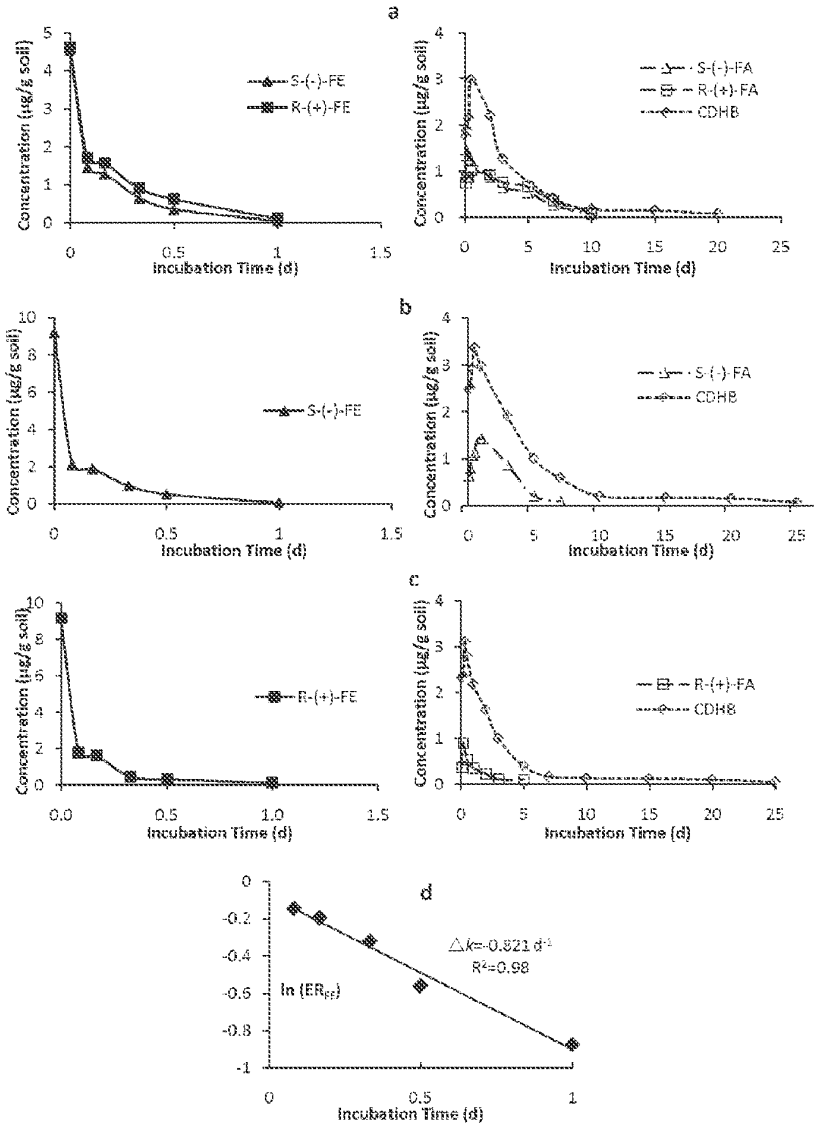


Figure 3. Degradation of FE in soil (expt SN1, SN2, and SN3 with rac-, *S*-(−)-, *R*-(+)-FE, respectively. Note the concurrent rapid formation and slower degradation of CDHB and FA arising from FE): (**a**) degradation of rac-FE (expt SN1); (**b**) degradation of *S*-(−)-FE (expt SN2); (**c**) degradation of *R*-(+)-FE (expt SN3); (**d**) the plot of ln(ER) from experiment SN1 (incubation of rac-FE) versus incubation time *t* showing a linear relationship.

S-(−)- and *R*-(+)-FE from samples of experiments SN2 and SN3 (**Figure 3b**,**c**), respectively. Experiments group 2 (SN2, SY2, SC2) and group 3 (SN3, SY3, SC3) revealed no formation of the *S*-(−)-FE from *R*-(+)-FE throughout the incubation time and vice versa. These data showed that inversion was insignificant compared to degradation indicating that FE configuration was stable in these soils. The results were attributed to rapid hydrolysis and different microbial community.

Formation of the Two Metabolites of FE. FA and CDHB, arising from breakdown of the ester bond and cleavage of the ether linkage, respectively, were the main metabolites of FE detected in this study. The chromatograms in **Figure 2** and the data plotted in **Figure 3a**−**c** showed that the persistent decrease of the unchanged parent compound was accompanied by the concurrent increase and subsequent decrease of FA and CDHB in Jiangxi soils. The hydrolysis of the rac-FE which yielded predominately *R*-(+)-FA residue and the ER values of acquired FA which consistently decreased with time (**Table 2**) showed enantioselectivity in the formation of the chiral metabolite FA in soils. The same formation trend was observed in the other two soil samples.

In Jiangxi soil samples spiked with rac-FE (expt SN1), the amounts of FA and CDHB detected during the initial day of incubation were about 2.22 and 1.76 μg/g, respectively. After further incubation, the concentration of FA reached a maximum of 2.25 μg/g at day 0.50 and then decreased to 0.17 μg/g at day 10. However, the concentration of CDHB reached a maximum of 2.99 μg/g at day 0.50 and then decreased to 0.08 μg/g at day 20. From *S*-(−)- and *R*-(+)-FE (expts SN2 and SN3, respectively) only the formation of the respective FA along with CDHB is observed, and these data indicated that the ester cleavage of *S*-(−)- and *R*-(+)-FE proceeded with retention of configuration, contrary to the activity of the other two soils.

In Shandong soil samples spiked with rac-FE (expt SY1), the amounts of FA and CDHB detected during the initial day of

COR-AAD1-00003739
Bayer EX1008 (Part 7 of 9)

Table 3. First-Order Rate Constant (k), Half-Life ($t_{1/2}$), and Correlation Coefficient (R^2) for the Degradation of Enantiomers FA in Soils

soil origins	experiment (incubated compound)	enantiomer	k (day^{-1})	$t_{1/2}$ (days)[a]	R^2
Neimenggu Chifeng soil	SC4	*S*-(−)-FA	0.134	5.17 ± 0.05	0.91
	(rac-FA)	*R*-(+)-FA	0.034	20.39 ± 0.03	0.96
	SC5 (*S*-(−)-FA)	*S*-(−)-FA	0.154	4.50 ± 0.07	0.96
	SC6 (*R*-(+)-FA)	*R*-(+)-FA	0.053	13.08 ± 0.06	0.95
Shandong Yanzhou soil	SY4	*S*-(−)-FA	0.280	2.48 ± 0.01	0.94
	(rac-FA)	*R*-(+)-FA	0.153	4.53 ± 0.06	0.95
	SY5 (*S*-(−)-FA)	*S*-(−)-FA	0.234	2.96 ± 0.03	0.98
	SY6 (*R*-(+)-FA)	*R*-(+)-FA	0.132	5.33 ± 0.04	0.92
Jiangxi Nanchang soil	SN4	*S*-(−)-FA	0.342	2.03 ± 0.01	0.96
	(rac-FA)	*R*-(+)-FA	0.286	2.42 ± 0.01	0.96
	SN5 (*S*-(−)-FA)	*S*-(−)-FA	0.280	2.39 ± 0.02	0.98
	SN6 (*R*-(+)-FA)	*R*-(+)-FA	0.242	2.86 ± 0.03	0.97

[a] Values represent the mean ± SD.

incubation were about 2.05 and 1.67 μg/g, respectively. After further incubation, the concentration of FA reached a maximum of 6.75 μg/g at day 2 and then decreased to 2.65 μg/g at day 25. Meanwhile, the concentration of CDHB reached a maximum of 4.04 μg/g at day 1 and then decreased to 0.82 μg/g at day 20. From *R*-(+)-FE (expts SY3) only the formation of the respective *R*-(+)-FA was observed, whereas from *S*-(−)-FE (expts SY2), both *R*-(+)-FA and *S*-(−)-FA appeared, indicating that the ester cleavage of *R*-(+)-FE proceeded with retention of configuration, whereas the ester cleavage of *S*-(−)-FE underwent inversion of the absolute configuration.

In Neimenggu soil samples spiked with rac-FE (expt SC1), the amounts of FA and CDHB detected during the initial day of incubation were about 0.81 and 0.60 μg/g, respectively, and then degraded slightly. After further incubation, the concentration of FA reached a maximum of 9.25 μg/g at day 0.5 and then decreased to 1.21 μg/g at day 25. However, the concentration of CDHB reached a maximum of 0.91 μg/g at day 0.33 and then decreased to 0.12 μg/g at day 25. From *R*-(+)-FE (expts SC3) only the formation of the respective *R*-(+)-FA was observed, whereas from *S*-(−)-FE (expts SC2), both *R*-(+)-FA and *S*-(−)-FA appeared, indicating that the ester cleavage of *R*-(+)-FE occurred with retention of configuration, but the ester cleavage of *S*-(−)-FE occurred with inversion of the optical configuration.

Enantioselective Degradation of the Chiral Metabolite FA in Soil. The degradation from the experiments group 4 (SN4, SY4, SC4), group 5 (SN5, SY5, SC5), and group 6 (SN6, SY6, SC6) with rac-, *S*-(−)-, *R*-(+)-FA, respectively, fitted a first-order kinetics decay model and the data were plotted respectively versus time t. Rate constants and R^2 were listed in **Table 3**. In **Figure 4a**−**c**, the chromatograms from the incubation of the rac-FA (expt SC4) in Neimenggu soil illustrated significant degradation of both enantiomers but with a clearly more rapid degradation of *S*-(−)- than *R*-(+)-FA, leading to residues enriched in *R*-(+)-enantiomer. Data from expt SY4 and expt SN4 showed similar degradation in Shandong soil and Jiangxi soil with varying degrees of enantioselectivity.

In Neimenggu soil samples, the ERs from the incubation of rac-FA (expt SC4) showed a continuous decrease with time from the initial value of 0.98 (racemic) to about 0.03 (concentration $[S] < [R]$, **Figure 5a**). A plot of ln(ER) versus time t was linear and the slope indicated a rate difference Δk ($k_{Racid} - k_{Sacid}$) of −0.093 day^{-1} (**Figure 5d**), which was in reasonable agreement with the above data ($k_{Racid} - k_{Sacid}$ = −0.100 day^{-1}). A t test between the means of ER values of spiked soil and ER = 0.98 yielded a $p < 0.001$. All of them indicated that the degradation of FA was highly enantioselective. In Jiangxi soil samples, the ERs from the incubation of rac-FA (expt SN4) showed a continuous decline with time from the initial value of 0.98 to about 0.69. A plot of

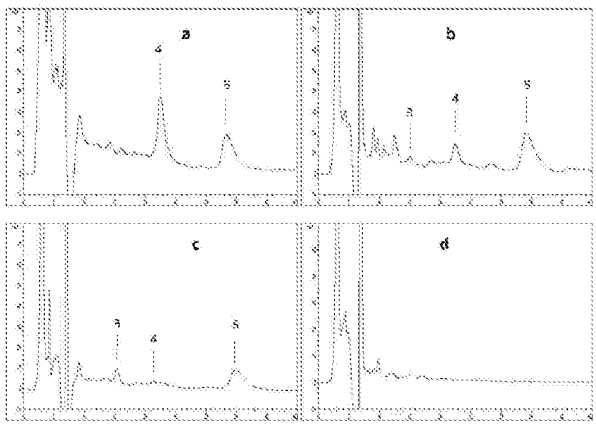


Figure 4. Chromatograms from the incubation of rac-FA in soil (expt SC4) under nonsterilized conditions: (**a**) 0 day; (**b**) 2 days; (**c**) 20 days; (**d**) blank soil. Peaks: 3, CDHB; 4, *S*-(−)-FA; 5, *R*-(+)-FA.

ln(ER) versus time t was linear and a rate difference Δk was −0.055 day^{-1}, which was in reasonable agreement with the above data ($k_{Racid} - k_{Sacid}$ = −0.056 day^{-1}). A t test between the means of the values of spiked soil and ER = 0.98 yielded a p value of 0.029. These indicated some degree of enantioselectivity. In Shandong soil samples, the ERs from the incubation of rac-FA (expt SY4) showed a continuous fall with time from the initial value of 0.98 to about 0.40. ln(ER) and time t was fitted with a linear correlation and the slope indicated a rate difference Δk of −0.104 day^{-1}, which was in reasonable agreement with the above data ($k_{Racid} - k_{Sacid}$ = −0.127 day^{-1}). A t test between the means of the values of spiked soil and ER = 0.98 yielded a p value of 0.030. Enantioselectivity also existed in the degradation of FA.

ES, which was defined as ES = $(k_S - k_R)/(k_S + k_R)$, is a measure of enantioselectivity (1). The fact that the two enantiomers of FA degraded at different rates ($k_{Sacid} > k_{Racid}$) and the ES value of 0.09, 0.29, and 0.56 were calculated from these rates in experiment SN4, SY4, and SC4, respectively, indicated low to high enantioselectivity of FA in the three soils, and *S*-(−)-FA degraded faster than *R*-(+)-FA. The highest ES was observed in Neimenggu soil with the highest pH (pH 8.1, ES = 0.56), and the lowest ES was found in Jiangxi soil with the lowest pH (pH 5.0, ES = 0.09). In addition, the ES in Neimenggu sandy loam soil is higher than that in Jiangxi clay soil, namely, the ES changed toward less positive values with decreasing sand content and increasing clay content. In control experiments (rac-FA) with

COR-AAD1-00003740
Bayer EX1008 (Part 7 of 9)

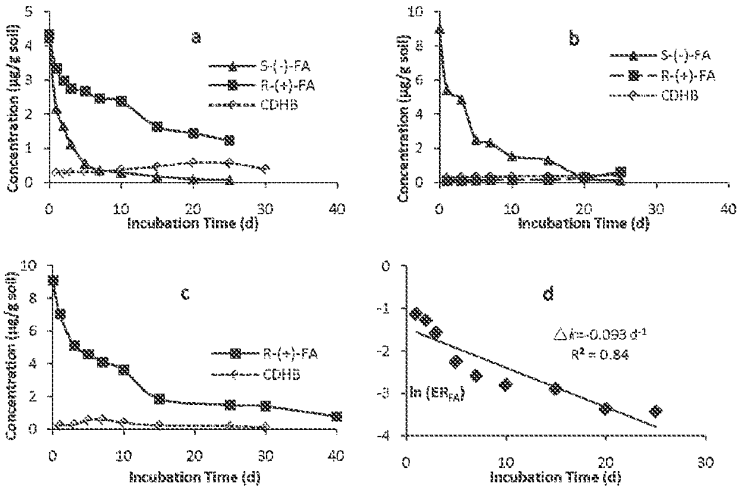


Figure 5. Degradation of FA in soil (expt SC4, SC5, and SC6 with rac-, *S*-(−)-, *R*-(+)-FA, respectively. Note the concurrent formation and degradation of CDHB arising from FA): (**a**) degradation of rac-FA (expt SC4); (**b**) degradation of *S*-(−)-FA (expt SC5); (**c**) degradation of *R*-(+)-FA (expt SC6); (**d**) the plot of ln(ER) from experiment SC4 (incubation of rac-FA) versus incubation time *t* showing a linear relationship.

sterilized soil samples, ER values were comparable to the ratio found for racemate. Thus, the degradation of FA in native soil samples was preponderantly mediated by biological processes.

Inversion of FA in Soil. Inversion was studied by separate incubations of the two enantiomers of FA under native conditions. We found *R*-(+)-FA and *S*-(−)-FA during the incubation of *S*-(−)-FE as mentioned above meaning there was inversion of *S*-(−)-FA to *R*-(+)-FA during the incubation of *S*-(−)-FA in Shangdong soil and Neimenggu soil but not in Jiangxi soil. Some studies suggested that soil properties such as soil pH, organic carbon, and soil texture have a major impact on the activity of the soil microbial community, and then could influence chiral signatures including enantiomerization in soils (*8*, *24*, *25*).

No indication for inversion was found in Jiangxi soil from the incubation of the pure *S*-(−)- and *R*-(+)-FA (expts SN5 and SN6, respectively), revealing no conversion of *S*-(−)- to *R*-(+)-FA during incubation and vice versa. *S*-(−)- and *R*-(+)-FA were both configurationally stable in Jiangxi soil.

The data from experiment SY5 and SC5 (incubation of the *S*-(−)-FA in Shandong soil and Neimenggu soil, respectively) showed a continuous decrease of the concentration of *S*-(−)-FA; meanwhile, the concentrations of *R*-(+)-FA in the two soils increased from initial values of 0 to 0.22 and 0.61 μg/g after 25 days of incubation, respectively (**Figure 5b**). The results illustrated conversion of the *S*-(−)-FA into *R*-(+)-FA. However, from experiment SY6 and SC6 (incubation of the *R*-(+)-FA in Shandong soil and Neimenggu soil, respectively), *R*-(+)-FA was configurationally stable (**Figure 5c**), and inversion was thus unimportant compared to degradation.

In this study, the stereochemistries of FE and its primary chiral product, FA, were investigated in soils using the racemic and the enantiopure compounds in combination with enantioselective analyses. The enantioselective degradation of FE occurred and the two enantiomers were configurationally stable in soils. Enantioselective degradation of FA was observed in the three soils, while there was inversion of *S*-(−)-FA to *R*-(+)-FA during the incubation of *S*-(−)-FA only in two soils. Moreover, enantioselectivity was attributed to microbial processes under native conditions. These results for major differences in the degradation of the enantiomers may have some implications for better environmental and ecological risk assessment for chiral pesticides.

LITERATURE CITED

(1) Müller, M. D.; Buser, H. R. Environmental behavior of acetamide pesticide stereoisomers. 2. Stereo- and enantioselective degradation in sewage sludge and soil. *Environ. Sci. Technol.* **1995**, *29*, 2031−2037.

(2) Monkiedje, A.; Spiteller, M.; Bester, K. Degradation of racemic and enantiopure metalaxyl in tropical and temperate soils. *Environ. Sci. Technol.* **2003**, *37*, 707−712.

(3) Liu, W. P.; Gan, J. Y.; Schlenk, D.; Jury, W. A. Enantioselectivity in environmental safety of current chiral insecticides. *Proc. Natl. Acad. Sci. U. S. A.* **2005**, *102* (3), 701−706.

(4) Diao, J. L.; Xu, P.; Wang, P.; Lu, D. H.; Lu, Y. L.; Zhou, Z. Q. Enantioselective degradation in sediment and aquatic toxicity to Daphnia magna of the herbicide lactofen enantiomers. *J. Agric. Food Chem.* **2010**, *58*, 2439−2445.

(5) Buser, H. R.; Müller, M. D.; Poiger, T.; Balmer, M. E. Environmental behavior of the chiral acetamide pesticide metalaxyl: enantioselective degradation and chiral stability in soil. *Environ. Sci. Technol.* **2002**, *36*, 221−226.

(6) Bewick, D. W. Stereochemistry of fluazifop-butyl transformations in soil. *Pestic. Sci.* **1986**, *17*, 349−356.

(7) Hegeman, W. J. M.; Laane, R. W. P. M. Enantiomeric enrichment of chiral pesticides in the environment. *Rev. Environ. Contam. Toxicol.* **2002**, *173*, 85−116.

(8) Lewis, D. L.; Garrison, A. W.; Wommack, K. E.; Whittemore, A.; Steudler, P.; Melillo, J. Influence of environmental changes on degradation of chiral pollutants in soils. *Nature* **1999**, *401*, 898−901.

(9) Bieringer, H. H.; Hörtlein, G.; Langelueddeke, P.; Handte, R. HOE 33171-a new selective herbicide for the control of annual and perennial warm climate grass weeds in broadleaf crops. *Proc. Brit. Crop Prot. Conf. Weeds* **1982**, *1*, 11−17.

(10) Tal, A.; Romano, M. L.; Stephenson, G. R.; Schwan, A. L.; Hall, J. C. Glutathione conjugation: A detoxification pathway for fenoxaprop-ethyl in barley, crabgrass, oat, and wheat. *Pestic. Biochem. Physiol.* **1993**, *46*, 190−199.

(11) Lee, W. M.; Elliott, J. E.; Brownsey, R. W. Inhibition of acetyl-CoA carboxylase isoforms by pyridoxal phosphate. *J. Biol. Chem* **2005**, *280*, 41385−41843.

(12) Lin, J.; Chen, J. W.; Cai, X. Y.; Qiao, X. L.; Huang, L. P.; Wang, D. G.; Wang, Z. Evolution of toxicity upon hydrolysis of fenoxaprop-*p*-ethyl. *J. Agric. Food Chem.* **2007**, *55* (18), 7626−7629.

(13) Smith, A. E.; Aubin, A. J. Degradation studies with ^{14}C-fenoxaprop in prairie soils. *Can. J. Soil Sci.* **1990**, *70*, 343−350.

COR-AAD1-00003741
Bayer EX1008 (Part 7 of 9)

(14) Lin, J.; Chen, J. W.; Wang, Y.; Cai, X. Y.; Wei, X. X.; Qiao, X. L. More toxic and photoresistant products from photodegradation of fenoxaprop-*p*-ethyl. *J. Agric. Food Chem.* **2008**, *56* (17), 8226−8230.

(15) Hoagland, R. E.; Zablotowicz, R. M. Biotransformations of fenoxaprop-ethyl by fluorescent Pseudomonas strains. *J. Agric. Food Chem.* **1998**, *46* (11), 4759−4765.

(16) Kurihara, N.; Miyamoto, J.; Paulson, G. D.; Zeeh, B.; Skidmore, M. W.; Hollingworth, R. M.; Kuiper, H. A. Chirality in synthetic agrochemicals: bioactivity and safety consideration. *Pure Appl. Chem.* **1997**, *69* (9), 2007−2025.

(17) Wiberg, K.; Letcher, R. J.; Sandau, C. D.; Norstrom, R. J.; Tyskind, M.; Bidleman, T. F. The enantioselective bioaccumulation of chiral chlordane and α-HCH contaminants in the polar bear food chain. *Environ. Sci. Technol.* **2000**, *34*, 2668−2674.

(18) Müller, M. D.; Poiger, T.; Buser, H. R. Isolation and identification of the metolachlor stereoisomers using high-performance liquid chromatography, polarimetric measurements, and enantioselective gas chromatography. *J. Agric. Food Chem.* **2001**, *49*, 42−49.

(19) Diao, J. L.; Lv, C. G.; Wang, X. Q.; Dang, Z. H.; Zhu, W. T.; Zhou, Z. Q. Influence of soil properties on the enantioselective degradation of the herbicide lactofen in soils. *J. Agric. Food Chem.* **2009**, *57*, 5865−5871.

(20) Müller, M. D.; Buser, H. R. Conversion reactions of various phenoxyalkanoic acid herbicides in soil. 1. Enantiomerization and enantioselective degradation of the chiral 2- phenoxyal-kanoic acid herbicides. *Environ. Sci. Technol.* **1997**, *31*, 1953−1959.

(21) Wink, O.; Luley, U. Enantioselective transformation of the herbicides diclofop-methyl and fenoxaprop-ethyl in soil. *Pestic. Sci.* **1988**, *22* (1), 31−40.

(22) Garrison, A. W. Probing the enantioselectivity of chiral pesticides. *Environ. Sci. Technol.* **2006**, *40*, 16−23.

(23) Moon, J. K.; Keum, Y. S.; Hwang, E. C.; Park, B. S.; Chang, H. R.; Li, Q. X.; Kim, J. H. Hapten syntheses and antibody generation for a new herbicide, metamifop. *J. Agric. Food Chem.* **2007**, *55* (14), 5416−5422.

(24) Buerge, I. J.; Poigner, T.; Müller, M. D.; Buser, H. R. Influence of pH on the stereoselective degradation of the fungicides epoxiconazole and cyproconazole in soils. *Environ. Sci. Technol.* **2006**, *40*, 5443−5450.

(25) Jones, W. J.; Mazur, C. S.; Kenneke, J. F.; Garrison, A. W. Enantioselective microbial transformation of the phenylpyrazole insecticide fipronil in anoxic sediments. *Environ. Sci. Technol.* **2007**, *41*, 8301−8307.

Received for review September 15, 2010. Revised manuscript received November 11, 2010. Accepted November 15, 2010. This work was supported by the National Natural Science Foundation of China (Contract Grant No. 20707038).

COR-AAD1-00003742
Bayer EX1008 (Part 7 of 9)

JOURNAL OF AGRICULTURAL AND FOOD CHEMISTRY

pubs.acs.org/JAFC

Rapid Biodegradation of the Herbicide 2,4-Dichlorophenoxyacetic Acid by *Cupriavidus gilardii* T-1

Xiangwei Wu, Wenbo Wang, Junwei Liu, Dandan Pan, Xiaohui Tu, Pei Lv, Yi Wang, Haiqun Cao, Yawen Wang, and Rimao Hua*

College of Resources and Environment, Key Laboratory of Agri-food Safety of Anhui Province, Anhui Agricultural University, Hefei 230036, People's Republic of China

Supporting Information

ABSTRACT: Phytotoxicity and environmental pollution of residual herbicides have caused much public concern during the past several decades. An indigenous bacterial strain capable of degrading 2,4-dichlorophenoxyacetic acid (2,4-D), designated T-1, was isolated from soybean field soil and identified as *Cupriavidus gilardii*. Strain T-1 degraded 2,4-D 3.39 times more rapidly than the model strain *Cupriavidus necator* JMP134. T-1 could also efficiently degrade 2-methyl-4-chlorophenoxyacetic acid (MCPA), MCPA isooctyl ester, and 2-(2,4-dichlorophenoxy)propionic acid (2,4-DP). Suitable conditions for 2,4-D degradation were pH 7.0−9.0, 37−42 °C, and 4.0 mL of inoculums. Degradation of 2,4-D was concentration-dependent. 2,4-D was degraded to 2,4-dichlorophenol (2,4-DCP) by cleavage of the ether bond and then to 3,5-dichlorocatechol (3,5-DCC) via hydroxylation, followed by ortho-cleavage to *cis*-2-dichlorodiene lactone (CDL). The metabolites 2,4-DCP or 3,5-DCC at 10 mg L^{-1} were completely degraded within 16 h. Fast degradation of 2,4-D and its analogues highlights the potential for use of *C. gilardii* T-1 in bioremediation of phenoxyalkanoic acid herbicides.

KEYWORDS: *2,4-D, biodegradation, Cupriavidus gilardii, phenoxyalkanoic acid herbicide, degradation pathway, degradation rate*

Downloaded via CORTEVA AGRISCIENCE on September 11, 2020 at 01:57:51 (UTC).
See https://pubs.acs.org/sharingguidelines for options on how to legitimately share published articles.

INTRODUCTION

2,4-Dichlorophenoxyacetic acid (2,4-D), a phenoxyalkanoic acid (PAA) herbicide, was first synthesized in 1941 and commercially marketed in the United States in 1944.[1] 2,4-D has been widely and intensively used for controlling some annual and perennial broad-leaved weeds in wheat, corn, cotton, soybean, and tobacco crops and nonagricultural soils.[2−4] However, this widespread and frequent application of 2,4-D might cause several toxicological, environmental contamination, and human health problems[5] and give rise to the emergence of herbicide-resistant weeds.[6,7] Despite its short half-life in soils or aquatic environment, 2,4-D has been frequently detected in soil, groundwater, and surface water at concentrations ranging from several to hundreds of micrograms per liter.[8−11]

A variety of toxic effects caused by 2,4-D have been reported. Previous studies have suggested that 2,4-D might influence the physiological and behavioral consequence of aquatic organisms[12] and be associated with gastric cancer, myocardial infarction, and type 2 diabetes in humans.[13,14] Also, 2,4-D may influence soil microbial communities by altering the balance between microbial populations.[5,15] In China, 2,4-D is mainly used to protect cereal crops at dosages ranging from 0.8 kg of active ingredient (ai) per hectare (ha^{-1}) to 1.5 kg ai ha^{-1}. The intensive use of 2,4-D in agriculture would lead to a negative effect on the environment such as pollutions of water and soil.[16] Although 2,4-D has a moderate persistence with relatively short half-lives in soils,[17] it is a potential surface water and groundwater contaminant due to its relatively high water solubility and low sorption by soils, accentuating the importance of 2,4-D-degrading bacteria in water and soil.[18] Therefore, biodegradation utilizing bacterial strains for efficient detoxification or removal of 2,4-D residues has attracted increasing attention for safe uses of 2,4-D and remediation of its pollution.

The predominant degradation of 2,4-D is caused by microbial action in soil.[19] At present, a variety of microorganisms capable of degrading 2,4-D have been isolated from various environments,[3] and most of them belong to the class of Proteobacteria.[20] Most of the 2,4-D-degrading bacteria are composed of various genera that belong to beta-proteobacteria and gamma-proteobacteria.[3,21] Those genera include *Achromobacter, Bordetella, Burkholderia, Cupriavidus, Delftia, Flavobacterium, Halomonas, Pseudomonas, Rhodoferax,* and *Variovorax*.[18,22−24] Furthermore, a few bacteria are members of genera belonging to alpha-proteobacteria, which contain the genera *Bradyrhizobium* and *Sphingomonas*.[24,25] These genera harbor *tfdA*-like genes (*tfdA* or *tfdA*α) or *cadAB* genes, which could express related enzymes to catalyze the degradation of PAA herbicides.[18] *Cupriavidus necator* JMP134 is a well-characterized 2,4-D-degrading bacteria and used as a model for the study of PAA herbicide biodegradation.[26] *C. necator* JMP134, formerly known as *Alcaligenes eutrophus, Ralstonia eutropha,* and *Waustersia eutropha*,[27] has a plasmid pJP4 containing the *tfd* gene cluster (*tfdABCDEF* genes), which can encode various enzymes for 2,4-D biodegradation.[3,26] *C. necator* JMP134 could degrade 70% of 2,4-D at 250 mg L^{-1} in 10 days, and its degradation rate was 17.5 mg L^{-1} day^{-1}.[28]

Although numerous strains have been reported to degrade 2,4-D, it would be still valuable for acquiring novel and fast

Received: February 4, 2017
Revised: April 19, 2017
Accepted: April 23, 2017
Published: April 24, 2017

ACS Publications © 2017 American Chemical Society

DOI: 10.1021/acs.jafc.7b00544
J. Agric. Food Chem. 2017, 65, 3711−3720

COR-AAD1-00003743
Bayer EX1008 (Part 7 of 9)

degradation strains as optional resources to detoxify 2,4-D in contamination sites. The aims of this study were to (i) isolate a highly efficient 2,4-D-degrading bacterium; (ii) evaluate the effects of pH, temperature, substrate concentration, and inoculation amount on 2,4-D biodegradation; (iii) assess its degradation capacity in soil and enzyme activity in solution; and (iv) elucidate the metabolic pathway of 2,4-D.

MATERIALS AND METHODS

Chemicals. 2,4-D (purity = 99.9%), 2,4-DCP (purity = 99.5%), 3,5-DCC (purity = 99.9%), 2,4-D sodium salt (purity = 98.5%), 2,4-D isooctyl ester (purity = 93.0%), MCPA (purity = 99.5%), MCPA isooctyl ester (purity = 95.0%), 2,4-DP (purity = 99.5%), 2,4-dichlorophenoxybutyric acid (2,4-DB) (purity = 99.0%), and 2,4,6-trichlorophenol (purity = 98.5%) were purchased from Dr. Ehrenstorfer GmbH, Augsburg, Germany. All other chemicals and solvents were of analytical or HPLC grade.

Enrichment and Isolation of 2,4-D-Degrading Bacteria. Soil samples used for isolating 2,4-D-degrading bacteria in this study were collected from a soybean field that had been spayed with 2,4-D over 10 years in Linyi, Shandong province, China. Mineral salt medium (MSM) consisted of 0.4 g L^{-1} of $MgSO_4{\cdot}7H_2O$, 0.002 g L^{-1} of $FeSO_4{\cdot}7H_2O$, 0.2 g L^{-1} of K_2HPO_4, 0.2 g L^{-1} of $(NH_4)_2SO_4$, 0.08 g L^{-1} of $CaSO_4$, and 1000 mL of deionized water at pH 7.0.[29] Ten gram soil samples were added to a 250 mL Erlenmeyer flask containing 100 mL of MSM, which was supplemented with 200 mg L^{-1} of 2,4-D as sole carbon and energy sources. The mixture was shaken and incubated at 30 °C and 150 rpm on a rotary shaker. After 7 days, 10 mL of the culture was transferred into a fresh MSM containing 2,4-D (40 mg L^{-1}) and incubated for 7 days under the same conditions described as above. Such an enrichment process was repeated three times in fresh MSM with the concentrations of 2,4-D increasing from 40 to 100 mg L^{-1}, and then the culture was dilution-plated and spread onto sterilized MSM agar plates containing 200 mg L^{-1} of 2,4-D and incubated at 30 °C in the dark. After incubation for 7 days, single colonies in the MSM plates containing 2,4-D were picked aseptically and tested for their degradation ability for the herbicide 2,4-D. Bacterial strain T-1 for degrading 2,4-D was obtained from these colonies formed on the plates and used to carry out further studies.

Identification of Bacterial Strain. To identify strain T-1, experiments including morphological observation, physico-biochemical tests, and 16S rRNA gene sequence analysis were performed. Strain T-1 grew in Luria−Bertani (LB) liquid medium for 20 h at 30 °C, and the cells were fixed by glutaraldehyde and freeze-dried, followed by morphological observation under a scanning electron microscope (SEM) (S-4800, Hitachi, Tokyo, Japan). Physico-biochemical characteristics were assayed by the Institute of Microbiology, Chinese Academy of Science (Beijing, China), according to the methods described by Dong and Cai.[30] The genomic DNA of strain T-1 was extracted using Tiangen Bacteria DNA Kit (Tiangen Biotech Co. Ltd., Beijing, China) according to the manufacturer's instructions. The 16S rRNA gene was amplified through polymerase chain reaction (PCR) using universal bacterial primers according to the method described by Liu et al.[29] 16S rRNA gene sequences were sequenced by Invitrogen Biotechnology Co. Ltd., (Shanghai, China). Assembled 16S rRNA gene sequences of strain T-1 were compared with that in the public domain through a BLAST search tool of NCBI.[31] Phylogenetic tree analysis was constructed using the neighbor-joining method with MEGA6.0 software.[32]

Inoculum Preparation. Strain T-1 was precultured overnight (24 h) in LB medium at 30 °C and 150 rpm on a rotary shaker. The cells were harvested after centrifugation (3380g, 10 min) and then immediately washed three times (3 × 20 mL) with sterilized MSM. The cells of T-1 were resuspended with MSM at pH 7.0. For all degradation experiments, the density of cells was adjusted to an OD_{600} of 0.6 (1.8×10^8 cfu mL^{-1}) determined by UV-1800 (Shimadzu Corp., Kyoto, Japan).

Biodegradation of 2,4-D by Strain T-1 in MSM. To assess the biodegradation of 2,4-D by strain T-1, MSM was supplemented with 2,4-D as the sole carbon and energy source. Each flask was inoculated with 0.5 mL suspensions of strain T-1 (OD_{600} = 0.6). All flasks were shaken at 150 rpm and 30 °C. For the control, the flask uninoculated T-1 was performed under the same conditions as described above. Each treatment and control were carried out in triplicate. At regular time intervals, the whole cultures were collected, followed by the addition of 20 mL of methanol. After sonication for 1 min, the mixture was transferred to a 50 mL volumetric flask and finally adjusted to 50 mL with 50% aqueous methanol. The solution was filtered through a 0.22 μm membrane prior to the analysis of 2,4-D residue.

The effect of the initial concentration of 2,4-D in MSM on the biodegradation of 2,4-D was tested at levels of 10−350 mg L^{-1}. Effects of temperature on 2,4-D biodegradation were evaluated at 20, 25, 30, 37, and 42 °C. The solution of MSM was adjusted with buffers (0.2 mol L^{-1} NaH_2PO_4 and Na_2HPO_4) at pH 5, 6, 7, 8, and 9 for the measurement of pH effect on the biodegradation of 2,4-D. Effects of inoculation volumes on 2,4-D biodegradation were examined with various amounts of cell suspensions (0.2, 0.5, 1.0, 2.0, and 4.0 mL of culture, OD_{600} = 0.6).

Biodegradation of Other PAA Herbicides. An aliquot of 0.5 mL of bacteria cell suspensions (OD_{600} = 0.6) was inoculated into 20 mL of MSM containing each 50 mg L^{-1} 2,4-D sodium salt, 2,4-D isooctyl ester, MCPA, MCPA isooctyl ester, 2,4-DP, 2,4-DB, or 2,4,6-trichlorophenol, followed by incubation at 30 °C in a rotary shaker at 150 rpm. After 4 and 7 days, the samples were taken for determination. All treatments were prepared separately in triplicate, and the controls were not inoculated with cell suspensions of T-1.

Determination of 2,4-D and Other PAA Herbicides. An aliquot of 20 mL of methanol was added to the above culture sample. The mixture was sonicated for 1 min, followed by adjustment of the volume to 50 mL for the analysis by a Waters Alliance e2695 high-performance liquid chromatograph (HPLC) equipped with a 2489 ultraviolet detector (Waters Co., Milford, MA, USA). 2,4-D, 2,4-DCP, 3,5-DCC, 2,4-D sodium salt, 2,4-DP, MCPA, 2,4-D isooctyl ester, MCPA isooctyl ester, 2,4-DB, and 2,4,6-trichlorophenol were detected with HPLC. The chromatographic separation was achieved on an Agilent Eclipse Plus C_{18} column (5 μm, 4.6 mm × 250 mm) at 40 °C. The flow rate was 1.0 mL min^{-1} with 60% aqueous acetonitrile (containing 0.5% acetic acid) as the elution solution except for 2,4-D isooctyl este and MCPA isooctyl ester. The sample injection volume was 20 μL. The detection wavelength was 230 nm. The detection of MCPA isooctyl ester and 2,4-D isooctyl ester was conducted according to the same method as described above besides the proportion of elution solution of 85% aqueous acetonitrile (containing 0.5% acetic acid).

Determination and Identification of 2,4-D Metabolites. An aliquot of 2.5 mL of bacteria cell suspensions (OD_{600} = 0.6) was inoculated in 100 mL of MSM containing 2,4-D (100 mg L^{-1}). After incubation for 0−36 h at 30 °C and 150 rpm, the cultures were extracted according to the following methods: (1) At 4, 8, 10, 12, 16, 20, 24, and 36 h, an aliquot of 2 mL of culture samples was filtered through a 0.22 μm membrane and analyzed on a HPLC and a Waters Acquity ultraperformance liquid chromatograph coupled to a XEVO triple-quadrupole mass spectrometer (UPLC-MS/MS, Waters). (2) After incubation for 8 and 16 h, the whole culture was frozen and dried by an FD5-4 freeze-dryer (SIM International Group Co., Ltd., Los Angeles, CA, USA) and then was dissolved in 5 mL of ethyl acetate or methyl alcohol. The dissolved sample was filtered through a 0.22 μm membrane prior to further analysis with an Agilent 7890B gas chromatograph equipped with an Agilent 7000C triple-quadrupole mass spectrometer (GC-MS/MS, Agilent Technology, Santa Clara, CA, USA) and an Agilent 1290 infinity II UPLC coupled to 6545 quadrupole time-of-flight mass spectrometer (UPLC-QTOFMS, Agilent Technology).

2,4-D metabolites were detected with UPLC-MS/MS. An analytical column (Waters BEH C_{18}, 1.7 μm, 2.1 mm × 100 mm) was used for chromatographic separation with a mobile phase of water containing 0.1% formic acid (A) and methanol (B) at a constant flow rate of 0.3 mL min^{-1}. The gradient elution program was isocratic 10% B for 0.5 min, from 10 to 70% of B over 7.5 min, from 70 to 10% of B over 0.2

DOI: 10.1021/acs.jafc.7b00544
J. Agric. Food Chem. 2017, 65, 3711−3720

COR-AAD1-00003744
Bayer EX1008 (Part 7 of 9)

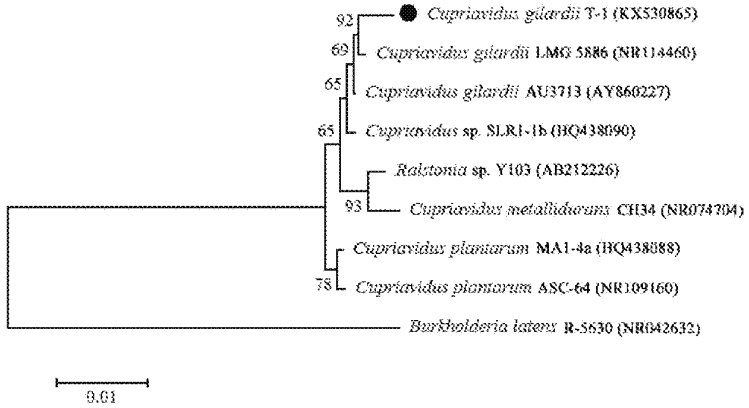


Figure 1. Phylogenetic tree constructed on the basis of 16S rRNA gene sequence of strain T-1 and other related species retrieved from the GenBank database according to neighbor joining. Bootstrap values are based on 1000 repetitions and indicated at branch points (>50%).

min, and 10% for 1.8 min prior to the next injection. The mass spectrometer was operated at electrospray ionization mode, and the scan ranged from m/z 100 to 300. Nitrogen was used as the desolvation and cone gases with 800 and 50 L h^{-1} flow rates, respectively. Desolvation (400 °C) and ion source (150 °C) were kept at constant temperatures. The voltage was 1000 and 21 V for capillary and cone, respectively.

The lyophilized samples were analyzed with GC-MS/MS. An HP-5 MS silica capillary column (0.25 μm, 30 m × 0.25 mm) was selected as the separation column. Helium was used as carrier gas at a flow rate of 1.2 mL min^{-1}. The oven temperature started at 60 °C for 0.5 min, then increased to 200 °C at a rate of 10 °C min^{-1}, held for 1 min, then raised to 280 °C at a rate of 15 °C min^{-1}, and held for 10 min. Interface (280 °C), injector (270 °C), and ion source (280 °C) were kept at constant temperatures. The mass spectrometer was operated with electron ionization (EI) source. Electron ionization energy was set at 70 eV. The MS detector was scanned from m/z 50 to 600.

The lyophilized samples were also analyzed with UPLC-QTOFMS. The analytical conditions of UPLC-QTOFMS were the same as those of UPLC-MS/MS except for some MS parameters. The mass spectrometer was operated with electrospray ionization (ESI) source at negative ion model with a voltage of 3.5 kV. Nitrogen was used as the sheath gas at a flow rate of 11 L min^{-1}, and the temperature was set at 350 °C. The fragmentor and skimmer voltages were set to 100 and 65 V, respectively. The TOF data were collected between m/z 50 and 350.

Biodegradation of the Metabolites 2,4-DCP and 3,5-DCC. An aliquot of 0.5 mL of bacterial cell suspensions (OD_{600} = 0.6) was inoculated in 20 mL of MSM containing 10 mg L^{-1} of 2,4-D, 2,4-DCP, 3,5-DCC, or their mixture. All flasks were incubated in a rotary shaker at 30 °C and 150 rpm in the dark. At certain time intervals, the whole culture was collected for determination of the concentration of 2,4-D, 2,4-DCP, or 3,5-DCC. Each treatment was carried out in triplicate, and the control treatment without T-1 was performed under the same conditions.

Biodegradation of 2,4-D in Soil. Soil used for degradation assays was collected from a field located in Changfeng county, Hefei, China. Surface soil taken from the top layer (0−15 cm) was mixed thoroughly and then passed through a 2 mm sieve to remove stones and debris. The soil was classified as silty clay loam, and its properties were as follows: sand, 25.4%; silt, 51.2%; clay, 24.1%; organic matter content, 4.19%; water-holding capacity, 30.4%; cation-exchange capacity, 18.1 cmol kg^{-1}; total nitrogen, 0.18%; and pH 7.4. Soil samples (0.5 kg dry weight equivalent) were treated with methanol solution of 2,4-D to obtain final concentrations of 10 and 50 mg kg^{-1} of dry soil and left for 1 h on a laminar flow bench for methanol evaporation. The soil samples were inoculated with strain T-1 preparation to give an initial inoculum density of 9.0 × 10^6 cfu g^{-1} soil, mixed thoroughly with a plastic spoon, and passed through a mesh (2 mm) to distribute 2,4-D and T-1 bacteria. Soil samples receiving the same amount of 2,4-D, but without inoculums, were used as controls. Soil water content was adjusted to 60% of water-holding content and maintained constantly by periodic addition of sterile distilled water. Soil samples were transferred to a 1 L conical flask with a stopper and incubated at 30 °C in the dark. Each treatment was performed in triplicate. After incubation for 0, 6, 12, 18, 24, 36, 48, 60, 72, and 96 h, 20 g soil samples from each treatment were taken for analysis of residual 2,4-D.

For determination of 2,4-D concentration in soil, soil samples (5 g) were extracted with 40 mL of 0.04 M NaOH solution for 50 min at 150 rpm on a rotary shaker and sonicated for 10 min. After centrifugation at 3380g for 5 min, 15 mL of the supernatant was transferred to a 50 mL centrifuge tube and adjusted to pH 3 with 85% phosphoric acid. Subsequently, 20 mL of ethyl acetate and 5 g of NaCl were added to the centrifuge tube. The mixtures were sonicated for 20 min and centrifuged at 3380g for 5 min. The ethyl acetate phase was collected, concentrated to dryness, and finally dissolved in 5 mL of methanol/water (1:1, v/v). The mean recoveries of fortified 2,4-D in soil at 0.05, 1, 10, and 50 mg kg^{-1} varied from 94 to 96% with a relative standard deviation (RSD) ≤7%. These data indicated that the method was satisfactory for the analysis of 2,4-D in soil.

Degradation of 2,4-D by Crude Enzyme. For the preparation of crude enzyme, cells of T-1 pregrown for 24 h in LB medium were exposed to 2,4-D at a concentration of 200 mg L^{-1} in MSM for 8 h at 30 °C for enzyme induction. The cells were collected by centrifugation (3380g, 10 min) at 4 °C and then immediately washed three times (3 × 20 mL) with sterilized phosphate buffer solution (PBS, 50 mM NaH_2PO_4−Na_2HPO_4, pH 7.0). The wet cells (1 g) were resuspended in 15 mL of PBS. Extraction of extracellular and intracellular crude enzymes of T-1 cells was referred to the method reported by Liu et al.[25] The cell debris containing membrane-bound enzymes was resuspended in 15 mL of PBS and kept at 4 °C for later use. The activities of different crude enzymes were determined by analyzing the amount of 2,4-D degraded. One unit of enzyme activity was defined as the amount of enzyme resulting in the degradation of 1 μmol of 2,4-D per minute at 30 °C.

To determine the effects of α-ketoglutarate (α-KG) and Fe^{2+} on enzyme activity, 0.5 mL of crude enzymes (extracellular, intracellular, or membrane-bound enzymes) was added to 2.5 mL of PBS containing 2,4-D, and the concentration of 2,4-D in mixed solution was 0.226 mM. The enzyme activities of the mixed solution were examined in the presence of 1 mM α-KG or 1 mM Fe^{2+} or with both compounds in comparison with no α-KG and Fe^{2+} as the control. Each treatment was performed in triplicate.

After incubation for 5 min at 30 °C, the enzyme reaction was stopped by the addition of 0.2 mL of hydrochloric solution (1 mM). Methanol (3 mL) was added to the culture sample, followed by sonication for 1 min. 2,4-D residues were determined according to the method described above.

DOI: 10.1021/acs.jafc.7b00544
J. Agric. Food Chem. 2017, 65, 3711−3720

COR-AAD1-00003745
Bayer EX1008 (Part 7 of 9)

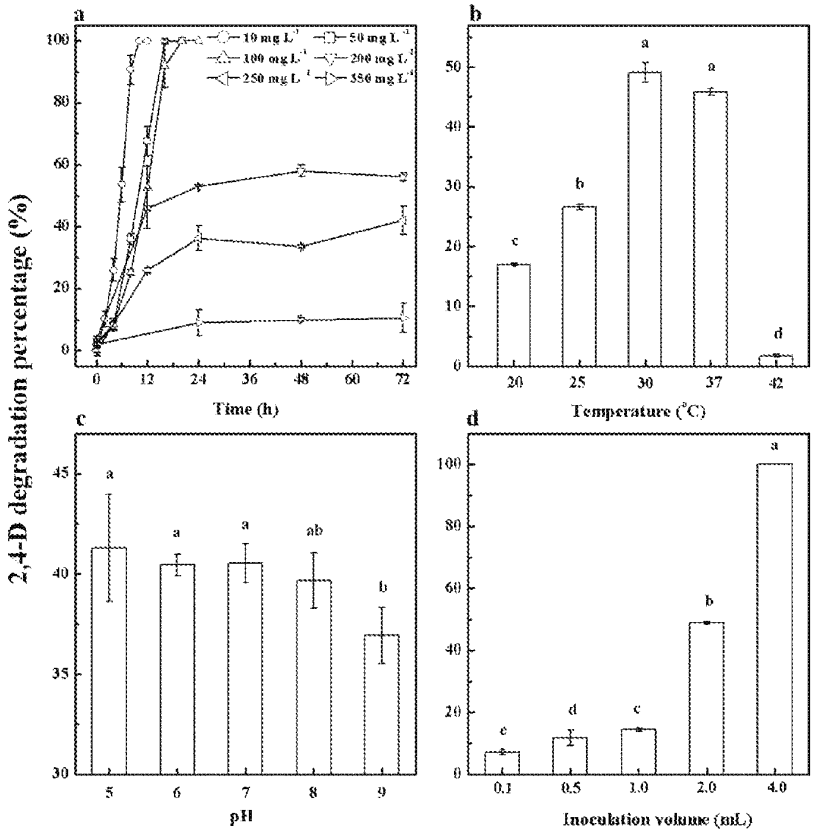


Figure 2. Effects of initial 2,4-D concentration (a), temperature (b), pH (c), and inoculation volume (d) on biodegradation of 2,4-D by strain T-1 in MSM. All values represent the mean ± standard deviation of triplicate samples.

Calculation and Statistical Analysis. The degradation percentage and degradation rate were calculated from eqs 1 and 2

$$X = \frac{C_{ck} - C_t}{C_{ck}} \times 100\% \quad (1)$$

$$V = \frac{C_{ck} - C_t}{t} \quad (2)$$

where X (%) is the degradation percentage of 2,4-D, V (mg L^{-1} h^{-1}) is the degradation rate of 2,4-D, C_{ck} and C_t are control concentration and treatment residual concentration (mg L^{-1}) of 2,4-D, respectively, and t is the culture time.

All treatments were performed in triplicate, and arithmetic averages were taken throughout the data analysis and calculation. The data were calculated using Excel (Microsoft 2010, USA) and then analyzed with the SPSS 19.0 software package (SPSS Inc., USA) and Origin 8.0 software (OriginLab Co., USA). The statistical significance was determined at $p < 0.05$.

RESULTS

Identification and Characterization of Strain T-1. Bacterial strain T-1 capable of utilizing 2,4-D as single carbon and energy source was isolated from a soil sample. T-1 is a Gram-negative, aerobic, and rod-shaped bacterium with the size of 0.25−0.35 μm × 0.85−0.95 μm (Figure S1). The colony morphology of T-1 on LB plate is light yellow, smooth, round, wet, and eminentia. It showed positive results in catalase, citrate utilization, and V.P test, whereas negative results in tests for methyl red, urease, and oxidase. It can hydrolyze arginine, pectin, and citrate, but cannot hydrolyze gelatin, starch, and casein. It can survive 4% of NaCl and utilize dextrin and lactate, but cannot utilize glucose and sucrose. The characteristics of T-1 are consistent with those of *C. gilardii*. The 16S rRNA gene sequence of T-1 (1347 bp) had been deposited in the NCBI GenBank database under accession no. KX530865. The 16S rRNA gene sequence alignment and phylogenetic tree analysis revealed that strain T-1 had 99% homology with *C. gilardii* (Figure 1). Therefore, strain T-1 was proposed to be *C. gilardii* T-1 on the basis of its 16S rRNA gene sequence analysis and morphological, physiological, and biochemical characteristics. It has been deposited in the China General Microbiological Culture Collection Center (CGMCC, no. 11179), Beijing, China.

Effect of 2,4-D Concentration on Its Biodegradation. Effects of 2,4-D concentrations at 10−350 mg L^{-1} on its biodegradation by strain T-1 were investigated in MSM at pH 7.0 and 30 °C (Figure 2a). In all controls without strain T-1, the 2,4-D concentrations remained unchanged during the experiment period. After incubation for 24 h, the degradation percentages of 2,4-D were approximately 100, 100, 100, 53.1, 36.3, and 9.0% at levels of 10, 50, 100, 200, 250, and 350 mg L^{-1}, respectively. The results showed that strain T-1 could rapidly degrade 2,4-D at concentrations of 10, 50, and 100 mg L^{-1}, and complete degradation of 2,4-D occurred at 10, 16, and 20 h, respectively. However, approximately 58.1, 33.6, and 10.0% of 2,4-D at concentrations of 200, 250, and 350 mg L^{-1} was degraded at 48 h, respectively, and then the degradation of

DOI: 10.1021/acs.jafc.7b00544
J. Agric. Food Chem. 2017, 65, 3711−3720

COR-AAD1-00003746
Bayer EX1008 (Part 7 of 9)

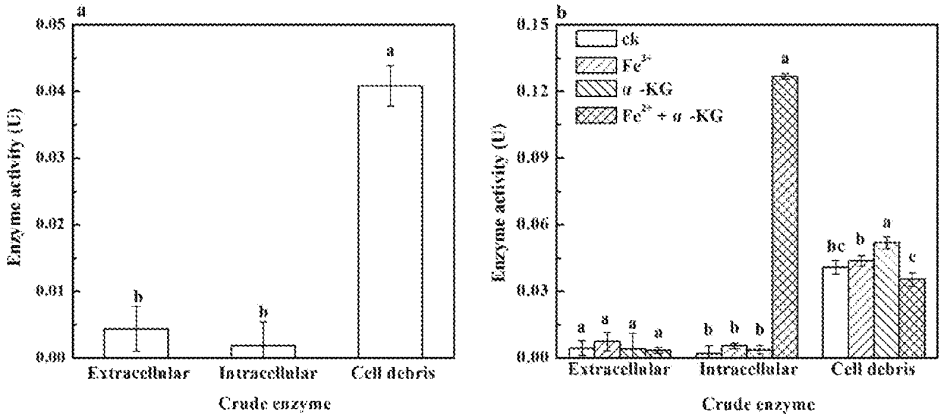


Figure 3. Enzyme activities of 2,4-D-degrading crude enzymes of strain T-1: (a) in the absence of Fe^{2+} and α-ketoglutarate (α-KG); (b) in the presence of Fe^{2+} or α-KG or with both Fe^{2+} and α-KG. Different letters above the bars indicate the values are significantly different ($p \leq 0.05$).

2,4-D was almost unchanged after 48 h. This indicated that the concentrations of 2,4-D ranging from 200 to 350 mg L^{-1} could inhibit the degradation capacity of strain T-1. The degradation inhibition might be caused by the toxicity of high concentrations of 2,4-D or their metabolites to strain T-1.

Effect of Temperature on 2,4-D Biodegradation. Effects of temperature (20−42 °C) on biodegradation of 50 mg L^{-1} 2,4-D in MSM (pH 7.0) are shown in Figure 2b. In all controls, the degradation percentages of 2,4-D were <0.5%. The degradation rates of 2,4-D were 0.86, 1.3, 2.5, 2.3, and 0.090 mg L^{-1} h^{-1} at 20, 25, 30, 37, and 42 °C after inoculation for 10 h, respectively. By contrast, the degradation percentages were >45% at temperatures between 30 and 37 °C after 10 h of inoculation. However, the degradation percentage was 1.8% at 42 °C, because the degradation ability of strain T-1 to 2,4-D could be inhibited at 42 °C. The degradation percentages of 2,4-D by strain T-1 at 30 and 37 °C were higher than those at the other temperatures ($p < 0.05$). Therefore, the optimal temperature for degrading 2,4-D by T-1 was 30−37 °C.

Effect of pH on 2,4-D Biodegradation. The biodegradation of 2,4-D of 50 mg L^{-1} in MSM of pH 5, 6, 7, 8, and 9 is revealed in Figure 2c. In all controls, the degradation percentages of 2,4-D were <2.4%. After incubation for 12 h, >36% of 2,4-D was removed at pH 5−9. The biodegradation rates of 2,4-D were 1.70, 1.68, 1.65, 1.64, and 1.53 mg L^{-1} h^{-1} at pH ranging from 5 to 9, respectively. The degradation percentage of 2,4-D by strain T-1 at pH 9 was lower than that at other pH values ($p < 0.05$). This indicated that the optimal pH range for 2,4-D degradation was 5−8.

Effect of Inoculation Volume on 2,4-D Biodegradation. The effect of inoculation volume on biodegradation of 50 mg L^{-1} 2,4-D in MSM at 30 °C and pH 7.0 is presented in Figure 2d. The degradation rates of 2,4-D were 0.45, 0.74, 1.5, 3.0, and 6.2 mg L^{-1} h^{-1} after incubation for 8 h when cell suspension volumes of T-1 were 0.2, 0.5, 1.0, 2.0, and 4.0 mL (OD_{600} = 0.6), respectively. The degradation rates increased with inoculation volumes ranging from 0.2 and 4.0 mL. The degradation rate constants were linearly related to the inoculation volumes increasing from 0.2 and 4.0 mL.

Degradation of 2,4-D by Strain T-1 in Soil. Biodegradation of 2,4-D was further investigated using soil microcosms inoculated with strain T-1. Approximately 21% of 2,4-D at an initial concentration of 50 mg kg^{-1} dissipated in the control soil without inoculation with T1 after incubation for 96 h because of biotic and abiotic factors (Figure S2a). A high content of soil organic matter (4.19%) may be responsible for the relatively rapid disappearance of 2,4-D in the control soil because a portion of 2,4-D applied to soil binds to the organic matter matrix and becomes nonextractable. Complete degradation of 2,4-D at 50 mg kg^{-1} occurred within 96 h in soil inoculated with T-1, and the degradation process could be described by pseudo-first-order kinetics. The degradation half-life ($T_{1/2}$) of 2,4-D at 50 mg kg^{-1} was 13.9 h in soil inoculated with T1. Similarly, approximately 98.0% of 2,4-D at 10 mg kg^{-1} was degraded within 36 h in soil inoculated with T-1, and the $T_{1/2}$ was 6.3 h (Figure S2b). The results revealed that strain T-1 had a strong potential for bioremediation of 2,4-D-contaminated soil.

2,4-D-Degrading Enzyme. The activity of 2,4-D degradation by crude enzymes was observed in the cell debris of T-1, whereas no activity was found in extracellular and intracellular crude enzymes (Figure 3a). Therefore, membrane-bound enzyme in cell debris may be responsible for 2,4-D degradation. A similar result was reported by Jaremko and Yu,[33] who showed the organic acid was converted by membrane-bound crude enzymes.

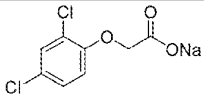
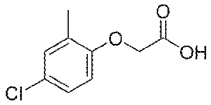
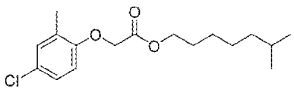
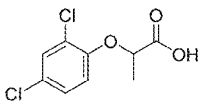
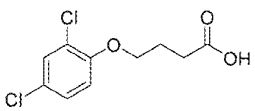
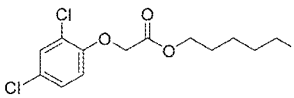
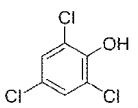
A previous study showed the 2,4-D-degrading enzyme involved in α-KG-dependent dioxygenase and Fe^{2+} was an important cofactor of 2,4-D dioxygenase.[34] The results for enzyme activity assays in the presence of α-KG or Fe^{2+} or with both compounds are shown in Figure 3b. The influence of different compounds on extracellular enzyme activities, including three treatments (α-KG, Fe^{2+}, and a mixture of α-KG and Fe^{2+}), was evaluated. Compared to the control, there was no significant difference in extracellular enzyme activities, suggesting extracellular enzyme had no 2,4-D degradation activity under three treatments. Similarly, with the addition of α-KG or Fe^{2+}, intracellular enzyme activities had no significant increase in comparison to the control. However, intracellular enzyme activity increased significantly from 0.002 to 0.127 U with the application of the combination of 1 mM α-KG and 1 mM Fe^{2+}. This indicated the 2,4-D-degrading intracellular enzyme was α-KG-dependent and required Fe^{2+} to degrade 2,4-D. With regard to membrane-bound enzyme, no obvious difference in enzyme activity was found between the control and the treatment (addition of a mixture of α-KG and Fe^{2+}).

It can be concluded that the intracellular and membrane-bound enzymes are involved in the biodegradation of 2,4-D.

DOI: 10.1021/acs.jafc.7b00544
J. Agric. Food Chem. 2017, 65, 3711−3720

COR-AAD1-00003747
Bayer EX1008 (Part 7 of 9)

Table 1. Degradation of Other PAA Compounds by StrainT-1

Compound	Structure	Degradation percentage (%) [a]	
		4 days	7 days
2,4-D sodium salt		100.0 ± 0.0	100.0 ±0.0
MCPA		93.3 ± 0.2	99.7 ± 0.0
MCPA isooctyl ester		20.0 ± 0.4	37.4 ± 1.4
2,4-DP		7.5 ± 0.0	12.7 ± 0.3
2,4-DB		-0.6 ± 0.4	-2.2 ± 0.4
2,4-D isooctyl ester		-0.2 ± 1.4	3.8 ± 0.1
2,4,6-trichlorophenol		-4.3 ± 0.7	-1.6 ± 0.4

[a]Values indicate means of triplicate samples and standard deviation (SD).

Also, Fe^{2+} and α-KG were essential to degrade 2,4-D by the intracellular enzymes.

Biodegradation of Other PAA Herbicides by Strain T-1. Strain T-1 could degrade 100% of 2,4-D sodium salt, 99.7% of MCPA, 37.4% of MCPA isooctyl ester, and 12.7% of 2,4-DP in MSM containing 50 mg L^{-1} of each substrate after incubation for 7 days (Table 1). Strain T-1 could rapidly degrade 2,4-D sodium salt and MCPA and could also degrade MCPA isooctyl ester and 2,4-DP, but could not degrade 2,4-DB, 2,4,6-trichlorophenol, and 2,4-D isooctyl ester.

Identification and Degradation of 2,4-D Metabolites. During the degradation of 2,4-D by strain T-1, after incubation for 16 h, two metabolites of 2,4-D (100 mg L^{-1}), namely, 2,4-DCP and 3,5-DCC, were identified and analyzed by HPLC according to the standards (Figure 4). At the same time, after incubation for 8 and 16 h, three metabolites from 2,4-D were identified with mass ion at m/z of 161.90 (EI^+) by GC-MS/MS, 176.68 (ESI^-, M − 1) by UPLC-MS/MS, and 172.9653 (ESI^-, M − 1) by UPLC-QTOFMS (Figure S3a–c). Compared to the reference standards and reported 2,4-D degradation pathway, these metabolites were identified to be 2,4-DCP, 3,5-DCC (Figure 4 and Figure S3a,b), and CDL (Figure S3c).

The degradation percentage of 2,4-D by strain T-1 was 97.8% at a concentration of 100 mg L^{-1} in 100 mL MSM, and the growth (OD_{600}) of strain T-1 reached a maximum at 20 h (Figure 5a). Because 2,4-D had been degraded completely by strain T-1, the density (OD_{600}) of strain T-1 decreased gradually after incubation for 20 h (Figure 5a). However, the concentrations of two 2,4-D metabolites (2,4-DCP and 3,5-DCC) were <0.5 mg L^{-1} (data not shown) at different incubation times. This result indicated that the degradations of the two metabolites were too fast and thus were hardly accumulated in the degradation system. Such small amounts of 2,4-D metabolites prompted us to further investigate the degradation of the two metabolites (2,4-DCP, 3,5-DCC) by strain T-1.

DOI: 10.1021/acs.jafc.7b00544
J. Agric. Food Chem. 2017, 65, 3711−3720

COR-AAD1-00003748
Bayer EX1008 (Part 7 of 9)

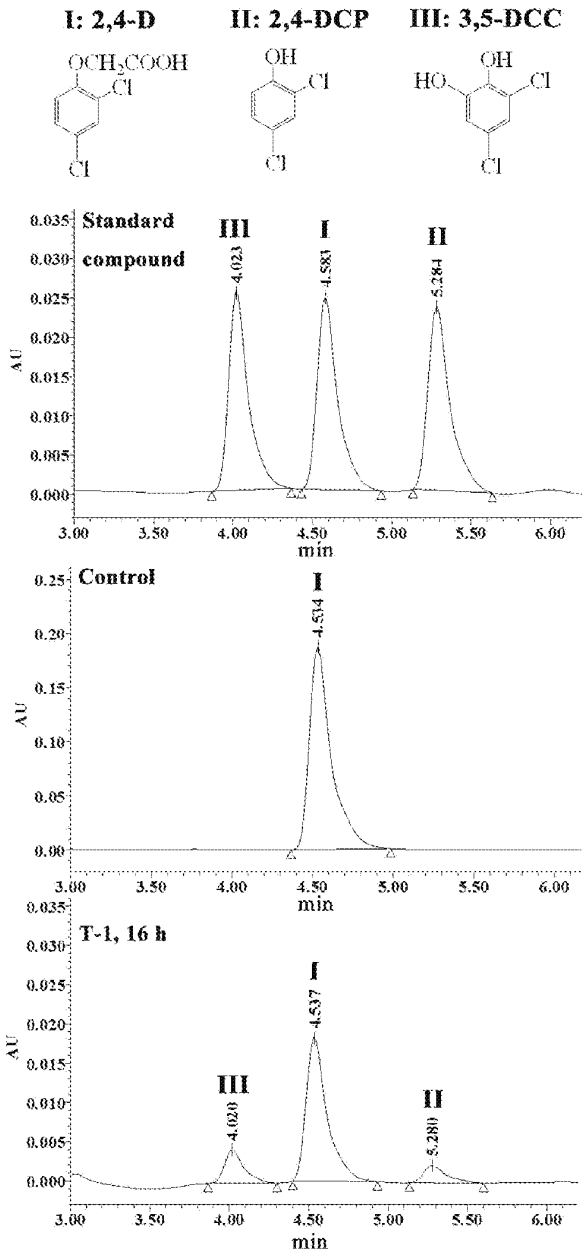


Figure 4. HPLC chromatograms of standard compounds, control, and degradation culture extracts of strain T-1 after incubation for 16 h.

The two metabolites (2,4-DCP, 3,5-DCC) can also be degraded by strain T-1. After incubation for 8 h, 90.6% of 2,4-D, 98.3% of 2,4-DCP, and 9.2% of 3,5-DCC at 10 mg L^{-1} of each compound inoculated in MSM alone were removed by strain T-1, respectively (Figure 5b). The complete degradation times of 2,4-D, 2,4-DCP, and 3,5-DCC at 10 mg L^{-1} were 10, 8, and 16 h, respectively. However, when these three compounds were mixed in MSM, they were degraded simultaneously and the degradation percentages of 2,4-D, 2,4-DCP, and 3,5-DCC were respectively 56.0, 99.4, and 89.1% at 10 mg L^{-1} of each compound after incubation for 12 h (Figure 5c). These results indicated that the degradation of each compound was more significant than that of the mixture of three compounds and that degradation rates were different between single compounds and the mixture.

Degradation Pathway of 2,4-D by Strain T-1. The degradation pathway of 2,4-D by strain T-1 was studied by metabolite analysis and identification. The degradation pathway of 2,4-D is proposed in Figure 6, where 2,4-D underwent decarboxymethylation to form 2,4-DCP. 2,4-DCP was then degraded to 3,5-DCC via a hydrolysis pathway. 3,5-DCC followed by ortho-cleavage of the catechol ring to CDL, and CDL formed presumably through hydrolysis reaction to CMA. CMA might participate in the tricarboxylic acid cycle and finally mineralized 2,4-D.

DISCUSSION

In this study, a new bacterial strain, T-1, capable of using 2,4-D as the sole carbon and energy sources was isolated and identified as *C. gilardii*. Up to now, a number of bacterial strains utilizing 2,4-D have been reported, such as *A. xylosoxidans* EST4002,[23] *Arthrobacter* sp.,[35] *Bradyrhizobium* sp. HW13,[36] *B. elkanii* USDA94,[37] *Burkholderia cepacia* DS-1,[17] *C. necator* JMP134,[28] *C. campinensis* BJ71,[38] *Cupriavidus* sp. TFD33,[39] *Novosphingobium* DY4,[40] *Pseudomonas* sp. NJ10,[41] *P. cepacia* DBO1,[42] *P. aeruginosa* NJ15,[43] *S. paucimobilis* DS-3,[17] and *V. paradoxus* TV1.[43] The degradation capacities of these 2,4-D-degrading bacteria have been well documented in previous literature.

The degradation rates of 2,4-D by the isolate strain T-1 were increased with increasing concentrations (10−100 mg L^{-1}). The degradation rate of strain T-1 at a concentration of 50 mg L^{-1} was 18.8 times greater than that of three other strains (*B. cepacia* DS-1, *Pseudomonas* sp. DS-2, and *S. paucimobilis* DS-3). For the concentration of 2,4-D at 200 mg L^{-1}, the degradation rate of 2,4-D by T-1 was approximately 1.5 times that of *C. campinensis* BJ71 and approximately 2.3 times that of *Novosphingobium* DY4. The degradation rate by T-1 to degrade 250 mg L^{-1} of 2,4-D was approximately 4.4 times that of the model 2,4-D-degrading bacterium (*C. necator* JMP134) (Table 2). Thus, strain T-1 manifests a faster degradation capacity in comparison with the other reported 2,4-D-degrading bacteria. Similar to our results, Han et al.[38] reported that the degradation rate of 2,4-D by *C. campinensis* BJ71 was 66.7−78.8 mg L^{-1} day^{-1} with concentrations increasing from 200 to 350 mg L^{-1}. In comparison, the 2,4-D degradation ability of strain T-1 was inhibited when the concentrations of 2,4-D were 200−350 mg L^{-1}. Similarly, Lu et al.[44] reported that the degradation of 3,5,6-trichloro-2-pyridinol (TCP) by *Cupriavidus* sp. DT-1 was inhibited with increasing concentrations of TCP (50−100 mg L^{-1}). Two microbial consortia (*Pseudomonas* sp. YT1 and *Stenotrophomonas maltophilia* YT2) had no effect on the degradation of 2,4-D with increasing concentrations of 2,4-D (50−200 mg L^{-1}) and were able to degrade up to 700 mg L^{-1}; however, both microbial consortia failed to degrade at 800 mg L^{-1}.[45]

The degradation rates of 2,4-D by strain T-1 were increased with temperatures ranging from 20 to 30 °C, whereas the ability of T-1 to degrade 2,4-D was inhibited at 42 °C. A similar result found was that the degradation rates of 2,4-D gradually increased at 22−30 °C, but significantly decreased at 42 °C.[38] The optimum degradation temperature of 2,4-D by microbial consortia (*Pseudomonas* sp. YT1 and *S. maltophilia* YT2) was 30 °C, whereas the microbial consortia could not degrade 2,4-D at 42 °C.[35] The degradation rate of 2,4-D by strain T-1 was not

DOI: 10.1021/acs.jafc.7b00544
J. Agric. Food Chem. 2017, 65, 3711−3720

COR-AAD1-00003749
Bayer EX1008 (Part 7 of 9)

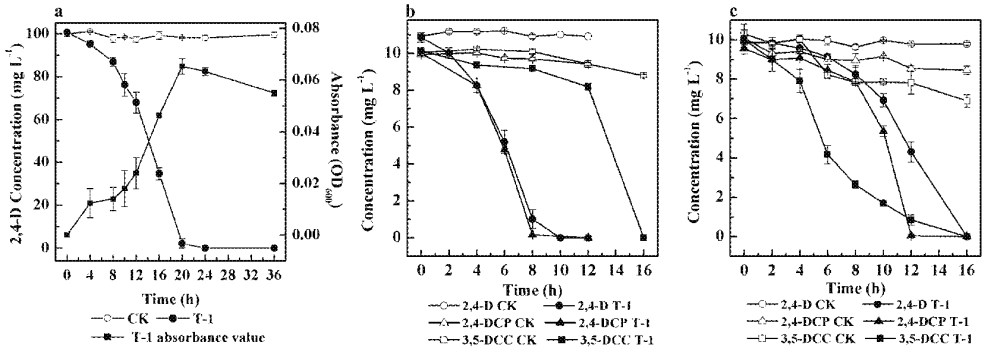


Figure 5. Degradation of 2,4-D and its metabolites by strain T-1 in MSM under different conditions: (a) 2,4-D alone; (b) three compounds alone; (c) mixture of three compounds.

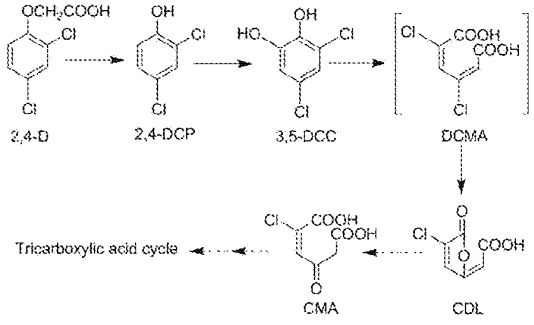


Figure 6. Proposed degradation pathway of 2,4-D by strain T-1. The solid line represents the determined pathway. The dotted line and bracket indicate the predicted pathway. 2,4-D, 2,4-dichlorophenoxyacetic acid; 2,4-DCP, 2,4-dichlorophenol; 3,5-DCC, 3,5-dichlorocatechol; DCMA, 2,4-dichloromuconic acid; CDL, *cis*-2-dichlorodiene lactone; CMA, chloromaleylacetic acid.

affected significantly at the pH range (5−8), except that the degradation ability decreased slightly at pH 9. These results agreed with the work of Greer et al.,[42] who found the optimal pH of 2,4-D degradation by *P. cepacia* BR16001 at 5.9−7.4. However, Han et al.[38] reported that the neutral condition was favorable for the degradation of 2,4-D by *C. campinensis* BJ71. The optimal pH of 2,4-D degradation by *Aeromonas* sp. NOH2 was 6.5.[46]

2,4-D could be rapidly degraded by strain T-1 and converted to 2,4-DCP, rapidly to 3,5-DCC, and then to CDL. CDL could be also further degraded by strain T-1. Similarly, Evans et al.[47] found that 2,4-D could be degraded to 2,4-DCP, then 3,5-DCC, and finally to α-chloromaleylacetate by *Pseudomonas* sp. N.C.I.B. 9340. *A. xylosoxidans* EST4002 and *C. necator* JMP134 containing *tfdABCDEF* genes could encode several 2,4-D-degrading enzymes and metabolize 2,4-D to 3,5-DCC, cleave the benzene ring, and then mineralize 2,4-D.[23,28]

Strain T-1 could degrade other PAA herbicides such as 2,4-D sodium salt, MCPA, MCPA isooctyl ester, and 2,4-DP. The result was similar to *C. campinensis* BJ71, which can degrade three PAA herbicides such as 2,4-D, MCPA, and mecoprop.[38] *Alcaligenes denitrificans* can also degrade various species of PAA herbicides such as 2,4-D, MCPA, 2,4-DP, and phenoxypropionic acid.[48] Compared to *C. campinensis* BJ71 and *A. denitrificans*, T-1 showed a wider degradation range to PAA herbicides.

Attaining a highly efficient degradation strain is critical to bioremediation of environmental pollutants. Strain T-1 isolated from the soil of a soybean field in this study could rapidly degrade 2,4-D, and its biodegradation rate was greater than that of the model strain *C. necator* JMP134 for degrading 2,4-D. Strain T-1 manifests a broad spectrum of degradation for PAA herbicides and has good degradation characteristics, such as rapid biodegradation of 2,4-D and good tolerance to a wide range of pH. It is likely that the findings of this study may provide guidance by utilizing strain T-1 to biodegrade and detoxify PAA herbicides in contaminated environments.

Table 2. Degradation Rates of Strain T-1 and Other 2,4-D-Degrading Microorganisms

strain	initial concn (mg L^{-1})	time (days)	degradation (%)	degradation rate (mg L^{-1} day^{-1})	ref
C. gilardii T-1	50	0.7	100	73	this study
C. gilardii T-1	100	0.8	100	127	this study
C. gilardii T-1	200	1	53	100	this study
C. gilardii T-1	250	1	36	77	this study
C. necator JMP134	250	10	70	17.5	28
C. necator EMA-G	250	1	100	250	49
C. necator EMA-K	250	3	100	83.3	49
Burkholderia cepacia DS-1	50	10	69	3.5	17
Pseudomonas sp. DS-2	50	10	73	3.7	17
s. paucimobilis DS-3	50	10	54	2.7	17
C. campinensis BJ71	200	3	100	66.7	38
Novosphingobium DY4	200	4.5	100	44.4	40

DOI: 10.1021/acs.jafc.7b00544
J. Agric. Food Chem. 2017, 65, 3711−3720

COR-AAD1-00003750
Bayer EX1008 (Part 7 of 9)

ASSOCIATED CONTENT

Supporting Information

The Supporting Information is available free of charge on the ACS Publications website at DOI: 10.1021/acs.jafc.7b00544.

Colony morphology and scanning electron micrograph of strain T-1; degradation of 2,4-D by strain T-1 in soil; total ion chromatograms, mass spectra, and proposed structures of 2,4-D metabolites (PDF)

AUTHOR INFORMATION

Corresponding Author

*(R.H.) Phone: +86 551 65786320. Fax: +86 551 65786296. E-mail: rimaohua@ahau.edu.cn.

ORCID

Xiangwei Wu: 0000-0003-3589-4051

Haiqun Cao: 0000-0001-9381-8896

Rimao Hua: 0000-0002-5601-6568

Funding

This work was supported in part by the National High Technology Research and Development Program of China (2013AA102804B), the National Natural Science Foundation of China (No. 31572033), the National Key Research and Development Program of China (2016YFD0200201-1), the Natural Science Foundation of Anhui Province of China (1408085MKL36), and the National Innovation and Entrepreneurship Program of College Students of China (201610364020).

Notes

The authors declare no competing financial interest.

REFERENCES

(1) IARC. Occupational exposures to chlorophenoxy herbicides. *IARC Monogr. Eval. Carcinog. Risk Chem. Hum.* **1986**, *41*, 357–406.

(2) Zhou, X.; Rotondaro, S. L.; Ma, M.; Rosser, S. W.; Olberding, E. L.; Wendelburg, B. M.; Adelfinskaya, Y. A.; Balcer, J. L.; Blewett, T. C.; Clements, B. Metabolism and residues of 2,4-dichlorophenoxyacetic acid in DAS-40278-9 maize (*Zea mays*) transformed with aryloxyalkanoate dioxygenase-1 gene. *J. Agric. Food Chem.* **2016**, *64*, 7438–7444.

(3) Zabaloy, M. C.; Garland, J. L.; Gomez, M. A. Assessment of the impact of 2,4-dichlorophenoxyacetic acid (2,4-D) on indigenous herbicide-degrading bacteria and microbial community function in an agricultural soil. *Appl. Soil Ecol.* **2010**, *46*, 240–246.

(4) Laurent, F.; Debrauwer, L.; Rathahao, E.; Scalla, R. 2,4-Dichlorophenoxyacetic acid metabolism in transgenic tolerant cotton (*Gossypium hirsutum*). *J. Agric. Food Chem.* **2000**, *48*, 5307–5311.

(5) Jones, G.; Vale, J. Mechanisms of toxicity, clinical features, and management of diquat poisoning: a review. *J. Toxicol., Clin. Toxicol.* **2000**, *38*, 123–128.

(6) Schulz, B.; Segobye, K. 2,4-D transport and herbicide resistance in weeds. *J. Exp. Bot.* **2016**, *67*, 3177–3179.

(7) Peterson, M. A.; McMaster, S. A.; Riechers, D. E.; Skelton, J.; Stahlman, P. W. 2,4-D past, present, and future: a review. *Weed Technol.* **2016**, *30*, 303–345.

(8) Felix-Cariedo, T. E.; Duran-Alvarez, J. C.; Jimenez-Cisneros, B. The occurrence and distribution of a group of organic micropollutants in Mexico City's water sources. *Sci. Total Environ.* **2013**, *454*, 109–118.

(9) Harrahy, E. A.; Edwards, D. S.; Hedman, C. J. Persistence of 2,4-D and its effects on benthic macroinvertebrates following spring treatment of Eurasian watermilfoil, *Myriophyllum spicatum* L. in two lakes in southeastern Wisconsin, USA. *Bull. Environ. Contam. Toxicol.* **2014**, *92*, 404–409.

(10) Ismail, B. S.; Sameni, M.; Halimah, M. Evaluation of herbicide pollution in the kerian ricefields of Perak, Malaysia. *World Appl. Sci. J.* **2011**, *15*, 05–13.

(11) Kuster, M.; Lopez de Alda, M. J.; Hernando, M. D.; Petrovic, M.; Martin-Alonso, J.; Barcelo, D. Analysis and occurrence of pharmaceuticals, estrogens, progestogens and polar pesticides in sewage treatment plant effluents, river water and drinking water in the Llobregat river basin (Barcelona, Spain). *J. Hydrol.* **2008**, *358*, 112–123.

(12) Browne, A. M.; Moore, P. A. The effects of sublethal levels of 2,4-dichlorophenoxyacetic acid herbicide (2,4-D) on feeding behaviors of the crayfish O-rusticus. *Arch. Environ. Contam. Toxicol.* **2014**, *67*, 234–244.

(13) Mills, P. K.; Yang, R. C. Agricultural exposures and gastric cancer risk in Hispanic farm workers in California. *Environ. Res.* **2007**, *104*, 282–289.

(14) Schreinemachers, D. M. Perturbation of lipids and glucose metabolism associated with previous 2,4-D exposure: a cross-sectional study of NHANES III data, 1988–1994. *Environ. Health* **2010**, *9*, 1–14.

(15) Chinalia, F. A.; Killham, K. S. 2,4-Dichlorophenoxyacetic acid (2,4-D) biodegradation in river sediments of northeast Scotland and its effect on the microbial communities (PLFA and DGGE). *Chemosphere* **2006**, *64*, 1675–1683.

(16) Paszko, T.; Muszynski, P.; Materska, M.; Bojanowska, M.; Kostecka, M.; Jackowska, I. Adsorption and degradation of phenoxyalkanoic acid herbicides in soils: a review. *Environ. Toxicol. Chem.* **2016**, *35*, 271–286.

(17) Cycon, M.; Zmijowska, A.; Piotrowska-Seget, Z. Biodegradation kinetics of 2,4-D by bacterial strains isolated from soil. *Central Eur. J. Biol.* **2011**, *6*, 188–198.

(18) Zaprasis, A.; Liu, Y. J.; Liu, S. J.; Drake, H. L.; Horn, M. A. Abundance of novel and diverse *tfdA*-like genes, encoding putative phenoxyalkanoic acid herbicide-degrading dioxygenases, in soil. *Appl. Environ. Microbiol.* **2010**, *76*, 119–128.

(19) Crespin, M. A.; Gallego, M.; Valcarcel, M.; Gonzalez, J. L. Study of the degradation of the herbicides 2,4-D and MCPA at different depths in contaminated agricultural soil. *Environ. Sci. Technol.* **2001**, *35*, 4265–4270.

(20) Kamagata, Y.; Fulthorpe, R.; Tamura, K.; Takami, H.; Forney, L.; Tiedje, J. Pristine environments harbor a new group of oligotrophic 2,4-dichlorophenoxyacetic acid-degrading bacteria. *Appl. Environ. Microbiol.* **1997**, 2266–2272.

(21) Lee, T. H.; Kurata, S.; Nakatsu, C. H.; Kamagata, Y. Molecular analysis of bacterial community based on 16S rDNA and functional genes in activated sludge enriched with 2,4-dichlorophenoxyacetic acid (2,4-D) under different cultural conditions. *Microb. Ecol.* **2005**, *49*, 151–162.

(22) Smith, A. E.; Mortensen, K.; Aubin, A. J.; Molloy, M. M. Degradation of MCPA, 2,4-D, and other phenoxyalkanoic acid herbicides using an isolated soil bacterium. *J. Agric. Food Chem.* **1994**, *42*, 401–405.

(23) Vedler, E.; Vahter, M.; Heinaru, A. The completely sequenced plasmid pEST4011 contains a novel IncP1 backbone and a catabolic transposon harboring *tfd* genes for 2,4-dichlorophenoxyacetic acid degradation. *J. Bacteriol.* **2004**, *186*, 7161–7174.

(24) Itoh, K.; Tashiro, Y.; Uobe, K.; Kamagata, Y.; Suyama, K.; Yamamoto, H. Root nodule *Bradyrhizobium* spp. Harbor *tfdAα* and *cadA*, homologous with genes encoding 2,4-dichlorophenoxyacetic acid-degrading proteins. *Appl. Environ. Microbiol.* **2004**, *70*, 2110–2118.

(25) Itoh, K.; Kanda, R.; Sumita, Y.; Kim, H.; Kamagata, Y.; Suyama, K.; Yamamoto, H.; Hausinger, R. P.; Tiedje, J. M. *tfdA*-like genes in 2,4-dichlorophenoxyacetic acid-degrading bacteria belonging to the *Bradyrhizobium-Agromonas-Nitrobacter-Afipia* cluster in alpha-proteobacteria. *Appl. Environ. Microbiol.* **2002**, *68*, 3449–3454.

(26) Pérez-Pantoja, D.; Iglesia, R. D.; Pieper, D. H.; González, B. Metabolic reconstruction of aromatic compounds degradation from

COR-AAD1-00003751
Bayer EX1008 (Part 7 of 9)

the genome of the amazing pollutant-degrading bacterium *Cupriavidus necator* JMP134. *FEMS Microbiol. Rev.* **2008**, *32*, 736−794.
(27) Lerch, T. Z.; Dignac, M. F.; Barriuso, E.; Bardoux, G.; Mariotti, A. Tracing 2,4-D metabolism in *Cupriavidus necator* JMP134 with ^{13}C-labelling technique and fatty acid profiling. *J. Microbiol. Methods* **2007**, *71*, 162−174.
(28) Lerch, T. Z.; Dignac, M. F.; Barriuso, E.; Mariotti, A. Effect of glucose on the fatty acid composition of *Cupriavidus necator* JMP134 during 2,4-dichlorophenoxyacetic acid degradation: implications for lioid-based stable isotone probing methods. *Appl. Environ. Microbiol.* **2011**, *77*, 7296−7306.
(29) Liu, J. W.; Hua, R. M.; Lv, P.; Tang, J.; Wang, Y.; Cao, H. Q.; Wu, X. W.; Li, Q. X. Novel hydrolytic de-methylthiolation of the *s*-triazine herbicide prometryn by *Leucobacter* sp. JW-1. *Sci. Total Environ.* **2017**, *579*, 115−123.
(30) Dong, X. Z.; Cai, M. Y. *Handbook of Common Bacterial System Identification*; Science Press: Beijing, China, 2001; pp 1−419.
(31) Altschul, S. F.; Madden, T. L.; Schäffer, A. A.; Zhang, J. H.; Zhang, Z.; Miller, W.; Lipman, D. J. Gapped BLAST and PSI-BLAST: a new generation of protein database search programs. *Nucleic Acids Res.* **1997**, *25*, 3389−3402.
(32) Tamura, K.; Peterson, D.; Peterson, N.; Stecher, G.; Nei, M.; Kumar, S. MEGA5: molecular evolutionary genetics analysis using maximum likelihood, evolutionary distance, and maximum parsimony methods. *Mol. Biol. Evol.* **2011**, *28*, 2731−2739.
(33) Jaremko, M.; Yu, J. The initial metabolic conversion of levulinic acid in *Cupriavidus necator*. *J. Biotechnol.* **2011**, *155*, 293−298.
(34) Hotopp, J. C. D.; Auchtung, T. A.; Hogan, D. A.; Hausinger, R. P. Intrinsic tryptophan fluorescence as a probe of metal and alpha-ketoglutarate binding to TfdA, a mononuclear non-heme iron dioxygenase. *J. Inorg. Biochem.* **2003**, *93*, 66−70.
(35) Chong, N. M.; Chang, H. W. Plasmid as a measure of microbial degradation capacity for 2,4-dichlorophenoxyacetic acid. *Bioresour. Technol.* **2009**, *100*, 1174−1179.
(36) Kitagawa, W.; Takami, S.; Miyauchi, K.; Masai, E.; Kamagata, Y.; Tiedje, J. M.; Fukuda, M. Novel 2,4-dichlorophenoxyacetic acid degradation genes from oligotrophic *Bradyrhizobium* sp. strain HW13 isolated from a pristine environment. *J. Bacteriol.* **2002**, *184*, 509−518.
(37) Hayashi, S.; Sano, T.; Suyama, K.; Itoh, K. 2,4-Dichlorophenoxyacetic acid (2,4-D)-and 2,4,5-trichlorophenoxyacetic acid (2,4,5-T)-degrading gene cluster in the soybean root-nodulating bacterium *Bradyrhizobium elkanii* USDA94. *Microbiol. Res.* **2016**, *188−189*, 62−71.
(38) Han, L. Z.; Zhao, D. G.; Li, C. C. Isolation and 2,4-D-degrading characteristics of *Cupriavidus campinensis* BJ71. *Brazilian J. Microbiol* **2015**, *46*, 433−441.
(39) Han, L. Z.; Liu, Y. B.; He, A. G.; Zhao, D. G. 16S rRNA gene phylogeny and *tfdA* gene analysis of 2,4-D-degrading bacteria isolated in China. *World J. Microbiol. Biotechnol.* **2014**, *30*, 2567−2576.
(40) Dai, Y.; Li, N. N.; Zhao, Q.; Xie, S. G. Bioremediation using *Novosphingobium* strain DY4 for 2,4-dichlorophenoxyacetic acid-contaminated soil and impact on microbial community structure. *Biodegradation* **2015**, *26*, 161−170.
(41) Musarrat, J.; Bano, N.; Rao, R. A. K. Isolation and characterization of 2,4-dichlorophenoxyacetic acid-catabolizing bacteria and their biodegradation efficiency in soil. *World J. Microbiol. Biotechnol.* **2000**, *16*, 495−497.
(42) Greer, C. W.; Hawari, J.; Samson, R. Influence of environmental factors on 2,4-dichlorophenoxyacetic acid degradation by *Pseudomonas cepacia* isolated from peat. *Arch. Microbiol.* **1990**, *154*, 317−322.
(43) Vallaeys, T.; Albino, L.; Soulas, G.; Wright, A. D.; Weightman, A. J. Isolation and characterization of a stable 2,4-dichlorophenoxy-acetic acid degrading bacterium, *Variovorax paradoxus*, using chemo-stat culture. *Biotechnol. Lett.* **1998**, *20*, 1073−1076.
(44) Lu, P.; Li, Q. F.; Liu, H. M.; Feng, Z. Z.; Yan, X.; Hong, Q.; Li, S. P. Biodegradation of chlorpyrifos and 3,5,6-trichloro-2-pyridinol by *Cupriavidus* sp. DT-1. *Bioresour. Technol.* **2013**, *127*, 337−342.
(45) Samir, R.; Essam, T.; Ragab, Y.; Hashem, A. Enhanced photocatalytic−biological degradation of 2,4-dichlorophenoxyacetic acid. *Bull. Fac. Pharm.* **2015**, *53*, 77−82.
(46) Kim, B.; Han, M.; Cho, S.; Ahn, S.; Lim, S. P.; Yoo, S. Statistical optimization for biodegradation of 2,4-dichlorophenoxyacetic acid by soil isolated bacterium. *Microbiol. Biotechnol. Lett.* **2003**, *31*, 83−89.
(47) Evans, W. C.; Smith, B. S.; Fernley, H. N.; Davies, J. I. Bacterial metabolism of 2,4-dichlorophenoxyacetate. *Biochem. J.* **1971**, *122*, 543−551.
(48) Marriott, M. W.; Smejkal, C. W.; Lappin-Scott, H. M. Biodegradation of mixtures of chlorophenoxyalkanoic acid herbicides by *Alcaligenes denitrificans*. *J. Ind. Microbiol. Biotechnol.* **2000**, *25*, 255−259.
(49) Zabaloy, M. C.; Gomez, M. A. Isolation and characterization of indigenous 2,4-D herbicide degrading bacteria from an agricultural soil in proximity of Sauce Grande River, Argentina. *Ann. Microbiol.* **2014**, *64*, 969−974.

DOI: 10.1021/acs.jafc.7b00544
J. Agric. Food Chem. 2017, 65, 3711−3720

COR-AAD1-00003752
Bayer EX1008 (Part 7 of 9)

ResearchGate

See discussions, stats, and author profiles for this publication at: https://www.researchgate.net/publication/259285953

Isolation and characterization of indigenous 2,4-D herbicide degrading bacteria from an agricultural soil in proximity of Sauce Grande River, Argentina

Article in Annals of Microbiology · September 2013

DOI: 10.1007/s13213-013-0781-9

CITATIONS
15

READS
86

2 authors:



María Celina Zabaloy
Centro de Recursos Naturales Renovables de la Zona Semiárida (CERZOS CONICET)
30 PUBLICATIONS **477** CITATIONS
SEE PROFILE



Marisa Anahi Gomez
Universidad Nacional del Sur
61 PUBLICATIONS **700** CITATIONS
SEE PROFILE

Some of the authors of this publication are also working on these related projects:



USDA-NIFA-AFRI 2018-67019-27807: Understanding shifts in the microbial N cycle with inclusion of cover crops into long-term agricultural experiments and their links to soil health and productivity View project



Understanding what's going on belowground: study of the interaction of soil-plant-microbes in agricultural managementsregarded as "sustainable" View project

All content following this page was uploaded by María Celina Zabaloy on 17 April 2019.

The user has requested enhancement of the downloaded file.

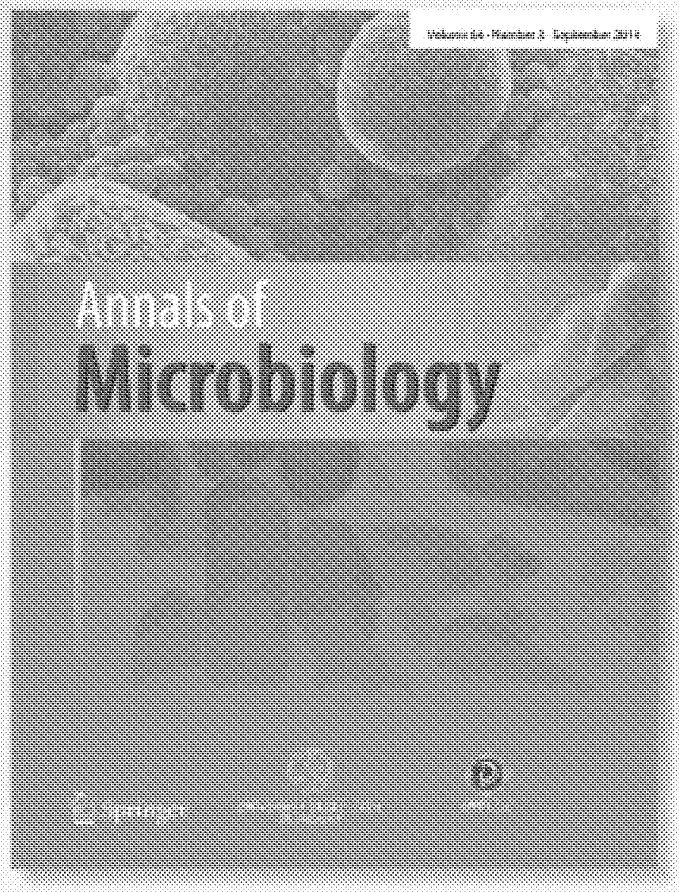
Isolation and characterization of indigenous 2,4-D herbicide degrading bacteria from an agricultural soil in proximity of Sauce Grande River, Argentina

M. Celina Zabaloy & Marisa A. Gómez

Annals of Microbiology

ISSN 1590-4261
Volume 64
Number 3

Ann Microbiol (2014) 64:969-974
DOI 10.1007/s13213-013-0731-9



Springer

COR-AAD1-00003754
Bayer EX1008 (Part 7 of 9)

Your article is protected by copyright and all rights are held exclusively by Springer-Verlag Berlin Heidelberg and the University of Milan. This e-offprint is for personal use only and shall not be self-archived in electronic repositories. If you wish to self-archive your article, please use the accepted manuscript version for posting on your own website. You may further deposit the accepted manuscript version in any repository, provided it is only made publicly available 12 months after official publication or later and provided acknowledgement is given to the original source of publication and a link is inserted to the published article on Springer's website. The link must be accompanied by the following text: "The final publication is available at link.springer.com".



COR-AAD1-00003755
Bayer EX1008 (Part 7 of 9)

Author's personal copy

Ann Microbiol (2014) 64:969–974
DOI 10.1007/s13213-013-0731-9

ORIGINAL ARTICLE

Isolation and characterization of indigenous 2,4-D herbicide degrading bacteria from an agricultural soil in proximity of Sauce Grande River, Argentina

M. Celina Zabaloy · Marisa A. Gómez

Received: 29 May 2013 / Accepted: 17 September 2013 / Published online: 4 October 2013
© Springer-Verlag Berlin Heidelberg and the University of Milan 2013

Abstract Our objective was to isolate and characterize indigenous bacteria able to use 2,4-D as a sole carbon (C) and energy source from an agricultural soil in the Sauce Grande River basin (Argentina). Culturable-dependant and molecular methods combined were used to identify and characterize putatively dominant indigenous degrading bacteria. Physiological traits, chloride release and biomass production showed the degradative capacity of the isolates obtained and high-performance liquid chromatography (HPLC) was used to corroborate the evidence. Degrading genes (*tfdA* and *tfdB*) were detected in all isolates, and their restriction fragment length polymorphisms (RFLP) were analyzed. Altogether, our results suggest that agricultural use of 2,4-D at recommended level leads to selection for a copiotrophic degrading population. The dominant genus able to metabolize 2,4-D in this soil was identified as *Cupriavidus* by 16S rRNA gene sequencing and the RFLP profiles of all isolates resembled that of *Cupriavidus necator* JMP134, the model organism for 2,4-D degradation. The strain EMA-G showed a remarkable performance in herbicide degradation (100 % removal in <1 day) in pure culture and is a favorite candidate for future biodegradation experiments.

Keywords 2,4-dichlorophenoxyacetic acid- degrading bacteria · *Cupriavidus* · *tfd* genes · Restriction fragment length polymorphism

M. C. Zabaloy (✉) · M. A. Gómez
Center of Renewable Resources of Semiarid Region (CERZOS-CONICET), Department of Agronomy, South National University, San Andrés 800, 8000 Bahia Blanca, Argentina
e-mail: mzabaloy@uns.edu.ar

Introduction

Phenoxy herbicides have been produced and commonly applied at a large scale since the first half of the twentieth century. The herbicide 2,4-dichlorophenoxyacetic acid (2,4-D) is extensively applied in agricultural fields worldwide to control dicotyledonous weeds in cereal crops and pastures, and to improve weed control obtained with glyphosate in no-till systems (Altieri and Pengue 2006; Roberts 1998). The herbicide is directly applied onto soil or sprayed over crops, and from there, often reaches superficial waters and sediments (Chinalia and Killham 2006). Later, animals and people may be exposed to 2,4-D through drinking water, which is worrisome as chlorophenoxyalkanoic acid herbicides (i.e., 2,4-D, 2,4-DB, MCPA and 2,4,5-T) are known endocrine-disrupting agents that have toxic effect to animals even at low concentrations (Pattanasupong et al. 2004)

Numerous work has been done to elucidate the physiological activity, mechanism of action, environmental fate of 2,4-D, and its potential for impacting soil microbial communities' structures and function (Baelum et al. 2008; Bouseba et al. 2009; Chinalia et al. 2007; Itoh et al. 2013). Yet fewer studies had dealt with the latest topic, particularly for low doses of herbicide (<5 mg kg^{-1} of active ingredient) simulating the agronomic use in the field (Bouseba et al. 2009; Ka et al. 1995; Merini et al. 2007; Vieuble-Gonod et al. 2005; Zabaloy et al. 2008, 2010).

2,4-D can be readily used as a carbon (C) and energy source by environmental microorganisms using at least two main different metabolic pathways, the α-ketoglutarate or the dehalogenase pathways (Ka et al. 1995; Kamagata et al. 1997; Kitagawa et al. 2002; Lerch et al. 2007; Muller et al. 2001; Vallaeys et al. 1996). The most studied catabolic pathway until

COR-AAD1-00003756
Bayer EX1008 (Part 7 of 9)

Author's personal copy

today follows the model encoded by plasmid pJP4 first isolated from *Cupriavidus necator* JMP134 (Lerch et al. 2007). *C. necator* JMP 134 harbors at least ten known genes involved in metabolism of 2,4-D; six of them are responsible for converting this compound to an intermediate of central metabolism (Chinalia et al. 2007). In the pathway initiated by the TfdA protein (a 2,4-D α-ketoglutarate dioxygenase encoded by *tfdA* gene) α–ketoglutarate is transformed into succinate and CO_2, and 2,4-D is converted into glyoxylate and 2,4-dichlorophenol (DCP). The next step in 2,4-D degradation is the transformation of DCP into 3,5-dichlorocatechol, which is catalyzed by a 2,4-dichlorophenol hydroxylase encoded in *tfdB* gene (Pérez-Pantoja et al. 2008). Most 2,4-D-degrading bacteria characterized to date are members of genera belonging to the β and γ subdivisions of the class *Proteobacteria* and were isolated from 2,4-D treated environments (Gonzalez et al. 2012; Kamagata et al. 1997; Lee et al. 2005). These β and γ subgroups carry 2,4-D degradation genes homologous to the canonical *tfdABCDEF* genes found in plasmid pJP4 of *C. necator* JMP134.

An understanding of the indigenous herbicide-degrading bacteria present in this agricultural soil is of the utmost importance, considering the high risk of herbicide contamination of the Sauce Grande River, a major water supply for the city of Bahía Blanca and the surrounding area (Orioli et al. 2008). Indigenous strains isolated in this work could be favorite candidates for bioaugmentation purposes for in situ cleanup strategies, as the survival and catabolic performance of exogenous introduced strains in bioremediation approaches is severely impaired by biotic and abiotic factors (Manzano et al. 2007; Marrón-Montiel et al. 2006). To provide de basis for testing these strains in future biodegradation studies, detailed knowledge on their biochemical and physiological properties and their genetic basis is required. The goal of this work was to isolate indigenous 2,4-D degraders from soil microcosms spiked with a low dose of 2,4-D, simulating agronomic use in the field. The putatively dominant population in microcosms was recovered by enrichment culture. Isolated degraders were identified by 16S rRNA gene sequencing, their degradation genes were characterized by restriction fragment length polymorphism (RFLP), and their 2,4-D degradation ability was confirmed by complementary methods.

Materials and methods

Soil sampling

The soil for this study was collected in an agricultural farm ("El Torino") in Saldungaray (38° 16′ S, 61° 41′ W) in the southern Pampas region, Buenos Aires, Argentina. The plot was selected because of its location in proximity of Sauce Grande River (< 100 m), where adequate herbicide management is critical to prevent water pollution. Soybean was cultivated for several years under no-till management, and pre-sowing weed control was done with 2,4-D and glyphosate until 2004. The last 2,4-D application occurred 29 months before the samples were taken. Since then, weed control was done with a mixture of fluorochloridone–cypermethrin–acetochlor for sunflower cultivation.

The soil is a sandy loam classified as Typic Argiudoll, with the following characteristics: pH (water) 6.6; total organic carbon, 20.1 g kg^{-1}, total nitrogen, 1.51 g kg^{-1} soil. Ten soil cores were randomly collected from the upper layer (0–10 cm) and then pooled to make a composite sample. Fresh, field-moist soil was sieved (< 5.6 mm) and kept at 4 °C until treatment within 2 weeks of sampling.

Chemicals

The herbicide 2,4-D (purity >98 %) was purchased from Fluka (Germany). All the other chemicals were of analytical reagent grade. The 2,4-D stock solution (25 mg ml^{-1}) was prepared by dissolving the necessary amount in methanol, filtered (<0. 22 μm) and stored at −20 °C.

Microcosms setup

Microcosms were prepared in 150-ml plastic flasks containing 40 g of soil, with caps loosely fitted to allow aeration. Before the experiment was initiated, soil microcosms were pre-incubated at their field moisture state for 7 days at 28 °C in the dark. One milliliter of a filter-sterilized aqueous solution of 2,4-D was spiked by dropping with pipette to give a final concentration of 5 mg kg^{-1} soil. Controls received only filter-sterilized distilled water. The dose of 2,4-D used here represents the concentration in soil after a single application of a commercial formulation (100 % isobutylic acid ester of 2,4-D) at the rate prescribed by the product label (0.4 l ha^{-1}), and expecting an interaction of herbicide and soil within the top 5 mm of the soil profile, for a soil with an apparent density of 1.3 ton m^{-3}. Further details on microcosms preparation can be found in a previous article (Zabaloy et al. 2010)

Enrichment cultures

Three replicate flasks per treatment were destructively sampled 1 month after treatment, and soil sub-samples (10 g dry wt. basis) were suspended in 0.85 % NaCl and used as the basis for a tenfold dilution series to estimate the most probable numbers of 2,4-D degrading bacteria ($MPN_{2,4\text{-}D}$) as described in Zabaloy et al. (2010). Enrichment cultures were prepared from the two most dilute positive tubes, using liquid mineral salts medium (MSM; K_2HPO_4 1.74 g l^{-1}, $NaHPO_4 \cdot 12H_2O$ 0.414 g l^{-1}, $(NH_4)SO_4$ 1.32 g l^{-1}, $MgSO_4 \cdot 7H_2O$ 0.246 g l^{-1}, $Ca(NO_3)_2$ 24 mg l^{-1}, $Fe(NO_3)_3 \cdot 9H_2O$ 4.4 mg l^{-1}, $MnSO_4 \cdot$

COR-AAD1-00003757
Bayer EX1008 (Part 7 of 9)

Author's personal copy

H_2O 2 μM, $ZnSO_4 \cdot 7H_2O$ 2 μM, $CuSO_4 \cdot 7H_2O$ 2 μM, $NiSO_4$ 0.2 μM, $Co(NO_3)_2$ 0.2 μM, $NaMoO_4$ 0.2 μM, distilled water). The herbicide was added aseptically after sterilization, by diluting an appropriate volume of the stock solution (section 2.2). After two sequential transfers in liquid MSM supplemented with 100 mg l^{-1} of 2,4-D (Focht 1994), a loop full of each enrichment was streaked on solid MSM (2,4-D 250 mg l^{-1}). Positive isolates were streaked on nutritive agar (Laboratorios Britania, Argentina) and incubated 7 days at 28 °C to check for purity, and well-separated colonies were transferred to MSM (2,4-D 250 mg l^{-1}) agar slants. Glycerol stocks were stored at −20 °C. Morphological and physiological traits of the isolates were assessed (Holt 1994).

2,4-D degradation

Ten isolates were cultured in 10 ml of MSM+2,4-D 250 mg l^{-1} (1:50 inoculum: medium) in triplicate 50-ml Erlenmeyer flasks. Cultures were incubated 72 h at 28 °C. At the end of the incubation, 4-ml aliquots were centrifuged (10 min, 12,500 rpm), the supernatant was preserved and used for chloride release and spectrophotometrical analyses, and the cell pellet was stored at −20 °C for protein analysis. 2,4-D degradation was confirmed by UV scanning at 230–310 nm (Shimadzu 2100 UV–vis), chloride release (Focht 1994) and biomass protein quantitation by Bradford method (Bradford 1976).

Based on physiological differences (protein biomass and chloride release) that suggested slight differences in growth and degradation rates, respectively, the isolates EMA-G and EMA-K were selected for further characterization. Overnight-grown liquid cultures (OD_{550nm}=0.1) of the isolates were inoculated in 120 ml of MSM+2,4-D 250 mg l^{-1} (1:50) in triplicate Erlenmeyer flasks and incubated in a rotary shaker (28 °C, 90 rpm) for 72 h. Aliquots of 3-ml volume were drawn every 24 h, centrifuged (10 min, 12,500 rpm) to remove biomass and quantitate 2,4-D and 2,4-dichlorophenol (DCP) in the supernatant by HPLC. The analytical phase was performed at the Industrial and Biotechnological Microbiology Laboratory, University of Buenos Aires, Argentina. Supernatant was diluted 1:3 in methanol (HPLC grade), filtered (<0.45 μm) and injected in a HPLC Jasco module, equipped with detector UV-975 and hybrid column MS-C18 full end-capped (250×4.6 mm- 5 μm particles and 100-Å pore diameter, Waters), mobile phase methanol: phosphoric acid (pH 2.5) 65:35 (isocratic, 1 ml min^{-1}) and detection at 230 nm.

DNA extraction and PCR

Isolates and reference bacteria *Alcaligenes* sp. JD6 and *Burkholderia cepacia* TFD3 (courtesy of F. Martin-Laurent, INRA Dijon, France) were continuously grown in liquid MSM supplemented with 2,4-D as C source (250 mg l^{-1}) at 28 °C for 72 h. UltraClean Microbial DNA isolation kit (MoBio Laboratories, Carlsbad, USA) was used to extract DNA from 2-ml aliquots of bacteria cultures, following manufacturer's instructions.

Specific primers sets for the *tfdA* and *tfdB* genes previously described by Vallaeys et al. (1996) were used for selective amplification of the respective genes. *Burkholderia cepacia* TFD3 (Tonso et al. 1995) and *Alcaligenes* sp. JD6 (Vallaeys et al. 1996) were used as positive controls. Reaction mixtures (25 μl) for amplification of each gene contained 3.5 μl of nuclease-free water, 12.5 μl of 2× Green Go Taq Master Mix (Promega, Madison, WI, USA), 1.0 μl each of two primers (10 μM, forward and reverse), and 4 μl of DNA template. A touchdown program was carried out using a My Cycler thermal cycler (Bio-Rad, Hercules, CA, USA). A hot-start (3 min at 94 °C) was followed by 8 touchdown cycles (45 s at 94 °C; 30 s at 57-50 °C [decreasing 1 °C/cycle]; 45 s at 72 °C), 30 regular cycles (45 s at 94 °C; 30 s at 50 °C; 45 s at 72 °C), and a final extension step of 10 min at 72 °C. PCR products were revealed by electrophoresis in a 2 % agarose gel.

RFLP of *tfd* genes

The PCR products obtained with *tfdA* and *tfdB* primers were digested overnight with the restriction enzymes AluI and BsuRI (HaeIII) (Fermentas, Canada) according to the conditions described by the manufacturer. Restriction fragments (RF) were electrophoresed in either a 3.5 % (*tfdA*) or 2.5 % (*tfdB*) agarose gel (Metaphor, FMC Bioproducts, France) prepared in TBE buffer (60 V, 90–120 min). Gels were stained with ethidium bromide and analyzed using Kodak Digital Science Image Analysis Software version 3.0 (Eastman Kodak Company, NY).

Sequencing of 16S rRNA gene

Taxonomic identification of three isolates (EMA-G, EMA-K and EMA-N) was done following sequencing of 16S rRNA gene with universal primers by Macrogen Inc. (Seoul, Korea), and alignment with known sequences in GenBank (blast.ncbi.nlm.nih.gov/Blast.cgi). The strain EMA-N was sent for 16S rRNA sequencing as the microscopic observation showed larger bacilli than the other isolates. Nucleotide sequences for isolates EMA-G, EMA-K and EMA-N were assigned the following accession numbers: JX627313, JX627314, and JX627315.

Results

Physiological characterization

Ten pure isolates grew stably on MSM supplemented with 250 mg l^{-1} of 2,4-D. Morphological and physiological

COR-AAD1-00003758
Bayer EX1008 (Part 7 of 9)

Author's personal copy

characterization showed that all isolates were motile Gram-negative rods, formed non-pigmented colonies, tested negative for O-F (glucose) and gelatin hydrolysis, were positive for oxidase and catalase tests, and reduced NO_3^- to NO_2^-. They were able to use carboxylic acids (fumarate, succinate, acetate), amino acids (asparagine, glutamate), benzoate and fructose as growth substrates, while other sugars were not used (rhamnose, arabinose, cellobiose, xylose).

2,4-D degradation

All isolates grew with up to 250 mg l^{-1} herbicide as sole C source with complete primary degradation in less than 72 h. This was confirmed for all isolates by UV spectrophotometry, chloride release and biomass synthesis as determined by protein quantitation (Table 1). Herbicide utilization was associated with disappearance of the 283 nm-absorbance peak and almost stoichiometric release of chloride ions (Table 1). In addition, strains were further tested by HPLC and complete 2,4-D degradation, with no DCP accumulation, was corroborated by this analytical approach (Fig. 1). The strain EMA-G showed better performance in 2,4-D degradation than EMA-K, as the former degraded 250 mg l^{-1} in less than 1 day, while the later initiated degradation (~5 % reduction in 2,4-D concentration) by that time.

Molecular analysis: presence and variability of *tfd*-genes

PCR amplification using the primers set specific for 2,4-D degrading genes *tfdA* (encoding a 2,4-D α-ketoglutarate dioxygenase) and *tfdB* (encoding a dichlorophenol hydroxylase) was done to elucidate the genetic basis for 2,4-D utilization in our isolates. With both *tfd*-specific primers, amplicons of the expected sizes for *tfdA* (370 bp) and *tfdB* (1.1 kb) were obtained from ten isolates and two reference strains (Fig. 2).

Table 2 shows the restriction patterns resulting from the digestion of *tfdA* and *tfdB* amplicons with two endonucleases (AluI and HaeIII). Restriction of *tfdA* amplicons from all

Table 1 Chloride release and biomass production of ten degrading isolates in MSM+2,4-D (250 mg l^{-1}≈1.1 mM)

Isolate	Released Cl^- (mM)	Protein (μg ml^{-1})[a]
EMA-A	1.1	2.5±0.1
EMA-E	1.1	2.5±0.2
EMA-F	1.1	1.1±0.3
EMA-F2	1.1	2.3±0.1
EMA-G	1.1	3.0±0.4
EMA-J	1.1	2.8±0.1
EMA-K	0.8	2.0±0.4
EMA-N	1.1	2.5±0.3
EMA-S	0.9	3.3±0.1
EMA-X	1.1	2.9±0.1

[a] Mean values±S.E (n=3)

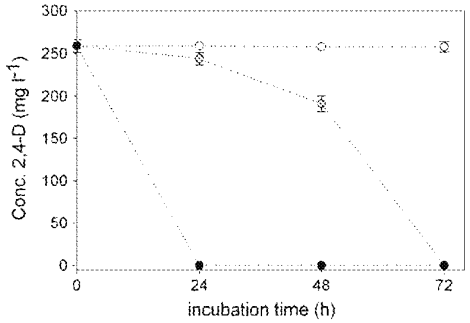


Fig. 1 Degradation of 2,4-D (250 mg l^{-1}) by selected isolates, measured by HPLC. Open circles: sterile control; filled circles: isolate G (black) and isolate K (gray). Values represent mean concentrations±S.E (n=3)

isolates and *Alcaligenes* sp. JD6 with AluI and HaeIII originated two and three neat restriction fragments (RFs) (Pattern I), respectively. Restriction of *tfdA* amplicon of *B. cepacia* TFD3 with AluI produced three RFs (Pattern II) clearly distinct from the RFs of Pattern I (digestion with HaeIII was not determined). Pattern A, resulting from digestion of *tfdB* amplicons from all isolates and *Alcaligenes* sp. JD6 with AluI and HaeIII, showed two and four RF, respectively. Pattern B resulting from the restriction of *tfdB* amplicon of *B. cepacia* TFD3 showed four neat RFs with each endonuclease.

The almost full-length 16S rRNA gene sequence determined showed that the isolates were closely related to *Cupriavidus necator* (β-proteobacteria, Burkholderiales) with 99 % identity to *Cupriavidus necator* strain N-1 (Accession N° NR 028766.1), type strain for the species.

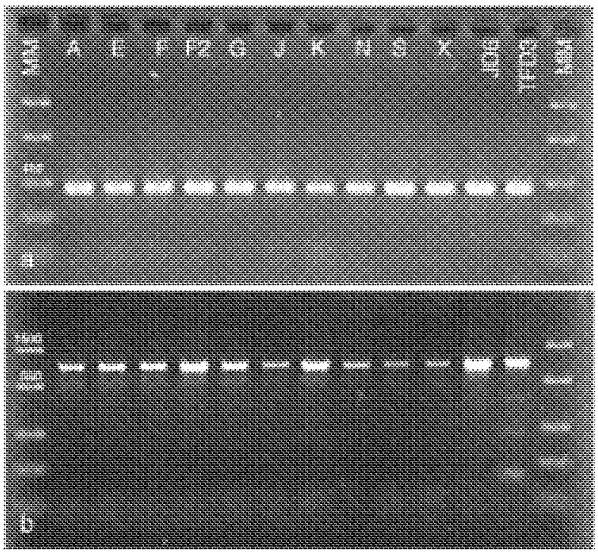


Fig. 2 PCR amplification of *tfdA* (**a**) and *tfdB* (**b**) genes from 10 isolates and two reference strains. Fragment sizes correspond to expected amplicon size for *tfdA* (370 pb) and *tfdB* (1.1 kb). MM=molecular size marker (50 bp-1.5 kb, Fermentas)

COR-AAD1-00003759
Bayer EX1008 (Part 7 of 9)

Author's personal copy

Table 2 Patterns observed after RFLP of *tfdA* and *tfdB* amplicons of ten isolates and two reference strains

Restriction Pattern	RF of *tfdA*[a](bp)		RF of *tfdB* (bp)	
	I	II	A	B
AluI	281	168	793	398
	90	119	322	307
		50		274
				138
BsuRI (HaeIII)	179 (12)	n.d	339 (1)	321 (6)
	115 (8)		262 (2)	268 (18)
	82 (8)		130 (2)	214 (14)
			58 (2)	89 (4)
				73 (8)

[a] Restriction fragment (RF) size in bp, corresponding to the average size of RFs of amplicons *tfdA* and *tfdB* obtained from ten isolates. In brackets, calculated differences with RFs for the canonical *tfd* genes digested with HaeIII as reported by Vallaeys et al. (1996). Italicized, estimated size of faint bands visualized in the gel

n.d not determined

Discussion

A previous study that evaluated the metabolic and degrading potential of this soil has shown it had a stable 2,4-D degrading population able to use the herbicide as C and energy source, which increased immediately after a low dose of 2,4-D and remained high for about 1 month after exposure had ceased (Zabaloy et al. 2010). In this study we isolated ten indigenous 2,4-D degrading bacteria belonging to the species *Cupriavidus necator* (formerly *Alcaligenes eutrophus, Ralstonia eutropha* and *Wautersia eutropha*) based on 16S rRNA gene sequence and physiological features in agreement with the genus description (Vandamme and Coenye 2004). This was consistent with our expectations, as the batch culture method used to enrich and isolate these bacteria is highly selective towards fast-growing copiotrophic microbes (Lee et al.2005; Macur et al. 2007). The fact that this taxonomic group was obtained from the most dilute positive MPN tubes may reflect its dominance in the 2,4-D degrading community in soil (Macur et al. 2007). In agreement, Cuadrado et al. (2010) reported that soils chronically exposed to phenoxy herbicides in the Humid Pampa in Argentina harbored a novel species of *Cupriavidus*, *Cupriavidus pampae*, able to degrade 4-(2,4-dichlorophenoxy) butyric acid (2,4-DB).

Degradation performance was different between two strains, EMA-G and EMA-K, even though both were able to degrade a high concentration of 2,4-D (250 mg l^{-1}) in less than 72 h. The reasons for that difference are unclear. It could be argued that one of them was in better metabolic shape to cope with the "stressful" initial 2,4-D concentration, given that this phenoxy herbicide causes energy spilling due to metabolic uncoupling in the cells (Marrón-Montiel et al. 2006). The recovery after the transient lag in herbicide degradation in EMA-K could be explained either by consumption of by-products accumulated during early phase in the batch culture, or by the decrease in herbicide concentration at the end of the culture, with the consequent reduction in the toxic effect of 2,4-D. EMA-G degradation performance (lag and % herbicide removal) in medium containing 2,4-D was comparable to that of a *Pseudomonas cepacia* strain harboring plasmid pJP4 (Ka et al. 1994) and to a *Delftia* sp. strain (Gonzalez et al. 2012) isolated from an agricultural soil and a polluted river, respectively. The efficiency of our strain was even better than that of *C. necator* JMP134 grown on 2,4-D as sole source of C (250 mg l^{-1}) (Lerch et al. 2007). The lack of lag in 2,4-D degradation observed in EMA-G strain could make it a better competitor in comparison to EMA-K (e.g. in soil inoculations) as lag is important in determining fitness (Ka et al. 1994). Therefore, future applications of our degrading strains should evaluate not only the overall performance in 2,4-D degradation but also growth rates, lag in degradation and other parameters reflecting fitness.

Presence of *tfdA* and *tfdB* genes was confirmed by PCR. This allows inference of the metabolic pathway for 2,4-D degradation present in our isolates, even though DCP could not be detected in the HPLC analysis due to its lability. The enzyme TfdA of these isolates degrade 2,4-D by initial removal of the acetate side chain of 2,4-D to produce DCP and glyoxylate while oxidizing α-ketoglutarate to CO_2 and succinate. Enzyme TfdB subsequently catalyzes DCP oxidation to 3, 5-dichlorocatechol. This compound then undergoes *orto*-cleavage and subsequent oxidation steps that yield intermediates that will be assimilated through Krebs cycle (Pérez-Pantoja et al. 2008). Restriction patterns of *tfdA* and *tfdB* with HaeIII give insight into the genetic basis of 2,4-D degrading enzymes present in our isolates. The sizes of the RF's of Pattern I and A observed in all isolates and *Alcaligenes* sp. JD6 were in accordance with the reported sizes for canonical type I *tfdA* and type I *tfdB* genes present in self-transmissible plasmid pJP4 in *C. necator* JMP134 (Vallaeys et al. 1996). Follow-up studies will aim at isolating their degradative plasmids and determining *tfdA* and *tfdB* sequences in these isolates in order to assess the homology with the canonical type I *tfd* genes.

Future perspectives

The isolation of ten native strains of *Cupriavidus necator* able to rapidly degrade a high concentration of 2,4-D in pure culture, harboring *tfd* degrading genes comparable to those of self-transmissible plasmid pJP4 of *C. necator* JMP134 is promising. These strains could be used in future cell or plasmid-mediated bioaugmentation tests (once their plasmids are isolated and characterized) with better chances to survive in soil and sediments of the Sauce Grande River basin than introduced exogenous bacteria.

COR-AAD1-00003760
Bayer EX1008 (Part 7 of 9)

Author's personal copy

Acknowledgements This study was partially supported by the National Agency for Promotion of Science and Technology (ANPCyT) through grant PICT 2007–00380. We thank employee Ana Zamponi from CONICET for technical assistance.

References

Altieri M, Pengue W (2006) GM soybean: Latin America's new coloniser. Seedling 13–17.

Baelum J, Nicolaisen MH, Holben WE, Strobel BW, Sørensen J, Jacobsen CS (2008) Direct analysis of tfdA gene expression by indigenous bacteria in phenoxy acid amended agricultural soil. ISMEJ 2:677–687

Bouseba B, Zertal A, Beguet J, Rouard N, Devers M, Martin C, Martin-Laurent F (2009) Evidence for 2,4-D mineralisation in Mediterranean soils: impact of moisture content and temperature. Pest Manag Sci 65:1021–1029

Bradford MM (1976) A rapid and sensitive method for the quantitation of microgram quantities of protein utilizing the principle of protein-dye binding. Anal Biochem 72:248–254

Chinalia FA, Killham KS (2006) 2,4-Dichlorophenoxyacetic acid (2,4-D) biodegradation in river sediments of Northeast Scotland and its effect on the microbial communities (PLFA and DGGE). Chemosphere 64:1675–1683

Chinalia FA, Regali-Seleghin ME, Correa EM (2007) 2,4-D toxicity: cause, effect and control. Terrest Acquat Environ Toxicol 1(2):24–33

Cuadrado V, Gomila M, Merini L, Giulietti AM, Moore ERB (2010) *Cupriavidus pampae* sp. nov., a novel herbicide –degrading bacterium isolated from agricultural soil. Int J Syst Evol Microbiol 60: 2606–2612

Focht DD (1994) Microbiological Procedures for Biodegradation Research. In: Angle S, Weaver R, Bottomley P, Bezdicek D, Smith S, Tabatabai A, Wollum A (eds) Methods of Soil Analysis: Part 2. Microbiological and Biochemical Properties. SSSA, Madison, pp 407–426

Gonzalez AJ, Gallego A, Gemini VL, Papalia M, Radice M, Gutkind G, Planes E, Korol SE (2012) Degradation and detoxification of the herbicide 2,4-dichlorophenoxyacetic acid (2,4-D) by an indigenous *Delftia* sp. strain in batch and continuous systems. Int Biodeterior Biodegradation 66:8–13

Holt JG (ed) (1994) Bergey's Manual of Determinative Bacteriology, 9thEdition. Williams and Wilkins, Baltimore

Itoh K, Kinoshita M, Morishita S, Chida M, Suyama K (2013) Characterization of 2,4-dichlorophenoxyacetic acid and 2,4,5-trichlorophenoxyacetic acid-degrading fungi in Vietnamese soils. FEMS Microbiol Ecol 84:1574–6941

Ka JO, Burauel P, Bronson JA, Holben W, Tiedje JM (1995) DNA probe analysis of microbial community selected in field by long-term 2,4-Dtreated field soils. Soil Sci Soc Am J 59:1581–1587

Ka JO, Holben WE, Tjedje JM (1994) Analysis of competition in soil among 2,4-dichlorophenoxy acetic acid-degrading bacteria. Appl Environ Microbiol 60:1121–1128

Kamagata Y, Fulthorpe R, Tamura K, Takami H, Forney L, Tiedje J (1997) Pristine environments harbor a new group of oligotrophic 2,4- dichlorophenoxyacetic acid-degrading bacteria. ApplEnviron Microbiol 63(6):2266–2272

Kitagawa W, Takami S, Miyauchi K, Masai E, Kamagata Y, Tiedje JM, Fukuda M (2002) Novel 2,4-dichlorophenoxyacetic acid degradation genes from *Bradyrhizobium* sp. strain HW13 isolated from a pristine environment. J Bacteriol 184:509–518

Lee T, Kurata S, Nakatsu C, Kamagata Y (2005) Molecular analysis of bacterial community based on 16S rDNA and functional genes in activated sludge enriched with 2,4-dichlorophenoxyacetic acid (2,4-D) under different cultural conditions. Microbiol Ecol 49:151–162

Lerch T, Dignac M-F, Barriuso E, Bardoux G, Mariotti A (2007) Tracing 2, 4-D metabolism in *Cupriavidus necator* JMP134 with ^{13}C-labelling technique and fatty acid profiling. J Microbiol Methods 71:162–174

Macur RE, Wheeler JT, Burr MD, Inskeep WP (2007) Impacts of 2,4-D application on soil microbial community and on populations associated with 2,4-D degradation. Microbiol Res 162:37–45

Manzano M, Morán AC, Tesser B, González B (2007) Role of eukaryotic microbiota in soil survival and catabolic performance of the 2,4-D herbicide degrading bacteria *Cupriavidus necator* JMP134. Anton van Leeuw 91:115–126

Marrón-Montiel E, Ordaz-Ruiz N, Rubio-Granados C, Juárez-Ramírez C, Galíndez-Mayer CJ (2006) 2,4-D-degrading bacterial consortium. Isolation, kinetic characterization in batch and continuous culture and application for bioaugmenting an activated sludge microbial community. Process Biochem 41:1521–1528

Merini LJ, Cuadrado V, Flocco CG, Giulietti AM (2007) Dissipation of 2, 4-D in soils of the Humid Pampa region, Argentina: a microcosm study. Chemosphere 68:259–265

Muller RH, Kleinsteuber S, Babel W (2001) Physiological and genetic characteristics of two bacterial strains utilizing phenoxypropionate and phenoxyacetate herbicides. Microbiol Res 156:121–131

Orioli G, Sabattini M, Marchena J, Vázquez R (2008) The impact of agricultural land use on stream chemistry and inputs to an inland reservoir: case of the Sauce Grande River, Argentina. Hydrolog Sci J 53(4):834–843

Pattanasupong A, Nagase H, Inoue M, Hirata K, Tani K, Nasu M et al (2004) Ability of a microbial consortium to remove pesticide, carbendazim and 2,4-dichlorophenoxyacetic acid. World J Microbiol Biotechnol 20(5):517–522

Pérez-Pantoja D, De la Iglesia R, Pieper DH, González B (2008) Metabolic reconstruction of aromatic compounds degradation from the genome of the amazing pollutant-degrading bacterium *Cupriavidus necator* JMP134. FEMS Microbiol Rev 32:736–794

Roberts TR (Ed.) (1998) Metabolic Pathways of Agrochemicals: Part 1. Herbicides and Plant Regulators. Royal Society of Chemistry.

Tonso NL, Matheson VG, Holben WE (1995) Polyphasic characterization of a suite of bacterial isolates capable of degrading 2,4-D. Microb Ecol 30:3–24

Vallaeys T, Fulthorpe RR, Wrigth AM, Soulas G (1996) The metabolic pathway of 2,4-dichlorophenoxyacetic acid degradation involves different families of *tfd*A and *tfdB* genes according to PCR-RFLP analysis. FEMS Microbiol Ecol 20:163–172

Vandamme P, Coenye T (2004) Taxonomy of the genus *Cupriavidus*: a tale of lost and found. Int J Syst Evol Micr 54:2285–2289

Vieuble-Gonod L, Chadoeuf J, Chenu C (2005) Spatial distribution of microbial 2,4-dichlorophenoxy acetic acid mineralization from field to microhabitat scales. Soil Sci Soc Am J 70(1):64–71

Zabaloy MC, Garland JL, Gomez MA (2008) An integrated approach to evaluate the impacts of the herbicides glyphosate, 2,4-D and metsulfuron methyl on soil microbial communities in the Pampas region, Argentina. Appl Soil Ecol 40:1–12

Zabaloy MC, Garland JL, Gomez MA (2010) Assessment of the impact of 2,4-dichlorophenoxy acetic acid (2,4-D) on indigenous herbicide-degrading bacteria and microbial community function in an agricultural soil. Appl Soil Ecol 46:240–246

COR-AAD1-00003761
Bayer EX1008 (Part 7 of 9)

PLOS ONE

Novel Insight into the Genetic Context of the *cadAB* Genes from a 4-chloro-2-methylphenoxyacetic Acid-Degrading *Sphingomonas*

Tue Kjærgaard Nielsen[1,2], Zhuofei Xu[2], Erkin Gözdereliler[1], Jens Aamand[1], Lars Hestbjerg Hansen[2*¤], Sebastian R. Sørensen[1]

1 Department of Geochemistry, Geological Survey of Denmark and Greenland, Copenhagen, Denmark, **2** Section for Microbiology, University of Copenhagen, Copenhagen, Denmark

Abstract

The 2-methyl-4-chlorophenoxyacetic (MCPA) acid-degrader *Sphingomonas* sp. ERG5 has recently been isolated from MCPA-degrading bacterial communities. Using Illumina-sequencing, the 5.7 Mb genome of this isolate was sequenced in this study, revealing the 138 kbp plasmid pCADAB1 harboring the 32.5 kbp composite transposon Tn6228 which contains genes encoding proteins for the removal of 2,4-dichlorophenoxyacetic acid (2,4-D) and MCPA, as well as the regulation of this pathway. Transposon Tn6228 was confirmed by PCR to be situated on the plasmid and also exist in a circular intermediate state - typical of IS3 elements. The canonical *tfdAα*-gene of group III 2,4-D degraders, encoding the first step in degradation of 2,4-D and related compounds, was not present in the chromosomal contigs. However, the alternative *cadAB* genes, also providing the initial degradation step, were found in Tn6228, along with the 2,4-D-degradation-associated genes *tfdBCDEFKR* and *cadR*. Putative reductase and ferredoxin genes *cadCD* of Rieske non-heme iron oxygenases were also present in close proximity to *cadAB*, suggesting that these might have an unknown role in the initial degradation reaction. Parts of the composite transposon contain sequence displaying high similarity to previously analyzed 2,4-D degradation genes, suggesting rapid dissemination and high conservation of the chlorinated-phenoxyacetic acid (PAA)-degradation genotype among the sphingomonads.

Citation: Nielsen TK, Xu Z, Gözdereliler E, Aamand J, Hansen LH, et al. (2013) Novel Insight into the Genetic Context of the *cadAB* Genes from a 4-chloro-2-methylphenoxyacetic Acid-Degrading *Sphingomonas*. PLoS ONE 8(12): e83346. doi:10.1371/journal.pone.0083346

Editor: Brian Stevenson, University of Kentucky College of Medicine, United States of America

Received August 28, 2013; **Accepted** November 1, 2013; **Published** December 31, 2013

Copyright: © 2013 Nielsen et al. This is an open-access article distributed under the terms of the Creative Commons Attribution License, which permits unrestricted use, distribution, and reproduction in any medium, provided the original author and source are credited.

Funding: This study was partly funded by the Center for Environmental and Agricultural Microbiology - CREAM and the Lundbeck Foundation (www.lundbeckfoundation.com) project DK nr R44-A4384 (Lars Hestbjerg Hansen). CREAM is funded by the VILLUM FOUNDATION (www.villumfoundation.dk). The funders had no role in study design, data collection and analysis, decision to publish, or preparation of the manuscript.

Competing Interests: The authors have declared that no competing interests exist.

* E-mail: lhha@dmu.dk

¤ Current address: ENVS - Department of Environmental Science, Aarhus University, Roskilde, Denmark

Introduction

2-methyl-4-chlorophenoxyacetic (MCPA) and 2,4-dichlorophenoxyacetic acid (2,4-D) are widely used phenoxyacetic acid herbicides that are occasionally found in the Danish groundwater aquifers [1]. The complete degradation of 2,4-D and MCPA have been described with the first step being performed by the products of the genes *tfdA*, *tfdAα* or *cadAB* [2–5]. The product of the first catabolic step is then further degraded by the products of genes *tfdBCDEF* to finally yield β-ketoadipate, which is degraded in the central metabolism [6]. Most attention has been paid to *tfdA* and *tfdAα* [3–5,7], while *cadAB* has been less described [2,8,9]. A recent study on MCPA degradation in soil microcosms showed that both the *cadA* and *tfdA* genes are simultaneously expressed during MCPA degradation in soil [10], indicating that additional knowledge should be gathered on the *cadAB* genes if they are to be compared with the well-studied *tfdA* gene.

Phenoxyacetic acid (PAA) herbicide degraders are generally divided into three categories [5,9,11]. The first group consists of β- and γ-proteobacteria, which are characterized by the involvement of the *tfdA* gene as the first step in the degradation of phenoxyacetic acid herbicides. Within group I degraders, three further subclasses have been described, based on the similarities of the *tfdA* sequences (class I–III) [12]. Group II consists of α-proteobacteria that are phylogenetically closely related to *Bradyrhizobium* sp. Remarkably, representatives of this group were initially isolated from pristine environments in Canada, Chile and Hawaii [11]. This group was shown to possess a *tfdA*-like gene, termed *tfdAα*, which is 56–60% similar to the representative *tfdA* gene of the canonical group I degrader *Cupriavidus pinatubonensis* JMP134 [5]. Group III degraders are α-proteobacteria closely related to the *Sphingomonas* genus, also harboring the *tfdAα* gene [9].

The CadAB catabolic proteins have been shown to perform the same initial step in 2,4-D degradation as TfdA. However, CadAB are subunits of a Rieske non-heme iron oxygenase, making its mode of action quite different from the α-ketoglutarate-dependent dioxygenase action of TfdA [2,3]. CadAB of *Bradyrhizobium* sp. HW13 shows homology to the benzoate dioxygenase BenAB and the 2,4,5-T catabolic protein TftAB [2]. The *cadA* gene has been found in members of both group II and III PAA-herbicide degraders [2,8,9,13]. Some of these bacteria also have the *tfdAα* gene, displaying a dual-system of degradative genes [9].

COR-AAD1-00003762
Bayer EX1008 (Part 7 of 9)

Previously, a gene cluster from *Sphingomonas* sp. 58-1 containing the genes *cadAB*, was cloned into an *E. coli*, resulting in 2,4-D degradation in this host. Mutational analysis showed that both *cadA* and *cadB* were essential for 2,4-D degradation [8]. In this study, the MCPA- and 2,4-D-degrading bacterium *Sphingomonas* sp. ERG5, recently isolated from the MCPA-degrading bacterial communities described in [14], had its genomic content shotgun sequenced using Illumina-sequencing. This bacterium was shown to have a transposon, harboring *cadAB* as well as other PAA-herbicide catabolic and regulatory genes, situated on a plasmid containing genes for conjugative transfer.

Methods

DNA extraction and Illumina sequencing

DNA was extracted from strain ERG5 grown on R2A (Difco™) plates at 20°C supplemented with 100 mg/l of MCPA (Fluka Chemie AG), using the PowerLyzer™ UltraClean® Microbial DNA Isolation kit (MOBIO). A swab of bacteria from a single colony was picked for DNA extraction. Cell lysis was performed using the FastPrep-24 instrument (MP Biomedicals) for 3×30 seconds at 4 m/s with samples chilled on ice between runs. The extracted DNA was quantified using a QUBIT® 2.0 fluorometer (Invitrogen) and was measured to be 7.82 ng/µl. The low quantity of DNA was presumably due to the low cell density of *Sphingomonas* sp. ERG5 when grown in the relatively low nutrient medium R2A (compared to e.g. LB). A paired-end sequencing library for the Illumina was built with an average insert-size of 500 bp using a modified protocol for the NEBNext® Ultra™ DNA Library Prep Kit for Illumina® (New England BioLabs Inc). The library was loaded onto approximately 1/15 of an Illumina flow-cell and 2×100 base paired-end sequencing was performed on an Illumina® HiSeq 2000 machine.

Genetic analysis

The raw reads were preprocessed using AdapterRemoval [15] and then assembled using the Velvet *de-novo* assembler (version 1.2.08) [16] with scaffolding switched off. An initial automated annotation was performed using the RAST service [17], while the sequences described in detail in this study were manually annotated using BLASTX with standard parameters [18] and Pfam domain search (version 27.0.) [19]. Open reading frames (ORFs) were predicted using the EasyGene server [20,21]. A genetic map of plasmid pCADAB1 was generated using DNAplotter [22]. Copy numbers of genetic elements was estimated by comparing sequence coverages, as seen elsewhere [23].

The following programs and scripts were used for identification and analysis of IS-elements: ISfinder [24], einverted from the EMBOSS software package [25] and COILS [26]. A genetic map of transposon Tn6228 showing nucleotide similarities to gene clusters from *Sphingomonas* sp. 58-1 (accession no. AB353895.1), *Sphingomonas* sp. tfd44 (accession no. AY598949.1) and *Sphingobium herbicidovorans* MH (accession no. AJ628861.1) was constructed using Easyfig [27] with BLASTN implemented. The figure was edited for visual improvement in Inkscape [28].

Phylogenetic analysis of CadA

The derived amino acid sequence of the *cadA* ORF from *Sphingomonas* sp. ERG5 was used as query for a BLASTX [18] search with standard parameters. Homologous sequences were chosen for analysis from the BLASTX hits with a cutoff value of 50% amino acid identity. The sequences were aligned using the Phylogeny.fr pipeline [29]: sequences were aligned with T-Coffee (v6.85) [30] using the pair-wise alignment methods Mlalign_id_-pair and Mslow_pair. Following alignment, ambiguous regions were removed using Gblocks (v0.91b) [31] with the following parameters: minimum length of a block after gap cleaning: 10, no gap positions allowed in final alignment, all segments with contiguous nonconserved positions bigger than 8 were rejected, minimum number of sequences for a flank position: 85%. A phylogenetic tree was constructed using the Maximum Likelihood method and the Jones-Taylor-Thornton (JTT) amino acid substitution model [32], implemented in the PhyML program (v3.0 aLRT) [33,34]. The reliability for internal branches was assessed using the bootstrapping method with 100 bootstrap replicates. The tree was visualized with MEGA4.0.2 [35]. Similar trees were constructed for CadBR and TfdBCDEFKR.

PCR for identification of transposon position

Primers for PCR amplification of DNA for capillary sequencing were designed using primer-BLAST [36] and synthesized by Eurofins MWG Operon (Ebersberg, Germany). All primers were designed to have a melting temperature (Tm) of approximately 63°C and are shown in Table 1. The primers were used in different combinations to test for 1) the presence/lack of transposon Tn6228 on plasmid pCADAB1, 2) circular intermediate state of Tn6228, 3) presence of Tn6228 in the pCADAB1 at 3′ end of transposon, 4) presence of Tn6228 in pCADAB1 at the 5′ end of transposon. The primed positions are shown in Figure 1 and the combinations of primers are shown in Table 2. PCRs were set up in 20 µl reactions containing 200 µM dNTPs, 0.5 µM of both forward and reverse primers, 0.2 µl of Phusion® High-Fidelity DNA Polymerase (New England Biolabs), 4 µl of 5× Phusion GC reaction buffer, 3% DMSO, 1 µl template DNA and up to 20 µl of Molecular Biology Grade Water (MOBIO). PCRs were performed on a S1000™ Thermal Cycler (BIO-RAD) using a Touch Down (TD) PCR program: an initial denaturation step at 98°C for 40 seconds followed by 15 cycles with denaturation at 98°C for 10 seconds, annealing starting at 72°C for 15 seconds and lowered by 1°C per cycle, elongation at 72°C for 80 seconds. After TD cycling, the protocol continued with 20 cycles of 98°C for 10 seconds, 57°C for 15 seconds, 72°C for 80 seconds and a final elongation step of 72°C for 5 minutes. TD-PCR products were run on a 1% agarose gel, which was cast using modified TAE-buffer from the Millipore DNA Gel Extraction Kit and containing 0.5 µg/ml ethidium bromide. The amplification products were excised from the gel using Millipore DNA Gel Extraction Kit and DNA concentrations were measured using the Qubit® 2.0 Fluorometer (Invitrogen). The extracted PCR products were shipped to Macrogen for capillary sequencing.

Nucleotide sequence accession numbers

The nucleotide sequence of plasmid pCADAB1 has been submitted to the GenBank database under accession number KF494257.

Results

Shotgun sequencing of *Sphingomonas* sp. ERG5

The MCPA-degrading *Sphingomonas* sp. ERG5 was sequenced using the Illumina HiSeq2000 platform. Preprocessing and assembly of 12,540,301 paired reads yielded 69 contigs larger than 500 bp. These contigs have a combined size of 5.7 Mb, a G+C content of 63.7% and an average coverage of approximately 91×. The 16S gene sequence of *Sphingomonas* sp. ERG5 showed 99% similarity to *Sphingomonas alpina* strain S8-3 (accession no. GQ161989.1).

COR-AAD1-00003763
Bayer EX1008 (Part 7 of 9)

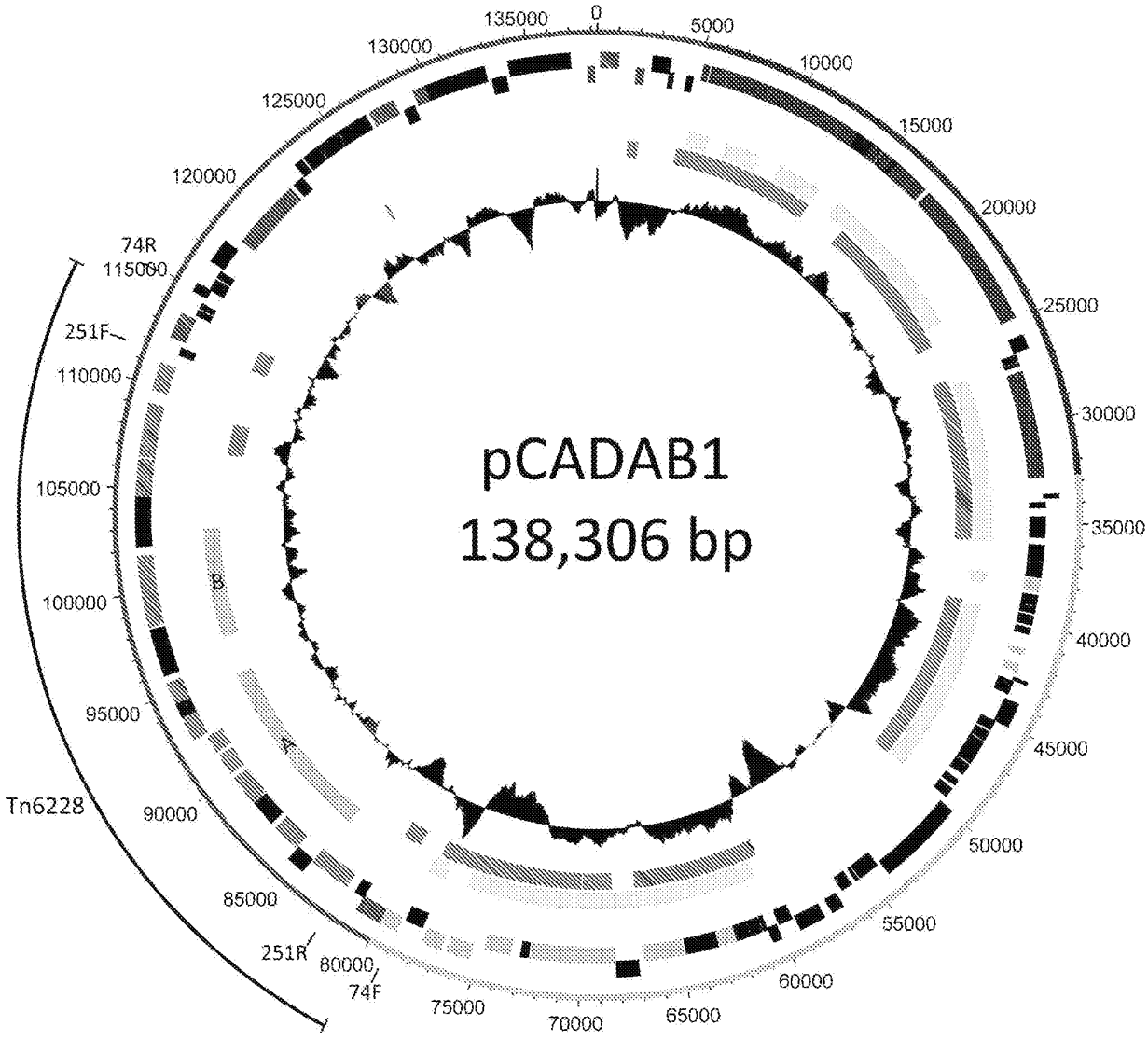


Figure 1. Genetic map of plasmid pCADAB1 and composite transposon Tn6228. The outer ring shows the functional regions of the plasmid: conjugative transfer (blue), plasmid stability and maintenance (yellow) and region containing multiple IS-elements (red). The composite transposon Tn6228 is displayed on the outside of the plasmid backbone (black line) Primers 74F, 74R, 251F and 251R for PCR have been marked on the outer ring. Inside of the backbone, predicted ORFs on either the positive strand (top blocks) or negative strand (bottom blocks) are displayed. Genes involved in degradation of MCPA are highlighted (green). Also highlighted are IS-elements (red), genes related to the type 4 secretion system (blue) and genes involved in plasmid maintenance and stability (yellow). The middle circle shows similarity to other sequences: Grey bars indicate collinear blocks of similarity to A) *Sphingomonas* sp. tfd44 (acc. no. AY598949.1) and B) *Sphingomonas* sp. 58-1 (acc. no. AB353895.1), while bright green bars indicate collinearity with plasmid pNL1 (acc. no. CP000676.1) and dark green with plasmid pCAR3 (acc. no. AB270530.1). The minimum nucleotide similarity in collinear blocks is 72%. The inner circle displays the G+C content (window size = 1000, step size = 10).
doi:10.1371/journal.pone.0083346.g001

A single homolog of the TfdA-related taurine catabolism dioxygenase (TauD) was found in the chromosomal contigs; however, the deduced amino acid sequence of this gene showed little similarity to any verified TfdA proteins. The closest TfdA 2,4-D dioxygenase homolog to this gene is that of *Ralstonia solanacearum* CMR15 (accession no. YP_008997670.1), which is only 31% identical to the taurine dioxygenase of *Sphingomonas* sp. ERG5.

However, genes homologous to *cadAB* were located on a 32.5 kbp contig containing a 1266 bp IS3 element. This contig had a G+C content of 62.4% and a coverage of 106.5×. An identical copy of the IS3 element was present in an approximately 106 kbp circular contig (circularity and size confirmed by PCR - data not shown) with a coverage of 97.5× and a G+C content of 63.4%, which contained genes involved in conjugative plasmid transfer, indicating that this contig represents a conjugative plasmid (pCADAB1). The total coverage of the IS3 elements was 199.8×, indicating that this insertion sequence has a copy number of approximately 2. It was hypothesized that the 32.5 kbp contig actually represents a composite transposon (Tn6228), flanked by identical, directly oriented copies of the IS3 elements,

COR-AAD1-00003764
Bayer EX1008 (Part 7 of 9)

Table 1. Primers used for TD-PCR.

Primer	Type	Target region	Sequence (5′-3′)	Anneal temp (°C)
251F	Forward primer	5′ end of transposon	AACCGGAACCCATCGGCATC	62.89
251R	Reverse primer	3′ end of transposon	CGGAACCGCTGCTCCATACC	63.25
74F	Forward primer	Upstream of transposon	CACCTTGACCACGGGTTCGG	63.33
74R	Reverse primer	Downstream of transposon	CCAAAGCGGTATCTGCCGTGA	63.02

doi:10.1371/journal.pone.0083346.t001

which is situated on the conjugative plasmid contig (review on composite transposons [37]). The length of the IS3 elements is longer than the insert-size of the paired-end Illumina sequencing, which prevents the Velvet program from correctly assembling this repeated structure as summarized by [38].

Genetic organization of transposon Tn6228 and plasmid pCADAB1

To investigate the possible position of Tn6228 in plasmid pCADAB1, PCRs were performed (Table 1+2 and Figure 1), followed by sequencing of the PCR products (results not shown). Primer set 1 was designed so that a 3373 bp product would result from the PCR if only the IS3 element is present and not the entire Tn6228. PCR with primer set 2 will yield a 3174 bp product if Tn6228 has a circular state outside pCADAB1, since primers 251F and 251R target the sequence at either end of Tn6228 and prime outwards. Primer sets 3 and 4 use combinations of primers targeting either Tn6228 or pCADAB1 sequence near the IS3 elements. PCR products from these primer sets with the predicted sizes (Table 2) will indicate that Tn6228 is situated on pCADAB1 in the predicted location. The PCR products had the expected sizes, except from that of primer set 1 which was larger than 3373 bp. The bands were excised from the gel and the PCR products were sequenced. The sequencing revealed that PCR using primer sets 3 and 4 had amplified DNA from the predicted location of Tn6228, confirming the predicted position on pCADAB1. The PCR using primer set 2 yielded a product with the predicted size, and sequencing of the PCR product confirmed that Tn6228 indeed has a circular state, as well as linearly inserted into pCADAB1. The product from the PCR with primer set 1 could not be sequenced properly, yielding only base calls of poor quality.

The organization of pCADAB1 with Tn6228 in the determined position is shown in Figure 1. Here, predicted genes, G+C content and regions of homology are shown. With PCR and PCR product sequencing it was confirmed that the transposon exists in a circular state, as well as in a linear state in the plasmid which is typical for IS3 elements [39] (reviewed by [40]). Identical copies of the IS3 element were determined to be flanking the composite transposon, when inserted into the plasmid. The IS3-like transposase found here contained a leucine-zipper motif, a DDE-motif and imperfect inverted repeats - all of which are expected to be present in a functional IS3-element [41].

Annotation of genes in transposon Tn6228

EasyGene ORF prediction of the transposon contig yielded 27 ORFs, which are numbered relative to plasmid start in the following sections. Manual annotation using BLASTX and Pfam domain search resulted in the predicted genes shown in Table S1 and Figure 2.

Within the Tn6228 transposon, three different gene clusters showed high similarity to previously identified clusters of 2,4-D catabolic genes (Figure 1 and 2). The first, 10493 bp in length, spans transposon-relative positions 2894–13386, contains 10 predicted ORFs and shares high nucleotide similarity (99% identity) to a chlorocatechol catabolic gene cluster from *Sphingomonas* sp. tfd44 [42] (accession no. AY598949.1). Due to sequence similarity, as well as BLASTX and Pfam results, ORFs 83–92 in this gene cluster were designated to encode putative LysR-type regulator, putative succinate-semialdehyde dehydrogenase GabD, hypothetical protein, hypothetical protein with Rieske domain, dienelactone hydrolase TfdE, chlorocatechol 1,2-dioxygenase TfdC, maleylacetate reductase TfdF, LysR-type regulator TfdR, muconate lactonizing enzyme TfdD and putative Tau/SafE sulfite exporter, respectively. The second gene cluster is 6182 bp in length and is located 2212 bp downstream of the first cluster in transposon-relative positions 15599–21780. It shows high nucleotide similarity (98% identity) to a clone fragment from *Sphingomonas* sp. 58-1 [8] (accession no. AB353895.1) and contains ORFs 95–98, which are annotated to encode pyridine nucleotide-disulphide oxidoreductase, large subunit of 2,4-D oxygenase CadA, small subunit of 2,4-D oxygenase CadB, and putative 2-hydroxybenzoate 5-hydroxylase ferredoxin CadC, respectively. Between the gene clusters, ORFs 93 and 94 encode transcriptional

Table 2. Combination of primers for TD-PCR and tested hypotheses.

Primerset (primers used)	Tested hypothesis	Predicted fragment size (bp)
P1 (74F+74R)	The plasmid only contains the transposase, not the transposon	3373
P2 (251F+251R)	The transposon has a circular state	3174
P3 (251F+74R)	The transposon is located on the plasmid in the predicted position. This primerset primes in the 3′-end of transposon	3333
P4 (74F+251R)	The transposon is located on the plasmid in the predicted position. This primerset primes in the 5′-end of transposon	3234

doi:10.1371/journal.pone.0083346.t002

COR-AAD1-00003765
Bayer EX1008 (Part 7 of 9)

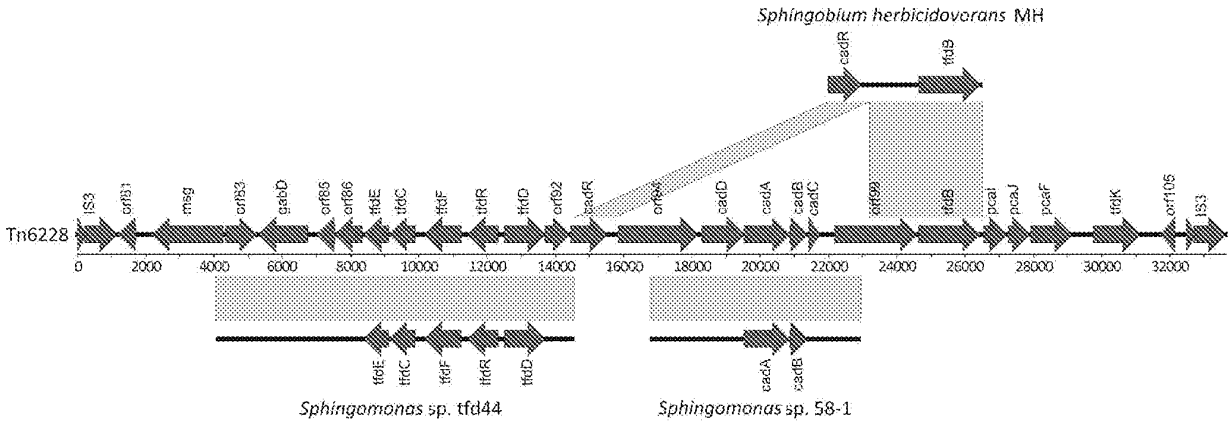


Figure 2. Genetic organization of the composite transposon Tn6228 and comparison to other gene clusters. Genes are marked with blue arrows. Gene abbreviations are *msg*: malate synthase G, *gabD*: putative succinate-semialdehyde dehydrogenase, *tfdE*: dienelacatone hydrolase, *tfdC*: chlorocatechol 1,2-dioxygenase, *tfdF*: maleylacetate reductase, *tfdR*: LysR family transcriptional regulator, *tfdD*: chloromuconate cycloisomerase, *tauE/safE*: sulfite exporter, *cadR*: AraC family transcriptional regulator, *cadD*: oxidoreductase component of Rieske non-heme iron oxygenase (RO), *cadA*: large subunit of 2,4-D oxygenase, *cadB*: small subunit of 2,4-D oxygenase, *cadC*: ferredoxin component of RO, *tfdB*: dichlorophenol hydroxylase, *pcaI*: 3-oxoacid CoA-transferase A subunit, *pcaJ*: 3-oxoacid CoA-transferase B subunit, *pcaF*: beta-ketoadipyl CoA thiolase, *tfdK*: transport protein. Nucleotide similarity is shown as gray bars linking to the corresponding gene clusters in *Sphingomonas* sp. tfd44 (acc. no. AY598949.1), *Sphingomonas* sp. 58-1 (acc. no. AB353895.1) and *Sphingobium herbicidovorans* MH (acc. no. AJ628861.1). Nucleotide similarities are shown with a cutoff value of 98% and were identified with BLASTN as implemented in Easyfig [27]. The composite figure shown here was compiled in Inkscape [28].
doi:10.1371/journal.pone.0083346.g002

regulator CadR and a putative TonB-dependent receptor, respectively. Upstream of the first gene cluster, ORFs 81 and 82 encode an unknown hypothetical protein and a malate synthase G, respectively. Downstream of the second gene cluster, ORFs 99–107 were predicted to encode a putative TonB-dependent receptor, dichlorophenol hydroxylase TfdB, A and B subunits of a 3-oxoacid CoA-transferase PcaIJ, a beta-ketoadipyl CoA thiolase PcaF, transport protein TfdK, a putative diguanylate cyclase and two ORFs constituting a transposase of the IS3 family. The genes *cadR*, *orf99* and *tfdB* showed high nucleotide similarity with a gene cluster from *Sphingobium herbicidovorans* MH (accession no. AJ628861.1), although *orf99* might be truncated in this bacterium (Figure 2).

A phylogenetic tree of 18 selected CadA amino acid sequences from the genera *Sphingomonas*, *Bradyrhizobium*, *Burkholderia* and *Arthrobacter* was constructed (Figure 3). This tree shows a clustering of CadA, similar to a clustering previously described [5], where CadA can be separated into 3 different clades: a *Sphingomonas* clade, a 2,4-D degrading *Bradyrhizobium* clade and a clade containing *Bradyrhizobium* not degrading 2,4-D. The *Sphingomonas* clade also contains a single member of the *Arthrobacter* genus, which has possibly acquired the *cadA* gene through horizontal gene transfer (HGT).

Properties of plasmid and transposon

EasyGene predicted 110 ORFs in the plasmid pCADAB1, and an automated annotation by RAST revealed that the predicted genes could be divided into cohesive regions of function: conjugal transfer, plasmid maintenance/stability and a region containing various IS-elements (Figure 1). The regions for conjugal transfer and maintenance/stability showed similarity in their nucleotide sequences to the sphingomonad plasmids pCAR3 (accession no. AB270530.1) and pNL1 (accession no. CP000676.1), which have been shown to harbor the genes involved in degradation of xenobiotics [43,44]. Within the conjugal transfer region, the genes *traALEKBVCFWUNFHGID*, *trbC* and *dsbC* encode a type 4 secretion system (T4SS) for conjugative transfer. These genes are very similar to those of pNL1 (Figure 1), which has been shown to be capable of conjugative transfer [44,45]. The maintenance/stability region of pERG5 contains genes encoding plasmid replication and partitioning systems, a toxin-antitoxin system, a multimer resolution system and restriction-modification systems.

The transposon was assembled by Velvet as one contig at a size of approximately 32.5 kbp, a G+C content of 62.4% and a coverage of 106.5×. Based on the average sequence coverages of the transposon, plasmid and chromosome, it was estimated that the transposon copy number is 1.17 relative to the chromosome and 1.09 relative to the plasmid. This approach for estimating copy numbers has been utilized previously [23]. Two ORFs (ORF 106–107) were predicted to constitute an IS-element gene, which was confirmed by ISfinder [24] and showed 84% identity with the IS3 family (group IS407) transposase ISSpma1 from *Sphingopyxis macrogoltabida* (accession no. AB196775). The IS-element has imperfect inverted repeats of 49 bp (32/49) (IRL: TGATCTGCCCCCTTCTGAGTGGTCCAAAATCTCTGT-TATTTTGGATCAT and IRR: ACAATGCACTAACAAT-CAACACGGACCACTCAGTGGGGGCCGGTCA). Furthermore, a leucine-zipper motif, involved in dimer formation of the transposase gene [41], was identified (data not shown) using the COILS program [26]. The conserved transposase-related DDE motif [41] was manually identified in the derived amino acid sequence as Dfv-55-sDngse-31-Esfngslr.

Discussion

In this study, we have identified a composite transposon (Tn6228) containing the complete genetic blueprint for degradation of 2,4-D and MCPA in a *Sphingomonas* sp. recently isolated from MCPA-degrading bacterial communities that originated from a herbicide-impacted groundwater aquifer [14]. This transposable element, which contains the catabolic genes cadAB in a novel genetic context, was situated on a conjugative plasmid. The plasmid contig, approximately 106 kbp in size, contains a single, perfectly identical copy of the IS3-element also present in

COR-AAD1-00003766
Bayer EX1008 (Part 7 of 9)

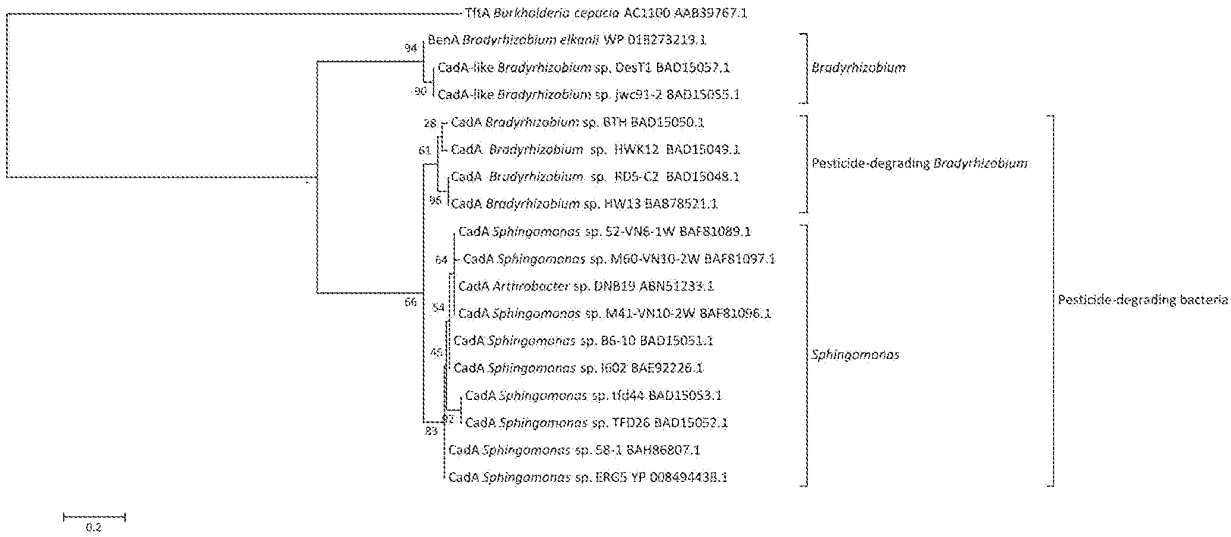


Figure 3. Dendrogram representing the phylogenetic relationship of representative CadA sequences. Representative sequences for alignment were identified from a BLASTX search using the derived amino acid sequence of CadA from *Sphingomonas* sp. ERG5 as query. BLASTX hits were picked for comparison with a cutoff value of 50% for amino acid identities. The support of each branch, as determined from 100 bootstrap samples, is indicated as a percentage at each node. Sequences were aligned with T-Coffee (v6.85) [30] and the alignment was curated with Gblocks (v0.91b) [31]. A phylogenetic tree was constructed using a maximum likelihood approach and the JTT substitution model [32] in the PhyML program (v3.0 aLRT) [33,34]. The resulting unrooted phylogenetic tree was visualized in MEGA4.0.2[35].
doi:10.1371/journal.pone.0083346.g003

the transposon contig. It was hypothesized that transposon Tn6228 would exist on the plasmid pCADAB1 flanked by identical IS3-elements, as well as in a circular intermediate state, typical of IS3-elements [39]. Due to the length of the transposase (1266 bp) being longer than the insert length in the Illumina library (500 bp), the assembler will not be able to solve the structure shown in Figure 1, where the transposon is inserted into the plasmid with IS3 elements flanking it. The structure displayed in Figure 1 was confirmed with PCR and product sequencing, using combinations (Table 2) of the primers shown in Figure 1 and Table 1. The PCR product sequencing from PCR primer set 1 did not provide any eligible sequence, while sequencing of the products from PCRs 3 and 4 (Table 2) confirmed that the transposon is situated on pCADAB1 (data not shown). The failure of PCR and product sequencing with primer set 1 indicates that a scenario with only an IS3 element and not Tn6228 in the predicted position is not plausible. The fact that the catabolic genes are located on a conjugative plasmid is in good agreement with previous observations in xenobiotic-degrading sphingomonads [45].

Catabolic genes involved in degradation of MCPA

The well-studied *tfdA*α gene could not be found in the assembled contigs of *Sphingomonas* sp. ERG5. However, the alternative Rieske non-heme iron oxygenase (RO) *cadAB* genes were found within the composite transposon Tn6228 also harboring the remaining genes in the degradation pathway of 2,4-D and related compounds [42]. The 1347 bp *cadA* ORF shows very high amino acid similarity (99% identity) to the α-subunit of 2,4-D oxygenase from *Sphingomonas* sp. 58-1 (accession no. BAH86807.1) and contains a Rieske motif and a catalytic domain, typical of RO enzymes. The 567 bp *cadB* ORF also shows high amino acid similarity (98% identity) to CadB from *Sphingomonas* sp. 58-1. β-subunits of RO oxygenases have been reported to be involved in substrate specificity [46].

In three-component RO-systems, a reductase receives electrons from NAD(P)H which is carried by a ferredoxin to the catabolic oxygenase, as reviewed in [47]. *orf95* is predicted to encode a putative oxidoreductase protein. This ORF shows high similarity to *orf*1 from *Sphingomonas* sp. 58-1 (98% identity). *orf98* is predicted to encode a Rieske ferredoxin component in the Rieske non-heme iron oxygenase (RO) family [48] and shows highest similarity (54% identity) to a 2-hydroxybenzoate 5-hydroxylase ferredoxin from *Achromobacter piechaudii* HLE (accession no. ZP_15933011.1). Even though all the parts of a three-component RO-system seem to be present in *Sphingomonas* sp. ERG5, the roles of the ferredoxin and oxidoreductase components in this RO system remain unknown, since it has previously been shown that the *cadAB* genes were necessary for conversion of 2,4-D to 2,4-DCP, but the oxidoreductase, putatively encoded by *orf95*, was not [8]. A ferredoxin component was not identified in the paper describing *Sphingomonas* sp. 58-1 [8], even though the sequence for a ferredoxin is present in the clone fragment in its GenBank entry (accession no. AB353895.1). The *cadABC* genes were first discovered in the strain *Bradyrhizobium* sp. HW3. Here it was shown that the ferredoxin component encoded by *cadC* indeed was essential for 2,4-D transformation, but no reductase was identified [2]. The finding of possible ferredoxin and reductase components of a three-component RO system in *Sphingomonas* sp. ERG5 suggests that these might be involved in the first catabolic step in 2,4-D and MCPA degradation, leading to the designation of putative *cadC* and putative novel gene *cadD* of the ferredoxin and reductase *orf*s, respectively.

Following the initial aryl ether linkage cleavage of MCPA and 2,4-D catalyzed by CadAB, the subsequent catabolic and regulatory pathway are represented by 8 ORFs in Tn6228: *tfdB, tfdC, tfdD, tfdE, tfdF, tfdK, tfdR* and *cadR*. These ORFs showed high amino acid similarity to previously described genes in the chlorophenoxyacetic acid metabolic pathway of strains *Sphingobium herbicidovorans* and *Sphingomonas* sp. TFD44 [42,49] (Table S1). The

COR-AAD1-00003767
Bayer EX1008 (Part 7 of 9)

tfd-genes are involved in the *ortho* cleavage pathway of 2,4-D and related compounds and were first studied in *Cupriavidus pinatubonensis* JMP134 [50]. The *tfdB* gene encodes a dichlorophenol hydroxylase, which converts 4-chloro-2-methylphenol (MCP) to 5-chloro-3-methyl-catechol (MCC), which is then converted to chloromuconate by a chlorocatechol 1,2-dioxygenase, encoded by *tfdC*. The product of *tfdD* then transforms chloromuconate to dienelactone. Finally, dienelactone is converted first to maleylacetate then to 3-oxoadipate by the gene products of *tfdE* and *tfdF*, respectively.

Additionally, *orf101* and *orf102* encode subunits A and B of a 3-oxoadipate CoA-transferase, enabling the reaction yielding 3-oxoadipyl-CoA and succinate from 3-oxoadipate and succinyl-CoA. The 3-oxoadipate for this reaction could be provided by the reaction catalyzed by TfdF. *orf103* is predicted to encode a 3-oxoadipyl CoA thiolase that can convert 3-oxoadipyl-CoA to succinyl-CoA and acetyl-CoA, both of which are further degraded the tricarboxylic acid cycle (TCA) [51]. *orf82* and *orf84* are designated to encode a malate synthase G and a putative succinate-semialdehyde dehydrogenase, respectively. Both of these enzymes are involved in the TCA and glyoxylate cycle; however homologs of these proteins were identified on chromosomal contigs (data not shown), suggesting that these plasmid-encoded enzymes are not essential for the host cell. Malate synthase G can convert acetyl-CoA into malate and succinate-semialdehyde dehydrogenase is possibly involved in the further degradation of succinyl-CoA.

In addition to the catabolic genes, regulatory genes *cadR* and *tfdR* as well as a gene encoding the transport protein TfdK are also present within the transposon. The deduced amino acid sequence of the *cadR* gene found here is 100% identical to that of *Sphingobium herbicidovorans* MH (accession no. CAF32814.1) and has an identity of 62% to the *cad* gene transcriptional regulator from *Bradyrhizobium* sp. HW13 (accession no. BAB78520.1). The *cadR* gene was found to be essential for 2,4-D degradation in *Bradyrhizobium* sp. HW13 and it was hypothesized, due to sequence similarity, that *cadR* encodes a positive transcriptional regulator [2].

orf90 was annotated as a LysR-type transcriptional regulator TfdR with high similarity (99% identity) to TfdR of *Sphingomonas* sp. TFD44 (accession no. AAT99366.1). It has been suggested that the transcriptional inducer of the 2,4-D pathway is the product of the TfdC protein, 2,4-dichloromuconate [52].

A homologue of the *tfdK* gene in *Sphingobium herbicidovorans* MH (accession no. CAF32820.1) encoding a protein of the major facilitator superfamily (MFS) was found to be encoded by *orf104*. In *Cupriavidus pinatubonensis* JMP134 it was shown that TfdK is an active transporter of 2,4-D and increases its uptake rate of 2,4-D up to 10 times compared to a tfdK mutant [53].

Evolution of genetic elements

Two of the three gene clusters in Tn6228 previously described, showed high degrees of collinearity and sequence similarity to previous isolates [8,42]. This could indicate that this specific genetic organization of the *cad*- and *tfd*-genes is highly conserved within sphingomonads capable of PAA-herbicide degradation or that these genes are an integral part of the genetic repertoire of sphingomonads. It has previously been discussed that sphingomonads harbor large numbers of mobile genetic elements [54] and that these are likely responsible for regular genetic exchange of biodegradative potential between sphingomonads [55]. The sequence conservation displayed in Figure 2 strongly supports that these catabolic enzymes are subject to HGT between sphingomonads. The non-collinearity between *Sphingomonas* sp. ERG5 and the gene cluster from *Sphingobium herbicidorans* MH could indicate that genetic rearrangements have occurred in one of the strains (Figure 2). The G+C values of Tn6228 shows that no internal regions with a markedly different G+C content are present within the transposon (Figure 1). However, when comparing with the plasmid backbone of pCADAB1, the region containing mobile genetic elements (including Tn6228) has a tendency towards slightly lower G+C contents. This suggests that the region with many mobile genetic elements might contain genes with an origin different from that of the plasmid backbone. Furthermore, the average G+C contents of pCADAB1 and Tn6228 are not different from that of the chromosomal contigs, suggesting that either these genetic entities were not recently acquired via horizontal gene transfer or that they originate from a bacteria with similar G+C content. Despite *Sphingomonas* sp. 58-1 being isolated in Japan, *Sphingomonas* sp. TFD44 being isolated in North America and *Sphingomonas* sp. ERG5 being isolated in Denmark, these strains show remarkable homology at the DNA level in the catabolic genes. All these were isolated from pesticide-polluted soils, and it would be interesting to attempt the isolation of *cadAB*-harboring sphingomonads from pristine environments for molecular comparisons in order to study the origin of this PAA degradation pathway initiated by the *cad*-genes.

Considering the phylogenetic separation of the CadA amino acid sequences shown in Figure 3 into a *Sphingomonas* and two *Bradyrhizobium* clades, it seems plausible that there exist multiple (at least three) classes of CadA that are each inherent to only the *Sphingomonas* or *Bradyrhizobium* genus. It was suggested that the *Sphingomonas* cluster and 2,4-D degrading *Bradyrhizobium* cluster had evolved from a shared ancestral gene, indicating different evolution of the *cadA* gene in 2,4-D degraders from that of non-2,4-D degraders [5]. Similar phylogenetic trees were constructed for the genes *tfdBCDEFRK* and *cadR*. The trees for *tfdBD* (Figures S1 and S2) contain monophyletic clades of the *Sphingomonadaceae* family, indicating that these genes are more similar within this family than with other phylogenetic groups (e.g. the *Bradyrhizobiaceae* family or *Burkholderiales* order). This suggests that parts of the 2,4-D-degradation pathway has evolved separately in the *Sphingomonadaceae* family, which is supported by others [9] who hypothesized that the *tfdA*α gene has evolved distinctly in sphingomonads and *Bradyrhizobium* without horizontal gene transfer. However, representatives of the downstream *tfd*-genes from *Sphingomonadaceae* are not yet abundant enough in the databases for proper evolutionary studies. The remaining phylogenetic trees suggest that horizontal gene transfer has had an effect on the evolution of the *tfdCEFRK* genes since no clear monophyletic groups are defined for any particular genera (data not shown).

The plasmid backbone of pCADAB1, encoding genes related to conjugative transfer and plasmid stability, showed high similarity and collinearity to plasmids pCAR3 (accession. no. AB270530.1) and pNL1 (accession. no. CP000676.1) from *Sphingomonas* sp. KA1 and *Novosphingobium aromaticivorans* DSM12444, respectively (Figure 1). Plasmid pNL1 has been shown to be able to transfer to other sphingomonads [45], and both pNL1 and pCAR3 have been suggested to be members of a novel incompatibility group of plasmids [43]. Though additional mating experiments should be carried out on this putatively novel incompatibility group, preliminary investigations on the plasmid replication and partitioning genes *repA* and *parA* of pCADAB1 indicates that this plasmid belongs to this group (data not shown). In fact, the backbones of the described plasmids are similar and collinear, while the region containing IS-elements and transposons is completely unrelated, suggesting that these mobile genetic elements might serve as the tools for acquiring new catabolic genes while the backbone is the unchangeable toolbox of these

COR-AAD1-00003768
Bayer EX1008 (Part 7 of 9)

sphingomonad strains. It has been shown that many sphingomonad strains contain degradative plasmids [45]. If these plasmids are restricted to reside in members of the sphingomonad genera, it could explain why genes such as *cadA* evolve separately from other *cadA*-harboring genera. Further studies on the plasmids of sphingomonads will possibly provide insight to the degradative capabilities of these bacteria and why they apparently are successfully thriving in polluted environments.

Conclusions

In this study, a composite transposon was identified which harbors the complete set of genes for MCPA and 2,4-D degradation, including initial steps of the TCA cycle and regulatory genes. The transposon was furthermore found to be situated on a putatively conjugative plasmid. The pathway initiates with the CadAB Rieske non-heme iron monooxygenase, rather than the α-ketoglutarate-dependent dioxygenase TfdA enzyme, that is most often associated with this pathway.

Supporting Information

Table S1 Predicted ORFs with annotations and putative protein properties.
(DOCX)

Figure S1 Dendrogram representing the phylogenetic relationship of representative TfdB sequences.
(TIF)

Figure S2 Dendrogram representing the phylogenetic relationship of representative TfdD sequences.
(TIF)

Acknowledgments

We would like to thank laboratory technicians Karin Pinholt Vestberg at University of Copenhagen and Pia Bach Jakobsen at GEUS for assistance.

Author Contributions

Conceived and designed the experiments: TKN ZX JA SRS LHH. Performed the experiments: TKN ZX. Analyzed the data: TKN ZX EG. Contributed reagents/materials/analysis tools: LHH JA SRS. Wrote the paper: TKN.

References

1. Thorling L, Hansen B, Langtofte C, Brüsch W, Møller RR, et al. (2011) Grundvand. Status og udvikling 1989–2010. Teknisk rapport, GEUS 2011.
2. Kitagawa W, Takami S, Miyauchi K, Masai E, Kamagata Y, et al. (2002) Novel 2,4-dichlorophenoxyacetic acid degradation genes from oligotrophic Bradyrhizobium sp. strain HW13 isolated from a pristine environment. J Bacteriol 184: 509–518.
3. Fukumori F, Hausinger RP (1993) Alcaligenes eutrophus JMP134 "2,4-dichlorophenoxyacetate monooxygenase" is an alpha-ketoglutarate-dependent dioxygenase. J Bacteriol 175: 2083–2086.
4. Streber WR, Timmis KN, Zenk MH (1987) Analysis, cloning, and high-level expression of 2,4-dichlorophenoxyacetate monooxygenase gene tfdA of Alcaligenes eutrophus JMP134. J Bacteriol 169: 2950–2955.
5. Itoh K, Kanda R, Sumita Y, Kim H, Kamagata Y, et al. (2002) tfdA-like genes in 2,4-dichlorophenoxyacetic acid-degrading bacteria belonging to the Bradyrhizobium-Agromonas-Nitrobacter-Afipia cluster in alpha-Proteobacteria. Appl Environ Microbiol 68: 3449–3454.
6. Ledger T, Pieper DH, Perez-Pantoja D, Gonzalez B (2002) Novel insights into the interplay between peripheral reactions encoded by xyl genes and the chlorocatechol pathway encoded by tfd genes for the degradation of chlorobenzoates by Ralstonia eutropha JMP134. Microbiology 148: 3431–3440.
7. Fukumori F, Hausinger RP (1993) Purification and characterization of 2,4-dichlorophenoxyacetate/alpha-ketoglutarate dioxygenase. J Biol Chem 268: 24311–24317.
8. Shimojo M, Kawakami M, Amada K (2009) Analysis of genes encoding the 2,4-dichlorophenoxyacetic acid-degrading enzyme from Sphingomonas agrestis 58-1. J Biosci Bioeng 108: 56–59.
9. Itoh K, Tashiro Y, Uobe K, Kamagata Y, Suyama K, et al. (2004) Root nodule Bradyrhizobium spp. harbor tfdAalpha and cadA, homologous with genes encoding 2,4-dichlorophenoxyacetic acid-degrading proteins. Appl Environ Microbiol 70: 2110–2118.
10. Ditterich F, Poll C, Pagel H, Babin D, Smalla K, et al. (2013) Succession of bacterial and fungal 4-chloro-2-methylphenoxyacetic acid degraders at the soil-litter interface. FEMS Microbiol Ecol.
11. Kamagata Y, Fulthorpe RR, Tamura K, Takami H, Forney LJ, et al. (1997) Pristine environments harbor a new group of oligotrophic 2,4-dichlorophenoxyacetic acid-degrading bacteria. Appl Environ Microbiol 63: 2266–2272.
12. McGowan C, Fulthorpe R, Wright A, Tiedje JM (1998) Evidence for interspecies gene transfer in the evolution of 2,4-dichlorophenoxyacetic acid degraders. Appl Environ Microbiol 64: 4089–4092.
13. Huong NL, Itoh K, Suyama K (2007) Diversity of 2,4-dichlorophenoxyacetic acid (2,4-D) and 2,4,5-trichlorophenoxyacetic acid (2,4,5-T)-degrading bacteria in Vietnamese soils. Microbes and Environments 22: 243–256.
14. Gözdereliler E, Boon N, Aamand J, De Roy K, Granitsiotis MS, et al. (2013) Comparing metabolic functionalities, community structures, and dynamics of herbicide-degrading communities cultivated with different substrate concentrations. Appl Environ Microbiol 79: 367–375.
15. Lindgreen S (2012) AdapterRemoval: easy cleaning of next-generation sequencing reads. BMC Res Notes 5: 337.
16. Zerbino DR, Birney E (2008) Velvet: algorithms for de novo short read assembly using de Bruijn graphs. Genome Res 18: 821–829.
17. Aziz RK, Bartels D, Best AA, DeJongh M, Disz T, et al. (2008) The RAST Server: rapid annotations using subsystems technology. BMC Genomics 9: 75.
18. Altschul SF, Gish W, Miller W, Myers EW, Lipman DJ (1990) Basic local alignment search tool. J Mol Biol 215: 403–410.
19. Bateman A, Birney E, Durbin R, Eddy SR, Howe KL, et al. (2000) The Pfam protein families database. Nucleic Acids Res 28: 263–266.
20. Nielsen P, Krogh A (2005) Large-scale prokaryotic gene prediction and comparison to genome annotation. Bioinformatics 21: 4322–4329.
21. Larsen TS, Krogh A (2003) EasyGene–a prokaryotic gene finder that ranks ORFs by statistical significance. BMC Bioinformatics 4: 21.
22. Carver T, Thomson N, Bleasby A, Berriman M, Parkhill J (2009) DNAPlotter: circular and linear interactive genome visualization. Bioinformatics 25: 119–120.
23. Rasko DA, Rosovitz MJ, Okstad OA, Fouts DE, Jiang L, et al. (2007) Complete sequence analysis of novel plasmids from emetic and periodontal Bacillus cereus isolates reveals a common evolutionary history among the B. cereus-group plasmids, including Bacillus anthracis pXO1. J Bacteriol 189: 52–64.
24. Siguier P, Perochon J, Lestrade L, Mahillon J, Chandler M (2006) ISfinder: the reference centre for bacterial insertion sequences. Nucleic Acids Res 34: D32–36.
25. Rice P, Longden I, Bleasby A (2000) EMBOSS: the European Molecular Biology Open Software Suite. Trends Genet 16: 276–277.
26. Lupas A, Van Dyke M, Stock J (1991) Predicting coiled coils from protein sequences. Science 252: 1162–1164.
27. Sullivan MJ, Petty NK, Beatson SA (2011) Easyfig: a genome comparison visualizer. Bioinformatics 27: 1009–1010.
28. Inkscape website. Available: http://www.inkscape.org. Accessed 2013 Jul 4.
29. Dereeper A, Guignon V, Blanc G, Audic S, Buffet S, et al. (2008) Phylogeny.fr: robust phylogenetic analysis for the non-specialist. Nucleic Acids Res 36: W465–469.
30. Notredame C, Higgins DG, Heringa J (2000) T-Coffee: A novel method for fast and accurate multiple sequence alignment. J Mol Biol 302: 205–217.
31. Castresana J (2000) Selection of conserved blocks from multiple alignments for their use in phylogenetic analysis. Mol Biol Evol 17: 540–552.
32. Jones DT, Taylor WR, Thornton JM (1992) The rapid generation of mutation data matrices from protein sequences. Comput Appl Biosci 8: 275–282.
33. Guindon S, Gascuel O (2003) A simple, fast, and accurate algorithm to estimate large phylogenies by maximum likelihood. Syst Biol 52: 696–704.
34. Anisimova M, Gascuel O (2006) Approximate likelihood-ratio test for branches: A fast, accurate, and powerful alternative. Syst Biol 55: 539–552.
35. Tamura K, Dudley J, Nei M, Kumar S (2007) MEGA4: Molecular Evolutionary Genetics Analysis (MEGA) software version 4.0. Mol Biol Evol 24: 1596–1599.
36. Ye J, Coulouris G, Zaretskaya I, Cutcutache I, Rozen S, et al. (2012) Primer-BLAST: a tool to design target-specific primers for polymerase chain reaction. BMC Bioinformatics 13: 134.
37. Nojiri H, Shintani M, Omori T (2004) Divergence of mobile genetic elements involved in the distribution of xenobiotic-catabolic capacity. Appl Microbiol Biotechnol 64: 154–174.
38. Nagarajan N, Pop M (2013) Sequence assembly demystified. Nat Rev Genet 14: 157–167.
39. Sekine Y, Aihara K, Ohtsubo E (1999) Linearization and transposition of circular molecules of insertion sequence IS3. J Mol Biol 294: 21–34.

COR-AAD1-00003769
Bayer EX1008 (Part 7 of 9)

40. Curcio MJ, Derbyshire KM (2003) The outs and ins of transposition: from mu to kangaroo. Nat Rev Mol Cell Biol 4: 865–877.
41. Ohtsubo E, Minematsu H, Tsuchida K, Ohtsubo H, Sekine Y (2004) Intermediate molecules generated by transposase in the pathways of transposition of bacterial insertion element IS3. Adv Biophys 38: 125–139.
42. Thiel M, Kaschabek SR, Groning J, Mau M, Schlomann M (2005) Two unusual chlorocatechol catabolic gene clusters in Sphingomonas sp. TFD44. Arch Microbiol 183: 80–94.
43. Shintani M, Urata M, Inoue K, Eto K, Habe H, et al. (2007) The Sphingomonas plasmid pCAR3 is involved in complete mineralization of carbazole. J Bacteriol 189: 2007–2020.
44. Romine MF, Stillwell LC, Wong KK, Thurston SJ, Sisk EC, et al. (1999) Complete sequence of a 184-kilobase catabolic plasmid from Sphingomonas aromaticivorans F199. J Bacteriol 181: 1585–1602.
45. Basta T, Keck A, Klein J, Stolz A (2004) Detection and characterization of conjugative degradative plasmids in xenobiotic-degrading Sphingomonas strains. J Bacteriol 186: 3862–3872.
46. Hurtubise Y, Barriault D, Sylvestre M (1998) Involvement of the terminal oxygenase beta subunit in the biphenyl dioxygenase reactivity pattern toward chlorobiphenyls. J Bacteriol 180: 5828–5835.
47. Ferraro DJ, Gakhar L, Ramaswamy S (2005) Rieske business: structure-function of Rieske non-heme oxygenases. Biochem Biophys Res Commun 338: 175–190.
48. Gibson DT, Parales RE (2000) Aromatic hydrocarbon dioxygenases in environmental biotechnology. Curr Opin Biotechnol 11: 236–243.
49. Muller TA, Byrde SM, Werlen C, van der Meer JR, Kohler HP (2004) Genetic analysis of phenoxyalkanoic acid degradation in Sphingomonas herbicidovorans MH. Appl Environ Microbiol 70: 6066–6075.
50. Don RH, Weightman AJ, Knackmuss HJ, Timmis KN (1985) Transposon mutagenesis and cloning analysis of the pathways for degradation of 2,4-dichlorophenoxyacetic acid and 3-chlorobenzoate in Alcaligenes eutrophus JMP134(pJP4). J Bacteriol 161: 85–90.
51. Harwood CS, Parales RE (1996) The beta-ketoadipate pathway and the biology of self-identity. Annu Rev Microbiol 50: 553–590.
52. Filer K, Harker AR (1997) Identification of the Inducing Agent of the 2,4-Dichlorophenoxyacetic Acid Pathway Encoded by Plasmid pJP4. Appl Environ Microbiol 63: 317–320.
53. Leveau JH, Zehnder AJ, van der Meer JR (1998) The tfdK gene product facilitates uptake of 2,4-dichlorophenoxyacetate by Ralstonia eutropha JMP134(pJP4). J Bacteriol 180: 2237–2243.
54. Aylward FO, McDonald BR, Adams SM, Valenzuela A, Schmidt RA, et al. (2013) Comparison of 26 Sphingomonad Genomes Reveals Diverse Environmental Adaptations and Biodegradative Capabilities. Applied and Environmental Microbiology.
55. Stolz A (2009) Molecular characteristics of xenobiotic-degrading sphingomonads. Appl Microbiol Biotechnol 81: 793–811.

COR-AAD1-00003770
Bayer EX1008 (Part 7 of 9)

Bulletin of Environmental Contamination and Toxicology (2020) 104:200–205
https://doi.org/10.1007/s00128-019-02760-5

Biodegradation Potential and Ecotoxicity Assessment in Soil Extracts Amended with Phenoxy Acid Herbicide (2,4-D) and a Structurally-Similar Plant Secondary Metabolite (Ferulic Acid)

Elżbieta Mierzejewska[1] · Agnieszka Baran[2] · Magdalena Urbaniak[1,3]

Received: 24 September 2019 / Accepted: 22 November 2019 / Published online: 28 November 2019
© Springer Science+Business Media, LLC, part of Springer Nature 2019

Abstract

Phenoxy acid 2,4-D (2,4-dichlorophenoxy acid) is one of the most commonly-used herbicide in agriculture. Biodegradation of 2,4-D can be stimulated by structurally-related plant secondary metabolites such as ferulic acid (FA). The aim of this study is to: (1) assess the potential of indigenous soil bacteria to degrade 2,4-D in the presence of FA by PCR analysis of functional *tfdA* genes, (2) to determine the influence of 2,4-D and FA on samples ecotoxicity using Phytotoxkit® and Microtox® biotests. The detection of *tfdA* genes varied depending on the enrichment of samples with FA. FA suppressed detection of the *tfdA* genes, 100 µM 2,4-D induced higher detection of studied amplicons, while 500 µM 2,4-D delayed their detection. The ecotoxicity response was specific and differed between plants (PE% *Lepidium sativum* > *Sinapis alba* > *Sorghum saccharatum*) and bacteria (PE% up to 99% for *Vibrio fischeri*). Our findings confirm that 2,4-D and FA had a toxic influence on the used organisms.

Keywords 2,4-D · Biodegradation · Plant secondary metabolites · Ferulic acid · *tfdA* gene · Ecotoxicity

Abbreviations

2,4-D	2,4-Dichlorophenoxy acid
PSM	Plant secondary metabolite
FA	Ferulic acid
PE%	Percentage effect

The development of herbicides and other easily-accessible crop protection agents has allowed significant increases in agricultural production. Nowadays, one of the most commonly-used active ingredient in herbicides is 2,4-D (2,4-dichlorophenoxy acid). Due to its low cost and good performance, its use has grown worldwide, and it is now the fifth most commonly-used active ingredient in the United States in the agricultural and home/garden market sector (U.S. EPA Report 2017); in addition, 6.5 million kg of 2,4-D was sold in the EU in 2016 (~2 million kg in Poland) (Eurostat 2018). Such significant usage, however, runs the risk of misuse. In particular, incorrect storage and usage practices can widen the dispersal of the compound and its metabolites throughout the environment, especially in soil and water ecosystems, resulting in disturbances in ecological sustainability. Hence, various methods have been developed for eliminating 2,4-D from the environment. One such approach employs degradation by soil microbiota (biodegradation), especially by bacteria harboring the functional genes from the *tfdABCDEF* cluster (Kitagawa et al. 2002). The first step of the 2,4-D biodegradation pathway is initiated by α-ketoglutarate-dependent dioxygenase encoded by genes from the *tfdA* cluster, including *tfdA Class I, II, III* and *tfdA α* (Kitagawa et al. 2002). Due to the high degree of homology between strains, the genes from the *tfdA* cluster

Electronic supplementary material The online version of this article (https://doi.org/10.1007/s00128-019-02760-5) contains supplementary material, which is available to authorized users.

✉ Elżbieta Mierzejewska
elzbieta.mierzejewska@unilodz.eu

[1] Department of Applied Ecology, Faculty of Biology and Environmental Protection, University of Lodz, Banacha 12/16, 90-237 Lodz, Poland

[2] Faculty of Agriculture and Economics, Department of Agricultural and Environmental Chemistry, University of Agriculture in Krakow, Mickiewicza 21, 31-120 Kraków, Poland

[3] Faculty of Food and Biochemical Technology, Department of Biochemistry and Microbiology, University of Chemistry and Technology in Prague, Technicka 3, 166 28 Prague, Czech Republic

COR-AAD1-00003771
Bayer EX1008 (Part 7 of 9)

have been selected as biomarkers of the capability of bacteria to metabolize 2,4-D (Kitagawa et al. 2002), and they are frequently used in studies of phenoxy acid biodegradation. Nevertheless, microbial degradation of 2,4-D might be very slow in the natural environment, especially in a temperate climate characterized by low winter temperatures and, in many regions, by depleted soil organic carbon content and acidic pH. Therefore, there is a need to identify nature-based solutions that can enhance the process of bacterial degradation. A promising way to enhance the removal of 2,4-D from the environment is rhizoremediation: a naturally occurring process which takes place in the soil immediately around the plant roots (rhizosphere); during this process, microbial growth and pollutant degradation are stimulated by root exudates enriched by plant secondary metabolites (PSMs). PSMs not only modify the chemical and physical properties of the soil and protect plants against phytopathogens, but also act as substrates or inducers on the catabolic pathways employed by rhizospheric microorganisms to remove contaminants (Uhlik et al. 2013). One common PSM is ferulic acid (FA; 4-hydroxy-3-methoxycinnamic acid), which is widely distributed throughout all plant tissues and excreted to the soil (Singh et al. 2014). Its structural similarity to 2,4-D suggests it may impact the degradation of the herbicide by soil microbiota by accelerating the catabolic activity of bacteria (i.e. the presence of functional degradative genes) thus lessening the ecotoxicity of the samples. Hence, the aim of this study was twofold: it firstly determines the potential of indigenous soil bacteria to degrade 2,4-D in the presence or absence of structurally-related PSM (FA); this is achieved by PCR analysis of the bacterial *16S rDNA* gene and the set of functional *tfdA* and *tfdA*-like genes involved in 2,4-D degradation. In addition, the study evaluates the influence of herbicide (2,4-D) and FA on the ecotoxicity of samples using two widely-used commercially-available biotests: Phytotoxkit® and Microtox®.

Materials and Methods

Liquid mineral salt medium (MSM) was prepared according to Gaunt and Evans (1971). The soil extract was prepared according to Strzelczyk (1968) with some modifications (see SI), using agricultural soil of known properties (see Table SI1). The study was conducted in bacterial cultures containing MSM enriched with soil microorganisms derived from the soil extract (50%:50%, v/v). Phenoxy herbicide i.e. 2,4-D stock solution concentration (7.5 µM) was controlled according to methods described below. Accurate dilutions were made in order to obtain samples with 2,4-D at doses of 100 and 500 µM and/or FA at a dose of 250 µM (see SI). Samples containing only sterile MSM, or a mixture of sterile MSM and sterile soil extract, were used as controls to assess the degree of 2,4-D physicochemical degradation. The samples were incubated in darkness at 25 °C for 24 days. Samples were collected for molecular analysis four times during the incubation period, i.e. every six days. Bacterial DNA extraction was performed using a EurX Bacterial & Yeast Genomic DNA Purification Kit. Sterile samples with no microorganisms were also isolated and the absence of DNA was determined on agarose gel. These samples were not used for further gene amplification. The PCR gene amplification itself was performed according to Poll et al. (2010) and Bælum et al. (2006, 2010) with minor modifications regarding the annealing temperature (see Table SI2). The bacterial DNA fragment was amplified using two primer pairs specific to bacterial *16S rDNA*, and five sets of primers specific to the *tfdA* gene (see Table SI2). PCR products were separated by 1.5% agarose gel electrophoresis in TBE buffer using constant voltage (70 V), and visualized using ethidium bromide (2 mg/mL), with DNA M100–500 (MR75) and DNA M600–1000 (MR85) markers (DNA Gdańsk). The gels were documented using the UVitec system (Cambridge, UK). The samples were also subjected to ecotoxicity analysis at the beginning (Phytotoxkit®) and at the end of incubation period (Phytotoxkit® and Microtox®). In the Phytotoxkit®, the inhibition of the root length of three plant species *Sorghum saccharatum* (L.) Moench, *Lepidium sativum* (L.) and *Sinapis alba* (L.) was measured in relation to control sample of soil after three days of exposure (ISO 18763:2016; Phytotoxkit 2004). The Microtox® bioassay, in contrast, uses the luminescent properties of *Vibrio fischeri*. The inhibition of luminescence was measured before and after a 15-min incubation of the bacterial suspension with the samples (Microbics Corporation 1992). The ecotoxicity testing procedures are described in more detail in our earlier studies (Baran and Tarnawski 2013; Urbaniak et al. 2016; Mierzejewska et al. 2017). The samples were classified as non-toxic when the percent effect (PE%) of root growth inhibition or luminescence inhibition was $\geq 20\%$, slightly toxic in the range $20\% \leq PE < 50\%$, toxic in the range $50\% \leq PE < 100\%$, and highly toxic at $PE = 100\%$ (Persoone et al. 2003).

The concentration of 2,4-D was assessed after 24 days of incubation using enzyme immunoassay (ELISA) RaPID Assay® 2,4-D Test Kit following the manufacturer procedure (Modern Water 2012). The % of 2,4-D reduction was calculated in reference to the initial concentration of herbicide used (100/500 µM). To assess the exact concentration of the herbicide used, its initial concentration was confirmed using RaPID Assay® 2,4-D Test Kit. Each analytical batch contained a sample blank, a control sample of known concentration, 4 calibration standards (0 µM; 0.0045 µM; 0.045 µM; 0.2262 µM) and tested samples. Zero standard (0 µM) contained diluent and it was used in the calibration standard as a negative control. The precision was verified by

COR-AAD1-00003772
Bayer EX1008 (Part 7 of 9)

duplicate analyses and the test reproducibility was measured using coefficient of variation (CVs). CVs should be lower than 10% for calibration standards and lower than 15% for samples. If the CVs exceeded the above values, the whole procedure was repeated in order to achieve good quality of the obtained results. The minimum detection level of the kit was 0.0032 µM. Before the analysis studied samples were appropriately diluted in order to fit in the calibration standard. The effect of dilution was taken into consideration during the calculation of 2,4-D concentration. Samples showing a concentration lower than minimum detection level were considered to be negative.

Results and Discussion

The microorganisms extracted from agricultural soil for the purpose of the current study were found to possess *tfdAα* and *tfdA Class III* gene fragments, which are responsible for the initial step of phenoxy acids degradation and were identified in a wide range of pristine and contaminated sites (Lappin et al. 1985).Their presence indicates that the soil microbiota are able to degrade 2,4-D (Mierzejewska et al. 2017). Our findings confirm the presence of bacterial DNA, including the conservative *16S rDNA* gene fragment, in all the samples amended with soil extract. Amplification of functional degradative *tfdA* genes revealed the abundance of almost all selected functional gene fragments in the studied samples, except for *tfdA Class II* (Table 1). Significant differences were also found between samples with PSM-FA and those without. *tfdAα* was observed in 75% of soil extract samples, irrespective of FA application. In the variants with soil extract and no FA, the gene was present during first 18 days of incubation but not on the last day; however, in samples enriched with FA, the gene wasn't detected on 12th day (Table 1). The application of herbicide also shifted the occurrence pattern of the gene: in the soil extract samples, *tfdAα* was only observed at the higher dose of 2,4-D (500 µM), and only at the end of the incubation period. When further supplemented with FA, *tfdAα* amplicons were observed in 50% of samples treated with the lower dose of herbicide (100 µM), but in no samples with the higher dose (500 µM) (Table 1). *tfdA Class I* was detected only in samples enriched with FA, while *tfdA Class III* was observed only in variants without FA. Both *Class I* and *III* were observed following the application of 100 µM 2,4-D, but their detection occurred later at the higher concentration (Table 1). Also *tfdA* gene fragments demonstrated different patterns depending on the enrichment of samples with FA: the addition of PSM suppressed detection of the gene (Table 1). The wide diversity of *tfdA*-like genes is partly due to the wide range of bacteria capable of degrading phenoxy acids in the environment. Three groups of bacteria harboring

Table 1 The results of the PCR amplification; '+' indicate the presence of a PCR product for the studied primers

Days of incubation	2,4-D concentration	Target gene										
		16S rDNA	tfdA alfa	tfdA cI	tfdA cII	tfdA cIII	tfdA	16S rDNA	tfdA alfa	tfdA cI	tfdA cII	tfdA cIII	tfdA
Sample		MSM + SE						MSM + SE + FA					
6	0 µM	+	+					+	+				
12		+	+					+					
18		+	+				+	+	+				
24		+					+	+	+	+			
6	100 µM	+				+		+		+			
12		+				+		+		+			
18		+				+		+	+	+			
24		+				+		+	+				
6	500 µM	+						+					
12		+				+		+		+			
18		+				+		+					
24		+	+					+					

MSM mineral salt medium, *SE* soil extract

COR-AAD1-00003773
Bayer EX1008 (Part 7 of 9)

tfdA-like genes have been identified based on their phylogeny and catabolic activity. The first group is that of the *α-Proteobacteria*, comprising bacteria closely related to *Bradyrhizobium* spp.; these carry the *tfdAα* gene (Nojiri et al. 2014). The two other groups are the *γ*- and *β-Proteobacteria*, which carry the *tfdA Class I, II* and *III* genes (Nojiri et al. 2014). *Class I* is found in *Cupriavidus pinatubonensis*, *Class II* is less widely distributed, being found only in *Burkholderia* spp., and *Class III* is found in *Comamonas acidovorans* (Kitagawa et al. 2002). Hence, the composition of *tfdA* genes in a particular environment can be used as an indicator to determine the predominant microbial populations. In our case, the addition of FA changed the observed patterns of *tfdA* and *tfdA-like* genes. This might indicate that different microbial populations were involved in the biodegradation process. In addition, other changes in gene patterns can occur following the addition of a carbon source, which will also influence the composition of *tfdA*-bearing bacteria. Such a process was observed by Kargi and Eker (2005), who demonstrated enhanced biodegradation of chlorophenols following the addition of carbohydrates, these being primary carbon substrates for bacteria, or other phenolic compounds used by bacteria as cometabolites. Our findings also indicate that the higher dose of 2,4-D inhibited the detection of functional genes, irrespective of whether FA was added; this suggests that the added compounds had a toxic effect on the growth of desired microorganisms. The high toxicity of 2,4-D is confirmed by the results of our ecotoxicity assessment (Table 2). In the case of Phytotoxkit®, all the herbicide-amended samples demonstrated strong inhibition of root elongation. The samples enriched with 2,4-D (100/500 µM), demonstrated root growth inhibition of 100% for *L. sativum* (100 and 500 µM), 98% (100 µM) and 94% (500 µM) for *S. alba*, 90% (100 µM) and 92% (500 µM) for *S. saccharatum* (Table 2). Samples with MSM and soil extract only were found to exhibit lower ecotoxicity (51–57%); however, these values still exceeded the ecotoxicity level of 20%, and should be considered as toxic for the test plants. The ecotoxicity of 2,4-D (100/500 µM) did not appear to differ after 24 days of incubation, even with the addition of FA (Table 2). Of the test plants, *L. sativum* was the most sensitive to treatment, displaying 100% root growth inhibition in all samples with 2,4-D. Root growth inhibition ranged between 94% and 98% for *S. alba*, and between 88% and 95% for *S. saccharatum*. Strong ecotoxic effects were also observed against samples treated with FA alone: 56% inhibition for *L. sativum*, 73% for *S. alba* and 22% for *S. saccharatum* (Table 2). It should be underlined that phenolic acids, such as FA, play roles in the biochemical interactions between plants. FA has been found to suppress plant growth

Table 2 Ecotoxicity assessment results (PE%) and 2,4-D reduction (%) after 24 days of incubation

Samples		Phytotoxkit			Microtox	2,4-D reduction (%)
		Roots growth inhibition			Luminescence inhibition	
2,4-D concentration	Sample variant	L. s.	S. a.	S. s.	V. f.	
		PE%				
Beginning of incubation						
0 µM	MSM + SE	51	57	51	n.a.	n.a.
100 µM	MSM + SE	100	98	90	n.a.	n.a.
500 µM	MSM + SE	100	94	92	n.a.	n.a.
After 24 days of incubation						
0 µM	MSM + SE + FA	56	73	22	99	n.a.
100 µM	MSM*	100	96	88	38	86
	MSM + FA[a]	98	95	84	40	93
	MSM + Sterile SE[a]	100	97	88	55	83
	MSM + SE	100	94	91	65	98
	MSM + SE + FA	100	98	90	83	100
500 µM	MSM[a]	10	96	95	45	100
	MSM + FA[a]	100	96	94	64	100
	MSM + Sterile SE[a]	100	96	95	53	99
	MSM + SE	100	97	90	72	100
	MSM + SE + FA	100	97	92	84	97

L.s., *Lepidium sativum*; S.a., *Sinapis alba*; S.s., *Sorghum saccharatum*; V.f., *Vibrio fischeri*; MSM, Mineral Salt Medium; SE, soil extract; *n.a*, not analysed; PE%, percent effect

[a]Samples without microorganisms

COR-AAD1-00003774
Bayer EX1008 (Part 7 of 9)

by the inhibition of seed germination, root and shoot growth and cell division, as well as by reduction of leaf chlorophyll content (Singh et al. 2014). In our case, the combined use of herbicide and FA induces strong ecotoxic effects on the studied species, with the most sensitive plants being dicotyledonous *L. sativum* and *S. alba*; this is consistent with our previous studies (Baran and Tarnawski 2015; Urbaniak et al. 2016; Mierzejewska et al. 2017). The high ecotoxicity of the studied samples was also confirmed by the Microtox® biotest. The lowest luminescence inhibition of *V. fischeri* (Table 2) was observed for pure 2,4-D (38% for 100 µM and 45% for 500 µM), with higher activity observed for sterile soil extract, i.e. no microbial activity (55%–53%), and soil extract with microorganisms (65%–72%) (Table 2). The addition of FA had varying effects on luminescence inhibition depending on the initial 2,4-D concentration: at 100 µM, the level was lower (40%) than that of samples with soil extract (55–99%), while at 500 µM, it was higher (64%) than the sterile soil extract (53%). The highest PE% was observed for samples treated with soil extract and FA: no herbicide—99%, 100 µM 2,4-D—83% and 500 µM 2,4-D—84% (Table 2). FA is a natural compound with antimicrobial properties, which acts by disrupting cell membranes and causing ion leakage (Jia et al. 2016). As 100 mg/L FA was sufficient to reduce the viability of *Campylobacter jejuni* (Jia et al. 2016), the FA concentration used in the present study (250 µM) could have had a toxic effect. Table 2 shows results of % 2,4-D reduction after 24 days of incubation. As no significant changes occurred over time both for samples ecotoxicity and 2,4-D reduction, neither in controls nor samples with microorganisms, it is possible that the intermediates formed during the physicochemical processes, such as 2,4-dichlorophenol (2,4-DCP) and 3,5-dichlorocatechol (3,5-DCC) exhibit a strong ecotoxic effect. For example, 50% inhibition of *N. tabacum* cells was observed following exposure to 10 mg/L 2,4-DCP (Perkins et al. 1987); however, other findings found 2,4-DCP to be lessphytotoxic than 2,4-D both in vitro and in vivo (Taylor et al. 1989). In addition, although the test organisms demonstrated varying responses, the studied samples were generally found to be toxic or highly toxic (*L. sativum*). 3,5-DCC can also exhibit higher toxicity than a parent compound (Schweigert et al. 2001). Low toxicity was demonstrated only against *S. saccharatum* and *V. fischeri* following exposure to combined 2,4-D and FA (Table 2). The ecotoxicity of 2,4-D against biota has been extensively studied, mainly by plant bioassays, e.g. inhibition of root and hypocotyl elongation (Wei et al. 2000), disturbances of mesophyll cell structure and proliferation of vascular tissue (Pazmiño et al. 2011). Its spread in the environment can also result in the contamination of water ecosystems, leading to cellular deformation of green algae (i.e. *Ankistrodesmus falcatus*) (Martínez-Ruiz and Martínez-Jerónimo 2018), malformations and behavioural changes to fish (i.e. *Cyprinus carpio*) (Sarikaya and Yilmaz 2003), abnormal cellular proliferation in amphibians (*Rhinella arenarum*) (Aronzon et al. 2011) and the development of non-viable embryous in invertebrates (*Biomphalaria glabrata*) (Estevam et al. 2006). Therefore, determining the biodegradation potential of soil microbiota and identifying methods of enhancing the in situ removal process, are of ecological significance and enhance the protection of the ecosystem as a whole. The growing application of 2,4-D not only results in inhibition of the growth of broad-leafed plants, but also an increase in the level of pollution in the environment. Hence, there is a need to identify nature-based methods that enable effective elimination of 2,4-D from the environment. The present findings not only identify changes in the detection of functional, bacterial degradative genes following FA application, but also indicate that the higher dose of 2,4-D suppressed the detection of these gene fragments. This suggests that both 2,4-D and FA had a toxic effect on the proliferation and catabolic activity of bacterial consortia in the amended samples. The ecotoxicity assessment also found 2,4-D to be highly toxic. Although the response of the indicator organisms was highly specific and differed significantly between higher plants (producers) and bacteria (decomposers), the herbicide and FA were found to be toxic to the test organisms for all the studied samples.

Acknowledgements The research was supported by the Student Research Grants programme at University of Lodz: Plants Secondary Metabolites as stimulators of bacterial degradation of 2,4-D and MCPA, and the European Structural and Investment Funds, OP RDE-funded project 'CHEMFELLS4UCTP' (No. CZ.02.2.69/0.0/0.0/17_050/0008485)".

References

Aronzon CM, Sandoval MT, Herkovits J, Pérez-Coll CS (2011) Stage-dependent toxicity of 2,4-dichlorophenoxyacetic on the embryonic development of a South American toad, *Rhinella arenarum*. Environ Toxicol 26:373–381. https://doi.org/10.1002/tox.20564

Bælum J, Henriksen T, Christian H et al (2006) Degradation of 4-chloro-2-methylphenoxyacetic acid in top- and subsoil is quantitatively linked to the class III tfdA gene. Appl Environ Microbiol 72:1476–1486. https://doi.org/10.1128/AEM.72.2.1476

Bælum J, Jacobsen CS, Holben WE (2010) Comparison of 16S rRNA gene phylogeny and functional tfdA gene distribution in thirty-one different 2, 4-dichlorophenoxyacetic acid and 4-chloro-2-methylphenoxyacetic acid degraders. Syst Appl Microbiol 33:67–70. https://doi.org/10.1016/j.syapm.2010.01.001

Baran A, Tarnawski M (2013) Phytotoxkit/Phytotestkit and Microtox?? As tools for toxicity assessment of sediments. Ecotoxicol Environ Saf 98:19–27. https://doi.org/10.1016/j.ecoenv.2013.10.010

Baran A, Tarnawski M (2015) Assessment of heavy metals mobility and toxicity in contaminated sediments by sequential extraction and a battery of bioassays. Ecotoxicology 24:1279–1293. https://doi.org/10.1007/s10646-015-1499-4

COR-AAD1-00003775
Bayer EX1008 (Part 7 of 9)

Estevam EC, Nakano E, Kawano T et al (2006) Dominant lethal effects of 2,4-D in *Biomphalaria glabrata*. Mutat Res 611:83–88. https://doi.org/10.1016/j.mrgentox.2006.07.001

Eurostat Sales of pesticides by type of pesticide (2018)

Gaunt JK, Evans WC (1971) Metabolism of 4-chloro-2-methylphenoxyacetate by a soil pseudomonad. Preliminary evidence for the metabolic pathway. Biochem J 122:519–526

Jia Z, Song K, Chen Y et al (2016) Antimicrobial activity of ferulic acid against *Cronobacter sakazakii* and possible mechanism of action. Foodborne Pathog Dis 13:196–204. https://doi.org/10.1089/fpd.2015.1992

Kargi F, Eker S (2005) Removal of 2,4-dichlorophenol and toxicity from synthetic wastewater in a rotating perforated tube biofilm reactor. Process Biochem 40:2105–2111. https://doi.org/10.1016/j.procbio.2004.07.013

Kitagawa W, Takami S, Miyauchi K et al (2002) Novel 2,4-dichlorophenoxyacetic acid degradation genes from oligotrophic. Society 184:509–518. https://doi.org/10.1128/JB.184.2.509

Lappin HM, Greaves MP, Slater JH (1985) Degradation of the herbicide mecoprop [2-(2-methyl-4-chlorophenoxy)propionic acid] by a synergistic microbial community. Appl Environ Microbiol 49:429–433

Martínez-Ruiz EB, Martínez-Jerónimo F (2018) Exposure to the herbicide 2,4-D produces different toxic effects in two different phytoplankters: A green microalga (*Ankistrodesmus falcatus*) and a toxigenic cyanobacterium (*Microcystis aeruginosa*). Sci Total Environ 619–620:1566–1578. https://doi.org/10.1016/j.scitotenv.2017.10.145

Microbics Corporation (1992) Microtox manual toxicity testing handbook

Mierzejewska E, Baran A, Urbaniak M (2017) The influence of MCPA on soil phytotoxicity and the presence of genes involved in its biodegradation. Arch Environ Prot 44:58–64. https://doi.org/10.24425/122303

Modern Water (2012) RaPID Assay ® 2,4-D

Nojiri H, Fukuda M, Tsuda M, Kamagata Y (2014) Biodegradative bacteria: how bacteria degrade, survive, adapt, and evolve. Springer, New York. pp 1–358. https://doi.org/10.1007/978-4-431-54520-0

Pazmiño DM, Rodríguez-Serrano M, Romero-Puertas MC et al (2011) Differential response of young and adult leaves to herbicide 2,4-dichlorophenoxyacetic acid in pea plants: role of reactive oxygen species. Plant Cell Environ 34:1874–1889. https://doi.org/10.1111/j.1365-3040.2011.02383.x

Perkins EJ, Stiff CM, Lurquin PF (1987) Use of *Alcaligenes eutrophus* as a source of genes for 2,4-D resistance in plants. Weed Sci 35:12–18. https://doi.org/10.1017/S0043174500060987 doi

Persoone G, Marsalek B, Blinova I et al (2003) A practical and user-friendly toxicity classification system with microbiotests for natural waters and wastewaters. Environ Toxicol 18:395–402. https://doi.org/10.1002/tox.10141

Phytotoxkit (2004) Seed germination and early growth microbiotest with higher plants. Standard Operational Procedure. MicroBioTest Inc., Nazareth. 24

Poll C, Pagel H, Devers-Lamrani M et al (2010) Regulation of bacterial and fungal MCPA degradation at the soil-litter interface. Soil Biol Biochem 42:1879–1887. https://doi.org/10.1016/j.soilbio.2010.07.013

Sarikaya R, Yilmaz M (2003) Investigation of acute toxicity and the effect of 2,4-D (2,4-dichlorophenoxyacetic acid) herbicide on the behavior of the common carp (*Cyprinus carpio* L., 1758; Pisces, Cyprinidae). Chemosphere 52:195–201. https://doi.org/10.1016/S0045-6535(03)00106-1

Schweigert N, Hunziker R, Escher B, Eggen R (2001) Acute toxicity of (chloro-)catechol-copper combinations in *Escherichia coil* corresponds to their membrane toxicity in vitro. Environ Toxicol Chem 20:239–247

Singh HP, Kaur S, Batish DR, Kohli RK (2014) Ferulic acid impairs rhizogenesis and root growth, and alters associated biochemical changes in mung bean (*Vigna radiata*) hypocotyls. J Plant Interact 9:267–274. doi:https://doi.org/10.1080/17429145.2013.820360

Strzelczyk A (1968) Methods of soil fungi analysis. Soil Sci Annu 19:56–73

Taylor SG, Shilling DG, Quesenberry KH, Chaudhry GR (1989) Phytotoxicity of 2,4-D and 2,4-Dichlorophenol to Red Clover (*Trifolium pratense*). Weed Sci 37:825–829

U.S. Environmental Protection Agency (2017) Pesticides Industry Sales and Usage. 2008–2012 Market Estimates. Washington

Uhlik O, Musilova L, Ridl J et al (2013) Plant secondary metabolite-induced shifts in bacterial community structure and degradative ability in contaminated soil. Appl Microbiol Biotechnol 97:9245–9256. https://doi.org/10.1007/s00253-012-4627-6

Urbaniak M, Wyrwicka A, Zieliński M, Mankiewicz-Boczek J (2016) Potential for phytoremediation of PCDD/PCDF-contaminated sludge and sediments using cucurbitaceae plants: a pilot study. Bull Environ Contam Toxicol 97:401–406. https://doi.org/10.1007/s00128-016-1868-6

Wei YD, Zheng HG, Hall JC (2000) Role of auxinic herbicide-induced ethylene on hypocotyl elongation and root/hypocotyl radial expansion. Pest Manag Sci 56:377–387

Publisher's Note Springer Nature remains neutral with regard to jurisdictional claims in published maps and institutional affiliations

COR-AAD1-00003776
Bayer EX1008 (Part 7 of 9)

Journal of Bioscience and Bioengineering
VOL. 108 No. 1, 56–59, 2009

www.elsevier.com/locate/jbiosc

Analysis of genes encoding the 2,4-dichlorophenoxyacetic acid-degrading enzyme from *Sphingomonas agrestis* 58-1

Mitsuhiro Shimojo,[1] Mitsuyasu Kawakami,[2] and Kei Amada[2,*]

Materials Science and Production Engineering, Graduate School of Engineering, Fukuoka Institute of Technology 3-30-1 Wajirohigashi, Higashi, Fukuoka 811-0295, Japan[1] and Department of Life, Environment and Materials Science, Faculty of Engineering, Fukuoka Institute of Technology 3-30-1 Wajirohigashi, Higashi, Fukuoka 811-0295, Japan[2]

Received 6 November 2008; accepted 24 February 2009

A 2,4-dichlorophenoxy acetic acid (2,4-D)-degrading bacterium, strain 58-1, was newly isolated from soil samples collected in the Fukuoka Prefecture, Japan, and grown on an enrichment culture medium containing 2,4-D as the sole carbon source. Phylogenic analysis identified strain 58-1 as *Sphingomonas agrestis*. In 2,4-D degraders, classes I, II, and III inherit the *tfdA*, *cadA*, and *tfdAα* genes, respectively, and the results from degenerate-PCR indicated that this strain belongs to the class II degraders. A clone that includes the *cadA* gene homolog of *S. agrestis* 58-1 was screened from a library by using the PCR amplified fragment as a DNA probe. The cloned fragment was sequenced and found to consist of 5043 nucleotides and include 3 open reading frames (orfs). The *orf1*, *orf2*, and *orf3* genes encode polypeptides consisting of 412, 448, and 177 amino acids, respectively. The *Orf2* product shares a high degree of sequence similarity (92%) with the large subunit of 2,4-D oxygenase from the *Bradyrhizobium* sp. strain HW13, which belongs to the class III 2,4-D degraders, while the *orf3* product shared 63% sequence similarity with the small subunit of 2,4-D oxygenase from the strain HW13. The results of the functional expression analysis using various deletion mutants in *Escherichia coli* revealed that the expression of both *orf2* and *orf3* genes, but not *orf1*, is essential for the conversion of 2,4-D to 2,4-DCP. From these results, we conclude the first isolation of 2,4-D oxygenase genes from a class II 2,4-D degrader.

© 2009, The Society for Biotechnology, Japan. All rights reserved.

[**Key words:** 2,4-dichlorophenoxyacetic acid-degrading bacterium; 2,4-D oxygenase; *cadAB* genes; *Sphingomonas agrestis* 58-1; Functional expression; Deletion mutants]

2,4-Dichlorophenoxyacetic acid (2,4-D) is a synthetic phytohormone that has been widely used as a herbicide for controlling broadleaf weeds. Many 2,4-D-degrading microorganisms have been isolated (1–3) and classified into 3 groups on the basis of their phylogeny and the sequences of the genes encoding the 2,4-D-degrading enzyme (4). Class I 2,4-D degraders include various copiotrophic, fast-growing bacteria that belong to the subdivisions of the β- and γ-*Proteobacteria*. In class I degraders, 2,4-D is converted to 2,4-dichlorophenol (2,4-DCP) by an α-ketoglutarate-dependent 2,4-D dioxygenase encoded by the *tfdA* gene (5). The *Ralstonia eutropha* JMP134, a class I degrader, has been extensively characterized (3, 6, 7). Class III degraders include oligotrophic, slow-growing strains belonging to the *Bradyrhizobium–Agromyces–Nitrobacter–Afipia* (BANA) cluster of α-*Proteobacteria*. Organisms belonging to this group were isolated from pristine soils and contained the *cad* gene cluster and a *tfdA*-like gene (*tfdAα*) that encodes the 2,4-D-degrading enzymes (8–11). Class II degraders include copiotrophic, fast-growing strains belonging to the subdivision of α-*Proteobacteria* and belonging to the genus *Sphingomonas* (12, 13). However, this group contains the *cadA* gene, but not the *tfdA* gene. The presence of the *cadA* homolog in class II 2,4-D degraders was confirmed by using Southern analysis and partial *cadA* amplification by PCR. However, it has not yet been determined whether these genes are expressed as the functional active enzymes.

In this report, we describe the cloning and characterization of the *cadAB* genes from a class II degrader, *Sphingomonas agrestis* 58-1, which encode the enzymes responsible for the conversion of 2,4-D to 2,4-dichlorophenol.

MATERIALS AND METHODS

Isolation of 2,4-D-degrading bacteria We collected 50 soil samples from various environments such as mountains, farmlands, riversides, and industrial areas in Northern Kyushu, to isolate 2,4-D-degrading bacteria. The soil samples were mixed with a basal medium (0.5 g K_2HPO_4, 0.5 g KH_2PO_4, 0.25 g NH_4NO_3, 0.002 g $NaMoO_4 \cdot 2H_2O$, 0.001 g $FeSO_4 \cdot 7H_2O$, and 0.001 g $MnSO_4 \cdot 7H_2O$ per liter) containing 2,4-D (0.005 g) as the sole carbon source, and enrichment culture was performed at 30 °C for 7 d. The culture broth was centrifuged, and the concentration of 2,4-D in the supernatant was measured using a DU 530 spectrophotometer (Beckman-Coulter Inc., Osaka, Japan) at 284 nm and a high-performance liquid chromatography (HPLC) system (LaChrom Elite system; Hitachi High-Technologies, Fukuoka, Japan) under the following conditions: column, YMC-Pack ODS-A A312 150*6.0 (YMC Co. Ltd., Kyoto, Japan); eluate, 75% acetonitrile, 0.5% acetic acid, and 24.5% water; and flow rate, 1.0 ml/min. A photodiode array detector was used to measure the absorbance at 284 nm. The culture broths with decreased 2,4-D concentration were then transferred to agar plates. Morphologically different colonies that formed on the plates were isolated, and their 2,4-D-degrading ability was examined.

* Corresponding author. Tel.: +81 92 606 3994; fax: +81 92 606 0728.
E-mail address: amada@fit.ac.jp (K. Amada).

1389-1723/$ – see front matter © 2009, The Society for Biotechnology, Japan. All rights reserved.
doi:10.1016/j.jbiosc.2009.02.018

COR-AAD1-00003777
Bayer EX1008 (Part 7 of 9)

Characterization of 2,4-D-degrading bacteria Biochemical analysis of the isolated 2,4-D-degrading bacteria was performed using the API20NE kit (Bio Merieux S.A., France). Gram staining was performed, and the cells were observed under a light microscope (Olympus IMT-2, Fukuoka, Japan). Cell growth was monitored by measuring the optical density of the cultures at 600 nm with a spectrophotometer. The concentration of 2,4-D in the medium was measured using a spectrophotometer as described above.

A partial gene fragment of the 16S rRNA was amplified by PCR using a thermal cycler (TaKaRa Bio, Kyoto, Japan) and a universal primer set corresponding to positions 8–27 (forward primer) and 1492–1510 (reverse primer), according to the *Escherichia coli* numbering system (14). The amplified DNA fragment was sequenced (15) using the Genome Lab DTCS quick start kit (Beckman-Coulter Inc., Osaka, Japan). The reacted DNA fragment was analyzed using a CEQ8800 Genetic Analysis System (Beckman-Coulter Inc., Osaka, Japan).

DNA manipulations, Southern hybridization, and sequencing DNA manipulations were performed as described elsewhere (16). Total DNA from *S. agrestis* 58-1 was extracted using the Marmur procedure (17). A partial *cadA* fragment was amplified from the total DNA using the primers 5′-AAGCTGCA(A/G)TTTGA(A/G)AA(C/T)GG-3′ and 5′-(A/C)GGATTGAAGAAATCCTG(A/G)TA-3′, as described by Itoh et al. 2004. Oligonucleotides for PCR and sequencing were obtained from Genenet Co., Ltd. (Fukuoka, Japan). The amplified partial *cadA* fragment was directly ligated into pBluescript II KS (+) T-vector, a phagemid vector (Stratagene, Tokyo, Japan), and introduced into *E. coli* DH5α cells (TOYOBO, Osaka, Japan) using an electroporator (EasyjecT Optima, COSMO BIO, Tokyo, Japan). *E. coli* DH5α cells were grown at 37 °C in LB medium (10 g Bacto tryptone, 5 g Bacto yeast extract, and 10 g NaCl per liter of the medium) and 50 μg/ml ampicillin. The amplified partial *cadA* fragment was labeled with digoxigenin (DIG) using a DNA Labeling Kit (Roche Molecular Biochemicals, Tokyo, Japan) and used as a probe for Southern hybridization analysis. Colony hybridization of the strain was also performed using the above mentioned procedure with the same probe. The insert region was sequenced using T7 and T3 primers (TaKaRa Bio, Kyoto, Japan) and the sequenced regions were analyzed using a CEQ8800 Genetic Analysis System. The nucleotide sequence analysis was performed using BLAST (18) and ClustalW programs (19) provided by the National Institute of Genetics, Shizuoka, Japan (DDBJ: DNA Data Bank of JAPAN).

Construction of the expression vector for the genes encoding the 2,4-D-converting enzyme Using the cloned DNA fragment and protein expression vectors (pBluescript II KS (+) and pUC19), we constructed the expression vector for the *cadAB* genes from *S. agrestis* 58-1 and its derivative in *E. coli* DH5α cells. The recombinant *E. coli* DH5α cells were grown overnight at 37 °C in LB medium containing ampicillin. Cell pellets were collected by centrifugation (3500 rpm, 10 min), resuspended in basal medium containing 2,4-D and grown overnight at 37 °C. The concentration of 2,4-D was determined spectrometrically and by HPLC.

The sequence data of the 16S rRNA and the DNA fragment including the *cadAB* genes from *S. agrestis* 58-1 have been submitted to the DDBJ/EMBL/GenBank databases under accession nos. AB459536 and AB353895, respectively.

RESULTS AND DISCUSSION

Isolation of 2,4-D-degrading bacteria The soil samples collected from various environments were inoculated directly into a basal liquid medium. The 2,4-D concentration was decreased in more than half of the soil samples after incubation in the basal medium for 7 days at 30 °C. We then attempted to obtain 2,4-D-degrading bacteria by using the enrichment cultivation method. Finally, we were able to obtain 11 isolates from the cultures grown on basal agar plates containing 2,4-D as the sole carbon source.

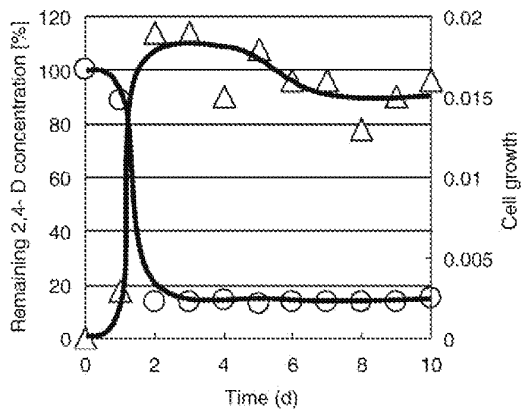


FIG. 1. Time course of 2,4-D degradation and cell growth curve of *S. agrestis* 58-1, measured spectrophotometrically. Symbols: circle, 2,4-D concentration; triangle, cell growth.

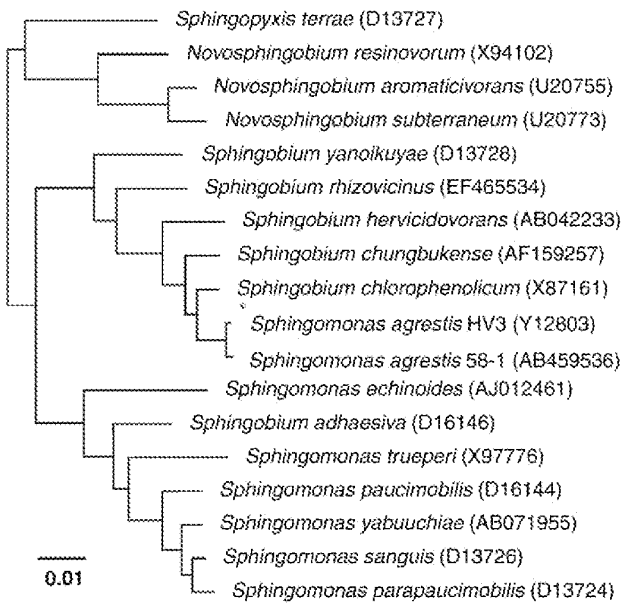


FIG. 2. Phylogenetic tree constructed by the neighbor-joining method on the basis of 16S rRNA gene sequence homology between *S. agrestis* 58-1 and members of the genus *Sphingomonas sensu lato*. The corresponding DDBJ accession numbers are shown in parentheses. The scale bar indicates 0.01 nucleotide substitutions per nucleotide position. * *Sphingomonas agrestis* (strain HV3; 21) has not been validly described.

Colony PCR was performed using primers for the *cadA* gene from *Sphingomonas sensu lato* to select the class II 2,4-D degrader belonging to that genus (20). Analysis by agarose gel electrophoresis revealed DNA fragments amplified from 5 colonies. Among these 5 positive strains, one that was fast growing, possessed the highest 2,4-D degradation ability, and displayed different colony morphology was selected and designated as strain 58-1.

Characterization of the 2,4-D-degrading bacterial strain 58-1 A typical growth curve and the 2,4-D degradation ability (with an initial 2,4-D concentration of 50 mg/l) of strain 58-1 are shown in Fig. 1. Strain 58-1 could completely degrade 2,4-D in the basal liquid medium within 2 days. No peak corresponding to the retention time of 2,4-D was observed for strain 58-1 in the HPLC assay.

The cells of strain 58-1 were motile, gram-negative, aerobic, and rod-shaped. The colony characteristics of this strain on nutrient agar plates were as follows: yellow color; convex; circular; and a smooth surface. This strain showed positive results for the oxidase test and for the assimilation of glucose, arabinose, and maltose.

An almost-complete 16S rRNA gene sequence (1378 bp) of strain 58-1 was isolated and registered in the DDBJ database (accession no. AB459536). A BLAST search for similar sequences in the DDBJ database revealed that this strain is closely related to members of the genus *Sphingobium* (20). Species belonging to the genus *Sphingobium*, including *S. agrestis* (21), *S. chlorophenolicum* (22), and *S. chungbukense* (23), are known to have the ability to degrade various aromatic compounds. The sequence of the strain showed a high level of similarity to that of *S. agrestis* HV3 (accession no. Y12803, 99.8%). It also showed similarities of 98.6% and 98.0% to the sequence of the strains *S. chlorophenolicum* (accession no. X87161) and *S. chungbukense* DJ77 (accession no. AF159257), respectively. A phylogenetic tree generated using the neighbor-joining method is shown in Fig. 2. In the

COR-AAD1-00003778
Bayer EX1008 (Part 7 of 9)

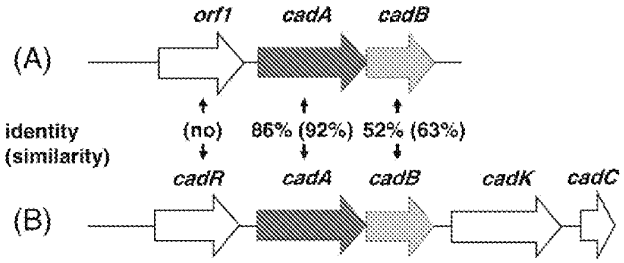


FIG. 3. Comparison of the *cad* gene cluster from (A) *S. agrestis* 58-1 and (B) *Bradyrhizobium* sp. strain HW13. The orfs containing *cad* genes are represented by large horizontal arrows and the identity (similarity) values of the corresponding gene products are represented between the vertical arrows.

phylogenetic tree constructed on the basis of 16S rRNA gene sequences, strain 58-1 is placed close to *S. agrestis*. Based on these results, we identified strain 58-1 as *S. agrestis*. *S. agrestis* HV3 was isolated as a 2-methyl-4-chlorophenoxyacetic acid (MCPA)- and 2,4-D-metabolizing strain (24) from the soil samples of Finnish fields, but the gene encoding the 2,4-D-degrading enzyme has not yet been analyzed. Incidentally, *S. agrestis* has not been validly described.

Cloning of the 2,4-D-degrading gene The total DNA of *S. agrestis* 58-1 was digested with *Eco*RI, *Bam*HI, and both enzymes (E–B), blotted onto nylon membranes, and hybridized with a labeled *cadA* probe. The *Eco*RI, *Bam*HI, and double digest (E–B) hybridization bands were observed at the positions of about 9, 15, and 5 kbp, respectively. The DNA fragments obtained after both *Eco*RI and *Bam*HI digestion were inserted into pBluescript II KS(+) and then introduced by electroporation into *E. coli* DH5α cells for colony hybridization. Among the 74 colonies, 1 positive clone was obtained from the E–B library. The plasmid that was purified from this positive clone was designated as pBBE58-1.

The entire nucleotide sequence of the cloned fragment was determined using dideoxy termination by the primer walking method. The nucleotide sequence was analyzed using the BLAST programs provided by the DDBJ. The 5-kbp E–B digested DNA fragment consisted of 5043 nucleotides. The nucleotide sequence of this fragment has been registered in the DDBJ/EMBL/GenBank database (accession no. AB353895). The fragment was comprised of 3 open reading frames (*orfs*), whose nucleotide lengths were 1239, 1347, and 534 bp. The *orf1*, *orf2*, and *orf3* genes likely encode polypeptides of 412, 448, and 177 amino acids, respectively.

The *orf1* product showed the highest identity with the genes encoding ferredoxin-NAD^+ reductase in *Rhizobium* sp. strain NGR234 (33%; accession no. AY316746) and initial carbazole dioxygenase reductase in *Sphingomonas* sp. strain CB3 (29%; accession no. AF060489). The *orf2* and *orf3* products showed 86% (92%) and 52% (63%) identities (similarities) with *cadA* and *cadB*, which correspond, respectively, to the large and small subunits of the 2,4-D oxygenase from the *Bradyrhizobium* sp. strain HW13 (accession no. AB062679). The *orf2* and *orf3* products also showed 52% and 45% identities with TftA and TftB of the 2,4,5-T degrader *B. cepacia* (accession no. U11420), which correspond to the large and small subunits of 2,4,5-trichlorophenoxyacetic acid oxygenase, respectively.

The 5-kbp DNA fragment from *S. agrestis* 58-1 was compared with the 2,4-D-degrading enzyme gene cluster from the *Bradyrhizobium* sp. strain HW13, which belongs to the class III 2,4-D degraders (Fig. 3). However, *orf1* of *S. agrestis* 58-1 shared no significant identity (<10%) or consensus sequence with *Bradyrhizobium* sp. strain HW13 *cadR*, which encodes an AraC/XylS type of transcriptional regulator (9). The incompletely sequenced gene located upstream of *tfdB*, which encodes dichlorophenol hydroxylase from *S. herbicidovorans* MH, was similar to *cadR* from the *Bradyrhizobium* sp. strain HW13 (9, 25) and was not located either upstream or downstream of the *cadAB* genes.

Expression of both the *orf2* and *orf3* genes was essential for the conversion of 2,4-D to 2,4-DCP in *E. coli* DH5α cells *E. coli* DH5α cells containing pBBE58-1 did not show any conversion of 2,4-D to 2,4-DCP. The insert DNA digested by *Eco*RI and *Bam*HI was subcloned downstream of the *lac* promoter in pUC19. *E. coli* DH5α cells containing the newly constructed plasmid displayed 2,4-D-degrading activity. This is because the gene fragment was inserted in the opposite orientation to *lac* promoter in pBluescript II KS(+) and in the same orientation as the *lac* promoter in pUC19 (Fig. 4). This was the first observation of 2,4-D-converting activity when using genes from a class II 2,4-degrader. This expression plasmid harboring the gene encoding the active 2,4-D-converting enzyme was designated as pUBE.

To examining whether each gene corresponding to *orfs 1*, *2*, and *3* is essential for 2,4-D conversion, the deletion mutants of pUBE were constructed in pBluescript II KS(+), as illustrated in Fig. 4. pBNN, pBXE, pBXN, and pBCE contained the entire *orf1* and *2* genes, the *orf2* and *3* genes, the *orf2* gene, and the *orf3* gene, respectively. These plasmids were introduced into *E. coli* DH5α cells by electroporation. Each transformant was grown in LB medium and incubated in basal medium containing 50 mg/l 2,4-D to determine the 2,4-D degradation activity. As seen in Fig. 4, pBNN, pBXN, and pBCE did not show converting activity, while pBXE retained the ability to convert 2,4-D to

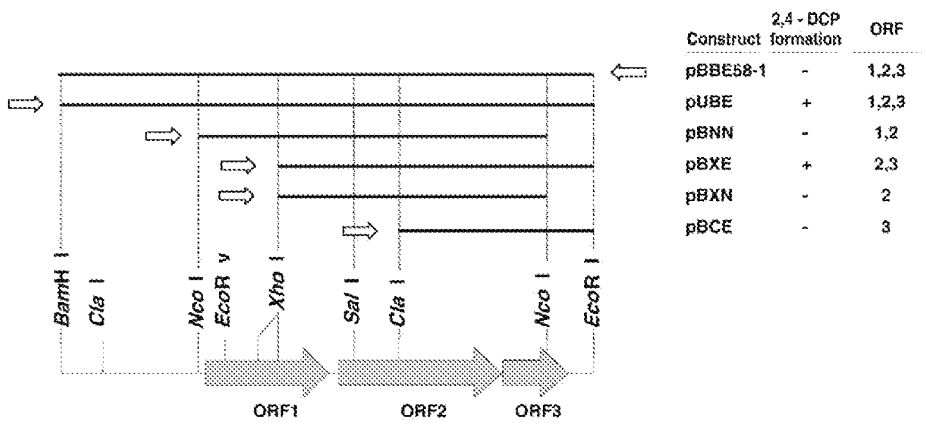


FIG. 4. Subcloning and identification of the genes encoding 2,4-D-degrading enzymes. The positions of deletion in the mutant derivatives are illustrated. The name of the construct, the 2,4-D degradation activity of each clone, and the orfs involved are summarized on the right. The orfs containing *cad* genes are represented by large horizontal arrows at the bottom, which correspond to the physical maps of pUBE. Small arrows indicate the direction of transcription by the *lac* promoter in the vectors.

COR-AAD1-00003779
Bayer EX1008 (Part 7 of 9)

2,4-DCP. These results indicate that the expression of both the *orf2* and *orf3* genes, but not the *orf1* gene, is essential to retain the ability to degrade 2,4-D in *E. coli* DH5α cells. These results differed from those obtained for the *Bradyrhizobium* sp. strain HW13, in which the 2,4-D oxygenase gene could not functionally express its enzyme activity in *E. coli* HB101 or *Pseudomonas putida* PpY101. This difference might indicate that, in the recombinant *E. coli*, the 2,4-D-converting activity of the oxygenase in strain 58-1 is higher than that of the oxygenase in strain HW13 (9).

The genus *Sphingomonas sensu lato* includes the class II 2,4-D degraders. Phylogenetic and classification analyses using the 16S rRNA and 2,4-D oxydase genes is a commonly used technique in 2,4-D-degrading bacteria (26, 27). The 2,4-D degradation activity has been well studied in class I and class III 2,4-D degraders, but the genetic and enzymatic background of this activity in class II 2,4-D degraders has not yet been elucidated. Based on sequence homology and enzymatic function analyses, we designated the *orf2* and *orf3* genes from *S. agrestis* 58-1 as *cadA* and *cadB*, respectively, for class II 2,4-D degrader.

Recently, we succeeded in inducing overexpression of the *cadAB* genes using *E. coli* as the host strain (unpublished data). Overexpression of the *cadAB* genes in *E. coli* is expected to be applicable for the biochemical and structural analysis of 2,4-D oxygenase and understanding the molecular mechanism of the conversion of 2,4-D to 2,4-DCP.

ACKNOWLEDGMENTS

This work was supported by funds from MEXT (Ministry of Education, Culture, Sports, Science and Technology), HAITEKU (2005–2009), and the Electronics Research Laboratory, Fukuoka Institute of Technology (2003 and 2005).

References

1. **Don, R. H. and Pemberton, J. M.:** Properties of six pesticide degradation plasmids isolated from *Alcaligenes paradoxus* and *Alcaligenes eutrophus*, J. Bacteriol., **145**, 681–686 (1981).
2. **Amy, P. S., Schulke, J. W., Frazier, L. M., and Seidler, R. J.:** Characterization of aquatic bacteria and cloning of genes specifying partial degradation of 2,4-dichlorophenoxyacetic acid, Appl. Environ. Microbiol., **49**, 1237–1245 (1985).
3. **Fulthorpe, R. R., McGowan, C., Maltseva, O. V., Holben, W. E., and Tiedje, J. M.:** 2,4-dichlorophenoxyacetic acid-degrading bacteria contain mosaics of catabolic genes, Appl. Environ. Microbiol., **61**, 3274–3281 (1995).
4. **Kamagata, Y., Fulthorpe, R. R., Tamura, K., Takami, H., Forney, L. J., and Tiedje, J. M.:** Pristine environments harbor a new group of oligotrophic 2,4-dichlorophenoxyacetic acid-degrading bacteria, Appl. Environ. Microbiol., **63**, 2266–2272 (1997).
5. **Fukumori, F. and Hausinger, R. P.:** *Alcaligenes eutrophus* JMP134 "2,4-dichlorophenoxyacetate monooxygenase" is an α-ketoglutarate-dependent dioxygenase, J. Bacteriol., **175**, 2083–2086 (1993).
6. **Fukumori, F. and Hausinger, R. P.:** Purification and characterization of 2,4-dichlorophenoxyacetate/α-ketoglutarate dioxygenase, J. Biol. Chem., **268**, 24311–24317 (1993).
7. **Haker, A. R., Olsen, R. H., and Seidler, R. J.:** Phenoxyacetic acid degradation by the 2,4-dichlorophenoxyacetic acid (TFD) pathway of plasmid pJP4: mapping and characterization of the TFD regulatory gene, *tfdR*, J. Bacteriol., **171**, 314–320 (1989).
8. **Itoh, K., Tashiro, Y., Uobe, K., Kamagata, Y., Suyama, K., and Yamamoto, H.:** Root nodule *Bradyrhizobium* spp. harbor *tfdA*α and *cadA*, homologous with genes encoding 2,4-dichlorophenoxyacetic acid-degrading proteins, Appl. Environ. Microbiol., **70**, 2110–2118 (2004).
9. **Kitagawa, W., Takami, S., Miyauchi, K., Masai, E., Kamagata, Y., Tiedje, J. M., and Fukuda, M.:** Novel 2,4-dichlorophenoxyacetic acid degradation genes from oligotrophic *Bradyrhizobium* sp. strain HW13 isolated from a pristine environment, J. Bacteriol., **184**, 509–518 (2002).
10. **Itoh, K., Kanda, R., Momoda, Y., Sumita, Y., Kamagata, Y., Suyama, K., and Yamamoto, H.:** Presence of 2,4-d-catabolozomg bacteria in a Japanese arable soil that belong to BANA (*Bradyrhizobium–Agromonas–Nitrobacter–Afipia*) cluster in α-*Proteobacteria*, Microbes. Environ., **15**, 113–117 (2000).
11. **Itoh, K., Kanda, R., Sumita, Y., Kim, H., Kamagata, Y., Suyama, K., Yamamoto, H., Hausinger, R. P., and Tiedje, M.:** *tfdA*-like genes in 2,4-dichlorophenoxyacetic acid-degrading bacteria belonging to the *Bradyrhizobium–Agromonas–Nitrobacter–Afipia* cluster in α-*Proteobacteria*, Appl. Environ. Microbiol., **68**, 3449–3454 (2002).
12. **Ka, J. O., Holben, W. E., and Tiedje, J. M.:** Genetic and phenotypic diversity of 2,4-dichlorophenoxyacetic acid (2,4-D)-degrading bacteria isolated from 2,4-D-treated field soils, Appl. Environ. Microbiol., **60**, 1106–1115 (1994).
13. **Vallaeys, T., Fulthorpe, R. R., Wright, A. M., and Soulas, G.:** The metabolic pathway of 2,4-dichlorophenoxyacetic acid degradation involves different families of *tfdA* and *tfdB* genes according to PCR-RFLP analysis, FEMS. Microb. Ecol., **20**, 163–172 (1996).
14. **Weisbur, G. W., Barns, S. M., Pelletier, D. A., and Lane, D. J.:** 16S ribosomal DNA amplification for phylogenetic study, J. Bacteriol., **173**, 697–703 (1991).
15. **Hiraishi, A.:** Direct automated sequencing of 16S rDNA amplified by polymerase chain reaction from bacterial cultures without DNA purification, Lett. Appl. Microbiol., **15**, 210–213 (1992).
16. **Sambrook, J. and Russell, D. W.:** Molecular cloning: a laboratory manual, 3rd edition, Cold Spring Harbor Laboratory Press, New York, 2001.
17. **Marmur, J.:** A procedure for the isolation of deoxyribonucleic acid from microorganisms, J. Mol. Biol., **3**, 208–218 (1961).
18. **Altschul, S. F., Gish, W., Miller, W., Myers, E. W., and Lipman, D. J.:** Basic local alignment search tool, J. Mol. Biol., **215**, 403–410 (1990).
19. **Thompson, J. D., Higgins, D. G., and Gibson, T. J.:** CLUSTAL W: improving the sensitivity of progressive multiple sequence alignment through sequence weighting, position-specific gap penalties and weight matrix choice, Nucleic Acids Res., **22**, 4673–4680 (1994).
20. **Takeuchi, M., Hamana, K., and Hiraishi, A.:** Proposal of the genus *Sphingomonas sensu stricto* and three new genera, *Sphingobium*, *Novosphingobium* and *Sphingopyxis*, on the basis of phylogenetic and chemotaxonomic analyses, Int. J. Syst. Evol. Microbiol., **51**, 1405–1417 (2001).
21. **Yrjälä, K., Suomalainen, S., Suhonen, E. L., Kilpi, S., Paulin, L., and Romantschuk, M.:** Characterization and reclassification of an aromatic- and chloroaromatic-degrading *Pseudomonas* sp., strain HV3, as *Sphingomonas* sp. HV3, Int. J. Syst. Bacteriol., **48**, 1057–1062 (1998).
22. **Ederer, M. M., Crawford, R. L., Herwig, R. P., and Orser, C. S.:** PCP degradation is mediated by closely related strains of the genus *Sphingomonas*, Mol. Ecol., **6**, 39–49 (1997).
23. **Pal, R., Bala, S., Dadhwal, M., Kumar, M., Dhingra, G., Prakash, O., Prabagaran, S. R., Shivaji, S., Cullum, J., Holliger, C., and Lal, R.:** Hexachlorocyclohexane-degrading bacterial strains *Sphingomonas paucimobilis* B90A, UT26 and Sp+, having similar lin genes, represent three distinct species, *Sphingobium indicum* sp. nov., *Sphingobium japonicum* sp. nov. and *Sphingobium francense* sp. nov., and reclassification of [*Sphingomonas*] *chungbukensis* as *Sphingobium chungbukense* comb. nov, Int. J. Syst. Evol. Microbiol., **55**, 1965–1972 (2005).
24. **Kilpi, S., Backström, V., and Korhola, M.:** Degradation of 2-methyl-4-chlorophenoxyacetic acid (MCPA), 2,4-dichlorophenoxyacetic acid (2,4-D), benzoic acid and salicylic acid by *Pseudomonas* sp. HV3, FEMS Microbiol. Lett., **8**, 177–182 (1980).
25. **Müller, T. A., Byrde, S. M., Werlen, C., van der Meer, J. R., and Kohler, H. P.:** Genetic analysis of phenoxyalkanoic acid degradation in *Sphingomonas herbicidovorans* MH, Appl. Environ. Microbiol., **70**, 6066–6075 (2004).
26. **Huong, N. L., Itoh, K., and Suyama, K.:** Diversity of 2,4-dichlorophenoxyacetic acid (2,4-D) and 2,4,5-trichlorophenoxyacetic acid (2,4,5-T)-degrading bacteria in Vietnamese soils, Microbes. Environ., **22**, 243–256 (2007).
27. **Huong, N. L., Itoh, K., and Suyama, K.:** 2,4-Dichlorophenoxyacetic Acid (2,4-D)- and 2,4,5-trichlorophenoxyacetic Acid (2,4,5-T)-degrading bacterial community in soil–water suspension during the enrichment process, Microbes. Environ., **23**, 142–148 (2008).

COR-AAD1-00003780
Bayer EX1008 (Part 7 of 9)

World J Microbiol Biotechnol (2015) 31:1021–1030
DOI 10.1007/s11274-015-1852-z

ORIGINAL PAPER

Cloning, expression, characterization and mutational analysis of the *tfdA* gene from *Cupriavidus campinensis* BJ71

Lizhen Han[1,2,3] · Yanbo Liu[1,2,3] · Cuicui Li[2,3] · Degang Zhao[1,2,3]

Received: 5 January 2015 / Accepted: 3 April 2015 / Published online: 8 April 2015
© Springer Science+Business Media Dordrecht 2015

Abstract 2,4-Dichlorophenoxyacetic acid (2,4-D)/α-ketoglutarate (α-KG) dioxygenase (TfdA) is an Fe(II)-dependent enzyme that catalyzes the first step in degradation of the herbicide 2,4-D. Previous studies focused on the *tfdA* gene in *Ralstonia eutropha* JMP134 isolated in Australia. In this study, a new *tfdA* gene was cloned from *Cupriavidus campinensis* BJ71, an effective degrading bacteria from China, based on the iCOnsensus-DEgenerate Hybrid Oligonucleotide Primers (iCODEHOPs) protocol, combined with high-efficiency Thermal Asymmetric Interlaced PCR (hiTAIL-PCR). The open reading frame of 861 bp encoded a putative 287 amino acid protein with a theoretical molecular mass of 32.32 kDa. The gene was overexpressed in *Escherichia coli* BL21 (DE3) and the purified TfdA showed optimal activity at pH 6.75 and 30 °C. This enzyme was more thermostable and it could use 3-hydrocinnamic acid as substrate, with a similar enzyme activity compared with 2,4-D. TfdA and its variants were created as maltose-binding protein (MBP) tagged fusion proteins to examine the roles of putative substrate-binding residues. The MBP-N110A, MBP-V198A and MBP-R207K proteins showed decreased k_{cat} and increased *Km*, and MBP-R278A was inactive, suggesting these residues may affect 2,4-D binding or catalysis.

Keywords *tfdA* · *Cupriavidus campinensis* BJ71 · 2,4-D/α-KG-dependent dioxygenase · Site-directed mutagenesis · Characterization

✉ Degang Zhao
dgzhao@gzu.edu.cn

Lizhen Han
hanlizhen11@163.com

[1] Key Laboratory of Green Pesticide and Agricultural Bioengineering, Ministry of Education, Guiyang 550025, China

[2] Key Laboratory of Plant Resources Conservation and Germplasm Innovation in Mountainous Region (Guizhou University), Ministry of Education, College of Life Sciences, Guizhou University, Guiyang 550025, China

[3] Guizhou Key Lab of Agro-Bioengineering, Guizhou University, Guiyang 550025, China

Introduction

2,4-Dichlorophenoxyacetic acid (2,4-D) is a phenoxy herbicide that has been used widely to control dicotyledonous weeds in cereal and grass crops for over 70 years. The herbicide is regarded as readily biodegradable, and a number of strains able to grow on 2,4-D as a sole carbon source have been isolated. These phylogenetically diverse bacteria, which belong to the α-, β-, and γ-*Proteobacteria* and the *Bacterioidetes/Chlorobi* group (Itoh et al. 2002, 2004; Ka et al. 1994; Lee et al. 2005; Suwa et al. 1996), harbor *tfdA*-like genes [*tfdA* or *tfdA*α; encoding (2,4-D)/α-ketoglutarate (α-KG) dioxygenase] and are categorized into three groups based on their evolution and physiology (Kamagata et al. 1997). The first group comprises species belonging to the β- and γ-*Proteobacteria* and can be further divided into three distinct classes based on their *tfdA* genes. Class I *tfdA* genes are closely related to those of *Cupriavidus necator* JMP134 (formerly *Alcaligenes eutrophus*, *Wautersia eutropha*, or *Ralstonia eutropha*), a well-studied 2,4-D degrader (Streber et al. 1987). Class II *tfdA* genes comprise those of *Burkholderia* sp. strain RASC and a few strains that are 76 % identical to class I *tfdA* genes. Class III *tfdA* genes are 77 and 80 % identical to the class I and class II *tfdA* genes, respectively, and are linked to 2-methyl-4-chlorophenoxyacetic acid (MCPA) degradation in soil (Baelum et al. 2006, 2008;

COR-AAD1-00003781
Bayer EX1008 (Part 7 of 9)

McGowan et al. 1998). The second and third groups comprise alphaproteobacterial *Bradyrhizobium*- and *Sphingomonas*-related organisms, respectively, and contain *tfdA* α genes with between 46 and 60 % identity to the canonical *tfdAs* of group 1 (Fulthorpe et al. 1995; Itoh et al. 2000, 2002, 2004; Kamagata et al. 1997). However, in these two groups, 2,4-D catabolism may involve the *cadABC* genes, which are predicted to encode functional components of a multicomponent 2,4-D oxygenase (Itoh et al. 2004; Kitagawa et al. 2002; Shimojo et al. 2009). Streber et al. (1987) isolated, sequenced and characterized the first gene, the canonical *tfdA*, from the bacterium *C. necator* JMP134. Its protein product, TfdA, is an Fe(II)/α-KG-dependent dioxygenase belonging to Group II α-KG dependent dioxygenases, and shows clear homology (30 % amino acid identity) to *Escherichia coli* taurine/α-KG dioxygenase (TauD) (Eichhorn et al. 1997). TfdA catalyzes 2,4-D into 2,4-dichlorophenol (2,4-DCP) and glyoxylate, while oxidizing α-KG to CO_2 and succinate, as an initial step of 2,4-D degradation (Fukumori and Hausinger 1993a, b; Vedler et al. 2000). Subsequently, additional complete *tfdA*-like genes and numerous partial *tfdA* gene sequences have been found in total genomic DNAs (Bælum et al. 2006; Gonod et al. 2006; Han et al. 2014; Hoffmann et al. 2003; Poh et al. 2002; Shaw and Burns 2004; Vedler et al. 2000; Zakaria et al. 2007). These nucleotide sequences identified >99 % within class I *tfdA* genes. The sequence data and phylogenetic tree demonstrated that this class shows very low diversity (Bælum et al. 2010).

In our previous study, we isolated an effective 2,4-D degrading bacterium, *C. campinensis* BJ71, from Beijing, China. This strain exhibited a degradation rate of up to 99.57 % (initial 2,4-D concentration of 350 mg L^{-1}) after 6 days of incubation (submitted for publication) and its 2,4-D degradation efficiency was greater than JMP134, the most intensively studied chloroaromatic-degrading microorganism to date, which showed a 70 % maximum degradation rate (initial concentration of 250 mg L^{-1}) after 10 days (Lerch et al. 2007). Interestingly, alignment of the TfdA sequence from BJ71 with that of JMP134 identified differences at 11 amino acid sites within the encoded product of the 365-bp *tfdA* fragments (Han et al. 2014). Hence, in the present study, the *tfdA* gene from *C. campinensis* BJ71 was cloned successfully and expressed to further study the essential differences in biodegradability compared with *C. necator* JMP134. The enzyme was purified and its biochemical properties were determined. In addition, site-directed mutagenesis was performed and the kinetic parameters of the mutants were examined to determine the effects of the mutations on enzyme activity. This study provides an insight into the diversity of class I TfdAs and may be useful for analyzing differences in degradation efficiency among 2,4-D-degrading bacteria strains.

Materials and methods

Strains, plasmids, growth conditions, and reagents

BJ71, an effective 2,4-D-degrading bacterial strain isolated from a wheat soil in China, was identified as *C. campinensis*, based on its 16S rRNA sequence analysis and morphological, physiological, and biochemical characteristics (submitted for publication). It was then preserved in our laboratory and deposited in the China Center for Type Culture Collection under accession number CCTCC M 2014006. BJ71 was grown aerobically in Luria–Bertani (LB) medium containing 500-mg L^{-1} 2,4-D at 30 °C with moderate stirring (150 rpm) and used as the plasmid DNA donor to clone the *tfdA* gene. *Escherichia coli* JM109 was used as the cloning host, whereas *E. coli* BL21 (DE3) was used as the expression host. The vectors used were pGEM-T Easy (Promega, Madison, WI, USA) for sequencing, pET28a (Novagen, Darmstadt, Germany) and pMAL-c5x (New England BioLabs, Beverly, MA, USA) for expression. *E. coli* JM109 and *E. coli* BL21 (DE3) cells were grown at 37 °C in LB medium with ampicillin (100 mg L^{-1}), unless stated otherwise. 2,4-D and all other chemicals were purchased from Sigma-Aldrich (St. Louis, MO, USA). The Gel DNA Extraction kit, In-Fusion HD Cloning kit (Clontech, San Francisco, CA, USA), PrimerSTAR HS DNA polymerase and all other enzymes used for molecular cloning, except *Xmn*I (from New England BioLabs), dNTP and isopropyl-β-d-thiogalactoside (IPTG), were purchased from Takara (Dalian, China). The Plasmid Mini Kit was purchased from Omega (Doraville, GA, USA). Takara synthesized all the primers. All other chemicals were of the highest grade available.

Isolation of the *tfdA* gene from BJ71 strain by degenerate PCR and hiTAIL-PCR

Plasmid DNA from *C. campinensis* strain BJ71 was extracted using a Plasmid Mini Kit and used as template. An iCODEHOPs strategy (Rose et al. 1998, 2003; Boyce et al. 2009) and hiTAIL-PCR (Liu and Huang 1998; Liu and Chen 2007) were used to amplify and clone the complete sequences of the *tfdA* gene of *C. campinensis* BJ71. Degenerate primers to amplify the partial nucleotide sequences of the *tfdA* gene were designed by iCODEHOPs (http://courses.washington.edu/bioinfo/CODEHOP/Codehop%20Genes.html) on the basis of a multiple sequence alignment of 42 published TfdA protein sequences from NCBI. Two highly conserved amino acid sequence motifs, DTEFC and NRCV, were chosen as targets. Primers *tfdA* F and *tfdA* R (Table 1) were derived from these motifs and amplifications were performed using a touchdown protocol (Han et al. 2014).

COR-AAD1-00003782
Bayer EX1008 (Part 7 of 9)

Table 1 Oligonucleotide primers used in the present study

Experiment	Primer name	Primer (5′–3′)
Degenerate PCR	COD *tfdA* F	CGACACCGAGTTCTGCgayatgmgngc
	COD *tfdA* R	CGCAGCGGTTGtcccanatnac
hiTAIL-PCR	*tfdA* LB-0a	AGCGATGGCGGTACACGAACTGGCG
	tfdA LB-1a	ACGATGGACTCCAGTCCGGCCTGGGCACCGATGAAGAGAAAGCGGCGTC
	tfdA LB-2a	GAGTAGTCGGTGTCGCCCAGAAGGAAG
	tfdA RB-0a	TTCCTTCTGGGCGACACCGACTACTCCG
	tfdA RB-1a	ACGATGGACTCCAGTCCGGCCGCTCGGGACGCCGCTTTCTCTTCATC
	tfdA RB-2a	GCAACGCCAGTTCGTGTACCGCCATC
	LAD1-1	ACGATGGACTCCAGAGCGGCCGC(G/C/A)N(G/C/A)NNNGGAA
	LAD1-2	ACGATGGACTCCAGAGCGGCCGC(G/C/T)N(G/C/T)NNNGGTT
	LAD1-3	ACGATGGACTCCAGAGCGGCCGC(G/C/A)(G/C/A)N(G/C/A)NNNCCAA
	LAD1-4	ACGATGGACTCCAGAGCGGCCGC(G/C/T)(G/A/T)N(G/C/T)NNNCGGT
	AC1	ACGATGGACTCCAGAG
Gene cloning	*tfdA* Up-F	CCGACCCCCTTGCGAGTTAGGAAAAGGAGA
	tfdA Down-R	GCGATTCGCGGCCAGCATGACTTCG
Gene expression	*tfdA* E-mF	CGGGATCCGAGGGAAGG'ATTTCAATGAGCGCAGTTGCCAACCC
	tfdA E-F	GGCA'TATGTCATGAGCGCAGTTGCCAACCC
	tfdA E-R	TACCTGCAGGG'AATTCCTAGGCGACGGCGTCGTCCA
Mutagenesis	N110A-F	GCGCAGACTAATTCGAGCTCGAAC
	N110A-R	TACCTGCAGGGAATTCCTAGGCGAC
	N110A-F01	TTCGCCGCGCAGCTCTGGCACAGC
	N110A-R01	TGCCAGAGCTGCGCGGCGAAATTGCCG
	V198A-F01	GCCGCTGGCGCGAACCCATGCCG
	V198A-R01	CATGGGTTCGCGCCAGCGGCCACC
	R207K-F01	TCGGGACGCAAATTTCTCTTCATC
	R207K-R01	AAGAGAAATTTGCGTCCCGAGCCG
	R278A-R	TACCTGCAGGGAATTCCTAGGCGACGGCGTCGTCCAGGGTCGTCGCCGCGCGCAGCTCGCGCC

Y = C/T, R = A/G, N = A/C/G/T

The flanking fragments of the conserved region were amplified using hiTAIL-PCR. The nested insertion-specific primers were designed based on the amplified partial *tfdA* gene fragment. Specific primers *tfdA* LB-0a, LB-1a and LB-2a were used to amplify the sequence upstream of the 5′ region, and primers *tfdA* RB-0a, RB-1a and RB-2a for amplified the sequence downstream of the 3′ region. Arbitrary degenerate primers LAD1-1, LAD1-2, LAD1-3, LAD1-4 and AC1 came from Liu and Chen (2007). Table 1 lists the primers used in this study. The detailed procedures of hiTAIL-PCR were according to the original publication, except that LA Taq and GC buffer II were used instead of Ex Taq and PCR buffer.

According to the sequences assembled by the DNAMAN program, primers *tfdA* Up-F/Down-R were designed to amplify the nucleotide sequence containing the full-length *tfdA* gene (Table 1). All PCR products were purified, ligated into pGEM-T Easy vector and sequenced by Takara. The pGEM-T Easy vector containing the complete *tfdA* gene sequence was named pGEM-T-*tfdA*.

Bioinformatic analysis of the *tfdA* gene

The ORF was predicted using the NCBI ORF Finder (http://www.ncbi.nlm.nih.gov/projects/gorf/). The BLAST programs (http://blast.ncbi.nlm.nih.gov/Blast.cgi) were used to perform similarity searches. Multiple sequence alignments were performed using CLUSTAL Omega (http://www.ebi.ac.uk/Tools/msa/clustalo) (Larkin et al. 2007). The phylogenetic tree was generated using the neighbor-joining method in the MEGA5.1 program (Tamura et al. 2011). A bootstrap analysis based on 1000 replicates was employed to place confidence estimates on the tree. The prediction of protein binding sites and evaluation of tertiary structure were made by RaptorX-*Binding* (http://raptorx.uchicago.edu/) (Källberg et al.

COR-AAD1-00003783
Bayer EX1008 (Part 7 of 9)

2012), and analysis of protein domains was made by ProDom (http://prodom.prabi.fr/prodom/current/html/home.php) (Servant et al. 2002).

Cloning of the *tfdA* gene in *E. coli*

Using pGEM-T-*tfdA* as the template, the entire ORF was amplified using primers *tfdA* E-F and *tfdA* E-R (Table 1, restriction sites underlined in primers) to create *Nde*I and *Eco*RI sites at the ends of the complete *tfdA* gene. The PCR product was cloned into vector pET-28a, which had been digested with the same enzymes, and transformed into *E. coli* BL21 (DE3). To create a construct expressing the MBP-TfdA fusion protein, the wild-type *tfdA* gene was amplified using primers *tfdA* E-mF (*Xmn*I site underlined) and *tfdA* E-R (*Eco*RI site underlined), and the product was inserted into pMAL-c5x. The identity of the newly created *malE-tfdA* gene fusion was confirmed by sequencing, and the expression plasmid pMAL-c5x-*tfdA* was transformed into *E. coli* BL21 (DE3).

Site-directed mutagenesis of TfdA

Mutants Asn110Ala, Val198Ala, Arg207Lys and Arg278Ala were generated using an In-Fusion PCR cloning kit and pMAL-c5x-*tfdA* as the template; the mutagenic primers are listed in Table 1. Mutations were confirmed by sequence analysis of both DNA strands. Mutated plasmids were transformed into *E. coli* strains as described above.

Heterologous expression and purification of the TfdA recombinant and mutants

Unless stated otherwise, all experiments were done at 4 °C. *E. coli* BL21 (DE3) cells were grown in LB medium supplemented with 2.0 g of glucose L^{-1} and 100 mg of ampicillin L^{-1} (For expression of wild-type TfdA, 20 mg L^{-1} kanamycin), with agitation, until they reached an OD_{600} of 0.5–0.6. IPTG (0.3 mM) was then added and the cultures incubated for a further 7 h at 30 °C. The cells were harvested by centrifugation (4000×*g*, 20 min) and suspended in a solution containing 20 mM Tris–HCl, 1 mM EDTA, 1 mM PMSF and 0.4 μg of leupeptin mL^{-1} (pH 7.6). The suspended cells were disrupted by ultrasonication on ice. Clear supernatants were obtained by centrifugation (20,000×*g*, 20 min) and used as a crude cell extract. The wild-type, MalE-TfdA and its variants were purified and subjected SDS-PAGE analysis.

Enzyme assays

The enzyme activities of the wild-type, MBP-TfdA and the variants were performed as described previously, by determining the amount of 2,4-DCP formed using the 4-aminoantipyrine method (King et al. 1991). The typical assay mixture (total volume of 1 mL) contained 1 mM α-KG, 50 μM ascorbic acid, 50 μM $(NH_4)_2Fe(SO_4)_2$ and 1 mM 2,4-D in 10 mM imidazole buffer (pH 6.75) at 30 °C. The reactions were quenched by the addition of EDTA to a concentration of 5 mM. Product formation was assayed by adding 100-μL borate buffer, 10-μL 2 % 4-aminoantipyrine (w/v), and 10-μL 8 % potassium ferricyanide (w/v). The concentration of released 2,4-DCP was quantified by reaction with 4-aminoantipyrene, followed by measurement of the absorbance at 510 nm after a 20 min reaction at 30 °C. All assays were performed in triplicate. One unit of activity was defined as the amount of enzyme that formed 1 μM of 2,4-DCP per min at 30 °C. Specific activity was expressed as units per milligram of protein. Protein concentrations were measured using the Bradford method, with bovine serum albumin as the standard. The optimal temperature for TfdA activity was determined by measuring enzyme activity at temperatures ranging from 25 to 55 °C after a 20 min reaction at pH 6.75, using 2,4-D as the substrate and following the same protocol. The optimal pH was measured at 30 °C using the same substrate over a pH range of 3.0–11.0. Thermal stability was determined by measuring the residual enzyme activity after 30 min of treatment at different temperatures (25–55 °C). pH stability was determined by analyzing residual enzyme activity after incubating in the pH range 3.0–11.0 at 4 °C for 20 h (Fukumori and Hausinger 1993b).

The substrate specificity was analyzed by measuring the relative enzyme activity with the following 2,4-D related compounds: phenoxyacetate, 4-chlorophenoxyacetic acid, 4-chlorocinnamic acid, 3-hydroxycinnamic acid, 2-naphthoxyacetic acid, 4-methoxycinnamic acid, hippuric acid, cinnamic acid.

Maximum rates (Vmax), affinities (K_m), and catalytic efficiencies (k_{cat}/K_m) of the wild-type, MBP-TfdA and variants were compared to study the influence of the mutations on the enzyme's activity. These kinetic parameters were calculated using a Lineweaver–Burk plot (based on a weighted nonlinear analysis of the Michaelis–Menten model). The TfdA variants were assumed to have an $Mr = 32{,}320$ according to the predicted molecular weight of TfdA ($Mr = 32{,}320$) by Protparam (Gasteiger et al. 2005). The MBP-TfdA variants were assigned an $Mr = 74{,}800$, representing the combined molecular weight of the maltose-binding protein (42,480) and TfdA, and used this to calculate the k_{cat} values. Enzyme assays was carried out under optimal conditions with varying 2,4-D concentrations (0.01–10 mM).

Nucleotide sequence accession number

The complete nucleotide sequence and partial nucleotide sequence of the *tfdA* gene from *C. campinensis* BJ71 were

COR-AAD1-00003784
Bayer EX1008 (Part 7 of 9)

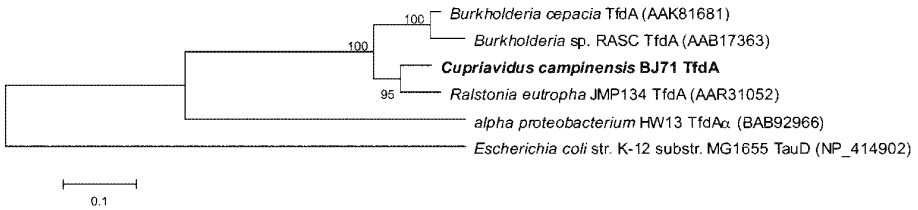


Fig. 1 Phylogenetic tree of TfdA/TauD amino acid sequences. The sequence alignment was performed using MEGA5.1 software. [*Cupriavidus campinensis* BJ71] AHN65070 (this paper); [*Ralstonia eutropha* JMP134] AAR31052 (class I TfdA); [*Burkholderia* sp. RASC] AAB17363 (class II TfdA); [*Burkholderia cepacia* 2a] AAK81681 (class III TfdA); [*Alphaproteobacterium* sp. HW13] BAB92966 (TfdAα); [*Escherichia coli* str. K-12 substr. MG1655] NP_414902 (TauD)

deposited into GenBank under accession numbers KJ028765 and KJ028762, respectively.

Results

Cloning *tfdA* gene from *C. campinensis* BJ71

Using the iCODEHOPs method, a partial 365-bp DNA fragment was obtained from the plasmid DNA of BJ71. Conserved domain searches indicated the peptide encoded by this fragment possessed characteristic residues within the active site of the 2,4-D/α-ketoglutarate dioxygenase TfdA family proteins. However, this nucleotide sequence did not match exactly to any previously reported *tfdA* gene sequences. To acquire the flanking sequences of the *tfdA* gene, nested specific primer sets (LB-0a/LB-1a/LB-2a, RB-0a/RB-1a/RB-2a) were designed based on the 365-bp nucleotide sequence. Target fragments were amplified by pre-amplification and two rounds of PCR with LA Taq and GCII buffer, according to the hiTAIL-PCR procedure. Based on the assembled sequences, including the 365-bp conserved region, and the 5′ and 3′ regions, primers *tfdA* Up-F and *tfdA* Down-R were designed and the 1080-bp length sequence was amplified and sequenced. ORF Finder identified an open reading frame of 861 bp.

Sequence analysis of *tfdA* gene from *C. campinensis* BJ71

The nucleotide sequence of the 861 bp ORF exhibited 87 % identity with the *tfdA* gene in *R. eutropha* JMP134 (M16730). The ORF encodes a putative 287 amino acid protein with a theoretical molecular mass and pI of 32.32 kDa and 6.01, respectively. The phylogenetic relationship among the amino acid sequences of TfdA from *C. campinensis* BJ71 strain and other TauD family proteins was constructed using MEGA 5.1 software. The highest sequence identity of this encoding product was 95 % with *R. eutropha* JMP134 TfdA, indicating that it belonged to the class I TfdA proteins (Fig. 1). The amino acid sequence alignment further showed that TfdA from *C. campinensis* BJ71 has the consensus motif HX(D/E)$X_{138-207}$HX_{10-13}(R/K), which was identified in the taurine dioxygenase (TauD) of *E. coli*, the representative of Group II α-KG-dependent dioxygenase. Differences were identified at 27 sites in TfdA from BJ71 compared with *R. eutropha* JMP134. In particular, 16 differences were observed for the identical and conserved residues of Group II α-KG-dependent dioxygenases (Fig. 2).

Physicochemical characterization of recombinant TfdA

The wild-type TfdA protein was expressed successfully in *E. coli* BL21 (DE3) by IPTG induction and purified using a Ni-NTA affinity chromatography column. The molecular mass of the protein was approximately 32 kDa. The effects of temperature and pH on TfdA activity were investigated using 2,4-D as the substrate. As shown in Fig. 3, the optimum temperature was 30 °C and more than 90 % of the initial activity was maintained when the reaction temperature ranged from 25 to 35 °C. However, relative activity decreased sharply at temperatures above 40 °C. The purified TfdA was relatively insensitive to thermal inactivation and the relative activities were 62, 27, and 5 % of the total after incubation for 30 min at 30, 40 and 55 °C, respectively. The pH dependence of TfdA was examined and the pH optimum was determined as 6.75. TfdA was stable over a wide pH range (7.0–10.0), with more than 90 % residual activity after incubation for 20 h at 4 °C. Among nine potential substrates tested, 34 and 7 % of the activity were observed with 4-chlorophenoxyacetic acid and MCPA as substrates, respectively. There was no activity with cinnamic acid. The enzyme exhibited similar catalytic efficiency when the substrate was phenoxyacetate, 4-chlorocinnamic acid, 2-naphthoxyacetic acid, 4-methoxycinnamic acid and hippuric acid, respectively. Surprisingly, the best substrate was 3-hydrocinnamic acid, which showed 102.59 % of the enzyme activity compared with 2,4-D (Table 2).

COR-AAD1-00003785
Bayer EX1008 (Part 7 of 9)

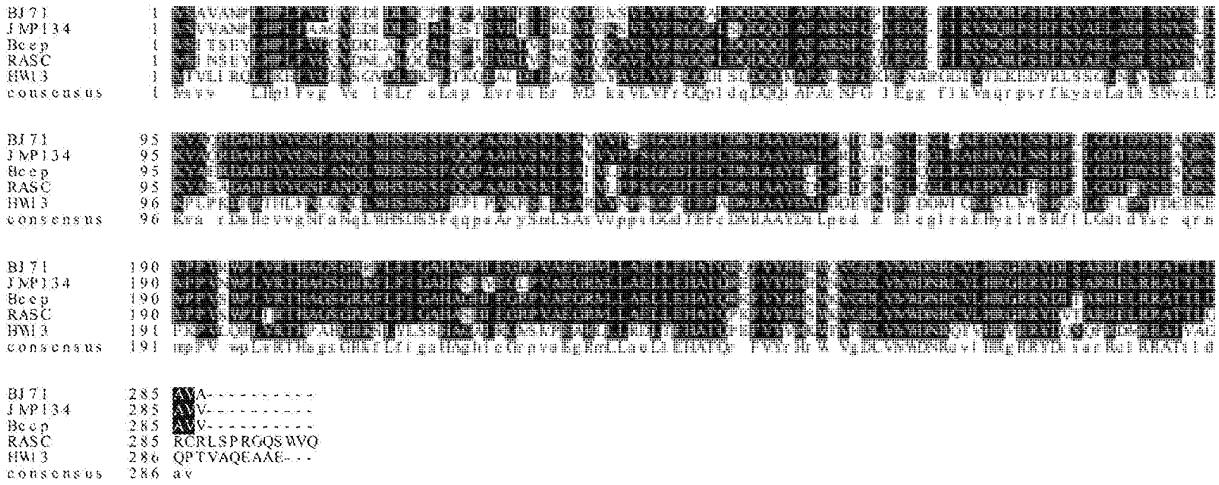


Fig. 2 Sequence alignment of TfdA from BJ71 with other group II α-KG-dependent dioxygenases. BJ71, *Cupriavidus campinensis* BJ71 TfdA (AHN65070); JMP134, *Ralstonia eutropha* JMP134 TfdA (AAR31052); Bcep, *Burkholderia cepacia* 2a TfdA (AAK81681); RASC, *Burkholderia* sp. RASC TfdA (AAB17363); and HW13, *Alphaproteobacterium* sp. HW13 TfdAα (BAB92966). The identical and conserved residues are highlighted in *white* on *black* and *gray* backgrounds, respectively

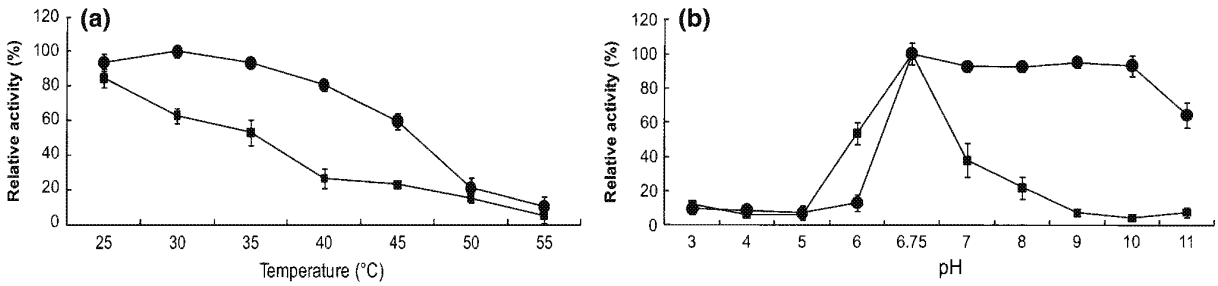


Fig. 3 Effect of temperature (**a**) and pH (**b**) on the activity of purified TfdA. **a**. Effect of temperature. The enzyme reactions to determine optimum temperature were assayed at 25 to 55 °C at pH 6.75. The thermostability of the purified enzyme was measured at 30 °C after preincubation at 25 to 55 °C for 30 min. The highest activity was considered 100 % when calculating the relative activities. All data shown are mean values from three replicate experiments. *Circle with solid line*, optimum temperature; *square with solid line*, thermostability. **b** Effect of pH. The enzyme reactions of the purified TfdA were assayed at pH 3.0–11.0 at 30 °C. The highest activity was considered 100 % when calculating the relative activities. *Circle with solid line*, optimum pH; *square with solid line*, pH stability. All data shown are mean values from at three replicate experiments

Site-directed mutagenesis of TfdA

Using the crystal structure of TauD (PDB number: 3pvjA) from *Pseudomonas putida* as the model, the protein binding sites and three-dimensional structure were predicted by RaptorX-*Binding*. Analysis of protein domains among Group II α-KG-dependent dioxygenase were made by ProDom. These results, combined with a sequence alignment of TfdA and TauD (Fig. 2), revealed conservation of certain active site residues (data not shown). To investigate the role of these active site residues on the enzyme's activity, three residues (N110, V198 and R278) in the active site of TfdA were targeted for alanine substitution, and R207 in the conserved site was targeted for lysine substitution, using site-directed mutagenesis. It was reported that wild-type TfdA and an MBP-TfdA fusion protein had essentially identical k_{cat} and very similar *Km* values for α-KG and 2,4-D; however, some TfdA variants were present as inclusion bodies when expressed in pET23a vector (Hogan et al. 2000). Our results showed similar effects (Table 3). Mutants MBP-N110A, MBP-V198A, MBP-R207 K and MBP-R278A were constructed, expressed and purified. The molecular weights of the expressed fusion protein and mutants were approximately 76 kDa, which comprised the maltose-binding protein and TfdA of 287 amino acids, whereas the molecular mass of the protein expressed from empty pMAL-c5 vector was approximately 42 kDa (data not shown). The enzyme

COR-AAD1-00003786
Bayer EX1008 (Part 7 of 9)

Table 2 Substrate specificities of TfdA

Substrate	Relative activity (%) (mean ± SD)	Specific activity (min^{-1})
2,4-D	100.00	115.02
MCPA	7.19 ± 0.45	8.27
Phenoxyacetate	18.32 ± 4.12	21.07
4-Chlorophenoxyacetic acid	34.20 ± 7.18	39.31
4-Chlorocinnamic acid	17.29 ± 3.36	19.89
3-Hydroxycinnamic acid	102.59 ± 6.75	117.98
2-Naphthoxyacetic acid	16.19 ± 5.00	18.62
4-Methoxycinnamic acid	14.05 ± 1.73	16.16
Hippuric acid	13.47 ± 3.07	15.50
Cinnamic acid	0	–

The substrate range was determined using TfdA purified from two independent batches; the enzyme activity of each batch was measured three times with all substrates

Table 3 Kinetic parameters for TfdA and three variants

TfdA sample	k_{cat} (min^{-1})	K_m (μM)	k_{cat}/K_m (min^{-1} mM^{-1})
TfdA	821.36 ± 35.91	1.19 ± 0.02	690218.47 ± 597.38
MBP-TfdA	815.87 ± 25.32	1.59 ± 0.04	513774.49 ± 505.81
MBP-N110A	29.24 ± 0.34	183.63 ± 16.53	159.22 ± 60.51
MBP-V198A	110.62 ± 15.84	9726.80 ± 268.09	11.37 ± 7.96
MBP-R207K	245.22 ± 18.30	12.36 ± 0.21	19839.75 ± 278.45

The specific activity of the TfdA was 115.02 min^{-1}

activities of these four mutants were analyzed using 2,4-D as the substrate. No activity was observed with mutant MBP-R278A, which confirmed the importance of residue R278 for TfdA activity. To our surprise, MBP-V198A exhibited a sevenfold reduction in k_{cat} and a 6117-fold increase in the *Km* for 2,4-D. In addition, the MBP-N110A variant showed a 27-fold reduction in k_{cat} and a 115-fold increase in *Km*, whereas the MBP-R207K variant showed an 8-fold increase and a 3-fold reduction, accordingly (Table 3). The large increases in *Km* and reductions in k_{cat} resulted in corresponding decreases in the catalytic efficiency (k_{cat}/Km) of these variants.

Discussion

In the current study, we successfully cloned the *tfdA* gene from *Cupriavidus campinensis* BJ71 and the nucleotide sequences exhibited identity of 87 % with the *tfdA* gene from *R. eutropha* JMP134. McGowan et al. (1998) amplified class I *tfdA* gene fragments (313-bp length) from 2,4-D-degrading strains JMP134, TFD39, TFD23, K712, and TFD9 and observed that they differed from each other by only 2 bp at most. Full-length CDSs of class I *tfdA* genes were amplified from ten strains and only three amino acids were different among their encoded proteins (Baelum et al. 2010). By contrast, we found 27 amino acid changes between the protein encoded by *tfdA* from BJ71 and that encoded by *tfdA* from JMP134. To the best of our knowledge, this is the largest difference observed compared with other class I *tfdA* genes. The difference in the TfdA protein sequences may affect its degradation capability.

To explore its activity, the *tfdA* gene from BJ71 was overexpressed and purified. It showed some differences compared with the canonical *tfdA* from JMP134. Fukumori and Hausinger (1993b) reported that the purified TfdA from JMP134 was very sensitive to thermal inactivation. It remained stable only up to 30 °C and was completely inactivated within 5 min at 40 °C. By contrast, TfdA from BJ71 was more thermostable and retained 27 % of its activity after incubation at 40 °C for 30 min. Previous studies evaluated the ability to purified TfdA to utilize various phenoxyacetic acids, thiophenoxyacetic acids, phenoxypropionic acids, and non-phenoxyacid, aromatic compounds. Non-halogenated phenoxyacetate possessed a larger *Km* value than did the halogenated substrates. TfdA exhibited no activity toward hydrocinnamic acid, and cinnamic acid was metabolized poorly. The substrate associated with the highest catalytic efficiency was identified as 2,4-D (Fukumori and Hausinger 1993b; Saari et al. 1999; Dunning Hotopp and Hausinger 2001). In the current study, TfdA from BJ71 could catalyze substrates containing different substituents, such as hydroxyl, methyl, and chloride groups on the aromatic ring. Many ring-substituted

COR-AAD1-00003787
Bayer EX1008 (Part 7 of 9)

compounds were also reasonable substrates with lower catalytic rates. TfdA does not use cinnamic acid. Interestingly, in contrast to TfdA from JMP134, this enzyme exhibited the highest turnover rates with 3-hydrocinnamic acid. It was suggested that the *tfdA*α genes could be the origin of the *tfdA* genes and naturally occurring aryl ethers and cinnamic acid were proposed as candidate substrates of TfdAα (Itoh et al. 2002, 2004). It was reported that several cinnamic acids, such as 2,4-dichlorocinnamic acid, 2- or 4-monochloro derivatives, unsubstituted cinnamic acid, were used as substrates by TfdA from JMP134 (Dunning Hotopp and Hausinger 2001). However, to the best of our knowledge, this is the first report of a thermostable TfdA that could degrade 3-hydrocinnamic acid. Accordingly, the substrate specificity and thermostability of the four mutants showed no significant differences with the wild-type (data not shown). Whether the improved thermostability and different substrate utilizations are attributable to other amino acid differences between the TfdA from *C. campinensis* BJ71 and *C. necator* JMP134 remains to be determined.

The 2,4-D/α-KG-dependent dioxygenase TfdA from *C. necator* JMP134 has been well characterized. Hogan et al. (2000) suggested that His-214 might aid in catalysis or binding of 2,4-D, and His-114, Asp-116 and His-263 were likely metal ligands in TfdA. Based on the X-ray crystal structure of TauD from *E. coli* (PDB number: 1gqw) in an oligomeric state, interactions with the 2,4-D carboxylic acid were proposed to involve Arg278, Lys71 and His214. The backbone amide of Ser117, Lys95 and probably Lys71 were hypothesized to interact with the 2,4-D ether atom, whereas Arg274 and Thr141 were suspected to bind αKG (Elkins et al. 2002). Kinetic characteristics of K71L, K71Q, K95L, K95Q, R274Q, R274L and R278Q variants confirmed this hypothesis (Dunning Hotopp and Hausinger 2002). However, Knauer et al. (2012) reported that both TauD from *P. putida* KT2440 ($TauD_{Pp}$) and from *E. coli* ($TauD_{Ec}$) were tetramers, based on crystal structures and kinetic characterizations. We observed some different results compared with TfdA from JMP134 when we predicted protein binding sites of TfdA from BJ71 using the crystal structure of $TauD_{Pp}$. Accordingly, MBP-N110A, MBP-V198A, MBP-R207 K and MBP-R278A variants of TfdA were created. Their activities were measured, and in selected cases, detailed kinetic experiments were performed. The most striking changes observed for these proteins involved the *Km*, which ranged from an 8-fold increase in the case of MBP-R207K to a 6117-fold increase for MBP-V198A. The large increases in *Km* resulted in corresponding decreases in the catalytic efficiency (k_{cat}/*Km*) of these variants, especially in MBP-N110A and MBP-V198A TfdA. In the present study, the TfdA protein from BJ71 has a predicted catalytic pocket, comprising Asn110, His114, Asp116, Ser117, Leu129, Thr141, His263, Gly265, Arg274, Leu276 and Arg278. The MBP-N110A variant exhibited an 115-fold increase in *Km*, which led us to hypothesize that the decreased binding to the substrate α-KG of N110A was because the hydrophilic nature of Asn110 is important for the catalytic center of enzyme. Val198 is a highly conserved amino acid residue among the TauD family and lies in the β-sheet, which is located outside of the catalytic domain. The secondary structure of MBP-V198A was changed from β-strand to α-helix in this site as Ala in replacement of Val198 and it affected the catalytic activity of MBP-TfdA immensely. Lys207 is the conserved residue in group II α-KG-dependent dioxygenases and Arg replaced Lys in this site in the TfdA from BJ71 (Fig. 2). The change in *Km* and k_{cat} of MBP-R207K mutant could have resulted from decreased ionic interaction. The results confirmed that Asn110, Val198, and Arg207 are involved in 2,4-D substrate binding and provide useful insights into the catalytic mechanism of TfdA from BJ71. However, additional studies are required to test this hypothesis.

In this work, a novel *tfdA* gene was cloned from *C. campinensis* BJ71 and overexpressed in *E. coli*. A detailed characterization of this enzyme was provided, including optimal activity and substrate specificity. TfdA from BJ71 was only 95 % identical to TfdA of *R. eutropha* JMP134, the largest difference reported between class I TfdAs to date. Recombinant MBP-tagged TfdA could utilize 3-hydrocinnamic acid with a similar catalytic efficiency to 2,4-D and was more thermostable. Variants of MBP-TfdA were constructed and analyzed; the results suggested that Asn110, Val198, Arg207 and Arg278 might be involved in 2,4-D binding or catalysis.

Acknowledgments The authors thank the Foundation of the National Transgenic Major Project of China (2013ZX08010-003, 2014ZX0801008B-002) and the Province Science Project in Guizhou (J [2013] 2123) for their support.

References

Bælum J, Henriksen T, Hansen HCB, Jacobsen CS (2006) Degradation of 4-chloro-2-methylphenoxyacetic acid in top- and subsoil is quantitatively linked to the class III *tfdA* gene. Appl Environ Microbiol 72(2):1476–1486

Bælum J, Nicolaisen MH, Holben WE, Strobel BW, Sørensen J, Jacobsen CS (2008) Direct analysis of *tfdA* gene expression by indigenous bacteria in phenoxy acid amended agricultural soil. ISME J 2(6):677–687

Bælum J, Jacobsen CS, Holben WE (2010) Comparison of 16S rRNA gene phylogeny and functional *tfdA* gene distribution in thirty-one different 2,4-dichlorophenoxyacetic acid and 4-chloro-2-methylphenoxy -acetic acid degraders. Syst Appl Microbiol 33(2):67–70

Boyce R, Chilana P, Rose TM (2009) iCODEHOPs: a new interactive program for designing COnsensus- Degenerate Hybrid

COR-AAD1-00003788
Bayer EX1008 (Part 7 of 9)

Oligonucleotide Primers from multiply aligned protein sequences. Nucleic Acids Res. doi:10.1093/nar/gkp379
Dunning Hotopp JC, Hausinger RP (2001) Alternative substrates of 2,4-dichlorophenoxy- acetate/α- ketoglutarate dioxygenase. J Mol Catal B Enzym 15:155–162
Dunning Hotopp JC, Hausinger RP (2002) Probing the 2,4-dichlorophenoxyacetate/α-ketoglutarate dioxygenase substrate-binding site by site-directed mutagenesis and mechanism-based inactivation. Biochemistry 41:9787–9794
Eichhorn E, van der Ploeg JR, Kertesz MA, Leisinger T (1997) Characterization of alpha-ketoglutarate- dependent taurine dioxygenase from *Escherichia coli*. J Biol Chem 272:23031–23036
Elkins JM, Ryle MJ, Clifton IJ, Dunning Hotopp JC, Lloyd JS, Burzlaff NI, Baldwin JE, Hausinger RP, Roach PL (2002) X-ray crystal structure of Escherichia coli taurine/α-ketoglutarate dioxygenase complexed to ferrous iron and substrates. Biochemistry 41:5185–5192
Fukumori F, Hausinger RP (1993a) Alcaligenes eutrophus JMP134 "2,4-dichlorophenoxy- acetate monooxygenase" is an & α;-ketoglutarate-dependent dioxygenase. J Bacteriol 175(7):2083–2086
Fukumori F, Hausinger RP (1993b) Purification and characterization of 2,4-dichlorophenoxy-acetate/α-ketoglutarate dioxygenase. J Biol Chem 268(32):24311–24317
Fulthorpe RR, McGowan C, Maltseva OV, Holben WE, Tiedje JM (1995) 2,4- Dichlorophenoxyacetic acid-degrading bacteria contain mosaics of catabolic genes. Appl Environ Microboil 61(9):3274–3281
Gasteiger E, Hoogland C, Gattiker A, Duvaud S, Wilkins MR, Appel RD, Bairoch A (2005) Protein identification and analysis tools on the ExPASy server. In: Walker JM (ed) The proteomics protocols handbook. Humana Press, Totowa, pp 571–607
Gonod LV, Martin-Laurent F, Chenu C (2006) 2,4-D impact on bacterial communities, and the activity and genetic potential of 2,4-D degrading communities in soil. FEMS Microbiol Ecol 58:529–537
Han L, Liu Y, He A, Zhao D (2014) 16S rRNA gene phylogeny and *tfdA* gene analysis of 2,4-D-degrading bacteria isolated in China. World J Microbiol Biotechnol 30(10):2567–2576
Hoffmann D, Kleinsteuber S, Müller RH, Babel W (2003) A transposon encoding the complete 2,4-dichlorophenoxyacetic acid degradation pathway in the alkalitolerant strain *Delftia acidovorans* P4a. Microbiology 149:2545–2556
Hogan DA, Smith SR, Saari EA, McCracken J, Hausinger RP (2000) Site-directed mutagenesis of 2,4-dichlorophenoxyacetic acid/α-ketoglutarate dioxygenase. J Biol Chem 275(17):12400–12409
Itoh K, Kanda R, Momoda Y, Sumita Y, Kamagata Y, Suyama K, Yamamoto H (2000) Presence of 2,4-D catabolizing bacteria in a Japanese arable soil that belong to BANA (Bradyrhizobium-Agromonas-Nitrobacter-Afipia) cluster in α-Proteobacteria. Microbes Environ 15(2):113–117
Itoh K, Kanda R, Sumita Y, Kim H, Kamagata Y, Suyama K, Yamamoto H, Hausinger RP, Tiedje JM (2002) tfdA-like genes in 2,4-dichlorophenoxyacetic acid-degrading bacteria belonging to the Bradyrhizobium-Agromonas-Nitrobacter-Afipia cluster in α-Proteobacteria. Appl Environ Microbiol 68(7):3449–3454
Itoh K, Tashiro Y, Uobe K, Kamagata Y, Suyama K, Yamamoto H (2004) Root nodule *Bradyhizobium* spp. harbor *tfdA*α and *cadA*, homologous with genes encoding 2,4-dichlorophenoxyacetic acid-degrading proteins. Appl Environ Microbiol 70:2110–2118
Ka JO, Holben WE, Tiedje M (1994) Genetic and phenotypic diversity of 2,4-dichlorophenoxy- acetic acid (2,4-D)-degrading bacteria isolated from 2,4-D-treated field soils. Appl Environ Microbiol 60(4):1106–1115
Källberg M, Wang H, Wang S, Peng J, Wang Z, Lu H, Xu J (2012) Template-based protein structure modeling using the RaptorX web server. Nat Protoc 7(8):1511–1522
Kamagata Y, Fulthorpe RR, Tamura K, Takami H, Formey LJ, Tiedje JM (1997) Pristine environments harbor a new group of oligotrophic 2,4-dichlorophenoxyacetic acid-degrading bacteria. Appl Environ Microbiol 63(6):2266–2272
King RJ, Short KA, Seidler RJ (1991) Assay for detection and enumeration of genetically engineered microorganisms which is based on the activity of a deregulated 2,4- dichlorophenoxyacetate monooxygenase. Appl Environ Microb 57(6):1790–1792
Kitagawa W, Takam S, Miyauchi K, Masai E, Kamagata Y, Tiedje JM (2002) Novel 2,4-dichloro phenoxyacetic acid degradation genes from oligotrophic *Bradyrhizobium* sp. strain HW13 isolated from a pristine environment. J Bacteriol 184:509–518
Knauer SH, Hartl-Spiegelhauer O, Schwarzinger S, Hänzelmann P, Dobbek H (2012) The Fe(II)/α- ketoglutarate-dependent taurine dioxygenases from *Pseudomonas putida* and *Escherichia coli* are tetramers. FEBS J 279(5):816–831
Larkin MA, Blackshields G, Brown NP, Chenna R, McGettigan PA, McWilliam H, Valentin F, Wallace IM, Wilm A, Lopez R, Thompson JD, Gibson TJ, Higgins DG (2007) Clustal W and clustal X version 2.0. Bioinformatics 23(21):2947–2948
Lee TH, Kurata S, Nakatsu CH, Kamagata Y (2005) Molecular analysis of bacterial community based on 16S rDNA and functional genes in activated sludge enriched with 2,4-dichlorophenoxyacetic acid (2,4-D) under different cultural conditions. Microb Ecol 49(1):151–162
Lerch TZ, Dignac MF, Barriuso E, Bardoux G, Mariotti A (2007) Tracing 2,4-D metabolism in *Cupriavidus necator* JMP134 with 13 C-labelling technique and fatty acid profiling. J Microbiol Methods 71:162–174
Liu YG, Chen Y (2007) High-efficiency thermal asymmetric interlaced PCR for amplification of unknown flanking sequences. Biotechniques 43:649–656
Liu YG, Huang N (1998) Efficient amplification of insert end sequences from bacterial artificial chromosome clones by thermal asymmetric interlaced PCR. Plant Mol Biol Rep 16:175–181
McGowan C, Fulthorpe R, Wright A, Tiedje JM (1998) Evidence for interspecies gene transfer in the evolution of 2,4-dichlorophenoxyacetic acid degraders. Appl Environ Microbiol 64(10):4089–4092
Poh RPC, Smith ARW, Bruce IJ (2002) Complete characterization of Tn5330 from *Burkholderia cepacia* strain 2a (pIJB1) and studies of 2,4-dichlorophenoxyacetate uptake by the organism. Plasmid 48:1–12
Rose TM, Schultz ER, Henikoff JG, Pietrokovski S, McCallum CM, Henikoff S (1998) Consensus-degenerate hybrid oligonucleotide primers for amplification of distantly related sequences. Nucleic Acids Res 26(7):1628–1635
Rose TM, Henikoff JG, Henikoff S (2003) CODEHOP (COnsensus-Degenerate Hybrid Oligonucleotide Primer) PCR primer design. Nucleic Acids Res 31(13):3763–3766
Saari RE, Hogan DA, Hausinger RP (1999) Stereospecific degradation of the phenoxypropionate herbicide dichlorprop 6(4):421–428
Servant F, Bru C, Carrère S, Courcelle E, Gouzy J, Peyruc D, Kahn D (2002) ProDom: automated clustering of homologous domains. Brief Bioinform 3(3):246–251
Shaw L, Burns RG (2004) Enhanced mineralization of [U-^{14}C]2,4-dichlorophenoxyacetic acid in soil from the rhizosphere of *Trifolium pretense*. Appl Environ Microbiol 70:4766–4774
Shimojo M, Kawakami M, Aamda K (2009) Analysis of genes encoding the 2,4- dichlorophenoxyacetic acid-degrading enzyme from *Sphingomonas agrestis* 58-1. J Biosci Bioeng 108:56–59

COR-AAD1-00003789
Bayer EX1008 (Part 7 of 9)

Streber WR, Timmis KN, Zenk MH (1987) Analysis, cloning, and high-level expression of 2,4-dichlorophenoxyacetate monooxygenase gene *tfdA* of *Alcaligenes eutrophus* JMP134. J Bacteriol 169(7):2950–2955

Suwa Y, Wright AD, Fukimori F, Nummy KA, Hausinger RP, Holben WE, Forney LJ (1996) Characterization of a chromosomally encoded 2,4-dichlorophenoxyacetic acid/α- ketoglutarate dioxygenase from *Burkholderia* sp. strain RASC. Appl Environ Microbiol 62(7):2464–2469

Tamura K, Peterson D, Peterson N, Stecher G, Nei M, Kumar S (2011) MEGA5: molecular evolutionary genetics analysis using maximum likelihood, evolutionary distance, and maximum parsimony methods. Mol Biol Evol 28(10):2731–2739

Vedler E, Kõiv V, Heinaru A (2000) Analysis of the 2,4-dichlorophenoxyacetic acid- degradative plasmid pEST4011 of *Achromobacter xylosoxidans* subsp. *denitrificans* strain EST4002. Gene 255:281–288

Zakaria D, Lappin-Scott H, Burton S, Whitby C (2007) Bacterial diversity in soil enrichment cultures amended with 2-methyl-4-chlorophenoxy)propionic acid (mecoprop). Environ Microbiol 9:2575–2587

COR-AAD1-00003790
Bayer EX1008 (Part 7 of 9)

environmental microbiology

Environmental Microbiology (2011) 13(6), 1513–1523 doi:10.1111/j.1462-2920.2011.02456.x

(*R,S*)-dichlorprop herbicide in agricultural soil induces proliferation and expression of multiple dioxygenase-encoding genes in the indigenous microbial community

Mélanie M. Paulin,* Mette H. Nicolaisen and Jan Sørensen

Section of Genetics and Microbiology, Department of Agriculture and Ecology, Faculty of Life Sciences, University of Copenhagen, Thorvaldsensvej 40, 1871 Frederiksberg C, Denmark.

Summary

We investigated the effect of (*R,S*)-dichlorprop herbicide addition to soil microcosms on the degrading indigenous microbial community by targeting multiple α-ketoglutarate-dependent (α-KG) dioxygenase-encoding genes (*rdpA*, *sdpA* and *tfdA* group I) at both gene and transcript level. The soil microbial community responded with high growth of potential degraders as measured by the abundance of dioxygenase-encoding genes using quantitative real-time PCR (qPCR). *rdpA* DNA was not detectable in unamended soil but reached over 10^6 copies g^{-1} soil after amendment. *sdpA* and *tfdA* were both present prior to amendment at levels of ~5×10^4 and ~10^2 copies g^{-1} soil, respectively, and both reached over 10^6 copies g^{-1} soil. While expression of all three target genes was detected during two cycles of herbicide degradation, a time-shift occurred between maximum expression of each gene. Gene diversity by denaturing gradient gel electrophoresis (DGGE) uncovered a diversity of *sdpA* and *tfdA* genes at the DNA level while *rdpA* remained highly conserved. However, mRNA profiles indicated that all transcribed *tfdA* sequences were class III genes while *rdpA* transcripts shared 100% identity to *rdpA* of *Delftia acidovorans* MC1 and *sdpA* transcripts shared 100% identity to *sdpA* from *Sphingomonas herbicidovorans* MH. This is the first report to describe expression dynamics of multiple α-KG dioxygenase-encoding genes in the indigenous microbial community as related to degradation of a phenoxypropionate herbicide in soil.

Received 13 September, 2010; accepted 30 January, 2011. *For correspondence. E-mail mel_paulin@yahoo.ca; Tel. (+45) 3533 2627; Fax (+45) 3533 2606.

Introduction

Soil serves as a biological filter through which most precipitation must pass before reaching the groundwater; this function is critical in order to avoid contamination of the groundwater with xenobiotics. One group of pollutants are the phenoxy acid herbicides which are frequently detected in Danish groundwater reservoirs (GEUS, 2009) at levels above the EU limit of 0.1 μg l^{-1}. To understand the ability of the soil to serve as a filter, more knowledge is needed on the actual degradation of these compounds under *in situ* soil conditions.

Microbial degradation of phenoxy acid herbicides is initiated by etherolytic cleavage of the side-chain, catalysed by a range of α-ketoglutarate-dependent (α-KG) dioxygenases, and conversion of the herbicide into the corresponding phenol (Fukumori and Hausinger, 1993; Tett *et al.*, 1997; Saari *et al.*, 1999; Itoh *et al.*, 2002). Two novel α-KG dioxygenases able to initiate the degradation of chiral phenoxypropionate acid herbicides (*R,S*)-dichlorprop and (*R,S*)-mecoprop have recently been discovered and are encoded by the *rdpA* and *sdpA* genes (Müller *et al.*, 2004; Schleinitz *et al.*, 2004). Culture-dependent studies show that the RdpA enzyme uses the herbicidal (*R*)-enantiomer of these chiral compounds as a substrate while SdpA uses only the non-herbicidal (*S*)-enantiomer (Nickel *et al.*, 1997; Zipper *et al.*, 1998; Müller and Babel, 1999; Müller *et al.*, 2001; 2006). Presence and organization of these novel genes have only recently been described from three different strains isolated for their ability to degrade (*R,S*)-dichlorprop (Müller *et al.*, 2004; Schleinitz *et al.*, 2004).

The *tfdA* gene encodes another α-KG dioxygenase involved in initiating the degradation pathway of many phenoxyalkanoic acid (PAA) herbicides. Unlike the *rdpA* and *sdpA* genes, this gene has been extensively studied and found to be widespread and described in a number of bacterial genera (Kamagata *et al.*, 1997; McGowan *et al.*, 1998; Itoh *et al.*, 2002; 2004; Kitagawa *et al.*, 2002). As a general consensus, PAA herbicide degraders have been classified into three major groups based on their physiological and evolutionary characteristics (Kamagata *et al.*, 1997), with group 1 being further divided into three

© 2011 Society for Applied Microbiology and Blackwell Publishing Ltd

COR-AAD1-00003791

Bayer EX1008 (Part 7 of 9)

classes (McGowan *et al.*, 1998). Recently, class III *tfdA* genes have been linked to the biodegradation activity of PAA herbicides such as 2-methyl-4-chlorophenoxyacetic acid (MCPA) (Bælum *et al.*, 2006) and 2,4-dichlorophenoxyacetic acid (2,4-D) (Bælum *et al.*, 2008) and have also been found in soil enrichment subcultures degrading the phenoxypropionate herbicide (*R*)- and (*R,S*)-mecoprop (Zakaria *et al.*, 2007). Furthermore, the class III *tfdA* genes were the only ones to proliferate during degradation of (*R*)-mecoprop at different depths of a sandy loam soil (Rodríguez-Cruz *et al.*, 2010). A high abundance of group 2 and 3 *tfdA*-related genes in four different types of soil has recently been reported (Zaprasis *et al.*, 2009), but involvement of these genes during degradation of PAA in soil has yet to be demonstrated.

Despite extensive efforts dedicated to studying α-KG dioxygenase-encoding genes related to *tfdA* and the fact that (*R,S*)-dichlorprop mineralization in soil is well documented, *in situ* detection of *rdpA* and *sdpA* genes from indigenous degrader populations in soil is still sorely lacking, prompting the need for investigating their involvement in phenoxypropionate herbicide degradation. It is also unclear whether multiple α-KG dioxygenase-encoding genes can be simultaneously expressed during microbial degradation of PAA herbicides in soil, but the enantiomeric nature of phenoxypropionate herbicides makes it plausible. Some bacterial isolates are able to degrade racemic herbicide mixtures, others degrade only one enantiomeric form (Tett *et al.*, 1994; 1997; Saari *et al.*, 1999), and *in situ* observations of preferential enantiomeric degradation of (*R,S*)-dichlorprop in soil have been reported (Garrison *et al.*, 1996; Müller and Buser, 1997; Lewis *et al.*, 1999). These findings only increase the likelihood that multiple genes may be involved.

The present study aimed to better understand which functional genes are present in indigenous (*R,S*)-dichlorprop degrader soil communities and how they are regulated in response to *in situ* herbicide amendment. One attractive approach for studying microbial activity during biological processes in soil is to follow expression of specific functional genes by targeting mRNA transcripts (Nicolaisen *et al.*, 2008; Freitag and Prosser, 2009; Di *et al.*, 2010; Freitag *et al.*, 2010). This approach was used to target multiple α-KG dioxygenase-encoding genes: *rdpA*, *sdpA* and *tfdA* group I including class I, II and III. Presence and activity of the genes were followed by quantitative real-time PCR (qPCR) of DNA and mRNA while denaturing gradient gel electrophoresis (DGGE) and cloning were used to analyse the diversity of genes and transcripts extracted from agricultural soil samples amended twice with 20 mg kg^{-1} (*R,S*)-dichlorprop.

Results

*Mineralization of (*R,S*)-dichlorprop in agricultural soil*

Over the course of 102 days, approximately 40% of the first amendment of 20 mg kg^{-1} ^{14}C-(*R,S*)-dichlorprop was mineralized by the indigenous microbial community (Fig. 1A). The mineralization curve could be divided into three segments with a long initial linear phase indicative of slow mineralization for approximately the first 40 days,

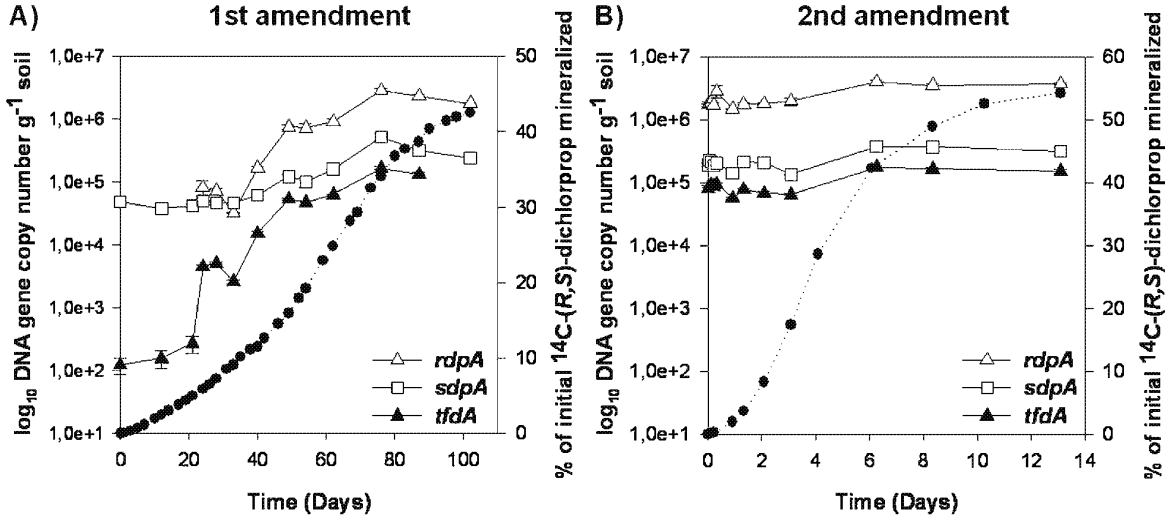


Fig. 1. Progress curves of *rdpA* (△), *sdpA* (□) and *tfdA* (▲) gene copy number and mineralization (●) data in soil spiked with (*R,S*)-dichlorprop. A first amendment of 20 mg kg^{-1} (*R,S*)-dichlorprop at 0 h (A) was followed by a similar second amendment after 102 days (B) of incubation when mineralization of the first amendment had reached a plateau phase.

COR-AAD1-00003792
Bayer EX1008 (Part 7 of 9)

followed by a steeper exponential phase between 40 and 80 days where maximum rates of mineralization were reached before ending in a plateau. A similar pattern of mineralization was observed for the second amendment of herbicide initiated at day 102 but with a considerably faster rate of degradation reaching maximum cumulative mineralization of 55% within only 13 days (Fig. 1B).

Abundance of rdpA, sdpA *and* tfdA *genes*

No *rdpA* genes were detected in the soil by qPCR prior to (*R,S*)-dichlorprop treatment. *sdpA* genes were present at approximately 5×10^4 copies g^{-1} soil and *tfdA* genes were detected but the low values at ~100–300 copies g^{-1} soil were outside the linear range of the standard curve.

Quantification of the three α-KG dioxygenase-encoding genes obtained by qPCR gave clear evidence that (*R,S*)-dichlorprop in the soil supported proliferation of bacteria harbouring *rdpA*, *sdpA* and *tfdA* genes. Addition of 20 mg kg^{-1} (*R,S*)-dichlorprop supported a dramatic increase in *rdpA* gene abundance from undetectable levels to 3×10^6 copies g^{-1} soil (Fig. 1A). In comparison with background levels found in the soil receiving no herbicide treatment, *sdpA* gene copies underwent a 10-fold increase from 5×10^4 to 5×10^5 copies g^{-1} soil while *tfdA* gene abundance rose from ~10^2 copies g^{-1} soil to a maximum of ~2×10^5 copies g^{-1} soil after 76 days of incubation. The second amendment of 20 mg kg^{-1} (*R,S*)-dichlorprop caused approximately a twofold increase for all three dioxygenase-encoding genes after 6 days of exposure but no significant growth was observed as in the initial herbicide treatment (Fig. 1B).

Expression of multiple α-KG dioxygenase-encoding genes

The microbial community actively transcribed all three genes during degradation of (*R,S*)-dichlorprop in soil. As measured by *rdpA* mRNA : DNA (transcript : gene ratio), expression was first detected at 40 days of incubation and rose quickly to reach and maintain a maximum level between 49 and 87 days before undergoing a decrease (Fig. 2A). *sdpA* expression was detected as early as 12 days after the initial treatment with (*R,S*)-dichlorprop and kept increasing until reaching a maximum after 54 days of incubation (Fig. 2B). While maximum expression of *rdpA*

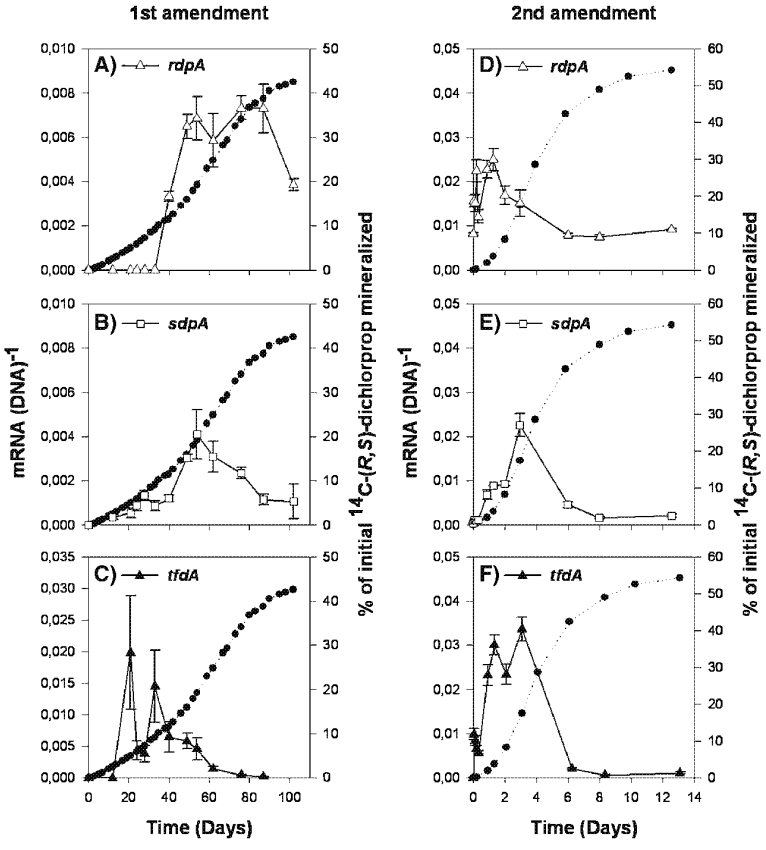


Fig. 2. Transcription dynamics of multiple α-KG dioxygenase genes represented as mRNA $(DNA)^{-1}$ ratios in soil spiked with (*R,S*)-dichlorprop. A first amendment of 20 mg kg^{-1} (*R,S*)-dichlorprop at 0 h was followed by a similar second amendment after 102 days of incubation when mineralization of the first amendment had reached a plateau phase. A time-course quantification of mRNA transcripts was made by RT-qPCR for *rdpA* (△), *sdpA* (□) and *tfdA* (▲) genes during mineralization (●). Error bars represent standard error of mean from a minimum of three replicates obtained from the RT-qPCR reactions. As a reference, mineralization curves (also shown in Fig. 1) are included.

COR-AAD1-00003793
Bayer EX1008 (Part 7 of 9)

and *sdpA* genes coincided with the steepest part of the curve when the rate of (*R,S*)-dichlorprop was at its highest, maximal expression of *tfdA* was detected earlier during the mostly linear part of mineralization (Fig. 2C). Hence, *tfdA* expression was first detected at day 21 but at a high transcript : gene ratio; transcription activity subsequently underwent a decrease before again increasing at 33 days and finally decreasing to barely detectable levels by 76–87 days. Comparison of expression between the three genes showed that despite having the highest abundance of DNA in soil, maximal expression of *rdpA* was approximately threefold lower than that of *tfdA*. The *sdpA* gene had levels of DNA similar to the *tfdA* gene but exhibited transcript : gene ratios fivefold and twofold lower than *tfdA* and *rdpA* respectively. No transcription activity was detected from microcosms receiving no herbicide amendment (data not shown).

While a marked time-shift in expression occurred between the enantiomer-specific genes and the *tfdA* genes during the first exposure to (*R,S*)-dichlorprop, a second amendment at day 102 induced a much faster response from all three genes. Contrary to the two other genes, *rdpA* was still being expressed right before the second amendment of 20 mg kg^{-1} (*R,S*)-dichlorprop and reached maximum expression after 32 h (Fig. 2D). Expression of both *sdpA* and *tfdA* started at barely detectable levels but quickly rose to a maximum at 74 h incubation for *sdpA* and between 22 h and 74 h for *tfdA* (Fig. 2E and F). Thereafter, expression of all three genes decreased and returned to levels observed before the second amendment of herbicide. Interestingly, the level of expression was higher for all three genes following the second amendment compared with the first amendment. Especially the *sdpA* expression increased significantly with a fivefold increase compared with the first amendment.

Dynamics and diversity of rdpA, sdpA *and* tfdA *genes and transcripts*

As DGGE-based analysis of *rdpA* and *sdpA* genes has not previously been reported, reference and environmental samples were chosen to determine if GC-clamps should be added to the reverse or forward primers for PCR amplification of each gene by running amplicons on the DGGE gel. No clear band separation and very cloudy profiles were obtained when the GC-clamp was added to the reverse rdpA and sdpA primers (Fig. 3). Alternatively, when the GC-clamp was added to the forward primers, this combination proved capable of distinguishing between *rdpA* and *sdpA* from reference samples *Delftia acidovorans* MC1 and *Sphingomonas herbicidovorans* MH as reflected by a shift in migration position of the bands (Fig. 3). Finally, while acceptable for cloned *tfdA* sequences, the forward GC-clamp primer yielded a faint and cloudy profile of bands from the environmental samples even though PCR amplicons were strong on agarose gels (Fig. 3). Here, the reverse GC-clamp primer yielded the stronger band intensities and was able to differentiate the *tfdA* sequences throughout the course of the soil microcosm experiment (Fig. 4C); it was however

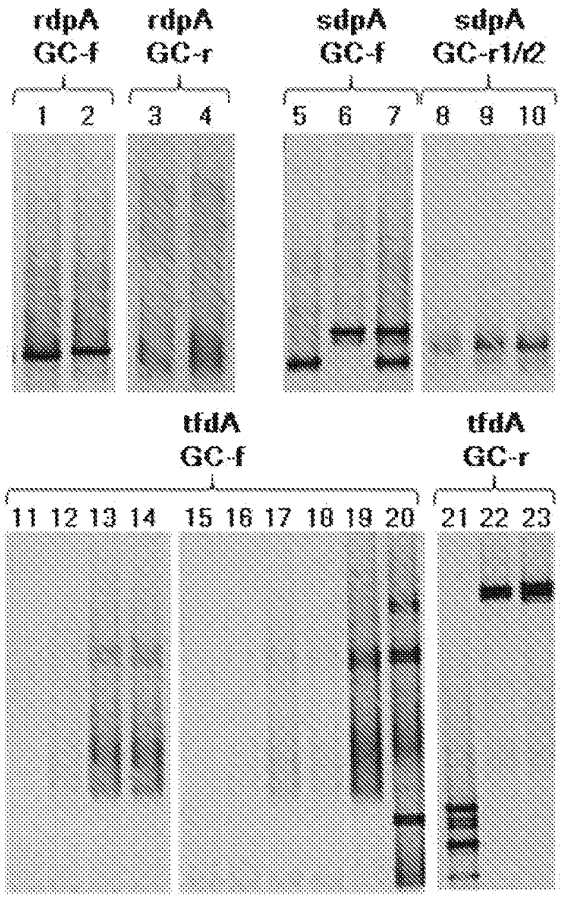


Fig. 3. DGGE optimization of GC-clamp primer combinations for *sdpA*, *rdpA* and *tfdA* genes. For *rdpA*, lanes 1 and 2 show amplifications with forward GC-clamp of DNA extracted from *D. acidovorans* MC1 and *S. herbicidovorans* MH respectively. Lanes 3 and 4 show results using a reverse GC-clamp. For *sdpA*, lanes 5–7 show amplifications with a forward GC-clamp of DNA extracted from reference strains *D. acidovorans* MC1, *S. herbicidovorans* MH and an equal mixture of the two strains respectively. Lanes 8–10 represent the same samples but amplified with a reverse GC-clamp. For *tfdA*, lanes 11–19 represent PCR-DGGE amplification of indigenous nucleic acids from the soil microcosms: (11–14) DNA of days 12, 33, 102 (first amendment) and 32 h (second amendment); (15–19) mRNA days 12, 21, 33 and 87 (first amendment) and 32 h (second amendment). Finally, lane 20 represents a mixture of the three *tfdA* clones from class I (lower band), class II (upper band) and class III (middle band) amplified with the forward GC-clamp while products in lanes 21–23 were amplified with the reverse GC-clamp and represent class I, class II and class III *tfdA* respectively.

COR-AAD1-00003794
Bayer EX1008 (Part 7 of 9)

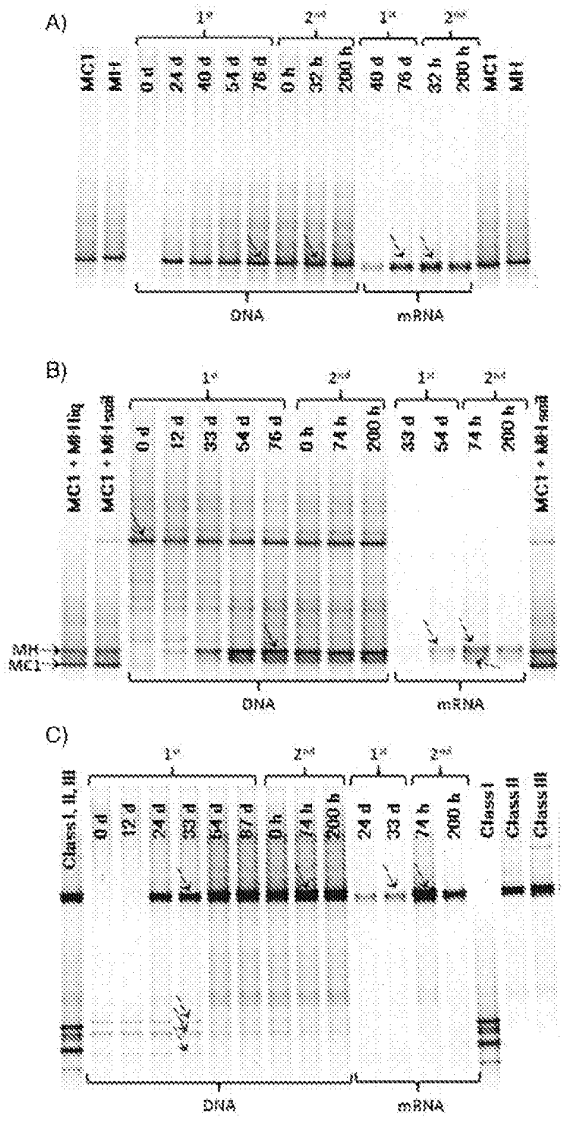


Fig. 4. DGGE profiles of PCR-amplified (A) *rdpA*, (B) *sdpA* and (C) *tfdA* DNA and mRNA fragments from the indigenous microbial community in agricultural soil amended twice with 20 mg kg^{-1} (*R,S*)-dichlorprop. Arrows indicate bands that were excised and sequenced. DGGE markers for *rdpA* and *sdpA* sequences were PCR-amplified from both *D. acidovorans* MC1 (MC1) and *S. herbicidovorans* MH (MH), using either total DNA extracted from pure cultures (liq) or total DNA extracted from soil samples inoculated with 5×10^7 cells g^{-1} soil for either strain (soil). Markers were generated from inoculated soil samples if not indicated otherwise. Markers for the *tfdA* gene were PCR-amplified from clones of class I, class II and class III *tfdA* genes. The number of incubation days (d) is indicated for samples collected after the first amendment of herbicide while the number of hours (h) is indicated for samples collected after the second amendment.

difficult to obtain separation of bands between cloned class II and class III *tfdA* sequences which migrated at the same position. Nonetheless, the reverse GC-clamp primer was chosen to conduct *tfdA* DGGE profiles because of the poor results obtained using the forward GC-clamp on environmental soil samples.

Several DNA and mRNA samples representing both amendments were chosen to assess the diversity of soil indigenous genes encoding α-KG dioxygenase enzymes by DGGE and melting curve analysis. Melting curve analysis following qPCR amplification indicated a single melting peak temperature (T_m) for *rdpA* and *sdpA*, respectively, and this T_m was the same for both DNA and mRNA sequences. While a single peak ($T_m = 89°C$) was observed in the qPCR melting curve of *tfdA* DNA amplicons from day 0 and day 12, products from day 21 generated a double peak with T_m of 89°C and 86°C indicating the presence of more than one product. From day 24 and forward, only the product with a T_m of 86°C was detected as was the case for all positive amplifications of mRNA samples, pointing to a shift in the population structure over time.

The *rdpA* DGGE profile produced a distinct single band appearing in all experimental samples in response to herbicide amendment; this band migrated at approximately the same position as the reference *rdpA* fragment from *D. acidovorans* MC1 amplified from inoculated soil DNA extracts. DGGE analysis of mRNA gave evidence that genes detected in the DNA analysis were the same as the ones being transcribed. This was confirmed by cloning and sequencing of *rdpA* DNA and mRNA cut from DGGE gels from day 76 of the first herbicide amendment and 32 h after the second amendment. BLASTN query of the GenBank database showed that all *rdpA* sequences recovered shared 100% identity to *rdpA* from *D. acidovorans* MC1 as well as a few *Burkholderia* sp. isolates recovered from agricultural soils and 99% identity to *S. herbicidovorans* MH.

In contrast to the *rdpA* community profile, both *sdpA* and *tfdA* profiles reflected a transition of the community in response to the (*R,S*)-dichlorprop amendment (Fig. 4B and C). Figure 4B shows the effect of adding (*R,S*)-dichlorprop on the indigenous microbial community harbouring *sdpA* genes. One dominant band present in the upper part of the gel prior to and following addition of the herbicide had a migration position identical to a band observed in the reference *sdpA* sequences prepared from spiking soil samples with known degraders. This band was exclusively associated with soil DNA extracts and was absent from pure culture DNA extracts. Sequencing and comparison to the GenBank database revealed that clones of this band showed closest match (≥ 90% identity) to uncultured bacterial clones of *sdpA* previously described in the same soil receiving no herbicide

COR-AAD1-00003795
Bayer EX1008 (Part 7 of 9)

treatment (Paulin *et al.*, 2010). However, these sequences were not detected in the mRNA samples and were presumably not actively involved in (*R,S*)-dichlorprop degradation. Another band appearing in response to (*R,S*)-dichlorprop grew stronger in intensity over time and seemed to be closely related to the *sdpA* sequence from *S. herbicidovorans* MH. This band was the only one to be detected both in DNA and in mRNA samples, thus representing actively transcribed genes during herbicide degradation. Sequencing of multiple clones confirmed 100% identity to the *sdpA* sequence of *S. herbicidovorans* MH which was also the case when sequencing clones obtained from the lower mRNA band at 74 h (Fig. 4B). Thus, DGGE and sequencing was able to uncover the diversity of the *sdpA* genes which was not possible by simple analysis of the qPCR melting curve.

From day 0, the DNA-based *tfdA* profile showed multiple bands of low intensity in the lower part of the gel presumably corresponding to *tfdA* class I sequences based on the positions in the gel and the melting curve profiles obtained by qPCR. However, cloning and sequencing of these bands from the day 33 sample as indicated in Fig. 4C revealed that the 215 bp gene fragments shared strongest similarity to a taurine catabolism dioxygenase Taud/TidA from *Variovorax paradoxus* S110 (80% identity). Translation into a 71-mer peptide fragment and BLASTP search of the database gave identical results of 80% identity to *V. paradoxus* S110. As first noticed in day 21 of the qPCR melting profiles, a shift in the nature of *tfdA* gene products was observed over time represented by the appearance of a strong upper band in the DGGE gel that aligned with the class II/class III *tfdA* reference genes. The community profile of transcribed genes showed a single band in all mRNA samples corresponding to the same intense upper band seen in the DNA profile. Multiple clones from these upper bands (Fig. 4C) were sequenced and all shared identities of at least 99% with other class III *tfdA* sequences.

Discussion

Genes encoding upper pathway enzymes are of particular importance for degradation of xenobiotics since microorganisms often broaden their substrate utilization spectrum by diversifying these genes (Khomenkov *et al.*, 2008). In this study, we report a change in the functional structure of the indigenous soil microbial community in response to degradation of (*R,S*)-dichlorprop which was reflected by an increase in the abundance of all three genes. While increased abundance of the *tfdA* genes has previously been reported in relation to 2,4-D, MCPA and (*R*)-mecoprop degradation (Bælum *et al.*, 2008; Rodríguez-Cruz *et al.*, 2010), this is the first time that the *rdpA* and *sdpA* genes are quantitatively linked to the degradation of any PAA herbicide in soil. Proliferation of these genes indicate that organisms harbouring one or more genes are able to grow using (*R,S*)-dichlorprop as a carbon substrate.

The RdpA and SdpA α-KG-dependent dioxygenases have narrow substrate specificity and are generally specific to the respective (*R*)- and (*S*)-enantiomers of dichlorprop and mecoprop (Westendorf *et al.*, 2003; Müller *et al.*, 2006). The substrate specificity of different types of TfdA towards the chiral herbicides remains unclear and the only founded reports of TfdA specificity are towards the (*S*)-enantiomer (Saari *et al.*, 1999). A recent look at genes potentially involved in mecoprop-degrading soil enrichment cultures revealed the presence of *sdpA*, class III *tfdA* and *cadA* genes in cultures grown on (*R,S*)-mecoprop while *rdpA* was the only gene present when cultures were grown solely on the (*R*)-enantiomer (Zakaria *et al.*, 2007). In contrast, we found *rdpA* genes to be highly abundant in soil mineralizing (*R,S*)-dichlorprop in parallel to a high abundance of *sdpA* and *tfdA*. *rdpA* and *sdpA* genes are most likely involved in degradation of (*R*)-dichlorprop and (*S*)-dichlorprop, respectively, but even though the *tfdA* genes have previously been detected during herbicide degradation, direct evidence proving that the TfdA enzyme is capable of using the (*R*)-enantiomer as a substrate has been lacking. Studies using separate (*R*)- and (*S*)-enantiomers of these chiral herbicides are thus needed to make further conclusions regarding substrate specificity.

Variations in mRNA transcript levels are the first signs of cellular response to changing environmental conditions, and hence are a suitable target for understanding environmental factors controlling initiation of herbicide degradation. Transcription dynamics showed strong evidence for involvement of *rdpA*, *sdpA* and *tfdA* genes since all three were induced upon exposure to (*R,S*)-dichlorprop. Interestingly, the degrader community responded with earlier maximal expression of *tfdA* genes in comparison with the *rdpA* and *sdpA* genes whose maximum expression levels were detected later and at lower levels. This later expression may in part account for the relatively slower mineralization of (*R,S*)-dichlorprop that was observed in comparison with its phenoxyacetate counterparts 2,4-D and MCPA (Bælum *et al.*, 2008). The faster response of *tfdA* expression in comparison with *rdpA* and *sdpA* could be a reflection of differences in the genetic organization of bacteria carrying these genes. In *Cupriavidus necator* JMP134, the *tfd* genes encoding metabolism of phenoxyacetates are found within a well-organized and tightly regulated operon structure (Leveau *et al.*, 1999; Pérez-Pantoja *et al.*, 2008). Although studies suggest that (*R,S*)-dichlorprop and (*R,S*)-mecoprop are metabolized through a similar modified *ortho*-cleavage pathway, evidence also points towards a recent acquisi-

COR-AAD1-00003796
Bayer EX1008 (Part 7 of 9)

tion of the α-KG dioxygenase-encoding genes *rdpA* and *sdpA* (Müller *et al.*, 2001; 2004; Benndorf *et al.*, 2004) and genes encoding the metabolic pathway for degradation are reported to be scattered over the genome in *S. herbicidovorans* MH with no tight regulation of gene expression (Müller *et al.*, 2004). Without isolation of host organisms, it remains impossible to determine if genetic organization was the source of this later gene activation and differences in the growth rates of host organism could be an alternative explanation. Growth rates in bacteria are known to vary substantially and growth rate-dependent factors such as the abundance of RNA polymerases and ribosomes are known to affect gene expression (Bremer and Dennis, 1996). In some bacteria, transcription rates of constitutively expressed genes increase during faster cell growth (Liang *et al.*, 1998) while regulated genes also subject to growth-related effects may additionally be influenced by the growth dependence of their regulators (Klumpp *et al.*, 2009). Based only on partial gene sequences, it is difficult to determine if host organisms of *rdpA* and *sdpA* genes had a slower growth rate, but the *tfdA* genes that were expressed in this study were identical to class III *tfdA* genes which are normally associated with fast-growing *Proteobacteria* of the β and γ subdivisions (McGowan *et al.*, 1998). The hypothesis that differential growth rates may have influenced the dynamics of expression between the three α-KG-encoding genes is reinforced by the observation that once a certain biomass of active (*R,S*)-dichlorprop degraders was achieved, a second amendment of herbicide produced a quick response with all three genes being upregulated within a few hours and without a noticeable lag. This was also accompanied by a higher mineralization rate as is typical of acclimatized herbicide-degrading populations where little growth is required to actively metabolize the compound (Arbeli and Fuentes, 2007).

Interestingly, *rdpA* and *sdpA* were still transcribed following the initial degradation event which is in agreement with our previous findings where low levels of constitutive gene expression were detected from *D. acidovorans* MC1 both prior to and after (*R,S*)-dichlorprop degradation but were further induced when re-exposed to the herbicide (Paulin *et al.*, 2010). Previous pure culture studies have also hinted towards constitutive expression of both genes through measurement of catalytic enzyme activity (Müller *et al.*, 2001; 2004). In contrast, the degrader population harbouring *tfdA* virtually shut down expression of the gene following the first degradation cycle, or at least to a level below our detection limit. This fits well with the suggested tight regulation of *tfdA* in *C. necator* JMP134 where the pathway intermediate 2,4-dichloromuconate acts as inducer of gene expression followed by a drop in the level of *tfdA* mRNA transcripts once the TfdD enzyme converting 2,4-dichloromuconate is present at high levels in the cell (Leveau *et al.*, 1999; Pérez-Pantoja *et al.*, 2008). Other studies of *tfdA* expression during degradation of 2,4-D and MCPA in soil also observed similar drops in expression but were still able to detect very low levels of transcripts once mineralization had ceased (Bælum *et al.*, 2008).

Several time points were chosen to follow the succession of the functional diversity of α-KG dioxygenase-encoding genes involved in degradation of (*R,S*)-dichlorprop by analysis of DNA and mRNA (converted to cDNA) DGGE profiles. Although DGGE may have limitations with regards to effectiveness of band separation, we believe that it can be a very useful tool particularly when studying diversity of functional genes which have an overall lower diversity in contrast to the very abundant and diverse 16S rDNA sequences which still suffer from limited resolution by DGGE analysis (Kisand and Wikner, 2003). The results presented here stress the importance of including simple optimization procedures that are often overlooked but can have a strong impact on the level of resolution obtained from environmental samples in comparison with pure culture samples (Fig. 3). Only one type of *rdpA* sequence identical to *D. acidovorans* MC1 *rdpA* clearly dominated the degrader population and mRNA profiles confirmed that indigenous soil bacteria expressing this gene were involved in degradation. Since very few studies have targeted *rdpA* genes, sequence information to date is limited and comes from just a few cultured strains including *S. herbicidovorans* MH (Müller *et al.*, 2004), *D. acidovorans* MC1 and *Rhodoferax* sp. P230 (Schleinitz *et al.*, 2004), and a *Burkholderia* sp. isolate (Zakaria *et al.*, 2007). However, they all indicate that *rdpA* is a well-conserved gene. Our findings are in agreement to this and are the first to demonstrate the importance of *rdpA* gene sequences during *in situ* degradation of phenoxypropionate herbicides in soil. In contrast, the natural *sdpA* gene pool has recently been reported as highly diverse in soils receiving no herbicides (Paulin *et al.*, 2010). While this diversity was reflected in the DNA DGGE profiles herein, one band in particular was dominant and consistently detected throughout the course of the experiment regardless of herbicide presence. Sequencing revealed this band to share over 90% identity to the *sdpA* clones retrieved previously (Paulin *et al.*, 2010), but analysis of mRNA DGGE profiles indicated that they were not involved in the degradation of (*R,S*)-dichlorprop. Rather, transcription was attributed to only one type of *sdpA* sequence that shared 100% identity to *S. herbicidovorans* MH and also corresponded to the DNA band that was exclusively associated to soil actively degrading (*R,S*)-dichlorprop. A similar occurrence has been reported previously where *tfdA* genes detected in soils prior to enrichment with PAA herbicides were not always the ones being expressed after enrichment (Kamagata *et al.*,

COR-AAD1-00003797
Bayer EX1008 (Part 7 of 9)

1997; Itoh *et al.*, 2000; Bælum *et al.*, 2006; Zaprasis *et al.*, 2009). Likewise, *tfdA* sequences initially detected here were not responsible for subsequent degradation after amendment. Instead, class III *tfdA* sequences proliferated and were the only ones expressed in response to both amendments of (*R,S*)-dichlorprop. Similar findings also highlighted the involvement of class III *tfdA* genes in response to degradation of (*R*)-mecoprop in soil (Rodriguez-Cruz *et al.*, 2010) and to (*R,S*)- and (*R*)-mecoprop degradation in soil enrichment cultures (Zakaria *et al.*, 2007). Furthermore, degradation of phenoxyacetic herbicides 2,4-D and MCPA both induced expression of class III genes in soil although class I genes were also expressed at a low level during 2,4-D degradation (Bælum *et al.*, 2008). The presence of α-KG dioxygenase-encoding genes in soil that are not activated by PAA herbicides might be explained by the presence of natural substrates in soil (Hogan *et al.*, 1997; Dunning Hotopp and Hausinger, 2001). Although multiple types of *sdpA*, *tfdA* and *tfdA*-like genes can be detected in soil, only very specific types of *sdpA*, *tfdA* (class III) and *rdpA* sequences seem to be of particular importance for degradation of various PAA herbicides.

The findings reported highlight the importance of multiple α-KG dioxygenase-encoding genes during *in situ* microbial degradation of a chiral phenoxypropionate herbicide. Although class III *tfdA* genes were clearly induced in response to (*R,S*)-dichlorprop degradation, parallel growth of degraders expressing the *rdpA* and *sdpA* genes indicate that the TfdA enzyme alone may not be sufficient to carry out the initial cleavage of both forms of the herbicide. Furthermore, gene diversity analysis clearly demonstrated that expressed α-KG dioxygenase-encoding genes related to (*R,S*)-dichlorprop degradation were highly conserved. Future research should take into consideration the contribution of catabolic dioxygenase-encoding genes other than *tfdA* and would certainly benefit from screening soils from different geographical regions to help determine if *rdpA* and *sdpA* genes are conserved and widespread in the environment.

Experimental procedures

Soil and herbicide application

Organic agricultural top soil classified as Typic Argiudoll (USDA Soil Taxonomy) with 19% clay, 18% silt, 62% sand, 1.2% carbon and pH 7.2 was obtained from Sjællands Odde, Zeeland, Denmark and stored at 4°C until use. Soil was passed through a 4 mm sieve prior to microcosm set-up and a subsample was baked at 105°C for 24 h to determine soil water content. Stock solutions of (*R,S*)-[Ring-U-^{14}C]-dichlorprop (specific activity 3.56 MBq mg^{-1}; radiochemical purity 97.41%; IZOTOP, Budapest, Hungary) were prepared in methanol (LabScan, Dublin, Ireland) whereas stock solutions of unlabelled (*R,S*)-dichlorprop were prepared in DMSO (VWR, Fontenay-sous-Bois, France). Water content of 30 g of soil was adjusted to 18% wet weight with sterile MilliQ water taking into account the subsequent addition of (*R,S*)-dichlorprop solution. Soil was then mixed mechanically in a plastic bag and transferred into a glass flask. (*R,S*)-dichlorprop was applied to the soil microcosm as a top amendment in a fixed volume solution of 1.1 ml prepared with 0.1 M Na_2HPO_4 (pH 8.45) at a final concentration of 20 mg kg^{-1} soil unlabelled (*R,S*)-dichlorprop and trace amounts of labelled (*R,S*)-dichlorprop (28 000 dpm g^{-1} soil). Mineralization was measured at appropriate time intervals as described previously (Nicolaisen *et al.*, 2008) by sampling the evolved $^{14}CO_2$ trapped in 1 ml of 1 M NaOH placed in a glass vial on top of the soil. The bottle was closed airtight and incubated in the dark at 20°C. Microcosms containing no herbicide and only 1.1 ml of 0.1 M Na_2HPO_4 were prepared as controls. After mineralization of the first amendment of (*R,S*)-dichlorprop had reached a plateau phase, a second amendment of 20 mg kg^{-1} soil was added in the same manner. Throughout both cycles of (*R,S*)-dichlorprop mineralization, 0.5 g of soil samples were taken at regular time intervals over 115 days and immediately frozen in liquid nitrogen and stored at −70°C until nucleic acid extraction. Mineralization data were corrected for removal of the 0.5 g of soil samples.

Nucleic acid extraction and cDNA synthesis

DNA and RNA were co-extracted from soil samples as previously described (Nicolaisen *et al.*, 2008). To assist nucleic acid extraction, 1 µl of glycogen (Roche, Basel, Switzerland) was added during precipitation with PEG 6000. Final extracts were resuspended in 50 µl of DNase- and RNase-free DEPC-treated water (Fluka; Sigma-Aldrich, Saint Louis, MO) and stored at −70°C. Following the extraction procedure, contaminating DNA was eliminated by treating 8 µl aliquots of each nucleic acid sample with 2 units of RQ1 RNase-free DNase 1 (Promega, Madison, WI) according to the manufacturer's protocol. cDNA was synthesized immediately after by using 4 µl of subsamples of each DNase-treated extract as a template for reverse transcription with the Omniscript reverse transcription kit (Qiagen, Crawly, UK). DNase-treated control reactions were prepared in parallel for each RNA sample without addition of the reverse transcriptase (RT) to ensure the absence of DNA contamination. RT reactions were prepared with 400 ng of random hexamer primers (Promega), 4 U of SUPER RNase inhibitor (Ambion, Austin, TX) and reagents provided in the kit for a final volume of 20 µl. Incubation conditions were followed as recommended by the manufacturer. Resulting cDNA samples were stored at −20°C until use for qPCR.

qPCR of the rdpA, sdpA *and* tfdA *genes*

DNA standard curves were prepared as previously described (Nicolaisen *et al.*, 2008; Paulin *et al.*, 2010) using known quantities of *D. acidovorans* MC1 for *rdpA* and *sdpA* genes and *C. necator* AEO106 (pRO101) that carries the class I *tfdA* gene. Ten-fold dilutions of washed cells were added in 100 µl volumes to Bio101 Lysing Matrix E tubes (MP Biomedicals,

COR-AAD1-00003798
Bayer EX1008 (Part 7 of 9)

Solon, OH) containing 500 mg of soil. Dilutions ranging from 10^8 to 10^3 cells g^{-1} soil were prepared for both *D. acidovorans* MC1 and *C. necator* AEO106 (pRO101) cells. Nucleic acids were then extracted as described above and 1/10 dilutions of DNA were used as templates for qPCR. The target genes in both organisms are single copy in the cells (Schleinitz *et al.*, 2004; Pérez-Pantoja *et al.*, 2008). Consequently, DNA standard curves were prepared from DNA/RNA extractions of cell dilutions and used to quantify both DNA and mRNA from *rdpA*, *sdpA* or *tfdA* with mRNA being quantified as DNA gene equivalents and presented as ratios of mRNA normalized to DNA as previously described (Nicolaisen *et al.*, 2008). Acceptable ranges of linearity were determined and used for each standard curve and corresponding gene: 10^6 to 10^3 copies g^{-1} soil for *rdpA*; 10^6 to 10^5 copies g^{-1} soil for *sdpA*; and 10^8 to 10^3 copies g^{-1} soil for *tfdA*. Presence of background levels of *sdpA* in soil caused the standard curve to have a non-linear relationship for dilutions ranging from 10^4 to 10^2 copies g^{-1} soil; extrapolation of the linear segment of the standard curve (10^8 to 10^5 copies g^{-1} soil) for quantification of lower copy numbers of *sdpA* was thus necessary.

Quantitative real-time PCR quantification of all samples collected during the soil microcosm experiment was performed on the DNA, cDNA and DNase-treated RNA fractions using the Brilliant SYBR Green qPCR Master Mix (Stratagene, La Jolla, CA) and the primer sets rdpA_f/rdpA_r and sdpA_f/sdpA_r1/sdpA_r2 for the *rdpA* and *sdpA* genes, respectively, using the conditions previously described (Paulin *et al.*, 2010). The tfdA** primer set was used with the same cycling conditions previously described (Bælum *et al.*, 2006), but using 0.4 μM of each primer and the same reaction mixture as for the *rdpA* and *sdpA* genes. All qPCR analyses were set up in triplicate including the standard curves. Amplification efficiency (E) was calculated from the slope of the standard curve using the equation $E = 10^{(-1/\text{slope})} - 1$.

Dioxygenase gene profiling by DGGE

For DGGE analysis, DNA and corresponding cDNA from soil extracts were selected to represent time points at the early, intermediate and late phases of mineralization over two cycles of (*R,S*)-dichlorprop amendment. PCR was performed with the same primers and cycling conditions as indicated above. Addition of a GC-clamp (5′-CGCCCGCCGCGCGCG GCGGGCGGGGCGGGGGCACGGGGG-3′) was tested on both forward and reverse primers for each target gene to determine which yielded a better band separation on the DGGE gel. Optimal results were obtained when the GC-clamp was added on the forward primer for *rdpA* and *sdpA* genes and the GC-clamp was added to the reverse primer for the *tfdA* gene. DGGE markers were prepared from DNA extracted from pure cultures of *D. acidovorans* MC1 and *S. herbicidovorans* MH harbouring the *rdpA* and *sdpA* genes as well as from soils inoculated with these strains. For *tfdA*, PCR products from cloned genes representing class I, II and III *tfdA* were used as markers for comparison within DGGE profiles obtained from the soil microcosms amended with (*R,S*)-dichlorprop. PCR reactions for DGGE analyses were prepared as indicated above with the Brilliant II SYBR Green qPCR Master Mix (Stratagene, La Jolla, CA) using 5 μl of 1/10 dilution DNA or cDNA template and DNase/RNase-free water (Sigma-Aldrich) in a final volume of 50 μl. DGGE analysis was performed using the D-Code system apparatus (Bio-Rad, Hercules, CA). PCR products were loaded on 8% polyacrylamide gels with a 40–80% (w/v) denaturing gradient of urea and formamide. Electrophoresis was carried out at 60°C in 1× TAE buffer and run initially at 200 V for 30 min, followed by 130 V for 4 h 30 min. Gels were then stained for 20 min with SYBR gold nucleic acid stain (Molecular Probes, Eugene, OR) in 200 ml of 1× TAE and visualized and photographed using UV transillumination. Bands of interest were stabbed with a sterile pipette tip, rinsed in 25 μl of DNase/RNase-free water (Sigma-Aldrich) and kept overnight at 4°C to elute the DNA. Two-microlitre aliquots were used as a template for PCR re-amplification using the same conditions as indicated above for first PCR amplifications. PCR re-amplification products were subjected to separation on DGGE along with original PCR products to ensure specificity of the excised band before cloning.

Cloning, sequencing and analysis of rdpA, sdpA *and* tfdA *genes*

Re-amplification products of interest were ligated into the pCR®2.1-TOPO® plasmid vector and transformed into TOP10 chemically competent *Escherichia coli* cells following the manufacturer's protocol (Invitrogen, Carlsbad, CA). A minimum of 10 clones for each cloning reaction were randomly selected and screened by PCR-DGGE to ensure appropriate product insertion by comparison with the original environmental sample. A few clones carrying the correct inserts were selected for each cloning reaction and sent for sequencing (Uppsala Genome Center, Uppsala, Sweden) using the M13 universal primers (Invitrogen). Resulting nucleic acid sequences were submitted to a BLASTN query of the GenBank database in order to find most homologous sequences. The nucleotide sequences determined in this study have been deposited in the GenBank database under the Accession No. HQ009355 to HQ009398.

Acknowledgements

This study was supported by the Center for Environmental and Agricultural Microbiology (CREAM) funded by the Villum Kann Rasmussen Foundation. We would like to thank D. Ganzhorn for excellent technical assistance during sample processing.

References

Arbeli, Z., and Fuentes, C.L. (2007) Accelerated biodegradation of pesticides: an overview of the phenomenon, its basis and possible solutions; and a discussion on the tropical dimension. *Crop Prot* **26:** 1733–1746.

Bælum, J., Henriksen, T., Hansen, H.C.B., and Jacobsen, C.S. (2006) Degradation of 4-chloro-2-methylphenoxyacetic acid in top- and subsoil is quantitatively linked to the class III *tfdA* gene. *Appl Environ Microbiol* **72:** 1476–1486.

Bælum, J., Nicolaisen, M.H., Holben, W.E., Strobel, B.W., Sørensen, J., and Jacobsen, C.S. (2008) Direct analysis of

COR-AAD1-00003799
Bayer EX1008 (Part 7 of 9)

tfdA gene expression by indigenous bacteria in phenoxy acid amended agricultural soil. *ISME J* **2:** 677–687.

Benndorf, D., Davidson, I., and Babel, W. (2004) Regulation of catabolic enzymes during long-term exposure of *Delftia acidovorans* MC1 to chlorophenoxy herbicides. *Microbiology* **150:** 1005–1014.

Bremer, H., and Dennis, P.P. (1996) Modulation of chemical composition and other parameters of the cell by growth rate. In Escherichia coli *and* Salmonella. Neidhardt, F.C. (ed.). Washington, DC, USA: ASM Press, pp. 1553–1569.

Di, H.J., Cameron, K.C., Shen, J.P., Winefield, C.S., O'Callaghan, M., Bowatte, S., and He, J.Z. (2010) Ammonia-oxidizing bacteria and archaea grow under contrasting soil nitrogen conditions. *FEMS Microbiol Ecol* **72:** 386–394.

Dunning Hotopp, J.C., and Hausinger, R.P. (2001) Alternative substrates of 2,4-dichlorophenoxyacetate/alpha-ketoglutarate dioxygenase. *J Mol Catal B-Enzym* **15:** 155–162.

Freitag, T.E., and Prosser, J.I. (2009) Correlation of methane production and functional gene transcriptional activity in a peat soil. *Appl Environ Microbiol* **75:** 6679–6687.

Freitag, T.E., Toet, S., Ineson, P., and Prosser, J.I. (2010) Links between methane flux and transcriptional activities of methanogens and methane oxidizers in a blanket peat bog. *FEMS Microbiol Ecol* **73:** 157–165.

Fukumori, F., and Hausinger, R.P. (1993) Purification and characterization of 2,4-dichlorophenoxyacetate/alpha- ketoglutarate dioxygenase. *J Biol Chem* **268:** 24311–24317.

Garrison, A.W., Schmitt, P., Martens, D., and Kettrup, A. (1996) Enantiomeric selectivity in the environmental degradation of dichlorprop as determined by high-performance capillary electrophoresis. *Environ Sci Technol* **30:** 2449–2455.

GEUS (2009) Grundvandsovervågning 2009. In *Grundvand, Status og udvikling 1989–2008*. Thorling, L. (ed.). [WWW document]. URL http://www.grundvandsovervaagning.dk (in Danish).

Hogan, D.A., Buckley, D.H., Nakatsu, C.H., Schmidt, T.M., and Hausinger, R.P. (1997) Distribution of the *tfdA* gene in soil bacteria that do not degrade 2,4-dichlorophenoxyacetic acid (2,4-D). *Microb Ecol* **34:** 90–96.

Itoh, K., Kanda, R., Momoda, Y., Sumita, Y., Kamagata, Y., Suyama, K., and Yamamoto, H. (2000) Presence of 2,4-D-catabolizing bacteria in a Japanese arable soil that belong to BANA (*Bradyrhizobium–Agromonas–Nitrobacter–Afipia*) cluster in α-*Proteobacteria*. *Microb Environ* **15:** 113–117.

Itoh, K., Kanda, R., Sumita, Y., Kim, H., Kamagata, Y., Suyama, K., *et al.* (2002) *tfdA*-like genes in 2,4-dichlorophenoxyacetic acid-degrading bacteria belonging to the *Bradyrhizobium–Agromonas–Nitrobacter–Afipia* cluster in α-*Proteobacteria*. *Appl Environ Microbiol* **68:** 3449–3454.

Itoh, K., Tashiro, Y., Uobe, K., Kamagata, Y., Suyama, K., and Yamamoto, H. (2004) Root nodule *Bradyrhizobium* spp. harbor *tfdAa* and *cadA*, homologous with genes encoding 2,4-dichlorophenoxyacetic acid-degrading proteins. *Appl Environ Microbiol* **70:** 2110–2118.

Kamagata, Y., Fulthorpe, R.R., Tamura, K., Takami, H., Forney, L.J., and Tiedje, J.M. (1997) Pristine environments harbor a new group of oligotrophic 2,4- dichlorophenoxyacetic acid-degrading bacteria. *Appl Environ Microbiol* **63:** 2266–2272.

Khomenkov, V., Shevelev, A., Zhukov, V., Zagustina, N., Bezborodov, A., and Popov, V. (2008) Organization of metabolic pathways and molecular-genetic mechanisms of xenobiotic degradation in microorganisms: a review. *Appl Biochem Microbiol* **44:** 117–135.

Kisand, V., and Wikner, J. (2003) Limited resolution of 16S rDNA DGGE caused by melting properties and closely related DNA sequences. *J Microbiol Methods* **54:** 183–191.

Kitagawa, W., Takami, S., Miyauchi, K., Masai, E., Kamagata, Y., Tiedje, J.M., and Fukuda, M. (2002) Novel 2,4-dichlorophenoxyacetic acid degradation genes from oligotrophic *Bradyrhizobium* sp. strain HW13 isolated from a pristine environment. *J Bacteriol* **184:** 509–518.

Klumpp, S., Zhang, Z., and Hwa, T. (2009) Growth rate-dependent global effects on gene expression in bacteria. *Cell* **139:** 1366–1375.

Leveau, J.H.J., Konig, F., Fuchslin, H., Werlen, C., and van der Meer, J.R. (1999) Dynamics of multigene expression during catabolic adaptation of *Ralstonia eutropha* JMP134 (pJP4) to the herbicide 2,4-dichlorophenoxyacetate. *Mol Microbiol* **33:** 396–406.

Lewis, D.L., Garrison, A.W., Wommack, K.E., Whittemore, A., Steudler, P., and Melillo, J. (1999) Influence of environmental changes on degradation of chiral pollutants in soils. *Nature* **401:** 898–901.

Liang, S.T., Dennis, P.P., and Bremer, H. (1998) Expression of *lacZ* from the promoter of the *Escherichia coli* sp. operon cloned into vectors carrying the W205 *trp–lac* fusion. *J Bacteriol* **180:** 6090–6100.

McGowan, C., Fulthorpe, R., Wright, A., and Tiedje, J.M. (1998) Evidence for interspecies gene transfer in the evolution of 2,4-dichlorophenoxyacetic acid degraders. *Appl Environ Microbiol* **64:** 4089–4092.

Müller, M.D., and Buser, H.R. (1997) Conversion reactions of various phenoxyalkanoic acid herbicides in soil. 1. Enantiomerization and enantioselective degradation of the chiral 2-phenoxypropionic acid herbicides. *Environ Sci Technol* **31:** 1953–1959.

Müller, R.H., and Babel, W. (1999) Separation of two dichlorprop/alpha-keloglutarate dioxygenases with enantiospecific properties from *Comamonas acidovorans* MC1. *Acta Biotechnol* **19:** 349–355.

Müller, R.H., Kleinsteuber, S., and Babel, W. (2001) Physiological and genetic characteristics of two bacterial strains utilizing phenoxypropionate and phenoxyacetate herbicides. *Microbiol Res* **156:** 121–131.

Müller, T.A., Byrde, S.A., Werlen, C., van der Meer, J.R., and Kohler, H.P.E. (2004) Genetic analysis of phenoxyalkanoic acid degradation in *Sphingomonas herbicidovorans* MH. *Appl Environ Microbiol* **70:** 6066–6075.

Müller, T.A., Fleischmann, T., van der Meer, J.R., and Kohler, H.P.E. (2006) Purification and characterization of two enantioselective α-ketoglutarate-dependent dioxygenases, RdpA and SdpA, from *Sphingomonas herbicidovorans* MH. *Appl Environ Microbiol* **72:** 4853–4861.

COR-AAD1-00003800
Bayer EX1008 (Part 7 of 9)

Nickel, K., Suter, M.J.F., and Kohler, H.P.E. (1997) Involvement of two α-ketoglutarate-dependent dioxygenases in enantioselective degradation of (R)- and (S)-mecoprop by *Sphingomonas herbicidovorans* MH. *J Bacteriol* **179:** 6674–6679.

Nicolaisen, M.H., Bælum, J., Jacobsen, C.S., and Sørensen, J. (2008) Transcription dynamics of the functional *tfdA* gene during MCPA herbicide degradation by *Cupriavidus necator* AEO106 (pRO101) in agricultural soil. *Environ Microbiol* **10:** 571–579.

Paulin, M.M., Nicolaisen, M.H., and Sørensen, J. (2010) Abundance and expression of enantioselective *rdpA* and *sdpA* dioxygenase genes during degradation of the racemic herbicide (R,S)-2-(2,4-dichlorophenoxy) propionate in soil. *Appl Environ Microbiol* **76:** 2873–2883.

Pérez-Pantoja, D., De la Iglesia, R., Pieper, D.H., and González, B. (2008) Metabolic reconstruction of aromatic compounds degradation from the genome of the amazing pollutant-degrading bacterium *Cupriavidus necator* JMP134. *FEMS Microbiol Rev* **32:** 736–794.

Rodríguez-Cruz, M.S., Bælum, J., Shaw, L.J., Sørensen, S.R., Shi, S., Aspray, T., *et al.* (2010) Biodegradation of the herbicide mecoprop-p with soil depth and its relationship with class III *tfdA* genes. *Soil Biol Biochem* **42:** 32–39.

Saari, R.E., Hogan, D.A., and Hausinger, R.P. (1999) Stereospecific degradation of the phenoxypropionate herbicide dichlorprop. *J Mol Catal B* **6:** 421–428.

Schleinitz, K.M., Kleinsteuber, S., Vallaeys, T., and Babel, W. (2004) Localization and characterization of two novel genes encoding stereospecific dioxygenases catalyzing 2(2,4-dichlorophenoxy)propionate cleavage in *Delftia acidovorans* MC1. *Appl Environ Microbiol* **70:** 5357–5365.

Tett, V.A., Willetts, A.J., and Lappin-Scott, H.M. (1994) Enantioselective degradation of the herbicide mecoprop [2-(2-methyl-4-chlorophenoxy)propionic acid] by mixed and pure bacterial cultures. *FEMS Microbiol Ecol* **14:** 191–199.

Tett, V.A., Willetts, A.J., and Lappin-Scott, H.M. (1997) Biodegradation of the chlorophenoxy herbicide (R)-(+)-mecoprop by *Alcaligenes denitrificans*. *Biodegradation* **8:** 43–52.

Westendorf, A., Müller, R.H., and Babel, W. (2003) Purification and characterisation of the enantiospecific dioxygenases from *Delftia acidovorans* MC1 initiating the degradation of phenoxypropionate and phenoxyacetate herbicides. *Acta Biotechnol* **23:** 3–17.

Zakaria, D., Lappin-Scott, H., Burton, S., and Whitby, C. (2007) Bacterial diversity in soil enrichment cultures amended with 2 (2-methyl-4-chlorophenoxy)propionic acid (mecoprop). *Environ Microbiol* **9:** 2575–2587.

Zaprasis, A., Liu, Y.J., Liu, S.J., Drake, H.L., and Horn, M.A. (2009) Novel and diverse *tfdA*-like genes encoding putative phenoxyalkanoic acid herbicide degrading dioxygenases are abundant in soil. *Appl Environ Microbiol* **12:** 2411–2425.

Zipper, C., Bunk, M., Zehnder, A.J.B., and Kohler, H.P.E. (1998) Enantioselective uptake and degradation of the chiral herbicide dichlorprop [(RS)-2-(2,4-dichlorophenoxy) propanoic acid] by *Sphingomonas herbicidovorans* MH. *J Bacteriol* **180:** 3368–3374.

COR-AAD1-00003801
Bayer EX1008 (Part 7 of 9)

Supplementary Table and Figures for "Structural Basis for the Enantiospecificities of *R*- and *S*-Specific Phenoxypropionate/α-Ketoglutarate Dioxygenases" by Tina A. Müller, Maria I. Zavodszky, Michael Feig, Leslie A. Kuhn, and Robert P. Hausinger

Table S1. *Sequences of mutagenesis primers used to create altered* rdpA- *and* sdpA *genes*

original gene	plasmid	mutant	primer sequence [a]
rdpA	pMec151	V80A	5'-CCC CGT CGA TCC CGC ACC CCT GCT CAA GA-3'
	pMec152	Q93A	5'-AGG GTA TCC AGA GGT GGC AAT GAT CCG CCG CGA AG-3'
	pMec153	Y221A	5'-TGT ACG TGA ACC AGG TCG CAT GCC AGC GCA TCG AG-3'
	pMec154	R285A	5'-CCG CTA CCT GAC GGC CAC CAC GGT CGG TG-3'
	pMec155	I106G/G107I	5'- GAA AGC GGG CGT GTG GGC ATA GAT GAC TGG CAC A-3'
	pMec156	I106G/107N	5'- GAA AGC GGG CGT GTG GGC AAT GAT GAC TGG CAC A -3'
	pMec157	L83A	5'-CCC GTG CCC CTG GCG AAG AGC ATC GAA G-3'
	pMec158	I106A	5'-GCG GGC GTG TGG CAG GTG ATG ACT G-3'
	pMec160	F171A	5'-CCA CGC GTG TGG CGG GCT CGC TCT AC-3'
	pMec161	F171Q	5'-CCA CGC GTG TGC AAG GCT CGC TCT AC-3'
sdpA	pMec191	E69A	5'-GGC CAC TCG AGT TCG CAA TGG CCG CGA TCA G-3'
	pMec192	H208A	5'-TGC TGA TCG GCC GCG CAG CCC ACG CCA TTC C-3'
	pMec193	H272A	5'-GAA GCG CAT CAT GTG GGC AAG CCG CAT CGC CGG-3'
	pMec194	R274A	5'-CAT CAT GTG GCA CAG CGC AAT CGC CGG CGA CCC-3'
	pMec195	G97N/N98G	5'- CAT GAT GAA GAT CCT GAA GAA CGG CAT GGG CTG GCA T -3'
	pMec196	G97I/N98G	5'- CAT GAT GAA GAT CCT GAA GAT CGG CAT GGG CTG GCA T -3'
	pMec197	Q162F	5'-CTG CAT TAC AGC TTT TCG AAG CTC GGC-3'
	pMec198	R207A	5'-CTG CTG ATC GGC GCC CAC GCC CAC G-3'
	pMec199	R207V	5'-CTG CTG ATC GGC GTG CAC GCC CAC GCC-3'

[a] The reverse primer used for the creation of all mutants was the complement of the forward primer.

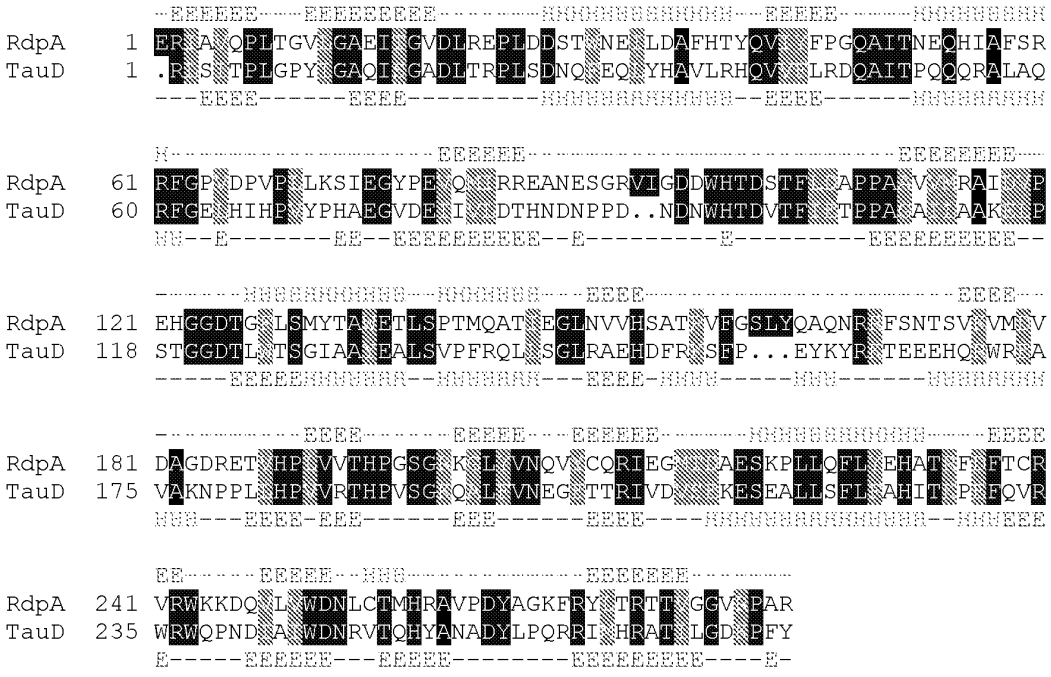
Figure S1. Amino acid sequences of RdpA (A) and SdpA (B) aligned to TauD. The predicted secondary structural elements for the query proteins are given above the sequences, and the secondary structure found in the TauD crystal structure is shown below. The letter H indicates helical structure and E stands for β sheet. Identical residues are depicted in white against a black background and similar residues are highlighted by gray boxes.

Figure S2. Homology models of RdpA (A) and SdpA (B). Ribbon diagrams (colored blue at the *N*-termini to red at the *C*-termini) are shown for the RdpA and SdpA monomers, in each case revealing the typical jellyroll motif of αKG dependent dioxygenases. Also shown as spheres are the bound iron atoms, and the side chains of the Fe^{II} binding ligands along with αKG are depicted in stick form.

Figure S3. Representative purification of variant forms of SdpA as analyzed by SDS-PAGE. Proteins were resolved by using 12% polyacrylamide gels and stained with Coomassie brillant blue. For each sample derived from BL21(DE3) cells containing the indicated plasmid, lane 1 contains cell extracts and lane 2 contains the proteins eluted from Ni-NTA resin. The final lane contains molecular weight markers (indicated in kDa).

Figure S1

A


RdpA 1 ERSAQPLTGVGAEIGVDLREPLDDSTGNELDAFHTYQVGFPGQAITNEQHIAFSR
TauD 1 .RSSTPLGPYGAQIGADLTRPLSDNQGEQLYHAVLRHQVGLRDQAITPQQQRALAQ
RdpA 61 RFGPGDPVPGLKSIEGYPEGQGRREANESGRVIGDDWHTDSTFGAPPAGVGRAIGP
TauD 60 RFGEGHIHPGYPHAEGVDEGIGDTHNDNPPD..NDNWHTDVTFGTPPAGAGAAKGP
RdpA 121 EHGGDTGGLSMYTAGETLSPTMQATGEGLNVVHSATGVEGSLYQAQNRGFSNTSVGVMGV
TauD 118 STGGDTLGTSGIAAGEALSVPFRQLGSGLRAEHDFRGSFP...EYKYRGTEEEHQGWRGA
RdpA 181 DAGDRETGHPGVVTHPGSGGKGLGVNQVGQRIEGGGAESKPLLQFLGEHATGFGFTCR
TauD 175 VAKNPPLGHPGVRTHPVSGGQGLGVNEGGTTRIVDGGKESEALLSFLGAHITGPGFQVR
RdpA 241 VRWKKDQGLGWDNLCTMHRAVPDYAGKFRYGTRTTGGVGPAR
TauD 235 WRWQPNDGAGWDNRVTQHYANADYLPQRRIGHRATGLGDGPFY

B

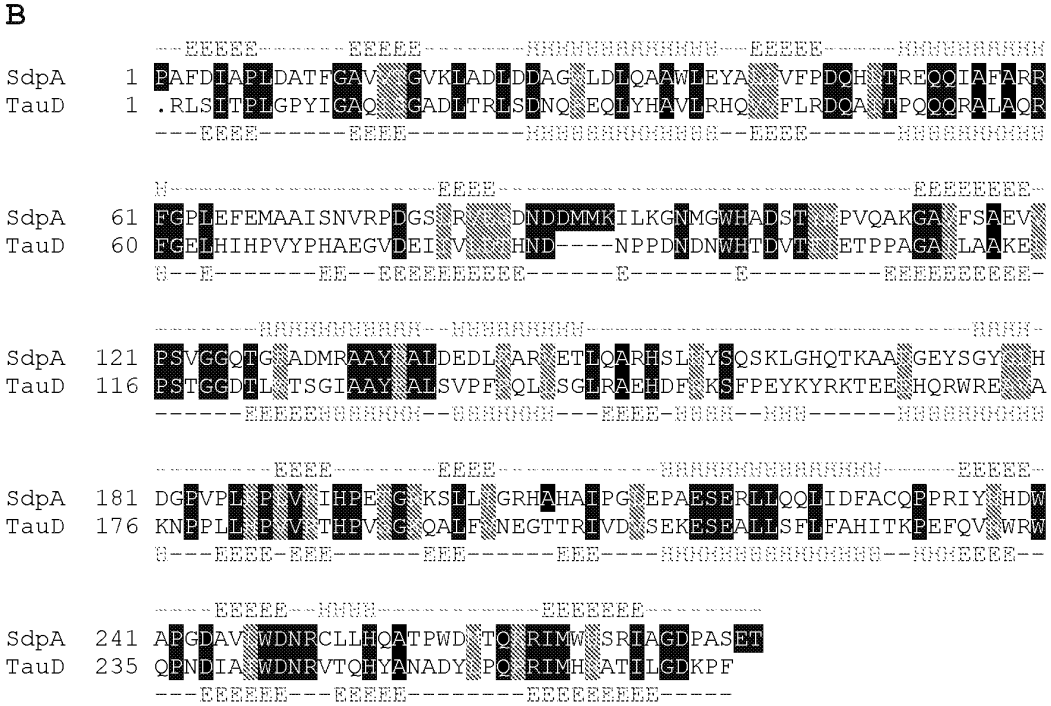

SdpA 1 PAFDIAPLDATFGAVGGVKLADLDDAGGLDLQAAWLEYAGVFPDQHGTREQQIAFARR
TauD 1 .RLSITPLGPYIGAQGGADLTRLSDNQGEQLYHAVLRHQGFLRDQAITPQQQRALAQR
SdpA 61 FGPLEFEMAAISNVRPDGSGRGGDNDDMMKILKGNMGWHADSTGPVQAKGAGFSAEVG
TauD 60 FGELHIHPVYPHAEGVDEIGVGGHND----NPPDNDNWHTDVTGETPPAGAGLAAKEG
SdpA 121 PSVGGQTGGADMRAAYGALDEDLGARGETLQARHSLGYSQSKLGHQTKAAGGEYSGYGGH
TauD 116 PSTGGDTLGTSGIAAYGALSVPFGQLGSGLRAEHDFGKSFPEYKYRKTEEGHQRWREGGA
SdpA 181 DGPVPLGPGVGIHPEGGKSLLGRHAHAIPGGEPAESERLLQQLIDFACQPPRIYGHDWG
TauD 176 KNPPLLGPGVGTHPVGGQALFGNEGTTRIVDGSEKESEALLSFLFAHITKPEFQVGWRW
SdpA 241 APGDAVGWDNRCLLHQATPWDGTQGRIMWGSRIAGDPASET
TauD 235 QPNDIAGWDNRVTQHYANADYGPQGRIMHGATILGDKPF

Figure S2

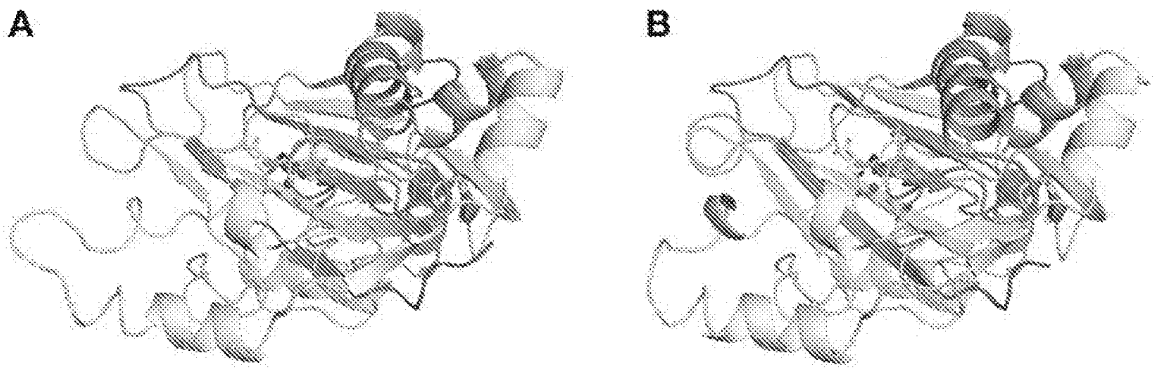
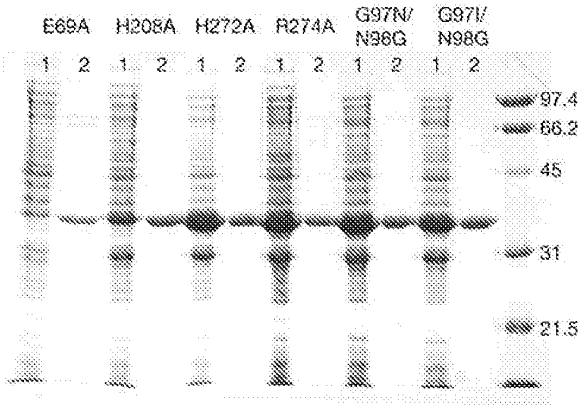


Figure S3


E69A
H208A
H272A
R274A
G97N/ N98G
G97I/ N98G
1 2 1 2 1 2 1 2 1 2 1 2
97.4
66.2
45
31
21.5

Supplementary Information

Molecular Basis for Enantioselective Herbicide Degradation Imparted by Aryloxyalkanoate Dioxygenases (AADs) in Transgenic Plants

Jonathan R. Chekan[1,2,#], Chayanid Ongpipattanakul[1,#], Terry R. Wright[3], Bo Zhang[4], J. Martin Bollinger, Jr.[4,5], Lauren J. Rajakovich[4], Carsten Krebs[4,5], Robert M. Cicchillo[3],and Satish K. Nair[1,2,6,*]

[1]Department of Biochemistry, [2]Carl R. Woese Institute for Genomic Biology, and [6]Center for Biophysics and Quantitative Biology; University of Illinois, 600 S Mathews Ave, Urbana, IL, 61801, USA
and
[3]Corteva Agriscience™, Agriculture Division of DowDuPont, 9330 Zionsville Road, Indianapolis, IN, 46268, USA
and
[4]Department of Chemistry and [5]Department of Biochemistry and Molecular Biology, The Pennsylvania State University, University Park, Pennsylvania 16802

These authors contributed equally to this work
Authors to whom correspondence should be addressed: snair@illinois.edu

COR-AAD1-00003807
Bayer EX1008 (Part 7 of 9)

TABLE OF CONTENTS

Supplementary Materials and Methods.....3

Supplementary Figure 1 – Genomic Context of TfdA from *Cupriavidua necator* JMP134..... .7

Supplementary Figure 2 – Phylogenetic tree of putative AAD sequences..... 8

Supplementary Figure 3 – Genomic Context of AAD-1 and AAD-12.....9

Supplementary Figure 4 – Analytical Gel Filtration and SDS-PAGE analysis of AADs.....10

Supplementary Figure 5 – Normalized activity of AAD-2 against a panel of substrates 11

Supplementary Figure 6 - Kinetic curves for the AAD-2 reaction using various substrates.....12

Supplementary Figure 7 – Activity of AAD-2 against MCPA 13

Supplementary Figure 8 – Kinetic-difference spectra from the stopped-flow absorption experiment....14

Supplementary Figure 9 – Mössbauer spectra of a sample of the AAD-1 reaction.....15

Supplementary Figure 10 – Sequence alignment of select AADs.....16

Supplementary Table 1 – List of putative AADs identified by EFI-EST.....17

Supplementary Table 2 – Kinetic parameters of AAD-1 and AAD-2 across a panel of substrates.....19

Supplementary Table 3 – List of primers used in this study.....20

Supplementary Table 4 – Data collection and refinement statistics..... 21

Supplementary References.....22

COR-AAD1-00003808
Bayer EX1008 (Part 7 of 9)

Supplementary Materials and Methods

General Procedures, Chemicals, and Reagents

All chemical reagents were purchased from Sigma-Aldrich unless otherwise noted. All of the material used for protein production and purification were purchased from GE Healthcare. *Escherichia coli* DH5α and BL21(DE3)Rosetta (Invitrogen) strains were used for plasmid maintenance and protein overexpression respectively unless otherwise noted.

Preparation of AAD-1 for Crystallographic Studies

Lyophilized AAD-1 supplied by Corteva Agriscience was resuspended in a buffer composed of 100 mM KCl and 20 mM HEPES free acid (pH 7.5) and further purified by size exclusion chromatography using a Superdex S75-16/60 column (GE Healthcare Life Sciences) equilibrated with the same buffer. Pure fractions were collected and concentrated to 50-60 mg/mL before storage in liquid nitrogen.

Cloning, Expression and Purification of AAD-2

The *aad2* gene from *Bradyrhizobium diazoefficiens* USDA 110 cloned into a pET28-a vector using the primer listed in **Supplementary Table S2**, and the resultant plasmid was transformed into *E. coli* containing the Rosetta plasmid for subsequent expression. AAD-2 was produced by growing the cells in shaking flask of LB media at a temperature of 37 °C. When the cells reached an $O.D._{600}$ of 0.6, the cells were cooled on ice for 15 minutes. Following the addition of 0.5 mM IPTG, the cells were placed in an 18 °C shaking incubator for 18 hours. The cells were then harvested by centrifugation and resuspended in a buffer composed of 500 mM NaCl, 20 mM Tris base (pH 8.0), and 10% glycerol. Resuspended cells were lysed by sonication and the lysate was centrifuged at 14,000 rpm to remove cell debris. The cleared cell lysate was loaded onto a HisTrap column, which was subsequently washed with 1 M NaCl, 30 mM imidazole, and 20 mM Tris base (pH 8.0). Polyhistidine tagged AAD-2 was eluted using a linear gradient beginning with 1 M NaCl, 20 mM Tris base (pH 8.0), and 30 mM imidazole and ending with 250 mM imidazole. Pure fractions, as judged by SDS-PAGE, were combined and treated with thrombin (final ratio of 1:100 (w/w)) for 18 hours at 4 °C to cleave the N-terminal tag. Tag-free AAD-2 was concentrated and loaded onto a size exclusion column (Superdex S75 16/60) pre-equilibrated with containing 100 mM KCl and 20 mM HEPES free acid (pH 7.5). Pure fractions were collected and concentrated to 25 mg/mL before storage in liquid nitrogen.

AAD-1 Activity under Conditions of Stopped-Flow and Freeze-Quench Experiments.

The stopped-flow absorption and freeze-quenched Mössbauer experiments were carried out essentially as previously described (1). The stopped-flow experiments were carried out at 5 °C on an Applied

COR-AAD1-00003809
Bayer EX1008 (Part 7 of 9)

Photophysics (Leatherhead, U.K.) SX20 instrument housed in a Labmaster MBraun glovebox. The instrument was configured for single mixing with an optical path length of 1 cm and detection with a photodiode-array (PDA). In the experiments shown in Figure 3A, an air-saturated buffer solution (50 mM sodium MOPS, pH 7.5, 10% glycerol) was mixed with an equal volume of an anoxic solution containing 1.1 mM AAD-1, 1.0 mM Fe(II), 10 mM αKG and either no primary substrate, 9 mM 2,4,-D, or 9 mM d_2-2,4-D. Owing to the complexity of the kinetic traces, no attempt was made to fit the data globally according to a necessarily elaborate kinetic model. Rather, traces were fit as the sum of exponentials to provide estimates for the observed rate constants characterizing the multiple phases of the reactions with and without the 2,4-D primary substrate (or its deuterium-containing isotopologue). In the freeze-quench Mössbauer experiment shown in Figure 3B, the reactant complex contained 2.2 mM AAD-1, 2.0 mM $^{57}Fe^{2+}$, 10 mM αKG, and 9.0 mM d_2-2,4D. It was mixed at 5 °C with an equal volume of O_2-saturated buffer (the same buffer used in the stopped-flow experiments), and the reaction was quenched by rapid freezing after 0.09 s. A second sample was quenched at a reaction time of 0.28 s to verify the transient nature of the new species detected in the 0.09-s sample. Mössbauer spectra were recorded on a constant acceleration Mössbauer spectrometer from Seeco (Edina, MN) equipped with a Janis SVT-400 variable temperature cryostat. Isomer shifts are reported with respect to the centroid of the spectrum of α-iron metal at room temperature. Simulations of Mössbauer spectra were carried out with the program WMOSS (Seeco, Edina, MN).

Determination of Substrate Scope and Kinetic Parameters

To determine the substrate scope for AAD-2, we used a coupled continuous assay monitoring the decrease in absorbance of NADH at 340nm using reactions in a 96-well microplate format. Reactions contained a total volume of 150 µL, with the following composition: 20 mM MOPS (pH 7.0), 200 µM $FeSO_4 \cdot 7H_20$, 200 µM L-ascorbic acid, 10µM AAD-2, 3 mM of each respective substrate, 14 units of lactate dehydrogenase (Roche), and 400 µM NADH. Assays were initiated by the addition of α-ketoglutarate to a final concentration of 1 mM. Plates were read using an Epoch Microplate Spectrophotometer (BioTek®) and monitored using the Gen5 software (BioTek®). Reactions were carried out in triplicate. Relative V_{max} over a linear range was determined for each substrate, and then the data was normalized against the highest relative V_{max}. Prism5 (GraphPad) was used to visualize the data.

To obtain kinetic parameters for AAD-2, an end point assay monitoring the emergence of a red quinone dye at 510 nm was utilized. Reactions contained 10 µM AAD-2, the appropriate volume of each serially diluted substrate, in the following buffer: 20 mM MOPS (pH 7.0), 200 µM $FeSO_4 \cdot 7H_20$, 200 µM L-ascorbic acid. Reactions were initiated in the same manner as aforementioned. All reactions were carried

COR-AAD1-00003810
Bayer EX1008 (Part 7 of 9)

out under ambient conditions: the system may have not necessarily been saturated in O_2. After the fifteen minutes, reactions were quenched with the addition of 10 μL of 100 mM EDTA (pH 8.0). To develop each reaction for absorbance readings at 510 nm, 15 μL of pH 10 buffer (3.09 g boric acid, 3.73 g KCl, 44 mL of 1N KOH), 0.2% 4-aminoantipyrine, and 0.8% potassium ferricyanide was added to each well. The resultant color was allowed to develop for three minutes before absorbance readings were performed. Additional kinetic parameters for AAD-1 were obtained using the same experimental procedures as for AAD-2, except that only 2 μM of enzyme was used. Reactions were carried out in triplicate; Prism5 (GraphPad) was used to analyze and visualize the data.

Crystallization of AAD-1 and AAD-2

Preliminary crystals of AAD-1 in complex with Mn^{2+}, αKG, and (*R*)-dichlorprop were obtained using a sparse matrix screen. Diffraction quality crystals were grown using hanging drop vapor diffusion with 8 mg/mL AAD-1 pre-incubated with 5 mM (*R*)-dichlorprop, 5 mM αKG, and 5 mM $MnCl_2$. The protein mixture was added to mother liquor containing 25% PEG 3350, 0.3 M Li_2SO_4, and 0.1 M bicine (pH 9.0) in a 1:1 ratio at 4 °C. Crystals of AAD-1 in complex with (*R*)-cyhalofop or (*R*)-diclofop were obtained in a similar manner. Diffraction quality crystals of AAD-1 (10-15 mg/mL) in complex with (*R*)-dichlorprop (5 mM), and vanadyl sulfate (1 mM) were obtained by seeding using the same conditions described above. Addition of succinate in the drop impeded crystallization, and complexes were obtained by soaking crystals of AAD-1/vanadyl/(*R*)-dichlorprop in crystallization media supplemented with 5 mM succinate. Crystals of AAD-2 in complex with Mn^{2+} and NOG were first observed using a sparse matrix screen and refined using the hanging drop method. Briefly, AAD-2 (8-12 mg/mL), was incubated with (*S*)-dichlorprop, Mn^{2+}, and NOG (each at 2 mM) for 20 minutes and then mixed with a solution containing 22-28% PEG 4000, 0.07 M $LiSO_4$, and 0.1 M MES (pH 6.0) and equilibrated against the same solution. Crystals of all samples were briefly soaked in mother liquor supplemented with either 15% glycerol (AAD-1) or 15% ethylene glycol (AAD-2) immediately prior to vitrification by direct immersion into liquid nitrogen.

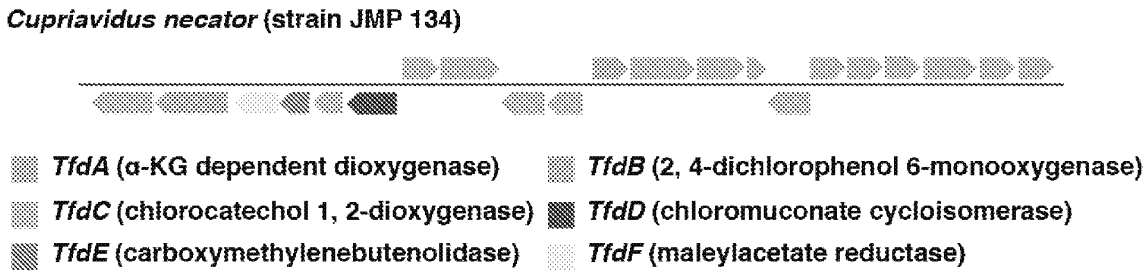
Bioinformatics

The sequence divergence of known AAD members limited identification of other AADs based solely on sequence similarities with select members of PF20668 (TauD) superfamily. Thus, the sequences of TfdA, AAD-1, and AAD-12 were each used to generate Sequence Similarity Networks (SSNs) (2) based on individual BLAST search (1000 sequences each). Gene Neighborhood Networks (GNNs) (3), using a gene window of 15 genes upstream and downstream of each sequence node, were then constructed for each SSN output. Each graphical GNN was then examined for presence for the following PFAMs:

COR-AAD1-00003811
Bayer EX1008 (Part 7 of 9)

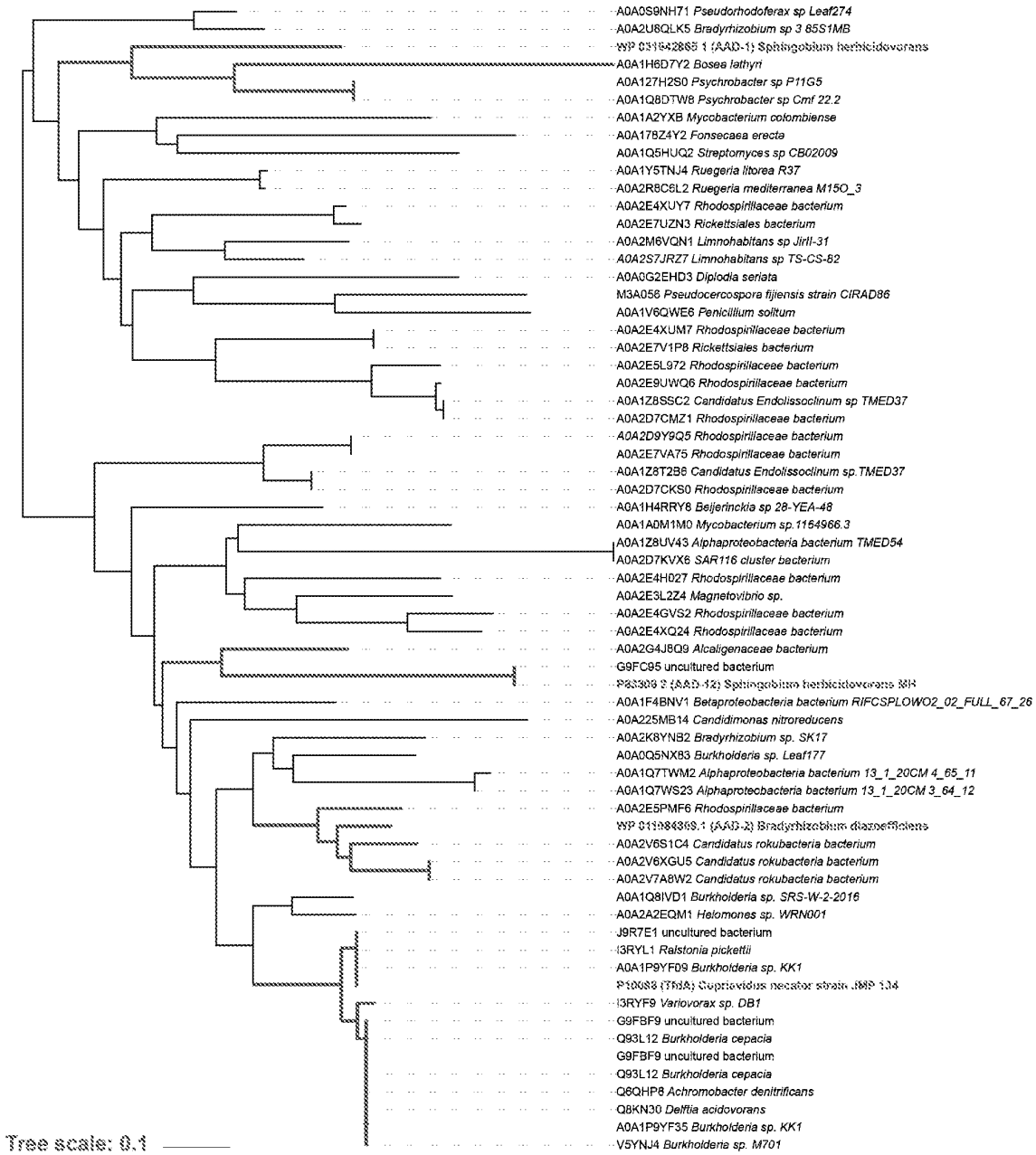
PF01494 (TfdB-like monooxygenases), or PF00775 fused to PF04444 (TfdC-like 1, 2 catechol dioxygenases). Clusters that contain mis-annotated PF01494, and PF00775 and PF04444 were included. Clusters that contained PF00775 fused to PF12391 (protocatechuate 3, 4-dioxygenases) were also included. The final SSN was generated using these sequences, along with sequences of TfdA, AAD-1, AAD-12, and 238 randomly selected members of the TauD superfamily (1/170 of all annotated TauD family members in the Uniref90 database). A representative node network at sequence similarity of 100% was used in order to filter through duplicate entries that were obtained during the initial query. Singletons (i.e. nodes with no other similar sequences) were omitted from Fig. 2 to concisely visualize the data.

COR-AAD1-00003812
Bayer EX1008 (Part 7 of 9)



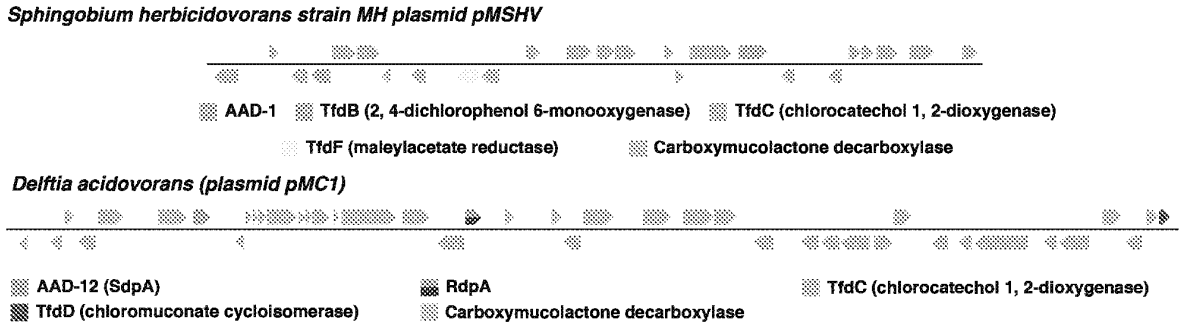
Supplementary Figure 1. Genomic context of *Tfd*A-F from the conjugative plasmid pJP4. Plasmid pJP4 was initially detected in the host bacterium *Cupriavidus necator* JMP134 (4). Genes of importance to degradation pathways are highlighted and annotated according to the legend below. Proteins that are non-essential to the pathway have been colored grey.

COR-AAD1-00003813
Bayer EX1008 (Part 7 of 9)



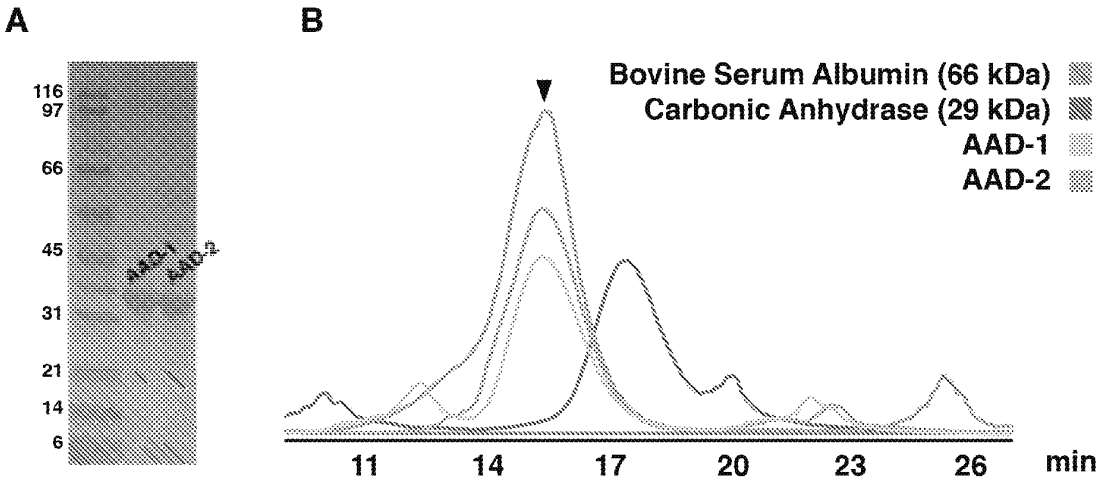
Supplementary Figure 2. Phylogenetic tree of putative AAD sequences. Sequences manually culled and used for the SNN/GNN analysis are shown in black, while sequences in blue are AADs of interest that have been biochemically characterized. Clades that contain the AADs of interest are also noted in blue.

COR-AAD1-00003814
Bayer EX1008 (Part 7 of 9)



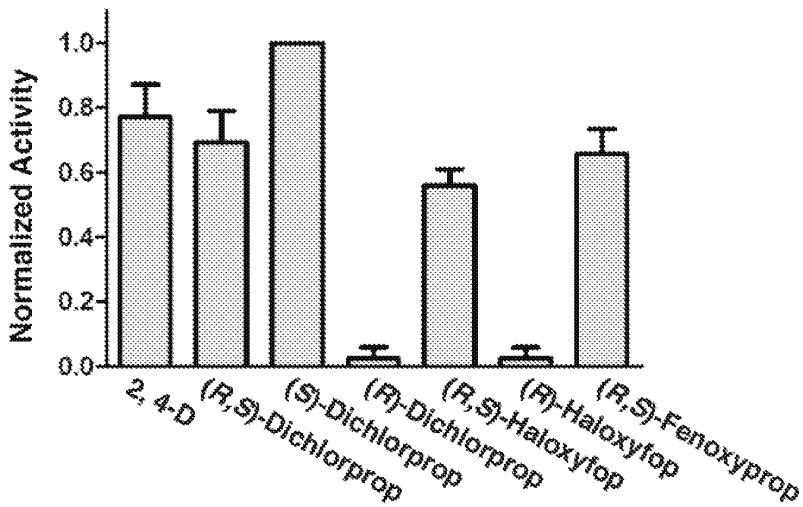
Supplementary Figure 3. Genomic context of AAD-1 and AAD-12. The genomic context highlights the distal nature of potential biosynthetic genes. We note that the genomic context of AAD-1 is that of a homolog (98% amino acid sequence similarity to the AAD-1 that was crystalized), as there is no annotated genomic data for corresponding organism and conjugative plasmid in public databases. Annotated genomic context of AAD-2 was also not available in public databases. Genes of importance to degradation pathways are highlighted and annotated according to the legend below. Proteins that are non-essential to the pathway have been colored grey.

COR-AAD1-00003815
Bayer EX1008 (Part 7 of 9)



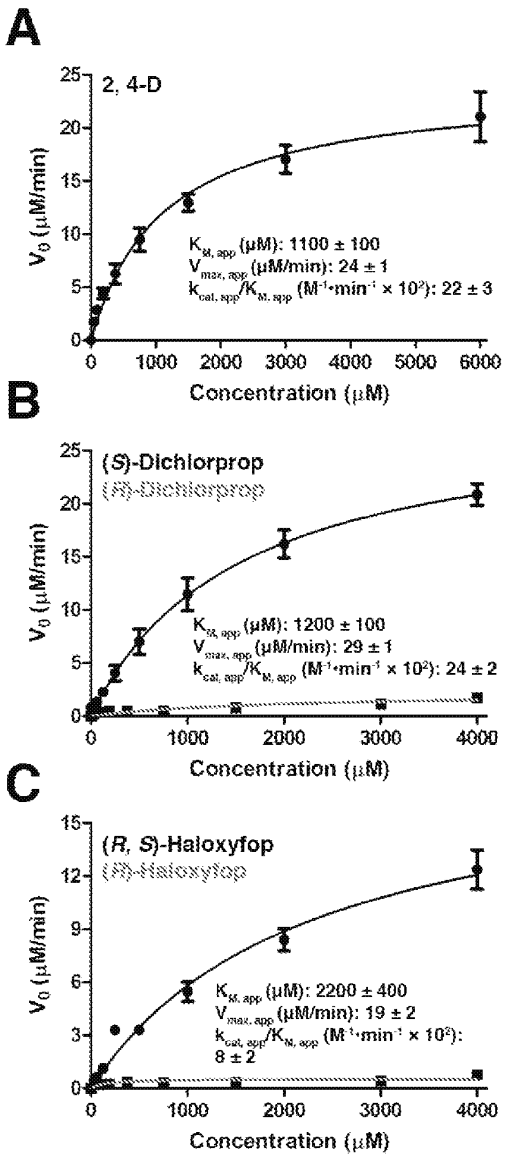
Supplementary Figure 4. Analytical Gel Filtration and SDS-PAGE analysis of AADs. (A) SDS-PAGE gel of AAD-1 and AAD-2 used for crystallographic and biochemical studies. (B) Analytical gel filtration of AAD-1 (33.2 kDa) and AAD-2 (33.6 kDa) against known standards. Elution profile suggests that AAD-1 and AAD-2 assemble as dimers in solution, denoted by the black arrow at ~15 min elution.

COR-AAD1-00003816
Bayer EX1008 (Part 7 of 9)



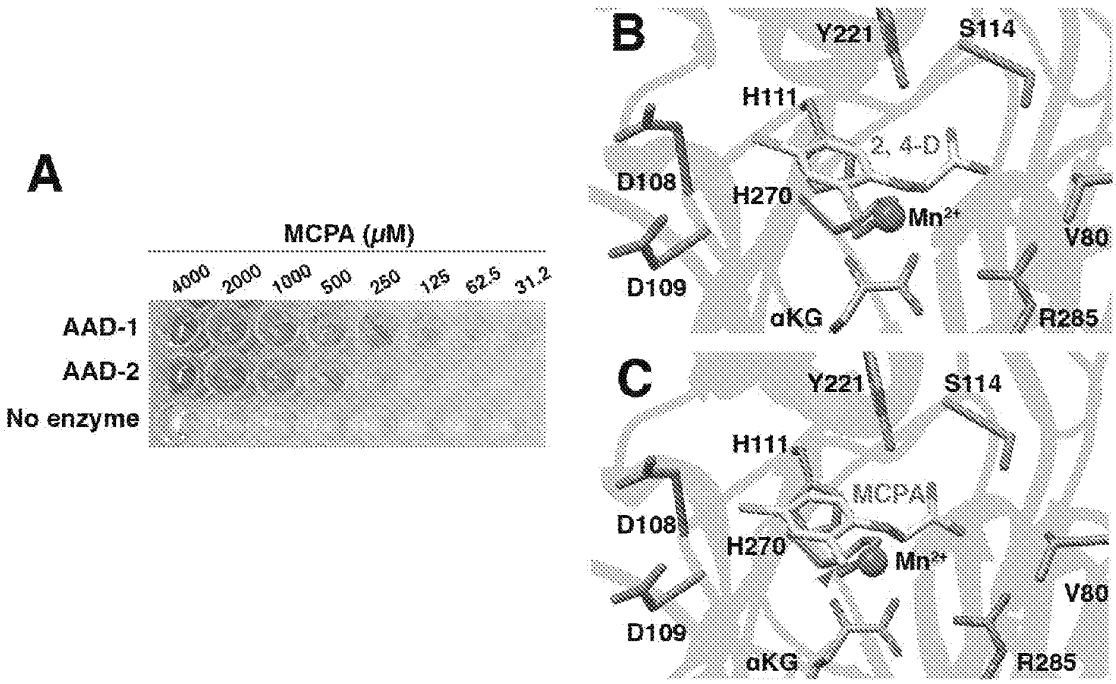
Supplementary Figure 5. Normalized activity of AAD-2 against a panel of substrates. The activity reported has been normalized to the activity of AAD-2 against (*S)*-dichlorprop, which was the substrate it most preferred amongst those tested.

COR-AAD1-00003817
Bayer EX1008 (Part 7 of 9)



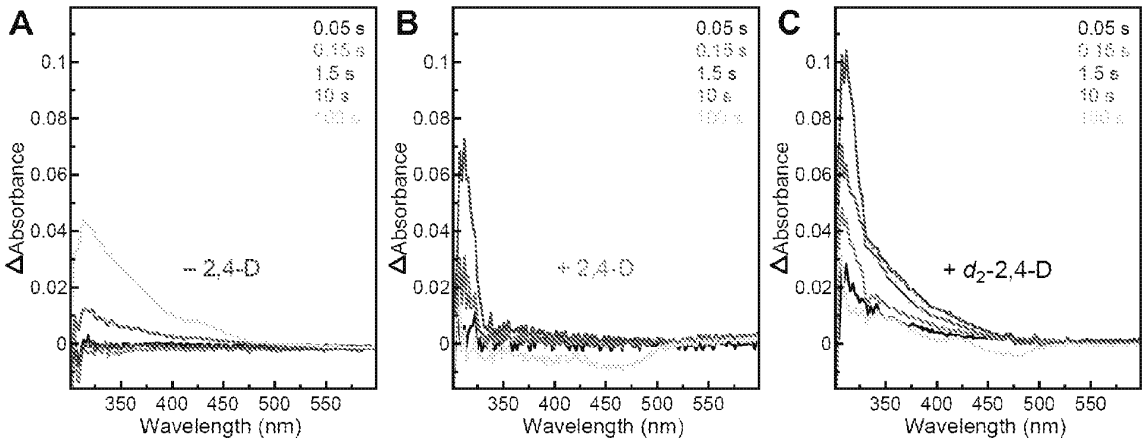
Supplementary Figure 6. Kinetic curves for the AAD-2 reaction using various substrates. (A) Kinetic curve of AAD-2 with 2,4-D at various concentrations. (B) Kinetic curves of AAD-2 with (*S*)-dichlorprop (black curve) or (*R*)-dichlorprop (red curve). (C) Kinetic curves of AAD-2 with (*R*,*S*)-haloxyfop (black curve) or (*R*)-haloxyfop (red curve). For racemic substrates, the concentration noted is the effective concentration of the (*S*) enantiomer in the sample. Kinetic parameters noted in each pane l correspond to values calculated using the black curve in each panel.

COR-AAD1-00003818
Bayer EX1008 (Part 7 of 9)



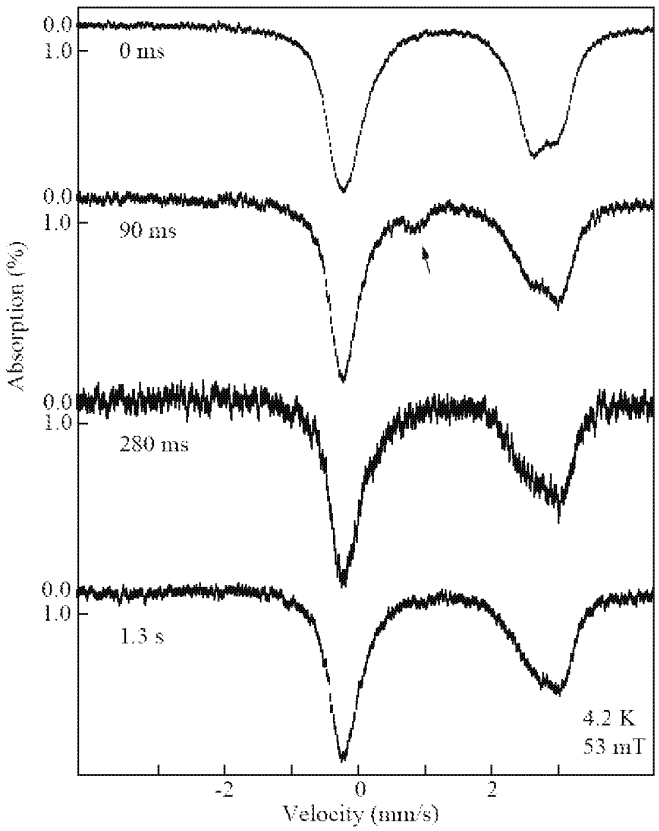
Supplementary Figure 7. AAD-1 and AAD-2 can accept MCPA as a substrate. (A) Select wells in a 96-well plate depicting the characteristic red color indicative of the presence of a phenol product (developed under basic conditions using 4-aminoantipyrine and potassium ferricyanate) as AAD-1 and AAD-2 react with MCPA at varying concentrations. The no enzyme control lane has been included to show that a null reaction will produce a pale yellow color. (B) Docking model depicting 2,4-D in the active site of AAD-1. (C) Docking model depicting MCPA in the active site of AAD-1. MCPA differs from 2,4-D only by the presence of a methyl group (brown arrow). AAD-1 was chosen to model in the achiral substrates as the structure of AAD-2 does not contain electron density for a herbicide substrate.

COR-AAD1-00003819
Bayer EX1008 (Part 7 of 9)



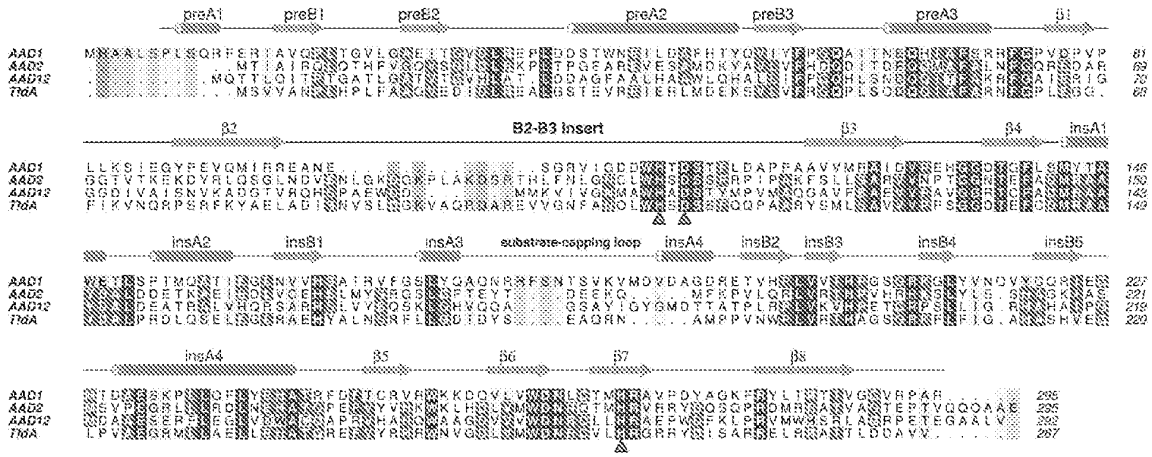
Supplementary Figure 8. Kinetic-difference spectra from the stopped-flow absorption experiment. The spectra shown here are the results of subtracting the experimental spectrum of an early reaction time (0.005 s) from the spectra taken at the reaction times indicated in the legend in the experiments with (A) no primary substrate, (B) unlabeled 2,4-D, and (C) d_2-2,4-D. The reaction conditions are given in Supplemental Materials and Methods.

COR-AAD1-00003820
Bayer EX1008 (Part 7 of 9)



Supplementary Figure 9. Mössbauer spectra of samples of the AAD-1 reaction. 4.2-K/53-mT Mössbauer spectra of a sample of the AAD-1•Fe(II) •αKG•d_2-2,4-D reactant complex (top) and samples, wherein the reactant complex was reacted for 90 ms, 280 ms, or 1.3 s. The position of the high-energy line of the ferryl intermediate is indicated with an arrow in the spectrum of the 90-ms sample. The reaction conditions are given in Supplemental Materials and Methods.

COR-AAD1-00003821
Bayer EX1008 (Part 7 of 9)



Supplementary Figure 10. Sequence alignment of select AADs. Sequence alignment of select AADs, noting secondary structure elements, and the β2β3 insert found in AAD-12 and AAD-2.

COR-AAD1-00003822
Bayer EX1008 (Part 7 of 9)

	Organism	Uniprot ID
Co-localizes with TfdB-like protein	Pseudocercospora fijiensis (strain CIRAD86)	M3A056
	Penicillium solitum	A0A1V6QWE6
	Fonsecaea erecta	A0A178Z4Y2
	Mycobacterium colombiense	A0A1A2YXB1
	Streptomyces sp. CB02009	A0A1Q5HUQ2
	Mycobacterium sp. 1164966.3	A0A1A0M1M0
	Alphaproteobacteria bacterium TMED54	A0A1Z8UV43
	SAR116 cluster bacterium	A0A2D7KVX6
	Rhodospirillaceae bacterium	A0A2D9Y9Q5
	Rhodospirillaceae bacterium	A0A2E7VA75
	Candidatus Endolissoclinum sp. TMED37	A0A1Z8T2B6
	Rhodospirillaceae bacterium	A0A2D7CKS0
	Rhodospirillaceae bacterium	A0A2E4GVS2
	Rhodospirillaceae bacterium	A0A2E4XQ24
	Magnetovibrio sp.	A0A2E3L2Z4
	Rhodospirillaceae bacterium	A0A2E4H027
	Alphaproteobacteria bacterium 13_1_20CM_4_65_11	A0A1Q7TWM2
	Alphaproteobacteria bacterium 13_1_20CM_3_64_12	A0A1Q7WS23
	Betaproteobacteria bacterium RIFCSPLOWO2_02_FULL_67_26	A0A1F4BNV1
	Alcaligenaceae bacterium	A0A2G4J8Q9
	Rhodospirillaceae bacterium	A0A2E5PMF6
	Candidatus Rokubacteria bacterium	A0A2V6XGU5
	Candidatus Rokubacteria bacterium	A0A2V7A8W2
	Burkholderia sp. SRS-W-2-2016	A0A1Q8IVD1
Co-localizes with TfdC-like protein	Diplodia seriata	A0A0G2EHD3
	Candidatus rokubacteria bacterium	A0A2V6S1C4
	Burkholderia sp. Leaf177	A0A0Q5NX83
	Bradyrhizobium sp. SK17	A0A2K8YNB2
	Halomonas sp. WRN001	A0A2A2EQM1
	Burkholderia sp. KK1	A0A1P9YF09
	Rhodospirillaceae bacterium	A0A2E4XUY7
	Rickettsiales bacterium	A0A2E7UZN3
	Rhodospirillaceae bacterium	A0A2E4XUM7
	Rickettsiales bacterium	A0A2E7V1P8

COR-AAD1-00003823
Bayer EX1008 (Part 7 of 9)

	Organism	UniprotID
Co-localizes with TfdC-like protein	Candidatus endolissoclinum sp. TMED37	A0A1Z8SSC2
	Rhodospirillaceae bacterium	A0A2D7CMZ1
	Rhodospirillaceae bacterium	A0A2E9UWQ6
	Rhodospirillaceae bacterium	A0A2E5L972
	Pseudorhodoferax sp. Leaf274	A0A0S9NH71
	Bradyrhizobium sp. 3 85S1MB	A0A2U8QLK5
	Bosea lathyri	A0A1H6D7Y2
	Beijerinckia sp. 28-YEA-48	A0A1H4RRY8
	Uncultured bacterium	G9FC95
Co-localizes with TfdB and TfdC-like proteins	uncultured bacterium	G9FBF9
	Burkholderia cepacia	Q93L12
	Achromobacter denitrificans	Q6QHP8
	Uncultured bacterium	G9FBF9
	Burkholderia cepacia	Q93L12
	Achromobacter denitrificans	Q6QHP8
	Delftia acidovorans	Q8KN30
	Burkholderia sp. KK1	A0A1P9YF35
	Burkholderia sp. M701	V5YNJ4
	Ralstonia pickettii	I3RYL1
	Uncultured bacterium	J9R7E1
	Variovorax sp. DB1	I3RYF9
	andidimonas nitroreducens	A0A225MB14
	Psychrobacter sp. P11G5	A0A127H2S0
	Psychrobacter sp. Cmf 22.2	A0A1Q8DTW8
	Ruegeria litorea R37	A0A1Y5TNJ4
	Ruegeria mediterranea M15O_3	A0A2R8C6L2
	Limnohabitans sp. JirII-31	A0A2M6VQN1
	Limnohabitans sp. TS-CS-82	A0A2S7JRZ7

Supplementary Table 1. List of Uniprot IDs of Putative AADs Identified by EFI-EST (2). The table above lists the UniprotIDs of putative AADs found using the EFI-FEST Sequence Similarity Network (SSN) and Genome Neighborhood Network (GNN) tools (3). Sequences are group to whether they co-occur (within a 15 gene window) with a TfdB homolog, TfdC homolog, or both.

COR-AAD1-00003824
Bayer EX1008 (Part 7 of 9)

Substrate	AAD-1		AAD-2	
	$K_{M,\ app}$ (μM)	$k_{cat,\ app}/K_{M,\ app}$ (M^{-1}·min^{-1} × 10^3)	$K_{M,\ app}$ (μM)	$k_{cat,\ app}/K_{M,\ app}$ (M^{-1}·min^{-1} × 10^2)
2, 4-D	683 ± 76*	27*	1100 ± 100	22 ± 3
(*R*)-dichlorprop	527 ± 38*	3380*	N. D.	N. D.
(*S*)-dichlorprop	N. D.	N. D.	1200 ± 100	24 ± 2
(*R*)-cyhalofop	96 ± 7*	1950*	N. D.	N.D.
(*R,S*)-diclofop	160 ± 40	97 ± 5	N. S.	N.A.
(*R,S*)-haloxyfop	330 ± 100	50 ± 2	2200 ± 300	8 ± 2
(*R,S*)-quizalofop	120 ±30	32 ± 3	N.S.	N.A

Supplementary Table 2. Kinetic parameters of AAD-1 and AAD-2 across a panel of substrates. Values denoted with an * were previously reported (5). The aforementioned values have been converted from $M^{-1}s^{-1} \times 10^3$ as reported, to $M^{-1}min^{-1} \times 10^3$ to provide a more direct means of comparison. Values noted with N. D. (not detected) indicate that the no activity was detected. Values noted with N. S. (not saturated) suggests that the enzyme does not prefer that compound as a substrate, i.e. only a subtle colorimetric change at 510nm was observed when 10 μM of enzyme was incubated with 4mM (effective concentration) of the accepted enantiomer of over a 15 minute incubation period. The lack in change of absorbance hindered our kinetic assays due to issues in detection. Unless otherwise noted, all other values were obtained during this study.

COR-AAD1-00003825
Bayer EX1008 (Part 7 of 9)

Primer	Sequence
AAD-2_NLIC_FP	TACTTCCAATCCAATGCAATGACGATCGCCATCCGGCAGCTT
AAD-2_NLIC_RP	TTATCCACTTCCAATGTTATTATCACTCCGCCGCCTGCTGCTG

Supplementary Table 3. List of primers used in this study.

COR-AAD1-00003826
Bayer EX1008 (Part 7 of 9)

Supplementary Table 3. Data collection, phasing and refinement statistics

	AAD-1 Mn^{2+}•αKG• (*R*)-dichlorprop	**AAD-1** Mn^{2+}•αKG• (*R*)-dicyhalofop	**AAD-1** Mn^{2+}•αKG• (*R*)-diclofop	**AAD-1** $(VO)^{2+}$•succ• (*R*)-dichlorprop	**AAD-2** Mn^{2+}•αKG
Data collection					
Space group	$P2_12_12$	$P2_12_12$	$P2_12_12$	$P2_12_12$	C2
Unit cell	85.9, 97.8, 69.9	85.5, 97.4, 69.8	85.8, 97.78, 69.9	85.9, 97.9, 69.9	266.5, 55.5, 183.7, 118.9°
Resolution	86-1.58 (1.59-1.58)	86-1.9 (1.91-1.9)	86-1.8 (1.81-1.8)	57-1.5 (1.54-1.5)	50-2.15 (2.19-2.15)
Total reflections	656,362	380,331	508,030	1,275,386	579,196
Unique	80,901	46,644	55,192	92,316	127,502
R_{sym} (%)[1]	0.093 (0.956)	0.119 (755)	0.111 (0.929)	0.072 (0.792)	0.088 (0.720)
I/σ(I) [1]	17.5 (2.1)	17.0 (2.9)	18.7 (2.6)	20.5 (2.2)	16.1 (1.6)
Completeness	100 (95.8)	100 (97.7)	100 (97.3)	99.2 (99.4)	99.0 (92.6)
Redundancy	8.1 (7.9)	8.2 (8.3)	9.2 (9.3)	13.8 (8.2)	4.6 (3.8)
Refinement					
Resolution (Å)	54.2-1.58	56.7-1.9	48.9-1.8	25.0-1.51	25.0-2.15
# reflections	80,828	46,591	55,138	87,655	107,559
R_{work} / R_{free}[2]	16.2/19.7	17.5/21.8	16.3/20.1	19.5/21.7	18.8/23.3
# of atoms					
Protein	4,497	4,500	4,482	4,498	15,111
αKG/succinate	20	20	20	8	70
Herbicide	14	44	21	14	-
Water	734	576	668	650	1,633
B-factors					
Protein	19.4	21.5	19.6	22.0	34.7
αKG/succinate	14.6	17.5	15.5	22.8	34.1
Herbicide	22.1	32.9	32.6	38.2	-
Water	30.3	28.7	29.6	32.4	38.1
RMS deviations					
Bond lengths (Å)	0.011	0.004	0.007	0.007	0.009
Bond angles (°)	1.249	0.865	1.066	1.16	1.29

1. Highest resolution shell is shown in parenthesis.

2. R-factor = $\Sigma(|F_{obs}|-k|F_{calc}|)/\Sigma|F_{obs}|$and R-free is the R value for a test set of reflections consisting of a random 5% of the diffraction data not used in refinement.

COR-AAD1-00003827
Bayer EX1008 (Part 7 of 9)

SUPPLEMENTAL REFERENCES

1. Price JC, Barr EW, Hoffart LM, Krebs C, & Bollinger JM, Jr. (2005) Kinetic dissection of the catalytic mechanism of taurine:alpha-ketoglutarate dioxygenase (TauD) from *Escherichia coli*. *Biochemistry* 44:8138-8147.

2. Gerlt JA, *et al.* (2015) Enzyme Function Initiative-Enzyme Similarity Tool (EFI-EST): A web tool for generating protein sequence similarity networks. *Biochim Biophys Acta* 1854:1019-1037.

3. Gerlt JA (2017) Genomic Enzymology: Web tools for leveraging protein family sequence-function space and genome context to discover novel functions. *Biochemistry* 56:4293-4308.

4. Don RH & Pemberton JM (1981) Properties of six pesticide degradation plasmids isolated from Alcaligenes paradoxus and Alcaligenes eutrophus. *J Bacteriol* 145:681-686.

5. Wright TR, *et al.* (2010) Robust crop resistance to broadleaf and grass herbicides provided by aryloxyalkanoate dioxygenase transgenes. *Proc Natl Acad Sci U S A* 107:20240-20245.

COR-AAD1-00003828
Bayer EX1008 (Part 7 of 9)

Protein

COVID-19 is an emerging, rapidly evolving situation.
Get the latest public health information from CDC: https://www.coronavirus.gov .
Get the latest research from NIH: https://www.nih.gov/coronavirus.
Find NCBI SARS-CoV-2 literature, sequence, and clinical content: https://www.ncbi.nlm.nih.gov/sars-cov-2/.

GenPept

alpha KG dependent 2,4-D dioxygenase [alpha proteobacterium RD5-C2]

GenBank: BAB92964.1

Identical Proteins FASTA Graphics

Go to:

```
LOCUS       BAB92964                295 aa            linear   BCT 02-JUL-2002
DEFINITION  alpha KG dependent 2,4-D dioxygenase [alpha proteobacterium
            RD5-C2].
ACCESSION   BAB92964
VERSION     BAB92964.1
DBSOURCE    accession AB074490.1
KEYWORDS    .
SOURCE      alpha proteobacterium RD5-C2
  ORGANISM  alpha proteobacterium RD5-C2
            Bacteria; Proteobacteria; Alphaproteobacteria.
REFERENCE   1
  AUTHORS   Itoh,K., Kanda,R., Sumita,Y., Kim,H., Kamagata,Y., Suyama,K.,
            Yamamoto,H., Hausinger,R.P. and Tiedje,J.M.
  TITLE     tfdA-like genes in 2,4-dichlorophenoxyacetic acid-degrading
            bacteria belonging to the
            Bradyrhizobium-Agromonas-Nitrobacter-Afipia cluster in
            alpha-Proteobacteria
  JOURNAL   Appl. Environ. Microbiol. 68 (7), 3449-3454 (2002)
   PUBMED   12089027
REFERENCE   2  (residues 1 to 295)
  AUTHORS   Itoh,K.
  TITLE     Direct Submission
  JOURNAL   Submitted (19-NOV-2001) Kazuhito Itoh, Shimane university, Life and
            Environmental Science; Nishikawatsu 1060, Matsue, Shimane 690-8504,
            Japan (E-mail:itohkz@life.shimane-u.ac.jp, Tel:81-852-32-6521,
            Fax:81-852-32-6597)
FEATURES             Location/Qualifiers
     source          1..295
                     /organism="alpha proteobacterium RD5-C2"
                     /strain="RD5-C2"
                     /db_xref="taxon:179278"
     Protein         1..295
                     /product="alpha KG dependent 2,4-D dioxygenase"
     Region          5..288
                     /region_name="TauD"
                     /note="Taurine dioxygenase, alpha-ketoglutarate-dependent
                     [Secondary metabolites biosynthesis, transport and
                     catabolism]; COG2175"
                     /db_xref="CDD:225086"
     Region          5..281
                     /region_name="TauD"
                     /note="Taurine catabolism dioxygenase TauD, TfdA family;
                     pfam02668"
                     /db_xref="CDD:280777"
     CDS             1..295
                     /gene="tfdA-like"
                     /coded_by="AB074490.1:82..969"
                     /transl_table=11
ORIGIN
        1 mtvlirqlhk hfvgevsgvd lrkpltkqea idieagmdky avlvfhgqdi sddqqmafal
       61 nfgerenarg gtvtkkedyr lssglndvsn lgkdgkplpk dhrthlfnlg nclwhsdssf
      121 rpipakfsll sarvvnpkgg ntefadmraa ydalddetkt eiddmicehs lmysrgslgf
      181 ldytdeekem fkpvlqrlvr thpahgrksl ylsshagair gmsmpearll lrdltehatq
      241 pefvyvhkwt vhdlvmwdnr qtvhrvrryd qsqprdmrra tvagtqptva qeaae
//
```


COR-AAD1-00003829
Bayer EX1008 (Part 7 of 9)

Expression of 2,4-Dichlorophenoxyacetic Acid Monooxygenase Gene in Tobacco Plants

Kwon, Jin Kyung[1] · Ka, Jong-Ok[2] · Kim, Byung-Dong[1]
[1]Dept. of Horticulture, Seoul National University, Suwon 441-744, Korea
[2]Dept. of Agricultural Biology, Seoul National University, Suwon 441-744, Korea

Abstract

The 2,4-D monooxygenase gene (*tfdA*) from *Alcaligenes eutrophus* was modified by PCR primer mutagenesis to produce a plant consensus translational start sequence by changing GTG to ATG. We confirmed the modified gene, *mfdA*, by sequencing. The *mfdA* gene was cloned into a cauliflower mosaic virus 35S promoter expression vector (pMBP-1/*mfdA*) and introduced into tobacco plants by *Agrobacterium*-mediated transformation. Introduction of the *mfdA* gene into genomic DNA of plants was confirmed by Southern blot hybridization analysis. Northern blot hybridization analysis showed that the *mfdA* gene was stably expressed in transformed tobacco plants. Transformed tobacco plants tolerated elevated level of 8 mg · L^{-1} 2,4-D in tissue culture and showed resistance when sprayed with 3 g · L^{-1} 2,4-D.

Additional key words: genetic engineering, herbicide resistance, *tfdA*, transformant plant

Introduction

The herbicide 2,4-dichlorophenoxyacetic acid (2,4-D) has been used as an auxin-like herbicide with high selectivity to control broad leaf weeds in lawn, and barley and rice fields. Because 2,4-D tends to drift in prevailing winds when sprayed, susceptible crops nearby can be damaged. To reduce this damage, resistant crops to 2,4-D has been developed in dicotyledonous plants by genetic engineering (Bayley et al., 1992).

Soil microorganisms that degrade 2,4-D were identified and multienzyme pathways for 2,4-D degradation have been demonstrated in several bacterial genera (Amy et al., 1983; Don and Pemberton, 1981). *Alcaligenes eutrophus* is one of the best characterized organisms. It contains a conjugative plasmid pJP4 which carries genes of *tfdA*, *tfdB*, *tfdC*, *tfdD*, *tfdE*, and *tfdF*. The first gene in the 2,4-D degradation pathway encodes 2,4-D monooxygenase which converts 2,4-D to 2,4-dichlorophenol (Fukumori and Hausinger, 1993; Perkins and Luquin, 1988). The 2,4-dichlorophenol is less toxic to plants than 2,4-D. The nucleotide sequence of the 2,4-D monooxygenase gene in *Alcaligenes eutrophus* was determined (Streber et al., 1989) and its open reading frame is 861 bp.

We modified the 2,4-D monooxygenase gene of bacterial origin to fit into plant codon usage and transformed into tobacco plants as a model system to render resistance to high levels of the herbicide 2,4-D.

Materials and Methods

Construction of plant expression vector

Standard techniques of gene cloning were used as described by Maniatis et al. (1989). The translation start codon of 2,4-D monooxygenase gene in *Alcaligenes eutrophus* JMP103 (Ka et al., 1994) is GTG whereas that in plants is ATG. We constructed a pair of primers (5'-GAGCATCTAGATGAGCGTCGTCGCA-3', and 5'-ATGGCGAGCTCTAGACACGGCATC-3') which contain ATG start codon and restriction sites of *Xba* I and *Sac* I, respectively (Fig. 1. A). The plasmid containing 2,4-D monooxygenase gene was used as templates for PCR amplification (1 min at 94℃, 1 min at 62℃ and 1 min at 72℃, for each cycle, and total of 35 cycles). PCR products were digested with *Xba* I /*Sac* I , and cloned into *Xba* I /*Sac* I sites of pGEM 7Zf(+) vector. To confirm sequences of the modified *tfdA* (*mfdA*) gene, chain termination method was used as modified by Tabor & Richardson (1995) with thermo sequenase and α-^{35}S]ATP from Amersham. The *mfdA* gene was inserted between the cauliflower mosaic virus 35S promoter and the NOS terminator of pMBP-1 which contains nopaline synthase terminator and neomycin phosphotransferase II gene for kanamycin resistance, and this gene construct was named pMBP-1/*mfdA* (Fig. 1. B). The pMBP-1/*mfdA* plasmid was transferred from *E. coli* into *Agrobacterium tumefaciens* LBA4404 by freeze-thaw method. To confirm insertion of pMBP-1/*mfdA* plasmid into *A. tumefaciens* LBA4404, PCR was performed as mentioned above.

Transformation into tobacco plants

Nicotiana tabacum cv. Xanthi plants were used as tissue donors. Leaf disc transformation was essentially done as described by Horsch et al. (1985). Direct shoot induction medium (DSIM) and root induction medium (RIM) were based on Murashige and Skoog (MS) medium containing 100 mg · L^{-1} and 50 mg · L^{-1} kanamycin, respectively (Kim et al., 1991). Discs of *N. tabacum* cv. Xanthi (1 cm × 1 cm) were excised from young leaves and placed on MS medium. *A. tumefaciens* LBA4404 containing pMBP-1/*mfdA* plasmid was added to the leaf discs and co-cultivated in the dark at 28℃ for 24 hours.

COR-AAD1-00003830
Bayer EX1008 (Part 7 of 9)

Leaf discs were transferred on RMM containing 2 mg · L⁻¹ benzylaminopurine and 500 mg · L⁻¹ kanamycin for selection of transformed shoots. Regenerated shoots on RMM were transferred onto RIM which is hormone free. Regenerated rooted plants were transferred to soil to grow and grown in the greenhouse.

Southern/Northern blot hybridization

Plant genomic DNA was prepared from young leaves as described by Murray and Thompson (1980). For Southern hybridization experiment plant DNA was cut with *Xba* I and *Sac* I and probed with a PCR product of the *aphA* gene. Total RNA of plant was isolated essentially as described by Chomczynski and Sacchi (1987) and transferred to a nylon membrane. PCR product containing the *aphA* gene was used as a probe to detect the *aphA* RNA.

Assay for 2,4-D resistance

To determine the 2,4-D concentration at which level shoot formation is inhibited, untransformed tobacco leaf discs were cultured on RMM containing 0.1, 0.2, 0.4, 0.8, 1.6, 3.2, 6.4, and 12.8 mg · L⁻¹ 2,4-D. To test resistance against 2,4-D, explants of transformed plants which expressed the *aphA* were cultured on RMM containing 0, 1, 2, 4, 8, and 16 mg · L⁻¹ 2,4-D. After one 3 g · L⁻¹ 2,4-D was directly sprayed to untransformed and transformed tobacco plants.

Results and Discussion

Construction of plant expression vector

The first enzyme in 2,4-D degradation pathway, 2,4-D monooxygenase, is encoded by *tfdA* gene. The translation start codon of 2,4-D monooxygenase gene was modified from GTC to the plant start codon ATG by PCR (Fig. 1. *A*) and the altered sequences were confirmed by plasmid sequencing method. One sequence was converted from C to T (data not shown). It must have been introduced by PCR amplification or by the synthetic primer, however, since the change did not affect amino acid sequence, the *aphA* gene was cloned into pMBP-1 with CaMV 35S promoter and nopaline synthase (nos) 3′ polyadenylation signal. The pMBP-1/*aphA* was transferred into *A. tumefaciens* LBA4404 and its transformation was confirmed by PCR (data not shown).

Transformation of tobacco plants

Leaf discs of *N. tabacum* cv. Xanthi plants were used for *Agrobacterium*-mediated transformation. Transformed shoots were selected on RMM containing 100 mg · L⁻¹ kanamycin and regenerated on RIM containing 50 mg · L⁻¹ kanamycin (data not shown). Total 45 putative transformed plants were obtained from this experiment and the transformation efficiency was about 9.3%. Positive transformed plants were transferred to soil and grown in the greenhouse. Growth of the transformants was not distinguishable from untransformed control plants except for the T12 plant which had white color flowers (data not shown).

Expression of the *aphA* gene in transformed plants

Southern hybridization analysis was performed to confirm integration of the *aphA* gene into plant genomic DNA. T2, T3, and T13 plants produced a positive hybridization band of 483 bp as expected (Fig. 2). The expression of the *aphA* gene was determined in these selected transformed tobacco plants by northern blot hybridization (Fig. 3). The *aphA* gene was expressed weakly in T3 (Fig. 3, Lane 4), and T12 (Fig. 3, Lane 2) plants and strongly in T2 (Fig. 3, Lane 3) plant.

The 2,4-D degradation assay

The wild-like tobaccos, 2,4-D is known to induce callus formation and to suppress shoot regeneration of tobacco leaf discs in tissue culture. Leaf discs of untransformed tobacco plants did not produce shoot in the presence of 2,4-D at concentrations higher than 0.2 mg · L⁻¹ (data not shown). But leaf discs of T2 transformants which expressed the *aphA* gene at high level were able to produce normal shoots on a RMM containing 8 mg · L⁻¹ 2,4-D (data not shown). When these transformed plants expressing the *aphA* gene were sprayed with 2,4-D at 3 g · L⁻¹, an ordinary field application concentration, they were not affected, whereas the untransformed plant withered (Fig. 4). These data were shown that transformed plants were resistant to 2,4-D.

Our purpose was to confirm the possibility that microbial gene could be expressed in the plant cell. *N. tabacum* cv. Xanthi as a model system. Expression of the 2,4-D degradation gene in tobacco to confer the plant 2,4-D resistance will act as example that can be applied to other agriculturally important crops (Shapiro et al., 1992). This system may also be applied to

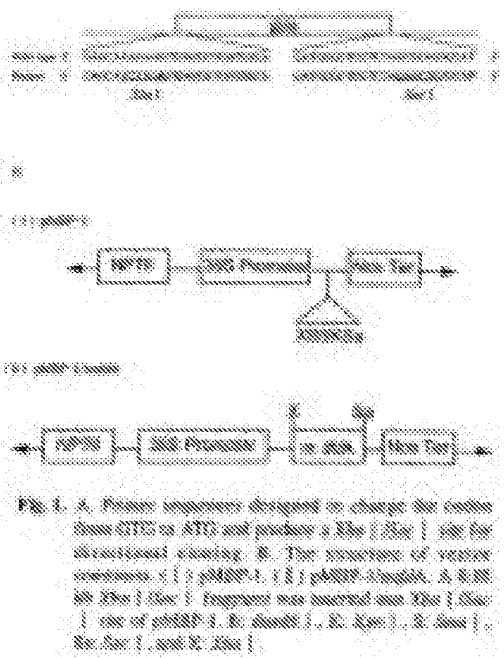


Fig. 1. *A.* Primer sequences designed to change the codon from GTC to ATG and produce a *Xba* I (*Sac* I) site for directional cloning. *B.* The structure of vector constructs. *(+)* pMBP-1, *(-)* pMBP-1/*aphA*. *A* 0.48 kb *Xba* I (*Sac* I) fragment was inserted into *Xba* I (*Sac* I) site of pMBP-1. *Bs*, plasmid; *E*, *Eco* I; *S*, *Sac* I; *Xb*, *Xba* I; and *X*, *Xho* I

COR-AAD1-00003831
Bayer EX1008 (Part 7 of 9)

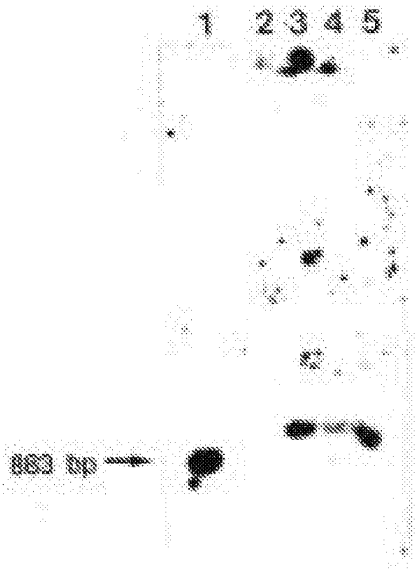


Fig. 3. Southern hybridization analysis of transformed soybean plants.
Genomic DNA was digested with *Sac* I and *Xba* I. Probe was the amplified PCR product.
Lane 1: mgDA PCR products. Lane 2: Genomic DNA from non-transformed soybean plants, and Lanes 3-5: transformed soybean plants T2, T3 and T12, respectively.

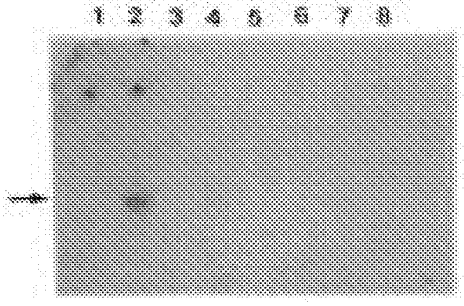


Fig. 5. Northern hybridization analysis of transformed soybean plants.
Total RNA from plants were separated on agarose-formaldehyde gels, transferred onto a nylon membrane and probed with the mgDA PCR products.
Lane 1: Non-transformed *Neodiprion sabinianus* cv. Xenik; Lanes 2-8: Transformed plants T2, T4, T5, T7, T9, T12, and T13. The predicted transcripts are indicated by the arrow.

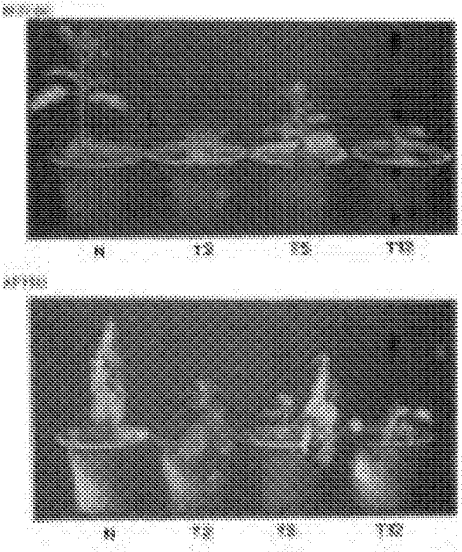


Fig. 4. Comparison of non-transformed and transformed soybean plants sprayed with 3 g/L 2,4-D ester once at a week interval. Photograph was taken 4 weeks after the second spray. N, Non-transformed, and T2, T5, and T12: Transformed soybean plants.

phytoremediation for removing organic compounds or heavy metals is met by plant (Cunningham and Ow, 1996).

Acknowledgment

We are grateful to B. J. Choi, J. W. Yu, and S. J. Kim for helpful suggestions on plant transformation. This study is supported by Korean Ministry of Education through Research Fund.

Literature cited

Amy, P.S., J.W. Schaller, L.M. Preuss and R.J. Seidler. 1985. Characterization of aquatic bacteria and cloning of genes specifying partial degradation of 2,4-dichlorophenoxyacetic acid. Appl. Environ. Microbiol. 49:1253-1260.

Bayley, C., N. Trolander, C. Ray, M. Morgan, J.E. Quesenberry, and D.W. Ow. 1992. Engineering 2,4-D resistance into maize. Theor. Appl. Genet. 83:645-649.

Chomczynski, P. and N. Sacchi. 1987. Single-step method of RNA isolation by acid guanidinium thiocyanate-phenol-chloroform extraction. Anal. Biochem. 162:156-159.

Cunningham, S.D. and D.W. Ow. 1996. Promises and prospects of phytoremediation. Plant Physiol. 110:715-719.

Frear, R.D. and J.M. Pemberton. 1981. Properties of six pesticide degradation plasmids isolated from *Alcaligenes paradoxus* and *Alcaligenes eutrophus*. J. Bact. 148:395-400.

Bayer EX1008 (Part 7 of 9)

COR-AAD1-00003832

The Journal of Microbiology, March 2003, p.7-15 Vol. 41, No. 1
Copyright © 2003, The Microbiological Society of Korea

Genetic and Phenotypic Diversity of Dichlorprop-Degrading Bacteria Isolated from Soils

Hae-Dong Park and Jong-Ok Ka*

School of Agricultural Biotechnology, Seoul National University, Suwon 441-744, Korea

(Received December 3, 2002 / Accepted February 11, 2003)

Nine dichlorprop-degrading bacteria and three pairs of bacteria showing syntrophic metabolism of the herbicide were isolated from soils, and their genetic and phenotypic characteristics were investigated. Analysis of 16S rDNA sequences indicated that the isolates were related to members of the genera, *Sphingomonas*, *Herbaspirillum*, and *Bradyrhizobium*. Twelve different chromosomal DNA patterns were obtained by polymerase-chain-reaction (PCR) amplification of repetitive extragenic palindromic (REP) sequences from the 15 isolates. The isolates were able to utilize the herbicide dichlorprop as a sole source of carbon and energy and their dichlorprop degradative pathways were induced by the presence of dichlorprop. Most of the isolates and syntrophic pairs were able to degrade both (*R*)- and (*S*)-dichlorprop, but strain DP522 exhibited enantioselective degradation of (*S*)-dichlorprop. The isolates degraded 2,4-dichlorophenoxyacetic acid, 2-methyl-4-chlorophenoxyacetic acid, and mecoprop, in addition to dichlorprop. Oxygen uptake experiments indicated that most of the isolates degraded dichlorprop through 2,4-dichlorophenol.

Key words: bacteria, biodegradation, dichlorprop, diversity

Chlorinated phenoxyalkanoates are widely used, and thus many studies have focused on their persistence and fate in the natural environment (Torstensson *et al.*, 1975; Smith and Hayden, 1981; Smith and Aubin, 1991). Some phenoxyacid herbicides, such as 2,4-dichlorophenoxy acetic acid (2,4-D) and 2-methyl-4-chlorophenoxyacetic acid (MCPA), are readily mineralized by a number of soil microorganisms and stimulate substantial growth of the corresponding microbial population (Foster and Mckercher, 1973; Loos *et al.*, 1979; Biederbeck *et al.*, 1987). In contrast, other closely related pesticides, such as 2,4,5-trichlorophenoxyacetic acid (2,4,5-T), are not easily degraded by soil microorganisms, and organisms able to degrade them are very rare in the environment (Alexander, 1965). 2-(2,4-dichlorophenoxy) propionic acid (dichlorprop, 2,4-DP) is one of the chlorinated phenoxy alkanoic herbicides and is used to control broad-leaved weeds in cereals and grassland. While the phenoxyacetic acids such as 2,4-D and MCPA are achiral, the phenoxypropionic acids including dichlorprop and 2-(2-methyl-4-chlorophenoxy) propionic acid (mecoprop, MCPP) are chiral because they possess an asymmetrically substituted C-atom. Most commercial formulations of dichlorprop are racemic mixtures, containing both the (*R*) and the (*S*) enantiomers of dichlorprop, though only the (*R*) enantiomer has been reported to be herbicidally active (Aberg, 1956).

Among the phenoxyalkanoic aicds, 2,4-D has been most extensively studied regarding its environmental fate, metabolizing microorganisms, degradation pathways, and degradative genes and enzymes (Loos *et al.*, 1967; Don *et al.*, 1985; Pieper *et al.*, 1988; Ka *et al.*, 1994; Chung and Ka, 1998). In contrast, relatively little information is available on the microorganisms able to degrade chiral phenoxyalkanoic acid herbicides such as dichlorprop and mecoprop (Horvath *et al.*, 1990; Tett *et al.*, 1994). The main limitation is that, unlike the 2,4-D-degrading organisms, the dichlorprop- and mecoprop-degrading microorganisms are not ubiquitous in the environment and thus not easily isolated in pure cultures on laboratory media. These chiral herbicides are considered more recalcitrant than 2,4-D due to the propionic acid side chain linked to the oxygen atom of the phenoxyacid moiety (Alexander and Aleem, 1961). It requires long continuous cultivation to obtain degradation-positive cultures of the herbicides and the prolonged enrichment often results in multi-membered mixed cultures (Lappin *et al.*, 1985; Tett *et al.*, 1994). The difficulty of obtaining pure cultures implies that the complete mineralization of the herbicides can only occur through the syntrophism of a consortium of microorganisms in nature (Tett *et al.*, 1994).

In this work, we studied the occurrence of dichlorprop-degrading microorganisms in two different types of natural

* To whom correspondence should be addressed.
(Tel) 82-31-290-2475; (Fax) 82-31-294-8533
(E-mail) kagil@plaza.snu.ac.kr

COR-AAD1-00003833
Bayer EX1008 (Part 7 of 9)

soils, i.e., agricultural soils with no history of dichlorprop amendments and golf course soils routinely treated with the herbicide for several years. Through a simple enrichment procedure, we were able to isolate nine dichlorprop-degrading bacteria and three pairs of syntrophic bacteria co-mineralizing the herbicide from golf course soils, but no microorganisms were purified from the agricultural soils. We investigated their species diversity by 16S rDNA sequence analysis and REP-PCR patterns of chromosomes, and described their physiological and genetic properties related to dichlorprop biodegradation.

Materials and Methods

Media and culture conditions

PTYG medium contained (in grams per liter) peptone (0.25), tryptone (0.25), yeast extract (0.5), glucose (0.5), magnesium sulfate (0.03), calcium chloride (0.003), and agar (for plates only, 15). The dichlorprop mineral medium used for enrichment, isolation, and maintenance of isolates contained (in grams per liter) dichlorprop (0.3), KH_2PO_4 (1.36), Na_2HPO_4 (1.41), $(NH_4)_2SO_4$ (0.3), $MgSO_4 \cdot 7H_2O$ (0.05), $CaCl_2 \cdot H_2O$ (0.0058), trace metal solution (5 ml/liter), and agar (for plates only, 15). The trace metal solution contained (in grams per liter) $FeSO_4 \cdot 7H_2O$ (0.55), $ZnSO_4 \cdot 7H_2O$ (0.23), $MnSO_4 \cdot 7H_2O$ (0.34), $Co(NO_3)_2 \cdot 6H_2O$ (0.075), $CuSO_4 \cdot 5H_2O$ (0.047), and $(NH_4)_6Mo_7O_{24} \cdot 4H_2O$ (0.025). Each of the bacteria showing syntrophic degradation of dichlorprop was maintained on PTYG medium. PTYG medium was also used for strain purification and colony production for the repetitive extragenic palindromic PCR (REP-PCR). All cultures were incubated at 30°C and liquid cultures were aerated by shaking at 200 rpm on a rotary shaker (Vision Co., Korea).

Chemicals

2-(2,4-dichlorophenoxy)propionic acid (2,4-DP, dichlorprop), 4-(2,4-dichlorophenoxy)butyric acid (2,4-DB), 4-(2-methyl-4-chlorophenoxy)butyric acid (MCPB), and 2-(2-methyl-4-chlorophenoxy)propionic acid (MCPP, mecoprop) were obtained from Aldrich Chemical Co., Milwaukee, USA, and analytical grade 2,4-dichlorophenoxyacetic acid (2,4-D), 2,4-dichlorophenol (2,4-DCP), 3,5-dichlorocatechol, 2-methyl-4-chlorophenoxyacetic acid (MCPA), and (*R*)-enantiomer of dichlorprop were purchased from Sigma Chemical Co., St. Louis, USA.

Isolation of dichlorprop-degraders

Soil samples were taken from golf courses and agricultural fields of various locations in South Korea. The golf courses selected in this study have been treated with racemic dichlorprop for several years, while the upland fields, which have been under normal agricultural practices growing dry crops, such as legumes and barley, for more than 10 years, have no history of dichlorprop amendments. Samples from the top 15 cm of soil were taken, sifted through a 2-mm-pore-size sieve, and kept at 4 °C prior to use. A 100 g of each soil sample was transferred to each 250 ml sterile beaker, and then treated with racemic dichlorprop dissolved in 0.1 M NaH_2PO_4 buffer (pH 7.0) to a concentration of 300 ppm and thoroughly mixed. Four weeks after the dichlorprop application, a 10 g soil sample from each beaker was homogenized with 95 ml of a sterile 0.85% saline solution by shaking the preparation at 200 rpm on a rotary shaker. Samples (0.1 ml) of appropriate 10-fold dilutions were inoculated into test tubes containing 3 ml of dichlorprop medium (300 ppm). The tubes were incubated at 30°C for 4 weeks and degradation of dichlorprop was analyzed by spectrophotometry and reverse-phase HPLC on μBondapack C18 column (3.9 by 300 mm; Waters, Milford, MA, USA) and a UV detector set at 282 nm; methanol 0.1% phosphoric acid (60 : 40) was used as the eluant. The culture of the terminal positive tube showing substantial cell growth and less than 20% of the dichlorprop remaining was enriched by two additional transfers into fresh medium. Each enriched culture was streaked onto PTYG agar medium and single colonies were then tested for dichlorprop degradation in fresh dichlorprop medium before strain purification.

16S rDNA sequence analysis

Total genomic DNA was isolated from the isolates and PCR amplification of 16S rRNA genes was performed with 27f and 1492r as previously described (Lane, 1991). The amplified 16S rRNA genes were sequenced using a ABI Prism BigDye Terminator Cycle Sequencing Ready Kit according to the manufacturers instruction (Perkin-Elmer) with the sequencing primers 27f and 519r (Hugenholtz *et al.*, 1998). Approximately 400 unambiguous nucleotide positions were used for comparison to the data in GenBank using the Basic Local Alignment Search Tool (BLAST) (Altschul *et al.*, 1990). Sequences from nearest relatives were identified from the Ribosome Database Project (RDP) using the SIMILARITY-RANK program of the RDP (Maidak *et al.*, 2000)

Colony REP-PCR

The colony REP-PCR was performed using BOXA1R as a primer as described previously (de Bruijn, 1992; Versalovic *et al.*, 1994). Each isolate was grown on the PTYG agar medium for 24 to 48 h, and then a small amount of cells was resuspended in 25 μl of PCR mixture. After PCR amplification, 10 μl samples of the REP-PCR products were separated by electrophoresis on horizontal 1% agarose gels.

Degradative phenotype analysis

Each strain was grown on dichlorprop medium (300 ppm) or on PTYG medium. Cells were then harvested by cen-

COR-AAD1-00003834
Bayer EX1008 (Part 7 of 9)

trifugation at 10,000 × g for 10 min at 4 °C, washed twice with an equal volume of 15 mM phosphate buffer (pH 7.0), and resuspended in the same buffer. Aliquots of suspended cells were inoculated into culture tubes, each of which contained the mineral medium supplemented with one of the structural analogs at a concentration of 300 μg/ml. After 4 week's incubation, the cultures were centrifuged to remove the cellular material, and the UV absorption was measured at 282 nm to determine the degradation of phenoxyacetates.

Axenic culture experiment

After growth in dichlorprop medium or PTYG medium, cells were harvested, washed, and resuspended in sodium phosphate buffer. Aliquots of suspended cells were inoculated into duplicate flasks containing 200 ml of dichlorprop medium at a final density of $OD_{550} = 0.005$. All cultures were incubated at 30°C and were aerated by shaking at 200 rpm on a rotary shaker. Aliquots of the cultures were regularly removed to determine cell growth and degradation of dichlorprop.

Plasmid detection and conjugation

For detection of plasmid DNA, cells were lysed using a modified form (Ka and Tiedje, 1994) of the procedure previously published (Kado and Liu, 1981). Curing of plasmid was performed by the sodium dodecyl sulfate method (Crosa *et al.*, 1994). To analyze the transferability of the dichlorprop degradative phenotype of the isolates, matings were performed on membrane filters as described by Willetts (Willetts, 1988), using *Alcaligenes eutrophus* JMP228 and *Pseudomonas cepacia* DBO1 as the recipients. Transconjugants were selected on dichlorprop mineral medium containing appropriate antibiotics, 1.5% Noble agar, and 300 μg/ml of dichlorprop.

Respirometric experiments

Each strain was grown in dichlorprop medium or glucose medium. Cells were then harvested at 4°C, washed twice, and resuspended in mineral medium. The resuspended cells were kept on ice prior to being added to the respiratory chambers. The initial rates of oxygen uptake were measured with Clark type polarographic oxygen probes of the YSI Model 5300 Biological Oxygen Monitor according to the manufacturers manual (Yellow Springs Instrument Co., Inc, Ohio). The sample chamber contained 100–300 ppm substrate and the equivalent of about 0.4 mg dry wt. bacteria in a total volume of 3.0 ml. The experiments were carried out at 28°C in replicates and the indicated rates of oxygen uptake have been corrected for indigenous respiratory rates measured in the absence of any added substrates. Protein content was measured by the method of Lowry *et al.*, using bovine serum albumin as a standard (Lowry *et al.*, 1951) and activities were expressed as μl O_2/h/mg protein.

PCR amplification of the tfd genes

The partial gene sequences specific to the 2,4-D degradation pathway were amplified by PCR with specific primers targeted for the *tfdA, B,* and *C* genes of the 2,4-D degradative plasmid pJP4 (Don *et al.*, 1985). The PCR cycles and primers for the *tfd* genes were previously reported (Berthelet *et al.*, 1996; Vallaeys *et al.*, 1996; Kamagata *et al.*, 1997). The amplification of the *tfdA, B,* and *C* genes with the corresponding primers was expected to produce a 362 bp, 205 bp, and 361 bp DNA fragment, respectively.

Results

Isolation of dichlorprop-degrading bacteria

Both agricultural soils and golf course soils were subjected to the simple enrichment procedure to isolate dichlorprop-degrading microorganisms. However, none of the 75 agricultural soil samples showed any detectable degradation of dichlorprop during the incubation time. Thus, no organisms able to degrade dichlorprop were purified from any of the agricultural soils. In contrast, 12 of the 17 golf course soils, which had been treated with dichlorprop for several years, exhibited positive degradation of the herbicide. Nine dichlorprop-degrading bacteria were isolated and purified from the positive tubes of 9 different soils (Table 1). Except for strain DP522, which degraded only about 50% of the racemic herbicide, dichlorprop in mineral medium was completely degraded by the isolates, and no dead-end products accumulated during biodegradation of the herbicide when analyzed with high-performance liquid chromatography. Since dichlorprop is highly water-soluble and not volatile, its disappearance is due to microbial degradation. Figure 1 shows typical growth and degradation curves by strain DP535 on dichlorprop medium. However, some enriched cultures failed to produce pure strains able to degrade dichlorprop. When the different colony types from each of these cultures were combined on dichlorprop

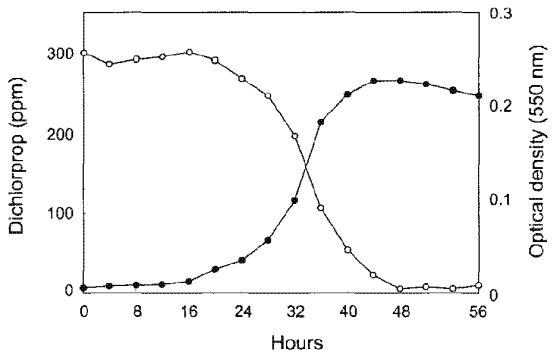


Fig. 1. Disappearance of dichlorprop (○) and growth of strain DP535 (●) during its growth in mineral medium. Each point is the mean for two replicate liquid cultures.

COR-AAD1-00003835
Bayer EX1008 (Part 7 of 9)

Table 1. Nearest relatives of the dichlorprop-degrading isolates based upon 16S rDNA sequence analysis

Isolate[a]	GenBank accession no.	Soil sites	Nearest relative	Similarity(%)[b]
DP522	AY227691	Koyang, Kyongggido	*Sphingomonas agrestis*	98
DP523	AY227692	Koyang, Kyongggido	*Sphingomonas asaccharolytica*	98
DP524	AY227693	Koyang, Kyongggido	*Sphingomonas* sp. CD	99
DP535	AY227694	Kimpo, Kyongggido	*Sphingomonas asaccharolytica*	98
DP542	AY227695	Koyang, Kyongggido	*Sphingomonas agrestis*	98
DP611	AY227696	Chungju, Chungbuk	*Bradyrhizobium* sp.	99
DP622	AY227697	Gwangju, Kyongggido	*Sphingomonas asaccharolytica*	98
DP661	AY227698	Gapyeong, Kyongggido	*Sphingomonas asaccharolytica*	98
DP682	AY227699	Yongin, Kyongggido	*Sphingomonas agrestis*	99
DP51a	AY227700	Yongin, Kyongggido	*Sphingomonas* sp. SRS2	99
DP51b	AY227701	Yongin, Kyongggido	*Herbaspirillum seropedicae*	98
DP52a	AY227702	Koyang, Kyongggido	*Sphingomonas* sp. SRS2	99
DP52b	AY227703	Koyang, Kyongggido	*Herbaspirillum frisingense*	100
DP67a	AY227704	Yongin, Kyongggido	Uncultured eubacterium WR1130	98
DP67b	AY227705	Yongin, Kyongggido	*Herbaspirillum seropedicae*	98

[a]Syntrophic bacteria were denoted by a and b.
[b]Based upon approximately 400 nucleotide positions at the 5' end of the 16S rRNA gene

medium, some mixed cultures were able to grow and mineralize the herbicide. From these mixed cultures, three pairs of presumably syntrophic bacteria (denoted by a and b) capable of degrading dichlorprop were isolated from three different soils (Table 1).

16S rDNA sequence and REP-PCR analyses

When analyzed by 16S rDNA sequences, the isolates were found to be related to members of the genera *Sphingomonas*, *Bradyrhizobium*, and *Herbaspirillum* (Table 1). All of the isolates were Gram-negative and belong to the alpha and beta subgroups of Proteobacteria. Although the dichlorprop-degrading strains were isolated from different soil locations, some isolates were most closely related to the same species, such as *Sphingomonas asaccharolytica* and *Sphingomonas agrestis*. A REP-PCR experiment was performed to study the genomic relatedness among the isolates closely related according to the 16S rDNA sequence analysis (Fig. 2). It was revealed that the 15 isolates produced 12 different DNA fingerprint patterns. An identical REP-PCR pattern was observed for strains DP523, DP535, DP622, and DP661, which were classified as *Sphingomonas asaccharolytica*. Identical patterns indicate that the strains are very closely related or siblings. Since all of the strains were isolated from different soil samples, their detection frequencies reflect their ubiquitousness in the soils examined. Interestingly, the three pairs of syntrophic bacteria produced six different DNA fingerprint patterns (Fig. 2), suggesting that each isolate is a distinct strain.

Growth of dichlorprop-degrading bacteria in axenic cultures

To understand axenic growth patterns of the dichlorprop degraders, the strains were inoculated into racemic dichlorprop medium after growth on the herbicide (inducing) or on PTYG (non-inducing). The growth curves of some representative strains are shown in Figure 3. Among the isolates capable of degrading dichlorprop alone, strains DP523, DP535, DP542, DP622, and DP661 grew quickly on dichlorprop medium, showing short lag period (ca. 16 h). Strains DP522 and DP682 exhibited relatively a longer lag periods (ca. 30 h), and strain DP524 and DP611 showed the longest lag periods (ca. 60−110 h) under uninduced conditions. In contrast, when adapted to dichlorprop metabolism, the isolates degraded the herbicide much more quickly, suggesting that the dichlorprop degradative pathways are inducible by the presence of the herbicide. The inducibility of dichlorprop degradative pathways of the isolates was confirmed in respirometry experiments conducted with adapted or not adapted cells. Respiratory activities on dichlorprop ranged from 42.4 (syntrophic pair DP67ab) to 227.7 (strain DP523) μl O_2/h/mg protein for the isolates grown on dichlorprop, but the cells cultivated on glucose oxidized the herbicide

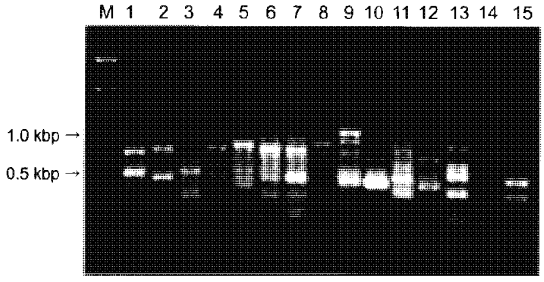


Fig. 2. REP-PCR band patterns of the isolates. Lanes: 1, DP522; 2, DP523; 3, DP524; 4, DP535; 5, DP542; 6, DP622; 7, DP661; 8, DP682; 9, DP611; 10, DP51a; 11, DP51b; 12, DP52a; 13, DP52b; 14, DP67a; 15, DP67b; M, DNA size marker.

COR-AAD1-00003836
Bayer EX1008 (Part 7 of 9)

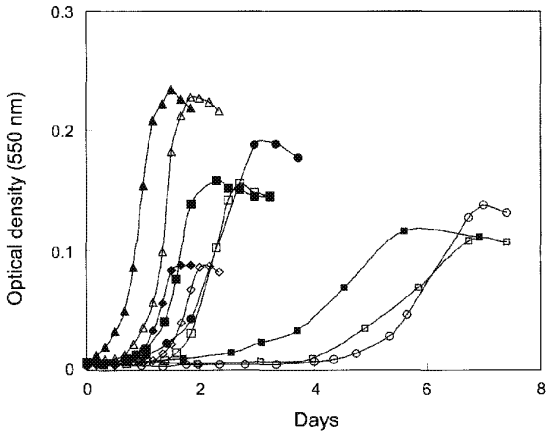


Fig. 3. Growth of dichlorprop-degrading bacteria on racemic dichlorprop. Symbols: ○ and ●, DP611; ◇ and ◆, DP522; □ and ■, DP682; △ and ▲, DP535; □ and ■, DP67ab. The inoculated bacteria were either adapted (solid symbol) or not adapted (open symbol) to dichlorprop metabolism. Each point is the mean for two replicate liquid cultures. OD, optical density.

much more slowly. For the syntrophic bacteria, groups DP51ab, DP52ab, and DP67ab showed a growth pattern similar to each other, exhibiting ca. 96 h of lag period.

Degradative diversity analysis

The isolates were grown on dichlorprop or PTYG medium, and then examined for their ability to degrade other compounds related to dichlorprop. All of the pure isolates capable of degrading dichlorprop independently were also able to mineralize 2,4-D, MCPP, and MCPA, whether they were adapted to dichlorprop metabolism or not (Table 2). When each strain was inoculated into minimal medium containing pure (*R*)-type dichlorprop as the sole carbon source, only strain DP522 of the isolates was not able to degrade and grow on it. In fact, this strain exhibited lower culture absorbance than the other pure isolates. About 50% of the initial racemic dichlorprop was not degraded during the axenic culture experiment. Thus, this strain has enantioselective degradation property on chiral dichlorprop, degrading only (*S*)-type dichlorprop. Interestingly, this strain was also able to degrade MCPB only under dichlorprop-adapted conditions, suggesting

Table 2. Patterns of utilization of substrates by the isolates

Isolate	Pregrowth condition[a]	Substrate[b]					
		2,4-DP	2,4-D	MCPP	MCPA	2,4-DB	MCPB
DP522	A	+	++	+	++	-	++
	U	+	++	+	++	-	-
DP523	A	++	++	++	++	-	-
	U	++	++	++	++	-	-
DP524	A	++	++	++	++	-	-
	U	++	++	++	++	-	-
DP535	A	++	++	++	++	-	-
	U	++	++	++	++	-	-
DP542	A	++	++	++	++	-	-
	U	++	++	++	++	-	-
DP611	A	++	++	++	++	-	-
	U	++	++	++	++	-	-
DP622	A	++	++	++	++	-	-
	U	++	++	++	++	-	-
DP661	A	++	++	++	++	-	-
	U	++	++	++	++	-	-
DP682	A	++	++	++	++	-	-
	U	++	++	++	++	-	-
DP51ab	A	++	++	++	-	++	-
	U	++	++	++	-	++	-
DP52ab	A	++	++	++	++	-	-
	U	++	++	++	++	-	-
DP67ab	A	++	++	-	++	-	-
	U	++	++	-	++	-	-

[a]The isolates were grown on 2,4-DP (A) or PTYG (U) before the test of substrate utilization.

[b]Test for the utilization of substrates. ++, >95% reduction in peak height as determined by UV scanning and substantial growth (optical density at 550 nm > 0.12); +, 40 to 60% reduction in peak height and moderate growth (optical density at 550 nm > 0.08); −, < 15% reduction in peak height and very scant growth (optical density at 550 nm <0.01). 2,4-DP, 2-(2,4-dichlorophenoxy)propionic acid; 2,4-D, 2,4-dichlorophenoxyacetic acid; MCPP, 2-(2-methyl-4-chlorophenoxy)propionic acid; MCPA, 2-methyl-4-chlorophenoxyacetic acid; 2,4-DB, 4-(2,4-dichlorophenoxy)butyric acid; MCPB, 4-(2-methyl-4-chlorophenoxy)butyric acid.

COR-AAD1-00003837
Bayer EX1008 (Part 7 of 9)

Table 3. Respiratory activities of whole cells of representative dichlorprop-degrading bacteria grown on dichlorprop

Substrate[a]	% Respiratory activity of bacterial cells[b]								
	DP522	DP523	DP524	DP542	DP682	DP611	DP51ab	DP52ab	DP67ab
dichlorprop	100 (115.0)	100 (227.7)	100 (102.4)	100 (145.3)	100 (116.3)	100 (109.8)	100 (88.7)	100 (155.9)	100 (42.4)
2,4-D	65	48	44	17	60	19	21	31	44
2,4-DCP	86	54	36	48	86	43	75	16	62
3,5-DCC	62	56	132	62	138	65	58	15	174
Glucose	15	2	12	10	6	4	5	12	6

[a]2,4-D, 2,4-dichlorophenoxyacetic acid; 2,4-DCP, 2,4-dichlorophenol; 3,5-DCC, 3,5-dichlorocatechol.
[b]Respiratory activities in [μl O_2 h^{-1} (mg protein)$^{-1}$] are given in parentheses. The values are the mean of two replicate assays of two independent cultures.

that this compound is probably metabolized because of its structural similarity to dichlorprop or its metabolites. None of the isolates could degrade 2,4-DB.

Each of the two-member communities was also able to degrade 2,4-D as well as dichlorprop syntrophically, while no single organism alone could degrade any of the compounds (Table 2). Interestingly, the DP51ab pair was capable of synergistically mineralizing 2,4-DB, which was not degraded by any of the pure isolates. The group DP52ab showed a similar utilization pattern to the pure isolates capable of independently degrading dichlorprop, while group DP67ab was not able to degrade MCPP.

Respirometric experiments

To investigate the diversity of dichlorprop degradation pathways among the isolates, each strain and the syntrophic pairs were grown on dichlorprop medium or on glucose medium. They were then analyzed for oxygen uptake with various substrates, including the assumed intermediates of dichlorprop, such as 2,4-D, 2,4-DCP and 3,5-DCC (Table 3). Dichlorprop-grown cells of strain DP682 rapidly oxidized dichlorprop, 2,4-D, 2,4-DCP, and 3,5-DCC. This result indicates that this strain degrades dichlorprop through the formation of 2,4-DCP and 3,5-DCC, which has been reported as a degradation pathway for dichlorprop in a *Flavobacterium* sp. strain MH (Horvath *et al.*, 1990). Other isolates, such as DP522, DP523, and DP67ab, exhibited similar oxygen uptake patterns to strain DP682. Strains DP542, DP611, and DP51ab also showed high oxygen consumption with 2,4-DCP and 3,5-DCC, but their oxygen uptake rates with 2,4-D were much lower compared to those of the DP682 type. At present, it is not clear whether dichlorprop is degraded via 2,4-D formed by decarboxylation of the herbicide in DP682 types. On the other hand, syntrophic group DP52ab adapted to dichlorprop metabolism had much lower oxygen consumption with 2,4-DCP and 3,5-DCC, suggesting that this syntrophic pair utilizes dichlorprop using a dissimilar degradation pathway from the DP682 types. Most of the cells grown on dichlorprop showed low oxygen consumption with glucose.

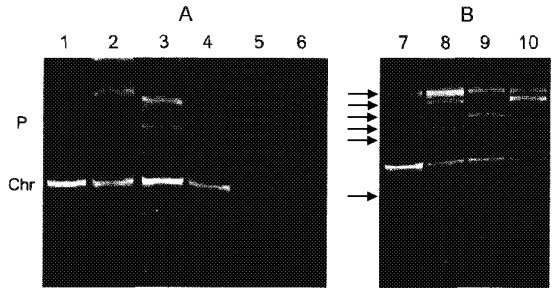


Fig. 4. Plasmid profiles of the isolates. Lanes: 1, DP522; 2, DP524; 3, DP542; 4, DP682; 5, DP51a; 6, DP67a; 7, DP542; 8, DP542-1; 9, DP542-2; 10, DP542-3. P, plasmid band; Chr, chromosomal band. The arrows indicate six plasmid bands.

Plasmid detection and transferability of dichlorprop degradation phenotype

When the isolates were subjected to Kado's plasmid detection procedure, six strains among the 15 isolates exhibited one to six plasmid DNA bands (Fig. 4A). These plasmids were stably maintained in cells cultivated for two months with repeated transfers in Luria-Bertani medium and were not easily cured with sodium dodecyl sulfate, except strain DP542. Initially, strain DP542 was able to degrade both (*S*)-and (*R*)-enantiomers of dichlorprop and MCPP. However, when the second and the sixth plasmids from the top were lost (Fig. 4B, lane 9), the cured strain DP542-2 could not degrade (*R*)-type enantiomers any more. Since cured strains (DP542-1 and DP542-3) without the third or the fourth plasmid (Fig. 4B, lanes 8 and 10) were still able to degrade the herbicides completely, the second and the sixth plasmids appeared to have crucial roles in degradation of (*R*)-type dichlorprop and MCPP in strain DP542. When the isolates containing plasmid were mated with two antibiotic-resistant recipients, *Pseudomonas cepacia* DBO1 and *Alcaligenes eutrophus* JMP228, the dichlorprop degradation phenotype was not transferred to any of the two recipients at a detectable frequency ($<10^{-9}$) from any of the isolates.

PCR amplification of the tfd genes

COR-AAD1-00003838
Bayer EX1008 (Part 7 of 9)

Since all of the pure isolates and the syntrophic pairs were able to degrade 2,4-D as well as dichlorprop, we investigated whether the isolates have any *tfd*-like genes of the 2,4-D degradative plasmid pJP4. When PCR amplification was performed for every isolate using specific primers selected from the internal sequences of the *tfdA*, *B*, and *C* genes, none of the isolates exhibited any PCR DNA bands (data not shown). The results indicate that the genes involved in 2,4-D degradation in these isolates do not have any significant homology with the well-known *tfd* genes of the 2,4-D degradative plasmid pJP4 (Don *et al.*, 1985).

Discussion

We isolated dominant dichlorprop-degrading bacteria from golf course soils and analyzed their diversity and properties on dichlorprop degradation. Unlike 2,4-D and MCPA, which are easily degraded by soil microorganisms, dichlorprop and MCPP have a propionic acid side chain linked to the chiral carbon atom, which decreases the susceptibility of the herbicide to microbial attack (Alexander and Aleem, 1961). It usually takes a long time to enrich microbial cultures able to degrade dichlorprop or MCPP, and many of the researches have had to use soil-column techniques and chemostat cultures to enrich them (Lappin *et al.*, 1985; Horvath *et al.*, 1990). The inability to easily isolate pure cultures capable of degrading dichlorprop or MCPP suggested that the soil microorganisms possessing the complete degradative pathway required to mineralize the herbicides are very rare in natural environments (Tett *et al.*, 1994). This was true for the agricultural soils tested in this work, showing no positive degradation of dichlorprop in all of the 75 different agricultural soil samples. In contrast, about 70% of the golf course soil samples exhibited positive degradation of the herbicide, and thus nine strains able to independently mineralize dichlorprop and three pairs of syntrophic degraders were readily isolated from these soils with a simple enrichment procedure. The results suggest that the dichlorprop-degrading microorganisms are ubiquitous in the soils routinely treated with dichlorprop, while they are very rare in the environments with no history of dichlorprop amendments.

Most of the previous dichlorprop- and MCPP-degrading microorganisms were isolated through long periods of subcultivation from multi-membered mixed cultures, suggesting that the degradative pathway of the herbicide in a pure culture resulted from the combination of the genetic information of several organisms in the mixed culture (Horvath *et al.*, 1990; Tett *et al.*, 1994). Genes specifying biodegradation of the pesticides are often contained on plasmids, which can facilitate the transfer of genetic information among microbial populations (Pemberton *et al.*, 1979). Among our isolates independently capable of degrading dichlorprop, most strains possessed one to six plasmids and only two species, *S. asaccharolytica* and *Bradyrhizobium* sp., did not show any plasmid DNA (Fig. 4), suggesting that the plasmids could have crucial roles in development of the dichlorprop degradative pathway. It is of note that strain DP542 harbored six different plasmids. This strain was initially able to mineralize 2,4-D, MCPA, and both (*R*)-and (*S*)-enantiomers of dichlorprop and MCPP. However, the cured strain without the second and the sixth plasmids could not degrade the (*R*)-enantiomers of the herbicides any more. The results suggest that the degradation of each enantiomer is catalyzed by each specific enzyme and the genetic information required for enantioselective degradation of the herbicides is on the separate plasmid in strain DP542.

The herbicidally active (*R*)-type enantiomers of dichlorprop and MCPP were found to be more slowly degraded than the inactive (*S*)-type enantiomers in environmental samples (Heron and Christensen, 1992; Müller and Buser, 1997). However, it is not yet known which enantiomer is perferentially utilized as a carbon and energy source by pure cultures. In the case of MCPP, both enantiomers were used as growth substrates by *S. herbicidovorans*, while *Alcaligenes denitrificans* degraded only the (*R*)-type enantiomer (Tett *et al.*, 1994; Zipper *et al.*, 1996). In our study, all of the isolates were able to utilize both enantiomers as growth substrates, except strain DP522 which could not mineralize the (*R*)-enantiomer. The results indicate that the microorganisms capable of degrading both enantiomers of the herbicides are dominant in natural environments, while the microbial populations degrading only one type of enantiomer could be rare.

All of our isolates and syntrophic pairs could degrade 2,4-D, in addition to dichlorprop, but none of them gave any PCR-amplified DNA bands with any of the primers of the *tfdA*, *B*, and *C* genes. It has been reported that about 25% of the forty-seven 2,4-D-degrading bacteria isolated under 2,4-D selection had all of the *tfdA, B, C*, and *D* genes (Ka *et al.*, 1994). Our results suggest that the isolates, which were isolated under dichlorprop selection, utilize 2,4-D using dissimilar degradative genes from those of the previously described 2,4-D-degrading strains, and thus that different groups of microorganisms are enriched depending on the applied selection, even though the enriched strains share a common property of degrading the same compound.

Acknowledgments

This study was in part supported by the BioGreen 21 Project.

References

Aberg, B. 1956. On the effects of para-substitution in some plant

COR-AAD1-00003839
Bayer EX1008 (Part 7 of 9)

growth regulators with phenyl nuclei, pp. 93-116. *In* R.L. Wain and F. Wightman (Eds.), The Chemistry and Mode of Action of Plant Growth Substances. Butterworth Scientific Publications, London

Alexander, M. 1965. Biodegradation: problems of molecular recalcitrance and microbial fallibility. *Adv. Appl. Microbiol.* 7, 35-80.

Alexander, M. and M.I.H. Aleem. 1961. Effect of chemical structure on microbial decomposition of aromatic herbicides. *J. Agric. Food Chem.* 9, 44-47.

Altschul, S.F., W. Gish, W. Miller, E.W. Myers, and D.J. Lipman. 1990. Basic local alignment tool. *J. Mol. Biol.* 215, 403-410.

Biederbeck, V.O., C.A. Campbell, and A.E. Smith. 1987. Effects of long-term 2,4-D field applications on soil biochemical processes. *J. Environ. Qual.* 16, 257-262.

Berthelet, M., L.G. Whyte, and C.W. Greer. 1996. Rapid, direct extraction of DNA from soils for PCR analysis using polyvinylpolypyrrolidone spin columns. *FEMS Microbiol. Lett.* 138, 17-22.

Chung, M.J. and J.O. Ka. 1998. Isolation and characterization of 2,4-dichlorophenoxyacetic acid-degrading bacteria from paddy soils. *J. Microbiol.* 36(4), 256-261.

Crosa, J.H., M.E. Tolmasky, L.A. Actis, and S. Falkow. 1994. Plasmids, p. 365-386. *In* P. Gerhardt, R.G.E. Murray, W.A. Wood, and N.R. Krieg (eds.), Methods for General and Molecular Bacteriology. Am. Soc. Microbiol., Washington.

de Bruijn, F.J. 1992. Use of repetitive (repetitive extragenic palindromic and enterobacterial repetitive intergeneric consensus) sequences and the polymerase chain reaction to fingerprint the genomes of *Rhizobium meliloti* isolates and other soil bacteria. *Appl. Environ. Microbiol.* 58, 2180-2187.

Don, R.H., A.J. Weightman, H.-J. Knackmuss, and K.N. Timmis. 1985. Transposon mutagenesis and cloning analysis of the pathways for degradation of 2,4-dichlorophenoxyacetic acid and 3-chlorobenzoate in *Alcaligenes eutrophus* JMP134(pJP4). *J. Bacteriol.* 161, 85-90.

Foster, R.K. and R.B. Mckercher. 1973. Laboratory incubation studies of chlorophenoxyacetic acids in chernozemic soils. *Soil Biol. Biochem.* 5, 333-337.

Heron, G. and T.H. Christensen. 1992. Degradation of the herbicide mecoprop in an aerobic aquifer determined by laboratory batch studies. *Chemosphere* 24, 547-557.

Horvath, M., G. Ditzelmüller, M. Loidl, and F. Streichsbier. 1990. Isolation and characterization of a 2-(2,4-dichlorophenoxy)propionic acid-degrading soil bacterium. *Appl. Microbiol. Biotechnol.* 33, 213-216.

Hugenholtz, P., C. Pitulle, K.L. Hershberger, and N.R. Pace. 1998. Novel division level bacterial diversity in a Yellowstone hot spring. *J. Bacteriol.* 180, 366-376.

Ka, J.O., W.E. Holben, and J.M. Tiedje. 1994. Genetic and phenotypic diversity of 2,4-dichlorophenoxyacetic acid (2,4-D)-degrading bacteria isolated from 2,4-D-treated field soils. *Appl. Environ. Microbiol.* 60, 1106-1115.

Ka, J.O. and J.M. Tiedje. 1994. Integration and excision of a 2,4-dichlorophenoxyacetic acid-degradative plasmid in *Alcaligenes paradoxus* and evidence of its natural intergeneric transfer. *J. Bacteriol.* 176, 5284-5289.

Kado, C.I. and S.T. Liu. 1981. Rapid procedure for detection and isolation of large and small plasmids. *J. Bacteriol.* 145, 1365-1373.

Kamagata, Y., R.A. Fulthorpe, K. Tamura, H. Takami, L.J. Forney, and J.M. Tiedje. 1997. Pristine environments harbor a new group of oligotrophic 2,4-dichlorophenoxyacetic acid-degrading bacteria. *Appl. Environ. Microbiol.* 63, 2266-2272.

Lane, D.J. 1991. 16S/23S rRNA sequencing, pp. 115-148. *In* E. Stackebrandt and M. Goodfellow (Eds.), Nucleic Acid Techniques in Bacterial Systematics. John Wiley and Sons, England.

Lappin, H.M., M.P. Greaves, and J.H. Slater. 1985. Degradation of the herbicide mecoprop [2-(2-methyl-4-chlorophenoxy)propionic acid] by a synergistic microbial community. *Appl. Environ. Microbiol.* 49, 429-433.

Loos, M.A., R.N. Roberts, and M. Alexander. 1967. Phenols as intermediates in the decomposition of phenoxyacetates by an *Arthrobacter* species. *Can. J. Microbiol.* 13, 679-690.

Loos, M.A., I.F. Schlosser, and W.R. Mapham. 1979. Phenoxy herbicide degradation in soils: quantitative studies of 2,4-D and MCPA-degrading microbial populations. *Soil Biol. Biochem.* 1, 377-385.

Lowry, O.H., N.J. Rosebrough, A.L. Farr, and R.J. Randall. 1951. Protein measurement with the Folin phenol reagent. *J. Biol. Chem.* 193, 265-275.

Maidak, B.L., J.R. Cole, T.G. Lilburn, C.T. Parker Jr, P.R. Saxman, J.M. Stredwick, G.M. Garrity, B. Li, G.J. Olsen, S. Pramanik, T.M. Schmidt, and J.M. Tiedje. 2000. The RDP (Ribosomal Database Project) continues. *Nucleic Acids Res.* 28(1), 173-174.

Müller, M.D. and H. Buser. 1997. Conversion reactions of various phenoxyalkanoic acid herbicides in soil. 1. Enantiomerization and enantioselective degradation of the chiral 2-phenoxypropionic acid herbicides. *Environ. Sci. Technol.* 31, 1953-1959.

Pemberton, J.M., B. Corney, and R.H. Don. 1979. Evolution and spread of pesticide degrading ability among soil microorganisms, pp. 287-299. *In* K.N. Timmis and A. Puhler (Eds.), Plasmids of Medical, Environmental and Commercial Importance. Elsevier/North-Holland Biomedical Press, Amsterdam.

Pieper, D.H., W. Reineke, K.-H. Engesser, and H.-J. Knackmuss. 1988. Metabolism of 2,4-dichlorophenoxyacetic acid, 4-chloro-2-methylphenoxyacetic acid and 2-methylphenoxyacetic acid by *Alcaligenes eutrophus* JMP134. *Arch. Microbiol.* 150, 95-102.

Smith, A.E. and A.J. Aubin. 1991. Effects of long-term 2,4-D and MCPA field applications on the soil breakdown of 2,4-D, MCPA, mecoprop, and 2,4,5-T. *J. Environ. Qual.* 20, 436-438.

Smith, A.E. and B.J. Hayden. 1981. Relative persistence of MCPA, MCPB and mecoprop in Saskatchewan soils, and the identification of MCPA in MCPB-treated soils. *Weed Res.* 21, 179-183.

Tett, V.A., A.J. Willetts, and H.M. Lappin-Scott. 1994. Enantioselective degradation of the herbicide mecoprop [2-(2-methyl-4-chlorophenoxy)propionic acid] by mixed and pure bacterial cultures. *FEMS Microbiol. Ecol.* 14, 191-200.

Torstensson, N.T.L., J. Stark, and B. Goransson. 1975. The effect of repeated applications of 2,4-D and MCPA on their breakdown in soil. *Weed Res.*15,159-164.

Vallaeys,T., R.R. Fulthorpe, A.M. Wright, and G. Soulas. 1996. The metabolic pathway of 2,4-dichlorophenoxyacetic acid degradation involves different families of *tfdA* and *tfdB* genes according to PCR-RFLP analysis. *FEMS Microbiol. Ecol.* 20, 163-172.

COR-AAD1-00003840
Bayer EX1008 (Part 7 of 9)

Versalovic, J., M. Schneider, F.J. de Bruijn, and J.R. Lupski. 1994. Genomic fingerprinting of bacteria using repetitive sequence-based polymerase chain reaction. *Methods Mol. Cell Biol.* 5, 25-40.

Willetts, N.S. 1988. Conjugation. *Methods Microbiol.* 21, 49-77.

Zipper, C., K. Nickel, W. Angst, and H.-P.E. Kohler. 1996. Complete microbial degradation of both enantiomers of the chiral herbicide mecoprop ((*RS*)-2-(4-chloro-2-methylphenoxy) propionic acid) in an enantioselective manner by *Sphingomonas herbicidovorans* sp. nov. *Appl. Environ. Microbiol.* 62, 4318-4322.

COR-AAD1-00003841
Bayer EX1008 (Part 7 of 9)

UNITED STATES PATENT AND TRADEMARK OFFICE

UNITED STATES DEPARTMENT OF COMMERCE
United States Patent and Trademark Office
Address: COMMISSIONER FOR PATENTS
P.O. Box 1450
Alexandria, Virginia 22313-1450
www.uspto.gov

APPLICATION NO.	FILING DATE	FIRST NAMED INVENTOR	ATTORNEY DOCKET NO.	CONFIRMATION NO.
15/288,406	10/07/2016	Terry WRIGHT	14764-258662	5402

107540 7590 12/08/2020
Barnes & Thornburg LLP (Dow)
11 South Meridian Street
Indianapolis, IN 46204

EXAMINER
KRUSE, DAVID H

ART UNIT	PAPER NUMBER
1663	

NOTIFICATION DATE	DELIVERY MODE
12/08/2020	ELECTRONIC

Please find below and/or attached an Office communication concerning this application or proceeding.

The time period for reply, if any, is set in the attached communication.

Notice of the Office communication was sent electronically on above-indicated "Notification Date" to the following e-mail address(es):

INDocket@btlaw.com

COR-AAD1-00003842
Bayer EX1008 (Part 7 of 9)

Office Action Summary	Application No. 15/288,406	Applicant(s) WRIGHT et al.	
	Examiner DAVID H KRUSE	Art Unit 1663	AIA (FITF) Status No

-- The MAILING DATE of this communication appears on the cover sheet with the correspondence address --

Period for Reply

A SHORTENED STATUTORY PERIOD FOR REPLY IS SET TO EXPIRE 3 MONTHS FROM THE MAILING DATE OF THIS COMMUNICATION.

- Extensions of time may be available under the provisions of 37 CFR 1.136(a). In no event, however, may a reply be timely filed after SIX (6) MONTHS from the mailing date of this communication.
- If NO period for reply is specified above, the maximum statutory period will apply and will expire SIX (6) MONTHS from the mailing date of this communication.
- Failure to reply within the set or extended period for reply will, by statute, cause the application to become ABANDONED (35 U.S.C. § 133). Any reply received by the Office later than three months after the mailing date of this communication, even if timely filed, may reduce any earned patent term adjustment. See 37 CFR 1.704(b).

Status

1)☑ Responsive to communication(s) filed on 09 September 2020.

☐ A declaration(s)/affidavit(s) under **37 CFR 1.130(b)** was/were filed on _____.

2a)☑ This action is **FINAL.** 2b) ☐ This action is non-final.

3)☐ An election was made by the applicant in response to a restriction requirement set forth during the interview on _____; the restriction requirement and election have been incorporated into this action.

4)☐ Since this application is in condition for allowance except for formal matters, prosecution as to the merits is closed in accordance with the practice under *Ex parte Quayle*, 1935 C.D. 11, 453 O.G. 213.

Disposition of Claims*

5) ☑ Claim(s) 15-16 and 18-49 is/are pending in the application.

5a) Of the above claim(s) _____ is/are withdrawn from consideration.

6) ☐ Claim(s) _____ is/are allowed.

7) ☑ Claim(s) 15-16 and 18-49 is/are rejected.

8) ☐ Claim(s) _____ is/are objected to.

9) ☐ Claim(s) _____ are subject to restriction and/or election requirement

* If any claims have been determined allowable, you may be eligible to benefit from the **Patent Prosecution Highway** program at a participating intellectual property office for the corresponding application. For more information, please see http://www.uspto.gov/patents/init_events/pph/index.jsp or send an inquiry to **PPHfeedback@uspto.gov.**

Application Papers

10)☐ The specification is objected to by the Examiner.

11)☐ The drawing(s) filed on _____ is/are: a)☐ accepted or b)☐ objected to by the Examiner.

Applicant may not request that any objection to the drawing(s) be held in abeyance. See 37 CFR 1.85(a).

Replacement drawing sheet(s) including the correction is required if the drawing(s) is objected to. See 37 CFR 1.121(d).

Priority under 35 U.S.C. § 119

12)☐ Acknowledgment is made of a claim for foreign priority under 35 U.S.C. § 119(a)-(d) or (f).

Certified copies:

a)☐ All b)☐ Some** c)☐ None of the:

1.☐ Certified copies of the priority documents have been received.

2.☐ Certified copies of the priority documents have been received in Application No. _____.

3.☐ Copies of the certified copies of the priority documents have been received in this National Stage application from the International Bureau (PCT Rule 17.2(a)).

** See the attached detailed Office action for a list of the certified copies not received.

Attachment(s)

1) ☐ Notice of References Cited (PTO-892)

2) ☑ Information Disclosure Statement(s) (PTO/SB/08a and/or PTO/SB/08b) Paper No(s)/Mail Date _____.

3) ☐ Interview Summary (PTO-413) Paper No(s)/Mail Date _____.

4) ☐ Other: _____.

Status of the Application

1. This Office action is in response to the Response filed 9 September 2020.

2. The rejection under 35 USC 112, first paragraph, for lack of written description is withdrawn in view of Applicant's response and the evidence made of record attached to the Applicant Initiated Interview Summary mailed 31 August 2020. Said evidence demonstrated variants of instant SEQ ID NO: 9 produced by truncations of both the N and C termini that retain the claimed function and that would describe the variation within the claimed genus. Further, these variants were described on page 34, paragraph 00141, of the instant Specification.

3. The rejection under 35 USC 103(a) is withdrawn in view of Applicant's Response. Specifically the ability of the AAD-1 gene to produce herbicide tolerance in a transgenic plant cell to two distinct type of herbicides.

Double Patenting

4. The nonstatutory double patenting rejection is based on a judicially created doctrine grounded in public policy (a policy reflected in the statute) so as to prevent the unjustified or improper time-wise extension of the "right to exclude" granted by a patent and to prevent possible harassment by multiple assignees. A nonstatutory double patenting rejection is appropriate where the conflicting claims are not identical, but at least one examined application claim is not patentably distinct from the reference claim(s) because the examined application claim is either anticipated by, or would have been obvious over, the reference claim(s). See, e.g., *In re Berg*, 140 F.3d 1428, 46 USPQ2d 1226 (Fed. Cir. 1998); *In re Goodman*, 11 F.3d 1046, 29 USPQ2d 2010 (Fed. Cir. 1993); *In re Longi*, 759 F.2d 887, 225 USPQ 645 (Fed. Cir. 1985); *In re Van Ornum*,

686 F.2d 937, 214 USPQ 761 (CCPA 1982); *In re Vogel*, 422 F.2d 438, 164 USPQ 619 (CCPA 1970); *In re Thorington*, 418 F.2d 528, 163 USPQ 644 (CCPA 1969).

A timely filed terminal disclaimer in compliance with 37 CFR 1.321(c) or 1.321(d) may be used to overcome an actual or provisional rejection based on nonstatutory double patenting provided the reference application or patent either is shown to be commonly owned with the examined application, or claims an invention made as a result of activities undertaken within the scope of a joint research agreement. See MPEP § 717.02 for applications subject to examination under the first inventor to file provisions of the AIA as explained in MPEP § 2159. See MPEP § 2146 *et seq.* for applications not subject to examination under the first inventor to file provisions of the AIA. A terminal disclaimer must be signed in compliance with 37 CFR 1.321(b).

The USPTO Internet website contains terminal disclaimer forms which may be used. Please visit www.uspto.gov/patent/patents-forms. The filing date of the application in which the form is filed determines what form (e.g., PTO/SB/25, PTO/SB/26, PTO/AIA/25, or PTO/AIA/26) should be used. A web-based e-Terminal Disclaimer may be filled out completely online using web-screens. An e-Terminal Disclaimer that meets all requirements is auto-processed and approved immediately upon submission. For more information about e-Terminal Disclaimers, refer to www.uspto.gov/patents/process/file/efs/guidance/eTD-info-I.jsp.

5. Claims 15, 16 and 18-49 remain rejected on the ground of nonstatutory double patenting as being unpatentable over claims 1-43 of U.S. Patent No. 7,838,733. Although the claims at issue are not identical, they are not patentably distinct from each other because the genus claimed in the '733 Patent represents a subgenus of the

instantly claimed invention and thus both anticipates and renders obvious the instantly claimed invention.

Applicant states that Applicant will file the necessary terminal disclaimer to overcome the rejection upon a finding of allowable subject matter (page 8, 3rd paragraph of the Remarks). Because the instant rejection is not provisional it is maintained for the reasons of record.

6. Claims 15, 16 and 18-49 remain rejected on the ground of nonstatutory double patenting as being unpatentable over claims 1-22 of U.S. Patent No. 9,127,289. Although the claims at issue are not identical, they are not patentably distinct from each other because the genus claimed in the '289 Patent represents a subgenus of the instantly claimed invention and thus both anticipates and renders obvious the instantly claimed invention.

Applicant states that Applicant will file the necessary terminal disclaimer to overcome the rejection upon a finding of allowable subject matter (page 8, 3rd paragraph of the Remarks). Because the instant rejection is not provisional it is maintained for the reasons of record.

7. Claims 15, 16 and 18-49 remain rejected on the ground of nonstatutory double patenting as being unpatentable over claims 1-13 of U.S. Patent No. 10,174,337 (which issued from US Patent Application 14/820,893). Although the claims at issue are not identical, they are not patentably distinct from each other because the genus claimed in the '337 patent represents a subgenus of the instantly claimed invention and thus both anticipates and renders obvious the instantly claimed invention.

This rejection has been modified because the Application has issued as a U.S. Patent. Applicant states that Applicant will file the necessary terminal disclaimer to overcome the rejection upon a finding of allowable subject matter (page 8, 3rd paragraph of the Remarks). Because the instant rejection is not provisional it is maintained for the reasons of record.

Conclusion

8. **THIS ACTION IS MADE FINAL.** Applicant is reminded of the extension of time policy as set forth in 37 CFR 1.136(a).

A shortened statutory period for reply to this final action is set to expire THREE MONTHS from the mailing date of this action. In the event a first reply is filed within TWO MONTHS of the mailing date of this final action and the advisory action is not mailed until after the end of the THREE-MONTH shortened statutory period, then the shortened statutory period will expire on the date the advisory action is mailed, and any extension fee pursuant to 37 CFR 1.136(a) will be calculated from the mailing date of the advisory action. In no event, however, will the statutory period for reply expire later than SIX MONTHS from the mailing date of this final action.

9. No claims are allowed.

10. Any inquiry concerning this communication or earlier communications from the examiner should be directed to David H. Kruse, Ph.D. whose telephone number is (571) 272-0799 and direct fax number (571) 273-0799. The examiner can normally be reached on Monday to Friday from 7:30 a.m. to 4:00 p.m.

If attempts to reach the examiner by telephone are unsuccessful, the examiner's supervisor, Amjad Abraham can be reached at (571) 270-7058. The central FAX number for official correspondence is 571-273-8300.

Any inquiry of a general nature or relating to the status of this application or proceeding should be directed to the Group Receptionist whose telephone number is (571) 272-1600.

/David H Kruse/
Primary Examiner, Art Unit 1663

Search Notes	Application/Control No.	Applicant(s)/Patent Under Reexamination
	15/288,406	WRIGHT et al.
	Examiner	Art Unit
	DAVID H KRUSE	1663

CPC - Searched*		
Symbol	Date	Examiner
C12N 9/0069	11/07/2018	/DK/

CPC Combination Sets - Searched*		
Symbol	Date	Examiner

US Classification - Searched*			
Class	Subclass	Date	Examiner

* See search history printout included with this form or the SEARCH NOTES box below to determine the scope of the search.

Search Notes		
Search Notes	Date	Examiner
Inventor Name Search	11/07/2018	/DK/
EAST: USPAT, USPGPUB, EPO, JPO, DERWENT	11/07/2018	/DK/
STN: AGRICOLA, BIOSIS, CAPLUS, EMBASE, CABA	11/07/2018	/DK/
Sequence Search of SEQ ID NO: 9	10/30/2018	/DK/
Update EAST	07/05/2019	/DK/
Update EAST	03/04/2020	/DK/
Update EAST	11/25/2020	/DK/
Sequence Search of SEQ ID NO: 9, included interference search	12/01/2020	/DK/

/DAVID H KRUSE/ Primary Examiner, Art Unit 1663	

COR-AAD1-00003849
Bayer EX1008 (Part 7 of 9)

Search Notes	Application/Control No.	Applicant(s)/Patent Under Reexamination
	15/288,406	WRIGHT et al.
	Examiner	Art Unit
	DAVID H KRUSE	1663

Interference Search			
US Class/CPC Symbol	US Subclass/CPC Group	Date	Examiner

/DAVID H KRUSE/ Primary Examiner, Art Unit 1663	

COR-AAD1-00003850
Bayer EX1008 (Part 7 of 9)

EAST Search History

EAST Search History (Prior Art)

Ref #	Hits	Search Query	DBs	Default Operator	Plurals	Time Stamp
L1	60	aad-1.clm.	US-PGPUB; USPAT; USOCR; FPRS; EPO; JPO; DERWENT	OR	OFF	2020/11/25 10:56
L2	17	dichlorophenoxypropionate with dioxygenase	US-PGPUB; USPAT; USOCR; FPRS; EPO; JPO; DERWENT	OR	OFF	2020/11/25 10:56
S1	688	aad-1	US-PGPUB; USPAT; USOCR; FPRS; EPO; JPO; DERWENT	OR	OFF	2018/11/07 08:20
S2	48	aad-1.clm.	US-PGPUB; USPAT; USOCR; FPRS; EPO; JPO; DERWENT	OR	OFF	2018/11/07 08:21
S3	14	dichlorophenoxypropionate with dioxygenase	US-PGPUB; USPAT; USOCR; FPRS; EPO; JPO; DERWENT	OR	OFF	2018/11/07 08:36
S4	15	dichlorophenoxypropionate with dioxygenase	US-PGPUB; USPAT; USOCR; FPRS; EPO; JPO; DERWENT	OR	OFF	2019/07/05 10:38
S5	1	("10323287").PN.	USPAT; USOCR	OR	OFF	2019/07/05 10:39
S6	1	("10174337").PN.	USPAT; USOCR	OR	OFF	2019/07/05 12:38
S7	54	aad-1.clm.	US-PGPUB; USPAT; USOCR; FPRS; EPO; JPO; DERWENT	OR	OFF	2020/03/04 12:46
S8	16	dichlorophenoxypropionate with dioxygenase	US-PGPUB; USPAT; USOCR; FPRS; EPO; JPO; DERWENT	OR	OFF	2020/03/04 12:46
S9	859	aad-1	US-PGPUB; USPAT; USOCR; FPRS; EPO; JPO; DERWENT	OR	OFF	2020/03/04 12:46
S10	1	("20030041357").PN.	US-PGPUB; USPAT; USOCR	OR	OFF	2020/03/05 12:37

EAST Search History (Interference)

<This search history is empty>

11/25/2020 10:58:26 AM
C:\Users\dkruse\Documents\EAST\Workspaces\15288406.wsp

BARNES & THORNBURG LLP

11 South Meridian Street
Indianapolis, Indiana 46204
(317) 236-1313

PATENT APPLICATION

IN THE UNITED STATES PATENT AND TRADEMARK OFFICE

Customer No.:	107540
Group:	1663
Confirmation No.:	5402
Application No.:	15/288,406
Invention:	**NOVEL HERBICIDE RESISTANCE GENES**
Applicant:	Terry Wright et al.
Filed:	October 7, 2016
Attorney Docket:	14764-258662
Examiner	David Kruse

FILED ELECTRONICALLY:

January 10, 2020

SUPPLEMENTAL INFORMATION DISCLOSURE STATEMENT

Mail Stop Amendment
Commissioner for Patents
P.O. Box 1450
Alexandria, Virginia 22313-1450

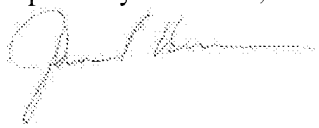
Sir:

This Statement is filed pursuant to 37 C.F.R. § 1.56. No representation is intended that a complete search has been made of the prior art or that no better art references than the references cited in this IDS are available. The filing of this IDS shall not be construed to be an admission that the information cited in the IDS is, or is considered to be, material to patentability as defined in §1.56(b). Pursuant to 37 C.F.R. § 1.98(a)(2)(ii), copies of cited U.S. patents and patent publications are not provided herewith; a copy of each cited foreign and non-patent reference is provided herewith for review by the Examiner.

As this IDS is being filed with an accompanying RCE, applicant believe no fees are required for this filing. However, the Commissioner is hereby authorized to charge any fee necessary to affect this filing to our Deposit Account No. 10-0435, with reference to our Matter No. 14764-258662.

Consideration of the claims, leading to their allowance and passage of the application to issuance, is respectfully requested. If any further discussion of this matter would speed prosecution of this application, the Examiner is invited to call the undersigned at (434) 220-2866.

Respectfully submitted,



John P. Breen
Registration No. 38,833
Attorney for Applicants

JPB:glt
(317) 261-7940
Indianapolis, Indiana 46204

COR-AAD1-00003854
Bayer EX1008 (Part 7 of 9)

SHEET 1 of 1

Form PTO-1449 (Modified)	Atty. Docket No.	Serial No.
INFORMATION DISCLOSURE STATEMENT	14764-258662	15/288,406
	Applicant(s) Terry Wright et al.	
	Filing Date October 7, 2016	Art Unit 1663

ALL REFERENCES CONSIDERED EXCEPT WHERE LINED THROUGH. /D.H.K/

U.S. PATENT DOCUMENTS

Examiner Initials	Document Number	Issue or Publication Date	Name	Class	Subclass	Filing Date (If Appropriate)

FOREIGN PATENT DOCUMENTS

Examiner Initials	Document Number	Publication Date	Country	Translation Yes	Translation No

OTHER DOCUMENTS

	Schleinitz et al., Appl. Env. Microbiol. 70:5357-5365, 2004
	Müller et al, Protein Science (2006), 15:1356–1368
	Hotopp et al, Biochemistry 2002, 41, 9787-9794

ALL REFERENCES CONSIDERED EXCEPT WHERE LINED THROUGH. /D.H.K/

EXAMINER: /DAVID H KRUSE/	DATE CONSIDERED: 03/03/2020

Doc code: IDS
Doc description: Information Disclosure Statement (IDS) Filed

PTO/SB/08a (02-18)
Approved for use through 11/30/2020. OMB 0651-0031
U.S. Patent and Trademark Office; U.S. DEPARTMENT OF COMMERCE

Under the Paperwork Reduction Act of 1995, no persons are required to respond to a collection of information unless it contains a valid OMB control number.

INFORMATION DISCLOSURE STATEMENT BY APPLICANT

(Not for submission under 37 CFR 1.99)

Application Number	15288406
Filing Date	2016-10-07
First Named Inventor	Terry Wright
Art Unit	1663
Examiner Name	KRUSE, David H.
Attorney Docket Number	14764-258662

ALL REFERENCES CONSIDERED EXCEPT WHERE LINED THROUGH. /D.H.K/

U.S.PATENTS Remove

Examiner Initial*	Cite No	Patent Number	Kind Code[1]	Issue Date	Name of Patentee or Applicant of cited Document	Pages, Columns, Lines where Relevant Passages or Relevant Figures Appear
	1	5910626		1999-06-08	Haselkorn and Gornicki	
	2	6087563		2000-07-11	DellaPenna and Norris	
	3	6107549		2000-08-22	Feng et al.	
	4	6268547		2001-07-31	Weeks	
	5	7405074		2008-07-29	Castle et al.	
	6	7462481		2008-12-09	Castle et al.	
	7	7659448		2010-02-09	Ahrens et al.	
	8	7863503		2011-01-04	Castle et al.	

/DAVID H KRUSE/ 11/25/2020

INFORMATION DISCLOSURE STATEMENT BY APPLICANT (Not for submission under 37 CFR 1.99)		
	Application Number	15288406
	Filing Date	2016-10-07
	First Named Inventor	Terry Wright
	Art Unit	1663
	Examiner Name	KRUSE, David H.
	Attorney Docket Number	14764-258662

ALL REFERENCES CONSIDERED EXCEPT WHERE LINED THROUGH. /D.H.K/

	9	7998703		2011-08-16	Castle et al.	
	10	8222489		2012-07-17	Castle et al.	
	11	9074007		2015-07-07	Danilevskaya et al,	

If you wish to add additional U.S. Patent citation information please click the Add button. Add

U.S.PATENT APPLICATION PUBLICATIONS Remove

Examiner Initial*	Cite No	Publication Number	Kind Code[1]	Publication Date	Name of Patentee or Applicant of cited Document	Pages,Columns,Lines where Relevant Passages or Relevant Figures Appear
	1	20020059659		2002-05-16	Stemmer	
	2	20030056245		2003-03-20	Chatterjee et al.	
	3	20090069182		2009-03-12	Castle et al.	
	4	20120245339		2012-09-27	Castle et al.	
	5	20140325713		2014-10-30	Kovalic et al.	

If you wish to add additional U.S. Published Application citation information please click the Add button. Add

FOREIGN PATENT DOCUMENTS Remove

/DAVID H KRUSE/ 11/25/2020

INFORMATION DISCLOSURE STATEMENT BY APPLICANT (Not for submission under 37 CFR 1.99)		
	Application Number	15288406
	Filing Date	2016-10-07
	First Named Inventor	Terry Wright
	Art Unit	1663
	Examiner Name	KRUSE, David H.
	Attorney Docket Number	14764-258662

ALL REFERENCES CONSIDERED EXCEPT WHERE LINED THROUGH. /D.H.K/

Examiner Initial*	Cite No	Foreign Document Number[3]	Country Code[2] ¡	Kind Code[4]	Publication Date	Name of Patentee or Applicant of cited Document	Pages,Columns,Lines where Relevant Passages or Relevant Figures Appear	T[5]
	1	1025250	EP		1999-05-14	Grimm and Tanaka	WO99/23231 and English counterpart US 6624342	☒
	2	2535414	EP		2012-12-19	Castle et al.		☐
	3	2005/287415	JP		2005-10-20	Kamagata et al.	Abstract trans only	☒
	4	9808963	WO		1998-03-05	Gengenback et al.		☐
	5	9820144	WO		1998-05-14	Thompson et al.		☐
	6	9838294	WO		1998-09-03	Kaphammer		☐
	7	9838336	WO		1998-09-03	Elsemore et al.		☐
	8	9844139	WO		1998-10-08	Horn and Hall		☐
	9	9910513	WO		1999-03-04	Daniell		☐
	10	1999/063092	WO		1999-12-06	Luschnig et al.		☐

EFS Web 2.1.18 /DAVID H KRUSE/ 11/25/2020

INFORMATION DISCLOSURE STATEMENT BY APPLICANT (Not for submission under 37 CFR 1.99)		
	Application Number	15288406
	Filing Date	2016-10-07
	First Named Inventor	Terry Wright
	Art Unit	1663
	Examiner Name	KRUSE, David H.
	Attorney Docket Number	14764-258662

ALL REFERENCES CONSIDERED EXCEPT WHERE LINED THROUGH. /D.H.K/

	11	2000/006757	WO		2000-02-10	Horn and Hall		☐
	12	2001/038513	WO		2001-05-31	Castle et al.		☐
	13	2003/056904	WO		2003-07-17	Raab		☐

If you wish to add additional Foreign Patent Document citation information please click the Add button — Add

NON-PATENT LITERATURE DOCUMENTS — Remove

Examiner Initials*	Cite No	Include name of the author (in CAPITAL LETTERS), title of the article (when appropriate), title of the item (book, magazine, journal, serial, symposium, catalog, etc), date, pages(s), volume-issue number(s), publisher, city and/or country where published.	T5
	1	BAYLEY et al., Engineering 2,4-D resistance into cotton, Theoretical and Applied Genetics (1992), 83(5), 645-9.	☐
	2	BHAT et al., Purification of 3,5-dichlorocatechol 1,2-dioxygenase, a nonheme iron dioxygenase and a key enzyme in the biodegradation of a herbicide, 2,4-dichlorophenoxyacetic acid (2,4-D), from Pseudomonas cepacia CSV90, Archives of Biochemistry and Biophysics (1993), 300(2), 738-46.	☐
	3	CHAUDHRY and HUANG, Isolation and characterization of a new plasmid from a Flavobacterium sp. which carries the genes for degradation of 2,4-dichlorophenoxyacetate, Journal of Bacteriology (1988), 170(9), 3897-902.	☐
	4	CHEN and MARTIN, Reasons for the acclimation for 2,4-D biodegradation in lake water, Journal of Environmental Quality (1989), 18(2), 153-6.	☐
	5	COSPER et al., X-ray absorption spectroscopic analysis of Fe(II) and Cu(II) forms of a herbicide-degrading ketoglutarate dioxygenase, JBIC, Journal of Biological Inorganic Chemistry (1999), 4(1), 122-129.	☐
	6	DAANE and HAGGBLOM, Earthworm egg capsules as vectors for the environmental introduction of biodegradative bacteria, Applied and Environmental Microbiology (1999), 65(6), 2376-2381.	☐

/DAVID H KRUSE/ 11/25/2020

INFORMATION DISCLOSURE STATEMENT BY APPLICANT (Not for submission under 37 CFR 1.99)		
	Application Number	15288406
	Filing Date	2016-10-07
	First Named Inventor	Terry Wright
	Art Unit	1663
	Examiner Name	KRUSE, David H.
	Attorney Docket Number	14764-258662

ALL REFERENCES CONSIDERED EXCEPT WHERE LINED THROUGH. /D.H.K/

	7	DE LIPTHAY et al., Enhanced degradation of phenoxyacetic acid in soil by horizontal transfer of the tfdA gene encoding a 2,4-dichlorophenoxyacetic acid dioxygenase, FEMS Microbiology Ecology (2001), 35(1), 75-84.	☐
	8	DE LIPTHAY et al., Expression of tfdA genes in aquatic microbial communities during acclimation to 2,4-dichlorophenoxyacetic acid, FEMS Microbiology Ecology (2002), 40(3), 205-214.	☐
	9	DE LIPTHAY et al., In situ exposure to low herbicide concentrations affects microbial population composition and catabolic gene frequency in an aerobic shallow aquifer, Applied and Environmental Microbiology (2003), 69(1), 461-467.	☐
	10	DUNBAR et al., Genetic diversity through the looking glass: effect of enrichment bias, Applied and Environmental Microbiology (1997), 63(4), 1326-1331.	☐
	11	FENG and KENNEDY, Biodegradation and plant protection from the herbicide 2,4-D by plant-microbial associations in cotton production systems, Biotechnology and Bioengineering (1997), 54(6), 513-519.	☐
	12	FUECHSLIN et al., Effect of integration of a GFP reporter gene on fitness of Ralstonia eutropha during growth with 2,4-dichlorophenoxyacetic acid, Environmental Microbiology (2003), 5(10), 878-887.	☐
	13	HARKER et al., Phenoxyacetic acid degradation by the 2,4-dichlorophenoxyacetic acid (TFD) pathway of plasmid pJP4: mapping and characterization of the TFD regulatory gene, tfdR, Journal of Bacteriology (1989), 171(1), 314-20.	☐
	14	HAWKINS and HARWOOD, Chemotaxis of Ralstonia eutropha JMP134(pJP4) to the herbicide 2,4-dichlorophenoxyacetate, Applied and Environmental Microbiology (2002), 68(2), 968-972.	☐
	15	HEGG et al., Herbicide-Degrading Keto Acid-Dependent Enzyme TfdA: Metal Coordination Environment and Mechanistic Insights, Biochemistry (1999), 38(50), 16714-16726.	☐
	16	HOFFMANN et al., A transposon encoding the complete 2,4-dichlorophenoxyacetic acid degradation pathway in the alkalitolerant strain Delftia acidovorans P4a, Microbiology (Reading, United Kingdom) (2003), 149(9), 2545-2556.	☐
	17	HOGAN et al., Distribution of the tfdA gene in soil bacteria that do not degrade 2,4-dichlorophenoxyacetic acid (2,4-D), Microbial Ecology (1997), 34(2), 90-96.	☐

INFORMATION DISCLOSURE STATEMENT BY APPLICANT (Not for submission under 37 CFR 1.99)		
	Application Number	15288406
	Filing Date	2016-10-07
	First Named Inventor	Terry Wright
	Art Unit	1663
	Examiner Name	KRUSE, David H.
	Attorney Docket Number	14764-258662

ALL REFERENCES CONSIDERED EXCEPT WHERE LINED THROUGH. /D.H.K/

	18	HOGAN et al., Site-directed mutagenesis of 2,4-dichlorophenoxyacetic acid/ketoglutarate dioxygenase. Identification of residues involved in metallocenter formation and substrate binding, Journal of Biological Chemistry (2000), 275(17), 12400-12409.	☐
	19	Poiger et al., J Agic Food Chem. (63)2583-2590 (2015), Environmental Behavior of the Chiral Herbicide Haloxyfop. 1. Rapid and Preferential Interconversion of the Enantiomers in Soil.	☐
	20	KANEKO et al., DNA Research (9)189-197 (2002), Complete Genomic Sequence of Nitrogen-fixing Symbiotic Bacterium Bradyrhizobium japonicum USDA110	☐
	21	JACKMAN et al., Electrokinetic movement and biodegradation of 2,4-dichlorophenoxyacetic acid in silt soil, Biotechnology and Bioengineering (2001), 74(1), 40-48.	☐
	22	KA and TIEDJE, Integration and excision of a 2,4-dichlorophenoxyacetic acid-degradative plasmid in Alcaligenes paradoxus and evidence of its natural intergeneric transfer, Journal of Bacteriology (1994), 176(17), 5284-9.	☐
	23	KA et al., Use of gene probes to aid in recovery and identification of functionally dominant 2,4-dichlorophenoxyacetic acid-degrading populations in soil, Applied and Environmental Microbiology (1994), 60(4), 1116-20.	☐
	24	KITAGAWA et al., Novel 2,4-dichlorophenoxyacetic acid degradation genes from oligotrophic Bradyrhizobium sp. strain HW13 isolated from a pristine environment, Journal of Bacteriology (2002), 184(2), 509-518.	☐
	25	KLEINSTEUBER et al., Expression of the 2,4-D degradative pathway of pJP4 in an alkaliphilic, moderately halophilic soda lake isolate, Halomonas sp. EF43, Extremophiles (2001), 5(6), 375-384.	☐
	26	LAEMMLI et al., Mutation analysis of the different tfd genes for degradation of chloroaromatic compounds in Ralstonia eutropha JMP134, Archives of Microbiology (2004), 181(2), 112-121. (Published online: 16 December 2003).	☐
	27	LAURENT et al., 2,4-Dichlorophenoxyacetic Acid Metabolism in Transgenic Tolerant Cotton (Gossypium hirsutum), Journal of Agricultural and Food Chemistry (2000), 48(11), 5307-5311.	☐
	28	LETOUZE and GASQUEZ, Enhanced activity of several herbicide-degrading enzymes: a suggested mechanism responsible for multiple resistance in blackgrass (Alopecurus myosuroides Huds.), Agronomie (2003), 23(7), 601-608.	☐

/DAVID H KRUSE/ 11/25/2020

INFORMATION DISCLOSURE STATEMENT BY APPLICANT (Not for submission under 37 CFR 1.99)		
	Application Number	15288406
	Filing Date	2016-10-07
	First Named Inventor	Terry Wright
	Art Unit	1663
	Examiner Name	KRUSE, David H.
	Attorney Docket Number	14764-258662

ALL REFERENCES CONSIDERED EXCEPT WHERE LINED THROUGH. /D.H.K/

	29	LEWIS et al., Influence of environmental changes on degradation of chiral pollutants in soils, Nature (London) (1999), 401(6756), 898-901.	☐
	30	LOOS et al., Phenoxyacetate herbicide detoxication by bacterial enzymes, Journal of Agricultural and Food Chemistry (1967), 15(5), 858-60.	☐
	31	LUDWIG et al., Chromatographic separation of the enantiomers of marine pollutants. Part 5: enantioselective degradation of phenoxycarboxylic acid herbicides by marine microorganisms, Chemosphere (1992), 24(10), 1423-9.	☐
	32	LYON et al., Expression of a bacterial gene in transgenic tobacco plants confers resistance to the herbicide 2,4-dichlorophenoxyacetic acid, Plant Molecular Biology (1989), 13(5), 533-40.	☐
	33	LYON et al., Cotton plants transformed with a bacterial degradation gene are protected from accidental spray drift damage by the herbicide 2,4-dichlorophenoxyacetic acid, Transgenic Research (1993), 2(3), 162-9.	☐
	34	MAE et al., Characterization of a new 2,4-dichlorophenoxyacetic acid degrading plasmid pEST4011: physical map and localization of catabolic genes, Journal of General Microbiology (1993), 139(12), 3165-70.	☐
	35	MALTSEVA et al., Degradation of 2,4-dichlorophenoxyacetic acid by haloalkaliphilic bacteria, Microbiology (Reading, United Kingdom) (1996), 142(5), 1115-1122.	☐
	36	MARRIOTT et al., Biodegradation of mixtures of chlorophenoxyalkanoic acid herbicides by Alcaligenes denitrificans, Journal of Industrial Microbiology & Biotechnology (2000), 25(5), 255-259.	☐
	37	MATHESON et al., Evidence for acquisition in nature of a chromosomal 2,4-dichlorophenoxyacetic acid/ketoglutarate dioxygenase gene by different Burkholderia spp, Applied and Environmental Microbiology (1996), 62(7), 2457-2463.	☐
	38	MCGOWAN et al., Evidence for interspecies gene transfer in the evolution of 2,4-dichlorophenoxyacetic acid degraders, Applied and Environmental Microbiology (1998), 64(10), 4089-4092.	☐
	39		☐

INFORMATION DISCLOSURE STATEMENT BY APPLICANT (Not for submission under 37 CFR 1.99)		
	Application Number	15288406
	Filing Date	2016-10-07
	First Named Inventor	Terry Wright
	Art Unit	1663
	Examiner Name	KRUSE, David H.
	Attorney Docket Number	14764-258662

ALL REFERENCES CONSIDERED EXCEPT WHERE LINED THROUGH. /D.H.K/

	40	MORTENSEN and JACOBSEN, Influence of Frozen Storage on Herbicide Degradation Capacity in Surface and Subsurface Sandy Soils, Environ Sci Technol 2004, 38, 6625-6632.	☐
	41	MULLER and BABEL, Pseudo-recalcitrance of chlorophenoxyalkanoate herbicides - correlation to the availability of ketoglutarate, Acta Biotechnologica (2001), 21(3), 227-242.	☐
	42	MULLER and BABEL, Separation of two dichlorprop/ketoglutarate dioxygenases with enantiospecific properties from Comamonas acidovorans MC1, Acta Biotechnologica (1999), 19(4), 349-355.	☐
	43	MULLER et al., Comamonas acidovorans strain MC1. A new isolate capable of degrading the chiral herbicides dichlorprop and mecoprop and the herbicides 2,4-D and MCPA, Microbiological Research (1999), 154(3), 241-246.	☐
	44	NICKEL et al., Involvement of two ketoglutarate-dependent dioxygenases in enantioselective degradation of (R)- and (S)-mecoprop by Sphingomonas herbicidovorans MH, Journal of Bacteriology (1997), 179(21), 6674-6679.	☐
	45	OHKOUCHI et al., Cloning and expression of DL-2-haloacid dehalogenase gene from Burkholderia cepacia, Water Science and Technology (2000), 42(7-8, Hazard Assessment and Control of Environmental Contaminants (Ecohazard 99)), 261-268.	☐
	46	PARKER and DOXTADER, Kinetics of microbial decomposition of 2,4-D in soil: effects of herbicide concentration, Journal of Environmental Quality (1982), 11(4), 679-84.	☐
	47	PERKINS et al., Use of Alcaligenes eutrophus as a source of genes for 2,4-D resistance in plants, Weed Science (1987), 35(Suppl. 1), 12-18.	☐
	48	PLUMEIER et al., Importance of different tfd genes for degradation of chloroaromatics by Ralstonia eutropha JMP134, Journal of Bacteriology (2002), 184(15), 4054-4064.	☐
	49	POH et al., Complete characterization of Tn5530 from Burkholderia cepacia strain 2a (plJB1) and studies of 2,4-dichlorophenoxyacetate uptake by the organism, Plasmid (2002), 48(1), 1-12.	☐
	50	PRESTON et al., Multiple resistance to dissimilar herbicide chemistries in a biotype of Lolium rigidum due to enhanced activity of several herbicide degrading enzymes, Pesticide Biochemistry and Physiology (1996), 54(2), 123-134.	☐

EFS Web 2.1.18 /DAVID H KRUSE/ 11/25/2020

	51	ROUSSEAUX et al., Isolation and characterisation of new Gram-negative and Gram-positive atrazine degrading bacteria from different French soils, FEMS Microbiology Ecology (2001), 36(2-3), 211-222.	☐
	52	SAARI et al., Stereospecific degradation of the phenoxypropionate herbicide dichlorprop, Journal of Molecular Catalysis B: Enzymatic (1999), 6(4), 421-428.	☐
	53	SCHNEIDERHEINZE et al., Plant and soil enantioselective biodegradation of racemic phenoxyalkanoic herbicides, Chirality (1999), 11(4), 330-337.	☐
	54	SEIFERT et al., Effect of tillage on microbial characteristics and herbicide degradation in a Sharkey clay soil, Weed Science (2001), 49(5), 685-693.	☐
	55	SHAW and BURNS, Enhanced mineralization of [U-14C]2,4-dichlorophenoxyacetic acid in soil from the rhizosphere of Trifolium pratense, Applied and Environmental Microbiology (2004), 70(8), 4766-4774.	☐
	56	SMEJKAL et al., Substrate specificity of chlorophenoxyalkanoic acid-degrading bacteria is not dependent upon phylogenetically related tfdA gene types, Biology and Fertility of Soils (2001), 33(6), 507-513.	☐
	57	STREBER and WILLMITZER, Transgenic tobacco plants expressing a bacterial detoxifying enzyme are resistant to 2,4-D, Bio/Technology (1989), 7(8), 811-16.	☐
	58	SWIEGERS et al., Carnitine biosynthesis in Neurospora crassa: identification of a cDNA coding for N-trimethyllysine hydroxylase and its functional expression in Saccharomyces cerevisiae, FEMS Microbiology Letters (2002), 210(1), 19-23.	☐
	59	TETT et al., Enantioselective degradation of the herbicide mecoprop [2-(2-methyl-4-chlorophenoxy)propionic acid] by mixed and pure bacterial cultures, FEMS Microbiology Ecology (1994), 14(3), 191-200.	☐
	60	TOP and SPRINGAEL, The role of mobile genetic elements in bacterial adaptation to xenobiotic organic compounds, Current Opinion in Biotechnology (2003), 14(3), 262-269.	☐
	61	TOP et al., Capture of a catabolic plasmid that encodes only 2,4-dichlorophenoxyacetic acid:ketoglutaric acid dioxygenase (TfdA) by genetic complementation, Applied and Environmental Microbiology (1996), 62(7), 2470-2476.	☐

ALL REFERENCES CONSIDERED EXCEPT WHERE LINED THROUGH. /D.H.K/

/DAVID H KRUSE/ 11/25/2020

INFORMATION DISCLOSURE STATEMENT BY APPLICANT (Not for submission under 37 CFR 1.99)		
	Application Number	15288406
	Filing Date	2016-10-07
	First Named Inventor	Terry Wright
	Art Unit	1663
	Examiner Name	KRUSE, David H.
	Attorney Docket Number	14764-258662

ALL REFERENCES CONSIDERED EXCEPT WHERE LINED THROUGH. /D.H.K/

	62	TOP et al., Methane oxidation as a method to evaluate the removal of 2,4-dichlorophenoxyacetic acid (2,4-D) from soil by plasmid-mediated bioaugmentation, FEMS Microbiology Ecology (1999), 28(3), 203-213.	☐
	63	TRAVKIN et al., Characterization of an intradiol dioxygenase involved in the biodegradation of the chlorophenoxy herbicides 2,4-D and 2,4,5-T, FEBS Letters (1997), 407(1), 69-72.	☐
	64	VALLAEYS et al., PCR-RFLP analysis of 16S rRNA, tfdA and tfdB genes reveals a diversity of 2,4-D degraders in soil aggregates, FEMS Microbiology Ecology (1997), 24(3), 269-278.	☐
	65	VALLAEYS et al., The metabolic pathway of 2,4-dichlorophenoxyacetic acid degradation involves different families of tfdA and tfdB genes according to PCR-RFLP analysis, FEMS Microbiology Ecology (1996), 20(3), 163-172.	☐
	66	VEDLER et al., Analysis of the 2,4-dichlorophenoxyacetic acid-degradative plasmid pEST4011 of Achromobacter xylosoxidans subsp. denitrificans strain EST4002, Gene (2000), 255(2), 281-288.	☐
	67	VEDLER et al., TfdR, the LysR-type transcriptional activator, is responsible for the activation of the tfdCB operon of Pseudomonas putida 2,4-dichlorophenoxyacetic acid degradative plasmid pEST4011, Gene (2000), 245(1), 161-168.	☐
	68	VELICER, Pleiotropic effects of adaptation to a single carbon source for growth on alternative substrates, Applied and Environmental Microbiology (1999), 65(1), 264-269.	☐
	69	WHITING et al., Metal Coordination Environment of a Cu(II)-Substituted Keto Acid-Dependent Dioxygenase That Degrades the Herbicide 2,4-D, Journal of the American Chemical Society (1997), 119(14), 3413-3414.	☐
	70	YI et al., Phylogenetic and phenotypic diversity of 4-chlorobenzoate-degrading bacteria isolated from soils, FEMS Microbiology Ecology (2000), 31(1), 53-60.	☐
	71	ZHANG et al., In vitro assay for 2,4-D resistance in transgenic cotton, In Vitro Cellular & Developmental Biology: Plant (2001), 37(2), 300-304.	☐
	72	ZHANG et al., Inheritance and segregation of exogenous genes in transgenic cotton, Journal of Genetics (2000), 79 (2), 71-75.	☐

EFS Web 2.1.18 /DAVID H KRUSE/ 11/25/2020

INFORMATION DISCLOSURE STATEMENT BY APPLICANT (Not for submission under 37 CFR 1.99)		
	Application Number	15288406
	Filing Date	2016-10-07
	First Named Inventor	Terry Wright
	Art Unit	1663
	Examiner Name	KRUSE, David H.
	Attorney Docket Number	14764-258662

ALL REFERENCES CONSIDERED EXCEPT WHERE LINED THROUGH. /D.H.K/

	73	ZIPPER et al., Complete microbial degradation of both enantiomers of the chiral herbicide mecoprop [(RS)-2-(4-chloro-2-methylphenoxy)propionic acid] in an enantioselective manner by Sphingomonas herbicidovorans sp. Nov, Applied and Environmental Microbiology (1996), 62(12), 4318-4322.	☐
	74	ZIPPER et al., Enantioselective uptake and degradation of the chiral herbicide dichlorprop [(RS)-2-(2,4-dichlorophenoxy)propanoic acid] by Sphingomonas herbicidovorans MH, Journal of Bacteriology (1998), 180(13), 3368-3374.	☐
	75	CHO ET AL, Agricultural Chemistry and Biotechnology (English Edition) (1999), 42(2), 57-61 , Isolation and characterization of 2-methyl-4-chlorophenoxyacetic acid-degrading bacteria from agricultural soils.	☐
	76	KWON et al J. Kor. Soc. Hort. Sci. (1997), 38(6), 796-799.	☐
	77	LIM ET AL, Journal of Microbiology (Seoul, Republic of Korea) (2004), 42(2), 87-93 Genetic and phenotypic diversity of (R/S)-mecoprop [2-(2-methyl-4-chlorophenoxy)propionic acid]-degrading bacteria isolated from soils	☐
	78	Tamura et al, Nippon Noyaku Gakkaishi (2001), 26(3), 309-314 , Microbial pesticide degradations and evolutionary analysis of degrading enzymes.	☐
	79	PARK ET AL, Journal of Microbiology (Seoul, Republic of Korea) (2003), 41(1), 7-15, Genetic and phenotypic diversity of dichlorprop-degrading bacteria isolated from soils.	☐
	80	VALLAEYS ET AL, Biotechnology Letters (1998), 20(11), 1073-1076 , Isolation and characterization of a stable 2,4-dichlorophenoxyacetic acid degrading bacterium, Variovorax paradoxus, using chemostat culture	☐
	81	(Book, will be provided upon request) Nakatsu CH, Fukumori F, Fulthorpe R, Hausinger R, Holben W, Kamagata Y, Korona R, Lenski R, Maltseva O, Matheson VG, McGowan C. Genetic diversity of 2, 4-dichlorophenoxyacetic acid (2, 4-D) catabolic genes. Microbial diversity and genetics of biodegradation. Japan Scientific Societies Press, Tokyo, Japan. 1997:197-206.	☐
	82	(Same book, will be provided upon request) Hausinger RP, Fukumori F, Hogan DA, Sassanella TM, Kamagata Y, Takami H, Saari RE, Horikoshi K, Fukuda M, Kudo T. Microbial diversity and genetics of biodegradation. by K. Horikoshi, M. Fukuda and T. Kudo, Japan Science Societies Press, Tokyo. 1997:35-51.	☐
	83	Fukamori and Hausinger, JBC (268)24311(1993), Purification and characterization of 2,4-Dichlorophenoxyacetate/a-ketogutarate dioxygenase.	☐

EFS Web 2.1.18 /DAVID H KRUSE/ 11/25/2020

INFORMATION DISCLOSURE STATEMENT BY APPLICANT (Not for submission under 37 CFR 1.99)		
	Application Number	15288406
	Filing Date	2016-10-07
	First Named Inventor	Terry Wright
	Art Unit	1663
	Examiner Name	KRUSE, David H.
	Attorney Docket Number	14764-258662

ALL REFERENCES CONSIDERED EXCEPT WHERE LINED THROUGH. /D.H.K/

	84	Fukamori and Hausinger, J Bacterioloogy (175)2083(1993), Alcaligenes eutrophus JMP134 "2,4-Dichlorophenoxyacetate monooxygenase" is an a-Ketoglutarate-dependent dioxygenase.	☐
	85		☐
	86		☐
	87		☐
	88	Ehrig et al., Acta Biotechologica (17)351-356(1997), Isolation of phenoxyherbicidedegrading Rhodoferax species from contaminated building material.	☐
	89	Hausinger, Critical Reviews in Biochemsitry (39)21-68(2004), Fe(II)/α-Ketoglutarate-Dependent Hydroxylases and Related Enzymes.	☐
	90	Kohler et al., J Ind Microbio biotech (23)336(1999), Sphingomonas herbicidovorans MH: a versatile phenoxyalkanoic acid herbicide degrader.	☐
	91	Hausinger and Fukamori, Env Health Perspectives (103)37-39(1995), Characterization of the first enzyme in 2,4-Dichlorphenoxyacetic acid metabolism.	☐
	92	Don et al., J Bacteriol (161)85(1985), Transposon Mutagenesis and Cloning Analysis of the Pathways for Degradation of 2,4-Dichlorophenoxyacetic Acid and 3-Chlorobenzoate in Alcaligenes eutrophus JMP134(pJP4).	☐
	93	Don et al.,J Bacteriol (161)466(1985), Genetic and Physical Map of the 2,4-Dichlorophenoxyacetic Acid-Degradative Plasmid pJP4	☐
	94	Hotopp et al., J. Molec. Catalysis B: Enzymatic (15)155-162(2001), Alternative substrates of 2,4-dichlorophenoxyacetate/-ketoglutarate dioxygenase.	☐

EFS Web 2.1.18 /DAVID H KRUSE/ 11/25/2020

INFORMATION DISCLOSURE STATEMENT BY APPLICANT (Not for submission under 37 CFR 1.99)		
	Application Number	15288406
	Filing Date	2016-10-07
	First Named Inventor	Terry Wright
	Art Unit	1663
	Examiner Name	KRUSE, David H.
	Attorney Docket Number	14764-258662

ALL REFERENCES CONSIDERED EXCEPT WHERE LINED THROUGH. /D.H.K/

	95	WESTENDORF ET AL., Microbiol. Res. 157 (4), 317-322 (2002), The two enantiospecific dichlorprop/α-ketoglutarate-dioxygenases from Delftia acidovorans MC1 –protein and sequence data of RdpA and SdpA.	☐
	96	PARK ET AL, Journal of Microbiology and Biotechnology (2003), 13(2), 243-250 , Isolation and characterization of 4-(2,4-dichlorophenoxy)butyric acid-degrading bacteria from agricultural soils.	☐
	97	Mueller RH, Babel W. Degradability and recalcitrance of phenoxyalkanoic acid herbicides- traits of the microbial metabolism. InSecond International Conferen~ce on Remediation of Chlorinated and Racalcitrant Compounds 2000 (pp. 229-236).	☐
	98	TETT, Biodegradation (1997), 8(1), 43-52 , Biodegradation of the chlorophenoxy herbicide (R)-(+)-mecoprop by Alcaligenes denitrificans.	☐
	99	Llewellyn et al, Herbicide-Resistant Crops (1996), 159-74, Genetic engineering of crops for tolerance to 2,4-D.	☐
	100		☐

	101	Baelum et al., Appl. Environ. Microbiol. (72)1476-1486 (2006), Degradation of 4-Chloro-2-Methylphenoxyacetic Acid in Top- and Subsoil Is Quantitatively Linked to the Class III tfdA Gene.	☐
	102	Baelum et al., Appl. Environ. Microbiol. (75)2969-2972 (2009), TaqMan Probe-Based Real-Time PCR Assay for Detection and Discrimination of Class I, II, and III tfdA Genes in Soils Treated with Phenoxy Acid Herbicides.	☐
	103	Griffin et al., J Agric Food Chem (61)6589-6596(2013), Characterization of Aryloxyalkanoate Dioxygenase-12, a Nonheme Fe(II)/α-Ketoglutarate-Dependent Dioxygenase, Expressed in Transgenic Soybean and Pseudomonas fluorescens.	☐
	104	Hausinger, RSC Metallobiology (2015) Chapter 1 of 2-Oxoglutarate-dependent oxygenases, Biochemical diversity of 2-oxoglytarate-dependent oxygenases.	☐
	105	Leibeling et al, Eng Life Sci (13)278(2013), Posttranslational oxidative modification of (R)-2-(2,4-dichlorophenoxy) propionate/α-ketoglutarate-dependent dioxygenases (RdpA) leads to improved degradation of 2,4-dichlorophenoxyacetate (2,4-D).	☐

/DAVID H KRUSE/ 11/25/2020

	106	Muller et al., Applied and Environmental Microbiology (72)4853(2006), Purification and Characterization of Two Enantioselective a-Ketoglutarate-Dependent Dioxygenases, RdpA and SdpA, from Sphingomonas herbicidovorans MH.	☐
	107	Paulin et al., Appl. Environ. Microbiol. (76)2873(2010), Abundance and Expression of Enantioselective rdpA and sdpA Dioxygenase Genes during Degradation of the Racemic Herbicide (R,S)-2-(2,4-Dichlorophenoxy)Propionate in Soil.	☐
	108	Zaprasis et al, Appl. Environ. Microbiol. (76)119(2010), Abundance of Novel and Diverse tfdA-Like Genes, Encoding Putative Phenoxyalkanoic Acid Herbicide-Degrading Dioxygenases, in Soil .	☐
	109	Zhang ET AL. Journal of Agricultural and Food Chemistry (2020), 68(26), 6967-6976 CODEN: JAFCAU; ISSN: 0021-8561 Enantioselective Catabolism of the Two Enantiomers of the Phenoxyalkanoic Acid Herbicide Dichlorprop by Sphingopyxis sp. DBS4.	☐
	110	Krausse et al., 4th biotechnology symposium of the University of Leipzig (abstract) pg 60 (2005), Crystal structure of the 2-oxoglutarate dependent dioxygenase RdpA.	☐
	111	Mueller et al., Un Mich ICBIC 2005 abstract, Insights into the enantiospecificities of (R)- and (S)-dichlorprop/a-ketoglutarate dioxygenases.	☐

ALL REFERENCES CONSIDERED EXCEPT WHERE LINED THROUGH. /D.H.K/

/DAVID H KRUSE/ 11/25/2020

INFORMATION DISCLOSURE STATEMENT BY APPLICANT (Not for submission under 37 CFR 1.99)		
	Application Number	15288406
	Filing Date	2016-10-07
	First Named Inventor	Terry Wright
	Art Unit	1663
	Examiner Name	KRUSE, David H.
	Attorney Docket Number	14764-258662

ALL REFERENCES CONSIDERED EXCEPT WHERE LINED THROUGH. /D.H.K/

	112	Krausse et al., Freiberg Un Deutschen Gesellschaft fur Kristallographie (2006), (Poster title 72L) Structure of the 2-Oxoglutarate Dependent Dioxygenase RdpA by X-ray Crystallography and Small Angle X-ray Scattering	☐
	113	Gazitua et al., Environ Microbiol (12)2411(2010), Novel α-ketoglutarate dioxygenase tfdA-related genes are found in soil DNA after exposure to phenoxyalkanoic herbicides.	☐
	114	Chekan et al., Proceedings of the National Academy of Sciences (116)13299-13304(2019), Molecular basis for enantioselective herbicide degradation imparted by aryloxyalkanoate dioxygenases in transgenic plants.	☐
	115	Larue et al, Pest Manag Sci (75)2086(2019), Development of enzymes for robust aryloxyphenoxypropionate and synthetic auxin herbicide tolerance traits in maize and soybean crops.	☐
	116	Liu et al., FEMS Microbiol Ecol (86)114-129(2013) , Consumers of 4-chloro-2-methylpheoxyacetic acid from agricultural soil and drilosphere harbor cadA, r/sdpA, and tfdA-like gene encoding oxygenases.	☐
	117	Muller et al., Protein Science (15)prot1356(2006), Structural basis for the enantiospecificities of R- and S-specific phenoxypropionate/a-ketoglutarate dioxygenases.	☐
	118	Muller, Eng Life Sci (7)311-321 (2007), Activity and Reaction Mechanism of the Initial Enzymatic Step Specifying the Microbial Degradation of 2,4-Dichlorophenoxyacetate.	☐
	119	Westendorf, Eng Life Sci (6)552-559(2006), Kinetic Traits and Enzyme Form Patterns of (R)-2-(2,4-Dichlorophenoxy) propionate/a-Ketoglutarate Dioxygenase (RdpA) after Expression in Different Bacterial Strains.	☐
	120	Wright et al., Proc Natl Acad Sci (107)20240(2010), Robust crop resistance to broadleaf and grass herbicides provided by aryloxyalkanoate dioxygenase transgenes.	☐
	121	GenBank accession no. AAA21983.1 tfdA Cupriavidus necator (replaced Ralstonia eutropha), April 23, 1993.	☐
	122	GenBank accession no. AAK81681.1 tfdA Burkholderia cepacia, August 24, 2020, July 23, 2016.	☐

EFS Web 2.1.18 /DAVID H KRUSE/ 11/25/2020

INFORMATION DISCLOSURE STATEMENT BY APPLICANT (Not for submission under 37 CFR 1.99)		
	Application Number	15288406
	Filing Date	2016-10-07
	First Named Inventor	Terry Wright
	Art Unit	1663
	Examiner Name	KRUSE, David H.
	Attorney Docket Number	14764-258662

ALL REFERENCES CONSIDERED EXCEPT WHERE LINED THROUGH. /D.H.K/

	123	UniProtKB accession no. Q45423.1 tfdA Burkholderia sp. RASC, Nov 1, 1996.	☐
	124	GenBank accession no. AAS49436 tfdA Achromobacter denitrificans, April 3, 2020.	☐
	125	GenBank accession no. AAB47567.1 tfdABurkholderia cepacia plJB, July 26,2016.	☐
	126	GenBank accession no. AAM76772.1 tfdADelftia acidovorans _-_287 aaProtein_-_NCBI July 26, 2016	☐
	127	GenBank accession no. BAB92965.1 tfdA alpha proteobacterium HWK12, July 2, 2002.	☐
	128	GenBank accession no. BAB92966.1 tfdA alpha proteobacterium HW13, July 2, 2002.	☐
	129	NCBI accession no. WP_011084309.1 tfdA Bradyrhizobium diazoefficiens (replaced B. japonicum), 27-JUL-2019.	☐
	130	UniProtKB accession no. P83309.2 sdpA MC1 Delftia aciovorans, Sep 18, 2019.	☐
	131	UniProtKB accession no. Q700X4.1 sdpA MH Shingobium herbicidovorans, Nov 1, 1996.	☐
	132	GenBank accession no. ABD67501.1 sdpA P230 Rhodoferax sp. P230, March 14, 2006.	☐
	133	UniProtKB accession no. Q8KSC8.2 RdpA Shingobium herbicidovorans, March 1, 2004.	☐

INFORMATION DISCLOSURE STATEMENT BY APPLICANT (Not for submission under 37 CFR 1.99)		
	Application Number	15288406
	Filing Date	2016-10-07
	First Named Inventor	Terry Wright
	Art Unit	1663
	Examiner Name	KRUSE, David H.
	Attorney Docket Number	14764-258662

ALL REFERENCES CONSIDERED EXCEPT WHERE LINED THROUGH. /D.H.K/

	134	Muller, Swiss Federal Institute of Technology thesis (Nov2004), Metabolism of phenoxyalkanoic acid herbicides in Sphingomonas herbicidovorans MH cloning and characterization of two enantiospecific α-ketoglutarate-dependent dioxygenases and degradation pathway analysis.	☐
	135	Westendorf Universität Leipzig thesis-German (2005), Enantioselektive Verwertung von Phenoxyalkanoat-Herbiziden durch Bakterien – Eine Charakterisierung der Dioxygenasen des initialen Abbau-Schrittes.	☐
	136	Baelum et al., System Appl Microbiol. (33)67(2010), Supplemental Material to Comparison of 16S rRNA gene phylogeny and functional tfdA gene distribution in thirty-one different 2, 4-dichlorophenoxyacetic acid and 4-chloro-2-methylphenoxyacetic acid degraders.	☐
	137	Zhang et al., J. Agric. Food Chem. (66)12217(2018), Two dcm Gene Clusters Essential for the Degradation of Diclofopmethyl in a Microbial Consortium of Rhodococcus sp. JT-3 and Brevundimonas sp. JT-9.	☐
	138	Jing et al., Ecological indicators (75)126(2017)-Enantioselective toxicity and degradation of chiral herbicidefenoxaprop-ethyl in earthworm Eisenia fetida.	☐
	139	HAN ET AL, World Journal of Microbiology & Biotechnology (2014), 30(10)2567-2576 , 16S rRNA gene phylogeny and tfdA gene analysis of 2,4-D-degrading bacteria isolated in China.	☐
	140	Zhang et al., J. Agric. Food Chem. (58)12878(2010), Enantioselective Environmental Behavior of the Chiral Herbicide Fenoxaprop-ethyl and Its Chiral MetaboliteFenoxaprop in Soil.	☐
	141	Wu et al., J. Agric. Food Chem. (65)3711(2017), Rapid Biodegradation of the Herbicide 2,4-Dichlorophenoxyacetic Acid by Cupriavidus gilardii T-1.	☐
	142	Zabaloy et al., Ann Microbiol (64)969(2014), Isolation and characterization of indigenous 2,4-D herbicide degrading bacteria from an agricultural soil in proximity of Sauce Grande River, Argentina.	☐
	143	Nielsen et al., PLOS One 8(12)e83346(2013), Novel Insight into the Genetic Context of the cadAB Genes from a 4- chloro-2-methylphenoxyacetic Acid-Degrading Sphingomonas.	☐
	144	Mierzejewska et al, Bulletin Env Contam Tox (104)200(2020), Biodegradation Potential and Ecotoxicity Assessment in Soil Extracts Amended with Phenoxy Acid Herbicide (2,4-D) and a Structurally-Similar Plant Secondary Metabolite (Ferulic Acid).	☐

EFS Web 2.1.18 /DAVID H KRUSE/ 11/25/2020

INFORMATION DISCLOSURE STATEMENT BY APPLICANT (Not for submission under 37 CFR 1.99)		
	Application Number	15288406
	Filing Date	2016-10-07
	First Named Inventor	Terry Wright
	Art Unit	1663
	Examiner Name	KRUSE, David H.
	Attorney Docket Number	14764-258662

ALL REFERENCES CONSIDERED EXCEPT WHERE LINED THROUGH. /D.H.K/

	145	Shimojo et al., J Biosc Bioengin. (108)56(2009), Analysis of genes encoding the 2,4-dichlorophenoxyacetic acid-degrading enzyme from Sphingomonas agrestis 58-1.	☐
	146	HAN ET AL, World Journal of Microbiology & Biotechnology (2015), 31(7), 1021-1030 , Cloning, expression, characterization and mutational analysis of the tfdA gene from Cupriavidus campinensis BJ71.	☐
	147	Paulin et al., Environ Micriobiol (13)1513-1523(2011), (R,S)-dichlorprop herbicide in agricultural soil induces proliferation and expression of multiple dioxygenase-encoding genes in the indigenous	☐
	148	Muller et al., Protein Science (15)prot1356(2006), Supplemental Table and Figures to Structural basis for the enantiospecificities of R- and S-specific phenoxypropionate/a-ketoglutarate dioxygenases.	☐
	149	Chekan et al., Proceedings of the National Academy of Sciences (116)13299-13304(2019), SUPPLEMENTAL Molecular basis for enantioselective herbicide degradation imparted by aryloxyalkanoate dioxygenases in transgenic plants.	☐
	150	GenBank accession no. BAB92964.1 tfdAa alpha proteobacterium RD5-C2 - NCBI. July 2, 2002.	☐

If you wish to add additional non-patent literature document citation information please click the Add button Add

EXAMINER SIGNATURE

Examiner Signature	/DAVID H KRUSE/	Date Considered	11/25/2020

*EXAMINER: Initial if reference considered, whether or not citation is in conformance with MPEP 609. Draw line through a citation if not in conformance and not considered. Include copy of this form with next communication to applicant.

[1] See Kind Codes of USPTO Patent Documents at www.USPTO.GOV or MPEP 901.04. [2] Enter office that issued the document, by the two-letter code (WIPO Standard ST.3). [3] For Japanese patent documents, the indication of the year of the reign of the Emperor must precede the serial number of the patent document. [4] Kind of document by the appropriate symbols as indicated on the document under WIPO Standard ST.16 if possible. [5] Applicant is to place a check mark here if English language translation is attached.

INFORMATION DISCLOSURE STATEMENT BY APPLICANT (Not for submission under 37 CFR 1.99)		
	Application Number	15288406
	Filing Date	2016-10-07
	First Named Inventor	Terry Wright
	Art Unit	1663
	Examiner Name	KRUSE, David H.
	Attorney Docket Number	14764-258662

CERTIFICATION STATEMENT

Please see 37 CFR 1.97 and 1.98 to make the appropriate selection(s):

☐ That each item of information contained in the information disclosure statement was first cited in any communication from a foreign patent office in a counterpart foreign application not more than three months prior to the filing of the information disclosure statement. See 37 CFR 1.97(e)(1).

OR

☐ That no item of information contained in the information disclosure statement was cited in a communication from a foreign patent office in a counterpart foreign application, and, to the knowledge of the person signing the certification after making reasonable inquiry, no item of information contained in the information disclosure statement was known to any individual designated in 37 CFR 1.56(c) more than three months prior to the filing of the information disclosure statement. See 37 CFR 1.97(e)(2).

☐

☒ See attached certification statement.

☒ The fee set forth in 37 CFR 1.17 (p) has been submitted herewith.

A certification statement is not submitted herewith.

SIGNATURE

A signature of the applicant or representative is required in accordance with CFR 1.33, 10.18. Please see CFR 1.4(d) for the form of the signature.

Signature	/John P. Breen/	Date (YYYY-MM-DD)	2020-09-22
Name/Print	John P. Breen	Registration Number	38833

This collection of information is required by 37 CFR 1.97 and 1.98. The information is required to obtain or retain a benefit by the public which is to file (and by the USPTO to process) an application. Confidentiality is governed by 35 U.S.C. 122 and 37 CFR 1.14. This collection is estimated to take 1 hour to complete, including gathering, preparing and submitting the completed application form to the USPTO. Time will vary depending upon the individual case. Any comments on the amount of time you require to complete this form and/or suggestions for reducing this burden, should be sent to the Chief Information Officer, U.S. Patent and Trademark Office, U.S. Department of Commerce, P.O. Box 1450, Alexandria, VA 22313-1450. DO NOT SEND FEES OR COMPLETED FORMS TO THIS ADDRESS. **SEND TO: Commissioner for Patents, P.O. Box 1450, Alexandria, VA 22313-1450.**

Privacy Act Statement

The Privacy Act of 1974 (P.L. 93-579) requires that you be given certain information in connection with your submission of the attached form related to a patent application or patent. Accordingly, pursuant to the requirements of the Act, please be advised that: (1) the general authority for the collection of this information is 35 U.S.C. 2(b)(2); (2) furnishing of the information solicited is voluntary; and (3) the principal purpose for which the information is used by the U.S. Patent and Trademark Office is to process and/or examine your submission related to a patent application or patent. If you do not furnish the requested information, the U.S. Patent and Trademark Office may not be able to process and/or examine your submission, which may result in termination of proceedings or abandonment of the application or expiration of the patent.

The information provided by you in this form will be subject to the following routine uses:

1. The information on this form will be treated confidentially to the extent allowed under the Freedom of Information Act (5 U.S.C. 552) and the Privacy Act (5 U.S.C. 552a). Records from this system of records may be disclosed to the Department of Justice to determine whether the Freedom of Information Act requires disclosure of these records.

2. A record from this system of records may be disclosed, as a routine use, in the course of presenting evidence to a court, magistrate, or administrative tribunal, including disclosures to opposing counsel in the course of settlement negotiations.

3. A record in this system of records may be disclosed, as a routine use, to a Member of Congress submitting a request involving an individual, to whom the record pertains, when the individual has requested assistance from the Member with respect to the subject matter of the record.

4. A record in this system of records may be disclosed, as a routine use, to a contractor of the Agency having need for the information in order to perform a contract. Recipients of information shall be required to comply with the requirements of the Privacy Act of 1974, as amended, pursuant to 5 U.S.C. 552a(m).

5. A record related to an International Application filed under the Patent Cooperation Treaty in this system of records may be disclosed, as a routine use, to the International Bureau of the World Intellectual Property Organization, pursuant to the Patent Cooperation Treaty.

6. A record in this system of records may be disclosed, as a routine use, to another federal agency for purposes of National Security review (35 U.S.C. 181) and for review pursuant to the Atomic Energy Act (42 U.S.C. 218(c)).

7. A record from this system of records may be disclosed, as a routine use, to the Administrator, General Services, or his/her designee, during an inspection of records conducted by GSA as part of that agency's responsibility to recommend improvements in records management practices and programs, under authority of 44 U.S.C. 2904 and 2906. Such disclosure shall be made in accordance with the GSA regulations governing inspection of records for this purpose, and any other relevant (i.e., GSA or Commerce) directive. Such disclosure shall not be used to make determinations about individuals.

8. A record from this system of records may be disclosed, as a routine use, to the public after either publication of the application pursuant to 35 U.S.C. 122(b) or issuance of a patent pursuant to 35 U.S.C. 151. Further, a record may be disclosed, subject to the limitations of 37 CFR 1.14, as a routine use, to the public if the record was filed in an application which became abandoned or in which the proceedings were terminated and which application is referenced by either a published application, an application open to public inspections or an issued patent.

9. A record from this system of records may be disclosed, as a routine use, to a Federal, State, or local law enforcement agency, if the USPTO becomes aware of a violation or potential violation of law or regulation.

Doc code: IDS
Doc description: Information Disclosure Statement (IDS) Filed

PTO/SB/08a (02-18)
Approved for use through 11/30/2020. OMB 0651-0031
U.S. Patent and Trademark Office; U.S. DEPARTMENT OF COMMERCE
Under the Paperwork Reduction Act of 1995, no persons are required to respond to a collection of information unless it contains a valid OMB control number.

INFORMATION DISCLOSURE STATEMENT BY APPLICANT

(Not for submission under 37 CFR 1.99)

Application Number	15288406
Filing Date	2016-10-07
First Named Inventor	Terry Wright
Art Unit	1663
Examiner Name	KRUSE, DAVID H
Attorney Docket Number	14764-258662

ALL REFERENCES CONSIDERED EXCEPT WHERE LINED THROUGH. /D.H.K/

U.S.PATENTS Remove

Examiner Initial*	Cite No	Patent Number	Kind Code[1]	Issue Date	Name of Patentee or Applicant of cited Document	Pages,Columns,Lines where Relevant Passages or Relevant Figures Appear
	1					

If you wish to add additional U.S. Patent citation information please click the Add button. Add

U.S.PATENT APPLICATION PUBLICATIONS Remove

Examiner Initial*	Cite No	Publication Number	Kind Code[1]	Publication Date	Name of Patentee or Applicant of cited Document	Pages,Columns,Lines where Relevant Passages or Relevant Figures Appear
	1					

If you wish to add additional U.S. Published Application citation information please click the Add button. Add

FOREIGN PATENT DOCUMENTS Remove

Examiner Initial*	Cite No	Foreign Document Number[3]	Country Code[2] i	Kind Code[4]	Publication Date	Name of Patentee or Applicant of cited Document	Pages,Columns,Lines where Relevant Passages or Relevant Figures Appear	T[5]
	1	WO 2005/107437	WO		2005-11-17	Dow Agrosciences LLC		

If you wish to add additional Foreign Patent Document citation information please click the Add button Add

NON-PATENT LITERATURE DOCUMENTS Remove

Examiner Initials*	Cite No	Include name of the author (in CAPITAL LETTERS), title of the article (when appropriate), title of the item (book, magazine, journal, serial, symposium, catalog, etc), date, pages(s), volume-issue number(s), publisher, city and/or country where published.	T[5]

/DAVID H KRUSE/ 11/25/2020

EFS Web 2.1.18

INFORMATION DISCLOSURE STATEMENT BY APPLICANT (Not for submission under 37 CFR 1.99)		
	Application Number	15288406
	Filing Date	2016-10-07
	First Named Inventor	Terry Wright
	Art Unit	1663
	Examiner Name	KRUSE, DAVID H
	Attorney Docket Number	14764-258662

ALL REFERENCES CONSIDERED EXCEPT WHERE LINED THROUGH. /D.H.K/

	1	STREBER et al., Analysis, cloning, and high-level expression of 2,4-dichlorophenoxyacetate monooxygenase gene tfdA of Alcaligenes eutrophus JMP134, Journal of Bacteriology (1987), 169(7), 2950-5.	
	2	Poh et al., 2,4-Dichlorophenoxyacetate / α-ketoglutarate dioxygenases from Burkholderia cepacia 2a and Ralstonia eutropha JMP134, Microbios 105 43-63 2001.	
	3	SUWA et al., Characterization of a chromosomally encoded 2,4-dichlorophenoxyacetic acid/ketoglutarate dioxygenase from Burkholderia sp. strain RASC, Applied and Environmental Microbiology (1996), 62(7), 2464-2469.	
	4	ITOH et al., tfdA-like genes in 2,4-dichlorophenoxyacetic acid-degrading bacteria belonging to the Bradyrhizobium-Agromonas-Nitrobacter-Afipia cluster in Proteobacteria, Applied and Environmental Microbiology (2002), 68(7), 3449-3454.	
	5	Vedler et al. The Completely Sequenced Plasmid pEST4011 Contains a Novel IncP1 Backbone and a Catabolic Transposon Harboring tfd Genes for 2,4-Dichlorophenoxyacetic Acid Degradation, JOURNAL OF BACTERIOLOGY, Vol. 186, No. 21, Nov. 2004, p. 7161–7174.	
	6	HOFFMANN et al., Development and application of PCR primers for the detection of the tfd genes in Delftia acidovorans P4a involved in the degradation of 2,4-D, Acta Biotechnologica (2001), 21(4), 321-331.	
	7	ITOH et al.,Root nodule Bradyrhizobium spp. harbor tfdA and cadA, homologous with genes encoding 2,4-dichlorophenoxyacetic acid-degrading proteins, Applied and Environmental Microbiology (2004), 70(4), 2110-2118.	
	8	Kaneko et al., Complete Genomic Sequence of Nitrogen-fixing Symbiotic Bacterium Bradyrhizobium japonicum USDA110 (Supplement). DNA Research 9, — Supplement, 225–256 (2002).	
	9	Schleinitz et al., Localization and Characterization of Two Novel Genes Encoding Stereospecific Dioxygenases Catalyzing 2(2,4-Dichlorophenoxy)propionate Cleavage in Delftia acidovorans MC1, APPLIED AND ENVIRONMENTAL MICROBIOLOGY, Sept. 2004, p. 5357–5365.	
	10	Muller et al., Genetic Analysis of Phenoxyalkanoic Acid Degradation in Sphingomonas herbicidovorans MH; APPLIED AND ENVIRONMENTAL MICROBIOLOGY, Oct. 2004, Vol. 70, No. 10, p. 6066–6075.	
	11	MULLER et al., Physiological and genetic characteristics of two bacterial strains utilizing phenoxypropionate and phenoxyacetate herbicides, Microbiological Research (2001), 156(2), 121-131.	

EFS Web 2.1.18 /DAVID H KRUSE/ 11/25/2020

INFORMATION DISCLOSURE STATEMENT BY APPLICANT (Not for submission under 37 CFR 1.99)		
	Application Number	15288406
	Filing Date	2016-10-07
	First Named Inventor	Terry Wright
	Art Unit	1663
	Examiner Name	KRUSE, DAVID H
	Attorney Docket Number	14764-258662

ALL REFERENCES CONSIDERED EXCEPT WHERE LINED THROUGH. /D.H.K/

If you wish to add additional non-patent literature document citation information please click the Add button Add

EXAMINER SIGNATURE

Examiner Signature	/DAVID H KRUSE/	Date Considered	11/25/2020

*EXAMINER: Initial if reference considered, whether or not citation is in conformance with MPEP 609. Draw line through a citation if not in conformance and not considered. Include copy of this form with next communication to applicant.

[1] See Kind Codes of USPTO Patent Documents at www.USPTO.GOV or MPEP 901.04. [2] Enter office that issued the document, by the two-letter code (WIPO Standard ST.3). [3] For Japanese patent documents, the indication of the year of the reign of the Emperor must precede the serial number of the patent document. [4] Kind of document by the appropriate symbols as indicated on the document under WIPO Standard ST.16 if possible. [5] Applicant is to place a check mark here if English language translation is attached.

INFORMATION DISCLOSURE STATEMENT BY APPLICANT (Not for submission under 37 CFR 1.99)		
	Application Number	15288406
	Filing Date	2016-10-07
	First Named Inventor	Terry Wright
	Art Unit	1663
	Examiner Name	KRUSE, DAVID H
	Attorney Docket Number	14764-258662

CERTIFICATION STATEMENT

Please see 37 CFR 1.97 and 1.98 to make the appropriate selection(s):

That each item of information contained in the information disclosure statement was first cited in any communication from a foreign patent office in a counterpart foreign application not more than three months prior to the filing of the information disclosure statement. See 37 CFR 1.97(e)(1).

OR

☐ That no item of information contained in the information disclosure statement was cited in a communication from a foreign patent office in a counterpart foreign application, and, to the knowledge of the person signing the certification after making reasonable inquiry, no item of information contained in the information disclosure statement was known to any individual designated in 37 CFR 1.56(c) more than three months prior to the filing of the information disclosure statement. See 37 CFR 1.97(e)(2).

See attached certification statement.

☒ The fee set forth in 37 CFR 1.17 (p) has been submitted herewith.

☒ A certification statement is not submitted herewith.

SIGNATURE

A signature of the applicant or representative is required in accordance with CFR 1.33, 10.18. Please see CFR 1.4(d) for the form of the signature.

Signature	/John P. Breen/	Date (YYYY-MM-DD)	2020-09-10
Name/Print	John P. Breen	Registration Number	38833

This collection of information is required by 37 CFR 1.97 and 1.98. The information is required to obtain or retain a benefit by the public which is to file (and by the USPTO to process) an application. Confidentiality is governed by 35 U.S.C. 122 and 37 CFR 1.14. This collection is estimated to take 1 hour to complete, including gathering, preparing and submitting the completed application form to the USPTO. Time will vary depending upon the individual case. Any comments on the amount of time you require to complete this form and/or suggestions for reducing this burden, should be sent to the Chief Information Officer, U.S. Patent and Trademark Office, U.S. Department of Commerce, P.O. Box 1450, Alexandria, VA 22313-1450. DO NOT SEND FEES OR COMPLETED FORMS TO THIS ADDRESS. **SEND TO: Commissioner for Patents, P.O. Box 1450, Alexandria, VA 22313-1450.**

Privacy Act Statement

The Privacy Act of 1974 (P.L. 93-579) requires that you be given certain information in connection with your submission of the attached form related to a patent application or patent. Accordingly, pursuant to the requirements of the Act, please be advised that: (1) the general authority for the collection of this information is 35 U.S.C. 2(b)(2); (2) furnishing of the information solicited is voluntary; and (3) the principal purpose for which the information is used by the U.S. Patent and Trademark Office is to process and/or examine your submission related to a patent application or patent. If you do not furnish the requested information, the U.S. Patent and Trademark Office may not be able to process and/or examine your submission, which may result in termination of proceedings or abandonment of the application or expiration of the patent.

The information provided by you in this form will be subject to the following routine uses:

1. The information on this form will be treated confidentially to the extent allowed under the Freedom of Information Act (5 U.S.C. 552) and the Privacy Act (5 U.S.C. 552a). Records from this system of records may be disclosed to the Department of Justice to determine whether the Freedom of Information Act requires disclosure of these record s.

2. A record from this system of records may be disclosed, as a routine use, in the course of presenting evidence to a court, magistrate, or administrative tribunal, including disclosures to opposing counsel in the course of settlement negotiations.

3. A record in this system of records may be disclosed, as a routine use, to a Member of Congress submitting a request involving an individual, to whom the record pertains, when the individual has requested assistance from the Member with respect to the subject matter of the record.

4. A record in this system of records may be disclosed, as a routine use, to a contractor of the Agency having need for the information in order to perform a contract. Recipients of information shall be required to comply with the requirements of the Privacy Act of 1974, as amended, pursuant to 5 U.S.C. 552a(m).

5. A record related to an International Application filed under the Patent Cooperation Treaty in this system of records may be disclosed, as a routine use, to the International Bureau of the World Intellectual Property Organization, pursuant to the Patent Cooperation Treaty.

6. A record in this system of records may be disclosed, as a routine use, to another federal agency for purposes of National Security review (35 U.S.C. 181) and for review pursuant to the Atomic Energy Act (42 U.S.C. 218(c)).

7. A record from this system of records may be disclosed, as a routine use, to the Administrator, General Services, or his/her designee, during an inspection of records conducted by GSA as part of that agency's responsibility to recommend improvements in records management practices and programs, under authority of 44 U.S.C. 2904 and 2906. Such disclosure shall be made in accordance with the GSA regulations governing inspection of records for this purpose, and any other relevant (i.e., GSA or Commerce) directive. Such disclosure shall not be used to make determinations about individuals.

8. A record from this system of records may be disclosed, as a routine use, to the public after either publication of the application pursuant to 35 U.S.C. 122(b) or issuance of a patent pursuant to 35 U.S.C. 151. Further, a record may be disclosed, subject to the limitations of 37 CFR 1.14, as a routine use, to the public if the record was filed in an application which became abandoned or in which the proceedings were terminated and which application is referenced by either a published application, an application open to public inspections or an issued patent.

9. A record from this system of records may be disclosed, as a routine use, to a Federal, State, or local law enforcement agency, if the USPTO becomes aware of a violation or potential violation of law or regulation.

Doc Code: DIST.E.FILE **Document Description: Electronic Terminal Disclaimer - Filed**	PTO/SB/26 U.S. Patent and Trademark Office Department of Commerce

Electronic Petition Request	**TERMINAL DISCLAIMER TO OBVIATE A DOUBLE PATENTING REJECTION OVER A "PRIOR" PATENT**
Application Number	15288406
Filing Date	07-Oct-2016
First Named Inventor	Terry WRIGHT
Attorney Docket Number	14764-258662
Title of Invention	NOVEL HERBICIDE RESISTANCE GENES

☒ Filing of terminal disclaimer does not obviate requirement for response under 37 CFR 1.111 to outstanding Office Action

☒ This electronic Terminal Disclaimer is not being used for a Joint Research Agreement.

Owner	Percent Interest
DOW AGROSCIENCES LLC	100%

The owner(s) with percent interest listed above in the instant application hereby disclaims, except as provided below, the terminal part of the statutory term of any patent granted on the instant application which would extend beyond the expiration date of the full statutory term of prior patent number(s)

7838733

9127289

10174337

as the term of said prior patent is presently shortened by any terminal disclaimer. The owner hereby agrees that any patent so granted on the instant application shall be enforceable only for and during such period that it and the prior patent are commonly owned. This agreement runs with any patent granted on the instant application and is binding upon the grantee, its successors or assigns.

In making the above disclaimer, the owner does not disclaim the terminal part of the term of any patent granted on the instant application that would extend to the expiration date of the full statutory term of the prior patent, "as the term of said prior patent is presently shortened by any terminal disclaimer," in the event that said prior patent later:
- expires for failure to pay a maintenance fee;
- is held unenforceable;
- is found invalid by a court of competent jurisdiction;
- is statutorily disclaimed in whole or terminally disclaimed under 37 CFR 1.321;
- has all claims canceled by a reexamination certificate;
- is reissued; or
- is in any manner terminated prior to the expiration of its full statutory term as presently shortened by any terminal disclaimer.

◉ Terminal disclaimer fee under 37 CFR 1.20(d) is included with Electronic Terminal Disclaimer request. ○ I certify, in accordance with 37 CFR 1.4(d)(4), that the terminal disclaimer fee under 37 CFR 1.20(d) required for this terminal disclaimer has already been paid in the above-identified application.	
Applicant claims the following fee status: ○ Small Entity ○ Micro Entity ◉ Regular Undiscounted I hereby declare that all statements made herein of my own knowledge are true and that all statements made on information and belief are believed to be true; and further that these statements were made with the knowledge that willful false statements and the like so made are punishable by fine or imprisonment, or both, under Section 1001 of Title 18 of the United States Code and that such willful false statements may jeopardize the validity of the application or any patent issued thereon.	
THIS PORTION MUST BE COMPLETED BY THE SIGNATORY OR SIGNATORIES I certify, in accordance with 37 CFR 1.4(d)(4) that I am: ◉ An attorney or agent registered to practice before the Patent and Trademark Office who is of record in this application Registration Number 38833 ○ A sole inventor ○ A joint inventor; I certify that I am authorized to sign this submission on behalf of all of the inventors as evidenced by the power of attorney in the application ○ A joint inventor; all of whom are signing this request	
Signature	/John P. Breen/
Name	John P. Breen

*Statement under 37 CFR 3.73(b) is required if terminal disclaimer is signed by the assignee (owner).
Form PTO/SB/96 may be used for making this certification. See MPEP § 324.

Electronic Patent Application Fee Transmittal

Application Number:	15288406
Filing Date:	07-Oct-2016
Title of Invention:	NOVEL HERBICIDE RESISTANCE GENES
First Named Inventor/Applicant Name:	Terry WRIGHT
Filer:	John P. Breen/Garla Twyman
Attorney Docket Number:	14764-258662

Filed as Large Entity

Filing Fees for Utility under 35 USC 111(a)

Description	Fee Code	Quantity	Amount	Sub-Total in USD($)
Basic Filing:				
STATUTORY OR TERMINAL DISCLAIMER	1814	1	170	170
Pages:				
Claims:				
Miscellaneous-Filing:				
Petition:				
Patent-Appeals-and-Interference:				
Post-Allowance-and-Post-Issuance:				

Description	Fee Code	Quantity	Amount	Sub-Total in USD($)
Extension-of-Time:				
Miscellaneous:				
			Total in USD ($)	**170**

Doc Code: DISQ.E.FILE
Document Description: Electronic Terminal Disclaimer – Approved

Application No.: 15288406

Filing Date: 07-Oct-2016

Applicant/Patent under Reexamination: WRIGHT

Electronic Terminal Disclaimer filed on December 8, 2020

☒ APPROVED

This patent is subject to a terminal disclaimer

☐ DISAPPROVED

Approved/Disapproved by: Electronic Terminal Disclaimer automatically approved by EFS-Web

U.S. Patent and Trademark Office

Electronic Acknowledgement Receipt	
EFS ID:	41320162
Application Number:	15288406
International Application Number:	
Confirmation Number:	5402
Title of Invention:	NOVEL HERBICIDE RESISTANCE GENES
First Named Inventor/Applicant Name:	Terry WRIGHT
Customer Number:	107540
Filer:	John P. Breen/Garla Twyman
Filer Authorized By:	John P. Breen
Attorney Docket Number:	14764-258662
Receipt Date:	08-DEC-2020
Filing Date:	07-OCT-2016
Time Stamp:	10:56:27
Application Type:	Utility under 35 USC 111(a)

Payment information:

Submitted with Payment	yes
Payment Type	CARD
Payment was successfully received in RAM	$170
RAM confirmation Number	E2020B8A56236991
Deposit Account	100435
Authorized User	Garla Twyman
The Director of the USPTO is hereby authorized to charge indicated fees and credit any overpayment as follows: 37 CFR 1.21 (Miscellaneous fees and charges) 37 CFR 1.20 (Post Issuance fees)	

37 CFR 1.19 (Document supply fees)

37 CFR 1.17 (Patent application and reexamination processing fees)

37 CFR 1.16 (National application filing, search, and examination fees)

File Listing:

Document Number	Document Description	File Name	File Size(Bytes)/ Message Digest	Multi Part /.zip	Pages (if appl.)
1	Terminal Disclaimer-Filed (Electronic)	eTerminal-Disclaimer.pdf	33917 3b51fa3e2ee7a9d0d2cd19e25e9581d840935b24	no	2
Warnings:					
Information:					
2	Fee Worksheet (SB06)	fee-info.pdf	30447 64052ba84fa530dcc1cdfe65be77f48934c20212	no	2
Warnings:					
Information:					
		Total Files Size (in bytes):	64364		

This Acknowledgement Receipt evidences receipt on the noted date by the USPTO of the indicated documents, characterized by the applicant, and including page counts, where applicable. It serves as evidence of receipt similar to a Post Card, as described in MPEP 503.

New Applications Under 35 U.S.C. 111
If a new application is being filed and the application includes the necessary components for a filing date (see 37 CFR 1.53(b)-(d) and MPEP 506), a Filing Receipt (37 CFR 1.54) will be issued in due course and the date shown on this Acknowledgement Receipt will establish the filing date of the application.
National Stage of an International Application under 35 U.S.C. 371
If a timely submission to enter the national stage of an international application is compliant with the conditions of 35 U.S.C. 371 and other applicable requirements a Form PCT/DO/EO/903 indicating acceptance of the application as a national stage submission under 35 U.S.C. 371 will be issued in addition to the Filing Receipt, in due course.
New International Application Filed with the USPTO as a Receiving Office
If a new international application is being filed and the international application includes the necessary components for an international filing date (see PCT Article 11 and MPEP 1810), a Notification of the International Application Number and of the International Filing Date (Form PCT/RO/105) will be issued in due course, subject to prescriptions concerning national security, and the date shown on this Acknowledgement Receipt will establish the international filing date of the application.

To: INDocket@btlaw.com,,
From: PAIR_eOfficeAction@uspto.gov
Cc: PAIR_eOfficeAction@uspto.gov
Subject: Private PAIR Correspondence Notification for Customer Number 107540

Dec 08, 2020 03:53:47 AM

Dear PAIR Customer:

Barnes & Thornburg LLP (Dow)
11 South Meridian Street
Indianapolis, IN 46204
UNITED STATES

The following USPTO patent application(s) associated with your Customer Number, 107540 , have new outgoing correspondence. This correspondence is now available for viewing in Private PAIR.

The official date of notification of the outgoing correspondence will be indicated on the form PTOL-90 accompanying the correspondence.

Disclaimer:
The list of documents shown below is provided as a courtesy and is not part of the official file wrapper. The content of the images shown in PAIR is the official record.

Application	Document	Mailroom Date	Attorney Docket No.
15288406	CTFR	12/08/2020	14764-258662
	1449	12/08/2020	14764-258662
	1449	12/08/2020	14764-258662
	1449	12/08/2020	14764-258662

To view your correspondence online or update your email addresses, please visit us anytime at https://sportal.uspto.gov/secure/myportal/privatepair.

If you have any questions, please email the Electronic Business Center (EBC) at EBC@uspto.gov with 'e-Office Action' on the subject line or call 1-866-217-9197 during the following hours:

Monday - Friday 6:00 a.m. to 12:00 a.m.

Thank you for prompt attention to this notice,

UNITED STATES PATENT AND TRADEMARK OFFICE

PATENT APPLICATION INFORMATION RETRIEVAL SYSTEM

UNITED STATES PATENT AND TRADEMARK OFFICE
COMMISSIONER FOR PATENTS
P.O.BOX 1450
ALEXANDRIA VA 22313-1451

PRESORTED
FIRST-CLASS MAIL
U.S. POSTAGE PAID
POSTEDIGITAL
NNNNN

Barnes & Thornburg LLP (Dow)
11 South Meridian Street
Indianapolis, IN 46204

Courtesy Reminder for
Application Serial No: 15/288,406

Attorney Docket No: 14764-258662
Customer Number: 107540
Date of Electronic Notification: 12/08/2020

This is a courtesy reminder that new correspondence is available for this application. If you have not done so already, please review the correspondence. The official date of notification of the outgoing correspondence will be indicated on the form PTOL-90 accompanying the correspondence.

An email notification regarding the correspondence was sent to the following email address(es) associated with your customer number:
INDocket@btlaw.com

To view your correspondence online or update your email addresses, please visit us anytime at **https://ppair-my.uspto.gov/pair/PrivatePair.**
If you have any questions, please email the Electronic Business Center (EBC) at EBC@uspto.gov or call 1-866-217-9197.

BARNES & THORNBURG

11 South Meridian Street
Indianapolis, Indiana 46204
(317) 236-1313
(317) 231-7433 Fax

IN THE UNITED STATES PATENT AND TRADEMARK OFFICE

Customer No.:	107540
Group:	1663
Confirmation No.:	5402
Application No.:	15/288,406
Invention:	**Novel Herbicide Resistance Genes**
Inventor:	Terry Wright et al.
Filed:	October 7, 2016
Attorney Docket:	14764-258662
Examiner:	David Kruse

FILED ELECTRONICALLY:

December 16, 2020

AMENDMENT AND RESPONSE UNDER 37 CFR 1.116

Commissioner for Patents
P.O. Box 1450
Alexandria, Virginia 22313-1450

Sir:

In response to the final Office Action dated December 8, 2020, Applicant requests entry of the following amendments and consideration of the accompanying remarks. Applicant believes that no fees are required for submission of this response. If any fees are required to effect this filing, the Commissioner is authorized to charge the same to the account of Barnes & Thornburg, Deposit Account No. 10-0435 with reference to our file 14764-258662.

Amendments to the Claims are submitted herewith beginning on page 2.

Remarks begin on page 8 of this paper.

AMENDMENTS TO THE CLAIMS:

This listing of claims will replace all prior versions, and listings of claims in the application:

Claims:

Claims 1-14. (Canceled).

15. (Previously Presented) A transgenic plant cell comprising a recombinant polynucleotide that encodes an AAD-1 protein that exhibits aryloxyalkanoate dioxygenase activity wherein said activity enzymatically degrades a phenoxy auxin herbicide and an (R)-aryloxyphenoxypropionate herbicide, further wherein said AAD-1 protein comprises:

i) an amino acid sequence having at least 85% sequence identity with SEQ ID NO: 9; and

ii) an AAD-1 motif having the general formula of:

$HX_{112}D(X)_{114\text{-}137}T(X)_{139\text{-}269}H(X)_{271\text{-}280}R$, wherein

X_{112} represents a single amino acid at position 112, relative to the sequence of SEQ ID NO: 9;

$(X)_{114\text{-}137}$ represents a sequence of 24 amino acids;

$(X)_{139\text{-}269}$ represents a sequence of 131 amino acids; and

$(X)_{271\text{-}280}$ represents a sequence of 10 amino acids.

16. (Previously Presented) The plant cell of claim 15 wherein said AAD-1 motif has the general formula of:

$HX_{112}D(X)_{114\text{-}137}T(X)_{139\text{-}269}H(X)_{271\text{-}280}R(X)_{282\text{-}284}R$, wherein $(X)_{282\text{-}284}$ represents a sequence of 3 amino acids.

17. (Canceled).

COR-AAD1-00003891
Bayer EX1008 (Part 7 of 9)

18. (Previously Presented) The plant cell of claim 15 wherein the AAD-1 protein comprises an amino acid sequence having at least 90% sequence identity with SEQ ID NO: 9.

19. (Previously Presented) The plant cell of claim 15 wherein said plant cell is dicotyledonous and selected from the group consisting of a cotton cell, a tobacco cell, a canola cell, a soybean cell, and an Arabidopsis cell.

20. (Previously Presented) The plant cell of claim 15 wherein said plant cell is a monocotyledonous cell selected from the group consisting of a rice cell and a maize cell.

21. (Currently Amended) A transgenic plant comprising a plurality of the plant cells of claim 15, wherein expression of said polynucleotide renders said plant tolerant to an aryloxyalkanoate herbicide.

22. (Previously Presented) The plant of claim 21 wherein said aryloxyalkanoate herbicide is a phenoxy auxin herbicide.

23. (Previously Presented) The plant of claim 21 wherein said aryloxyalkanoate herbicide is selected from the group consisting of 2,4-dichlorophenoxyacetic acid, MCPA, dichlorprop, and mecoprop.

24. (Previously Presented) The plant of claim 21 wherein said aryloxyalkanoate herbicide is an (R)-aryloxyphenoxypropionate.

25. (Previously Presented) The plant of claim 21 wherein said aryloxyalkanoate herbicide is selected from the group consisting of (R)-fluazifop, (R)-haloxyfop, (R)-diclofop, (R)-quizalofop, (R)-fenoxaprop, (R)-metamifop, (R)-cyhalofop, and (R)-clodinofop.

COR-AAD1-00003892
Bayer EX1008 (Part 7 of 9)

26. (Previously Presented) The plant of claim 21 wherein said plant further comprises a second herbicide resistance gene.

27. (Previously Presented) The plant of claim 26 wherein said second herbicide resistance gene renders said plant resistant to an herbicide selected from the group consisting of glyphosate, glufosinate, acetolactate synthase (ALS) inhibitors, inhibitors of 4-hydroxyphenyl-pyruvate-dioxygenase (HPPD), dicamba, and inhibitors of protoporphyrinogen oxidase (PPO).

28. (Previously Presented) A method of controlling at least one weed in a field, wherein said field contains at least one plant of claim 21, wherein said method comprises applying to at least a portion of said field a first herbicide selected from the group consisting of a phenoxy auxin herbicide and an (R)-aryloxyphenoxypropionate herbicide.

29. (Previously Presented) The method of claim 28 wherein said phenoxy auxin herbicide is an R-enantiomer of a chiral phenoxy auxin.

30. (Previously Presented) The method of claim 28 wherein said phenoxy auxin herbicide is an achiral phenoxy auxin selected from the group consisting of 2,4-D and MCPA.

31. (Previously Presented) The method of claim 28 wherein said (R)-aryloxyphenoxypropionate herbicide is selected from the group consisting of (R)-fluazifop, (R)-haloxyfop, (R)-diclofop, (R)-quizalofop, (R)-fenoxaprop, (R)-metamifop, (R)-cyhalofop, and (R)-clodinofop.

32. (Previously Presented) The method of claim 28 wherein said method comprises applying a second herbicide.

33. (Previously Presented) The method of claim 32 wherein said first herbicide and said second herbicide are applied sequentially.

COR-AAD1-00003893
Bayer EX1008 (Part 7 of 9)

34. (Previously Presented) The method of claim 32 wherein said first herbicide and said second herbicide are applied concurrently.

35. (Previously Presented) The method of claim 32 wherein said first herbicide is a phenoxy auxin and said second herbicide is an (R)-aryloxyphenoxypropionate.

36. (Previously Presented) The method of claim 32 wherein said second herbicide is selected from the group consisting of glyphosate, glufosinate, dicamba, acetolactate synthase (ALS) inhibitors, protoporphyrinogen oxidase (PPO) inhibitors, and 4-hydroxyphenyl-pyruvate-dioxygenase (HPPD) inhibitors.

37. (Previously Presented) The method of claim 32, wherein said first herbicide is 2,4-D and said second herbicide is glyphosate or glufosinate.

38. (Previously Presented) The method of claim 32, wherein said first herbicide is an (R)-aryloxyphenoxypropionate and said second herbicide is glyphosate or glufosinate.

39. (Previously Presented) The method of claim 32 wherein said plant further comprises a second herbicide resistance gene that renders said plant resistant to said second herbicide.

40. (Currently Amended) The method of claim 39 wherein said second herbicide resistance gene is selected from the group consisting of a modified acetolactate synthase (ALS) gene, a glyphosate resistance gene, a glufosinate resistance gene, and a dicamba-degrading enzyme gene.

41. (Currently Amended) The method of claim 40 wherein:

(a) said modified ALS gene is selected from the group consisting of [[a]] SurA, SurB, Csr1, Csr1-1, and Csr1-2;

COR-AAD1-00003894
Bayer EX1008 (Part 7 of 9)

(b) said glyphosate resistance gene is selected from the group consisting of modified EPSPS (5-enolpyruvylshikimate-3-phosphate synthase), GOX, and GAT; and,

(c) said glufosinate resistance gene is selected from the group consisting of phosphinothricin-N-acetyltransferase (PAT) and bar.

42. (Previously Presented) The method of claim 32 wherein said method further comprises applying a third herbicide.

43. (Previously Presented) The method of claim 42, wherein said third herbicide is selected from the group consisting of glyphosate, glufosinate, HPPD-inhibitors, PPO-inhibitors, ALS inhibitors, and dicamba.

44. (Previously Presented) The method of claim 43 wherein said first, second and third herbicides are 2,4-D, quizalofop, and glyphosate.

45. (Currently Amended) A seed comprising a plurality of the plant cells of claim 15.

46. (Previously Presented) A method of controlling weeds in a field, wherein said method comprises applying an aryloxyalkanoate herbicide to said field and planting a seed of claim 45 in said field within 14 days of applying said aryloxyalkanoate herbicide.

47. (Previously Presented) A plant grown from the seed of claim 45.

48. (Previously Presented) A part, progeny, or asexual propagate of the plant of claim 47, wherein said part, progeny, or sexual propagate comprises said polynucleotide.

49. (Previously Presented) An (R)-aryloxyphenoxypropionate herbicide tolerant transgenic plant cell comprising a recombinant polynucleotide that encodes an AAD-1 protein that exhibits aryloxyalkanoate dioxygenase activity wherein said activity enzymatically

COR-AAD1-00003895
Bayer EX1008 (Part 7 of 9)

degrades a phenoxy auxin herbicide and an (R)-aryloxyphenoxypropionate herbicide, further wherein said AAD-1 protein comprises:

i) an amino acid sequence having at least 85% sequence identity with SEQ ID NO: 9; and

ii) an AAD-1 motif having the general formula of:

$HX_{112}D(X)_{114-137}T(X)_{139-269}H(X)_{271-280}R$, wherein

X_{112} represents a single amino acid at position 112, relative to the sequence of SEQ ID NO: 9;

$(X)_{114-137}$ represents a sequence of 24 amino acids;

$(X)_{139-269}$ represents a sequence of 131 amino acids; and

$(X)_{271-280}$ represents a sequence of 10 amino acids, wherein said motif has 90% sequence identity with corresponding amino acids of position 111 to 281 of SEQ ID NO: 9.

COR-AAD1-00003896
Bayer EX1008 (Part 7 of 9)

REMARKS

Claim Amendments

Claim 41 has been amended to conform to the Markush format using the conjunction "and" between the penultimate and final listed elements. Claims 21 and 45 have been amended to correct prepositional phrases, and Claim 40 has been amended to clarify antecedent basis. No new matter is added by way of these amendments.

Accordingly, applicant respectfully requests entry of the amendments and consideration of the following remarks.

Double Patenting Rejections – Terminal Disclaimers Were Filed & Accepted

Claims 15, 16 and 18-49 are rejected for obviousness type double patenting over claims 1-43 of US Patent No. 7,838,733. Claims 15, 16 and 18-49 are rejected for obviousness type double patenting over claims 1-22 of US Patent No. 9,127,289. Claims 15, 16 and 18-49 are rejected for obviousness type double patenting over claims 1-13 of US Patent No. 10,174,337. On December 8, 2020, Applicant filed e-terminal disclaimers over each of US Patent No. 7,838,733, US Patent No. 9,127,289 and US Patent No. 10,174,337, which have been accepted, thus obviating the obviousness type double patenting rejections of claims 15, 16 and 18-49.

Remarks

Applicant appreciates the Examiner's withdrawal of the written description and obviousness rejections. As a minor clarification, and as the Examiner correctly noted in the Interview Summary, the referenced variants contained amino acid modifications throughout their sequences (but outside of the recited AAD-1 motif)—not truncations at the C- and N- termini, as the final Office Action states. *See* Interview Summary (August 31, 2020); Office Action, 2; Wright-II Declaration ¶ 18 (September 9, 2020).

COR-AAD1-00003897
Bayer EX1008 (Part 7 of 9)

The application is now believed to be in condition for allowance, and allowance of the application is respectfully requested. If any further discussion of this matter would speed prosecution of this application, the Examiner is invited to call the undersigned at (434) 220-2866.

Respectfully submitted,

/John P. Breen/

John P. Breen
Registration No. 38,833
Attorney for Applicants

(317) 261-7940
Indianapolis, Indiana 46204

COR-AAD1-00003898
Bayer EX1008 (Part 7 of 9)

BARNES & THORNBURG LLP

11 South Meridian Street
Indianapolis, Indiana 46204
(317) 236-1313

PATENT APPLICATION

IN THE UNITED STATES PATENT AND TRADEMARK OFFICE

Customer No.:	107540	**FILED ELECTRONICALLY:**
Group:	1663	
Confirmation No.:	5402	
Application No.:	15/288,406	
Invention:	**NOVEL HERBICIDE RESISTANCE GENES**	**December 16, 2020**
Applicant:	Terry Wright et al.	
Filed:	October 7, 2016	
Attorney Docket:	14764-258662	
Examiner	David Kruse	

SUPPLEMENTAL INFORMATION DISCLOSURE STATEMENT

Mail Stop Amendment
Commissioner for Patents
P.O. Box 1450
Alexandria, Virginia 22313-1450

Sir:

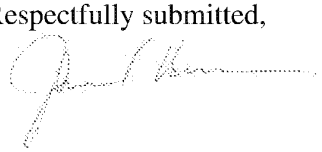
This Statement is filed pursuant to 37 C.F.R. § 1.56. No representation is intended that a complete search has been made of the prior art or that no better art references than the references cited in this IDS are available. The filing of this IDS shall not be construed to be an admission that the information cited in the IDS is, or is considered to be, material to patentability as defined in §1.56(b).

Pursuant to 37 C.F.R. § 1.98(a)(2)(ii), copies of cited U.S. patents and patent publications are not provided herewith; a copy of each cited foreign and non-patent reference is provided herewith.

Applicant submits herewith the fee set forth in 37 CFR 1.17 (p) and authorize the Commissioner to charge any additional fee necessary to affect this filing to our Deposit Account No. 10-0435, with reference to our Matter No. 14764-258662.

Consideration of the claims, leading to their allowance and passage of the application to issuance, is respectfully requested. If any further discussion of this matter would speed prosecution of this application, the Examiner is invited to call the undersigned at (434) 220-2866.

Respectfully submitted,



John P. Breen
Registration No. 38,833
Attorney for Applicants

JPB:glt
(317) 261-7940
Indianapolis, Indiana 46204

Doc code: IDS
Doc description: Information Disclosure Statement (IDS) Filed

PTO/SB/08a (02-18)

INFORMATION DISCLOSURE STATEMENT BY APPLICANT (**Not for submission under 37 CFR 1.99)**	Application Number	15288406
	Filing Date	2016-10-07
	First Named Inventor	Terry Wright
	Art Unit	1663
	Examiner Name	KRUSE, David H.
	Attorney Docket Number	14764-258662

U.S.PATENTS Remove

Examiner Initial*	Cite No	Patent Number	Kind Code[1]	Issue Date	Name of Patentee or Applicant of cited Document	Pages,Columns,Lines where Relevant Passages or Relevant Figures Appear
	1	5463175		1995-10-31	Barry et al.	
	2	6518222		2003-02-11	Arndt et al	

If you wish to add additional U.S. Patent citation information please click the Add button. Add

U.S.PATENT APPLICATION PUBLICATIONS Remove

Examiner Initial*	Cite No	Publication Number	Kind Code[1]	Publication Date	Name of Patentee or Applicant of cited Document	Pages,Columns,Lines where Relevant Passages or Relevant Figures Appear
	3	2003135879		2003-07-17	Weeks et al.	

If you wish to add additional U.S. Published Application citation information please click the Add button. Add

INFORMATION DISCLOSURE STATEMENT BY APPLICANT (Not for submission under 37 CFR 1.99)		
	Application Number	15288406
	Filing Date	2016-10-07
	First Named Inventor	Terry Wright
	Art Unit	1663
	Examiner Name	KRUSE, David H.
	Attorney Docket Number	14764-258662

FOREIGN PATENT DOCUMENTS

Examiner Initial*	Cite No	Foreign Document Number[3]	Country Code[2] ¡	Kind Code[4]	Publication Date	Name of Patentee or Applicant of cited Document	Pages,Columns,Lines where Relevant Passages or Relevant Figures Appear	T[5]
	4	03/013224	WO		2003-02-20	BAYER BIOSCIENCE N.V.		☐
	5	87/05629	WO		1987-09-24	PLANT GENETIC SYSTEMS N.V.		☐
	6	97/13402	WO		1997-04-17	DOW AGROSCIENCES LLC		☐
	7	96/33270	WO		1996-10-24	AMERICAN CYANAMID COMPANY		☐
	8	1167531	EP		2002-01-02	Monsanto Technology LLC		☐
	9	0009727	WO		2000-02-24	MAXYGEN, INC.		☐
	10	0066748	WO		2000-11-09	SYNGENTA LIMITED		☐
	11	1471533	CN		2004-01-28	DOW AGROSCIENCES LLC	English Abstract	☐

INFORMATION DISCLOSURE STATEMENT BY APPLICANT (Not for submission under 37 CFR 1.99)		
	Application Number	15288406
	Filing Date	2016-10-07
	First Named Inventor	Terry Wright
	Art Unit	1663
	Examiner Name	KRUSE, David H.
	Attorney Docket Number	14764-258662

If you wish to add additional Foreign Patent Document citation information please click the Add button		Add	
NON-PATENT LITERATURE DOCUMENTS		Remove	
Examiner Initials*	Cite No	Include name of the author (in CAPITAL LETTERS), title of the article (when appropriate), title of the item (book, magazine, journal, serial, symposium, catalog, etc), date, pages(s), volume-issue number(s), publisher, city and/or country where published.	T5
	12	HULSE J D ET AL: "CARNITINE BIOSYNTHESIS BETA HYDROXYLATION OF TRI METHYL LYSINE BY AN ALPHA KETO GLUTARATE DEPENDENT MITOCHONDRIAL DI OXYGENASE", JOURNAL OF BIOLOGICAL CHEMISTRY, vol. 253, no. 5, 1978, pages 1654-1659, ISSN: 0021-9258	☐
	13	EICHHORN ERIC ET AL: "Characterization of alpha-ketoglutarate-dependent taurine dioxygenase from Escherichia coli", JOURNAL OF BIOLOGICAL CHEMISTRY, vol. 272, no. 37, 1997, pages 23031-23036, ISSN: 0021-9258	☐
	14	BISHT NA VEEN CHANDRA ET AL: "Development of 2,4-O-resistant transgenics in Indian oilseed mustard (Brassica juncea)", CURRENT SCIENCE (BANGALORE), vol. 87, no. 3, 10 August 2004 (2004-08-10), pages 367-370, ISSN: 0011-3891	☐
	15	PRINS M: "Broad virus resistance in transgenic plants", TRENDS IN BIOTECHNOLOGY, ELSEVIER PUBLICATIONS, CAMBRIDGE, GB, vol. 21, no. 9, 1 September 2003 (2003-09-01), pages 373-375, XP004450444, ISSN: 0167-7799, DOI: 10.1016/S0167-7799(03)00183-5	☐
	16	DELLAPORTA S L ET AL: "A PLANT DNA MINIPREPARATION: VERSION 11", PLANT MOLECULAR BIOLOGY REPORTER, SPRINGER SCIENCE +BUSINESS MEDIA B.V, NL, vol. 1, no. 4, 1 January 1983 (1983-01-01), pages 19-21, XP001016105, ISSN: 0735-9640	☐
	17	Opposition filed against EP 10012200.1, filed on 2013-12-20	☐
	18	Opposition filed against EP 10012201.9, filed on 2013-12-06	☐
	19	Opposition filed against EP 10012202.7, filed on 2013-12-20	☐
	20	Opposition filed against EP 10012199.5, filed on 2014-06-18	☐

	21	Molecular Cloning, A Laboratory Manual, Cold Spring Harbor Laboratory Press, SECOND EDITION., 1989, Vol.2, p.11.45	☐
	22	Applicant Response to Opposition filed against EP 10012200.1, filed on 2014-08-08	☐
	23	Applicant Response to Opposition filed against EP 10012201.9, filed on 2014-07-28	☐
	24	Applicant Response to Opposition filed against EP 10012202.7, filed on 2014-07-28	☐
	25	Applicant Response to Opposition filed against EP 10012199.5, filed on 2014-11-22	☐
	26	Final Decision in Opposition filed against EP 10012200.1, filed on 2016-08-01	☐
	27	Final Decision in Opposition filed against EP 10012201.9, filed on 2016-08-01	☐
	28	Final Decision in Opposition filed against EP 10012202.7, filed on 2016-08-01	☐
	29	Final Decision in Opposition filed against EP 10012199.5, issued on 2016-02-09	☐

CERTIFICATION STATEMENT

X The fee set forth in 37 CFR 1.17 (p) has been submitted herewith.

X A certification statement is not submitted herewith.

SIGNATURE

A signature of the applicant or representative is required in accordance with CFR 1.33, 10.18. Please see CFR 1.4(d) for the form of the signature.

Signature	/John P. Breen/	Date (YYYY-MM-DD)	2020-12-16
Name/Print	John P. Breen	Registration Number	38833

This collection of information is required by 37 CFR 1.97 and 1.98. The information is required to obtain or retain a benefit by the public which is to file (and by the USPTO to process) an application. Confidentiality is governed by 35 U.S.C. 122 and 37 CFR 1.14. This collection is estimated to take 1 hour to complete, including gathering, preparing and submitting the completed application form to the USPTO. Time will vary depending upon the individual case. Any comments on the amount of time you require to complete this form and/or suggestions for reducing this burden, should be sent to the Chief Information Officer, U.S. Patent and Trademark Office, U.S. Department of Commerce, P.O. Box 1450, Alexandria, VA 22313-1450. DO NOT SEND FEES OR COMPLETED FORMS TO THIS ADDRESS. **SEND TO: Commissioner for Patents, P.O. Box 1450, Alexandria, VA 22313-1450.**

(12) INTERNATIONAL APPLICATION PUBLISHED UNDER THE PATENT COOPERATION TREATY (PCT)

(19) World Intellectual Property Organization
International Bureau

(43) International Publication Date
20 February 2003 (20.02.2003)

PCT

(10) International Publication Number
WO 03/013224 A2

(51) International Patent Classification[7]: A01H

(21) International Application Number: PCT/EP02/08136

(22) International Filing Date: 19 July 2002 (19.07.2002)

(25) Filing Language: English

(26) Publication Language: English

(30) Priority Data:
09/921,922 6 August 2001 (06.08.2001) US

(71) Applicant: **BAYER BIOSCIENCE N.V.** [BE/BE]; Jozef Plateaustraat 22, B-9000 Gent (BE).

(72) Inventors: **TROLINDER, Linda**; 1004 Dogwood St, Idalout, TX 79329 (US). **JEFFERSON, Gwyn**; 2787 Marico Place, Green Ville, MS 38701 (US). **DE BEUCKELEER, Marc**; Hekers 36, B-9052 Zwijnaarde (BE).

(81) Designated States *(national)*: AE, AG, AL, AM, AT, AU, AZ, BA, BB, BG, BR, BY, BZ, CA, CH, CN, CO, CR, CU, CZ, DE, DK, DM, DZ, EC, EE, ES, FI, GB, GD, GE, GH, GM, HR, HU, ID, IL, IN, IS, JP, KE, KG, KP, KR, KZ, LC, LK, LR, LS, LT, LU, LV, MA, MD, MG, MK, MN, MW, MX, MZ, NO, NZ, OM, PH, PL, PT, RO, RU, SD, SE, SG, SI, SK, SL, TJ, TM, TN, TR, TT, TZ, UA, UG, UZ, VN, YU, ZA, ZM, ZW.

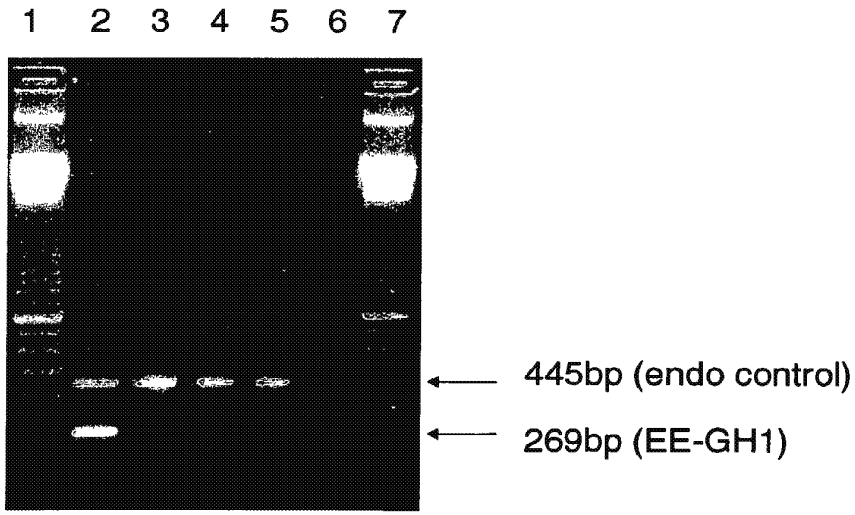
(84) Designated States *(regional)*: ARIPO patent (GH, GM, KE, LS, MW, MZ, SD, SL, SZ, TZ, UG, ZM, ZW), Eurasian patent (AM, AZ, BY, KG, KZ, MD, RU, TJ, TM), European patent (AT, BE, BG, CH, CY, CZ, DE, DK, EE, ES, FI, FR, GB, GR, IE, IT, LU, MC, NL, PT, SE, SK, TR), OAPI patent (BF, BJ, CF, CG, CI, CM, GA, GN, GQ, GW, ML, MR, NE, SN, TD, TG).

Declarations under Rule 4.17:
— *as to the identity of the inventor (Rule 4.17(i)) for all designations*
— *as to applicant's entitlement to apply for and be granted a patent (Rule 4.17(ii)) for all designations*
— *as to the applicant's entitlement to claim the priority of the earlier application (Rule 4.17(iii)) for all designations*

Published:
— *without international search report and to be republished upon receipt of that report*

For two-letter codes and other abbreviations, refer to the "Guidance Notes on Codes and Abbreviations" appearing at the beginning of each regular issue of the PCT Gazette.

(54) Title: HERBICIDE TOLERANT COTTON PLANTS AND METHODS FOR PRODUCING AND IDENTIFYING SAME



(57) Abstract: The invention pertains to transgenic cotton plants, plant material and seeds, characterized by harboring a specific transformation event, particularly by the presence of a gene encoding a protein that confers herbicide tolerance, at a specific location in the cotton genome. The cotton plants of the invention combine the herbicide tolerant phenotype with optimal agronomic performance.

WO 03/013224 A2

Title of the invention

HERBICIDE TOLERANT COTTON PLANTS AND METHODS FOR PRODUCING AND IDENTIFYING SAME

Field of the invention

This invention pertains to transgenic cotton plants, plant material and seeds, characterized by harboring a specific transformation event, particularly by the presence of a gene encoding a protein that confers herbicide tolerance, at a specific location in the cotton genome. The cotton plants of the invention combine the herbicide tolerant phenotype with an agronomic performance, genetic stability and adaptability to different genetic backgrounds equivalent to the non-transformed cotton line in the absence of weed pressure.

All documents cited herein are hereby incorporated herein by reference.

Background of the invention

The phenotypic expression of a transgene in a plant is determined both by the structure of the gene itself and by its location in the plant genome. At the same time the presence of the transgene at different locations in the genome will influence the overall phenotype of the plant in different ways. The agronomically or industrially successful introduction of a commercially interesting trait in a plant by genetic manipulation can be a lengthy procedure dependent on different factors. The actual transformation and regeneration of genetically transformed plants are only the first in a series of selection steps, which include extensive genetic characterization, breeding, and evaluation in field trials.

Cotton fiber is the single most important textile worldwide. About 80 million acres of cotton are harvested annually across the globe. Cotton is the fifth largest crop in the U.S. in terms of acreage production, with over 15 million acres planted in 2000. Primary weed

CONFIRMATION COPY

COR-AAD1-00003908
Bayer EX1008 (Part 7 of 9)

species for cotton are *Ipomoea sp.* (morning glory), *Amaranthus spp.* (pigweed), *Cyperus spp.* (nutsedge), *Xanthium spp.* (cocklebur) and *Sorghum spp.* (johnsongrass). Before the introduction of broad-leaf herbicides that could be used on a growing cotton field, growers used directed, post-emergence applications of nonselective herbicides taking care not to contact the growing crop plants. As this requires a difference in height between the weeds and the crop, this is not always possible. Especially for small cotton, this practice is time-consuming and potentially damaging to the crop.

The *bar* gene (Thompson et al, 1987, EMBO J 6:2519-2523; Deblock *et al.* 1987, EMBO J. 6:2513-2518) is a gene encoding the enzyme phosphinothricin acetyl transferase (PAT), which, when expressed in a plant, confers resistance to the herbicidal compounds phosphinothricin (also called glufosinate) or bialaphos (see also for example US patents, 5,646,024 and 5,561,236) and salts and optical isomers thereof. Phosphinothricin controls broadleaf weeds including morning glory and has a wide window of application.

Successful genetic transformation of cotton has been obtained by a number of methods including *Agrobacterium* infection of cotton explants (Firoozabady et al. 1987, Plant Molecular Biology 10:105-116; Umbeck et al. 1987, Bio/Technology 5:263-266 and in WO 00/71733, US 5,004,863, and US 5,159,135), as well as direct gene transfer by microprojectile bombardment of meristematic cotton tissues (Finer and Mc Mullen, 1990, Plant Cell Reports, 5:586-589; McCabe and Martinell, 1993, Bio/Technology 11:596-598, WO92/15675, EP0 531 506). Increased transformation efficiency for *Agrobacterium* transformation has been reported using the methods described by Hansen et al. (1994, Proc. Nat. Acad. Sci. 91:7603-7607) Veluthambi et al. (1989, Journal of Bacteriology 171:3696-3703) and WO 00/71733.
Different methods for regeneration of cotton plants have also been described (WO 89/05344, US 5,244,802, US 5,583,036, WO89/12102, WO98/15622, and WO97/12512).

However, the foregoing documents fail to teach or suggest the present invention.

COR-AAD1-00003909
Bayer EX1008 (Part 7 of 9)

Summary of the invention

The present invention relates to a transgenic cotton plant, or seed, cells or tissues thereof, comprising, stably integrated into its genome, an expression cassette which comprises a herbicide tolerance gene comprising the coding sequence of the *bar* gene (as described in Example 1.1 herein), which is herbicide tolerant and, in the absence of weed pressure, has an agronomic performance which is substantially equivalent to the non-transgenic isoline. Under weed pressure and the appropriate Liberty™ treatment, the plant will have a superior agronomic phenotype compared to the non-transgenic plant.

In one embodiment of the invention, the cotton plant or seed, cells or tissues thereof, comprises the expression cassette of pGSV71 (as described in Example 1.1, Table 1 herein). In the preferred embodiment of the invention the cotton plant or seed, cells or tissues thereof comprise elite event EE-GH1.

In another embodiment of the invention, the transgenic cotton plant or seed, cells or tissues thereof comprises:

(i) event EE-GH1 in its genome ;or

(ii) event EE-GH1 with the proviso that the *bar* gene used in the event is substituted with a nucleic acid sequence that hybridizes to the complement of the *bar* gene under stringent conditions.

More specifically, the present invention relates to a transgenic cotton plant, seed, cells or tissues thereof, the genomic DNA of which is characterized by the fact that, when analyzed in a PCR identification protocol as described herein, using two primers directed to the 5' or 3' flanking region of EE-GH1 and the foreign DNA, respectively, yields a fragment which is specific for EE-GH1. Preferably the primers are directed against the 5' flanking region within SEQ ID NO: 1 and the foreign DNA respectively; most preferably, the primers comprise the nucleotide sequence of SEQ ID NO: 2 and SEQ ID NO: 3 respectively, and yield a DNA fragment of between 250 and 290 bp, preferably of about 269 bp.

COR-AAD1-00003910
Bayer EX1008 (Part 7 of 9)

Reference seed comprising the elite event of the invention has been deposited at the ATCC under accession number PTA-3343. Thus, a preferred embodiment of the invention is the seed comprising elite event EE-GH1 deposited as ATTC accession number PTA-3343, which will grow into a cotton plant resistant to glufosinate. The seed of ATCC deposit number PTA-3343, which is a seed lot consisting of about 50% non-transgenic kernels and 50% transgenic kernels hemizygous for the transgene, comprising the elite event of the invention, which will grow into glufosinate tolerant plants. The seed can be sown and the growing plants can be treated with PPT or Liberty™ as described herein to obtain 100% glufosinate tolerant plants, comprising the elite event of the invention. The invention further relates to cells, tissues, progeny, and descendants from a plant comprising the elite event of the invention grown from the seed deposited at the ATCC having accession number PTA-3343. The invention further relates to plants obtainable by propagation of and/or breeding with a cotton plant comprising the elite event of the invention grown from the seed deposited at the ATCC having accession number PTA-3343.

The invention further relates to plants, seeds, cells or tissues comprising a foreign DNA sequence, preferably a herbicide tolerance gene as described herein, integrated into the chromosomal DNA in a region which comprises the plant DNA sequence of SEQ ID NO: 1 and/or SEQ ID NO: 4, more particularly which comprises the DNA sequence of SEQ ID NO: 5, or a sequence which hybridizes under stringent conditions to a sequence that is complementary to a sequence comprising the plant DNA sequence of SEQ ID NO: 1, SEQ ID NO: 4 and/or SEQ ID NO: 5.

The invention further provides a process for producing a transgenic cell of a cotton plant, which comprises inserting a recombinant DNA molecule into a region of the chromosomal DNA of a cotton cell, tissue or callus which comprises the plant DNA sequence of SEQ ID NO: 1 and/or SEQ ID NO: 4, or which comprises a sequence which hybridizes under stringent conditions to a sequence that is complementary to a sequence comprising the plant DNA sequence of SEQ ID NO: 1 and/or SEQ ID NO: 4.

COR-AAD1-00003911
Bayer EX1008 (Part 7 of 9)

The invention further relates to a method for identifying a transgenic plant, or cells or tissues thereof, comprising elite event EE-GH1 which method is based on identifying the presence of characterizing DNA sequences or amino acids encoded by such DNA sequences in the transgenic plant, cells or tissues. According to a preferred embodiment of the invention, such characterizing DNA sequences are sequences of 15bp, preferably 20bp, most preferably 30bp or more which comprise the insertion site of the event, i.e. both a part foreign DNA and a part of the cotton genome (either the 5' or 3' flanking region) contiguous therewith, allowing specific identification of the elite event.

According to another aspect of the invention, DNA sequences are disclosed comprising the insertion site of the event and sufficient length of polynucleotides of both the cotton genomic DNA and the foreign DNA (transgene), so as to be useful as primer or probe for the detection of EE-GH1. Preferably, such sequences comprise at least 9 nucleotides of the cotton genomic DNA and a similar number of nucleotides of the foreign DNA (transgene) of EE-GH1 therewith at each side of the insertion site respectively. Most preferably, such DNA sequences comprise at least 9 nucleotides of the cotton genomic DNA and a similar number of nucleotides of the foreign DNA contiguous with the insertion site in SEQ ID NO: 1 or SEQ ID NO: 4.

According to another preferred aspect of the invention, the method for identifying a transgenic plant, or cells or tissues thereof, comprising elite event EE-GH1, comprises amplifying a sequence of a nucleic acid present in biological samples, using a polymerase chain reaction, with at least two primers, one of which recognizes the plant DNA in the 5' or 3' flanking region of EE-GH1, the other which recognizes a sequence within the foreign DNA. Preferably, the genomic DNA is analyzed using primers which recognize a sequence within the plant 5' flanking region of EE-GH1, most preferably within the plant DNA sequence in SEQ ID NO: 1, and a sequence within the foreign DNA, respectively. Especially preferably, the genomic DNA is analyzed according to the PCR identification protocol described herein whereby the primer recognizing a sequence within the 5' flanking region comprises the nucleotide sequence of SEQ ID NO: 2. Particularly, the

COR-AAD1-00003912
Bayer EX1008 (Part 7 of 9)

primer recognizing a sequence within the 5' flanking region comprises the nucleotide sequence of SEQ ID NO: 2 and the primer recognizing a sequence within the foreign DNA comprises the nucleotide sequence of SEQ ID NO: 3, so that the amplified fragment is a fragment preferably of between 250 and 290 bp, more preferably of between 260 and 270 bp, most preferably of about 269 bp.

Accordingly, the present invention relates to the transgenic plant, cells or tissues thereof which can be identified according the above-described identification methods for EE-GH1.

The present invention relates to methods for identifying elite event EE-GH1 in biological samples, which methods are based on primers or probes that specifically recognize the 5' and/or 3' flanking sequence of EE-GH1. In a preferred embodiment of the invention these methods are based on primers or probes which recognize a sequence within SEQ ID NO: 1 and/or SEQ ID NO: 4, more particularly primers or probes comprising the sequence of SEQ ID NO: 2. According to another embodiment of the invention such methods are based on primers or probes which recognize a characterizing sequence of EE-GH1, which is a DNA sequence comprising the insertion site of the event, including sufficient nucleotides of the 5' or 3' flanking DNA and the foreign DNA contiguous therewith so as to be diagnostic for the event. Most particularly, such methods are based on sequences comprising sufficient nucleotides of the 5' or 3' flanking DNA and the foreign DNA contiguous therewith of SEQ ID NO: 1 or SEQ ID NO: 4. Such methods are known in the art and include, but are not limited to, the method described by Lyamichev et al. (1999, Nature Biotechn 17:292-296).

The present invention further relates to the specific flanking sequences of EE-GH1 described herein, which can be used to develop specific identification methods for EE-GH1 in biological samples. More particularly, the invention relates to the 5' and or 3' flanking regions of EE-GH1, which can be used for the development of specific primers and probes as well as to the specific primers and probes developed from the 5' and/or 3' flanking sequences of EE-GH1 and the insertion site adjacent thereto. The invention

COR-AAD1-00003913
Bayer EX1008 (Part 7 of 9)

further relates to identification methods for the presence of EE-GH1 in biological samples based on the use of such specific primers or probes.

The invention thus also relates to a kit for identifying elite event EE-GH1 in biological samples, the kit comprising at least one primer or probe which specifically recognizes the 5' or 3' flanking region of EE-GH1.

Preferably the kit of the invention comprises, in addition to a primer which specifically recognizes the 5' or 3' flanking region of EE-GH1, a second primer which specifically recognizes a sequence within the foreign DNA of EE-GH1, for use in a PCR identification protocol. Preferably, the kit of the invention comprises two (or more) specific primers, one of which recognizes a sequence within the 5' flanking region of EE-GH1, most preferably a sequence within the plant DNA region of SEQ ID NO: 1, and an other which recognizes a sequence within the foreign DNA. Especially preferably, the primer recognizing the plant DNA sequence within 5' flanking region comprises the nucleotide sequence of SEQ ID NO: 2. Particularly, the primer recognizing the plant DNA sequence within 5' flanking region comprises the nucleotide sequence of SEQ ID NO: 2 and the primer recognizing the foreign DNA comprises the nucleotide sequence of SEQ ID NO: 1 described herein.

According to a further embodiment, the invention relates to a kit for identifying elite event EE-GH1 in biological samples, which kit comprises at least one specific primer or probe having a sequence which corresponds (or is complementary to) a sequence that hybridizes under stringent conditions to a specific or characterizing region of EE-GH1. Preferably the sequence of the probe corresponds to a specific region comprising part of the foreign DNA and part of the 5' or 3' flanking region (plant DNA) of EE-GH1 contiguous therewith. Most preferably the specific probe comprises (or is complementary to) a sequence that hybridizes under stringent conditions to a sequence of 15 to 30 nucleotides spanning the insertion site at the 5' or 3' region of the foreign DNA within SEQ ID NO: 1 or SEQ ID NO: 4. Especially preferably the specific probe comprises (or is complementary to) a sequence that hybridizes under stringent conditions to a sequence

COR-AAD1-00003914
Bayer EX1008 (Part 7 of 9)

of 9 nucleotides of plant DNA and a similar number of nucleotides of the foreign DNA contiguous with the insertion site, within the sequences of SEQ ID NO:1 or SEQ ID NO:4. According to a particular embodiment, such a primer comprises a sequence that is identical to a sequence of 9 nucleotides of plant DNA and a similar number of nucleotides of the foreign DNA contiguous with the insertion site, within the sequences of SEQ ID NO: 1 or SEQ ID NO: 4.

The methods and kits encompassed by the present invention can be used for different purposes such as, but not limited to the following: to identify EE-GH1 in plants, plant material or in products such as, but not limited to food or feed products (fresh or processed) comprising or derived from plant material; additionally or alternatively, the methods and kits of the present invention can be used to identify transgenic plant material for purposes of segregation between transgenic and non-transgenic material; additionally or alternatively, the methods and kits of the present invention can be used to determine the quality (i.e. percentage pure material) of plant material comprising EE-GH1.

The present invention further relates to a method for tracking plants comprising elite event EE-GH1 in their genome upon introduction into different cultivars.

It will be understood that particular embodiments of the invention are described by the dependent claims cited herein.

Brief description of the Figure

The following detailed description, given by way of example, but not intended to limit the invention to specific embodiments described, may be understood in conjunction with the accompanying Figure, incorporated herein by reference, in which:

COR-AAD1-00003915
Bayer EX1008 (Part 7 of 9)

Fig. 1. PCR analysis of other events and elite event EE-GH1 using the EE-GH1 PCR identification protocol. Loading sequence of the gel: lane 1, molecular weight marker (100bp ladder), lane 2, DNA sample from a cotton plant comprising the transgenic event EE-GH1, lane 3, DNA samples from a cotton plant comprising another transgenic event, lane 4, DNA from wild-type cotton, lane 5, wild-type + 1 copy of the pGSV71-BamHI digest (positive control), lane 6, negative control (no template), lane 8, molecular weight marker (100bp ladder).

Detailed Description of Preferred Embodiments

The term "gene" as used herein refers to any DNA sequence comprising several operably linked DNA fragments such as a promoter region, a 5' untranslated region (the 5'UTR), a coding region (which may or may not code for a protein), and an untranslated 3' region (3'UTR) comprising a polyadenylation site. Typically in plant cells, the 5'UTR, the coding region and the 3'UTR are transcribed into an RNA of which, in the case of a protein encoding gene, the coding region is translated into a protein. A gene may include additional DNA fragments such as, for example, introns. As used herein, a genetic locus is the position of a given gene in the genome of a plant.

The term "chimeric" when referring to a gene or DNA sequence is used to refer to the fact that the gene or DNA sequence comprises at least two functionally relevant DNA fragments (such as promoter, 5'UTR, coding region, 3'UTR, intron) that are not naturally associated with each other and/or originate, for example, from different sources. "Foreign" referring to a gene or DNA sequence with respect to a plant species is used to indicate that the gene or DNA sequence is not naturally found in that plant species, or is not naturally found in that genetic locus in that plant species. The term "foreign DNA" will be used herein to refer to a DNA sequence as it has incorporated into the genome of a plant as a result of transformation. The "transforming DNA" as used herein refers to a recombinant DNA molecule used for transformation. The transforming DNA usually comprises at least one "gene of interest" (e.g. a chimeric gene) which is capable of

COR-AAD1-00003916
Bayer EX1008 (Part 7 of 9)

conferring one or more specific characteristics to the transformed plant. The term "recombinant DNA molecule" is used to exemplify and thus can include an isolated nucleic acid molecule which can be DNA and which can be obtained through recombinant or other procedures.

As used herein the term "transgene" refers to a gene of interest (or the whole of the foreign DNA) as incorporated in the genome of a plant. A "transgenic plant" refers to a plant comprising at least one transgene in the genome of all of its cells.

The foreign DNA present in the plants of the present invention will preferably comprise a herbicide tolerance gene, more specifically a 35S-*bar* gene as the gene of interest.

A "herbicide tolerance" gene as used herein refers to a gene that renders the plant tolerant to a herbicide. An example of a herbicide tolerance gene is gene comprising a sequence encoding the enzyme phosphinothricin acetyl transferase, which detoxifies phosphinothricin, under the control of a constitutive promoter. More specifically, in the elite event of the present invention the herbicide tolerance gene comprises the coding sequence of the bialaphos resistance gene (*bar*) of *Streptomyces hygroscopicus* (Thompson *et al.* (1987) EMBO J 6: 2519-2523) under control of the 35S promoter from Cauliflower Mosaic Virus (Odell et al., (1985), Nature 313: 810-812), also referred to as "35S-*bar*" herein. The expression of the 35S-*bar* gene confers tolerance to herbicidal compounds phosphinothricin or bialaphos or glufosinate, or more generally, glutamine synthase inhibitors, or salts or optical isomers thereof which will generally be referred to as "glufosinate tolerance" herein.

By hybridizing under "stringent conditions" is meant the conventional hybridizing conditions as described by Sambrook et al. (1989) (Molecular Cloning: A Laboratory Manual, Second Edition, Cold Spring Harbour Laboratory Press, NY) which for instance can comprise the following steps: 1) immobilizing plant genomic DNA fragments on a filter, 2) prehybridizing the filter for 1 to 2 hours at 42°C in 50% formamide, 5 X SSPE, 2 X Denhardt's reagent and 0.1% SDS, or for 1 to 2 hours at 68°C in 6 X SSC, 2 X Denhardt's reagent and 0.1% SDS, 3) adding the hybridization probe which has been

COR-AAD1-00003917
Bayer EX1008 (Part 7 of 9)

labeled, 4) incubating for 16 to 24 hours, 5) washing the filter for 20 min. at room temperature in 1X SSC, 0.1 %SDS, 6) washing the filter three times for 20 min. each at 68°C in 0.2 X SSC, 0.1 %SDS, and 7) exposing the filter for 24 to 48 hours to X-ray film at -70°C with an intensifying screen.

The incorporation of a recombinant DNA molecule in the plant genome typically results from transformation of a cell, tissue or callus (or from another genetic manipulation). The particular site of incorporation is either random or is at a predetermined location (if a process of targeted integration is used).

The DNA introduced into the plant genome as a result of transformation of a plant cell or tissue with a recombinant DNA or "transforming DNA" is hereinafter referred to as "foreign DNA" comprising one or more "transgenes". Thus, foreign DNA may comprise both recombinant DNA as well as newly introduced, rearranged DNA of the plant. However, the term "plant DNA" in the context of the present invention will refer to DNA of the plant which is generally found in the same genetic locus in the corresponding wild-type plant.

The foreign DNA can be characterized by the location and the configuration at the site of incorporation of the recombinant DNA molecule in the plant genome. The site in the plant genome where a recombinant DNA has been inserted is also referred to as the "insertion site" or "target site". Insertion of the recombinant DNA into the plant genome can be associated with a deletion of plant DNA, referred to as "target site deletion". A "flanking region" or "flanking sequence" as used herein refers to a sequence of at least 20 bp, preferably at least 50 bp, and up to 5000 bp of the plant genome which is located either immediately upstream of and contiguous with or immediately downstream of and contiguous with the foreign DNA. Transformation procedures leading to random integration of the foreign DNA will result in transformants with different flanking regions, which are characteristic and unique for each transformant. When the recombinant DNA present in a transgenic plant is introduced into a different plant through traditional crossing, its insertion site in the plant genome, or its flanking regions will generally not be changed (apart from occasional changes due to mutations or cross-

COR-AAD1-00003918
Bayer EX1008 (Part 7 of 9)

over and transposons). An "insertion region" as used herein refers to the region corresponding to the region of at least 40 bp, preferably at least 100 bp, and up to more than 10000 bp, encompassed by the sequence which comprises the upstream and/or the downstream flanking region of a foreign DNA in the (untransformed) plant genome (and including the insertion site and possible target site deletion). Taking into consideration minor differences due to mutations within a species, an insertion region will retain at least 85%, preferably 90%, more preferably 95%, and most preferably 100% sequence identity with the sequence comprising the upstream and downstream flanking regions of the foreign DNA in a given plant of that species.

Expression of a gene of interest refers to the fact that the gene confers on the plant one or more phenotypic traits (e.g. herbicide tolerance) that were intended to be conferred by the introduction of the recombinant DNA molecule – the transforming DNA - used during transformation (on the basis of the structure and function of part or all of the gene(s) of interest).

An "event" is defined as a (artificial) genetic locus that, as a result of genetic engineering, carries a foreign DNA comprising at least one copy of the gene(s) of interest (also referred to as a transformation event). An event is characterized phenotypically by the expression of the transgenes. At the genetic level, an event is part of the genetic makeup of a plant. At the molecular level, an event is characterized by the restriction map (e.g. as determined by Southern blotting) and/or by the upstream and/or downstream flanking sequences of the foreign DNA, and/or the molecular configuration of the foreign DNA comprising the transgenes. Usually when transforming a plant cell, tissue or callus with a transforming DNA, a multitude of events are generated, each of which is unique.

An "elite event", as used herein, is an event which is selected from a group of events, obtained by transformation with the same transforming DNA or by back-crossing with plants obtained by such transformation, based on the phenotypic expression and stability of the transgenes and the absence of negative impact on the agronomic characteristics of the plant comprising it (i.e., selected transformation event). Thus the criteria for elite

COR-AAD1-00003919
Bayer EX1008 (Part 7 of 9)

event selection are one or more, preferably two or more, advantageously all of the following:

a) That the presence of the foreign DNA in the plant does not compromise other desired characteristics of the plant, such as those relating to agronomic performance or commercial value;

b) That the event is characterized by a well defined molecular configuration which is stably inherited and for which appropriate diagnostic tools for identity control can be developed;

c) That the gene(s) of interest show(s) an appropriate and stable spatial and temporal phenotypic expression in homozygous condition of the event, at a commercially acceptable level in a range of environmental conditions in which the plants carrying the event are likely to be exposed in normal agronomic use.

It is preferred that the foreign DNA is associated with a position in the plant genome that allows introgression into desired commercial genetic backgrounds.

The status of an event as an elite event is confirmed by introgression of the elite event in different relevant genetic backgrounds and observing compliance with one, two or all of the criteria e.g. a), b) and c) above.

An "elite event" thus refers to a genetic locus comprising a foreign DNA, which answers to the above-described criteria. A plant, plant material or progeny such as seeds can comprise one or more elite events in its genome. Thus, when referring to a plant, seed cell or tissue comprising elite event EE-GH1 in its genome, a plant, seed cell or tissue is intended which comprises the foreign DNA described herein (comprising the 35S-*bar* gene) integrated in its genome at the integration site described herein.

The tools developed to identify an elite event or the plant or plant material comprising an elite event, or products which comprise plant material comprising the elite event are based on the specific genomic characteristics of the elite event, such as, a specific restriction map of the genomic region comprising the foreign DNA, molecular markers or the sequence of the flanking region(s) of the foreign DNA.

COR-AAD1-00003920
Bayer EX1008 (Part 7 of 9)

Once one or both of the flanking regions of the foreign DNA have been sequenced, primers and probes can be developed which specifically recognize this (these) sequence(s) in the nucleic acid (DNA or RNA) of a sample by way of a molecular biological technique. For instance a PCR method can be developed to identify the elite event in biological samples (such as samples of plants, plant material or products comprising plant material). Such a PCR is based on at least two specific "primers" one recognizing a sequence within the 5' or 3' flanking region of the elite event and the other recognizing a sequence within the foreign DNA. The primers preferably have a sequence of between 15 and 35 nucleotides which under optimized PCR conditions "specifically recognize" a sequence within the 5' or 3' flanking region of the elite event and the foreign DNA of the elite event respectively, so that a specific fragment ("integration fragment") is amplified from a nucleic acid sample comprising the elite event. This means that only the targeted integration fragment, and no other sequence (of that size) in the plant genome or foreign DNA, is amplified under optimized PCR conditions.

Preferably, the integration fragment has a length of between 50 and 500 nucleotides, most preferably of between 100 and 350 nucleotides. Preferably the specific primers have a sequence which is between 80 and 100% identical to a sequence within the 5' or 3' flanking region of the elite event and the foreign DNA of the elite event, respectively, provided the mismatches still allow specific identification of the elite event with these primers under optimized PCR conditions. The range of allowable mismatches however, can easily be determined experimentally and are known to a person skilled in the art.

As the sequence of the primers and their recognized sequence in the genome are unique for the elite event, amplification of the integration fragment will occur only in biological samples comprising (the nucleic acid of) the elite event. Preferably when performing a PCR to identify the presence of EE-GH1 in unknown samples, a control is included of a set of primers with which a fragment within a "housekeeping gene" of the plant species of the event can be amplified. Housekeeping genes are genes that are expressed in most cell types and which are concerned with basic metabolic activities common to all cells. Preferably, the fragment amplified from the housekeeping gene is a fragment which is

COR-AAD1-00003921
Bayer EX1008 (Part 7 of 9)

larger than the amplified integration fragment. Depending on the samples to be analyzed, other controls can be included.

Standard PCR protocols are described in the art, such as in 'PCR Applications Manual" (Roche Molecular Biochemicals, 2nd Edition, 1999). The optimal conditions for the PCR, including the sequence of the specific primers, is specified in a "PCR identification protocol" for each elite event. It is however understood that a number of parameters in the PCR identification protocol may need to be adjusted to specific laboratory conditions, and may be modified slightly to obtain similar results. For instance, use of a different method for preparation of DNA may require adjustment of, for instance, the amount of primers, polymerase and annealing conditions used. Similarly, the selection of other primers may dictate other optimal conditions for the PCR identification protocol. These adjustments will however be apparent to a person skilled in the art, and are furthermore detailed in current PCR application manuals such as the one cited above.

Alternatively, specific primers can be used to amplify an integration fragment that can be used as a "specific probe" for identifying EE-GH1 in biological samples. Contacting nucleic acid of a biological sample, with the probe, under conditions which allow hybridization of the probe with its corresponding fragment in the nucleic acid, results in the formation of a nucleic acid/probe hybrid. The formation of this hybrid can be detected (e.g. labeling of the nucleic acid or probe), whereby the formation of this hybrid indicates the presence of EE-GH1. Such identification methods based on hybridization with a specific probe (either on a solid phase carrier or in solution) have been described in the art. The specific probe is preferably a sequence which, under optimized conditions, hybridizes specifically to a region comprising part of the 5' or 3' flanking region of the elite event and also comprising part of the foreign DNA contiguous therewith (hereinafter also referred to as a "specific region" of the event). Depending on the method used, such a specific probe can comprise a sequence of between 15 and 30 bp or of between 50 and 500 bp, preferably of 100 to 350 bp which hybridizes under stringent conditions to the nucleotide sequence (or the complement of such sequence) of a specific region. Preferably, the specific probe will comprise a sequence of about 15 to about 100

COR-AAD1-00003922
Bayer EX1008 (Part 7 of 9)

contiguous nucleotides identical (or complementary) to a specific region of the elite event. Most preferably such a probe comprises at least 9 nucleotides identical to (or complementary to the 3' or 5' flanking region and a similar number of nucleotides in the foreign DNA contiguous therewith. Most preferably, such a probe comprises at least 9 nucleotides identical to (or complementary to the 3' or 5' flanking region and a similar number of nucleotides in the foreign DNA contiguous therewith of SEQ ID NO: 1 or SEQ ID NO: 4.

A "restriction map" as used herein refers to a set of Southern blot patterns obtained after cleaving plant genomic DNA (and/or the foreign DNA comprised therein) with a particular restriction enzyme, or set of restriction enzymes and hybridization with a probe sharing sequence similarity with the foreign DNA under standard stringency conditions. Standard stringency conditions as used herein refers to the conditions for hybridization described herein or to the conventional hybridizing conditions as described by Sambrook *et al.* (1989) (Molecular Cloning: A Laboratory Manual, Second Edition, Cold Spring Harbour Laboratory Press, NY) which for instance can comprise the following steps: 1) immobilizing plant genomic DNA fragments on a filter, 2) prehybridizing the filter for 1 to 2 hours at 42°C in 50% formamide, 5 X SSPE, 2 X Denhardt's reagent and 0.1% SDS, or for 1 to 2 hours at 68°C in 6 X SSC, 2 X Denhardt's reagent and 0.1% SDS, 3) adding the hybridization probe which has been labeled, 4) incubating for 16 to 24 hours, 5) washing the filter for 20 min. at room temperature in 1X SSC, 0.1 %SDS, 6) washing the filter three times for 20 min. each at 68°C in 0.2 X SSC, 0.1 %SDS, and 7) exposing the filter for 24 to 48 hours to X-ray film at -70°C with an intensifying screen.

Due to the (endogenous) restriction sites present in a plant genome prior to incorporation of the foreign DNA, insertion of a foreign DNA will alter the specific restriction map of that genome. Thus, a particular transformant or progeny derived thereof can be identified by one or more specific restriction patterns.

Alternatively, plants or plant material comprising an elite event can be identified by testing according to a PCR identification protocol. This is a PCR which specifically

COR-AAD1-00003923
Bayer EX1008 (Part 7 of 9)

recognizes the elite event. Essentially, a set of PCR primers is developed which recognizes a) a sequence within the 3' or 5' flanking sequence of the elite event and b) a sequence within the foreign DNA, which primers amplify a fragment (integration fragment) preferably of between 100 and 300 nucleotides. Preferably, a control is included of a set of primers which amplifies a fragment within a housekeeping gene of the plant species (preferably a fragment which is larger than the amplified integration fragment). The optimal conditions for the PCR, including the sequence of the specific primers is specified in a PCR identification protocol.

Other methods for identifying plants, plant material or products comprising plant material comprising elite event EE-GH1 are also envisaged. These methods include all methods based on the detection of the foreign DNA sequence and flanking sequence(s) of the elite event with a specific probe. More particularly, chip-based technologies, such as those described by Hacia *et al.* 1996 (Nat Genet 14(4):441-447) and Shoemaker *et al.* 1996 (Nat Genet 14(4):450-456) are envisaged. These methods allow segregation of target molccules as high-density arrays by using fixed probe arrays or by tagging of the genes with oligonucleotides, after which they can be screened by hybridization. Alternatively, third wave detection methods, such as those described by Lyamichev *et al.* (1999, above) are envisaged.

Identification of the protein(s) encoded by the foreign DNA of the elite event can be done by classical protein detection methods described in the art, such as those based on chromatographic or electromagnetic properties of the protein or the detection by specific monoclonal antibodies (as described in "Guide to protein purification, Murray P. Deutscher editor).

A "kit" as used herein refers to a set of reagents for the purpose of performing the method of the invention, more particularly, the identification of the elite event EE-GH1 in biological samples. More particularly, a preferred embodiment of the kit of the invention comprises at least one or two specific primers, as described above. Optionally, the kit can further comprise any other reagent described herein in the PCR identification protocol.

COR-AAD1-00003924
Bayer EX1008 (Part 7 of 9)

Alternatively, according to another embodiment of this invention, the kit can comprise a specific probe, as described above, which specifically hybridizes with nucleic acid of biological samples to identify the presence of EE-GH1 therein. Optionally, the kit can further comprise any other reagent (such as but not limited to hybridizing buffer, label) for identification of EE-GH1 in biological samples, using the specific probe.

The kit of the invention can be used, and its components can be specifically adjusted, for purposes of quality control (e.g., purity of seed lots), detection of the elite event in plant material or material comprising or derived from plant material, such as but not limited to food or feed products.

The present invention relates to the development of an elite event in cotton, EE-GH1, to the plants comprising this event, the progeny obtained from these plants and to the plant cells, or plant material derived from this event. Plants comprising elite event EE-GH1 were obtained through transformation with pGSV71 as described in example 1.

Cotton plants or plant material comprising EE-GH1 can be identified according to the PCR identification protocol described for EE-GH1 in Example 4 herein. Briefly, cotton genomic DNA is amplified by PCR using a primer which specifically recognizes a sequence within the 5' or 3' flanking sequence of EE-GH1, particularly the primer with the sequence of SEQ ID NO: 2, and a primer which recognizes a sequence in the foreign DNA, particularly the primer with the sequence of SEQ ID NO: 3. Endogenous cotton DNA primers are used as controls. If the plant material yields a fragment of between 250 and 290 bp, preferably of about 269 bp, the cotton plant is determined to harbor elite event EE-GH1.

Plants harboring EE-GH1 are characterized by their glufosinate tolerance, which in the context of the present invention includes that plants are tolerant to the herbicide Liberty™. Tolerance to Liberty™ can be tested in different ways. The leaf paint method as described herein, is most useful when you wish to identify both resistant and sensitive plants, but do not want to kill the sensitive ones. Alternatively, tolerance can be tested by

COR-AAD1-00003925
Bayer EX1008 (Part 7 of 9)

Liberty™ spray application. Spray treatments should be made between the leaf stages V3 and V4 for best results. Tolerant plants are characterized by the fact that spraying of the plants with at least 200 grams active ingredient/hectare (g.a.i./ha), preferably 400 g.a.i./ha, and possibly up to 1600 g.a.i./ha (4X the normal field rate), does not kill the plants. A broadcast application should be applied at a rate of 28-34 oz Liberty™. It is best to apply at a volume of 20 gallons of water per acre using a flat fan type nozzle while being careful not to direct spray applications directly into the whorl of the plants to avoid surfactant burn on the leaves. The herbicide effect should appear within 48 hours and be clearly visible within 5-7 days.

Plants harboring EE-GH1 can further be characterized by the presence in their cells of phosphinothricin acetyl transferase as determined by a PAT assay (De Block et al, 1987, supra).

Plants harboring EE-GH1 can, for example, be obtained from seeds deposited at the ATCC under accession number PTA-3343, which contain 50% kernels that are hemizigous for the elite event. Such plants can be further propagated to introduce the elite event of the invention into other cultivars of the same plant species. Selected seeds obtained from these plants contain the elite event stably incorporated into their genome. The invention further relates to plants derived from the ATCC accession number PTA-334, comprising EE-GH1. The term "derived from" herein indicates that the plants are related, i.e. they are both progeny (direct or of two or more generations) of the same transformant by crossing.

Plants harboring EE-GH1 are also characterized by having agronomical characteristics that are comparable to commercially available varieties of cotton in the US, in the absence of weed pressure and use of Liberty™ for weed control. It has been observed that the presence of a foreign DNA in the insertion region of the cotton plant genome described herein, confers particularly interesting phenotypic and molecular characteristics to the plants comprising this event. More specifically, the presence of the foreign DNA in this particular region in the genome of these plants, results in plants which display a stable phenotypic expression of the gene of interest without significantly compromising

COR-AAD1-00003926
Bayer EX1008 (Part 7 of 9)

any aspect of desired agronomic performance of the plants. Thus, the insertion region, corresponding to a sequence comprising the plant DNA of SEQ ID NO: 1 and/or SEQ ID NO: 4, more particularly a sequence corresponding to SEQ ID NO: 5, most particularly the insertion site of EE-GH1 therein, is shown to be particularly suited for the introduction of a gene(s) of interest. More particularly, the insertion region of EE-GH1 (corresponding to a DNA sequence of at least 40 bp in the cotton genome within SEQ ID NO: 5), or a sequence of at least 40 bp which hybridizes under stringent conditions to the complement of the sequence of SEQ ID NO: 5, is particularly suited for the introduction of foreign DNA comprising a herbicide tolerance gene, ensuring expression of each of these genes in the plant without compromising agronomic performance.

A recombinant DNA molecule can be specifically inserted in an insertion region by targeted insertion methods. Such methods are well known to those skilled in the art and comprise, for example, homologous recombination using a recombinase such as, but not limited to the FLP recombinase from *Saccharomyces cerevisiae* (published PCTP application WO 99/25821), the CRE recombinase from *Escherichia coli* phage P1 (published PCT application WO 99/25840), the recombinase from pSR1 of *Saccharomyces rouxii* (Araki *et al.* 1985, J Mol Biol 182:191-203), the Gin/gix system of phage Mu (Maeser and Kahlmann, 1991, Mol Gen Genetics 230:170-176) or the lambda phage recombination system (such as described in US Patent 4,673,640).

As used herein, "sequence identity" with regard to nucleotide sequences (DNA or RNA), refers to the number of positions with identical nucleotides divided by the number of nucleotides in the shorter of the two sequences. The alignment of the two nucleotide sequences is performed by the Wilbur and Lipmann algorithm (Wilbur and Lipmann, 1983, Proc Nat Acad Sci USA 80:726) using a window-size of 20 nucleotides, a word length of 4 nucleotides, and a gap penalty of 4. Computer-assisted analysis and interpretation of sequence data, including sequence alignment as described above, can, e.g., be conveniently performed using the programs of the Wisconsin Package (from the Genetics Computer Group, Inc). Sequences are indicated as "essentially similar" when such sequences have a sequence identity of at least about 75%, particularly at least about

COR-AAD1-00003927
Bayer EX1008 (Part 7 of 9)

80%, more particularly at least about 85%, quite particularly about 90%, especially about 95%, more especially about 100%, quite especially are identical. It is clear that when RNA sequences are said to be essentially similar or have a certain degree of sequence identity with DNA sequences, thymine (T) in the DNA sequence is considered equal to uracil (U) in the RNA sequence. "Complementary to" as used herein refers to the complementarity between the A and T (U), and G and C nucleotides in nucleotide sequences.

As used in herein, a "biological sample" is a sample of a plant, plant material or products comprising plant material. The term "plant" is intended to encompass cotton (such as but not limited to *Gossypium hirsutum*) plant tissues, at any stage of maturity, as well as any cells, tissues, or organs taken from or derived from any such plant, including without limitation, any seeds, leaves, stems, flowers, roots, single cells, gametes, cell cultures, tissue cultures or protoplasts. "Plant material", as used herein refers to material which is obtained or derived from a plant. Products comprising plant material relate to food, feed or other products which are produced using plant material or can be contaminated by plant material. It is understood that, in the context of the present invention, such biological samples are preferably tested for the presence of nucleic acids specific for EE-GH1, implying the presence of nucleic acids in the samples. Thus the methods referred to herein for identifying elite event EE-GH1 in biological samples, preferably relate to the identification in biological samples of nucleic acids which comprise the elite event.

As used herein "comprising" is to be interpreted as specifying the presence of the stated features, integers, steps or components as referred to, but does not preclude the presence or addition of one or more features, integers, steps or components, or groups thereof. Thus, e.g., a nucleic acid or protein comprising a sequence of nucleotides or amino acids, may comprise more nucleotides or amino acids than the actually cited ones, i.e., be embedded in a larger nucleic acid or protein. A chimeric gene comprising a DNA sequence which is functionally or structurally defined, may comprise additional DNA sequences, etc.

COR-AAD1-00003928
Bayer EX1008 (Part 7 of 9)

The following examples describe the development and characteristics of cotton plants harboring the elite events EE-GH1 as well as the development of tools for the identification of elite event EE-GH1 in biological samples.

Unless otherwise stated, all recombinant DNA techniques are carried out according to standard protocols as described in Sambrook *et al.* (1989) *Molecular Cloning: A Laboratory Manual*, Second Edition, Cold Spring Harbour Laboratory Press, NY and in Volumes 1 and 2 of Ausubel *et al.* (1994) *Current Protocols in Molecular Biology*, Current Protocols, USA. Standard materials and methods for plant molecular work are described in Plant Molecular Biology Labfax (1993) by R.D.D. Croy published by BIOS Scientific Publications Ltd (UK) and Blackwell Scientific Publications, UK.

In the description and examples, reference is made to the following sequences:

SEQ ID NO: 1:	sequence comprising the 5' flanking region
SEQ ID NO: 2:	primer GHI06
SEQ ID NO: 3:	primer GHI05
SEQ ID NO: 4:	sequence comprising the 3' flanking region
SEQ ID NO: 5:	insertion region
SEQ ID NO: 6:	plasmid pGSV71
SEQ ID NO: 7:	plasmid pRVA44
SEQ ID NO: 8	primer MDB327
SEQ ID NO: 9:	primer MLD015
SEQ ID NO: 10:	primer MLD016
SEQ ID NO: 11:	primer MDB612
SEQ ID NO: 12:	primer MDB053
SEQ ID NO: 13:	primer MDB356
SEQ ID NO: 14:	primer DPA017
SEQ ID NO: 15:	primer MLD019
SEQ ID NO: 16:	sequence comprising target site deletion
SEQ ID NO: 17:	primer GHI01
SEQ ID NO: 18:	primer GHI02

COR-AAD1-00003929
Bayer EX1008 (Part 7 of 9)

EXAMPLES

Example 1: Transformation of cotton with a herbicide tolerance gene

1.1. Construction of the chimeric DNA comprising the *bar* gene under the control of a constitutive promoter

A plasmid pGSV71 was constructed following standard procedures. The sequence of the genetic elemennts of plasmid pGSV71 is given in table 1 (SEQ ID NO: 6):

Table 1. Nucleotide positions of the genetic elements in pGSV71

Nt positions	Abbreviation	Description and references
198-222	-	Right border Repeat from the TL-DNA from pTiB6S3 (Gielen *et al.*, 1984, EMBO J. 3:835-846)
223-249	-	Polylinker
250-1634	P35S3	Promoter of the 35S RNA of Cauliflower Mosaic Virus (Odell *et al.*, (1985), Nature 313: 810-812)
1635-2186	*bar*	Coding sequence encoding phosphinothricine-acetyl-transferase from *Streptomyces hygroscopicus* (Thompson *et al.*, (1987) EMBO J. 6: 2519-2523). The N-terminal two codons of the wild-type *bar* coding region have been substituted for codons ATG and GAC respectively.
2187-2205	-	Polylinker
2206-2465	*3'nos*	A 260 bp TaqI fragment from the 3'untranslated region of the nopaline-synthase gene originating from the T-DNA of pTiT37 (Depicker *et al.*, 1982, J. Mol. Appl. Genet. 1: 561-573)
2466-2519	-	Polylinker
2520-2544	-	Left border Repeat from the TL-DNA from pTiB6S3 (Gielen *et al.*, 1984, EMBO J. 3:835-846)

1.2. Transformation of *Gossypium hirsutum*

Cotton tissue from Coker312 plants was transformed with pGSV71 using *Agrobacterium* transformation (US 5,986,181) and regenerated to plants on appropriate media.

COR-AAD1-00003930
Bayer EX1008 (Part 7 of 9)

The small plantlets initiated on the selective regeneration media were transferred to new medium for germination (all medium is hormone-free). Plantlets were then transferred to the growth chambers or to the greenhouses.

Selection was done on phosphinothricin (PPT) at all stages except plantlet regeneration, which was done in the absence of PPT to accelerate growth. This resulted in a set of primary transformants (plants of generation T0).

Example 2: Development of events

2.1. Development of lines carrying the event trait

T0 shoots were transferred to greenhouse soil and plants were screened for glufosinate tolerance and for the presence of the PAT enzyme with a PAT ELISA (Steffens Biotechnische Analysen GmbH, Ebringen, Germany).

T1 to T3 plants were grown in the greenhouse and tested for Liberty™ tolerance at a 2x rate (by spraying 56 oz/ha). Positive plants were tested for expression of the bar gene using the Pat assay as described by Deblock et al. 1987 (EMBO J. 6:2513-2518).

Presence of the foreign DNA and copy number was checked by Southern blot analysis. Total genomic DNA was isolated from 1g of leaf tissue according to the CETAB method of Doyle *et al.* (1987, Phytochem. Bull. 19:11) and digested with EcoRI restriction enzyme.

Probes such as the following were used for Southern analysis :

"*bar*" probe: 474 bp KpnI-BglI digest of plasmid pDE110 (WO 92/09696)

"35S" probe: 892 bp NcoI-MunI digest of plasmid pRVA44 (SEQ ID NO: 7)

T2 Plants were also evaluated for general phenotypic characteristics compared to the non-transgenic isogenic lines. In later generations, the lines for which no negative penalties on phenotype or agronomic performance was observed for the presence of the transgene

COR-AAD1-00003931
Bayer EX1008 (Part 7 of 9)

either in hemizygous or in homozygous condition, as compared to wild-types were selected.

T4 material was grown in the field and tested under field conditions for Liberty™ tolerance according to different schedules.

In later generations, plants were compared to commercial varieties for yield, fiber quality and plant mapping data. Agronomic characteristics, such as plant height, height to node, boll retention, stand, vigor, fiber length, fiber strength and lint yield were evaluated.

It was determined that one event performed equally or better than the comparable checks and that for this event yield was dependent on background rather than on presence of the transgene.

2.2. Selection of an elite event

This selection procedure, yielded one elite event which displayed optimal expression of the 35S-*bar* gene, i.e. tolerance to glufosinate ammonium, without penalty on agronomic performance and yield. This elite event was named EE-GH1.

2.3. Testing of EE-GH1 in cotton varieties with different genetic backgrounds and in different locations

The selected event was introduced into different commercial genetic backgrounds, including FM989, FM 832, FM958, and FM966 and results of field trials of four different locations were compared. Plants were sprayed with 1600 g.a.i./ha, using different treatments (1x3-5 leaf stage, 4x, 3-5 leaf stage, 1x+1x, 3-5 leaf stage, 4x+4x, 3-5 leaf stage, 0 as control).
Seedling emergence and vigor rating for the elite event was very good.

COR-AAD1-00003932
Bayer EX1008 (Part 7 of 9)

No visible damage as a result of herbicide application was ever observed after application regardless of rate or stage of development at the time of application. There were no detrimental effects on morphology or growth habit of plants by herbicide application

Furthermore, the event had normal leaf, flower and boll morphology, excellent fertility, and showed no disease or abnormal insect susceptibility in multiple genetic backgrounds. During introgression into multiple genetic backgrounds no aberrant problems or abnormalities were observed over four generations.

2.4. Genetic analysis of the locus

The genetic stability of the insert for the EE-GH1 event was checked by molecular and phenotypic analysis in the progeny plants over several generations.
Southern blot analyses of plants of the T1, T2 and T3 generation were compared for the EE-GH1 event. The patterns obtained were found to be identical in the different generations. This proves that the molecular configuration of the foreign DNA in EE-GH1 was stable.

The EE-GH1 event displayed Mendelian segregation for the transgene as a single genetic locus in at least three subsequent generations indicating that the insert is stable.

Example 3: Characterization of elite event EE-GH1

3.1 In-depth molecular and genetic analysis of the locus

Once the EE-GH1 event was identified as the event in which expression of the transgene as well as overall agronomic performance were optimal, the locus of the transgene was analyzed in detail on a molecular level. This included sequencing of the flanking regions of the transgene.

COR-AAD1-00003933
Bayer EX1008 (Part 7 of 9)

The sequence of the regions flanking the inserted transgene in the EE-GH1 event was determined using the TAIL-PCR protocol as described by Liu *et al.* (1995, Plant J. 8(3): 457-463).

a) Determination of the 5' flanking region

The primers used were:

		Sequence (5' → 3')	**Position in pGSV71**
Degenerate primer	MDB327	NTg.Agg.WTC.NWg.TSA.T (SEQ ID NO: 8)	-
Primary TAIL	MLD015	Tgg.TTC.CTA.gCg.TgA.gCC.AgT.g (SEQ ID NO: 9)	606→585
Second. TAIL	MLD016	AgC.TgC.TgC.TCT.TgC.CTC.TgT (SEQ ID NO: 10)	467→447
Tertiary TAIL	GHI05	ggA.CCg.TTA.TAC.ACA.ACg.Tag (SEQ ID NO: 3)	358→338

Whereby N=A,C, T or g; S=C or g; W=A or T

The fragment amplified using MDB327-GHI05 was ca. 1200 bp which was sequenced (5'flank: SEQ ID NO: 1). The sequence between bp 1 and bp 677 comprised plant DNA, while the sequence between bp 678 and bp 850 corresponded to pGSV71 DNA.

b) Determination of the 3' flanking region

The primers used were:

COR-AAD1-00003934
Bayer EX1008 (Part 7 of 9)

		Sequence (5' → 3')	Position in pGSV71
Degenerate primer	MDB612	NgT.gCT.SWg.ANA.WgA.T (SEQ ID NO: 11)	-
Primary TAIL	MDB053	CAT.gAC.gTg.ggT.TCC.Tgg.Cag.C (SEQ ID NO: 12)	2109-2130
Secondary TAIL	MDB356	AAT.CCT.gTT.gCC.ggT.CTT.gCg (SEQ ID NO: 13)	2252-2272
Tertiary TAIL	DPA017	gAT.TAg.AgT.CCC.gCA.ATT.ATA.C (SEQ ID NO: 14)	2362-2383

Whereby: N = A,C,T or g; S = C or g; W = A or T

The fragment amplified using MDB612-DPA017 was ca. 400 bp, the complete sequence of which was determined (SEQ ID NO: 4). The sequence between nucleotide 1 and 179 corresponds to T-DNA, while the sequence between nucleotide 180 and 426 corresponds to plant DNA.

c) Identification of the target site deletion

Using primers corresponding to sequences within the flanking regions of the transgene on the wildtype *Gossypium hirsutum* as a template, the insertion site of the transgene was identified.

The following primers were used:

	Sequence (5' → 3')	Position in 5'flank (SEQ ID NO: 1)	Position in 3'flank (SEQ ID NO: 4)
GHI06	TTg.CAC.CAT.CTA.gCT.CAC.TC (SEQ ID NO: 2)	815 → 795	- - - - -

COR-AAD1-00003935
Bayer EX1008 (Part 7 of 9)

MLD019	CAA.gAT.gCg.AgC.AAC.TAT.gT (SEQ ID NO: 15)	-----	285 → 266

This yielded a 200 bp fragment (SEQ ID NO: 16) in which bp 85 to 122 corresponds to a target site deletion.

Thus, the insertion region (SEQ ID NO: 5) as sequenced comprises:

1-677:	5' flanking region	bp 1 to 677 of SEQ ID NO: 1
678-714:	target site deletion	bp 85 to 122 of SEQ ID NO: 16
715-916:	3' flanking region	bp 180 to 426 of SEQ ID NO: 4

3.2. Genetic analysis of the locus

The genetic stability of the insert was checked by molecular and phenotypic analysis in the progeny plants over several generations.

Southern blot analyses on glufosinate tolerant plants of EE-GH1 cotton plants of the T_0, T_1 and T_2 generation were compared and were found to be identical. This proves that the molecular configuration of the transgene in EE-GH1 containing plants was stable.

The EE-GH1 event displayed Mendelian segregation for the transgene as a single genetic locus in at least three subsequent generations indicating that the insert is stable.

On the basis of the above results EE-GH1 was identified as an elite event.

Example 4: Development of diagnostic tools for identity control

A EE-GH1 Elite event PCR Identification protocol was developed to identify the presence of EE-GH1 in plants, plant material or biological samples.

COR-AAD1-00003936
Bayer EX1008 (Part 7 of 9)

EE-GH1 Elite event Polymerase Chain Reaction identification protocol

A test run, with all appropriate controls, has to be performed before attempting to screen unknowns. The presented protocol might require optimization for components that may differ between labs (template DNA preparation, Taq DNA polymerase, quality of the primers, dNTP's, thermocyler, etc.).

Amplification of the endogenous sequence plays a key role in the protocol. One has to attain PCR and thermocycling conditions that amplify equimolar quantities of both the endogenous and transgenic sequence in a known transgenic genomic DNA template. Whenever the targeted endogenous fragment is not amplified or whenever the targeted sequences are not amplified with the same ethidium bromide staining intensities, as judged by agarose gel electrophoresis, optimization of the PCR conditions may be required.

Template DNA

Template DNA is prepared according to the CTAB method described by Doyle and Doyle (1987, Phytochem. Bull. 19: 11). When using DNA prepared with other methods, a test run utilizing different amounts of template should be done. Usually 50 ng of genomic template DNA yields the best results.

Assigned positive and negative controls

The following positive and negative controls should be included in a PCR run:

- Master Mix control (DNA negative control). This is a PCR in which no DNA is added to the reaction. When the expected result, no PCR products, is observed this indicates that the PCR cocktail was not contaminated with target DNA.

COR-AAD1-00003937
Bayer EX1008 (Part 7 of 9)

- A DNA positive control (genomic DNA sample known to contain the transgenic sequences). Successful amplification of this positive control demonstrates that the PCR was run under conditions which allow for the amplification of target sequences.

- A wildtype DNA control. This is a PCR in which the template DNA provided is genomic DNA prepared from a non-transgenic plant. When the expected result, no amplification of the transgene PCR product but amplification of the endogenous PCR product, is observed this indicates that there is no detectable transgene background amplification in a genomic DNA sample.

Primers

The following primers, which specifically recognize the transgene and a flanking sequence of EE-GH1 are used:

Primer	Sequence (5' → 3')	Position in SEQ ID NO: 1	Target
GHI05	ggA.CCg.TTA.TAC.ACA.ACg.Tag (SEQ ID NO: 3)	758→ 738	pGSV71 sequence
GHI06	TTg.CAC.CAT.CTA.gCT.CAC.TC (SEQ ID NO: 2)	815→ 795	Plant DNA Sequence

Primers targeting an endogenous sequence are always included in the PCR cocktail. These primers serve as an internal control in unknown samples and in the DNA positive control. A positive result with the endogenous primer-pair demonstrates that there is ample DNA of adequate quality in the genomic DNA preparation for a PCR product to be generated. The endogenous primers used are:

GHI01: 5'-AAC.CTA.ggC.TgC.TgA.Agg.AgC-3' (SEQ ID NO: 17)

(Alcohol dehydrogenase gene Acc. NO: AF036569, 1070→1090)

COR-AAD1-00003938
Bayer EX1008 (Part 7 of 9)

GHI02: 5'-CAA.CTC.CTC.CAg.TCA.TCT.CCg-3' (SEQ ID NO: 18)

(Alcohol dehydrogenase gene Acc. NO: AF036569, 1515→1495)

Amplified fragments

The expected amplified fragments in the PCR reaction are:

For primer pair GHI01-GHI02: 445bp (endogenous control)

For primer pair GHI05-GHI06: 269bp (EE-GH1 Elite Event)

PCR conditions

The PCR mix for 50µl reactions contains:

5 µl template DNA

5 µl 10x Amplification Buffer (supplied with Taq polymerase)

1 µl 10 mM dNTP's

0.5 µl GHI01 (10pmoles/µl)

0.5 µl GHI02 (10pmoles/µl)

1 µl GHI05 (10pmoles/µl)

1 µl GHI06 (10pmoles/µl)

0.2 µl Taq DNA polymerase (5 units/µl)

water up to 50 µl

The thermocycling profile to be followed for optimal results is the following:

4 min. at 95°C

Followed by: 1 min. at 95°C

1 min. at 57°C

2 min. at 72°C

For 5 cycles

Followed by: 30 sec. at 92°C

30 sec. at 57°C

COR-AAD1-00003939
Bayer EX1008 (Part 7 of 9)

1 min. at 72°C
For 25 cycles
Followed by: 5 minutes at 72°C

Agarose gel analysis

Between 10 and 20µl of the PCR samples should be applied on a 1.5% agarose gel (Tris-borate buffer) with an appropriate molecular weight marker (e.g. 100bp ladder PHARMACIA).

Validation of the results

Data from transgenic plant DNA samples within a single PCR run and a single PCR cocktail should not be acceptable unless 1) the DNA positive control shows the expected PCR products (transgenic and endogenous fragments), 2) the DNA negative control is negative for PCR amplification (no fragments) and 3) the wild-type DNA control shows the expected result (endogenous fragment amplification).

Lanes showing visible amounts of the transgenic and endogenous PCR products of the expected sizes, indicate that the corresponding plant from which the genomic template DNA was prepared, has inherited the EE-GH1 elite event. Lanes not showing visible amounts of the transgenic PCR product and showing visible amounts of the endogenous PCR product, indicate that the corresponding plant from which the genomic template DNA was prepared, does not comprise the elite event. Lanes not showing visible amounts of the endogenous and transgenic PCR products, indicate that the quality and/or quantity of the genomic DNA didn't allow for a PCR product to be generated. These plants cannot be scored. The genomic DNA preparation should be repeated and a new PCR run, with the appropriate controls, has to be performed.

COR-AAD1-00003940
Bayer EX1008 (Part 7 of 9)

Use of discriminating PCR protocol to identify EE-GH1

Cotton leaf material from plants comprising different transgenic events (samples 1 to 4) was tested according to the above-described protocol. Samples from cotton wild-type were taken as negative controls.

The results of the PCR analysis are illustrated in Figure 1. Sample 1 is recognized as comprising elite event EE-GH1. All other tested lines do not comprise this elite event.

Example 5: Introgression of EE-GH1 into preferred cultivars

Elite event EE-GH1 is introduced by repeated back-crossing into the following commercial cotton cultivars: FM5013, FM5015, FM5017, FM989, FM832, FM966 and FM958.

It is observed that the introgression of the elite event into these cultivars does not significantly influence any of the desirable phenotypic or agronomic characteristics of these cultivars (no linkage drag) while expression of the transgene, as determined by glufosinate tolerance, meets commercially acceptable levels. This confirms the status of event EE-GH1 as an elite event.

As used in the claims below, unless otherwise clearly indicated, the term "plant" is intended to encompass plant tissues, at any stage of maturity, as well as any cells, tissues, or organs taken from or derived from any such plant, including without limitation, any seeds, leaves, stems, flowers, roots, single cells, gametes, cell cultures, tissue cultures or protoplasts.

Reference seed comprising elite event EE-GH1 was deposited as EE-GH1 at the ATCC (10801 University Blvd., Manassas, VA 20110-2209) on April 26, 2001, under ATCC accession number PTA-3343.

COR-AAD1-00003941
Bayer EX1008 (Part 7 of 9)

As used in the claims below, unless otherwise clearly indicated, the term "plant" is intended to encompass plant tissues, at any stage of maturity, as well as any cells, tissues, or organs taken from or derived from any such plant, including without limitation, any seeds, leaves, stems, flowers, roots, single cells, gametes, cell cultures, tissue cultures or protoplasts.

The above description of the invention is intended to be illustrative and not limiting. Various changes or modifications in the embodiments described may occur to those skilled in the art. These can be made without departing from the spirit or scope of the invention.

COR-AAD1-00003942
Bayer EX1008 (Part 7 of 9)

WHAT IS CLAIMED IS:

1. A transgenic cotton plant or seed, cells or tissues thereof comprising event EE-GH1 in its genome.

2. The transgenic cotton plant, or seed, cells or tissues of claim 1, the genomic DNA of which, when analyzed using the Elite event identification protocol for EE-GH1 with two primers comprising the nucleotide sequence of SEQ ID NO: 2 and SEQ ID NO: 3 respectively, yields a DNA fragment of between 250 and 290 bp.

3. The cotton plant, or seed, cells or tissues thereof, according to claim 2, wherein said DNA fragment is a fragment of about 269 bp.

4. A cotton plant, or seed, cells or tissues thereof, obtained by propagation of and/or breeding with a cotton plant grown from the seed deposited at the ATCC under accession number PTA-3343.

5. A cotton plant, seed, cells or tissues thereof which is the progeny of the seed deposited at the ATCC under accession number PTA-3343.

6. A method for identifying elite event EE-GH1 in biological samples, which method comprises detecting an EE-GH1 specific region with a primer or probe which specifically recognizes the 5' flanking region of SEQ ID NO: 3 or the 3' flanking region of SEQ ID NO: 4 of EE-GH1.

7. The method of claim 6, said method comprising amplifying a DNA fragment of between 100 and 350 bp from a nucleic acid present in said biological samples using a polymerase chain reaction with at least two primers, one of which recognizes the 5' or 3' flanking region of EE-GH1 and the other which recognizes a sequence within the foreign DNA of EE-GH1.

COR-AAD1-00003943
Bayer EX1008 (Part 7 of 9)

8. The method of claim 7, wherein said one primer recognizes a sequence within the 5' flanking region of SEQ ID NO: 3 and said other primer recognizes a sequence within the foreign DNA of EE-GH1.

9. The method of claim 8, wherein said primer recognizing a sequence within the 5' flanking region of EE-GH1 comprises the sequence of SEQ ID NO: 2.

10. The method of any one of claims 6 to 9, wherein said primer recognizing a sequence within the foreign DNA comprises the sequence of SEQ ID NO: 1.

11. A method for identifying EE-GH1 in a biological sample, which method comprises detecting an EE-GH1 specific region with a specific primer or probe which hybridizes under stringent conditions to a sequence within the 5' of SEQ ID NO: 3 or within the 3' flanking sequence of SEQ ID NO: 4 of EE-GH1.

12. A method for identifying a transgenic plant, or cells or tissues thereof, comprising the elite event EE-GH1, which method comprises establishing that genomic DNA can be used, according to a PCR identification protocol, to amplify a DNA fragment of between 250 and 290 bp, using a polymerase chain reaction with two primers having the nucleotide sequence of SEQ ID NO: 1 and SEQ ID NO: 2, respectively.

13. A kit for identifying elite event EE-GH1 in biological samples, said kit comprising at least one PCR primer or probe, which recognizes a sequence within the 5' flanking region of SEQ ID NO: 3 or the 3' flanking region of SEQ ID NO: 4 of EE-GH1.

14. The kit of claim 13, wherein said at least one PCR primer recognizes a sequence within the plant DNA in SEQ ID NO: 3.

COR-AAD1-00003944
Bayer EX1008 (Part 7 of 9)

15. The kit of claim 14, wherein said primer recognizing a sequence within the plant DNA in SEQ ID NO: 3 comprises the sequence of SEQ ID NO: 2.

16. The kit of Claims 13 to 15, which further comprises at least a second PCR primer or probe which recognizes a sequence within the foreign DNA of EE-GH1.

17. The kit of claim 16, wherein said primer recognizing a sequence within the foreign DNA of EE-GH1 comprises the sequence of SEQ ID NO: 1.

18. A method for confirming seed purity, which method comprises detecting an EE-GH1 specific DNA sequence with a specific primer or probe which specifically recognizes a sequence within the 5' flanking region of SEQ ID NO: 3 or the 3' flanking region of SEQ ID NO: 4 of EE-GH1, in seed samples.

19. A method for screening seeds for the presence of EE-GH1, which method comprises detecting an EE-GH1 specific DNA sequence with a specific primer or probe which specifically recognizes a sequence within the 5' flanking region of SEQ ID NO: 3 or the 3' flanking region of SEQ ID NO: 4 of EE-GH1, in samples of seed lots.

20. A seed deposited at the ATCC under accession number PTA-3343.

21. A cotton seed comprising elite event EE-GH1, reference seed comprising said event having been deposited at the ATCC under accession number PTA-3343.

22. A cotton plant, cell or tissue or plant material thereof comprising elite event EE-GH1, derived from the seed of claim 21.

23. Transgenic cotton plants, seeds, cells or tissues, the genomic DNA of which comprises a transgene integrated into the chromosomal DNA in a region which

COR-AAD1-00003945
Bayer EX1008 (Part 7 of 9)

comprises a sequence of at least 40 bp which hybridizes under stringent conditions with a sequence which is complementary to the sequence of SEQ ID NO: 5.

24. A process for producing a transgenic cotton plant or cell or tissue of a cotton plant, said process comprising introducing a recombinant DNA molecule into a region of cotton chromosomal DNA corresponding to a sequence of at least 40 bp that hybridizes under stringent conditions with a sequence that is complementary to the sequence of SEQ ID NO: 5, and, optionally, regenerating a cotton plant from the transformed cotton cell or tissue.

25. The process of claim 24, wherein said recombinant DNA molecule comprises an herbicide resistance gene.

26. The plant or cell or tissue of a cotton plant obtained by the process of claims 24 or 25.

27. A transgenic cotton plant or seed, cells or tissues thereof comprising

(i) event EE-GH1 in its genome ;or

(ii) event EE-GH1 with the proviso that the *bar* gene used in the event is substituted with a nucleic acid sequence that hybridizes to the complement of the *bar* gene under stringent conditions.

28. A DNA molecule which can be amplified from a nucleic acid sample of cotton, using a set of primers the first of which comprises a sequence of 15 to 30 nucleotides complementary to a sequence within SEQ ID NO:1 or SEQ ID NO:4, the second of which comprises a sequence complementary to the foreign DNA present in said nucleic acid sample of corn.

29. The DNA molecule of claim 28, which can be amplified from a nucleic acid sample of cotton, using a set of primers, the first of which comprising SEQ ID NO:2, the second of which comprising SEQ ID NO:3.

COR-AAD1-00003946
Bayer EX1008 (Part 7 of 9)

30. A detection kit comprising the DNA of claim 28 or 29.

31. A DNA molecule isolated from corn tissue, comprising the sequence of SEQ ID NO:1 or SEQ ID NO:4

32. A DNA molecule comprising a sequence which is identical to or complementary to the sequence of 9 nucleotides of plant DNA and foreign DNA at each side contiguous with the insertion site contained in SEQ ID NO: 1 or SEQ ID NO: 4.

COR-AAD1-00003947
Bayer EX1008 (Part 7 of 9)

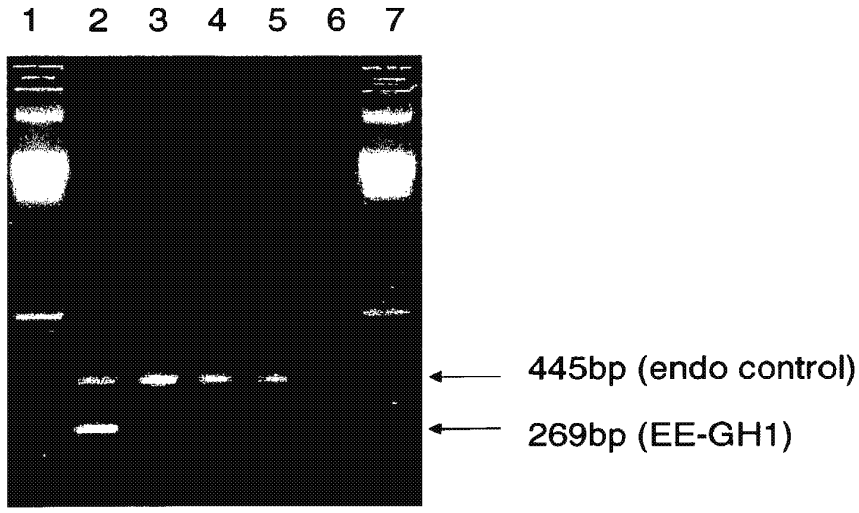


Figure 1

SEQUENCE LISTING

<110> Aventis CropScience N.V.

<120> Herbicide tolerant cotton plants and methods for producing and identifying same

<130> EE-GH1

<150> US 09/921,922
<151> 2001-08-06

<160> 18

<170> PatentIn version 3.1

<210> 1
<211> 850
<212> DNA
<213> Artificial: sequence comprising 5' flanking region

<400> 1
aaaggggatg agattgaatg ttaccttatc aacaaaagga gttgtagctc atggaacaac 60

aatagtcttt tccacggaaa cctagatgat gtttctccaa tgcttgataa atctttaaca 120

ttgtcatcat aagttgcaac ctcatgtttc acacaagcat caatcaaatg ttgatcttca 180

ttactaaaat gtgcttgatc cttccttaca caaatctacc tatgttgtgg tattttgttc 240

tattcatcat tctaacaagt tttgcaattg agttgaactt cttccaatct cgtatcagcc 300

tataatagtg gggtctaata tgtccatttt tcccacaata atgacatata atctttctaa 360

agcttttatt ctctgcctta tgatgaaaag aacccaaatc tttaacttta acaaaaataa 420

gatgagcgat aggttcttca cctttattga tgtaaccaag tcctctatgg catggttcaa 480

ttctcattga agccaaaatt tcatgaaact tctcacattg gcctctaaac ttcttcaaga 540

tagcctttgc accatctagc tcactcttgg ttgttttcaa aacatcatcc gtttcttgga 600

ccacaatttt gagcttttca ttttctattt tgaggataat agtttattcc ctcaaggaac 660

tattcaactg agcttaacag tactcggccg tcgaccgcgg tacccggaat tccaatccca 720

caaaaatctg agcttaacag cacagttgct cctctcagag cagaatcggg tattcaacac 780

cctcatatca actactacgt tgtgtataac ggtccacatg ccggtatata cgatgactgg 840

ggttgtacaa 850

<210> 2
<211> 20
<212> DNA
<213> Artificial: primer GHI06

<400> 2
ttgcaccatc tagctcactc 20

COR-AAD1-00003949
Bayer EX1008 (Part 7 of 9)

<210> 3
<211> 21
<212> DNA
<213> Artificial: primer GHI05

<400> 3
ggaccgttat acacaacgta g 21

<210> 4
<211> 426
<212> DNA
<213> Artificial: sequence comprising 3'flanking region

<400> 4
gattagagtc ccgcaattat acatttaata cgcgatagaa aacaaaatat agcgcgcaaa 60

ctaggataaa ttatcgcgcg cggtgtcatc tatgttacta gatcgggaag atcctctaga 120

gtcgacctgc aggcatgcaa gcttagatcc atggagccat ttacaattga atatatcctc 180

caaatattta aaaagaatat caccattatc cgaatcttct ttaaaatctg ttagaacacg 240

gtttggaata gtggtagtaa aagtaacata gttgctcgca tcttgatcta cattaaactt 300

tcttcatcac tccaagtgat tgtaaatgac ttctatttct tcttagtatt agcacattct 360

aatttttaagt gaaacaatcc cttacattca taacattgaa tatccttcta tcatctcaca 420

gcacga 426

<210> 5
<211> 961
<212> DNA
<213> Gossypium hirsutum: insertion region

<400> 5
aaaggggatg agattgaatg ttaccttatc aacaaaagga gttgtagctc atggaacaac 60

aatagtcttt tccacggaaa cctagatgat gtttctccaa tgcttgataa atctttaaca 120

ttgtcatcat aagttgcaac ctcatgtttc acacaagcat caatcaaatg ttgatcttca 180

ttactaaaat gtgcttgatc cttccttaca caaatctacc tatgttgtgg tattttgttc 240

tattcatcat tctaacaagt tttgcaattg agttgaactt cttccaatct cgtatcagcc 300

tataatagtg gggtctaata tgtccatttt tcccacaata atgacatata atctttctaa 360

agcttttatt ctctgcctta tgatgaaaag aacccaaatc tttaacttta acaaaaataa 420

gatgagcgat aggttcttca cctttattga tgtaaccaag tcctctatgg catggttcaa 480

ttctcattga agccaaaatt tcatgaaact tctcacattg gcctctaaac ttcttcaaga 540

tagcctttgc accatctagc tcactcttgg ttgttttcaa aacatcatcc gtttcttgga 600

ccacaatttt gagcttttca ttttctattt tgaggataat agtttattcc ctcaaggaac 660

COR-AAD1-00003950
Bayer EX1008 (Part 7 of 9)

tattcaactg agcttaaatc tcaatttttt ttaacatatg actataagta tcctccaaat 720

atttaaaaag aatatcacca ttatccgaat cttctttaaa atctgttaga acacggtttg 780

gaatagtggt agtaaaagta acatagttgc tcgcatcttg atctacatta aactttcttc 840

atcactccaa gtgattgtaa atgacttcta tttcttctta gtattagcac attctaattt 900

taagtgaaac aatcccttac attcataaca ttgaatatcc ttctatcatc tcacagcacg 960

a 961

<210> 6
<211> 9555
<212> DNA
<213> Artificial: plasmid pGSV71

<400> 6
agattcgaag ctcggtcccg tgggtgttct gtcgtctcgt tgtacaacga aatccattcc 60

cattccgcgc tcaagatggc ttcccctcgg cagttcatca gggctaaatc aatctagccg 120

acttgtccgg tgaaatgggc tgcactccaa cagaaacaat caaacaaaca tacacagcga 180

cttattcaca cgcgacaaat tacaacggta tatatcctgc cagtactcgg ccgtcgaccg 240

cggtacccgg aattccaatc ccacaaaaat ctgagcttaa cagcacagtt gctcctctca 300

gagcagaatc gggtattcaa caccctcata tcaactacta cgttgtgtat aacggtccac 360

atgccggtat atacgatgac tggggttgta caaaggcggc aacaaacggc gttcccggag 420

ttgcacacaa gaaatttgcc actattacag aggcaagagc agcagctgac gcgtacacaa 480

caagtcagca aacagacagg ttgaacttca tccccaaagg agaagctcaa ctcaagccca 540

agagctttgc taaggcccta acaagcccac caaagcaaaa agcccactgg ctcacgctag 600

gaaccaaaag gcccagcagt gatccagccc caaaagagat ctcctttgcc ccggagatta 660

caatggacga tttcctctat ctttacgatc taggaaggaa gttcgaaggt gaaggtgacg 720

acactatgtt caccactgat aatgagaagg ttagcctctt caatttcaga aagaatgctg 780

acccacagat ggttagagag gcctacgcag caggtctcat caagacgatc tacccgagta 840

acaatctcca ggagatcaaa taccttccca agaaggttaa agatgcagtc aaaagattca 900

ggactaattg catcaagaac acagagaaag acatatttct caagatcaga agtactattc 960

cagtatggac gattcaaggc ttgcttcata aaccaaggca agtaatagag attggagtct 1020

ctaaaaaggt agttcctact gaatctaagg ccatgcatgg agtctaagat tcaaatcgag 1080

gatctaacag aactcgccgt gaagactggc gaacagttca tacagagtct tttacgactc 1140

aatgacaaga agaaaatctt cgtcaacatg gtggagcacg acactctggt ctactccaaa 1200

aatgtcaaag atacagtctc agaagaccaa agggctattg agacttttca acaaaggata 1260

COR-AAD1-00003951
Bayer EX1008 (Part 7 of 9)

atttcgggaa acctcctcgg attccattgc ccagctatct gtcacttcat cgaaaggaca 1320

gtagaaaagg aaggtggctc ctacaaatgc catcattgcg ataaaggaaa ggctatcatt 1380

caagatgcct ctgccgacag tggtcccaaa gatggacccc cacccacgag gagcatcgtg 1440

gaaaaagaag acgttccaac cacgtcttca aagcaagtgg attgatgtga catctccact 1500

gacgtaaggg atgacgcaca atcccactat ccttcgcaag acccttcctc tatataagga 1560

agttcatttc atttggagag gacacgctga aatcaccagt ctctctctat aaatctatct 1620

ctctctctat aaccatggac ccagaacgac gcccggccga catccgccgt gccaccgagg 1680

cggacatgcc ggcggtctgc accatcgtca accactacat cgagacaagc acggtcaact 1740

tccgtaccga gccgcaggaa ccgcaggagt ggacggacga cctcgtccgt ctgcgggagc 1800

gctatccctg gctcgtcgcc gaggtggacg gcgaggtcgc cggcatcgcc tacgcgggcc 1860

cctggaaggc acgcaacgcc tacgactgga cggccgagtc gaccgtgtac gtctcccccc 1920

gccaccagcg gacgggactg ggctccacgc tctacaccca cctgctgaag tccctggagg 1980

cacagggctt caagagcgtg gtcgctgtca tcgggctgcc caacgacccg agcgtgcgca 2040

tgcacgaggc gctcggatat gccccccgcg gcatgctgcg ggcggccggc ttcaagcacg 2100

ggaactggca tgacgtgggt ttctggcagc tggacttcag cctgccggta ccgccccgtc 2160

cggtcctgcc cgtcaccgag atctgagatc acgcgttcta ggatccgaag cagatcgttc 2220

aaacatttgg caataaagtt tcttaagatt gaatcctgtt gccggtcttg cgatgattat 2280

catataattt ctgttgaatt acgttaagca tgtaataatt aacatgtaat gcatgacgtt 2340

atttatgaga tgggttttta tgattagagt cccgcaatta tacatttaat acgcgataga 2400

aaacaaaata tagcgcgcaa actaggataa attatcgcgc gcggtgtcat ctatgttact 2460

agatcgggaa gatcctctag agtcgacctg caggcatgca agcttagatc catggagcca 2520

tttacaattg aatatatcct gccgccgctg ccgctttgca cccggtggag cttgcatgtt 2580

ggtttctacg cagaactgag ccggttaggc agataatttc cattgagaac tgagccatgt 2640

gcaccttccc cccaacacgg tgagcgacgg ggcaacggag tgatccacat gggactttta 2700

aacatcatcc gtcggatggc gttgcgagag aagcagtcga tccgtgagat cagccgacgc 2760

accgggcagg cgcgcaacac gatcgcaaag tatttgaacg caggtacaat cgagccgacg 2820

ttcacggtac cggaacgacc aagcaagcta gcttagtaaa gccctcgcta gattttaatg 2880

cggatgttgc gattacttcg ccaactattg cgataacaag aaaaagccag cctttcatga 2940

tatatctccc aatttgtgta gggcttatta tgcacgctta aaaataataa aagcagactt 3000

gacctgatag tttggctgtg agcaattatg tgcttagtgc atctaacgct tgagttaagc 3060

cgcgccgcga agcggcgtcg gcttgaacga attgttagac attatttgcc gactaccttg 3120

COR-AAD1-00003952
Bayer EX1008 (Part 7 of 9)

gtgatctcgc ctttcacgta gtggacaaat tcttccaact gatctgcgcg cgaggccaag 3180

cgatcttctt cttgtccaag ataagcctgt ctagcttcaa gtatgacggg ctgatactgg 3240

gccggcaggc gctccattgc ccagtcggca gcgacatcct tcggcgcgat tttgccggtt 3300

actgcgctgt accaaatgcg ggacaacgta agcactacat ttcgctcatc gccagcccag 3360

tcgggcggcg agttccatag cgttaaggtt tcatttagcg cctcaaatag atcctgttca 3420

ggaaccggat caaagagttc ctccgccgct ggacctacca aggcaacgct atgttctctt 3480

gcttttgtca gcaagatagc cagatcaatg tcgatcgtgg ctggctcgaa gatacctgca 3540

agaatgtcat tgcgctgcca ttctccaaat tgcagttcgc gcttagctgg ataacgccac 3600

ggaatgatgt cgtcgtgcac aacaatggtg acttctacag cgcggagaat ctcgctctct 3660

ccaggggaag ccgaagtttc caaaaggtcg ttgatcaaag ctcgccgcgt tgtttcatca 3720

agccttacgg tcaccgtaac cagcaaatca atatcactgt gtggcttcag gccgccatcc 3780

actgcggagc cgtacaaatg tacggccagc aacgtcggtt cgagatggcg ctcgatgacg 3840

ccaactacct ctgatagttg agtcgatact tcggcgatca ccgcttccct catgatgttt 3900

aactttgttt tagggcgact gccctgctgc gtaacatcgt tgctgctcca taacatcaaa 3960

catcgaccca cggcgtaacg cgcttgctgc ttggatgccc gaggcataga ctgtacccca 4020

aaaaaacagt cataacaagc catgaaaacc gccactgcgc cgttaccacc gctgcgttcg 4080

gtcaaggttc tggaccagtt gcgtgagcgc atacgctact tgcattacag cttacgaacc 4140

gaacaggctt atgtccactg ggttcgtgcc ttcatccgtt tccacggtgt gcgtcacccg 4200

gcaaccttgg gcagcagcga agtcgaggca tttctgtcct ggctggcgaa cgagcgcaag 4260

gtttcggtct ccacgcatcg tcaggcattg gcggccttgc tgttcttcta cggcaagtgc 4320

tgtgcacgga tctgccctgg cttcaggaga tcggaagacc tcggccgtcc gggcgcttgc 4380

cggtggtgct gaccccggat gaagtggttc gcatcctcgg ttttctggaa ggcgagcatc 4440

gtttgttcgc ccagcttctg tatggaacgg gcatgcggat cagtgagggt ttgcaactgc 4500

gggtcaagga tctggatttc gatcacggca cgatcatcgt gcgggagggc aagggctcca 4560

aggatcgggc cttgatgtta cccgagagct tggcacccag cctgcgcgag cagggatcga 4620

tccaacccct ccgctgctat agtgcagtcg gcttctgacg ttcagtgcag ccgtcttctg 4680

aaaacgacat gtcgcacaag tcctaagtta cgcgacaggc tgccgccctg ccctttttcct 4740

ggcgttttct tgtcgcgtgt tttagtcgca taaagtagaa tacttgcgac tagaaccgga 4800

gacattacgc catgaacaag agcgccgccg ctggcctgct gggctatgcc cgcgtcagca 4860

ccgacgacca ggacttgacc aaccaacggg ccgaactgca cgcggccggc tgcaccaagc 4920

COR-AAD1-00003953
Bayer EX1008 (Part 7 of 9)

tgttttccga gaagatcacc ggcaccaggc gcgaccgccc ggagctggcc aggatgcttg 4980

accacctacg ccctggcgac gttgtgacag tgaccaggct agaccgcctg gcccgcagca 5040

cccgcgacct actggacatt gccgagcgca tccaggaggc cggcgcgggc ctgcgtagcc 5100

tggcagagcc gtgggccgac accaccacgc cggccggccg catggtgttg accgtgttcg 5160

ccggcattgc cgagttcgag cgttccctaa tcatcgaccg cacccggagc gggcgcgagg 5220

ccgccaaggc ccgaggcgtg aagtttggcc cccgccctac cctcaccccg gcacagatcg 5280

cgcacgcccg cgagctgatc gaccaggaag gccgcaccgt gaaagaggcg gctgcactgc 5340

ttggcgtgca tcgctcgacc ctgtaccgcg cacttgagcg cagcgaggaa gtgacgccca 5400

ccgaggccag gcggcgcggt gccttccgtg aggacgcatt gaccgaggcc gacgccctgg 5460

cggccgccga gaatgaacgc caagaggaac aagcatgaaa ccgcaccagg acggccagga 5520

cgaaccgttt ttcattaccg aagagatcga ggcggagatg atcgcggccg ggtacgtgtt 5580

cgagccgccc gcgcacgtct caaccgtgcg gctgcatgaa atcctggccg gtttgtctga 5640

tgccaagctg gcggcctggc cggccagctt ggccgctgaa gaaaccgagc gccgccgtct 5700

aaaaaggtga tgtgtatttg agtaaaacag cttgcgtcat gcggtcgctg cgtatatgat 5760

gcgatgagta aataaacaaa tacgcaaggg gaacgcatga aggttatcgc tgtacttaac 5820

cagaaaggcg ggtcaggcaa gacgaccatc gcaacccatc tagcccgcgc cctgcaactc 5880

gccggggccg atgttctgtt agtcgattcc gatccccagg gcagtgcccg cgattgggcg 5940

gccgtgcggg aagatcaacc gctaaccgtt gtcggcatcg accgcccgac gattgaccgc 6000

gacgtgaagg ccatcggccg gcgcgacttc gtagtgatcg acggagcgcc ccaggcggcg 6060

gacttggctg tgtccgcgat caaggcagcc gacttcgtgc tgattccggt gcagccaagc 6120

ccttacgaca tatgggccac cgccgacctg gtggagctgg ttaagcagcg cattgaggtc 6180

acggatggaa ggctacaagc ggcctttgtc gtgtcgcggg cgatcaaagg cacgcgcatc 6240

ggcggtgagg ttgccgaggc gctggccggg tacgagctgc ccattcttga gtcccgtatc 6300

acgcagcgcg tgagctaccc aggcactgcc gccgccggca caaccgttct tgaatcagaa 6360

cccgagggcg acgctgcccg cgaggtccag gcgctggccg ctgaaattaa atcaaaactc 6420

atttgagtta atgaggtaaa gagaaaatga gcaaaagcac aaacacgcta agtgccggcc 6480

gtccgagcgc acgcagcagc aaggctgcaa cgttggccag cctggcagac acgccagcca 6540

tgaagcgggt caactttcag ttgccggcgg aggatcacac caagctgaag atgtacgcgg 6600

tacgccaagg caagaccatt accgagctgc tatctgaata catcgcgcag ctaccagagt 6660

aaatgagcaa atgaataaat gagtagatga attttagcgg ctaaaggagg cggcatggaa 6720

aatcaagaac aaccaggcac cgacgccgtg gaatgcccca tgtgtggagg aacgggcggt 6780

COR-AAD1-00003954
Bayer EX1008 (Part 7 of 9)

tggccaggcg taagcggctg ggttgtctgc cggccctgca atggcactgg aacccccaag 6840

cccgaggaat cggcgtgacg gtcgcaaacc atccggcccg gtacaaatcg gcgcggcgct 6900

gggtgatgac ctggtggaga agttgaaggc cgcgcaggcc gcccagcggc aacgcatcga 6960

ggcagaagca cgccccggtg aatcgtggca agcggccgct gatcgaatcc gcaaagaatc 7020

ccggcaaccg ccggcagccg gtgcgccgtc gattaggaag ccgcccaagg gcgacgagca 7080

accagatttt ttcgttccga tgctctatga cgtgggcacc cgcgatagtc gcagcatcat 7140

ggacgtggcc gttttccgtc tgtcgaagcg tgaccgacga gctggcgagg tgatccgcta 7200

cgagcttcca gacgggcacg tagaggtttc cgcagggccg gccggcatgg ccagtgtgtg 7260

ggattacgac ctggtactga tggcggtttc ccatctaacc gaatccatga accgataccg 7320

ggaagggaag ggagacaagc ccggccgcgt gttccgtcca cacgttgcgg acgtactcaa 7380

gttctgccgg cgagccgatg gcggaaagca gaaagacgac ctggtagaaa cctgcattcg 7440

gttaaacacc acgcacgttg ccatgcagcg tacgaagaag gccaagaacg gccgcctggt 7500

gacggtatcc gagggtgaag ccttgattag ccgctacaag atcgtaaaga gcgaaaccgg 7560

gcggccggag tacatcgaga tcgagctagc tgattggatg taccgcgaga tcacagaagg 7620

caagaacccg gacgtgctga cggttcaccc cgattacttt ttgatcgatc ccggcatcgg 7680

ccgttttctc taccgcctgg cacgccgcgc cgcaggcaag gcagaagcca gatggttgtt 7740

caagacgatc tacgaacgca gtggcagcgc cggagagttc aagaagttct gtttcaccgt 7800

gcgcaagctg atcgggtcaa atgacctgcc ggagtacgat ttgaaggagg aggcggggca 7860

ggctggcccg atcctagtca tgcgctaccg caacctgatc gagggcgaag catccgccgg 7920

ttcctaatgt acggagcaga tgctagggca aattgcccta gcaggggaaa aaggtcgaaa 7980

aggtctcttt cctgtggata gcacgtacat tgggaaccca aagccgtaca ttgggaaccg 8040

gaacccgtac attgggaacc caaagccgta cattgggaac cggtcacaca tgtaagtgac 8100

tgatataaaa gagaaaaaag gcgatttttc cgcctaaaac tctttaaaac ttattaaaac 8160

tcttaaaacc cgcctggcct gtgcataact gtctggccag cgcacagccg aagagctgca 8220

aaaagcgcct acccttcggt cgctgcgctc cctacgcccc gccgcttcgc gtcggcctat 8280

cgcggccgct ggccgctcaa aaatggctgg cctacggcca ggcaatctac cagggcgcgg 8340

acaagccgcg ccgtcgccac tcgaccgccg gcgcccacat caaggcaccc tgcctcgcgc 8400

gtttcggtga tgacggtgaa aacctctgac acatgcagct cccggagacg gtcacagctt 8460

gtctgtaagc ggatgccggg agcagacaag cccgtcaggg cgcgtcagcg ggtgttggcg 8520

ggtgtcgggg cgcagccatg acccagtcac gtagcgatag cggagtgtat actggcttaa 8580

COR-AAD1-00003955
Bayer EX1008 (Part 7 of 9)

ctatgcggca tcagagcaga ttgtactgag agtgcaccat atgcggtgtg aaataccgca 8640

cagatgcgta aggagaaaat accgcatcag gcgctcttcc gcttcctcgc tcactgactc 8700

gctgcgctcg gtcgttcggc tgcggcgagc ggtatcagct cactcaaagg cggtaatacg 8760

gttatccaca gaatcagggg ataacgcagg aaagaacatg tgagcaaaag gccagcaaaa 8820

ggccaggaac cgtaaaaagg ccgcgttgct ggcgtttttc cataggctcc gccccctga 8880

cgagcatcac aaaaatcgac gctcaagtca gaggtggcga aacccgacag gactataaag 8940

ataccaggcg tttccccctg gaagctccct cgtgcgctct cctgttccga ccctgccgct 9000

taccggatac ctgtccgcct ttctcccttc gggaagcgtg gcgctttctc atagctcacg 9060

ctgtaggtat ctcagttcgg tgtaggtcgt tcgctccaag ctgggctgtg tgcacgaacc 9120

ccccgttcag cccgaccgct gcgccttatc cggtaactat cgtcttgagt ccaacccggt 9180

aagacacgac ttatcgccac tggcagcagc cactggtaac aggattagca gagcgaggta 9240

tgtaggcggt gctacagagt tcttgaagtg gtggcctaac tacggctaca ctagaaggac 9300

agtatttggt atctgcgctc tgctgaagcc agttaccttc ggaaaaagag ttggtagctc 9360

ttgatccggc aaacaaacca ccgctggtag cggtggtttt tttgtttgca agcagcagat 9420

tacgcgcaga aaaaaaggat ctcaagaaga tccggaaaac gcaagcgcaa agagaaagca 9480

ggtagcttgc agtgggctta catggcgata gctagactgg gcggttttat ggacagcaag 9540

cgaaccggaa ttgcc 9555

<210> 7
<211> 4182
<212> DNA
<213> Artificial: plasmid pRVA44

<400> 7
tcgcgcgttt cggtgatgac ggtgaaaacc tctgacacat gcagctcccg gagacggtca 60

cagcttgtct gtaagcggat gccgggagca gacaagcccg tcagggcgcg tcagcgggtg 120

ttggcgggtg tcggggctgg cttaactatg cggcatcaga gcagattgta ctgagagtgc 180

accatacctg caggcaattg gtacctacgt atgcatggcg cgccatatgc ccgggccctg 240

tacagcggcc gcgttcctac gcagcaggtc tcatcaagac gatctacccg agtaacaatc 300

tccaggagat caaatacctt cccaagaagg ttaaagatgc agtcaaaaga ttcaggacta 360

attgcatcaa gaacacagag aaagacatat ttctcaagat cagaagtact attccagtat 420

ggacgattca aggcttgctt cataaaccaa ggcaagtaat agagattgga gtctctaaaa 480

aggtagttcc tactgaatct aaggccatgc atggagtcta agattcaaat cgaggatcta 540

acagaactcg ccgtgaagac tggcgaacag ttcatacaga gtcttttacg actcaatgac 600

COR-AAD1-00003956
Bayer EX1008 (Part 7 of 9)

aagaagaaaa tcttcgtcaa catggtggag cacgacactc tggtctactc caaaaatgtc 660

aaagatacag tctcagaaga ccaaagggct attgagactt ttcaacaaag gataatttcg 720

ggaaacctcc tcggattcca ttgcccagct atctgtcact tcatcgaaag gacagtagaa 780

aaggaaggtg gctcctacaa atgccatcat tgcgataaag gaaaggctat cattcaagat 840

gcctctgccg acagtggtcc caaagatgga cccccaccca cgaggagcat cgtggaaaaa 900

gaagacgttc caaccacgtc ttcaaagcaa gtggattgat gtgacatctc cactgacgta 960

agggatgacg cacaatccca ctatccttcg caagaccctt cctctatata aggaagttca 1020

tttcatttgg agaggacacg ctgaaatcac cagtctctct ctataaatct atctctctct 1080

ctataaccat ggacccagaa cgacgcccgg ccgacatccg ccgtgccacc gaggcggaca 1140

tgccggcggt ctgcaccatc gtcaaccact acatcgagac aagcacggtc aacttccgta 1200

ccgagccgca ggaaccgcag gagtggacgg acgacctcgt ccgtctgcgg gagcgctatc 1260

cctggctcgt cgccgaggtg gacggcgagg tcgccggcat cgcctacgcg ggcccctgga 1320

aggcacgcaa cgcctacgac tggacggccg agtcgaccgt gtacgtctcc ccccgccacc 1380

agcggacggg actgggctcc acgctctaca cccacctgct gaagtccctg gaggcacagg 1440

gcttcaagag cgtggtcgct gtcatcgggc tgcccaacga cccgagcgtg cgcatgcacg 1500

aggcgctcgg atatgccccc cgcggcatgc tgcgggcggc cggcttcaag cacgggaact 1560

ggcatgacgt gggtttctgg cagctggact tcagcctgcc ggtaccgccc cgtccggtcc 1620

tgcccgtcac cgagatctga tctcacgcgt ctaggatccg aagcagatcg ttcaaacatt 1680

tggcaataaa gtttcttaag attgaatcct gttgccggtc ttgcgatgat tatcatataa 1740

tttctgttga attacgttaa gcatgtaata attaacatgt aatgcatgac gttatttatg 1800

agatgggttt ttatgattag agtcccgcaa ttatacattt aatacgcgat agaaaacaaa 1860

atatagcgcg caaactagga taaattatcg cgcgcggtgt catctatgtt actagatcgg 1920

gaagatcctc tagagcgatc gcaagcttgg cgtaatcatg gtcatagctg tttcctgtgt 1980

gaaattgtta tccgctcaca attccacaca acatacgagc cggaagcata aagtgtaaag 2040

cctggggtgc ctaatgagtg agctaactca cattaattgc gttgcgctca ctgcccgctt 2100

tccagtcggg aaacctgtcg tgccagctgc attaatgaat cggccaacgc gcggggagag 2160

gcggtttgcg tattgggcgc tcttccgctt cctcgctcac tgactcgctg cgctcggtcg 2220

ttcggctgcg gcgagcggta tcagctcact caaaggcggt aatacggtta tccacagaat 2280

caggggataa cgcaggaaag aacatgtgag caaaaggcca gcaaaaggcc aggaaccgta 2340

aaaaggccgc gttgctggcg tttttccata ggctccgccc ccctgacgag catcacaaaa 2400

atcgacgctc aagtcagagg tggcgaaacc cgacaggact ataaagatac caggcgtttc 2460

COR-AAD1-00003957
Bayer EX1008 (Part 7 of 9)

ccccctggaag ctccctcgtg cgctctcctg ttccgaccct gccgcttacc ggatacctgt 2520

ccgcctttct cccttcggga agcgtggcgc tttctcaaag ctcacgctgt aggtatctca 2580

gttcggtgta ggtcgttcgc tccaagctgg gctgtgtgca cgaacccccc gttcagcccg 2640

accgctgcgc cttatccggt aactatcgtc ttgagtccaa cccggtaaga cacgacttat 2700

cgccactggc agcagccact ggtaacagga ttagcagagc gaggtatgta ggcggtgcta 2760

cagagttctt gaagtggtgg cctaactacg gctacactag aagaacagta tttggtatct 2820

gcgctctgct gaagccagtt accttcggaa aaagagttgg tagctcttga tccggcaaac 2880

aaaccaccgc tggtagcggt ggtttttttg tttgcaagca gcagattacg cgcagaaaaa 2940

aaggatctca agaagatcct ttgatctttt ctacggggtc tgacgctcag tggaacgaaa 3000

actcacgtta agggattttg gtcatgagat tatcaaaaag gatcttcacc tagatccttt 3060

taaattaaaa atgaagtttt aaatcaatct aaagtatata tgagtaaact tggtctgaca 3120

gttaccaatg cttaatcagt gaggcaccta tctcagcgat ctgtctattt cgttcatcca 3180

tagttgcctg actccccgtc gtgtagataa ctacgatacg ggagggctta ccatctggcc 3240

ccagtgctgc aatgataccg cgagacccac gctcaccggc tccagattta tcagcaataa 3300

accagccagc cggaagggcc gagcgcagaa gtggtcctgc aactttatcc gcctccatcc 3360

agtctattaa ttgttgccgg gaagctagag taagtagttc gccagttaat agtttgcgca 3420

acgttgttgc cattgctaca ggcatcgtgg tgtcacgctc gtcgtttggt atggcttcat 3480

tcagctccgg ttcccaacga tcaaggcgag ttacatgatc ccccatgttg tgcaaaaaag 3540

cggttagctc cttcggtcct ccgatcgttg tcagaagtaa gttggccgca gtgttatcac 3600

tcatggttat ggcagcactg cataattctc ttactgtcat gccatccgta agatgctttt 3660

ctgtgactgg tgagtactca accaagtcat tctgagaata gtgtatgcgg cgaccgagtt 3720

gctcttgccc ggcgtcaata cgggataata ccgcgccaca tagcagaact ttaaaagtgc 3780

tcatcattgg aaaacgttct tcggggcgaa aactctcaag gatcttaccg ctgttgagat 3840

ccagttcgat gtaacccact cgtgcaccca actgatcttc agcatctttt actttcacca 3900

gcgtttctgg gtgagcaaaa acaggaaggc aaaatgccgc aaaaaaggga ataagggcga 3960

cacggaaatg ttgaatactc atactcttcc tttttcaata ttattgaagc atttatcagg 4020

gttattgtct catgagcgga tacatatttg aatgtattta gaaaaataaa caaatagggg 4080

ttccgcgcac atttccccga aaagtgccac ctgacgtcta agaaaccatt attatcatga 4140

cattaaccta taaaaatagg cgtatcacga ggccctttcg tc 4182

<210> 8

COR-AAD1-00003958
Bayer EX1008 (Part 7 of 9)

<211> 16
<212> DNA
<213> Artificial: primer MDB327

<220>
<221> misc_feature
<222> (1)..(16)
<223> "n" = a,c,t or g; "s" = c or g; "w" = a or t

<400> 8
ntgaggwtcn wgtsat 16

<210> 9
<211> 22
<212> DNA
<213> Artificial: primer MLD015

<400> 9
tggttcctag cgtgagccag tg 22

<210> 10
<211> 21
<212> DNA
<213> Artificial: primer MLD016

<400> 10
agctgctgct cttgcctctg t 21

<210> 11
<211> 16
<212> DNA
<213> Artificial: primer MDB612

<220>
<221> misc_feature
<222> (1)..(16)
<223> "n" = a,c,t or g; "s" = c or g; "w" = a or t

<400> 11
ngtgctswga nawgat 16

<210> 12
<211> 22
<212> DNA
<213> Artificial: primer MDB053

<400> 12
catgacgtgg gtttctggca gc 22

<210> 13
<211> 21
<212> DNA
<213> Artificial: primer MDB356

COR-AAD1-00003959
Bayer EX1008 (Part 7 of 9)

<400> 13
aatcctgttg ccggtcttgc g 21

<210> 14
<211> 22
<212> DNA
<213> Artificial: primer DPA017

<400> 14
gattagagtc ccgcaattat ac 22

<210> 15
<211> 20
<212> DNA
<213> Artificial: primer MLD019

<400> 15
caagatgcga gcaactatgt 20

<210> 16
<211> 200
<212> DNA
<213> Artificial: sequence comprising target site deletion

<400> 16
tcttggacca caattttgag cttttcattt tctattttga ggataatagt ttattccctc 60

aaggaactat tcaactgagc ttaatatctc aatttttttt aacatatgac tataagtatc 120

ctccaaatat ttaaaaagaa tatcaccatt atccgaatct tctttaaaat ctgttagaac 180

acggtttgga atagtggtag 200

<210> 17
<211> 21
<212> DNA
<213> Artificial: primer GHI01

<400> 17
aacctaggct gctgaaggag c 21

<210> 18
<211> 21
<212> DNA
<213> Artificial: primer GHI02

<400> 18
caactcctcc agtcatctcc g 21

COR-AAD1-00003960
Bayer EX1008 (Part 7 of 9)

CORRECTED VERSION *

PCT

WORLD INTELLECTUAL PROPERTY ORGANIZATION
International Bureau

INTERNATIONAL APPLICATION PUBLISHED UNDER THE PATENT COOPERATION TREATY (PCT)

(51) International Patent Classification 4 :
C12N 15/00, A01H 1/00
C12N 5/00, A01H 5/10
// C12N 9/10

A1

(11) International Publication Number: WO 87/ 05629

(43) International Publication Date:
24 September 1987 (24.09.87)

(21) International Application Number: PCT/EP87/00141

(22) International Filing Date: 11 March 1987 (11.03.87)

(31) Priority Application Numbers: 86400521.0 (EP)
87400141.5 (EP)

(32) Priority Dates: 11 March 1986 (11.03.86)
21 January 1987 (21.01.87)

(33) Priority Countries: GB, et al.

(71) Applicants *(for all designated States except US):* PLANT GENETIC SYSTEMS N.V. [BE/BE]; Kunstlaan 46, B-1040 Brussels (BE). BIOGEN N.V. [NL/NL]; Pieterma A 1 15, Willemstad, Curaçao (AN).

(72) Inventors; and
(75) Inventors/Applicants *(for US only) :* LEEMANS, Jan [BE/BE]; Ellebochten 38, B-9210 Heusden (BE). BOTTERMAN, Johan [BE/BE]; Eedstraat 37, B-9710 Zwijnaarde (BE). DE BLOCK, Marc [BE/BE]; Vogelhoekstraat 32, B-9219 Gentbrugge (BE). THOMPSON, Charles [US/CH]; 19, chemin des Palettes, CH-1212 Grand-Lancy (CH). MOUVA, Rao [IN/CH]; 10, avenue Secheron, CH-1202 Genève (CH).

(74) Agent: GUTMANN, Ernest; S.C. Ernest Gutmann - Yves Plasseraud, 67, boulevard Haussmann, F-75008 Paris (FR).

(81) Designated States: AU, BJ (OAPI patent), BR, CF (OAPI patent), CG (OAPI patent), CM (OAPI patent), DK, FI, GA (OAPI patent), HU, JP, KR, ML (OAPI patent), MR (OAPI patent), NO, SN (OAPI patent), SU, TD (OAPI patent), TG (OAPI patent), US.

Published
With international search report.
Before the expiration of the time limit for amending the claims and to be republished in the event of the receipt of amendments.

(54) Title: PLANT CELLS RESISTANT TO GLUTAMINE-SYNTHETASE INHIBITORS, MADE BY GENETIC ENGINEERING

(57) Abstract

DNA fragment containing a determined gene, the expression of which inhibits the antibiotic and herbicidal effects of Bialaphos and related products. It also relates to recombinant vectors, containing such DNA fragment, which enable this protective gene to be introduced and expressed into cells and plant cells.

* (Referred to in PCT Gazette No. 25/1987, Section II)

COR-AAD1-00003961
Bayer EX1008 (Part 7 of 9)

FOR THE PURPOSES OF INFORMATION ONLY

Codes used to identify States party to the PCT on the front pages of pamphlets publishing international applications under the PCT.

AT	Austria
AU	Australia
BB	Barbados
BE	Belgium
BG	Bulgaria
BJ	Benin
BR	Brazil
CF	Central African Republic
CG	Congo
CH	Switzerland
CM	Cameroon
DE	Germany, Federal Republic of
DK	Denmark
FI	Finland
FR	France
GA	Gabon
GB	United Kingdom
HU	Hungary
IT	Italy
JP	Japan
KP	Democratic People's Republic of Korea
KR	Republic of Korea
LI	Liechtenstein
LK	Sri Lanka
LU	Luxembourg
MC	Monaco
MG	Madagascar
ML	Mali
MR	Mauritania
MW	Malawi
NL	Netherlands
NO	Norway
RO	Romania
SD	Sudan
SE	Sweden
SN	Senegal
SU	Soviet Union
TD	Chad
TG	Togo
US	United States of America

PCT WORLD INTELLECTUAL PROPERTY ORGANIZATION
International Bureau

INTERNATIONAL APPLICATION PUBLISHED UNDER THE PATENT COOPERATION TREATY (PCT)

(51) International Patent Classification [4] : C12N 15/00, A01H 1/00 C12N 5/00, A01H 5/10 // C12N 9/10	A1	(11) International Publication Number: **WO 87/ 05629** (43) International Publication Date: 24 September 1987 (24.09.87)

(21) International Application Number: PCT/EP87/00141

(22) International Filing Date: 11 March 1987 (11.03.87)

(31) Priority Application Numbers: 86400521.0 (EP)
87400141.5 (EP)

(32) Priority Dates: 11 March 1986 (11.03.86)
21 January 1987 (21.01.87)

(33) Priority Countries: GB, et al.

(71) Applicants *(for all designated States except US):* PLANT GENETIC SYSTEMS N.V. [BE/BE]; Kunstlaan 46, B-1040 Brussels (BE). BIOGEN N.V. [NL/NL]; Pietermaai 15, Willemstad, Curaçao (AN).

(72) Inventors; and
(75) Inventors/Applicants *(for US only) :* LEEMANS, Jan [BE/BE]; Ellebochten 38, B-9210 Heusden (BE). ROTTERMAN, Johan [BE/BE]; Eedstraat 37, B-9710 Zwijnaarde (BE). DE BLOCK, Marc [BE/BE]; Vogelhoekstraat 32, B-9219 Gentbrugge (BE). THOMPSON, Charles [US/CH]; 19, chemin de Palettes, CH-1212 Grand-Lancy (CH). MOUVA, Rao [IN/CH]; 10, avenue Secheron, CH-1202 Genève (CH).

(74) Agent: GUTMANN, Ernest; S.C. Ernest Gutmann - Yves Plasseraud, 67, boulevard Haussmann, F-75008 Paris (FR).

(81) Designated States: AU, BJ (OAPI patent), BR, CF (OAPI patent), CG (OAPI patent), CM (OAPI patent), DK, FI, GA (OAPI patent), HU, JP, KR, ML (OAPI patent), MR (OAPI patent), NO, SN (OAPI patent), SU, TD (OAPI patent), TG (OAPI patent), US.

Published
With international search report.
Before the expiration of the time limit for amending the claims and to be republished in the event of the receipt of amendments.

(54) Title: PLANT CELLS RESISTANT TO GLUTAMINE-SYNTHETASE INHIBITORS, MADE BY GENETIC ENGINEERING

(57) Abstract

DNA fragment containing a determined gene, the expression of which inhibits the antibiotic and herbicidal effects of Bialaphos and related products. It also relates to recombinant vectors, containing such DNA fragment, which enable this protective gene to be introduced and expressed into cells and plant cells.

COR-AAD1-00003963
Bayer EX1008 (Part 7 of 9)

FOR THE PURPOSES OF INFORMATION ONLY

Codes used to identify States party to the PCT on the front pages of pamphlets publishing international applications under the PCT.

AT	Austria	**FR**	France	**ML**	Mali
AU	Australia	**GA**	Gabon	**MR**	Mauritania
BB	Barbados	**GB**	United Kingdom	**MW**	Malawi
BE	Belgium	**HU**	Hungary	**NL**	Netherlands
BG	Bulgaria	**IT**	Italy	**NO**	Norway
BJ	Benin	**JP**	Japan	**RO**	Romania
BR	Brazil	**KP**	Democratic People's Republic of Korea	**SD**	Sudan
CF	Central African Republic			**SE**	Sweden
CG	Congo	**KR**	Republic of Korea	**SN**	Senegal
CH	Switzerland	**LI**	Liechtenstein	**SU**	Soviet Union
CM	Cameroon	**LK**	Sri Lanka	**TD**	Chad
DE	Germany, Federal Republic of	**LU**	Luxembourg	**TG**	Togo
DK	Denmark	**MC**	Monaco	**US**	United States of America
FI	Finland	**MG**	Madagascar		

Plant cells resistant to glutamine-synthetase inhibitors, made by genetic engineering.

The invention relates to a process for protecting plant cells and plants against the action of glutamine synthetase inhibitors.

It also relates to applications of such process, particularly to the development of herbicide resistance into determined plants.

It relates further to non-biologically transformed plant cells and plants displaying resistance to glutamine synthetase inhibitors as well as to suitable DNA fragments and recombinants containing nucleotide sequences encoding resistance to glutamine synthetase inhibitors.

Glutamine synthetase (hereafter simply designated by GS) constitutes in most plants one of the essential enzymes for the development and life of plant cells. It is known that GS converts glutamate into glutamine. GS is involved in an efficient pathway (the only one known nowadays) in most plants for the detoxification of ammonia released by nitrate reduction, aminoacid degradation or photorespiration. Therefore potent inhibitors of GS are very toxic to plant cells. A particular class of herbicides has been developped, based on the toxic effect due to inhibit inhibition of GS in plants.

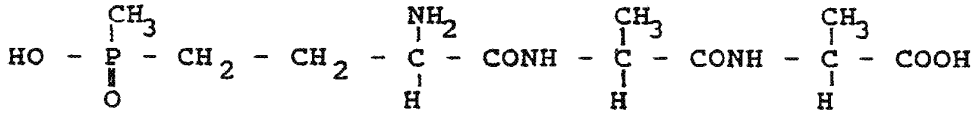
These herbicides comprise as active ingredient a GS inhibitor.

There are at least two possible ways which might lead to plants resistant to the inhibitors of the action of glutamine synthetase ; (1) by changing the target. It can be envisaged that mutations in the GS enzyme can lead to insensitivity towards the herbicide ; (2) by inactivation of the herbicide. Breakdown or modification of the herbicide inside the plant could lead to resistance.

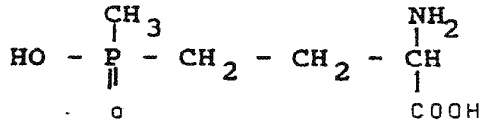
COR-AAD1-00003965
Bayer EX1008 (Part 7 of 9)

Bialaphos and phosphinothricin (hereafter simply designated by PPT) are two such inhibitors of the action of GS, (ref. 16, 17) and have been shown to possess excellent herbicidal properties (see more particularly ref. 2 as concerns Bialaphos).

Bialaphos has the following formula (I) :



PPT has the following formula (II) :



Thus the structural difference between PPT and Bialaphos resides in the absence of two alanine aminoacids in the case of PPT.

These two herbicides are non selective. They inhibit growth of all the different species of plants present on the soil, accordingly cause their total destruction.

Bialaphos was first disclosed as having antibiotic properties, which enabled it to be used as a pesticide or a fungicide. Bialaphos can be produced according to the process disclosed in united-states patent n° 3 832 394, assigned to MEIJI SEIKA KAISHA LTD., which patent is incorporated herein by reference. It comprises cultivating Streptomyces hygroscopicus, such as the strain available at the American Type Culture Collection, under the ATCC number 21,705, and recovering Bialaphos from its culture medium. However, other strains, such as Streptomyces viridochromogenes, also produce this compound (ref. 1).

Other tripeptide antibiotics which contain a PPT moiety are or might be discovered in nature as well, e.g. phosalacin (ref. 15).

PPT is also obtained by chemical synthesis and is commercially distributed by the industrial Company

COR-AAD1-00003966
Bayer EX1008 (Part 7 of 9)

HOECHST.

A number of Streptomyces species have been disclosed which produce highly active antibiotics which are known to incapacitate procaryotic cell functions or enzymes. The Streptomyces species which produce these antibiotics would themselves be destroyed if they had not a self defence mechanism against these antibiotics. This self defence mechanism has been found in several instances to comprise an enzyme capable of inhibiting the antibiotic effect, thus of avoiding autotoxicity for the Streptomyces species concerned. This modification is generally reversed when the molecule is exported from the cell.

The existence of a gene which encodes an enzyme able to modify the antibiotic so as to inhibit the antibiotic effect against the host has been demonstrated in several Streptomyces producing antibiotics, for example, in S. fradiae, S. azureus, S. vinaceus, S. erythreus, producing neomycin, thiostrepton, viomycin, and MLS (Macrolide Lincosamide Streptogramin) antibiotics respectively (ref. 4), (ref. 5), (ref. 6),(ref.14 by CHATER et al., 1982 describes standard techniques which can be used for bringing these effects to light).

In accordance with the present invention, it has been found that Streptomyces hygroscopicus ATCC 21,705, also possesses a gene encoding an enzyme responsible of the inactivation of the antibiotic properties of Bialaphos. Experiments carried out by the applicants have lead to the isolation of such a gene and its use in a process for controlling the action of GS inhibitors, based on PPT or derived products.

An object of the invention is to provide a new process for controlling the action in plant cells and plants of GS inhibitors.

Another object of the invention is to provide DNA

COR-AAD1-00003967
Bayer EX1008 (Part 7 of 9)

fragments and DNA recombinants, particularly modified vectors containing said DNA fragments, which DNA fragments contain nucleotide sequences capable, when incorporated in plant cells and plants, to protect them against the action of GS inhibitors.

A further object of the invention is to provide non-biologically transformed plant cells and plants capable of neutralizing or inactivating GS inhibitors.

A further object of the invention is to provide a process for selectively protecting plant species against herbicides of a GS inhibitor type.

More specifically an object of the invention is to provide a DNA fragment transferable to plant cells- and to whole plants- capable of protecting them against the herbicidal effects of Bialaphos and of structurally analogous herbicides.

A further object of the invention is to provide plant cells resistant to the products of the class examplified by Bialaphos, which products possess the PPT unit in their structure.

The process according to the invention for controlling the action in plant cells and plants of a GS inhibitor when contacted therewith, comprises providing said plants with a heterologous DNA fragment including a foreign nucleotide sequence, capable of being expressed in the form of a protein in said plant cells and plants, under condition such as to cause said heterologus DNA fragment to be integrated stably through generations in the cells of said plants, and wherein said protein has an enzymatic activity capable of inactivating or neutralization of said glutamine synthetase inhibitor.

A preferred DNA fragment is one derived from an antibiotic-producing-Streptomyces strain (or a sequence comprising a nucleotide sequence encoding the same activity) and which encodes resistance to a said GS

COR-AAD1-00003968
Bayer EX1008 (Part 7 of 9)

inhibitors.

Preferred nucleotide sequences for use in this invention encode a protein which has acetyl tranferase activity with respect to said GS inhibitors.

A most preferred DNA fragment according to the invention comprises a nucleotide sequence coding for a polypeptide having a PPT acetyl transferase activity.

A particular DNA fragment according to the invention, for the subsequent transformation of plant cells, consists of a nucleotide sequence coding for at least part of a polypeptide having the following sequence :

```
                                                    X SER PRO GLU
  183
ARG ARG PRO ALA ASP ILE ARG ARG ALA THR GLU ALA ASP MET PRO
  228
ALA VAL CYS THR ILE VAL ASN HIS TYR ILE GLU THR SER THR VAL
  273
ASN PHE ARG THR GLU PRO GLN GLU PRO GLN GLU TRP THR ASP ASP
  318
LEU VAL ARG LEU ARG GLU ARG TYR PRO TRP LEU VAL ALA GLU VAL
  363
ASP GLY GLU VAL ALA GLY ILE ALA TYR ALA GLY PRO TRP LYS ALA
  408
ARG ASN ALA TYR ASP TRP THR ALA GLU SER THR VAL TYR VAL SER
  453
PRO ARG HIS GLN ARG THR GLY LEU GLY SER THR LEU TYR THR HIS
  498
LEU LEU LYS SER LEU GLU ALA GLN GLY PHE LYS SER VAL VAL ALA
  543
VAL ILE GLY LEU PRO ASN ASP PRO SER VAL ARG MET HIS GLU ALA
  588
LEU GLY TYR ALA PRO ARG GLY MET LEU ARG ALA ALA GLY PHE LYS
  633
HIS GLY ASN TRP HIS ASP VAL GLY PHE TRP GLN LEU ASP PHE SER
  678
LEU PRO VAL PRO PRO ARG PRO VAL LEU PRO VAL THR GLU ILE
  723
```

COR-AAD1-00003969
Bayer EX1008 (Part 7 of 9)

in which X represents MET or VAL, which part of said polypeptide is of sufficient length to confer protection against Bialaphos to plant cells, when incorportated genetically and expressed therein, i.e. as termed hereafter "plant-protecting capability" against Bialaphos.

A preferred DNA fragment consists of the following nucleotide sequence :

```
                                                    GTG AGC CCA GAA
   183
CGA CGC CCG GCC GAC ATC CGC CGT GCC ACC GAG GCG GAC ATG CCG
  228
GCG GTC TGC ACC ATC GTC AAC CAC TAC ATC GAG ACA AGC ACG GTC
  273
AAC TTC CGT ACC GAG CCG CAG GAA CCG CAG GAG TGG ACG GAC GAC
  318
CTC GTC CGT CTG CGG GAG CGC TAT CCC TGG CTC GTC GCC GAG GTG
  363
GAC GGC GAG GTC GCC GGC ATC GCC TAC GCG GGC CCC TGG AAG GCA
  408
CGC AAC GCC TAC GAC TGG ACG GCC GAG TCG ACC GTG TAC GTC TCC
  453
CCC CGC CAC CAG CGG ACG GGA CTG GGC TCC ACG CTC TAC ACC CAC
  498
CTG CTG AAG TCC CTG GAG GCA CAG GGC TTC AAG AGC GTG GTC GCT
  543
GTC ATC GGG CTG CCC AAC GAC CCG AGC GTG CGC ATG CAC GAG GCG
  588
CTC GGA TAT GCC CCC CGC GGC ATG CTG CGG GCG GCC GGC TTC AAG
  633
CAC GGG AAC TGG CAT GAC GTG GGT TTC TGG CAG CTG GAC TTC AGC
  678
CTG CCG GTA CCG CCC CGT CCG GTC CTG CCC GTC ACC GAG ATC
  723
```

or of a part thereof expressing a polypeptide having

COR-AAD1-00003970
Bayer EX1008 (Part 7 of 9)

plant-protecting capability against Bialaphos.

The invention also relates to any DNA fragment differing from the preferred one indicated hereabove by the replacement of any of its nucleotides by others, yet without modifying the genetic information of the preferred DNA sequence mentioned hereabove (normally within the meaning of the universal genetic code), and furthermore to any equivalent DNA sequence which would encode a polypeptide having the same properties, particularly a Bialaphos-resistance-activity.

It will be understood that the man skilled in the art should be capable of readily assessing those parts of the nucleotide sequences that could be removed from either side of any of the DNA fragments according to the invention, for instance by removing terminal parts on either side of said DNA fragment, such as by an exonucleolytic enzyme, for instance Bal31, by recloning the remaining fragment in a suitable plasmid and by assaying the capacity of the modified plasmid to transform appropriate cells and to protect it against the Bialaphos antibiotic or herbicide as disclosed later, whichever assay is appropriate.

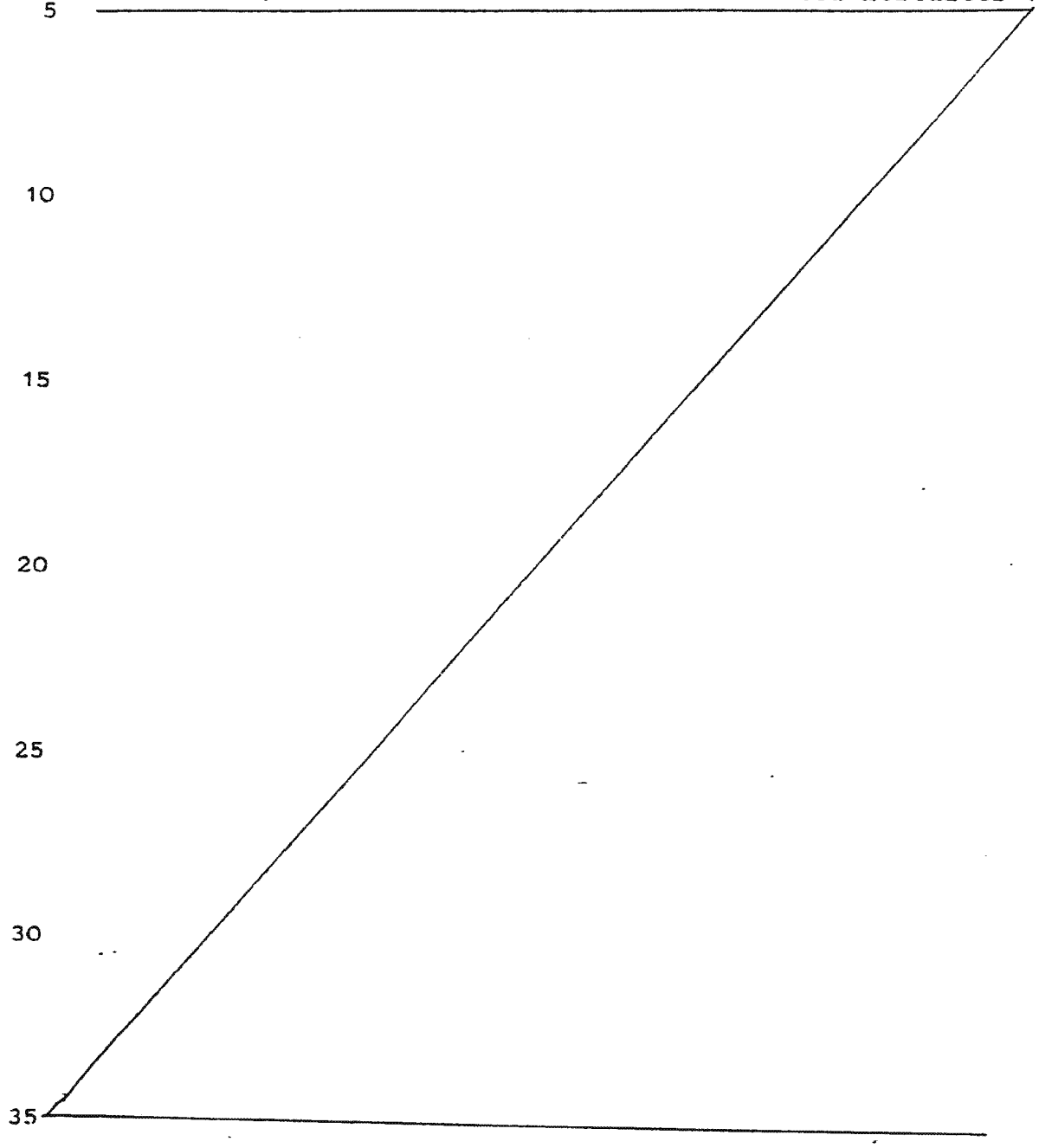
For the easiness of language, these DNA fragments will be termed hereafter as "Bialaphos-resistance DNA". In a similar manner, the corresponding polypeptide will be termed as "Bialaphos-resistance enzyme".

While in the preceding discussion particular emphasis has been put on DNA fragments capable, when introduced into plant cells and plants, to confer on them protection against Bialaphos or PPT, it should be understood that the invention should in no way be deemed as limited thereto.

In a same manner, the invention pertains to DNA fragments which, when introduced into such plant cells, would also confer on them a protection against other GS

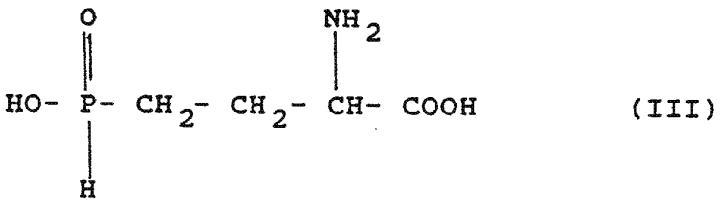
COR-AAD1-00003971
Bayer EX1008 (Part 7 of 9)

inhibitors, for instance of intermediate products involved in the natural biosynthesis of phosphinotricin, such as the compounds designated by the abbreviations MP101 (III), MP102 (IV), the formula of which are indicated hereafter :

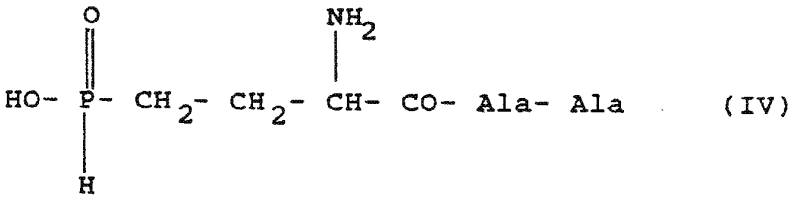


COR-AAD1-00003972

Bayer EX1008 (Part 7 of 9)



(III)



(IV)

More generally, the invention has opened the route to the production of DNA fragments which, upon proper incorporation into plant cells and plants, can protect them against GS inhibitors when contacted therewith, as this will be shown in a detailed manner in relation to Bialaphos and PPT in the examples which will follow.

This having been established, it will be appreciated that any fragment encoding an enzymatic activity which would protect plant cells and plants against said GS inhibitors, by inactivationg, should be viewed as an equivalent of the preferred fragments which have been disclosed hereabove. This would apply especially to any DNA fragments that would result from genetic screening of the genomic DNAs of strains, particularly of antibiotic-producing strains, likely to possess genes which, even- though structurally different, would encode similar activity with respect to Bialaphos or PPT, or even with respect to other GS inhibitors. This applies to any gene in other strains producing a PPT derivative.

Therefore, it should be understood that the language "Bialaphos-resistance DNA" or "Bialaphos-resistance enzyme" used thereafter as a matter of convenience is intended to relate not only to the DNAs and

COR-AAD1-00003973
Bayer EX1008 (Part 7 of 9)

enzymes specifically concerned with resistance to PPT or most directly related derivatives, but more generally with other DNAs and enzymes which would be capable, under the same circumstances, of inactivating the action in plants of GS inhibitors.

The invention also relates to DNA recombinants containing the above defined Bialaphos-resistance DNA fragments recombined with heterologous DNA, said heterologous DNA containing regulation elements and said Bialaphos-resistance DNA being under the control of said regulation elements in such manner as to be expressible in a foreign cellular environment compatible with said regulation elements. Particularly the abovesaid Bialaphos-resistance-DNA fragments contained in said DNA recombinants are devoid of any DNA region involved in the biosynthesis of Bialaphos, when said Bialaphos-resistance-DNA fragment originate themselves from Bialaphos-producing strains.

By "heterologous DNA" is meant a DNA of an other origin than that from which said Bialaphos-resistance-DNA originated, e.g. is different from that of a Streptomyces hygroscopicus or Streptomyces viridochromogenes or even more preferably a DNA foreign to Streptomyces DNA. Particularly said regulation elements are those which are capable of controlling the transcription and translation of DNA sequences normally associated with them in said foreign environment. "Cellular" refers both to micro-organisms and to cell cultures.

This heterologous DNA may be a bacterial DNA, particularly when it is desired to produce a large amount of the recombinant DNA, such as for amplification purposes. In that respect a preferred heterologous DNA consists of DNA of E. coli or of DNA compatible with E. coli. It may be DNA of the same origin as that of the cells concerned or other DNA, for instance viral or plasmidic DNA known as

COR-AAD1-00003974
Bayer EX1008 (Part 7 of 9)

capable of replicating in the cells concerned.

Preferred recombinant DNA contains heterologous DNA compatible with plant cells, particularly Ti-plasmid DNA.

Particularly preferred recombinants are those which contain GS inhibitor inactivating DNA under the control of a promoter recognized by plant cells, particularly those plant cells on which inactivation of GS inhibitors is to be conferred.

Preferred recombinants according to the invention further relate to modified vectors, particularly plasmids, containing said GS-inhibitor-inactivating DNA so positioned with respect to regulation elements, including particularly promoter elements, that they enable said GS inhibitor-inactivating DNA to be transcribed and translated in the cellular environment which is compatible with said heterologous DNA. Advantageous vectors are those so engineered as to cause stable incorporation of said GS inhibitor inactivating DNA in foreign cells, particularly in their genomic DNA. Preferred modified vectors are those which enable the stable transformation of plant cells and which confer to the corresponding cells, the capability of inactivating GS inhibitors.

It seems that, as described later, the initiation codon of the Bialaphos-resistance-gene of the Streptomyces hygroscopicus strain used herein is a GTG codon. But in preferred recombinant DNAs or vectors, the Bialaphos-resistance-gene is modified by substitution of an ATG initiation codon for the initiation codon GTG, which ATG enables translation initiation in plant cells.

In the example which follows, the plant promoter sequence which has been used was constituted by a promoter of the 35 S cauliflower mosaic virus. Needless to say that the man skilled in the art will be capable of selecting other plant promoters, when more appropriate in relation

COR-AAD1-00003975
Bayer EX1008 (Part 7 of 9)

to the plant species concerned.

According to an other preferred embodiment of the invention, particularly when it is desired to achieve transport of the enzyme encoded by the Bialaphos-resistance-DNA into the chloroplasts, the heterologous DNA fragment is fused to a gene or DNA fragment encoding a transit peptide, said last mentioned fragment being then intercalated between the GS inhibitor inactivating gene and the plant promoter selected.

As concerns means capable of achieving such constructions, reference can be made to the following British applications 84 32757 filed on December 28, 1984 and 85 00336 filed on January 7, 1985 and to the related applications filed in the United-States of America (n° 755,173, filed on July 15, 1985), in the European Patent Office (n° 85 402596.2, filed on December 20,1985), in Japan (n° 299 730, filed on December 27, 1985), in Israel (n° 77 466 filed on December 27, 1985) and in Australia (n° 5 165 485, filed on December 24, 1985), all of which are incorporated herein by reference.

Reference can also be made to the scientific literature, particularly to the following articles :

- VAN DEN BROECK et al., 1985, Nature, 313, 358-363 ;
- SCHREIER and al., Embo. J., vol. 4, n° 1, 25-32.

These articles are also incorporated herein by reference.

For the sake of the record, be it recalled here that under the expression "transit peptide", one refers to a polypeptide fragment which is normally associated with a chloroplast protein or a chloroplast protein sub-unit in a precursor protein encoded by plant cell nuclear DNA. The transit peptide then separates from the chloroplast protein or is proteolitically removed, during the translocation process of the latter protein into the chloroplasts.

COR-AAD1-00003976
Bayer EX1008 (Part 7 of 9)

Examples of suitable transit peptides are those associated with the small subunit of ribulose-1,5 biphosphate (RuBP) carboxylase or that associated with the chlorophyl a/b binding proteins.

There is thus provided DNA fragments and DNA recombinants which are suitable for use in the process defined hereafter.

More particularly the invention also relates to a process, which can be generally defined as a process for producing plants and reproduction material of said plants including a heterologous genetic material stably integrated therein and capable of being expressed in said plants or reproduction material in the form of a protein capable of inactivating or neutralizing the activity of a glutamine synthetase-inhibitor, comprising the non biological steps of producing plants cells or plant tissue including said heterologous genetic material from starting plant cells or plant tissue not able to express that inhibiting or neutralizing activity, regenerating plants or reproduction material of said plants or both from said plant cells or plant tissue including said genetic material and, optionally, biologically replicating said last mentioned plants or reproduction material or both, wherein said non-biological steps of producing said plant cells or plant tissue including said heterologous genetic material, comprises transforming said starting plant cells or plant tissue with a DNA-recombinant containing a nucleotide sequence encoding said protein, as well as the regulatory elements selected among those which are capable of enabling the expression of said nucleotide sequence in said plant cells or plant tissue, and to cause the stable integration of said nucleotide sequence in said plant cells and tissue, as well as in the plant and reproduction material processed therefrom throughout generations.

The invention also relates to the cell cultures

COR-AAD1-00003977
Bayer EX1008 (Part 7 of 9)

containing Bialaphos-resistance-DNA, or more generally said GS-inhibitor-inactivating DNA, which cell cultures have the property of being resistant to a composition containing a GS inhibitor, when cultured in a medium containing a such composition at dosages which would be destructive for non transformed cells.

The invention concerns more particularly those plant cells or cell cultures in which the Bialaphos-resistance DNA is stably integrated and which remains present over successive generations of said plant cells. Thus the resistance to a GS inhibitor, more particularly Bialaphos or PPT, can also be considered as a way of characterizing the plant cells of this invention.

Optionally one may also resort to hybridization experiments between the genomic DNA obtained from said plant cells with a probe containing a GS inhibitor inactivating DNA sequence.

More generally the invention relates to plant cells, reproduction material, particularly seeds, as well as plants containing a foreign or heterologous DNA fragment stably integrated in their respective genomic DNAs, said fragments being transferred throughout generations of such plant cells, reproduction material, seeds and plants, wherein said DNA fragment encodes a protein inducing a non-variety-specific enzymatic activity capable of inactivating or neutralizing GS inhibitors, particularly Bialaphos and PPT, more particularly to confer on said plant cells, reproduction material, seeds and plants a corresponding non-variety-specific phenotype of resistance to GS inhibitors.

"Non-variety-specific" enzymatic activity or phenotype aims at referring to the fact that they are not characteristic of specific plant genes or species as this will be illustrated in a non-limitative way by the examples which will follow. They are induced in said plant

COR-AAD1-00003978
Bayer EX1008 (Part 7 of 9)

materials by essentially non-biological processes applicable to plants belonging to species normally unrelated with one another and comprising the incorporation into said plant material of heterologous DNA, e.g. bacterial DNA or chemically synthesized DNA, which does not normally occur in said plant material or which normally cannot be incorporated therein by natural breeding processes, and which yet confers a common phenotype (e.g. herbicide resistance) to them.

The invention is of particular advantageous use in processes for protecting field-cultivated plant species against weeds, which processes comprise the step of treating the field with an herbicide, e.g. Bialaphos or PPT in a dosage effective to kill said weeds, wherein the cultivated plant species then contains in their genome a DNA fragment encoding a protein having an enzymatic activity capable of neutralizing or inactivating said GS inhibitor.

By way of illustration only, effective doses for use in the abovesaid process range from about 0.4 to about 1.6 kg/Hectare of Bialaphos or PPT.

There follows now a disclosure of how the preferred DNA fragment described hereabove was isolated starting from the Streptomyces hygroscopicus strain available at the American Type Culture Collection under deposition number ATCC 21 705, by way of examplification only.

The following disclosure also provides the technique which can be applied to other strains producing compounds with a PPT moiety.

The disclosure will then be completed with the description of the insertion of a preferred DNA fragment conferring to the transformed cells the capability of inactivating Bialaphos and PPT. Thus the Bialaphos-inactivating-DNA fragment designated thereafter by

COR-AAD1-00003979
Bayer EX1008 (Part 7 of 9)

Bialaphos-resistance gene or "sfr" gene, isolated by the above described technique into plasmids which can be used for transforming plant cells and conferring to them a resistance against Bialaphos, also merely by way of example for non-limitative illustration purposes.

The following disclosure is made with reference to the drawings in which :

- fig. 1 is a restriction map of a plasmid containing a Streptomyces hygroscopicus DNA fragment encoding Bialaphos-resistance, which plasmid, designated hereafter as pBG1 has been constructed according to the disclosure which follows ;

- fig. 2 shows the nucleotide sequence of a smaller fragment obtained from pBG1, subcloned into another plasmid (pBG39) and containing the resistance gene ;

- fig. 3 shows the construction of a series of plasmids given by way of example, which plasmids aim at providing suitable adaptation means for the insertion therein of the Bialaphos-resistance gene or "sfr" gene ;

- fig. 4A and 4B show the construction of a series of plasmids given by way of example, which plasmids contain suitable plant cell promoter sequences able to initiate transcription and expression of the foreign gene inserted under their control into said plasmids ;

- fig. 5A shows a determined fragment of the nucleotide sequence of the plasmid obtained in figure 3 ;

- fig. 5B shows the reconstruction of the first codons of a Bialaphos-resistance gene, from a FokI/BglII fragment obtained from pBG39 and the substitution of an ATG initiation codon for the GTG initiation codon of the natural "sfr" gene ;

- fig. 5C shows the reconstruction of the entire "sfr" gene, namely the last codons thereof, and its insertion into a plasmid obtained in figures 4A and 4B ;

- fig. 6A shows an expression vector containing

COR-AAD1-00003980
Bayer EX1008 (Part 7 of 9)

the "sfr" gene placed under the control of a plant cell promoter ;

- fig. 6B shows another expression vector deriving from the one shown in fig. 6A, by the substitution of some nucleotides.

- fig. 7 shows the construction of a series of plasmids given by way of examples, to ultimately produce plasmids containing the promoter region and the transit peptide sequence of a determined plant cell gene, for the insertion of the "sfr" gene under the control of said promoter region and downstream of said transit peptide sequence.

- fig. 8 to 11 will be referred to hereafter.

The following experiment was set up to isolate a Bialaphos-resistance-gene from S. hygroscopicus, according to standard techniques for cloning into Streptomyces.

2.5 µg of S. hygroscopicus genomic DNA and 0.5 µg of Streptomyces vector pIJ61 were cleaved with PstI according to the method described in ref. 6. The vector fragments and genomic fragments were mixed and ligated (4 hours at 10°C followed by 72 hours at 4°C in ligation salts which contain 66 mM Tris-HCl (pH 7.5), 1 mM EDTA, 10 mM $MgCl_2$, 10 mM 2-mercaptoethanol and 0.1 mM ATP) at a total DNA concentration of 40 µg ml^{-1} with T4 DNA ligase. Ligation products were introduced into 3 x 10^9 S. lividans strain 66 protoplasts by a transformation procedure mediated by polyethylene-glycol (PEG) as described hereafter. These protoplasts gave rise to 5 x 10^7 colonies and 4 x 10^4 pocks after regeneration on 20 plates of R2 agar containing 0.5 % of Difco yeast extract (R2 YE). Preparation and composition of the different mediums and buffers used in the disclosed experiments are described hereinafter. When these lawns were replica-plated on minimal

COR-AAD1-00003981
Bayer EX1008 (Part 7 of 9)

medium plates containing 50 µg ml^{-1} Bialaphos, drug resistant colonies appeared at a frequency of 1 per 10^4 transformants. After purification of the drug resistant colonies, there plasmid DNA was isolated and used to retransform S. lividans protoplasts. Non selective regeneration followed by replication to Bialaphos-containing-medium demonstrated a 100 % correlation between pocks and Bialaphos resistant growth. The recombinant plasmids of several resistant clones all contained a 1.7 Kb PstI insert (see fig. 1).

Subcloning of the herbicide resistance gene

The 1.7 Kb PstI insert was then subcloned into the high copy number streptomycete vector pIJ385 to generate plasmid pBG20. S. lividans strains which contained pBG20 were more than 500 times more resistant to Bialaphos. S. lividans growth is normally inhibited in minimal medium containing 1 µg/ml Bialaphos ; growth of transformants containing pBG20 was not noticeably inhibited in a medium containing 500 µg/ml Bialaphos. The PstI fragment was also subcloned in either orientation into the PstI site of the plasmid pBR322, to produce plasmids pBG1 and pBG2, according to their orientation. A test on minimal M9 medium demonstrated that E. coli E8767 containing pBG1 or pBG2 was resistant to Bialaphos.

A ± 1.65 Kb PstI - BamHI fragment was subcloned from pBG1 into the plasmid pUC19 to produce the plasmid pBG39, and conferred Bialaphos resistance to E. coli, W3110, C600 and JM83.

Using an in vitro coupled transcription-translation system (ref. 5) from S. lividans extracts, the 1,65 Kb PstI - BamHI fragment in pBG39 was shown to direct the synthesis of a 22 Kd protein. In the following, this 1,65 Kb insert includes a fragment coding for a 22 Kd protein and will be called "sfr" gene.

COR-AAD1-00003982
Bayer EX1008 (Part 7 of 9)

Fine mapping and sequencing of the gene

A 625 bp Sau3A fragment was subcloned from pBG39 into pUC19 and still conferred Bialaphos resistance to a E. coli W3110 host. The resulting clones were pBG93 and pBG94, according to the orientation.

The orientation of the gene in the Sau3A fragment was indicated by experiments which have shown that Bialaphos resistance could be induced with IPTG from the pUC19 lac promoter in pBG93. In the presence of IPTG (0.5 mM) the resistance of pBG93/W3110 increased from 5 to 50 µg/ml on a M9 medium containing Bialaphos. The W3110 host devoid of pBG93, did not grow on M9 medium containing 5 µg/ml Bialaphos. These experiments demonstrated that the Sau3A fragment could be subcloned without loss of activity. They also provided for the proper orientation as shown in the fig. 2, enclosed thereafter. The protein encoded by these clones was detected by using coupled transcription-translation systems derived from extracts of S. lividans (ref. 7). Depending on the orientation of the Sau3A fragment, translation products of different sizes were observed ; 22 Kd for pBG94 and ± 28 Kd for pBG93. This indicated that the Sau3A fragment did not contain the entire resistance gene and that a fusion protein was formed which included a polypeptide sequence resulting from the translation of a pUC19 sequence.

In order to obtain large amounts of the protein, a 1.7 Kb PstI fragment from pBG1 was cloned into the high copy number Streptomycete replicon pIJ385. The obtained plasmid, pBG20, was used to transform S. hygroscopicus. Transformants which contained this plasmid had more than 5 times as much PPT acetylating activity and also had increased amounts of a 22 kd protein on sodium dodecylsulfate gels (SDS gels). Furthermore, both the acetyl transferase and the 22 kd protein appeared when the production of Bialaphos begun. The correlation of the in

COR-AAD1-00003983
Bayer EX1008 (Part 7 of 9)

vitro data, kinetics of synthesis, and amplified expression associated with pBG20 transformants strongly implied that this 22 Kd band was the gene product.

The complete nucleotide sequence of the 625 bp Sau3A fragment was determined as well as of flanking sequences. Computer analysis revealed the presence of an open reading frame over the entire length of the Sau3A fragment.

Characterization of the sfr gene product

A series of experiments were performed to determine that the open reading frame of the "sfr" gene indeed encoded the Bialaphos resistance enzyme. To determine the 5' end of the resistance gene, the NH_2-terminal sequence of the enzyme was determined. As concerns more particularly the technique used to determine the said sequence, reference is made to the technique developed by J. VANDEKERCKHOVE, Eur. J. Bioc. 152, p. 9-19, 1985, and to French patent applications n° 85 14579 filed on October 1st, 1985 and n° 85 13046 filed on September 2nd, 1985, all of which are incorporated herein by reference.

This technique allows the immobilization on glass fibre sheets coated with the polyquaternary amine commercially available under the registered trademark POLYBRENE of proteins and of nucleic acids previously separated on a sodium dodecylsulfate containing polyacrylamide gel. The transfer is carried out essentially as for the protein blotting on nitrocellulose membranes (ref. 8). This allows the determination of amino-acid composition and partial sequence of the immobilized proteins. The portion of the sheet carrying the immobilized 22 kd protein produced by S. hygroscopicus pBG20 was cut out and the disc was mounted in the reaction chambre of a gas-phase sequenator to subject the glass-fibre bound 22 Kd protein to the Edman degradation procedure. The following amino-acid sequence was obtained :

COR-AAD1-00003984
Bayer EX1008 (Part 7 of 9)

Pro-Glu-Arg-Arg-Pro-Ala-Asp-Ile-Arg-Arg

This sequence matched an amino-acid sequence which was deduced from the open reading frame of the 625 bp Sau3A fragment. It corresponded to the stretch from codon 3 to codon 12.

Thus, the NH_2-terminus of the 22 Kd protein was upstream of this sequence. It was determined that translation of the actual protein was likely to be initiated 2 amino-acids earlier at a GTG initiation codon. GTG is often used as initiator codon in Streptomyces and translated as methionine. The protein translated from the GTG initiation codon would be 183 amino-acids long and would have a molecular weight of 20 550. This was in good agreement with the observed approximate molecular weight of 22 000.

Furthermore, the termination codon, TGA, was located just downstream of the Sau3A site. Cloning of the 625 bp Sau3A fragment in a BamHI site digested pUC19 did not result in the reconstruction of the termination codon. This explained the fusion proteins which were observed in the in vitro transcription-translation analysis.

Mechanism of PPT-resistance

Having defined a first phenotype and some of the physical characteristics of the resistance gene and its gene product, a series of experiments was then carried out to understand the mechanism by which it confers resistance. As described hereabove, PPT is the portion of Bialaphos which inhibits glutamine synthetase (GS) and that N-acetyl PPT is not an inhibitor. Using a standard assay (ref. 9), S. hygroscopicus ATCC 21 705 derivates were shown to contain a PPT acetyl transferase which was not found in S. lividans. The activity does not acetylate the Bialaphos tripeptide. S. lividans carrying the resistance gene cloned in pBG20 or pBG16 (a plasmid containing the 625 bp Sau3A fragment cloned into another

COR-AAD1-00003985
Bayer EX1008 (Part 7 of 9)

streptomycete vector, pIJ680) also contained the activity which could acetylate PPT but not Bialaphos. The PPT derived reaction product produced by extracts of pBG20/ S. lividans was isolated in order to confirm that it was indeed acetyl-PPT. Analysis by mass spectroscopy showed that the molecular weight had increased relative to PPT by the equivalent of one acetyl group. It was thus concluded that the 625 bp Sau3A fragment contained sequences which code for PPT acetyl transferase.

The experimental conditions and reagents used in the techniques disclosed hereabove were as follows :

Preparation and composition of the mediums and buffers above used

1° P medium : 10.3 g of sucrose, 0.025 g of K_2SO_4, 0.203 g of $MgCl_2.6H_2O$ and 0.2 ml of a trace element solution are dissolved in 80 ml of distilled water and autoclaved. Then in order, 1 ml of KH_2PO_4 (0.5 %), 10 ml of $CaCl_2$, $2H_2O$ (3.68 %), and 10 ml of TES buffer (0.25 M), pH : 7.2) are added. Trace element solution (per litre) : $ZnCl_2$, 40 mg ; $FeCl_3.6H_2O$, 200 mg ; $CuCl_2.2H_2O$, 10 mg ; $MnCl_2.4H_2O$, 10 mg ; $Na_2B_4O_7.10H_2O$, 10 mg ; $(NH_4)_6Mo_7O_{24}.4H_2O$, 10 mg.

2° R2YE : 10.3 g of sucrose, 0.025 g of K_2SO_4, 1.012 g of $MgCl_2.6H_2O$, 1 g of glucose, 0.01 g of Difco casamino acids, and 2.2 g of Difco agar are dissolved in 80 ml distilled water and autoclaved. 0.2 ml of trace element solution, 1 ml of KH_2PO_4 (0.5 %), 8.02 ml of $CaCl_2.2H_2O$ (3.68 %), 1.5 ml of L-proline (20 %), 10 ml of TES buffer (0.25 M) (pH : 7.2), 0.5 ml of (1 M) NaOH, 5 ml of yeast extract (10 %) are sequentially added.

3° TE : 10 mM TRIS HCl, 1 mM EDTA, pH 8.0.

4° YEME : Difco yeast extract (0.3 %), Difco peptone (0.5 %), oxoid malt extract (0.3 %), glucose (1 %).

Transformation of S. lividans protoplasts

1. A culture composed of 25 ml YEME, 34 % sucrose, 0.005 M

COR-AAD1-00003986
Bayer EX1008 (Part 7 of 9)

$MgCl_2$, 0.5 % glycine, in a 250 ml baffled flask, is centrifuged during 30 to 36 hours.

2. The pellet is suspended in 10.3 % sucrose and centrifuged. This washing is repeated once.

3. The mycelium is suspended in 4 ml lysozyme solution (1 mg/ml in P medium with $CaCl_2$ and $MgCl_2$ concentrations reduced to 0.0025 M) and incubated at 30°C for 15 to 60 minutes.

4. The solution is mixed by pipetting three times in a 5 ml pipette and incubated for further 15 minutes.

5. P medium (5 ml) is added and mixed by pipetting as in step 4.

6. The solution is filtered through cotton wool and protoplasts are gently sedimented in a bench centrifuge at 800 x G during 7 minutes.

7. Protoplasts are suspended in 4 ml P medium and centrifuged again.

8. Step 7 is repeated and protoplasts are suspended in the drop of P medium left after pouring off the supernatant (for transformation).

9. DNA is added in less than 20 µl TE.

10. 0.5 ml PEG 1 000 solution (2.5 g PEG dissolved in 7.5 ml of 2.5 % sucrose, 0.0014 K_2SO_4, 0.1 M $CaCl_2$, 0.05 M TRIS-maleic acid, pH 8.0, plus trace elements) is immediately added and pipetted once to mix the components.

11. After 60 seconds, 5 ml of P medium are added and the protoplasts are sedimented by gentle centrifugation.

12. The pellet is suspended in P medium (1 ml).

13. 0.1 ml is plated out on R2YE plates (for transformation dry plates to 85 % of their fresh weigh e. g. in a laminar flow cabinet).

14. Incubation at 30°C.

A - Construction of a "sfr" gene cassette

A "sfr" gene cassette was constructed to allow subsequent cloning in plant expression vectors.

COR-AAD1-00003987
Bayer EX1008 (Part 7 of 9)

Isolation of a FokI-BglII fragment from the plasmid pBG39 containing a "sfr" gene fragment led to the loss of the first codons, including the initiation codon, and of the last codons, including the stop codon.

This fragment of the "sfr" gene could be reconstructed in vitro with synthetic oligonucleotides which encode appropriate amino-acids.

The complementary synthetic oligonucleotides were 5'-CATGAGCCCAGAAC and 3'-TCGGGTCTTGCTGC.

By using such synthetic oligonucleotides, the 5' end of the "sfr" gene could be reformed and the GTG initiation codon substituted for a codon well translated by plant cells, particularly an ATG codon.

The DNA fragment containing the oligonucleotides linked to the "sfr" gene was then inserted into an appropriate plasmid, which contained a determined nucleotide sequence thereafter designated by an "adapter" fragment.

This adapter fragment comprised :

- a TGA termination codon which enabled the last codons of the "sfr" gene to be reformed ;
- appropriate restriction sites which enabled the insertion of the fragment of the nucleotide sequence comprising the "sfr" gene partially reformed with the synthetic oligonucleotides ; this insertion resulted in the reconstruction of an intact "sfr" gene ;
- appropriate restriction sites for the isolation of the entire "sfr" gene.

The "sfr" gene was then inserted into another plasmid, which contained a suitable plant promoter sequence. The plant promoter sequence consisted of the cauliflower mosaïc virus promoter sequence (p35S). Of course the invention is not limited to the use of this particular promoter. Other sequences could be chosen as promoters suitable in plants, for example the TR 1'-2' promoter region and the promoter fragment of a Rubisco small

COR-AAD1-00003988
Bayer EX1008 (Part 7 of 9)

subunit gene from Arabidopsis thaliana hereafter described.

1° Construction of the plasmid pLK56.2 (fig. 3)

The construction of plasmid pLK56.2 aimed at obtaining a suitable adaptor including the following sequence of restriction sites : SmaI, BamHI, NcoI, KpnI, BglII, MluI, BamHI, HindIII and XbaI.

The starting plasmids used for this construction, pLK56, pJB64 and pLK33 were those disclosed by BOTTERMAN (ref. 11).

The DNA fragments hereafter described were isolated and separated from low melting point agarose (LGA).

The plasmid pLK56 was cleaved by the enzymes BamHI and NdeI. A NcoI-NdeI fragment (referred to in the drawings by arc "a" in broken line) obtained from plasmid pJB64 was substituted in pLK56 for the BamHI-NdeI fragment shown at "b". Ligation was possible after filling in the BamHI and NcoI protruding ends with the DNA polymerase I of E. coli (Klenow's fragment).

Particularly recircularization took place by means of a T4 DNA ligase. A new plasmid pLK56.3 was obtained.

This plasmid was cleaved by the enzymes XbaI and PstI.

The BamHI-PstI fragment of pLK33 (c) (on fig. 3) was substituted for the XbaI-PstI fragment (d) of pLK56.3, after repairing of their respective ends by Klenow's fragment.

After recircularization by means of the T4 DNA ligase, the obtained plasmid pLK56.2 contained a nucleotide sequence which comprised the necessary restriction sites for the subsequent insertion of the "sfr" gene.

2° Construction of the plasmid pGSH150 (fig. 4A)

Parallel with the last discussed construction,

COR-AAD1-00003989
Bayer EX1008 (Part 7 of 9)

there was produced a plasmid containing a promoter sequence recognized by the polymerases of plant cells and including suitable restriction sites, downstream of said promoter sequence in the direction of transcription, which restriction sites are then intented to enable the accomodation of the "sfr" gene then obtainable from pLK56.2, under the control of said plant promoter.

Plasmid pGV825 is described in DEBLAERE et al. (ref. 10). Plasmid pJB63 is from BOTTERMAN (ref. 11).

pGV825 was linearized with PvuII and recircularized by the T4 DNA ligase, resulting in the deletion of an internal PvuII fragment shown at (e), (plasmid pGV956).

pGV956 was then cleaved by BamHI and BglII.

The BamHI-BglII fragment (f) obtained from pJB63 was dephosphorylated with calf intestine phosphatase (CIP) and substituted for the BamHI-BglII fragment of pGV956.

Plasmid pGV1500 was obtained after recircularization by means of T4 DNA ligase.

An EcoRI-HindIII fragment obtained from plasmid pGSH50 was purified. The latter plasmid carried the dual TR 1'-2' promoter fragment described in VELTEN et al., (ref.13). This fragment was inserted in pGV1500, digested with HpaI and HindIII and yielded pGSH150.

This plasmid contains the promoter fragment in front of the 3' end of the T-DNA transcript 7 and a BamHI and ClaI sites for cloning.

3° Construction of the plasmid pGSJ260 (fig. 4B)

CP3 is a plasmid derived from pBR322 and which contains the 35S promoter region of cauliflower mosaic virus within a BamHI fragment.

pGSH150 was cut by BamHI and BglII.

The BamHI-BglII fragment (h) of CP3, which contained the nucleotide sequence of p35S promoter, was substituted for the BamHI-BglII fragment (i) in pGSH150 to form plasmid pGSJ250. pGSJ250 was then opened at its BglII

COR-AAD1-00003990
Bayer EX1008 (Part 7 of 9)

restriction site.

A BamHI fragment obtained from mGV2 (ref. 12) was inserted in pGSJ250 at the BglII site to form plasmid pGSJ260.

However prior to inserting the "sfr" gene obtainable from pLK56.2 into plasmid pGSJ260, it was still desirable to further modify the first in order to permit insertion in a more practical manner. Thus pLK56.2 was further modified as discussed below to yield pGSR1.

Starting from plasmid pGSJ260, two plasmid constructions for subsequent transformations of plant cells were made :

- a first plasmid permitting the expression of the "sfr" gene in the cytoplasm of plant cells, and
- a second plasmid so modified as to achieve transport of the Bialaphos-resistance enzymes to the chloroplasts of plant cells.

First case : plasmid enabling the expression of the "sfr" gene in the cytoplasm of plant cells

Cloning of the sfr gene cassette in a plant expression vector (pGSR2) (fig. 5)

On figure 5A, the nucleotide sequence of the adapter of pLK56.2 is shown. In particular, the locations of BamHI, NcoI, BglII restriction sites are shown.

This adapter fragment was cleaved by the enzymes NcoI and BglII.

Figure 5B shows the FokI-BglII fragment (j) obtained from pBG39. The locations of these two restriction sites are shown on figure 2.

Using synthetic oligonucleotides, the first codons of the "sfr" gene were reformed, particularly the 5' end of the gene in which a ATG initiation codon was substituted for the initial GTG codon.

This FokI-BglII fragment completed with the synthetic oligonucleotides was then substituted in pLK56.2

COR-AAD1-00003991
Bayer EX1008 (Part 7 of 9)

for the NcoI-BglII fragment of the adapter. The 3' end of the gene was thus reformed too, after recircularization with T4 DNA ligased. The plasmid obtained, pGSR1, thus contained the entire "sfr" gene inserted in its adapter.

The plasmid pGSJ260 was then opened by BamHI (fig. 5C) and the BamHI fragment obtained from pGSR1, which contained the entire "sfr" gene, was inserted into pGSJ260.

The obtained plasmid, pGSR2 (see fig. 6A) contained a pBR322 replicon, a bacterial streptomycin resistance gene (SDM-SP-AD-transferase) and an engineered T-DNA consisting of :

- the border fragments of the T-DNA ;
- a chimeric kanamycin gene which provided a dominant selectable marker in plant cells ; and
- a chimeric "sfr" gene.

The chimeric "sfr" gene consisting of :

- the promoter region of the cauliflower mosaïc virus (p35S) ;
- the "sfr" gene cassette as described in fig. 5 ;
- the 3' untranslated region, including the polyadenylation signal of T-DNA transcript 7.

pGSR2 was introduced into Agrobacterium tumefaciens recipient C58ClRif^R (pGV2260) according to the procedure described by DEBLAERE et al. (ref. 10).

This strain was used to introduce the chimeric "sfr" gene in N. tabacum SR_1 plants.

Two variant plasmids deriving from pGSR2, namely pGSFR280 and pGSFR281, have been constructed. They differ in the untranslated sequence following the transcription initiation site. In pGSR2, this fragment consists of the following sequence :

GAGGACACGCTGAAATCACCAGTCTCGGATCCATG ;

while it consists of :

GAGGACACGCTGAAATCACCAGTCTCTCTACAAATCGATCCATG

COR-AAD1-00003992
Bayer EX1008 (Part 7 of 9)

in pGSR280 and of

GAGGACACGCTGAAATCACCAGTCTCTCTACAAATCGATG

in pGSFR281, with an ATG codon being the initiation codon of the "sfr" gene. The "sfr" gene is also fused to the TR1'-2' promoter in the plasmid pGSH150 (fig. 4A) yielding pGSFR160 and pGSFR161 (fig. 6B). These plasmids contain slight differences in the pTR2 "sfr" gene configuration : the "sfr" gene is correctly fused to the endogenous gene 2' ATG in pGSFR161 (for sequences see ref. 13), whereas 4 extra base pairs (ATCC) are present just ahead of the ATG codon in pGSFR160. Otherwise, plasmids p65FR161 and p65FR160 are completely identical.

All plasmids are introduced in Agrobacterium by cointegration in the acceptor plamids pGV2260 yielding the respective plasmids pGSFR1280, pGSFR1281, pGSFR1160 and pGSFR1161.

Second case : construction of a plasmid containing the "sfr" gene downstream of a DNA sequence encoding a transit peptide and suitable for achieving subsequent translocation of the "sfr" gene expression product into plant-cell-chloroplasts

In another set of experiments, the nucleotide sequence which contained the "sfr" gene was fused to a DNA sequence encoding a transit peptide so as to enable its transport into chloroplasts.

A fragment of the "sfr" gene was isolated from the adapter fragment above described and fused to a transit peptide. With synthetic oligonucleotides, the entire "sfr" gene was reconstructed and fused to a transit peptide.

The plasmid (plasmid pATS3 mentioned below) which contained the nucleotide sequence encoding the transit peptide comprised also the promoter sequence thereof.

Construction of the plasmid pGSR4 which contains the "sfr" gene fused to a DNA sequence encoding transit peptide (fig. 7)

COR-AAD1-00003993
Bayer EX1008 (Part 7 of 9)

Plasmid pLK57 is from BOTTERMAN, (ref.11). Plasmid pATS3 is a pUC19 clone which contains a 2 Kb EcoRI genomic DNA fragment from Arabidopsis thaliana comprising the promoter region and the transit peptide nucleotide sequence of the gene, the expression thereof is the small subunit of ribulose biphosphate carboxylase (ssu). The A. thaliana small subunit was isolated as a 1 500 bp EcoRI-SphI fragment. The SphI cleavage site exactly occurs at the site where the coding region of the mature ssu protein starts.

Plasmids pLK57 and pATS3 were opened with EcoRI and SphI. After recircularization by means of the T4 DNA ligase, a recombinant plasmid pLKAB1 containing the sequence encoding the transit peptide (Tp) and its promoter region (Pssu) was obtained.

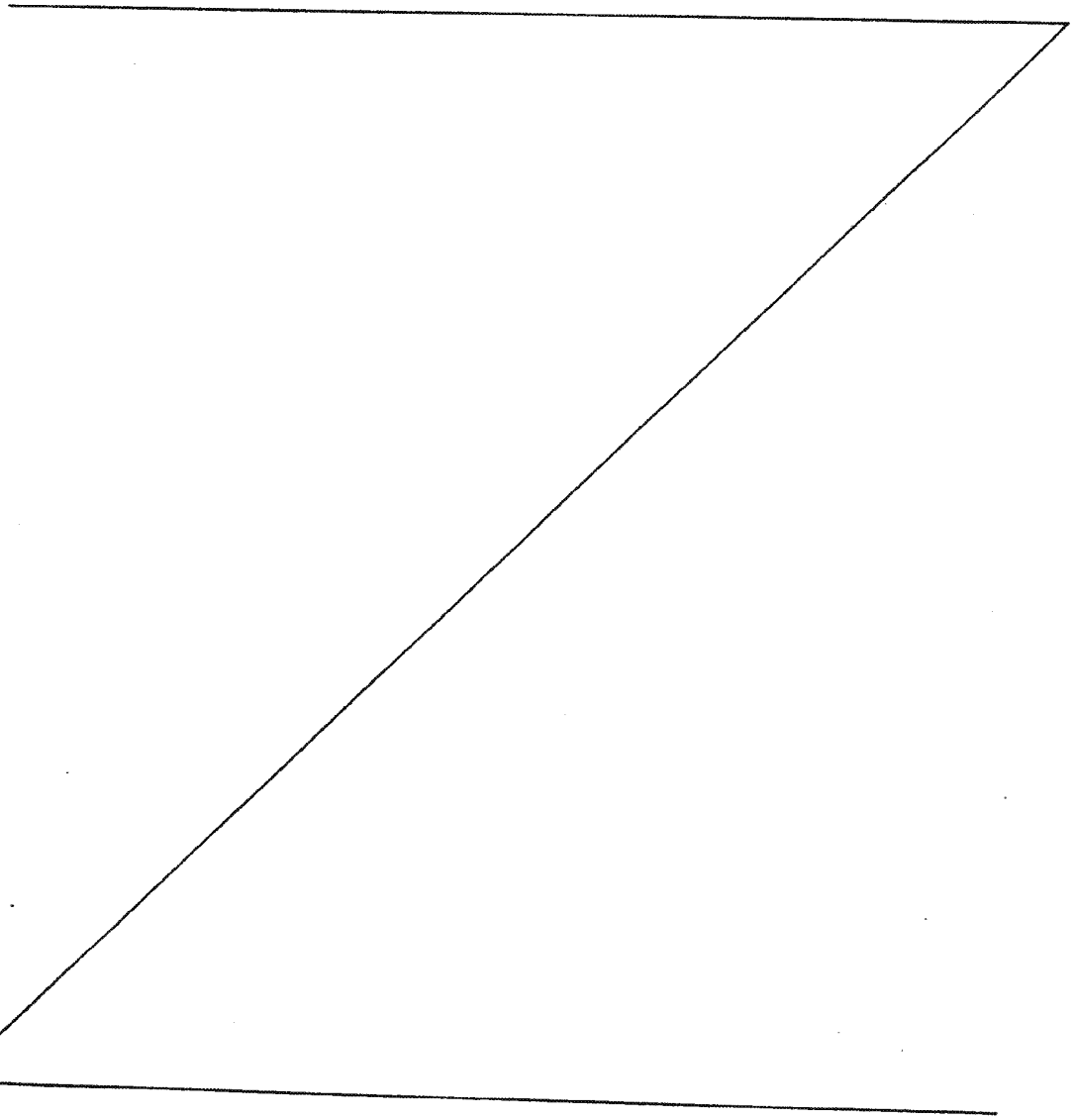
In order to correctly fuse the "sfr" gene at the cleavage site of the signal peptide, the N-terminal gene sequence was first modified. Since it was observed that N-terminal gene fusions with the "sfr" gene retain their enzymatic activity, the second codon (AGC) was modified to a GAC, yielding an NcoI site overlapping with the ATG initiator site. A new plasmid, pGSSFR2 was obtained. It only differs from pGSR1 (fig. 5B), by that mutation. The NcoI-BamHI fragment obtained from pGSFR2 was fused at the SphI end of the transit peptide sequence. In parallel, the "sfr" gene fragment was fused correctly to the ATG initiator of the ssu gene (not shown in figures).

Introduction of the "sfr" gene into a different plant species

The Bialaphos-resistance induced in plants by the expression of chimeric genes, when the latter have been transformed with appropriate vectors containing said chimeric genes, has been demonstrated as follows. The recombinant plasmids containing the "sfr" gene were introduced separately by mobilization into Agrobacterium strain $C58C_1$ Rif^R (pGV2260) according to the procedure described

COR-AAD1-00003994
Bayer EX1008 (Part 7 of 9)

by DEBLAERE and al., Nucl. Acid. Res., 13, p. 1 477, 1985. Recombinant strains containing hybrid Ti plasmides were formed. These strains were used to infect and transform leaf discs of different plant species, according to a method essentially as described by HORSH and al., 1985, Science, vol. 227. Transformation procedure of these different plant species given by way of example, is described thereafter.



COR-AAD1-00003995
Bayer EX1008 (Part 7 of 9)

1. Leaf disc transformation of Nicotiana tabacum

Used Media are described thereafter :

A_1 MS salt/2 + 1% sucrose
0.8 % agar
pH 5.7

A_{10} B5-medium + 250 mg/l NH_4NO_3
750 mg/l $CaCl_2\ 2H_2O$
0.5 g/l 2-(N-Morpholino)ethane-sulfonic acid (MES) pH 5.7
30 g/l sucrose

A_{11} B5-medium + 250 mg/l NH_4NO_3
0.5 g/l MES pH 5.7
2 % glucose
0.8 % agar
40 mg/l adenine

+ 1 mg/l 6-Benzylaminopurine (BAP)
0.1 mg/l Indole-3-acetic acid (IAA)
500 mg/l Claforan

A_{12} B5-medium + 250 mg/l NH_4NO_3
0.5 g/l MES pH 5.7
2 % glucose
0.8 % agar
40 mg/l adenine

+ 1 mg/l BAP
200 mg/l claforan

COR-AAD1-00003996
Bayer EX1008 (Part 7 of 9)

33

A_{13} MS-salt/2 + 3 % sucrose
0.5 MES g/l pH 5.7
0.7 % agar
200 mg/l claforan

Bacterial medium = min A : (Miller 1972) 60 mM K_2HPO_4, $3H_2O$, 33 mM KH_2PO_4 ; 7.5 mM $(NH_4)_2SO4$ 1.7 M trinatriumcitrat; 1 mM $MgSO_4$; 2 g/l glucose ; 50 mg/l vitamine B1

- Plant material :

Nicotiana tabacum cv. Petit Havana SR1

Plants are used 6 to 8 weeks after subculture on medium A_1

- Infection :

- midribs and edges are removed from leaves.
- Remaining parts are cut into segments of about 0.25 cm^2 and are placed in the infection medium A_{10} (about 12 segments in a 9 cm Petri dish containing 10 ml A_{10}).
- Segments are then infected with 25 µl per Petri dish of a late log culture of the Agrobacterium strain grown in min A medium.
- Petri dish are incubated for 2 to 3 days at low light intensity.
- After 2 to 3 days medium is removed and replaced by 20 ml of medium A_{10} containing 500 mg/l clarofan.

- Selection and shoot induction

- The leaf discs are placed on medium A_{11} containing a selective agent :

100 mg/l kanamycin and
10 to 100 mg/l phosphinotricin.

COR-AAD1-00003997
Bayer EX1008 (Part 7 of 9)

- Leaf discs are transferred to fresh medium weekly.

- After 3 to 4 weeks regenating calli arise. They are separated and placed on medium A_{12} with the same concentration of selective agent as used for the selection.

- Rooting

- After 2 to 3 weeks the calli are covered with shoots, which can be isolated and transferred to rooting medium A_{13} (without selection).

- Rooting takes 1 to 2 weeks.

- After a few more weeks, these plants are propagated on medium A_1.

2. Tuber disc infection of Solanum tuberosum (potato)

Used media are described thereafter :

C_1 B5-medium	+ 250 mg/l NH_4NO_3 300 mg/l $(CaCH_2PO_4)_2$ 0.5 g/l MES pH 5.7 0.5 g/l polyvinylpyrrolidone (PVP) 40 g/l mannitol (=0.22M) 0.8 % agar 40 mg/l adenine
C_2 B5-medium	+ 250 mg/l NH_4NO_3 400 mg/l glutamine 0.5 g/l MES pH 5.7 0.5 g/l PVP 40 g/l mannitol 40 mg/l adenine 0.8 % agar

COR-AAD1-00003998
Bayer EX1008 (Part 7 of 9)

35

+ 0.5 mg/l transzeatine
0.1 mg/l IAA
500 mg/l clarofan

C_5 MS salt/2 + 3 % sucrose
0.7 % agar
pH 5.7

C_7 B5-medium + 250 mg/l NH_4NO_3
400 mg/l glutamine
0.5 g/l MES pH 5.7
0.5 g/l PVP
20 g/l mannitol
20 g/l glucose
40 mg/l adenine
0.6 % agarose

+ 0.5 mg/l transzeatine
0.1 mg/l IAA
500 mg/l clarofan

C_8 B5-medium + 250 mg/l NH_4NO_3
400 mg/l glutamine
0.5 g/l MES pH 5.7
0.5 g/l PVP
20 g/l mannitol
20 g/l glucose
40 mg/l adenine
0.6 % agarose

+ 200 mg/l clarofan
1 mg/l transzeatine

COR-AAD1-00003999
Bayer EX1008 (Part 7 of 9)

C_9 B5-medium	+ 250 mg/l NH_4NO_3 400 mg/l glutamine 0.5 g/l MES pH 5.7 0.5 g/l PVP 20 g/l mannitol 20 g/l glucose 40 mg/l adenine 0.6 % agarose
	+ 1 mg/l transzeatine 0.01 mg/l Gibberellic acid A_3 (GA_3) 100 mg/l clarofan
C_{11} MS salt/2	+ 6 % sucrose 0.7 % agar

Bacterial medium = min A : (Miller 1972 60 mM $K_2HPO_4.3H_2O$; 33 mM KH_2PO_4; 7.5 mM $(NH_4)_2SO_4$; 1.7 trinatriumcitrat; 1 mM $MgSO_4$;
2 g/l glucose; 50 mg/l vitamine B1.

- PLant material

Tubers of Solanum tuberosum c.v Berolina
c.v Désirée

- Infection

- Potatoes are peeled and washed with water.
- Then they are washed with concentrated commercial bleach for 20 minutes, and
- rinsed 3 to 5 times with sterile water.
- The outer layer is removed (1 to 1.5 cm)
- The central part is cut into discs of about 1 cm^2 and 2 to 3 mm thick.
- Discs are placed on medium C_1 (4 pieces in a 9

COR-AAD1-00004000
Bayer EX1008 (Part 7 of 9)

cm Petri dish).

- 10 µl of a late log culture of an Agrobacterium strain grown in min A medium is applied on each disc.
- Discs are incubated for 2 days at low light intensity.

- Selection and shoot induction

- Discs are dried on a filter paper and transferred to medium C_2 with 100 mg/l kanamycin.
- After one month small calli are removed from the discs and transferred to medium C_7 containing 50 mg/l kanamycin.
- After a few more weeks, the calli are transferred to medium C_8 containing 50 mg/l kanamycin.
- If little shoots start to develop, the calli are transferred to elongation medium C_9 containing 50 mg/l Kanamycin.

- Rooting

- Elongated shoots are separated and transferred to rooting medium C_{11}.
- Rooted shoots are propagated on medium C_5.

3. Leaf disc infection of Lycopersicum esculentum (tomato)

Used media are described thereafter

A_1	MS salt/2	+ 1 % sucrose 0.8 % agar pH 5.7
B_1	B5-medium	+ 250 mg/l NH_4NO_3 0.5 g/l MES pH 5.7 0.5 g/l PVP 300 mg/l Ca $(H_2PO_4)_2$ 2 % glucose 40 mg/l adenine 40 g/l mannitol

B_2 B5-medium + 250 mg/l NH_4NO_3
0.5 g/l MES pH 5.7
0.5 g/l PVP
400 mg/l glutamine
2 % glucose
0.6 % agarose
40 mg/l adenine
40 g/l mannitol

+ 0.5 mg/l transzeatine
0.01 mg/l IAA
500 mg/l claforan

B_3 B5-medium + 250 mg/l NH_4NO_3
0.5 g/l MES pH 5.7
0.5 g/l PVP
400 mg/l glutamine
2 % glucose
0.6 % agarose
40 mg/l adenine
30 g/l mannitol

+ 0.5 mg/l transzeatine
0.01 mg/l IAA
500 mg/l clarofan

B_4 B5-medium + 250 mg/l NH_4NO_3
0.5 g/l MES pH 5.7
0.5 g/l PVP
400 mg/l glutamine
2 % glucose
0.6 % agarose
40 mg/l adenine
20 g/l mannitol

COR-AAD1-00004002
Bayer EX1008 (Part 7 of 9)

	+ 0.5 mg/l transzeatine 0.01 mg/l IAA 500 mg/l clarofan
B_5 B5-medium	+ 250 mg/l NH_4NO_3 0.5 g/l MES pH 5.7 0.5 g/l PVP 400 mg/l glutamine 2 % glucose 0.6 % agarose 40 mg/l adenine 10 g/l mannitol
	+ 0.5 mg/l transzeatine 0.01 mg/l IAA 500 mg/l clarofan
B_6 B5-medium	+ 250 mg/l NH_4NO_3 0.5 g/l MES pH 5.7 0.5 g/l PVP 400 mg/l glutamine 2 % glucose 0.6 % agarose 40 mg/l adenine
	+ 0.5 mg/l transzeatine 0.01 mg/l IAA 200 mg/l clarofan
B_7 B5-medium	+ 250 mg/l NH_4NO_3 0.5 g/l MES pH 5.7 0.5 g/l PVP 400 mg/l glutamine 2 % glucose 0.6 % agarose

COR-AAD1-00004003
Bayer EX1008 (Part 7 of 9)

40

40 mg/l adenine

+ 1 mg/l transzeatine
200 mg/l clarofan

B_8 MS salt/2 + 2 % sucrose
0.5 g/l MES pH 5.7
0.7 % agar

B_9 B5-medium + 250 mg/l NH_4NO_3
0.5 g/l MES pH 5.7
0.5 g/l PVP
2 % glucose
0.6 % agarose
40 mg/l adenine

+ 1 mg/l transzeatine
0.01 mg/l GA_3

Bacterial medium = min A : (Miller 1972) 60 mM $K_2HPO_4.3H_2O$; 33 mM KH_2PO_4; 7.5 mM $(NH_4)_2SO_4$; 1.7 M trinatriumcitrat; 1 mM $MgSO_4$; 2 g/l glucose; 50 mg/l vitamine B1

- Plant material

Lycopersicum esculentum cv. Lucullus.

Plants are used 6 weeks after subculture on medium A_1.

- Infection

- Midrib is removed from the leaves.
- Leaves are cut in segments of about 0.25 to 1 cm^2 (the edges of the leaves are not wounded, so that only maximum 3 sides of the leaf pieces is wounded).
- Segments are placed in infection medium B_1

COR-AAD1-00004004
Bayer EX1008 (Part 7 of 9)

(upside down), about 10 segments in a 9 cm Petri dish.

- Segments are then infected wiht 20 µl per Petri dish of a late log culture of the Agrobacterium strain grown in min A medium.
- Petri dishes incubate for 2 days at low light intensity.
- Medium is removed after 2 days and replaced by 20 ml of medium B_1 containing 500 mg/l clarofan.

- Selection and shoot induction

- The leaf discs are placed in medium B_2 + 50 or 100 mg/l kanamycin.
- Each 5 days the osmotic pressure of the medium is lowered by decreasing the mannitol concentration, transfers are done consecutively in medium B_3, B_4, B_5, and B_6.
- After one month calli with meristems are separated from the leaf discs and placed on medium B_7 with 50 or 100 mg/l kanamycin.
- Once little shoots have formed, calli are transferred to elongation medium B_9 with 50 or 100 mg/l kanamycin.

- Rooting

- Elongated shoots are separated and transferred to medium B_8 for rooting.
- Plants are propagated on medium A_1.

Greenhouse tests for herbicide resistance

Material and method

In this experiment, two herbicides comprising phosphinotricin as active ingredient, are used.

These compounds are those commercially available under the registered trademarks BASTA^R and MEIJI HERBIACE^R.

These products are diluted to 2 % with tap water. Spraying is carried out on a square metre area from the

COR-AAD1-00004005
Bayer EX1008 (Part 7 of 9)

four corners. Temperature of the greenhouse is about 22°C for tobaccos and tomato, and above 10°C to 15°C for potato.

Results

- Tobacco spraytest

a) Nicotiana tabacum cv. Petit Havana SR1 plants transformed with the chimeric "sfr" genes as present in pGSFR1161 or pGSFR1281, as well as unstransformed control plants (from 10 cm to 50 cm high) are treated with 20 l BASTA^{R}/ha. Control SR1 plants die after 6 days, while transformed plants are fully resistant to 20 l BASTA^{R}/ha and continue growing undistinguishable from untreated plants. No visible damage is detected, also the treatment is repeated every two weeks. The treatment has no effect in subsequent flowering. The recommended dose oF BASTA^{R} herbicide in agriculture is 2.5-7.5 l/ha.

b) A similar experiment is performed using 8 l/ha MEIJI HERBIACE^{R}. The transformed plants (the same as above) are fully resistant and continue growing undistinguishable from untreated plants. No visible damage is detectable.

- Potato spraytest

Untransformed and transformed potato plants (Solanum tuberosum cv. Berolina) (20 cm high) with the chimeric "sfr" gene as present in pGSFR1161 or pGSFR1281 are treated with 20 l BASTA^{R}/ha. Control plants die after 6 days while the transformed plants do not show any visible damage. They grow undistiguishable from untreated plants.

- tomato spraytest

Untransformed and transformed tomato plants (lycopersium esculentum c.v. luculus) (25 cm high) with the chimeric "sfr" gene as present in pGSFR1161 and pGSFR1281 are treated with 20 l BASTA^{R}/ha. control plants

COR-AAD1-00004006
Bayer EX1008 (Part 7 of 9)

die after six days while transformed plants are fully resistant. They do not show any visible damage and grow undistiguishable from untreated plants.

- Growth control of phytopathogenic fungi with transformed plants

In another set of experiments, potato plants expressing chimeric "sfr" genes as present in pGSFR1161 or pGSFR1281 are grown in a greenhouse compartment at 20°C under high humidity. Plants are innoculated by spraying 1 ml of a suspension of 10^6 Phytophtora infestans spores per ml. Plants grow in growth chambers (20°c, 95 % humidity, 4 000 lux) until fungal disease symptoms are visible (one week). One set of the plants are at that moment sprayed with Bialaphos at a dose of 8 l/ha. Two weeks later, untreated plants are completely ingested by the fungus. The growth of the fungus is stopped on the Bialaphos treated plants and no further disease symptoms evolve. The plants are effectively protected by the fungicide action of Bialaphos.

- Transmission of the PPT resistance through seeds

Transformed tobacco plants expressing the chimeric "sfr" gene present in pGSFR1161 and pGSFR1281 are brought to flowering in the greenhouse. They show a normal fertility.

- About 500 F1 seeds of each plant are sown in soil, F1 designating seeds of the first generation, i.e directly issued from the originally transformed plants. When seedlings are 2-3 cm high, they are sprayed with 8 l BASTA^R/ha. 7 days later, healthy and damaged plants can be distinguished in a ratio of approximately 3 to 1. this shows that PPT resistance is inherited as a dominant marker encoded by a single locus.

10 resistant F1 seedlings are grown to maturity and seeds are harvested. F2 seedlings are grown as described above and tested for PPT-resistance by spraying

COR-AAD1-00004007
Bayer EX1008 (Part 7 of 9)

BASTA^{R} at a dose of 8 l/ha. Some of the F1 plants produce F2 seedlings which are all PPT-resistant showing that these plants are homozygous for the resistance gene.The invention also concerns plant cells and plants non-essentially-biologically-transformed with a GS inhibitor-inactivating-gene according to the invention.

In a preferred embodiment of the invention, plant cells and plants are non-biologically-transformed with the "sfr" gene hereabove described.

Such plant cells and plants possess, stably integrated in their genome, a non-variety-specific character which render them able to produce detectable amounts of phosphinotricin-acetyl transferase.

This character confers to the transformed plant cells and plants a non-variety-specific enzymatic activity capable of inactivating or neutralizing GS inhibitors like Bialaphos and PPT.

Accordingly, plant cells and plants transformed according to the invention are rendered resistant against the herbicidal effects of Bialaphos and related compounds.

Since Bialaphos was first described as a fungicide, transformed plants can also be protected against fungal diseases by spraying with the compound several times.

In a preferred embodiment, Bialaphos or related compounds is applied several times, particularly at time intervals of about 20 to 100 days.

The invention also concerns a new process for selectively protecting a plant species against fungal diseases and selectively destroying weeds in a field comprising the steps of treating a field with an herbicide, wherein the plant species contain in their genome a DNA fragment encoding a protein having an enzymatic activity capable of neutralizing or inactivating GS inhibitors and wherein the used herbicide comprises as

COR-AAD1-00004008
Bayer EX1008 (Part 7 of 9)

active ingredient a GS inhibitor.

It comes without saying that the process according to the invention can be employed with the same efficiency, either to only destroy weeds in a field, if plants are not infected with fungi , either to only stop the development of fungi if the latter appears after destruction of weeds.

In a preferred embodiment of the process according to the invention, plant species are transformed with a DNA fragment comprising the "sfr" gene as described hereabove, and the used herbicide is PPT or a related compound.

Accordingly, a solution of PPT or related compound is applied over the field, for example by spraying, several times after emergence of the plant species to be cultivated, until early and late germinating weeds are destroyed.

It is quite evident that before emergence of plant species to be cultivated, the field can be treated with an herbicidal composition to destroy weeds.

On the same hand, fields can be treated even before the plant species to be cultivated are sowed.

Before emergence of the desired plant species, fields can be treated with any available herbicide, including Bialaphos-type herbicides.

After emergence of the desired plant species, Bialaphos or related compound is applied several times.

In a preferred embodiment, the herbicide is applied at time intervals of about from 20 to 100 days.

Since plants to be cultivated are transformed in such a way as to resist to the herbicidal effects of Bialaphos-type herbicides, fields can be treated even after emergence of the cultivated plants.

This is particularly useful to totally destroy early and late germinating weeds, without any effect on the plants to be produced.

Preferably, Bialaphos or related compoud is

COR-AAD1-00004009
Bayer EX1008 (Part 7 of 9)

applied at a dose ranging from about 0.4 to about 1.6 kg/ha, and diluted in a liquid carrier at a concentration such as to enable its application to the field at a rate ranging from about 2 to about 8 l/ha.

There follows examples, given by way of illustration, of some embodiments of the process with different plant species.

- Sugarbeets

The North European sugarbeet is planted from March 15 up to April 15, depending upon the weather condition and more precisely on the precipitation and average temperature. the weeds problems are more or less the same in each country and can cause difficulties until the crop closes its canopy around mid-July.

Weed problems can be separated in three situations :

- early germination of the grassy weeds,
- early germinating broadleaved weeds,
- late germinating broadleaved weeds.

Up to now, pre-emergence herbicides have been succesfully used. Such compounds are for example those commercially available under the registered trademarks : PYRAMIN^{R}, GOLTIX^{R} and VENZAR^{R}. However, the susceptibility to dry weather conditions of these products as well as the lack of residual activity to control late germinating weeds have led the farmer to use post-emergence products in addition to pre-emergence ones.

Table (I) thereafter indicates the active ingredients contained in the herbicidal compositions cited in the following examples.

COR-AAD1-00004010
Bayer EX1008 (Part 7 of 9)

TABLE (I)

Commercial Name	Active Ingredient	Formulation
AVADEX^{R}	Diallate	EC 400 g/l
AVADEX BW^{R}	Triallate	EC 400 g/l
GOLTIX^{R}	Metamitron	WP 70 %
RONEET^{R}	Cycloate	EC 718 g/l
TRAMAT^{R}	Ethofumerate	EC 200 g/l
FERVINAL^{R}	Alloxydime-sodium	SP 75 %
BASTA^{R}	Phosphinotricin	200 g/l
PYRAMIN FL^{R}	Chloridazon	SC 430 g/l

According to the invention, post-emergence herbicides consist of Bialaphos or related compounds, which offer a good level of growth control of annual grasses (Bromus, Avena spp., Alopecurus, POA) and broadleaves (Galium, Polygonum, Senecio, Solanum, Mercurialis).

Post-emergence herbicides can be applied at different moments of the growth of sugarbeet ; at a cotyledon level, two-leave level or at a four-leave level.

Table (II) thereafter represents possible systems of field-treatment, given by way of example.

In those examples, the post-emergence herbicide of the class of Bialaphos used is BASTA^{R}, in combination with different pre-emergence herbicides. Concentrations are indicated in l/ha or kg/ha.

COR-AAD1-00004011
Bayer EX1008 (Part 7 of 9)

TABLE (II)

POSSIBLE WEEDCONTROL SYSTEMS IN SUGARBEETS, BASED ON THE USE OF BASTA^{R} , PROVIDING BEETS ARE MADE RESISTANT AGAINST THE LATTER CHEMICAL (in lt or kg/ha).

	Pre-sowing	Pre-emergence	Cotyledons	Two-leaves	Four leaves
1.	AVADEX^{R} 3.5 lt	-	BASTA^{R} 3 lt	BASTA^{R}/tramat 3 lt 1.5 lt	-
2.	AVADEX^{R} 3.5 lt	GOLTIX^{R} 4 kg	-	-	-
3	RONEET^{R} 4 lt	GOLTIX^{R} 5 kg	-	-	-
4.	RONEET^{R} 4 lt	GOLTIX^{R} 2.5 kg	-	BASTA^{R} 3 lt	-
5.	TRAMAT^{R} 5 lt	-	-	BASTA^{R} 3 lt	BASTA^{R}/GOLTIX^{R} 2 lt 2 kg
6.	-	GOLTIX^{R} 2.5 kg	-	BASTA^{R} 3 lt	-
7.	-	-	BASTA^{R}/tramat 3 lt 1.7 lt	-	BASTA^{R}/GOLTIX^{R} 3 lt 2 kg
8.	PYRAMIN^{R} 6 lt	-	BASTA^{R} 3 lt	Venzar 1 kg	-
9.	-	-	BASTA^{R} 3 lt	BASTA^{R}/GOLTIX^{R} 3 lt 2 kg	-
10.	DIALLATE^{R} 3.5 lt	PYRAMIN^{R} 6 lt		BASTA^{R}/Metamitron 3 lt 1 kg	-

COR-AAD1-00004012

Bayer EX1008 (Part 7 of 9)

- Potatoes

Potatoes are grown in Europe on about 8.10^6 Ha. The major products used for weed control are Linuron/monolinuron or the compound commercially available under the denomination METRABUZIN

These products perform well against most weedspecies.

However, weeds such as Galium and Solanum plus late germinating Chenopodium and Polygonum are not always effectively controlled, while control of the annual grasses is also sometime erratic.

Once again, late germinating broadleaved weeds are only controllable by post-emergence applications of herbicides such as BASTA^R.

Table (III) thereafter represents some examples given by way of example of field-treatment in the case of potatoes.

TABLE (III)

Weeds control systems in potatoes, based on the use of BASTA^R, providing potatoes are rendered resistant to BASTA^R.

Linuron + monolinuron (375 g + 375 g/ha) prior to emergence	
BASTA^R	3-4 lt/ha after emergence (5-15 cm)
BASTA^R/fluazifop-butyl	3-4 lt/ha + 2 lt/ha after emergence (5-15 cm)

Linuron	WP 50 % (AFALON^R)
Monolinuron	WP 47.5 % (ARESSIN^R)
fluazifop-butyl	EL 250 g/l (FUSILADE^R)

The strains pGSJ260 and pBG39 used hereabove have

COR-AAD1-00004013
Bayer EX1008 (Part 7 of 9)

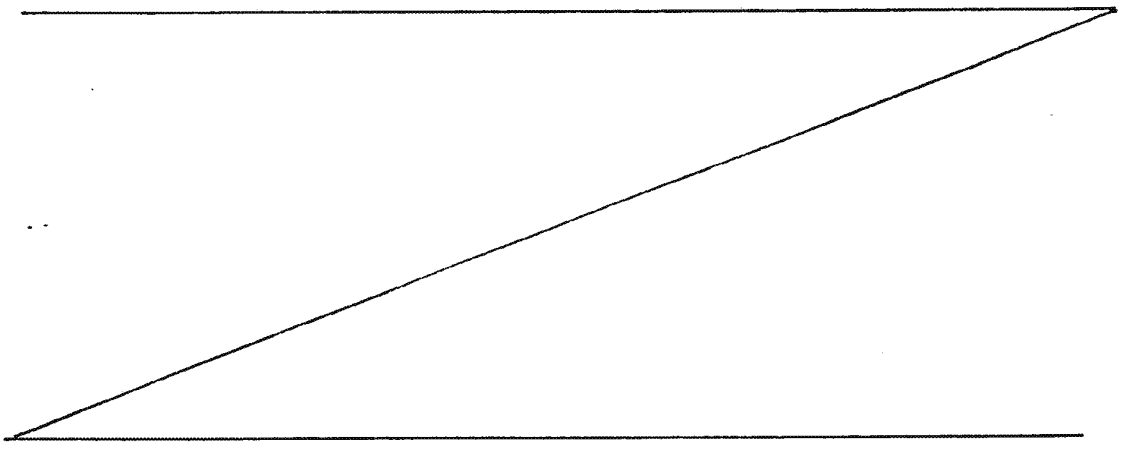
been deposited on December 12nd, 1985, at the "German Collection of Micro-organisms" (DEUTSCHE SAMMLUNG VON MIKROORGANISMEN) at Göttingen, Germany. They received the deposition numbers DSM 3 606 and DSM 3 607 respectively.

Further embodiments of the invention are described hereafter with reference to the figures in which :

- fig. 8 shows the restriction map of a plasmid pJS1 containing another Bialaphos-resistance-gene ;
- fig. 9 shows the nucleotide sequence of the "sfrsv" gene containing the resistance gene ;
- fig. 10 shows the amino acid homology of "sfrsv" gene and "sfr" gene,
- fig. 11 shows the construction of a plasmid, given by way of example, which contains the "sfrsv" gene and suitable for the transformation of plant cells.

Another Bialaphos-resistance-gene has been isolated form another Bialaphos-producing-strains, i.e. streptomyces viridochromogenes. This second resistance-gene is thereafter designated by "sfrsv" gene.

This second preferred DNA fragment according to the invention, for the subsequent transformation of plant cells, consists of a nucleotide sequence coding for at least part of a polypeptide having the following sequence :



51

V S P E R R P V E I R P A T A A D M

A A V C D I V N H Y I E T S T V N F

R T E P Q T P Q E W I D D L E R L Q

D R Y P W L V A E V E G V V A G I A

Y A G P W K A R N A Y D W T V E S T

V Y V S H R H Q R L G L G S T L Y T

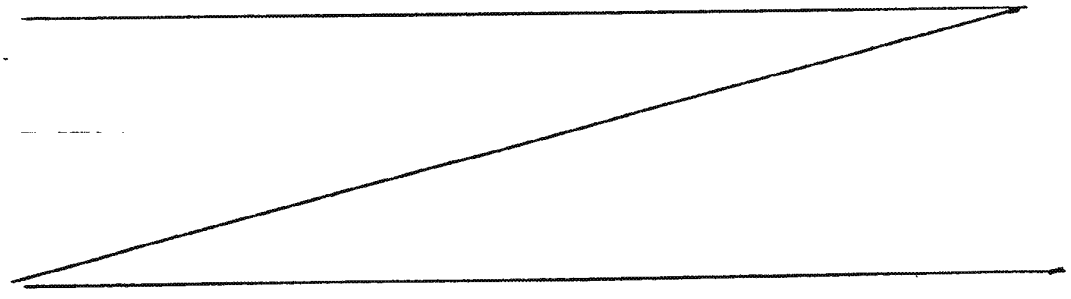
H L L K S M E A Q G F K S V V A V I

G L P N D P S V R L H E A L G Y T A

R G T L R A A G Y K H G G W H D V G

F W Q R D F E L P A P P R P V R P V

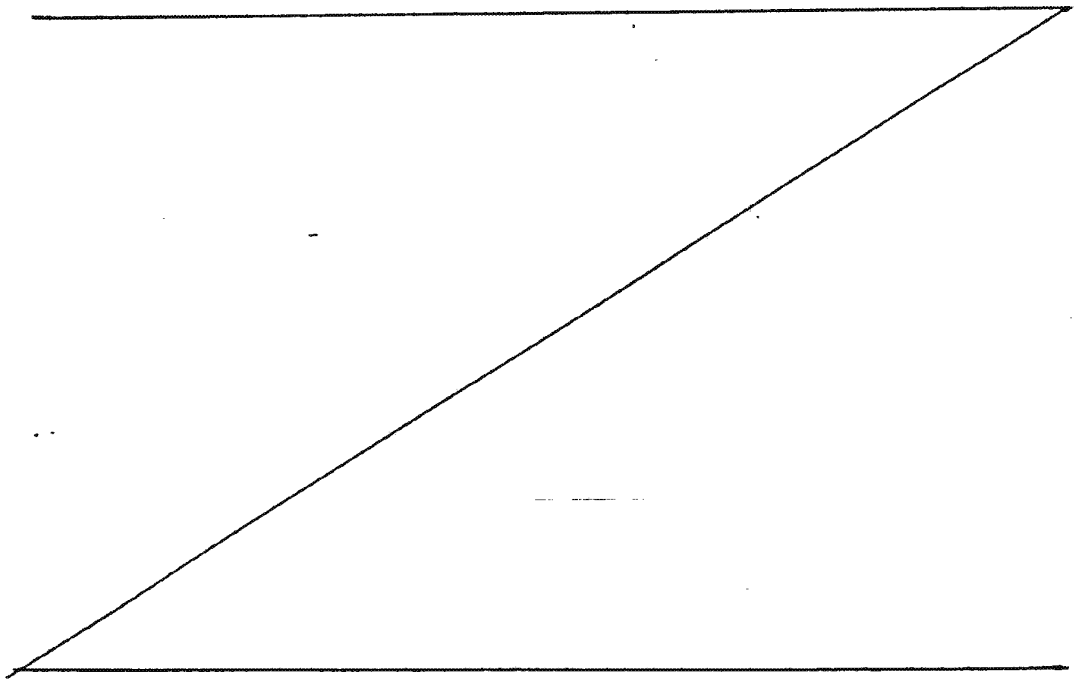
T Q I *



which part of said polypeptide is of sufficient length to confer protection against Bialaphos-"plant-protecting-capability" to plant cells, when incorporated genetically and expressed therein. Reference will also be made hereafter to the "plant-protecting-capability" against Bialaphos of the abovesaid nucleotide sequence.

Meaning of the designation of amino acids by a single letter is given therafter.

Alanine	A	Leucine	L
Arginine	R	Lysine	K
Asparagine	N	Methionine	M
Aspartic Acid	D	Phenylalanine	F
Cysteine	C	Proline	P
Cystine	C	Serine	S
Glycine	G	Threonine	T
Glutamic Acid	E	Tryptophan	W
Glutamine	Q	Tyrosine	Y
Histidine	H	Valine	V
Isoleucine	I		



This second preferred DNA fragment consists of the following nucleotide sequence :

TAAAGAGGTGCCCGCCACCCGCTTTCGCAGAACACCGAAGGAGACCACAC

GTGAGCCCAGAACGACGCCCGGTCGAGATCCGTCCCGCCACCGCCGCCGA

CATGGCGGCGGTCTGCGACATCGTCAATCACTACATCGAGACGAGCACGG

TCAACTTCCGTACGGAGCCGCAGACTCCGCAGGAGTGGATCGACGACCTG

GAGCGCCTCCAGGACCGCTACCCCTGGCTCGTCGCCGAGGTGGAGGGCGT

CGTCGCCGGCATCGCCTACGCCGGCCCCTGGAAGGCCCGCAACGCCTACG

ACTGGACCGTCGAGTCGACGGTGTACGTCTCCCACCGGCACCAGCGGCTC

GGACTGGGCTCCACCCTCTACACCCACCTGCTGAAGTCCATGGAGGCCCA

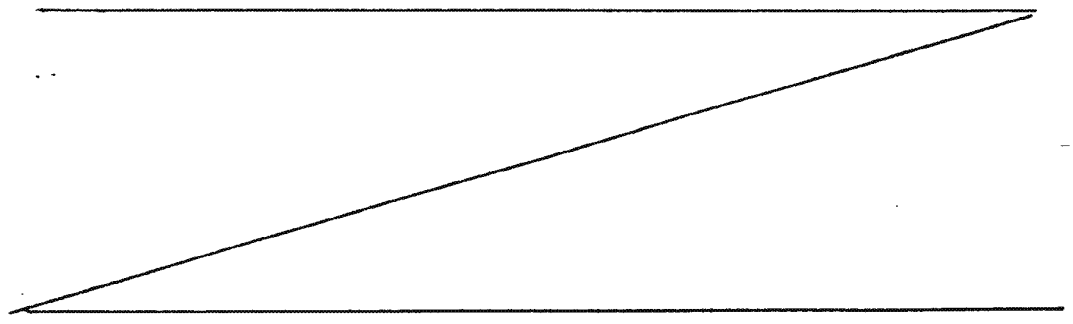
GGGCTTCAAGAGCGTGGTCGCCGTCATCGGACTGCCCAACGACCCGAGCG

TGCGCCTGCACGAGGCGCTCGGATACACCGCGCGCGGGACGCTGCGGGCA

GCCGGCTACAAGCACGGGGGCTGGCACGACGTGGGGTTCTGGCAGCGCGA

CTTCGAGCTGCCGGCCCCGCCCCGCCCCGTCCGGCCCGTCACACAGATCT

GAGCGGAGAGCGCATGGC

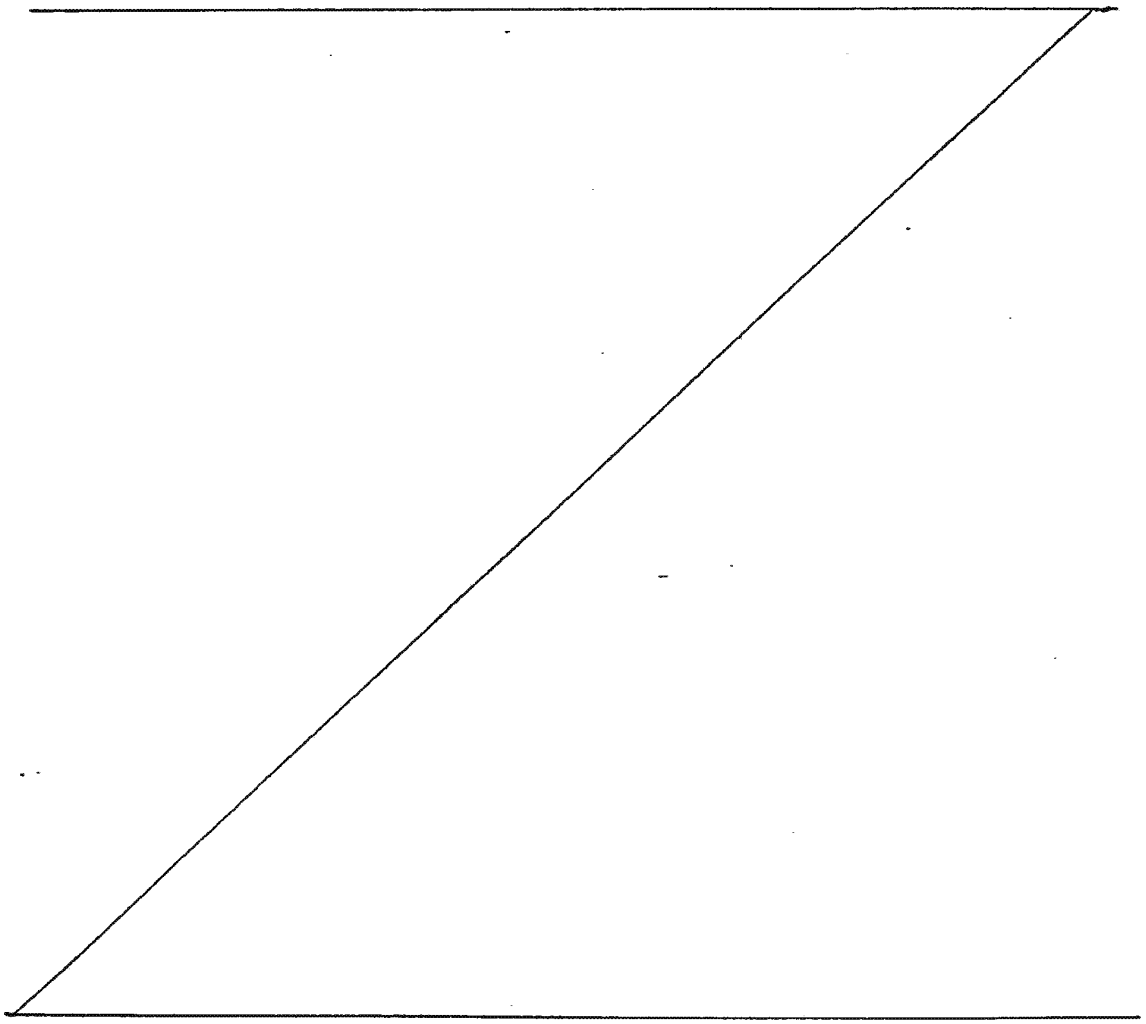


or of a part thereof expressing a polypeptide having plant-protecting capability against Bialaphos ;

There follows hereafter the description of experiments carried out for the isolation of the "sfrsv" resistance gene, the construction of expression vectors which contain the resistance gene and which allow the subsequent transformation of plant cells, in order to render them resistant to GS inhibitors.

Cloning of the bialaphos-resistance-"sfrsv" gene from Streptomyces viridochromogenes

The strain Streptomyces viridochromogenes DSM



COR-AAD1-00004018
Bayer EX1008 (Part 7 of 9)

40736 (ref 1) was grown and total DNA of this strain was prepared according to standard techniques. DNA samples were digested respectively with PstI, SmaI and Sau3AI in three different reactions and separated on an agarose gel, together with plasmid DNA from pGSR1 (fig. 5B) digested with BamHI. In a Southern analysis the DNA was blotted on a nitrocellulose filter and hybridized with the labbeled BamHI fragment from pGSR1 containing the "sfr" gene. In all four lanes of the gel, a restriction fragment was showing strong homology with the probe : a PstI fragment of about 3 kb, a SmaI fragment of about 1.2 kb and Sau3AI fragment of 0.5 kb. In order to clone this gene, PstI restriction fragments were directly cloned in the Escherichia coli vector pUC8. 3000 colonies obtained after transformation were transferred to nitrocellulose filters, and hybridized with the "sfr" probe. Positive candidates were further tested for their growth on minimal medium plates containing 300 µg/ml PPT. One transformant that grew on PPT-containing-medium was further analysed. The plasmid map and relevant restriction sites of this plasmid pJS1 are represented in fig. 8. The strain MC1061 (pJS1) has been deposited on March 06, 1987 at the DEUTSCHE SAMMLUNG VON MIKROORGANISMEN (DSM) under deposition number DSM 4023. The clone restriction fragment has been sequenced according to the Maxam and Gilbert method and the coding region of the gene could be identified through homology. The sequence of the "sfrsv" gene is represented in fig.9 and the homology on the nucleotide and amino acid sequence level with "sfr" gene is shown in fig. 10.

Expression of the "sfrsv" gene

A "sfrsv gene cassette" was also constructed to allow subsequent cloning in plant expression vectors. A BanII-BglII fragment containing the "sfrsv" coding region without the initiation codon GTG was isolated from pJS1.

COR-AAD1-00004019
Bayer EX1008 (Part 7 of 9)

This fragment was ligated in the vector pLK56-2 digested with NcoI and BglII, together with a synthetic oligonucleotide 5'-CATGAGCC-3', similar with the one described for "sfr" gene and shown in fig. 5. The construction of pGSR1SV is schematically shown in fig. 11. Since similar cassettes of both genes are present in respectively pGSR1 and pGSR1SV, previous described constructions for the expression of the "sfr" gene in plants can be repeated.

Enzymatic analysis of crude extracts from E. coli strains carrying plasmid pGSR1SV demonstrated the synthesis of an acetylase which could acetylate PPT. This was shown by thin layer chromotography of the reaction porducts.

The "sfrsv" gene was then inserted into the plasmid vector pGSJ260 (fig. 4B) under the control of the CaMV 35s promoter, to yield a plasmid pGS2SV, similar to pGSR2 (fig. 6A) except that the "sfrsv" gene is substituted for the "sfr" gene.

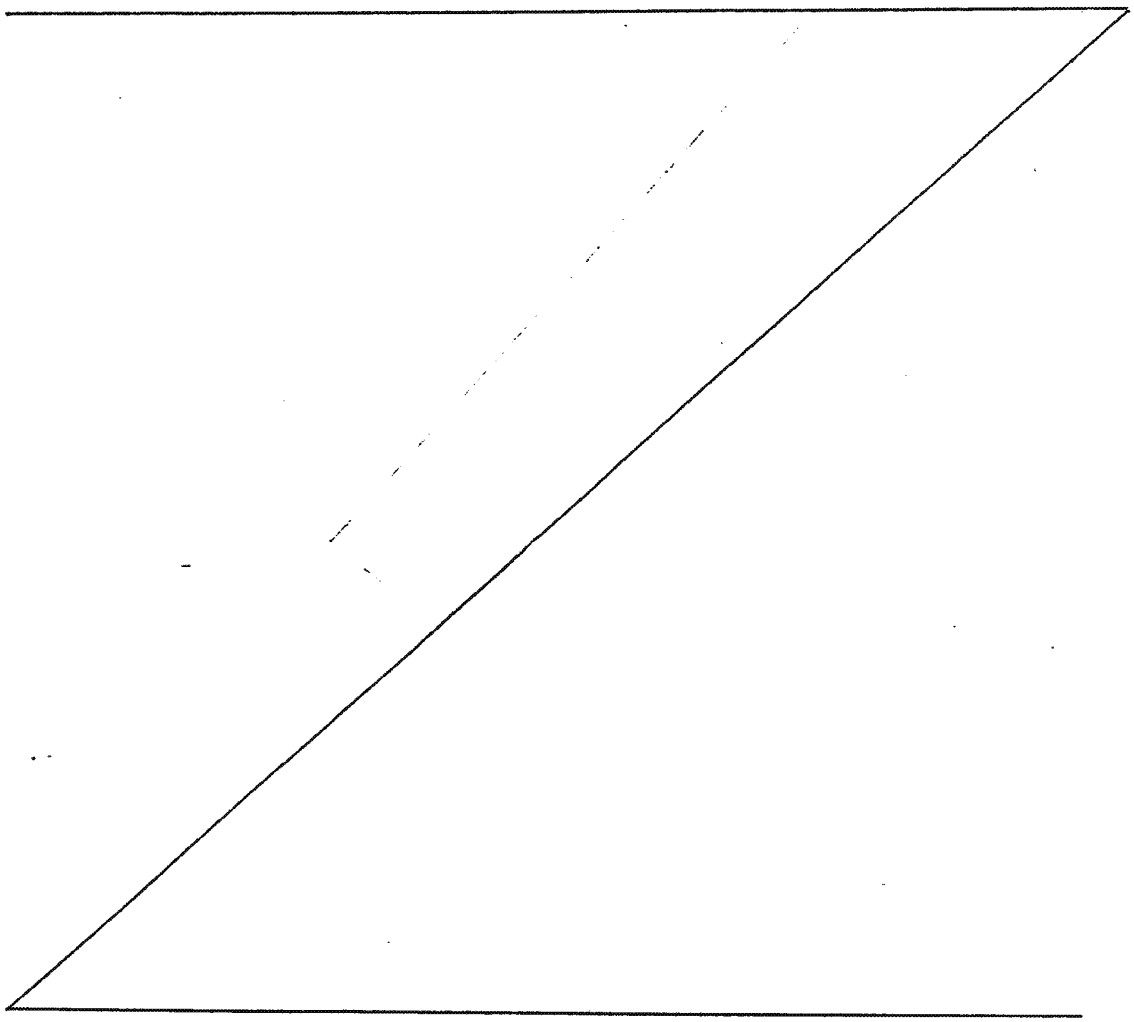
It is clear that herbicide resistance gene of the above type may be obtained from many other microorganism that produce PPT or PPT derivatives. Herbicide resistance gene can then be incorporated in plant cells with a view of protecting them against the action of such Glutamine Synthetase inhibitors. For instance, a Bialaphos-resistance-gene is obtained from Kitasotosporia (ref. 15).

Transformed plant cells and plants which contain the "sfrsv" resistance gene can be obtained with plasmid pGSR2SV, using the same Agrobacterium-mediated-transformation system as hereabove described for the transformation of different plant species with the "sfr" gene.

COR-AAD1-00004020
Bayer EX1008 (Part 7 of 9)

Plants are regenerated and tested for their resistance with similar spraying tests as described hereabove. All plants behaved similarly and show resistance against herbicides consisting of glutamine synthetase inhibitors.

Finally, the invention also pertains to the combination of the plants resistant to an inhibitor of glutamine synthetase as defined above with the corresponding inhibitor of glutamine synthetase for use in the production of the cultures of said plants free from weeds.



COR-AAD1-00004021
Bayer EX1008 (Part 7 of 9)

REFERENCES

1. BAYER et al., HELVETICA CHEMICA ACTA, 1972
2. WAKABAYASHI K. and MATSUNAKA S., Proc. 1982, British Crop Protection Conference, 439-450
3. M. MASON et al., PHYTOCHEMISTRY, 1982, vol. 21, n° 4, p. 855-857.
4. C. J. THOMPSON et al., NATURE, July 31, 1980, vol. 286, n° 5 772, p. 525-527
5. C. J. THOMPSON et al., JOURNAL OF BACTERIOLOGY, August 1982, p. 678-685
6. C. J. THOMPSON et al., GENE 20, 1982, p. 51-62
7. C. J. THOMPSON et al., MOL. GEN. GENET., 1984, 195, p. 39-43
8. TOWBIN et al., PROC. NATL. ACAD. SCI. USA, 1979, 76, p. 4 350-4 354
9. METHODS OF ENZYMOLOGY, V.XLIII, p. 737-755
10. DEBLAERE H. et al., 1985, Nucl. Acid. Res., 13, 1 477
11. BOTTERMAN J., February 1986, Ph. D. Thesis, State University of Ghent
12. DEBLAERE R., february 1986, Ph. D Thesis, Free University of Brussel, Belgium
13. VELTEN et al, EMBO J. 1984, vol. 3, n°12, p. 2 723-2 730
14. CHATER et al, Gene cloning in Streptomyces. Curr. Top. Microbiol. Immunol., 1982, 96, p. 69-75
15. OMURA et al, J. of Antibiotics, Vol. 37, 8, 939-940, 1984
16. MURAKAMI et al, Mol. Gen. Genet., 205, 42-50, 1986
17. MANDERSCHEID and WILD, J. Plant Phys., 123, 135-142, 1986

COR-AAD1-00004022
Bayer EX1008 (Part 7 of 9)

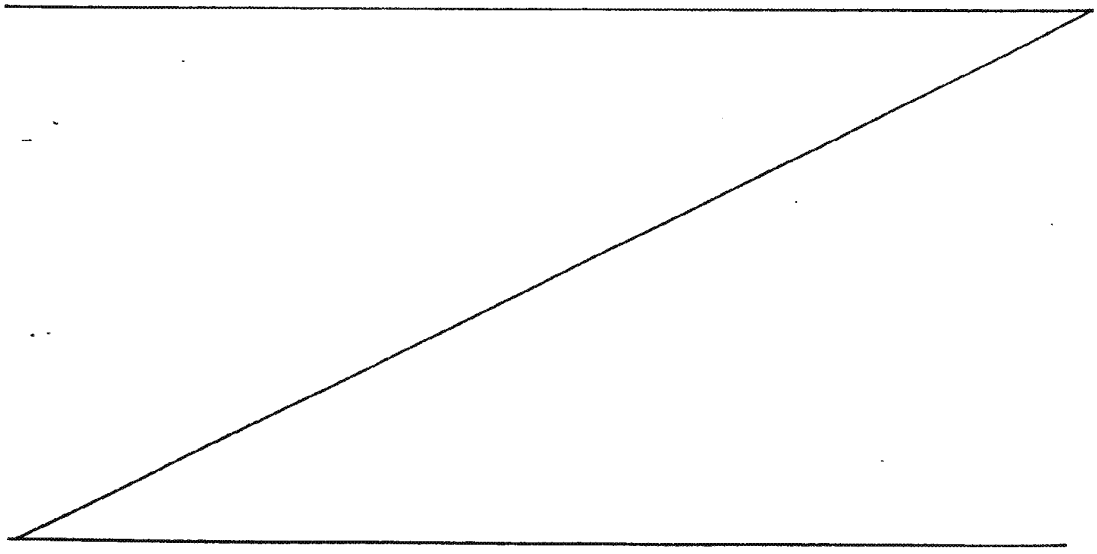
CLAIMS

1. Process for controlling the action in plant cells and plants of a glutamine synthetase inhibitor when contacted herewith, which comprises providing said plants with a heterologous DNA including a foreign nucleotide sequence, capable of being expressed in the form of a protein in said plant cells and plants, under conditions such as to cause said heterologous DNA to be integrated stably through generations in the cells of said plants, and wherein said protein has an enzymatic activity capable of causing inactivation or neutralization of said glutamine synthetase inhibitor.

2. Process according to claim 1, wherein the heterologous DNA fragment comprises a foreign nucleotide sequence coding for a polypeptide having a PPT acetyl transferase activity.

3. Process according to the claims 1 to 2, wherein the heterologous DNA fragment belongs to the genome of a Streptomyces.

4. Process according to any of the claims 1 to 3, wherein the heterologous DNA fragment comprises a foreign



COR-AAD1-00004023
Bayer EX1008 (Part 7 of 9)

nucleotide sequence coding for the following amino acid sequence :

```
                                                    X SER PRO GLU

  183
ARG ARG PRO ALA ASP ILE ARG ARG ALA THR GLU ALA ASP MET PRO

  228
ASP VAL CYS THR ILE VAL ASN HIS TYR ILE GLU THR SER THR VAL

  273
ASN PHE ARG THR GLU PRO GLN GLU PRO GLN GLU TRP THR ASP ASP

  318
LEU VAL ARG LEU ARG GLU ARG TYR PRO TRP LEU VAL ALA GLU VAL

  363
ASP GLY GLU VAL ALA GLY ILE ALA TYR ALA GLY PRO TRP LYS ALA

  408
ARG ASN ALA TYR ASP TRP THR ALA GLU SER THR VAL TYR VAL SER

  453
PRO ARG HIS GLN ARG THR GLY LEU GLY SER THR LEU TYR THR HIS

  498
LEU LEU LYS SER LEU GLU ALA GLN GLY PHE LYS SER VAL VAL ALA

  543
VAL ILE GLY LEU PRO ASN ASP PRO SER VAL ARG MET HIS GLU ALA

  588
LEU GLY TYR ALA PRO ARG GLY MET LEU ARG ALA ALA GLY PHE LYS

  633
HIS GLY ASN TRP HIS ASP VAL GLY PHE TRP GLN LEU ASP PHE SER

  678
LEU PRO VAL PRO PRO ARG PRO VAL LEU PRO VAL THR GLU ILE

  723
```

in which X represents MET or VAL, or a part of a polypeptide of sufficient length to possess said enzymatic activity and, when said DNA fragment is expressed in plant cells, to protect the latter against the herbicidal activity of glutamine synthetase inhibitors.

5. Process according to any of the claims 1 to 4, wherein the heterologous DNA fagment comprises the following nucleotide sequence :

```
                                                    GTG AGC CCA GAA
  183
CGA CGC CCG GCC GAC ATC CGC CGT GCC ACC GAG GCG GAC ATG CCG
  228
GCG GTC TGC ACC ATC GTC AAC CAC TAC ATC GAG ACA AGC ACG GTC
  273
AAC TTC CGT ACC GAG CCG CAG GAA CCG CAG GAG TGG ACG GAC GAC
  318
CTC GTC CGT CTG CGG GAG CGC TAT CCC TGG CTC GTC GCC GAG GTG
  363
GAC GGC GAG GTC GCC GGC ATC GCC TAC GCG GGC CCC TGG AAG GCA
  408
CGC AAC GCC TAC GAC TGG ACG GCC GAG TCG ACC GTG TAC GTC TCC
  453
CCC CGC CAC CAG CGG ACG GGA CTG GGC TCC ACG CTC TAC ACC CAC
  498
CTG CTG AAG TCC CTG GAG GCA CAG GGC TTC AAG AGC GTG GTC GCT
  543
GTC ATC GGG CTG CCC AAC GAC CCG AGC GTG CGC ATG CAC GAG GCG
  588
CTC GGA TAT GCC CCC CGC GGC ATG CTG CGG GCG GCC GGC TTC AAG
  633
CAC GGG AAC TGG CAT GAC GTG GGT TTC TGG CAG CTG GAC TTC AGC
  678
CTG CCG GTA CCG CCC CGT CCG GTC CTG CCC GTC ACC GAG ATC
  723
```

COR-AAD1-00004025
Bayer EX1008 (Part 7 of 9)

or a part thereof expressing a polypeptide capable of inactivating said glutamine synthetase inhibitor.

6. Process according to any of claims 1 to 5, wherein the initiation codon ATG is substituted for the inititiation codon GTG of the sequence defined in claim 5.

7. Process according to any of claims 1 to 3, wherein the heterologous DNA fragment comprises a foreign nucleotide sequence coding for the following amino acid sequence :

V S P E R R P V E I R P A T A A D M

A A V C D I V N H Y I E T S T V N F

R T E P Q T P Q E W I D D L E R L Q

D R Y P W L V A E V E G V V A G I A

Y A G P W K A R N A Y D W T V E S T

V Y V S H R H Q R L G L G S T L Y T

H L L K S M E A Q G F K S V V A V I

G L P N D P S V R L H E A L G Y T A

R G T L R A A G Y K H G G W H D V G

F W Q R D F E L P A P P R P V R P V

T Q I *

or a part of a polypeptide of sufficient length to possess said enzymatic activity and, when said DNA fragment is expressed in plant cells, to protect the latter against the herbicidal activity of glutamine synthetase inhibitors.

8. Process according to claim 7, wherein the heterologous DNA fragment comprises the following nucleotide sequence :

TAAAGAGGTGCCCGCCACCCGCTTTCGCAGAACACCGAAGGAGACCACAC

GTGAGCCCAGAACGACGCCCGGTCGAGATCCGTCCCGCCACCGCCGCCGA

CATGGCGGCGGTCTGCGACATCGTCAATCACTACATCGAGACGAGCACGG

TCAACTTCCGTACGGAGCCGCAGACTCCGCAGGAGTGGATCGACGACCTG

GAGCGCCTCCAGGACCGCTACCCCTGGCTCGTCGCCGAGGTGGAGGGCGT

CGTCGCCGGCATCGCCTACGCCGGCCCCTGGAAGGCCCGCAACGCCTACG

ACTGGACCGTCGAGTCGACGGTGTACGTCTCCCACCGGCACCAGCGGCTC

GGACTGGGCTCCACCCTCTACACCCACCTGCTGAAGTCCATGGAGGCCCA

GGGCTTCAAGAGCGTGGTCGCCGTCATCGGACTGCCCAACGACCCGAGCG

TGCGCCTGCACGAGGCGCTCGGATACACCGCGCGCGGGACGCTGCGGGCA

GCCGGCTACAAGCACGGGGGCTGGCACGACGTGGGGTTCTGGCAGCGCGA

CTTCGAGCTGCCGGCCCCGCCCCGCCCCGTCCGGCCCGTCACACAGATCT

GAGCGGAGAGCGCATGGC

or a part thereof expressing a polypeptide capable of inactivating said glutamine synthetase inhibitor.

9. In a process for producing plants and reproduction material of said plants including a heterologous genetic material stably integrated therein and capable of being expressed in said plants or reproduction material in the form of a protein capable of inactivating or neutralizing the activity of a glutamine synthetase inhibitor, comprising the non biological steps of producing plants cells or plant tissue including said heterologous genetic material from starting plant cells or plant tissue not able to express that inhibiting or neutralizing activity, regenerating plants or reproduction material of said plants or both from said plant cells or plant tissue including said genetic material and, optionally, biologically replicating said last mentioned plants or reproduction material or both, wherein said steps of producing said plant cells or plant tissue including said heterologous genetic material comprises transforming said starting plant cells or plant tissue with a DNA recombinant containing a nucleotide sequence encoding said protein as well as the regulatory elements selected among those which are capable of enabling the expression of said nucleotide sequence in said plant cells or plant tissue and to cause the stable integration of said nucleotide sequence in said plant cells and tissue, as well as in the plant and reproduction material processed therefrom throughout generations.

10. The process according to claim 9, wherein starting cells are transformed with a recombinant DNA which contains the fragment of any one of the claims 1 to 8 recombined with heterologous DNA, and wherein said recombinant DNA is devoid of any DNA region involved in the biosynthesis of Bialaphos, when said fragment originates itself from a Bialaphos-producing strain.

11. The process according to claim 10, wherein the recombinant DNA is a vector suitable for the transformation of a cellular host and, when introduced therein, for allowing for the neutralization or inhibition of glutamine synthetase inhibitors.

12. The process according to claim 11, wherein the vector comprises said recombinant DNA under the control of replicon elements suitable for the transformation of bacteria, particularly E.coli.

13. The process of claim 11, wherein the vector comprises said recombinant DNA fragment under the control of a plant promotor region, which vector further comprises regulation elements allowing for the expression of said DNA fragments in plant cells, when the latter are later transformed with said vector.

14. The process of any of claims 10 to 13, which confers resistance against herbicidal effects of Bialaphos, PPT or related derivatives to the transformed plant cells.

15. The process of claim 13 or 14, wherein the vector comprises a nucleotide sequence encoding a transit peptide intercalated between said plant promotor region and said recombinant DNA fragment.

16. The process of claim 15, wherein the transit peptide is selected from ribulose-1,5 biphosphate carboxylase and chlorophyl a/b binding proteins.

17. The process of any of claims 11 to 16, wherein said vector is a Ti plasmid.

18. Plant cells, non biologically transformed, wherein they possess, stably integrated in their genome, a DNA fragment encoding a protein having a non-variety-specific enzymatic activity capable of neutralizing or inactivating glutamine synthetase inhibitors.

19. Plant cells according to claim 18, wherein they are capable of generating a plant capable of

producing seeds, said seeds having a non-variety-specific enzymatic activity capable of inactivating or neutralizing glutamine synthetase inhibitors.

20. Plant cells according to claim 18 or 19, wherein they are transformed by the process of any of claims 9 to 17.

21. Plant cells according to any of claims 18 to 20, which produce detectable amounts of phosphinotricin acetyl transferase.

22. Seeds, non biologically transformed, which possess, stably integrated in their genome, a DNA fragment encoding a protein having a non-variety-specific enzymatic activity capable of inactivating or neutralizing glutamine synthetase inhibitors.

23. Seeds according to claim 22, which are capable of germinating into a plant capable of producing seeds having a non-variety-specific enzymatic activity capable of inactivating or neutralizing glutamine synthetase inhibitors.

24. Seeds according to claim 22 or 23, which are transformed by the process of any one of the claims 9 to 17.

25. Plants, non biologically transformed, which possess, stably integrated in their genome, a DNA fragment encoding a protein having a non-variety-specific enzymatic activity capable of neutralizing or inactivating glutamine synthetase inhibitors.

26. Plants according to claim 25, which are capable of producing seeds having a non-variety specific enzymatic activity capable of inactivating or neutralizing glutamine synthetase inhibitors.

27. Plants according to claim 25 or 26, which are transformed by the process of any of claims 9 to 17.

28. Process for protecting a plant species and selectively destroying weeds in a field comprising the

COR-AAD1-00004030
Bayer EX1008 (Part 7 of 9)

steps of treating a field with an herbicide, wherein the plant species contain in their genome a DNA fragment encoding a protein having an enzymatic activity capable of neutralizing or inactivating glutamine synthetase inhibitors, and wherein the used herbicide is a glutamine synthetase inhibitor.

29. Process according to claim 28, wherein the plant species contains a DNA fragment according to any one of claims 1 to 8.

30. Process according to claim 28 or 29, wherein the plant species are transformed according to the process of any one of claims 9 to 17.

31. Process according to any one of claims 28 to 30, wherein a solution of a glutamine synthetase inibitor is applied on the field, after emergence of the cultivated plant species, several times, particularly at time intervals of about 20 to 100 days, until early and late germinating weeds are destroyed.

32. Process according to any of claims 28 to 31, wherein glutamine synthetase inhibitors comprise Bialaphos, phosphinotricin and related compounds.

33. Process for selectively protecting a plant species in a field against fungal diseases comprising the steps of treating a field with an herbicide, wherein the plant species contain in their genome a DNA fragment encoding a protein having an enzymatic activity capable of neutralizing an inactivating glutamine synthetase inhibitors and wherein the used herbicide is a glutamine synthetase inhibitor.

34. Process according to claim 33, wherein the plant species contain a DNA fragment according to any of claims 1 to 8.

35. Process according to claim 33 or 34, wherein the plant species are transformed according to the process of any one of claims 9 to 17.

COR-AAD1-00004031
Bayer EX1008 (Part 7 of 9)

36. Process according to any one of claims 33 to 35, wherein a solution of a glutamine synthetase inhibitor is applied on the field, after emergence of the cultivated plant species, several times, particularly at time intervals of about 20 to 100 days until fungi are destroyed.

37. Process according to any one of claims 33 to 36, wherein glutamine synthetase inhibitor is selected from a group which comprises Bialaphos, phosphinotricin and related compounds.

38. Process according to claim 32 or 37, wherein Bialaphos, PPT or related compound is applied at a dose ranging from about 0.4 to about 1.6 kg/ha.

39. Process according to claim 38, wherein Bialaphos, PPT or related compound is diluted in a liquid carrier at a concentration such as to enable its application to the field at a rate ranging from about 2 l/ha to about 8 l/ha.

40. Process according to any of claim 38 or 39, wherein selectively protected plant species comprise sugar-beet, rice, potato, tomato, maize, tobacco.

41. Vector which contains a DNA fragment encoding a polypeptide having an enzymatic activity capable of causing inactivation of glutamine synthetase inhibitors.

42. Vector according to claim 41, which is suitable for the transformation of plant cells and plants.

43. Vector according to claim 41 or 42, which contains a DNA fragment belonging to the genome of a Streptomyces.

44. Vector according to any of claims 41 to 43, which contains the DNA fragment recombined with heterologous DNA, wherein said recombinant DNA is devoid of any DNA region involved in the biosynthesis of Bialaphos.

45. The vector of claim 44 suitable for the transformation of a cellular host and, when introduced therein, for allowing for expression of a polypeptide capable of inactivating glutamine synthetase inhibitor.

46. The vector of claim 45, wherein said DNA fragment is under the control of replicon elements suitable for the transformation of bacteria, particularly E. coli.

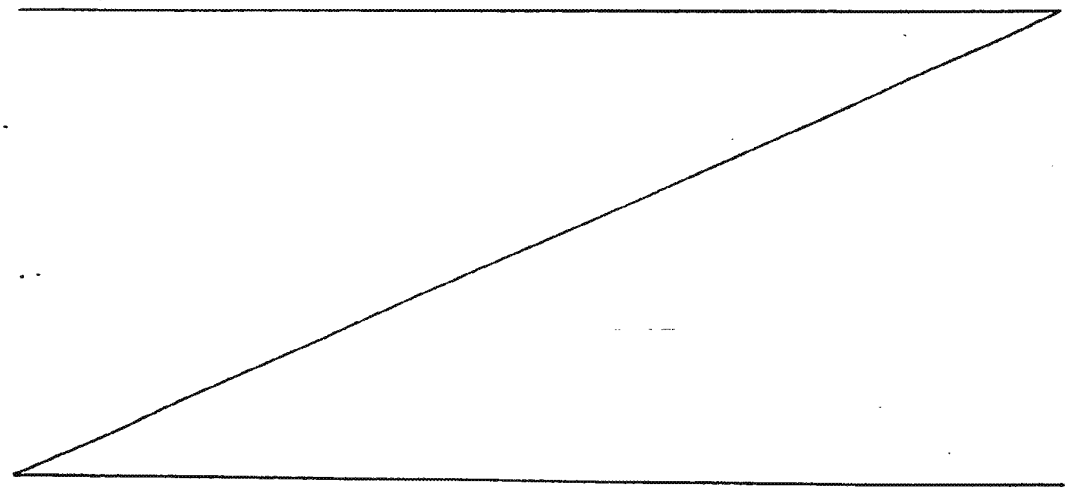
47. The vector of claim 46, wherein said DNA fragment is under the control of a plant promoter region, and of regulation elements allowing for the expression of said DNA fragments in plant cells, when the latter are later transformed with said vector.

48. The vector of claim 47, which confers bialaphos-resistance to the transformed plant cells.

49. The vector of claim 48, wherein a sequence encoding a transit peptide is intercalated between said plant promoter region and said DNA fragment.

50. The vector of claim 49, wherein the transit peptide is selected from ribulose-1,5 biphosphate carboxylase and chlorophyl a/b binding proteins.

51. The vector of any of claims 45 to 50, wherein said vector is a modified Ti plasmid.



COR-AAD1-00004033
Bayer EX1008 (Part 7 of 9)

52. Vector according to any of claims 41 to 51, which comprises the following nucleotide sequence :

```
                                                        GTG AGC CCA GAA
    183
CGA CGC CCG GCC GAC ATC CGC CGT GCC ACC GAG GCG GAC ATG CCG
  228
GCG GTC TGC ACC ATC GTC AAC CAC TAC ATC GAG ACA AGC ACG GTC
  273
AAC TTC CGT ACC GAG CCG CAG GAA CCG CAG GAG TGG ACG GAC GAC
  318
CTC GTC CGT CTG CGG GAG CGC TAT CCC TGG CTC GTC GCC GAG GTG
  363
GAC GGC GAG GTC GCC GGC ATC GCC TAC GCG GGC CCC TGG AAG GCA
  408
CGC AAC GCC TAC GAC TGG ACG GCC GAG TCG ACC GTG TAC GTC TCC
  453
CCC CGC CAC CAG CGG ACG GGA CTG GGC TCC ACG CTC TAC ACC CAC
  498
CTG CTG AAG TCC CTG GAG GCA CAG GGC TTC AAG AGC GTG GTC GCT
  543
GTC ATC GGG CTG CCC AAC GAC CCG AGC GTG CGC ATG CAC GAG GCG
  588
CTC GGA TAT GCC CCC CGC GGC ATG CTG CGG GCG GCC GGC TTC AAG
  633
CAC GGG AAC TGG CAT GAC GTG GGT TTC TGG CAG CTG GAC TTC AGC
  678
CTG CCG GTA CCG CCC CGT CCG GTC CTG CCC GTC ACC GAG ATC
  723
```

53. The vector of claim 52, wherein the initiation codon ATG is substituted for the initiation codon GTG of the sequence defined in claim 52.

54. Vector according to any of claims 41 to 51, which comprises the following nucleotide sequence :

TAAAGAGGTGCCCGCCACCCGCTTTCGCAGAACACCGAAGGAGACCACAC

GTGAGCCCAGAACGACGCCCGGTCGAGATCCGTCCCGCCACCGCCGCCGA

CATGGCGGCGGTCTGCGACATCGTCAATCACTACATCGAGACGAGCACGG

TCAACTTCCGTACGGAGCCGCAGACTCCGCAGGAGTGGATCGACGACCTG

GAGCGCCTCCAGGACCGCTACCCCTGGCTCGTCGCCGAGGTGGAGGGCGT

CGTCGCCGGCATCGCCTACGCCGGCCCCTGGAAGGCCCGCAACGCCTACG

ACTGGACCGTCGAGTCGACGGTGTACGTCTCCCACCGGCACCAGCGGCTC

GGACTGGGCTCCACCCTCTACACCCACCTGCTGAAGTCCATGGAGGCCCA

GGGCTTCAAGAGCGTGGTCGCCGTCATCGGACTGCCCAACGACCCGAGCG

TGCGCCTGCACGAGGCGCTCGGATACACCGCGCGCGGGACGCTGCGGGCA

GCCGGCTACAAGCACGGGGGCTGGCACGACGTGGGGTTCTGGCAGCGCGA

CTTCGAGCTGCCGGCCCCGCCCCGCCCCGTCCGGCCCGTCACACAGATCT

GAGCGGAGAGCGCATGGC

55. A DNA fragment, for the subsequent transformation of plant cells, coding for a polypeptide having phosphinothricin-acetyl-transferase activity, which consists of a nucleotide sequence coding for the following amino acid sequence :

X SER PRO GLU

183
ARG ARG PRO ALA ASP ILE ARG ARG ALA THR GLU ALA ASP MET PRO

228
ALA VAL CYS THR ILE VAL ASN HIS TYR ILE GLU THR SER THR VAL

273
ASN PHE ARG THR GLU PRO GLN GLU PRO GLN GLU TRP THR ASP ASP

318
LEU VAL ARG LEU ARG GLU ARG TYR PRO TRP LEU VAL ALA GLU VAL

363
ASP GLY GLU VAL ALA GLY ILE ALA TYR ALA GLY PRO TRP LYS ALA

408
ARG ASN ALA TYR ASP TRP THR ALA GLU SER THR VAL TYR VAL SER

453
PRO ARG HIS GLN ARG THR GLY LEU GLY SER THR LEU TYR THR HIS

498
LEU LEU LYS SER LEU GLU ALA GLN GLY PHE LYS SER VAL VAL ALA

543
VAL ILE GLY LEU PRO ASN ASP PRO SER VAL ARG MET HIS GLU ALA

588
LEU GLY TYR ALA PRO ARG GLY MET LEU ARG ALA ALA GLY PHE LYS

633
HIS GLY ASN TRP HIS ASP VAL GLY PHE TRP GLN LEU ASP PHE SER

678
LEU PRO VAL PRO PRO ARG PRO VAL LEU PRO VAL THR GLU ILE

723

COR-AAD1-00004036
Bayer EX1008 (Part 7 of 9)

in which X represents MET or VAL, or of a part of said nucleotide sequence of sufficient length to code for a polypeptide still having phosphinotricin-acetyl-transferase activity.

56. The DNA fragment of claim 55 which comprises the following nucleotide sequence :

```
                                                    GTG AGC CCA GAA
      183
CGA CGC CCG GCC GAC ATC CGC CGT GCC ACC GAG GCG GAC ATG CCG
      228
GCG GTC TGC ACC ATC GTC AAC CAC TAC ATC GAG ACA AGC ACG GTC
      273
AAC TTC CGT ACC GAG CCG CAG GAA CCG CAG GAG TGG ACG GAC GAC
      318
CTC GTC CGT CTG CGG GAG CGC TAT CCC TGG CTC GTC GCC GAG GTG
      363
GAC GGC GAG GTC GCC GGC ATC GCC TAC GCG GGC CCC TGG AAG GCA
      408
CGC AAC GCC TAC GAC TGG ACG GCC GAG TCG ACC GTG TAC GTC TCC
      453
CCC CGC CAC CAG CGG ACG GGA CTG GGC TCC ACG CTC TAC ACC CAC
      498
CTG CTG AAG TCC CTG GAG GCA CAG GGC TTC AAG AGC GTG GTC GCT
      543
GTC ATC GGG CTG CCC AAC GAC CCG AGC GTG CGC ATG CAC GAG GCG
      588
CTC GGA TAT GCC CCC CGC GGC ATG CTG CGG GCG GCC GGC TTC AAG
      633
CAC GGG AAC TGG CAT GAC GTG GGT TTC TGG CAG CTG GAC TTC AGC
      678
CTG CCG GTA CCG CCC CGT CCG GTC CTG CCC GTC ACC GAG ATC
      723
```

or a part thereof expressing a polypeptide having phosphinotricin-acetyl-transferase activity.

57. A DNA fragment, for the subsequent transformation of plant cells, coding for a polypeptide having phosphinotricin-acetyl-transferase activity, which consists of a nucleotide sequence coding for the following amino acid sequence :

V S P E R R P V E I R P A T A A D M

A A V C D I V N H Y I E T S T V N F

R T E P Q T P Q E W I D D L E R L Q

D R Y P W L V A E V E G V V A G I A

Y A G P W K A R N A Y D W T V E S T

V Y V S H R H Q R L G L G S T L Y T

H L L K S M E A Q G F K S V V A V I

G L P N D P S V R L H E A L G Y T A

R G T L R A A G Y K H G G W H D V G

F W Q R D F E L P A P P R P V R P V

T Q I *

COR-AAD1-00004038
Bayer EX1008 (Part 7 of 9)

or of a part of said nucleotide sequence of sufficient length to code for a polypeptide still having phosphinotricin-acetyl-transferase activity.

58. The DNA fragment of claim 57, which comprises the following nucleotide sequence :

TAAAGAGGTGCCCGCCACCCGCTTTCGCAGAACACCGAAGGAGACCACAC

GTGAGCCCAGAACGACGCCCGGTCGAGATCCGTCCCGCCACCGCCGCCGA

CATGGCGGCGGTCTGCGACATCGTCAATCACTACATCGAGACGAGCACGG

TCAACTTCCGTACGGAGCCGCAGACTCCGCAGGAGTGGATCGACGACCTG

GAGCGCCTCCAGGACCGCTACCCCTGGCTCGTCGCCGAGGTGGAGGGCGT

CGTCGCCGGCATCGCCTACGCCGGCCCCTGGAAGGCCCGCAACGCCTACG

ACTGGACCGTCGAGTCGACGGTGTACGTCTCCCACCGGCACCAGCGGCTC

GGACTGGGCTCCACCCTCTACACCCACCTGCTGAAGTCCATGGAGGCCCA

GGGCTTCAAGAGCGTGGTCGCCGTCATCGGACTGCCCAACGACCCGAGCG

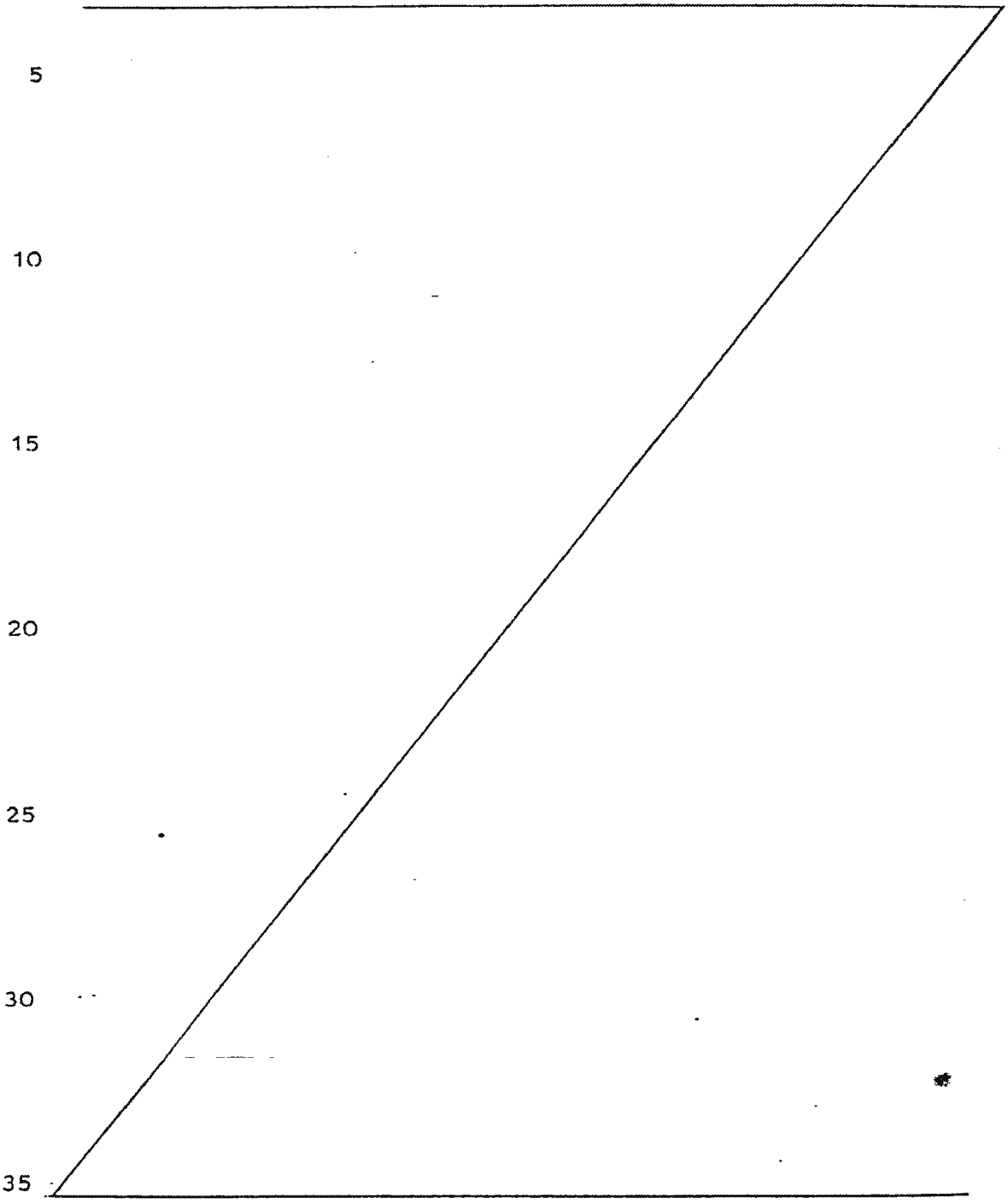
TGCGCCTGCACGAGGCGCTCGGATACACCGCGCGCGGGACGCTGCGGGCA

GCCGGCTACAAGCACGGGGGCTGGCACGACGTGGGGTTCTGGCAGCGCGA

CTTCGAGCTGCCGGCCCCGCCCCGCCCCGTCCGGCCCGTCACACAGATCT

GAGCGGAGAGCGCATGGC

or of a part thereof expressing a polypeptide having phosphinotricin-acetyl-transferase activity.



COR-AAD1-00004040
Bayer EX1008 (Part 7 of 9)

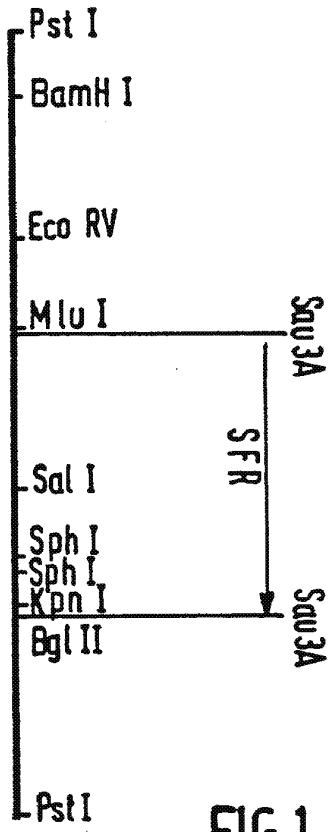


FIG.1

COR-AAD1-00004041
Bayer EX1008 (Part 7 of 9)

CCC GCT CAA GCT CGC TGT CAT TTT CGA GAC GCC ATC TTT GGA AGC
GGT GGC CGA ATC CGT ACT GCG CGG ACT CGA CGA CGC GTA AAA CGA
TCG ACC ACG TAC ACG AGT CCG GAC ACG GGG CGA GGA GGC CCG GTT
CCG GCA CCG AGG AAG ACC GAA GGA AGA CCA CAC GTG AGC CCA GAA
CGA CGC CCG GCC GAC ATC CGC CGT GCC ACC GAG GCG GAC ATG CCG
FokI
GCG GTC TGC ACC ATC GTC AAC CAC TAC ATC GAG ACA AGC ACG GTC
AAC TTC CGT ACC GAG CCG CAG GAA CCG CAG GAG TGG ACG GAC GAC
CTC GTC CGT CTG CGG GAG CGC TAT CCC TGG CTC GTC GCC GAG GTG
GAC GGC GAG GTC GCC GGC ATC GCC TAC GCG GGC CCC TGG AAG GCA
CGC AAC GCC TAC GAC TGG ACG GCC GAG TCG ACC GTG TAC GTC TCC
CCC CGC CAC CAG CGG ACG GGA CTG GGC TCC ACG CTC TAC ACC CAC
CTG CTG AAG TCC CTG GAG GCA CAG GGC TTC AAG AGC GTG GTC GCT
GTC ATC GGG CTG CCC AAC GAC CCG AGC GTG CGC ATG CAC GAG GCG
CTC GGA TAT GCC CCC CGC GGC ATG CTG CGG GCG GCC GGC TTC AAG
CAC GGG AAC TGG CAT GAC GTG GGT TTC TGG CAG CTG GAC TTC AGC
CTG CCG GTA CCG CCC CGT CCG GTC CTG CCC GTC ACC GAG ATC TGA
BglII
ACG GAG TGC GCG TGG GCA TCG CCC GAG TTG GAG CTG GTA CGG GAA
CTC ATC GAA CTC AAC TGG CAT ACC CGC AAT GGT GAG GTG GAA CCG
CGG CGG ATC GCG TAC GAC CGT GCC CAG G

FIG.2

COR-AAD1-00004042
Bayer EX1008 (Part 7 of 9)

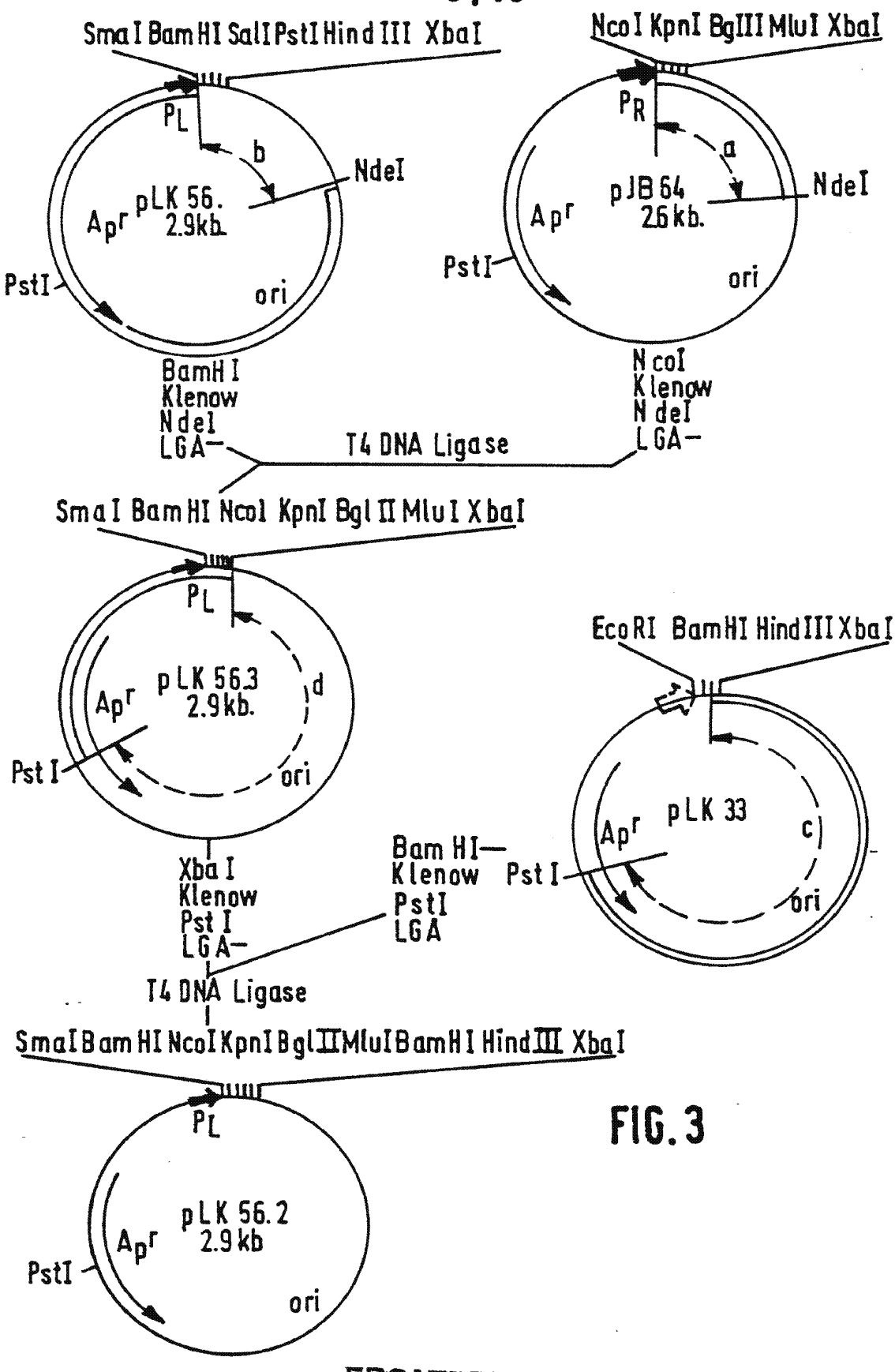


FIG. 3

COR-AAD1-00004043
Bayer EX1008 (Part 7 of 9)

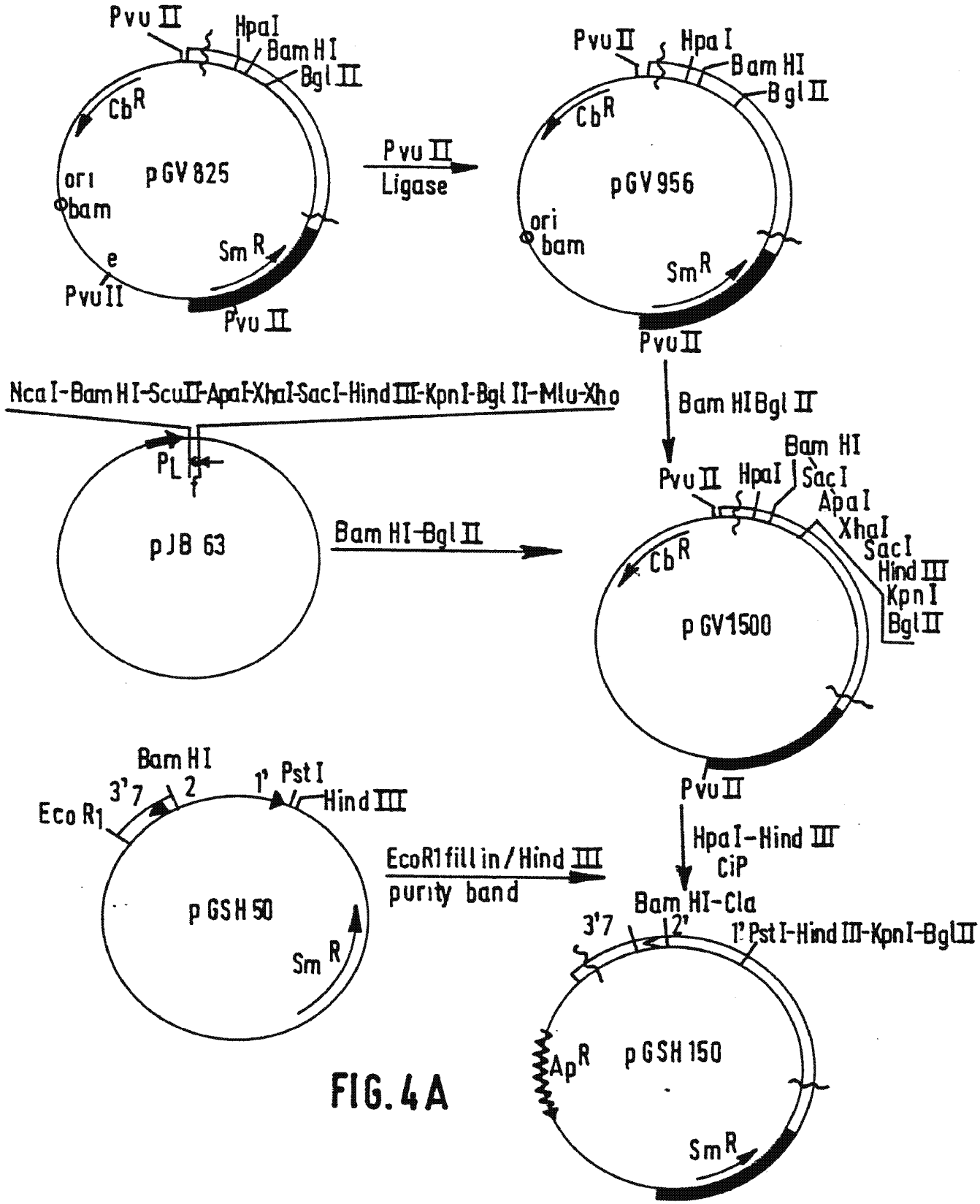


FIG. 4A

COR-AAD1-00004044
Bayer EX1008 (Part 7 of 9)

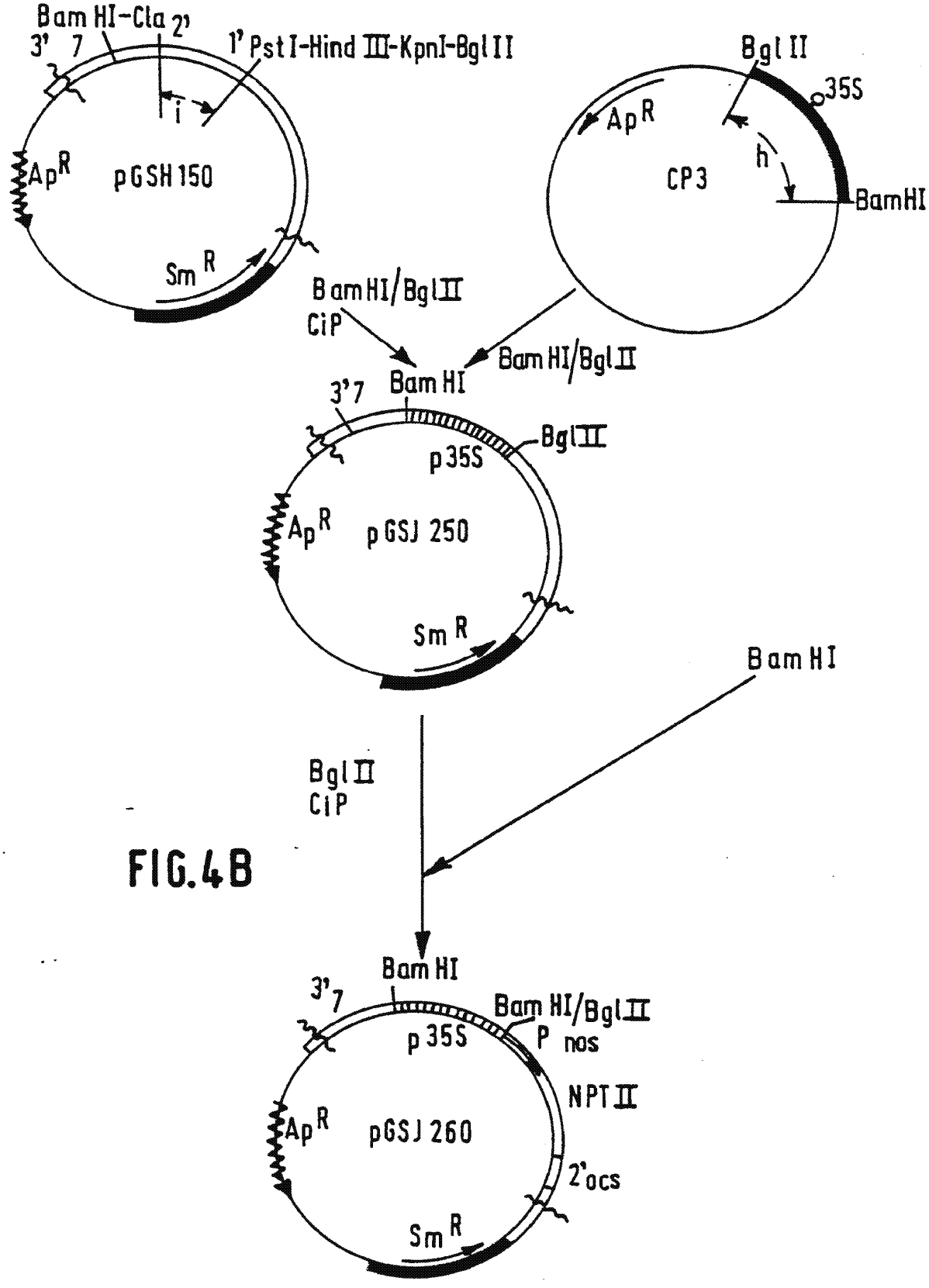


FIG.4B

COR-AAD1-00004045
Bayer EX1008 (Part 7 of 9)

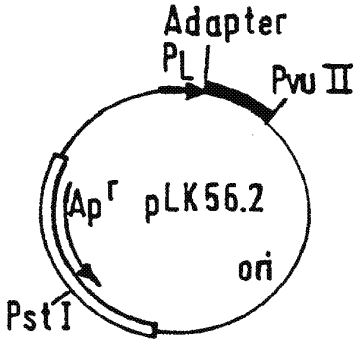




FIG.5A

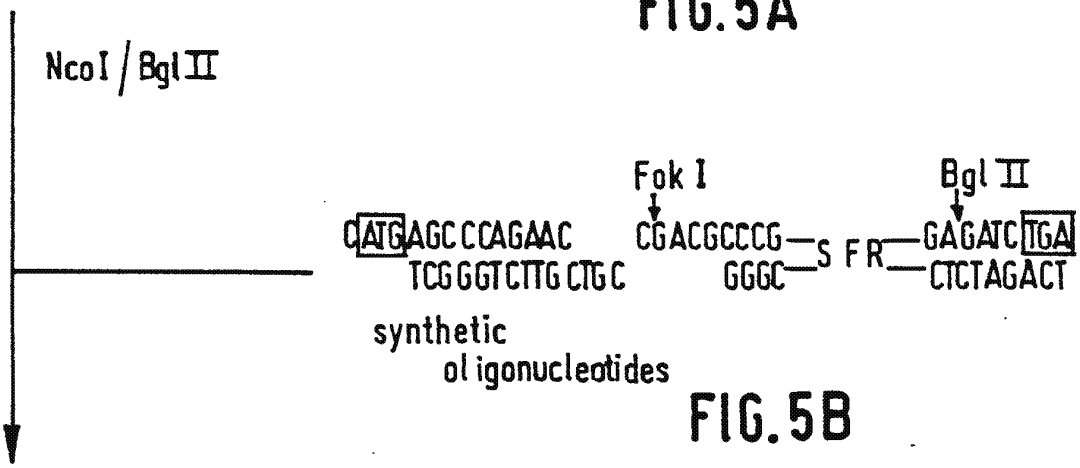


FIG.5B

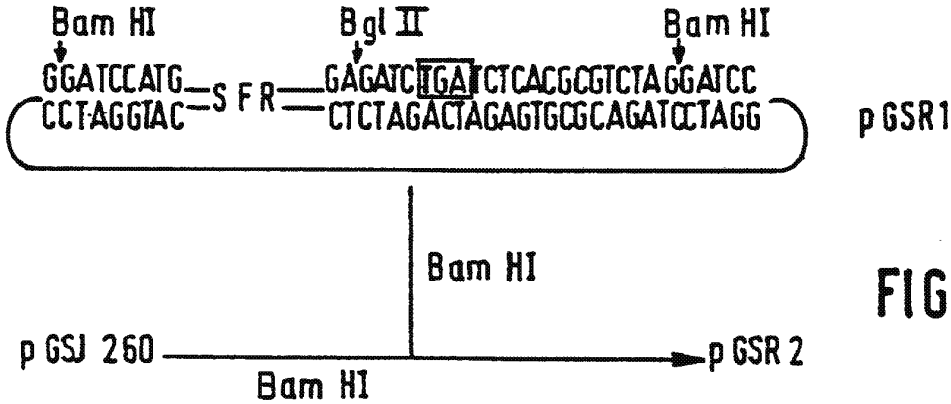


FIG.5C

COR-AAD1-00004046
Bayer EX1008 (Part 7 of 9)

Bayer EX1008 (Part 7 of 9)

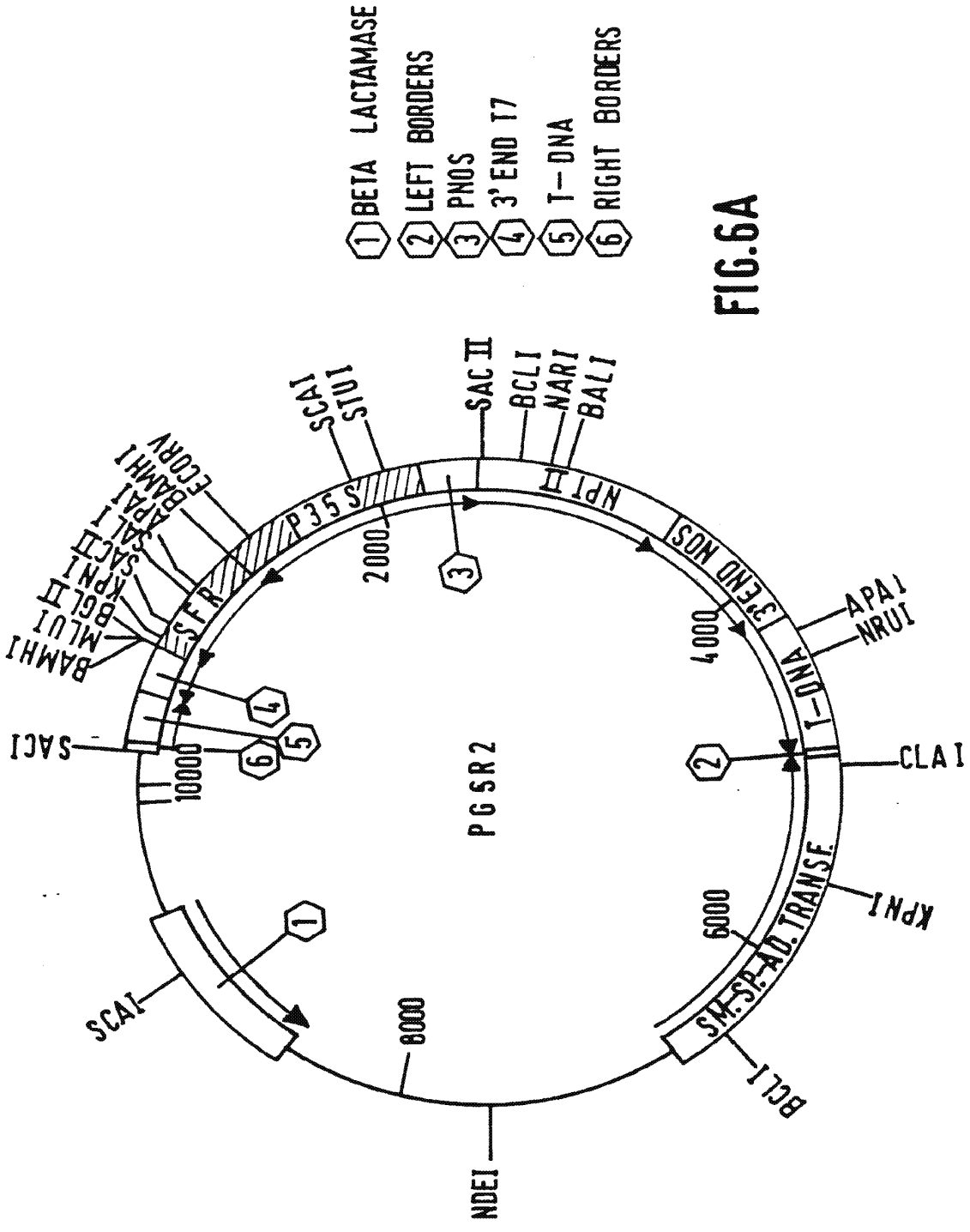


FIG.6A

COR-AAD1-00004047

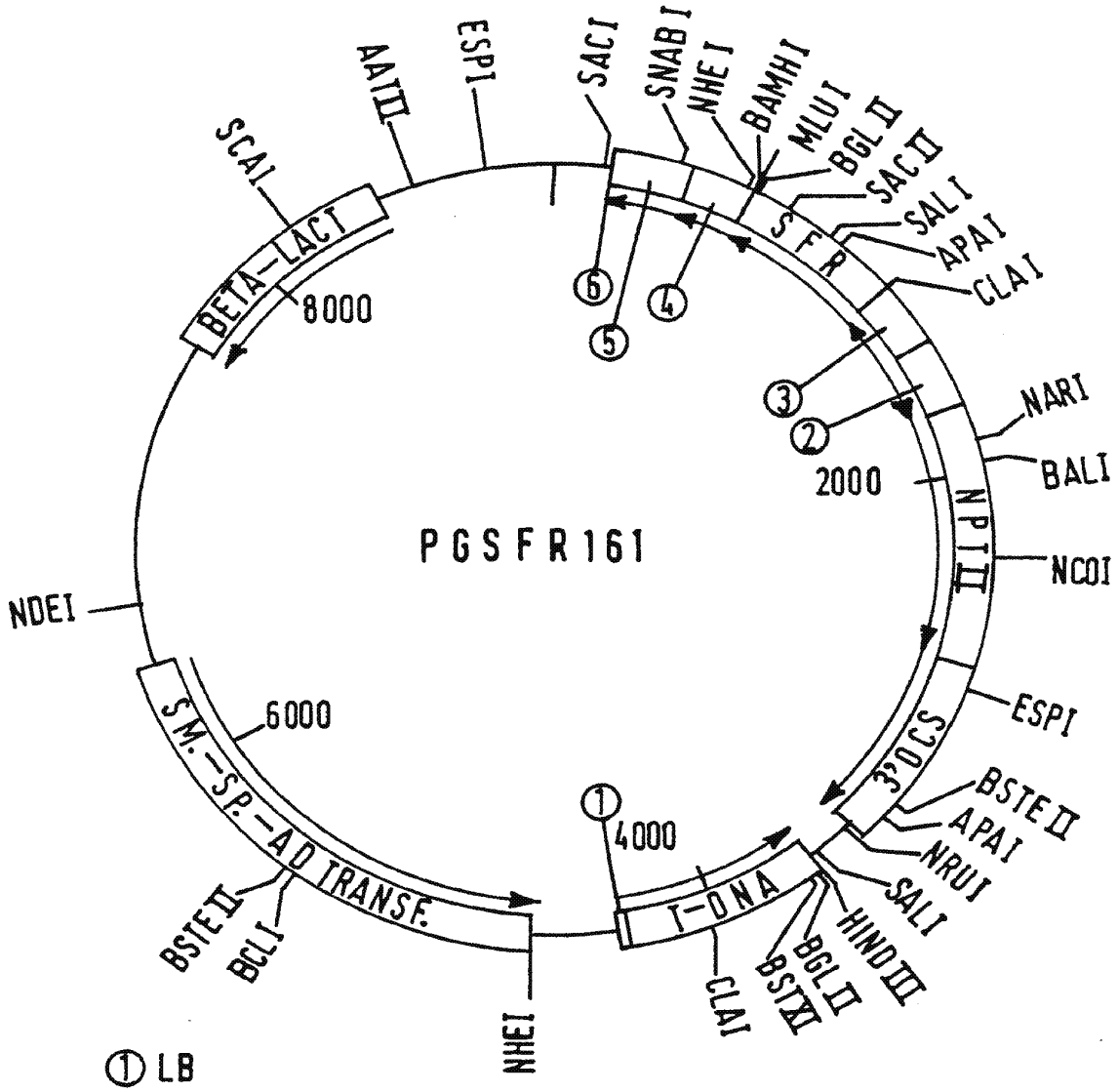


FIG.6B

COR-AAD1-00004048
Bayer EX1008 (Part 7 of 9)

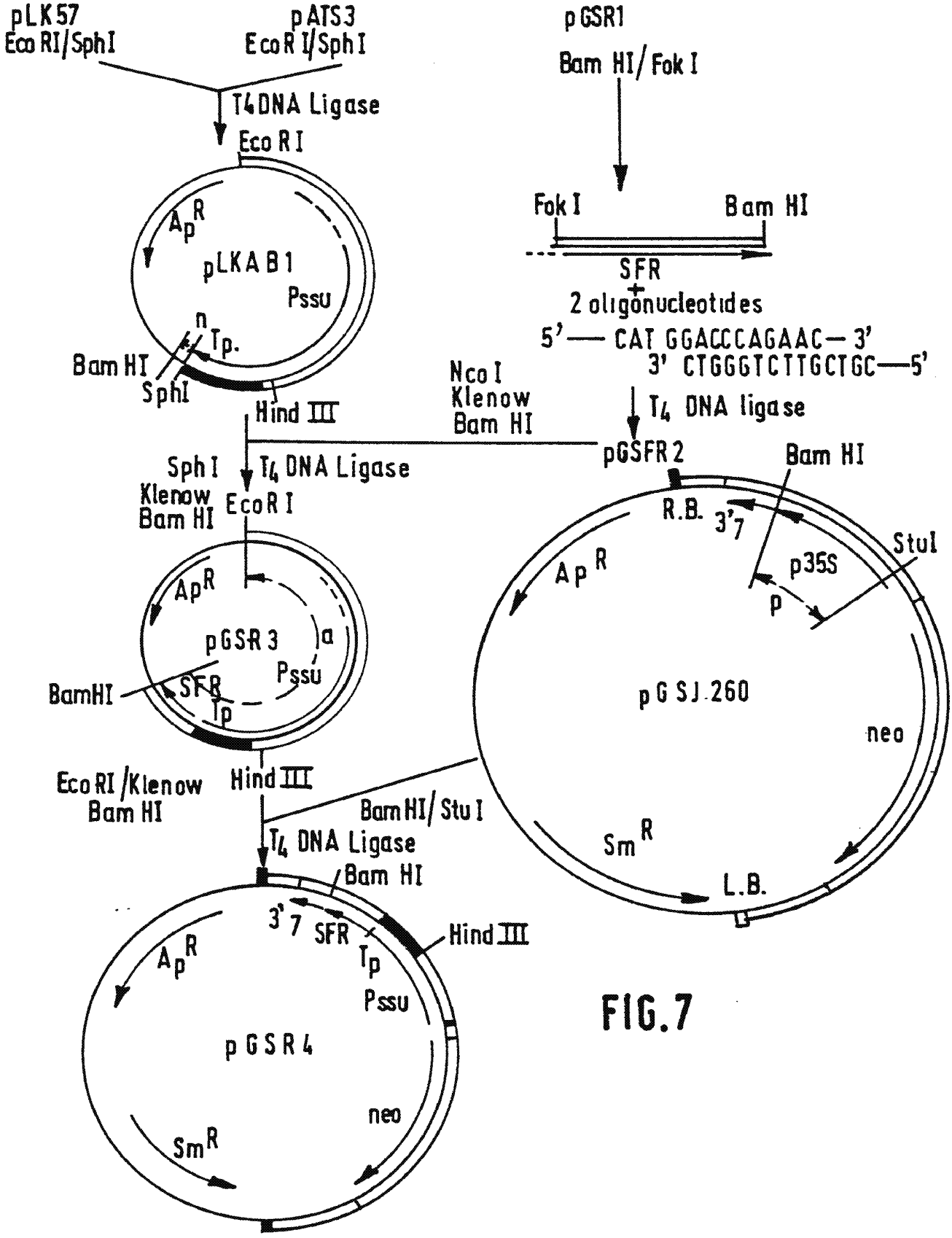


FIG.7

COR-AAD1-00004049
Bayer EX1008 (Part 7 of 9)

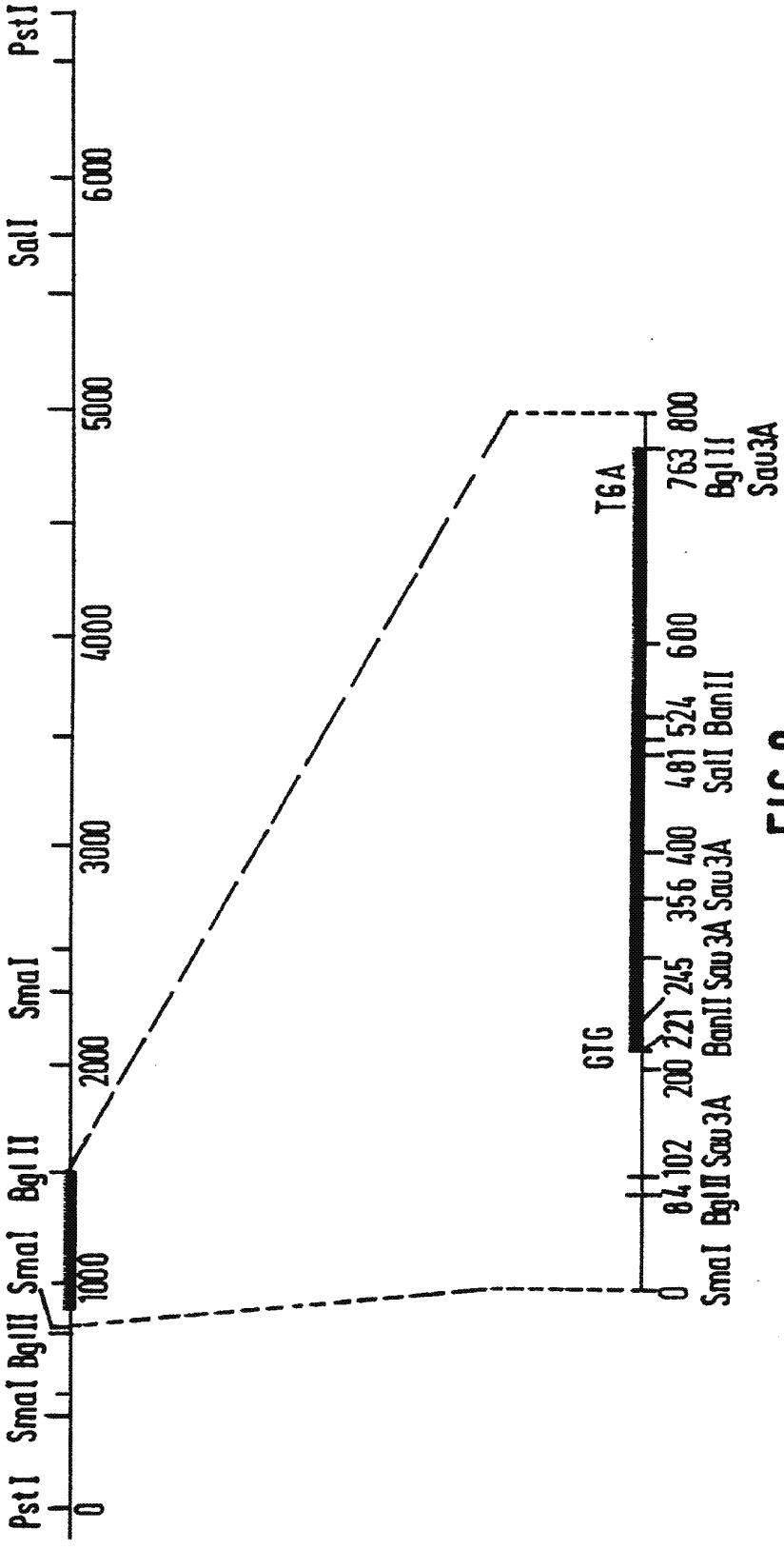


FIG.8

COR-AAD1-00004050
Bayer EX1008 (Part 7 of 9)

TAAAGAGGTGCCCGCCACCCGCTTTCGCAGAACACCGAAGGAGACCACAC

GTGAGCCCAGAACGACGCCCGGTCGAGATCCGTCCCGCCACCGCCGCCGA

CATGGCGGCGGTCTGCGACATCGTCAATCACTACATCGAGACGAGCACGG

TCAACTTCCGTACGGAGCCGCAGACTCCGCAGGAGTGGATCGACGACCTG

GAGCGCCTCCAGGACCGCTACCCCTGGCTCGTCGCCGAGGTGGAGGGCGT

CGTCGCCGGCATCGCCTACGCCGGCCCCTGGAAGGCCCGCAACGCCTACG

ACTGGACCGTCGAGTCGACGGTGTACGTCTCCCACCGGCACCAGCGGCTC

GGACTGGGCTCCACCCTCTACACCCACCTGCTGAAGTCCATGGAGGCCCA

GGGCTTCAAGAGCGTGGTCGCCGTCATCGGACTGCCCAACGACCCGAGCG

TGCGCCTGCACGAGGCGCTCGGATACACCGCGCGCGGGACGCTGCGGGCA

GCCGGCTACAAGCACGGGGGCTGGCACGACGTGGGGTTCTGGCAGCGCGA

CTTCGAGCTGCCGGCCCCGCCCCGCCCCGTCCGGCCCGTCACACAGATCT

GAGCGGAGAGCGCATGGC

FIG.9

COR-AAD1-00004051
Bayer EX1008 (Part 7 of 9)

ERSATZBLATT

```
                    10         20         30         40         50
PBG39_____ MSPERRPADI RRATEADMPA VCTIVNHYIE TSTVNFRTEP QEPQEWTDDL
PJS1______  VSPERRPVEI RPATAADMAA VCDIVNHYIE TSTVNFRTEP QTPQEWIDDL

                    60         70         80         90         100
PBG39_____ VRLRERYPWL VAEVDGEVAG IAYAGPWKAR NAYDWTAEST VYVSPRHQRT
PJS1______ ERLQDRYPWL VAEVEGVVAG IAYAGPWKAR NAYDWTVEST VYVSHRHQRL

                    110        120        130        140        150
PBG39_____ GLGSTLYTHL LKSLEAQGFK SVVAVIGLPN DPSVRMHEAL GYAPRGMLRA
PJS1______ GLGSTLYTHL LKSMEAQGFK SVVAVIGLPN DPSVRLHEAL GYTARGTLRA

                    160        170        180
PBG39_____ AGFKHGNWHD VGFWQLDFSL PVPPRPVLPV TEI*
PJS1______ AGYKHGGWHD VGFWQRDFEL PAPPRPVRPV TQI*
```

FIG.10

COR-AAD1-00004052

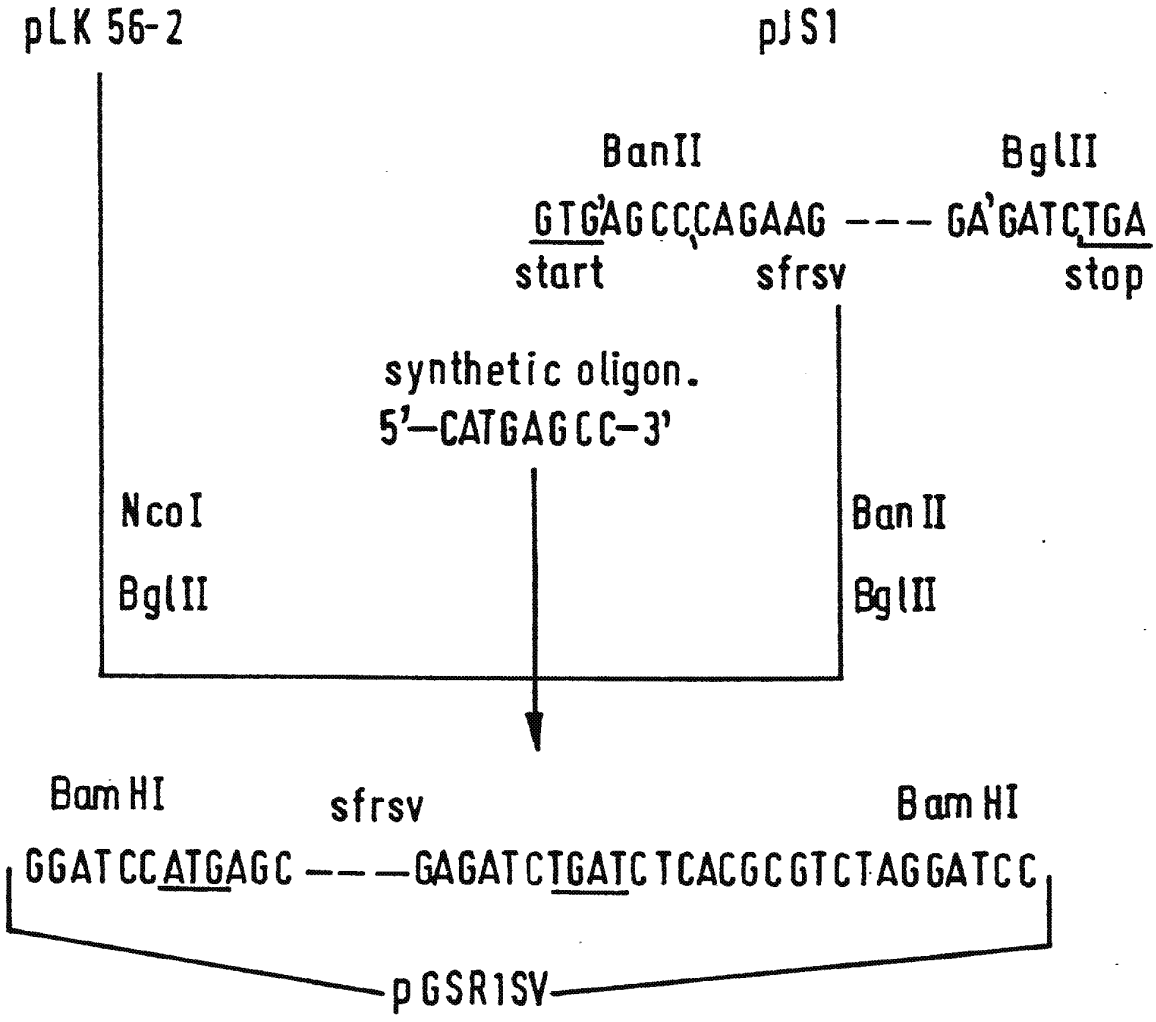


FIG. 11

COR-AAD1-00004053
Bayer EX1008 (Part 7 of 9)

INTERNATIONAL SEARCH REPORT

International Application No PCT/EP 87/00141

I. CLASSIFICATION OF SUBJECT MATTER (if several classification symbols apply, indicate all) [6]

According to International Patent Classification (IPC) or to both National Classification and IPC

IPC[4]: C 12 N 15/00; A 01 H 1/00; C 12 N 5/00; A 01 H 5/10; // C 12 N 9/10

II. FIELDS SEARCHED

Minimum Documentation Searched [7]

Classification System	Classification Symbols
IPC[4]	C 12 N; A 01 H; A 01 N

Documentation Searched other than Minimum Documentation to the Extent that such Documents are included in the Fields Searched [8]

III. DOCUMENTS CONSIDERED TO BE RELEVANT [9]

Category [10]	Citation of Document, [11] with indication, where appropriate, of the relevant passages [12]	Relevant to Claim No. [13]
X	EP, A, 0173327 (MEIJA SEIKA KAISHA) 5 March 1986 see page 19, lines 28-36; figure 7	12,41,43, 45,46,52, 55,56
Y		1-40,42,44, 47-51,53,54, 57,58
Y	WO, A, 84/02920 (MONSANTO) 2 August 1984 see page 12, lines 13-18; page 39, lines 1-16; claims 29-34	1-58
Y	Journal of Molecular and Applied Genetics, volume 2, no. 6, 1984, Raven Press, (New York, US), G. Donn et al.: "Herbicide-resistant alfalfa Cells: An example of gene amplification in plants", pages 621-635 see page 625, right-hand column, last paragraph	1-58

./.

* Special categories of cited documents: [10]

"A" document defining the general state of the art which is not considered to be of particular relevance

"E" earlier document but published on or after the international filing date

"L" document which may throw doubts on priority claim(s) or which is cited to establish the publication date of another citation or other special reason (as specified)

"O" document referring to an oral disclosure, use, exhibition or other means

"P" document published prior to the international filing date but later than the priority date claimed

"T" later document published after the international filing date or priority date and not in conflict with the application but cited to understand the principle or theory underlying the invention

"X" document of particular relevance; the claimed invention cannot be considered novel or cannot be considered to involve an inventive step

"Y" document of particular relevance; the claimed invention cannot be considered to involve an inventive step when the document is combined with one or more other such documents, such combination being obvious to a person skilled in the art.

"&" document member of the same patent family

IV. CERTIFICATION

Date of the Actual Completion of the International Search	Date of Mailing of this International Search Report
4th July 1987	18 AUG 1987
International Searching Authority: EUROPEAN PATENT OFFICE	Signature of Authorized Officer: M. VAN MOL

Form PCT/ISA/210 (second sheet) (January 1985)

COR-AAD1-00004054

Bayer EX1008 (Part 7 of 9)

International Application No. PCT/EP 87/00141

III. DOCUMENTS CONSIDERED TO BE RELEVANT (CONTINUED FROM THE SECOND SHEET)

Category *	Citation of Document, with indication, where appropriate, of the relevant passages	Relevant to Claim No
Y	Nature, volume 317, 24 October 1985, R. Shields: "Engineering herbicide resistance", page 668 see the whole article	1-17,47-51
Y	WO, A, 84/02913 (MONSANTO) 2 August 1984 see page 4, lines 17-28; page 5, lines 9-20; claims 17-19; page 41; figures 18, 21,27,37	6,12,15-17, 47-51,53
Y	Gene, volume 33, no. 2, 1985, Elsevier Science Publishers, (Amsterdam, NL), J. Vara et al.: "Cloning and expression of a puromycin N-acetyl transferase gene from Streptomyces alboniger in Streptomyces lividans and Escherichia coli", pages 197-206 see summary; page 204, right-hand column, paragraph 1	12,46
Y	Biotechnology, volume 4, no. 9, September 1986, (New York, US), J.T. Fayerman: "New developments in gene cloning in antibiotic producing microorganisms", pages 786-789 see page 788, bottom of left-hand column - top of right-hand column	7,8,54,57, 58
Y	Helvetica Chimica Acta, volume 55, fasc. 1, no. 25, 1972, E. Bayer et al.: "Stoffwechselprodukte von Mikroorganismen. Phosphinothricin und Phosphinothricyl-Alanyl-Alanin", pages 224-239 see summary	7,8,54,57, 58
Y	WO, A, 86/02097 (GENERAL HOSPITAL CORP.) 10 April 1986 see page 13, last paragraph - page 14, paragraph 1; page 26; claim 23	28-40
Y	The Pesticide Manual, A World Compendium, 7th edition, 1983, ed. by Charles R. Worthing, published by The British Crop Protection Council, (London, GB), see page 302, no. 6930	28-40
P,X	Chemical Abstracts, volume 106, 1987, (Columbus, Ohio, US), T. Murakami et al.: "The bialaphos biosynthetic genes of Streptomyces hygroscopicus: molecular cloning and ./.	

Form PCT ISA.210 (extra sheet) (January 1985)

COR-AAD1-00004055
Bayer EX1008 (Part 7 of 9)

International Application No. PCT/EP 87/00141

III. DOCUMENTS CONSIDERED TO BE RELEVANT (CONTINUED FROM THE SECOND SHEET)

Category *	Citation of Document, with indication, where appropriate, of the relevant passages	Relevant to Claim No
	characterization of the gene cluster, see page 1149, abstract 1151u, MGG, Mol. Gen. Genet. 1986, 205(1), 42-50	12,41,43,45, 46,52,55,56
P,Y		1-40,42,44, 47-51,53,54, 57-58
	--	
A	EMBO Journal, volume 4, 1985, IRL Press Limited, (Oxford, GB), P.H. Schreier et al.: "The use of nuclear-encoded sequences to direct the light-regulated synthesis and transport of a foreign protein into plant chloroplasts", pages 25-32 see page 30, right-hand column - page 31	13-17,47-51
	--	
A	Proceedings of the Nationale Academy of Sciences of USA, volume 81, May 1984, A.R. Cashmore: "Structure and expression of a pea nuclear gene encoding a chlorophyll a/b-binding polypeptide", pages 2960-2964 see page 2964	13-17,47-51
	--	
A	Chemical Abstracts, volume 98, 1983, (Columbus, Ohio, US), P. Langelueddeke et al.: "Glufosinate (HOE 39866), a new non-selective contact herbicide: results of several years' experimentation in orchards and vineyards from different European countries", see pages 242-243, abstract 48585v, Meded. Fac. Landbouwwet., Rijksuniv. Gent 1982, 47(1), 95-104	31,32,36
	--	
A	Chemical Abstracts, volume 104, no. 5, February 1986, (Columbus, Ohio, US), J.D.G. Jones et al.: "High level expression of introduced chimeric genes in regenerated transformed plants", see page 152, abstract 29747a, EMBO J. 1985, 4(10), 2411-18	16,50
	--	
A	Nucleic Acids Research, volume 14, no. 4, February 1986, IRL Press Limited, (Oxford, GB), M. Zalacain et al.: "Nucleotide sequence of the hygromycin B phospho-transferase gene from Streptomyces hygroscopicus", pages 1565-1581, see page 1573, paragraph 1; page 1577, paragraph 2	6,53
	-- ./...	

Form PCT ISA.210 (extra sheet) (January 1985)

COR-AAD1-00004056
Bayer EX1008 (Part 7 of 9)

International Application No. PCT/EP 87/00141

III. DOCUMENTS CONSIDERED TO BE RELEVANT _ (CONTINUED FROM THE SECOND SHEET)

Category *	Citation of Document, with indication, where appropriate, of the relevant passages	Relevant to Claim No
A	Nucleic Acids Research, volume 13, no. 19, October 1985, IRL Press Limited, (Oxford, GB), J. Velten et al.: "Selection-expression plasmid vectors for use in genetic transformation of higher plants", pages 6981-6998 --	
A	Chemical Abstracts, volume 104, no. 9, 3 March 1986, (Columbus, Ohio, US), M.C. Erickson et al.: "Purification and properties of glutamine synthetase from spinach leaves", see page 311, abstract 64619g, Plant Physiol. 1985, 79(4), 923-7 --	
P,A	The Journal of Antibiotics, volume 49, no. 5, May 1986, (Tokyo, JP), T. Kobayashi et al.: "Cloning and characterization of the strepto-thricin-resistance gene which encodes streptothricin acetyltransferase from streptomyces lavendulae", pages 688-693 --	
A	GB, A, 2007976 (MEIJI SEIKA) 31 May 1979	

Form PCT ISA.210 (extra sheet) (January 1985)

COR-AAD1-00004057
Bayer EX1008 (Part 7 of 9)

ANNEX TO THE INTERNATIONAL SEARCH REPORT ON

INTERNATIONAL APPLICATION NO. PCT/EP 87/00141 (SA 16647)

This Annex lists the patent family members relating to the patent documents cited in the above-mentioned international search report. The members are as contained in the European Patent Office EDP file on 28/07/87

The European Patent Office is in no way liable for these particulars which are merely given for the purpose of information.

Patent document cited in search report	Publication date	Patent family member(s)		Publication date
EP-A- 0173327	05/03/86	JP-A-	61058589	25/03/86
WO-A- 8402920	02/08/84	AU-A-	2436384	15/08/84
		EP-A-	0131620	23/01/85
		JP-T-	60500795	30/05/85
		AU-B-	559562	12/03/87
WO-A- 8402913	02/08/84	EP-A-	0131623	23/01/85
		JP-T-	60500796	30/05/85
WO-A- 8602097	10/04/86	AU-A-	4952985	17/04/86
		EP-A-	0200746	12/11/86
		JP-T-	62500769	02/04/87
GB-A- 2007976	31/05/79	DE-A,C	2848224	10/05/79
		JP-A-	54067026	30/05/79
		AU-A-	4130978	17/05/79
		AU-B-	514686	19/02/81
		CA-A-	1120280	23/03/82
		DE-C-	2857693	09/10/86
		FR-A,B	2407671	01/06/79
		JP-A-	54119034	14/09/79
		US-A-	4309208	05/01/82
		US-A-	4448601	15/05/84
		US-A-	4455163	19/06/84
		US-A-	4552584	12/11/85
		US-A-	4622060	11/11/86

For more details about this annex :
see Official Journal of the European Patent Office, No. 12/82

PCT WORLD INTELLECTUAL PROPERTY ORGANIZATION
International Bureau

INTERNATIONAL APPLICATION PUBLISHED UNDER THE PATENT COOPERATION TREATY (PCT)

(51) International Patent Classification 6 :
A01H 5/00, 5/10, C12N 15/32, 15/82

A1

(11) International Publication Number: **WO 97/13402**

(43) International Publication Date: 17 April 1997 (17.04.97)

(21) International Application Number: PCT/US96/16582

(22) International Filing Date: 11 October 1996 (11.10.96)

(30) Priority Data:
60/005,405 13 October 1995 (13.10.95) US

(71) Applicant: DOWELANCO [US/US]; 9330 Zionsville Road, Indianapolis, IN 45268-1054 (US).

(72) Inventors: MERLO, Donald, J.; 11845 Durbin Drive, Carmel, IN 46032 (US). FOLKERTS, Otto; 159 Red Oak Lane, Carmel, IN 46033 (US).

(74) Agents: SAMPLES, Kenneth, H. et al.; Fitch, Even, Tabin & Flannery, Room 900, 135 S. LaSalle Street, Chicago, IL 60603 (US).

(81) Designated States: AL, AM, AT, AU, AZ, BB, BG, BR, BY, CA, CH, CN, CZ, DE (Utility model), DK, EE, ES, FI, GB, GE, HU, IL, IS, JP, KE, KG, KP, KR, KZ, LK, LR, LS, LT, LU, LV, MD, MG, MK, MN, MW, MX, NO, NZ, PL, PT, RO, RU, SD, SE, SG, SI, SK, TJ, TM, TR, TT, UA, UG, UZ, VN, ARIPO patent (KE, LS, MW, SD, SZ, UG), Eurasian patent (AM, AZ, BY, KG, KZ, MD, RU, TJ, TM), European patent (AT, BE, CH, DE, DK, ES, FI, FR, GB, GR, IE, IT, LU, MC, NL, PT, SE), OAPI patent (BF, BJ, CF, CG, CI, CM, GA, GN, ML, MR, NE, SN, TD, TG).

Published
With international search report.
Before the expiration of the time limit for amending the claims and to be republished in the event of the receipt of amendments.

(54) Title: MODIFIED BACILLUS THURINGIENSIS GENE FOR LEPIDOPTERAN CONTROL IN PLANTS

(57) Abstract

Synthetic DNA sequences which are optimized for expression in plants, particularly maize, and which encode a *Bacillus thuringiensis* protein that is toxic to specific insects are provided, along with methods for the engineering of any synthetic insecticidal gene in maize.

FOR THE PURPOSES OF INFORMATION ONLY

Codes used to identify States party to the PCT on the front pages of pamphlets publishing international applications under the PCT.

AM	Armenia	**GB**	United Kingdom	**MW**	Malawi
AT	Austria	**GE**	Georgia	**MX**	Mexico
AU	Australia	**GN**	Guinea	**NE**	Niger
BB	Barbados	**GR**	Greece	**NL**	Netherlands
BE	Belgium	**HU**	Hungary	**NO**	Norway
BF	Burkina Faso	**IE**	Ireland	**NZ**	New Zealand
BG	Bulgaria	**IT**	Italy	**PL**	Poland
BJ	Benin	**JP**	Japan	**PT**	Portugal
BR	Brazil	**KE**	Kenya	**RO**	Romania
BY	Belarus	**KG**	Kyrgystan	**RU**	Russian Federation
CA	Canada	**KP**	Democratic People's Republic of Korea	**SD**	Sudan
CF	Central African Republic			**SE**	Sweden
CG	Congo	**KR**	Republic of Korea	**SG**	Singapore
CH	Switzerland	**KZ**	Kazakhstan	**SI**	Slovenia
CI	Côte d'Ivoire	**LI**	Liechtenstein	**SK**	Slovakia
CM	Cameroon	**LK**	Sri Lanka	**SN**	Senegal
CN	China	**LR**	Liberia	**SZ**	Swaziland
CS	Czechoslovakia	**LT**	Lithuania	**TD**	Chad
CZ	Czech Republic	**LU**	Luxembourg	**TG**	Togo
DE	Germany	**LV**	Latvia	**TJ**	Tajikistan
DK	Denmark	**MC**	Monaco	**TT**	Trinidad and Tobago
EE	Estonia	**MD**	Republic of Moldova	**UA**	Ukraine
ES	Spain	**MG**	Madagascar	**UG**	Uganda
FI	Finland	**ML**	Mali	**US**	United States of America
FR	France	**MN**	Mongolia	**UZ**	Uzbekistan
GA	Gabon	**MR**	Mauritania	**VN**	Viet Nam

MODIFIED *BACILLUS THURINGIENSIS* GENE FOR LEPIDOPTERAN CONTROL IN PLANTS

The present invention relates to the design, synthesis and expression in plants of a DNA sequence that encodes a *Bacillus thuringiensis* protein that is toxic to specific insects. More particularly, the invention is directed to a synthetic DNA sequence which is optimized for expression in plants, a vector containing the synthetic DNA sequence which is suitable for transforming plants, and plants which stably express the protein coded for by the synthetic DNA sequence.

BACKGROUND OF THE INVENTION

A widely used microbial pesticide is derived from the soil microbe *Bacillus thuringiensis* (*Bt*). *Bt* is a gram-positive, spore-forming bacterium characterized by parasporal crystalline protein inclusions. The crystal protein, often referred to as the δ-endotoxin, has two forms: a nontoxic protoxin with an approximate molecular weight (MW) of 130 kilodaltons (kD); and a toxic form having an approximate MW of 68 kD. The crystalline protein inclusions contain the protoxin protein which is activated in the gut of larvae of a number of insect species. During activation, the protoxin is cleaved, the toxic moiety residing in an amino-proximal 58-68 kD polypeptide. In vivo, the crystal is activated by being solubilized and converted to toxic form by the alkalinity and proteases of the insect gut.

The toxic activity of the protein produced by *Bt* is highly specific to particular insect species and is recognized as safe to higher vertebrates. Numerous reports have shown that the intrasporal crystal proteins isolated from many strains of *Bt* possess extremely high

COR-AAD1-00004061
Bayer EX1008 (Part 7 of 9)

levels of toxicity specific for Lepidopteran larvae, or Coleopteran larvae, with an effective concentration required to inhibit 50% of larval growth in the range of 1 ng/ml of diet for the most sensitive insects (MacIntosh et al., J. Invert. Pathol. 565 (1990) 258).

The cloning, sequencing and expression of the *Bt* protein gene in other bacterial hosts has been described (International Publication No. WO 93/04587, EP Appln. No. 89300388.9, EP Appln. No. 90304996.3, and U.S. Patent No. 5,286,485). However, expression of insecticidal protein genes derived from *Bt* in plants has been extremely difficult, and typically, only low levels of protein have been obtained in transgenic plants (Vaeck et al., Nature, 328 (1987) 33; Barton et al., Plant Physiol., 85 (1987) 1103; and Fischoff et al., Bio/Technology, 5 (1987) 807).

One possible explanation for low expression of the native *Bt* gene in transgenic plants is that the codon usage in a native *Bt* protein gene is significantly different from that of a typical plant gene (EP Appln. No. 89309069.6). Codon usage may influence the expression of genes at the level of translation, transcription or mRNA processing.

Another possible reason for low levels of expression of the native *Bt* gene in transgenic plants may be due to fortuitous transcription processing sites which produce aberrant forms of mRNA (International Publication No. WO 93/07278). Possible processing sites include polyadenylation sites, intron splicing sites, transcriptional termination signals and transport signals. Fortuitous occurrence of such processing sites in a coding region may complicate the expression of a gene in a transgenic host.

COR-AAD1-00004062
Bayer EX1008 (Part 7 of 9)

To optimize an insecticidal gene for expression in plants, attempts have been made to alter the native *Bt* gene to resemble, as much as possible, genes naturally contained within the host plant to be transformed. For example, U.S. Patent No. 5,380,831 to Adang et al. describes a chemically synthesized gene encoding an insecticidal protein which is functionally equivalent to a native insecticidal protein of *Bt*, and which is designed to be expressed in plants at a level higher than a native *Bt* gene. The synthetic gene is at least approximately 85% homologous to a native insecticidal protein gene of *Bt* and is designed such that its distribution frequency of codon usage deviates no more than 25% of highly expressed plant genes, and preferably no more than about 10%. The synthetic gene has GC and TA doublet avoidance indices, based on the frequency in a host gene sequence, that deviates from that of the host plant by no more than about 10-15%, and has a GC content of about 45%.

International Publication No. WO 93/07278 describes a synthetic *Bt* crystal protein gene in which codon usage has been altered in order to increase expression in maize. The synthetic gene is at least approximately 66% homologous to a native insecticidal protein gene of *Bt* and 98% homologous to a pure maize optimized gene. The synthetic gene has a GC content of from 50-64% and does not have prolines at the 3' end of the sequence.

SUMMARY OF THE INVENTION

The present invention is directed to the design, synthesis, and expression in both bacterial and plant cells of a plant optimized DNA sequence that encodes a *Bacillus thuringiensis* HD73 protein which is toxic to Lepidopteran insects. The invention is further related to a method of designing a synthetic gene. The

COR-AAD1-00004063
Bayer EX1008 (Part 7 of 9)

plant optimized DNA sequence comprises codons effective to encode an insecticidal plant protein (hereinafter ICP) with about 589 to about 619 amino acids. The nucleotide sequence coding for ICP is about 70 to about 71% homologous to a native *Bt* nucleotide sequence encoding ICP, and about 63% homologous to a pure maize nucleotide sequence. Codon usage in the plant optimized nucleotide sequence has a deviation from that of the host plant of about 0.23 to about 3.48, preferably about 1.075.

The present invention is also directed to plant expression vectors capable of expression in plant cells, such as maize. The plant expression vector comprising in sequence 5' to 3', a promoter sequence effective to initiate transcription in plant cells; a translational enhancer sequence specific to maize; a first vector unique restriction enzyme cleavage site; a coding sequence coding for a protein typically of less than about 620 amino acids, the protein preferably being substantially homologous with the amino-proximal portion of a *Bt* ICP; a second vector unique restriction enzyme cleavage site; and a polyadenylation sequence.

Another aspect of the invention is directed to a transgenic plant and seeds from a transgenic plant. The transgenic plant and seeds from a transgenic plant comprising in their genome the inheritable synthetic *Bt* gene described herein. This *Bt* synthetic gene is expressed in the cells of the plant or a plant grown from the seeds of the transgenic plant, in sufficient amounts to control lepidopteran insects.

The present invention also provides methods of engineering any structural gene so that it may be optimally expressed in plants, in particular maize. Due to the plasticity afforded by the redundancy of the genetic code (i.e. some amino acids are specified by more than one codon) the invention prescribes a method of

COR-AAD1-00004064
Bayer EX1008 (Part 7 of 9)

modifying the genetic sequence of any gene so that the resulting protein that is expressed is unchanged, but the codons are modified to optimize the expression of the protein in the particular plant of interest.

In practicing the method of the invention, the codon bias of the plant is determined. The codon bias is the statistical codon distribution that the plant uses for coding its proteins. After determining the bias, the percent frequency of the codons in the gene of interest, such as a native *Bacillus thuringiensis*, is determined. The amino acid sequence of the protein of interest is reverse translated so that the resulting nucleic acid sequence codes for the same protein as the native gene, but the resulting nucleic acid sequence corresponds to the first preferred codons of the desired plant. The new sequence is analyzed for restriction enzyme sites that might have been created by the modification. The identified sites are further modified by replacing the codons with second or third choice preferred codons. Other sites in the sequence which could affect the transcription or translation of the gene of interest are the exon:intron 5' or 3' junctions, poly A addition signals, or RNA polymerase termination signals. The sequence is further analyzed and modified to reduce the frequency of TA or GC doublets. In addition to the doublets, G or C sequence blocks that have more than about four residues that are the same can affect transcription of the sequence. Therefore, these blocks are also modified by replacing the codons of first or second choice, etc. with the next preferred codon of choice. The method described above enables one skilled in the art to modify gene(s) that are foreign to a particular plant so that the genes are optimally expressed in plants.

It is an overall interest of the present invention to provide a means for protection of plants

COR-AAD1-00004065
Bayer EX1008 (Part 7 of 9)

against insect damage. More specifically, it is of particular interest to provide a maize optimized nucleotide sequence coding for an insecticidal protein from *Bt* having the nucleotide sequence in SEQ. ID. NO. 1.

The invention further provides a doubly enhanced 35S or 19S promoter which expresses foreign proteins, including *Bt* crystal protein or *Bt* insecticidal crystal proteins more effectively than a 35S or 19S promoter as well as a MSV leader sequence that could be further modified for use with other promoters.

In another aspect, the invention provides a leader sequence which could be used to enhance the expression of any promoter.

Other aspects, advantages, features and characteristics of the present invention will become more apparent upon consideration of the following description and the appended claims.

BRIEF DESCRIPTION OF THE FIGURES

Fig. 1 illustrates the PCR synthesis strategy. Fig. 1A is a graphic representation of the modified ICP gene with key restriction sites indicated above the bar, numbers underneath denote their locations in the gene. The three gene parts that were synthesized separately are shown underneath the gene, the cloning sites incorporated into the ends of each part are shown at the ends of each fragment. Fig. 1B sets forth the PCR synthesis of the 5' end fragment of the ICP gene. The 12 oligonucleotides used in the synthesis are indicated by arrows. The direction of the arrows correspond to the polarity of synthesis of the nascent DNA strand. The location of each oligonucleotide in the gene fragment is indicated between the parentheses, the reverse order of the nucleotide location of the bottom set of oligonucleotides

COR-AAD1-00004066
Bayer EX1008 (Part 7 of 9)

indicates their reverse complementarity to the top (coding) strand of the gene.

Fig. 2 shows the resulting gel from the purification of ICP oligonucleotides by denaturing PAGE. ICP oligonucleotides Bt6 through Bt10 were fractionated by electrophoresis on 12% denaturing PAGE as described in Example 1. Oligonucleotide identities are shown above each lane, and the size of each (nucleotides) is shown below the lane. The mobilities of the tracking dyes xylene cyanol (XC) and bromophenol blue (BPB) are indicated on the right.

Fig. 3 shows a gel which illustrates the progression in the synthesis of the three ICP gene parts. For each section, products of PCR steps 1-6 (5' and 3' sections) or 1-5 (center section) are shown in the lanes marked 1-6 or 1-5, respectively. Each lane contains 5 µl of gel purified DNA from the previous PCR step. Unmarked lanes at the outside of the gel contain 100 bp ladder DNA size standards (GIBCO/BRL).

Fig. 4 shows a gel that illustrates the expression of ICP in *E. coli*. ICP expressed in *E. coli* cells from a cytoplasmic expression vector was analyzed by SDS-PAGE and Western blotting as described in Example 4. Lane 1 contains an amount of *E. coli* total cell protein corresponding to about a 50 ng pellet of protein extract of *E. coli* cells expressing the cytoplasmic expression vector; lane 2 contains about 50 ng of cytoplasmic expression vector extract pellet; lane 3 contains about 10 ng of pellet extract. The negative control lane 4 contains 100 ng of extract pellet of *E. coli* cells expressing pET-9d. Lanes 5, 6 and 7 contain 20, 50 and 100 ng, respectively, of purified native *Bt* ICP.

COR-AAD1-00004067
Bayer EX1008 (Part 7 of 9)

Fig. 5 is a graphical representation which sets forth the results of *Manduca sexta* bioassays. Feeding assays with 500 ng each of *E. coli* extract protein (pET-9d pellet), pellet protein from extract of cells containing the ICP cytoplasmic expression plasmid cytoplasmic expression vector (CEV pellet), cytoplasmic expression vector expressing cells (CEV cells), and native ICP (*Bt* protein) were carried out as described in Example 6. Larval weight and mortality were scored 4 days after placing neonate larvae on the diets.

Fig. 6 is a map of plasmid vector pDAB 910 as further described in Example 7.

Fig. 7 is a map of plasmid vector pDAB 911 as further described in Example 7.

Fig. 8 is a map of plasmid vector pDAB 917 as further described in Example 7.

Fig. 9 is a gel that illustrates the expression of ICP in transgenic MSD callus. ICP expressed in MSD callus isolates was detected by SDS-PAGE and western blotting as described in Example 8. Lanes 1 through 7 contain callus extracts of maize isolates obtained by transformation of MSD line #4 with plasmid pDAB 911; lane 8 contains callus extract of nontransformed MSD line #4; lanes 9 and 10 contain 10 and 1 ng, respectively, of purified ICP.

Fig. 10 is a map of plasmid vector pDAB303 as further described in Example 7.

Fig. 11 illustrates several maps of tested promoters in plasmids pKA882, PDAB305, pDAB310, pDAB348 and pDAB353. More specifically, **pKA882** contains the native 35S promoter, as embodied within CaMV nts 6605 to

COR-AAD1-00004068
Bayer EX1008 (Part 7 of 9)

7439 (MCASTRAS), followed by Linker Sequence A (SEQ. ID. NO. 3)

XbaI BamHI BamHI SalI NcoI
GGGGAC TCTAGAGGATCCGGATCCGTGACCATGG

wherein the ATG (underlined) encoded within the Nco I recognition sequence is the GUS translational start codon. Transcripts from this promoter contain as the 5' untranslated leader sequence essentially the above polylinker sequence.

pDAB348 contains an enhanced 35S promoter with additional 3' sequences and embodied as nucleotides 7093 to 7344 of CaMV DNA, the linker sequence CATCGATG, nucleotides 7093 to 7439 of CaMV, followed by the Linker Sequence A from above.

pDAB305 contains an enhanced 35S promoter with additional 3' sequences and embodied as nucleotides 7093 to 7344 of CaMV DNA, the linker sequence CATCGATG, nucleotides 7093 to 7439 of CaMV, the linker sequence GGGGACTCTAGAGGATCCAG (SEQ. ID. NO. 4), nucleotides 167 to 186 of MSV, nucleotides 188 to 277 of MSV, a C residue followed by nucleotides 120 to 210 of maize Adh1.S, nucleotides 555 to 672 of maize Adh1.S, the linker sequence GACGGATCTG (SEQ. ID. NO. 5), nucleotides 278 to 317 of MSV, and a G residue that represents the final base of an Nco I recognition sequence CCATGG. As above, the GUS translational start codon is part of the Nco I site. Transcripts from this promoter contain as the 5' untranslated leader essentially the MSV coat protein leader sequence, into which has been inserted a deleted version of the maize Adh1.S intron 1.

pDAB310 contains an enhanced 35S promoter with additional 3' sequences and embodied as nucleotides 7093 to 7344 of CaMV DNA, the linker sequence CATCGATG, nucleotides 7093 to 7439 of CaMV, the linker sequence GGGGACTCTAGAGGATCCAG (SEQ. ID. NO. 6), nucleotides 167 to 186 of MSV, nucleotides 188 to 317 of MSV, and a G residue that represents the final base of an Nco I

COR-AAD1-00004069
Bayer EX1008 (Part 7 of 9)

recognition sequence, CCATGG. As above, the GUS translational start codon is part of the Nco I site. Transcripts from this promoter contain the 5' untranslated leader essentially the MSV coat protein leader sequence.

pDAB353 contains an enhanced 35S promoter with additional 3' sequences and embodied as nucleotides 7093 to 7344 of CaMV DNA, the linker sequence CATCGATG, nucleotides 7093 to 7439 of CaMV, the linker sequence GGGGACTCTAGAG (SEQ. ID. NO. 7), nucleotides 120 to 210 of maize Adh1.S, nucleotides 555 to 672 of maize Adh1.S, and the sequence CCGTCGACCATGG (SEQ. ID. NO. 8). As above, the GUS translational start codon is part of the Nco I site. Transcripts from this promoter contain as the 5' untranslated leader essentially a deleted version of the maize Adh.S intron 1.

DETAILED DESCRIPTION OF THE INVENTION

Definitions

The following definitions are provided in order to provide clarity as to the intent or scope of their usage in the specification and claims. All patents and publications referred to herein are incorporated by reference herein.

Crystal protein or *insecticidal crystal protein* (ICP) or *crystal toxin* refers to the major protein component of the parasporal crystals formed in strains of *Bt*. This protein component exhibits selective toxicity to different species of insects. The molecular size of the major protein isolated from parasporal crystals varies depending on the strain of *Bt* from which it is derived. Crystal proteins having molecular weights of approximately 132, 65, and 28 kDa have been reported. It has been shown that the approximately 132 kDa protein is

COR-AAD1-00004070
Bayer EX1008 (Part 7 of 9)

a protoxin that is cleaved to form an amino proximal insect toxin of approximately 65 kDa.

The *crystal protein gene* refers to the DNA sequence encoding the insecticidal crystal protein in either full length protoxin or toxin form, depending on the strain of *Bt* from which the gene is derived.

As used herein, the term *nucleotide* refers to monomeric unit of DNA or RNA consisting of a sugar moiety (pentose), a phosphate, and a nitrogenous heterocyclic base. The base is linked to the sugar moiety via the glycosidic carbon (1' carbon of the pentose). The combination of base and sugar is called a nucleoside; the base characterizes the nucleotide. The four DNA bases are adenine ("A"), guanine ("G"), cytosine ("C"), and thymine ("T"). The four RNA bases are A, G, C, and uracil ("U").

A *structural gene* is that portion of a gene comprising a DNA segment encoding a protein, polypeptide or a portion thereof, and excluding the 5' sequence which drives the initiation of transcription. The structural gene may be one which is normally found in the cell or one which is not normally found in the cellular location wherein it is introduced, in which case it is termed a *heterologous gene*. A heterologous gene may be derived in whole or in part from any source known to the art, including a bacterial genome or episome, eukaryotic, nuclear or plasmid DNA, cDNA, viral DNA or chemically synthesized DNA. A structural gene may contain one or more modifications in either the coding or the untranslated regions which could affect the biological activity or the chemical structure of the expression product, the rate of expression or the manner of expression control. Such modifications include, but are not limited to, mutations, insertions, deletions and substitutions of one or more nucleotides. The structural

COR-AAD1-00004071
Bayer EX1008 (Part 7 of 9)

gene may constitute an uninterrupted coding sequence or it may include one or more introns, bounded by the appropriate splice junctions. The structural gene may be a composite of segments derived from a plurality of sources (naturally occurring or synthetic, where synthetic refers to DNA that is chemically synthesized). The structural gene may also encode a fusion protein.

Operably linked refers to a juxtaposition wherein the components are configured so as to perform their usual function. Thus, control sequences operably linked to a coding sequence are capable of effecting the expression of the coding sequence.

Plant tissue includes differentiated and undifferentiated tissues of plants, including, but not limited to, roots, shoots, leaves, pollen, seeds, tumor tissue and various forms of cells in culture, such as single cells, protoplasts, embryos and callus tissue. The plant tissue may be in planta or in organ, tissue or cell culture.

Plant cell as used herein includes plant cells in planta and plant cells and protoplasts in culture.

Homology refers to identity or near identity of nucleotide or amino acid sequences. As is understood in the art, nucleotide mismatches can occur at the third or wobble base in the codon without causing amino acid substitutions in the final polypeptide sequence. Also, minor nucleotide modifications (e.g., substitutions, insertions or deletions) in certain regions of the gene sequence can be tolerated whenever such modifications result in changes in amino acid sequence that do not alter functionality of the final product. It has been shown that chemically synthesized copies of whole, or parts of, gene sequences can replace the corresponding regions in the natural gene without loss of gene

COR-AAD1-00004072
Bayer EX1008 (Part 7 of 9)

function. Homologs of specific DNA sequences may be identified by those skilled in the art using the test of cross-hybridization of nucleic acids under conditions of stringency as is well understood in the art (as described in Hames et al., Nucleic Acid Hybridisation, (1985) IRL Press, Oxford, UK). Extent of homology is often measured in terms of percentage of identity between the sequences compared.

Preferred codon or *frequency of preferred codon usage* refers to the preference exhibited by a specific host cell in usage of nucleotide codons to specify a given amino acid. To determine the frequency of usage of a particular codon in a gene, the number of occurrences of that codon in the gene is divided by the total number of occurrences of all codons specifying the same amino acid in the gene. The frequency of preferred codon usage exhibited by a host cell can be calculated by averaging the frequency of preferred codon usage in a large number of genes expressed by the host cell.

The percent deviation of the frequency of preferred codon usage for a synthetic gene from that employed by a host cell is calculated first by determining the percent deviation of the frequency of usage of a single codon from that of the host cell followed by obtaining the average deviation over all codons. As defined herein, this calculation includes unique codons (i.e., ATG and TGG). In general terms the overall average deviation of the codon usage of a synthetic gene from that of a host cell is calculated using the equation

$$A=\sum_{n=1}^{Z}\frac{\frac{|X_n-Y_N|}{X_N}X\ 100}{Z}$$

where X_n = frequency of usage for codon n in the host cell; Y_n = frequency of usage for codon n in the synthetic

COR-AAD1-00004073
Bayer EX1008 (Part 7 of 9)

gene; where n represents an individual codon that specifies an amino acid; and where the total number of codons is Z.

The term *pure plant optimized nucleotide sequence* refers to a gene or DNA sequence comprising 100% of the host plant preferred codon sequences for a particular polypeptide. A *pure maize optimized sequence* is a gene or DNA sequence which comprises 100% of the maize preferred codon sequence for a particular polypeptide.

As used herein, a *plant optimized nucleotide sequence* refers to a gene or DNA sequence produced from variations of the pure plant optimized sequence. The variations as described herein include alterations of the pure plant optimized nucleotide sequence to permit manipulation of the gene, such as by altering a nucleotide to create or eliminate restriction sites; and variations to eliminate potentially deleterious processing sites, such as potential polyadenylation sites or intron splicing recognition sites. A *maize optimized nucleotide sequence* refers to a gene or DNA sequence produced from variations of a pure maize optimized sequence. In one aspect of the invention, the plant optimized nucleotide sequence is about 70 to about 71% homologous with a native *Bt* nucleotide sequence encoding ICP, and about 63% homologous based on first choice codon usage and about 83% homologous to a pure maize optimized nucleotide sequence.

Derived from is used to mean taken, obtained, received, traced, replicated or descended from a source (chemical and/or biological). A derivative may be produced by chemical or biological manipulation (including, but not limited to, substitution, addition, insertion, deletion, extraction, isolation, mutation and replication) of the original source.

COR-AAD1-00004074
Bayer EX1008 (Part 7 of 9)

Chemically synthesized, as related to a sequence of DNA, means that the component nucleotides were assembled in vitro. Manual chemical synthesis of DNA may be accomplished using well established procedures (Caruthers, Methodology of DNA and RNA Sequencing, (1983), Weissman (ed.), Praeger Publishers, New York, Chapter 1); automated chemical synthesis can be performed using one of a number of commercially available machines.

The term *designed to be highly expressed* as used herein refers to a level of expression of a designed gene wherein the amount of its full-length specific mRNA transcripts produced is sufficient to be quantified in Northern blots and, thus, represents a level of specific mRNA expressed corresponding to greater than or equal to approximately 0.001% of the poly(A)+mRNA. Before this invention, natural *Bt* genes were transcribed at levels wherein the amount of full-length specific mRNA produced was insufficient to be estimated using the Northern blot technique. However, in the present invention, transcription of a synthetic maize optimized *Bt* ICP gene designed to be highly expressed, is increased to the extent that sufficiently high levels of the ICP accumulate to kill feeding insects.

Design of a Maize Optimized *Bt* ICP Gene Sequence

The design and synthesis strategy set forth herein represents the generally preferred methods for design and synthesis of a plant, specifically maize, optimized ICP gene. Those of ordinary skill in the art will recognize that changes to this protocol are possible without undue experimentation to design and synthesize an ICP gene for expression in other plant species.

The DNA sequence of the ICP gene from *Bacillus thuringiensis* subsp. *kurstaki* HD73, as reported by Adang et al., Gene, 36 (1985) 289, was used as a starting

COR-AAD1-00004075
Bayer EX1008 (Part 7 of 9)

sequence for the design of a maize optimized *Bt* ICP gene. The resulting maize optimized *Bt* ICP gene is identified in SEQ. ID. NO. 1. The maize specific optimized insecticidal gene sequence contains about 63% first choice codons, between about 22% to about 37% second choice codons and between about 15% to about 0% third and/or fourth choice codons, wherein the total percentage is 100%. More preferably, the maize specific optimized insecticidal gene sequence contains about 63% first choice codons, between about 22% to about 37% second choice codons, and between 15% and 0% third choice codons, wherein the total percentage is 100%. Most preferably, the maize specific optimized insecticidal gene sequence contains about 63% first choice codons, at least about 22% second choice codons, about 7.5% third choice codons, and about 7.5% fourth choice codons, wherein the total percentage is 100%.

More specifically, *B. thuringiensis* CrylA(c) was used as the starting material. Analysis of the base composition of the native gene reveals significant disparity from maize genes. For example, the guanosine plus cytosine (G+C) composition of the native ICP gene is 37%, whereas maize genes fall into the G+C range of 45-75% (Table 1).

COR-AAD1-00004076
Bayer EX1008 (Part 7 of 9)

Table 1. Compilation of G+C contents of protein coding regions of maize genes

Protein Class[a]	Range %G+C	Mean %G+C[b]
Metabolic Enzymes (40)	44.4-75.3	59.0 (8.0)
Storage Proteins		
Group I (23)	46.0-51.9	48.1 (1.3)
Group II (13)	60.4-74.3	67.5 (3.2)
Group I + II (36)	46.0-74.3	55.1 (9.6)[c]
Structural Proteins (18)	48.6-70.5	63.6 (6.7)
Regulatory Proteins (5)	57.2-68.9	62.0 (4.9)
Uncharacterized Proteins (9)	51.5-70.3	64.3-(7.2)
All Proteins (108)	**44.4-75.3**	**60.8 (5.2)**

[a] Numbers of genes in class given in parentheses.

[b] Standard deviations given in parentheses.

[c] Combined groups mean ignored in calculation of overall mean.

For the data in Table 1, coding regions of the genes were extracted from GenBank (Release 71) entries, and base compositions were calculated using the MacVector™ program (IBI, New Haven, CT). Intron sequences were ignored in the calculations. Group I and II storage protein gene sequences were distinguished by their marked difference in base composition.

The very low G+C content of the native *Bt* ICP gene (and consequent skewing towards high A+T content) results in the generation of sequences mimicking or duplicating plant gene control sequences that are known to be highly A+T rich. The presence of some A+T-rich sequences within the DNA of the introduced gene (e.g. TATA box regions normally found in gene promoters) may result in aberrant transcription of the gene. On the other hand, the presence of other regulatory sequences residing in the transcribed mRNA (e.g. polyadenylation signal sequences (AAUAAA), or sequences complementary to small nuclear RNAs involved in pre-mRNA splicing) may

COR-AAD1-00004077
Bayer EX1008 (Part 7 of 9)

lead to RNA instability. Therefore, one goal in the design of a maize optimized *Bt* ICP gene was to generate a DNA sequence having a higher G+C content, and preferably one close to that of maize genes coding for metabolic enzymes. Another goal in the design of the maize optimized *Bt* ICP gene was to generate a DNA sequence that not only has a higher G+C content, but by modifying sequence changes should be made so as to not hinder translation.

Due to the plasticity afforded by the redundancy of the genetic code (i.e. some amino acids are specified by more than one codon), evolution of the genomes of different organisms or classes of organisms has resulted in differential usage of redundant codons. This "codon bias" is reflected in the mean base composition of protein coding regions. For example, organisms with relatively low G+C contents utilize codons having A or T in the third position of redundant codons, whereas those having higher G+C contents utilize codons having G or C in the third position. It is thought that the presence of "minor" codons within a gene's mRNA may reduce the absolute translation rate of that mRNA, especially when the relative abundance of the charged tRNA corresponding to the minor codon is low. An extension of this is that the diminution of translation rate by individual minor codons would be at least additive for multiple minor codons. Therefore, mRNAs having high relative contents of minor codons would have correspondingly low translation rates. This rate would be reflected by the synthesis of low levels of the encoded protein.

A comparison of the codon composition of the *Bt* ICP gene and the codon compositions of maize genes (Table 2) reveals a large disparity in codon bias.

COR-AAD1-00004078
Bayer EX1008 (Part 7 of 9)

Table 2. Comparison of codon usage between 26 maize genes and a gene encoding a *Bacillus thuringiensis* Cry1A(c) protein[a]

Amino Acid	Codon[a]	Maize[b] %	Bt[b] %	Amino Acid	Codon[a]	Maize[b] %	Bt[b] %
Gly	GGG	16	22	Ile	ATA	8	24
Gly	GGA	13	**40**	Ile	ATT	24	**53**
Gly	GGT	21	28	Ile	ATC	**68**	23
Gly	GGC	**50**	10				
				Thr	ACG	26	22
Glu	GAG	**81**	21	Thr	ACA	11	**39**
Glu	GAA	19	**79**	Thr	ACT	16	22
				Thr	ACC	**47**	17
Asp	GAT	24	**75**				
Asp	GAC	**76**	25	Trp	TAG	**100**	**100**
Val	GTG	**40**	20	End	TGA	26	0
Val	GTA	6	**40**	End	TAG	**52**	**100**
Val	GTT	17	30	End	TAA	22	0
Val	GTC	37	10				
				Cys	TGT	21	**62**
Ala	GCG	24	23	Cys	TGC	**79**	38
Ala	GCA	13	26				
Ala	GCT	27	**39**	Tyr	TAT	14	**81**
Ala	GCC	**36**	12	Tyr	TAC	**86**	19
Arg	AGG	26	14	Leu	TTG	13	9
Arg	AGA	7	**42**	Leu	TTA	3	**42**
Arg	CGG	13	1	Leu	CTG	**31**	9
Arg	CGA	3	14	Leu	CTA	9	18
Arg	CGT	11	25	Leu	CTT	16	16
Arg	CGC	**40**	4	Leu	CTC	28	6
Ser	AGT	5	**27**	Phe	TTT	20	**80**
Ser	AGC	**28**	7	Phe	TTC	**80**	20
Ser	TCG	16	13				
Ser	TCA	10	20	Gln	CAG	**59**	13
Ser	TCT	14	18	Gln	CAA	41	**87**
Ser	TCC	27	15				
				His	CAT	29	**82**
Lys	AAG	**90**	32	His	CAC	**71**	18
Lys	AAA	10	**68**				
				Pro	CCG	27	21
Asn	AAT	19	**72**	Pro	CCA	23	**49**
Asn	AAC	**81**	28	Pro	CCT	20	26
				Pro	CCC	**30**	4
Met	ATG	**100**	**100**				

[a] Maize codon usage adapted from Murray et al. (Nucl. Acids Res., 17 (1989) 477). A compilation of 62 maize genes (Wada et al., Nucl. Acids Res., 18 (1990) 2367) indicated the same most commonly used codons, although differences between extremes were lessened.

COR-AAD1-00004079
Bayer EX1008 (Part 7 of 9)

Numbers represent the frequencies at which each codon appears in a gene sequence as a percentage of the total number of times that all codons for that particular amino acid occur. Underlined numbers signify the "preferred" codons for each organism or gene.

Without exception, any redundant codon present in the *Bacillus* gene is a nonpreferred maize codon. These differences in codon bias are particularly evident in those cases where only two codon choices exist (i.e. Glu, Asp, Lys, Asn, Cys, Tyr, Phe, Gln, and His).

In designing the maize optimized *Bt* ICP gene the amino acid sequence of ICP was reverse translated into a DNA sequence, utilizing a nonredundant genetic code established from the codon bias table compiled for maize gene DNA sequences. The resulting DNA sequence, which was completely homogeneous in codon usage, was further modified in five reiterations to establish a DNA sequence that, besides having a higher degree of codon diversity, also contained strategically placed restriction enzyme recognition sites, desirable base composition, and a lack of sequences that might interfere with transcription of the gene, or translation of the product mRNA.

Mze HD73 #1 trnc: Synthesis of an ICP gene with preferred maize codons. As a starting point for creating a new ICP gene sequence, a "Maize Genetic Code" was created, wherein each amino acid is specified by a unique codon chosen on the basis of the most commonly occurring maize codons from Table 2 (frequencies as underlined numerals in the "Maize %" columns). The native *Bt* ICP DNA sequence was translated into the corresponding protein sequence, and the amino-terminal 610 amino acids (which comprise the minimal insecticidal peptide of the ICP) were reverse-translated into a new DNA sequence based on the Maize Genetic Code. This sequence, designated Mze HD73 #1 trnc was therefore comprised

COR-AAD1-00004080
Bayer EX1008 (Part 7 of 9)

entirely of "preferred" maize codons and had a G+C content of 66%, somewhat higher than a "typical" maize gene (Table 1). The new DNA sequence had 624 base changes from the native *Bacillus* ICP DNA sequence.

Mze HD73 #2 trnc: Elimination of enzyme recognition sites. The restriction enzymes *BamH I*, *Bgl II*, *Bcl I*, and *Nco I* are routinely used for the construction of gene expression cassettes. Therefore, it is preferable that a DNA sequence that encodes a protein of interest not contain recognition sites for these enzymes. Analysis of the DNA sequence of Mze HD73 #1 trnc revealed recognition sequences for three *Bcl I* sites, three *Bgl I* sites, two *Bgl II* sites, one *BamH I* site, and one *Nco I* site. Alteration of the DNA sequence in such a fashion as to eliminate these sites forces the use of codons that are not the "preferred" maize codons, but rather are second or lower choice codons. For example, nucleotide 249 of the sequence was changed from G to C, changing a leucine codon from CTG (the preferred maize codon, being present 31% of the time, Table 2), to CTC (the second most frequently used leucine codon, occurring 28% of the time). This single change eliminated a *Bcl I* recognition site and an overlapping *Pvu II* site. Twelve other changes and their rationales are given in Table 3.

COR-AAD1-00004081
Bayer EX1008 (Part 7 of 9)

Table 3. Changes made in Mze HD73 #1 trnc → Mze HD73 #2 trnc

Position	Change	Rationale
249	G>C	Eliminate *Bcl I*h site
295	C>A	Eliminate *Bgl I* site
297	C>G	Eliminate *Bgl I* site
324	G>A	Eliminate *Bgl II* site
592	C>A	Eliminate *Bgl I* site
594	C>G	Eliminate *Bgl I* site
801	C>T	Eliminate *Bgl II* site
970	A>T	Eliminate *Bgl I* site
971	G>C	Eliminate *Bgl I* site
1020	C>G	Eliminate *Nco I* site
1368	C>T	Eliminate *BamH I* site
1461	G>C	Eliminate *Bcl I* site
1794	G>C	Eliminate *Bcl I* site

The resulting sequence was designated Mze HD73 #2 trnc, and encoded the identical protein as Mze HD73 #1 trnc.

Analysis of the sequence revealed no recognition sites for *BamH I, Bgl II, Bcl I, Nco I,* or several other commonly used enzymes. The analysis also revealed that the ICP coding strand of Mze HD73 #2 trnc contains an entire Open Reading Frame (ORF) in reading frames 1 and 3. The ORF in frame 1 corresponds to that of the ICP, and verifies that no stop codons were inadvertently generated by the changes made to the sequence. The single ORF in frame 3 begins with the G of the ICP start codon, and continues uninterrupted to the end of the sequence.

COR-AAD1-00004082
Bayer EX1008 (Part 7 of 9)

Mze HD73 #3 trnc: Modification of enzyme recognition sites to facilitate synthesis. Current technology (using a combination of automated and enzymatic DNA syntheses) has an upper limit in the range of a few hundred base pairs for the size of fragments that can be reasonably synthesized *in vitro*. Consequently, it was necessary to divide the 1830 bp of DNA sequence for the ICP into several sections, each one flanked by appropriate restriction enzyme recognition sequences. The spacing of these sites was such that the corresponding DNA fragments were of a size that could be easily synthesized and manipulated *in vitro*. Site introduction was accomplished by making 6 base changes in the sequence of Mze HD73 #2 (summarized in Table 4).

Table 4. Changes made in Mze HD73 #2 trnc → Mze HD73 #3 trnc

Position	Change	Rationale
645	G>C	Create *Xho I* site
841	C>A	Eliminate *Sst II* site
843	C>G	Eliminate *Sst II* site
1221	G>C	Create *Sal I* site
1531	C>A	Eliminate *Sst II* site
1533	C>G	Eliminate *Sst II* site

These changes were made to eliminate two of three *Sst II* sites (leaving an appropriately positioned, unique *Sst II* site), and to create new restriction enzyme recognition sites with appropriate spacing. Again, these changes did not alter the amino acid sequence of the encoded protein, and did not utilize any very low frequency maize codons. The strategy employed to identify the positions of the new sites was based on analysis of the codon usage frequencies (Table 2). Preferred or frequently used maize codon pairs were chosen that generated restriction sites when juxtaposed.

COR-AAD1-00004083
Bayer EX1008 (Part 7 of 9)

For example, paired codons CTC (Leu) and GAG (Glu) form an *Xho I* recognition site (CTCGAG), and paired codons GTC (Val) and GAC (Asp) form a *Sal I* site (GTCGAC). Analysis of the ICP sequence identified a Leu/Glu pair at residues 215/216, and a Val/Asp pair at residues 407/408. Appropriate base substitutions were made to generate the recognition sequences at these sites (Table 4). Analysis of the sequence of this gene (Mze HD73 #3 trnc) revealed the same ORF's as in version #2.

A search of the DNA sequence of Mze HD73 #3 trnc with a plant consensus sequence for exon:intron 5' junctions [AG:GTAAGT] revealed a 4/8 match [GGTA] at 629-632, and 3/8 matches [GGT] at eight other positions. The (T)GGTA(C) at 629 could not be changed without changing the encoded amino acids, since the genetic code utilizes a unique Trp codon (TGG), and both codons for the following Tyr begin with TA [TAC and TAT]. However, the sequence GGTA is probably not sufficient to serve as a splice recognition site, since the 5' A residue of the consensus sequence is highly conserved in splice recognition sites for both plant and animal RNAs, and the GGTA sequence occurs in the *E. coli* ß-glucuronidase coding region (which is expressed well in plant cells), and in exon 1 of maize alcohol dehydrogenase (Adh) 1. In addition, GGTA is found as part of all *Kpn I* recognition sites [GGTACC] which occur naturally in some plant genes, so it likely does not represent a potential splice donor site *per se*.

The Mze HD73 #3 trnc DNA sequence was then searched for sequences similar to or identical with the poly A addition site signal consensus AATAAA. A perfect match was found in the native ICP gene sequence, but no homology was found to this engineered sequence, or shorter versions of it (down to AATA) in Mze HD73 #3 trnc.

COR-AAD1-00004084
Bayer EX1008 (Part 7 of 9)

Sequences resembling an RNA polymerase II termination sequence were searched using the template CAN-_AGTNNAA, where N represents any of the four bases found in DNA. There were no matches at any level with N set 7 to 9.

It is thought that the formation of intrastrand self-complementary structures ("hairpins") in mRNAs inhibits the progression of ribosomes along the mRNA during translation, and that the hairpin formers CTTCGG and its same-strand complement CCGAAG are particularly disadvantageous. Two perfect matches of CTTCGG were found in Mze HD73 #3 trnc (at 201-206 and 1707-1712). However, there were no matches to CCGAAG, CCGAA, CGAAG, or CGAA. Since the importance of hairpins is uncertain, the ICP sequence was not examined for any other self-complementary sequence blocks.

Mze HD73 #3 trnc: Elimination of TA or GC doublets. Eukaryotic genes are relatively deficient in the nucleotide doublets TA and GC, and enriched in doublets TG and CT. Only two "preferred" maize codons (Table 2) contain TA or CG doublets: TAC (Tyr) and CGC (Arg). The use of these codons in the synthetic sequence necessitates the generation of doublets we wished to avoid. Therefore, the benefit of using the preferred codon must be balanced against the detriment of creating an overabundance of "forbidden" doublets. In the Tyr case, substitution by the second choice codon does not eliminate the TA doublet, since it is also a component of that codon (TAT). In the Arg case, however, the second choice codon (AGG) is used in maize only slightly less frequently than the first choice (26% vs 40% of the time), so the substitution of CGC by AGG was completed. The other codons that contain TA or CG doublets [GTA (Val); ATA (Ile); TAG, TAA (End); TTA, CTA (Leu); GCG (Ala); CGG, CGA, CGT (Art); ACG (Thr); and CCG (Pro)] are either not acceptable for use in coding regions (e.g. the

COR-AAD1-00004085
Bayer EX1008 (Part 7 of 9)

stop codons), are found so infrequently in maize genes that they are not suitable for inclusion in a codon-biased sequence, or are members of codons sets that have acceptable synonyms (Table 2).

In addition to occurring within a single codon, CG and TA doublets are generated by juxtaposition of codons ending in C or T and codons beginning with G or A. Since none of the maize preferred codons end in T, T/A juxtapositions are necessarily due to doublets internal to single codons, in gene versions using only preferred codons. CG doublets generated by amino acid pairs are located by reviewing the protein sequence for juxtapositions of amino acids that are represented by maize preferred codons ending in C, with amino acids represented by maize preferred codons starting with G. The "C-enders" are Gly (GGC), Asp (GAC), Ala (GCC), Arg (CGC, Ser (AGC), Asn (AAC), lle (ATC), Thr (ACC), Cys (TGC), Tyr (TAC), Phe (TTC), His (CAC, and Pro (CCC); the "G-starters" are Gly (GGC), Glu (GAG), Asp (GAC), Val (GTG), and Ala (GCC) (Table 5).

COR-AAD1-00004086
Bayer EX1008 (Part 7 of 9)

Table 5. Amino Acid Juxtapositions That Generate CG Doublets

AMINO ACIDS WITH CODONS THAT START WITH G					
Amino Acids with Codons That End with C[a]	**Glycine (G)**	**Glutamic Acid (E)**	**Aspartic Acid (D)**	**Valine (V)**	**Alanine (A)**
Glycine (G) GGC(50)>GGT(21)	Gly/Gly G/G	Gly/Gly G/E	Gly/Asp G/D	Gly/Val G/V	Gly/Ala G/A
Alanine (A) GCC(36)>GCT(27)	Ala/Gly A/G	Ala/Glu A/E	Ala/Asp A/D	Ala/Val A/V	Ala/Ala A/A
Arginine (R) CGC(40)>AGG(26)	Arg/Gly R/G	Arg/Glu R/E	Arg/Asp R/D	Arg/Val R/V	Arg/Ala R/A
Serine (S) AGC(28)>TCG(16) AGC(28)>TCT(14)	Ser/Gly S/G	Ser/Glu S/E	Ser/Asp S/D	Ser/Val S/V	Ser/Ala S/A
Isoleucine (I) ATC(68)>ATT(24)	Ile/Gly I/G	Ile/Glu I/E	Ile/Asp I/D	Ile/Val I/V	Ile/Ala I/A
Threonine (T) ACC(47)>ACG(26)	Thr/Gly T/G	Thr/Glu T/E	Thr/Asp T/D	Thr/Val T/V	Thr/Ala T/A
Proline (P) CCC(30)>CCG(27)	Pro/Gly P/G	Pro/Glu P/E	Pro/Asp P/D	Pro/Val P/V	Pro/Ala P/A

[a]Recommended codon substitutions and the relative frequencies of the codons in maize genes are given below the amino acid names.

Having identified such amino acid doublets, one could then try to change either of the codons to minimize the occurrence of CG doublets, without sacrificing an inordinate amount of codon bias. However, since all of the alternate codons for the preferred codon "G-starters" also begin with G, the G of these CG doublets can not be changed, and one is confined to changes in the codons for the first amino acid of the pair, when appropriate alternate codons exist. In some instances [e.g. Asp: GAC (76) > GAT (24); Asn: AAC (81) > AAT (19); Cys: TGC (79) > TGT (21); Tyr: TAC (86) > TAT (14); Phe: TTC (80) > TTT (20); and His: CAC (71) > CAT (29)], the alternate codon is found in maize genes at such a significantly lower frequency than the preferred codons that substitution is

COR-AAD1-00004087
Bayer EX1008 (Part 7 of 9)

not an option. Therefore, doublets generated by those juxtapositions can be ignored.

Accordingly, a list of 128 doublets that comprised juxtapositions of the above amino acids that generate CG in the Mze HD73 #3 trnc protein sequence was compiled (Table 6). Changes to the sequence of the codons corresponding to 74 of the amino acid doublets (underlined position numbers in Table 6) were made to eliminate the CG base doublets.

Table 6. Amino Acid Juxtapositions in Mze HD73 #3 trnc That Generate CG Doublets[a]

Position	Amino Acids	Position	Amino Acids	Position	Amino Acids
8/9	ASN/GLU	206/207	TYR/ALA	438/439	SER/GLY
19/20	PRO/GLUE	207/208	ALA/VAL	444/445	SER/VAL
25/26	GLY/GLY	213/214	THR/GLY	449/450	ARG/ALA
26/27	GLY/GLU	217/218	ARG/VAL	459/460	SER/ALA
29/30	ILE/GLU	221/222	PRO/ASP	460/461	ALA/GLU
31/32	THR/GLY	224/225	ARG/ASP	466/467	ILE/ALA
36/37	ILE/ASP	234/235	ARG/GLU	468/469	SER/ASP
48/49	SER/GLU	239/240	THR/VAL	475/476	PRO/ALA
50/51	PHE/VAL	243/244	ILE/VAL	476/477	ALA/VAL
52/53	PRO/GLY	250/251	TYR/ASP	484/485	ASN/GLY
53/54	GLY/ALA	259/260	THR/VAL	486/487	SER/VAL
54/55	ALA/GLY	265/266	ARG/GLU	489/490	SER/GLY
56/57	PHE/VAL	271/272	PRO/VAL	491/492	PRO/GLY
68/69	PHE/GLY	276/277	PHE/ASP	494/495	THR/GLY
74/75	ASP/ALA	277/278	ASP/GLY	495/496	GLY/GLY
80/81	ILE/GLU	281/282	ARG/GLY	496/497	GLY/ASP
88/89	ILE/GLU	283/284	SER/ALA	504/505	SER/GLY
91/92	PHE/ALA	287/288	ILE/GLU	511/512	ARG/GLY
110/111	TYR/ALA	307/308	THR/ASP	514/515	ILE/GLU
111/112	ALA/GLU	308/309	ASP/ALA	528/529	ARG/VAL
115/116	ARG/GLU	311/312	ARG/GLY	530/531	ARG/VAL
119/120	ALA/ASP	317/318	SER/GLY	533/534	TYR/ALA
124/125	PRO/ALA	325/326	PRO/VAL	535/536	SER/VAL
127/128	ARG/GLU	329/330	SER/GLY	542/543	ASN/VAL
135/136	ASN/ASP	331/332	PRO/GLU	554/555	THR/VAL
139/140	SER/ALA	338/339	TYR/GLY	556/557	PRO/ALA
143/144	THR/ALA	343/344	ASN/ALA	558/559	THR/ALA
148/149	PHE/ALA	344/345	ALA/ALA	568/569	SER/ASP
149/150	ALA/VAL	350/351	ILE/VAL	570/571	PHE/GLY

COR-AAD1-00004088
Bayer EX1008 (Part 7 of 9)

Position	Amino Acids	Position	Amino Acids	Position	Amino Acids
159/160	SER/VAL	**357/358**	GLY/VAL	573/574	PHE/GLU
161/162	TYR/VAL	**373/374**	ILE/GLY	575/576	SER/ALA
164/165	ALA/ALA	**381/382**	SER/VAL	577/578	ASN/ALA
170/171	SER/VAL	**384/385**	ASP/GLY	586/587	ILE/VAL
173/174	ARG/ASP	**386/387**	THR/GLU	**588/589**	GLY/VAL
174/175	ASP/VAL	388/389	PHE/ALA	**593/594**	SER/GLY
176/177	SER/VAL	390/391	TYR/GLY	**595/596**	THR/ALA
178/179	PHE/GLY	398/399	SER/ALA	**596/597**	ALA/GLY
184/185	PHE/ASP	399/400	ALA/VAL	**597/598**	GLY/VAL
185/186	ASP/ALA	**404/405**	SER/GLY	600/601	ILE/ASP
186/187	ALA/ALA	406/407	THR/VAL	603/604	PHE/GLU
194/195	ASN/ASP	412/413	ASP/GLU	**607/608**	PRO/VAL
200/201	ILE/GLY	419/420	ASN/VAL	**609/610**	THR/ALA
204/205	THR/ASP	432/433	HIS/GLY		

* Bases in positions in bold type were changed as documented in Table 7 below.

The choice of which alternate codons to substitute for the preferred ones is largely determined by the fact that the alternate should not be amongst the class of very infrequently used codons. One factor to consider is that a DNA sequence comprised of only the preferred maize codons may suffer from expression problems, since an unnatural reliance on a single codon for each amino acid may deplete the pool of tRNAs or aminoacyl-tRNA synthetases for that codon. It is thought to be beneficial to introduce some diversity in codon composition by using second (or third) choice codons, as long as the natural usage of the codon in maize genes seems to accommodate the choice. In this regard, it is important to note that the frequency of codon occurrence in any organism's genes must be weighted relative to the number of synonymous codons that exist for the particular amino acid in the universal genetic code. For example, the relative frequencies of maize usage of the Phe codon TTT (20%) clearly reflects a greater amount of counterselection (codon bias) than the identical relative frequency of the Pro codon CCT (20%), since there are only two Phe codons, and four Pro codons (Table 2). The

COR-AAD1-00004089
Bayer EX1008 (Part 7 of 9)

acceptability of an alternate codon as a substitute for a preferred one is therefore not a straightforward choice.

Additional factors come into play when making the choice of acceptable alternative codons to reduce the numbers of CG doublets. For example, when the preferred Arg codon CGC (40%) occurs in the context CGCG, two CG doublets are eliminated simultaneously by substitution with the second choice Arg codon AGG (26%). Clearly, such substitutions are desirable from the dual standpoints of reducing CG doublets, as well as generating codon diversity. On a more subtle basis, substitution of the preferred Thr codon ACC (47%) in the context ACCG by the second choice codon ACG (26%), or substitution of the preferred Ser codon AGC (28%) in the context AGCG by the third choice codon TCG (16%), does not change the overall numbers of CG doublets, but generates desirable codon diversity. Finally, substitution of the preferred Ser codon AGC (28%) in the context AGCG with the fourth choice codon TCT (14%) eliminates the CG doublet, generates codon diversity, and increases the overall number of CT doublets as well.

Table 7 summarizes these and other changes made to the sequence of Mze HD73 #3 trnc to generate Mze HD73 #4 trnc.

Table 7. Changes made in Mze HD73 #3 trnc → Mze HD73 #4 trnc

Position	Change	Basis	Position	Change	Basis	Position	Change	Basis
75	C>T	1	949	A>T	3, 9	1470	C>T	3, 4
78	C>T	1	950	G>C	3, 9	1473	C>A	1, 3, 4
156	C>A	1	951	C>T	1, 9	1476	C>T	3, 4
159	C>T	1, 10	975	C>A	1	1482	C>G	3
162	C>T	1, 9	985	A>T	3, 9	1485	C>T	1
183	G>C	2	986	G>C	3, 9	1488	C>T	1
264	C>T	1	987	C>T	1, 9	1510	A>T	3, 9

COR-AAD1-00004090
Bayer EX1008 (Part 7 of 9)

Position	Change	Basis	Position	Change	Basis	Position	Change	Basis
333	C>T	1, 9	993	C>A	1	1511	G>C	3
343	C>A	3	1032	C>T	1, 9	1512	C>G	1
345	C>G	1	1050	C>T	1	1515	C>T	3, 4
357	C>T	1, 9	1071	C>T	1	1582	C>A	1
372	C>A	1	1119	C>T	1	1583	C>G	1
379	C>A	1	1141	A>T	3	1587	G>C	3
381	C>G	1	1142	G>C	3	1588	C>A	1
429	C>G	3	1143	C>G	1	1590	C>G	1
447	C>T	1, 9	1152	C>T	1	1593	G>C	3
480	G>C	3, 9	1158	C>T	1, 9	1594	C>A	1, 3, 4
492	C>T	1, 9	1167	C>T	3, 4, 9	1596	C>G	3, 4
508	A>T	3	1210	A>T	3, 9	1602	C>T	3, 4, 9
509	G>C	3	1211	G>C	3, 9	1603	A>T	3, 9
510	C>G	1	1212	C>T	1, 9	1604	G>C	3, 9
517	C>A	1	1215	C>T	5	1605	C>T	1, 9
519	C>G	1	1221	C>G	6	1662	C>G	1
555	C>T	1	1312	A>T	3	1668	C>A	1
558	C>T	1, 9	1313	G>C	3	1674	C>G	1
600	C>T	1	1314	C>G	1	1699	A>T	3
612	C>G	3	1330	A>T	3, 4	1700	G>C	3
639	C>G	3	1331	G>C	3, 4	1702	A>T	3, 9
649	C>A	1	1332	C>T	1	1703	G>C	3
651	C>G	1	1345	C>A	1	1704	C>G	1
663	C>A	1	1347	C>G	1	1723	A>T	3
670	C>A	1	1353	C>A	3, 4	1724	G>C	3
672	C>G	1	1375	A>T	3, 9	1725	C>G	1
700	C>A	3	1376	G>C	3, 9	1764	C>T	1
702	C>G	1	1377	C>T	1, 9	1777	A>T	3, 9
717	C>G	1	1380	C>T	1, 9	1778	G>C	3, 9
729	C>T	1	1398	C>T	1	1779	C>T	1
777	C>G	1	1402	A>T	3, 9	1785	C>G	1
793	C>A	1	1403	G>C	3, 9	1788	C>T	1, 9
795	C>G	1	1404	C>T	1, 9	1791	C>T	1
813	C>A	1	1428	C>T	1, 9	1821	C>A	1
847	A>T	3	1456	A>T	3	1827	C>G	1
848	G>C	3	1457	G>C	3	1831-33	CCA	7

COR-AAD1-00004091
Bayer EX1008 (Part 7 of 9)